VOLUME 29 / NUMBER 18
SEPTEMBER 23, 1991
ACC. NOS. N91-26113 TO N91-27119

STAR
AN ABSTRACT JOURNAL

Scientific and Technical Aerospace Reports

PRODUCED BY THE
SCIENTIFIC AND TECHNICAL
INFORMATION
PROGRAM

NASA

NATIONAL AERONAUTICS AND SPACE ADMINISTRATION

***Scientific and Technical Aerospace Reports* (*STAR*)** is an abstract journal that provides comprehensive coverage of worldwide aerospace-related reports. It is a major product of the International Aerospace Database managed by the NASA Scientific and Technical Information (STI) Program. The coverage includes reports on aeronautics, space, and supporting disciplines. *STAR* lists current, publicly available reports entered into the NASA STI Database during the 2-week period preceding publication. A typical citation and abstract appear on page viii. They explain how to read the items that are announced in this journal.

NASA sponsors a companion journal, *International Aerospace Abstracts* (*IAA*), that lists abstracts of the open literature on aerospace subjects available worldwide. *IAA* is available through the American Institute of Aeronautics and Astronautics.

Entries found in *STAR* and *IAA* are available through NASA's online service, RECON, as the International Aerospace Database and through DIALOG as the Aerospace Database.

Information on aerospace and related subjects is gathered by the NASA STI Program through national and international agreements and exchanges and is made available to the NASA community as well as to the public in many forms through various outlets. The section on NASA STI Program Products and Services contains additional information.

US ISSN 0036-8741

Volume 29 Number 18 / September 23, 1991

TABLE OF CONTENTS

AERONAUTICS For related information see also *Astronautics.*

01 AERONAUTICS (GENERAL) **2921**

02 AERODYNAMICS **2921**
Includes aerodynamics of bodies, combinations, wings, rotors, and control surfaces; and internal flow in ducts and turbomachinery. For related information see also *34 Fluid Mechanics and Heat Transfer.*

03 AIR TRANSPORTATION AND SAFETY **2923**
Includes passenger and cargo air transport operations; and aircraft accidents. For related information see also *16 Space Transportation* and *85 Urban Technology and Transportation.*

04 AIRCRAFT COMMUNICATIONS AND NAVIGATION **2923**
Includes digital and voice communication with aircraft; air navigation systems (satellite and ground based); and air traffic control. For related information see also *17 Space Communications, Spacecraft Communications, Command and Tracking* and *32 Communications and Radar.*

05 AIRCRAFT DESIGN, TESTING AND PERFORMANCE **2924**
Includes aircraft simulation technology. For related information see also *18 Spacecraft Design, Testing and Performance* and *39 Structural Mechanics.* For land transportation vehicles see *85 Urban Technology and Transportation.*

06 AIRCRAFT INSTRUMENTATION **2926**
Includes cockpit and cabin display devices; and flight instruments. For related information see also *19 Space craft Instrumentation* and *35 Instrumentation and Photography.*

07 AIRCRAFT PROPULSION AND POWER **2926**
Includes prime propulsion systems and systems components, e.g., gas turbine engines and compressors; and onboard auxiliary power plants for aircraft. For related information see also *20 Spacecraft Propulsion and Power, 28 Propellants and Fuels,* and *44 Energy Production and Conversion.*

08 AIRCRAFT STABILITY AND CONTROL **2927**
Includes aircraft handling qualities; piloting; flight controls; and autopilots. For related information see also *05 Aircraft Design, Testing and Performance.*

09 RESEARCH AND SUPPORT FACILITIES (AIR) **2929**
Includes airports, hangars and runways; aircraft repair and overhaul facilities; wind tunnels; shock tubes; and aircraft engine test stands. For related information see also *14 Ground Support Systems and Facilities (Space).*

ASTRONAUTICS For related information see also *Aeronautics.*

12 ASTRONAUTICS (GENERAL) **2930**
For extraterrestrial exploration see *91 Lunar and Planetary Exploration.*

13 ASTRODYNAMICS **2933**
Includes powered and free-flight trajectories; and orbital and launching dynamics.

14 GROUND SUPPORT SYSTEMS AND FACILITIES (SPACE) **2934**
Includes launch complexes, research and production facilities; ground support equipment, e.g., mobile transporters; and simulators. For related information see also *09 Research and Support Facilities (Air).*

15 LAUNCH VEHICLES AND SPACE VEHICLES ..... **N.A.**
Includes boosters; operating problems of launch/space vehicle systems; and reusable vehicles. For related information see also *20 Spacecraft Propulsion and Power.*

16 SPACE TRANSPORTATION **2935**
Includes passenger and cargo space transportation, e.g., shuttle operations; and space rescue techniques. For related information see also *03 Air Transportation and Safety* and *18 Spacecraft Design, Testing and Performance.* For space suits see *54 Man/System Technology and Life Support.*

17 SPACE COMMUNICATIONS, SPACECRAFT COMMUNICATIONS, COMMAND AND TRACKING . **N.A.**
Includes telemetry; space communications networks; astronavigation and guidance; and radio blackout. For related information see also *04 Aircraft Communications and Navigation* and *32 Communications and Radar.*

N.A.—no abstracts were assigned to this category for this issue.

18 SPACECRAFT DESIGN, TESTING AND PERFORMANCE **2935**
Includes satellites; space platforms; space stations; spacecraft systems and components such as thermal and environmental controls; and attitude controls. For life support systems see *54 Man/System Technology and Life Support.* For related information see also *05 Aircraft Design, Testing and Performance, 39 Structural Mechanics,* and *16 Space Transportation.*

19 SPACECRAFT INSTRUMENTATION ..... **N.A.**
For related information see also *06 Aircraft Instrumentation* and *35 Instrumentation and Photography.*

20 SPACECRAFT PROPULSION AND POWER **2936**
Includes main propulsion systems and components, e.g., rocket engines; and spacecraft auxiliary power sources. For related information see also *07 Aircraft Propulsion and Power, 28 Propellants and Fuels, 44 Energy Production and Conversion,* and *15 Launch Vehicles and Space Vehicles.*

CHEMISTRY AND MATERIALS

23 CHEMISTRY AND MATERIALS (GENERAL) **2938**

24 COMPOSITE MATERIALS **2939**
Includes physical, chemical, and mechanical properties of laminates and other composite materials. For ceramic materials see *27 Nonmetallic Materials.*

25 INORGANIC AND PHYSICAL CHEMISTRY **2944**
Includes chemical analysis, e.g., chromatography; combustion theory; electrochemistry; and photochemistry. For related information see also *77 Thermodynamics and Statistical Physics.*

26 METALLIC MATERIALS **2953**
Includes physical, chemical, and mechanical properties of metals, e.g., corrosion; and metallurgy.

27 NONMETALLIC MATERIALS **2958**
Includes physical, chemical, and mechanical properties of plastics, elastomers, lubricants, polymers, textiles, adhesives, and ceramic materials. For composite materials see *24 Composite Materials.*

28 PROPELLANTS AND FUELS **2968**
Includes rocket propellants, igniters and oxidizers; their storage and handling procedures; and aircraft fuels. For related information see also *07 Aircraft Propulsion and Power, 20 Spacecraft Propulsion and Power,* and *44 Energy Production and Conversion.*

29 MATERIALS PROCESSING **2971**
Includes space-based development of products and processes for commercial application. For biological materials see *55 Space Biology.*

ENGINEERING For related information see also *Physics.*

31 ENGINEERING (GENERAL) **2971**
Includes vacuum technology; control engineering; display engineering; cryogenics; and fire prevention.

32 COMMUNICATIONS AND RADAR **2972**
Includes radar; land and global communications; communications theory; and optical communications. For related information see also *04 Aircraft Communications and Navigation* and *17 Space Communications, Spacecraft Communications, Command and Tracking.* For search and rescue see *03 Air Transportation and Safety,* and *16 Space Transportation.*

33 ELECTRONICS AND ELECTRICAL ENGINEERING **2977**
Includes test equipment and maintainability; components, e.g., tunnel diodes and transistors; microminiaturization; and integrated circuitry. For related information see also *60 Computer Operations and Hardware* and *76 Solid-State Physics.*

34 FLUID MECHANICS AND HEAT TRANSFER **2982**
Includes boundary layers; hydrodynamics; fluidics; mass transfer and ablation cooling. For related information see also *02 Aerodynamics* and *77 Thermodynamics and Statistical Physics.*

35 INSTRUMENTATION AND PHOTOGRAPHY **2987**
Includes remote sensors; measuring instruments and gauges; detectors; cameras and photographic supplies; and holography. For aerial photography see *43 Earth Resources and Remote Sensing.* For related information see also *06 Aircraft Instrumentation* and *19 Spacecraft Instrumentation.*

36 LASERS AND MASERS **2988**
Includes parametric amplifiers. For related information see also *76 Solid-State Physics.*

37 MECHANICAL ENGINEERING **2993**
Includes auxiliary systems (nonpower); machine elements and processes; and mechanical equipment.

38 QUALITY ASSURANCE AND RELIABILITY **2996**
Includes product sampling procedures and techniques; and quality control.

39 STRUCTURAL MECHANICS **2998**
Includes structural element design and weight analysis; fatigue; and thermal stress. For applications see *05 Aircraft Design, Testing and Performance* and *18 Spacecraft Design, Testing and Performance.*

GEOSCIENCES For related information see also *Space Sciences.*

42 GEOSCIENCES (GENERAL) **3001**

43 EARTH RESOURCES AND REMOTE SENSING **3003**
Includes remote sensing of earth resources by aircraft and spacecraft; photogrammetry; and aerial photography. For instrumentation see *35 Instrumentation and Photography.*

44 ENERGY PRODUCTION AND CONVERSION **3004**
Includes specific energy conversion systems, e.g., fuel cells; global sources of energy; geophysical conversion; and windpower. For related information see also *07 Aircraft Propulsion and Power, 20 Spacecraft Propulsion and Power,* and *28 Propellants and Fuels.*

45 ENVIRONMENT POLLUTION **3005**
Includes atmospheric, noise, thermal, and water pollution.

46 GEOPHYSICS **3008**
Includes aeronomy; upper and lower atmosphere studies; ionospheric and magnetospheric physics; and geomagnetism. For space radiation see *93 Space Radiation.*

47 METEOROLOGY AND CLIMATOLOGY **3013**
Includes weather forecasting and modification.

48 OCEANOGRAPHY **3017**
Includes biological, dynamic, and physical oceanography; and marine resources. For related information see also *43 Earth Resources and Remote Sensing.*

LIFE SCIENCES

51 LIFE SCIENCES (GENERAL) **3019**

52 AEROSPACE MEDICINE **3022**
Includes physiological factors; biological effects of radiation; and effects of weightlessness on man and animals.

53 BEHAVIORAL SCIENCES **3031**
Includes psychological factors; individual and group behavior; crew training and evaluation; and psychiatric research.

54 MAN/SYSTEM TECHNOLOGY AND LIFE SUPPORT **3034**
Includes human engineering; biotechnology; and space suits and protective clothing. For related information see also *16 Space Transportation.*

55 SPACE BIOLOGY ..... **N.A.**
Includes exobiology; planetary biology; and extraterrestrial life.

MATHEMATICAL AND COMPUTER SCIENCES

59 MATHEMATICAL AND COMPUTER SCIENCES (GENERAL) ..... **N.A.**

60 COMPUTER OPERATIONS AND HARDWARE **3037**
Includes hardware for computer graphics, firmware, and data processing. For components see *33 Electronics and Electrical Engineering.*

61 COMPUTER PROGRAMMING AND SOFTWARE **3038**
Includes computer programs, routines, algorithms, and specific applications, e.g., CAD/CAM.

62 COMPUTER SYSTEMS **3043**
Includes computer networks and special application computer systems.

63 CYBERNETICS **3044**
Includes feedback and control theory, artificial intelligence, robotics and expert systems. For related information see also *54 Man/System Technology and Life Support.*

64 NUMERICAL ANALYSIS **3049**
Includes iteration, difference equations, and numerical approximation.

65 STATISTICS AND PROBABILITY **3053**
Includes data sampling and smoothing; Monte Carlo method; and stochastic processes.

66 SYSTEMS ANALYSIS **3054**
Includes mathematical modeling; network analysis; and operations research.

67 THEORETICAL MATHEMATICS ..... **N.A.**
Includes topology and number theory.

PHYSICS For related information see also *Engineering.*

70 PHYSICS (GENERAL) **3055**
For precision time and time interval (PTTI) see *35 Instrumentation and Photography;* for geophysics, astrophysics or solar physics see *46 Geophysics, 90 Astrophysics,* or *92 Solar Physics.*

71 ACOUSTICS **3055**
Includes sound generation, transmission, and attenuation. For noise pollution see *45 Environment Pollution.*

72 ATOMIC AND MOLECULAR PHYSICS **3058**
Includes atomic structure, electron properties, and molecular spectra.

73 NUCLEAR AND HIGH-ENERGY PHYSICS **3062**
Includes elementary and nuclear particles; and reactor theory. For space radiation see *93 Space Radiation.*

74 OPTICS **3062**
Includes light phenomena and optical devices. For lasers see *36 Lasers and Masers.*

75 PLASMA PHYSICS **3066**
Includes magnetohydrodynamics and plasma fusion. For ionospheric plasmas see *46 Geophysics.* For space plasmas see *90 Astrophysics.*

76 SOLID-STATE PHYSICS **3068**
Includes superconductivity. For related information see also *33 Electronics and Electrical Engineering* and *36 Lasers and Masers.*

77 THERMODYNAMICS AND STATISTICAL PHYSICS **3074**
Includes quantum mechanics; theoretical physics; and Bose and Fermi statistics. For related information see also *25 Inorganic and Physical Chemistry* and *34 Fluid Mechanics and Heat Transfer.*

SOCIAL SCIENCES

80 SOCIAL SCIENCES (GENERAL) ..... **N.A.**
Includes educational matters.

81 ADMINISTRATION AND MANAGEMENT **3075**
Includes management planning and research.

82 DOCUMENTATION AND INFORMATION SCIENCE **3076**
Includes information management; information storage and retrieval technology; technical writing; graphic arts; and micrography. For computer documentation see *61 Computer Programming and Software.*

83 ECONOMICS AND COST ANALYSIS ..... **N.A.**
Includes cost effectiveness studies.

84 LAW, POLITICAL SCIENCE AND SPACE POLICY **3083**
Includes NASA appropriation hearings; aviation law; space law and policy; international law; international cooperation; and patent policy.

85 URBAN TECHNOLOGY AND TRANSPORTATION ..... **N.A.**
Includes applications of space technology to urban problems; technology transfer; technology assessment; and surface and mass transportation. For related information see *03 Air Transportation and Safety, 16 Space Transportation,* and *44 Energy Production and Conversion.*

SPACE SCIENCES For related information see also *Geosciences.*

88 SPACE SCIENCES (GENERAL) ..... **N.A.**

89 ASTRONOMY **3083**
Includes radio, gamma-ray, and infrared astronomy; and astrometry.

90 ASTROPHYSICS **3084**
Includes cosmology; celestial mechanics; space plasmas; and interstellar and interplanetary gases and dust. For related information see also *75 Plasma Physics.*

91 LUNAR AND PLANETARY EXPLORATION **3084**
Includes planetology; and manned and unmanned flights. For spacecraft design or space stations see *18 Spacecraft Design, Testing and Performance.*

92 SOLAR PHYSICS **3090**
Includes solar activity, solar flares, solar radiation and sunspots. For related information see *93 Space Radiation.*

93 SPACE RADIATION ..... **N.A.**
Includes cosmic radiation; and inner and outer earth's radiation belts. For biological effects of radiation see *52 Aerospace Medicine.* For theory see *73 Nuclear and High-Energy Physics.*

GENERAL

Includes aeronautical, astronautical, and space science related histories, biographies, and pertinent reports too broad for categorization; histories or broad overviews of NASA programs.

99 GENERAL **3091**

SUBJECT INDEX **I-1**

PERSONAL AUTHOR INDEX **I-77**

CORPORATE SOURCE INDEX **I-85**

CONTRACT NUMBER INDEX **I-99**

REPORT/ACCESSION NUMBER INDEX **I-103**

APPENDIX **A-1**

TYPICAL CITATION AND ABSTRACT

NASA SPONSORED
ON MICROFICHE
ACCESSION NUMBER
N91-10047*# Georgia Inst. of Tech., Atlanta. School of Aerospace Engineering.
CORPORATE SOURCE
TITLE
NONLINEAR FEEDBACK CONTROL FOR HIGH ALPHA FLIGHT Final Report, Jan. 1989 - Apr. 1990
PUBLICATION DATE
AUTHOR
Harold Stalford Apr. 1990 15 p
CONTRACT OR GRANT
(Grant NAG1-959)
AVAILABILITY SOURCE
REPORT NUMBERS
(NASA-CR-186545; NAS 1.26;186545) Avail: NTIS HC/MF A03
PRICE CODE
COSATI CODE
CSCL 01C
Analytical aerodynamic models are derived from a high alpha 6 DOF wind tunnel model. One detail model requires some interpolation between nonlinear functions of alpha. One analytical model requires no interpolation and as such is a completely continuous model. Flight path optimization is conducted on the basic maneuvers: half-loop, 90 degree pitch-up, and level turn. The optimal control analysis uses the derived analytical model in the equations of motion and is based on both moment and force equations. The maximum principle solution for the half-loop is poststall trajectory performing the half-loop in 13.6 seconds. The agility induced by thrust vectoring capability provided a minimum effect on reducing the maneuver time. By means of thrust vectoring control the 90 degrees pitch-up maneuver can be executed in a small place over a short time interval. The agility capability of thrust vectoring is quite beneficial for pitch-up maneuvers. The level turn results are based currently on only outer layer solutions of singular pertrubation. Poststall solutions provide high turn rates but generate higher losses of energy than that of classical sustained solutions.
Author

VOLUME 29 NUMBER 18 / SEPTEMBER 23, 1991

Scientific and Technical Aerospace Reports

A Semimonthly Publication of the National Aeronautics and Space Administration

01 AERONAUTICS (GENERAL)

N91-26113*# National Aeronautics and Space Administration. Hugh L. Dryden Flight Research Facility, Edwards, CA.
DEVELOPMENT OF AN INTEGRATED AEROSERVOELASTIC ANALYSIS PROGRAM AND CORRELATION WITH TEST DATA
K. K. Gupta, M. J. Brenner, and L. S. Voelker Washington May 1991 105 p
(NASA-TP-3120; H-1543; NAS 1.60:3120) Avail: NTIS HC/MF A06 CSCL 01B

The details and results are presented of the general-purpose finite element STructural Analysis RoutineS (STARS) to perform a complete linear aeroelastic and aeroservoelastic analysis. The earlier version of the STARS computer program enabled effective finite element modeling as well as static, vibration, buckling, and dynamic response of damped and undamped systems, including those with pre-stressed and spinning structures. Additions to the STARS program include aeroelastic modeling for flutter and divergence solutions, and hybrid control system augmentation for aeroservoelastic analysis. Numerical results of the X-29A aircraft pertaining to vibration, flutter-divergence, and open- and closed-loop aeroservoelastic controls analysis are compared to ground vibration, wind-tunnel, and flight-test results. The open- and closed-loop aeroservoelastic control analyses are based on a hybrid formulation representing the interaction of structural, aerodynamic, and flight-control dynamics. Author

02 AERODYNAMICS

Includes aerodynamics of bodies, combinations, wings, rotors, and control surfaces; and internal flow in ducts and turbomachinery.

For related information see also *34 Fluid Mechanics and Heat Transfer.*

N91-26114*# Nevada Univ., Reno. Engineering Research and Development Center.
NUMERICAL INVESTIGATIONS IN THREE-DIMENSIONAL INTERNAL FLOWS Semiannual Status Report, 1 Jan. - 30 Jun. 1991
William C. Rose 30 Jun. 1991 32 p
(Contract NCC2-507)
(NASA-CR-188615; NAS 1.26:188615) Avail: NTIS HC/MF A03 CSCL 01A

The present study is a preliminary investigation into the behavior of the flow within a 28 degree total geometric turning angle hypothetical Mach 10 inlet as calculated with the full three-dimensional Navier-Stokes equations. Comparison between the two-dimensional and three-dimensional solutions have been made. The overall compression is not significantly different between the two-dimensional and center plane three dimensional solutions. Approximately one-half to two-thirds of the inlet flow at the exit of the inlet behave nominally two-dimensionally. On the other hand, flow field non-uniformities in the three-dimensional solution indicate the potential significance of the sidewall boundary layer flows ingested into the inlet. The tailoring of the geometry at the inlet shoulder and on the cowl obtained in the two-dimensional parametric design study have also proved to be effective at controlling the boundary layer behavior in the three-dimensional code. The three-dimensional inlet solution remained started indicating that the two-dimensional design had a sufficient margin to allow for three-dimensional flow field effects. Although confidence is being gained in the use of SCRAM3D (three-dimensional full Navier-Stokes code) as applied to similar flow fields, the actual effects of the three-dimensional flow fields associated with sidewalls and wind tunnel installations can require verification with ground-based experiments. Author

N91-26115# Aerospace Corp., El Segundo, CA. Lab. Operations.
PRESSURE DISTRIBUTION AND INDUCED FORCE FIELD ON A CONICAL NOZZLE DUE TO IMPINGEMENT OF A NORMAL JET INTO THE SUPERSONIC CROSS-FLOW
Farzad Baban, Emil M. Kaegi, Munson A. Kwok, Robert L. Vaewig, and Richard G. Aurandt 15 Feb. 1991 31 p
(Contract F04701-88-C-0089)
(AD-A233981; TR-0090(5930-01)-2; SSD-TR-91-05) Avail: NTIS HC/MF A03 CSCL 20/4

An experimental investigation was undertaken to study the pressure distribution and induced side force on the wall of a conical nozzle due to intrusion of a jet into a supersonic cross flow. The experiment was carried out to simulate the side injection of fuel coolant from the regenerative cooling system into the supersonic exhaust gas discharging through the nozzle of a rocket engine. The motivation was to shed light on an engine anomaly that occurred during the first Titan IV launch, and thereby to reject or to substantiate the hypothesis that two or three ruptured regenerative cooling tubes caused the near-normal injection of liquid fuel (Aerozine-50) into the exhaust gas in the expansion nozzle section. This scenario was the prime reason for one of the engines to gimbal over to its extreme stop position. The flow of nitrogen (700 psi plenum pressure) through a 1/30th subscale converging-diverging nozzle simulated the main exhaust flow. Injection of a liquid (Freon-11, water) or a gas (nitrogen) from an injection port drilled at the most probable wall location provided the penetrating side jet. Mass flow rate ratios (jet-to-main flow rates), as well as local Mach number, were matched as closely as possible with those reported from actual flight data. The mass flow ratio was varied to assess the sensitivity of the results to the relative momentum of the jet. GRA

N91-26116# Ballistic Research Labs., Aberdeen Proving Ground, MD.
AERODYNAMICS OF A 0.60 CALIBER ELECTROMAGNETIC PROJECTILE Final Report, Jun. - Oct. 1990
James M. Garner Apr. 1991 23 p
(AD-A234660; BRL-MR-3907) Avail: NTIS HC/MF A03 CSCL 19/10

Spark photography range tests of a 0.60 caliber electromagnetic projectile were conducted to determine the aerodynamic characteristics at supersonic velocities. The design demonstrated adequate stability and typical drag characteristics. The effect of an asymmetric base geometry on the location of the aerodynamic center of pressure is also shown. GRA

N91-26117# Virginia Polytechnic Inst. and State Univ., Blacksburg. Interdisciplinary Center for Applied Mathematics.
STATE SPACE MODELS FOR AEROELASTIC AND VISCOELASTIC SYSTEMS Final Report, 1 Jan. 1988 - 31 Dec. 1990
T. L. Herdman 6 Mar. 1991 10 p
(Grant AF-AFOSR-0074-88; AF Proj. 2304)
(AD-A234730; AFOSR-91-0272TR) Avail: NTIS HC/MF A02 CSCL 01/1

We develop state space models for aeroelastic systems including unsteady aerodynamics. We establish the applicability of semigroup theory for these systems on weighted product spaces by showing well-posedness and obtaining a dissipative estimate for the infinitesimal generator of the associated Cauchy problem. Numerical techniques are developed for the singular neutral functional differential equation that model the aeroelastic systems. Also, we present a technique based on quasilinearization for identifying unknown coefficients in parabolic partial differential equations. This technique is applied to both linear and nonlinear equations with spatially varying unknown coefficients. GRA

N91-26118# Ballistic Research Labs., Aberdeen Proving Ground, MD.
THE EFFECT OF SABOT WHEELBASE AND POSITION ON THE LAUNCH DYNAMICS OF FIN-STABILIZED KINETIC ENERGY AMMUNITION Final Report, 1 Jan. - 31 Dec. 1990
Peter Plostins, Jonathan A. Bornstein, and Ilmars Celmins Apr. 1991 47 p
(DA Proj. 1L1-62618-AH-80)
(AD-A234945; BRL-TR-3225) Avail: NTIS HC/MF A03 CSCL 19/1

A test program was performed to determine the effects of changes in sabot wheelbase and position on the launch dynamics of fin-stabilized kinetic energy penetrators. The launch sequence was measured; the measurements covered the gun dynamics, transitional ballistics, and free-flight aeroballistics of the projectile trajectory. All of the projectile jump components were measured independently, summed, and the result compared with the projectile impact on the target. The dispersion of each of the components was computed and compared to the target impact dispersion. The dispersion computed using the dispersion model compared well with the target impact dispersion. Both low and high dispersion was observed for the different configurations. Low dispersion was the result of strong biases or low component magnitudes. Each configuration responded differently to the inbore launch sequence; therefore, the key to understanding the origins of the dispersion phenomenon lies in understanding the inbore dynamic response of sabot/penetrator designs. GRA

N91-26119# Nielsen Engineering and Research, Inc., Mountain View, CA.
THE EFFECTS OF COMPRESSIBILITY ON A SUPERSONIC MIXING LAYER Final Report, 1 Dec. 1987 - 30 Nov. 1990
D. Nixon, L. R. Keefe, and G. D. Kuhn 30 Jan. 1991 53 p
(Contract F49620-88-C-0003)
(AD-A234992; NEAR-TR-421) Avail: NTIS HC/MF A04 CSCL 20/4

The objective of the work is to identify the flow mechanisms that cause the decrease in spreading rate of supersonic mixing layers as the convective Mach number increases and to suggest a means of enhancing the mixing. Two approaches have been taken, one numerical and one analytic. A computer code, TMRC, has been used to simulate both time and space developing two-dimensional mixing layers to get some indication of the flow physics. In addition, three-dimensional spatially developing mixing layers have been simulated. The numerical studies indicate that some accuracy problems may exist in existing algorithms. To complement the numerical study, a simple analysis has been developed which explains the variation of mixing rate with convective Mach number. The analysis seems to indicate that little can be done to enhance mixing as such, although the real problem of simultaneous mixing and combustion may be more amenable to control. The analysis has been extended to include heat release as a first step in this direction. GRA

N91-26120# Massachusetts Inst. of Tech., Cambridge.
CALCULATED AERODYNAMICS OF WINGS IN SEVERE MANEUVER Final Report, 1 May 1986 - 30 Nov. 1990
J. E. McCune 18 Mar. 1991 6 p
(Grant AF-AFOSR-0157-86; AF Proj. 2307)
(AD-A235241; AFOSR-91-0380TR) Avail: NTIS HC/MF A02 CSCL 01/1

This report briefly summarizes the overall effort concerning the aerodynamics and basic fluid mechanics of slender wings with leading-edge separation, including cases involving severe unsteady maneuver. New and efficient methods have been developed and important new insights gained in the understanding of intense wing-wake interaction. Two just-completed Ph.D. theses, which are noted, document many of the principal new contributions of this research. A complete list of publications and theses completed under the grant is included in the report. GRA

N91-26121*# National Aeronautics and Space Administration. Lewis Research Center, Cleveland, OH.
CONTROL OF AN AXISYMMETRIC TURBULENT JET BY MULTI-MODAL EXCITATION
Ganesh Raman, Edward J. Rice, and Eli Reshotko (Case Western Reserve Univ., Cleveland, OH.) 1991 8 p Presented at the Eighth Symposium on Turbulent Shear Flows, Munich, Fed. Republic of Germany, 9-11 Sep. 1991; sponsored by the Turbulent Shear Flow Committee
(NASA-TM-104483; E-6243; NAS 1.15:104483) Avail: NTIS HC/MF A02 CSCL 01A

Experimental measurements of naturally occurring instability modes in the axisymmetric shear layer of high Reynolds number turbulent jet are presented. The region up to the end of the potential core was dominated by the axisymmetric mode. The azimuthal modes dominated only downstream of the potential core region. The energy content of the higher order modes (m is greater than 1) was significantly lower than that of the axisymmeteric and m = + or - 1 modes. Under optimum conditions, two-frequency excitation (both at m = 0) was more effective than single frequency excitation (at m = 0) for jet spreading enhancement. An extended region of the jet was controlled by forcing combinations of both axisymmetric (m = 0) and helical modes (m = + or - 1). Higher spreading rates were obtained when multi-modal forcing was applied. Author

N91-26122*# National Aeronautics and Space Administration. Lewis Research Center, Cleveland, OH.
A STUDY OF HIGH SPEED FLOWS IN AN AIRCRAFT TRANSITION DUCT Ph.D. Thesis - Iowa State Univ.
Bruce A. Reichert Jun. 1991 270 p
(NASA-TM-104449; E-6290; NAS 1.15:104449) Avail: NTIS HC/MF A12 CSCL 01A

The study of circular-to-rectangular transition duct flows with and without inlet swirl is presented. A method was devised to create a swirling, solid body rotational flow with minimal associated disturbances. Details of the swirl generator design and construction are discussed. Coefficients based on velocities and total and static pressures measured in cross stream planes at four axial locations within the transition duct along with surface static pressures and surface oil film visualization are presented for both nonswirling and swirling incoming flows. A method was developed to acquire trace gas measurements within the transition duct at high flow velocities. Statistical methods are used to help interpret the trace gas results. Author

N91-26123*# Old Dominion Univ., Norfolk, VA. Dept. of Mechanical Engineering and Mechanics.
VISCOUS FLOW SIMULATIONS OF INTERNAL STORE CARRIAGE AND SEPARATION Final Report, 15 May 1991
Oktay Baysal Jul. 1991 35 p
(Grant NAG1-664)

(NASA-CR-185343; NAS 1.26:185343) Avail: NTIS HC/MF A03 CSCL 01A

The internal carriage of stores by the military aircraft is an option for possible reductions in the aerodynamic drag and the observability. Trade studies of this option require considering the aircraft and the stores together. In an effort to develop a computational fluid dynamic (CFD) code for such studies, an investigation was conducted from 1986 to 1990. The study was divided into five building-block steps. First, a full Navier-Stokes code was developed to simulate the unsteady, three-dimensional cavity flow. As the second step, this code was then used to simulate the flows past various missile configurations at angles of attack up to 44 deg. The effects of incidence as well as the turbulence on the leeside flows were computationally captured. The objective of this study has involved the interference flows of rather complex configurations with multiple, joint or disjoint, components of nonsimilar geometries. Hence, a hybrid domain decomposition (HDD) method was developed as the third step of the investigation. The strengths of the multiblock, zonal, and overlapped grids were judiciously combined and employed for the present problem. In the fourth step, the interference flow past a missile near a flat-plate wing was simulated using the HDD method. Finally, the fifth step involved the simulation of the internal store carriage and separation. Four different cases for two different configurations were simulated. The computational results of all five steps were successfully compared with the available wind tunnel test data. The unsteady aerodynamic forces on the separating store were computationally predicted. The CFD code developed for this project is called Viscous Internal Store Carriage Code (VISCC). Author

N91-26124# Advisory Group for Aerospace Research and Development, Neuilly-Sur-Seine (France). Fluid Dynamics Panel.
EXPERIMENTAL TECHNIQUES IN THE FIELD OF LOW DENSITY AERODYNAMICS
J. Allegre, M. Raffin, and J. J. Bernard, ed. (Paris VI Univ., France) Apr. 1991 60 p Original contains color illustrations
(AGARD-AG-318(E); ISBN-92-835-0613-8) Copyright Avail: NTIS HC/MF A04; Non-NATO Nationals requests available only from AGARD/Scientific Publications Executive

Over the course of the past few decades, space programs have engendered a great deal of experimental and theoretical research aimed at improving the understanding of the characteristics and properties of flows in rarefied gas dynamics. A few of the more common measurement techniques used in low-density wind tunnels and altitude simulation chambers, for subsonic, supersonic, and hypersonic flows at low Reynolds numbers, chiefly compatible with spacecraft reentry flight conditions, are discussed. The instrumentation used in low-density testing is fundamentally different from that which is used in conventional wind tunnels, because of the level of rarefaction of the flows, which limits the forces, pressures, and mass densities to be measured and modifies the flow viscosity and interaction conditions. The rarefaction of flows generally tends to thicken the boundary layers and changes the structure of the shock waves. Author

03 AIR TRANSPORTATION AND SAFETY

Includes passenger and cargo air transport operations; and aircraft accidents.

For related information see also *16 Space Transportation* and *85 Urban Technology and Transportation.*

N91-26125# Aeronautical Systems Div., Wright-Patterson AFB, OH.
KC-135 GROUND COLLISION AVOIDANCE SYSTEM QUESTIONNAIRE Final Report, Dec. 1989 - Mar. 1990
Justin D. Rueb and John A. Hassoun Aug. 1990 40 p
(AD-A234385; ASD-TR-90-5010) Avail: NTIS HC/MF A03 CSCL 01/2

Crew Station Evaluation Facility engineers collected subjective data from a sample of 82 operational SAC crew members. The data provide information needed in the design of the Ground Collision Avoidance System (GCAS) for all KC-135 aircraft. The GCAS is designed to alert aircrews of an impending ground impact, should current flight conditions/aircraft configuration remain unchanged. This study found that KC-135 aircrews would prefer a multi-faceted, bimodal GCAS warning system. This should consist of a light/tone or light/voice warning. The light nomenclature, altitude, and the voice message, pullup were the most preferred warning messages. The GCAS warning should be present for as long as the warning conditions exist or until the pilot activates a GCAS system reset switch. The GCAS should begin coverage from 200 ft (AGL) and remain active until 5000 ft (AGL). It should cover roll angles from zero degrees to a minimum upper limit of 45 degrees. Subject data and comments are discussed in further detail. GRA

N91-26126*# Boeing Commercial Airplane Co., Seattle, WA.
CIVIL TILTROTOR MISSIONS AND APPLICATIONS. PHASE 2: THE COMMERCIAL PASSENGER MARKET Final Report
P. Thompson, R. Neir, R. Reber, R. Scholes, H. Alexander, D. Sweet, and D. Berry, ed. Feb. 1991 58 p Original contains color illustrations
(Contract NAS2-12393)
(NASA-CR-177576; NAS 1.26:177576; D6-55699-1-Phase-2)
Avail: NTIS HC/MF A04 CSCL 01C

The commercial passenger market for the civil tiltrotor was examined in phase 2. A market responsive commercial tiltrotor was found to be technically feasible, and a significant worldwide market potential was found to exist for such an aircraft, especially for relieving congestion in urban area-to-urban area service and for providing cost effective hub airport feeder service. Potential technical obstacles of community noise, vertiport area navigation, surveillance, and control, and the pilot/aircraft interface were determined to be surmountable. Nontechnical obstacles relating to national commitment and leadership and development of ground and air infrastructure were determined to be more difficult to resolve; an innovative public/private partnership is suggested to allow coordinated development of an initial commercial tiltrotor network to relieve congestion in the crowded US Northeast corridor by the year 2000. Author

04 AIRCRAFT COMMUNICATIONS AND NAVIGATION

Includes digital and voice communication with aircraft; air navigation systems (satellite and ground based); and air traffic control.

For related information see also *17 Space Communications, Spacecraft Communications, Command and Tracking* and *Communications and Radar.*

N91-26127# Range Commanders Council, White Sands Missile Range, NM.
IRIG STANDARD FORMAT FOR GLOBAL POSITIONING SYSTEM (GPS) DATA FOR POST-OPERATION INTERRANGE EXCHANGE
Apr. 1991 69 p
(AD-A234932; RCC-164-91; IRIG-STANDARD-164-91) Avail: NTIS HC/MF A04 CSCL 17/7

Document provides standard format for post-operation exchange of NAVSTAR/Global Positioning system (GPS) data between the ranges and is designed to produce an efficient and cost effective GPS data exchange format. This format is independent of the GPS receiver and provides a common exchange format minimizing range reformatting of GPS data and cost of processing GPS data and maximizing the speed and ease of GPS data exchange. GRA

N91-26128# Analytic Sciences Corp., Reading, MA.
OMEGA SYSTEM PERFORMANCE ASSESSMENT AND COVERAGE EVALUATION (PACE) WORKSTATION DESIGN AND IMPLEMENTATION, VOLUME 1
George R. Desrochers Feb. 1991 39 p
(Contract DTCG23-89-C-20008)
(AD-A235225; TIM-5834-2-2-Vol-1; USCG/ONSCEN-02.1-91-Vol-1) Avail: NTIS HC/MF A03 CSCL 17/7

The Performance Assessment and Coverage Evaluation (PACE) workstation is a microcomputer-based tool to assist Omega Navigation System Center personnel in answering questions regarding Omega system performance. The workstation implements a probabilistic model of Omega system availability for user-selected coverage and other criteria. This memorandum provides information on the design and implementation of the PACE workstation software. GRA

N91-26129# Analytic Sciences Corp., Reading, MA.
OMEGA/VLF SIGNAL COVERAGE DATABASE DEVELOPMENT Final Report, Jul. 1989 - Jan. 1991
Radha R. Gupta Jan. 1991 70 p
(Contract DTCG23-89-C-20008)
(AD-A235226; TIM-5834-3-1; USCG/ONSCEN-03-91) Avail: NTIS HC/MF A04 CSCL 12/7

The performance assessment and coverage evaluation (PACE) workstation used for Omega system performance analysis incorporates a 24-hour/ 4 month/ 2-frequency/ cell-format Omega system signal coverage database. PACE uses this database, in addition to other databases, to compute expected availability of the Omega system using 10.2 and/or 13.6 kHz Omega signals in a specified geographic region at a specified time (UT hour and month). The signal coverage database contains the signal coverage elements needed to establish usability/ non-usability of the 10.2/13.6 kHz Omega signals at a given location (cell) and time. This report describes the methodology used to generate the Omega signal covering database. In addition, the report presents candidate approaches, including the associated labor/computer resources, that could be used to generate a modal-signal database for the VLF communications network station. GRA

N91-26130# Aeronautical Systems Div., Wright-Patterson AFB, OH.
EVALUATION OF THE C/EC/KC-135 GROUND COLLISION AVOIDANCE SYSTEM (GCAS), STUDY 1 Final Report, Jan. 1990 - Jan. 1991
Justin D. Rueb and John A. Hassoun Mar. 1991 156 p
(AD-A235301; ASD-TR-91-5004-Study-1) Avail: NTIS HC/MF A08 CSCL 01/5

In support of the KC-135 Avionics modernization Program, subjective and performance data were collected in order to provide the Government and contractor engineers with information needed in the design of a Ground Collision Avoidance System (GCAS) for all C/EC/KC-135 aircraft. The GCAS will serve to alert the crew of an impending ground impact. This decision will be based on data collected from various aircraft sensors (e.g., radio altimeter). The GCAS, due to the downward looking nature of the radio altimeter, will not be as effective as a forward looking Terrain Following Radar (TFR) and would only serve to complement this system. This evaluation was Study 1 of a two-part study. Study 1 was comprised of four phases. Throughout the four phases, concerns and recommendations were forwarded to the System Program Office and to the Cubic Corporation. This resulted in modification of the algorithm prior to the next phase of the evaluation. GRA

05 AIRCRAFT DESIGN, TESTING AND PERFORMANCE

Includes aircraft simulation technology.

For related information see also *18 Spacecraft Design, Testing and Performance* and *39 Structural Mechanics.* For land transportation vehicles see *85 Urban Technology and Transportation.*

N91-26131# Aeronautical Systems Div., Wright-Patterson AFB, OH. Directorate of Flight Systems Engineering.
A LOOK AT DIGITAL NOSE WHEEL STEERING Final Report, Feb. - Aug. 1990
Mark L. Nowack 24 Sep. 1990 37 p
(AD-A233944; ASD-TR-90-5018; ENF-TM-90-6) Avail: NTIS HC/MF A03 CSCL 01/3

This report examines the impact of digital control on nose wheel steering of aircraft. The development of steering systems is reviewed from early mechanical systems through integrated brake control systems. The value of digital control is then examined based on unique capabilities, performance improvement, and fault detection. Cost, weight, and maintainability impacts are discussed. GRA

N91-26132# General Accounting Office, Washington, DC. National Security and International Affairs Div.
UNMANNED AERIAL VEHICLES. MEDIUM RANGE SYSTEM COMPONENTS DO NOT FIT
Mar. 1991 33 p
(AD-A234131; GAO/NSIAD-91-2) Avail: NTIS HC/MF A03 CSCL 01/3

DOD has encountered a major problem in developing the Medium-Range UAV for common-service use because the ATARS payload will not fit in the UAV. If this problem is not satisfactorily solved, it could undermine the program goals of having a common-service UAV, reconnaissance payload, and image processing system for UAV, and manned aircraft. In addition to the payload fit problem, the program has encountered several other problems. To solve the problems, the program manager is proposing numerous changes that, when taken together, would represent a vastly different UAV. The new UAV would include a larger payload bay to accommodate ATARS and would incorporate various other features to solve the current system's existing problems. GRA

N91-26133# North American Aircraft Operations, Los Angeles, CA.
HIGH PERFORMANCE TRANSPARENCY DESIGN Final Report, Sep. 1986 - Dec. 1989
F. F. Abdi and G. M. Clark Nov. 1990 146 p
(Contract F33615-86-C-3414)
(AD-A234456; NA-89-1122L; WRDC-TR-90-3061) Avail: NTIS HC/MF A07 CSCL 01/3

Aircraft transparency design requirements continue to become more complex and typically require more iterations to establish a successful configuration. These iterations are costly in terms of schedules, funds, or operational changes and design changes. The objective of the program was to define and demonstrate application of computerized analysis tools to a transparency design method for high performance crew compartment enclosure. The program used MAGNA and STAPAT together with a microbased initial cross-section code to achieve the objective. A case study based on a TF-15 transparency demonstrated preliminary design for birdstrike and thermal conditions at $M = 0.76$ and $M = 1.1$. The study also included a discussion of failure criteria and the result of an advanced transparency materials survey. GRA

N91-26134# Florida Atlantic Univ., Boca Raton. Dept. of Mechanical Engineering.
DYNAMICS OF ELASTIC BENDING AND TORSION OF HINGELESS ROTORS WITH DYNAMIC STALL
Gopal H. Gaonkar and Dinesh Barwey 23 Feb. 1991 51 p

(Contract DAAL03-87-K-0037)
(AD-A234775; ARO-24738.7-EG) Avail: NTIS HC/MF A04 CSCL 01/1

The effects of dynamic stall lift and drag on the flap-lag stability of a hingeless rotor are investigated, both experimentally and analytically. The emphasis is on the correlation with measured regressing lead-lag mode damping levels of a soft-inplane, three-bladed model rotor, operated untrimmed. The correlation covers a wide range of test conditions for several values of rotor speed, collective pitch angle, shaft tilt angle and advance ratio. It includes cases that vary from near zero thrust conditions in hover to highly stalled forward flight conditions with advance ratios as high as 0.55 and shaft tilt angles as high as 20 deg. Both the experimental and analytical blade models represent a simple model of a hingeless rotor with rigid blades and spring restrained flap-lag hinges. The aerodynamic representation is based on the ONERA dynamic stall models comprising virtually independent unified lift and drag models. The nonlinear equations of blade motion and stall dynamics are perturbed about a periodic forced response, and the damping is evaluated by the Floquet eigenanalysis. In comparison to the linear and quasisteady stall aerodynamic theories, the theory with dynamic stall lift and quasisteady stall drag qualitatively improves the correlation, and adding dynamic stall drag provides further quantitative improvement. GRA

N91-26135# Naval Postgraduate School, Monterey, CA.
ESTABLISHMENT OF A REMOTELY PILOTED HELICOPTER TEST FLIGHT PROGRAM FOR HIGHER HARMONIC CONTROL RESEARCH M.S. Thesis
James G. Scott Jun. 1990 71 p
(AD-A234978) Avail: NTIS HC/MF A04 CSCL 01/4

An analytical research study was begun on a helicopter vibration reduction concept known as higher harmonic control (HHC). To supplement this research, a helicopter flight test program was established to generate flight test data in support of the NPS HHC research efforts. To accomplish this task, a remotely piloted helicopter was chosen as the test vehicle. The research efforts encompassed by this thesis are the determination of attributes required of a RPH used for HHC studies, the selection and acquisition of an RPH capable of completing the intended research mission, and the preliminary analysis of the RPH's flight control system for modification to an HHC configuration. A brief overview of helicopter vibrations and HHC fundamentals, along with an in-depth description of the selected RPH, is presented. Preliminary analysis of the RPH's flight control system includes the determination of associated freeplay and torsional constant values for the flight control components and the calculation of the necessary actuator torque requirements for HHC actuation. This research effort is the first stage of a long term program designed to provide NPS with an in house asset capable of generating HHC flight test data in support of analytical research. GRA

N91-26136# School of Aerospace Medicine, Brooks AFB, TX.
REFURBISHING AV-8 ON-BOARD OXYGEN GENERATION SYSTEM BEDS Interim Report, May - Aug. 1990
Kenneth G. Ikels and Aaron M. Shakocius Dec. 1990 26 p
(AF Proj. 7930)
(AD-A235083; USAFSAM-TP-90-22) Avail: NTIS HC/MF A03 CSCL 23/5

The Crew Systems Branch, Crew Technology Div, USAF SAM, has carefully prepared specific procedures and instructions to provide users of the AV-8 On-Board Oxygen Generation System (OBOGS) with detailed information and requirements on refurbishing OBOGS beds. Included in the instructions on disassembling, repacking, and assembling the OBOGS beds, are specific procedures for determining the activity and, if necessary, activating the molecular sieve before the beds are repacked. In addition, technics and procedures are detailed for testing the repacked beds prior to reassembly of the concentrator to ensure efficient air separation. GRA

N91-26137*# National Aeronautics and Space Administration. Langley Research Center, Hampton, VA.
PERFORMANCE OPTIMIZATION OF HELICOPTER ROTOR BLADES
Joanne L. Walsh Apr. 1991 22 p Presented at the Third Air Force/NASA Symposium on Recent Advances in Multi-Disciplinary Analyses and Optimization, San Francisco, CA, 24-26 Sep. 1990
(NASA-TM-104054; NAS 1.15:104054) Avail: NTIS HC/MF A03 CSCL 01C

As part of a center-wide activity at NASA Langley Research Center to develop multidisciplinary design procedures by accounting for discipline interactions, a performance design optimization procedure is developed. The procedure optimizes the aerodynamic performance of rotor blades by selecting the point of taper initiation, root chord, taper ratio, and maximum twist which minimize hover horsepower while not degrading forward flight performance. The procedure uses HOVT (a strip theory momentum analysis) to compute the horse power required for hover and the comprehensive helicopter analysis program CAMRAD to compute the horsepower required for forward flight and maneuver. The optimization algorithm consists of the general purpose optimization program CONMIN and approximate analyses. Sensitivity analyses consisting of derivatives of the objective function and constraints are carried out by forward finite differences. The procedure is applied to a test problem which is an analytical model of a wind tunnel model of a utility rotor blade. Author

N91-26138# RAND Corp., Santa Monica, CA.
HOW LOW CAN AN UNMANNED AIR VEHICLE FLY? Thesis
William E. Dean Oct. 1990 36 p
(RAND-P-7680-RGS) Avail: NTIS HC/MF A03

The issue of unmanned air vehicles (UAVs) as candidates for reconnaissance platforms was studied. A model was constructed to simulate preprogrammed smooth paths from peak to peak in hilly terrain. Some commaned altitude was added to all the points of the flight path. Then the clobber probability was calculated by introducing navigational error, so that the UAV could encounter hills unexpectedly. Finally, the intervisibility between a radar site and the UAV was calculated. As an excursion, a downward-looking altimeter was simulated. The true altitude above ground level (AGL) was compared with the expected AGL. The case runs are described and the results presented. The modeling environment, the models, and the limitations are discussed. B.G.

N91-26139*# Boeing Helicopter Co., Philadelphia, PA.
TECHNOLOGY NEEDS FOR HIGH-SPEED ROTORCRAFT, VOLUME 1
J. B. Wilkerson, J. J. Schneider, and K. M. Bartie May 1991 250 p
(Contract NAS2-13041)
(NASA-CR-177585; A-91159; NAS 1.26:177585) Avail: NTIS HC/MF A11 CSCL 01C

High-speed rotorcraft concepts and the technology needed to extend rotorcraft cruise speeds up to 450 knots (while retaining the helicopter attributes of low downwash velocities) were identified. Task I identified 20 concepts with high-speed potential. These concepts were qualitatively evaluated to determine the five most promising ones. These five concepts were designed with optimum wing loading and disk loading to a common NASA-defined military transport mission. The optimum designs were quantitatively compared against 11 key criteria and ranked accordingly. The two highest ranking concepts were selected for the further study. Author

N91-26140*# G and C Systems, Inc., San Juan Capistrano, CA.
AUTONOMOUS AIRCRAFT INITIATIVE STUDY Final Report
Marle D. Hewett Jul. 1991 92 p Prepared in cooperation with PRC Systems Services Co., Edwards, CA
(Contracts NAS2-12722; ATD-89-GNC-1504)
(NASA-CR-186013; H-1609; NAS 1.26:186013) Avail: NTIS HC/MF A05 CSCL 01C

The results of a consulting effort to aid NASA Ames-Dryden in defining a new initiative in aircraft automation are described. The

initiative described is a multi-year, multi-center technology development and flight demonstration program. The initiative features the further development of technologies in aircraft automation already being pursued at multiple NASA centers and Department of Defense (DoD) research and Development (R and D) facilities. The proposed initiative involves the development of technologies in intelligent systems, guidance, control, software development, airborne computing, navigation, communications, sensors, unmanned vehicles, and air traffic control. It involves the integration and implementation of these technologies to the extent necessary to conduct selected and incremental flight demonstrations. Author

N91-26141# General Accounting Office, Washington, DC. National Security and International Affairs Div.
AEROSPACE PLANE TECHNOLOGY: RESEARCH AND DEVELOPMENT EFFORTS IN EUROPE. REPORT TO THE CHAIRMAN, COMMITTEE ON SCIENCE, SPACE, AND TECHNOLOGY, HOUSE OF REPRESENTATIVES
Jul. 1991 148 p
(GAO/NSIAD-91-194) Avail: NTIS HC/MF A07; also available from GAO, Gaithersburg, MD HC first five copies free, additional copies $2.00

Investment in foreign aerospace vehicle research and technological development efforts are reviewed. Supporters of the National Aero-Space Plane Program in the Congress are concerned about foreign competition to the program and its impact on U.S. technological leadership. The following subject areas are covered: European space policies and aerospace goals and objectives; European aerospace vehicle programs; development of enabling technologies; U.S and European investment in aerospace vehicle research and technological development efforts; European aerospace test facilities and their capabilities; and international cooperation. Author

06 AIRCRAFT INSTRUMENTATION

Includes cockpit and cabin display devices; and flight instruments.

For related information see also *19 Spacecraft Instrumentation* and *35 Instrumentation and Photography.*

N91-26142*# National Aeronautics and Space Administration. Ames Research Center, Moffett Field, CA.
FORMAT AND BASIC GEOMETRY OF A PERSPECTIVE DISPLAY OF AIR TRAFFIC FOR THE COCKPIT
Michael Wallace McGreevy and Stephen R. Ellis Jun. 1991 48 p
(NASA-TM-86680; A-85126; NAS 1.15:86680) Avail: NTIS HC/MF A03 CSCL 01D

The design and implementation of a perspective display of air traffic for the cockpit is discussed. Parameters of the perspective are variable and interactive so that the appearance of the projected image can be widely varied. This approach makes allowances for exploration of perspective parameters and their interactions. The display was initially used to study the cases of horizontal maneuver biases found in experiments involving a plan view air traffic display format. Experiments to determine the effect of perspective geometry on spatial judgements have evolved from the display program. Several scaling techniques and other adjustments to the perspective are used to tailor the geometry for effective presentation of 3-D traffic situations. Author

N91-26143# RAND Corp., Santa Monica, CA.
VHSIC ELECTRONICS AND THE COST OF AIR FORCE AVIONICS IN THE 1990s
Paul S. Killingsworth and Jeanne M. Jarvaise Nov. 1990 101 p
(Contract F49620-86-C-0008)
(RAND-R-3843-AF; ISBN-0-8330-1026-3; LC-89-70202) Avail: NTIS HC/MF A06

Discussed here are the cost issues for avionics systems using very high speed integrated circuits (VHSIC) and VHSIC-like technology. Also given is some background on integrated circuit technology and a method for checking the reasonableness of cost estimates on avionics systems that incorporate highly integrated electronics. Author

07 AIRCRAFT PROPULSION AND POWER

Includes prime propulsion systems and systems components, e.g., gas turbine engines and compressors; and onboard auxilliary power plants for aircraft.

For related information see also *20 Spacecraft Propulsion and Power, 28 Propellants and Fuels,* and *44 Energy Production and Conversion.*

N91-26144# Coordinating Research Council, Inc., Atlanta, GA.
SURVEY OF CURRENT AIRCRAFT ENGINE CONDITIONS
Kurt Strauss Feb. 1991 20 p
(AD-A235143; CRC-573) Avail: NTIS HC/MF A03 CSCL 21/4

In the letter of March 15, 1989, concern was expressed over the fact that existing specification test methods did not detect a thermal stability problem when fuel was used in an advanced turbine engine. The same letter, which is attached as Appendix B, suggested several research approaches to resolve the problem. As a result the CRC Group on Oxidation Stability of Gas Turbine Fuels formed a panel to develop a plan to meet the ASTM request. Panel membership is shown in Appendix A. The detailed plan was prepared by panel leader and is given in Appendix C. The first item in the plan was to conduct a survey of engine/airframe manufacturers to develop fuel system parameters for typical past, present and future aircraft. GRA

N91-26145# United Technologies Research Center, East Hartford, CT.
INVESTIGATION OF HOT STREAK MIGRATION AND FILM COOLING EFFECTS ON THE HEAT TRANSFER IN ROTOR/STATOR INTERACTING FLOWS Quarterly Progress Report, 1 Jan. 1990 - 31 Mar. 1991
Daniel J. Dorney and Roger L. Davis 31 Mar. 1991 22 p
(Contract N00140-88-C-0677)
(AD-A235420) Avail: NTIS HC/MF A03 CSCL 20/13

This effort extended the three-dimensional unsteady rotor/stator interaction code, ROTOR3, to investigate hot streak migration and film cooling effects on the passage flow and blade surface heat transfer for an axial flow turbine stage. These objectives are part of an overall plan to extend the capabilities of this numerical procedure and to determine the potential of this technique to impact the design of future rotating turbomachinery components. The principal benefits that will result from this effort are: (1) a diagnostic analysis and code which can be used to help design turbine blades with increased efficiency and reduced cooling requirements; (2) an open literature demonstration on the use of computational simulation and scientific visualization for gaining insight into complex turbomachinery flows; (3) acceleration of the transition of large-scale computational analyses to the turbomachinery design process through joint involvement between UTRC and Pratt and Whitney turbine engineers; and (4) a useful and proven design tool which can be used with existing and future engine design procedures. GRA

N91-26146*# National Aeronautics and Space Administration. Lewis Research Center, Cleveland, OH.
CFD ANALYSIS OF JET MIXING IN LOW NOx FLAMETUBE COMBUSTORS
M. V. Talpallikar, C. E. Smith, M. C. Lai (Wayne State Univ., Detroit, MI.), and J. D. Holdeman 1991 11 p Presented at the 36th International Gas Turbine and Aeroengine Congress and Exposition, Orlando, FL, 3-6 Jun. 1991; sponsored by ASME Original contains color illustrations
(Contract NAS3-25834)

(NASA-TM-104466; E-6313; NAS 1.15:104466; ASME-91-GT-217) Avail: NTIS HC/MF A03; 1 functional color page CSCL 21E

The Rich-burn/Quick-mix/Lean-burn (RQL) combustor was identified as a potential gas turbine combustor concept to reduce NO(x) emissions in High Speed Civil Transport (HSCT) aircraft. To demonstrate reduced NO(x) levels, cylindrical flametube versions of RQL combustors are being tested at NASA Lewis Research Center. A critical technology needed for the RQL combustor is a method of quickly mixing by-pass combustion air with rich-burn gases. Jet mixing in a cylindrical quick-mix section was numerically analyzed. The quick-mix configuration was five inches in diameter and employed twelve radial-inflow slots. The numerical analyses were performed with an advanced, validated 3-D Computational Fluid Dynamics (CFD) code named REFLEQS. Parametric variation of jet-to-mainstream momentum flux ratio (J) and slot aspect ratio was investigated. Both non-reacting and reacting analyses were performed. Results showed mixing and NO(x) emissions to be highly sensitive to J and slot aspect ratio. Lowest NO(x) emissions occurred when the dilution jet penetrated to approximately mid-radius. The viability of using 3-D CFD analyses for optimizing jet mixing was demonstrated. Author

08 AIRCRAFT STABILITY AND CONTROL

Includes aircraft handling qualities; piloting; flight controls; and autopilots.

For related information see also *05 Aircraft Design, Testing and Performance.*

N91-26147# Department of the Navy, Washington, DC.
APPARATUS FOR GUIDING A MISSILE Patent
Daniel C. Barnes, inventor (to Navy), Wendell J. Bridges, inventor (to Navy), and Jon R. Carr, inventor (to Navy) 19 Feb. 1991 7 p Filed 7 Jul. 1970
(AD-D014866; US-Patent-4,993,662; US-Patent-Appl-SN-056014; US-Patent-Class-244-3.17) Avail: US Patent and Trademark Office CSCL 17/7

This patent discloses a device for correcting the flight path of an air to surface missile and guiding said missile to a target. A first map of a strip of ground which is transverse to the direction of flight is provided on a rotatable drum along with a second map of a strip of ground which is parallel with the direction of flight. A live image of the ground over which said missile is traveling is projected first through the first map to provide a position fix of the missile in range and azimuth relative to a target and after a correction has been made to the flight path of the missile, the live image of the ground is projected through the second map to provide guidance correction to direct the missile to the target. GRA

N91-26148# Air Force Inst. of Tech., Wright-Patterson AFB, OH. Foreign Technology Div.
APPLICATION OF TRANSFORMATIONAL IDEAS TO AUTOMATIC FLIGHT CONTROL DESIGN
Li Wenhua and Liang Feng 21 Mar. 1991 17 p Transl. into ENGLISH from Acta Aeronautica et Astronautica Sinica (China), v. 11, no. 4, p 165-170
(AD-A234758; FTD-ID(RS)T-1276-90) Avail: NTIS HC/MF A03 CSCL 01/4

To opt to use geometrical methods to design actual nonlinear systems, one must, first of all, resolve the problems of the complexity of transformations, the great amount of calculations, and other similar problems. Because of this, simplifying the design process is extremely important. In this article, based on transformational ideas, we have obtained two methods and used them in the design of the U.S. F-8 Crusader fighter plane's vertical control system. The simulation results clearly demonstrate that the new control laws are obviously superior to the original nonlinear optimization control laws. Moreover, it is possible to guarantee that aircraft can make high angle attack flights. GRA

N91-26149# Naval Air Development Center, Warminster, PA. Air Vehicle and Crew Systems Technology Dept.
FLIGHT CONTROL LAW SYNTHESIS USING NEURAL NETWORK THEORY Interim Report, Oct. 1989 - Sep. 1990
Robert D. DiGirolamo and Shawn T. Donley 31 Oct. 1990 20 p
(AD-A234990; NADC-91004-60) Avail: NTIS HC/MF A03 CSCL 01/4

A commonly used technique for advanced fighter aircraft control law development involves a lengthy process of linearizing the aircraft model and calculating many control system gains via conventional linear methods. This process must be repeated for a number of trim points within the flight envelope to achieve the aircraft stability and flying qualities mandated by various military specifications. Neural networks have been used extensively in many applications such as pattern recognition and optimization because of their ability to create nonlinear mappings of continuous valued inputs through supervised learning. This report outlines a concept which incorporates emerging neural network technology with present-day control theory to produce a system by which optimal controller gains can be automatically generated. The research completed to date and the results contained in this report are intended to provide a proof of concept by applying the neural network synthesis technique to some simplified linear and nonlinear examples. GRA

N91-26150# Advisory Group for Aerospace Research and Development, Neuilly-Sur-Seine (France). Structures and Materials Panel.
MANUAL ON THE FLIGHT OF FLEXIBLE AIRCRAFT IN TURBULENCE
John C. Houbolt, ed. May 1991 173 p In FRENCH and ENGLISH
(AGARD-AG-317; ISBN-92-835-0617-0) Copyright Avail: NTIS HC/MF A08; Non-NATO Nationals requests available only from AGARD/Scientific Publications Executive

In the course of the past few years, the Structures and Materials Panel of AGARD has considered a number of aspects of the turbulence problem as it affects aircraft. The presented publication constitutes a review document in which is distilled the experience of specialists from amongst the aircraft manufacturing nations of NATO. It is aimed at those in design offices concerned with the problems of turbulences and resultant loads. For individual titles, see N91-26151 through N91-26158.

N91-26151*# National Aeronautics and Space Administration. Langley Research Center, Hampton, VA.
MEASUREMENT OF ATMOSPHERIC TURBULENCE c46
Harold N. Murrow *In* AGARD, Manual on the Flight of Flexible Aircraft in Turbulence May 1991 p 1-30 (For primary document see N91-26150 18-08)
Copyright Avail: NTIS HC/MF A08; Non-NATO Nationals requests available only from AGARD/Scientific Publications Executive CSCL 04A

The material contained is primarily a compilation of information that has already been published. The attached reference list should be adequate for clarifying points to any detail desired. The purpose is to provide a description of the methodology required for measuring atmospheric turbulence in the form of true gust velocity. The content will include instrumentation requirements and selections used, flight assessments of the measurement system, some data reduction considerations, and finally some typical data obtained. Author

N91-26152# National Aerospace Lab., Emmeloord (Netherlands).
ACQUISITION OF STATISTICAL GUST LOAD DATA BY COMMERCIAL AIRPLANES
J. B. deJonge *In* AGARD, Manual on the Flight of Flexible Aircraft in Turbulence May 1991 p 31-40 (For primary document see N91-26150 18-08)
Copyright Avail: NTIS HC/MF A08; Non-NATO Nationals requests available only from AGARD/Scientific Publications Executive

Knowledge about the nature and properties of atmospheric turbulence was and is being obtained from measurements with specially instrumented 'research' aircraft. On the other hand, statistical information on the frequency of occurrence and intensity of gusts is largely based on relatively simple measurements, using simple recording devices, obtained over a period of more than half a century in commercial aircraft during normal operations. These measurements are of an indirect nature, that means not the gust velocity itself but the aircraft response due to the gust is measured. Universally, the c.g vertical acceleration was taken as the response quantity to be measured. This choice is quite understandable: in the first place the incremental vertical acceleration is directly proportional to the incremental lift force due to the gust and thus an obvious measure of gust strength; in the second place, the c.g acceleration is easy to measure with simple and reliable instrumentation. A brief review is presented of 'historical' acceleration recording programs carried out by NACA (and its successor NASA) and the RAE. Next, more recent recording programs making use of acceleration data recorded with so-called ACMS (Aircraft Collision Monitoring System) is discussed. The methods used to reduce the acceleration data to 'gust velocities' is briefly described with specific reference to the differences in the various programs. In a summarizing discussion the possibility and desirability to extend the gust data base using 'routine' ACMS recorded c.g acceleration data will come forward. To compared data from different sources it is essential that agreement on data reduction procedures be reached. It is argued that for this, a reduction method based on a continuous gust concept and an aircraft response including pitch appears the most appropriate.

Author

N91-26153# Office National d'Etudes et de Recherches Aerospatiales, Paris (France).

IMPROVED REDUCTION OF GUST LOADS DATA FOR GUST INTENSITY

Gabriel Coupry *In* AGARD, Manual on the Flight of Flexible Aircraft in Turbulence May 1991 p 41-57 (For primary document see N91-26150 18-08)

Copyright Avail: NTIS HC/MF A08; Non-NATO Nationals requests available only from AGARD/Scientific Publications Executive

The reduction of load factor data to turbulence data, in view of proposing improved statistics of gusts is examined. The different methods available to achieve this process are reviewed. A comprehensive analysis is made to highlight the shortcomings and their consequences on the regulations. The renewal of interest in turbulence comes from the new problems industry has to face: large aspect ratio commercial aircraft, penetration of military aircraft at low altitude and high velocity, active control of flight and of loads, and justification of increased fatigue life of existing commercial aircraft. The philosophy underlying the data reduction is examined, and it raises the question of the meaning of a gust deduced from acceleration data. Some of the methods are then described. Finally, the shortcomings (especially those due to the effect of pilot maneuvers) and their impact on the requirements are highlighted.

Author

N91-26154# Federal Aviation Administration, Seattle, WA.

CERTIFICATION PROCEDURES AND REQUIREMENTS

Terence J. Barnes and Victor Card (Civil Aviation Authority, Redhill, England) *In* AGARD, Manual on the Flight of Flexible Aircraft in Turbulence May 1991 p 58-65 (For primary document see N91-26150 18-08)

Copyright Avail: NTIS HC/MF A08; Non-NATO Nationals requests available only from AGARD/Scientific Publications Executive

The mathematical models of aircraft and atmospheric turbulence and their rationale are described. Emphasis is given to the revisions and refinements made starting in the 1920s up to the present time. The major steps, beginning with the sharp edged gust formulate, are traced through the modified formula specifying ramp-platform gusts and later to one-minus-cosine gusts and finally to criteria for continuous gust analyses. The influence of aircraft design developments on design criteria development needs is also addressed. A brief summary of military criteria is included. Significant discussion is devoted to measurements that have been made, including onboard recordings, to provide an extensive data base of: (1) atmospheric turbulence experience in routine flight operations; (2) specifically-instrumented research aircraft measurements to provide atmospheric characterization for various flight and meteorological conditions; and (3) comparisons of measured and calculated aircraft responses in turbulence.

Author

N91-26155# Deutsche Airbus G.m.b.H., Hamburg (Germany, F.R.).

GUST DESIGN PROCEDURES

Helmut Lusebrink and Rainer Sonder *In* AGARD, Manual on the Flight of Flexible Aircraft in Turbulence May 1991 p 66-116 (For primary document see N91-26150 18-08)

Copyright Avail: NTIS HC/MF A08; Non-NATO Nationals requests available only from AGARD/Scientific Publications Executive

One of the most important structural design conditions for civil and military transport aircraft are the vertical and lateral gust loads, which the aicraft experiences, when flying in a turbulent atmosphere. Complying with U.S. and European Airworthiness Regulations, the aircraft manufacturer has to consider two basic gust concepts or models: the discrete gust model, and the continuous turbulence power spectrum density (PSD) gust models. During the years of application, the gust shape and intensities changed and are now the well-known truncated 1-cos shape with a constant gust gradient distance (USA/Europe) or a variable one for U.K. The aircraft manufacturer has to apply both the Discrete and one of the PSD methods to find the most critical one for each aircraft component and then design the structure for the envelope loads. The dynamic gust load analysis should be performed in the frequency domain by means of transfer or frequency response functions. The PSD methods cannot be directly applied to nonlinear dynamic models. Approximative methods which have the statistical characteristics given in the requirements have to be applied. Acceptance of the airworthiness authorities will be obtained, if the linearization methods provide conservative design loads. The influence of automatic control systems on structural loads due to discrete gust and PSD methods, including their failed and degraded states, has to be investigated. From the variety of unsteady aerodynamic theories, the 3-dimensional doublet lattice method was selected. Time plane analysis of the dynamical gust problem has to be performed for modern aircraft with digital flight control and alleviation systems containing a variety of nonlinear elements. For this purpose, the unsteady aerodynamic forces have to be transformed from the frequency plane to the time plane. This is achieved by approximating the elements of the modalized unsteady aerodynamic force matrix by PADE-type approximants, which allow generations of the Delta-pulse response matrix kernels used in the convolution integral representation of the unsteady aerodynamic forces in the time plane.

B.G.

N91-26156# Boeing Canada, Toronto (Ontario).

ANALYSIS BY THE STATISTICAL DISCRETE GUST METHOD

John Glaser *In* AGARD, Manual on the Flight of Flexible Aircraft in Turbulence May 1991 p 117-134 (For primary document see N91-26150 18-08)

Copyright Avail: NTIS HC/MF A08; Non-NATO Nationals requests available only from AGARD/Scientific Publications Executive

The general formulation of the Statistical Discrete Gust (SDG) model for atmospheric turbulence proposed by J. Glynn Jones for the von Karman spectrum in its higher frequency range is defined and illustrative results are presented. The equivalence of the two models, SDG PSD (power spectrum density), is confirmed by showing that the dynamic response ratios, bar gamma/bar A, for both rigid and elastic aircraft loads are reasonably constant and approximately equal to the expected value of 10.4 ft.(sup 1/3). Although the SDG method is more complex to implement and more costly to run than the PSD method of FAR/JAR 25, its implementation for routine calculations of linear aircraft structures is confirmed by the present study. The SDG model offers an alternative time domain analysis method for calculating response loads to continuous turbulence for both linear and nonlinear aircraft

structures (active controls). In addition, the ADG method can potentially provide a more representative model for extreme gust processes, but this requires further development. Author

N91-26157# National Aerospace Lab., Amsterdam (Netherlands).
MATCHING OF PSD-DESIGN LOADS
Roel Noback *In* AGARD, Manual on the Flight of Flexible Aircraft in Turbulence May 1991 p 135-149 (For primary document see N91-26150 18-08)
Copyright Avail: NTIS HC/MF A08; Non-NATO Nationals requests available only from AGARD/Scientific Publications Executive

The PSD (power spectrum density) method as described in the requirements produces the design loads, however not the mutual relation or phasing. For stressing purposes and also for testing, realistic load combinations or design load conditions are needed. In the discrete gust case design load conditions almost naturally consist of the loads occurring at the same time, usually at the time that one of the loads reaches its maximum values. The PSD method is based on statistical considerations and PSD degree load conditions should have the same basis. A method to generate design load conditions or to match design loads, obtained with the design envelope analysis of the PSD method is described. The method is based on the statistical correlation between outputs (loads) of a linear system, the aircraft, to a common input, atmospheric turbulence. For design loads obtained with the mission analysis such a direct relationship does not exist and the generation of design load conditions is more involved and will not be treated here. An approximate method is proposed. A design load condition should be in equilibrium, that is the equations of equilibrium should be valid for these loads. This is proven for the design load conditions as generated with the described method. The derivation of the design load conditions will be given for the case that only two loads are involved. The derivation for the general case with N loads is given. Only the results are presented. Author

N91-26158# Civil Aviation Authority, Redhill (England).
TRENDS IN CERTIFICATION PROCEDURES AND DESIGN ANALYSIS
Victor Card and Terence J. Barnes (Federal Aviation Administration, Seattle, WA.) *In* AGARD, Manual on the Flight of Flexible Aircraft in Turbulence May 1991 p 150-160 (For primary document see N91-26150 18-08)
Copyright Avail: NTIS HC/MF A08; Non-NATO Nationals requests available only from AGARD/Scientific Publications Executive

In the past various gust load formulas were developed for the calculation of design gust loads on aircraft. Since the time it was first published in 1954, the alleviation factor approach of Pratt and Walker has gained almost universal acceptance. The problem of using the gust load requirements is discussed. Discrete gust statistics and power spectral density (PSD) concept are explained. B.G.

09 RESEARCH AND SUPPORT FACILITIES (AIR)

Includes airports, hangars and runways; aircraft repair and overhaul facilities; wind tunnels; shock tubes; and aircraft engine test stands.

For related information see also *14 Ground Support Systems and Facilities (Space).*

N91-26159*# National Aeronautics and Space Administration. Langley Research Center, Hampton, VA.
LIQUID COOLED SUPERSONIC TOTAL TEMPERATURE PROBE Patent Application
Nicholas T. Lagen, inventor (to NASA) (George Washington Univ., Hampton, VA.) and Garland D. Reece, inventor (to NASA) 23 Apr. 1991 32 p
(NASA-Case-LAR-14435-1-CU; NAS 1.71:LAR-14435-1-CU; US-Patent-Appl-SN-690144) Avail: NTIS HC/MF A03 CSCL 14B

A total temperature probe is provided for use in a supersonic environment. An outer shell, which can be L-shaped, defines an internal chamber and test chamber. The test chamber is located at a distal end of the outer shell and has a test inlet. A thermocouple is located within the internal chamber and has a temperature of the supersonic external flow environment. A portion of the thermocouple adjacent to the thermocouple distal end forms a liquid tight seal between the reservoir and the test chamber. A supply tube is provided for supplying a liquid coolant through the internal chamber and terminates at the thermocouple portion adjacent to the thermocouple distal end and an exit conduit is provided for removing liquid coolant from the reservoir. The outer shell of the probe is thus internally cooled by the liquid coolant when being subjected to intense supersonic temperatures of up to 2000 F. The novelty of the invention lies in the unique structure which permits effective cooling of a total temperature probe. NASA

N91-26160# Army Engineer Waterways Experiment Station, Vicksburg, MS. Geotechnical Lab.
GEOGRID REINFORCED BASE COURSE FOR FLEXIBLE PAVEMENTS FOR LIGHT AIRCRAFT: LITERATURE REVIEW AND TEST SECTION DESIGN Interim Report
Steve L. Webster May 1991 40 p
(Contract DTFA01-89-Z-02029)
(DOT/FAA/RD-90/28) Avail: NTIS HC/MF A03

The results are presented of a literature review investigating geogrid reinforced base courses for flexible pavements for light aircraft and the design of a geogrid test section for field testing the validity of potential geogrid reinforcement results. The literature review included related areas such as geogrid ballast reinforcement for railroad track bed, reinforcement for aggregate surface pavements, and reinforcement for flexible pavements. Based on the literature review, geogrids have application in ballast reinforcement for railroad track bed and in reinforcement for aggregate surface pavements. Full-scale field tests have verified that for subgrade CBR strengths of 1.5 to 5.0, geogrid reinforced aggregate surface pavement can carry about 3.5 times more traffic repetitions than equivalent nonreinforced pavements before a 1.5-in. rut depth is reached. Author

N91-26161# Illinois Univ., Urbana. Dept. of Civil Engineering.
GUIDELINES FOR DESIGN, CONSTRUCTION, AND EVALUATION OF AIRPORT PAVEMENT DRAINAGE Final Report
Barry J. Dempsey and Richard A. Pur Oct. 1990 166 p
(Contracts DACA88-85-M-0271; DACA88-85-M-0786; DACW88-85-D-0004)
(DOT/FAA/RD-90/31) Avail: NTIS HC/MF A08

Comprehensive guidelines are provided for the design, construction, and evaluation of airport pavement drainage. Procedures for considering climatic effects on airport drainage are described. Brief summaries of several climatic models which can be used to generate temperature and moisture conditions in pavements are presented. A review of the FAA design procedures for airport surface drainage is presented in order to maintain comprehensive coverage of all aspects of drainage in a single report. Pavement surface drainage is discussed in terms of pavement grooving and the use of porous friction courses. Pavement subsurface drainage is discussed in detail. Methods for determining the sources and quantity of water which enter the pavement are provided. Procedures for designing subbase drainage layers, blankets and filter layers have been presented. Based on the sources and quantity of water which enters the pavement, methods for selecting and sizing the subdrainage collectors and outlets are discussed. Both the used conventional circular pipe systems and prefabricated geocomposite subdrainage (PGS) systems are described. Author

N91-27065*# Iowa State Univ. of Science and Technology, Ames. Dept. of Aerospace Engineering.
THE AEOLIAN WIND TUNNEL
J. D. Iversen *In* NASA. Ames Research Center, Sand and Dust

on Mars May 1991 p 24-25 (For primary document see N91-27057 18-91)
Avail: NTIS HC/MF A04 CSCL 14B

12 ASTRONAUTICS (GENERAL)

For extraterrestrial exploration see *91 Lunar and Planetary Exploration.*

N91-26162# Joint Publications Research Service, Arlington, VA.
JPRS REPORT: SCIENCE AND TECHNOLOGY. USSR: SPACE
16 Apr. 1991 104 p Transl. into ENGLISH of various Russian Articles
(JPRS-USP-91-002) Avail: NTIS HC/MF A06

Topics addressed include: manned mission highlights; space sciences; interplanetary sciences; space policy and administration; life sciences; space engineering; and space applications. For individual titles, see N91-26163 through N91-26179.

N91-26163# Joint Publications Research Service, Arlington, VA.
EVOLUTION OF SOME TYPES OF EARTH SATELLITE ORBITS Abstract Only **c13**
M. A. Vashkovyak and M. L. Lidov *In its* JPRS Report: Science and Technology. USSR: Space 16 Apr. 1991 p 33 Transl. into ENGLISH from Kosmicheskiye Issledovaniya (Moscow, USSR), v. 28, no. 6, Nov.-Dec. 1990 p 803-807 (For primary document see N91-26162 18-12)
Avail: NTIS HC/MF A06

The search continues for an orbit suitable for very long baseline interferometry. The eccentricity and semimajor axis should be large, and the orbital elements will undergo large changes over the span of several years. This work examines numerically and analytically the evolution of elements of separatrix and near-equilibrium orbits. These orbits have a perigee near Earth and an apogee of several hundreds of thousands of kilometers. It is found that the phase trajectory of the separatrix orbit falls in the areas of libration change, and the period of libration is about seven years. The greatest changes in orbit are experience in the first six months; thereafter they are attenuated. Highly elliptical near-equilibrium orbits with a large inclination to the ecliptic plane have variations of a librational character, the rate of evolution increases as the apogee distance increases. Author

N91-26164# Joint Publications Research Service, Arlington, VA.
SPATIAL ROTATIONS OF A SATELLITE IN A CIRCULAR THREE-BODY PROBLEM FOR THE CASE OF GENERAL RESONANCE Abstract Only **c13**
P. S. Krasilnikov *In its* JPRS Report: Science and Technology. USSR: Space 16 Apr. 1991 p 33 Transl. into ENGLISH from Kosmicheskiye Issledovaniya (Moscow, USSR), v. 28, no. 6, Nov.-Dec. 1990 p 808-819 (For primary document see N91-26162 18-12)
Avail: NTIS HC/MF A06

The problem of the resonant rotation of spacecraft around the center of mass in the gravitational field of two very heavy homogeneous spherical bodies moving in a circular orbit relative to each other is examined. The spacecraft is considered an infinitely small solid body. It is shown that the averaged equations of a dynamically symmetrical satellite can be integrated in quadratures. Two or four equilibrium points may exist. The satellite's motion is described by quasi-periodic time functions. Its central ellipsoid of inertia is near spherical. The gravitational momenta cause a slow shift in the direction of the kinetic momenta. Possible loops in the spatial orbits are classified. Planar satellite orbits constitute a deformation of the loop into a closed curve of degree zero. Critical values of parameters at which the degree of the loop changes are found. The effect of the satellite's trajectory on its movement around the center of mass is studied. Author

N91-26165# Joint Publications Research Service, Arlington, VA.
OSCILLATIONS OF A SMALL-MASS SATELLITE PROBE CAUSED BY AERODYNAMIC AND GRAVITATIONAL FORCES Abstract Only **c13**
V. I. Zhuk and Ye. M. Shakhov *In its* JPRS Report: Science and Technology. USSR: Space 16 Apr. 1991 p 33-34 Transl. into ENGLISH from Kosmicheskiye Issledovaniya (Moscow, USSR), v. 28, no. 6, Nov.-Dec. 1990 p 820-830 (For primary document see N91-26162 18-12)
Avail: NTIS HC/MF A06

The three-dimensional oscillations of a satellite tethered to a main satellite are examined in the context of a model that considers diurnal variations in atmospheric density and the rotation of the atmosphere. The tether is an inextensible, flexible cable. The frequency of oscillations at the transversal point of relative equilibrium may substantially exceed the frequency of revolution of the main satellite, which is in a circular orbit. Because of this, several characteristic times can be determined in the system, and these may be used in space experiments. This is in contrast to other works which consider such oscillations undesirable. Oscillations are the result of aerodynamic drag, and may depend not only on the density of the atmosphere, but also on the density gradient. When the probe is heavy, gravity plays a greater role than drag. The oscillations may be used to study atmospheric density and other geophysical characteristics. Author

N91-26166# Joint Publications Research Service, Arlington, VA.
ANALYSIS OF NECESSARY AND SUFFICIENT CONDITIONS FOR THE EQUILIBRIUM STABILITY OF A GYROSTATIC SATELLITE Abstract Only **c18**
A. A. Anchev and V. A. Atanasov *In its* JPRS Report: Science and Technology. USSR: Space 16 Apr. 1991 p 34 Transl. into ENGLISH from Kosmicheskiye Issledovaniya (Moscow, USSR), v. 28, no. 6, Nov.-Dec. 1990 p 831-836 (For primary document see N91-26162 18-12)
Avail: NTIS HC/MF A06

The gyrostatic satellite had three rotors whose axes of rotation are along the main central axis of inertia of the satellite. The central axes of the satellite are directed along the axes of the orbital coordinate system. The satellite moves in a circular orbit. The necessary and sufficient conditions for stability of equilibrium attitude are calculated and analyzed. These results are compared with the results of other authors. Author

N91-26167# Joint Publications Research Service, Arlington, VA.
CALCULATION OF THE POINTING ACCURACY OF SPACECRAFT EQUIPMENT USING AUTONOMOUS MEASUREMENTS OF THE ANGULAR POSITION OF THE OBJECT OF INVESTIGATION Abstract Only **c13**
A. A. Chernov *In its* JPRS Report: Science and Technology. USSR: Space 16 Apr. 1991 p 34 Transl. into ENGLISH from Kosmicheskiye Issledovaniya (Moscow, USSR), v. 28, no. 6, Nov.-Dec. 1990 p 837-845 (For primary document see N91-26162 18-12)
Avail: NTIS HC/MF A06

The pointing accuracy of a star tracking system is determined that uses indirect pointing. Data on the position of the target are sent to the tracking system from the spacecraft's information and measurement system. The information and measurement system has only an angle measuring channel, which consists of an optical telescope and a radiation detector whose plane is orthogonal to the optical axis of the telescope. The pointing system uses combined control with compensation of perturbations. Delays in signal propagation are considered. It is assumed that there are no systematic pointing errors. Portions of the article are devoted to calculation of pointing errors in the scientific equipment and the scatter of positions in the photodetector. It is also assumed that the spacecraft moves without angular acceleration during the experiment. The probability of capture of the target in the instrument's field of view is calculated. Author

N91-26168# Joint Publications Research Service, Arlington, VA.
ANALYTICAL ALGORITHMS TO SOLVE AN INVERSE NAVIGATION PROBLEM FOR A SYSTEM OF SATELLITES Abstract Only **c13**
R. I. Braslavets *In its* JPRS Report: Science and Technology. USSR: Space 16 Apr. 1991 p 34 Transl. into ENGLISH from Kosmicheskiye Issledovaniya (Moscow, USSR), v. 28, no. 6, Nov.-Dec. 1990 p 846-853 (For primary document see N91-26162 18-12)
Avail: NTIS HC/MF A06

A methodical approach is proposed for the development of analytical algorithms for the navigation of an observer-spacecraft from synchronous measurements of angular and linear parameters of the positions of several (two to six) reference satellites chosen from a system of satellites. Reference satellites create a navigation field that enables the unambiguous determination of the position vector of the observer. Formulas are obtained to calculate various types of navigation algorithms differing in their navigation algorithms. Recommendations are given for formalizing the structure of several elements of navigational algorithms. The relative simplicity of the finite formulas of navigation algorithms and their independence from a-priori information on the position of the observer-spacecraft will make it possible to implement them in future spacecraft to increase the reliability of navigation.
Author

N91-26169# Joint Publications Research Service, Arlington, VA.
STUDY OF THE PROPERTIES OF THE AUTONOMOUS OPTICAL NAVIGATION OF A SPACE PROBE IN A RENDEZVOUS WITH AN ASTEROID Abstract Only **c13**
V. V. Ivashkin *In its* JPRS Report: Science and Technology. USSR: Space 16 Apr. 1991 p 34-35 Transl. into ENGLISH from Kosmicheskiye Issledovaniya (Moscow, USSR), v. 28, no. 6, Nov.-Dec. 1990 p 854-864 (For primary document see N91-26162 18-12)
Avail: NTIS HC/MF A06

Several countries are developing programs to send probes to small solar system objects. Properties of autonomous navigation are examined for a spacecraft on such a mission. In this case the main spacecraft approaches the object for remote study, then releases a probe for a closer study. The probe brakes as it approaches the surface and releases rods which embed in the surface to study the soil. While a high landing speed is required for the soil study rods, a soft landing is desired for the probe. It is necessary to know the probe's exact distance from the surface. Previously, radar altitude measurements were made. The possibility of using optical navigation is examined. The object of the study is the asteroid Vesta. Navigation by measurements of the angular diameter of Vesta may be unsuitable. Sighting the asteroid on a star field is examined, and this method yields adequate results. Cases are examined where the distance to the target is known, as are cases where it must be determined. The examination includes a consideration of error analysis, and an analysis is made of the probe position determination accuracy and the landing speed accuracy of the probe.
Author

N91-26170# Joint Publications Research Service, Arlington, VA.
FLUID DAMPING OF THE OSCILLATIONS OF SATELLITES WITH A LARGE MAGNETIC MOMENT Abstract Only **c18**
M. L. Pivovarov *In its* JPRS Report: Science and Technology. USSR: Space 16 Apr. 1991 p 35 Transl. into ENGLISH from Kosmicheskiye Issledovaniya (Moscow, USSR), v. 28, no. 6, Nov.-Dec. 1990 p 865-873 (For primary document see N91-26162 18-12)
Avail: NTIS HC/MF A06

The rotation of a satellite with a permanent magnet in the plane of a polar Keplerian elliptical orbit is examined. The damping of oscillations relative to a line of magnetic force by a viscous fluid which completely fills a cavity is considered. The period of the satellite's movement relative to the force line is much smaller than its period of rotation. Two cases are examined: when the cavity is of an arbitrary shape and its Reynolds number is small, and when it is toroidal and its Reynolds number is arbitrary. It is assumed the magnetic moment of the satellite is large. An averaging method is used to obtain analytical expressions which describe the decrease in rotational energy of the satellite and the damping of oscillations relative to the force line of the magnetic field. The effectiveness of the damper is proportional to the moment of inertia of the field. To decrease the volume of the damper, a dense fluid like mercury can be used.
Author

N91-26171# Joint Publications Research Service, Arlington, VA.
MEASUREMENTS OF THE LONGITUDINAL MOVEMENTS OF O(+) IONS IN THE SUBAURORAL UPPER ATMOSPHERE FROM THE AUREOL 3 SATELLITE Abstract Only **c46**
L. V. Zinin, V. S. Solovyev, Yu. I. Galperin, V. A. Gladyshev, and S. A. Grigoryev *In its* JPRS Report: Science and Technology. USSR: Space 16 Apr. 1991 p 35 Transl. into ENGLISH from Kosmicheskiye Issledovaniya (Moscow, USSR), v. 28, no. 6, Nov.-Dec. 1990 p 886-889 (For primary document see N91-26162 18-12)
Avail: NTIS HC/MF A06

The study of the longitudinal movements of thermal ions in the upper ionosphere, which dictate their outflow into the magnetosphere, is important in the physics of ionosphere-magnetosphere interaction. The main mechanism for this transfer is the polar wind. Recent experimental data have confirmed the polar wind theory for light ions, and indicated significant upward fluxes of thermal O(+) ions from the high latitude ionosphere. The question then arises of how well these longitudinal movements of O(+) are described by a non-steady state hydrodynamic model of the polar wind. These fluxes were measured from the F layer to 1,500 to 2,000 km by the Aureol 3 satellite, part of a Soviet-French collaboration. The DYCTION instrument used to make the measurements is described. It was found that at night there was a downward flux of O(+) ions, especially at high altitudes. In the early morning, the opposite was true for the F layer; O(+) ions moved upward at speeds reaching 400 to 700 m/s. The upwelling is due to a sharp increase in electron temperature due to the appearance of photoelectrons against a background of decreased nighttime electron concentration and temperature. There is qualitative agreement between the model and experimental data. Differences in the speed of ion avalanche are due to the actual nonMaxwellian distribuiton of velocities. Deviations in observed data are due to measurement error and the changing effects of geomagnetic activity and variations in ion temperature.
Author

N91-26172# Joint Publications Research Service, Arlington, VA.
DYNAMICS OF EQUATORIAL AND POLAR BOUNDARIES OF PENETRATION OF SOLAR PROTONS WITH ENERGY ABOUT 1 MeV INTO MAGNETOSPHERE DURING STRONG MAGNETIC STORM Abstract Only **c92**
L. A. Darchiyeva, T. A. Ivanova, E. N. Sosnovets, and L. V. Tverskaya *In its* JPRS Report: Science and Technology. USSR: Space 16 Apr. 1991 p 37-38 Transl. into ENGLISH from Geomagnetizm i Aeronomiya (Moscow, USSR), v. 30, no. 5, Sep.-Oct. 1990 p 856-858 (For primary document see N91-26162 18-12)
Avail: NTIS HC/MF A06

Research on the asymmetric injection of ring current particles on the basis of direct measurements on a single satellite does not make it possible to obtain the global picture of particle injection because the satellite intersects only two narrow sectors LT. Accordingly, a study was made of the dynamics of the equatorial and polar boundaries of penetration of solar protons into the magnetosphere on the basis of published data from simultaneous measurements on three artificial satellites during the phase of development and at onset of the recovery phase of the strong magnetic storm of 3 to 4 Apr. 1979, supplemented by data from the world network of magnetic observatories. It was found that the extremal approach of the boundary of penetration of solar protons with an energy about 1 MeV to the Earth occurred several hours before the storm maximum and with a minimal latitudinal position of the polar electrojet. Quasiperiodic movements of the

polar boundaries of solar protons in the magnetosphere, associated with a series of substorms in the process of development of a world magnetic storm, were discovered. Author

N91-26173# Joint Publications Research Service, Arlington, VA.
MODELLING THE DYNAMICS OF FLUXES OF ELECTRONS WITH ENERGIES 30-300 keV IN GEOSTATIONARY ORBIT Abstract Only **c93**
V. I. Degtyarev, G. V. Popov, and S. S. Sheshukov *In its* JPRS Report: Science and Technology. USSR: Space 16 Apr. 1991 p 38 Transl. into ENGLISH from Geomagnetizm i Aeronomiya (Moscow, USSR), v. 30, no. 5, Sep.-Oct. 1990 p 866-868 (For primary document see N91-26162 18-12)
Avail: NTIS HC/MF A06

A model of the dynamics of electrons with energies 30 to 300 keV along a geostationary orbit was constructed. The purpose of the model was a diagnosis or prediction of the state of the medium at a specific moment in time on the basis of input parameters (geophysical and heliophysical indices). In this model the electron flux I with energy E acting on a satellite in a geostationary orbit at a specific moment in universal time can be described by three components: (1) asymmetry of drift shells of electrons in a 'stationary' magnetosphere; (2) adiabatic change in fluxes of electrons associated with slow deformation of drift shells with a change in solar wind parameters; and (3) nonadiabatic changes in electron fluxes occurring during a substorm and 'injection' events. The model was used in an analysis of data for the period 10 Mar. to 16 Jun., 1986. Measurements were made in six channels in the energy range 30 to 300 keV on three satellites situated approximately uniformly along a geostationary orbit. Each of the satellites carried identical particle spectrometers. An analysis of the spectra of variations gives the basis for representation of the change in electron fluxes in the course of a 24 hour period in the form of an expansion into a Fourier series. As an illustration, the results of use of the model for a retrospective prediction of the mean hourly fluxes of electrons in a geostationary orbit are given for a day with average magnetic activity during which several substorms were observed. Author

N91-26174# Joint Publications Research Service, Arlington, VA.
TURBULENT PROCESSES OF MASS-LOADING OF NEW IONS ON VENUS AND MARS AND THE PROBLEMS OF NUMERICAL MODELS OF THE INTERACTION OF SOLAR WIND WITH THESE PLANETS. 1: CHARACTERISTICS OF THE FLOW OF SOLAR WIND AROUND THE PLANETS Abstract Only **c91**
T. K. Breus and A. M. Krymskiy *In its* JPRS Report: Science and Technology. USSR: Space 16 Apr. 1991 p 40 Transl. into ENGLISH from Kosmicheskiye Issledovaniya (Moscow, USSR), v. 28, no. 6, Nov.-Dec. 1990 p 923-935 (For primary document see N91-26162 18-12)
Avail: NTIS HC/MF A06

Initially thought to be due only to solar wind/comet interactions, loading of the solar wind with heavy ions has been found to be the result also of interactions with planets. Is is a universal phenomenon near nonmagnetic and slightly magnetic solar system objects. An overview of previous investigations is given. On Venus, loading is most intense in the transition region near the ionopause. The ions are rapidly accelerated in laminar and turbulent fields. The conditions for the capture of new heavy ions by the solar wind vary substantially with distance from the planet surface and the solar zenith angle. It is impossible to determine the pressure of heavy ions for hydrodynamic calculations without kinetic calculations. Hydrodynamic models developed at solar minimum were found to be inadequate at solar maximum. A two-fluid model with anomalous friction between species of ions is used to described the flow of the solar wind around Venus and Mars. The friction is due to turbulent acceleration processes in the transition region. Author

N91-26175# Joint Publications Research Service, Arlington, VA.
CHARACTERISTICS OF AEROSOL IN THE ATMOSPHERE OF MARS ACCORDING TO DATA FROM THE KRFM EXPERIMENT Abstract Only **c91**
V. I. Moroz, Ye. V. Petrova, L. V. Ksanformaliti, L. Esposito, J. P. Bibring, M. Combes, A. Soufflot, O. F. Ganpantserova, N. V. Goroshkova, and A. V. Zharkov et al *In its* JPRS Report: Science and Technology. USSR: Space 16 Apr. 1991 p 40 Transl. into ENGLISH from Kosmicheskiye Issledovaniya (Moscow, USSR), v. 28, no. 6, Nov.-Dec. 1990 p 936-942 (For primary document see N91-26162 18-12)
Avail: NTIS HC/MF A06

The KRFM experiment on Fobos 2 consisted of an infrared radiometer and filters, and a 0.32 to 0.60 micron prism spectrometer. Photometric profiles of Mars were obtained in eight spectral bands from 320 to 550 nm. The equatorial region of Mars was studied from limb to limb. Some details of the profiles are associated with atmospheric aerosol. Quantitative analysis of aerosol properties is difficult because of the number of parameters needed. An interpretation of the data yielded three types of aerosol: (1) constant haze (mineral dust) mixed with gas; (2) ice haze at the surface at night; and (3) high-altitude clouds. The article examines types 1 and 3. THe absorption properties are those of basalt mixed with goethite. The optical depth, 0.3, is virtually independent of wavelength. The particle size distribution is wide. Author

N91-26176# Joint Publications Research Service, Arlington, VA.
RESULTS OF MORPHOMETRIC ANALYSIS OF THE TESSERAE SURFACE OF VENUS ACCORDING TO VENERA-15 AND -16 DATA Abstract Only **c91**
M. A. Ivanov *In its* JPRS Report: Science and Technology. USSR: Space 16 Apr. 1991 p 40 Transl. into ENGLISH from Astronomicheskiy Vestnik (Moscow, USSR), v. 24, no. 4, Oct.-Dec. 1990 p 288-295 (For primary document see N91-26162 18-12)
Avail: NTIS HC/MF A06

Tesserae occupy nine million square kilometers of the surface of Venus. Tesserae are raised above the surrounding surface and are crossed by systems of intersecting and parallel ridges and linear depressions. Ridges are peaked and depressions are V-shaped. Tesserae regions can be differentiated by the distances between their ridges, the spacing. The purpose of this article is to determine the spacing of various tesserae regions and to determine the patterns of the distribution of the spacing. The distance between ridges was found to vary from 2 to 38 km, with an average of 6 to 11 km. The global dependence between the area of the tesserae and their average height is calculated. A two-layer model of tesserae structure is presented, and calculations are done to determine the thickness of the upper deformed layer, which is estimated to be 1-2 to 3-7 km thick or 0.5-1 to 1-2 km thick, depending on the model used. It may be defined by the topography of the tesserae. Topography may be supported by upwelling matter or by buoyancy. Buoyance is assumed, and values are determined for different tesserae regions (Fortuna, Tellura, and Laima) and composition (basalt, feldspar). Author

N91-26177# Joint Publications Research Service, Arlington, VA.
DETERMINATION OF THE MASSES AND DENSITIES OF METEOROIDS FROM RADAR OBSERVATIONS FROM ONE POINT Abstract Only
P. Sh. Bibarsov, M. Narziyev, and R. P. Chebotarev *In its* JPRS Report: Science and Technology. USSR: Space 16 Apr. 1991 p 40-41 Transl. into ENGLISH from Astronomicheskiy Vestnik (Moscow, USSR), v. 24, no. 4, Oct.-Dec. 1990 p 326-332 (For primary document see N91-26162 18-12)
Avail: NTIS HC/MF A06

The location of the reflecting point on a meteor trail is examined relative to the point of maximum ionization according to the results of radar observations of meteoroids from five points and a method is proposed which considers the processes affecting the shape of the ionization curve in determining mass and density from radar observations of meteors from one point. On the average the reflecting poing is 0.4 km below the point of maximum ionization. Equations are presented to calculate the mass of the meteoroid and correct for factors which affect the ionization curve. The density and mass of meteoroids can be calculated from the length of the meteoroid ratio echo measured at one point or from radar

observations from one point when the proposed method is used. Two methods of calculating mass are presented. For a meteoroid of mass 10(exp -3) to 10 (exp -1) g, density varies from 0.5 to 5.2 g/cu cm, with an average value of 1.9 g/cu cm. Author

N91-26178# Joint Publications Research Service, Arlington, VA.
REVIEW OF PRIMARY MEDICAL RESULTS OF YEAR-LONG FLIGHT ON MIR STATION **c52**
A. I. Grigoryev, S. A. Bugrov, V. V. Bogomolov, A. D. Yegorov, I. B. Kozlovskaya, I. D. Pestov, and I. K. Tarasov *In its* JPRS Report: Science and Technology. USSR: Space 16 Apr. 1991 p 42-49 Transl. into ENGLISH from Kosmicheskaya Biologiya i Aviakosmicheskaya Meditsina (USSR), v. 24, no. 5, Sep.-Oct. 1990 p 3-10 (For primary document see N91-26162 18-12)
Avail: NTIS HC/MF A06

The objective of medical investigations during and after the 366 day manned mission was to accumulate information about human responses to long-term effects of microgravity. To do this, cardiovascular and other systems were examined in detail during and after exposure. The results gave evidence that the crewmembers well adapted to the long-term flight effects. Their good health and high work capacity were supported by adequate medical procedures. Postflight readaptation developed similarly to what was seen after previous flights of shorter duration (6 to 11 months). No qualitatively new changes in the physiological systems were detected during or after this mission. Author

N91-26179# Joint Publications Research Service, Arlington, VA.
LIMITED CURRENT CAPABILITIES FOR COSMONAUT RESCUE Abstract Only
O. Burluka and D. Dmitriadi *In its* JPRS Report: Science and Technology. USSR: Space 16 Apr. 1991 p 50-51 Transl. into ENGLISH from NTR Tribuna (Moscow, USSR), no. 15-16, 1990 p 14 (For primary document see N91-26162 18-12)
Avail: NTIS HC/MF A06

A recent incident in space - the damage to the thermal insulation of the Soyuz spacecraft - has raised concern for the safety of the cosmonauts. A rescue operation scenario is discussed. Also discussed is the modified version of the new Soyuz. A conference, held in Saudi Arabia, was specially devoted to the problem of rescuing cosmonauts. B.G.

N91-26180# Air Force Inst. of Tech., Wright-Patterson AFB, OH. Foreign Technology Div.
CHINESE SPACE SCIENCE AND TECHNOLOGY (SELECTED ARTICLES)
21 Mar. 1991 27 p Transl. into ENGLISH from Zhongguo Kongjian Kexue Jishu (China), v. 10, no. 2, 1990 p 5-9, 25-29
(AD-A234798; FTD-ID(RS)T-1273-90) Avail: NTIS HC/MF A03 CSCL 22/2

Two articles are presented: (1) control of solid-apogee motor during orbit transfer maneuver; and (2) application of split-phase code PSK signal in data transmission of meteorological satellite remote sensing image. The first article provides a method for determining the optimum time and attitude at which the solid apogee motor should be fired in the launching of a geostationary satellite. In the second article, the split-phase code signal is analyzed, and its characteristics are reviewed. GRA

N91-26181# Air Force Inst. of Tech., Wright-Patterson AFB, OH. Foreign Technology Div.
PRIME MINISTER LI PENG TALKS WITH REPRESENTATIVES TO A DISCUSSION MEETING ON SATELLITE APPLICATIONS AND APPLIED SATELLITE TECHNOLOGY ABOUT THE DEVELOPMENT OF OUR COUNTRY'S ACTIVITIES IN SPACE
Qinglin Zhu 21 Mar. 1991 10 p Transl. into ENGLISH from Yuhang Xuebao (China), no. 4, 1989 p 1-2
(AD-A234801; FTD-ID(RS)T-1368-90) Avail: NTIS HC/MF A02 CSCL 22/1

On August 26, 1989, in Zhongnanhai, the Prime Minister of the State Council and the Team Leader of the National Space Team, Li Peng, met with the representatives to the initial meeting of the discussion forum on satellite applications and applied technology, and held long discussions with these same delegates. An account of these discussions is presented. GRA

N91-26182*# Contel Technology Center, Chantilly, VA.
ADVANCED SATELLITE RESEARCH PROJECT: SCAR RESEARCH DATABASE. BIBLIOGRAPHIC ANALYSIS Final Report, Sep. 1990 - Mar. 1991
Joseph N. Pelton 30 Mar. 1991 109 p
(Contract NASw-4520)
(NASA-CR-186086; NAS 1.26:186086) Avail: NTIS HC/MF A06 CSCL 22A

The literature search was provided to locate and analyze the most recent literature that was relevant to the research. This was done by cross-relating books, articles, monographs, and journals that relate to the following topics: (1) Experimental Systems - Advanced Communications Technology Satellite (ACTS), and (2) Integrated System Digital Network (ISDN) and Advance Communication Techniques (ISDN and satellites, ISDN standards, broadband ISDN, flame relay and switching, computer networks and satellites, satellite orbits and technology, satellite transmission quality, and network configuration). Bibliographic essay on literature citations and articles reviewed during the literature search task is provided. Author

N91-27108*# Houston Univ., TX. Coll. of Architecture.
DEVELOPING A TAXONOMY FOR MISSION ARCHITECTURE DEFINITION Final Report
Deborah J. Neubek *In its* NASA/ASEE Summer Faculty Fellowship Program, 1990, Volume 2 Dec. 1990 9 p (For primary document see N91-27103 18-99)
(Grant NGT-44-005-803)
Avail: NTIS HC/MF A09 CSCL 22A

13 ASTRODYNAMICS

Includes powered and free-flight trajectories; and orbital and launching dynamics.

N91-26183# Aerospace Corp., El Segundo, CA.
TRACE TRAJECTORY ANALYSIS AND ORBIT DETERMINATION PROGRAM. VOLUME 13: SQUARE ROOT INFORMATION FILTERING AND SMOOTHING Final Report
L. A. Campbell 15 Mar. 1991 91 p
(Contract F04701-88-C-0089)
(AD-A234957; TR-0059(9320)-1-Vol-13; SSD-TR-91-07-Vol-13)
Avail: NTIS HC/MF A05 CSCL 22/3

The TRACE Trajectory Analysis and Orbit Determination Program is a general purpose orbital analysis program. It was developed specifically to assist technical personnel in the analysis and design of satellite orbits and tracking systems. Volume 13 is a technical reference for the square root information filtering and smoothing (SRIF/S) capabilities, which are used for high precision orbit determination and error analysis. GRA

N91-26163# Joint Publications Research Service, Arlington, VA.
EVOLUTION OF SOME TYPES OF EARTH SATELLITE ORBITS Abstract Only
M. A. Vashkovyak and M. L. Lidov *In its* JPRS Report: Science and Technology. USSR: Space 16 Apr. 1991 p 33 Transl. into ENGLISH from Kosmicheskiye Issledovaniya (Moscow, USSR), v. 28, no. 6, Nov.-Dec. 1990 p 803-807 (For primary document see N91-26162 18-12)
Avail: NTIS HC/MF A06

N91-26164# Joint Publications Research Service, Arlington, VA.
SPATIAL ROTATIONS OF A SATELLITE IN A CIRCULAR THREE-BODY PROBLEM FOR THE CASE OF GENERAL RESONANCE Abstract Only
P. S. Krasilnikov *In its* JPRS Report: Science and Technology. USSR: Space 16 Apr. 1991 p 33 Transl. into ENGLISH from Kosmicheskiye Issledovaniya (Moscow, USSR), v. 28, no. 6,

Nov.-Dec. 1990 p 808-819 (For primary document see N91-26162 18-12)
Avail: NTIS HC/MF A06

N91-26165# Joint Publications Research Service, Arlington, VA.
OSCILLATIONS OF A SMALL-MASS SATELLITE PROBE CAUSED BY AERODYNAMIC AND GRAVITATIONAL FORCES Abstract Only
V. I. Zhuk and Ye. M. Shakhov *In its* JPRS Report: Science and Technology. USSR: Space 16 Apr. 1991 p 33-34 Transl. into ENGLISH from Kosmicheskiye Issledovaniya (Moscow, USSR), v. 28, no. 6, Nov.-Dec. 1990 p 820-830 (For primary document see N91-26162 18-12)
Avail: NTIS HC/MF A06

N91-26167# Joint Publications Research Service, Arlington, VA.
CALCULATION OF THE POINTING ACCURACY OF SPACECRAFT EQUIPMENT USING AUTONOMOUS MEASUREMENTS OF THE ANGULAR POSITION OF THE OBJECT OF INVESTIGATION Abstract Only
A. A. Chernov *In its* JPRS Report: Science and Technology. USSR: Space 16 Apr. 1991 p 34 Transl. into ENGLISH from Kosmicheskiye Issledovaniya (Moscow, USSR), v. 28, no. 6, Nov.-Dec. 1990 p 837-845 (For primary document see N91-26162 18-12)
Avail: NTIS HC/MF A06

N91-26168# Joint Publications Research Service, Arlington, VA.
ANALYTICAL ALGORITHMS TO SOLVE AN INVERSE NAVIGATION PROBLEM FOR A SYSTEM OF SATELLITES Abstract Only
R. I. Braslavets *In its* JPRS Report: Science and Technology. USSR: Space 16 Apr. 1991 p 34 Transl. into ENGLISH from Kosmicheskiye Issledovaniya (Moscow, USSR), v. 28, no. 6, Nov.-Dec. 1990 p 846-853 (For primary document see N91-26162 18-12)
Avail: NTIS HC/MF A06

N91-26169# Joint Publications Research Service, Arlington, VA.
STUDY OF THE PROPERTIES OF THE AUTONOMOUS OPTICAL NAVIGATION OF A SPACE PROBE IN A RENDEZVOUS WITH AN ASTEROID Abstract Only
V. V. Ivashkin *In its* JPRS Report: Science and Technology. USSR: Space 16 Apr. 1991 p 34-35 Transl. into ENGLISH from Kosmicheskiye Issledovaniya (Moscow, USSR), v. 28, no. 6, Nov.-Dec. 1990 p 854-864 (For primary document see N91-26162 18-12)
Avail: NTIS HC/MF A06

14 GROUND SUPPORT SYSTEMS AND FACILITIES (SPACE)

Includes launch complexes, research and production facilities; ground support equipment, e.g., mobile transporters; and simulators.

For related information see also *09 Research and Support Facilities (Air).*

N91-26184# Army Armament Research, Development and Engineering Center, Picatinny Arsenal, NJ. Fire Support Armaments Center.
RAIL CIRCUIT AUGMENTATION
William H. Davis May 1991 19 p
(AD-A234944; ARFSD-TR-91008) Avail: NTIS HC/MF A03
CSCL 10/2

A concept for an augmented railgun barrel and integrated projectile/armature system is presented. The system makes use of the rail geometry to expose the augmenting rails to the bore, and incorporates dual tandem armatures in the launch package. Benefits include reduced current and power required to launch a given mass and a modest reduction in sabot mass due to creation of multiple tension and compression regions resulting from the use of dual armatures. Radial and axial plasma confinement techniques may be required to take advantage to system benefits. Application to an antiarmor mission is proposed. GRA

N91-26185# Battelle Columbus Labs., OH. Tactical Technology Center.
ELECTROMAGNETIC LAUNCH TECHNOLOGY ASSESSMENT. SCIENTIFIC BASIS AND UNIFIED TREATMENT: FORCES AND ELECTROMECHANICAL POWER CONVERSION (ANALYTICAL AND NUMERICAL METHODS)
M. D. Driga Jun. 1990 127 p
(Contract DAAH01-88-C-0131; ARPA Order 6049)
(AD-A235028; TACTEC-R-6266) Avail: NTIS HC/MF A07
CSCL 20/3

This report suggests that one of the reasons why the electromagnetic (EM) hypervelocity launchers and associated power supply technologies have not reached their expectations is that most research has focused on simple railgun accelerators and homopolar generators. Complex rotating flux compressors would drastically improve the performance of EM launchers. This report explores the computations for the design of such complex magnetic flux compressors and heteropolar hypervelocity accelerators. It presents a finite element method formulation for electromagnetic field diffusion. GRA

N91-26186# Sandia National Labs., Albuquerque, NM.
HYPERVELOCITY LAUNCH CAPABILITIES TO OVER 10.4 km/s
L. C. Chhabildas, L. M. Barker, J. R. Asay, T. G. Trucano, and G. I. Kerley 1990 28 p Presented at the Annual Meeting of the Aeroballistic Range Association, San Diego, 22-25 Oct. 1990
(Contract DE-AC04-76DP-00789)
(DE91-010859; SAND-90-2474C; CONF-9010227-3) Avail: NTIS HC/MF A03

A systematic study is described which addresses the technical issues associated with launching flier-plates intact to hypervelocities. First, very high pressures are needed to launch the flier plates to hypervelocities, and second this high pressure loading must be uniform and nearly shockless. To achieve both these criteria, a graded-density material referred to as a pillow is used to impact a flier plate. When this graded-density material is used to impact a flier plate at high velocities on a two-stage light-gas gun, nearly shockless megabar pressure pulses are introduced into the flier plate. Since the loading on the flier plate is shockless, melting of the flier plate is prevented. This technique has been used to launch a 2-mm thick titanium alloy (Ti-6Al-4V) plate to a velocity of 8.1 km/s, and a 1-mm thick aluminum alloy (6061-T6) plate to a velocity of 10.4 km/s. A method is described by which the flier plate velocities could be further augmented to velocities approaching 14 km/s. DOE

N91-26187# Lawrence Livermore National Lab., CA.
PERFORMANCE OF HYPERVELOCITY ARMATURES WITH REPLENISHED METAL VAPOR PLASMAS
R. S. Hawke, A. R. Susoeff, J. A. Ang, C. H. Konrad, C. A. Hall, J. L. Sauve, and A. R. Vasey (Edgerton, Germeshausen and Grier, Inc., Albuquerque, NM.) 14 Mar. 1991 10 p Presented at the 3rd European Electromagnetic Launcher Symposium, London, England, 16-18 Apr. 1991
(Contract W-7405-eng-48)
(DE91-011931; UCRL-JC-106828; CONF-9104240-1) Avail: NTIS HC/MF A02

The joint SNL/LLNL STARFIRE project has employed a two-stage light-gas gun (2SLGG) injector, extensive diagnostics and emphasis on advanced projectile concept development. The 2SLGG injector enables the study of armature behavior at high velocity. Extensive diagnostics provides detailed measurements of armature performance. A new projectile concept was developed which has mitigated the loss of performance by feeding metal vapor from the projectile into the plasma armature thereby maintaining a high conductivity region at the front of the armature and enabling the current density to remain high in this region.

With this technique, nearly ideal performance up to 6.7 km/s was achieved. DOE

15 LAUNCH VEHICLES AND SPACE VEHICLES

Includes boosters; operating problems of launch/space vehicle systems; and reusable vehicles.

For related information see also *20 Spacecraft Propulsion and Power.*

No abstracts in this category.

16 SPACE TRANSPORTATION

Includes passenger and cargo space transportation, e.g., shuttle operations; and space rescue techniques.

For related information see also *03 Air Transportation and Safety* and *18 Spacecraft Design, Testing and Performance.* For space suits see *54 Man/System Technology and Life Support.*

N91-26188# Arnold Engineering Development Center, Arnold Air Force Station, TN.

BIDIRECTIONAL REFLECTANCE DISTRIBUTION (BRDF) OF NASA SHUTTLE TILES Final Report, 2-18 Jan. 1991

R. P. Young and B. E. Wood (Calspan Field Services, Inc., Arnold AFS, TN.) Apr. 1991 49 p

(AD-A235115; AEDC-TSR-91-V1) Avail: NTIS HC/MF A03 CSCL 14/4

Ground-based infrared IR cameras, located on a Maui mountaintop, are used to support a series of experiments associated with studying the condition of space shuttle tiles while in flight. This includes studying the reflective properties of the shuttle tiles while the shuttle is in orbit. Since the IR cameras used are sensitive in the 2.0 to 5.5 micron wavelength range the shuttle tile optical properties are required for the same spectral range. The optical property of particular interest is the tile Bidirectional Reflectance Distribution Function (BRDF). The tile BRDF is input into radiation models to help predict the expected power levels observed by the IR cameras. The objective of the tests reported was to measure the tile BRDF over the range of 2.0 to 5.5 micron as a function of reflectance angle. The BRDF of both black and white (flown and unflown) shuttle tiles were measured. This report describes the apparatus and method used to measure the BRDF of both black and white, flown and unflown, NASA space shuttle tiles. Measured data are included in the report appendix. GRA

17 SPACE COMM., SPACECRAFT COMM., COMMAND & TRACKING

Includes telemetry; space communications networks; astronavigation and guidance; and radio blackout.

For related information see also *04 Aircraft Communications and Navigation* and *32 Communications and Radar.*

No abstracts in this category.

18 SPACECRAFT DESIGN, TESTING AND PERFORMANCE

Includes satellites; space platforms; space stations; spacecraft systems and components such as thermal and environmental controls; and attitude controls.

For life support systems see *54 Man/System Technology and Life Support.* For related information see also *05 Aircraft Design, Testing and Performance, 39 Structural Mechanics,* and *16 Space Transportation.*

N91-26189# Atmospheric and Environmental Research, Inc., Cambridge, MA.

SATELLITE DATA DERIVED ESTIMATES OF EROSION PARAMETERS FOR REENTRY VEHICLES Final Report, Feb. - Nov. 1990

R. G. Isaacs, J. S. Belfiore, and H. C. Huang 5 Feb. 1991 163 p

(Contract F19628-90-C-0048)

(AD-A234792; GL-TR-90-0317) Avail: NTIS HC/MF A08 CSCL 04/2

This study investigates the derivation of reentry-vehicle erosion parameter estimates based on the inference of rain rate and hydrometeor liquid water content from microwave imagery data from the Defense Meteorological Satellite Program (DMSP) sensors. Specifically, this research focusers on evaluation of Special Sensor Microwave/Imager (SSM/I) brightness temperature data to obtain a climatology of intense atmospheric precipitation at selected relevant land based sites for a four month summer period. An integral element of the study is identification of convective cloud models to support the analysis of hydrometeor liquid water content from the inferred surface rainfall rates. Tasks include: (1) development of SSM/I rain rate climatology; (2) development of hydrometeor liquid water content parameterization; (3) application of liquid water parameterization; and (4) documentation. Software was implemented to: (1) read the SSM/I TDRs from the acquired SSM/I data tapes; (2) calibrate and antenna pattern correct the data to obtain brightness temperatures; (3) bin the data according to the location of each desired site by latitude and longitude; (4) apply the rain rate retrieval algorithm to the data; and (5) evaluate relevant climatologies. The latter included four month summer time series of average rainfall rate, spatial standard deviation, and hydrometeor integrated liquid water content for eleven Eurasian sites. GRA

N91-26190# Georgia Inst. of Tech., Atlanta. Computational Mechanics Center.

STUDIES IN MODELING, DYNAMICS, AND CONTROL OF SPACE STRUCTURES Final Technical Report

Satya N. Atluri Feb. 1991 12 p

(Grant AF-AFOSR-0020-84; AF Proj. 2302)

(AD-A235059; CMC-GIT-90-1; AFOSR-91-0248TR) Avail: NTIS HC/MF A03 CSCL 12/4

This report presents a summary of 30 papers published in archival literature, dealing with the issues of reduced order modeling, dynamics and control of space structures. Field/boundary element methods for control of nonlinear dynamic response of continuum models of space structures are discussed. Explicit expressions for tangent stiffnesses of truss and frame-type lattice structures are presented. Weak formulations of multibody dynamics problems with constraint are presented. GRA

N91-26191# Cornell Univ., Ithaca, NY.

NONLINEAR DYNAMICS AND CONTROL OF FLEXIBLE STRUCTURES Final Report, Oct. 1986 - Jun. 1990

Francis C. Moon 1 Mar. 1991 171 p

(Grant AF-AFOSR-0211-90; AF Proj. 3484)

(AD-A235186; AFOSR-91-0250TR) Avail: NTIS HC/MF A08 CSCL 22/2

The goals of these research projects were to examine the nonlinear dynamics and control of flexible structures, some of which might be used for space applications. This project was a collaborative one involving structural, electrical and mechanical

engineers. A major part of the research was on trusses/frames structures. Five different truss structures from three to ten meters in size were constructed, two with active controls. However, nonlinear dynamics of continuous beam type structures were also investigated. One of the principal themes was to explore what types of nonlinearities would result in chaotic and unpredictable vibrations. Loose joints in truss structures, friction, buckling and geometric nonlinearities were all found to lead to chaotic motions under certain periodic forcing conditions. Actuators and sensors for space truss active vibration suppression was investigated. New methods were developed for structural control using techniques for simulated annealing for actuator placement, nonlinear random vibrations of pin-jointed trusses, vibration analysis and new models to analyze chaotic dynamics in nonlinear structures with large deformations and friction forces. Finally, a major numerical effort resulted in new codes to predict large motions of structures under active control using parallel processing algorithms. GRA

N91-26192# Phillips Lab., Edwards AFB, CA.
THE EFFECTS OF SPACE DEBRIS ON SOLAR PROPULSION Final Report, Jun. - Jul. 1990
Mark Skibinski Mar. 1991 35 p
(AF Proj. 3056)
(AD-A235257; PL-TR-91-3001) Avail: NTIS HC/MF A03
CSCL 22/2

This research sought to determine the impact of space debris on solar propulsion for orbital transfer missions from low Earth Orbit (LEO) to Geosynchronous Earth Orbit (GEO). Orbital debris is a major concern because the present solar propulsion development calls for two 40 x 30 m inflatable concentrators which present a large area for space debris impact. The initial questions to be researched were: (1) How much extra inflationary gas will be required to make up for meteoroid and artificial space debris leaks? and (2) What is the probability of a catastrophic collision with the concentrators? Numerous debris models and many assumptions were used to calculate answers for these questions, but overall the inflatable reflectors were judged to be a plausible concept. It is plausible in that the amount of helium inflatent needed to keep the concentrators rigid is an acceptable weight (12 lbm). Also the probability of a catastrophic collision for a 40 day mission is minimal (0.1 percent). Further research and computer simulation is needed to better define the man-made debris distribution for elliptical (transfer) orbits due to their constant changing altitude. GRA

N91-26193*# National Aeronautics and Space Administration. Marshall Space Flight Center, Huntsville, AL.
ILLUMINANCE AND LUMINANCE DISTRIBUTIONS OF A PROTOTYPE AMBIENT ILLUMINATION SYSTEM FOR SPACE STATION FREEDOM
R. C. Mullican (McGown-Mullican-Dunn, Architects, Nashville, TN.) and B. C. Hayes Jun. 1991 33 p
(NASA-TM-103541; NAS 1.15:103541) Avail: NTIS HC/MF A03
CSCL 22B

Preliminary results of research conducted in the late 1970's indicate that perceptual qualities of an enclosure can be influenced by the distribution of illumination within the enclosure. Subjective impressions such as spaciousness, perceptual clarity, and relaxation or tenseness, among others, appear to be related to different combinations of surface luminance. A prototype indirect ambient illumination system was developed which will allow crew members to alter surface luminance distributions within an enclosed module, thus modifying perceptual cues to match crew preferences. A traditional lensed direct lighting system was compared to the prototype utilizing the full-scale mockup of Space Station Freedom developed by Marshall Space Flight Center. The direct lensed system was installed in the habitation module with the indirect prototype deployed in the U.S. laboratory module. Analysis centered on the illuminance and luminance distributions resultant from these systems and the implications of various luminaire spacing options. All test configurations were evaluated for compliance with NASA Standard 3000, Man-System Integration Standards. Author

N91-26194# General Accounting Office, Washington, DC. National Security and International Affairs Div.
WEATHER SATELLITES: ACTION NEEDED TO RESOLVE STATUS OF THE US GEOSTATIONARY SATELLITE PROGRAM. REPORT TO THE CHAIRMAN, COMMITTEE ON SCIENCE, SPACE, AND TECHNOLOGY, HOUSE OF REPRESENTATIVES
Jul. 1991 40 p
(GAO/NSIAD-91-252; B-233745) Avail: NTIS HC/MF A03; also available from GAO, Gaithersburg, MD HC first five copies free, additional copies $2.00

The National Oceanic and Atmospheric Administration (NOAA) and the National Aeronautics and Space Administration (NASA) joint efforts to develop and acquire the next generation of geostationary weather satellites (GOES-Next) are reviewed. The current cost, schedule, and technical status of the GOES-Next program; reasons for program problems that led to cost increases and schedule delays; and options available for precluding a gap in geostationary weather satellite coverage of the United States is discussed. B.G.

N91-26166# Joint Publications Research Service, Arlington, VA.
ANALYSIS OF NECESSARY AND SUFFICIENT CONDITIONS FOR THE EQUILIBRIUM STABILITY OF A GYROSTATIC SATELLITE Abstract Only
A. A. Anchev and V. A. Atanasov *In its* JPRS Report: Science and Technology. USSR: Space 16 Apr. 1991 p 34 Transl. into ENGLISH from Kosmicheskiye Issledovaniya (Moscow, USSR), v. 28, no. 6, Nov.-Dec. 1990 p 831-836 (For primary document see N91-26162 18-12)
Avail: NTIS HC/MF A06

N91-26170# Joint Publications Research Service, Arlington, VA.
FLUID DAMPING OF THE OSCILLATIONS OF SATELLITES WITH A LARGE MAGNETIC MOMENT Abstract Only
M. L. Pivovarov *In its* JPRS Report: Science and Technology. USSR: Space 16 Apr. 1991 p 35 Transl. into ENGLISH from Kosmicheskiye Issledovaniya (Moscow, USSR), v. 28, no. 6, Nov.-Dec. 1990 p 865-873 (For primary document see N91-26162 18-12)
Avail: NTIS HC/MF A06

19 SPACECRAFT INSTRUMENTATION

For related information see also *06 Aircraft Instrumentation* and *35 Instrumentation and Photography.*

No abstracts in this category.

20 SPACECRAFT PROPULSION AND POWER

Includes main propulsion systems and components, e.g., rocket engines; and spacecraft auxilliary power sources.

For related information see also *07 Aircraft Propulsion and Power, 28 Propellants and Fuels, 44 Energy Production and Conversion,* and *15 Launch Vehicles and Space Vehicles.*

N91-26195*# Thiokol Corp., Brigham City, UT. Space Operations.
FOLLOW-ON CABLE COUPLING LIGHTNING TEST. VOLUME 2: APPENDIXES A, B, C, AND D Final Test Report
31 Oct. 1990 489 p
(Contract NAS8-30490)
(NASA-CR-184124; NAS 1.26.184124; DR-5-3; WBS-4B102-11-10; ECS-SS3900; TWR-60187) Avail: NTIS HC/MF A21 CSCL 21H

The following information from the follow-on cable coupling lightning test of the Space Shuttle Booster is presented: (1) resistance measurements (cover-to-cover and cover-to-floor plate); (2) resistance measurements (external bond strap-to-case); (3) resistance measurements (internal bond strap-to-case) and; (4) follow-on cable coupling lightning test data plots. The bulk of the document comprises the follow-on cable coupling lightning test data plots. K.S.

N91-26196*# Aerojet TechSystems Co., Sacramento, CA.
ALS LIQUID HYDROGEN TURBOPUMP: ADVANCED DEVELOPMENT PROGRAM Monthly Progress Report, 20 May - 23 Jun. 1989
Nancy R. Shimp and George J. Claffy 21 Jul. 1989 134 p
(Contract NAS8-37593)
(NASA-CR-183730; NAS 1.26:183730; KGC4-M-2) Avail: NTIS HC/MF A07 CSCL 21H

The point of departure (POD) turbopump concept was reviewed and finalized. The basis for the POD was the configuration presented in the Aerojet proposal. After reviewing this proposal concept, several modifications were made. These modifications include the following: (1) the dual pump discharge arrangement was changed to a single discharge; (2) commonality of the turbine inlet manifold with the advanced launch system (ALS) liquid oxygen (LOX) TPA was dropped for this program; (3) the turbine housing flange arrangement was improved by relocating it away from the first stage nozzles; (4) a ten percent margin (five percent diameter increase) was built into the impeller design to ensure meeting the required discharge pressure without the need for increasing speed; (5) a ten percent turbine power margin was imposed which is to be obtained by increasing turbine inlet pressure if required; and (6) the backup concept, as an alternative to the use of cast impellers, now incorporates forged/machined shrouded impellers, rather than the unshrouded type originally planned. Author

N91-26197# Morehouse Coll., Atlanta, GA.
LIQUID FILM COOLING IN ROCKET ENGINES Final Report, Jun. 1987 - Dec. 1989
William M. Grisson Mar. 1991 74 p
(Contract F49620-85-C-0013)
(AD-A234288; AEDC-TR-91-1) Avail: NTIS HC/MF A04 CSCL 21/8

A one-dimensional analytical model of liquid film cooling in rocket engine combustion chambers is developed and compared with existing data. The vapor generated at the liquid interface greatly decreases the convective heat flux and is treated as a 'transition' process. The radiant heat is absorbed at the walls and transmitted to the liquid film by boiling, which can lead to burnout of the film. Downstream of the liquid film, the vapor provides continued thermal protection to the wall and is treated as a gaseous film cooling process. A standard correlation is expressed in differential form to allow for the nonuniform free-stream flow in the nozzle. Liquid film lengths are well predicted by the model. Downstream of the dry-out point, wall temperatures are well predicted up to the start of convergence. Downstream of the converging turn, a correction term, correlated by a centrifugal parameter, is required to account for increased mixing at the converging turn. Downstream of the throat, wall temperatures decrease very quickly because of acceleration of the boundary-layer gases, an effect not included in the model. GRA

N91-26198# Rocket Research Corp., Redmond, WA.
ARCJET ENDURANCE TEST PROGRAM Final Report, Dec. 1988 - Sep. 1990
Joseph Cassady, Paul G. Lichon, and David Q. King Mar. 1991 67 p
(Contract F04611-89-C-0013)
(AD-A235232; AL-TR-90-069) Avail: NTIS HC/MF A04 CSCL 21/3

A program of testing was conducted to improve the performance of the ammonia arcjet thruster. Prior data was found to be in error by approximately 20 percent resulting in a baseline Isp value of 740 s. Several configurations were tested in an attempt to restore the Isp to greater than 800 s. Results showed beneficial effects on both Isp and efficiency due to reduced constrictor diameter and increased electrode gap. The goal was achieved, with one configuration reaching 819 s. GRA

N91-26199# Phillips Lab., Edwards AFB, CA.
ENGINE CYCLE ANALYSIS FOR A PARTICLE BED REACTOR NUCLEAR ROCKET Final Report, May - Jul. 1990
David E. Suzuki Mar. 1991 61 p
(AF Proj. 3058)
(AD-A235258; PL-TR-91-3002) Avail: NTIS HC/MF A04 CSCL 21/6

This report addresses three candidate engine cycles for a particle bed nuclear rocket; bleed cycle with uncooled carbon - carbon composite nozzle; bleed cycle with regeneratively cooled Aluminum nozzle; expander cycle with regeneratively cooled Aluminum nozzle. The analysis was performed using the SALT System Analysis Language Translator code with the following amendments; particle bed reactor was modeled as a simple heater; a regeneratively cooled nozzle model was added which includes the heating of the coolant due to hot exhaust gases and nuclear heating of nozzle. The conclusion of the analysis were the topping cycle should be pursued for Mars missions and the bleed cycle should be pursued for OTV (Orbital Transfer Vehicle) missions. This study indicates that a regeneratively cooled aluminum nozzle can be sufficiently cooled to allow its use with a PBR rocket engine. This result is based on nozzle heating due to hot exhaust gases at a maximum chamber temperature and nuclear heating effects. The highest temperatures occur at the nozzle throat, where a composite or alloy coating could protect the aluminum. Further investigation of nozzle cooling should include modeling the nozzle with more nodes, and including more accurate dimensions for the nozzle wall thicknesses and coolant flow passages. The study also indicates that an expander cycle with a cooled aluminum nozzle can operate with a high pressure PBR at realistic TPA efficiencies. GRA

N91-26200*# National Aeronautics and Space Administration. Lewis Research Center, Cleveland, OH.
METHOD OF INJECTING FLUID PROPELLANTS INTO A ROCKET COMBUSTION CHAMBER Patent Application
Steven J. Schneider, inventor (to NASA) 31 May 1991 9 p
(NASA-Case-LEW-14846-2; NAS 1.71:14846-2; US-Patent-Appl-SN-709907) Avail: NTIS HC/MF A02 CSCL 21H

A rocket injector is provided with multiple sets of manifolds for supplying propellants to injector elements. Sensors transmit the temperatures of the propellants to a suitable controller which is operably connected to valves between these manifolds and propellant storage tanks. Additional valves are opened to furnish propellants to more of the manifolds when cryogenic propellant temperatures are sensed. Only a portion of the valves are opened to furnish propellants to some of the manifolds when lower temperatures are sensed. NASA

N91-26201*# Alabama Univ., Huntsville.
PROPULSION STABILITY CODES FOR LIQUID PROPELLANT PROPULSION SYSTEMS DEVELOPED FOR USE ON A PC COMPUTER Final Technical Report, 12 Jul. 1990 - 11 Jul. 1991
George B. Doane, III and Wilbur C. Armstrong 11 Jul. 1991 239 p
(Contract NAS8-36955)
(NASA-CR-184983; NAS 1.26:184983) Avail: NTIS HC/MF A11 CSCL 21H

Research into component modeling and system synthesis leading to the analysis of the major types of propulsion system instabilities and the characterization of various components characteristics are presented. Last year, several programs designed to run on a PC were developed for Marshall Space Flight Center. These codes covered the low, intermediate, and high frequency modes of oscillation of a liquid rocket propulsion system. No graphics were built into these programs and only simple piping

layouts were supported. This year's effort was to add run time graphics to the low and intermediate frequency codes, allow new types of piping elements (accumulators, pumps, and split pipes) in the low frequency code, and develop a new code for the PC to generate Nyquist plots. Author

N91-26202*# National Aeronautics and Space Administration. Lewis Research Center, Cleveland, OH.
DEVELOPMENT AND TESTING OF A SOURCE SUBSYSTEM FOR THE SUPPORTING DEVELOPMENT PMAD DC TEST BED
Robert M. Button 1991 8 p Presented at the 26th Intersociety Energy Conversion Engineering Conference, Boston, MA, 4-9 Aug. 1991; sponsored by ANS, SAE, ACS, AIAA, ASME, IEE, and AIChe
(NASA-TM-104510; E-6378; NAS 1.15:104510) Avail: NTIS HC/MF A02 CSCL 10B

The supporting Development Power Management and Distribution (PMAD) DC Test Bed is described. Its benefits to the Space Station Freedom Electrical Power System design are discussed along with a short description of how the PMAD DC Test Bed was systematically integrated. The Source Subsystem of the PMAD DC Test Bed consisting of a Sequential Shunt Unit (SSU) and a Battery Charge/Discharge Unit (BCDU) is introduced. The SSU is described in detail and component level test data is presented. Next, the BCDU's operation and design is given along with component level test data. The Source Subsystem is then presented and early data given to demonstrate an effective subsystem design. Author

N91-26203*# Thiokol Corp., Brigham City, UT. Space Operations.
TECHNICAL EVALUATION MOTOR NO. 7 (TEM-7) Final Test Report
Phil Hughes Apr. 1991 154 p
(Contract NAS8-30490)
(NASA-CR-184163; NAS 1.26:184163; TWR-17659; Publ-911520) Avail: NTIS HC/MF A08 CSCL 21H

The Technical Evaluation Motor No. 7 (TEM-7) test was a full-scale, full duration static test firing of a high performance motor-configuration solid rocket motor with nozzle vectoring. The final test report documents the procedures, performance, and results of the static test firing of TEM-7. All observations, discussions, conclusions, and recommendations included in the report are complete and final except for the TEM-7 fixed housing unbond investigation. A presentation and discussion of TEM-7 performance, anomalies, and test result concurrence with the objectives outlined in CTP-0107, Rev A, Space Shuttle Technical Evaluation Motor No. 7 (TEM-7) Static Fire Test Plan are included. Author

N91-26204*# Virginia Polytechnic Inst. and State Univ., Blacksburg. Dept. of Electrical Engineering.
SPACE PLATFORM POWER SYSTEM HARDWARE TESTBED Final Report, Sep. 1990 - Apr. 1991
D. Sable, A. Patil, T. Sizemore, S. Deuty, J. Noon, B. H. Cho, and F. C. Lee 21 Jun. 1991 410 p
(Grant NAG5-1232)
(NASA-CR-185839; NAS 1.26:185839) Avail: NTIS HC/MF A18 CSCL 10B

The scope of the work on the NASA Space Platform includes the design of a multi-module, multi-phase boost regulator, and a voltage-fed, push-pull autotransformer converter for the battery discharger. A buck converter was designed for the charge regulator. Also included is the associated mode control electronics for the charger and discharger, as well as continued development of a comprehensive modeling and simulation tool for the system. The design of the multi-module boost converter is discussed for use as a battery discharger. An alternative battery discharger design is discussed using a voltage-fed, push-pull autotransformer converter. The design of the charge regulator is explained using a simple buck converter. The design of the mode controller and effects of locating the bus filter capacitor bank 20 feet away from the power ORU are discussed. A brief discussion of some alternative topologies for battery charging and discharging is included. The power system modeling is described. Author

N91-26205*# Aerojet-General Corp., Sacramento, CA. Propulsion Div.
DEVELOPMENT OF LIFE PREDICTION CAPABILITIES FOR LIQUID PROPELLANT ROCKET ENGINES. POST-FIRE DIAGNOSTIC SYSTEM FOR THE SSME SYSTEM ARCHITECTURE STUDY Final Report, May 1990 - Aug. 1990
Mark Gage and Ronald DeHoff (Systems Control Technology, Inc., Palo Alto, CA.) 31 Jul. 1991 89 p
(Contract NAS3-25883)
(NASA-CR-187112; NAS 1.26:187112) Avail: NTIS HC/MF A05 CSCL 21H

This system architecture task (1) analyzed the current process used to make an assessment of engine and component health after each test or flight firing of an SSME, (2) developed an approach and a specific set of objectives and requirements for automated diagnostics during post fire health assessment, and (3) listed and described the software applications required to implement this system. The diagnostic system described is a distributed system with a database management system to store diagnostic information and test data, a CAE package for visual data analysis and preparation of plots of hot-fire data, a set of procedural applications for routine anomaly detection, and an expert system for the advanced anomaly detection and evaluation. Author

23 CHEMISTRY AND MATERIALS (GENERAL)

N91-26206# York Univ. (Ontario). Dept. of Chemistry.
MOLECULAR ORIENTATION OF THE SILVER TETRA NEOPENTOXY PHTHALO CYANINE AND STEARIC ACID MIXED LANGMUIR-BLODGETT FILM AND ITS CHEMICAL AND ELECTROCHEMICAL BEHAVIOUR
Yansong Fu and A. B. Lever 4 Apr. 1991 33 p
(Contract N00014-84-G-0201)
(AD-A234601; TR-39) Avail: NTIS HC/MF A03 CSCL 09/1

Mixed Langmuir-Blodgett films comprised of various relative concentration of silver tetra neopentoxy phthalo cyanine (AgTNPc) and stearic acid are reported. Electronic spectroscopic polarization data are discussed in terms of the relative orientation of aggregated AgTNPc domains in the film. Electrochemical data confirm the oxidation of AgIITNPc(-2) successively to AgIIITNPc(-2)+ and AgIIITNPc(-1)2+ in the film phase without loss of orientation. The film was also subject to chemical oxidation and reduction and the degree of organization following such chemistry is discussed. AGIITNPc(-2) aggregates, even when diluted following such chemistry is discussed. AgIITNPc(-2) aggregates, even when diluted with stearic acid, do not display resolved ESR spectra but ternary film mixtures of AgIITNPc(-2)/H2TNPc(-2)/ stearic acid do exhibit such resolved spectra. GRA

N91-26207# Utah Univ., Salt Lake City. Dept. of Chemistry.
STRUCTURE OF ALKYLATED SILICA SURFACES: QUENCHING OF FLUORESCENCE FROM COVALENTLY BOUND PYRENE Technical Report, Jun. 1990 - May 1991
A. L. Wong, M. L. Hunnicutt, and J. M Harris 22 Apr. 1991 11 p
(Contract N00014-89-J-1412)
(AD-A234642; TR-25-ONR) Avail: NTIS HC/MF A03 CSCL 07/3

The influence of overlying solvent on the structure of alkylated silica surfaces is studied. In these experiments, 3-(1-PYRENYL)PROPYL dimethylchlorosilane (3PPS) was chemically bonded at low coverages to silica gel, which was further modified with monomeric C1, C8, and C18 ligands. Fluorescence lifetimes of 3PPS were measured to determine the differences in the interfacial polarity of these materials in methanol and

methanol/water solution. Rates of quenching by mercuric chloride were also measured to correlate differences in polarity with the exposure of the immobilized probe to solvent. For C1-modified and bare silica, the results indicate an interfacial environment that is dominated by exposure to solvent. On C18-modified silica, access by the surface-bound probe to the quencher is minimal, indicating that the long alkyl chains limit exposure of the underlying silica to the solvent. The most interesting behavior was exhibited by C8 ligands, which produce an interfacial environment where the probe has limited contact with the solvent in methanol but becomes much more exposed in 75/25 pct. methanol/water. This change in environment was attributed to the collapse of the alkyl ligands, driven by hydrophobic interactions that reduce their contact with the aqueous solution. GRA

N91-26208# Massachusetts Inst. of Tech., Cambridge. Dept. of Chemistry.
ISOTROPIC EXCHANGE IN THE PLATINUM-CATALYZED REDUCTION OF OLEFINS IN PROTIC SOLVENTS
T. R. Lee and George M. Whitesides 23 Apr. 1991 29 p
(AD-A234828; TR-6) Avail: NTIS HC/MF A03 CSCL 07/3

This paper reports the isotopic compositions of alkanes obtained by the catalytic reductions of olefins using Hydrogen or Deuterium and platinum black in alcoholic and mixed organic/aqueous solvents. The isotope found in the product alkanes was predominantly that present in the solvent (ROH or ROD) regardless of the isotope present in the gas (H2 or D2). The rate of exchange of isotopes of hydrogen between the protic solvent and the surface of the catalyst was fast relative to the rate of production of alkanes; consequently, the content of excess deuterium in the alkanes provided a measure of the rate of activation of the C-H bonds of the intermediate surface alkyls relative to the rate of their reductive elimination as alkanes. In deuterated alcohols (ROD), under conditions in which the rates of reduction were limited by mass transport of H2 or D2 to the catalyst surface (the mass-transport limited regime, MTL: T = 40 C, PH(2) = 0.17 atm), the alkanes contained deuterium atoms in excess of that required for stoichiometric reduction of the double bond; for example, the average isotopic content of cyclooctane from reduction of cis-cyclooctene in ethyl alcohol-d was C8H4D12. GRA

24 COMPOSITE MATERIALS

Includes physical, chemical, and mechanical properties of laminates and other composite materials.
For ceramic materials see *27 Nonmetallic Materials*.

N91-26209 Cincinnati Univ., OH.
THERMOELASTIC WAVE PROPAGATION IN LAMINATED COMPOSITES Ph.D. Thesis
Muhammad A. Hawwa 1990 125 p
Avail: Univ. Microfilms Order No. DA9108617

The propagation of generalized thermoelastic waves in laminated composites is studied. The study starts with the development of a continuum mixture theory for a bilaminated isotropic waveguide. The approximate analytical results are found to be useful in getting a qualitative picture of the response. Next, a direct approach is used in order to check the validity of the theory against the exact solution. The work is then extended to consider multilayered media. The transfer matrix method is used to study obliquely travelling waves. Different modes are influenced by the thermoelastic coupling. However, for the case of normal incidence, it is shown that the transverse motion remains purely elastic. Further generalization is made by allowing the laminates of the multilayered media to be monoclinic. The exact solution obtained by the transfer matrix method can be used for higher symmetry materials such as orthotropic, transversely isotropic, and cubic by specializing the constitutive constants for these cases. For the situations when waves propagate in the direction of the axes of symmetry, the SH mode remains purely elastic. Numerical illustrations are given in the form of dispersion, and attenuation or damping. Dissert. Abstr.

N91-26210# Gordon Research Conferences, Inc., Kingston, RI.
GORDON RESEARCH CONFERENCE ON COMPOSITES Final Report, 1 Dec. 1990 - 30 Nov. 1991
Alan N. Gent 5 Feb. 1991 19 p Conference held in Ventura, CA, 14-18 Jan. 1991
(Contract DAAL03-01-G-0006; DA Proj. 1L1-61102-BH-57)
(AD-A233778; ARO-28321.1-MS-CF) Avail: NTIS HC/MF A03 CSCL 11/4

The conference consisted of a diverse series of lectures covering the synthesis and properties of new high-performance resins, properties of the interphase that develops between a resin and a fibrous or particulate inclusion, and mechanisms of failure of composite materials, particularly failures associated with cavitation or void formation in the resin that later develop into cracks. GRA

N91-26211# Air Force Occupational and Environmental Health Lab., Brooks AFB, TX.
COMPOSITE FIBER HAZARDS Final Report
John F. Seibert Dec. 1990 21 p
(AD-A233924; AFOEHL-EI00178MGA) Avail: NTIS HC/MF A03 CSCL 11/4

This report reviews potential health hazards from carbon/graphite and boron composite materials used in aircraft. Carbon and boron fibers are used as reinforcement in an epoxy matrix to form composite material aircraft parts. There is increasing concern over the potential health effects of these fibers released during sanding and grinding of composite parts in structural repair shops, and during clean up operations following aircraft accidents involving fire and/or breakage of composite parts. With the demise of the term CORKER, hazards from carbon composite materials were deemphasized. However, the CORKER annotation only addressed the electrical shorting hazards from airborne fibers following a fire and did not examine in detail potential health effects. Maintenance workers fear that carbon fibers are carcinogens. A review of the current literature on carbon fiber indicates it is relatively inert. Industrial hygiene evaluations should include sampling for total dust and comparing the levels to the ACGIH TLV for nuisance dust. Occupational health efforts should focus on problems with contact dermatitis from the resins systems and toxic effects of resin hardeners. GRA

N91-26212# Illinois Univ., Urbana-Champaign. National Center for Composite Materials Research.
EFFECT OF A VISCOELASTIC INTERFACE ON THE TRANSVERSE BEHAVIOR OF FIBER-REINFORCED COMPOSITES
M. Gosz, B. Moran, and J. D. Achenbach Apr. 1990 25 p
(AD-A233986; UIUC-NCCMR-90-07) Avail: NTIS HC/MF A03 CSCL 11/4

In this paper we investigate the effect of an inelastic interface layer on the mechanical behavior of a transversely loaded fiber-reinforced composite. A simple linearly viscoelastic model is used to characterize the stiffness and viscosity of the interface separating the fiber and matrix phases. The mechanical response is obtained using the finite element method and calculations are carried out for a unit cell in a periodic array of hexagonally packed fibers. An approximate representation of the time dependent macroscopic behavior of the micromechanical perspective, the influence of interfacial stress relaxation on the stress fields in the matric material contiguous to the interface is examined. GRA

N91-26213# Thermo-Systems, Inc., Saint Louis, MO.
TESTING OF A COMPOSITE THERMAL STRUCTURE TO INSULATE THE DRIVERS OF A LARGE SCALE BLAST/THERMAL SIMULATOR Final Report, Sep. 1986 - Jun. 1988
L. F. McCue Mar. 1991 92 p
(Contract DAAA15-86-C-0098; DA Proj. 1L1-62120-AH-25)

(AD-A234014; TSI-8152-BRL; BRL-CR-658) Avail: NTIS HC/MF A05 CSCL 11/4

This report describes the developmental testing of the thermal and mechanical properties of two versions of a composite structure which were developed for insulating the walls of high-pressure vessels containing hot nitrogen gas against heat loss and the results of these tests are presented. Included herein are data on thermal diffusivity, specific heat, density, expansion coefficients, thermal conductivity and mechanical properties, as well as energy transfer and temperature profiles for each of the composite systems. A subscale driver tube assembly modeling a driver tube of a Large Blast/Thermal Simulator and consisting of a nitrogen supply system, a gas heater, and the heat-insulated driver tube complete with instrumentation was designed and constructed. A future testing program under actual operating conditions is recommended. GRA

N91-26214# Illinois Univ., Urbana-Champaign. National Center for Composite Materials Research.

DEVELOPMENT OF A TEST SYSTEM AND EXPERIMENTAL METHOD FOR IN-PLANE BIAXIAL COMPRESSIVE DEFORMATION AND FAILURE OF FIBER COMPOSITE MATERIALS

S. H. Doong, J. E. Faoro, D. F. Socie, and S. S. Wang Apr. 1990 26 p

(AD-A234062; UIUC-NCCMR-90-06) Avail: NTIS HC/MF A03 CSCL 11/4

This paper presents the development of a test system and associated experimental procedure for evaluating in-plane biaxial compressive deformation and failure of fiber composite laminates. A description of the test system and the design of fixtures and specimen are given. Critical buckling stress of the specimen is determined analytically and compared to the experimentally obtained compressive strength. The capability of this testing system and accuracy of the experimental results are discussed and evaluated. A series of tests have been on E-glass/epoxy composite laminates with different lamination variables and stress biaxiality ratios. Compressive failure strengths of composite materials are determined in various in-plane biaxial loading conditions. GRA

N91-26215# Illinois Univ., Urbana-Champaign. National Center for Composite Materials Research.

A MODEL FOR WET FILAMENT WINDING OF COMPOSITE CYLINDERS WITH ARBITRARY THICKNESS

A. Agah-Tehrani and Hong Teng Jan. 1991 36 p

(AD-A234102; UIUC-NCCMR-91-02) Avail: NTIS HC/MF A03 CSCL 11/4

A continuum consolidation is purposed for analyzing the filament winding of thermoset composite cylinders with arbitrary thickness. The model takes account of the variation of both the instantaneous stiffness and the permeability of the mixture with fiber compaction. Due to resin filtration, the structure of the resulting initial-boundary value problem is similar to that of a moving boundary problem. Based on this analogy, a finite difference scheme is devised for the solution of the problem. For the case of winding onto a rigid mandrel, the results point to the existence of an active and a passive zone of consolidation. The results further indicate the possibility that during hoop winding of relatively thick cylinders, the tension can be completely lost in the portion of the passive zone away from the mandrel. GRA

N91-26216# Illinois Univ., Urbana-Champaign. National Center for Composite Materials Research.

INTERFACIAL SLIPPAGE OF A UNIDIRECTIONAL FIBER COMPOSITE UNDER LONGITUDINAL SHEARING

Hong Teng and A. Agah-Tehrani Jan. 1991 23 p

(AD-A234186; UIUC-NCCMR-91-01) Avail: NTIS HC/MF A03 CSCL 11/4

Interfacial slippage of a unidirectional fiber composite under longitudinal shearing is analyzed. The finite concentration of fibers has been taken into account by utilizing the composite cylinder model in the formulation of the problem. The resulting mixed boundary value problem leads to a system of dual series equations, which are then reduced to a Fredholm integral equation of the first kind with a logarithmic singularity. The extent of slip region, which depends on the level of loading, along with the distribution of shear tractions at the fiber-matrix interface is determined by solving the integral equation numerically. GRA

N91-26217# Illinois Univ., Urbana-Champaign. National Center for Composite Materials Research.

STATIC AND CYCLIC COMPRESSIVE FATIGUE OF THERMOPLASTIC-MATRIX COMPOSITE IN AMBIENT AND MOISTURE ENVIRONMENTS

Kiet VanChau Aug. 1990 56 p

(AD-A234187; UIUC-NCCMR-90-09) Avail: NTIS HC/MF A04 CSCL 11/9

Advanced fiber-reinforced thermoplastic-matrix composites are being considered for many advanced engineering applications. Among various issues involved in these applications, deformation and failure behavior of the composites under static and cyclic compressive loading in ambient and moisture environments are significant concern. In this study, a graphite-fiber/polyamide thermoplastic (AS4/J1) composite system is considered. Monotonic and cyclic fatigue compressive loadings are applied to the composite in ambient and moisture environments. The objectives of this research are to study: (1) compressive fatigue strength and failure modes; (2) compressive fatigue damage process and associated property degradation; (3) effect of water absorption on compressive fatigue failure behavior; and (4) effect of lamination parameters on compressive fatigue properties. GRA

N91-26218# Illinois Univ., Urbana-Champaign. National Center for Composite Materials Research.

NONLINEAR BEHAVIOR OF FIBER COMPOSITE MATERIALS AND ITS EFFECT ON THE POSTBUCKLING RESPONSE OF LAMINATED PLATES

Rami HajAli and Su S. Wang Dec. 1990 74 p

(AD-A234203; UIUC-NCCMR-90-10) Avail: NTIS HC/MF A04 CSCL 11/4

The nonlinear stress-strain behavior of unidirectional fiber composite material was examined. Two approaches were adopted. The first approach considers the stress-strain as nonlinear elastic relations, which are derived at through the use of a complementary energy density function, and takes into account the material symmetry. The second approach adopts the Ramberg-Osgood representation of one-dimensional stress-strain curves. By utilizing the deformation theory to express the nonlinear parts of the strain, a nonlinear stress-strain behavior was obtained. An incremental formulation of these theories was implemented in a finite element analysis. These approaches were examined in the context of postbuckling analysis of thick-section laminated plates. GRA

N91-26219# Pittsburgh Univ., PA. Dept. of Physics and Astronomy.

FAR- AND MID-INFRARED PROPERTIES OF METAL-INSULATOR COMPOSITE MATERIALS Final Technical Report, 1 Sep. 1985 - 31 Dec. 1990

Robert P. Devaty 28 Mar. 1991 24 p

(Contract N00014-85-K-0808)

(AD-A234264) Avail: NTIS HC/MF A03 CSCL 11/4

The goal of this research program was to investigate the infrared properties of metal-insulator granular composite materials in order to better understand the relationships between the observed electromagnetic properties, particularly the absorption, and the underlying physical mechanisms. There are several contributions to the observed infrared behavior of a composite material. First is the optical behavior of the individual metallic and insulating grains that make up the material. An important issue is the dependence of these properties on particle size due to boundary effects, quantum size effects, etc. The shapes of the particles is also important. Second is the effect of composition. The electromagnetic properties of a metal and an insulator differ greatly. The infrared properties of the composite material will clearly depend on the volume fraction of metal. The percolation threshold, which specifies

the composition for the onset of electrical conduction for a conductor mixed with an insulating host, is a fundamental parameter that characterizes the composition dependence. GRA

N91-26220# Massachusetts Inst. of Tech., Cambridge. Dept. of Materials Science and Engineering.
CORROSION OF GRAPHITE ALUMINUM METAL MATRIX COMPOSITES Technical Report, 1 Mar. - 31 Dec. 1990
M. A. Buonanno, R. M. Latanision, L. H. Hihara, and J. F. Chiang Feb. 1991 21 p
(Contract N00014-89-J-1588)
(AD-A234322; TR-3) Avail: NTIS HC/MF A03 CSCL 11/4

Several commercial G/Al metal matrix composites (MMC) have been studied by potentiodynamic polarization in deaerated 0.5 M Na2SO4. The results have been compared with those which were predicted by the mixed electrode theory. The results indicate that processing conditions, especially the cooling rate, had a strong influence on the corrosion behavior of the G/Al MMCs. Large scale G/Al model MMCs were fabricated at MIT in order to study the corrosion behavior of G/Al galvanic couples with the scanning potential microprobe (SPM). Preliminary results indicate that coating graphite with discontinuous alumina did not reduce the corrosion rate of the G/Al galvanic couple. Ion implanting the surface of G/Al model MMCs with zinc, a cathodic inhibitor, did reduce the corrosion G/Al galvanic couple; however, the protection was incomplete. GRA

N91-26221# California Univ., Santa Barbara. Dept. of Materials.
EFFECT OF SURFACE FORCES ON THE RHEOLOGY OF PARTICLE-LIQUID SYSTEMS AND THE CONSOLIDATION OF CERAMIC POWDERS Annual Report Nos. 1-3, 1 Feb. 1990 - 31 Jan. 1991
Fred F. Lange and Dale S. Pearson Feb. 1991 58 p
(Contract N00014-90-J-1441)
(AD-A234375) Avail: NTIS HC/MF A04 CSCL 11/4

More reliable ceramics require improved processing reliability. Heterogeneities bought with powders and those inadvertently introduced during processing as well as non-uniform and undefined phase distributions contribute to unreliable processing. Colloidal powder treatments can eliminate many heterogeneities and ensure more uniform phase distributions. To ensure that new heterogeneities are not introduced, colloidally treated powders must be piped, as slurries, directly to a die cavity. Slurry consolidation methods based on particle partitioning, e.g., pressure filtration and centrifugation are emphasized. Interparticle potentials play a dominant role in governing the slurry viscosity, maximum particle packing density and the rheology of the consolidated body. These roles are reviewed with the objective to understand how damage free bodies can be consolidated from slurries to increase the structural reliability of ceramics and their composites. GRA

N91-26222# Naval Air Development Center, Warminster, PA. Air Vehicle and Crew Systems Technology Dept.
AN ANISOTROPIC LAMINATED DAMPED PLATE THEORY Progress Report, Apr. 1989 - Apr. 1990
David J. Barrett 30 Jul. 1990 56 p
(AD-A234446; NADC-90066-60) Avail: NTIS HC/MF A04 CSCL 11/4

This report describes the formulation of a structural theory for the analysis of laminated anisotropic damped plates. The plates consist of laminated face sheets sandwiching a single damping layer. The displacement degrees of freedom used to construct the analytical model are a generalization of those found in constrained layer theory. Variational principles are used to form the equations of motion which are solved for the steady state response of simply supported semi-infinite plates. The analysis is used to examine the effect of stress coupling and compliant layering on improving the dynamic resistance of damped structures loaded in flexure. GRA

N91-26223# Lawrence Livermore National Lab., CA.
ON THE FINITE-STRAIN-INVARIANT FAILURE CRITERION FOR COMPOSITES Final Report, Feb. 1987 - Sep. 1989
William W. Feng and Scott E. Groves Mar. 1991 18 p
(Contract W-7405-eng-48; DA Proj. 1L1-62618-AH-80)
(AD-A234493; BRL-CR-655) Avail: NTIS HC/MF A03 CSCL 11/4

The finite-strain-invariant failure criterion, developed by Feng (to be published), was evaluated with the experimental data for a boron/epoxy, symmetrically balanced, angle-ply laminate. The results indicate that the failure-criterion prediction agrees with the experimental data and that the failure criterion also predicts the matrix or fiber-dominated modes of failure. Two special isotropic cases in infinitesimal strain theory are obtained. The failure criteria for these special cases preserve the mathematical forms of both the generalized Von Mises yield criterion and the Von Mises yield criterion in plasticity. GRA

N91-26224# Department of the Navy, Washington, DC.
INDIA-STABILIZED ZIRCONIA COATING FOR COMPOSITES Patent Application
Robert L. Jones, inventor (to Navy) 26 Sep. 1990 19 p
(AD-D014857; US-Patent-Appl-SN-589230) Avail: NTIS HC/MF A03 CSCL 11/3

The present invention relates to a thermally and chemically protective coating of india stabilized zirconia and a method for making the coating. As demands on fuel resources increase and as manufacturing techniques become more complex, industrial equipment is exposed to fuels and materials which contain corrosive contaminants. These corrosive contaminants can cause extensive damage to the surface and structure of industrial equipment, particularly to all types of motors, turbines, engines, furnaces, stacks, fluidized beds and the like. In addition, it is often necessary to protect industrial parts from damage and fatigue caused by operation at high temperatures. Ceramic coatings have been used to protect exposed surfaces from heat deterioration and corrosion. GRA

N91-26225# Grace (W. R.) and Co., Columbia, MD.
REACTION PROCESSING OF CERAMIC PARTICULATE AND WHISKER COMPOSITES
Carig P. Cameron and Roy W. Rice 1991 7 p
(Contract N00014-87-C-0515)
(AD-A234951) Avail: NTIS HC/MF A02 CSCL 11/2

Advanced ceramic materials such as, non-oxides and ceramic composites have attracted substantial attention because of the promising properties they offer. However, application of these materials has been severely limited by their cost. An important example of this cost constraint is the limited use of non-oxides ceramics, or non-oxide containing ceramic composites in armor applications. In many cases, the cost of the raw materials alone equals or exceeds the target price $10 to $20 per pound for finished armor tile. A class of reaction processed composites (e.g., of an oxide with one or more non-oxide phases) has been identified that offer promising performance potential but with raw material costs 1/3 to 1/10 of those for the analogous conventionally processed composites. It was also recognized that such reaction processing presented opportunities for both process and resultant property control. GRA

N91-26226# Pratt and Whitney Aircraft, West Palm Beach, FL.
FIBER COATING BY SPUTTERING FOR HIGH TEMPERATURE COMPOSITES Annual Report, 15 May 1989 - 14 Nov. 1990
M. L. Emiliani 10 Dec. 1990 44 p
(Contract F49620-89-C-0066)
(AD-A234994; PWA-FR-21539) Avail: NTIS HC/MF A03 CSCL 11/3

The purpose of this research, in collaboration with the University of California at Santa Barbara, is to identify fiber coatings that promote interfacial debonding in intermetallic and ceramic matrix composites. Numerous coatings have been deposited in support of allied research programs at UCSB. The present study examines the cause of improved fracture toughness in Y2O3 coated

Nb-toughened TiAl. Sputtered Y2O3 coatings were characterized. It is postulated that yttrium oxide coatings applied to niobium have an atomically sharp interface which has a lower fracture energy compared to Nb/Al2O3, resulting in improved debonding and fracture toughness. The results were related to indentation-derived fracture toughness data, as well as factors that may affect debonding of thin coatings. Reactive and non-reactive metal-ceramic systems are reviewed in an effort to understand why Y2O3 coatings perform well. GRA

N91-26227# Washington Univ., Seattle. Dept. of Mechanical Engineering.
DAMAGE ACCUMULATION IN ADVANCED METAL MATRIX COMPOSITES UNDER THERMAL CYCLING Final Report, 1 Oct. 1987 - 15 Oct. 1990
Minoru Taya, Mamidala Ramulu, William Armstrong, and Marty Dunn 25 Feb. 1991 196 p
(Grant AF-AFOSR-0059-89; AF Proj. 2302)
(AD-A235002; UW-ME-91-001; AFOSR-91-0261TR) Avail: NTIS HC/MF A09 CSCL 11/4

This research investigates the response to thermal cycling of a set of W-1 percent THO2 reinforced Fe-25CR-8A1-50Y superalloy matrix composites. During this research, unique composite materials were produced by powder metallurgical processing. These materials were three aligned composites of differing reinforcement aspect ratio, and a hierarchic composite which included fine diameter Al2O3 fibers. After hot isostatic pressing processing, specimen blanks were cut from the HIP billets by abrasive water jets after which specimens were turned using a conventional engine lathe. The specimens were then thermal sprayed with an oxidation resistant FeCrAlY coating identical to the matrix material. The specimens were then thermal cycled between 1100 C and 352 C and between 1100 C and 534 C for 100,500, or 750 cycles on a specially built thermal cycling machine. The dimensional change of each specimen was measured. It was found that the initial longitudinal growth per thermal cycle was small. After many thermal cycles however the longitudinal growth per thermal cycle became much larger. A severe growth of fiber-matrix interfacial damage was documented with scanning electron microscopy. The growth of two interfacial reaction phases was determined with a KEVEX dispersive x-ray analysis. The mechanical properties of the interfacial material were investigated with a Vickers microhardness test. Finally, the basic mechanical response of the material was investigated with room temperature tensile tests. GRA

N91-26228# Hughes Aircraft Co., El Segundo, CA. Electro-Optical and Data Systems Group.
INVESTIGATION OF POLYBENZOCYCLOBUTENE RESINS IN MULTILAYER THIN FILMS FOR ELECTRONIC PACKAGING Final Report, Jan. 1989 - Sep. 1990
S. O. Fong and J. W. Peters Feb. 1991 57 p
(Contract F33615-88-C-5509)
(AD-A235223; WRDC-TR-90-4135) Avail: NTIS HC/MF A04 CSCL 11/4

Polybenzocyclobutene dielectric films were found to exhibit significant advantages compared to polyimides for multichip multilayer packaging applications. Although PBCB films must be cured in an oxygen-free environment and are somewhat more sensitive to warpage/stress than polyimides, they are significantly superior with respect to moisture resistance, lower dielectric constant and leveling or planarization over rough surface topography. The adhesion of PBCB films to copper, aluminum and silicon without adhesion promoters is excellent. Tests to date with PBCB as a multilevel dielectric with both a counter/decoder circuit and an analog circuit, in conjunction with via post interconnects, reveal the potential for the reliable fabrication of high speed and high density multichip/multilayer modules. GRA

N91-26229# Washington Univ., Seattle. Dept. of Mechanical Engineering.
DYNAMIC FRACTURE RESPONSES OF Al2O3, Si3N4, AND SiC(w)/Al2O3 Technical Report, Aug. 1989 - Mar. 1991
Y. Takagi and A. S. Kobayashi 4 Apr. 1991 15 p
(Contract N00014-87-K-0326)
(AD-A235286; UWA/DME/TR-91/5) Avail: NTIS HC/MF A03 CSCL 11/2

A hybrid experimental-numerical procedure was used to characterize the dynamic fracture responses of alumina (Al2O3), silicon nitrides, (Si3N4) and silicon-carbide whisker/alumina matrix (SiC sub W/Al2O3) composite. A laser interferometric displacement gage was used to determine through the crack opening displacement (COD), the instantaneous crack tip location during rapid fracture at room temperature and 1000 C. Consistent with previous finding, the dynamic crack arrest stress intensity factor did not exist in the ceramics and ceramic matrix composite studied. GRA

N91-26230# North Carolina State Univ., Raleigh.
COMPOSITE DATABASE INTERFACE USERS MANUAL Final Report, Jun. 1989 - Sep. 1990
Lisa K. Spainhour and William J. Rasdorf Apr. 1991 142 p
(DA Proj. 1L1-62618-AH-80)
(AD-A235327; BRL-CR-663) Avail: NTIS HC/MF A07 CSCL 12/7

The information presented in this document provides a description of the composites database interface (CDI) program and its use and functionality. Section 1 explains the purpose of the composites database and the interface programs. Section 2 describes the language in which the system programs are written. Section 3 provides a system description, including an enumeration of the required hardware and software. Section 4 describes the computer start-up procedure which enables the user to operate the CDI system. Section 5 provides an overall description of the CDI system and how it is run. Section 6 demonstrates the use of the CDI system with a complete example. Section 7 lists and describes the schema of the composites database. The Appendices contain useful reference information for the CDI program, including sample reports and copies of all data entry forms, help screens and input/output files associated with the database and program. Complete program listings and a listing of the database schema are also provided. GRA

N91-26231# Army Lab. Command, Watertown, MA. Material Technology Lab.
EVALUATION OF ENVIRONMENTALLY AGED POLYMER/COMPOSITE MATERIAL BY ULTRASONIC INSPECTION Final Report
Robert F. Anastasi Mar. 1991 26 p
(AD-A235343; MTL-TR-91-10) Avail: NTIS HC/MF A03 CSCL 11/4

Ultrasonic nondestructive evaluation (NDE) techniques are being explored for application in monitoring the deterioration of glass fiber reinforced polymer matrix composite materials. Conventional ultrasonic equipment and testing arrangements were used that consisted of transducer, materials sample, and coupling medium (gel for contact and water for immersion methods). The sound generated by the transducer propagates through the coupling, into the sample, and is reflected from acoustic interfaces (flaws, material discontinuities, and sample surfaces). These reflections are either received by another transducer using a through transmission technique or by the sending transducer using a pulse echo technique. A typical A-scan signal (time versus voltage display) consists of an initial pulse (main bang), a front surface echo (in water immersion method), and a series of back surface echoes of decreasing amplitude. GRA

N91-26232 Tel-Aviv Univ. (Israel). Dept. of Solid Mechanics Materials and Structures.
BUCKLING OF LAMINATED COMPOSITE PLATES M.S. Thesis
Rivka Gilat-Cygeilman Dec. 1988 118 p
(ITN-91-85101) Copyright Avail: Tel-Aviv Univ., Exact Sciences Library, Ramat Aviv 69978, Israel

The Ritz method was used to obtain approximate solutions to the buckling problem of rectangular general laminated composite plates having various boundary conditions and subjected to various load conditions. The developed computer program was shown to

be reliable by comparing numerical results obtained using this program with solutions presented by others. The effects of a limited number of parameters on the buckling behavior were studied for certain orthotropic, anisotropic, symmetric and asymmetric laminated plates. Present results show that for certain cases, the buckling load of an asymmetric plate exceeds that of a symmetric plate, both built of the same number of layers having the same elastic and geometric properties. For asymmetric laminated plates, owing to the stretching-bending coupling, lateral deflection begins simultaneously with the application of compressive loads. The influence of this effect is not included in the present results since this work has been limited to the linear buckling problem of laminated plates. A nonlinear analysis must be used in order to get a more complete picture. Owing to the limitations of the classical thin laminated plate theory, the effect of transverse shear deformations has not been taken into account. This work deals with the buckling of thin elastic plates of high width-to-thickness ratio. For such plates, the classical theory is valid. Refined plate theories have to be employed to study the buckling of thick laminated plates, or composite laminated plates whose materials exhibit high E(sub i1)/G(sub i3), in which i = 1 or 2.

Author (ISA)

N91-26233*# National Aeronautics and Space Administration. Lewis Research Center, Cleveland, OH.

INVESTIGATION OF INTERFACIAL SHEAR STRENGTH IN SiC/Si3N4 COMPOSITES

J. I. Eldridge, R. T. Bhatt (Army Aviation Systems Command, Cleveland, OH.), and J. D. Kiser 1991 20 p Presented at the 15th Annual Conference on Composites and Advanced Ceramics, Cocoa Beach, FL, 13-16 Jan. 1991; sponsored by the American Ceramic Society

(DA Proj. 1L1-61102-AH-45)

(NASA-TM-103739; E-5979; NAS 1.15:103739; AVSCOM-TR-91-C-006) Avail: NTIS HC/MF A03 CSCL 11D

A fiber push-out technique was used to determine fiber/matrix interfacial shear strength (ISS) for silicon carbide fiber reinforced reaction-bonded silicon nitride (SiC/RBSN) composites in the as-fabricated condition and after consolidation by hot isostatic pressing (HIPing). In situ video microscopy and acoustic emission detection greatly aided the interpretation of push-out load/displacement curves. Author

N91-26234*# National Aeronautics and Space Administration. Lewis Research Center, Cleveland, OH.

POLYMERIC ROUTES TO SILICON CARBIDE AND SILICON OXYCARBIDE CMC

Frances I. Hurwitz, Paul J. Heimann, John Z. Gyekenyesi, John Masnovi, and Xin Ya Bu (Cleveland State Univ., OH.) 1991 13 p Presented at the 15th Annual Conference on Composites and Advanced Ceramics, Cocoa Beach, FL, 13-16 Jan. 1991; sponsored by the American Ceramic Society

(Contract NCC3-63; NAG3-749)

(NASA-TM-104372; E-6054; NAS 1.15:104372) Avail: NTIS HC/MF A03 CSCL 11D

An overview of two approaches to the formation of ceramic composite matrices from polymeric precursors is presented. Copolymerization of alkyl- and alkenylsilanes (RSiH3) represents a new precursor system for the production of Beta-SiC on pyrolysis, with copolymer composition controlling polymer structure, char yield, and ceramic stoichiometry and morphology. Polysilsesquioxanes which are synthesized readily and can be handled in air serve as precursors to Si-C-O ceramics. Copolymers of phenyl and methyl silsesquioxanes display rheological properties favorable for composite fabrication; these can be tailored by control of pH, water/methoxy ratio and copolymer composition. Composites obtained from these utilize a carbon coated, eight harness satin weave Nicalon cloth reinforcement. The material exhibits nonlinear stress-strain behavior in tension. Author

N91-26235# Southwest Research Inst., San Antonio, TX.

CHARACTERIZATION OF MECHANICAL DAMAGE MECHANISMS IN CERAMIC COMPOSITE MATERIALS

Technical Report, Sep. 1988 - Sep. 1989

James Lankford, Jr. and Cheryl R. Blanchard Sep. 1989 36 p (Contract N00014-84-C-0123; SwRI Proj. 8124)

(NR-032-553; SwRI-06-8124) Avail: NTIS HC/MF A03 CSCL 11D

The principal object of the program was to establish the loading rate dependence of compressive deformation and fracture micromechanisms in particulate and fiber reinforced ceramic matrix composites. Work during the last year has emphasized two types of composite in particular, i.e., SiC fiber reinforced pyroceram and SiC whisker-reinforced Si3N4. For individual titles, see N91-26236 through N91-26237.

N91-26236# Southwest Research Inst., San Antonio, TX. Dept. of Materials and Mechanics.

RESPONSE OF WHISKER-REINFORCED CERAMIC MATRIX COMPOSITES TO DYNAMIC COMPRESSIVE LOADING

James Lankford, Jr. and Cheryl R. Blanchard *In its* Characterization of Mechanical Damage Mechanisms in Ceramic Composite Materials Sep. 1989 p 1-16 Submitted for publication (For primary document see N91-26235 18-24)

Avail: NTIS HC/MF A03

The compressive strength of SiC whisker reinforced hot-pressed nitride was characterized over a wide range in strain rate. It was found that the strength of the matrix alone is extremely strain rate sensitive under impact loading, and that this sensitivity is retained in the reinforced condition, irrespective of whisker orientation. Superimposed on this effect is a peculiar strength decrease for slightly lower strain rates; it is suggested that the origin of this decrease lies in grain boundary residual tensile stresses. Author

N91-26237# Southwest Research Inst., San Antonio, TX. Dept. of Materials and Mechanics.

FRAGMENTATION OF BRITTLE MATERIALS AT HIGH RATES OF LOADING

James Lankford, Jr. and Cheryl R. Blanchard *In its* Characterization of Mechanical Damage Mechanisms in Ceramic Composite Materials Sep. 1989 p 17-33 Submitted for publication (For primary document see N91-26235 18-24)

Avail: NTIS HC/MF A03

Experiments involving the fragmentation of SiC during both quasistatic and high rate compressive loading are described. Measured fragment size distributions are considered in terms of current ideas regarding high strain rate damage and microfracture. It is concluded that both crack dynamics and crack nucleation via plastic flow mechanisms may be important elements in the failure process. Author

N91-26238*# Virginia Polytechnic Inst. and State Univ., Blacksburg. Dept. of Engineering Science and Mechanics.

DEVELOPMENT AND VERIFICATION OF GLOBAL/LOCAL ANALYSIS TECHNIQUES FOR LAMINATED COMPOSITES

Interim Report, 1 Jan. - 31 Dec. 1990

Danniella Muheim Thompson and O. Hayden Griffin, Jr. Jun. 1991 222 p

(Grant NAG1-675)

(NASA-CR-185060; NAS 1.26:185060; VPI-E-91-12) Avail: NTIS HC/MF A10 CSCL 11D

A two-dimensional to three-dimensional global/local finite element approach was developed, verified, and applied to a laminated composite plate of finite width and length containing a central circular hole. The resulting stress fields for axial compression loads were examined for several symmetric stacking sequences and hole sizes. Verification was based on comparison of the displacements and the stress fields with those accepted trends from previous free edge investigations and a complete three-dimensional finite element solution of the plate. The laminates in the compression study included symmetric cross-ply, angle-ply and quasi-isotropic stacking sequences. The entire plate was

selected as the global model and analyzed with two-dimensional finite elements. Displacements along a region identified as the global/local interface were applied in a kinematically consistent fashion to independent three-dimensional local models. Local areas of interest in the plate included a portion of the straight free edge near the hole, and the immediate area around the hole. Interlaminar stress results obtained from the global/local analyses compares well with previously reported trends, and some new conclusions about interlaminar stress fields in plates with different laminate orientations and hole sizes are presented for compressive loading. The effectiveness of the global/local procedure in reducing the computational effort required to solve these problems is clearly demonstrated through examination of the computer time required to formulate and solve the linear, static system of equations which result for the global and local analyses to those required for a complete three-dimensional formulation for a cross-ply laminate. Specific processors used during the analyses are described in general terms. The application of this global/local technique is not limited software system, and was developed and described in as general a manner as possible. Author

N91-26239# Northwestern Univ., Evanston, IL. Dept. of Physics and Astronomy.
ENERGETICS, BONDING MECHANISM AND ELECTRONIC STRUCTURE OF METAL/CERAMIC INTERFACES
Arthur J. Freeman Mar. 1991 18 p
(Contract DE-FG02-88ER-45372)
(DE91-009787; DOE/ER-45372/2) Avail: NTIS HC/MF A03

Insight is provided into the energetics and nature of bonding, the bonding mechanism, and structure of the interface for metal and ceramic materials. Results are reported for: (1) the metal (Ag, Fe and Co)/MgO interface; (2) the metal Pd/Al2O3 interface - including a first study of the noble metal oxides, PdO, AgO and PtO; and (3) ferroelectric ceramic materials. The precise full potential linearized augmented plane wave method was used to study the structural properties and electronic structure of bulk MgO, the clean MgO(001) surface, a free standing Ag monolayer, and an Ag monolayer adsorbed on the Mg(001) surface with Ag atoms located either above the O, the Mg or the hollow site. Plans for future research are mentioned. DOE

N91-26240# Oak Ridge National Lab., TN.
INVESTIGATION INTO THE EFFECT OF HEAT TREATMENT ON THE THERMAL CONDUCTIVITY OF 3-D CARBON/CARBON FIBER COMPOSITES
R. B. Dinwiddie, T. D. Burchell, and C. F. Baker 1991 3 p Presented at the 20th Biennial Conference on Carbon, Santa Barbara, 24-28 Jun. 1991
(Contract DE-AC05-84OR-21400)
(DE91-010388; CONF-910645-2) Avail: NTIS HC/MF A01

The material used was a carbon-carbon fiber composite manufactured from precursor yarn and petroleum based pitch through a process of repetitive densification of a woven preform. The resultant high temperature-high strength material exhibits relatively high thermal conductivity and is thus of interest to the fusion energy, plasma materials interactions (PMI) and plasma facing components (PFC) communities. Carbon-carbon fiber composite manufacture involves two distinct processes, preform weaving and component densification. Three samples were subjected to an additional heat treatment of 2550, 2750 or 3000 C subsequent to their fourth graphitization at 2400 C. It should be noted that no effort was made to optimize the composite for thermal conductivity, but rather only to provide a material with which to evaluate the effect of the final heat treatment temperature on the thermal conductivity. The fiber is the primary source of heat conduction in the composite. Consequently, increasing the fiber volume fraction, and/or the fiber thermal conductivity is expected to increase the composite thermal conductivity. DOE

N91-26241# Lawrence Livermore National Lab., CA.
MAGNETRON SPUTTER DEPOSITION OF BORON AND BORON CARBIDE
M. A. McKernan, D. Makowiecki, P. Ramsey, and A. Jankowski 13 Mar. 1991 20 p Presented at the International Conference on Metallurgical Coatings and Thin Films (ICMCTF), Waldorf, 22-26 Apr. 1991
(Contract W-7405-eng-48)
(DE91-011194; UCRL-JC-106571; CONF-9104231-1) Avail: NTIS HC/MF A03

The fabrication of x-ray optical coatings with greater reflectivity required the development of sputter deposition processes for boron and boron carbide. The use of high density boron and boron carbide and a vacuum brazed target design was required to achieve the required sputter process stability and resistance to the thermal stress created by high rate sputtering. The results include a description of the target fabrication procedures and sputter process parameters necessary to fabricate B4C1 and B2 modulated thin film structures. DOE

N91-26242# Oak Ridge National Lab., TN.
MICROSTRUCTURE DEVELOPMENT DURING MICROWAVE ANNEALING OF DENSE SILICON NITRIDE
T. N. Tiegs, M. K. Ferber, J. O. Kiggans, K. L. More, C. M. Hubbard, and D. W. Coffey 1991 10 p Presented at the 93rd Annual Meeting and Exposition of the American Ceramic Society (ACerS), Cincinnati, 28 Apr. - 2 May 1991
(Contract DE-AC05-84OR-21400)
(DE91-012069; CONF-910430-2) Avail: NTIS HC/MF A02

Microwave annealing of dense silicon nitride-based ceramics can result in substantial SiO volatilization from the grain boundary phases and compositional changes of those phases. It also results in further alpha-to-beta Si3N4 transformation accompanied by grain growth. These changes occur at bulk temperatures well below comparable observations in conventional heating. The differences are believed due to enhanced diffusion within the intergranular phases. DOE

25 INORGANIC AND PHYSICAL CHEMISTRY

Includes chemical analysis, e.g., chromatography; combustion theory; electrochemistry; and photochemistry.

For related information see also *77 Thermodynamics and Statistical Physics.*.

N91-26243# Lehigh Univ., Bethlehem, PA.
PARTIAL OXIDATION OF LIGHT ALKANES IN TRANSITION-METAL ION CONTAINING ZEOLITES
K. Klier, R. G. Herman, Jiann Lin, and J. P. Lange Oct. 1990 168 p
(Contract DE-FG22-86PC-90526)
(DE91-008202; DOE/PC-90526/T2) Avail: NTIS HC/MF A08

The purpose was to provide the scientific foundation for the conversion of C(sub 1)-C(sub 3) alkanes to oxygenates, particularly alcohols, and to higher hydrocarbons. The objectives were (1) to prepare selected transition metal ion zeolites by ion exchange with metal ions that are capable of undergoing redox reactions; (2) to characterize the transition metal ion containing zeolites experimentally and theoretically; (3) to characterize the adsorbed species formed between reactive gas phase molecules such as O2 and NO and the transition metal ions held in the zeolite matrix; and (4) to investigate the reactivity of those species for methane activation and conversion. Direct conversion of methane by low temperature partial oxidation to C2 hydrocarbons, oxygenated products such as methanol, or even to CO/H2 would be of significant interests for improvements in the economics of natural gas conversion. It would also open the bottle neck in the overall conversion scheme beginning with coal gasification and ending with the Mobil methanol-to-gasoline (MTG) process that produces a high octane liquid fuel. Sections of this report describe: the introductory background on transition metal zeolites; preparation and optical studies of Co(II)A zeolites; ligand field theory and dynamic Jahn-Teller effect for Co(II)A zeolite; scattered-wave x-alpha calculations of spectra of copper centers in oxide and zeolites; and studies of Fe(II)A zeolite. DOE

N91-26244# Pennsylvania Univ., Philadelphia. Dept. of Chemistry.
NEW DEVELOPMENTS IN THE SYNTHESIS AND DOPING OF POLYACETYLENE AND POLYANILINE Technical Report, 1 Jun. 1990 - 31 Oct. 1991
Alan G. MacDiarmid and A. J. Epstein 15 Mar. 1991 13 p
(Contract N00014-90-J-1559)
(AD-A233702; Rept-1990-1) Avail: NTIS HC/MF A03 CSCL 07/6

A study of cis-rich N-(CH)x and ARA-(CHA)x forms of B.A.S.F. polyacetylene involving elemental analysis of the pristine polymer and conductivities of the I2/CCl4 doped polymer are reported. Even though significant quantities of catalyst residue are present, the conductivity of the doped polymer is comparable to that of doped Shirakawa (CH)x. The synthesis of polyaniline in its fully oxidized, fully reduced and selected average intermediate oxidation states is described. The processing of polyaniline films and fibers by thermal stretching to give conductivities up to 100 S/cm is reported. Both doped and undoped polyaniline fibers have tensile strengths approaching those of commercial polymers. GRA

N91-26245# Pennsylvania Univ., Philadelphia. Dept. of Chemistry.
POLYANILINE: SYNTHESIS AND PROPERTIES OF PERNIGRANILINE
Alan G. MacDiarmid, S. K. Manohar, J. G. Masters, Y. Sun, and H. Weiss 15 Mar. 1991 8 p
(Contract N00014-90-J-1559)
(AD-A233706; Rept-1990-7) Avail: NTIS HC/MF A02 CSCL 07/3

The most highly oxidized polyaniline, in the form of pernigraniline base, can be synthesized as an analytically and oxidatively pure solid (powder or large free-standing films) by the controlled oxidation of emeraldine base by m-chloroperbenzoic acid or directly from aniline by oxidative polymerization with (NH4)2SO8. In the first method, the emeraldine oxidation state is converted directly to the pernigraniline oxidation state without passing through any intermediate discrete oxidation state at the molecular level. Treatment of pernigraniline base with aqueous HCl results not in protonated pernigraniline but in reductive ring chlorination to give the emeralidine oxidation state. GRA

N91-26246# Texas Univ., Austin. Dept. of Chemistry.
SURFACE MEDIATED PHOTOCATALYSIS Final Report, 15 Oct. 1987 - 15 Jan. 1991
Marye A. Fox 1 Mar. 1991 3 p
(Contract DAAL03-88-K-0012)
(AD-A233748; ARO-25169.13-CH) Avail: NTIS HC/MF A01 CSCL 07/4

Three methods for spacially controlled, photoinitiated degradation of organic materials have been conducted. These involve: (1) investigation of photochemical conversions of organic substances on metal oxides and semiconductor surfaces; (2) the preparation and evaluation of new soluble heteropolyoxonanion photooxidation catalysts; and (3) the synthesis of supported photocatalysts in macroscopic arrays. Reaction conditions to allow for chemical conversions under carefully contained conditions have shown that these routes are useful in the destruction of undesired toxic agents. GRA

N91-26247# California Univ., Los Angeles. Dept. of Chemistry and Biochemistry.
LASER IONIC MULTIPHOTON DISSOCIATION OF SOME ACRYLATE CLUSTERS
Hiroshi Morita, John E. Freitas, and Mostafa A. El-Sayed 18 Mar. 1991 22 p
(Contract N00014-89-J-1350)
(AD-A233801; TR-67) Avail: NTIS HC/MF A03 CSCL 07/3

Clusters of methyl acrylate (MA), methyl methacrylate (MMA) and ethyl acrylate (EA) are formed by supersonic expansion techniques. The clusters of these acrylates are ionized and decomposed by dominant channel of decomposition is the loss of the methoxy group in MA and MMA, and the loss of the ethoxy group in EA. A stable structure for the remaining neutral species is proposed. It is suggested that the charge on the cluster products is on the parent monomer unit while the decomposition occurs on other neutral monomer units within the clusters. The absorption of a number of photons leads to the decomposition of one, two or three monomers. The dynamics leading to energy pooling and localization are briefly discussed. GRA

N91-26248# Pittsburgh Univ., PA. Dept. of Chemistry.
ADSORPTION AND DECOMPOSITION OF ACETYLENE ON Si(100)-(2X1)
P. A. Taylor, R. M. Wallace, C. C. Cheng, W. H. Weinberg, and M. J. Dresser 5 Mar. 1991 43 p
(Contract N00014-82-K-0280)
(AD-A233808; TR-37) Avail: NTIS HC/MF A03 CSCL 07/2

The adsorption and decomposition of acetylene on Si(100)-(2x1) has been studied in ultrahigh vacuum by Auger spectroscopy, temperature programmed desorption, and changes in the partial pressure of acetylene as measured by a quadruple mass spectrometer during the formation of a monolayer. At a low surface temperature, reaction from the precursor state dominates, giving a chemisorption probability of unity at submonolayer coverages. The saturated acetylene coverage is measured to be one C2H2/Si2 dimer. Thermochemical arguments are presented which indicate that acetylene bonds as a di-sigma species to dimer sites in which the Si-Si dimer bond has been cleaved. Chemisorbed acetylene was found to undergo two thermal reactions. A minor pathway (less than five percent) involves acetylene desorption, and a major pathway (greater than 95 percent) involves the dissociation of acetylene to produce chemisorbed carbon and H2(g). At temperatures above 800 K, the surface carbon begins to diffuse into the bulk of the silicon crystal. GRA

N91-26249# California Univ., Los Angeles. Dept. of Chemistry and Biochemistry.
SIZE DEPENDENCE OF GASEOUS CLUSTER REACTIVITY AND EVAPORATION DYNAMICS AS A MECHANISTIC PROBE
M. A. El-Sayed 18 Mar. 1991 51 p
(Contract N00014-89-J-1350)
(AD-A233811; TR-68) Avail: NTIS HC/MF A04 CSCL 07/4

Two different types of cluster studies were carried out in the laboratory. In one, gaseous niobium metal clusters are synthesized by laser ablation and supersonic expansion in helium and detected by using excimer one-photon ionization-mass spectrometry methods. The dependence of their chemical reactivity (towards some carbon compounds) on size examined and used as a new mechanistic probe. In the other type of cluster studies, the mechanisms of the evaporation of one and two CsI molecules from individual mass selected (Cs(CsI)n)+ clusters (made by sputtering techniques) are determined from a study of the kinetic energy released and its distribution during evaporation process. GRA

N91-26250# Pennsylvania Univ., Philadelphia. Dept. of Chemistry.
PHOTOEXCITATION SPECTROSCOPY OF PERNIGRANILINE
J. M. Leng, J. M. Ginder, R. P. McCall, H. J. Ye, and A. J. Epstein 18 Mar. 1991 6 p
(Contract N00014-90-J-1559)
(AD-A233841; Rept-1990-22) Avail: NTIS HC/MF A02 CSCL 20/5

Absorption and photoinduced absorption spectroscopies are reported for pernigraniline base (PNB). Direct absorption of PNB shows the band gap energy at 2.3 eV and transition energies at 3.8 and 4.3 eV. The photoinduced absorption (PA) spectrum at room temperature shows three induced absorption peaks at 1.0 (LE), 1.5 (ME) and 3.0 eV (HE). At a temperature of 10 K, the LE peak becomes two peaks at 1.0 eV (LE1) and 1.3 eV (LE2). The ME peak is very long-lived; in addition, there are very long-lived relatively weak infrared vibrations. Light-induced ESR studies show the long-lived 1.5 eV peak has spin-1/2. GRA

N91-26251# Pennsylvania Univ., Philadelphia. Dept. of Chemistry.
POLYANILINE: ALLOWED OXIDATION STATES
J. G. Masters, Y. Sun, Alan G. MacDiarmid, and A. J. Epstein 18 Mar. 1991 6 p
(Contract N00014-90-J-1559)
(AD-A233842; Rept-1990-15) Avail: NTIS HC/MF A02 CSCL 07/6

The interconversion of different oxidation states of polyanilines has been studied. It is concluded that the polyaniline bases (NMP solution) exist only in three discrete oxidation states at the molecular level. The polyanilines refer to a class of polymers which can be considered as being derived from a polymer. The terms leucoemeraldine, emeraldine and pernigraniline refer to the different oxidation states of the polymer where (1-y) = 0, 0.5 and 1.0. No evidence has been obtained hitherto to indicate whether the polyanilines exist in a continuum of oxidation states at the molecular level ranging from (1-y) values of 0 to 1. Early work suggested that polyaniline could be isolated in five distinct oxidation states having (1-y) values of 0.0, 0.25, 0.50, 0.75 and 1.0. GRA

N91-26252# Pittsburgh Univ., PA. Surface Science Center.
ADSORPTION AND THERMAL BEHAVIOR OF ETHYLENE ON Si(100)-(2X1)
L. Clemen, R. M. Wallace, P. A. Taylor, M. J. Dresser, and W. J. Choyke 5 Mar. 1991 39 p
(Contract N00014-82-K-0280)
(AD-A234098; TR-38) Avail: NTIS HC/MF A03 CSCL 07/4

The study of the interaction of hydrocarbons with silicon is of importance in understanding the thermally activated formation of adsorbed carbon on silicon. This is the first step in the formation of silicon carbide thin films by chemical vapor deposition (CVD). Silicon carbide is an important material because of its strength, refractory properties, chemical inertness, resistance to radiation damage, and its ability to be used as an electronic material in a high temperature environment. Simple electronic devices made from silicon carbide have been produced, and progress in this area is actively continuing. Extensive research has been performed to determine the geometric and electronic structure of the Si(100) crystalline surface, as recently reviewed by Haneman. It has been found that the surface consists of rows of Si2 dimers yielding a (2x1) superstructure. Here, formally, a one half-filled dangling bond protrudes from the surface at each surface silicon atom. GRA

N91-26253# State Univ. of New York, Albany. Dept. of Chemistry.
CLUSTER BEAM ANALYSIS VIA PHOTOIONIZATION
J. R. Grover, W. J. Heron, M. T. Coolbaugh, W. R. Peifer, and James F. Garvey 1991 47 p
(Contract N00014-88-K-0483)
(AD-A234111; TR-21) Avail: NTIS HC/MF A03 CSCL 07/5

A photoionization method for quantitatively analyzing the neutral products of free jet expansions is described. The basic principle is to measure the yield of an ion characteristic of each component cluster at a photon energy just below that at which production of the same ion from larger clusters can be detected. Since there is then no problem with fragmentation, the beam density of each neutral cluster can be measured in the presence of larger clusters. Although these measurements must be done in test ions onset regions where their yields are often quite small, the technique is made highly practicable by the large intensities of widely tunable vacuum-UV synchrotron light now available at the electron storage rings. As an example, the method is applied to the analysis of cluster beams collimated from the free jet expansion of a 200:1 ammonia-chlorobenzene mixture. GRA

N91-26254# Naval Research Lab., Washington, DC.
FLEXURAL PLATE WAVE DEVICES FOR CHEMICAL ANALYSIS
Jay W. Grate, Stuart W. Wenzel, and Richard M. White 16 Apr. 1991 49 p
(AD-A234129; NRL-MR-6815) Avail: NTIS HC/MF A03 CSCL 07/4

The mass-sensitivities, vapor sensitivities, and vapor detection limits of flexural plate wave (FPW) and surface acoustic wave (SAW) vapor sensors are compared both theoretically and experimentally. FPW devices offer high mass sensitivity at much lower operating frequency. Mass sensitivity increases as membranes thickness decreases; frequency decreases at the same time. This scaling law is in contrast to SAW devices where mass sensitivity increases as frequency increases. FPW devices with sorbent polymer films respond to vapors in a manner similar to SAW devices coated with the same polymer. The FPW vapor sensor, however, offers lower absolute noise levels and hence lower vapor detection limits. It is also demonstrated experimentally that FPW devices can monitor changes in polymer films as the polymer undergoes the glass transition. Plots of frequency vs. temperature show a discontinuity in slope at the static glass transition. GRA

N91-26255# State Univ. of New York, Buffalo. Dept. of Chemistry.
CATIONIC POLYMERIZATION WITHIN VAN DER WAALS CLUSTERS OF THE FORM (CH2=R)n WHERE R=CH2, CF2 AND CHCH3
M. T. Coolbaugh, Gopal Vaidyanathan, William R. Peifer, and James F. Garvey 1990 32 p Submitted for publication
(Contract N00014-88-K-0483)
(AD-A234233; SUNY/AB/TR-20) Avail: NTIS HC/MF A03 CSCL 07/6

The cluster ion mass spectra resulting from electron ionization of van der Waals clusters composed of ethene, 1, 1-difluoroethene or propene molecules were observed as a function of expansion and ionization conditions. Expansion conditions favoring the formation of large neutral clusters lead to the observation of anomalous ion intensity distributions characterized by strong peaking as a function of cluster size. Comparisons are made between the present results and previous observations in both the gas and condensed phases. We propose that the anomalous cluster ion distributions arise as a consequence of the production of molecular (i.e., covalently bonded) ions produced by a series of intracluster addition (polymerication) reactions. GRA

N91-26256# California Univ., Berkeley. Dept. of Chemistry.
STUDY OF THE LOW-LYING ELECTRONIC STATES OF Si2 AND Si2(-) USING NEGATIVE ION PHOTODETACHMENT TECHNIQUES Interim Technical Report No. 6, Dec. 1990 - Mar. 1991
T. N. Kitsopoulos, C. J. Chick, Y. Zhao, and Daniel M. Neumark 1 Apr. 1991 36 p
(Contract N00014-87-K-0495)
(AD-A234336) Avail: NTIS HC/MF A03 CSCL 20/5

The spectroscopy of elemental clusters has become the focus of much experimental and theoretical research in recent years. A primary goal of these studies is to determine how chemical bonding in a cluster evolves as the number of atoms is varied. A full understanding of bonding in a cluster requires the characterization not only of its ground electronic state, but also of its low-lying excited electronic states. This is a formidable challenge due to the likely presence of a large number of low-lying electronic states in a many-atom cluster. As a first step towards understanding the nature of electronic states in larger clusters, we report here the results of two types of photodetachment experiments on Si2(-) which yield a detailed picture of low-lying electronic states of Si2 as well as the lowest two electronic states of Si2(-). GRA

N91-26257# Vermont Univ., Burlington. Dept. of Chemistry.
REGIO- AND STEREOCHEMICAL CONTROL IN SUBSTITUTION REACTIONS OF CYCLOPHOSPHAZENES
Christopher W. Allen 26 Mar. 1991 72 p
(Contract N00014-89-J-1041)
(AD-A234376; TR-16) Avail: NTIS HC/MF A04 CSCL 07/3

A comprehensive review of the factors leading to regio- and stereochemical control in the reactions of the cyclophosphazenes was prepared. Information from product distribution, kinetic and mechanistic studies was collected and used as a basis for predictive

guide lines for various classes of reactions including: reactions with amines, metathetical halogen and pseudohalogen exchange, reactions of oxyanions and thiolates, reactions with main group organometallics, the Friedel-Crafts reaction, reactions with transition metal organometallics. GRA

N91-26258# Pennsylvania Univ., Philadelphia. Dept. of Chemistry.
INTERACTION OF CATIONIC POLYPEPTIDES WITH ELECTROACTIVE POLYPYRROLE/POLY(STYRENESULFONATE) AND POLY(N-METHYLPYRROLE)/POLY(STYRENESULFONATE) FILMS Technical Report, 1 Jun. 1990 - 31 Oct. 1991
L. A. Prezyna, Y. J. Qiu, J. R. Reynolds, and G. E. Wnek 29 Mar. 1991 21 p
(Contract N00014-90-J-1559)
(AD-A234469; Rept-1990-36) Avail: NTIS HC/MF A03 CSCL 01/3

The binding of cationic polypeptides to polypyrrole PP/poly(styrenesulfonate)PSS and poly(N-methylpyrrole) PNMP/pss films, along with the effect of binding on film electroactivity, have been studied using the electrochemical quartz-crystal microbalance (EQCM). Two polypeptides were studied, namely poly(l-lysine hydrocholride) and the arginine-rich histone H3. Poly(l-lysine hydrochloride) binds to either the oxidized or reduced forms of the films, although the electroactivity and ability of the films to transport small cations upon electrochemical cycling remains intact. Histone H3 shows little tendency to bind to oxidized films, but upon electrochemical reduction PSS is extracted. This unusual behavior is thought to be the result of strong electrostatic and hydrophobic interactions between PSS and H3 at the PP/PSS surface. The films retain their electroactivity after interaction with H3. GRA

N91-26259# Naval Research Lab., Washington, DC.
WATER SOLUBILITY OF BIS(2-ETHYLHEXYL) HYDROGEN PHOSPHITE Memorandum Report
Robert E. Pellenbarg and Kia Cephas 17 Apr. 1991 12 p
(AD-A234561; NRL-MR-6795) Avail: NTIS HC/MF A03 CSCL 15/6

Chemical warfare defense research routinely utilizes simulants for chemical agents. This substitutive approach offers several advantages. Specifically, procedures relying on simulants can be much less rigid and dangerous than those which use live agents. Simulants, in contrast to lethal agents, can be more readily disseminated in the open environment. Thus, with appropriate non-toxic simulants, one can contaminate a large piece of military equipment, and study the decontamination (simulant removal) of the impacted device in a non-lethal setting. Such a decontamination exercise would be profoundly more difficult if one were to use live chemical agents. GRA

N91-26260# York Univ. (Ontario). Dept. of Chemistry.
THE CONTROL OF ORBITAL MIXING IN RUTHENIUM COMPLEXES CONTAINING QUINONE RELATED LIGANDS
H. Masui, A. B. Lever, and P. R. Auburn 4 Apr. 1991 41 p
(Contract N00014-84-G-0201)
(AD-A234602; TR-38) Avail: NTIS HC/MF A03 CSCL 20/5

Three redox series of complexes of the general formula Ru(II)(bpy)2LL and Ru(II)(Py)4LL (bpy=2,2'-bipyridine) are reported, where LL are the ligands, 1,2-dihydroxybenzen, 2-aminophenol or 1,2-diaminobenzene. These ligands can exist in the fully reduced catechol form, or the one and two electron oxidized semiquinone and quinone forms. Electronic and electron spin resonance spectroscopic, and electrochemical data are discussed in terms of orbital mixing and electronic structure, and the number of oxygen or nitrogen atoms in the coordinating ligand. GRA

N91-26261# York Univ. (Ontario). Dept. of Chemistry.
TETRA NEOPENTOXY PHTHALO CYANINE LANGMUIR-BLODGETT FILMS: SPECTROSCOPY AT THE AIR/WATER INTERFACE
Jiangbo Ouyang and A. B. Lever 4 Apr. 1991 26 p
(Contract N00014-84-G-0201)
(AD-A234603; TR-40) Avail: NTIS HC/MF A03 CSCL 07/4

A series of tetra neopentoxy phthalo cyanine (Ag2+, Ni2+, Zn2+, and Co2+) compounds are used in the study of Langmuir monolayers at the air/water interface. Isotherm measurements and absorption spectra of the standing monolayers are presented to discuss the mechanism of monolayer formation with tetra neopentoxy phthalo cyanines. The MTNPc species from self-assembled domains when the coverage is less than 1 monolayer. Combing exciton coupling theory with the isotherm measurement provides a consistent representation of the orientation angle of the MTNPc units at the air/water interface. GRA

N91-26262# Stanford Univ., CA. Dept. of Chemistry.
COMPARISON OF HYDROGEN DESORPTION KINETICS FROM Si(111)7X7 AND Si(100)2X1
M. L. Wise, B. G. Koehler, P. Gupta, P. A. Coon, and S. M. George 12 Apr. 1991 39 p
(Contract N00014-90-J-1281)
(AD-A234633; SU-TR-22) Avail: NTIS HC/MF A03 CSCL 07/4

The desorption kinetics of hydrogen from the 1 H2-TPD state on silicon (111) 7x7 and Si(100) 2x1 were studied using laser-induced thermal studies of H2 desorption from Si(111) 7x7 revealed second-order kinetics with a desorption activation barrier of Ed=62 kcal/mol. In contrast, the desorption of hydrogen from Si(100) 2x1 revealed first-order kinetics with an activation barrier of Ed=58 kcal/mol and a preexponential factor. The desorption kinetics yielded similar upper limits for the Si-H bond energies, but differnt desorption mechanisms on Si(111) 7x7 and Si(100)2x1. The TPD results were also in agreement with second-order H2 desorption kinetics on Si(111) 7x7 were consistent with a recombinatory desorption mechanism involving randomly positioned hydrogen atoms. The first-order H2 desorption mechanism involving randomly positioned hydrogen atoms. The first-order H2 desorption of H2 from two hydrogen atoms paired on the same silicon dimer on Si(100) 2x1. GRA

N91-26263# Stanford Univ., CA. Dept. of Chemistry.
COMPARISON OF H2 DESORPTION KINETICS FROM Si(111)7X7 AND Si(100)2X1
M. L. Wise, B. G. Koehler, P. Gupta, P. A. Coon, and S. M. George 12 Apr. 1991 9 p
(Contract N00014-90-J-1281)
(AD-A234634; SU-TR-17) Avail: NTIS HC/MF A02 CSCL 07/3

Hydrogen plays an important role in reactions important to semiconductor processing chemistry. Many species such as H2O, NH3, PH3, and SiH4 have been determined to chemisorb dissociatively on silicon and form silicon-hydrogen bonds. The kinetics of these reactions are believed to be rate-limited by H2 desorption. Laser induced thermal desorption techniques (LITD) have been utilized recently to measure H2 desorption kinetics from Si(111) 7x7 and Si (100) 2x1. Second-order H2 desorption kinetics were observed from Si(111) 7x7, whereas first-order kinetics were monitored from Si(100)2x1. GRA

N91-26264# Stanford Univ., CA. Dept. of Chemistry.
DESORPTION PRODUCT YIELDS FOLLOWING Cl2 ADSORPTION ON Si(111)7X7: COVERAGE AND TEMPERATURE DEPENDENCE
P. Gupta, P. A. Coon, B. G. Koehler, and S. M. George 12 Apr. 1991 34 p
(Contract N00014-90-J-1281)
(AD-A234635; SU-TR-15) Avail: NTIS HC/MF A03 CSCL 07/2

Chlorine plays an essential role during the plasma etching of silicon surfaces. The interaction between chlorine and silicon is also important in the epitaxial growth of silicon during chemical vapor deposition with SiCl4 + H2 or SiCl2H2(4-6). An understanding of the structure and stability of chlorine on silicon

surfaces is essential for a complete description of the surface reaction steps that define plasma etching and epitaxial growth processes. Previous work on chlorine adsorption on silicon surfaces has focused on the nature of the chloride species obtained after various stages of chlorine adsorption. X-ray photoemission spectroscopy (XPS) studies have monitored the silicon oxidation state after a saturation chlorine exposure Si(111)7x7 at 300 K. These XPS investigations measure oxidation states that were consistent with the bonding one, two and three chlorine atoms to individual silicon surface atoms. The photoemission studies also demonstrated that monochloride species were present at low chlorine coverages and di- and trichloride species were formed at higher chlorine coverages. Only monochloride species were observed to remain on the Si(111) 7x7 surface after annealing to 673 K (7). GRA

N91-26265# Stanford Univ., CA. Dept. of Chemistry.
FTIR STUDIES OF WATER AND AMMONIA DECOMPOSITION ON SILICON SURFACES
A. C. Dillon, P. Gupta, M. B. Robinson, A. S. Bracker, and S. M. George 12 Apr. 1991 8 p
(Contract N00014-90-J-1281)
(AD-A234637; SU-TR-18) Avail: NTIS HC/MF A02 CSCL 07/4

Fourier transform infrared (FTIR) transmission spectroscopy was used to monitor the decomposition of H2O(D2O) and NH3 (ND3) on silicon surfaces. Experiments were performed in-situ in an ultra-high vacuum (UHV) chamber using high surface area porous-silicon samples. The FTIR spectra revealed that H2O dissociates upon adsorption at 300 K to form SiH and SiOH surface species. NH3 also dissociates upon adsorption at 300 K to form SiH and SiNH2 species. Silicon samples with saturation exposures of H2O and NH3 were progressively annealed from 300 to 860 K. The FTIR spectra of an H2O-saturated silicon surface revealed that the SiOH species decomposed to form a silicon oxide species and additional surface hydrogen between 460 and 580 K. Likewise, the SiNH2 species decomposed between 540 and 660 K to produce silicon nitride and additional surface hydrogen. In both cases, the SiH surface species decreased as H2 desorption from the silicon surface was observed above 700 K. GRA

N91-26266# Stanford Univ., CA. Dept. of Chemistry.
DIETHYLSILANE DECOMPOSITION ON SILICON SURFACES STUDIED USING TRANSMISSION FTIR SPECTROSCOPY
A. C. Dillon, M. B. Robinson, M. Y. Han, and S. M. George 12 Apr. 1991 23 p
(Contract N00014-90-J-1281)
(AD-A234638; SU-TR-21) Avail: NTIS HC/MF A03 CSCL 20/12

Fourier transform infrared (FTIR) transmission spectroscopy was used to monitor the decomposition of diethylsilane (DES) (CH3CH2)2SiH2 on high-surface-area porous silicon samples. The FTIR spectra revealed that DES dissociatively adsorbs on porous silicon to form SiH and SiCH2CH3 species. The infrared absorbances of the CH2CH3 stretches at (2955 to 2879)/cm and the SiH stretch at 2088/cm were employed to monitor the decomposition of the SiCh2CH3 surface species. As the silicon surface was annealed to 500 to 750 K, the SiCH2CH3 species decomposed to produce gas phase ethylene CH2=CH2 and additional SiH surface species. These reaction products were consistent with a -hydride elimination reaction. Above 700 K, the SiH surface species decreased concurrently with the desorption of H2 from the porous silicon surface. In additional experiments, isothermal FTIR studies were performed the characterize the decomposition kinetics of SiCH2CH3 by -hydride elimination. The uptake of surface species was also monitored at various adsorption temperatures to determine the optimal DES exposure temperatures for carbon-free silicon deposition. GRA

N91-26267# Stanford Univ., CA. Dept. of Chemistry.
ADSORPTION AND DECOMPOSITION OF DIETHYLSILANE ON SILICON SURFACES
P. A. Coon, M. L. Wise, A. C. Dillon, M. B. Robinson, and S. M. George 12 Apr. 1991 9 p
(Contract N00014-90-J-1281)
(AD-A234639; SU-TR-19) Avail: NTIS HC/MF A02 CSCL 07/3

Diethylsilane (DES), Si(C2H5)2H2, is a promising candidate for the atomic layer epitaxy of silicon. The adsorption and decomposition kinetics of DES on silicon surfaces were studied using laser-induced thermal desorption (LITD), temperature programmed desorption (TPD), and Fourier transform infrared (FTIR) spectroscopy. FTIR studies on porous silicon surfaces indicated that DES dissociatively adsorbs below 600 K and produces Si-H and Si-C2H5 surface species. The desorption products following DES adsorption on Si(111) 7x7 were C2H4 and H2 for all surface coverages using both LITD and TPD techniques. Ethylene and H2 desorption occurred at 700 and 810 K, respectively, during TPD experiments with a heating rate of B = 9 K/s. Ethylene desorption was consistent with a beta hydrogen elimination mechanism from the Si-C2H5 surface species. Isothermal LITD studies monitored the desorption kinetics of C2H2 from Si(111) 7x7 as a function of time following DES exposures. GRA

N91-26268# Utah Univ., Salt Lake City. Dept. of Chemistry.
SURFACE DIFFUSION AT THE LIQUID-SOLID INTERFACE: QUENCHING OF FLUORESCENCE FROM PYRENE COVALENTLY BOUND TO METHYLATED SILICA Technical Report, Jun. 1990 - May 1991
A. L. Wong and J. M. Harris 22 Apr. 1991 34 p
(Contract N00014-89-J-1412)
(AD-A234645; TR-24-ONR) Avail: NTIS HC/MF A03 CSCL 07/2

The rates of iodine quenching of fluorescence from immobilized pyrene on methylated and bare porous silica gels suspended in methanol and aqueous methanol solvents are measured and compared. The interfacial quenching rate of 3-(1-pyrenyl) propyl-dimethyl monochlorosilane (3PPS) on C1-modified silica in methanol is significantly larger than the rate observed on bare silica. The enhanced rate on C1-silica is attributed to surface transport whereby iodine quencher molecules adsorb onto the hydrophobic surface and diffuse laterally to collide with the excited pyrene probe. This mechanism is supported by chromatographic data indicating that adsorbed iodine on the C1-silica is 100 times higher in concentration than on bare silica. GRA

N91-26269# Washington Univ., Seattle. Dept. of Chemistry.
A COMBINED XPS-ISS MODULATED MOLECULAR BEAM INVESTIGATION OF THE REACTIONS OF OXYGEN AND FLUORINE WITH SILICON SURFACES Final Report, 1987 - 1991
Thomas Engel 15 Feb. 1991 11 p
(Grant AF-AFOSR-0166-87)
(AD-A234867; AFOSR-91-0256TR) Avail: NTIS HC/MF A03 CSCL 07/4

The chemical reaction between Si(100) and molecular and atomic oxygen and fluorine has been studied. Using modulated molecular beam mass spectrometry, XPS, and ISS, the kinetics of adsorption reaction and desorption have been studied in detail. Atomic fluorine and oxygen are much more reactive at high coverages than their molecular counterparts. At low coverages, this is true for O, but not for F. GRA

N91-26270# Stanford Univ., CA. Dept. of Chemistry.
THEORY AND EXPERIMENTAL AND CHEMICAL INSTABILITIES Final Technical Report, 1 Jan. 1987 - 31 Dec. 1990
John Ross Mar. 1991 16 p
(Grant AF-AFOSR-0120-87; AF Proj. 2303)
(AD-A234916; AFOSR-91-0382TR) Avail: NTIS HC/MF A03 CSCL 07/4

Progress was made in understanding thermodynamics, kinetics and stochastic theories for non-linear chemical reactions far from equilibrium. Thermodynamics analysis for systems far from equilibrium has established necessary and sufficient criteria of

global stability and relative stability. Evaluations of transitions between periodic and aperiodic conditions in combustion kinetics have been classified based on the instable feature and the type of feedback loop. This study may contribute to finding an operational way to develop a mechanism from experimental results. GRA

N91-26271# Utah Univ., Salt Lake City. Dept. of Chemistry.
RAMAN SPECTROSCOPY STUDY OF SOLVATION STRUCTURE IN ACETONITRILE/WATER MIXTURES Technical Report, Jun. 1990 - May 1991
K. L. Rowlen and J. M. Harris 22 Apr. 1991 15 p
(Contract N00014-89-J-1412)
(AD-A234921; TR-23-ONR) Avail: NTIS HC/MF A03 CSCL 14/2

Raman spectroscopy is used to probe the CN stretching frequency of acetonitrile as a function of concentration in water. The CN band is modeled as the sum of two Gaussians. The concentration dependence of area and width for each of the Gaussian components provides experimental support of an equilibrium between two forms of acetonitrile in solution. In addition, the concentration dependence of each of the bands correlates well with the thermodynamically related Kirkwood-Buff integrals. The frequency shift of the CN band exhibits a linear dependence on the dielectric constant of protic solvents. There has been considerable effort to define and understand the fundamental molecular interactions important in liquid chromatography. Although the solvophobic theory is commonly invoked to explain retention in reversed-phase liquid chromatography (RPLC), recent studies have pointed out shortcomings in this model. GRA

N91-26272# International Business Machines Corp., Yorktown Heights, NY.
CHEMISTRY OF FLUORINE IN THE OXIDATION OF SILICON Technical Report, 1 Jun. 1990 - 1 Mar. 1991
S. R. Kasi, M. Liehr, and S. Cohen 3 Apr. 1991 18 p
(Contract N00014-89-C-0104)
(AD-A234959; TR-14) Avail: NTIS HC/MF A03 CSCL 07/2

The chemical environment of fluorine in the oxide layer of metal-oxide-semiconductor (MOS) structures has been examined by surface analytical spectroscopies. The HF treatment of Si(100) results in subsurface SiF formation. Upon oxidation, oxyfluoride moieties are formed with a significant accumulation of fluorine throughout the oxide layer. These changes are correlated to the electrical integrity of MOS interfaces by performing Fowler-Nordheim electron injection studies. GRA

N91-26273# AeroChem Research Labs., Inc., Princeton, NJ.
COMPUTER MODELING OF SOOT FORMATION COMPARING FREE RADICAL AND IONIC MECHANISMS Final Report, 1 Oct. 1987 - 30 Sep. 1990
H. F. Calcote and Robert J. Gill Feb. 1991 44 p Prepared in cooperation with Pennsylvania State Univ., University Park and Iowa State Univ. of Science and Technology, Ames
(Contract F49620-88-C-0007)
(AD-A235007; AEROCHEM-TP-495; AFOSR-91-0229TR) Avail: NTIS HC/MF A03 CSCL 07/4

A collaborative effort among AeroChem Research Laboratories Inc., Pennsylvania State University, and Iowa State University has been pursued to compare the relative importance of the free radical and the ionic mechanisms of soot formation. A detailed ionic reaction mechanism was developed; the rate coefficients were obtained from the literature or estimated; ambipolar diffusion and ion-electron recombination coefficients were calculated; and thermodynamic data for the ions were either compiled from the literature or calculated. Computer runs were made at Penn State using our ionic mechanism to simulate the well documented sooting acetylene/oxygen/argon flat flame at a pressure of 2.67 kPa and a linear flow rate of 50 cm/s. The calculated peak ion concentrations was consistent with experimental peak concentrations, but the calculated ion profiles appeared much earlier in time and decayed very rapidly compared to the experimental ion profiles. This was suspected to be dependent upon the calculated neutral species profiles from the free radical mechanism for small neutrals, which are required to form chemiions. GRA

N91-26274# Pittsburgh Univ., PA. Dept. of Chemistry.
THE STEPWISE DISSOCIATION OF NH3 ON THE Si(111)-(7X7) SURFACE: LOW TEMPERATURE DISSOCIATIVE ADSORPTION AND THERMAL EFFECTS
M. L. Colaianni, P. J. Chen, and J. T. Yates, Jr. 10 Apr. 1991 49 p
(Contract N00014-82-K-0280)
(AD-A235009; TR-39) Avail: NTIS HC/MF A03 CSCL 07/2

The molecular and dissociative adsorption of NH3 on a clean Si(111)-(7x7) surface has been studied using HREELS, AES and TPD. All NHx species have been vibrationally observed under varying experimental conditions. Adsorbed molecular ammonia is observed by both HREELS and TPD below 200 K. The absence of a strong delta s(NH3) mode in our vibrational spectra suggests NH3 is bound as a tilted species to the Si(111)-(7x7) surface. Ammonia exposures above 1.7 x 10 14 NH3/sq cm at 110 K populate a weakly bound NH3(a) state which desorbs upon heating with a peak desorption temperature of 115 K. The NH2(a) species is observed to form at 80 K at all coverages and exhibits an enhanced thermal stability at higher ammonia exposures. The NH(a) species is detected above 300 K by an energy loss feature at 1100 cm-1, which we assign to the delta (NH) mode. NH(a) is stable to 750 K on high coverage layers. Finally, we observe an increase in the Si-H stretching frequency as the concentration of -NH(a) and =N(a) species is increased by heating. GRA

N91-26275# Pittsburgh Univ., PA. Surface Science Center.
SURFACE CHEMISTRY OF SILICON: THE BEHAVIOR OF DANGLING BONDS
J. T. Yates, Jr. 22 Apr. 1991 32 p
(Contract N00014-82-K-0280)
(AD-A235011; TR-40) Avail: NTIS HC/MF A03 CSCL 07/2

The role of surface dangling bonds in controlling the surface chemistry of Si(100) and Si(111) has been investigated using surface science methods. The adsorption and decomposition of acetylene on Si(100) has been shown to occur by means of mobile precursor mechanism, leading to a di-sigma chemisorbed ethylenic species occupying Si dimer sites on Si(100). This species decomposes at elevated temperatures to produce adsorbed carbon and hydrogen (800 K) and then silicon carbide (1000 K). The activity of Si(111) for the adsorption of species such as ammonia and atomic hydrogen can be significantly reduced by doping of the surface region with boron. It has been shown that subsurface boron significantly changes the structure of Si(111)-(7x7) to a (sq rt 3 x sq rt 3) R 30 deg structure. In addition, the local doping of the surface reduces the chemical activity of the dangling bonds so that neither the dissociation of NH3 nor the adsorption of atomic hydrogen will occur. GRA

N91-26276# California Univ., Los Angeles. Dept. of Materials Science and Engineering.
INTERNATIONAL COLLABORATION PROGRAM ON INNOVATIVE CHEMICAL PROCESSING OF SUPERIOR ELECTRONIC AND OPTICAL MATERIALS Final Report, 14 Sep. 1987 - 14 Sep. 1990
J. D. Mackenzie Mar. 1991 38 p
(Contract F49620-87-K-0011)
(AD-A235030; AFOSR-91-0391TR) Avail: NTIS HC/MF A03 CSCL 20/3

A small team comprised of scientists from France, the United Kingdom, Japan and the U.S., has performed collaborative research on high transition temperature ceramic superconductors and inorganic nonlinear optical composites, the BiCuSrCaOx system was found to be glass-forming. The glass can be crystallized to give a superconducting glass-ceramic was machinable. The glass was also infrared transmitting to about 7 microns. Nanocomposites containing crystallites of CdS in both glass and organically-modified silicates (ORMOSIL) have been prepared via the sol-gel technique.

Quantum confinement was demonstrated in these nonlinear optical materials. GRA

N91-26277# Massachusetts Inst. of Tech., Cambridge. Dept. of Chemistry.
THE REDUCTION BY DEUTERIUM ON PLATINUM BLACK OF EXO-2-NORBORNYL AND ENDO-2-NORBORNYL TO NORBORNANE-2-d OCCURS WITH PREDOMINANT RETENTION OF CONFIGURATION
T. R. Lee and George M. Whitesides 1991 4 p
(Contract N00014-88-K-0731)
(AD-A235057; TR-3) Avail: NTIS HC/MF A01 CSCL 07/3

The stereochemistry of the reaction of C bonds is investigated in heterogeneous hydrogenations, based on the absorption of (DO)PtR2 on platinum black to generate R groups. It was concluded that the reduction of exo 2-norbornyl, and endo 2-norbornyl moities occurs with predominant retention of stereochemistry. B.G.

N91-26278# Michigan Univ., Ann Arbor. Dept. of Aerospace Engineering.
TURBULENT PREMIXED HYDROGEN/AIR FLAMES Final Report, 1 Aug. 1987 - 31 Dec. 1990
S. Kwon, M. S. Wu, J. F. Driscoll, and G. M. Faeth 15 Feb. 1991 108 p
(Contract N00014-87-K-0698)
(AD-A235109) Avail: NTIS HC/MF A06 CSCL 21/2

The properties of turbulent premixed flames were investigated both theoretically and experimentally. Attention was limited to hydrogen/air mixtures burning as either turbulent jet flames or a freely propagating flames in isotropic turbulence. The research has application to a variety to premixed turbulent combustion processes: underwater metal cutting at great depth, primary combustors for high-speed airbreathing propulsion systems, afterburners, fuel/air explosions, and spark-ignition internal combustion engines. Major findings of this phase of the investigation are as follows: (1) effects of preferential diffusion are relevent for flames at high Reynolds number, retarding and enhancing the distortion of the flame surface by turbulence for stable and unstable conditions, respectively; (2) local turbulent burning velocity, flame brush thickness and the fractal dimension of the flame surface all increase with distance from the flameholder, with larger rates of increases at larger turbulence intensities; (3) estimates of flame properties using contemporary turbulence models were only fair because these methods cannot account for effects of preferential diffusion, distance from the flameholder and finite laminar flame speeds; and (4) the stochastic simulation duplicated measured trends of flame surface properties for neutral preferential diffusion conditions (the only case considered) but underestimated effects of turbulence (particularly near the flame tip) due to the limitations of a two-dimensional simulation. GRA

N91-26279# Pennsylvania State Univ., University Park. Materials Research Lab.
MICROSTRUCTURE, POROSITY, AND MECHANICAL PROPERTY RELATIONSHIPS OF CALCIUM-SILICATE-HYDRATE Final Report, 15 Sep. 1987 - 14 Dec. 1990
M. W. Grutzeck, S. Hoyle, S. Kwan, J. LaRosa, and S. Bozich 15 Feb. 1991 117 p
(Grant AF-AFOSR-0395-87; AF Proj. 2306)
(AD-A235191; PSU-AFOSR-91-1; AFOSR-91-0257TR) Avail: NTIS HC/MF A06 CSCL 11/2

The structure of calcium silicate hydrate (C-S-H) formed as a result of solution/sol mixing, and hydration of tricalcium silicate (C3S) under fixed pH conditions was studied. MAS NMR and related analytical techniques (x-ray diffraction, SEM/TEM, and TGA) were used to characterize the hydration products. Two C-S-H phases having distinctly different structures (molecular and micro) and weight loss characteristics exist in the system CaO-SiO2-H2O and along the 10 wt. percent isoalumina join through the system CaO-Al2O3-SiO2-H2O. Coexisting phases form somewhere between 10 and 20 wt. percent alumina. C3S hydrated as a function of pH (11-12) confirmed that at low pHs (less than 11.5), a C-S-H consisting predominantly of Q2 silicate chains forms. At pH greater than or equal to 11 .5, a second C-S-H formed which consists of a combination of Q1Q2 silicate units. This C-S-H is more typical of that normally associated with the hydration of C3S or portland cement without pH control. The C3S hydrated at pH 13 contained only silicate dimer (Q1) and large quantities of crystalline Ca(OH)2. In this instance an entirely different gel (perhaps an alkali aluminosilicate hydrate) might be forming. In a parallel study, zeolites have been synthesized from synthetic and waste glasses (fly ash) mixed with alkali hydroxide solutions. Linde B1, chabazite and gobbinsite have been observed under certain conditions (relatively high Ca and alkali content). These data have been used to evaluate the feasibility of producing zeolite-cement composites. GRA

N91-26280# University of Northern Illinois, De Kalb. Dept. of Chemistry.
GEL SOLIDIFIED MICROINTERFACE BETWEEN TWO IMMISCIBLE ELECTROLYTES APPLIED TO AMPEROMETRIC DETECTION OF PICRATE AND TETRAMETHYLAMMONIUM Technical Report No. 39, 1 Jan. - 15 Apr. 1991
P. Vanysek and J. Xu 26 Apr. 1991 24 p
(Contract N00014-88-K-0075; NR Proj. RR0-4108)
(AD-A235260) Avail: NTIS HC/MF A03 CSCL 07/4

Transport of picrate and tetramethylammonium ions across an agar or PVC gel/liquid boundary formed between water and nitrobenzene has been investigated as a model for a study to determine electrochemically various semihydrophobicions. Linear calibration curves were obtained for concentrations greater than or equal to 10(exp -4) mol/l. Charge transport due to ion transfer between water and nitrobenzene was studied in either direction. Cyclic voltammetry, as a main investigative tool, indicated reversible transfer and diffusion control both in the solution and in the gel. Utilization of a small contact area (microinterface) was suggested for a practical analytical application. The microscopic size limits greatly the effect of a potential drop arising from the solution resistance. This follows the principle used in the work with ultramicroelectrodes. The gel solidification has been used to stabilize mechanically the interface. GRA

N91-26281# California Inst. of Tech., Pasadena. Graduate Aeronautical Labs.
AN EXPERIMENTAL INVESTIGATION OF STRUCTURE, MIXING, AND COMBUSTION IN COMPRESSIBLE TURBULENT SHEAR LAYERS Ph.D. Thesis
Jeffery L. Hall 1991 139 p
(Grant AF-AFOSR-0155-88; AF Proj. 2308)
(AD-A235278) Avail: NTIS HC/MF A07 CSCL 21/2

Two-dimensional, compressible, turbulent shear layers are studied in a new wind tunnel facility. Both reacting and non-reacting flows are investigated, with one free stream velocity supersonic and the other subsonic. The combustion experiments are based on use of low concentrations of hydrogen, nitric oxide and fluorine gases. Side-view Schlieren photographs of these reacting and non-reacting flows appear devoid of the 2-D, large scale structures seen in incompressible flow. Comparison with all-subsonic flows produced in the same facility suggests that this lack of two-dimensional structure is due to the presence of the supersonic high-speed free stream velocity. Travelling shock and expansion waves are observed in the high compressibility flows, evidently created by turbulent structures convecting at supersonic velocities. Such waves are seen only in the low-speed fluid, with apparent convection velocities much higher than those predicted on the basis of isentropic pressure-matching arguments. The measured shear layer growth rates agree with previous results by other experiments, except for a few cases at low compressibility and low density ratio. The fast chemistry regime is attained in some of the high compressibility flows tested. Flip experiments conducted in this regime indicated that the volume fraction of mixed fluid in the layer is substantially reduced as compared to previous incompressible results. GRA

N91-26282# Texas A&M Univ., College Station. Dept. of Chemistry.
THERMAL DEGRADATION CHEMISTRY OF POLY(DIPHENOXY PHOSPHAZENE) Technical Report No. 8, 1 Jun. 1989 - 31 May 1990
Shawn Maynard, Tom Sharp, and James F. Haw 25 Apr. 1991 9 p
(Contract N00014-88-K-0239)
(AD-A235284) Avail: NTIS HC/MF A02 CSCL 07/6

The thermal degradation of poly(diphenoxy phosphazene) has been reexamined with emphasis on the roles of P-Cl and P-OH weak links. The polymers studied had residual chlorine contents of less than 0.05, 2.4, and 9.9 percent. Thermal degradations were performed either in a synamic mode on the direct insertion probe of a mass spectrometer or under isothermal conditions in sealed ampules at temhperatures up to 40 C. Several model compounds (products observed from the synamic degradation of the polymers) were also subjected to isothermal degradation in order to better distinguish between primary and secondary products. The primary degradation products included chlorine-containing cyclic trimer and tetramer species, which were themselves too unstable to be observed in isothermal degradation of the cyclic oligomers rather than as a primary product from polymer chain ends, as had been previously suggested. Hydrolysis of P-Cl weak links was obtained only with difficulty, requiring steam treatment. Steam hydrolysis reduced the thermal stability of polymers with high initial P-Cl contents. GRA

N91-26283# Aerodyne Research, Inc., Billerica, MA.
BORON COMBUSTION MODEL DEVELOPMENT WITH KINETIC SENSITIVITY ANALYSIS AND MEASUREMENT OF KEY CHEMICAL RATE PARAMETERS Final Report, 1 Jan. 1988 - 31 Dec. 1990
R. C. Brown, C. E. Kolb, S. Y. Cho, R. A. Yetter, and H. R. Rabitz Jan. 1991 109 p
(Contract F49620-88-C-0048)
(AD-A235309; AFOSR-91-0387TR) Avail: NTIS HC/MF A06 CSCL 07/4

Kinetic models are presented for the chemically facilitated gasification of the ubiguitous boron oxide coating that inhibits particulate boron ignition and the second stage high temperature boron surface burning that occurs once the oxide coating has been removed. These models include a homogeneous gas phase oxidation mechanism consisting of 19 chemical species and 58 forward and reverse elementary reactions, multicomponent gas phase diffusion and heterogeneous reactions between gas phase oxidation products and the boron oxide/boron surface. Kinetic mechanisms are formulated to describe the heterogeneous surface reactions for both B2O3(1) and B(s) surfaces in terms of simple adsorption and desorption reaction steps. Thermochemical parameters for these reaction steps are estimated from the current heats of formation and gas phase bond energies for the major reactants. Reaction rate parameters are estimated from available experimental data or using elementary transition state theory arguments. GRA

N91-26284# Rensselaer Polytechnic Inst., Troy, NY. Dept. of Chemical Engineering.
TRANSPORT PROCESSES AND INTERFACIAL PHENOMENA IN AN EVAPORATING MENISCUS
M. Sujanani and P. C. Wayner, Jr. 1991 16 p Presented at the ASME/AIChE/ANS National Heat Transfer Conference, Minneapolis, 26-31 Jul. 1991
(Contract DE-FG02-89ER-14045)
(DE91-005561; CONF-910739-2) Avail: NTIS HC/MF A03

When a liquid film wets a solid surface, a contact line region is formed where the vapor, liquid and solid phases are in close proximity. The film thickness in this region varies from about 10 micron (Capillary Meniscus) to less than about 100 nm (Adsorbed film). In addition to being functions of temperature and pressure (as for a bulk phase), the thermodynamic properties (e.g., chemical potential) of these thin films depend on their shape (curvature) and thickness due to surface forces. The coupled transport processes and interfacial phenomena occurring in this microscopic region are also controlled by these surface forces. The objective is to report experimental data which complement earlier analytical models of this region. The experimental setup consists of a flat silicon plate partially immersed at a small angle, theta, in a pool of liquid. The plate is in a closed cell and a spreading liquid (1,1,2-Trichloro trifluoro ethane), in equilibrium with its own vapor, forms a zero contact angle with the plate. The plate can be electrically heated at the upper end by supplying power to a thin, rectangular platinum heater which is painted on the backside of the silicon wafer. The meniscus thickness profile, which is related to the effective pressure in the liquid, was used as a probe for understanding the sensitivity of the meniscus to the non-equilibrium effects associated with evaporation/condensation mechanisms. DOE

N91-26285# Sandia National Labs., Albuquerque, NM.
SURFACE CHEMKIN (VERSION 3.7): A FORTRAN PACKAGE FOR ANALYZING HETEROGENEOUS CHEMICAL KINETICS AT A SOLID-SURFACE-GAS-PHASE INTERFACE
M. E. Coltrin, R. J. Kee, and F. M. Rupley (Sandia National Labs., Livermore, CA.) Aug. 1990 145 p
(Contract DE-AC04-76DP-00789)
(DE91-010840; SAND-90-8003) Avail: NTIS HC/MF A07

Chapter 2 introduces the formalism developed to describe surface chemistry behavior. Unlike for gas-phase chemistry, where much software has been written to analyze mass-action kinetics and chemically reacting flow, elementary heterogeneous reactions are nowhere else (to our knowledge) treated with the generality provided in this package. For the treatment we first had to define a systematic convention to translate heterogeneous reaction ideas into a form that was amenable to efficient computation. Chapter 3 is a compendium of important equations in heterogeneous chemical kinetics. Many of the equations are simply definitions; but, in any case, derivations are either sketchy or not given. Although some readers will find many of the equations quite familiar, we find it useful to have them stated concisely in one document. For most equations, the package contains a subroutine that, when given the variables on the right-hand side, returns the variable on the left. Below some of the equation numbers is stated (in brackets) the name of the subroutine that provides information about that equation. Chapter 4 explains the mechanics of using these software packages and describes the job-control logic for running a typical problem. Chapter 5 explains the Surface Chemkin Interpreter and how to set up the required symbolic input to define a reaction mechanism. We have allowed the possibility of including multiple site types and multiple mixtures of bulk species. Each site type and bulk mixture may contain several species. Therefore, the data structures needed to refer to the phases and the species can be complex. Chapter 6 provides detailed information on the computational data structures that we use to refer to phases and species in each phase. Chapters 7 and 8 describe the Surface Subroutine Library, Chapter 7 being composed of short descriptions for quick reference and Chapter 8 explaining the input and output in the call sequence. DOE

N91-26286# Harvard Univ., Cambridge, MA.
FUNDAMENTAL STUDIES OF CARBENES AND HYDROCARBON RADICALS
P. Thaddeus and C. Gottlieb Apr. 1991 15 p
(Contract DE-FG02-88ER-13912)
(DE91-011029; DOE/ER-13912/3) Avail: NTIS HC/MF A03

Our research program provides definitive spectroscopic identification, highly accurate spectroscopic constants in the lowest vibrational states of the ground electronic state, and accurate structures of many of the important reactive intermediates in combustion chemistry. In the production of polycyclic aromatic hydrocarbons and soot in flames of aliphatic fuels, the rate controlling steps are the reactions responsible for ring formation. Mechanisms of these key reactions not yet understood, are believed to involve highly reactive hydrocarbons that result from pyrolysis of the fuel, but little is known about most of these reactive species and their structures have generally not yet been

determined. What is needed is high resolution spectroscopy, best achieved between the microwave and ir region of the spectrum (i.e., the millimeter and submillimeter regions) because of the excellent sensitivity, and ease of predictability and identification of pure rotational spectra. A further advantage of millimeter and submillimeter-wave over other wavelength regions is that, owing to high symmetry, gases such as acetylene, allene, and benzene have no permanent dipole moments and therefore no interfering transitions. DOE

N91-26287# Ames Lab., IA.
CROSS-LINKING AND MODIFICATION OF CYTOCHROME c WITH REDOX-ACTIVE METAL COMPLEXES Ph.D. Thesis
A. Lukes 2 May 1991 68 p
(Contract W-7405-eng-82)
(DE91-012023; IS-T-1522) Avail: NTIS HC/MF A04

This thesis consists of two parts. The first part shows that a redox-active trinuclear metal cluster may be used as a cross-linking reagent for proteins. Electron transfer is observed in the protein oligomers. The second part involves labelling the cysteine residue of baker's yeast cytochrome c with chloromercuriferrocene. Chloromercuriferrocene reacts with cytochrome c in two interesting ways. Symmetrization produces two products; two proteins cross-linked with mercury and diferrocenylmercury. Simple substitution of FeHgCl onto the protein followed by the addition of a proton by electrophilic substitution affords ferrocene and the mercuric chloride modified protein. DOE

N91-26288# California Univ., Santa Barbara. Quantum Inst.
THE CHEMISTRY OF SODIUM WITH SULFUR IN FLAMES
M. Steinberg and K. Schofield Feb. 1991 52 p
(Contract DE-FG21-86MC-23135)
(DE91-002060; DOE/MC-23135/2980) Avail: NTIS HC/MF A04

An experimental and analytical program examining sodium/sulfur chemistry has been conducted in a series of fuel rich and lean H2/O2/N2 flames, with and without added sulfur, and covering a wide range of temperatures and stoichiometries. Fluorescence measurements of OH and Na downstream profiles and sodium line reversal temperatures provided a broad data base for kinetic modeling. Analysis indicated NaSO2 to be the only significant sodium/sulfur product formed in the lean flames. Even so, its concentrations remain an extremely small fraction of the total sodium. The more important perturbation of the distribution of sodium over its molecular forms results from the catalytic effect of sulfur on the flame radical concentration levels rather than the formation of additional species. A bond dissociation energy of (Na-SO2) = 197 + or - 20 kJ/mol is derived assuming a non-planar structure or 210 + or - 20 kJ/mol if the molecule is planar. NaOS is dominant in the rich flames, coupled with small contributions from NaSO2, NaSH, NaS, and NaS2. Together, these can constitute from about 10 to 20 percent of the total flame sodium and do represent in this case an enhancement of molecular formation. Preliminary data in fuel rich C2H2/O2/N2 flames are consistent with this model. This further illustrates the general insensitivity of alkali chemistry to fuel type. DOE

N91-26289# Tufts Univ., Medford, MA. Dept. of Chemical Engineering.
ELECTROCATALYTIC STUDY OF AMMONIA SYNTHESIS AND METHANE DIMERIZATION IN HIGH TEMPERATURE SOLID ELECTROLYTE CELLS
M. Stoukides 28 Jan. 1991 8 p
(Contract DE-FG02-89CE-90048)
(DE91-009797; DOE/CE-90048/2) Avail: NTIS HC/MF A02

The dehydrogenative dimerization of methane is summarized. Two reactor cell configurations were used, and they are illustrated herein. Pt, Ag, Pd, Fe, Au, Y2O3-ZrO2/Au and SrCeO3 were investigated as catalysts using both cells. Methane conversion to ethane and ethylene in the absence of oxygen was found to be high, but in most cases carbonaceous deposits were formed. Steam co-fed with methane helped avoid these deposits. DOE

N91-26290# Northwestern Univ., Evanston, IL.
DEFECT CLUSTERING AND RELATED PROPERTIES OF OXIDES
J. B. Cohen, D. E. Ellis, and T. O. Mason Apr. 1991 5 p
(Contract DE-FG02-84ER-45097)
(DE91-011072; DOE/ER-45097/6) Avail: NTIS HC/MF A01

High temperature neutron diffraction patterns from Fe(1-x)O and Mn(1-x)O were analyzed by the Rietveld technique. The ratio of vacancies to interstitials in Fe(1-x)O, rho, was determined with a high degree of precision, enabling certain defect clusters to be eliminated from consideration. Electrical properties were modeled with 4:1 clusters at high temperatures or at Fe-rich compositions and 7:2 and 10:3 clusters as temperature or Fe content decreases. An extensive analysis of the high temperature electrical property measurements in Ba-doped La2CuO4 and Ce-doped Nd2CuO4. Each system displays an intrinsic regime where the carrier content is determined by oxygen nonstoichiometry, followed by an extrinsic electronic regime. Thereafter, however, evidence is seen of an extrinsic ionic regime, where the dopant is compensated by oxygen defects. Ultimately, a defect association regime is detected in Ba-doped La2CuO4. Self-consistent-field embedded cluster calculations on these materials and YBa2Cu3O(y) have been carried out for comparison with NMR, Moessbauer, and X-ray K-edge absorption studies. No indication is found at any geometry or local oxygen coordination for trivalent copper. Current work is focusing on vacancy ordering in YBaCu3O(y) with the aim to explore charge transfer between chain and plane sites. Proposed work for 1991/1992 is discussed. DOE

N91-26291# Pittsburgh Univ., PA. Dept. of Chemical and Petroleum Engineering.
THE SYNTHESIS OF METHANOL BY A NOVEL METHOD
V. Palekar, J. W. Tierney, and I. Wender 14 Sep. 1990 29 p Presented at the American Institute of Chemical Engineers (AIChE) Fall Annual Meeting, Chicago, 11-16 Nov. 1990
(Contract DE-FG22-89PC-89786)
(DE91-011131; CONF-901155-7) Avail: NTIS HC/MF A03

A new method for synthesizing methanol from CO and H2 in a slurry reactor is described and some recent experimental results are presented. At the temperatures and pressures used (100 to 160 C, 50 atm) the methanol product remains in the liquid phase and constitutes the bulk of the liquid phase. Small amounts of other products (less than 6 percent total) are also present. Methanol is both a reactant and a product. The reaction is believed to proceed in two steps. In the first, methanol is carbonylated to methyl formate, and then the methyl formate is hydrogenated to methanol. A homogeneous catalyst such as potassium methoxide is used for the carbonylation reaction and a heterogeneous catalyst such as copper chromite is used for the hydrogenation reaction. Rates for the concurrent reaction (both reactions taking place in the same reactor) are greater than predicted from studies of the individual reactions. The improved performance can be explained by an interaction between the two catalysts in the surface layer adjacent to the heterogeneous catalyst. DOE

N91-26292# Los Alamos National Lab., NM.
INVESTIGATION OF A HAMILTONIAN WITH TWO SOURCES OF ANISOTROPY: THE DZYALOSHINSKII-MORIYA AND SINGLE-SIZE INTERACTIONS
D. Coffey Jun. 1991 13 p Presented at the 5th Joint Magnetism and Magnetic Materials (MMM/INTERMAG) Conference, Pittsburgh, 18-21 Jun. 1991
(Contract W-7405-eng-36)
(DE91-011381; LA-UR-91-1275; CONF-910608-2) Avail: NTIS HC/MF A03

La2CuO4 is an S = 1/2 system with almost tetragonal symmetry so that there is no single site interaction term giving rise to anisotropy and the magnetic anisotropy of the system can be explained in terms of the Dzyaloshinskii-Moriya interaction. The Dzyaloshinskii-Moriya interaction can lead to weak ferromagnetism even in a system with predominantly antiferromagnetic interactions. However the closely related compounds, La2NiO4 and La2CoO4 are S = 1 and S = 3/2 systems respectively so that a single-site

interaction term is present and it is of interest to see how this interaction changes the magnetic properties of these compounds. Here the classical magnetic ground states are calculated for model Hamiltonians, appropriate to the different low temperature structural phases of the compounds, containing both interactions. DOE

N91-26293# Oak Ridge National Lab., TN.
MEASUREMENT OF THE NITROGEN TOTAL CROSS SECTION FROM 0.5 eV TO 50 MeV AND ANALYSIS OF THE 433-keV RESONANCE
J. A. Harvey, N. W. Hill, N. M. Larson, and D. C. Larson 1991 4 p Presented at the International Conference on Nuclear Data for Science and Technology, Juelich, Fed. Republic of Germany, 13-17 May 1991
(Contract DE-AC05-84OR-21400)
(DE91-012222; CONF-910503-9) Avail: NTIS HC/MF A01

High-resolution neutron transmission measurements have been made on several thicknesses of nitrogen gas samples from 0.5 eV to 50 MeV at the Oak Ridge Electron Linear Accelerator (ORELA). A preliminary R-matrix analysis has been done for resonances up to 800 keV. An R-matrix analysis of previous data was done by LANL and ENDF/B-VI, including the lowest energy resonance in (sup 14)N at 433 keV. They found a spin of 3/2 (with l = 1) and a peak cross section of 7.0 b. Analysis of the present data yield a spin of 7/2 (requiring l greater than or equal to 2) and a peak cross section of 11.5 b for this resonance. These results are important for transport calculations of neutrons through air. Scattering measurements are planned to determine the parity of this resonance. DOE

26 METALLIC MATERIALS

Includes physical, chemical, and mechanical properties of metals, e.g., corrosion; and metallurgy.

N91-26294# Argonne National Lab., IL.
CHEMICAL PHASE SEPARATION IN BINARY IRON-CHROMIUM ALLOYS
K. A. Hawick, J. E. Epperson, C. G. Windsor, and V. S. Rainey (AEA Technology, London, England) Dec. 1990 7 p Presented at the Fall Meeting of the Materials Research Society (MRS), Boston, 24 Nov. - 1 Dec. 1990
(Contract W-31-109-eng-38)
(DE91-010282; ANL/CP-70860; CONF-901105-114) Avail: NTIS HC/MF A02

A study of chromium-enriched domain growth occurring binary Fe-Cr alloys quenched from above to various temperatures within the miscibility gap has been made. We present kinetic sequences of in-situ small angle neutron scattering (SANS) data for aging times up to 75 hours on alloys containing 20, 30, and 40 atomic percent chromium. The SANS measurements are compared with partial structure functions obtained from computer simulations performed on a distributed array processor (DAP). We use a pair-potential lattice model, but simulate large systems containing up to 16 million lattice sites. We find good agreement between the scaled structure factors for our SANS data and computer simulated system. DOE

N91-26295# Systems Research Labs., Inc., Dayton, OH.
MATERIALS/MICROSTRUCTURES CHARACTERIZATION Final Report, 2 Sep. 1986 - 30 Apr. 1990
E. E. Keppler Jan. 1991 226 p
(Contract F33615-86-C-5013)
(AD-A233751; SRL-6921-F; WRDC-TR-90-4110) Avail: NTIS HC/MF A11 CSCL 11/6

Characterization research was conducted on titanium, aluminum and magnesium base alloys and nonmetallic polymers using electron-optical and light microscopy, electron microprobe, interference layer microscopy, and various light optical methods. Research was performed on twinning in TiAl. GRA

N91-26296# Army Armament Research, Development and Engineering Center, Watervliet, NY. Weapons Lab.
MICROALLOYED STEEL PREFORMS Final Report
Mara Brodsky Mar. 1991 36 p
(AD-A234039; ARCCB-TR-91012) Avail: NTIS HC/MF A03 CSCL 11/6

An analysis was conducted on two types of microalloyed steel to study their metallurgical, mechanical, and processing characteristics, and also to evaluate the suitability of utilizing these alloys as forgings for small gun tube components. The primary benefit associated with these steels is that optimum properties can be attained by direct quenching from the forging temperature. Presently, typical hot forgings must be thermally treated after forging to obtain desired properties. A test matrix was constructed to facilitate examination of the previously stated characteristics. The criteria included alloy type, heat-treatment temperature, forging reduction, tempering temperature, and bar diameter. Test results were compiled in a mechanical property data base that included hardness, tensile strength and yield strength, impact toughness, and ductile-to-brittle transition temperature. Further evaluation of these data enabled the determination of a desired processing route to achieve optimum properties. Based on the limited drawing specification requirements of only hardness, it was determined that several different processing combinations could yield acceptable results. However, for optimum properties (hardness), it was found that section thickness should be limited to one inch or less. GRA

N91-26297# Wright State Univ., Dayton, OH.
MECHANICAL BEHAVIOR AND FLOW MECHANISMS IN REFRACTORY METAL COMPOSITION Annual Report, 1 Mar. 1990 - 28 Feb. 1991
I. Weiss and R. Srinivasan 1 Apr. 1991 46 p
(Grant AF-AFOSR-0204-90; AF Proj. 3484)
(AD-A234701; AFOSR-91-0451TR) Avail: NTIS HC/MF A03 CSCL 11/6

Silicon alloy is a metastable material consisting of a silicide matrix with randomly dispersed large primary niobium dendrites and smaller secondary niobium particles. The various microstructures were studied with an SEM in the backscatter electron mode to provide atomic number contrast. Quantitative electron probe microanalysis (EPMA) using ZAF iterative corrections was carried out to identify the chemistry of the various phases. The extruded alloy consists essentially of the same phases: primary Nb dendrites and Nb3Si matrix with dispersed secondary Nb. The deformation by extrusion resulted in an elongation of the different phases in the material. GRA

N91-26298# Northwestern Univ., Evanston, IL. Dept. of Physics and Astronomy.
QUANTUM MECHANICAL APPROACH TO UNDERSTANDING MICROSTRUCTURAL AND MECHANICAL PROPERTIES OF INTERMETALLICS Annual Report, 1 Oct. 1989 - 30 Sep. 1990
Arthur J. Freeman 31 Oct. 1990 21 p
(Grant AF-AFOSR-0346-88; AF Proj. 2306)
(AD-A234702; AFOSR-91-0450TR) Avail: NTIS HC/MF A03 CSCL 11/6

The primary goal was to study and develop alloying concepts for understanding intermetallic alloys as derived from a first principles quantum mechanical approach. Thus, a major part of the effort was to study and determine ductilizing effects of alloying elements in several intermetallic compounds and to work closely with experimental efforts to evaluate the applicability of the theoretical approach to alloy design. Specifically, highly precise all-electron quantum mechanical electronic structure methods was applied to the study of a number of materials problems in order to obtain from first principles information of relevance to alloy stability and design of structural materials. Using state of the art all-electron self-consistent total energy methods which give precise solutions of the local density equations, fundamental information was sought about the structural and electronic properties of these alloys in order to predict stable and metastable phases and how alloying effects bonding, crystal ordering and crystal symmetry.

The first principles approach used here addresses questions of a metallurgical nature, such as phase stability, crystal structure, equilibrium lattice constants, and mechanical properties. For the ordered compounds, tailoring the chemistry of these alloys to obtain higher symmetry (and thus more ductile) crystalline phases is extremely important. GRA

N91-26299# Pennsylvania State Univ., University Park. Dept. of Materials Science and Engineering.
ADVANCED PROCESSING AND PROPERTIES OF HIGH PERFORMANCE ALLOYS Final Report
D. A. Koss 4 Apr. 1991 32 p
(Contract N00014-86-K-0381)
(AD-A234746; TR-18) Avail: NTIS HC/MF A03 CSCL 11/6

Progress is reviewed for a research program whose purpose was to establish a broad based understanding of the application and consequences of advanced processing techniques, especially as they influence the strength and fracture resistance of high performance structural alloys. The research areas are as follows: (1) the mechanism of strain induced void/pore linking during ductile fracture; (2) the influence of porosity of low cycle fatigue mechanics; (3) processing and properties of copper/niobium alloys; (4) the deformation of rapidly solidified titanium alloys at elevated temperatures; (5) strain path effects on fracture; and (6) a new age hardenable beta titanium alloy. GRA

N91-26300# Air Force Inst. of Tech., Wright-Patterson AFB, OH. Foreign Technology Div.
TITANIUM ALLOY INTEGRATED CENTRIFUGAL IMPELLER 5 COORDINATE COMPUTER ASSISTED MANUFACTURING TECHNOLOGY
Dianzhong Wen, Youlin Bao, and Zhongshu Ren 29 Nov. 1990 12 p Transl. into ENGLISH from Guoji Hangkong (China), no. 9, 1989 p 37-38
(AD-A234797; FTD-ID(RS)T-0754-90) Avail: NTIS HC/MF A03 CSCL 11/6

In a cooperation between the aerospace industry's No. 608 Aeroengine Research Institute and the South Motive Power and Machinery Complex, there has been successful research and an associated promoting of titanium alloy integrated centrifugal impeller 5 coordinate or axis computer assisted manufacturing (TICAM5NC) technology. Along with this, in November of 1988, it smoothly went through a ministry level technology evaluation. As far as the successful research on this new item of technology is concerned, it breaks through a big stumbling block in the process of production and test manufacture of medium and small model aviation engine centrifugal gas compressors. As far as a speed up in the development of our country's medium and small model aviation motive technology is concerned, the test manufacture of high efficiency, high pressure ratio centrifugal gas compressors will lead to a serious promotional effect. GRA

N91-26301# Carnegie-Mellon Univ., Pittsburgh, PA. Dept. of Metallurgical Engineering and Materials Science.
FUNDAMENTALS OF MECHANICAL BEHAVIOR IN INTERMETALLIC COMPOUNDS Annual Report, 1 Oct. 1989 - 30 Sep. 1989
James M. Howe and Anthony W. Thompson 1 Feb. 1991 42 p
(Grant AF-AFOSR-0033-90; AF Proj. 2306)
(AD-A235016; MEMS-ALC-14; AFOSR-91-0400TR) Avail: NTIS HC/MF A03 CSCL 11/6

Research in the first year of this program has examined mechanical behavior and creep of titanium aluminide alloys, both based on Ti3Al and TiAl, with the goal being better understanding of relationships between microstructure and mechanical properties of these intermetallic compound-based alloys. Detailed microstructural characterization has been conducted for both types of aluminide alloys. For Ta additions to TiAl alloys, which are thought to improve ductility, lowered stacking fault energy and increased twinning have been found. For a Ti3Al-based alloy, detailed stress and temperature dependences of creep have been measured, and a strong microstructural dependence of creep properties has been established. GRA

N91-26302# Massachusetts Inst. of Tech., Cambridge. Dept. of Chemistry.
HETEROGENEOUS CATALYSIS ON PLATINUM AND SELF-ASSEMBLED MONOLAYERS ON METAL AND METAL OXIDE SURFACES
T. R. Lee, Paul E. Laibinis, John P. Folkers, and George M. Whitesides 23 Apr. 1991 13 p
(Contract N00014-88-K-0731)
(AD-A235055; TR-2) Avail: NTIS HC/MF A03 CSCL 07/4

This paper describes research in two areas: heterogeneous catalysis and molecular self-assembly. The work in heterogeneous catalysis used the platinum-catalyzed hydrogenation of diolefin (diakyl) platinum (II) complexes to generate platinum surface alkyls of known structure. The structure and reactivity of these surface alkyls were inferred from characteristic processes occurring on the surface. The incorporation of deuterium from isotopically labelled protic solvents (e.g., EtOD) was particularly useful mechanistically. The technique of self-assembly was used to form organic monolayers by coordination of a ligand to a metal or metal oxide surface. In addition to the chemisorption of alkyl thiois on gold (as alkyl thiolates, RS(-)Au(+)), a number of other systems were demonstrated to give ordered organic surface species. GRA

N91-26303# Illinois Inst. of Tech., Chicago. Dept. of Metallurgical and Materials Engineering.
MICROSTRUCTURE, PLASTIC DEFORMATION AND MECHANICAL PROPERTIES OF MECHANICALLY ALLOYED NiAl AND NiAl BASED ALLOYS Annual Technical Report, 15 Feb. 1990 - 15 Feb. 1991
Marek Doliar, Philip Nash, Stanislaw Dymek, and Seung J. Hwang 12 Apr. 1991 56 p
(Grant AF-AFOSR-0152-90; AF Proj. 3484)
(AD-A235135; IIT-5-54718-1; AFOSR-91-0449TR) Avail: NTIS HC/MF A04 CSCL 11/6

Nickel aluminide (NiAl) and NiAl based alloys have been produced by mechanical alloys (MA) and hot extrusion, resulting in material which was fully dense, with a homogeneous, bimodal distribution of oxide paricles and with a fine grain size of less than 1 micrometers. Mechanical properties of the MA alloys have been studied by compression testing from room temperature to 1300 K in air. Yield strengths ranged from 1453 to 32 MPa depending on material and test temperature. The MA materials showed a considerable compressive ductility at room temperature (greater than 11.5 percent) without any microcracking being observed. A ductility minimum was observed at 800 K in all MA materials which is deduced to be due to dynamic strain aging. The effects of microstructure on the mechanical properties are discussed. Transmission electron microscopy has been carried out in order to characterize deformation mechanisms. The group of zone axes (001) slip was found to be predominant but a strong evidence of the group of zone axes (011) slip was also gathered. The occurrence of the group of zone axes (001) and (011) slip vectors satisfies general requirement for plasticity and explains significant room temperature ductility of MA NiAl. Cast NiAl has been also investigated for comparison with the MA materials. It exhibited a poor ductility (2.3 percent) and only the group of zone axes (001) dislocations were observed. The group of zone axes (001) slip provides only three independent slip systems and the number of independent slip systems is insufficient. The differences between cast and MA NiAl are discusse GRA

N91-26304# Georgia Inst. of Tech., Atlanta. School of Materials Engineering.
CYCLIC DEFORMATION, DAMAGE, AND EFFECTS OF ENVIRONMENT IN THE Ni3Al ORDERED ALLOY AT ELEVATED TEMPERATURE Final Technical Report, 1 Dec. 1987 - 1 Dec. 1990
Stephen D. Antolovich and Graham Webb 29 Mar. 1991 104 p

(Grant AF-AFOSR-0162-87; AF Proj. 2306)
(AD-A235168; AFOSR-91-0446TR) Avail: NTIS HC/MF A06 CSCL 11/6

The objective of this study is an experimental determination of the effect of composition, temperature, and environment of the fatigue crack propagation resistance of Ni3Al polycrystalline alloys. An analytical model for yield strength is introduced. The model utilizes a thermodynamic framework which is consistent with presently observed characteristics of yielding in Ni3Al, including strain rate independence and thermal reversibility. Two alloy compositions were evaluated with the same equivalent stoichiometry and processing history. Both alloys were single phase, substoichiometric B-doped compositions, one binary Ni-Al, one ternary Ni-Al-Cr. The mean linear intercept grain size of the ternary alloy was 3 times smaller than that of the binary alloy. An additional heat treatment was used to grow identical grain sizes in the binary and ternary alloys. These alloys were then used to evaluate the Chromium effect on the elevated temperature deformation properties. The materials were subjected to tensile cyclic loads and fatigue crack propagation testing at ambient and elevated temperature in both air and vacuum environments. Results from static and cyclic testing indicated that the grain boundary cohesive strength of the Ni-Al-Cr ternary alloys was lower than that of the Ni-Al alloys at ambient temperatures. At elevated temperatures stress-assisted oxygen diffusion along grain boundaries significantly reduces the grain boundary strength of the Ni-Al alloys and results in degradation of the mechanical properties. GRA

N91-26305# Aerospace Corp., El Segundo, CA. Lab. Operations.
LIFETIMES AND FAILURE MECHANISMS OF W/Re HAIRPIN FILAMENTS
Kenneth T. Luey 26 Feb. 1991 31 p
(Contract F04701-88-C-0089)
(AD-A235199; TR-0090(5945-09)-1; SSD-TR-91-06) Avail: NTIS HC/MF A03 CSCL 11/6

A life test of tungsten or tungsten alloys hairpin filaments used in a high-reliability electron beam instrument has been carried out to improve knowledge of filament life and failure mechanisms as a function of temperature. These filaments are made of non-sag tungsten/3 percent rhenium (W/3 percent Re) wire. A steep reduction in filament life is observed at 2760 K which is not predicted by models which assume thermal evaporation as the principal failure mechanism. Failure analysis of the filaments shows that the sudden loss of life at 2760 K is the result of localized formation of hot spots caused by the accumulation of voids at grain boundaries. Examination of the crystal growth rates indicates that the recrystallization temperature, occurs near 2760 K for the non-sag W/3 percent Re wire used in these filaments. This suggests that void accumulation acts as the principal life-limiting failure mechanism; spontaneous recrystallization at 2760 K increases the rate of voids growth and causes a severe reduction of filament life. GRA

N91-26306# Naval Air Development Center, Warminster, PA. Air Vehicle and Crew Systems Technology Dept.
MECHANICAL PROPERTIES OF SPRAY ATOMIZED SIC PARTICLE REINFORCED ALUMINUM-TITANIUM ALLOYS Final Report, Oct. 1989 - Oct. 1990
E. J. Lavernia, T. Chanda, F. A. Mohamed, and W. E. Frazier 31 Dec. 1990 29 p
(AD-A235231; NADC-90119-60) Avail: NTIS HC/MF A03 CSCL 11/6

In the present study, the elevated temperature mechanical behavior and microstructure of Al-Ti-Silicon carbide particulates SiCp metal matrix composites (MMCs) processed by spray atomization and co-deposition were investigated. The elevated temperature mechanical properties of the spray deposited and hot extruded materials were studied following a 100 hour exposure at 250, 350, 450 C; the mechanical properties at room temperature were also determined. The results of the present study show that the elevated temperature yield strength of the spray deposited and extruded materials compared favorably to those of an equivalent alloy made by powder metallurgical materials, were superior to those of the ingot material, but were inferior to those of mechanically alloyed Al-Ti materials. The evolution of the microstructure as a result of the thermal annealing was investigated using X-ray diffraction, TEM, and optical microscopy. The results from X-ray diffractometry studies showed extensive precipitation of the equilibrium Al3Ti phase during thermal exposure. In addition, no interfacial reactions were observed in Al-Ti-SiCp samples annealed at 500 C for 24 hrs. GRA

N91-26307# California Univ., Irvine.
GRAIN BOUNDARY CAVITATION PROCESSES IN A Ni3Al ALLOY AT ELEVATED TEMPERATURES Final Report, 1 Jul. 1989 - 30 Dec. 1990
James C. Earthman and Enrique J. Lavernia 25 Mar. 1991 65 p
(Grant AF-AFOSR-0435-89)
(AD-A235279; AFOSR-91-0398TR) Avail: NTIS HC/MF A04 CSCL 11/6

Fundamental studies of directional solidification and the mechanisms of intergranular cavitation in an advanced Ni3Al allow have been conducted. The experimental program includes a detailed examination of the growth kinetics of grain boundary cavities that lead to high temperature rupture. The results obtained have been analyzed and compared to those anticipated from existing theoretical models. GRA

N91-26308# Argonne National Lab., IL.
ADSORPTION OF AMMONIA ON IRON CLUSTERS
G. P. Das 1991 14 p
(Contract W-31-109-eng-38)
(DE91-011125; ANL/PP-66981) Avail: NTIS HC/MF A03

We describe here some preliminary calculations to shed light on the nature of interactions in small absorbate systems, in particular, ammonia with iron clusters. The calculations are based on an approximate ab initio formalism accompanied by several simplifying assumptions, and predict significant bonding. DOE

N91-26309# Ames Lab., IA.
EPITAXY OF METAL ATOMS ON METAL SURFACES: DEPOSITION AND DIFFUSION Ph.D. Thesis
D. E. Sanders 16 Apr. 1991 199 p
(Contract W-7405-eng-82)
(DE91-011142; IS-T-1530) Avail: NTIS HC/MF A09

We have investigated the dynamics of adsorption of a metal atom on a FCC(001) metal substrate of the same atom type. Two points were considered in detail: (1) the extent of ballistic or transient mobility (i.e., ability of the adatom to transform kinetic energy gained by adsorption into motion parallel to the substrate); (2) convergence of results with the number of moving atoms retained in the simulation. Using the molecular dynamics technique with four different types of potential energy surfaces (PES), we have discovered there is no transient mobility for the Cu/Cu(001) system at a surface temperature of 80 K and an incident gas atom kinetic energy of 0.25 eV. We have also discovered an important pitfall in such simulations: use of an insufficient number of active substrate layers leads to incorrect results displaying significant ballistic motion of the adsorbate. Using our most accurate many-body density functional based MD/MC-CEM PES and retaining sufficient number of active layers, we have also found an absence of transient mobility for the Ni/Ni(001), Rh/Rh(001), Pd/Pd(001), Pt/Pt(001), and Au/Au(001) systems. Only the Ag/Ag(001) system, with a very small diffusion barrier, was found to display any mobility. DOE

N91-26310# Argonne National Lab., IL.
MECHANICAL BEHAVIOR OF NANOCRYSTALLINE Cu, Pd, AND Ag SAMPLES
G. W. Nieman, J. R. Weertman (Northwestern Univ., Evanston, IL.), and R. W. Seigel Mar. 1991 11 p Presented at the Annual Meeting and Exhibition of the Minerals, Metals and Materials Society (TMS), New Orleans, 17-21 Feb. 1991

(Contract W-31-109-eng-38)
(DE91-011747; ANL/CP-72791; CONF-910202-14) Avail: NTIS HC/MF A03

Bulk samples of Cu with grain sizes in the range of 5 to 61 nm were produced from high purity Cu by inert gas condensation (IGC) in vacuum (approximately 10(exp -5) Pa), and samples of Cu-Cu2O with grain sizes of 5 to 7 nm were produced by IGC followed by consolidation in air. Samples produced by IGC from a Cu-7 at. (percent) Si alloy and consolidated in vacuum have grain sizes of 8 to 20 nm and small to negligible Si contents. Densities of all samples range from 82 to 99 (percent) of standard density. Mechanical properties measurements on nanocrystalline Cu and Pd samples show that strength is increased over that of conventional material, with a slight 1/(radical)d dependence. Two nanocrystalline Ag samples (21,51 nm) show apparent work hardening. Constant load creep tests performed at room temperature on nanocrystalline Cu and Pd indicate logarithmic creep typical of coarse-grained samples. High resolution electron microscopy shows nanostructural features, including multiple twinning, that may influence strain behavior. DOE

N91-26311# California Univ., Berkeley. Lawrence Berkeley Lab.
THE CRYOGENIC MECHANICAL PROPERTIES OF VINTAGE 3 Al-Li-Zr ALLOY 2090-T81
D. Chu and J. W. Morris, Jr. Feb. 1991 24 p Presented at the Annual Meeting and Exhibition of the Minerals, Metals and Materials Society (TMS), New Orleans, 17-21 Feb. 1991
(Contract DE-AC03-76SF-00098)
(DE91-011897; LBL-29395; CONF-910202-15) Avail: NTIS HC/MF A03

The cryogenic mechanical properties of a 12.7 mm (0.5 in.) Vintage III 2090-T81 (Al-3.05Cu-2.16Li-0.11Zr in weight percent) plate material are studied. The results indicate that the through-thickness and in-plane anisotropies in the yield strength of Vintage I 2090-T81 are reduced in the Vintage III material by utilizing a partial recrystallization step during the thermomechanical processing, but at some cost to the elongation and cryogenic fracture toughness. Sharp discontinuities in the microstructure resulting from this thermomechanical treatment give rise to distinct differences in the mechanical behavior between those regions that undergo recrystallization and those that do not. The reduced ductility observed in Vintage III 2090-T81 relative to Vintage I 2090-T81 is a result of an overall decrease in slip homogeneity and subsequent work hardening ability, while the reduced cryogenic toughness is due in part to the disruption of the monolithic unrecrystallized grain structure previously observed in Vintage I 2090-T81. A comparative study between the microstructural and mechanical properties of the two vintages of 2090 indicates that a fully unrecrystallized structure is essential for excellent cryogenic toughness. DOE

N91-26312*# National Aeronautics and Space Administration. Marshall Space Flight Center, Huntsville, AL.
THE CORROSION PROTECTION OF 2219-T87 ALUMINUM BY ANODIZING
M. D. Danford Jun. 1991 30 p
(NASA-TM-103540; NAS 1.15:103540) Avail: NTIS HC/MF A03 CSCL 11F

Various types of anodizing coatings were studied for 2219-T87 aluminum. These include both type II and type III anodized coats which were water sealed and a newly developed and proprietary Magnaplate HCR (TM) coat. Results indicate that type II anodizing is not much superior to type II anodizing as far as corrosion protection for 2219-T87 aluminum is concerned. Magnaplate HCR (TM) coatings should provide superior corrosion protection over an extended period of time using a coating thickness of 51 microns (2.0 mils). Author

N91-26313*# Fisk Univ., Nashville, TN. Dept. of Physics
US AND FOREIGN ALLOY CROSS-REFERENCE DATABASE Final Report
John M. Springer and Steven H. Morgan 31 May 1991 150 p
(Contract NAS8-36166)
(NASA-CR-184166; NAS 1.26:184166) Avail: NTIS HC/MF A07 CSCL 11F

Marshall Space Flight Center and other NASA installations have a continuing requirement for materials data from other countries involved with the development of joint international Spacelab experiments and other hardware. This need includes collecting data for common alloys to ascertain composition, physical properties, specifications, and designations. This data is scattered throughout a large number of specification statements, standards, handbooks, and other technical literature which make a manual search both tedious and often limited in extent. In recognition of this problem, a computerized database of information on alloys was developed along with the software necessary to provide the desired functions to access this data. The intention was to produce an initial database covering aluminum alloys, along with the program to provide a user-interface to the data, and then later to extend and refine the database to include other nonferrous and ferrous alloys. Author

N91-26314# Westinghouse Electric Corp., Pittsburgh, PA. Science and Technology Center.
PRECIPITATION IN ALLOY 718: A COMBINED AEM AND APFIM INVESTIGATION
M. G. Burke and M. K. Miller (Oak Ridge National Lab., TN.) 1991 14 p Presented at the Special Emphasis Symposium on Superalloys 718, 625, and Various Derivatives, Pittsburgh, 23-26 Jun. 1991
(Contract DE-AC05-84OR-21400)
(DE91-009918; CONF-910614-3) Avail: NTIS HC/MF A03

The desirable mechanical properties of nickel-base superalloy Alloy 718 are associated with a complex multiphase microstructure that is produced by a multistage heat treatment. The primary matrix strengthening phases (gamma double prime) and (gamma prime) and grain boundary phases (delta and Laves) formed during various aging treatments were characterized by a combination of analytical electron microscopy and atom probe field ion microscopy. Detailed structural and chemical analyses were performed to identify the phases and provide information concerning the precipitation sequence for the primary (gamma double prime) and delta phases. The results have revealed that there is a wide variation in the composition of the phases and that their compositions are affected by the thermal treatment and location within the complex microstructure. DOE

N91-26315# Edgerton, Germeshausen and Grier, Inc., Idaho Falls, ID.
CURRENT DISTRIBUTION MODELING FOR NOVEL ALUMINA ELECTROLYSIS
D. P. Ziegler (Aluminum Co. of America, Alcoa Center, PA.) 1991 11 p Presented at the American Institute of Mining Engineers (AIME) Meeting, New Orleans, 17-21 Feb. 1991 Prepared in cooperation with Aluminum Co. of America, Alcoa Center, PA
(Contract DE-FC07-89ID-12848)
(DE91-010060; EGG-M-91092; CONF-9102101-1) Avail: NTIS HC/MF A03

One-, two- and three-dimensional secondary current distributions are calculated for anode designs and electrolysis being investigated for a novel alumina electrolysis process using a three dimensional or extended area anode design. Agreement with measured polarization is good. The results indicate that for a particular configuration and electrolyte, the maximum local current density will be 28 pct. of the superficial current density. An alternative design giving a maximum of 15 pct. of the superficial current density was also investigated with the models. Evaluation of some other electrolyte systems indicates that they will not be suitable for use in the high surface area configuration. DOE

N91-26316# Oak Ridge National Lab., TN.
EFFECT OF BACTERIAL BIOFILMS ON CARBON STEEL PIT PROPAGATION IN PHOSPHATE CONTAINING MEDIUM
M. J. Franklin and D. C. White (Tennessee Univ., Knoxville.)

1990 22 p Presented at the International Congress on Microbially Influenced Corrosion, Knoxville, 7-12 Oct. 1990
(Contracts DE-AC05-84OR-21400; DE-AC02-76CH-00016)
(DE91-010806; CONF-9010138-2) Avail: NTIS HC/MF A03

Chemical corrosion inhibitors are commonly added to aqueous systems to minimize the oxidation of steel. The efficacy of certain inhibitors may be reduced by bacteria. The effect of microbial biofilms on carbon steel corrosion inhibition by phosphate was analyzed, using the scanning vibrating electrode technique (SVET) and monitoring of open circuit potential. Previous results have shown that in sterile medium containing 0.2 mM phosphate, as well as 1.0 mM chloride and 0.2 mM sulfate, carbon steel samples showed small anodic sites which subsequently became inactive. Whereas, in the presence of bacteria pits failed to become inactive and continued to propagate. Comparisons between viable bacteria and formaldehyde fixed bacteria on the pit propagation was analyzed. The results indicated that biofilms containing viable bacteria and fixed bacteria could cause pits to propagate. The time required for pit propagation was dependent on the concentration of bacteria as well as the viability of the bacteria. The results indicate that bacterial biofilms can cause pits, initiated by chemical corrosion, to continue to propagate either by reducing the efficacy of phosphate as a corrosion inhibitor or by maintaining the aggressive environment within pits. DOE

N91-26317# Oak Ridge National Lab., TN.
PERFORMANCE OF A 22Cr-20Ni-18Co-Fe ALLOY FOR SERVICE TO 870 C
R. W. Swindeman and T. H. Krukemyer (Toledo Univ., OH.) 1991 12 p Presented at the American Society of Mechanical Engineers (ASME) Pressure Vessels and Piping Conference, San Diego, 23-27 Jun. 1991
(Contract DE-AC05-84OR-21400)
(DE91-011366; CONF-910602-31) Avail: NTIS HC/MF A03

Tensile, creep, relaxation, and cyclic tests were performed on a 22Cr-20Ni-18Co-Fe alloy that was a candidate for the fabrication of a tubesheet to support ceramic particulate barrier filters in a hot-gas cleanup system. The tubesheet was expected to operate at temperatures to 870 C, and the duty cycle involved several hundred thermal cycles. Tensile data and vendor creep data were used to formulate a simple deformation model to describe tensile and creep behavior. The applicability of the model to problems involving relaxation and cyclic hardening was examined and an assessment was made regarding the importance of hardening and recovery at temperatures in the range 800 to 870 C. Finally, the model was applied to the problem of stress versus strain response during thermal cycling between 300 and 870 C. Results were compared with experimental thermal cycling test results and reasonable agreement was obtained. A stress rupture correlation based on vendor-supplied data was then produced and used to calculate life damage summation for three creep-fatigue tests at 870 C. It was found that the experimentally observed lives were substantially greater than those calculated from linear damage summation. Thus linear damage summation was judged to be a conservative approach to life prediction for thermal cycling conditions of the tubesheet. DOE

N91-26318# Lawrence Livermore National Lab., CA.
STRAIN ENHANCED MICROSTRUCTURAL EVOLUTION
M. L. Meier, A. K. Mukherjee (California Univ., Davis.), and D. R. Lesuer Feb. 1991 36 p
(Contract W-7405-eng-48)
(DE91-011921; UCRL-CR-106563) Avail: NTIS HC/MF A03

The elevated temperature deformation behavior of Ti-6Al-4V was investigated in the temperature range between 775 and 925 C and true strain rates 2 x 10(exp -5) to 0.05 s(exp -1). Region 3 was characterized by m = 0.13 and q = 602 kJ/mole. Region 2 is subdivided into a low temperature region 2a and a high temperature region 2b. Region 2a is characterized by m = 0.77, Q = 216 kJ/mole and relatively low ductility while region 2b is characterized by n = 1.3, an identical value of Q and high ductility. Low and high Beta-phase proportions are responsible for regions 2a and 2b, respectively. An apparent region 1 was accounted for by concurrent grain growth utilizing a grain size sensitivity parameter that is dependent on the Beta-phase volume fraction. The strain rate temperature regimes of regions 2a, 2b and 3 are illustrated in a region map. DOE

N91-26319# Sandia National Labs., Albuquerque, NM.
GRAIN BOUNDARY CHEMISTRY IN Al-Cu METALLIZATIONS AS DETERMINED BY ANALYTICAL ELECTRON MICROSCOPY
J. R. Michael, A. D. Romig, Jr., and D. R. Frear 1991 16 p Presented at the Spring Meeting of the Materials Research Society (MRS), Anaheim, 29 Apr. - 3 May 1991
(Contract DE-AC04-76DP-00789)
(DE91-012007; SAND-91-0933C; CONF-910406-6) Avail: NTIS HC/MF A03

Al with additions of Cu is commonly used as the conductor metallizations for integrated circuits (ICs). As the packing density of ICs increases, interconnect lines are required to carry ever higher current densities. Consequently, reliability due to electromigration failure becomes an increasing concern. Cu has been found to increase the lifetimes of these conductors, but the mechanism by which electromigration is improved is not yet fully understood. In order to evaluate certain theories of electromigration it is necessary to have a detailed description of the Cu distribution in the Al microstructure, with emphasis on the distribution of Cu at the grain boundaries. In this study analytical electron microscopy (AEM) has been used to characterize grain boundary regions in an Al-2 wt pct Cu thin film metallization on Si after a variety of thermal treatments. The results of this study indicate that the Cu distribution is dependent on the thermal annealing conditions. At temperatures near the theta phase CuAl2 solvus, the Cu distribution may be modelled by the collector-plate mechanism, in which the grain boundary is depleted in Cu relative to the matrix. At lower temperatures, Cu enrichment of the boundaries occurs, perhaps as a precursor to second phase formation. Natural cooling from the single phase field produces only grain boundary depletion of Cu consistent with the collector-plate mechanism. The kinetic details of the elemental segregation behavior derived from this study can be used to describe microstructural evolution in actual interconnect alloys. DOE

N91-26320# Sandia National Labs., Albuquerque, NM.
METASTABLE PITTING CORROSION OF ALUMINUM, Al-Cu, AND Al-Si THIN FILMS IN DILUTE HF SOLUTIONS AND ITS RELEVANCY TO THE PROCESSING OF INTEGRATED CIRCUIT INTERCONNECTIONS
J. R. Scully (Virginia Univ., Charlottesville.) and D. E. Peebles 1991 6 p Presented at the Spring Meeting of the Materials Research Society (MRS), Anaheim, 29 Apr. - 3 May 1991
(Contract DE-AC04-76DP-00789)
(DE91-012014; SAND-90-3144C; CONF-910406-7) Avail: NTIS HC/MF A02

We have investigated the pitting corrosion of Al, Al-Cu, and Al-Si thin films in dilute hydrofluoric acid solution. Additions of Cu and, to a lesser extent, Si cause an increase in open circuit potentials (OCP), pit densities and pit sizes as compared to pure Al. Pits in Al-Cu alloys are associated with Cu depleted grain boundaries which are galvanically coupled to adjacent (theta)-phase precipitates. Pits formed in Al-Si alloys are associated with the Al matrix which is galvanically coupled to Si nodules. Theta Al2Cu has different electrochemical characteristics than Al even though both maintain a thin Al surface oxide. Theta Al2Cu has a more positive OCP, above the average pit repassivation potential for pure Al. Since theta Al2 Cu supports cathodic reactions at enhanced rates compared to pure Al, its presence raises the potential of the adjacent pure Al grain boundary to values near its average breakdown potential and above its average repassivation potential. DOE

N91-26321# Oak Ridge National Lab., TN.
ENVIRONMENTAL EMBRITTLEMENT OF ORDERED INTERMETALLIC ALLOYS AT ROOM TEMPERATURE IN MOIST ATMOSPHERES
C. T. Liu 1991 10 p Presented at the 6th Japan Institute of

Metals (JIM) International Symposium on Intermetallic Compounds: Structure and Mechanical Properties, Sendai (Japan), 17-20 Jun. 1991
(Contract DE-AC05-84OR-21400)
(DE91-012051; CONF-9106146-5) Avail: NTIS HC/MF A02

This paper provides a comprehensive review of recent research on environmental embrittlement of ordered intermetallic alloys at ambient temperatures. Ordered intermetallics containing reactive elements such as Al, Si, Ti and V exhibit a severe reduction in ductility when tested in moisture-containing environments (e.g., moist air), instead of dry environments. The embrittlement involves the reaction of the reactive elements with moisture in air and generation of atomic hydrogen at crack tips. The loss in ductility is generally accompanied by a change in fracture mode from ductile rupture to brittle grain-boundary fracture in fcc-ordered intermetallics, and to brittle cleavage in bcc-ordered intermetallics. The underlying mechanisms of the hydrogen embrittlement are also discussed in this paper. DOE

N91-26322# Oak Ridge National Lab., TN.
TEM IN-SITU STRAINING OF B2 COMPOUNDS
Ian Baker, P. Nagpal, S. Guha (Materials and Electrochemical Research Corp., Tucson, AZ.), and J. A. Horton 1991 6 p Presented at the 6th Japan Institute of Metals (JIM) International Symposium on Intermetallic Compounds: Structure and Mechanical Properties, Sendai (Japan), 17-20 Jun. 1991
(Contracts DE-AC05-84OR-21400; DE-AC05-76OR-00033)
(DE91-012062; CONF-9106146-3) Avail: NTIS HC/MF A02

This paper reports preliminary observations of in-situ straining experiments performed using transmission electron microscopy on thin foils of the B2 compounds FeAl and NiAl, and of a two-phase B2/(f.c.c.)L1(sub 2) alloy containing a B2 phase Ni-30Al-20Fe. The first compound slips by movement of a/2(111) dislocation pairs, whereas the latter two exhibit (100) slip. NiAl and FeAl both showed intense dislocation activity ahead of growing cracks. In both cases, slip occurred in several places within the thin foils and not just ahead of the cracks. Slip in NiAl was wavy and the ease of cross slip was such that at higher strains a cell structure formed during in-situ straining. In contrast, FeAl showed planar slip in broad bands consisting of several parallel slip planes. Ni-30Al-20Fe also exhibited planar slip, but on individual planes not in bands. Dislocation pile-ups were also observed in the latter compound. DOE

N91-26323# Oak Ridge National Lab., TN.
MICROSTRUCTURE AND HARDNESS OF NiAl/Ni2AlX TWO-PHASE ORDERED INTERMETALLIC ALLOYS
Masao Takeyama (National Research Inst. for Metals, Tokyo, Japan), C. T. Liu, and C. J. Sparks, Jr. 1991 6 p Presented at the 6th Japan Institute of Metals (JIM) International Symposium on Intermetallic Compounds: Structure and Mechanical Properties, Sendai (Japan), 17-20 Jun. 1991
(Contract DE-AC05-84OR-21400)
(DE91-012068; CONF-9106146-6) Avail: NTIS HC/MF A02

Microstructures of several NiAl/Ni2AlX two-phase alloys with a composition of Ni-35 at. percent Al-13 at. percent X (X = Ti, Zr, Hf, V, Nb, Ta) have been studied by X-ray diffraction and scanning electron microscopic analyses. The alloy with vanadium exhibits a single phase of B2 structure, and others have two phases of B2 and L2(sub 1) structures. The lattice parameter of the B2 phase in these alloys remains almost unchanged of about 2.888 (angstrom), whereas the lattice parameter of the L2(sub 1) phase in the two-phase alloys varies in the range of 5.876 to 6.110 (angstrom), depending on the atomic radii of the elements X. The lattice misfit between the two phases is the smallest (1.5 percent) in the alloy with titanium and is the largest (6.1 percent) in the alloy with zirconium. The smaller the misfit, the more stable is the microstructure at elevated temperatures. DOE

N91-26324# Boston Univ., MA. Dept. of Chemistry.
STUDY OF INTERMEDIATES FROM TRANSITION METAL EXCITED-STATE ELECTRON-TRANSFER REACTIONS
M. Z. Hoffman 31 Mar. 1991 5 p
(Contract DE-FG02-86ER-13603)
(DE91-012182; DOE/ER-13603/4) Avail: NTIS HC/MF A01

This report contains sections entitled: (1) Cage escape yields in the quenching of Ru(II) photosensitizers; (2) Characterization of one-electron reduced Ru(II) complexes; (3) Synthesis and characterization of new Ru(II) photosensitizers; (4) Reductive quenching of Ru(II) and Cr(III) complexes; and (5) Photosensitized initiation of polymerization. DOE

N91-26325# Oak Ridge National Lab., TN.
THE ROLE OF ELECTRONIC STRUCTURE IN THE MECHANICAL BEHAVIOR OF ALUMINIDES
C. L. Fu 1991 10 p Presented at the 6th Japan Institute of Metals (JIM) International Symposium on Intermetallic Compounds: Structure and Mechanical Properties, Sendai (Japan), 17-20 Jun. 1991
(Contract DE-AC05-84OR-21400)
(DE91-012508; CONF-9106146-7) Avail: NTIS HC/MF A02

First-principles calculations based on local-density-functional theory have been used together with the anisotropic elasticity theory of dislocations to study the structural and electronic properties of aluminides. The bonding mechanism can be described by the combination of charge transfer and strong p-d hybridization effects. Elastic constants, various shear fault energies, and cleavage energies are calculated to interpret the slip behavior and the brittleness of B2 alloys and trialuminides. While the brittleness of trialuminides can be attributed mainly to their low cleavage strengths, cleavage fracture of B2 alloys is, in general, related to both the cleavage strength and crack tip plasticity. The effect of interstitially absorbed H on the bonding strength of Fe-Al is also investigated. DOE

N91-27089*# Xavier Univ. of Louisiana, New Orleans. Dept. of Physics.
LIF AND EMISSION STUDIES OF COPPER AND NITROGEN Final Report
Murty A. Akundi *In* Houston Univ., NASA/ASEE Summer Faculty Fellowship Program, 1990, Volume 1 Dec. 1990 16 p (For primary document see N91-27088 18-99)
(Grant NGT-44-005-803)
Avail: NTIS HC/MF A10 CSCL 11F

27 NONMETALLIC MATERIALS

Includes physical, chemical, and mechanical properties of plastics, elastomers, lubricants, polymers, textiles, adhesives, and ceramic materials.

For composite materials see *24 Composite Materials.*

N91-26326# Idaho National Engineering Lab., Idaho Falls.
AN ANALYTICAL METHODOLOGY TO PREDICT THE COATING CHARACTERISTICS OF PLASMA-SPRAYED CERAMIC POWDERS
D. J. Varacalle, Jr. 1990 13 p Presented at the Advanced Aerospace Materials/Processes Conferences and Exposition, Long Beach, 21-24 May 1990
(Contract DE-AC07-76ID-01570)
(DE91-010088; EGG-M-90209; CONF-900593-2) Avail: NTIS HC/MF A03

Experimental and analytical studies have been conducted at the Idaho National Engineering Laboratory (INEL) to investigate gas, particle, and coating dynamics in the plasma spray process. Nine experiments were conducted using a Taguchi statistical parametric approach. The thermal plasma produced by the commercial plasma spray torch and the related plasma/particle interaction were then numerically modeled from the cathode tip to varied standoff distances in the free plume for the nine experiments, which ranged in power from 28 to 43 kW. The flow and temperature fields in the plasma were solved using the governing conservation equations with suitable boundary conditions. This information was then used as boundary conditions to solve the plasma/particle

interaction problem for the nine experiments. The particle dynamics (10 to 75 micron particles) for a yttria-stabilized zirconia powder were then simulated by computer. Particle morphology is discussed with respect to the changes in the process parameters. The predicted temperature and velocity of the zirconia particles were then used as initial conditions to a coating dynamics code. The code predicts the thickness and porosity of the zirconia coatings for the specific process parameters. The predicted coating characteristics exhibit reasonable correlation with the actual characteristics obtained from the Taguchi experimental studies. DOE

N91-26327# Air Force Inst. of Tech., Wright-Patterson AFB, OH. Foreign Technology Div.

METHOD OF OBTAINING PHENOL-FURFURAL RESINS

D. R. Tursunova, N. U. Rizayev, A. Yu. Yuldashev, and Ya. Z. Rakhman-Zade 30 Oct. 1990 7 p Transl. into ENGLISH of Russian Patent No. 423794, (27 Jun. 1972) p 1-2

(AD-A233746; FTD-ID(RS)T-0958-90) Avail: NTIS HC/MF A02 CSCL 07/6

This invention relates to improvement of a method of obtaining phenol-furfural resins utilized in different branches of the national economy as cationites (for purification of waste water from ions of calcium, magnesium, etc., sorption of different metals). A method of obtaining phenol-furfural resins by polycondensation of sulfonated phenol with furfural is known; as obtained in this case, the resin has small exchange capacity, low swelling, and insufficient strength, which causes a low quality of cationites. The target of this invention is improvement in mechanical properties of phenol-furfural resins and an increase in its exchange capacitance. GRA

N91-26328# Pennsylvania Univ., Philadelphia. Dept. of Chemistry.

SYNTHESIS, POLYMERIZATION AND THERMAL PROPERTIES OF A NEW ACETYLENE-TERMINATED SCHIFF BASE

Technical Report, 1 Jun. 1990 - 31 Oct. 1991

Yen Wei, Ramakrishnan Hariharan, and Jayanta K. Ray 29 Mar. 1991 30 p

(Contract N00014-90-J-1559)

(AD-A233806; Rept-1990-34) Avail: NTIS HC/MF A03 CSCL 07/6

A new acetylene-terminated Schiff base monomer, N,N'-(1,4-phenylene dimethylidyne) bis-(4-ethynyl aniline) (PPP), was synthesized and was characterized by nuclear magnetic resonance and infrared spectroscopy. This monomer was then polymerized to yield a new polymer (PPPP) with alternating units of aromatic imine and diacetylene via an oxidative coupling polymerization of the acetylenic terminal groups. The monomer was also polymerized by thermal curing at elevated temperatures up to 400 C to afford a crosslinked polymer network without significant structural decomposition. Thermal properties and thermal reactions of the monomer and the polymers were studied by differential scanning calorimetry (DSC) and thermogravimetric analysis (TGA). The polymers exhibit excellent thermal stabilities in an inert atmosphere. Electronic properties of the polymers are also discussed. GRA

N91-26329# Pennsylvania Univ., Philadelphia. Dept. of Chemistry.

THERMAL TRANSITIONS AND MECHANICAL PROPERTIES OF THE FILMS OF CHEMICALLY PREPARED POLYANILINE

Technical Report, 1 Jun. 1990 - 31 Oct. 1991

Yen Wei, Guang-Way Jang, Kesyin F. Hsueh, Elliot M. Scherr, and Alan G. MacDiarmid 29 Mar. 1991 30 p

(Contract N00014-90-J-1559)

(AD-A233807; Rept-1990-35) Avail: NTIS HC/MF A03 CSCL 07/3

The mechanical and thermal properties of the solution-cast films of chemically prepared polyaniline have been studied by means of dynamic mechanical analysis (DMA), differential scanning calorimetry (DSC) and thermogravimetric analysis (TGA). The glass transition temperature (Tg) of the polyaniline films in emeraldine base form was determined and characterized for the first time to be in the range of ca. 105 to 220 C for the films containing ca. 16 to 0 percent of 1-methyl 2-pyrrolidinone (NMP) residual solvent, respectively, from a decrease in the storage modulus in DMA and from DSC studies. Depending on the content of NMP, the thin films of polyaniline have a storage modulus of ca. 200 MPa to 2 GPa at temperatures below Tg. Other thermal transitions and reactions in the temperature range of ca. 25 to 500 C are also characterized by infrared spectroscopy, x-ray diffraction, and cyclic voltammetry are discussed in relation to the mechanical properties of polyaniline. GRA

N91-26330# Pennsylvania Univ., Philadelphia. Dept. of Chemistry.

POLYANILINE: PERNIGRANILINE, AN ISOLABLE INTERMEDIATE IN THE CONVENTIONAL CHEMICAL SYNTHESIS OF EMERALDINE

S. K. Manohar, Alan G. MacDiarmid, and A. J. Epstein 18 Mar. 1991 6 p

(Contract N00014-90-J-1559)

(AD-A233840; Rept-1990-13) Avail: NTIS HC/MF A02 CSCL 07/6

The conventional chemical oxidative polymerization of aniline to polyaniline in the emeraldine oxidation state using acidic ammonium peroxydisulfate (aniline:peroxydisulfate 4:1; aq. 1.ON HCl; 0 C) was found to proceed via the intermediacy of the fully oxidized pernigraniline oxidation state (readily isolable as the base form). The intermediacy of the pernigraniline oxidation state was first detected by using a novel potential profiling technique in which the oxidation potential of the system was continuously monitored as a function of polymerization time. GRA

N91-26331# Pennsylvania Univ., Philadelphia. Dept. of Chemistry.

LIGHT INDUCED ELECTRON SPIN RESONANCE IN POLYANILINE

K. Cromack, A. J. Epstein, J. G. Masters, Y. Sun, and Alan G. MacDiarmid 18 Mar. 1991 6 p

(Contract N00014-90-J-1559)

(AD-A233847; Rept-1990-18) Avail: NTIS HC/MF A02 CSCL 20/5

Light induced electron spin resonance (LESR) is reported for members of the polyaniline family of polymers. The LESR is composed of a single line at g approximately 2 whose width and intensity are dependent on the time of exposure and temperature. The LESR line intensity shows a very long growth and decay time that can be fit to a Kohlrausch stretched exponential type law with coefficients that follow a Vogal-Fulcher law. There is a direct dependence of the linewidth of the photo-induced spins on the concentration of induced spins suggesting a strong interaction between induced defects and leading to the postulation of a phase segregation of defect. GRA

N91-26332# Pennsylvania Univ., Philadelphia. Dept. of Chemistry.

X RAY STRUCTURE OF POLYANILINES

M. E. Jozefowicz, A. J. Epstein, J. P. Pouget, J. G. Masters, and A. Ray 18 Mar. 1991 6 p

(Contract N00014-90-J-1559)

(AD-A233848; Rept-1990-20) Avail: NTIS HC/MF A02 CSCL 07/6

We describe two classes of the emeraldine form of polyaniline. Class I exhibits ES-I crystal structure in the HCl salt form and in the base form it is amorphous EB-I. Class II materials form partially crystalline structures EB-II and ES-II in base and HCl salt forms, respectively. We compare structural results on emeraldine with data for partially crystalline leucoemeraldine base (LEB) and pernigraniline base (PNB) - the fully reduced and oxidized forms of polyaniline, respectively. We contrast our studies of the EB-I/ES-I system with results for poly(o-toluidine) base, POT-EB and hydrochloride, POT-ES. GRA

N91-26333# Pennsylvania Univ., Philadelphia. Dept. of Chemistry.
THERMAL STABILITIES OF POLYANILINES
J. Yue, A. J. Epstein, Z. Zhong, P. K. Gallagher, and Alan G. MacDiarmid 18 Mar. 1991 6 p
(Contract N00014-90-J-1559)
(AD-A233849; Rept-1990-23) Avail: NTIS HC/MF A02 CSCL 07/3

Thermal stabilities of chemically synthesized polyaniline insulating and conducting forms which are doped with external and internal dopants have been studied by thermogravimetry (TG). The insulating forms have higher stability than their corresponding conducting forms. Polyaniline doped externally by HCl shows two major weight losses: The first loss is assigned to removal of water and dopant, and the second one is attributed to the decompositions of the backbone. Polyaniline doped internally by SO3H only shows one major weight loss up to 600C; the doping level is stabilized by SO3H covalently bonded on the polymer backbone. Preliminary data suggest that the covalently bonded sulfonic groups on the polyaniline chain increase the stability of the polyaniline backbone for both conducting and insulating forms. GRA

N91-26334# Air Force Systems Command, Griffiss AFB, NY. Dept. of Chemistry.
SYNTHETIC METALS: A NOVEL ROLE FOR ORGANIC POLYMERS
Alan G. MacDiarmid and Arthur J. Epstein 1991 19 p Presented at the International Symposium on Specialty Polymers, Singapore, 7-9 Nov. 1990
(Contract N00014-90-J-1559; NSF DMR-88-19885)
(AD-A233862; Rept-1991-5) Avail: NTIS HC/MF A03 CSCL 07/6

The synthesis p- and n-doping of polyactylene, (CH)x, the prototype conducting polymer or synthetic metal is described together with a qualitative description of its band structure and changes in band structure on doping to yield positive and negative solitons. Other conducting polymers are briefly discussed. The polyanilines, a large class of versatile conducting polymers involving a novel non-redox doping process, considered as being of significant commercial technological importance are discussed in particular with reference to their ease of processing. Present and future technological uses of conducting polymers are noted. GRA

N91-26335# Pennsylvania Univ., Philadelphia. Dept. of Chemistry.
ELECTRON LOCALIZATION IN POLYANILINE AND ITS DERIVATIVES
Z. H. Wang, A. J. Epstein, A. Ray, and Alan G. MacDiarmid 18 Mar. 1991 6 p
(Contract N00014-90-J-1559)
(AD-A233934; TR-1990-19) Avail: NTIS HC/MF A02 CSCL 07/6

Electron localization in the HCl salt form of polyaniline (PAN-ES) and its methyl ring-substituted derivative, poly-(o-toluidine)(POT-ES0) were investigated by optical, transport and magnetic studies. Compared with PAN-ES, POT-ES has increased electron localization though the band structure, crystallinity and intrachain coherence length are similar for two polymers. The localization is proposed to be induced by a CH3 group on each C6 ring which decreases the interchain diffusion rate through reduction of interchain coherence and increased interchain separation. GRA

N91-26336# Pennsylvania Univ., Philadelphia. Dept. of Chemistry.
STRUCTURE, ORDER AND THE METALLIC STATE IN POLYANILINE AND ITS DERIVATIVES
A. J. Epstein and Alan G. MacDiarmid 18 Mar. 1991 8 p
(Contract N00014-90-J-1559)
(AD-A233935; TR-1990-21) Avail: NTIS HC/MF A02 CSCL 07/S

The origin of high conductivity in various conducting polymers remains of considerable interest. The polyaniline family of polymers provides a means of sensitively testing the effects of crystal structure, coherence, order and chain separation on the conductivity. Extensive comparative study of emeraldine hydrochloride, oriented emeraldine hydrochloride, poly(ortho-toluidine) hydrochloride, and sulfonated polyaniline demonstrate the importance of interchain diffusion of charge in achieving high conductivities. These results are in accord with magnetotransport studies of polyacetylene which similarly demonstrate the importance of three-dimensional charge diffusion. GRA

N91-26337# Pennsylvania Univ., Philadelphia. Dept. of Chemistry.
IMPEDANCE PROFILING: A CONVENIENT TECHNIQUE FOR DETERMINING THE REDOX OR PROTONIC ACID DOPING CHARACTERISTICS OF CONDUCTING POLYMERS Technical Report, 1 Jun. - 31 Oct. 1990
D. B. Swanson, Alan G. MacDiarmid, and A. J. Epstein 18 Mar. 1991 6 p Prepared in cooperation with Ohio State Univ., Columbus, OH
(Contract N00014-90-J-1559)
(AD-A233941; Rept-1990-16) Avail: NTIS HC/MF A02 CSCL 07/6

A technique for rapidly determining the conductivity of a conducting polymer film as it is doped in an aqueous or non-aqueous medium is presented. The technique is particularly useful for rapid screening of new potential dopants. It is applicable to redox or protonic acid doping. Experimental conditions can be modified to optimize conductivity and study other related effects; these optimum conditions can subsequently be used for large scale doping by conventional synthetic methods. GRA

N91-26338# Illinois Univ., Urbana-Champaign. National Center for Composite Materials Research.
CHARACTERIZATION STUDIES OF FLUORINATED EPOXY RESINS: NAVAL EXPERIMENTAL RESIN C8/1SA AS A STRUCTURAL MATERIAL AND FOR USE IN BLENDS AND COMPOSITES
T. E. Twardowski and P. H. Geil 1 Jun. 1990 78 p
(AD-A234188; UIUC-NCCMR-89-0013) Avail: NTIS HC/MF A05 CSCL 11/9

Epoxy thermosets are currently the material of choice for high performance composite materials. They have high modulus, low weight, excellent adhesion to the filler component, and high dimensional and thermal stability as well as processing characteristics much more tractable than thermoplastics. Unfortunately, epoxies are often attacked by environmental elements, especially water, resulting in a degradation of properties. As such, modification of epoxies to improve their environmental resistance is valuable consideration. Epoxy resins incorporating large fluorine contents have met this challenge, showing low contact angle, low measure uptake, and improved flame resistance. What remains is the need to investigate the suitability of such resins for use in structural materials. GRA

N91-26339# Pennsylvania Univ., Philadelphia. Dept. of Chemistry.
NOVEL CONCEPTS IN ELECTRONIC POLYMERS: POLYANILINE AND ITS DERIVATIVES
A. J. Epstein and Alan G. MacDiarmid 3 Apr. 1991 21 p
(Contract N00014-90-J-1559)
(AD-A234214; Rept-1991-6) Avail: NTIS HC/MF A03 CSCL 07/6

Polyanilines have been known for over one hundred years. Recent studies of this chemically flexible polymer have demonstrated unusual chemical, electrical, and optical phenomena, both in insulating forms and conducting forms. The polyanilines differ substanially from earlier studied polyacetylene, polythiophene, polypyrrole, polydiacetylene, and other polymers in that their electronic structure is based on the overlap of alternating nitrogen atoms and C6 rings. Two classes of the emeraldine form of polyaniline are distinguished by preparation route and crystal

structure. For both classes, the Pauli susceptibility indicative of metallic state is correlated with the formation of a three dimensionally crystalline region. Charge conduction studies oriented films and fibers demonstrate that three-dimensional order between chains is critical for high conductivities. GRA

N91-26340# Pennsylvania Univ., Philadelphia. Dept. of Chemistry.
SPECTROSCOPY AND PHOTOEXCITATION SPECTROSCOPIES OF POLYANILINE: A MODEL SYSTEM FOR NEW PHENOMENA
A. J. Epstein, R. P. McCall, J. M. Ginder, and Alan G. MacDiarmid 3 Apr. 1991 82 p
(Contract N00014-90-J-1559)
(AD-A234215; Rept-1991-7) Avail: NTIS HC/MF A05 CSCL 20/5

Spectroscopy applied to solids is well established as an important means of determining the electronic structure as well as the vibrational normal modes of solids. More recently, photoexcitation spectroscopy has been developed and applied to numerous materials. These techniques have been extensively applied to polyacetylene and other conjugated carbon backbone polymers. They have played a central role in developing an understanding of these electronic polymers. The polyanilines are a large versatile family of polymers that differ substantially from earlier studied electronic polymers. Spectroscopy plays an essential role in determining the electronic structure of these materials and how they vary with oxidation state, protonation, and derivatization. The electronic structure reflects important differences between the polyanilines and other earlier-studied electronic polymers, including the absence of charge conjugation symmetry. GRA

N91-26341# Phasex Corp., Lawrence, MA.
SUPERCRITICAL FLUID PROCESSING OF PROPELLANT POLYMERS Final Report, Sep. 1989 - Sep. 1990
James J. Watkins and Val J. Krukonis Jan. 1991 62 p
(Contract F04611-89-C-0042)
(AD-A234285; PL-TR-91-3003) Avail: NTIS HC/MF A04 CSCL 07/6

Polymeric pre-propellant binders are known to be heterogeneous materials exhibiting significant variation with respect to molecular weight, structure, functionally, and related performance properties. The objective of this program was to demonstrate the feasibility of fractionating propellant binders with supercritical fluid (SCF) solvents. Hydroxy-terminated polybutadiene (HTPB) (R-45M, Atochem North America) was fractionated with supercritical propane yielding ten fractions with number average molecular weights ranging from 780 to 11760 and polydispersities of approximately 1.2. The increase in hydroxyl equivalent weight with nonlinear, with functionality increasing rapidly in the higher molecular weight fractions. Non-functional cyclic and other low molecular weight components were effectively extracted from glycidyl azide polymer (GAP) using supercritical carbon dioxide as evidenced by HPLC analysis. GRA

N91-26342# Rensselaer Polytechnic Inst., Troy, NY. Dept. of Chemistry.
A PROGRAM IN THE CHEMISTRY OF ELECTRONIC MATERIALS. TASK 1: NEW ORGANOMETALLIC PRECURSORS FOR THE LOW PRESSURE CHEMICAL VAPOR DEPOSITION OF REFRACTORY MATERIALS FOR ELECTRONICS Final Report, 1 Jul. 1985 - 31 Dec. 1990
L. V. Interrante, J. A. Moore, and R. R. Reeves 28 Feb. 1991 13 p
(Contract N00014-85-K-0632)
(AD-A234315) Avail: NTIS HC/MF A03 CSCL 11/6

The principal focus of this Project was the design and synthesis of volatile organometallic precursors for the low pressure chemical vapor deposition (LPCVD) of AlN, SiC, and other materials of interest for applications in electronics. The pyrolytic decomposition of these compounds were investigated using mass spectrometry and IR spectroscopy and the resultant thin films examined by Auger spectroscopy and SEM/TEM to determine the composition, microstructure, and purity of the phases present. Through the use of selected precursors of this type, high quality films of stoichiometric AlN and SiC were obtained at temperatures (500 to 800 C), well below that employed in previous investigations. Thin films of both AlN and the cuprate superconductors were also prepared by pyrolysis of solution-applied polymeric precursor films. GRA

N91-26343# State Univ. of New York, Buffalo. Dept. of Chemistry.
CLUSTER BEAM DEPOSITION OF HIGH TEMPERATURE MATERIALS
William J. Herron and James F. Garvey 1991 8 p
(Contract N00014-88-K-0483)
(AD-A234358; TR-18) Avail: NTIS HC/MF A02 CSCL 09/1

The latest attempts is present which use a Smalley-type source to generate novel thin films. This technique employs entraining, within a high pressure molecular beam expansion, the products generated from laser ablation of a rotating target rod. It is shown how just such a cluster beam source can be used to generate a high temperature material within a molecular beam and deposit it intact on a relatively cool substrate. By tailoring the various expansion conditions (i.e., expansion pressure, laser fluence, type of carrier gas, pulse delay, etc.) one can drastically effect the morphology and chemical nature of the surface generated. This technique has promise that it may be able to fabricate a wide variety of thin films with obvious industrial applications such as superconducting thin films, diamond-like carbon films, patterned or multilayered thin films. GRA

N91-26344# Pennsylvania State Univ., University Park. Dept. of Chemistry.
SYNTHESIS AND STRUCTURE OF SMALL-MOLECULE CYCLIC PHOSPHAZENES BEARING ORTHO-SUBSTITUTED ARYLOXY AND PHENOXY SUBSTITUENTS
H. R. Allock, A. A. Dembek, M. N. Mang, G. H. Riding, and M. Parvez 26 Mar. 1991 39 p
(Contract N00014-91-J-1194)
(AD-A234377; TR-2) Avail: NTIS HC/MF A03 CSCL 07/3

A series of cyclic, trimeric, and tetrameric phosphazenes with ortho-substituted aryloxy side groups were synthesized. The ortho-substituents are methyl and phenyl groups. These compounds are structural models for the corresponding high polymeric phosphazenes. GRA

N91-26345# Pennsylvania Univ., Philadelphia. Dept. of Chemistry.
RING-TORSIONAL POLARONS IN POLYANILINE AND POLYPARAPHENYLENE SULFIDE
J. M. Ginder, A. J. Epstein, and Alan G. MacDiarmid 15 Mar. 1991 8 p
(Contract N00014-90-J-1559)
(AD-A234384; TR-1990-12) Avail: NTIS HC/MF A02 CSCL 07/6

The role of the dihedral angle of the backbone phenyl rings in determining the electronic structure and charge storage mechanism in polyaniline (PAN) and polyparaphenylene sulfide (PPS) is reviewed. The sensitivity of the average ring torsion angle to the effects of steric repulsion and electron delocalization is manifest in the effects of derivatization and temperature on the optical spectra of these materials. It is shown that charge is self-trapped into localized defect states in part via changes in ring angle, leading to novel ring torsional polarons which induce only one defect level into the energy gap and possess a very large kinetic mass (50 to 500 me). Evidence for the existence of these defects in PAN and PPS is discussed. GRA

N91-26346# Imperial Coll. of Science and Technology, London (England). Dept. of Chemistry.
ENERGY MIGRATION, MOTION AND ORDER IN SYNTHETIC POLYMERS Periodic Report No. 7
David Phillips 1991 13 p

(Contract DAJA87-87-C-0031)
(AD-A234403; R/D-5718-CH-01) Avail: NTIS HC/MF A03 CSCL 07/6

This report is on the final phase of the three year program of work supported under the terms of this contract. The report is divided into two sections, that dealing with evanescent wave-induced fluorescence of polymer surface interactions, and that dealing with the fluorescence of synthetic polymers in solution. The emission properties of soluble polydiacetylenes have received considerable attention over the past few years, since they exhibit dramatic solvato, thermo and electrochromic effects. The evidence for 1D exciton diffusion in conjugated polymeric systems of this type promotes investigations for the theoretical modelling as well as the technological importance in optical molecular electronics. GRA

N91-26347# Pennsylvania Univ., Philadelphia. Dept. of Chemistry.
POLYANILINE: ORIENTED FILMS AND FIBERS Technical Report, 1 Jun. 1990 - 31 Oct. 1991
E. M. Scheer, Alan G. MacDiarmid, S. K. Manohar, J. G. Masters, and Y. Sun 18 Mar. 1991 6 p
(AD-A234414; Rept-1990-14) Avail: NTIS HC/MF A02 CSCL 07/6

The dependency of the conductivity of polyaniline (emeraldine oxidation state) on its molecular weight has been determined. Uni- and biaxially oriented films and uniaxially oriented fibers of emeraldine base have been studied and the dependency of their degree of crystallinity, tensile strength, and conductivity (after doping) on draw ratio has been determined. GRA

N91-26348# Army Cold Regions Research and Engineering Lab., Hanover, NH.
LUBRICANTS AT LOW TEMPERATURES
Deborah Diemand Dec. 1990 25 p
(AD-A234536; CRREL-TD-90-1) Avail: NTIS HC/MF A03 CSCL 11/8

Lubricants represent the single most critical problem encountered by vehicles in cold regions. A vehicle lubricated for use in temperature regions will simply not operate in an extremely cold environment. A chunk of heavy gear oil can be used to pound nails at -40C. Thus, it is of the utmost importance to ensure that all lubricants used in the vehicle be chosen with low-temperature operation in mind, including engine oil, gear oil, grease transmission fluid, hydraulic fluid, and brake fluid. Lubricants must have a sufficiently low viscosity for low-temperature use and must also be able to diffuse over all surfaces requiring lubrication and to permeate the pores and surface cracks of metals. The use of unsuitable lubricants may result in channeling, dry gears and bearings, difficult starting and shifting, quick wear, and deterioration of engines, engine attachments, and chassis. GRA

N91-26349# Texas A&M Univ., College Station. Dept. of Chemistry.
IONICALLY AND ELECTRONICALLY CONDUCTIVE COMPOSITE POLYMER MEMBRANES Final Report, 1 Apr. 1987 - 30 Jun. 1990
Charles R. Martin Feb. 1991 5 p
(Grant AF-AFOSR-0173-87; AF Proj. 2303)
(AD-A234587; AFOSR-91-0270) Avail: NTIS HC/MF A01 CSCL 20/3

The research accomplishments are briefly reviewed. The proposed research had two objectives: (1) to investigate selectivity and facility on ion transport in ionically conductive composite polymer membranes (these membranes were prepared by incorporating an ion exchange polymer into the pore system of a microporous support membrane); and (2) to investigate ion transport and electronic conductivity in electronically conductive polymers which had a molecular engineered fibrillar morphology. This unique fibrillar morphology was obtained by synthesizing the polymer within the pores of a microporous host membrane. These membranes contained linear, cylindrical pores, with equivalent pore diameters. We call this process 'template synthesis' because the pores in the membrane act as templates for the nascent electronically conductive polymer. GRA

N91-26350# Texas Univ., Arlington. Center for Advanced Polymer Research.
ELECTROACTIVE, NEAR INFRARED ABSORBING NICKEL BIS(DITHIOLENE) COMPLEX POLYCARBONATES AND POLYURETHANES
Fei Wang, Yong-Jian Qiu, and John R. Reynolds 12 Apr. 1991 47 p
(Contract N00014-90-J-1320)
(AD-A234595; TR-28) Avail: NTIS HC/MF A03 CSCL 11/9

A new series of polycarbonates and polyurethanes, containing nickel bis(dithiolene) (Ni-BDT) complexes in the main chain, have been synthesized via polymerization of a functionalized Ni-BDT complex. These polymers are highly soluble in common organic solvents, and free-standing films can be cast from solution. Gel permeation chromatographic analysis on these polymers indicates hydrodynamic volumes comparable to polystyrene standards having weight average mo'ecular weights (Mw) ranging from 1.35 x 10(exp 4) to 9.8 x 10(exp 4). These polymers exhibit a near-IR absorbance between 830-940 nm in solution due to the Ni-BDT complex and solvatochromism is observed with more polar solvents shifting the near-IR absorbance band to higher wavelength. A single glass transition (Tg) is observed for all polymers, suggesting a relatively random polymerization (no phase separation). The Tg's of the polycarbonates decrease with increased Ni-BDT, while the Tg's of the polyurethanes increase, as expected for changes in chain rigidity. Most of the Ni-BDT complex polymers are electroactive with a two step redox process, typical for Ni-BDT complexes, observed in cyclic voltammograms of the polymers in solution. The results presented herein indicate that the incorporation of Ni-BDT complexes into polymer main chains impart the unique optoelectronic properties of Ni-BDT's to the polymer. GRA

N91-26351# Texas Univ., Arlington. Center for Advanced Polymer Research.
PROCESSABLE POLYMERS AND COPOLYMERS OF 3-ALKYLTHIOPHENES AND THEIR BLENDS
Martin Pomerantz, John J. Tseng, Hong Zhu, Steven J. Sproull, and John R. Reynolds 12 Apr. 1991 8 p
(Contract N00014-90-J-1320)
(AD-A234596; TR-30) Avail: NTIS HC/MF A02 CSCL 07/6

Poly(3-alkylthiophenes) have been prepared using anhydrous FeCl3 while dry air was bubbled through the reaction mixture. Molecular weight studies via GPC, using polystyrene standards in conjunction with RI and UV detection along with absolute determinations using a multiangle laser light scattering (MALLS) detector, have shown these materials are of high molecular weight (Mw of up to 400,000) and relatively low polydispersity (Mw/Mn less than 3). Further, the MALLS detector (absolute molecular weights) provides weight average molecular weights 2 to 5 times larger than those obtained using polystyrene standards showing that polystyrene is a rather poor standard for these materials. A series of copolymers of the 3-alkylthiophenes was prepared using a 1:1 molar feed ratio of the two monomers and the molecular weights of the materials decreased with decreasing side chain length. Poly(3-alkylthiophenes) were processable via a variety of methods, including melt spinning to form soft fibers. The films and fibers were dopable with typical oxidants. The solution pulled fibers were observed to be birefringent with considerable orientation along the fiber axis. EDAX studies have shown that the doping of melt-spun fibers was quite uniform. Blends of poly(3-decylthiophene) with low density polyethylene have been prepared and melt-spun into fibers. Blends prepared by melt-blending the components were seen by electron microscopy to be phase separated into large domains while those prepared from xylene solution were much more uniform. GRA

N91-26352# Texas Univ., Arlington. Arlington Center for Advanced Polymer Research.
ELECTRONIC AND IONIC TRANSPORT IN PROCESSABLE CONDUCTING POLYMERS
Martin Pomerantz, John R. Reynolds, Krishnan Rajeshwar, and Dennis S. Marynick 12 Apr. 1991 6 p
(Contract N00014-90-J-1320)
(AD-A234597; TR-25) Avail: NTIS HC/MF A02 CSCL 07/3

A series of poly 1,4-bis(2-furanyl) 2,5-disubstituted p-phenylenes has been prepared electrochemically. They exhibit conductivities of up to 0.1 S/cm when doped electrochemically. The nature of the substituent has been shown to affect the cyclic voltammetric E(sub 1/2) potentials and bandgaps, but these are independent of the length of the alkyl chain in the substituents. Interestingly, electrogravimetric analysis has shown greater mass increase upon electrochemical oxidation with longer alkoxy chains. Poly (P-phenyl eneterephthalamido) propane sulfonate (PPTA PS) has been prepared and studied extensively. The ternary phase behavior of poly(p-phenylene benzo bisthiazole)/-PPTA-PS/methane sulfonic acid has been examined, and the intermolecular coil/rod interactions have been shown to cause the phase behavior to deviate from Flory's theory for molecular composites. The mechanistic aspects of the chemical reduction of polypyrrole naphthalene sulfonate thin films by hydrazine have been elucidated. The self exidation of polypyrrole in N2 and O2, and the involvement of polaron and bipolaron states, has been studied by UV-visible spectroelectrochemistry. Conformational analyses and electronic structures have been calculated for a variety of systems including copolymers of heterocyclic rings (e.g., furan and pyrrole) and disubstituted (methyl or methoxy)-p-phenylene systems, copolymers of heterocyclic rings and dimethoxy vinylene and a thienothiophene system. GRA

N91-26353# Texas Univ., Arlington. Center for Advanced Polymer Research.
SURFACE CHARACTERIZATION OF ELECTRICALLY CONDUCTING NICKEL TETRATHIOOXALATE/POLY(VINYL ALCOHOL) COMPOSITES
W. F. Stickle, John R. Reynolds, and C. A. Jolly 12 Apr. 1991 17 p
(Contract N00014-90-J-1320)
(AD-A234598; TR-26) Avail: NTIS HC/MF A03 CSCL 07/4

Nickel (II) acetate, complexed in poly(vinyl alcohol) (Ni/PVA) has been reacted with tetraethylammonium tetrathiooxalate (TEATTO) to form a semiconductive composite (NiTTO/PVA). The resulting materials are air stable and mechanically durable with conductivities up to .001/ohm cm. Examination of the surfaces by X-ray photoelectron spectroscopy (XPS) prior to treatment with TEATTO indicates the Ni/PVA surface to contain Ni(II) in an octahedral coordination. After reaction with TEATTO to form NITTO/PVA the Ni(II) is observed to be in a square planar coordination. The chemistry and composition of the Ni/PVA precursors, their TEATTO reaction products and model compounds, as characterized by XPS and static secondary ion mass spectrometry (SSIMS), are compared and contrasted. GRA

N91-26354# Texas Univ., Arlington. Center for Advanced Polymer Research.
ELECTROCHEMICALLY INDUCED CHARGE AND MASS TRANSPORT IN POLYPYRROLE/POLY(STYRENE SULFONATE) MOLECULAR COMPOSITES
Charles K. Baker, Yong-Jian Qiu, and John R. Reynolds 12 Apr. 1991 36 p
(Contract N00014-90-J-1320)
(AD-A234599; TR-27) Avail: NTIS HC/MF A03 CSCL 07/4

Polypyrrole/poly(styrene sulfonate) (PP/PSS) molecular composites have been synthesized by the electrochemical polymerization of pyrrole in the presence of sodium poly(styrene sulfonate) (PSS-Na+). Their synthesis and charge transport properties have been investigated by a combination of electrochemical and gravimetric techniques using the Electrochemical Quartz Crystal Microbalance (EQCM). Electropolyamerization in water at 0.8 V vs. Ag/AgCl yields a partially hydrated polymer complex with sulfonate dopant anions from the PSS. Mass transport is found to be cation specific, as expected for a composite system, with the polyelectrolyte chains physically entrapped within the polymer membrane. Frequency responses of the EQCM during electrochemical switching are found to increase with increasing electrolyte cation mass as Li+ is equivalent to Na+ is less than Cs+ is less than Et4N+ is less than Bu4N+. Chronogravimetric and chronocoulometric analyses of PP/PSS-Na+ yield apparent diffusion constants, Dapp, between 10 to (exp -9 to -11) sq cm/s for mobile hydrated Na+ species. Though the determination of theses values are complicated by the exact determination of the concentration of electroactive sites (C sub O), it is evident that reductive transport processes are faster than oxidative transport processes during switching. GRA

N91-26355# Dayton Univ., OH. Research Inst.
CHEMICAL SYNTHESIS STUDY OF DEUTERATED EPOXY RESINS Final Report, Sep. 1988 - Mar. 1990
Shwn-Meei Linden, Steven A. Sims, Richard P. Chartoff, and John M. Butler Apr. 1990 187 p
(Contract N62269-88-C-0253)
(AD-A234666; UDR-TR-90-31; NADC-91016-60) Avail: NTIS HC/MF A09 CSCL 11/9

Both the hydrogenated and deuterated epoxy resins of bisphenol A and epichlorohydrin were synthesized using the same synthetic procedure. Mixtures of deuterated resin with piperidine-D11 were cured side by side with the comparable hydrogenated mixtures. The decomposition temperatures observed in Thermal Gravimetric Analysis under both air and inert atmospheres for the cured deuterated resins are in general 10 to 30 C higher than the hydrogenated versions. The former also had lower percentage weight loss in the first stage of decomposition, most notably in the inert atmosphere. The data obtained lead to the conclusion tha the replacement of C-H bonds with C-D bonds indeed improves the thermal stability of epoxy resins. GRA

N91-26356# Pennsylvania Univ., Philadelphia. Dept. of Materials Science and Engineering.
PLASTICITY OF SINGLE CRYSTALLINE Al3X INTERMETALLIC COMPOUNDS Annual Report, 3 Jul. 1990 - 31 Mar. 1991
David E. Luzzi, David P. Pope, and Vaclay Vitek 6 Apr. 1991 17 p
(Grant AF-AFOSR-0062-89; AF Proj. 2306)
(AD-A234699; AFOSR-91-0453TR) Avail: NTIS HC/MF A03 CSCL 20/2

Progress in three areas is summarized: Deformation of LI2 single crystalline Al3Ti + Fe, high resolution transmission electron microscopy of dislocations and faults in this material, and computer simulations of dislocations and faults in both the DO22 and LI2 form. The slip systems were determined from macroscopic and microscopic analysis, and a new form of dislocation dissociation was observed. The computer simulations have shown why the temperature dependence of the flow strength is so distinct at low temperatures and why the DO22 form is always so brittle. GRA

N91-26357# Wright Research Development Center, Wright-Patterson AFB, OH.
SYNTHESIS AND PROPERTIES OF RIGID-ROD BENZOBISAZOLE POLYMERS CONTAINING BENZOTHIAZOLE PENDENT GROUPS Final Report, Oct. 1987 - Oct. 1988
Tsu-Tzu Tsai and Fred E. Arnold 16 Nov. 1990 24 p
(AD-A234742; WRDC-TR-90-4092) Avail: NTIS HC/MF A03 CSCL 07/6

Novel polybenzobisazoles containing benzothiazole pendents were prepared by the reaction of 2-benzothiazole or 2,5-dibenzothiazole terephthalic acids with the appropriate aminomercapto, aminohydroxy or tetraamino monomers in polyphosphoric acid at elevated temperatures. The polymerizations were carried out at concentrations (10 to 18 percent) which would promote anisotropic reaction mixtures. Intrinsic viscosities in range of 4 to 19 dl/g were measured in methanesulfonic acid at 30 C. Thermogravimetric-mass spectral analysis in vacuo showed that

the pendent benzothiazole group was the initial product of thermal degradation, maximizing at 590 C. Anisotropic polymerization mixtures could be wet-spun into fiber with modulus values between 25 to 30 MSI and tenacity values up to 350 KSI. GRA

N91-26358# General Atomic Co., San Diego, CA.
CERAMIC FIBER COATING DEVELOPMENT AND DEMONSTRATION Annual Technical Report, 1 Jul. 1989 - 31 Dec. 1990
H. Streckert, D. Hazelbeck, F. Montgomery, K. Norton, and I. Glatter 31 Jan. 1991 115 p
(Contract F49620-89-C-0078; ARPA Order 6808)
(AD-A234773; GA-C-20422; AFOSR-91-0225TR) Avail: NTIS HC/MF A06 CSCL 11/3

The objective of this program is to develop fiber coating techniques by gas phase and liquid phase processes. Thermochemical evaluation of fiber/coating/matrix systems was completed. Experimental studies on chemical and mechanical interaction between coating and substrate materials indicate no reaction zones in samples treated up to 1400 C. Mechanical tests revealed that the strength of interfaces decreases with increasing temperature treatment. Nicalon, Nextel and FR-PRD-166 fibers were coated with SiC and Si3N4 from preceramic polymer solutions. The same fibers were coated with Y2O3, Al2O3, MgAl2O4. YAlO3 and MgO from aqueous nitrate sols. Tensile strengths for Y2O3 coated Nicalon are comparable to as received fibers while Al2O3 coated Nicalon exhibits a 20 percent degradation. Nicalon, HPZ, Nextel and FP-PRD-166 were CVD coated with SiC. TEM data for Al2O3 coatings show evidence of crystallinity above 800 C annealing temperature. GRA

N91-26359# Rockwell International Science Center, Thousand Oaks, CA.
TRANSFORMATION TOUGHENING OF CERAMICS Annual Report No. 2, 15 Jan. 1990 - 11 Jan. 1991
D. B. Marshall Feb. 1991 93 p
(Contract F49620-89-C-0031)
(AD-A234926; SC71002.AR) Avail: NTIS HC/MF A05 CSCL 11/2

The transformation strains responsible for toughening of ZrO2 materials have been measured directly using Moire interferometry and a high resolution strain mapping technique based on digital image correlation. Results were correlated with Raman spectroscopy and finite element calculations. Calculations of the crack tip shielding in Ce-ZrO2 indicated that the fracture toughness could be increased by a factor of 2 by modifying the microstructure to change the shape of the transformation zone ahead of the crack tip. Layered composites of Ce-ZrO2 and Al2O3/Ce-ZrO2 have been explored as a means of achieving such zone modifications. Using a colloidal technique, multilayered composites with layer thickness as small as 10 microns have been fabricated. These layered structures have been observed to interact much more strongly than expected with the transformation zones, causing widening of the zone to the side of cracks as well as modification of the frontal region. The potential exists for extremely high fracture toughness in such systems. GRA

N91-26360# Army Natick Labs., MA.
MECHANICAL PROPERTIES OF POLYCARBONATE-POLYSULFONE AND POLYCARBONATE-POLYETHERIMIDE BLENDS Final Report, Oct. 1987 - Sep. 1990
William G. Kohlman Apr. 1991 28 p
(DA Proj. 1L1-61102-AH-52)
(AD-A234939; NATICK/TR-91/025) Avail: NTIS HC/MF A03 CSCL 11/9

This project is an attempt to produce a ballistic impact resistant transparent eye armor with improved scratch and chemical resistance over polycarbonate. The first stage of the project examines the thermal and mechanical properties of the polymers. Five, ten, and twenty percent by weight blends of polysulfone in polycarbonate and polyetherimide in polycarbonate were produced by melt blending using a counter-rotating twin screw extruder at 320 C. The materials were injected molded into plaques 11.4 cm square by 3.2 mm and 1.6 mm thick. Mechanical analysis consisting of tensile, pendulum impact, and ballistic impact testing was conducted using the plaques or samples machined from the plaques. Dynamic mechanical testing was performed using bars machined from the 3/2 mm plaques to observe the low temperature loss peak and determine the activation energy of the loss mechanism. Differential scanning calorimetry was conducted to measure the glass transition temperatures of the material. The presence of two glass transition temperatures and lack of transparency have indicated that the blends are immiscible. Both sets of blends exhibit fair to good ballistic impact properties up to at least 20 percent polysulfone or polyetherimide. The tensile data of the blends show an increase in tensile strength over the same range. GRA

N91-26361# Clark-Atlanta Univ., GA.
ORGANOSILICON POLYMERS INCORPORATING THE BICYCLO(2.2.2)-OCTANE MOIETY Final Report, 1 Jan. 1987 - 31 Jan. 1991
Yitbarek Habte-Mariam 31 Mar. 1991 11 p
(Grant AF-AFOSR-0123-87; AF Proj. 2484)
(AD-A234966; AFOSR-91-0251TR) Avail: NTIS HC/MF A03 CSCL 07/6

The efforts in this project has involved two goal s: the synthesis of main chain (MC) liquid crystalline (LC) polysiloxanes on one hand, and the determination of the utility of an integrated system for TGA/FTIR analysis in studying the conversion of precursor polymers to ceramic materials. Two approaches were used for the synthesis of MC LC polysiloxanes. In one case, diols such as highenol and hisphenol a ere reacted with bifunctional Si-H compounds such as diphenylsilane using Zn octoate as catalyst. In another case, diols were reacted with dichlorosilanes such as dimethyldichlorosilane. Characterization of the polymers by NMR, DSC, polarizing optical microscopy, TGA, FTIR, etc. has been completed. Additionally, the pyrolysis of simple alkylamide containing Si and Ti had been initiated. This will serve as model systems for ceramic precursors we are investigating in our laboratories. GRA

N91-26362# Missouri Univ., Rolla.
PRESSURELESS DENSIFICATION OF CERAMIC MATRIX COMPOSITES Annual Report, Mar. 1990 - Feb. 1991
M. N. Rahaman, L. R. Dharani, and R. E. Moore 22 Mar. 1991 83 p
(Grant AF-AFOSR-0267-90; AF Proj. 2306)
(AD-A235031; AFOSR-91-0399TR) Avail: NTIS HC/MF A05 CSCL 11/2

In the first reporting period, experimental and theoretical studies were performed to determine the effect of key material and processing parameters on the sintering of model ceramic composites. Experimentally, the effect of coarse inclusions (Zirconium oxide) on the sintering of a fine-grained matrix (Zinc oxide) was highly dependent on the forming method. Kinetic data and microstructural observations indicated that the main factors controlling sintering were the packing of the matrix immediately surrounding the inclusions and interactions between the inclusions. A forming method for alleviating these two problems was investigated. Using this method, composites with up to 35 V percent inclusions were sintered to full density under identical conditions used for the pure matrix. Theoretically, a finite element program was developed to describe the kinetic data over the entire sintering process. Transient stresses were calculated incrementally from the density-time data and used to predict the reduction in the sintering rate. The effects of single and multiple inclusions and heterogeneity in the matrix density were calculated. GRA

N91-26363# Naval Surface Warfare Center, Silver Spring, MD.
SYNTHESIS OF ENERGETIC SINGLE PHASE AND MULTI-PHASE POLYMERS Annual Progress Report, 1 Jan. - 31 Dec. 1990
H. G. Adolph and L. A. Nock 31 Mar. 1991 72 p
(AD-A235104) Avail: NTIS HC/MF A04 CSCL 07/6

The synthesis of ABA polymers with nitropolyformal and azidopolyether soft blocks and alkane hard blocks was continued. A higher molecular weight, isocyanate-terminated C30 hydrocarbon hard block was synthesized and characterized. Higher energy polyformal soft blocks were synthesized by copolymerization of a tetranitro dioxatridecanediol and a hexanitro dioxadiaza pentadecanediol. Three hundred grams of tetranitrodioxatridecanediol polyformal were prepared for use in ABA polymer synthesis. This polyformal was chain-extended with phosgene to increase its molecular weight. GRA

N91-26364# University of Southern California, Los Angeles. Dept. of Chemistry.
DESIGN OF POLYMERS WITH SEMICONDUCTOR, NLO, AND STRUCTURAL PROPERTIES Final Technical Report, 15 Aug. 1987 - 14 Feb. 1991
Larry R. Dalton 22 Apr. 1991 47 p
(Contract F49620-87-C-0100)
(AD-A235215; AFOSR-91-0497TR) Avail: NTIS HC/MF A03 CSCL 07/6

A major objective of this research program has been to explore unique optical effects which we have speculated to exist in ladder polymers. By steadily improving the solubility and processability through utilization of derivitization and precursor routes we have been able to form the first optical quality films of a ladder polymer and have achieved high resolution characterization of optical nonlinearity in these materials. We have thus succeeded in all our stated objectives, in addition we have examined for the first time numerous other systems of promising optical nonlinearity. Details of the synthesis, characterization and optical measurements of the most promising of the systems examined is contained in the body of this report. At the moment it is sufficient to say that an enormous amount of original research has been achieved through direct support of this grant, a measure of this can be readily seen if one examines the accompanying bibliography of manuscripts published through AFOSR support. GRA

N91-26365# Massachusetts Inst. of Tech., Cambridge. Dept. of Chemistry.
LIVING RING-OPENING METATHESIS POLYMERIZATION OF 7-OXA-2,3-DIFUNCTIONALIZED NORBORNENES AND NORBORNADIENES BY Mo(CHCMe2R) (N-2,6-C6H3-i-Pr2) (O-t-Bu)2 AND Mo(CHCMe2R) (N-2,6-C6H3-i-Pr2) (OCMe2CF3)2
Guillermo C. Bazan, John H. Oskam, Hyun-Nam Cho, Lee Y. Park, and Richard R. Schrock 18 Apr. 1991 49 p
(Contract N00014-89-J-1542)
(AD-A235235; TR-12) Avail: NTIS HC/MF A03 CSCL 07/3

An important class of readily prepared norbornenes and norbornadienes are those that contain oxygen in the 7 position. The 7-Oxanorbornenes and norbornadienes were polymerized by Ru and Os-based classical catalysts in ethanol and in water and the resulting polymers were shown to act as acyclic ionophores. Poly 7-oxa 2,3-dicarbo methoxynorbornadiene also was reported to be converted into a polyene upon dehydrogenation with DDQ. But from the point of view of mechanistic understanding, an important finding is that 7-oxanorbornene and norbornadiene derivatives are necessary to generate especially active and long-lived Ru catalysts in water. If it is assumed that ruthenium alkylidene complexes are involved in ring opening of norbornenes and norbornadienes in water it is important to determine how 7-oxa derivatives behave in a relatively well-understood and well-behaved ring opening catalyst system. GRA

N91-26366# North Dakota State Univ., Fargo. Dept. of Chemistry.
SECOND MINI-CONFERENCE ON KEY PROBLEMS IN SILICON CHEMISTRY Final Technical Report, 1 Apr. - 31 Dec. 1990
Mark S. Gordon Mar. 1991 3 p Conference held in Boulder, CO
(Grant AF-AFOSR-0153-90; AF Proj. 2303)
(AD-A235243; AFOSR-91-0383TR) Avail: NTIS HC/MF A01 CSCL 07/3

Leading researchers, both experimentalists and theoreticians, from a broad variety of disciplines were brought together, in order to promote interactions and to identify and address key problems in the field of silicon chemistry. The Symposium was divided into three subsections, with a Discussion Leader coordinating each subsection and leading a Forum on the appropriate topic at the end of the series of talks in that subsection: (1) Materials and Polymer Science; (2) Organosilicon Chemistry; and (3) Theoretical Chemistry. GRA

N91-26367# Colorado State Univ., Fort Collins. Dept. of Chemistry.
TEMPLATE SYNTHESIS OF POLYMERIC AND METAL MICROTUBULES
Charles R. Martin 13 Apr. 1991 13 p
(Contract N00014-82-K-0612)
(AD-A235307; TR-59) Avail: NTIS HC/MF A03 CSCL 14/2

An elegant new method is described for the synthesis of organic microtubules. This new method is based on the use of a microporous membrane as a template during tubule synthesis. This template method produces tubules with monodisperse lengths and diameters, and length, diameter, and wall thickness can be varied at will. This type of precise control over tubule geometry is not possible with the existing synthetic method. The tubules obtained are composed of chemically and mechanically robust heterocyclic polymers. A template was recently described for the synthesis of organic microtubules. This method entails the use of the pores in a microporous membrane as templates for tubule formation. The key to the tubule formation process is the presence of molecular anchors on the pore walls. These anchors insure that the tubule forming materials deposits as a thin skin which lines the pore wall. An electrochemical template method is herein described for the synthesis of metal (Au) microtubules. A general paradigm is also presented for the formation of molecular anchors on the pore walls of alumina template membranes. It is believed that this paradigm should allow for the synthesis of microtubules composed of any desired material. GRA

N91-26368# Carnegie-Mellon Univ., Pittsburgh, PA. Dept. of Chemistry.
CATALYSTS AND INITIATORS AS INSTRUMENTS CONTROLLING STRUCTURE OF POLYMERS WITH INORGANIC BACKBONE Technical Report No. 26, May 1990 - May 1991
Krzysztof Matyjaszewski 2 May 1991 23 p
(Contract N00014-90-J-1186)
(AD-A235350) Avail: NTIS HC/MF A03 CSCL 07/2

Importance of catalysts and initiators as factors which control macromolecular structure of various polymers with inorganic backbone is discussed. Chemoselectivity, regioselectivity, stereoselectivity and supramolecular control in the synthesis of polysiloxanes, polysilanes and polyphosphazenes is described. GRA

N91-26369# Carnegie-Mellon Univ., Pittsburgh, PA. Dept. of Chemistry.
POLYSILANES, SYNTHESIS, MODIFICATION, AND PROPERTIES Technical Report No. 22, May 1990 - May 1991
Krzysztof Matyjaszewski 2 May 1991 6 p
(Contract N00014-90-J-1186)
(AD-A235351) Avail: NTIS HC/MF A02 CSCL 07/2

Synthesis, modifications and characterization of various homopolysilanes and copolysilanes is reviewed with the main emphasis on the modification route and reductive coupling with various reducing agents and under various conditions. GRA

N91-26370# Carnegie-Mellon Univ., Pittsburgh, PA. Dept. of Chemistry.
SYNTHESIS AND CHARACTERIZATION OF POLYSILANES Technical Report No. 24, May 1990 - May 1991
Krzysztof Matyjaszewski, Martin Moeller, Karen Ruehl, Michael White, and Marek Cypryk 2 May 1991 24 p
(Contract N00014-90-J-1186)
(AD-A235357) Avail: NTIS HC/MF A03 CSCL 07/2

Preparation of polysilanes by sonochemical reductive coupling, modifications, and ring-opening polymerization is discussed. Various random copolysilanes are prepared by reductive coupling in order to control phase transition in solid copolymers. Polymers are characterized by GPC, NMR, UV, DSC, and electron microscopy. GRA

N91-26371# Carnegie-Mellon Univ., Pittsburgh, PA. Dept. of Chemistry.
PREPARATION OF INORGANIC AND ORGANOMETALLIC POLYMERS WITH CONTROLLED STRUCTURES Technical Report No. 27, May 1990 - May 1991
Krzysztof Matyjaszewski 2 May 1991 30 p
(Contract N00014-90-J-1186)
(AD-A235359) Avail: NTIS HC/MF A03 CSCL 07/6

Preparative and mechanistic aspects of polysilanes and polyphosphazenes are reviewed based on the several synthetic methods developed in the author's laboratories. Polysilanes are prepared by sonochemical reductive coupling, modifications and ring opening polymerization. Polyphosphazenes are prepared by the catalyzed polycondensation of phosphoranimines and by the direct reaction of phosphonites and phosphinites with silyl azides. GRA

N91-26372# Carnegie-Mellon Univ., Pittsburgh, PA. Dept. of Chemistry.
ANIONIC RING-OPENING POLYMERIZATION OF CYCLOTETRASILANES Technical Report No. 23, May 1990 - May 1991
Krzysztof Matyjaszewski 2 May 1991 14 p
(Contract N00014-90-J-1186)
(AD-A235360) Avail: NTIS HC/MF A03 CSCL 07/6

Various aspects of Silicon-Silicon bond cleavage are discussed in model and in macromolecular systems. Action of nucleophiles, electrophiles, and radicals are compared. Available cyclosilanes are described in view of their polymerizability. Preparation of strained and polymerizable rings is discussed. Anionic polymerization of various cycles with silicon atoms substituted by methyl and phenyl groups is shown. GRA

N91-26373# University of Southern Mississippi, Hattiesburg.
NOVEL LIQUID CRYSTALLINE POLYMERS AS NONLINEAR OPTICAL MATERIALS Final Report, 1 Apr. 1988 - 31 Aug. 1990
Anselm C. Griffin 31 Aug. 1990 13 p
(Contract F49620-88-C-0068)
(AD-A235371; AFOSR-91-0498TR) Avail: NTIS HC/MF A03 CSCL 07/5

Research results are presented for side-chain liquid crystalline polymers as NLO materials. Design criteria are discussed for temporally stabilized SHG (Second Harmonic Generation) in these polymers. The importance of liquid crystallinity on SHG is described. Main-chain liquid crystalline polymers for both second- and third-order NLO are presented. A photo-Fries reaction on polyarylcinnamates leads to a potential second-order chromophore while in the third-order area, siloxane and methylene spacers between defined pi-conjugated segments confers solubility and lowered melting temperatures to these polymers. GRA

N91-26374# National Inst. of Standards and Technology, Gaithersburg, MD. Ceramics Div.
STRENGTH AND MICROSTRUCTURE OF CERAMICS
S. J. Bennison, H. M. Chan, P. Chantikul, J. Kelly, and S. Lathabai Nov. 1990 152 p
(Grant AF-AFOSR-ISSA-91-002)
(AD-A235424; AFOSR-91-0448TR) Avail: NTIS HC/MF A08 CSCL 11/2

Results of a program on the toughness properties of monophase ceramics that toughen by bridging are presented. Fracture mechanics models describing this behavior, in the particular context of strength, are developed. Results of strengths tests confirming the essential predictions of the theory are presented. Innovative processing routes suggested by the models are shown to lead to two-phase composites with impressive flaw insensitivity. Titles of appended articles included: in situ measurements of bridged crack interfaces in the SEM; a loading device for fracture testing of compact tension specimens in the scanning electron microscope; cyclic fatigue from frictional degradation at bridging grains in alumina; the role of grain size in the strength an R-curve properties of alumina; the role of crystallization of an intergranular glassy phase in determining grain boundary residual stresses in debased aluminas; fabrication of flaw-tolerant aluminum-titanate-reinforced alumina; and fundamental condition for existence of microcrack clouds in monophase ceramics. GRA

N91-26375*# National Aeronautics and Space Administration. Lewis Research Center, Cleveland, OH.
OXIDATION RESISTANT COATINGS FOR TITANIUM ALLOYS AND TITANIUM ALLOY MATRIX COMPOSITES Patent Application
William J. Brindley, inventor (to NASA), James L. Smialek, inventor (to NASA), and Carl J. Rouge, inventor (to NASA) 1 Apr. 1991 9 p
(NASA-Case-LEW-15155-1; NAS 1.71:LEW-15155-1; US-Patent-Appl-SN-682160) Avail: NTIS HC/MF A02 CSCL 11C

An oxidation resistant coating for titanium alloys and titanium alloy matrix composites comprises an MCrAlX material. M is a metal selected from nickel, cobalt, and iron. X is an active element selected from Y, Yb, Zr, and Hf. NASA

N91-26376*# National Aeronautics and Space Administration. Lewis Research Center, Cleveland, OH.
METHOD OF PREPARING A THERMAL BARRIER COATING Patent Application
I. Zaplatynsky, inventor (to NASA) 1 Mar. 1991 10 p
(NASA-Case-LEW-14999-2; NAS 1.71:LEW-14999-2; US-Patent-Appl-SN-662684) Avail: NTIS HC/MF A02 CSCL 11C

A composite thermal barrier coating is plasma sprayed onto a substrate. This coating has a first layer including a first ceramic material and a second layer including a second ceramic material impregnated with a glass, the glass being a ternary eutectic. The glass may consist of about 14.6 weight percent Al_2O_3, about 23.3 weight percent CaO, and about 62.1 weight percent SiO_2. The first and second ceramic materials may include yttria-stabilized zirconia. NASA

N91-26377*# National Aeronautics and Space Administration. Langley Research Center, Hampton, VA.
EFFECT OF MOLECULAR WEIGHT ON POLYPHENYLQUINOXALINE PROPERTIES
Brian J. Jensen May 1991 36 p
(NASA-TM-104100; NAS 1.15:104100) Avail: NTIS HC/MF A03 CSCL 11C

A series of polyphenyl quinoxalines with different molecular weight and end-groups were prepared by varying monomer stoichiometry. Thus, 4,4'-oxydibenzil and 3,3'-diaminobenzidine were reacted in a 50/50 mixture of m-cresol and xylenes. Reaction concentration, temperature, and stir rate were studied and found to have an effect on polymer properties. Number and weight average molecular weights were determined and correlated well with viscosity data. Glass transition temperatures were determined and found to vary with molecular weight and end-groups. Mechanical properties of films from polymers with different molecular weights were essentially identical at room temperature but showed significant differences at 232 C. Diamine terminated polymers were found to be much less thermooxidatively stable than benzil terminated polymers when aged at 316 C even though dynamic thermogravimetric analysis revealed only slight differences. Lower molecular weight polymers exhibited better processability than higher molecular weight polymers. Author

N91-26378*# National Aeronautics and Space Administration. Langley Research Center, Hampton, VA.
LaRC-ITPI/ARYLENE ETHER COPOLYMERS

Brian J. Jensen and Dennis C. Working (Analytical Services and Materials, Inc., Hampton, VA.) May 1991 12 p
(NASA-TM-104099; NAS 1.15:104099) Avail: NTIS HC/MF A03 CSCL 11C

As part of an effort to develop high performance structural resins for aerospace applications, work has continued on block copolymers containing imide and arylene ether segments. The arylene ether block used in this study contains a bulky fluorene group in the polymer backbone while the imide block contains an arylene ketone segment similar to that in the arylene ether block and has been named LaRC-ITPI. A series of imide/arylene ether block and segmented copolymers were prepared and characterized. Films were prepared from these copolymers and mechanical properties were measured. Author

N91-26379# Argonne National Lab., IL.
A TRIBOLOGICAL INVESTIGATION OF THE GRAPHITE-TO-DIAMOND-LIKE BEHAVIOR OF AMORPHOUS CARBON FILMS ION-BEAM-DEPOSITED ON CERAMIC SUBSTRATES
A. Erdemir, M. Switala, R. Wei, and P. Wilbur (Colorado State Univ., Fort Collins.) Mar. 1991 25 p Presented at the Symposium on Tribological Coatings Surface Modification in Conjunction with the International Conference on Metallurgical Coating and Thin Films, San Diego, 22-26 Apr. 1991
(Contract W-31-109-eng-38)
(DE91-010816; ANL/CP-72657; CONF-910485-1) Avail: NTIS HC/MF A03

A tribological investigation was conducted on the graphite-to-diamond-like behavior of hard carbon films produced on SiC, Si3N4, and ZrO2 substrates by means of ion-beam-deposition. Friction tests were performed on a ball-on-disk machine with pairs of various ceramic balls and disks coated with hard carbon films in dry and humid air, Ar, and N2. The friction coefficients of carbon films sliding against Si3N4 and sapphire balls were in the range of 0.02 to 0.04 in N2 and Ar but significantly higher (approximately 0.15) in humid air. The wear rates of ceramic disks coated with carbon films were unmeasurable, and, depending on the test environment, the wear rates of counterface ceramic balls were reduced by factors of two to four orders of magnitude below those of balls that were slid against uncoated ceramic disks. Graphite disks were also tested, to obtain friction data that can help us understand the graphite-to-diamond-like tribological behavior of carbon films. Micro laser-Raman spectroscopy and scanning electron microscopy were employed to analyze the structure and chemistry of worn surfaces and to elucidate the graphite-to-diamond-like tribological behavior of amorphous carbon films. DOE

N91-26380# Oak Ridge National Lab., TN.
STRENGTH OF SiC- AND Si-N-C-CERAMIC FIBERS EXPOSED TO HIGH-TEMPERATURE GASEOUS ENVIRONMENTS
A. J. Moorhead and Hyoun-Ee Kim 1991 12 p Presented at the 8th International Conference on Composite Materials, Honolulu, 15-19 Jul. 1991
(Contract DE-AC05-84OR-21400)
(DE91-011099; CONF-910731-1) Avail: NTIS HC/MF A03

The effects of exposures to high-temperature gaseous environments on the strengths of Nicalon SiC fiber and HPZ Si-N-C fiber were investigated. The exposure conditions included: (1) Ar with various P(sub O2) at 1000 C and 1200 C for 10 h, and (2) air at 1000, 1200, and 1400 C for times up to 100 h. Individual fibers were tested in tension at room temperature following exposure, and correlations were made between the measured strengths and observed changes in surface morphology including that of the fracture surfaces. Thermal degradation of both fibers occurred under all conditions investigated. In fact, the effect of temperature far outweighed the effect of any other variable including the level of oxidant in the atmosphere, or exposure time. Although of significant different chemistry, degree of crystallinity (Nicalon is crystalline, HPZ is amorphous), and cross-sectional geometry, the strengths of the fibers and their response to the various exposures were remarkably similar with one exception. The strength of the HPZ fiber was significantly less degraded by exposure in air at 1400 C for times greater than two hours. DOE

N91-26381# Lawrence Livermore National Lab., CA.
NUMERICAL SIMULATIONS OF THE INDENTATION OF GLASS WITH IMPLICATIONS TO DUCTILE GRINDING
K. L. Blaedel and D. J. Nikkel, Jr. 25 Feb. 1991 30 p
(Contract W-7405-eng-48)
(DE91-011512; UCRL-ID-106838) Avail: NTIS HC/MF A03

The effect of grit geometry on the ability to precision grind brittle materials such as glass in a ductile manner is investigated using numerical simulations. The finite element code NIKE2D is used to simulate isolated indentations for various different indenter (grit) geometries and different indentation depths. A scalar function of the stress field is used to characterize whether or not a given state could lead to fracture of the glass under the indenter. It is found that while there are clear differences between the results for different indenter geometries, these differences are not so great that one would expect grit geometry to be a critical factor in the ability to grind in the ductile regime. DOE

N91-26382# Sandia National Labs., Albuquerque, NM.
POLYMER CHARACTERIZATION USING SINGLET OXYGEN PHOSPHORESCENCE AS A SPECTROSCOPIC PROBE
P. R. Ogilby, M. P. Dillon, Yuanping Gao, Kai-Kong lu, M. Kristiansen (New Mexico Univ., Albuquerque.), V. L. Taylor, and R. L. Clough 1991 50 p Presented at the 201st American Chemical Society (ACS) National Meeting, Atlanta, 14-19 Apr. 1991
(Contract DE-AC04-76DP-00789)
(DE91-011735; SAND-91-0988C; CONF-910402-13) Avail: NTIS HC/MF A03

Singlet molecular oxygen (1 Delta g O2) can be produced in solid organic polymers by a variety of different methods. The phosphorescence of singlet oxygen can be monitored in both steady-state and time-resolved experiments, yielding valuable information on the structure and properties of (1) the polymer, and (2) solutes dissolved in the polymer. With this spectroscopic probe, we are also able to comment on specific processes that can have important practical ramifications including, for example, the degradation of polymers. In addition, this probe provides a method by which oxygen diffusion/permeation coefficients can rapidly and accurately be determined in polymer films over a wide temperature range. DOE

N91-26383# Oak Ridge National Lab., TN.
SLIDING WEAR-TESTING AND DATA ANALYSIS STRATEGIES FOR ADVANCED ENGINEERING CERAMICS
P. J. Blau and C. S. Yust 1990 14 p Presented at the ASTM Symposium on the Cyclic Deformation, Fracture, and Nondestructive Evaluation of Advanced Materials, San Antonio, 12 Nov. 1990
(Contract DE-AC05-84OR-21400)
(DE91-009524; CONF-901184-1) Avail: NTIS HC/MF A03

Thousands of wear tests are conducted each year on advanced engineering ceramics, and the number will undoubtedly continue to grow. The motivation for conducting most of these tests is to screen or evaluate ceramic-based materials for specific applications, though a smaller number are ostensibly conducted for more basic research purposes. Significantly, even the more generic testing is often justified by identifying potential applications for the results of that work. Most of the wear test methodology in use today is derived from wear tests developed for metals and alloys. Use of such traditional methods is often adequate, especially if the method was based on a close simulation of the intended application. Differences in response to environment, fracture, and fatigue related factors embodied in wear testing ceramics may, however, require modifications in testing strategy and in interpreting the significance of the results. Long period incubation times for catastrophic wear transitions in ceramics may make accelerated or short term testing a risky matter. A strategy is outlined for for designing sliding wear tests for ceramic materials using several examples for polycrystalline ceramics and ceramic composites,

and one procedure is described in which wear transition diagram methodology, developed for lubricated metals, can be adapted for use with ceramics. DOE

N91-26384# Oak Ridge National Lab., TN.
CERAMIC TECHNOLOGY FOR ADVANCED HEAT ENGINES PROJECT
Dec. 1990 462 p
(Contract DE-AC05-84OR-21400)
(DE91-010451; ORNL/TM-11719) Avail: NTIS HC/MF A20

Significant accomplishments in fabricating ceramic components for the Department of Energy (DOE), National Aeronautics and Space Administration (NASA), and Department of Defense (DoD) advanced heat engine programs have provided evidence that the operation of ceramic parts in high-temperature engine environments is feasible. However, these programs have also demonstrated that additional research is needed in materials and processing development, design methodology, and data base and life prediction before industry will have a sufficient technology base from which to produce reliable cost effective ceramic engine components commercially. The objective is to develop the industrial technology base required for reliable ceramics for application in advanced automotive heat engines. The project approach includes determining the mechanisms controlling reliability, improving processes for fabricating existing ceramics, developing new materials with increased reliability, and testing these materials in simulated engine environments to confirm reliability. Although this is a generic materials project, the focus is on the structural ceramics for advanced gas turbine and diesel engines, ceramic bearings and attachments, and ceramic coatings for thermal barrier and wear applications in these engines. This advanced materials technology is being developed in parallel and close coordination with the ongoing DOE and industry proof of concept engine development programs. To facilitate the rapid transfer of this technology to U.S. industry, the major portion of the work is being done in the ceramic industry, with technological support from government laboratories, other industrial laboratories, and universities. DOE

N91-26385# Sandia National Labs., Albuquerque, NM.
PROCESS MONITORING OF POLYURETHANE FOAM USING FOURIER TRANSFORM INFRARED SPECTROSCOPY
J. C. Alberti, K. J. Ward, and D. S. Blair 20 Feb. 1991 28 p
Presented at the Environmentally Conscious Manufacturing/ Technology Applications Workshop, Albuquerque, 20-21 Feb. 1991
(Contract DE-AC04-76DP-00789)
(DE91-010578; SAND-91-0469C; CONF-910279-14) Avail: NTIS HC/MF A03

Polyurethane foams are dispensed into firesets to protect their electrical integrity under extreme environmental conditions. Although the production process has generally high precision, reliability problems were identified. Preliminary results from a research program involving the use of rapid infrared sensors combined with multivariate analysis to monitor the blend of raw materials in near real time are presented. Two distinct regions of the infrared spectrum are considered. The mid infrared region is shown to make sufficiently precise concentration predictions while the near infrared region will require more experimentation. Both infrared regions will be considered for pilot and/or plant scale studies in order to completely specify the infrared sensor. The concentration predictions from the infrared sensor will be used in a closed loop control system in order to improve the reliability of the process. DOE

N91-26386# Jet Propulsion Lab., California Inst. of Tech., Pasadena.
ADDITIVES FOR HIGH TEMPERATURE LIQUID LUBRICANTS
C. Moran and A. H. Yavrouian 1 Apr. 1991 7 p
(Contract DE-AI02-89CE-90023)
(DE91-011018; DOE/CE-90023/T1) Avail: NTIS HC/MF A02

The purpose of this task is to perform research for the Department of Energy (DOE) on the synthesis and characterization of additives for liquid lubricants which will lead to significant improvements in the major tribology task area of friction and wear reductions at high temperature. To this end JPL is surveying candidate precursor compounds which are soluble in liquid lubricants, synthesizing the most promising of these materials, characterizing them, and submitting these additives to NIST for evaluation. Calculations have been made to estimate the Hildebrand solubility parameters for candidate precursor compounds. The initial listing is confined to dinitrites which can form chelates with metals or their compounds. The goal is to find soluble additives that can react in situ with the bearing surface to form adherent lubricating film. Although none of the compounds listed match the solubility parameters of liquid lubricants, the lowest solubility parameters were calculated for dialkyl substituted compounds. In this case, there is probably sufficient solubility to provide adequate amounts of reactants on the metal surfaces. The conclusions are based on previous results where only 0.5 to 1 percent solubility was sufficient to give excellent lubrication. DOE

28 PROPELLANTS AND FUELS

Includes rocket propellants, igniters, and oxidizers; their storage and handling procedures; and aircraft fuels.

For related information see also *07 Aircraft Propulsion and Power, 20 Spacecraft Propulsion and Power,* and *44 Energy Production and Conversion.*

N91-26387# Army War Coll., Carlisle Barracks, PA.
WHAT FUELS OUR FUTURE? Final Report
Robert L. Jarvis 26 Mar. 1991 46 p
(AD-A233674) Avail: NTIS HC/MF A03 CSCL 11/7

This study project reviews the recent history of fuels usage and product evolution (since WWII) and presents current doctrine. The conclusion and recommendation of this project is that the Army of 2001 should have a single fuel on the battlefield. This fuel should be readily available at a reasonable cost, worldwide. The fuel chosen should be safe to transport and store while meeting the requirements of a wide variety of military equipment. This project also addresses current misconceptions, perceived problems, and issues to be resolved about a single fuel concept. Both commercial jet fuel (Jet A1) and its military counterpart, jet propulsion fuel (JP8) offer a safe, relatively available, versatile, and logistically supportable compromise to the varying needs of the majority of ground and air equipment. GRA

N91-26388# Imperial Coll. of Science and Technology, London (England).
LASER INITIATED IGNITION OF LIQUID PROPELLANT Final Technical Report
F. B. Carleton, K. Krallis, and F. J. Weinberg 31 Jan. 1991 26 p
(Contract DAJA45-87-C-0010)
(AD-A233777; R/D-5462-AN-01) Avail: NTIS HC/MF A03 CSCL 21/2

As a result of our studies, we conclude that liquid propellant is permanently altered by precursory electrolysis and that focusing outside the drop produces more decomposition. This is attributed to the combined effects of the plasma and shock wave generated during breakdown. It is shown that the NO formed in the air plasma also plays a part. There is little or no difference between the results for Q-switched and free running pulses at the same total energy. Heat treatment followed by varying rest periods has much the same effect as electrolysis. Three propellant mixtures were used for this test: LP-101, HAN/SBAN, and HAN.DEAN. Following previous studies of electrical ignition initiation of liquid propellants in plasma jets by focused laser beams is studied both by fast cine shadowgraphy and by recording permanent gas release as a measure of decomposition. Unlike military propellants, droplets of aqueous mixtures of nitrate salts of hydroxylamine with a 4-carbon aliphatic amine do not ignite when an approx 10 J laser pulse is focused within the liquid. Ignition is achieved by producing

breakdown in air in the vicinity of propellant droplets, though little decomposition results, at atmospheric pressure. Precursory electrolysis of varying duration is attempted in view of postulated chemical mechanisms which suggest that solution of NO in the propellant should enhance ignition. This indeed greatly promotes the vigor of the reaction and leads to an amount of decomposition which increases with increasing time of electrolysis. It appears that the propellant is permanently modified by this simple procedure, leading to obvious practical as well as fundamental conclusions. GRA

N91-26389# Army Armament Research and Development Command, Dover, NJ. Armament Engineering Directorate.
MOLECULAR MECHANICS CALCULATIONS FOR NITRO AND AMINO SUBSTITUTED CONJUGATED SYSTEMS CONTAINING OXYGEN AND NITROGEN Final Report, Dec. 1989 - Dec. 1990
T. Vladimiroff Apr. 1991 24 p
(AD-A233928; ARAED-TR-91002) Avail: NTIS HC/MF A03 CSCL 19/1

The Army is interested in developing new energetic materials which are highly resistant to initiation by heat and shock. Some of the most stable energetic materials known to man can be characterized as nitroaromatics. However, molecules like TNT and TATB do not have enough energy to make good propellants. One way to increase the energy of a molecule is to achieve a more favorable oxygen balance. Thus it would seem reasonable to consider aromatic systems which incorporate oxygen or nitrogen into the aromatic ring. Nitro and amino substituted pyridines, diazines, triazines, tetrazines, pyrroles and furans are investigated. First the heat of formation for these new materials is computed using additivity rules and an estimate of the propellant performance is made. Then the method of molecular mechanics is used to calculate the structure and properties of the various isomers of these molecules. It is found that nitro groups placed next to each other increases the steric energy while an amine group placed between nitro groups stabilizes the system. Diamiontrinitropyridine seems to be particularly attractive candidate molecule for use in low vulnerability propellants. GRA

N91-26390# Army Armament Research and Development Command, Dover, NJ. Armament Engineering Directorate.
MODIFICATION OF THE USER FRIENDLY THERMODYNAMIC CODE TO INCLUDE THE EFFECTS OF MINOR SPECIES Final Report, Dec. 1989 - Dec. 1990
T. Valdimiroff Apr. 1991 21 p
(AD-A233929; ARAED-TR-91001) Avail: NTIS HC/MF A03 CSCL 20/13

Three years ago, a user friendly thermodynamic code was developed at Picatinny Arsenal for the personal computer. This code enabled the engineer to calculate the flame temperature of a new propellant formulation on a personal computer thus eliminating the need for access to a mainframe computer. The new code uses the highly accurate equation of state for propellant gases developed by Powell, Wilmot, Haar and Klein and does not rely on the two term virial expansion employed in BLAKE and the ICT codes. This equation of state was developed to accurately calculate the pressure of mixtures of water, carbon monoxide, carbon dioxide, hydrogen, and nitrogen but was not designed to take into account the contributions of minor species. As a result, the effects of all minor species were described in a very approximate way. This defect in the code has now been removed. For many minor species which are predicted to occur in a propellant gas after combustion the equation of state parameters are not known. Both BLAKE and the ICT codes assign generic parameters to all of these minor species. Second and third viral coefficients are then calculated and used in their virial expansion. GRA

N91-26391# Ballistic Research Labs., Aberdeen Proving Ground, MD.
A NEW HIGH-PROGRESSIVITY/HIGH-DENSITY PROPULSION CONCEPT: PARTIALLY CUT MULTIPERFORATED STICK PROPELLANT Final Report, Jan. - Oct. 1987
Carl R. Ruth, Frederick W. Robbins, Thomas C. Minor, and Arthur A. Koszoru Mar. 1991 54 p
(DA Proj. 1L1-62618-AH-80)
(AD-A234255; BRL-TR-3189) Avail: NTIS HC/MF A04 CSCL 19/1

This report presents the results from investigations with a high progressive/high density (HPD) propelling charge concept using partially-cut, multiperforated stick propellant. While multiperforated stick propellant is attractive both for its progressivity and loading density, the internal pressurization of the long, unvented perforations is of considerable concern. Such internal pressurization may result in mechanical failure of the grains, exposing unprogrammed burning surfaces and leading to overpressurization of the chamber. In the partially cut configuration, the perforations are vented via cuts made through the perforations perpendicular to the axis of the grain at periodic locations along the axis. In order for the partial cutting to be effective, the spacing of the cuts must take into account the diameter of the perforation and the burning rate of the propellant in the perforation. GRA

N91-26392 Department of the Navy, Washington, DC.
BONDING AGENT FOR COMPOSITE PROPELLANTS Patent
John P. Consaga, inventor (to Navy) 31 Jul. 1990 5 p Filed 24 Jul. 80
(AD-D014876; US-Patent-4,944,815; US-Patent-Appl-SN-178258; US-Patent-Class-149-19.1) Avail: US Patent and Trademark Office CSCL 19/1

The invention pertains generally to composite propellants and in particular to strengthening composite propellants through a binder-filler interaction. Composite propellants are nonhomogenous propellants and comprise primarily crystalline oxidizers and metal fuels uniformally suspended in a resin binder. The crystalline oxidizers are usually inorganic compounds, such as ammonium perchlorate or potassium nitrate but can also be organic, for example, cyclotrimethylenetrinitramine (RDX) or cyclotetramethylenetetranitramine (HMX). The metal fuels are powders of elemental metals, such as, aluminum and magnesium. In contrast with these ingredients, the binders are organic polymers such as urethanes, polyamides, or vinyl polymers. Often as much as 80 weight percent of the propellant is oxidizer along about 10 weight percent of metal fuel, thus, giving a solids loading of around 90 weight percent of the total composition. GRA

N91-26393# Pennsylvania State Univ., University Park.
A STUDY OF THE GAS PHASE CHEMISTRY OF SOLID PROPELLANTS USING A MICROPROBE MASS SPECTROMETER (MPMS) SYSTEM: INITIAL DEVELOPMENT OF THE MPMS SYSTEM Annual Report No. 1
Thomas A. Litzinger 1990 22 p
(Contract N00014-89-J-1238)
(AD-A234839) Avail: NTIS HC/MF A03 CSCL 21/2

Detailed knowledge of the gas-phase reactions which occur during propellant ignition and combustion are required to understand and model these processes. If detailed models were available, modification of propellant formulations for improved combustion behavior could be achieved with much less trial-and-error testing. Furthermore, detailed models could be used to generate simplified kinetics schemes for use in propellant models. Without a firm basis for these simplified kinetic schemes, the kinetic parameters are often adjusted to fit burning rate and ignition data; thus, the propellant models are reduced to sophisticated curve fits to experimental data. The present research program, centers around the development and application of a microprobe, mass spectrometer (MPMS) system to study the gas phase chemistry of solid propellant ingredients and solid propellants during heating by a CO2 laser and during steady combustion. The MPMS system uses quartz microprobes with orifice sizes of 100 microns or less to withdraw gases from the region above the sample material. Through a two stage pumping system, the sample is delivered to a quadrupole mass spectrometer for analysis. Sampling is continuous throughout the combustion event so that species profiles of stable intermediates above the sample are obtained during the experiments. GRA

N91-26394# Pennsylvania State Univ., University Park.
A STUDY OF THE GAS PHASE CHEMISTRY OF SOLID PROPELLANTS USING A MICROPROBE MASS SPECTROMETER (MPMS) SYSTEM: PRELIMINARY RESULTS FOR SOLID FUELS (HTPB/ZECOREZ AND BAMO/NMMO), SINGLE-BASE PROPELLANT (M10) AND AN RDX-BASED PROPELLANT (BLX-9) Annual Report No. 2
Thomas A. Litzinger 1991 26 p
(Contract N00014-89-J-1238)
(AD-A234840) Avail: NTIS HC/MF A03 CSCL 21/2

Detailed knowledge of the gas-phase reactions which occur during propellant ignition and combustion are required to understand and model these processes. If detailed models were available, modification of propellant formulations for improved combustion behavior could be achieved with much less trial-and-error testing. Furthermore, detailed models could be used to generate simplified kinetics schemes for use in propellant models. This research program centers around the development and application of a microprobe, mass spectrometer (MPMS) system to study the gas phase chemistry of solid propellant ingredients and solid propellants during heating by a CO2 laser and during steady combustion. The MPMS system uses quartz microprobes with orifice sizes of 100 microns or less to withdraw gases from the region above the sample material. Through a two stage pumping system, the sample is delivered to a quadrupole mass spectrometer for analysis. Sampling is continuous throughout the combustion event so that species profiles of stable intermediates above the sample are obtained during the experiments. In addition to the MPMS system, existing experimental methods to be used in the work include high speed direct photography, high speed Schlieren photography, microthermocouple probes, and photodiodes (for first visible light). GRA

N91-26395# Department of Defense Explosives Safety Board, Alexandria, VA.
MINUTES OF THE 24TH EXPLOSIVES SAFETY SEMINAR, VOLUME 1
30 Aug. 1990 1202 p Seminar held in Saint Louis, MO, 28-30 Aug. 1990
(AD-A235005) Avail: NTIS HC/MF A99 CSCL 19/1

Session topics covered in this volume include: Quantity-distance assessments; Structural concepts and design; Insensitive munitions; Explosives disposal; Structural predictions; Explosives demolition disposal; Lightning protection; Explosion hazard ranges; Explosives facility design considerations; Hazard classifications; and Explosives waste management. GRA

N91-26396# Department of Defense Explosives Safety Board, Alexandria, VA.
MINUTES OF THE 24TH EXPLOSIVES SAFETY SEMINAR, VOLUME 2
30 Aug. 1990 1331 p Seminar held in Saint Louis, MO, 28-30 Aug. 1990
(AD-A235006) Avail: NTIS HC/MF A99 CSCL 19/1

Session topics covered in this volume include: Klotz Club underground testing; Liquid explosion hazards; Explosion propagation tests; Explosion hazards reduction; Lightning protection; Accidents; Explosion containment; Unexploded ordnance clearance; Debris hazards; Site plans and surveys; Explosives manufacturing considerations; Space vehicle explosive hazards; Concrete response testing; Far-field airblast effects; Fragment hazards. GRA

N91-26397# General Accounting Office, Washington, DC. National Security and International Affairs Div.
AIR FORCE STOCK FUND: HYDRAZINE SALES CONSISTENT WITH THE COMMERCIAL SPACE LAUNCH ACT. REPORT TO THE CHAIRMAN, COMMITTEE ON SCIENCE, SPACE AND TECHNOLOGY, HOUSE OF REPRESENTATIVES
May 1991 18 p
(GAO/NSIAD-91-196) Avail: NTIS HC/MF A03; also available from GAO, Gaithersburg, MD HC first five copies free, additional copies $2.00

The Air Force's sales of hydrazine propellants to private firms for use in commercial space launches was reviewed to determine if such sales complied with the intent of the Commercial Space Launch Act (CSLA). CSLA is intended to encourage and facilitate commercial space launches by the private sector. The Air Force purchases hydrazine propellants from Olin Chemicals and sells the propellant from its stock fund to both government and authorized commercial customers. Olin, which would like to increase its direct commercial sales, has alleged that the Air Force is competing with it by making hydrazine propellants available to private firms and by depriving it of the opportunity to sell its product directly to commercial customers. No basis was found on which to conclude that the Air Force's selling of hydrazine propellants to commercial customers was contrary to the requirements or the intent of CSLA. Further, the Air Force has authority, separate from CSLA, for its sales practices in support of commercial space launch activities. A major purpose of CSLA was for the Federal government to encourage and promote private sector participation in the national space program. While CSLA does not specifically address the issue of government agency competition with private sector interests, it gives agencies considerable discretion in balancing the private sector's commercial interests and the government's interest regarding public health and safety, safety of property, or national security interests. B.G.

N91-26398# Sandia National Labs., Albuquerque, NM.
COMMERCIALIZING SOLAR HYDROGEN PRODUCTION
J. T. Holmes and M. R. Prairie 1991 8 p Presented at the 2nd Annual US Hydrogen Meeting, Washington, 13-15 Mar. 1991
(Contract DE-AC04-76DP-00789)
(DE91-011232; SAND-90-2994C; CONF-9103164-1) Avail: NTIS HC/MF A02

This paper discusses the need for a government-supported program to commercialize hydrogen production methods which use solar energy as the main source of energy. Current methods use hydrocarbons and generate large amounts of carbon dioxide. The paper describes results from a literature survey performed to identify technologies using direct solar energy that were likely to succeed on an industrial scale in the near term. Critical parameters included calculated efficiencies, measured efficiencies, and development status. The cost of solar collectors is cited as the reason most promising solar hydrogen research is not taken to the pilot plant stage. The author recommends use of existing DOE facilities already in operation for pilot plant testing. DOE

N91-26399# Lawrence Livermore National Lab., CA.
SHOCK RESPONSE OF DETASHEET
B. W. Asay, J. B. Ramsay, M. U. Anderson, and R. A. Graham (Sandia National Labs., Albuquerque, NM.) 1991 10 p Presented at the Joint Army/Navy/NASA/Air Force (JANNAF) Propulsion Systems Hazards Subcommittee Meeting, Albuquerque, 18-22 Mar. 1991
(Contract DE-AC04-76DP-00789)
(DE91-010923; SAND-91-0632C; CONF-9103131-4) Avail: NTIS HC/MF A02

Detasheet(reg sign) is a DuPont sheet explosive that consists of 68 pct. PETN, 8 pct. nitrocellulose, and 24 pct. acetyl tributyl citrate. It is used extensively in metal forming and other industrial applications, as well as in military applications. Its shock and initiation response are incompletely understood. The results are summarized which were obtained on the nonreactive Hugoniot for Detasheet, the results of two wedge tests, a measurement of the bulk sound speed, and two different measures of the detonation pressure. A more complete description of the experimental techniques used and the data analyses are being prepared for publication. The piezoelectric polymer stress-rate gauge, polyvinylidine fluoride (PVDF), was used to measure the input pressure profiles, the transmitted stress wave profiles, and the transit times through the samples. Because of the extraordinary sensitivity of the PVDF gauge and the flexible nature of Detasheet, special procedures were developed to achieve intimate contact

with the samples while preserving a known sample thickness. Viscoplastic and initiation phenomena in Detasheet were clearly observed using the PVDF gauges. The shock initiation behavior of this material was investigated with the conventional wedge test as well as plane wave experiments using disks of Detasheet and PVDF gauges. The shock sensitivity is compared with that of XTX 8003 (80 pct. PETN/20 pct. Sylgard 182(reg sign)). The detonation pressure was measured with a simple plate dent test as well as with a Manganin stress gauge. DOE

29 MATERIALS PROCESSING

Includes space-based development of products and processes for commercial applications.
For biological materials see *55 Space Biology.*

N91-26400# General Accounting Office, Washington, DC. National Security and International Affairs Div.
COMMERCIAL USE OF SPACE: MANY GRANTEES MAKING PROGRESS, BUT NASA OVERSIGHT COULD BE IMPROVED. REPORT TO THE CHAIR, SUBCOMMITTEE ON VA, HUD, AND INDEPENDENT AGENCIES, COMMITTEE ON APPROPRIATIONS, U.S. SENATE
May 1991 46 p
(GAO/NSIAD-91-142) Avail: NTIS HC/MF A03; also available from GAO, Gaithersburg, MD HC first five copies free, additional copies $2.00

The National Aeronautics and Space Administration (NASA) has long recognized that to help the United States maintain a technological edge throughout the world, it must find ways to encourage and support the development of a domestic commercial space industry. In 1985, NASA began to provide grants and other types of support to the Centers for Commercial Development of Space to encourage the melding of the resources and talents of government, industry, and academic institutions for researching and developing space-related technologies that have potential commercial applications. After a limited period of grant support of 5 to 7 years, NASA expected the centers to become self-sufficient. GAO was asked to review the extent of private sector involvement in the Centers' programs, the centers' progress toward and prospects for self-sufficiency, and NASA's management of the program. Since the inception of the program, the centers have been increasing the number of organizations and companies with which they have become affiliated. More importantly, the number of such affiliates that represent industry has also been increasing. The proportion of centers; support provided by NASA grants has been increasing, not decreasing. The main reason for this pattern of increasing support is that NASA's overall grant support to help the centers fund the cost of access to space and the cost of unique hardware and facilities has increased. None of the center directors believe that their centers will be able to continue at their present levels of activity if grant support is withdrawn before 1995. B.G.

N91-27092*# Mankato State Coll., MN. Dept. of Mathematics, Astronomy and Statistics.
MATHEMATICAL MODELING OF THE FLOW FIELD AND PARTICLE MOTION IN A ROTATING BIOREACTOR AT UNIT GRAVITY AND MICROGRAVITY Final Report
Ernest J. Boyd *In* Houston Univ., NASA/ASEE Summer Faculty Fellowship Program, 1990, Volume 1 Dec. 1990 17 p (For primary document see N91-27088 18-99)
(Grant NGT-44-005-803)
Avail: NTIS HC/MF A10 CSCL 12A

31 ENGINEERING (GENERAL)

Includes vacuum technology; control engineering; display engineering; cryogenics; and fire prevention.

N91-26401 Maryland Univ., College Park.
GEOMETRY, DYNAMICS AND CONTROL OF COUPLED SYSTEMS Ph.D. Thesis
Li-Sheng Wang 1990 205 p
Avail: Univ. Microfilms Order No. DA9110367

The dynamics and control of coupled mechanical systems are studied. A key feature is the systematic use of modern geometric mechanics, including methods based on symplectic geometry, Lie symmetry groups, reductions, Lagrangian mechanics, and Hamiltonian mechanics to study specific Eulerian many body problems. A general framework for gyroscopic systems with symmetry is introduced and analyzed. The influence of the gyroscopic term (linear term in Lagrangian) on the dynamical behavior is exploited. The notion of gyroscopic control is proposed to emphasize the role of the gyroscopic term in designing control algorithms. The block diagonalization techniques associated to the energy momentum method which proved to be very useful in determining stability for simple mechanical systems with symmetry are successfully extended to gyroscopic systems with symmetry. The techniques developed are applied to several interesting mechanical systems. These examples include the dual spin method of attitude control for artificial satellites, a multibody analog of the dual spin problem, a rigid body with momentum wheels in a central gravitational force field, and a rigid body with momentum wheels and a flexible attachment. Dissert. Abstr.

N91-26402# Army Cold Regions Research and Engineering Lab., Hanover, NH.
INTERNATIONAL STATE-OF-THE-ART COLLOQUIUM ON LOW-TEMPERATURE ASPHALT PAVEMENT CRACKING Summary Report
James A. Scherocman Feb. 1991 57 p Colloquium held in Hanover, NH, 6-8 May 1987
(DA Proj. 4A7-62730-AT-42)
(AD-A233663; CRREL-SR-91-5) Avail: NTIS HC/MF A04 CSCL 15/6

The International State-of-the-Art Colloquium on Low-Temperature Asphalt Pavement Cracking was held in Hanover, N.H., on 6-8 May 1987. The objective was to review and summarize the existing knowledge of the causes of low-temperature transverse cracking of asphalt concrete pavement. Discussion also suggested directions for future research needed to more fully understand the mechanisms of the causes of low-temperature cracking. Overlays were not discussed. GRA

N91-26403# Washington Univ., Seattle.
A BASIC GUIDE TO OVERLAY DESIGN USING NONDESTRUCTIVE TESTING EQUIPMENT DATA M.S. Thesis
Vernon R. Turner Aug. 1990 39 p
(AD-A234472) Avail: NTIS HC/MF A03 CSCL 13/2

The purpose of this paper is to provide a basic and concise guide to designing asphalt concrete (AC) overlays over existing AC pavements. The basis for these designs is deflection data obtained from nondestructive testing (NDT) equipment. This data is used in design procedures which produce required overlay thickness or an estimate of remaining pavement life. This guide enables one to design overlays or better monitor the designs being performed by others. This paper will discuss three types of NDT equipment, the Asphalt Institute Overlay Designs by Deflection Analysis and by the effective thickness method as well as a method of estimating remaining pavement life, correlations between NDT equipment and recent correlations in Washington State. Asphalt overlays provide one of the most cost effective methods of improving existing pavements. Asphalt overlays can be used to strengthen existing pavements, to reduce maintenance costs, to increase pavement life, to provide a smoother ride, and to improve skid resistance. GRA

N91-26404# Georgia Inst. of Tech., Atlanta.
ANALYSIS OF KNOWLEDGE-BASED EXPERT SYSTEMS AS TOOLS FOR CONSTRUCTION DESIGN M.S. Thesis
Arthur N. Cole Mar. 1991 52 p
(AD-A234473) Avail: NTIS HC/MF A04 CSCL 13/2

Because construction costs are continuously rising, Congress mandated that those within the respective branches of military service who are responsible for planning and executing construction programs develop policies and procedures that ensure that the individual projects are designed, bid, and constructed as rapidly as possible. This requires an approach that demands maximum efficiency from the design process. Reviews are necessary to ensure that designs meet all requirements, but the reviews themselves must be conducted in the least amount of time so as to preclude delays. Design tools that increases efficiency are knowledge-based expert systems which are interactive computer programs that incorporate judgement, experience, rules of thumb, and other expertise, so as to provide knowledgeable advice about a specific domain. They mimic the thought process employed by a human expert in solving a problem. GRA

N91-26405# Quest Integrated, Inc., Kent, WA.
ABRASIVE-WATERJET MACHINING OF ISOGRID STRUCTURES Final Report, 14 May - 13 Nov. 1990
Mohamed Hashish, Mark Marvin, and David Monserud 18 Dec. 1990 63 p
(Contract F04704-90-C-0033)
(AD-A234628; QUEST-TR-508; BMO-TR-91-03) Avail: NTIS HC/MF A04 CSCL 11/6

An experimental investigation was conducted to determine the feasibility of machining isogrid structures with abrasive-waterjets (AWJs). The main objective was to mill isogrid patterns in surfaces with accurate depth control using an AWJ. Three different approaches using AWJs were tested: linear cutting of isogrid patterns for diffusion bonding, milling with conventional AWJ nozzles, and milling with a single-angled rotary AWJ nozzle. It was shown that pocket milling with conventional AWJs is the most feasible of those tested. The milling can be done internally on preformed aluminum tubes, and the AWJ can also be used on materials other than aluminum. Accurate depth control can be achieved at high productivity rates. As an example, it is projected that a 48-inch-diameter skirt 12 inches high could be milled with an isogrid pattern in 6.3 hours. Milled isogrid patterns can be controlled to 0.001 inch, and thin walls of less than 0.025 inch are achievable. Milling isogrid patterns with conventional AWJs could be very economical, but additional development efforts are required to optimize the milling process and to demonstrate the milling of prototype parts. GRA

N91-26406# Naval Civil Engineering Lab., Port Hueneme, CA.
LIQUID WATER PRODUCTION FROM ATMOSPHERIC SOURCES Final Report, Oct. 1984 - Jun. 1987
John D. Matthews and Norman P. Clarke Feb. 1991 22 p
(NR Proj. RZ6-6512)
(AD-A235090; NCEL-TN-1825) Avail: NTIS HC/MF A03 CSCL 13/2

The purpose of this effort was to assess the feasibility of developing a desiccant system to produce potable water from atmospheric sources that is compatible with military constraints. Goals were: (1) to examine desiccant technology, investigate methods of using available desiccants to collect atmospheric moisture, (2) develop a conceptual model of a desiccant water production system, and (3) develop a mathematical model to simulate the operation of the conceptual model. Results show that a desiccant system can produce large quantities of potable water using relatively small amounts of fuel for heat and fan power. The focus of this project was using a liquid desiccant (such as triethylene glycol) in an absorption-distillation cycle. This report documents the theoretical analysis of a hypothetical liquid desiccant based system for producing liquid water through collection of atmospheric moisture. Estimates are made of cost, weight and water production rate for the hypothetical system. GRA

N91-27109*# Prairie View Agricultural and Mechanical Coll., TX. Dept. of Civil Engineering.
DESIGN OF A LUNAR OXYGEN PRODUCTION PLANT Final Report
Ramalingam Radhakrishnan *In* Houston Univ., NASA/ASEE Summer Faculty Fellowship Program, 1990, Volume 2 Dec. 1990 12 p (For primary document see N91-27103 18-99)
(Grant NGT-44-005-803)
Avail: NTIS HC/MF A09 CSCL 13B

32 COMMUNICATIONS AND RADAR

Includes radar; land and global communications; communications theory; and optical communications.

For related information see also *04 Aircraft Communications and Navigation* and *17 Space Communications, Spacecraft Communications, Command and Tracking.* For search and rescue see *03 Air Transportation and Safety,* and *16 Space Transportation.*

N91-26407* Alabama Univ., Huntsville. Dept. of Physics.
GAMMA RAY ASTRONOMY Final Technical Progress Report, 13 Jul. 1989 - 12 Jan. 1991
William S. Paciesas Jan. 1991 33 p
(Contract NAS8-36955)
(NASA-CR-187774; NAS 1.26:187774) Avail: NTIS HC/MF A03 CSCL 17I

Miscellaneous tasks related to the development of the Bursts and Transient Source Experiment on the Gamma Ray Observatory and to analysis of archival data from balloon flight experiments were performed. The results are summarized and relevant references are included. Author

N91-26408# Defence Research Establishment, Ottawa (Ontario).
EVALUATION OF THE MARISAT SATELLITE UHF WIDEBAND CHANNEL
W. R. Seed Nov. 1990 36 p
(AD-A233666; DREO-TN-90-25) Avail: NTIS HC/MF A03 CSCL 25/2

The use of the MARISAT satellite UHF wideband channel as a radio link for multiple users is investigated. An analytical evaluation of the link is performed for up to 10 users sharing the non-processing transponder's 500 kHz bandwidth. The terminal link carrier-power-to-noise-power-spectral-density ratio, C/N(sub 0), is evaluated for data rates of 2.4, 4.8 and 16 kbps, and for terminal effective isotropic radiated power (EIRP) levels from 17 to 30 dBW. Analyses are performed for cases in which all terminals transmit with the same EIRP and also for cases in which a single user is either 3 dB above or below the other users. A variety of loading schemes are considered to demonstrate the variation in user SNR degradation due to hardlimiting on-board the transponder. The terminal C/N(sub 0) is compared to the minimum performance requirement plus a 3 dB margin to determine the link capacity. Two experiments which were run to evaluate the MARISAT UHF wideband channel spectrum usage and to measure the terminal C/N(sub 0) are described. Power spectral density graphs of the wideband channel and individual subchannels are presented. The results of a 24-hour test to monitor the terminal C/N(sub 0) are discussed in terms of the observed C/N(sub 0) fluctuations and spectrum anomalies. GRA

N91-26409# Illinois Univ., Urbana. Coordinated Science Lab.
SPREAD SPECTRUM COMMUNICATION NETWORKS Final Report, 15 Aug. 1987 - 31 Jan. 1991
Michael B. Pursley and Dilip V. Sarwate Feb. 1991 13 p
(Contract DAAL03-87-K-0097)
(AD-A233696; ARO-25342.28-EL) Avail: NTIS HC/MF A03 CSCL 25/2

One of the difficulties that arises in the analysis of codeword and packet error probabilities in asynchronous frequency-hop (FH) multiple-access communication systems and networks is the

statistical dependence between symbol errors within a codeword or packet in FH communications with multiple symbols per dwell interval. The basic problem is that the hits by other transmissions are statistically dependent. In one paper, we developed improved bounds on the codeword error probability for such FH multiple-access systems and networks. This was accomplished by investigating models in which hits are conditionally independent given the number of interfering packets and choosing the conditional probability of a hit in such a way that a bound on the performance of the actual system can be obtained. We showed that if the ratio of the number of interfering packets to the number of frequency slots is held constant, hits the asynchronous FH networks are asymptotically independent in the limits as the number of frequency slots increases. Thus, when the number of frequency slots is large, the error probabilities can be closely approximated by using the simplified model with independent hits. We published a related paper which shows that, contrary to a paper published by another author, the sequence of hits in an asynchronous FH multiple-access communication system does not form a Markov process. GRA

N91-26410# Massachusetts Inst. of Tech., Lexington. Lincoln Lab.
WIDEBAND HETERODYNE SPATIAL TRACKING FOR OPTICAL SPACE COMMUNICATIONS
D. J. Bernays, G. M. Carter, and K. A. Winick 8 Feb. 1991 39 p
(Contract F19628-90-C-0002)
(AD-A233722; TR-910; ESD-TR-90-147) Avail: NTIS HC/MF A03 CSCL 12/9

A wideband optical heterodyne spatial tracker for use in diode laser-based heterodyne optical space communications is described. The tracking error signals are formed by correlating the output of an intensity noise-cancelling communications receiver with the outputs of the tracking photodetectors. This correlation technique removes noise induced offsets which may significantly limit performance of other wideband tracking schemes and is an alternative to adding amplitude modulation in the track channel relative to square-law based demodulation of the track channel alone. The correlation concept is experimentally verified, and closed-loop tracking performance is demonstrated. GRA

N91-26411# Massachusetts Inst. of Tech., Lexington. Lincoln Lab.
OPTIMAL WALSH MODULATIONS IN THE PRESENCE OF DOPPLER
A. L. Kachelmyer and K. W. Forsythe 11 Feb. 1991 44 p
(Contract F19628-90-C-0002)
(AD-A233723; TR-905; ESD-TR-90-134) Avail: NTIS HC/MF A03 CSCL 12/9

The performance loss of an M-ary orthogonal keying (MOK) system can be minimized by selecting good signaling sets, due to relative motion between its transmitter and receiver. The formulation for evaluating good signaling sets, or codesets, is developed for Walsh function data modulations. A union bound performance measure, which closely approximates the exact probability of a demodulation error, is devised to allow for convenient evaluation of Walsh function codesets. The best Walsh function codesets for codevectors up to length 10 and for M = 2,4,8, and 16 are presented along with their performance. In addition, codesets based on error-correcting codes are supplied along with a performance bound expressed in terms of the code's minimum distance. GRA

N91-26412# Massachusetts Inst. of Tech., Lexington. Lincoln Lab.
OPPORTUNITIES FOR ADVANCED SPEECH PROCESSING IN MILITARY COMPUTER-BASED SYSTEMS
C. J. Weinstein 11 Feb. 1991 51 p
(Contract F19628-90-C-0002)
(AD-A233724; TR-904; ESD-TR-90-133) Avail: NTIS HC/MF A04 CSCL 25/4

This report presents a study of military applications of advanced speech processing technology which includes three major elements: (1) review and assessment of current efforts in military applications of speech technology; (2) identification of opportunities for future military applications of advanced speech technology; and (3) identifications of problem areas where research in speed processing is needed to meet application requirements and of current research thrusts which appear promising. The relationship of this study to previous assessments of military applications of speech technology is discussed, and substantial recent progress is noted. Current efforts in military applications of speech technology which are highlighted include: (1) narrowband (2400 b/s) and very-low-rate (50-1200 b/s) secure voice communication; (2) voice/data integration in computer networks; (3) speech recognition in fighter aircraft, military helicopters, battle management, and air traffic control training systems; and (4) noise and interference removal for human listeners. Opportunities for advanced applications are identified by means of descriptions of several generic systems which would be possible with advances in speech technology and in system integration. GRA

N91-26413# Massachusetts Inst. of Tech., Lexington. Lincoln Lab.
A TEST VECTOR GENERATOR FOR A RADAR SIGNAL PROCESSOR Technical Report, 1 Nov. 1988 - 30 Sep. 1989
C. B. Robins 7 Feb. 1991 86 p
(Contract F19628-90-C-0002)
(AD-A233725; TR-827; ESD-TR-90-117) Avail: NTIS HC/MF A05 CSCL 17/9

This report documents the test vector generator (TVG) system developed for the purpose of testing a radar signal processor. This system simulates an eight channel radar receiver by providing input data for testing the signal processor test bed. The TVG system outputs 128-bit wide data samples at variable rates up to and including 10 million samples per second. The VTG memory array is one million samples deep. Variably sized output vectors can be addressed within the memory array and the vectors can be concatenated, repeated, and reshuffled in real time under the control of a single board computer. The TVG is seen having applications on a variety of programs. Discussions of adapting and scaling the system to these other applications are presented. GRA

N91-26414# Massachusetts Inst. of Tech., Lexington. Lincoln Lab.
A PHYSIOLOGICALLY MOTIVATED FRONT END FOR SPEECH RECOGNITION
Thao K. Nguyen, Richard P. Lippmann, Bernard Gold, and Douglas B. Paul 26 Feb. 1991 42 p
(Contract F19628-90-C-0002)
(AD-A233727; TR-893; ESD-TR-90-139) Avail: NTIS HC/MF A03 CSCL 25/4

A physiological front-end preprocessor for speech recognition was evaluated using a large isolated word database in noisy and quiet environments. The front end was based on the ensemble interval histogram (EIH) model developed by Oded Ghitza, which provides phase or synchrony information similar to that available on the auditory nerve. A modified EIH front end was implemented and tested using a Lincoln hidden Markov model (HMM) isolated word recognizer with a large stress/style speech database at various signal-to-noise ratios (SNRs). The modified EIH front end performed as well as the conventional mel-filter bank (MFB) front for normal speech. It provided only a slight reduction in error rate at very low SNRs when trained with clean speech and no improvements in error rate compared with the MFB front end when both trained and tested in noise. Excessive computation requirements - more than 200 times that of our best performing conventional front end - currently limit the practicality of the EIH front end. GRA

N91-26415# Aerospace Corp., El Segundo, CA.
APPLICATION OF A CONJUGATE GRADIENT METHOD TO THE SYNTHESIS OF PHASE-ONLY PLANAR ARRAYS
Timothy J. Peters 15 Feb. 1991 60 p

(Contract F04701-88-C-0089)
(AD-A233756; TR-0090(5925-05)-1; SSD-TR-91-03) Avail: NTIS HC/MF A04 CSCL 09/1

The problem of minimizing the peak sidelobe level of a planar array of dipoles using phase-only synthesis is investigated. A hybrid nonlinear function minimization scheme is developed using a Taylor series approximation and a conjugate gradient algorithm. A weighted average peak sidelobe level function is introduced to yield a more stable numerical procedure. The peak sidelobe level is found to decrease in proportion to the logarithm of the aperture behavior. GRA

N91-26416# Naval Research Lab., Washington, DC.
THE EFFECT OF THE IONOSPHERE ON RADIOWAVE SIGNALS AND SYSTEMS PERFORMANCE BASED ON IONOSPHERIC EFFECTS SYMPOSIUM
John M. Goodman, J. A. Klobuchar, R. G. Joiner, and H. Solcher 3 May 1990 589 p Symposium held in Washington, DC, 1-3 May 1990
(AD-A233797) Avail: NTIS HC/MF A25 CSCL 20/14

Topics addressed include: Topical Reviews, High Latitude Phenomena, Scintillation Effects, Radar System Effects, High Frequency, Meteor, and Miscellaneous Systems, Total Electron Content and Global Positioning System, Longwave Systems and Modification. GRA

N91-26417# Telecommunication Science Associates, Inc., San Diego, CA.
VLF NIGHTTIME DATA ANALYSIS Final Report
Mar. 1991 125 p
(Contract N66001-88-D-0033)
(AD-A234006; TCS-TP-89-368; NOSC-TD-2042) Avail: NTIS HC/MF A06 CSCL 20/14

This paper documents a very low frequency/low frequency (VLF/LF) Data Analysis task by the Naval Ocean Systems Center to improve the modeling of the nighttime ionosphere when making propagation predictions with the Long Wave Propagation Capability (LWPC) computer program. The task utilizes an extensive database of VLF measured data recorded during the 1985 to 1986 trips of the merchant ship GTS Callaghan in the North Atlantic area. By constraining the Callaghan data to those periods when both the ship and the distant transmitters were in time zones consistent with all-nighttime propagation, and by eliminating data from trips outside the principal area of interest, an aggregated set of recorded data was assembled for each frequency of concern. Four frequencies were examined: 16.0, 19.0, 21.4 and 24.0 kHz. Recorded data sets were graphed as signal vs. distance plots, computing distance from the transmitter for each ship's location. The LWPC program was then utilized to compute signal vs. distance along a typical path in the same ocean area, and the predicted and recorded data were compared. By changing the LWPC parameters different propagation predictions were compared with the recorded data until a best fit was obtained. GRA

N91-26418# Mission Research Corp., Santa Barbara, CA.
PROPAGATION OF RF SIGNALS THROUGH STRUCTURED IONIZATION: THE GENERAL MODEL Technical Report, 1 Jan. - 31 Dec. 1989
Roger A. Dana 1 Mar. 1991 138 p
(Contract DNA001-87-C-0169)
(AD-A234051; MRC-R-1262R; DNA-TR-90-9) Avail: NTIS HC/MF A07 CSCL 20/14

Design and evaluation of radio frequency (RF) systems that must operate through ionospheric disturbances requires an accurate channel model. Such a model can be used to construct realizations of the received signal for use in digital simulations of transionospheric communications links and radars or hardware channel simulators. This report presents a review of RF propagation through structured ionization, starting with Maxwell's equations and ending with the two-position, two-frequency, two-time mutual coherence function of the received signal. The derivation of the mutual coherence function requires a model for the temporal and spatial variations of the electron density fluctuations in the ionosphere. Under Taylor's frozen in hypothesis, the electron density fluctuations are described as a rigid structure that drifts past the line-of-sight. In the fully turbulent case, the spatial and temporal fluctuations of the electron density are uncorrelated. Reality should lie somewhere between these two limiting models. GRA

N91-26419# University of Southern California, Los Angeles. Communications Sciences Inst.
ADAPTIVE SPREAD SPECTRUM NETWORKS Final Report, 1 May 1988 - 31 Dec. 1990
John Silvester Mar. 1991 36 p
(Contract DAAL03-88-K-0050)
(AD-A234084; ARO-25507-31-EL) Avail: NTIS HC/MF A03 CSCL 25/2

Abstracts are presented of papers processed, submitted, and published and Ph.D. theses. GRA

N91-26420# Washington Univ., Saint Louis, MO. Dept. of Physics.
THEORY OF RADAR TARGET DISCRIMINATION Final Report, period ending Feb. 1991
E. T. Jaynes and C. R. Smith Feb. 1991 32 p
(Contract DAAL03-86-D-0001)
(AD-A234172; AD-E951634; ASMI-CR-RD-AS-91-6) Avail: NTIS HC/MF A03 CSCL 17/9

After a brief discussion of the radar target identification program, a direct application of probability theory is given to the problem of deciding which of a set of possible targets is present. The reliability of discrimination depends on the noise level, the back ground hash, the variation of echo with target aspect angles, the energy and shape of the transmitted pulse, and the number of pulses. The effect of each of these variables is calculated and discussed, leading to some new conclusions about optimal radar design and optimal data processing. The tactics which might succeed are quite different from those that have been tried in the past, and give elementary intuitive explanations why this is so. GRA

N91-26421# Mitre Corp., Bedford, MA.
INPUT IMPEDANCE AND GAIN OF MONOPOLE ELEMENTS WITH DISK GROUND PLANES ON FLAT EARTH
M. M. Weiner Dec. 1990 25 p
(AD-A234284; MTR-M90-92) Avail: NTIS HC/MF A03 CSCL 09/1

This paper extends previously reported results for a quarterwave monopole element on a disk ground plane in free space to the case where the disk ground plane rests on flat earth. Numerical results are obtained by utilizing Richmond's method of moments computer program for disk ground planes over flat earth. GRA

N91-26422# Syracuse Univ., NY. Dept. of Electrical and Computer Engineering.
UNCERTAINTY HANDLING AT SPEECH/NATURAL LANGUAGE INTERFACE, VOLUME 1 Final Technical Report, Jan. 1988 - Jan. 1989
Can Isik Dec. 1990 24 p
(Contract F30602-88-D-0027)
(AD-A234310; RADC-TR-90-412-Vol-1) Avail: NTIS HC/MF A03 CSCL 25/4

VoiceScribe 1000 Speech Recognition System provides a discrete utterance, speaker dependent recognition system capability. The speech driver interface routines give a confidence level, which is a number between 0 and 100, for the word that best matches the uttered word. For the alternate choices it provides distances between those words and the uttered word, which are numbers between 0 and 254. To modify the VoiceScribe 1000 Speech Recognition System to give not only the best match, but a set of close matches for each utterance and their levels of match, the distance measures were utilized to calculate the certainty levels for alternate choices, and the confidence level for the best matched word was used directly as its certainty level. Further work needs to be done for more consistent confidence level assignments. GRA

N91-26423# Texas A&M Univ., College Station. Dept. of Electrical Engineering.
RADIATION, SCATTERING, AND GUIDANCE OF ELECTROMAGNETIC FIELDS BY ARBITRARILY SHAPED STRUCTURES EMBEDDED IN LAYERED DIELECTRIC MEDIA Quarterly Progress Report, 1 Jan. - 31 Mar. 1991
K. A. Michalski 31 Mar. 1991 1 p
(Contract N00014-91-J-1197)
(AD-A234434) Avail: NTIS HC/MF A01 CSCL 20/14

The study has been completed for an aperture-coupled microstrip patch antennas with uniaxial substrates. In particular, by a rigorous spectral domain approach - a circular microstrip antenna excited by a fundamental microstrip line mode is analyzed through a rectangular aperture in a ground plane. A more efficient, but approximate, reciprocity theorem based method, has also been implemented. Finally, a mixed, spectral and space domain approach has been developed to analyze an arbitrarily shaped microstrip patch antenna coupled to a microstrip transmission line through an arbitrarily shaped aperture. The space domain method is used to model the arbitrarily shaped patch and aperture, and the semiinfinite transmission line is modeled in spectral domain. To corroborate the validity of the analysis, we have built a circular patch test antenna coupled to the transmission line through a rectangular aperture and measured its input impedance over a broad frequency range. GRA

N91-26424# Lowell Univ., MA. Center for Atmospheric Research.
METEOR SCATTER COMMUNICATION BETWEEN THULE AND STATION NORD, GREENLAND
Jens Ostergaard Sep. 1990 161 p
(Contract F19628-88-K-0004)
(AD-A234440; ULRF-462/CAR; GL-TR-90-0248; SR-3) Avail: NTIS HC/MF A08 CSCL 25/2

Meteor scatter as a mode of communication was first examined in Canada in the late 1940's and later in Europe in 1960. It was found to provide a good, but relatively low capacity digital communication channel. In comparison with high yield satellite links, meteor scatter was too complex for widespread utilization then. However, the advent of the microprocessor has removed the most costly obstacles of its economical use in areas where no regular communication systems exist. This report examines such meteor scatter paths between selected Greenland sites and Station Nord. A 1800 km link was found to provide virtually no throughput and discussion focuses on probable causes. In contrast, a 1150 km link traversing northern Greenland produced very high throughput. Extensive analyses are presented of propagation properties and potential communication capabilities. These are discussed extensively in light of several scenarios. GRA

N91-26425# Naval Research Lab., Washington, DC.
PLASMA REFLECTORS FOR ELECTRONIC BEAM STEERING IN RADAR SYSTEMS Memorandum Report
Wallace M. Manheimer 17 Apr. 1991 24 p
(AD-A234560; NRL-MR-6809) Avail: NTIS HC/MF A03 CSCL 20/9

Methods of generating a planar plasma are investigated. The application is a reflector for radar waves. The use of the plasma reflector could allow electronic beam steering at frequencies above what is generally viable for phased arrays. Three aspects of the planar plasma production are investigated: the localization of the plasma; the main plasma production; and the long term viability of the system. Possible applications include ship based antenna at X-Band and space based antenna at 60 GHz. GRA

N91-26426# Colorado School of Mines, Golden. Dept. of Mathematics and Computer Sciences.
BACKSCATTERING ENHANCEMENT FROM ROUGH SURFACES Final Report, 15 Dec. 1988 - 14 Dec. 1990
John A. DeSanto 11 Mar. 1991 5 p
(Contract DAAL03-89-K-0024)
(AD-A234707; ARO-26275.3-GS) Avail: NTIS HC A02/MF A01 CSCL 20/3

Several classical theoretical developments are available to treat rough surface scattering, each with a limited parameter domain of validity. Recent experimental work uses manufactured surfaces whose parameters (height and slope) are outside these domains. Predictions include an enhancement of the scattering in the backscatter directions for random surfaces of large rms height and slope. New methods to treat these problems have been obtained. Results include further development of the mixed spectral and coordinate method for both scalar and electromagnetic problems. For the scalar case we have used this method to generate algorithms which are used to reconstruct rough surfaces from scattered field data. Two versions of the reconstruction are possible. The first is valid for small roughness and is FFT based. It reconstructs the profile using fixed frequency and fixed illumination angle data for the Dirichlet boundary condition. The second is valid in the domain of the Kirchoff approximation and is FFT based, but here on a prescribed data set involving both incident and scattered angles. For larger roughness surfaces we have observed enhancement effects using a different numerical approach. GRA

N91-26427# Aerospace Medical Research Labs., Wright-Patterson AFB, OH.
INTELLIGIBILITY OF DIGITAL SPEECH MASKED BY NOISE: NORMAL HEARING AND HEARING IMPAIRED LISTENERS Summary Report, Oct. 1988 - Jun. 1990
Charles W. Nixon, Mark S. Stephenson, Richard L. McKinley, Vernie G. Fisher, and Michael J. Jacobs Jun. 1990 37 p
(AF Proj. 7231)
(AD-A234852; AAMRL-TR-90-026) Avail: NTIS HC/MF A03 CSCL 25/4

The intelligibility in noise of normal and digital speech (ADPCM, CVSD, LPC-10 vocoders) was measured for normal hearing and hearing impaired listeners. The digitally coded speech was generally less intelligible than normal speech; however, the highest quality digital system provided speech that was similar in intelligibility to normal speech. The speech from some digital systems was more vulnerable to noise masking than from others. Hearing impaired persons with no prior experience listening to digital speech required more time to attain maximum listening performance than normal hearing listeners. The rank ordering of intelligibility of the three types of digital speech was the same for the hearing impaired as for the normal hearing listeners. Persons with moderate hearing loss will have greater difficulty than normal hearing listeners in understanding digital speech in noise. Personnel with hearing impairment using digital speech systems in operational noise environment may be contributing to voice communication problems attributed only to the digital speech. GRA

N91-26428# Range Commanders Council, White Sands Missile Range, NM.
HORACE: PRESENTATION-LEVEL PROTOCOL STANDARD FOR DIGITAL TRANSMISSION OF MONOCHROME TELEVISION IMAGES
Mar. 1991 62 p
(AD-A235276; RCC-210-91) Avail: NTIS HC/MF A04 CSCL 25/5

This document establishes a single digital television transmission standard with sufficient versatility to meet a large variety of instrumentation needs for DOD test ranges. Within the framework of the standard, the user can specify transmission rate, horizontal and temporal resolutions, and can determine what picture quality is required for any particular use. Additional data, not intended to be part of the displayed picture, can be added between picture fields and between horizontal lines. The decoder requires almost no adjustment when digitized video data and clock signal are fed and can indicate the type of error if errors are detected. This standard defines a presentation-level protocol syntax and concerns itself with operation at the user, presentation, and session levels at both ends of the one-way link. The action of the HORACE protocol is unaffected by changes below these levels as long as the received signal associated with it, and the order of data bits is unchanged from those sent. GRA

N91-26429# BBN Systems and Technologies Corp., Cambridge, MA.
ARCHITECTURES FOR A HIGH PERFORMANCE DISTRIBUTED OPERATING SYSTEM Final Report, Mar. 1989 - Mar. 1990
Kenneth J. Schroder, Richard E. Schantz, and Stephen T. Vinter Mar. 1991 54 p
(Contract F30602-87-D-0093)
(AD-A235333; RL-TR-91-19) Avail: NTIS HC/MF A04 CSCL 12/6

This document focused on how object oriented distributed system architecture adapt to incorporate the benefits of high performance communication technology. The introduction of fiber optic digital technology over the next decade will lead to a dramatic increase in communication bandwidth. Other technologies will lead to comparable improvements in processor, memory, and device speeds. These advances will result in changes to communication protocols, networks, and operating systems, and growing distribution of functions across multiple computers both locally and globally. These major underlying changes will have to be reflected in the design of new distributed systems. The growth trends of these related technologies are surveyed, followed by a brief characterization of the applications that will benefit from these advances. The key goals of software development in high performance environments are to enable new classes of applications by exploiting performance and to develop better application structures to encourage scalability. This report discusses such goals of distributed systems and the impact of higher performance technology on each. Detailed architectural issues are covered with specific recommendations for further investigation. Suggestions for improvements to the Cronus distributed operating system to adapt it to higher performance environments are given. GRA

N91-26430# Rensselaer Polytechnic Inst., Troy, NY.
SPREAD SPECTRUM COMMUNICATIONS EMULATOR DESIGN Final Report, Jan. 1989 - Jun. 1990
Gary J. Saulnier, Pankaj K. Das, and Joseph M. Pennisi Mar. 1991 54 p
(Contract F30602-88-D-0025)
(AD-A235403; RL-TR-91-32) Avail: NTIS HC/MF A04 CSCL 17/4

This report describes a simulation which was developed to emulate a spread spectrum communication system. The simulation was developed to allow test and evaluation of advanced signal processing concepts, which will be used by the Air Force in developing next-generation jam resistant, covert communication systems. GRA

N91-26431# RAND Corp., Santa Monica, CA.
THE WILD WEASEL DEVELOPMENT PROGRAMS, ONE RUN, ONE HIT, ONE ERROR
Gerald J. Stiles Jul. 1990 51 p
(RAND-P-7661-RGS) Avail: NTIS HC/MF A04

Traced here are the development and upgrade programs for a specialized program, the F-4G Wild Weasel. Potential reasons why the initial development program for the aircraft succeeded, whereas the follow-on program failed, are examined. Author

N91-26432# Advisory Group for Aerospace Research and Development, Neuilly-Sur-Seine (France). Flight Mechanics Panel.
DIGITAL SIGNAL CONDITIONING FOR FLIGHT TEST, VOLUME 19
G. A. Bever (National Aeronautics and Space Administration. Ames Research Center, Moffett Field, CA.) Jun. 1991 92 p
(AGARD-AG-160-Vol-19; ISBN-92-835-0621-9) Copyright Avail: NTIS HC/MF A05; Non-NATO Nationals requests available only from AGARD/Scientific Publications Executive

Flight test instrumentation engineers are provided with an introduction to digital processes on aircraft. Flight test instrumentation systems are rapidly evolving from analog intensive to digital intensive systems, including the use of onboard digital computers. Topics include: measurements that are digital in origin, sampling, encoding, transmitting, and storing of data. Particular emphasis is placed on modern avionic data bus architectures and what to be aware of when extracting data from them. Some example data extractions are given. Tradeoffs between digital logic families, trends in digital development, and design testing techniques are discussed. An introduction to digital filtering is also covered. Author

N91-26433# Mitre Corp., McLean, VA. Civil Systems Div.
FUNCTIONAL BASELINE SPECIFICATION FOR ATC DATA LINK SERVICE IMPLEMENTATION IN THE HOST COMPUTER SYSTEM Final Report
F. Buck, P. Cratch, H. Gabrieli, and D. Sweeney Jun. 1991 134 p
(Contract DTFA01-89-C-00001)
(DOT/FAA/CT-91/12; MTR-90W00164) Avail: NTIS HC/MF A07

This specification defines the requirements for implementing the initial air traffic control (ATC) data link services in the host computer system. In addition to describing how each of the initial services operate in the context of current host processing, the new controller data entries and display features associated with each of the initial data link services are defined. System supervisory and support functions are also specified. Author

N91-26615*# Kyoto Univ. (Japan). Radio Atmospheric Science Center.
RADAR PRINCIPLES
Toru Sato *In* International Council of Scientific Unions, Kyoto Middle Atmosphere Program. Handbook for MAP. Volume 30: International School on Atmospheric Radar Oct. 1989 p 19-53 (For primary document see N91-26613 18-46)
Avail: NTIS HC/MF A16; also available from SCOSTEP Secretariat, Illinois Univ., 1406 Green Street, Urbana, IL 61801 CSCL 17I

N91-26616*# EISCAT Scientific Association, Kiruna (Sweden).
THE INSTRUMENTAL PRINCIPLES OF MST RADARS AND INCOHERENT SCATTER RADARS AND THE CONFIGURATION OF RADAR SYSTEM HARDWARE
Juergen Roettger (Max-Planck-Inst. fuer Aeronomie, Katlenburg-Lindau, Germany, F.R.) *In* International Council of Scientific Unions, Kyoto Middle Atmosphere Program. Handbook for MAP. Volume 30: International School on Atmospheric Radar Oct. 1989 p 54-113 (For primary document see N91-26613 18-46)
Avail: NTIS HC/MF A16; also available from SCOSTEP Secretariat, Illinois Univ., 1406 Green Street, Urbana, IL 61801 CSCL 17I

N91-26617*# Instituto Geofisico del Peru, Lima. Jicamarca Radio Observatory.
STATISTICAL CHARACTERISTICS OF MST RADAR ECHOES AND ITS INTERPRETATION
Ronald F. Woodman *In* International Council of Scientific Unions, Kyoto Middle Atmosphere Program. Handbook for MAP. Volume 30: International School on Atmospheric Radar Oct. 1989 p 114-150 (For primary document see N91-26613 18-46)
Avail: NTIS HC/MF A16; also available from SCOSTEP Secretariat, Illinois Univ., 1406 Green Street, Urbana, IL 61801 CSCL 17I

N91-26618*# Kyoto Univ. (Japan). Radio Atmospheric Science Center.
DATA ACQUISITION AND PROCESSING
Toshitaka Tsuda *In* International Council of Scientific Unions, Kyoto Middle Atmosphere Program. Handbook for MAP. Volume 30: International School on Atmospheric Radar Oct. 1989 p 151-183 (For primary document see N91-26613 18-46)
Avail: NTIS HC/MF A16; also available from SCOSTEP Secretariat, Illinois Univ., 1406 Green Street, Urbana, IL 61801 CSCL 17I

N91-26619*# Case Western Reserve Univ., Cleveland, OH. Dept. of Electrical Engineering and Applied Physics.
SPECTRAL AND CORRELATION ANALYSIS WITH APPLICATIONS TO MIDDLE-ATMOSPHERE RADARS
Prabhat K. Rastogi *In* International Council of Scientific Unions, Kyoto Middle Atmosphere Program. Handbook for MAP. Volume 30: International School on Atmospheric Radar Oct. 1989 p 184-227 (For primary document see N91-26613 18-46)
Avail: NTIS HC/MF A16; also available from SCOSTEP Secretariat, Illinois Univ., 1406 Green Street, Urbana, IL 61801 CSCL 17I

N91-26620*# Kyoto Univ. (Japan). Radio Atmospheric Science Center.
TARGET PARAMETER ESTIMATION
W. K. Hocking (Adelaide Univ., Australia) *In* International Council of Scientific Unions, Kyoto Middle Atmosphere Program. Handbook for MAP. Volume 30: International School on Atmospheric Radar Oct. 1989 p 228-268 (For primary document see N91-26613 18-46)
Avail: NTIS HC/MF A16; also available from SCOSTEP Secretariat, Illinois Univ., 1406 Green Street, Urbana, IL 61801 CSCL 17I

N91-27100*# Stevens Inst. of Tech., Hoboken, NJ. Dept. of Electrical Engineering.
APPLICATIONS OF FORMAL SIMULATION LANGUAGES IN THE CONTROL AND MONITORING SUBSYSTEMS OF SPACE STATION FREEDOM Final Report
R. C. Lacovara *In* Houston Univ., NASA/ASEE Summer Faculty Fellowship Program, 1990, Volume 1 Dec. 1990 13 p (For primary document see N91-27088 18-99)
(Grant NGT-44-005-803)
Avail: NTIS HC/MF A10 CSCL 17B

33 ELECTRONICS AND ELECTRICAL ENGINEERING

Includes test equipment and maintainability; components, e.g., tunnel diodes and transistors; microminiaturization; and integrated circuitry.

For related information see also *60 Computer Operations and Hardware* and *76 Solid-State Physics.*

N91-26434*# Cincinnati Univ., OH. Dept. of Electrical and Computer Engineering.
MMIC INTEGRATION TECHNOLOGY INVESTIGATION Final Technical Report, 5 Mar. 1990 - 15 Jun. 1991
Vik J. Kapoor 15 Jun. 1991 74 p
(Contract NCC3-167)
(NASA-CR-188035; NAS 1.26:188035) Avail: NTIS HC/MF A04 CSCL 09A

Final technical report on NASA cooperative agreement NCC-167 is presented for the period March 5, 1990 to June 15, 1991. The following topics are included: (1) four to one power combiner for 20 GHz phased array antenna using RADC MMIC phase shifters; and (2) testing of indium phosphide devices. For individual titles, see N91-26435 through N91-26436.

N91-26435*# Cincinnati Univ., OH.
FOUR-TO-ONE POWER COMBINER FOR 20 GHz PHASED ARRAY ANTENNA USING RADC MMIC PHASE SHIFTERS
In its MMIC Integration Technology Investigation 15 Jun. 1991 p 1-42 (For primary document see N91-26434 18-33)
Avail: NTIS HC/MF A04 CSCL 09A

The design and microwave simulation of two-to-one microstrip power combiners is described. The power combiners were designed for use in a four element phase array receive antenna subarray at 20 GHz. Four test circuits are described which were designed to enable testing of the power combiner and the four element phased array antenna. Test Circuit 1 enables measurement of the two-to-one power combiner. Test Circuit 2 enables measurement of the four-to-one power combiner. Test Circuit 3 enables measurement of a four element antenna array without phase shifting MMIC's in order to characterize the power combiner with the antenna patch-to-microstrip coaxial feedthroughs. Test circuit 4 is the four element phased array antenna including the RADC MMIC phase shifters and appropriate interconnects to provide bias voltages and control phase bits. Author

N91-26436*# National Aeronautics and Space Administration. Lewis Research Center, Cleveland, OH.
SUBMICRON GATE InP POWER MISFET'S WITH IMPROVED OUTPUT POWER DENSITY AT 18 AND 20 GHz
M. D. Biedenbender, Vik J. Kapoor, K. A. Shalkhauser, L. J. Messick, R. Nguyen, D. Schmitz, and H. Juergensen (Aixtron Corp., Aachen, Germany, F.R.) *In* Cincinnati Univ., OH, MMIC Integration Technology Investigation 15 Jun. 1991 p 44-69 (For primary document see N91-26434 18-33)
Avail: NTIS HC/MF A04 CSCL 09A

The microwave characteristics are presented at 18 and 20 GHz of submicron gate indium phosphide (InP) metal-insulator-semiconductor field-effect transistors (MISFET's) for high output power density applications. InP power MISFET's were fabricated and the output power density was investigated as a function of drain-source spacing. The best output power density and gain were obtained for drain-source spacing of 3 microns. The output power density is 2.7 times greater than was previously measured for InP MISFET's at 18 and 20 GHz, and the power-added efficiency also increased. Author

N91-26437# National Inst. of Standards and Technology, Gaithersburg, MD. Semiconductor Electronics Div.
CENTER FOR ELECTRONICS AND ELECTRICAL ENGINEERING. TECHNICAL PROGRESS BULLETIN COVERING CENTER PROGRAMS, JULY TO SEPTEMBER 1990, WITH 1991 CEEE EVENTS CALENDAR
J. A. Gonzalez Jan. 1991 48 p
(PB91-159749; NISTIR-4496) Avail: NTIS HC/MF A03 CSCL 09C

The report is the thirty-second issue of a quarterly publication providing information on the technical work of the National Institute of Standards and Technology (formerly the National Bureau of Standards) Center for Electronics and Electrical Engineering (CEEE). The issue of the CEEE Technical Progress Bulletin covers the third quarter of calendar year 1990. Abstracts are provided by technical area for both published papers and papers approved by NIST for publication. General topics discussed include the following: Semiconductor Technology Program; Signals and Systems Metrology Program; Additional Information; 1991 CEEE Calendar; Sponsor List; and Key Contacts in Center, Center Organization. Author

N91-26438* National Aeronautics and Space Administration. Goddard Space Flight Center, Greenbelt, MD.
SYNCHRONOUS DEMODULATOR Patent
John F. Sutton, inventor (to NASA) 14 May 1991 8 p Filed 29 Sep. 1989
(NASA-Case-GSC-13179-1; US-Patent-5,015,963;
US-Patent-Appl-SN-414815; US-Patent-Class-329-361;
US-Patent-Class-329-349; US-Patent-Class-307-353;
Int-Patent-Class-H03D-1/04) Avail: US Patent and Trademark Office CSCL 09C

A synchronous demodulator includes a switch which is operated in synchronism with an incoming periodic signal and both divides and applies that signal to two signal channels. The two channels each include a network for computing and holding, for a predetermined length of time, the average signal value on that channel and applies those valves, in the form of two other signals, to the inputs of a differential amplifier. The networks may be R-C networks. The output of the differential amplifier may or may not form the output of the synchronous detector and may or may not be filtered. The output will not include a periodic signal due to the presence of a dc offset. Additionally, the output will not contain any substantial ripple due to periodic components in the input

signal. In a somewhat more complex version, containing twice the structural components of the above synchronous demodulator with a more complex switching mechanism, essentially all ripple due to periodic components in the input signal are eliminated. Author

N91-26439# Cree Research, Inc., Durham, NC.
DEVELOPMENT AND TESTING OF RADIATION AND ELECTROMAGNETIC PULSE HARDENED SILICON CARBIDE BASED ELECTRONICS Quarterly Report, 1 Sep. - 30 Nov. 1990
J. A. Edmond and J. W. Palmour 28 Feb. 1991 10 p
(Contract N00014-90-C-0037)
(AD-A233744; TR-901008-5) Avail: NTIS HC/MF A02 CSCL 09/1

There were three primary objectives for this reporting period. The first was to epitaxially grow and fabricate low voltage (50 to 70 V) p-n junction rectifiers for subsequent avalanche energy testing (AET) at 10 micro second pulse widths. The results of this test are compared to the AET results for higher voltage rectifiers (400 to 500 V) reported last quarter. The second was to design and epitaxially grow a gated thyrister structure. Two structures yielding 80 to 150 V and 200 to 350 V breakover voltage at zero gate current have been grown. The third objective was to fabricate JFET devices with higher power output than those discussed in the previous report. As in the last report, to simulate the effects of an electromagnetic pulse (EMP) on a p-n junction device, reverse bias AET was performed. The difference between this experiment and those performed in the previous reporting period was that the breakdown voltage (Vbr) of the present diodes was substantially lower than in the former test. Previously, the Vbr of the diodes was generally in the 400 to 500 V range where one would expect that the passivating layer on the junction may greatly affect its avalanche energy capability. In this experiment, diodes with a Vbr of 50 to 70 V were fabricated and tested for their resistance to EMP effects. GRA

N91-26440# North Carolina State Univ., Raleigh.
ACTIVE DEVICES FOR MONOLITHIC MILLIMETER-WAVE INTEGRATED CIRCUITS Final Report
D. E. Stoneking and R. J. Trew 15 Mar. 1991 22 p
(Contract DAAL03-86-G-0056)
(AD-A234033; ARO-23788.2-EL-F) Avail: NTIS HC/MF A03 CSCL 09/1

The purpose of this project was to develop an advanced computer aided design (CAD) tool that can be used for the design of microwave and millimeter-wave solid-state integrated circuits. The completed work consists of major improvements to a large-signal, physics based model for GaAs field effect transistor (MESFET) integrated circuits previously developed at North Carolina State University (NCSU). New features for the model include a large-signal load-pull algorithm and RF sensitivity and process yield capability. The new algorithms significantly enhance the use of the simulator in design applications. The new capability permits the simulator to be used for both MESFET and RF circuit process yield optimization. Author (GRA)

N91-26441# Rome Air Development Center, Griffiss AFB, NY.
DIGITAL LOGIC TESTING AND TESTABILITY
Warren H. Debany, Jr. Feb. 1991 59 p
(AF Proj. 2338)
(AD-A234123; RL-TR-91-6) Avail: NTIS HC/MF A04 CSCL 09/1

Electronic hardware is subject to defects that are introduced at the time of manufacture and failures that occur in the field. Because of the complexity of digital logic circuits, they are difficult to test. This report provides an overview of digital logic testing. It provides access to the literature and unifies terminology and concepts that have evolved in this field. It discusses the types and causes of failures in digital logic. This report presents the topics of logic and fault simulation, fault grading, test generation algorithms, and fault isolation. The discussion of testability measurement is useful for understanding testability requirements and analysis techniques. Design-for-testability and built in test techniques are presented. GRA

N91-26442# Naval Ocean Systems Center, San Diego, CA.
DE-EMBEDDING MILLIMETER-WAVE INTEGRATED CIRCUITS WITH TRL
David Rubin Jan. 1991 31 p
(AD-A234194; NOSC/TD-2020) Avail: NTIS HC/MF A03 CSCL 09/1

Through the use of a modification of the TRL (Through-Reflect-Line) method, integrated circuits contained within transitions have been successfully de-embedded. Two waveguide-to-suspended substrate fixtures of different lengths were fabricated on a computer-controlled mill. Printed circuit waveguide probes were intentionally shortened to make them very reactive. Transmission and reflection measurement of a filter placed between the probes highlight the differences between measured and de-embedded results. This report reviews the theory behind TRL, explains the modifications used, and presents a computer program to de-embedded measurements from a Wiltron 360 network analyzer. GRA

N91-26443# Frequency and Time Systems, Inc., Beverly, MA.
TACTICAL QUARTZ OSCILLATOR DEVELOPMENT Final Report, 1983 - 1989
Donald A. Emmons Sep. 1990 60 p
(Contract F19628-81-C-0148)
(AD-A234308; RADC-TR-90-232) Avail: NTIS HC/MF A04 CSCL 20/2

This report presents results on development, fabrication, and testing of precision oscillators utilizing the miniature SC-cut 10MHz BVA resonator. Performance characteristics of ten engineering development model oscillators, FTS Model 2000B, were evaluated. Important results include the demonstration of low g-sensitivity, very good frequency stability, and low aging rate. GRA

N91-26444# Rome Air Development Center, Griffiss AFB, NY.
RADC CATHODE LIFE TEST FACILITY Report, Oct. 1981 - Jun. 1990
Mark E. Novak, Dirk T. Bussey, and Edward J. Daniszewski Feb. 1991 59 p
(AD-A234309; RL-TR-91-10) Avail: NTIS HC/MF A04 CSCL 14/2

This report provides a basic introduction to the Rome Laboratory Cathode Life Test Facility, followed by a compilation of life test data. The Cathode Life Test Facility has been in operation for nine years and has tested 10 different cathode types for a total of approximately 1.5 million hours of life test data. GRA

N91-26445# Texas Univ., Austin. Electrical Engineering Research Lab.
HIGH TEMPERATURE SUPERCONDUCTING PLANAR CIRCUIT STRUCTURES FOR HIGH FREQUENCY APPLICATIONS Final Report, Oct. 1988 - Dec. 1990
Tatsuo Itoh 20 Jan. 1991 7 p
(Contract N00014-89-J-1006)
(AD-A234335) Avail: NTIS HC/MF A02 CSCL 20/12

This report summarizes technical activities and accomplishments under the support from Office of Naval Research in the area of electromagnetic analysis of planar circuit structures that contain high Tc superconductors. The report is divided into two parts. The first part is concerned with the numerical methods developed for characterizations of discontinuities in the planar circuit. The second part is on the development of a new method for characterizing a conductor loss in the high Tc planar transmission lines. GRA

N91-26446# Massachusetts Inst. of Tech., Cambridge. Artificial Intelligence Lab.
PIEZOELECTRIC MICROMOTORS FOR MICROROBOTS Memorandum Report
Anita M. Flynn, Lee S. Tavrow, Stephen F. Bart, and Rodney A. Brooks Feb. 1991 22 p

(Contract N00014-85-K-0685)
(AD-A234423; AI-M-1269) Avail: NTIS HC/MF A03 CSCL 10/2

Mobile robots are able to carry more and more intelligence (and in smaller packages) onboard everyday. Now we would like to match the brawn of our robots to the same scale as the brain. Towards this end, we have fabricated some small, a few millimeters in diameter, piezoelectric motors using ferroelectric thin films. These motors consist of two pieces: a stator and a rotor. The stationary stator includes a piezoelectric film in which we induce bending in the form of a traveling wave. Anything which sits atop the stator is propelled by the wave. A small glass lens placed upon the stator becomes the spinning rotor. Piezoelectric micromotors overcome the problems currently associated with electrostatic micromotors such as low torque, friction, and the need for high voltage excitation. GRA

N91-26447# Harry Diamond Labs., Adelphi, MD.
AN ELECTRON-BEAM DOSE DEPOSITION EXPERIMENT: TIGER 1-D SIMULATION CODE VERSUS THERMOLUMINESCENT DOSIMETRY Final Report, Jan. - Sep. 1989
Steven R. Murrill, Charles W. Tipton, and Charles T. Self Mar. 1991 29 p
(AD-A234507; HDL-TM-91-3) Avail: NTIS HC/MF A03 CSCL 20/3

The dose absorbed in an integrated circuit (IC) die exposed to a pulse of low-energy electrons is a strong function of both electron energy and surrounding packaging materials. This report describes an experiment designed to measure how well the Integrated TIGER Series one-dimensional (1-D) electron transport simulation program predicts dose correction factors for a state-of-the-art IC package and package/printed circuit board (PCB) combination. These derived factors are compared with data obtained experimentally using thermoluminescent dosimeters (TLD's) and the FX-45 flash x-ray machine (operated in electron-beam (e-beam) mode). The results of this experiment show that the TIGER 1-D simulation code can be used to accurately predict FX-45 e-beam dose deposition correction factors for reasonably complex IC packaging configurations. GRA

N91-26448# Department of the Navy, Washington, DC.
HIGH POWER KLYSTRON AMPLIFIER Patent Application
M. Friedman, inventor (to Navy), Y. Y. Lau, inventor (to Navy), J. Krall, inventor (to Navy), and V. Serlin, inventor (to Navy) 16 Jan. 1991 15 p
(AD-D014862; US-Patent-Appl-SN-641997) Avail: NTIS HC/MF A03 CSCL 09/1

A klystron amplifier is disclosed in which the drift tube is in the form of a casing and a central member disposed coaxially about the same centerline to form a coaxial space between the central member and the casing which runs parallel to the centerline, and through which the klystron's electron beam flows. The casing and central member are maintained at ground potential, which maintains the space charge of the electron beam at low level, permitting the klystron to operate more efficiently and output higher power. GRA

N91-26449 Department of the Navy, Washington, DC.
MAGNETIC FIELD GENERATOR Patent
James C. Slone, Jr., inventor (to Navy), John A. Hudson, inventor (to Navy), and Bernard Deleman, inventor (to Navy) 19 Feb. 1991 10 p Filed 2 Jun. 70
(AD-D014869; US-Patent-4,993,325; US-Patent-Appl-SN-059796; US-Patent-Class-102-402) Avail: US Patent and Trademark Office CSCL 10/2

This invention discloses a magnetic field generator employing a direct current electromagnetic coil which is swept through a predetermined area by a drive motor and transmission means. Circuit means are disclosed to periodically reverse the polarity of the generated magnetic field either in synchronism with the sweeping of the electromagnetic coil or at a time related frequency. GRA

N91-26450 Department of the Navy, Washington, DC.
BLOCK PATTERNING OF THE METALLIZATION OF POLYVINYLIDENE FLUORIDE TRANSDUCERS Patent
Gee-In Goo, inventor (to Navy) and Thomas A. Waters, inventor (to Navy) 3 Jul. 1990 7 p Filed 5 Jul. 88
(AD-D014872; US-Patent-4,939,407; US-Patent-Appl-SN-215136; US-Patent-Class-310-366) Avail: US Patent and Trademark Office CSCL 09/1

A composite sheet transducer for producing voltage in response to stimuli is described. The transducer is composed of a polymeric sheet sandwiched between a plurality of thin film conductive blocks arranged in non-conductive blocks with the block patterns of opposed electrode assemblies isolated to establish a network of closed circuit segments of sensors. electric shorting between opposed overlapping blocks is thereby limited to circuit segment areas of the composite sheet to avoid interference with voltage production in other areas of the composite sheet. GRA

N91-26451# Defense Logistics Agency, Alexandria, VA.
FORECASTING DIGITAL MICROCIRCUIT OBSOLESCENCE Final Report
Nandakumar M. Balwally Mar. 1991 16 p
(AD-A234573; DLA-91-P00177) Avail: NTIS HC/MF A03 CSCL 09/1

This report documents a procedure for forecasting digital microcircuit obsolescence at the Defense Electronics Supply Center, Dayton, OH. Obsolescence is caused by rapid advancement in digital technology and decrease in commercial demand while military demand still continues. In logistics parlance, parts obsolescence is known as a diminishing manufacturing source (DMS) problem. Continued supply of an obsolete DMS item is assured via substitution, alternate sourcing or a one time buy equal to the lifetime requirements of the item. Emulation is a recent alternative which explores the possibility of replacing obsolete digital microcircuits with state of the art devices which can be manufactured and supplied on demand. The report recommends use of a statistical model which forecasts DMS items from a population of presently non-DMS items belonging to obsolete digital microcircuit technologies. The items forecast by the model should be evaluated for their emulation potential. GRA

N91-26452# Illinois Univ., Chicago. Dept. of Chemistry.
SCANNING TUNNELLING MICROSCOPE FOR BORON SURFACE STUDIES Final Report, 1 Dec. 1988 - 1 May 1990
Michael Trenary 31 Oct. 1990 4 p
(Grant AF-AFOSR-0146-89; AF Proj. 3442)
(AD-A234716; AFOSR-91-0269TR) Avail: NTIS HC/MF A01 CSCL 09/1

The equipment purchased is to be used in an experimental study of the relationship between atomic structure and chemical reactivity for boron and carbon surfaces. This research is currently being supported by grant AFOSR-88-0111. A renewal proposal is currently pending with AFOSR to continue these studies. Carbon and boron are exceptionally stable, covalently bonded solids with highly unique crystal structures. The specific reactions to be studied are loosely related to the problems of oxidation and oxidation inhibition of carbon/carbon composites. The main experimental instrument to be used is a scanning tunneling microscope (STM) purchased under grant number AFSOR-89-0146. Other techniques to be used include Auger electron spectroscopy, X-ray photoelectron spectroscopy (XPS), ultraviolet photoelectron spectroscopy (UPS), low energy electron diffraction (LEED), temperature programmed desorption (TPD) and scanning tunneling microscopy (STM). GRA

N91-26453# Air Force Inst. of Tech., Wright-Patterson AFB, OH. Foreign Technology Div.
METHODS OF OBTAINING AN ELECTRICAL CONTACT
L. Z. Shenfil, V. Ye. Gul, G. K. Melnikova, N. I. Siprikova, and M. K. Rozhdestvenskaya 15 Mar. 1991 7 p Transl. into ENGLISH of Russian Patent No. 228147, (9 Dec. 1964) p 1-2
(AD-A234800; FTD-ID(RS)T-1080-90) Avail: NTIS HC/MF A02 CSCL 09/1

There is a known method for obtaining an electrical contact between connectable parts by hardening a polymer film with ferromagnetic filler in an electrical field. If the film is hardened in a uniform magnetic field, the induced chains are isolated from each other only with very low doses of filler (less than 2 percent by volume). The chains in such a low-filled film are very thin and the specific resistance rho approximately equal to 0.15 does not ensure a sufficiently reliable electrical contact. In order to obtain smaller values of rho, it is necessary to increase the dosing of the filler. In this case, the number of chains per unit of film area increases, the distance between the chains diminishes, and for dosings over 2 percent by volume, connectors are formed between the chains that close them among themselves. Thus, the electrical conductivity along the film is raised, and no reliable multispot electrical contact is obtained in the uniform field. GRA

N91-26454# Army Lab. Command, Fort Monmouth, NJ. Electronics Technology and Devices Lab.
THE ROLE OF EEPROM DEVICES IN UPCOMING ISDN APPLICATIONS Technical Report, 1990 - 1991
Herbert L. Nette Feb. 1991 16 p
(AD-A234837; SLCET-TR-91-5) Avail: NTIS HC/MF A03 CSCL 09/1

Integrated Services Digital Network (ISDN) equipments are rapidly becoming a major market for semiconductor chips. Although at first glance this growing market appears to be geared at logic chips, nonvolatile memories represent important support chips and will become a significant segment of this market. Challenges in these applications consist in operating EEPROMs at lower voltages and lower power and embedding them on ever more complex communications processor chips. GRA

N91-26455# State Univ. of New York, Buffalo. Dept. of Chemistry.
FIELD WORK AND DISPERSION RELATIONS OF EXCITATIONS ON FRACTALS
Mark I. Stockman, Thomas F. George, and Valdimir M. Shalaev Apr. 1991 24 p
(Contract N00014-90-J-1193)
(AD-A234953; UBUFFALO/DC/91/TR-46) Avail: NTIS HC/MF A03 CSCL 09/5

An approach to finding the dispersion law of excitations on fractals for an arbitrary interaction is developed. It is based on the scale invariance of the probe-field work and allows one to express exponents of the dispersion law in terms of the spectral and Hausdorff dimensions. The expressions obtained for the dispersion-law exponent are different for vibrational (Goldstone-type) and dipolar (non-Goldstone-type) excitations. GRA

N91-26456# International Business Machines Corp., Yorktown Heights, NY.
SURFACE ETCHING AND ROUGHENING IN INTEGRATED PROCESSING OF THERMAL OXIDES Technical Report, 1 Jul. 1989 - 1 Dec. 1990
M. Offenberg, M. Liehr, and G. W. Rubloff 3 Apr. 1991 35 p
(Contract N00014-89-C-0104)
(AD-A234960; TR-15) Avail: NTIS HC/MF A03 CSCL 09/1

A multichamber UHV processing and analysis system has been used to study integrated thermal oxide processing, in which the final precleaning process and the thermal oxidation process are integrated by employing transfer of the wafers through ultraclean, inert ambients (purified, dry N2 and then ultrahigh vacuum). The Al-gate MOS capacitors show high breakdown fields (approximately 12 MV/cm) when a thin oxide passivation layer is present prior to oxidation, but low fields (less than 6 MV/cm) when the Si surface is initially oxygen free. This contrasting behavior is caused by the etching of Si surfaces which occurs at elevated temperature in the presence of trace concentration (approximately 100 ppb) of oxygen (e.g., 2 Si + O2 yields 2SiO2), leading to surface roughening and then field enhancement at asperities in the structure. Oxide surface passivation prevents etching and assures the dielectric integrity of the structure. GRA

N91-26457# California Univ., Irvine.
WORK PERFORMED EXPERIMENTS: 1989-1990 Report, 1 May 1989 - 30 Sep. 1990
Gregory Benford 30 Sep. 1990 21 p
(Contract N00014-89-J-1759)
(AD-A235221) Avail: NTIS HC/MF A03 CSCL 09/1

Studied was an X-band Backward Wave Oscillator (BWO) which could be filled both with a hard vacuum and with plasma. The observed power output was about 40MW in the vacuum BWO with a frequency of 8.5 GHz and a bandwidth of 0.5GHz. After filling with plasma, the power output increased by a factor of 6. The bandwidth increased to 2 GHz, with a frequency up-shift of about 1 GHz. In addition, we tested four different shapes of cathode, and found an optimum shape. GRA

N91-26458# Princeton Univ., NJ. Dept. of Civil Engineering and Operations Research.
ACCELERATION INSENSITIVE RESONATORS Final Report, 1 Oct. 1987 - 30 Nov. 1990
Peter C. Lee Feb. 1991 7 p
(Contract DAAL03-87-K-0125)
(AD-A235400; ARO-25289.7-EG) Avail: NTIS HC/MF A02 CSCL 09/1

The objective of the research is to study the sensitivity of frequency changes when the crystal resonator is subject to an acceleration of arbitrary direction. The acceleration produces body force which causes stresses in the resonator. These stresses, in turn, affect the frequency shift. A numerical analytical approach has been developed and employed to compute systematically how the acceleration sensitivity depends on a number of parameters, such as the support orientation, support structures, plate thickness, plate orientation, ratio of mass of electrodes to mass of the plate, and the location of electrode mass. It is found that by controlling one or a combination of these parameters, the acceleration sensitivity can be reduced for resonators without electrodes. For resonators with electrodes, the unevenly distributed electrode masses may be one of the dominating causes of the wide variations of observed acceleration sensitivity. Acceleration sensitivity may, therefore, be reduced significantly by placing electrode mass symmetrically with respect to the center of the plate. GRA

N91-26459*# National Aeronautics and Space Administration. Marshall Space Flight Center, Huntsville, AL.
CONTROL CIRCUITRY USING ELECTRONIC EMULATION OF A SYNCHRO SIGNAL FOR ACCURATE CONTROL OF POSITION AND RATE OF ROTATION FOR SHAFTS Patent Application
David E. Howard, inventor (to NASA) and Dennis A. Smith, inventor (to NASA) 3 Jun. 1991 16 p
(NASA-Case-MFS-28458-1; NAS 1.71:MFS-28458-1; US-Patent-Appl-SN-710192) Avail: NTIS HC/MF A03 CSCL 09A

The invention disclosed is a digital circuit which emulates a synchro signal in a synchro-resolver follower system for precise control of shaft position and rotation at very low rotational rates. The invention replaces the synchro and drive motor in a synchro-resolver follower system with a digital and analog synchro emulation circuit for generating the resolver control signal. The synchro emulation circuit includes amplitude modulation means to provide relatively high frequency resolver excitation signals for accurate resolver response even with very low shaft rotation rates. NASA

N91-26460 Tel-Aviv Univ. (Israel). School of Physics and Astronomy.
CALCULATION OF THE CONDUCTANCE OF TWO DIMENSIONAL NARROW WIRES M.S. Thesis
Ilan Kander May 1989 99 p In HEBREW; ENGLISH summary
(ITN-91-85109) Copyright Avail: Tel-Aviv Univ., Exact Sciences Library, Ramat Aviv 69978, Israel

There is an interest in the quantum transport of electrons in systems where the sample dimensions are less than a phase

coherence length L(sub phi) which is the distance across which the electrons lose phase memory (typically by inelastic scattering). The two-contact conductance is examined of 2-D systems (strips) as functions of Fermi energy system dimensions as is the amount of disorder at zero temperature. Under these conditions all scattering processes are elastic. The term channel is used in order to describe a quantum state with a given transverse quantum number and the appropriate longitudinal momentum. A channel is considered conducting if its longitudinal momentum is real, and decaying if its longitudinal momentum is imaginary. The calculation of the conductance is done in two ways. Transfer matrix for very long systems and Green's function for relatively short ones. The conductance curve in an ordered system is quantized and in a disordered system it is smeared. Interesting changes in the conductance near the thresholds for changes in the quantized value of the conductance are observed. Author (ISA)

N91-26461*# Maxwell Labs., Inc., San Diego, CA.
HIGH-POWER CONVERTERS FOR SPACE APPLICATIONS Final Report
J. N. Park and Randy Cooper Jun. 1991 133 p Prepared in cooperation with General Electric Co., Schenectady, NY
(Contract NAS3-25800)
(NASA-CR-187116; NAS 1.26:187116; Rept-90SRD008) Avail: NTIS HC/MF A07 CSCL 10B

Phase 1 was a concept definition effort to extend space-type dc/dc converter technology to the megawatt level with a weight of less than 0.1 kg/kW (220 lb./MW). Two system designs were evaluated in Phase 1. Each design operates from a 5 kV stacked fuel cell source and provides a voltage step-up to 100 kV at 10 A for charging capacitors (100 pps at a duty cycle of 17 min on, 17 min off). Both designs use an MCT-based, full-bridge inverter, gaseous hydrogen cooling, and crowbar fault protection. The GE-CRD system uses an advanced high-voltage transformer/rectifier filter is series with a resonant tank circuit, driven by an inverter operating at 20 to 50 kHz. Output voltage is controlled through frequency and phase shift control. Fast transient response and stability is ensured via optimal control. Super-resonant operation employing MCTs provides the advantages of lossless snubbing, no turn-on switching loss, use of medium-speed diodes, and intrinsic current limiting under load-fault conditions. Estimated weight of the GE-CRD system is 88 kg (1.5 cu ft.). Efficiency of 94.4 percent and total system loss is 55.711 kW operating at 1 MW load power. The Maxwell system is based on a resonance transformer approach using a cascade of five LC resonant sections at 100 kHz. The 5 kV bus is converted to a square wave, stepped-up to a 100 kV sine wave by the LC sections, rectified, and filtered. Output voltage is controlled with a special series regulator circuit. Estimated weight of the Maxwell system is 83.8 kg (4.0 cu ft.). Efficiency is 87.2 percent and total system loss is 146.411 kW operating at 1 MW load power.
Author

N91-26462*# Catholic Univ. of America, Washington, DC. Vitreous State Lab.
LONG-TERM PREDICTION TEST PROCEDURE FOR MOST ICs, BASED ON LINEAR RESPONSE THEORY Final Report
V. Litovchenko and I. Ivakhnenko 1 Apr. 1991 58 p
(Grant NAG5-864)
(NASA-CR-185843; NAS 1.26:185843) Avail: NTIS HC/MF A04 CSCL 09C

Experimentally, thermal annealing is known to be a factor which enables a number of different integrated circuits (IC's) to recover their operating characteristics after suffering radiation damage in the space radiation environment; thus, decreasing and limiting long term cumulative total-dose effects. This annealing is also known to be accelerated at elevated temperatures both during and after irradiation. Linear response theory (LRT) was applied, and a linear response function (LRF) to predict the radiation/annealing response of sensitive parameters of IC's for long term (several months or years) exposure to the space radiation environment were constructed. Compressing the annealing process from several years in orbit to just a few hours or days in the laboratory is achieved by subjecting the IC to elevated temperatures or by increasing the typical spaceflight dose rate by several orders of magnitude for simultaneous radiation/annealing only. The accomplishments are as follows: (1) the test procedure to make predictions of the radiation response was developed; (2) the calculation of the shift in the threshold potential due to the charge distribution in the oxide was written; (3) electron tunneling processes from the bulk Si to the oxide region in an MOS IC were estimated; (4) in order to connect the experimental annealing data to the theoretical model, constants of the model of the basic annealing process were established; (5) experimental data obtained at elevated temperatures were analyzed; (6) time compression and reliability of predictions for the long term region were shown; (7) a method to compress test time and to make predictions of response for the nonlinear region was proposed; and (8) nonlinearity of the LRF with respect to log(t) was calculated theoretically from a model. Author

N91-26463# Sandia National Labs., Albuquerque, NM.
PROOF-OF-CONCEPT ZINC/BROMINE ELECTRIC VEHICLE BATTERY
J. Bolsted, P. Eidler, R. Miles, R. Petersen, K. Yaccarino, and S. Lott Apr. 1991 98 p Prepared in cooperation with Johnson Controls, Inc., Milwaukee, WI
(Contracts DE-AC04-76DP-00789; DE-AC04-88AL-54304)
(DE91-011767; SAND-91-7029) Avail: NTIS HC/MF A05

Johnson Controls acquired and tested the zinc/bromine battery design developed by Exxon Research and Engineering Corporation (the Z-design) and, with Exxon, determined the key problems in this design: expansion and warping of electrodes, leaking of electrolyte from the battery stack, and excessive self-discharge brought about by transfer of bromine across the separator. The problems of electrode expansion and high self-discharge were mitigated by developing improved electrode and separator materials. Starting in the second year of the contract, JCI developed a new V-design battery stack which used different hardware and tooling to address the problem of stack leakage. The V-design uses thermal welding to achieve a hermetically sealed construction. The flow distribution is improved, and the massive endblocks of the original system were replaced by thinner, lighter endblocks which are stiffened by means of rigid aluminum honeycomb inserts. Highlights of performance characteristics of batteries built and tested under the contract given. DOE

N91-26464# California Univ., Berkeley. Lawrence Berkeley Lab.
LOW FREQUENCY NOISE IN RESONANT JOSEPHSON SOLITON OSCILLATORS
J. B. Hansen, T. Holst (Technical Univ. of Denmark, Lyngby.), F. C. Wellstood, and J. Clarke Sep. 1990 7 p Presented at the Applied Superconductivity Conference, Aspen, 24-28 Sep. 1990
(Contract DE-AC03-76SF-00098)
(DE91-011911; LBL-28891; CONF-900944-44) Avail: NTIS HC/MF A02

The noise in the resonant soliton mode of long and narrow Josephson tunnel junctions (Josephson Transmission Lines, JTLs) was measured in the frequency range from 0.1 Hz to 25 kHz by means of a dc SQUID. To within a factor of 2 the measured white noise was found to be equal to the Nyquist voltage noise in a resistance equal to the dynamic resistance R(sub D) of the current voltage characteristic at the bias point. In contrast, measurements of the linewidth of the microwave radiation from the same JTL showed that the spectral density of the underlying noise voltage scaled as R(sub D)(exp 2)/R(sub S) where R(sub S) is the static resistance. The origin of the different behavior is not known. DOE

N91-27105*# Florida Inst. of Tech., Melbourne. Dept. of Computer Science.
A DESIGN FOR AN INTELLIGENT MONITOR AND CONTROLLER FOR SPACE STATION ELECTRICAL POWER USING PARALLEL DISTRIBUTED PROBLEM SOLVING Final Report

Robert A. Morris *In* Houston Univ., NASA/ASEE Summer Faculty Fellowship Program, 1990, Volume 2 Dec. 1990 15 p (For primary document see N91-27103 18-99)
(Grant NGT-44-005-803)
Avail: NTIS HC/MF A09 CSCL 09C

N91-27110*# Tennessee Technological Univ., Cookeville. Dept. of Electrical Engineering.
DESIGN OF OPTIMAL CORRELATION FILTERS FOR HYBRID VISION SYSTEMS Final Report
Periasamy K. Rajan *In* Houston Univ., NASA/ASEE Summer Faculty Fellowship Program, 1990, Volume 2 Dec. 1990 15 p (For primary document see N91-27103 18-99)
(Grant NGT-44-005-803)
Avail: NTIS HC/MF A09 CSCL 09C

34 FLUID MECHANICS AND HEAT TRANSFER

Includes boundary layers; hydrodynamics; fluidics; mass transfer; and ablation cooling.

For related information see also *02 Aerodynamics* and *77 Thermodynamics and Statistical Physics.*

N91-26465*# National Aeronautics and Space Administration. Ames Research Center, Moffett Field, CA.
THE KINEMATICS OF TURBULENT BOUNDARY LAYER STRUCTURE
Stephen Kern Robinson Apr. 1991 333 p Seminar held at College Park, MD Original contains color illustrations
(NASA-TM-103859; A-91123; NAS 1.15:103859) Avail: NTIS HC/MF A15; 50 functional color pages CSCL 20D

The long history of research into the internal structure of turbulent boundary layers has not provided a unified picture of the physics responsible for turbulence production and dissipation. The goals of the present research are to: (1) define the current state of boundary layer structure knowledge; and (2) utilize direct numerical simulation results to help close the unresolved issues identified in part A and to unify the fragmented knowledge of various coherent motions into a consistent kinematic model of boundary layer structure. The results of the current study show that all classes of coherent motion in the low Reynolds number turbulent boundary layer may be related to vortical structures, but that no single form of vortex is representative of the wide variety of vortical structures observed. In particular, ejection and sweep motions, as well as entrainment from the free-streem are shown to have strong spatial and temporal relationships with vortical structures. Disturbances of vortex size, location, and intensity show that quasi-streamwise vortices dominate the buffer region, while transverse vortices and vortical arches dominate the wake region. Both types of vortical structure are common in the log region. The interrelationships between the various structures and the population distributions of vortices are combined into a conceptual kinematic model for the boundary layer. Aspects of vortical structure dynamics are also postulated, based on time-sequence animations of the numerically simulated flow. Author

N91-26466# Aeronautical Research Inst. of Sweden, Stockholm.
METHODS TO ENHANCE THE ACCURACY OF FINITE VOLUME SCHEMES 2
Thilo Schoenfeld (Centre Europeen Recherche et de Formation Advance en Calcul Scientific, Toulouse, France) and Peter Wilde 1991 32 p Sponsored in part by Swedish National Board for Technical Development, and by Defence Materiel Administration of Sweden
(FFA-147) Avail: NTIS HC/MF A03

Several compact higher order schemes to solve the three dimensional Euler equations are constructed. The methods are based on the finite volume technique with a cell-vertex space discretization. Different explicit time integration schemes of Runge-Kutte type are compared in connection with the higher order schemes. The stability behavior of the methods is analyzed and their usefulness is demonstrated by results obtained for the transonic flow around a delta wing at incidence. Author

N91-26467# Westinghouse Electric Corp., Pittsburgh, PA. Science and Technology Center.
ADVANCED STUDY IN SOLID TRANSPORT: RHEOLOGICAL BEHAVIOR OF DENSE SUSPENSION
H. J. Kim, J. L. S. Chen (Pittsburgh Univ., PA.), R. M. Roidt, and H. A. Burgman 23 Oct. 1990 168 p
(Contract DE-AC22-88PC-88949)
(DE91-009428; DOE/PC-88949/T8) Avail: NTIS HC/MF A08

The objective of the present research is to develop a basic understanding of the fundamental rheological properties of high solids concentration slurries or wet cake. A dynamic shear cell test device has been constructed and operated to measure dynamic shear stress and determine the effects of experimental parameters upon the dynamic shear stress of the materials. The solids used are glass beads and coal powders. The experimental parameters investigated are: water fraction, normal stress, speed, gap height, size, and size distribution. A statistical method is adapted to evaluate the effects of the experimental parameters. The experiments with glass beads show that the dynamic shear stress is independent of shear rate, providing the gap height is larger than about 27 times the bead diameter, but is a functional of normal stress and water fraction. The dynamic friction coefficient increases sharply as the water fraction increases up to 10 percent, and decreases gradually for water fractions greater than 10 percent. Dynamic experiments with coal-water mixtures show that the coal-water mixtures behave like the glass beads when water fraction is lower than a certain value. However, as the water fraction increases beyond that value, the coal-water mixtures display the characteristics of thixotropic fluids with shear thinning. The flow index of the coal-water mixtures is independent of normal stress, but decreases as the water fraction decreases. DOE

N91-26468# Institute of Gas Technology, Chicago, IL.
DETERMINATION OF FLOW-REGIME BOUNDARIES FOR COHESIVE PARTICLES
T. M. Knowlton and J. G. Findlay Feb. 1991 25 p
(Contract DE-AC22-88PC-88951)
(DE91-010552; DOE/PC-88951/7) Avail: NTIS HC/MF A03

Cohesive powders are composed of fine particles (particles generally less than 44 microns in size). Interparticle forces are extremely large and cause clumping, sticking, and channeling when attempts are made to fluidize these powders. Although flow problems can be experienced in the transport of free-flowing solids, they are pale in comparison to the problems experienced with the flow of cohesive powders. Most process designers have shied away from using cohesive powders. However, cohesive powders are often produced in processes by attrition. Also, because cohesive solids have an extremely high surface area per unit volume, they are potentially desirable feed stocks for many processes. In addition, recent research has shown that beneficiation of oil shale and coal is possible after grinding these materials down to cohesive size range. The purpose of this work is to develop a hydrodynamic model capable of predicting the choking/non-choking flow regime boundary for cohesive solids. There are six tasks in this study: preparation of a project work plan; hydrodynamic model development; determination of solid rheological properties for incorporation into the hydrodynamic model; small-scale flow tests; large-scale flow tests; and comparison of model with data and preparation of final report. Analysis of the mass flux, particle velocity, and solids density radial profiles obtained on the 7.6-cm-diameter test unit was started this quarter. Additional work was conducted on the construction of a test unit to be used to measure the particle velocity of cohesive solids in a dilute-phase transfer system using laser Doppler velocimetry (LDV). DOE

N91-26469# David Taylor Research Center, Bethesda, MD.
REFLECTION OF INCIDENT PRESSURE WAVES BY RIBBED PANELS Research and Development Report
G. Maidanik and J. Dickey Feb. 1991 56 p
(AD-A233671; DTRC-91/006) Avail: NTIS HC/MF A04 CSCL 20/4

The definitions of the reflection coefficients, in the absence of ribs and due to ribs, of an incident pressure wave on a plane at the surface of a ribbed fluid loaded panel are defined, examined, and computed. The incident pressure wave is described by a plane wave and by a collimated beam. The results of representative computations are displayed. Through these displays, some aspects of the influence on the reflection coefficients caused by changes in the parameters that describe the ribbed panel, the fluid loading, and the incidence are investigated. These aspects include wavenumber aliasing and symmetries in some of the terms and factors that compose the expressions for the reflection coefficients; the wavenumber of concern lies across the ribs. Aliasings are present, however, only when the separations between adjacent ribs are conditioned to be equal. Moreover, in some of these aliased terms and factors, symmetry is present only when the incidence obeys specific conditions. Disturbing either of these conditions tends to spoil the aliasing and/or the symmetries in these terms and factors. It is shown, however, that the aliasing and symmetry properties are invariant to changes in the parameters that describe the ribbed panel and/or the fluid loading to which it is subjected. GRA

N91-26470# Naval Research Lab., Washington, DC.
DIRECT AND LARGE-EDDY SIMULATIONS OF THREE-DIMENSIONAL COMPRESSIBLE NAVIER-STOKES TURBULENCE Interim Report
T. A. Zang, R. B. Dahlburg, and J. P. Dahlburg 2 Apr. 1991 56 p
(NR Proj. RR0-1109)
(AD-A233717; NRL-MR-6799) Avail: NTIS HC/MF A04 CSCL 20/4

This paper reports results from the numerical implementation and testing of the compressible large eddy-simulation (LES). Relevant quantities from 32-cubed coarse grid LES solutions are compared with results generated from direct numerical simulations (DNS) of three-dimensional compressible turbulence that have been run both with sufficient resolution, at 96 cubed. The 32 cubed LES results overall agree well with their 96 cubed DNS counterparts. Moreover, the new DNS results confirm several recent conclusions about compressible turbulence that have been based primarily on two-dimensional simulations. GRA

N91-26471# Houston Univ., TX. Dept. of Mechanical Engineering.
BASIC STUDIES OF MICROSTRUCTURE OF COMBUSTING TURBULENT FLOWS Final Technical Report, for period ending 30 Jun. 1990
Fazle Hussain 4 Mar. 1991 30 p
(Contract N00014-87-K-0670)
(AD-A234222) Avail: NTIS HC/MF A03 CSCL 21/2

The goal is to develop a state-of-the-art measurement technique, Holographic Particle Displacement Velocimetry (HPV), which can provide instantaneous velocities everywhere in the flow field simultaneously. Another goal is to use the power of supercomputers to simulate 3D flows with heat release to study the physics of combusting turbulent flows. Computations suffer from limited flow times and Reynolds number but can provide flow properties in more detail than possible by any existing experimental techniques. Moreover, numerical simulations can provide quantities almost impossible to measure experimentally. This article discusses efforts to develop the holographic particle displacement velocimetry system and results of direct numerical numerical simulations of combusting flows. GRA

N91-26472# Wisconsin Univ., Madison. Center for Mathematical Sciences.
ANALYTICAL SOLUTION OF PLANE POISEUILLE FLOW OF A JOHNSON-SEGALMAN FLUID Technical Summary Report
M. Yao and D. S. Malkus May 1990 34 p
(Grants AF-AFOSR-0141-85; NSF DMS-87-12058; NSF DMS-89-07264)
(AD-A234313; CMS-TSR-90-24) Avail: NTIS HC/MF A03 CSCL 20/4

The pressure driven plane Poiseuille flow of the Johnson-Segalman fluid is studied. By changing integral variable and solving a cubic equation at each location, the exact steady solutions for this flow was obtained. Both monotone and non-monotone stress strain rate relations are considered and complete formulation and solution procedures are developed. The flow curves from Vinogradov et al's spurt data capillary flow are simulated analytically with encouraging agreement between the analytical results and the experimental data. The analytical solution technique and results are also applied to the hole pressure problem and an analytical prediction of hole pressure presented. GRA

N91-26473# Ballistic Research Labs., Aberdeen Proving Ground, MD.
OPTICAL STUDIES OF THE FLOW START-UP PROCESSES IN FOUR CONVERGENT-DIVERGENT NOZZLES Final Report, Jun. 1989 - Sep. 1990
Klaus O. Opalka Mar. 1991 117 p
(DA Proj. 1L1-62120-AH-25)
(AD-A234552; BRL-TR-3215) Avail: NTIS HC/MF A06 CSCL 20/4

In the context of design studies for the U.S. Large Blast/Thermal Simulator, BRL has sponsored optical studies of the flow start-up in convergent-divergent nozzles which have the flow-initiating diaphragm located in the nozzle throat. The experiments were performed in the 200 mm shock tube at the Ernst-Mach Institute in Freiburg (Breisgau), West-Germany. The scope of the studies included divergent nozzles with half cone angles of 6, 16, 45 and 90 deg tested at seven diaphragm pressure ratios ranging from 4 to 188 and resulting in shock strengths ranging from 1.4 to 4.4. Results were summarized in graphs of significant parameters, e.g., shock formation time, flow start-up period, flow expansion angle, and shock strength versus the driver pressure ratio and further compared with numerical results obtained with the BRL-Q1D hydrocode. The numerical-experimental comparison shows qualitative agreement. The flow phenomena are generally reproduced by the computations as long as they are not strongly dependent on viscous effects. The study shows that a pressure loss of 10 percent is connected to the presence of a large area discontinuity at the exit plane of the nozzle throat when no divergent nozzle is attached. Results suggest that a 45 deg divergent nozzle may present an acceptable compromise for minimizing these pressure losses by reducing the associated area discontinuities. GRA

N91-26474# Naval Research Lab., Washington, DC.
USE OF A ZONE MODEL FOR VALIDATION OF A HORIZONTAL CEILING/FLOOR VENT ALGORITHM Memorandum Report
J. L. Bailey, F. W. Williams, and P. A. Tatem 26 Apr. 1991 42 p
(NR Proj. RH2-1522)
(AD-A234553; NRL-MR-6811) Avail: NTIS HC/MF A03 CSCL 21/2

An algorithm has been developed to describe the exchange flow through a horizontal vent, such as a ship's hatch. Until recently, there was no way to fully characterize the flow through a horizontal vent. A zone model is used to test the validity of a horizontal ceiling/floor vent flow algorithm. Development of this algorithm makes it possible to fully characterize vertical flow through a horizontal vent. The algorithm is incorporated into a computer model written to simulate a compartment, with a fire inside, ventilated only through a hole in the ceiling. Model predictions

are shown to be comparable to small scale experimental results. To further test and confirm this algorithm, a similar comparison should be made on a larger scale. GRA

N91-26475# Naval Underwater Systems Center, New London, CT.
COMPARISONS OF BACKSCATTERING FROM CYLINDRICAL SHELLS DESCRIBED BY THIN SHELL AND ELASTICITY THEORIES
Ronald P. Radlinski, Richard D. Vogelsong, and Louis R. Dragonette 4 Mar. 1991 23 p Presented at the 120th Meeting of the Acoustical Society of America, San Diego, CA, Nov. 1990
(AD-A234745; NUSC-TD-8835) Avail: NTIS HC/MF A03 CSCL 20/1

For kh less than or equal to 0.65, where k is the fluid wavenumber and h is the shell wall thickness, scattering from infinite cylindrical shells at normal incidence can be described by a combination of specular reflection and the zeroth order symmetric Lamb waves that correspond to extensional and inextensional modes of shell theory. Love-Timoshenko thin shell theory is found to closely describe the resonance scattering behavior from these types of structural modes. At higher values of kh, scattering from the antisymmetric Lamb-type flexural modes is predicted by full elasticity theory. For materials in which the plate and modified shear wave speeds can be either greater or less than the wave speed in the backscattering predictions of fluid, the accuracy of Love-Timoshenko thin shell theory will be investigated near the excitation of the antisymmetric Lamb-type flexural waves by comparisons with full elasticity theory. Plate theories will be used to develop a physical explanation of the resulting differences. GRA

N91-26476# Georgia Inst. of Tech., Atlanta.
IMPROVED ALGORITHMS FOR TRANSIENT AND STEADY-STATE FLUID-STRUCTURE INTERACTION Final Report
Jerry H. Ginsberg 1990 19 p
(Contract N00014-84-K-0713)
(AD-A235172) Avail: NTIS HC/MF A03 CSCL 20/1

The interaction between a vibrating submerged structure and the surrounding fluid, which features coupling between the surface pressure distribution and the structural displacement, is an inherent feature for sound radiation and target strength analyses. A variety of approaches have been implemented in the past, but each suffers from serious limitations. Formal mathematical analysis using separation of variables or integral transform techniques is suitable only for the simplest structural models, while full finite element descriptions of realistic structures and the surrounding medium lead to excessively large computer simulations. One approach uses approximate impedance-type boundary condition of uncertain accuracy to model the fluid response. The initial effort within the project was devoted to deriving the variational principle and validating it through the solution of canonical problems whose solutions had already been obtained by other methods. This work involved cylinder, spherical, and disk geometries. Because of the presence of singularities in the formulation associated with free space Green's function, much effort was expended in the early phase of the project to develop numerical techniques that were both efficient and robust. That effort was a continuing theme of the research program, whenever the generality of the principle was extended. GRA

N91-26477# Colorado Univ., Boulder.
THEORETICAL STUDIES OF THE KINEMATICS, DYNAMICS, STABILITY, AND CONTROL OF UNSTEADY/VORTICAL FLOWS Final Report, 1 Aug. 1988 - 31 Dec. 1990
Chuen-Yen Chow Feb. 1991 4 p
(Contract F49620-88-C-0098)
(AD-A235190; Rept-1-5-36452; AFOSR-91-0235TR) Avail: NTIS HC/MF A01 CSCL 20/4

Several unsteady vortical flows have been computed with success. A free vortex might be trapped by an oscillating airfoil for lift augmentation. Numerical simulations of streaklines have shown some pitfalls that might be encountered when interpreting photographs of unsteady vortical flows. Traveling acoustic waves are found to have the effect of either re-orienting a cluster of vortices or destabilizing the otherwise stable Karman vortex street. The onset of instability of boundary layers along semi-infinite circular cylinders is analyzed, including the effects of transverse curvature and spin motion of the cylinders. Some important mechanisms that are responsible for vorticity generation and flow separation on bodies in unsteady motion have been identified. GRA

N91-26478# Army Construction Engineering Research Lab., Champaign, IL.
RESEARCH IN NONLINEAR WATER WAVES Quarterly Letter Progress Report, 1 Jan. - 31 Mar. 1991
P. G. Saffman 2 Apr. 1991 1 p
(AD-A235410) Avail: NTIS HC/MF A01 CSCL 20/4

Work during the quarter concentrated on the effect of a thin shear layer on the generation of waves by wind. The case of no shear layer, i.e., the Miles mechanism, has been re-examined and it was found, as mentioned in an earlier letter, that the method of solution adopted by Miles and later justified physically by Lighthill is not very accurate, both qualitatively and quantitatively. The discrepancy is not as large as preliminary calculations indicated, but it is still significant. A search of the literature is now in progress to see if the more accurate calculations give results which agree better with observation, and the work is being prepared for publication. GRA

N91-26479*# Carnegie-Mellon Univ., Pittsburgh, PA. Dept. of Mechanical Engineering.
DYNAMICS OF FACE AND ANNULAR SEALS WITH TWO-PHASE FLOW Final Report
William F. Hughes, Prithwish Basu, Paul A. Beatty, Richard M. Beeler, and Stephen Lau Washington NASA Oct. 1989 269 p
(Grant NAG3-166)
(NASA-CR-4256; E-4999; NAS 1.26:4256) Avail: NTIS HC/MF A12 CSCL 20D

A detailed study was made of face and annular seals under conditions where boiling, i.e., phase change of the leaking fluid, occurs within the seal. Many seals operate in this mode because of flashing due to pressure drop and/or heat input from frictional heating. High pressure, water pumps, industrial chemical pumps, and cryogenic pumps are mentioned as a few of many applications. The initial motivation was the LOX-GOX seals for the space shuttle main engine, but the study was expanded to include any face or annular seal where boiling occurs. Some of the distinctive behavior characteristics of two-phase seals were discussed, particularly their axial stability. While two-phase seals probably exhibit instability to disturbances of other degrees of freedom such as wobble, etc., under certain conditions, such analyses are too complex to be treated at present. Since an all liquid seal (with parallel faces) has a neutral axial stiffness curve, and is stabilized axially by convergent coning, other degrees of freedom stability analyses are necessary. However, the axial stability behavior of the two-phase seal is always a consideration no matter how well the seal is aligned and regardless of the speed. Hence, axial stability is thought of as the primary design consideration for two-phase seals and indeed the stability behavior under sub-cooling variations probably overshadows other concerns. The main thrust was the dynamic analysis of axial motion of two-phase face seals, principally the determination of axial stiffness, and the steady behavior of two-phase annular seals. The main conclusions are that seals with two-phase flow may be unstable if improperly balanced. Detailed theoretical analyses of low (laminar) and high (turbulent) leakage seals are presented along with computer codes, parametric studies, and in particular a simplified PC based code that allows for rapid performance prediction. A simplified combined computer code for the performance prediction over the laminar and turbulent ranges of a two-phase seal is described and documented. The analyses, results, and computer codes are summarized. Author

N91-26480 Tel-Aviv Univ. (Israel). Dept. of Fluid Mechanics and Heat Transfer.

RICOCHET OF SPHERE OFF WATER M.S. Thesis

Joseph Shoockron Jun. 1989 159 p In HEBREW; ENGLISH summary

(ITN-91-85102) Copyright Avail: Tel-Aviv Univ., Exact Sciences Library, Ramat Aviv 69978, Israel

This work deals with the analysis and calculation of the critical angle for the ricochet of a sphere off water. The critical angle is defined as the maximum incidence angle of a sphere over water which enables it to ricochet. This work presents the development and calculation of the forces acting on the sphere during its entry into the water. Since the critical angle is very sensitive to the hydrodynamic forces, the accurate development and calculation of these forces has been emphasized in some previous methods. There is a simple empirical formula for calculation of the critical angle, which is theta(sub c) = 18 deg/square root of zeta, where theta(sub c) is the critical angle and zeta is the ratio between the density of the sphere and the density of the water. Likewise, there are works which give a theoretical basis to the above-mentioned formula. This formula does not depend on the incidence velocity of the sphere or on the sphere radius, these being parameters that affect the critical angle. In this work it is verified that the critical angle depends on these added parameters, in the form of the F(sub r) number, where F(sub r) = V(exp 2)/Rg. Author (ISA)

N91-26481 Tel-Aviv Univ. (Israel). Dept. of Fluid Mechanics and Heat Transfer.

AN EXPERIMENTAL AND NUMERICAL STUDY OF WAVEMAKER DISSIPATION IN THE PROCESS OF DIRECT GENERATION OF THE RESONANT SLOSHING WAVES IN A RECTANGULAR TANK M.S. Thesis

Chemesse Melad Jun. 1989 99 p In HEBREW; ENGLISH summary

(ITN-91-85103) Copyright Avail: Tel-Aviv Univ., Exact Sciences Library, Ramat Aviv 69978, Israel

Nonlinear resonant standing waves, directly excited in a rectangular tank, were studied experimentally and numerically. Emphasis was placed on steady nonlinear standing waves. The experiments demonstrated the existence of a well defined hysteresis between two quite different wave distributions in the tank, under identical forcing conditions. The complex dissipation coefficient at the wavemaker was measured under a wide range of experimental conditions; calculation of the coefficient was based on the assumption of a linear relation between the shear stress at the wavemaker and the velocity in the potential core at the outer edge of the boundary layer. The dissipation coefficient thus calculated showed pronounced hysteresis, similar to that observed in the wave field, and the results indicate that the absolute value of the wavemaker dissipation coefficient significantly exceeds the estimated value based on purely viscous dissipation. This was attributed to turbulence effects arising from the vortex shedding at the discontinuities of the wavemaker surface. It is shown that the incorporation of this dissipation in the boundary condition at the wavemaker, as a nonlinear term in a form generally used to describe dissipation in a turbulent boundary layer, is more appropriate, allowing hysteresis to be removed from the wavemaker dissipation coefficient. Numerical simulation, based on the solution of the nonlinear Schroedinger equation, with the dissipation coefficient at the wavemaker obtained experimentally, showed that the hysteresis may be reproduced in computations when the nonlinear boundary condition at the wavemaker is adopted. Good qualitative and quantitative agreement between the experimental and the numerical results was obtained in these calculations. On the other hand, calculations based on linear boundary conditions at the wavemaker could only reproduce correctly one of the two possible wave distributions in the tank. ISA

N91-26482 Tel-Aviv Univ. (Israel). Dept. of Fluid Mechanics and Heat Transfer.

THE DELAY OF TURBULENT BOUNDARY LAYER SEPARATION BY OSCILLATORY ACTIVE CONTROL M.S. Thesis

Boaz Nishri Dec. 1989 110 p In HEBREW; ENGLISH summary

(ITN-91-85104) Copyright Avail: Tel-Aviv Univ., Exact Sciences Library, Ramat Aviv 69978, Israel

The aims were to develop an active method to control turbulent boundary layer separation, to study its efficiency, and to study the flow regime after its activation. In a subsonic open-ended wind tunnel, a sharp angle in a flat plate created a local discontinuity and a strong downstream positive pressure gradient, causing boundary layer separation from the plate. A vibrating flap at the discontinuity constituted the active means of separation control. A hot-wire probe was used to measure the velocity field along the length of the plate. The data were processed to obtain information on the fluid behavior, averaged over frequency and time. The similarity of the velocity profile of the upper part of the separated flow to the average velocity profile in a 2-dimensional mixing layer in which a vibrating flap increased the mixing among different velocities, led to the suggestion that, in the present case of a separated boundary layer, a vibrating flap would enhance the mixing of the energy-rich upper part of the flow with the energy-poor lower part, leading to reattachment of the flow. Reattachment occurred, characterized by 3 regions: a small region of large 2-dimensional vortices; a region in which the vortices decayed, whose location depended on vibration frequency, and in which the boundary layer was characteristic of a vibrating fluid moving against a positive pressure gradient; and a region where the decaying large vortices no longer affected the flow near the plate surface, and with a classic turbulent boundary layer. The principle conclusion was that a vibrating flap provides an effective active control means for a turbulent boundary layer, and can prevent flow separation. ISA

N91-26483 Tel-Aviv Univ. (Israel). Dept. of Fluid Mechanics and Heat Transfer.

INVESTIGATION OF LAMINAR, FULLY DEVELOPED FLOW IN ANNULUS BY FINITE DIFFERENCE MODEL M.S. Thesis

Edi Mazor Aug. 1989 95 p In HEBREW; ENGLISH summary

(ITN-91-85116) Copyright Avail: Tel-Aviv Univ., Exact Sciences Library, Ramat Aviv 69978, Israel

In previous studies of flow in an annular tank, driven by a rotating screen, a 2-D model, which considered the effects of radial stratification of turbulence but neglected secondary flow effects, accurately predicted entrainment but failed to predict some features of the velocity field, including the appearance of a velocity tongue in the vicinity of the outer layer. Herein, secondary flow effects were introduced into the model, but simplification was achieved by using laminar flow. The governing equations describing steady laminar flow in an annulus with one or two rotating screens were solved by the finite difference method. The resulting algorithm was checked against published results. A special procedure of hot and cold conditions for initial velocity distributions in an iteration process yielded multiple solutions for the flow in a curved channel, in accordance with earlier theoretical predictions, and various secondary flow patterns were obtained, comprising two or four vortices, for identical pressure gradients. In contrast, in an annulus, no multiple solutions were obtained for the full range of angular velocities of the screens. When the flow was generated by one screen the secondary flow comprised one vortex; in the case of two rotating screens, two vortices were always obtained. The momentum transport in the central part of the annulus is mainly due to the secondary flow; consequently, good agreement was obtained between the calculated and measured laminar velocity profiles, indicating that any turbulent model used to describe the flow in an annulus should account for the secondary flow. The suggested next step in refining the theoretical model should involve inclusion of the turbulent diffusion coefficient, to evaluate the entrainment processes in an annulus. ISA

N91-26484# Los Alamos National Lab., NM.
SIMULATION OF PORE SCALE POROUS MEDIA FLOW USING LATTICE GAS METHODS
K. Eggert, Shiyi Chen, B. Travis, D. Grunau, E. Loh, and F. Kovarik (Houston Univ., TX.) 1991 12 p Presented at the SPE/UA Emerging Technologies Conference, Houston, 5-7 Jul. 1991
(Contract W-7405-eng-36)
(DE91-004829; LA-UR-90-3782; CONF-910759-1) Avail: NTIS HC/MF A03

Carbon dioxide-foam injection is an important technique for improving the recovery of oil from porous rocks. Huh, et. al. (1989) recently presented results of two-dimensional laboratory micromodel studies conducted to better understand this process for improved oil recovery. These experimental results indicate that the introduction of CO2 foam may be expected to have a substantial effect on the relative permeability curves that would be used to model improved oil recovery in a reservoir. However, in order to determine expected changes in relative permeability a computational technique is required to quantify the experimental results, and to help determine the appropriate relative permeability curves for reservoir scale calculation. Two computational methodologies are needed to utilize the experimental information to improve reservoir simulations. First, a method is needed for quantitatively describing the phenomena observed in the micromodel geometry. Second, a method is needed to extend these effects to the different scales of heterogeneity that may be expected to exist between the laboratory and the field. The focus is on the first of these methods, and although it does not yet fully solve the problem of representing these fluid systems in the laboratory, it presents a promising approach to this problem. The application of the lattice gas method is discussed for solution of the nondimensional Navier-Stokes equations for flow of fluids through the complex microscopic geometry of porous media. In particular, the approach presented allows the simulation not only of single fluids through the media, but of systems of two or more fluids ranging from fully miscible to completely immiscible. DOE

N91-26485# Lawrence Livermore National Lab., CA.
COMPUTATIONAL MODEL FOR OPTIMIZING LONGITUDINAL FIN HEAT TRANSFER IN LAMINAR INTERNAL FLOWS
C. S. Landram Nov. 1990 35 p Presented at the ASME/AIChE/ANS National Heat Transfer Conference, Minneapolis, 26-31 Jul. 1991
(Contract W-7405-eng-48)
(DE91-005070; UCRL-JC-105437; CONF-910739-1) Avail: NTIS HC/MF A03

Optimal configurations are identified, based on a numerical model, for fully developed laminar internal flows whose base boundary walls have perpendicular fins extending longitudinally into the fluid. The optimum coolant flow channel, formed between each fin, has an aspect ratio dependent on the coolant to wall thermal conductivity ratio and on the fin to channel width ratio, which is optimally about unity. A base thickness exists which minimizes the base hot-spot temperature, and its value is dependent on the fin to channel width ratio. DOE

N91-26486# Sandia National Labs., Albuquerque, NM.
BENCHMARK STUDY BETWEEN FIDAP AND A CELLULAR AUTOMATA CODE
R. L. Akau and H. W. Stockman 1991 34 p Presented at the 4th FIDAP Users Conference, Evanston, 14-16 Apr. 1991
(Contract DE-AC04-76DP-00789)
(DE91-011224; SAND-91-0160C; CONF-9104202-4) Avail: NTIS HC/MF A03

A fluid flow benchmark exercise was conducted to compare results between a cellular automata code and FIDAP. Cellular automata codes are free from gridding constraints, and are generally used to model slow (Reynolds number approximately 1) flows around complex solid obstacles. However, the accuracy of cellular automata codes at higher Reynolds numbers, where inertial terms are significant, is not well-documented. In order to validate the cellular automata code, two fluids problems were investigated. For both problems, flow was assumed to be laminar, two-dimensional, isothermal, incompressible and periodic. Results showed that the cellular automata code simulated the overall behavior of the flow field. DOE

N91-26487# Argonne National Lab., IL.
SLOSHING RESPONSE IN A TANK CONTAINING TWO LIQUIDS
Y. Tang, D. C. Ma, and Y. W. Chang 1991 9 p Presented at the American Society of Mechanical Engineers (ASME) Pressure Vessels and Piping Conference, San Diego, 23-27 Jun. 1991
(Contract W-31-109-eng-38)
(DE91-011844; ANL/CP-72401; CONF-910602-39) Avail: NTIS HC/MF A02

A study on the sloshing response in a tank containing two different liquids under seismic excitation is presented. Both analytical and numerical (FEM) methods are employed in the analysis. The results obtained by the two methods are in good agreement. The response quantities examined include the sloshing wave height, the natural frequencies of the sloshing motion, and the vertical displacement at the interface of the two liquids. It is shown that the maximum sloshing wave height may increase significantly, and the fundamental period of the sloshing motion is longer than that in an identical tank containing only one liquid. DOE

N91-26488*# Old Dominion Univ., Norfolk, VA. Dept. of Mechanical Engineering and Mechanics.
NAVIER-STOKES CALCULATIONS OF SCRAMJET-NOZZLE-AFTERBODY FLOWFIELDS Final Report, period ending 15 Aug. 1991
Oktay Baysal Jul. 1991 32 p
(Grant NAG1-811)
(NASA-CR-185356; NAS 1.26:185356) Avail: NTIS HC/MF A03 CSCL 20D

A comprehensive computational fluid dynamics effort was conducted from 1987 to 1990 to properly design a nozzle and lower aft end of a generic hypersonic vehicle powered by a scramjet engine. The interference of the exhaust on the control surfaces of the vehicle can have adverse effects on its stability. Two-dimensional Navier-Stokes computations were performed, where the exhaust gas was assumed to be air behaving as a perfect gas. Then the exhaust was simulated by a mixture of Freon-12 and argon, which required solving the Navier-Stokes equations for four species: (nitrogen, oxygen, Freon-12, and argon). This allowed gamma to be a field variable during the mixing of the multispecies gases. Two different mixing models were used and comparisons between them as well as the perfect gas air calculations were made to assess their relative merits. Finally, the three dimensional Navier-Stokes computations were made for the full-span scramjet nozzle afterbody module. Author

N91-26489# Argonne National Lab., IL.
IMPLEMENTATION OF THE FLOW-MODULATED SKEW-UPWIND DIFFERENCE SCHEME IN THE COMMIX-1C CODE: A FIRST ASSESSMENT
M. Bottoni, T. H. Chien, H. M. Dommanus, W. T. Sha, Y. Shen, and R. Laster (Texas A&M Univ., College Station.) 1991 52 p Presented at the 14th Meeting of the Liquid Metal Boiling Working Group (LMBWG), Brasimon, Italy, 1 6-18 Apr. 1991
(Contract W-31-109-eng-38)
(DE91-011168; ANL/CP-72421; CONF-9104226-1) Avail: NTIS HC/MF A04

The implementation of the Flow-Modulated Skew-Upwind Difference (FMSUD) scheme in the momentum equation of the COMMIX-1C computer program, where the scheme has been used so far only in the energy equation, is described in detail. Because the three scalar components of the momentum equation are solved in different meshes, staggered with respect to the mesh used for the energy equation and displaced in the respective coordinate direction, implementation of the FMSUD scheme in the momentum equations is by far more demanding than the implementation of a single scalar equation in centered cells. For this reason, a new approach has been devised to treat the problem, from the

mathematical viewpoint, in the maximum generality and for all flow conditions, taking into account automatically the direction of the velocity vector and thus choosing automatically the weighting factors to be associated to different cells in the skew-upwind discretization. The new mathematical approach is straightforward for the treatment of inner cells of the fluid-dynamic definition domain, but particular care must be paid to its implementation for boundary cells where the appropriate boundary conditions must be applied. The tests cases are explained in which the implementation of the FMSUD method has been applied and the quality of the numerical results against the correct solution, when the latter is known, is explained. DOE

N91-27071*# Arizona State Univ., Tempe. Dept. of Geology.
SALTATION THRESHOLD REDUCTION DUE TO THE ELECTROSTATIC AGGLOMERATION OF FINE PARTICLES
Rodman N. Leach and Ronald Greeley *In* NASA. Ames Research Center, Sand and Dust on Mars May 1991 p 38 (For primary document see N91-27057 18-91)
Avail: NTIS HC/MF A04 CSCL 20D

N91-27098*# Texas Univ., San Antonio. Div. of Engineering.
REEXAMINATION OF METMAN, RECOMMENDATIONS ON ENHANCEMENT OF LCVG, AND DEVELOPMENT OF NEW CONCEPTS FOR EMU HEAT SINK Final Report
Amir Karimi *In* Houston Univ., NASA/ASEE Summer Faculty Fellowship Program, 1990, Volume 1 Dec. 1990 16 p (For primary document see N91-27088 18-99)
(Grant NGT-44-005-803)
Avail: NTIS HC/MF A10 CSCL 20D

35 INSTRUMENTATION AND PHOTOGRAPHY

Includes remote sensors; measuring instruments and gages; detectors; cameras and photographic supplies; and holography.

For aerial photography see *43 Earth Resources and Remote Sensing.* For related information see also *06 Aircraft Instrumentation,* and *19 Spacecraft Instrumentation.*

N91-26490*# National Aeronautics and Space Administration. Lewis Research Center, Cleveland, OH.
APPLIED HIGH-SPEED IMAGING FOR THE ICING RESEARCH PROGRAM AT NASA LEWIS RESEARCH CENTER
Howard Slater, Jay Owens (Cortez 3 Services Corp., Brook Park, OH.), and Jaiwon Shin 1991 18 p Presented at the 1991 International Symposium on Optical Applied Science and Engineering, San Diego, CA, 21-26 Jul. 1991; sponsored by the Society of Photo-Optical Instrumentation Engineers
(Contract NAS3-24816)
(NASA-TM-104415; E-6246; NAS 1.15:104415) Avail: NTIS HC/MF A03 CSCL 14B

The Icing Research Tunnel at NASA Lewis Research Center provides scientists a scaled, controlled environment to simulate natural icing events. The closed-loop, low speed, refrigerated wind tunnel offers the experimental capability to test for icing certification requirements, analytical model validation and calibration techniques, cloud physics instrumentation refinement, advanced ice protection systems, and rotorcraft icing methodology development. The test procedures for these objectives all require a high degree of visual documentation, both in real-time data acquisition and post-test image processing. Information is provided to scientific, technical, and industrial imaging specialists as well as to research personnel about the high-speed and conventional imaging systems will be on the recent ice protection technology program. Various imaging examples for some of the tests are presented. Additional imaging examples are available from the NASA Lewis Research Center's Photographic and Printing Branch. Author

N91-26491# Naval Ocean Systems Center, San Diego, CA.
BACKPLANE BUS DISTRIBUTED REALTIME CLOCK SYNCHRONIZATION
D. R. Wilcox Dec. 1990 58 p
(AD-A234476; NOSC/TR-1400) Avail: NTIS HC/MF A04 CSCL 25/5

This report presents methods of synchronizing the realtime clocks associated with a set of respective digital processing modules interconnected through a backplane bus. All the methods are based on the broad cast of a strobe signal over the backplane bus, which simultaneously samples all the realtime clocks being synchronized. The report describes and compares various methods of implementing realtime clocks, designed to permit their rate of advance with respect to physical time to be adjusted. It examines and makes recommendations on various interface standardization issues related to variable rate realtime clocks. It also gives and evaluates software algorithms for synchronizing variable rate realtime clocks. GRA

N91-26492# Naval Research Lab., Washington, DC.
DEPRESSED COLLECTOR EXPERIMENTS ON A QUASIOPTICAL GYROTRON Memorandum Report
T. A. Hardgreaves, A. W. Fliflet, R. P. Fischer, and M. L. Barsanti 17 Apr. 1991 15 p Prepared in cooperation with JAYCOR, Vienna, VA
(AD-A234559) Avail: NTIS HC/MF A03 CSCL 09/1

A simple, single, single-stage collector has been tested on the quasioptical gyrotron (QOG) experiment at the Naval Research Laboratory (NRL). This is the first application of a depressed collector to a high power gyrotron, and was relatively easily accomplished due to the natural separation of the electron beam and the output radiation in the QOC. Collector efficiencies as high as 50 percent and overall efficiencies up to 16 percent were observed. The output power reached 431 kW with an overall efficiency of 13 percent and a collector efficiency of 41 percent The collector efficiency was limited in this experiment due to interception of approximately 15 percent of the electron beam on an undepressed section of the beam guide, a problem readily correctable with a small change in the beam guide dimensions. If this part of the electron beam was collected at the collector potential, the overall and collector efficiency would increase to 16 percent and 55 percent respectively. The maximum collector efficiency would increase to 58 percent (at high output power) and the best overall efficiency would increase to 20 percent (at lower output power). GRA

N91-26493# Air Force Systems Command, Wright-Patterson AFB, OH. Foreign Technology Div.
WPG-30 MODEL MICROPROCESSOR CONTROLLED ROTATING BERYLLIUM MIRROR SCANNING CAMERA AND ITS APPLICATIONS
Xianxiang Tan, Wanqing Xu, and Meijuan Zhu 21 Mar. 1991 15 p Transl. into ENGLISH from Baozha Yu Chongji (Peoples Rep. of China), v. 9, no. 1, Jan. 1989 p 49-54
(AD-A234802; FTD-ID(RS)T-1277-90) Avail: NTIS HC/MF A03 CSCL 14/4

This article elucidates the principal technical capabilities of the newly test manufactured WPG-30 Model microprocessor controlled rotating beryllium mirror scanning or streak camera, its special features and the status of its initial applications in experiments on the mechanics or dynamics of explosions. This camera opts for the use of beryllium mirror turbines, a scanning or streak speed (writing time) of 15km/s, and, in conjunction with this, maintains strong optical energy. Because of this, it raises its interval resolution capability. It makes use of a microprocessor controlled unit raising the camera's degree of automatic control and measurement speed precision. Through detonation experiments, it has been clearly shown that this type of new camera, both in its ability to discriminate or resolve differences in wave forms and in its ability to discriminate or resolve differences in wave forms and in its precision of measurement of time duration intervals, represents a very large increase. GRA

N91-26494# Massachusetts Inst. of Tech., Cambridge. Research Lab. of Electronics.
ATOM WAVE INTERFEROMETER Annual Report, 1 Dec. 1989 - 30 Nov. 1990
David E. Pritchard 5 Apr. 1991 6 p
(Contract N00014-89-J-1207)
(AD-A234863) Avail: NTIS HC/MF A02 CSCL 14/2

Using fabricated transmission gratings as optical elements for the matter waves, we are constructing an atom interferometer which will physically separate atom waves before recombining them. Atom interferometers will be useful in studies of atomic properties, tests of basic quantum physics, for metrology, as a rotation sensor, and perhaps ultimately as devices to make ultra-small structures using atom holograms. GRA

N91-26495# Sandia National Labs., Albuquerque, NM.
INTERFACIAL FORCE SENSOR WITH FORCE-FEEDBACK CONTROL
S. A. Joyce, J. E. Houston, and B. K. Smith 1990 11 p
Presented at the 1990 International Electron Device Conference, San Francisco, 10-12 Dec. 1990
(Contract DE-AC04-76DP-00789)
(DE91-004897; SAND-90-2558C; CONF-901244-3) Avail: NTIS HC/MF A03

A new interfacial force microscope capable of measuring the forces between two surfaces over the entire range of surface separations, up to contact, has been developed. The design is centered around a differential capacitance displacement sensor where the common capacitor plate is supported by torsion bars. A force-feedback control system balances the interfacial forces at the sensor, maintaining the common capacitor plate at its rest position. This control eliminates the instability which occurs with the conventional cantilever-based force sensors when the attractive force gradient exceeds the mechanical stiffness of the cantilever. The ability to measure interfacial forces at surface separations smaller than this instability point using the feedback control is demonstrated. DOE

N91-27094*# Texas A&M Univ., Galveston. Dept. of Marine Science.
PHOTOGRAPHIC IMAGE ENHANCEMENT Final Report
Gerald E. Hite *In* Houston Univ., NASA/ASEE Summer Faculty Fellowship Program, 1990, Volume 1 Dec. 1990 14 p (For primary document see N91-27088 18-99)
(Grant NGT-44-005-803)
Avail: NTIS HC/MF A10 CSCL 14E

36 LASERS AND MASERS

Includes parametric amplifiers.
For related information see also *76 Solid-State Physics.*

N91-26496# Rochester Univ., NY. Inst. of Optics.
PROCEEDINGS OF THE OPTOELECTRONIC WORKSHOP 27: SEMICONDUCTOR LASERS AND THEIR APPLICATIONS Interim Technical Report
Govind Agrawal and C. W. Trussell 17 Dec. 1990 161 p
Workshop held in Rochester, NY, 17 Dec. 1990; sponsored in part by Rochester Univ., and Army
(Contract DAAL03-86-K-0173)
(AD-A233779; ARO-24626.209-PH-UIR) Avail: NTIS HC/MF A08 CSCL 09/3

This workshop represents the twenty-seventh of a series of intensive academic/government interactions in the field of advanced electro-optics, as part of the Army sponsored University Research Initiative. By documenting the associated technology status and dialogue it is hoped that this baseline will serve all interested parties towards providing a solution to high priority Army requirements. GRA

N91-26497# Air Force Systems Command, Wright-Patterson AFB, OH. Foreign Technology Div.
LASER APPLICATIONS IN MACHINING SLAB MATERIALS
Xiaoping Zhang 23 Oct. 1990 18 p Transl. into ENGLISH from Duanya Jishu (China), v. 14, no. 3, 35039, 1989 p 25
(AD-A233823; FTD-ID(RS)T-0550-90) Avail: NTIS HC/MF A03 CSCL 09/3

Since the invention of the laser back in 1960, laser technology has been extensively applied in many fields of science and technology. These has been a history of nearly two decades of using lasers as an energy source in machining materials, such as cutting, welding, ruling and boring, among other operations. With the development of flexible automation in production, the advantages of laser machining have has grown more and more obvious. The combination of laser technology and computer science further promotes the enhancement and upgrading of laser machining and related equipment. At present, many countries are building high quality laser equipment for machining slab materials, such as the Coherent and Spectra Physics corporations in the United States, the Trumpf Corporation in West Germany, the Amada Corporation in Japan, and the Bystronic Corporation in Switzerland, among other companies. GRA

N91-26498# Naval Postgraduate School, Monterey, CA.
SEA TEST DEVELOPMENT OF LASER ALTIMETER Final Report, Oct. 1988 - Dec. 1990
E. C. Crittenden, Jr., G. W. Rodeback, E. A. Milne, and A. W. Cooper Jan. 1991 25 p
(AD-A233824; NPS-PH-91-006) Avail: NTIS HC/MF A03 CSCL 17/5

Low altitude (81 m.) narrow-beam laser reflectance measurements were made from the nearly ocean-like water surface under the Golden Gate Bridge. For short wavelength waterways superimposed on swell, the signal amplitude probability distribution showed periods of zero return signal, even for vertical incidence, apparently due to tipping of the average water surface. The nonzero signals show an antilog-normal probability distribution, skewed toward higher signal than that provide by a normal (Gaussian) distribution. With incidence angle displaced from the vertical, the distribution shape is retained but with more frequent zero reflections. The decrease with angle of the average signal, including the zeros, is well fitted with a Gram-Charlier distribution, as seen by earlier observers using photographic techniques which masked these details of the structure. For the simpler wave pattern due to a long sustained wind direction, the signal amplitude probability distribution is log-normal with no zero signal periods, for this case, the distribution shifts toward exponential at large angles from the vertical. For surface states intermediate between the above two extremes the distribution is often normal. The larger return signal resulting from the skew toward larger amplitudes from lognormal are more favorable for disposable laser altimeters than previously believed. Also for an altimeter which may be swinging from a parachute or balloon, the return at angles from the vertical remains high. The presence of occasional zero return signal does degrade the accuracy of altitude somewhat for a descending altimeter, but the signal available assures performance at larger altitudes than previously expected. GRA

N91-26499# Philadelphia Coll. of Pharmacy and Science, PA. Dept. of Chemistry.
HIGH PULSE-ENERGY FLASHLAMP-PUMPABLE LASER DYES Final Technical Report, 1 Oct. 1989 - 30 Sep. 1990
Joel M. Kauffman and John A. Novinski 31 Dec. 1990 59 p
(Contract DAAL03-89-K-0160)
(AD-A233837; ARO-27514.2-CH) Avail: NTIS HC/MF A04 CSCL 09/3

To obtain higher pulse energies from laser dyes by means of flashlamp pumping in solution, several new prototype dyes were synthesized and submitted for testing. The dyes were intended to display high pulse energy either in a flowing solution in a non-flammable solvent or in the solid poly methyl methacrylate. The class of laser dye known as 4PyMPO was given an expanded fluorophor by substitution of a biphenylene for the phenylene (P)

group. None of the expected increases in extinction coefficient (e), fluorescence quantum yield and emission wavelength were obtained. GRA

N91-26500# Oklahoma State Univ., Stillwater. Center for Laser Research.
LASER SPECTROSCOPY CHARACTERIZATION OF MATERIALS FOR FREQUENCY AGILE SOLID STATE LASER SYSTEMS Final Report, 15 Jan. 1988 - 14 Jan. 1991
Richard C. Powell 15 Mar. 1991 176 p
(Contract DAAL03-88-K-0025)
(AD-A233916; ARO-25478.19-PH) Avail: NTIS HC/MF A09 CSCL 09/3

This research involves the use of laser spectroscopy techniques to investigate materials which include laser crystals such as Cr3+ -doped alexandrite, emerald, garnets, and glass ceramics as well as Nd3+ -doped garnets and germinates and Ho3+ -doped fluorides. In addition, photorefractive processes were studied in potassium niobate crystals and in rare earth doped glasses. Some of the results of major importance from this work are: (1) The characterization of the properties of laser-induced gratings in glasses; (2) The elucidation of the effects of dopant ions on the photorefractive response of potassium niobate; (3) The observation of a new type of picosecond nonlinear optical response in potassium niobate associated with scattering from a Nb hopping mode; (4) The characterization of the properties of energy migration and radiationless relaxation processes in Cr3+ doped laser crystals; (5) The characterization of the pumping dynamics and lasing properties of Ho+3 in BaYb2F8; and (6) The characterization of the pumping dynamics and lasing properties of several Nd3+ -doped crystals. GRA

N91-26501# New Mexico State Univ., Las Cruces. Dept. of Physics.
ATMOSPHERIC PROPAGATION OF LASER BEAMS Report, 1 Oct. 1987 - 31 Dec. 1990
Robert L. Armstrong Feb. 1991 21 p
(Contract DAAL03-87-K-0144)
(AD-A234314; ARO-25003.1-GS) Avail: NTIS HC/MF A03 CSCL 09/3

The enclosed report describes experimental and theoretical results obtained under this contract. Experimental work emphasized nonlinear interactions of an intense laser beam with micrometer-sized liquid droplets, including nonlinear optical effects such as stimulated Raman scattering (SRS) and lasing, plasma studies, and superheating. Theoretical analyses served both to aid in the understanding of the experimental investigations and to undertake studies of related theoretical interest, notably analysis of the companion problem of the propagation of an intense laser beam through a medium containing interaction aerosols. GRA

N91-26502# State Univ. of New York, Albany.
EFFECT OF AEROSOLS ON LASER-INDUCED BREAKDOWN Final Report, 15 Aug. 1987 - 31 Dec. 1990
Petr Chylek 20 Feb. 1991 66 p
(Contract DAAL03-87-K-0093)
(AD-A234324; ARO-24803.5-GS) Avail: NTIS HC/MF A04 CSCL 20/6

We have discovered the time delay of the order of a few nanoseconds in the emitted stimulated Raman scattering by micron-size droplets. We have verified experimentally that a certain class of mixing rules lead to an effective refractive index of composite particles which is in agreement with experimental measurements. We have derived an analytical expression for the distance between the Mie resonances as a function of the size parameter, refractive index, and the order of the resonance. We have obtained an analytical form for the adsorption and extinction cross sections of nonspherical particles in the form of prismatic columns and plates using the anomalous diffraction approximation. GRA

N91-26503# Naval Research Lab., Washington, DC.
FREQUENCY UPSHIFTING OF LASER PULSES BY IONIZATION FRONTS
E. Esarey, G. Joyce, and P. Sprangle 14 Mar. 1991 12 p
(Contract DE-AI05-83ER-40017; ARPA Order 7412-A)
(AD-A234354; NRL-MR-6737) Avail: NTIS HC/MF A03 CSCL 20/6

A novel method for upshifting the frequency of a laser pulse is examined, which utilizes the interaction of the pulse with a co-propagating relativistic ionization front. The induced frequency shift is found to initially scale linearly with the propagation time tau. Asymptotically, the frequency scales as sq. rt. tau. Phase slippage limitations may be overcome by appropriately increasing the plasma density as a function of tau, thus allowing for substantially higher frequency shifts. GRA

N91-26504# Naval Research Lab., Washington, DC.
X RAY LASER PROGRAM Final Report, 1 Oct. 1989 - 30 Sep. 1990
18 Apr. 1991 154 p
(AD-A234390; NRL-MR-6817) Avail: NTIS HC/MF A08 CSCL 20/9

Calculations of Photoionization, Photoexcitation, and Gain Production in a Neon Gas Cell Irradiated by a Sodium Z-Pinch on Saturn; the Naval Research Laboratory (NRL) Experimental Pulsed Power X-Ray Laser Program; Improving Plasma Uniformity in Z-Pinch Driven Neonlike Krypton X-Ray Lasers; Analysis of Pumping Mechanisms Significantly Affecting the Gain of Soft X-Ray Lines in Neonlike Selenium; and Prospects for X-Ray Lasing in Ultra Short-Pulse Laser/Plasma Interactions are among the topics discussed. GRA

N91-26505# Department of the Navy, Washington, DC.
A NARROW-BANDWIDTH UNSTABLE RESONATOR LASER CAVITY Patent Application
John Cooper, inventor (to Navy), John F. Reintjes, inventor (to Navy), Lawrence Tankesley, inventor (to Navy), and James L. Dexter, inventor (to Navy) 16 Oct. 1990 23 p
(AD-D014865; US-Patent-Appl-SN-598513) Avail: NTIS HC/MF A03 CSCL 09/3

An unstable resonator laser cavity providing high power radiation with diffraction-limited divergence and narrow-bandwidth comprise a gain medium for generating and amplifying laser radiation optically coupled to a reflector via a frequency narrowing element for providing feedback and bandwidth-narrowing of the laser radiation travelling between the gain medium and the reflector. A telescopic ring is optically coupled to the gain medium opposing the reflector. The telescopic ring comprises: a polarized beam splitter, which transmits a first polarization polarized laser radiation into the telescopic ring travelling in a first direction and reflects a second polarization polarized laser radiation into the telescopic ring traveling in a second direction; first and second rotators for rotating the first polarization polarized laser radiation to provide second polarization polarized laser radiation travelling in the first direction; and lenses for magnifying the second polarization polarized laser radiation travelling in the first direction onto the polarized beam splitter, which reflects the second polarization polarized laser radiation produced by the first and second rotators back into the gain medium. A scraper mirror, located between the gain medium and the reflector, provides the output beam. GRA

N91-26506# Department of the Navy, Washington, DC.
A ROOM-TEMPERATURE, FLASHPUMPED, 2.09 MICRON SOLID STATE LASER Patent Application
G. J. Quarles, inventor (to Navy) and Leon Esterowitz, inventor (to Navy) 30 Apr. 1990 21 p
(AD-D014871; US-Patent-Appl-SN-516943) Avail: NTIS HC/MF A03 CSCL 09/3

This patent application discloses a room-temperature solid state laser for producing a laser emission at a wavelength of substantially 2.09 microns. In a preferred embodiment, the laser includes: a laser cavity defined by first and second reflective elements opposing each other on a common axis to form a path

therebetween; a laser crystal disposed in the laser cavity, the laser crystal having a host material capable of accepting Cr(3+) sensitizer ions, Tm(3+) sensitizer ions and Ho(3+) activator ions; effective amounts of Cr(3+) sensitizer ions, Tm(3+) sensitizer ions and Ho(3+) activator ions dispersed within the host material; and means for exciting the laser crystal to produce a laser emission at substantially 2.09 microns with slope efficiency of at least 4 percent, and preferably of at least 5 percent. GRA

N91-26507# Rochester Univ., NY. Dept. of Physics and Astronomy.
LASER SWITCHED POWER LINAC Final Report, 1 Sep. 1987 - 31 Dec. 1990
A. C. Melissinos 8 Apr. 1991 57 p
(Grant AF-AFOSR-0328-87)
(AD-A234581; AFOSR-91-0378TR) Avail: NTIS HC/MF A04 CSCL 09/3

A short pulse (2 ps) infrared laser was used to activate photoconductive switches (Si and GaAs) which applied up to 2.5 kV to the outer circumference (R = 3cm) of two parallel metal discs. With a disc spacing of 0.5 mm, the best observed voltage multiplication of the pulse when it reached the center was a factor of 3.4 compared to a predicted gain of 6. GRA

N91-26508# Stanford Univ., CA. Dept. of Chemistry.
LASER-INDUCED DESORPTION OF H2 FROM Si(111)7X7
B. G. Koehler and S. M. George 12 Apr. 1991 40 p
(Contract N00014-90-J-1281)
(AD-A234636; SU-TR-14) Avail: NTIS HC/MF A03 CSCL 09/3

Laser excitation can lead to desorption when silicon surfaces are exposed to laser pulses at a frequency above the band gap. To determine whether a thermal or a photochemical desorption mechanism is operative, this study compared experimental measurements and numerical calculations for the laser-induced desorption (LID) of H2 from Si(111)7x7. The surface-temperature rise on Si(111)7x7 produced by laser pulses from a TEM-OO Q-switched Ruby laser at wavelength=694 nm was calculated using temperature-dependent physical and optical parameters and a finite penetration depth. The laser-induced surface heating results were then used to calculate laser-induced thermal desorption (LITD) yields for H2 from Si(111)7x7. The calculated H2 yields as a function of laser energy, surface temperature, and hydrogen coverage were compared with the corresponding experimental H2 LID measurements. GRA

N91-26509# Potomac Photonics, Inc., Lanham, MD.
QUASI-CW EXCIMER LASER, PHASE 2 Final Report, 1 Aug. 1988 - 31 Dec. 1990
C. P. Cristensen 15 Feb. 1991 19 p
(Contract F49620-88-C-0092)
(AD-A234771; Rept-0092F-Phase-2; AFOSR-91-0238TR-Phase-2) Avail: NTIS HC/MF A03 CSCL 09/3

A Phase 2 SBIR investigation of small high-repetition-rate waveguide excimers lasers is described. Techniques for fabrication of halogen-compatible discharge structures were investigated, and a KrF laser based on electrodeless microwave discharge technology was constructed. A solid-state magnetron driver for waveguide excimer lasers was developed, and studies of KrF laser gas consumption rates were conducted. A preliminary investigation of ArF laser operation was carried out and operation of a XeCl laser at pulse repetition rates as high as 13 kHz was demonstrated. In addition, waveguide XeCl laser pumping of a jet-stream dye laser and high prf photoablation by KrF and XeCl lasers was investigated. GRA

N91-26510# Rockwell International Corp., Newbury Park, CA. Microelectronics Technology Center.
MULTIGIGAHERTZ SEMICONDUCTOR LASERS Progress Report, 28 Sep. 1990 - 8 Feb. 1991
8 Feb. 1991 4 p
(Contract N00014-90-C-2354)
(AD-A234776) Avail: NTIS HC/MF A01 CSCL 09/3

The vendor has completed the processing of the first batch of high speed lasers. Device testing is in progress. In addition, the development of a package suitable for 20 GHz operation and 0.5 micron lithography to reduce the laser channel width are in process and on schedule. GRA

N91-26511# Air Force Systems Command, Wright-Patterson AFB, OH. Foreign Technology Div.
ARRAY-TYPED, SEALED-OFF MINI TEA CO2 LASER
Chengzhi Pan, Ming Zhai, Xiping Li, and Xiuyun Liu 21 Mar. 1991 18 p Transl. into ENGLISH from Zhongguo Jigung (Peoples Rep. of China), v. 17, no. 5, May 1990, p 264, 269-272
(AD-A234804; FTD-ID(RS)T-1181-90) Avail: NTIS HC/MF A03 CSCL 09/3

An array-typed sealed-off mini TEA CO2 laser is reported. This device can not only deliver parallel multi-beams, but also various CO2 laser outputs with high quality by using optical systems combinations, thereby it has wide potential applications in many scientific and technical fields. GRA

N91-26512# Missouri Univ., Saint Louis. Dept. of Physics.
CHAOTIC AND BIFURCATING NONLINEAR SYSTEMS DRIVEN BY NOISE WITH APPLICATIONS TO LASER DYNAMICS Final Report, 1 Dec. 1987 - 31 Oct. 1989
Frank Moss 31 Oct. 1989 5 p
(Contract N00014-88-K-0084)
(AD-A234841) Avail: NTIS HC/MF A01 CSCL 20/5

One aspect of the research was focused on the effects of noise as a driving force in various nonlinear dynamical systems. The effects studied were: postponements of bifurcations; state dependent diffusion; a mean first passage time in a system with both random temporal forcing in a random potential; and a mean first passage time problem with colored noise. A second aspect involved studies on switching properties of nonlinear systems in the presence of noise, and a special application of the results to a noise quenched, correlated, spontaneous emission laser. A third major effort was devoted to studies on stochastic resonance (SR) with a remark on the theory, a long work on the use of analog simulations in studies of SR, and a study of order and disorder in SR. At this point, a study was performed on noise induced topological transitions in the two dimensional stationary probability density of an archetypal bistable system. Finally, a new quantity was introduced to general studies on SR: the escape time probability distribution, wherein the theory, digital, and analog simulations were accomplished. These studies hold great promise for applications in a number of fields, including the creation of a deeper understanding of how noise assisted information is transmitted in biological neurons. GRA

N91-26513# Science Research Lab., Inc., Somerville, MA.
SCALING CW ELECTRON BEAM PUMPED RARE GAS LASERS TO ULTRA-HIGH AVERAGE POWER Final Report, 16 May - 15 Nov. 1990
11 Apr. 1991 35 p
(Contract DASG60-90-C-0061)
(AD-A235120; SRL-05-F-1991) Avail: NTIS HC/MF A03 CSCL 09/3

The overall objective of this program is to demonstrate the feasibility of efficiently scaling Ar:Xe lasers to ultra-high average power levels for strategic defense applications. The contractor has experimentally verified that the Ar:Xe laser system, which operates at near-IR wavelengths (1.73 micrometers), can achieve laser efficiencies of 4 percent with electron beam pumping at pump power densities as low as 10 watts/cc. This new efficient electron beam pumping regime promises cost-effective scaling of Ar:Xe laser systems to multi-megawatt average power levels while maintaining high electrical efficiency (4 to 6 percent) and near-diffraction-limited beam quality. In the Phase 2 effort, detailed experiments will be performed on an electron beam pumped Ar:Xe laser with a closed cycle flow loop at pump power densities of 10 to 20 W/cc. The objective of these experiments is to validate methods for correction and control of the optical distortions resulting from experiments is to validate methods for correction

and control of the optical distortions resulting from CW pumping. Control of thermal distortions will be achieved by optimally contouring the spatial profile of electron beam power deposition in the active volume. With the optimal deposition profile, higher order optical distortions will be negligible and a diffraction limited beam will be obtained after tilt and focus corrections are made. These corrections can be made by a simple local loop by an adaptive optics system in the beam train. GRA

N91-26514# Harry Diamond Labs., Adelphi, MD.
ENERGY LEVELS AND BRANCHING RATIOS OF Tm(3)+ IN TEN GARNET LASER MATERIALS Interim Report, 15 Jun. 1990 - 15 Jan. 1991
Clyde A. Morrison, Elizabeth D. Filer, and Norman P. Barnes Apr. 1991 23 p
(AD-A235274; HDL-TR-2196) Avail: NTIS HC/MF A03 CSCL 09/3

A prediction of laser performance of Tm transitions from the F4 to the H6 manifolds in ten garnets has been made by using a quantum-mechanical model. Theoretical energy levels, branching ratios, and population inversion percentages were calculated to determine threshold as a function of temperature. GRA

N91-26515# Los Alamos National Lab., NM.
DIAGNOSTIC STUDIES OF YBa2Cu3O(7-DELTA) LASER ABLATION
N. S. Nogar, R. C. Dye, S. R. Foltyn, R. E. Muenchausen, X. D. Wu, and R. C. Estler (Fort Lewis A&M Coll., Durango, CO.) 1991 10 p Presented at the HASRD Workshop on Laser Ablation: Mechanisms and Application, Oak Ridge, 8-10 Apr. 1991
(Contract W-7405-eng-36)
(DE91-011382; LA-UR-91-1267; CONF-9104192-3) Avail: NTIS HC/MF A02

The use of a variety of diagnostics can offer significant insight into the mechanisms of laser ablation and film growth. It seems clear that under conditions of optimum film growth that significant collisional processes occur both within the laser-desorbed plume, and between the plume and the processing gas. These collisional processes are responsible for the macroscopic characteristics of the plume, including velocity and spatial distributions, the ratio of ions and particles to neutral atoms and molecules, and the incorporation of oxygen into the film. It is also obvious that real-time diagnostics, applicable under conditions relevant to film production, could provide useful process monitors and feedback control for the production of high-temperature superconducting (HTSC) thin films. DOE

N91-26516# Argonne National Lab., IL.
ELEMENTARY REACTION RATE MEASUREMENTS AT HIGH TEMPERATURES BY TUNABLE-LASER FLASH-ABSORPTION
J. P. Hessler Mar. 1991 4 p Presented at the Department of Energy-Basic Energy Sciences (DOE-BES) Combustion Research Meeting, Lake Geneva, 28-31 May 1991
(Contract W-31-109-eng-38)
(DE91-011850; ANL/CP-70076; CONF-9105162-3) Avail: NTIS HC/MF A01

The major objective of this program is to measure thermal rate coefficients and branching ratios of elementary reactions which involve atomic and diatomic reactants or products. To perform these measurements, we have constructed an ultrahigh-purity shock tube to generate temperatures between 1500 and 5500 K. A high-resolution, laser light source is being used to measure the rate of change of the concentration of species which absorb below 50,000 per cm e.g.: OH, CH, CH3. State-of-the-art laser techniques are being used to extend the technique into the vacuum-ultraviolet spectral region where we can measure atomic species e.g.: H, D, C, O, and N; and diatomic species e.g.: O2 and OH. DOE

N91-26517# Lawrence Livermore National Lab., CA.
SATURATION AND KINETIC ISSUES FOR OPTICAL-FIELD-IONIZED PLASMA X RAY LASERS
D. C. Eder, P. Amendt, M. D. Rosen, J. K. Nash, and S. C. Wilks 29 Apr. 1991 7 p Presented at the Conference on Short-Wavelength Coherent Radiation: Generation and Application, Monterey, 4-10 Apr. 1991
(Contract W-7405-eng-48)
(DE91-012079; UCRL-JC-105738; CONF-9104164-4) Avail: NTIS HC/MF A02

Lasing between excited states and the ground state following optical-field ionization is studied. Saturation of an x ray laser when the lower lasing level is a ground state of a H-like or Li-like ion is discussed. Efficiencies of 10(exp -5) to 10(exp -4) are calculated for the 3d(sub 5/2)-2p(sub 3/2) transition at 98 A in Li-like Ne. The assumption that the fine-structure levels are populated according to their statistical weights is shown to be justified through comparisons with calculations using a detailed atomic model. The effect of saturation by a given fine-structure transition on the populations of the fine-structure levels is analyzed. DOE

N91-26518# Lawrence Livermore National Lab., CA.
DETERMINATION OF SBS INDUCED DAMAGE LIMITS IN LARGE FUSED SILICA OPTICS FOR INTENSE, TIME VARYING LASER PULSES
D. T. Kyrazis and T. L. Weiland 19 Oct. 1990 22 p Presented at the 22nd Boulder Damage Symposium, Boulder, 25-26 Oct. 1990
(Contract W-7405-eng-48)
(DE91-012080; UCRL-JC-105107; CONF-9010287-8) Avail: NTIS HC/MF A03

The propagation of intense 3rd harmonic light (0.351 micron) through large optical components of the Nova laser results in fracture damage of the center of the component. This damage is caused by an intense acoustical wave brought to focus in the center by reflecting off the circular edge of the optic. The source of this wave is light generated by transverse stimulated Brillouin scattering (SBS). By taking into account the transient gain characteristics of the SBS, the pulse energy can be correctly predicted that would cause damage for any time variation in intensity in the pump beam, and predict the relative intensity of the Brillouin light. The model is based on the transient behavior of a first order linear system. DOE

N91-26519# Lawrence Livermore National Lab., CA.
X RAY SPOT MOTION DURING 220 ps LASER PULSES
S. H. Langer 1 May 1991 7 p
(Contract W-7405-eng-48)
(DE91-012111; UCRL-ID-107120) Avail: NTIS HC/MF A02

To meet the goals of the Precision NOVA campaign, we need to discover how to accurately and repeatably position all 10 x ray spots at the desired location. As part of this effort, a series of shots sending all 10 beams onto a gold disk are made. There are 5 beams per side and the individual beams are aimed at 5 equally spaced points around a circle. Each beam has an incidence angle of 50 degrees relative to the disk normal. The laser pulse is a 100 or 200 ps Gaussian and each beam has an energy of roughly 200 J of 3(omega) light. A pinhole camera (PHC) with a 9 (mu)m aluminum filter is used to measure the emitted x rays. The transmission of the filter and the response of the detector means that most of the signal comes from below the aluminum K-edge at 1.6 keV if only the aluminum filter is present. If the beryllium filter is also used, half of the remaining signal is due to the gold M-band. The sub-critical portions of the ablated gold produce M-band emission, so some of the PHC signal comes from significantly in front of the disk. The direction of the offset is consistent with the hypothesis that the spot has shifted backward along the beam in a fashion similar to the spot motion that has been measured in longer pulse shots. On the other hand, there is no obvious reason why spot motion would leave 4 beams at their intended positions and 6 beams with large repeatable offsets of 100 microns. The goal is to find out if LASNEX models support the suggestion that the offset between the measured x ray spot positions and the point at which the laser beams were aimed can be explained by spot motion. Ron Thiessen's modeling in support of indirect drive implosions has shown that the spot motion reaches 100 to 150 microns at the end of a 1 ns pulse, so the motion

should be quite small for the 100 or 200 ps pulses considered here. The models run for this paper show the expected result, they predict roughly 10 microns of spot motion for the 200 ps pulse. DOE

N91-26520*# Stanford Univ., CA. Ginzton Lab.
SUNLITE PROGRAM. SUB-HERTZ RELATIVE FREQUENCY STABILIZATION OF TWO DIODE LASER PUMPED Nd:YAG LASERS LOCKED TO A FABRY-PEROT INTERFEROMETER
Final Report
R. L. Byer 1990 35 p
(Grant NAG1-839)
(NASA-CR-184957; NAS 1.26:184957) Avail: NTIS HC/MF A03 CSCL 20E

Two laser pumped Nd:YAG lasers were frequency stabilized to a commercial 6.327 GHz free spectral range Fabry-Perot interferometer yielding a best case beatnote linewidth of 330 MHz. In addition, a Fabry-Perot interferometer with a free spectral range of 680 MHz, a linewidth of 25 kHz, and a finesse of 27,500 was built, and when it was substituted in place of the commercial interferometer, it produced a robust and easily repeatable beatnote linewidth of 700 MHz. Author

N91-26521*# Massachusetts Inst. of Tech., Cambridge. Advanced Solid State Laser Materials Lab.
NEW LASER MATERIALS FOR LASER DIODE PUMPING
Annual Report, Jan. - Dec. 1990
H. P. Jenssen Dec. 1990 14 p
(Grant NAG1-924)
(NASA-CR-187786; NAS 1.26:187786) Avail: NTIS HC/MF A03 CSCL 20E

The potential advantages of laser diode pumped solid state lasers are many with high overall efficiency being the most important. In order to realize these advantages, the solid state laser material needs to be optimized for diode laser pumping and for the particular application. In the case of the Nd laser, materials with a longer upper level radiative lifetime are desirable. This is because the laser diode is fundamentally a cw source, and to obtain high energy storage, a long integration time is necessary. Fluoride crystals are investigated as host materials for the Nd laser and also for IR laser transitions in other rare earths, such as the 2 micron Ho laser and the 3 micron Er laser. The approach is to investigate both known crystals, such as BaY2F8, as well as new crystals such as NaYF8. Emphasis is on the growth and spectroscopy of BaY2F8. These two efforts are parallel efforts. The growth effort is aimed at establishing conditions for obtaining large, high quality boules for laser samples. This requires numerous experimental growth runs; however, from these runs, samples suitable for spectroscopy become available. Author

N91-26522# Los Alamos National Lab., NM.
TUNABLE EXCIMER LASERS
R. C. Sze 1990 7 p Presented at the International Conference on Lasers 1991, San Diego, 3-7 Dec. 1990
(Contract W-7405-eng-36)
(DE91-011399; LA-UR-91-1077; CONF-901293-1) Avail: NTIS HC/MF A02

The wide bandwidth nature of the rare-gas halide excimer transitions allow reasonable tuning of the laser oscillation wavelength that makes it useful for a number of applications. At the same time this wide bandwidth makes narrow band operation difficult and special techniques are needed to insure narrow frequency lasing as well as absolute frequency resettability. The author discusses briefly some of the classical frequency narrowing techniques and then goes on to some recent work that require lasers of special frequency characteristics for special applications including KrF laser fusion. DOE

N91-26523# Lawrence Livermore National Lab., CA.
PRECISION HIGH-POWER SOLID-STATE LASER DIAGNOSTICS FOR TARGET-IRRADIATION STUDIES AND TARGET-PLANE IRRADIATION MODELING
P. J. Wegner and M. A. Henesian Mar. 1991 15 p Presented at the OE/LASE 1991: 4th Society of Photo-Optical Instrumentation Engineers (SPIE) International Symposium, Los Angeles, 20-25 Jan. 1991
(Contract W-7405-eng-48)
(DE91-012036; UCRL-JC-106786; CONF-910123-28) Avail: NTIS HC/MF A03

A 0.74-m aperture laser diagnostic system has been designed and built and is an operational part of target irradiation experiments being conducted at the Nova Two Beam facility at Lawrence Livermore National Laboratory. These experiments examine the effects of laser beam conditioning on laser-plasma interaction, and include the use of full-aperture (0.74-m diameter) distributed phase element optics for fundamentally altering the irradiance distribution at either the second or third harmonic wavelengths of the Nova Nd:Glass laser system. The two beam laser diagnostic system (TBLDS) provides the suite of laser diagnostics essential to interpreting the results of these studies: (1) full-aperture energy measurement, (2) near-field imaging of planes up to 15 m ahead of the target chamber focusing lens, (3) far-field imaging of equivalent target planes within 5 mm on either side of best focus, (4) time-resolved power measurement using 10 to 20-ps resolution streak camera systems, (5) spectral measurement using a 1-m grating spectrometer with option for temporal streaking. The diagnostic is also equipped with a self referencing interferometer for measuring the wavefront at various near-field planes; however, this feature is still under activation. The diagnostic system can flexibly handle either the fundamental, second or third harmonic wavelengths on alternate laser pulses, and an energy range of 50 Joules/pulse to 12.5 kJ/pulse. In this paper we discuss the design of the TBLDS, and present results from ongoing measurements of the Nova irradiance without wavefront modifications. We also discuss our numerical simulation techniques for modeling the laser irradiance at the target plane. DOE

N91-26524# Oak Ridge National Lab., TN.
IN-SITU MONITORING OF LASER ABLATION OF SUPERCONDUCTORS
C. H. Chen, R. C. Phillips, and P. W. Morrison (Advanced Fuel Research, Inc., East Hartford, CT.) 1991 8 p Presented at the HASRD Workshop on Laser Ablation: Mechanisms and Application, Oak Ridge, 8-10 Apr. 1991
(Contract DE-AC05-84OR-21400)
(DE91-012057; CONF-9104192-4) Avail: NTIS HC/MF A02

In general, the preparation of superconductive thin film involves the vaporization of various chemicals. The species deposited on substrates include neutral atoms or molecules in ground states, atoms and molecules in excited states, ions in ground states and ions in excited states. An instrument which has the capability of the quantitative determination of atoms, molecules, and ions in various electronic states should provide very detailed information on the mechanism of formation of superconductive films. A position sensitive monitor of various oxide compounds relative to the flow and pressure of oxygen should reveal the role of oxygen, in superconductive film preparation. An ideal method of monitoring the deposition process is to continuously track the deposition in situ and automatically maintain optimum film growth. With this goal in mind, we have investigated several diagnostic methods. In this work, fluorescence spectra are presented which indicate suitability for monitoring excited atoms, molecules and ions; mass analysis of laser desorbed ions is described; and the application of resonance ionization spectroscopy (RIS) to monitor desorbed neutral atoms and molecules is discussed. Fourier Transform Infrared (FTIR) spectroscopy is used to measure substrate temperatures and the components on the surfaces. DOE

N91-26525# Lawrence Livermore National Lab., CA.
RADIO FREQUENCY AND MICROWAVE PLASMA FOR OPTICAL THIN FILM DEPOSITION
J. Otto, V. Paquet, R. T. Kersten, J. W. Etzkorn (Schott Glaswerke, Mainz, Germany, F.R.), R. M. Brusasco, J. Britten, J. H. Campbell, and J. B. Thorsness 18 Oct. 1990 14 p Presented at the SPIE Conference on Mathematical Imaging, San Diego, Jul. 1990

(Contract W-7405-eng-48)
(DE91-012081; UCRL-JC-105105; CONF-9007117-4) Avail: NTIS HC/MF A03

For the next generation of fusion lasers reflecting mirrors with laser damage thresholds of at least 40 J/sq cm for 10 ns laser pulses at 1.064 microns are needed. Up to now, no deposition technique has been developed to produce such mirrors. Best R and D-values realized today are around 30 J/sq cm for e-beam evaporated mirrors. R and D on conventional e-beam coating processes over the last 10 years has come up with marginal improvements in laser damage thresholds only. However, new technologies, like PICVD developed for the fabrication of ultra-low loss fiber preforms, seem to offer the potential to solve this problem. It is well known that fused silica produced by CVD processes can have laser damage thresholds as high as 80 J/sq cm. However, the thickness of a single deposited film is in the micron-range for most of the CVD processes used for preform manufacturing; since interference optics need films in the lambda/4n range the use of preform-fabrication processes for the purpose of interference mirror fabrication is limited to a few plasma based CVD technologies, namely PCVD. Especially PICVD is a very powerful technology to fabricate thin film multilayers for interference mirrors, because this technique is able to produce films down to monolayer thickness with nearly perfect stoichiometry and morphology. In first and preliminary experiments the usual deposition in a circular tube at high temperatures has been used for simplicity. However, to produce large area high quality laser mirrors this principle know-how has to be transferred from circular to planar geometry. Experiments showed, that there may be some limitations with respect to the homogeneity of a planar deposition using microwave excitation for the plasma. Therefore experiments have been performed in parallel with both RF and microwave excitation for comparison. In the following we will restrict ourselves to the description and discussions of the planar processes. DOE

N91-26526# Lawrence Livermore National Lab., CA.
DEVELOPMENT OF A SUBPICOSECOND, TUNABLE LiCAF (Cr:LiCaAlF6) LASER
M. D. Perry and F. G. Patterson 28 Mar. 1991 8 p Presented at the CLEO 1991: Conference on Lasers and Electro-Optics, Baltimore, 12-17 May 1991
(Contract W-7405-eng-48)
(DE91-012082; UCRL-JC-106926; CONF-910595-9) Avail: NTIS HC/MF A02

A new solid-state laser material, Cr:LiCaAlF6 (Li:CAF), developed originally for the Inertial Confinement Fusion program, holds great promise as a broad bandwidth exhibits a combination of properties (a broad emission spectrum, long-lifetime of the upper lasing level, low thermal lensing, and low excited state absorption) which make this a unique source for tunable and/or short-pulse lasers. We propose to demonstrate the full potential of LiCAF as a tunable, short pulse laser source by developing a high repetition rate, 100 GW, 100 femtosecond LiCAF laser. DOE

37 MECHANICAL ENGINEERING

Includes auxiliary systems (nonpower); machine elements and processes; and mechanical equipment.

N91-26527*# ST Systems Corp., Lanham, MD.
CONSTRAINED TRAJECTORY OPTIMIZATION FOR KINEMATICALLY REDUNDANT ARMS
Craig R. Carignan and Janice M. Tarrant 1990 9 p Presented at the ISRAM 1990 Third International Symposium on Robotics and Manufacturing, Vancouver, British Columbia, 18-20 Jul. 1990
(Contract NAS5-30440)
(NASA-CR-183477; NAS 1.26:183477) Avail: NTIS HC/MF A02 CSCL 13I

Two velocity optimization schemes for resolving redundant joint configurations are compared. The Extended Moore-Penrose Technique minimizes the joint velocities and avoids obstacles indirectly by adjoining a cost gradient to the solution. A new method can incorporate inequality constraints directly to avoid obstacles and singularities in the workspace. A four-link arm example is used to illustrate singularity avoidance while tracking desired end-effector paths. Author

N91-26528# North Dakota Univ., Grand Forks. Energy and Environmental Research Center.
PERFORMANCE EVALUATION OF A NOVEL EROSION-RESISTANT PUMP DESIGN
W. B. Hauserman and M. A. Musich 12 Sep. 1990 25 p
(Contract DE-FG22-89PC-89864)
(DE91-008201; DOE/PC-89864/T2) Avail: NTIS HC/MF A03

This is the final report on the evaluation of the Burly pump: a novel, semi-open impeller pump designed to offer exceptional resistance to wear by erosive slurries. It has a recessed or pocket type impeller, with a pattern of vanes designed to transfer momentum from the impeller to a vortex of fluid, consequently minimizing either the frequency or velocity of impact of suspended solids upon the impeller. This study compared the Burly pump with a more conventional Gorman-Rupp slurry pump by the method of accelerated wear simulation. Both pumps, with aluminum replicas of their standard impellers, were operated with a highly erosive slurry of quartz in water, achieving a degree of impeller destruction in hours compared to days using conventional cast iron impellers with a slurry of coal. The Gorman-Rupp pump, as expected, showed a rapid decrease in delivered hydraulic horsepower as the vanes on its impeller were worn away. The Burly pump, though delivering less hydraulic horsepower at the same speed, substantially improved its performance as the surface details of the impeller were worn away. No loss of performance by the Burly pump was found during this study. The limiting factor was the life of seals and bearings after exposure to the intentionally highly erosive slurries used. DOE

N91-26529# Johnson Matthey Environmental Products, Wayne, PA.
DEVELOPMENT OF A LOW TEMPERATURE CATALYTIC COMBUSTOR FOR SMALL GAS TURBINE APPLICATIONS Final Report, Mar. 1988 - Apr. 1989
M. Kosanovich and M. Wyatt Oct. 1990 129 p
(Contract GRI-5087-293-1565)
(PB91-161273; GRI-90/0339) Avail: NTIS HC/MF A07 CSCL 13I

The objective was to develop a catalytic combustion system for use with a 50 kW gas turbine cogeneration unit (advanced energy system). A combustor catalyst was developed based on a stabilized palladium formulation and supported on a thermally durable, high surface area alumina support. A lanthana stabilized, high surface area alumina was identified which maintained 90 to 100 sq m/g following 2500 hours of exposure to 1800 F. A metal monolith was utilized as the substrate and was constructed for a high temperature, oxidation resistant, aluminized ferric stainless steel. Subscale combustion experiments demonstrate the combustor catalyst maintains greater than 99.7 percent combustion efficiency for 500 hours at a gas hourly space velocity of 64,000. A full-scale combustion unit was designed and fabricated to demonstrate the technology on a commercial scale. Short-term experiments in the full-scale unit reveal favorable agreement with subscale data. GRA

N91-26530# Tecogen, Inc., Waltham, MA.
VARIABLE SPEED GAS ENGINE-DRIVEN AIR COMPRESSOR SYSTEM. PHASE 1: SYSTEM ANALYSIS Topical Report, Oct. 1989 - Oct. 1990
J. Morgan, A. Ruggles, and T. N. Chen Dec. 1990 39 p
(Contract GRI-5089-291-1846)
(PB91-159533; TR4489-096-90; GRI-91/0001) Avail: NTIS HC/MF A03 CSCL 13I

A nominal 150-hp gas engine driven air compressor using the TECODRIVE 8000 engine and the Ingersoll-Rand 178.5-mm twin screw compressor was designed. Phase 1 included the system engineering and design, economic and applications studies, and a draft commercialization plan. Author

N91-26531# Rensselaer Polytechnic Inst., Troy, NY. Dept. of Engineering and Mechanics.
IMPROVED MODELING AND PERFORMANCE OF SQUEEZE FILM DAMPER BEARINGS Final Report, 20 Sep. 1987 - 31 Dec. 1990
John A. Tichy 12 Feb. 1991 16 p
(Contract DAAL03-87-K-0113)
(AD-A233694; ARO-24839.7-EG) Avail: NTIS HC/MF A03
CSCL 13/9

The squeeze film damper is a bearing used in high speed turbomachinery to reduce rotor dynamics problem. A pure squeezing action in a thin film of lubricating fluid provides the desired damping. Due to the unsteady nature of the problem, a key assumption inherent in Reynolds' theory is not force, that of neglecting the inertia of the fluid. In addition, the fluid pressure often seeks a level lower than the vapor pressure, in which case a vapor cavity forms. Numerical calculations and supporting experiments are performed for a damper operating in the regime in which fluid inertia effects are important. A large error in the classical theory is seen at modified Reynolds number up to 30. These are the highest Reynolds numbers, heretofore reported, approaching those of actual practice. Regarding cavitation, a simplified model is developed. Compared to results obtained using the finite element method, considerable numerical work is saved and little accuracy is lost. Agreement with experimental measurements of cavity size and pressure is excellent. Preliminary studies have been undertaken concerning the use of electrorheological fluids in squeeze film dampers. GRA

N91-26532# Naval Postgraduate School, Monterey, CA.
ADAPTIVE CONTROL OF DIRECT DRIVE DEXTEROUS ROBOTIC HAND WITH BILATERAL TACTILE SENSING Final Report, 20 Sep. 1989 - 30 Sep. 1990
Morris R. Driels Dec. 1990 37 p
(AD-A233980; NPS69-90-06) Avail: NTIS HC/MF A03 CSCL 12/9

The work addresses the problem of identifying objects using a remote teleoperator. The application of the research is part of the development of demonstration technologies for the next generation of remotely operated vehicles (ROVs) currently under development by the US Navy. Two related research issues are developed. The first deals with determining how a teleoperator would remotely probe an unidentified object, and attempt to determine what the object is based only of force feedback through the teleoperator mechanism. Haptic models are tested against experimental data. The second issue addressed is the design of a dexterous, direct drive and effector for use on a teleoperator system. Results concerning the mechanic design of a small scale mechanical hand are discussed. GRA

N91-26533# New Mexico Univ., Albuquerque. Dept. of Mechanical Engineering.
DYNAMIC STABILITY OF FLEXIBLE ROBOT MANIPULATORS Final Report
Mo Shahinpoor and Gary L. Anderson 25 Feb. 1991 141 p
(Contract DAAL03-87-K-0114)
(AD-A234297; ARO-24867.8-EG) Avail: NTIS HC/MF A07
CSCL 12/9

This ARO-sponsored research investigation has led to a much better understanding of the means to control the dynamic stability of elastically flexible multi-axes robot manipulators as fully described in this final report and its enclosures and attachments. The acquired knowledge in this research effort will be applicable to a large number of military applications and needs such as the use of robotically automated fast moving and light weight gun barrels, target finders, directed laser or particle beams, tank auto-loaders, robot-equipped military vehicles, helicopters, and planes. The goals are the following: (1) to achieve stability of motion and computer control of precise positioning of fast moving (light-weight, flexible) robot manipulators, military aiming devices, and robotic tank autoloaders; (2) to explore stability of motion problems associated with robot arm-equipped military transports such as helicopters, tanks, and armored vehicles; (3) to construct an experimental set up for the simulation of the motion of a flexible robot attached to a moving base; and (4) to conduct experiments to confirm the results obtained in items 1 and 2 of the above goals. GRA

N91-26534# Southwest Research Inst., San Antonio, TX.
LONG-ROD PENETRATION OF CONFINED CERAMIC TILES Final Report, 1 Sep. 1988 - 31 Dec. 1990
Charles E. Anderson, Jr., Bruce L. Morris, James D. Walker, and James Lankford, Jr. Mar. 1991 7 p
(Contract DAAL03-88-K-0068)
(AD-A234312; ARO-26067.5-MS-A) Avail: NTIS HC/MF A02
CSCL 11/2

A multifaceted study of long-rod penetration of confined ceramic tiles was performed. Numerical and experimental efforts were pursued. An experimental methodology was developed to measure the ballistic response of confined ceramic tiles to impact at approx. 1.5 km/s by tungsten alloy long-rod projectiles. The depth of penetration into a backup steel substrate was the experimental observable. These data were then used to estimate more fundamental measures of ballistic performance such as the target resistance and the ability of the ceramic to erode the projectile. Numerical simulations of long-rod penetration were also performed to complement the experimental study and provide a baseline against which to compare ballistic performance. Further, a fundamental advance was made in the ability of Eulerian wavecodes (hydrocodes) to track accurately history-dependent, i.e., evolutionary, constitutive parameters, e.g., damage. GRA

N91-26535# Massachusetts Inst. of Tech., Cambridge. Artificial Intelligence Lab.
LINE KINEMATICS FOR WHOLE-ARM MANIPULATION Memorandum Report
Brian Eberman and David L. Brock Oct. 1990 16 p
(Contracts N00014-86-K-0685; N00014-85-K-0124)
(AD-A234422; AI-M-1255) Avail: NTIS HC/MF A03 CSCL 12/9

A Whole-Arm Manipulator uses every surface to both sense and interact with the environment. To facilitate the analysis and control of a Whole-Arm Manipulator, line geometry is used to describe the location and trajectory of the links. Applications of line kinematics are discussed and implemented on the MIT Whole-Arm Manipulator (WAM-1). GRA

N91-26536# Department of the Navy, Washington, DC.
MAGNETOSTRICTIVE ANGULAR POSITIONING MOTOR Patent Application
Arthur E. Clark, inventor (to NAVY) and Joseph P. Teter, inventor (to Navy) 11 Oct. 1990 14 p
(AD-D014858; US-Patent-Appl-SN-607345) Avail: NTIS HC/MF A03 CSCL 20/3

This patent application discloses a device in which a plurality of axially elongated drive modules are interconnected at their opposite ends in a polygonal arrangement to angularly spaced locations on an outer annular ring to establish compressive stress. Intermediate portions of the modules are radially spaced form an inner shaft through which a common rotational axis extends. Each module includes at least two magnetostrictive rod elements held in axial alignment at their adjacent ends by a coupling through which the module is radially spaced from the common axis and drive coils electrically energized to generate magnetic fields of opposite polarity causing simultaneous elongation and contraction of the rod elements to apply unidirectional torque to a rotor formed by either the outer ring or the inner shaft. GRA

N91-26537# Department of the Navy, Washington, DC.
VEHICLE STEERING DEVICE Patent Application
Bruce W. Travor, inventor (to Navy) and Roger A. Holler, inventor (to Navy) 3 Aug. 1990 12 p
(AD-D014861; US-Patent-Appl-SN-579921) Avail: NTIS HC/MF A03 CSCL 01/2

This patent application discloses a vehicle steering device that can be joined to any air-dropped, free-falling component and steers

that component directly down to a pre-determined location on the earth's surface. The device is comprised of an aerodynamically-shaped housing that is joined to the front of the component, and which carries orientation means in a nose portion, high-density gravity-reaction means, and steering fins rotatably joined. After the combination is dropped, at a pre-determined altitude and airspeed, the orientation means causes it to assume the most efficient aerodynamic position and then the gravity-reaction means forces the nose, which is joined to and leads the component, to dive into the earth. The reaction means are connected to the fins and force a controlled and predictable descent. GRA

N91-26538# Air Force Systems Command, Wright-Patterson AFB, OH. Foreign Technology Div.
ROBOT: A JOURNAL OF CHINESE SOCIETY OF AUTOMATION
7 Mar. 1991 209 p Transl. into ENGLISH of Jiqiren (Peoples Rep. of China), v. 3, no. 4, 1989 p 1-64
(AD-A234808; FTD-ID(RS)T-0466-90) Avail: NTIS HC/MF A10 CSCL 12/9

Topics addressed include: Hybrid Model Following Adaptive Control of Manipulators with Gravity Compensation; Dynamic Analysis of Robot with Five Degrees of Freedom; An Analysis of the Controllability of an Electrically Driven Robot Arm; and A New Type of Structure of Robot Finger with Synchronous Movement. GRA

N91-26539# Massachusetts Inst. of Tech., Cambridge. Artificial Intelligence Lab.
PASSIVE AND ACTIVE GRASPING WITH A PREHENSILE ROBOT END-EFFECTOR M.S. Thesis
Helen Greiner May 1990 75 p
(Contract N00014-86-K-0685)
(AD-A235085; AI-TR-1235) Avail: NTIS HC/MF A04 CSCL 12/9

This report presents a design of a new type of robot end-effector with inherent mechanical grasping capabilities. Concentrating on designing an end-effector to grasp a simple class of objects, cylindrical, allowed a design only one degree of actuation. The key features of this design are high bandwidth response to forces, passive grasping capabilities, ease of control, and ability to wrap around objects with simple geometries providing form closure. A prototype of this mechanism was built to evaluate these features. GRA

N91-26540# Naval Civil Engineering Lab., Port Hueneme, CA.
ADVANCED MATERIAL HANDLING EQUIPMENT CONTROLS Final Report, Oct. 1988 - Sep. 1990
William V. Miller and J. A. Lusher Jan. 1991 72 p Sponsored by Marine Corps Research, Development, and Acquisition Command
(AD-A235091; NCEL-R-931) Avail: NTIS HC/MF A04 CSCL 15/5

In order to improve the productivity, safety and reliability of Marine Corps Material Handling Equipment (MHE) in a combat environment, this investigation was divided between two specific aspects of MHE operations. The predominant of these is High Speed Control (HSC). This concept involves the coupling of high flow hydraulics with an appropriately synthesized feedback control network in order to achieve system dynamic response two to three times faster than that achieved with conventional control systems, along with rapid convergence (seemingly critical damping following command signal crossover). The second aspect of MHE operations investigated is the enhancement of palletized cargo acquisition from ISO containers using the Marine Corps Extendable Boom Fork-lift (EBFL). Enhancement is by way of providing the EBFL operator with a stereoscopic three-dimensional video image, inside the cab, of the cargo-acquisition area, showing both the cargo pallet slots and the fork lift tines. Subsequently computer control can be integrated with the video image processing so as to facilitate or automate acquisition. GRA

N91-26541# Texas A&M Univ., College Station. Turbomachinery Labs.
ROTORDYNAMIC AND LEAKAGE CHARACTERISTICS OF A 4-STAGE BRUSH SEAL Final Report, Oct. 1988 - Aug. 199U
Kelly J. Conner and Dara W. Childs Dec. 1990 147 p
(Contract F33615-88-C-2908)
(AD-A235336; TL-SEAL-4-90; WL-TR-91-2013) Avail: NTIS HC/MF A07 CSCL 11/1

Experimental results are presented for the direct and cross-coupled stiffness and damping coefficients as well as the leakage performance for a 4-stage brush seal. Variable test parameters include the inlet pressure, pressure ratio, shaft speed, fluid pre-rotation, and seal spacing. Direct damping is shown to increase with running speed; otherwise, the rotordynamic coefficients are relatively insensitive to changes in the test parameters. Cross-coupled stiffness is generally unchanged by increasing the inlet tangential velocity to the seals, suggesting that the brush seal is not effected by inlet swirl. Direct stiffness is shown to increase with frequency; however, the magnitudes of direct stiffness are always positive. Cross-coupled stiffness increases slightly with frequency, yet not as drastically as direct stiffness. Comparisons of test results for the 4-stage brush seal with an 8-cavity labyrinth showed superior rotordynamic performance for the brush seal, viz., larger values for direct stiffness and damping and lower values for the (destabilizing) cross-coupled stiffness coefficient. GRA

N91-26542*# National Aeronautics and Space Administration. Marshall Space Flight Center, Huntsville, AL.
DOUBLE FACE SEALING DEVICE Patent Application
Bruce Weddendorf, inventor (to NASA) 19 Feb. 1991 16 p
(NASA-Case-MFS-28521-1; NAS 1.71:MFS-28521-1; US-Patent-Appl-SN-657586) Avail: NTIS HC/MF A03 CSCL 11A

A double face sealing device is disclosed for mounting between two surfaces to provide an air-tight and fluid-tight seal between a closure member bearing one of the surfaces and a structure or housing bearing the other surface which extends around the opening or hatchway to be closed. The double face sealing device includes a plurality of sections or segments mounted to one of the surfaces, each having a main body portion, a pair of outwardly extending and diverging, cantilever, spring arms, and a pair of inwardly extending and diverging, cantilever, spring arms, an elastomeric cover on the distal, free ends of the outwardly extending and diverging spring arms, and an elastomeric cover on the distal, free, ends of the outwardly extending and diverging spring arms, and an elastomeric cover on the distal, free ends of the inwardly extending and diverging spring arms. The double face sealing device has application or use in all environments requiring a seal, but is particularly useful to seal openings or hatchways between compartments of spacecraft or aircraft. Author

N91-26543*# National Aeronautics and Space Administration. Lewis Research Center, Cleveland, OH.
REMOVABLE HAND HOLD Patent Application
Robert D. Corrigan, inventor (to NASA) and Robert L. Hauer, inventor (to NASA) 15 Apr. 1991 13 p
(NASA-Case-LEW-15196-1; NAS 1.71:LEW-15196-1; US-Patent-Appl-SN-687606) Avail: NTIS HC/MF A03 CSCL 13K

A hand hold utilizes joining means which comprises two different mounting brackets that are permanently fastened to a supporting structure. An alignment/capture bracket is disposed at one end of the hand rail or hand hold which mates with one of the mounting brackets. A securing bracket is disposed at the opposite end of the hand rail/hand hold which connects with the other mounting bracket by means of a locking device. The alignment/capture bracket has a central tapered tongue with two matching slots disposed on each side. NASA

N91-26544*# Washington Univ., Richland. Tri-Cities Univ. Center.
INVESTIGATION OF AXIAL POSITIONING FOR FLEXURAL COMPRESSORS Final Technical Report, 1 Dec. 1988 - 31 Jul. 1990
Peter Riggle 10 Jul. 1991 33 p
(Grant NAG5-1038)
(NASA-CR-185711; NAS 1.26:185711) Avail: NTIS HC/MF A03 CSCL 13I

The testing of the research compressor is presented. The research compressor was assembled and disassembled in order to show the consistency in which the piston and rod could be aligned with a .0004 inch radial gap around the piston. A full set of tests was completed for the first assembly, which is referred to as assembly no. 1. The compressor was disassembled and assembled a second time (assembly no. 2). Assembly no. 2 was only tested statically due to the time constraint. Results are discussed. B.G.

N91-27106*# Houston Univ., TX. Dept. of Applied Math. Sciences.
FUZZY LOGIC CONTROL SYSTEM TO PROVIDE AUTONOMOUS COLLISION AVOIDANCE FOR MARS ROVER VEHICLE Final Report
Michael G. Murphy *In its* NASA/ASEE Summer Faculty Fellowship Program, 1990, Volume 2 Dec. 1990 13 p (For primary document see N91-27103 18-99)
(Grant NGT-44-005-803)
Avail: NTIS HC/MF A09 CSCL 13F

38 QUALITY ASSURANCE AND RELIABILITY

Includes product sampling procedures and techniques; and quality control.

N91-26545# Defense Logistics Agency, Alexandria, VA.
QUALITY EFFECTIVENESS SENSING TECHNIQUE RELEASE 3.0 Final Report
Paul E. Grover Mar. 1991 68 p
(AD-A233651; DLA-91-P90272) Avail: NTIS HC/MF A04 CSCL 05/1

This report documents the logic, structure, and code for QUEST Release 3.1. QUEST Release 3.0 measures the effectiveness of the contractor's QA operations by comparing the contractor's key indicators with those of similar contractors (or peers). Based on those peer comparisons and trends, an effectiveness score for each indicator is computed and weighted average of all indicators produces a bottom line effectiveness rating. Release 3.0 was validated by incorporating the profound knowledge of experts in the weighting factors and program logic. A study advisory group, consisting of field and Headquarters DLA QA personnel guided the effort. A statistical test was passed which compared QUEST Release 3.0 results with expert opinion on certain contractors. Because of the track record of earlier releases, the use of knowledgeable experts in the development process, and the results of validity tests, it is concluded the QUEST 3.0 is implementable, valid, and meets the objective of measuring contractor QA effectiveness. It is recommended that Release 3.0 be implemented throughout the Defense Contract Management Command (DCMC). GRA

N91-26546# Florida State Univ., Tallahassee.
STATISTICAL ASPECTS OF RELIABILITY, MAINTAINABILITY, AND AVAILABILITY Final Summary Report, 1 Oct. - 31 Dec. 1990
Hani Doss, Frank Proschan, and Myles Hollander Feb. 1991 10 p
(Grant AF-AFOSR-0040-88; AF Proj. 2304)
(AD-A234546; AFOSR-91-0276TR) Avail: NTIS HC/MF A02 CSCL 12/3

The research performed under this grant developed theory, concepts, and methods in reliability, availability, and maintainability, applicable or potentially applicable to the programs of the U.S. Air Force in particular and the Department of Defense in general. In addition, because of the general nature of the mathematical and statistical approaches used, the results obtained are of value in a variety of other applied and theoretical areas of statistics and probability used by the USAF. GRA

N91-26547# Connecticut Univ., Storrs. Dept. of Statistics.
FIXED SAMPLE AND SEQUENTIAL PROBLEMS WITH APPLICATIONS IN RELIABILITY Final Report, 1 Jan. 1989 - 31 Dec. 1990
Dipak K. Dey and Nitis Mukhopadhyay 31 Dec. 1990 16 p
(Grant AF-AFOSR-0225-89; AF Proj. 2304)
(AD-A234547; AFOSR-91-0275TR) Avail: NTIS HC/MF A03 CSCL 12/3

The principal focus of this grant period had been on fixed-sample problems for the estimation of parameters and reliability functions from different parametric families of distributions. Professor Dey and his Ph.D. student (Ms. Pei-San Liu) first considered the estimation problems from generalized life distributions. They considered a decision theoretic route to obtain improved estimators of parameters and parametric functions. Professor Dey also considered the estimation of parameters from mixture distributions. Next, Professor Dey and his colleagues considered some related problems one for the estimation of the Poisson parameter under an asymmetric loss and the other is the determination of the class of minimax estimators of the scale parameter of the uniform distribution. Both these problems also have important applications in reliability. Professor Dey and his student (Mr. Y. Chung) then considered the estimation problems from the mixture of discrete exponential distributions. Through a mixing process, several complicated discrete multivariate distributions were created which included compound Poisson and negative binomial distributions. Improved estimators were then obtained under several plausible loss functions. In a related problem (in the mixture distribution scenario) Professor Dey and his colleagues considered the problem of estimation of parameters and reliability from a multivariate survival distribution generated by Weilbull-Inverse Gaussian mixture. GRA

N91-26548# Boeing Aerospace and Electronics Co., Seattle, WA.
X RAY TOMOGRAPHIC INSPECTION OF PRINTED WIRING ASSEMBLIES AND ELECTRICAL COMPONENTS Interim Report, Jul. 1989 - Jun. 1990
Richard H. Bossi and Robert J. Kruse 31 Oct. 1990 86 p
(Contract F33615-88-C-5404)
(AD-A234748; WRDC-TR-90-4091) Avail: NTIS HC/MF A05 CSCL 14/2

The visibility of X-ray tomography techniques for printed wiring assembly (PWA) solder bond evaluation and several categories of electronic components has been studied. The effort was performed as a final testing task assignment in the Advanced Development of X-Ray Computed Tomography Application program. The primary area for testing was surface mount technology solder bonds. During the course of the task assignment several other categories of electronic devices were examined including transformers, connectors, and an optical transducer. Five different X-ray systems for computed tomography (CT), laminography and radioscopy were used. The results of this final task assignment indicate that X-ray tomographic techniques can be useful for solder bond evaluation, and innerlayer trace analysis for PWA's and as a failure analysis tool for a broad range of electrical and electronic components. Investment in PWA solder bond evaluation systems using X-rays commonly show a short term (less than 1 year) payback. The particular system to be used and the economic payback rate depends on the assembly design and manufacturing throughput. Radioscopy (real-time radiography) and scanned beam laminography are the primary techniques recommended for solder bond evaluation. Printed wiring board innerlayer copper traces were imaged with laminographic inspection using industrial CT systems. GRA

N91-26549# WEA, Cambridge, MA.
NDE PATTERN RECOGNITION OF LSS STATES VIA WAVE PROPAGATION Final Report, 15 Jan. 1988 - 15 Jan. 1991
James H. Williams, Jr. 15 Jan. 1991 28 p
(Contract F49620-88-C-0036)
(AD-A234772; AFOSR-91-0230TR) Avail: NTIS HC/MF A03 CSCL 22/2

Nondestructive characterizations of structural states and structural parameters of large space structures (LSS) (i.e., space stations and space platforms) via wave propagation are considered. If a wave is introduced into or is generated within a structure, the existing structural states and parameters govern its propagation and detection. The structural states and parameters of LSS can be described by material properties, geometric forms and properties, environmental conditions and measurement conditions. Some of these structural properties and conditions are modulus of elasticity, structural dimensions, joint details, lattice patterns of structural components, lattice element connectivities, structural discontinuities and material defects states. There are many wave propagation parameters that can be measured by monitoring waves. A few of these are the initial wave arrival time, maximum wave amplitude, wave duration, and wave amplitude at specified frequencies evaluated using the Fourier transform. Thus, a large amount of data can be generated from a single wave propagation measurement. GRA

N91-26550# Douglas Aircraft Co., Inc., Long Beach, CA.
NONDESTRUCTIVE EVALUATION (NDE) OF FIBERGLASS MARINE STRUCTURES STATE-OF-THE ART REVIEW Final Report
Yoseph Bar-Cohen Nov. 1990 108 p
(Contract DTCG39-89-R-80812)
(AD-A234785; USCG-D-02-91) Avail: NTIS HC/MF A06 CSCL 13/10

This report reviews the methods of nondestructive evaluation (NDE) of glass-reinforced plastics as applicable to common marine sandwich construction. Forty panels of various cored and solid construction were built with implanted defects, such as dry fibers, uncured resin, air gaps, delaminations, cracks and impact damage. The panels were then subjected to a variety of testing techniques such as ultrasonics, tapping, thermography, radiography and visual inspection. Some of the results are highly varied, pointing out the difficulty of locating certain defects and the comparative ease of finding others. GRA

N91-26551# Vanderbilt Univ., Nashville, TN.
RESEARCH ON INTELLIGENT FAULT DETECTION AND REPAIR ADVISORY SYSTEMS Final Technical Report, 1 Feb. 1987 - 31 Oct. 1990
G. Collins, John Bourne, and A. J. Brodersen Oct. 1990 13 p
(Grant AF-AFOSR-0144-87; AF Proj. 2304)
(AD-A235267; AFOSR-91-0499TR) Avail: NTIS HC/MF A03 CSCL 12/9

During the grant extension period, all of the original objectives of the proposed research were met (where objective number 3 was modified early in the original grant period in involve the study of models of diagnostic belief rather than models based upon constraint propagation). The Adaptive Heuristic Reasoner system provides a consistent knowledge representation paradigm based upon flexible associative network constructions which maximize the use of domain specific terminology (objective one). All internal knowledge is consistently represented in belief function form (objective four), a form which supersedes rules in expressiveness yet which externally retains the flavor of if-then constructs. GRA

N91-26552# Michigan Univ., Ann Arbor. Dept. of Materials Science and Engineering.
NON-DESTRUCTIVE EVALUATION OF RESIDUAL STRESSES IN THIN FILMS VIA X RAY DIFFRACTION TOPOGRAPHY METHODS Final Report, Sep. 1987 - Nov. 1989
John C. Bilello 1 Mar. 1991 33 p
(Contract DAAL03-87-K-0049)
(AD-A235328; ARO-25077.6-MS) Avail: NTIS HC/MF A03 CSCL 04/2

Quantitative x ray diffraction topography techniques have been used to measure the residual strain magnitude and uniformity of deposition for Mo and W sputtered films on Si(100) substrates. High sensitivity rocking curve measurements were able to determine differential strains for films as thin as 2.5 nm; while Bragg angle contour mapping had similar sensitivity and was also able to assess coating uniformity and stress distribution over areas covering a whole wafer. Measurements of strain versus film thickness over a range of 2.5 to 80 nm showed that a critical thickness exists for maximum residual strain. Growth beyond this range produces stress relaxation. This non-destructive type of analysis could be employed on a wide range of film-substrate combinations. GRA

N91-26553 Tel-Aviv Univ. (Israel). Dept. of Statistics.
QUALITY BY DESIGN USING STATISTICALLY PLANNED EXPERIMENTS M.S. Thesis
Dizza Bursztyn May 1989 74 p In HEBREW; ENGLISH summary
(ITN-91-85119) Copyright Avail: Tel-Aviv Univ., Exact Sciences Library, Ramat Aviv 69978, Israel

A new method for analyzing parameter design experiments is proposed, and compared with Taguchi's Parameter Design method as a means to design experiments to analyze the effects of design factors on product quality. Taguchi suggested dividing design factors into specifiable Control Factors and unspecifiable Noise Factors. Taguchi's analysis is based on a variability measure, designated Signal to Noise Ratio. A suggested alternative method for analyzing parameter design experiments involves seeking an appropriate data transformation. A parameter design experiment is then considered as a large factorial experiment in which some of the factors are control factors and some noise factors. It is suggested that the experiment be analyzed as a simple factorial experiment, estimating main effects and interactions. If a noise factor has a large effect, through the interactions between control and noise factors, settings of the control factors are sought, for which the effect of the noise factor is close to zero. Taguchi's design ensures that all the interactions between control and noise factors are estimable. Examples are presented to compare Taguchi's method with factorial analysis. Taguchi's method is shown to be inefficient in many cases; a data analysis using this method can lead to wrong conclusions. Models are developed to analyze experiments which were planned according to Taguchi's suggestions, and an alternative planning method is suggested for the case where there may be squared effects. ISA

N91-26554# Los Alamos National Lab., NM.
X RAY-COMPUTED TOMOGRAPHY FOR INSPECTING INDUSTRIAL PARTS
D. A. Viskoe, D. M. Stupin, K. R. Greichen, and J. P. Ortega 1991 6 p Presented at the 2nd American Society for Nondestructive Testing (ASNT) on Industrial Computed Tomography Conference, San Diego, 20-24 May 1991
(Contract W-7405-eng-36)
(DE91-011390; LA-UR-91-1196; CONF-9105166-1) Avail: NTIS HC/MF A02

We are building a tomographic x-ray scanner to inspect cast explosives and industrial parts and to study new materials. We will use the scanner to examine parts up to 38 cm, in height, 25 cm in diameter, and 25 kg in weight. We tested our reconstruction program by comparing the results of a computer experiment with the input data. The program can complete a 128-by-128 pixel reconstruction in about 10 minutes. The tomographic x-ray scanner rotates and translates the sample through a second-generation scan. We use a 32-detector array with a 16-bit analog-to-digital converter purchased from Bio-Imaging Research. The detector and source are mounted on optical tables; one is a base for the entire assembly, and the other supports the detector array. We use an x-ray source from IRT Corporation with an output of 2 mA at 320 kV. The source spot size is 0.8 mm and the output is stable to +/- 1 percent over 5 hours. DOE

N91-26555# Pacific Northwest Lab., Richland, WA.
QUALITY ASSURANCE MANUAL
R. L. Shaub and D. E. Ryder Apr. 1991 72 p
(Contract DE-AC06-76RL-01830)
(DE91-012618; PNL-MA-70) Avail: NTIS HC/MF A04

In order to provide clients with quality products and services, Pacific Northwest Laboratory (PNL) has established and implemented a formal quality assurance program. These management controls are documented in this manual (PNL-MA-70) and its accompanying standards and procedures. The QA Program meets the basic requirements and supplements of ANSI/ASME NQA-1-1986 Edition, Quality Assurance Program Requirements for Nuclear Facilities, except as noted in specific sections of this manual. This manual provides topical requirements and an overview of the administrative procedures that apply to Impact Level 1 and 2 projects and activities. DOE

N91-27090*# Houston Univ., TX. Dept. of Applied Mathematical Sciences.
COMPOUND ESTIMATION PROCEDURES IN RELIABILITY Final Report
Ron Barnes *In its* NASA/ASEE Summer Faculty Fellowship Program, 1990, Volume 1 Dec. 1990 16 p (For primary document see N91-27088 18-99)
(Grant NGT-44-005-803)
Avail: NTIS HC/MF A10 CSCL 14D

N91-27107*# Virginia Commonwealth Univ., Richmond. Dept. of Mathematical Sciences.
EVALUATING THE EFFECT OF ACCURACY RATIOS ON THE PERCENT OF CALIBRATIONS WHICH ARE OUT OF TOLERANCE Final Report
Sharon E. Navard *In* Houston Univ., NASA/ASEE Summer Faculty Fellowship Program, 1990, Volume 2 Dec. 1990 15 p (For primary document see N91-27103 18-99)
(Grant NGT-44-005-803)
Avail: NTIS HC/MF A09 CSCL 14D

39 STRUCTURAL MECHANICS

Includes structural element design and weight analysis; fatigue; and thermal stress.

For applications see *05 Aircraft Design, Testing and Performance* and *18 Spacecraft Design, Testing and Performance.*

N91-26556# Overseas Relations Branch Translation Service, London (England).
INVESTIGATIONS INTO FRACTURE MECHANICS FAILURE CONCEPTS WITH THERMOMECHANICALLY ROLLED STEELS
K. E. Hagedorn and M. Eckel 1991 28 p Transl. into ENGLISH from German document, May 1991 27 p Presented at the 16th MPA Seminar, 4-5 Oct. 1990
(BLL-OA-Trans-4238-(6196.3)) Avail: NTIS HC/MF A03

The suitability of modern fracture mechanics failure concepts to ensure the safety of components made of thermomechanically rolled steels was investigated. The new versions of the PD 6493 method based on crack tip opening CTOD and the R6 method were of particular interest. The investigations also dealt with the problem of extremely brittle areas in the heat-affected zone (HAZ) of submerged arc welded joints of TM steels. Special attention was paid to instrumented notched-bar impact bending tests and metallographic investigations on fracture mechanics test specimens with notch position in the HAZ during determination of parameters. The bearing load behavior of medium-sized tensile plates with inner and double outer notches up to 4 MN maximum load was evaluated by the failure concepts in order to obtain information on the suitability of the concepts by comparison with the test results. Author

N91-26557# Overseas Relations Branch Translation Service, London (England).
LOAD-BEARING CAPACITY OF LARGE PIPES WITH CIRCUMFERENTIAL DEFECTS UNDER TENSILE STRESS: COMPARISON OF EXPERIMENTS WITH CALCULATED ESTIMATES
W. Stadtmueller, U. Eisele, P. Julisch, and D. Sturm 1991 34 p Transl. into ENGLISH from German document, May 1991 33 p Presented at the 16th MPA Seminar, 4-5 Oct. 1990
(BLL-OA-Trans-4233-(6196.3)) Avail: NTIS HC/MF A03

The common aim of many research projects concerning reactor safety in Germany is to prove that the integrity of components important for safety remains ensured even under the most unfavorable operating and accident conditions. Both component tests and calculations are performed for this purpose. Within the framework of a research project which investigated the behavior of pipes particularly from the point of view of dynamic stresses, pipe sections were tested quasistatically in the tensile test. To simulate crack formations as ascertained during overhauls of pipelines, the pipe sections were provided with partial circumferential defects of various depths, but uniform length. Several engineering calculation methods, which in contrast to calculations by the finite element method can be applied relatively easily, are known from the literature for pipes with circumferential defects under tensile stresses. With the aid of the results of the quasistatic tests with pipes the most commonly used approximation methods for calculation of the maximum force and, insofar as possible, also the force in the case of crack initiation, will be checked to determine their informativeness. Author

N91-26558# Virginia Polytechnic Inst., Blacksburg.
NONLINEAR OSCILLATIONS OF MECHANICAL SYSTEMS UNDER MULTIFREQUENCY PARAMETRIC EXCITATION Final Report
Raymond H. Plaut and Dean T. Mook 15 Feb. 1991 5 p
(AD-A233800; ARO-24720.24-EG) Avail: NTIS HC/MF A01 CSCL 20/11

Various problems related to the nonlinear oscillations of mechanical and structural systems were investigated. They involved the following topics: (1) Resonances in weakly nonlinear systems subjected to multifrequency parametric and/or external excitation, with one case being a self-excited system; (2) Dynamic behavior of cracked bars and rotating shafts, for the purpose of detecting cracks; (3) Vibrations of cylindrical membranes, with applications to inflatable dams; (4) Vibrations and stability of structures whose support resistance changes as the structure is loaded: (5) Dynamic instability of laminated composite plates under in-plane harmonically-varying loads; (6) Application of vibration data to nondestructively predict buckling loads; (7) Nonlinear oscillations of slender cantilevered beams under harmonically-varying loads; and (8) Prediction of a large jump in deflection, such as snap-through instability, under harmonically-varying loads. The results improve our understanding of the dynamics of mechanical and structural systems, and will be useful in the prevention of excessively large motions and unstable behavior. GRA

N91-26559# Virginia Polytechnic Inst. and State Univ., Blacksburg. Dept. of Engineering Science and Mechanics.
THE DEVELOPMENT OF PIEZOELECTRIC POLY(VINYLIDENE FLUORIDE) SENSORS FOR MEASURING PEEL STRESSES IN ADHESIVE JOINTS Final Report, 1 Aug. 1986 - 31 Dec. 1990
G. L. Anderson and D. A. Dillard 28 Feb. 1991 8 p
(Contract DAAL03-86-G-0041)
(AD-A233880; ARO-23759.3-EG-F) Avail: NTIS HC/MF A02 CSCL 17/8

Multi-point sensors for measuring peel stresses within adhesively bonded joints were developed using poly(vinylidene fluoride) films. Plasma and acid etch methods were explored and compared for improving bond strength for these in-situ sensors. Experimental evaluation of several joint geometries revealed good correlation between measured and analytically predicted peel stresses. The method holds considerable promise for laboratory

evaluation of the peel stress state in bonded joints and structures. GRA

N91-26560# Lawrence Livermore National Lab., CA.
VISCOELASTIC BEHAVIOR OF ELASTOMERIC MEMBRANES Final Report, Sep. 1988 - Aug. 1990
William W. Feng Mar. 1991 32 p
(Contract W-7405-eng-48; DA Proj. 1L1-62618-AH-80)
(AD-A234496; BRL-CR-656) Avail: NTIS HC/MF A03 CSCL 11/1

The formulation for large deformations of an axisymmetric nonlinear plane viscoelastic membrane is developed. The solutions from the formulation for both creep and relaxation of a circular membrane are presented. An experiment that demonstrates the relaxation phenomenon was performed, and the experimental data are used to determine the constitutive equation of an elastomer. GRA

N91-26561# Pennsylvania State Univ., University Park. Applied Research Lab.
THE WAVENUMBER-FREQUENCY FILTERING CHARACTERISTICS OF COMPLIANT LAYERS
J. E. Phillips, C. B. Burroughs, and W. J. Hughes Apr. 1991 131 p
(Contract N00039-88-C-0051)
(AD-A234768; PSU/ARL-TR-91-004) Avail: NTIS HC/MF A07 CSCL 13/7

Techniques for the measurement of the wavenumber-frequency filtering characteristics of compliant layers mounted on an elastic structure and subject to unsteady pressures are developed and demonstrated. In order to measure the performance of the layer at arbitrary wavenumbers and frequencies, an array of shakers was fabricated and used to generate a standing wavepattern of force where the maximum spectrum levels of the input forces could be concentrated at selected wavenumbers independent of the selected frequency. Arrays of thin film transducers were designed, fabricated, and used to measure the wavenumber-frequency pressure spectra above and below compliant layers. The wave-number frequency admittances of a coated and uncoated beam were used to determine the effectiveness of compliant layers in reducing the vibration response of the beam as a function of wavenumber and frequency. The development of the shakers, transducers, and data processing algorithms is described. Measurement results of the effectiveness and pressure transmission loss are presented as functions of frequency at different drive wavenumbers for several compliant layers with different properties. The pressure spectra above and below the layers, velocity spectra of the beam response, and admittances of the coated and uncoated beam are presented and analyzed as functions of wavenumber and frequency. GRA

N91-26562# Air Force Inst. of Tech., Wright-Patterson AFB, OH. Foreign Technology Div.
METHODS FOR DETERMINING CRACK DEPTH
Qianyuan He 21 Mar. 1991 15 p Transl. into ENGLISH from Wusun Jiance (China), v. 12, no. 4, 1990 p 96-99
(AD-A234799; FTD-ID(RS)T-1062-90) Avail: NTIS HC/MF A03 CSCL 20/11

With the growing progress and applications of fracture mechanics, determination of the actual depth of a crack in a workpiece is required. Some methods for determining crack depths with ultrasonics are presented and include: (1) determination of crack depth with surface waves; (2) measurement of crack depth with slant probe; (3) crack depth measurements with creep wave probe; (4) measurement of crack depth and height by using tip echo wave method; and (4) determination of crack height by using sound shadow method. GRA

N91-26563# Illinois Inst. of Tech., Chicago. Dept. of Civil Engineering.
THE HYSTERESIS AND INCREMENTAL COLLAPSE OF COMPLEX STRUCTURES: A PARADIGM FOR THE FATIGUE FAILURE OF MATERIALS Final Report, 1 Jan. 1988 - 31 Dec. 1990
S. A. Guralnick and T. Erber Mar. 1991 53 p
(Grant AF-AFOSR-0171-89; AF Proj. 2302)
(AD-A234831; AFOSR-91-0379TR) Avail: NTIS HC/MF A04 CSCL 13/13

The basic objective of this research program is to characterize the development of material fatigue by means of stress-strain hysteresis and acoustic emission measurements. We have conjectured that the accumulation and organization of damage in material fatigue is similar to the progressive failure of structures under cyclic loading, and, specifically, that the endurance limit of a material in fatigue is the analogue of the incremental collapse load of a structure. Since the principal features of the service life and failure of structures can be completely described by hysteresis methods, it is plausible that similar means can be used to characterize the inception and organization of microplastic processes in materials. All of the experimental results obtained during the current research program confirm these conjectures. GRA

N91-26564# California Univ., Berkeley. Dept. of Mechanical Engineering.
DYNAMIC ENERGY ABSORPTION OF SANDWICH STRUCTURES BY INELASTIC DEFORMATION Final Report, 1 Sep. 1988 - 31 Dec. 1990
Werner Goldsmith and Jerome L. Sackman 15 Feb. 1991 101 p
(Contract F49620-88-C-0131)
(AD-A234903; AFOSR-91-0233TR) Avail: NTIS HC/MF A06 CSCL 13/13

An investigation concerned with Inelastic Deformation of sandwich plates and shells under dynamic loading consisted of an experimental and an analytical study of the energy absorption capability of honeycomb and honeycomb sandwich structures. Laboratory tests of both types of samples were performed using both static loads and dynamic loads. The targets were attached to a ballistic pendulum arrangement either by a rigid backing or else by means of a simple support. Force-deformation curves were obtained by means of displacement and acceleration transducers. An analysis based on perfectly plastic behavior of the sandwich was obtained that permitted partial integration and hence minimized the computational procedure for the case of the backed sandwich; this was found to be in very good agreement with test results. Aluminum and Nomex honeycombs were employed as cores, while mostly aluminum face plates were employed, although polycarbonate, ABS and fiberglass materials were also investigated. GRA

N91-26565# Puerto Rico Univ., Mayaguez. Dept. of General Engineering.
FATIGUE CRACK TIP PLASTIC STRAIN RANGE MEASUREMENT STUDIES IN TWO TITANIUM ALLOYS Final Report, 1 Jun. 1989 - 31 May 1990
Pranab K. Mazumdar Jan. 1991 47 p
(Contract F49620-89-C-0064)
(AD-A234973; AFOSR-91-0234TR) Avail: NTIS HC/MF A03 CSCL 11/6

This program started with objectives to: (1) improve existing laboratory facilities to enhance research capabilities; (2) create interest of science and engineering among undergraduate students; and (3) conduct analytical and experimental works on localized deformation in fatigue. Although frequent breakdown and malfunction of our servohydraulic testing machine has halted our progress in experimentations with titanium alloys, we have been able to do quite well in improving the laboratory facilities. To avoid such unfortunate situations in the future, measures are now being taken to further improve our current facilities. Emphasis is placed

on the analytical efforts which have yielded two technical papers. GRA

N91-26566# Northwestern Univ., Evanston, IL. Dept. of Materials Science.
NATO ADVANCED RESEARCH WORKSHOP ON MEASUREMENT OF RESIDUAL AND APPLIED STRESS USING NEUTRON DIFFRACTION
R. A. Winholtz Apr. 1991 19 p Workshop held in Oxford, England, 18-22 Mar. 1991
(Contract N00014-80-C-1116)
(AD-A235103; TR-30) Avail: NTIS HC/MF A03 CSCL 20/11

In two phase or composite materials it is possible to determine both the macrostresses in the material and the average microstresses present in each phase. The stress equilibrium relations allowing this separation are outlined. It is shown that errors in the unstressed lattice parameter lead to errors in only the hydrostatic component of the stress tensor. It is thus possible to accurately determine the entire deviatoric macrostress and microstress tensors without the unstressed lattice parameters of the individual phases. Two examples of the usefulness of macrostress and microstress measurements are given. In a SiC-TiB2 microcracking ceramic composite large hydrostatic microstresses develop during consolidation due to differential thermal contraction. Microcracks form during stressing, relaxing the thermal microstresses. Measurements of this relaxation have helped quantify the toughening in this system associated with microcracking. Measurements in both the ferrite and cementite phases of 1080 steel during low cycle fatigue show the proportion of the applied load carried by each phase. These results show that as the material yields in both tension and compression, the carbides take a higher fraction of the load and thus the stress range experienced by the carbide phase is much higher. GRA

N91-26567# Texas A&M Univ., College Station. Research Foundation.
STABILIZATION AND CONTROL PROBLEMS IN STRUCTURAL DYNAMICS Final Report, Sep. 1988 - Dec. 1990
G. Chen and J. Zhou 26 Feb. 1991 9 p
(Grant AF-AFOSR-0334-87; AF Proj. 2304)
(AD-A235189; AFOSR-91-0264TR) Avail: NTIS HC/MF A02 CSCL 12/1

Drs. G. Chen and J. Zhou investigated various problems in the analysis, control, optimization and computation of structural mechanical systems and distributed parameter systems in general. In particular, they developed the wave method and boundary element methods and used functional analysis to study partial differential equation models of plates, solids and fluids, and other abstract mathematical systems. GRA

N91-26568# David Taylor Research Center, Bethesda, MD. Ship Materials Engineering Dept.
THE RELATIONSHIP OF TRADITIONAL DAMPING MEASURES FOR MATERIALS WITH HIGH DAMPING CAPACITY Research and Development Report, Jan. 1990 - Jan. 1991
E. J. Graesser and C. R. Wong Jan. 1991 46 p
(AD-A235347; DTRC/SME-91/05) Avail: NTIS HC/MF A03 CSCL 20/11

Simply stated, damping is the dissipation of energy in vibrating systems which results in either the control of the amplitude of oscillations or their eventual decay. In mechanical systems damping can be classified as passive or active. Active damping uses externally applied feedback control forces to limit the deformation and motion of large structural configurations. Passive damping makes use of properties which are inherent to the system and which arise from energy dissipation taking place within stressed elements of a vibrating system or from energy being imparted to a surrounding dissipative medium. The passive damping which is of interest in this discussion involves mechanically stressed materials or structural elements and the energy dissipation associated with cyclic strain or stress. GRA

N91-26569*# National Aeronautics and Space Administration. Langley Research Center, Hampton, VA.
EFFECT OF INITIAL DELAMINATION ON MODE 1 AND MODE 2 INTERLAMINAR FRACTURE TOUGHNESS AND FATIGUE FRACTURE THRESHOLD
Gretchen Bostaph Murri and Roderick H. Martin (Analytical Services and Materials, Inc., Hampton, VA.) May 1991 40 p Prepared in cooperation with Army Aviation Systems Command, Hampton, VA
(NASA-TM-104079; NAS 1.15:104079; AVSCOM-TR-91-B-005) Avail: NTIS HC/MF A03 CSCL 20K

Static and fatigue double-cantilever beam (DCB) and end-notch flexure (ENF) tests were conducted to determine the effect of the simulated initial delamination in interlaminar fracture toughness, G(sub c), and fatigue fracture threshold, G(sub th). Unidirectional, 24-ply specimens of S2/SP250 glass/epoxy were tested using Kapton inserts of four different thickness - 13, 25, 75, and 130 microns, at the midplane at one end, or with tension or shear precracks, to simulate an initial delamination. To determine G(sub c), the fatigue fracture threshold below which no delamination growth would occur in less than 1 x 10(exp 6) cycles, fatigue tests were conducted by cyclically loading specimens until delamination growth was detected. Consistent values of model 1 fracture toughness, G(sub Ic), were measured from DCB specimens with inserts of thickness 75 microns or thinner, or with shear precracks. The fatigue DCB tests gave similar values of G(sub Ith) for the 13, 25, and 75 microns specimens. Results for the shear precracked specimens were significantly lower that for specimens without precracks. Results for both the static and fatigue ENF tests showed that measured G(IIc) and G(IIth) values decreased with decreasing insert thickness, so that no limiting thickness could be determined. Results for specimens with inserts of 75 microns or thicker were significantly higher than the results for precracked specimens or specimens with 13 or 25 microns inserts. Author

N91-26570# Sandia National Labs., Albuquerque, NM.
RESIDUAL STRESSES IN METAL/CERAMIC BRAZES: EFFECT OF CREEP ON FINITE ELEMENT ANALYSIS RESULTS
J. J. Stephens, S. N. Burchett, and F. M. Hosking 1990 38 p Presented at the Fall Meeting of the Minerals, Metals and Materials Society (TMS) on Physical Metallurgy and Materials in Conjunction with Materials Week and the Material Applications and Services Exposition, Detroit, 7-11 Oct. 1990
(Contract DE-AC04-76DP-00789)
(DE91-011233; SAND-90-0973C; CONF-901008-11) Avail: NTIS HC/MF A03

Creep-induced stress relaxation of a braze alloy can be an important factor in successful processing of certain metal/ceramic braze joint geometries where there is a mismatch in thermal expansion. The inclusion of a creep constitutive law in finite element analysis (FEA) codes makes it possible to calculate the effect of a particular cooling rate from the braze temperature on residual stresses in the ceramic. Valid calculations require a constitutive law for creep of the brazement which accurately predicts the minimum strain rate over a wide range of temperatures. Using data from previous investigations on the creep of recrystallized Cu, we have developed minimum strain rate creep correlations at both high and intermediate temperatures for pure Cu. At the higher temperatures, a power law is used, with the activation energy obtained by regression analysis quite close to the value of lattice self diffusion in Cu. At intermediate temperatures (350 to 600 C), we have found that the Garofalo sinh equation obtains the best fit to the data, with an activation energy approximately equal to 2/3 of the activation energy for lattice diffusion, attributable to dislocation core diffusion. Results for FEA calculations of the residual stresses obtained in Cu brazing of a metallic feedthrough pin to a metallized alumina ceramic are presented using both time-independent and creep constitutive laws for pure Cu. At higher temperatures, the creep law predicts lower residual stresses in the alumina compared to the elastic/plastic constitutive law. However, at lower temperatures, the results obtained with the elastic/plastic constitutive law indicate lower stress levels in the

ceramic compared to the predictions obtained with the various creep constitutive relations. The lower temperature results are discussed in the context of primary creep behavior. DOE

N91-26571# California Univ., Berkeley. Lawrence Berkeley Lab.
SHELL HOOP PRESTRESS GENERATED BY WELDING
R. B. Meuser Mar. 1991 8 p Presented at the 3rd Annual International Industrial Symposium on the Super Collider (IISSC), Atlanta, 13-15 Mar. 1991
(Contract DE-AC03-76SF-00098)
(DE91-011892; LBL-29702; CONF-910340-8) Avail: NTIS HC/MF A02

For some magnet designs it is desirable to generate a prestress, approaching the yield strength, in the shell surrounding the yoke. If that prestress can be generated by weld shrinkage, then more expensive methods of prestressing can be avoided. Shell-to-yoke friction can reduce the prestress, so it is desirable to minimize it. A quick-and-dirty test was performed to address these matters. While the scatter of the data was large, it appears that weld shrinkage can indeed generate the required prestress. The scatter was too large to give any information about the friction, however. The experiment raised more questions than it answered. DOE

N91-26572# Oak Ridge National Lab., TN.
PRELIMINARY TEST RESULTS FROM THE HSST SHALLOW-CRACK FRACTURE TOUGHNESS PROGRAM
T. J. Theiss, G. C. Robinson, and S. T. Rolfe (Kansas Univ., Lawrence.) 1991 14 p Presented at the American Society of Mechanical Engineers (ASME) Pressure Vessels and Piping Conference, San Diego, 23-27 Jun. 1991
(Contract DE-AC05-84OR-21400)
(DE91-010147; CONF-910602-22) Avail: NTIS HC/MF A03

The Heavy Section Steel Technology (HSST) Program under sponsorship of the Nuclear Regulatory Commission (NRC) is investigating the influence of crack depth on the fracture toughness of reactor pressure vessel steel. The ultimate goal is the generation of a limited data base of elastoplastic fracture toughness values appropriate for shallow flaws in a reactor pressure vessel and the application of this data to reactor vessel life assessments. It was shown that shallow flaws play a dominant role in the probabilistic fracture mechanics analysis of reactor pressure vessels during a pressurized thermal shock event. In addition, recent research has shown that the crack initiation toughness measured using specimens with shallow flaws is greater that the toughness determined with conventional, deeply notched specimens at temperatures within the transition region for non-nuclear steels. The influence of crack depth on the elastoplastic fracture toughness for prototypic reactor material is being investigated. Preliminary results indicate a significant increase in the toughness associated with shallow flaws which has the potential to significantly impact the conditional probability of vessel failure. DOE

N91-27111*# California Univ., San Diego, La Jolla. Dept. of AMES.
DEVELOPMENT OF LOAD-DEPENDENT RITZ VECTOR METHOD FOR STRUCTURAL DYNAMIC ANALYSIS OF LARGE SPACE STRUCTURES Final Report
James M. Ricles *In* Houston Univ., NASA/ASEE Summer Faculty Fellowship Program, 1990, Volume 2 Dec. 1990 16 p (For primary document see N91-27103 18-99)
(Grant NGT-44-005-803)
Avail: NTIS HC/MF A09 CSCL 20K

N91-27117*# Coast Guard Academy, New London, CT. Dept. of Engineering.
STRUCTURAL CONCEPT STUDIES FOR A HORIZONTAL CYLINDRICAL LUNAR HABITAT AND A LUNAR GUYED TOWER Final Report
Paul K. Yin *In* Houston Univ., NASA/ASEE Summer Faculty Fellowship Program, 1990, Volume 2 Dec. 1990 15 p (For primary document see N91-27103 18-99)
(Grant NGT-44-005-803)
Avail: NTIS HC/MF A09 CSCL 20K

42 GEOSCIENCES (GENERAL)

N91-26573*# National Aeronautics and Space Administration. Goddard Space Flight Center, Greenbelt, MD.
WEST ANTARCTIC ICE SHEET INITIATIVE. VOLUME 2: DISCIPLINE REVIEWS
Robert A. Bindschadler, ed. Washington May 1991 147 p Workshop held in Greenbelt, MD, 16-18 Oct. 1990; sponsored in part by NASA, Washington, and NSF, Washington, DC
(NASA-CP-3115-Vol-2; Rept-91A01040-Vol-2; NAS 1.55:3115-Vol-2) Avail: NTIS HC/MF A07 CSCL 08C

Seven discipline review papers are presented on the state of the knowledge of West Antarctica and opinions on how that knowledge must be increased to predict the future behavior of this ice sheet and to assess its potential to collapse, rapidly raising the global sea level. These are the goals of the West Antarctic Ice Sheet Initiative (WAIS). For individual titles, see N91-26574 through N91-26580.

N91-26574*# Ohio State Univ., Columbus. Byrd Polar Research Center.
A REVIEW OF PRECIPITATION-RELATED ASPECTS OF WEST ANTARCTIC METEOROLOGY **c45**
David H. Bromwich, Andrew M. Carleton, and Thomas R. Parish (Wyoming Univ., Laramie.) *In* NASA. Goddard Space Flight Center, West Antarctic Ice Sheet Initiative. Volume 2: Discipline Reviews May 1991 p 1-22 (For primary document see N91-26573 18-42)
Avail: NTIS HC/MF A07 CSCL 13B

An overview is presented of the factors associated with snowfall over the West Antarctic Ice Sheet. The flux of atmospheric moisture across the coast, the synoptic processes over the South Pacific Ocean, the large scale atmospheric controls, and numerical modeling of the West Antarctic environment are all discussed. Suggestions are made for research needed to substantially upgrade the status of knowledge in these closely interrelated topic areas. Author

N91-26575*# Lamont-Doherty Geological Observatory, Palisades, NY.
SEA-LEVEL RESPONSE TO ICE SHEET EVOLUTION: AN OCEAN PERSPECTIVE **c48**
Stanley S. Jacobs *In* NASA. Goddard Space Flight Center, West Antarctic Ice Sheet Initiative. Volume 2: Discipline Reviews May 1991 p 23-47 (For primary document see N91-26573 18-42)
Avail: NTIS HC/MF A07 CSCL 08C

The ocean's influence upon and response to Antarctic ice sheet changes is considered in relation to sea level rise over recent and future decades. Assuming present day ice fronts are in approximate equilibrium, a preliminary budget for the ice sheet is estimated from accumulation vs. iceberg calving and the basal melting that occurs beneath floating ice shelves. Iceberg calving is derived from the volume of large bergs identified and tracked by the Navy/NOAA Joint Ice Center and from shipboard observations. Basal melting exceeds 600 cu km/yr and is concentrated near the ice fronts and ice shelf grounding lines. An apparent negative mass balance for the Antarctic ice sheet may result from an anomalous calving rate during the past decade, but there are large uncertainties associated with all components of the ice budget. The results from general circulation models are noted in the context of projected precipitation increases and ocean temperature changes on and near the continent. An ocean research program that could help refine budget estimates is consistent with goals of the West Antarctic Ice Sheet Initiative. Author

N91-26576*# Wisconsin Univ., Madison. Geophysical and Polar Research Center.

TERRESTRIAL GEOPHYSICS IN THE SEARISE PROJECT c46

C. R. Bentley *In* NASA. Goddard Space Flight Center, West Antarctic Ice Sheet Initiative. Volume 2: Discipline Reviews May 1991 p 49-54 (For primary document see N91-26573 18-42)

Avail: NTIS HC/MF A07 CSCL 08G

Some areas of research in the SeaRISE project are briefly discussed. They are as follows: (1) Radar Sounding serves multiple purposes. The most general and obvious is mapping ice thickness and the surface and bedrock topography of the ice sheet. (2) The purpose of Seismic Shooting, in addition to water depth measurements on floating ice, is to provide information about the internal physical characteristics of the ice sheet, the rock beneath it, and the interface between the two. (3) Passive Seismic monitoring of microearthquakes can be used to study brittle fracture within the ice or the rock beneath it. Common parameters available from these studies are fault location, orientation, and displacement, as well as the size of the rupture area, stress drop, and energy released. (4) There is a large contrast in Electrical Resistivity between ice or permafrost on the one hand and liquid water or wet rock on the other hand. Thus, electrical resistivity profiles have the ability of revealing the depth to the melting point, whether it is found at the base of the ice or in the subglacial rock. (5) Gravity anomalies, especially combined with seismic measurements, are an effective tool for determining deeper crustal structure. Anomalies averaged over extensive areas are useful also for their potential to reveal isostatic imbalance, which is a measure of average glacial change over the last several hundred years. E.R.

N91-26577*# Maine Univ., Orono. Dept. of Geological Sciences.

LATE WISCONSIN AND EARLY HOLOCENE GLACIAL HISTORY, INNER ROSS EMBAYMENT, ANTARCTICA c46

George H. Denton, James G. Bockheim, Scott C. Wilson, and Minze Stuiver (Washington Univ., Seattle.) *In* NASA. Goddard Space Flight Center, West Antarctic Ice Sheet Initiative. Volume 2: Discipline Reviews May 1991 p 55-86 Sponsored in part by NSF and Navy (For primary document see N91-26573 18-42)

Avail: NTIS HC/MF A07 CSCL 08G

Lateral drift sheets of outlet glaciers that pass through the Transantarctic Mountains constrain past changes of the huge Ross ice drainage system of the Antarctic Ice Sheet. Drift stratigraphy suggests correlation of Reedy III (Reedy Glacier), Beardmore, Britannia (Hatherton/Darwin Glaciers), Ross Sea (McMurdo Sound), and younger (Terra Nova Bay) drifts; radiocarbon dates place the outer limits of Ross Sea drift in late Wisconsin time at 24,000 to 13,000 yr B.P. Outlet glacier profiles from these drifts constrain late Wisconsin ice sheet surface elevations. Within these constraint, two extreme late Wisconsin reconstructions are given of the Ross ice drainage system. Both show little elevation change of the polar plateau coincident with extensive ice shelf grounding along the inner Ross Embayment. However, in the central Ross Embayment, one reconstruction shows floating shelf ice, where as the other shows a grounded ice sheet. Massive late Wisconsin/Holocene recession of grounded ice from the western Ross Embayment, which was underway at 13,040 yr B.P. and completed by 6600 to 6020 yr B.P., was accompanied by little change in plateau ice levels inland of the Transantarctic Mountains. Author

N91-26578*# Rice Univ., Houston, TX. Dept. of Geology and Geophysics.

MARINE RECORD OF LATE QUATERNARY GLACIAL-INTERGLACIAL FLUCTUATIONS IN THE ROSS SEA AND EVIDENCE FOR RAPID, EPISODIC SEA LEVEL CHANGE DUE TO MARINE ICE SHEET COLLAPSE c48

John B. Anderson *In* NASA. Goddard Space Flight Center, West Antarctic Ice Sheet Initiative. Volume 2: Discipline Reviews May 1991 p 87-110 (For primary document see N91-26573 18-42)

Avail: NTIS HC/MF A07 CSCL 08C

Some of the questions to be addressed by SeaRISE include: (1) what was the configuration of the West Antarctic ice sheet during the last glacial maximum; (2) What is its configuration during a glacial minimum; and (3) has it, or any marine ice sheet, undergone episodic rapid mass wasting. These questions are addressed in terms of what is known about the history of the marine ice sheet, specifically in Ross Sea, and what further studies are required to resolve these problems. A second question concerns the extent to which disintegration of marine ice sheets may result in rises in sea level that are episodic in nature and extremely rapid, as suggested by several glaciologists. Evidence that rapid, episodic sea level changes have occurred during the Holocene is also reviewed. Author

N91-26579*# Pennsylvania State Univ., University Park. Dept. of Geosciences.

ICE CORES AND SEARISE: WHAT WE DO (AND DON'T) KNOW c48

Richard B. Alley *In* NASA. Goddard Space Flight Center, West Antarctic Ice Sheet Initiative. Volume 2: Discipline Reviews May 1991 p 111-130 Sponsored in part by NSF (For primary document see N91-26573 18-42)

Avail: NTIS HC/MF A07 CSCL 08C

Ice core analyses are needed in SeaRISE to learn what the West Antarctic ice sheet and other marine ice sheets were like in the past, what climate changes led to their present states, and how they behave. The major results of interest to SeaRISE from previous ice core analyses in West Antarctic are that the end of the last ice age caused temperature and accumulation rate increases in inland regions, leading to ice sheet thickening followed by thinning to the present. Author

N91-26580*# Ohio State Univ., Columbus. Byrd Polar Research Center.

GLACIAL DYNAMICS (GLACIOLOGY) c46

Ian Whillans *In* NASA. Goddard Space Flight Center, West Antarctic Ice Sheet Initiative. Volume 2: Discipline Reviews May 1991 p 131-143 (For primary document see N91-26573 18-42)

Avail: NTIS HC/MF A07 CSCL 08G

Recent results are reviewed from studies of ice dynamics that relate to the objectives of the West Antarctic Ice Sheet initiative. The large amount of knowledge gained is emphasized. The best evidence shows that the ice sheet in West Antarctic is the most rapidly changing ice sheet on earth today. Its rate of change is much faster than most glaciologists had expected and it is changing in a manner much more complex than foreseen. It appears that the changes have two broad causes: a delayed but ongoing response to the termination of the last glaciation about 10,000 years ago; and automatic, internally caused flow adjustments. It is not fully known why the response to the last global termination is so delayed, nor is the operation of internal instabilities understood, and certainly the position has not yet been attained to predict the future course of the evolution of the ice sheet. Author

N91-26581# Joint Publications Research Service, Arlington, VA.

JPRS REPORT: SCIENCE AND TECHNOLOGY. USSR: EARTH SCIENCES

6 Mar. 1991 38 p Transl. into ENGLISH from various Russian articles

(JPRS-UES-91-002) Avail: NTIS HC/MF A03

Topics addressed include: Arctic and Antarctic research; geology; meteorology; oceanography; atmospheric physics; and ecology. B.G.

N91-26582# Joint Publications Research Service, Arlington, VA.

JPRS REPORT: SCIENCE AND TECHNOLOGY. USSR: EARTH SCIENCES

12 Apr. 1991 32 p Transl. into ENGLISH from various Russian articles

(JPRS-UES-91-003) Avail: NTIS HC/MF A03

The topics addressed include: Soviet-American naval arms control experiment; energy active region of the ocean; and the effect of turbulence on upper atmospheric impurity observation using lidar. For individual titles, see N91-26583 through N91-26584.

N91-26583# Joint Publications Research Service, Arlington, VA.
IN THE ENERGY ACTIVE REGION OF THE OCEAN c48
R. V. Ozmidov *In its* JPRS Report: Science and Technology. USSR: Earth Sciences 12 Apr. 1991 p 16-23 Transl. into ENGLISH from Zemlya i Vselennaya (Moscow, USSR), no. 4, Jul.-Aug. 1990 p 59-64 (For primary document see N91-26582 18-42)
Avail: NTIS HC/MF A03

The possibility of predicting weather and climate on the European continent depends significantly on the knowledge of the Gulf Stream and its variability; on the mechanisms of heat and moisture transfer from the ocean to the atmosphere; and on their dynamic interactions. All of these, unfortunately, have been insufficiently studied, because in the Newfoundland region of the Atlantic, where storms are commonplace, it is difficult to make observations. A study of the structure and variability of hydrophysical fields in the Newfoundland test site, one of the energy active regions of the world ocean, a study of the atmosphere above the test site, and determination of the interaction of the air and water are the tasks of the expedition on the Akademik Kurchatov. B.G.

N91-26584# Joint Publications Research Service, Arlington, VA.
EFFECT OF TURBULENCE ON IMPURITY OBSERVATION IN UPPER ATMOSPHERE USING LIDAR METHOD c46
M. F. Lagutin, D. M. Smagin, and A. D. Pivnenko *In its* JPRS Report: Science and Technology. USSR: Earth Sciences 12 Apr. 1991 p 24-29 Transl. into ENGLISH from Izvestiya Akademii Nauk Turkmenskoy SSR: Seriya Fiziko-Tekhnicheskikh, Khimicheskikh i Geologicheskikh Nauk (Ashkhabad, USSR), no. 5, Sep.-Oct. 1990 p 18-22 (For primary document see N91-26582 18-42)
Avail: NTIS HC/MF A03

The lidar method of studying the behavior of man-made impurity releases has been widely used in recent years in studies of the upper atmosphere dynamics and parameters. The method is very sensitive, and this significantly affects the impurity observation process, which has long duration, unlike observation methods such as meteor radar, and photography of meteors and man-made glowing clouds. The analysis of the space-time behavior of impurity pertains to 80 to 100 km altitudes at medium latitudes and applies to the optical detection and ranging method. Turbulence develops at these altitudes. It is assumed that impurity consists of a monocomponent neutral conservative gas and that its diffusion occurs in the uniform stationary turbulence field. A moving coordinate system was chosen whose origin coincides with the impurity release point and is moving at the regular wind velocity. Under these conditions the process of impurity diffusion is described in mathematical computations. Author

43 EARTH RESOURCES AND REMOTE SENSING

Includes remote sensing of earth resources by aircraft and spacecraft; photogrammetry; and aerial photography.

For instrumentation see *35 Instrumentation and Photography.*

N91-26585# Winand Staring Centre, Wageningen (Netherlands).
APPLICATION OF THEMATIC MAPPER IMAGES TO DETERMINE REGIONAL EVAPORATION FROM THE PLAYAS IN THE WESTERN DESERT OF EGYPT
W. G. M. Bastiaanssen and M. H. AbdElKarim (Research Inst. for Groundwater, Cairo, Egypt) 1990 24 p Presented at Application of Remote Sensing in Hydrology and Water Resources, Damascus, Syria, 12-18 Mar. 1990
(Rept-31; ISSN-0924-3062; ETN-91-99440) Copyright Avail: NTIS HC/MF A03

To estimate actual evaporation from playas or sebkhas, a technique based on analysis of LANDSAT Thematic Mapper images and field measurements was developed. Surface reflectance and surface temperature are obtained with Thematic Mapper measurements. Effective properties of nonhomogeneous land surfaces, could be derived from the satellite image. This information is applied to classify soils and to determine the transfer of sensible and latent heat into the atmosphere. An algorithm is developed to obtain maps of latent heat flux with measurements of surface reflectance and surface temperature on a pixel by pixel basis. The so obtained values are validated with ground based observations of latent heat flux, obtained by means of the Bowen ratio energy balance method. Combination of daily evaporation values, calculated by means of models to simulate soil water flow through the unsatured zone, with instantaneous latent heat flux values, gives maps of daily and annual evaporation rates. The overall conclusion is that evaporation from playas is significantly higher than previously estimated. This has an important impact on the total regional groundwater development schemes. ESA

N91-26586# Dartmouth Coll., Hanover, NH. School of Engineering.
THE EXAMINATION OF DISLOCATIONS IN ICE Final Report, 1 Jan. 1986 - 31 Dec. 1990
Ian Baker and Fuping Liu 19 Feb. 1991 10 p
(Contract DAAG29-85-K-0251)
(AD-A233716; ARO-23056.1-GS) Avail: NTIS HC/MF A02 CSCL 08/12

Attempts have been made to examine dislocation structures in ice using transmission electron microscopy and x-ray topography. The examination of dislocations in thin foils of ice prepared from bulk samples in the transmission electron microscope, using a special liquid nitrogen-cooled double-tilt specimen holder, had little success. The chief reasons for this were the difficulty of thin foil preparation and the fact that dislocation densities in ice are very low. Some fractography of ice surfaces was successfully performed using the electron microscope in scanning mode. In contrast to the TEM work, examination of dislocations in ice samples up to 2 mm thick using x-ray topography were very successful. The work was performed at the National Synchrotron Light Source at Brookhaven National Laboratory. Ice is the ideal material for x-ray topography because it consists of light elements (allowing thick samples to be made) and because dislocation densities are low. Studies of grain boundaries, dislocation dissociations, fault formation and disappearance, dislocation pile-ups, and dislocation loops were performed in polycrystalline ice. GRA

N91-26587# Naval Oceanographic and Atmospheric Research Lab., Bay Saint Louis, MS.
THE NAVY STANDARD COMPRESSED AERONAUTICAL CHART DATABASE Final Report
Maura C. Lohrenz and James E. Ryan Jul. 1990 78 p
(AD-A235340; AD-E040002; NOARL-8) Avail: NTIS HC/MF A05 CSCL 08/2

Interface control criteria for exchange of chart image data from NOARL's Map Data Formatting Facility to Fleet's aircraft mission planning systems and digital moving map systems are described. The Compressed Aeronautical Chart database consists of compressed and otherwise transformed aeronautical chart images stored on Compact Disk-Read Only Memory optical disks. The Compressed Aeronautical Chart is created from standard mapping, charting, and geodesy products distributed by the Defense Mapping Agency. Development and creation of this library is part of a NOARL effort to provide the Fleet with Navy standard digital mapping, charting and geodesy products when the DMA's products cannot be used in their original form. The Compressed Aeronautical Chart data is now a mission requirement for the successful flights of an increasing number of U.S. Navy and U.S. Marine Corps aircraft. This report is required by the Naval Air Systems Command in order to ensure that future aircraft mission planning systems

and digital moving map systems are built to be compatible with this Navy standard database. It is also required as an engineering aid in developing future databases that will be used with the Compressed Aeronautical Chart. GRA

44 ENERGY PRODUCTION AND CONVERSION

Includes specific energy conversion systems, e.g., fuel cells; global sources of energy; geophysical conversion; and windpower.

For related information see also *07 Aircraft Propulsion and Power, 20 Spacecraft Propulsion and Power,* and *28 Propellants and Fuels.*

N91-26588# Midwest Research Inst., Golden, CO.
PHOTOVOLTAICS: FROM THE LABORATORY TO THE MARKETPLACE
T. S. Basso, T. Surek, and J. Thornton Mar. 1991 10 p Presented at the 2nd American Society of Mechanical Engineers (ASME)/Japan Solar Energy Society (JSES)/Japan Society of Mechanical Engineers (JSME) International Solar Energy Conference, Reno, 17-22 Mar. 1991
(Contract DE-AC02-83CH-10093)
(DE91-002151; SERI/TP-211-3971; CONF-910318-16) Avail: NTIS HC/MF A02

Photovoltaics (PV), the direct conversion of sunlight to electricity, is experiencing significant improvements in technology performance and lowered costs. Fostering these improvements, the SERI Photovoltaic Advanced Research and Development (PVAR and D) Project supports research and provides services to the U.S. PV industry. This paper presents the recent advances and future direction of the PV project. Research areas are fundamental and supporting research, advanced thin-film materials, high-efficiency materials, module development, and systems development. Materials of interest include amorphous silicon, copper indium diselenide, cadmium telluride, crystalline silicon, gallium arsenide and related alloys, transparent conductors, antireflection coatings, substrates, and encapsulants. The PV project inherently provides technology transfer that helps industry shorten the time to bring R and D advances to the marketplace. SERI annually performs over 10,000 measurements for the entire PV community, participates in collaborative research, and welcomes visiting scientists. Two specific areas of recently increased national focus are: (1) manufacturing processes for cost-effective PV modules, and (2) systems development for high-value utility applications. The SERI research approach is based on facilitating direct contact between industry, electric utilities, and others interested in PV technology. This approach heavily relies on SERI/industry partnerships. The arrangements vary to address generic and company-specific problems to improve the US industry's competitive position and accelerate greater electric utility deployment of PV systems. DOE

N91-26589# Battery Engineering, Inc., Hyde Park, MA.
IMPROVEMENT IN THE CAPACITY AND SAFETY OF LITHIUM/INORGANIC ELECTROLYTE SULFUR DIOXIDE RECHARGEABLE CELLS, PHASE 2 Final Report, Sep. 1988 - Nov. 1990
Carl R. Schlaikjer, Medlinda D. Jones, Arden P. Johnson, James E. Torkelson, and Walter VanSchalkwijk Nov. 1990 219 p
(Contract DAAL01-88-C-0845; DA Proj. 1L1-62705-AH-94)
(AD-A235303; SLCET-TR-88-0845-F-Phase-2) Avail: NTIS HC/MF A10 CSCL 10/2

The objective was to develop a prototype rechargeable lithium/sulfur dioxide/carbon cell, using practical AA size hardware, in which the electrolyte was to be a sulfur dioxide solution of lithium bromide or thiocyanate, together with a highly soluble cosolute, a second non-lithium salt of the same anion. The cosolute was intended to replace the organic cosolvents familiar from the primary cells, and hopefully, to improve lithium plating efficiency and electrolyte stability during cycling. The primary discharge capacities for AA size cells containing 1.25M CsBr/0.12 M LiBr/SO2 were only about 400mAh, while secondary and subsequent capacities were less than 200 mAh. The rates of solvolysis of bromide and of thiocyanate were exacerbated apparently both by the high anion concentrations and by increased lithium ion concentration. Lithium/sulfur dioxide/carbon rechargeable cells were examined in which the electrolytes were mixtures of tetrachloro aluminate salts in sulfur dioxide, to take advantage of the better performance, but to face the problem of limited capacity. It was determined that the capacity of lithium/bromine soluble positive cells was being limited by the loss of electrical contact between the carbon and the positive electrode current collector. Also, lithium plating efficiency was poor. GRA

N91-26590 Tel-Aviv Univ. (Israel). Dept. of Electron Devices and Materials and Electromagnetic Radiation.
INVESTIGATION AND CHARACTERIZATION OF ITO/POLY-Si PHOTOVOLTAIC JUNCTIONS M.S. Thesis
Shaul Eliahou Dec. 1989 138 p In HEBREW; ENGLISH summary
(ITN-91-85105) Copyright Avail: Tel-Aviv Univ., Exact Sciences Library, Ramat Aviv 69978, Israel

An ion implantation method of neutralization was developed, to reduce the effects of grain boundaries and surface defects in polycrystalline silicon, a promising material for low-cost terrestrial solar cells. Neutralization was performed by using a glow discharge in the relevant gas to implant ions of iodine, nitrogen, oxygen, hydrogen and nitrogen + hydrogen into the poly-Si. The small radii of the implanted ions enabled them to penetrate into the grain boundaries and neutralize dangling bonds by forming stable bonds. The observed characteristics of junctions formed between indium tin oxide (ITO) and poly-Si indicated that nitrogen was the most promising neutralizing agent. Auger electron spectroscopy analysis showed the presence of the neutralizing elements at the interface of the ITO/poly-Si junctions. Measurement of the photovoltaic spectral response showed that nitrogen neutralization caused a shift from 680 to 770 nanometers, which is approximately the value characteristic of a Si single crystal. Electron Beam Induced Current (EBIC) measurement before neutralization showed signals only on the crystallites and not on the grain boundaries; after neutralization, EBIC signals were obtained on the whole crystal surface. Neutralization was shown to improve the junctions current-voltage characteristics and to increase the short-circuit current, open-circuit voltage, efficiency and fill factor. It was concluded that neutralization could provide a means of obtaining efficient, inexpensive polycrystalline solar cells. ISA

N91-26591# Midwest Research Inst., Golden, CO.
RESEARCH ON STABLE, HIGH-EFFICIENCY AMORPHOUS SILICON MULTIJUNCTION MODULES
P. K. Bhat, S. Brown, R. Hollingsworth, D. S. Shen, J. delCueto, E. Iwanicko, C. Marshall, C. DeHart, D. Mentor, and A. Benson et al Apr. 1991 69 p Prepared in cooperation with Glasstech Solar, Inc., Golden, CO
(Contract DE-AC02-83CH-10093)
(DE91-002159; SERI/TP-214-4292) Avail: NTIS HC/MF A04

This report describes a contract to produce multijunction modules based entirely on amorphous silicon alloys, the modules having an aperture area of at least 900 sq cm and a stable, reproducible conversion efficiency of at least 6.5 percent after 600 hours of light exposure (air mass 1.5) at 50 C. The work focussed on (1) producing opto-electronic-grade amorphous silicon material for band gaps of about 1.7 and 1.9 eV by changing the hydrogen content in the film bonded to the silicon, (2) studying and obtaining data on the light stability of single-junction p-i-n solar cells with gaps of about 1.7 and 1.9 eV, and (3) analyzing losses in a silicon/silicon multijunction cell. New results are reported on an indium tin oxide (ITO)/silver back contact and the deposition of granular tin oxide by atmospheric-pressure chemical vapor deposition. Progress toward module fabrication at the end of six months has been good, with the demonstration of 5.4 percent initial efficiency in a silicon/silicon multijunction submodule with

an aperture area of 4620 sq cm and incorporating devices with 2nd-junction i-layer thicknesses of about 3500 A. A single-junction silicon submodule with an aperture area of 4620 sq cm, a thickness of about 3500 A, and an initial efficiency of 6.5 percent was demonstrated. DOE

N91-26592*# National Aeronautics and Space Administration. Lewis Research Center, Cleveland, OH.
A RELIABILITY AND MASS PERSPECTIVE OF SP-100 STIRLING CYCLE LUNAR-BASE POWERPLANT DESIGNS
Harvey S. Bloomfield Jun. 1991 31 p
(NASA-TM-103736; E-5974; NAS 1.15:103736) Avail: NTIS HC/MF A03 CSCL 10B

The purpose was to obtain reliability and mass perspectives on selection of space power system conceptual designs based on SP-100 reactor and Stirling cycle power-generation subsystems. The approach taken was to: (1) develop a criterion for an acceptable overall reliability risk as a function of the expected range of emerging technology subsystem unit reliabilities; (2) conduct reliability and mass analyses for a diverse matrix of 800-kWe lunar-base design configurations employing single and multiple powerplants with both full and partial subsystem redundancy combinations; and (3) derive reliability and mass perspectives on selection of conceptual design configurations that meet an acceptable reliability criterion with the minimum system mass increase relative to reference powerplant design. The developed perspectives provided valuable insight into the considerations required to identify and characterize high-reliability and low-mass lunar-base powerplant conceptual design. Author

N91-26593# Technical Research Centre of Finland, Espoo. LVI-Tekniikan Lab.
ABSORPTION HEAT PUMP IN HEATING AND COOLING SYSTEMS OF BUILDINGS
I. Aho, ed. 1990 97 p In FINNISH; ENGLISH summary
(DE91-752988; VTT/LVIS-20009) Avail: NTIS HC/MF A05

This report focuses on the operation and applicability of absorption heat pumps (AHP) in building heating and cooling systems. Examples are presented on heating systems of residential buildings and a heating/cooling system of an office building. Despite the limitations of present AHP technology the examples assume AHPs which produce heat at an appropriate temperature level for each application. According to the calculations the primary energy saving potential of AHPs in building specific heat production is 20 to 40 percent. For AHPs coupled with district heating systems the primary energy saving potential can not be unambiguously defined because it is influenced by the production form of district heat, the influence of district heat demand on power generation etc. For the time being economical aspects limit the application potential of AHPs. The profitability of AHP investments is quite poor because of present energy prices, the price ratio of different energy forms and the high investment cost of AHP-systems. The environmental impact of AHPs depend on the fuel used in the generator. Using fuel oil or gas will decrease sulphur and particle emissions but might increase the emissions of NO(x) and hydrocarbons because of the smaller size of combustion units. CFC-emissions will be decreased because AHPs apply alternative refrigerants. DOE

45 ENVIRONMENT POLLUTION

Includes atmospheric, noise, thermal, and water pollution.

N91-26594# Corvallis Environmental Research Lab., OR.
ECOLOGICAL EXPOSURE AND EFFECTS OF AIRBORNE TOXIC CHEMICALS: AN OVERVIEW
T. J. Moser, J. R. Barker, and D. T. Tingey Jan. 1991 171 p Prepared in cooperation with ManTech Environmental Technology, Inc., Research Triangle Park, NC
(PB91-148460; EPA/600/3-91/001) Avail: NTIS HC/MF A08 CSCL 13B

Since the release of the Environmental Protection Agency's toxic release inventory estimates of 1987, there was a heightened concern over the nation's air quality. Primarily, the concern was directed at human health effects in industrial-urban areas. The fact that many airborne chemicals pose hazards to human health is only one aspect of the problem. The continued deposition of airborne toxic chemicals pose threats to both terrestrial and aquatic ecosystems, the discussion is limited to terrestrial vegetation. Author

N91-26595# Argonne National Lab., IL.
ACID RAIN IN ASIA
N. Bhatti, D. G. Streets, and W. K. Foell (Resource Management Associates, Inc., Madison, WI.) 1991 40 p Presented at the Energy and Environment in the Asia-Pacific Region: Planning for An Uncertain Future, Honolulu, 13-15 Feb. 1991
(Contract W-31-109-eng-38)
(DE91-011160; ANL/CP-72383; CONF-9102110-1) Avail: NTIS HC/MF A03

Acid rain has been an issue of widespread concern in North America and Europe for more than fifteen years. However, there is an emerging feeling that the problem in Europe and North America is nearing solution, largely as a result of existing and newly enacted legislation, decreased energy use due to conservation and efficiency improvements, and/or trends in energy policy away from fossil fuels. The situation in Asia appears much bleaker. Fossil fuels are already used in large quantities, such that local air pollution is becoming a serious problem and high deposition levels are being measured. Emission regulations in most countries (with the notable exception of Japan) are not very stringent. Energy plans in many countries (particularly PRC, India, Thailand, and South Korea) call for very large increases in coal combustion in the future. Finally, there is not presently a strong scientific or public constituency for action to mitigate the potential effects of acid deposition. These factors imply potentially serious problems in the future for long-range transport and deposition of sulfur and nitrogen species and consequent damage to ecosystems and materials. The political ramifications of transboundary environmental pollution in this region are also potentially serious. The purpose of this paper is to provide background information on the acid deposition situation in Asia, with the intention of laying the foundation for the development of a possible research program for this region. DOE

N91-26596*# Michigan Univ., Ann Arbor. Space Physics Research Lab.
THE ANALYSIS OF A ROCKET TOMOGRAPHY MEASUREMENT OF THE N2+3914A EMISSION AND N2 IONIZATION RATES IN AN AURORAL ARC Final Technical Report, 15 May 1990 - 15 Jul. 1991
Ian C. McDade 12 Jul. 1991 119 p
(Grant NAG5-670)
(NASA-CR-188622; NAS 1.26:188622) Avail: NTIS HC/MF A06 CSCL 13B

Techniques were developed for recovering two-dimensional distributions of auroral volume emission rates from rocket photometer measurements made in a tomographic spin scan mode. These tomographic inversion procedures are based upon an algebraic reconstruction technique (ART) and utilize two different iterative relaxation techniques for solving the problems associated with noise in the observational data. One of the inversion algorithms is based upon a least squares method and the other on a maximum probability approach. The performance of the inversion algorithms, and the limitations of the rocket tomography technique, were critically assessed using various factors such as (1) statistical and non-statistical noise in the observational data, (2) rocket penetration of the auroral form, (3) background sources of emission, (4) smearing due to the photometer field of view, and (5) temporal variations in the auroral form. These tests show that the inversion procedures may be successfully applied to rocket observations made in medium intensity aurora with standard rocket photometer instruments. The inversion procedures have been used to recover two-dimensional distributions of auroral emission rates and ionization rates from an existing set of N2+3914A rocket

photometer measurements which were made in a tomographic spin scan mode during the ARIES auroral campaign. The two-dimensional distributions of the 3914A volume emission rates recoverd from the inversion of the rocket data compare very well with the distributions that were inferred from ground-based measurements using triangulation-tomography techniques and the N2 ionization rates derived from the rocket tomography results are in very good agreement with the in situ particle measurements that were made during the flight. Three pre-prints describing the tomographic inversion techniques and the tomographic analysis of the ARIES rocket data are included as appendices. Author

N91-26597# Radian Corp., Sacramento, CA.
IMPROVEMENT OF PROCEDURES FOR EVALUATING PHOTOCHEMICAL MODELS Final Report
T. W. Tesche, F. R. Lurmann, P. M. Roth, P. Georgopoulos, and J. H. Seinfeld Aug. 1990 176 p Prepared in cooperation with Alpine Geophysics, Placerville, CA; Sonoma Technology, Inc., Santa Rosa, CA; and California Inst. of Technology, Pasadena, CA Sponsored by California State Air Resources Board, Sacramento
(Contract ARB-A832-103)
(PB91-160374; ARB-R-91/453) Avail: NTIS HC/MF A09 CSCL 13B

The study establishes a set of procedures that should be used by all groups evaluating the performance of a photochemical model application. A set of ten numerical measures are recommended for evaluating a photochemical model's accuracy in predicting ozone concentrations. Nine graphical methods and six investigative simulations are also recommended to give additional insight into model performance. Standards are presented that each study should try to meet. To complement the operational model evaluation procedures, several diagnostic procedures are suggested. The sensitivity of the model to uncertainties in hydrocarbon emission rates and speciation, and other parameters should be assessed. Uncertainty bounds of key input variables and parameters can be propagated through the model to provide estimated uncertainties in the ozone predictions. Comparisons between measurements and predictions of species other than ozone will help ensure that the model is predicting the right ozone for the right reasons. Plotting concentrations residuals (differences) against a variety of variables may give insight into the reasons for poor model performance. Mass flux and balance calculations can identify the relative importance of emissions and transport. The study also identifies testing a model's response to emission changes as the most important research need. Another important area is testing the emissions inventory. GRA

N91-26598# Computer Sciences Corp., Research Triangle Park, NC.
MODAL AEROSOL DYNAMICS MODELING
E. R. Whitby, P. H. McMurry, U. Shankar, and F. S. Binkowski Feb. 1991 281 p Prepared in cooperation with Minnesota Univ., Minneapolis
(Contract EPA-68-01-7365)
(PB91-161729; EPA/600/3-91/020) Avail: NTIS HC/MF A13 CSCL 13B

The report presents the governing equations for representing aerosol dynamics, based on several different representations of the aerosol size distribution. Analytical and numerical solution techniques for these governing equations are also reviewed. Described in detail is a computationally efficient numerical technique for simulating aerosol behavior in systems undergoing simultaneous heat transfer, fluid flow, and mass transfer in and between the gas and condensed phases. The technique belongs to a general class of models known as modal aerosol dynamics (MAD) models. These models solve for the temporal and spatial evolution of the particle size distribution function. Computational efficiency is achieved by representing the complete aerosol population as a sum of additive overlapping populations (modes), and solving for the time rate of change of integral moments of each mode. Applications of MAD models for simulating aerosol dynamics in continuous stirred tank aerosol reactors and flow aerosol reactors are provided. For the application to flow aerosol reactors, the discussion is developed in terms of considerations for merging a MAD model with the SIMPLER routine described by Patankar (1980). Considerations for incorporating a MAD model into the U.S. Environmental Protection Agency's Regional Particulate Model are also described. Author

N91-26599# Office of Technology Assessment, Washington, DC.
CHANGING BY DEGREES: STEPS TO REDUCE GREENHOUSE GASES
Feb. 1991 359 p
(PB91-163428; OTA-O-482) Avail: NTIS HC/MF A16; also available SOD HC $16.00 as 052-003-01223-5 CSCL 13B

The focus is on the potential emissions reductions in the next 25 years. The analysis is structured around six key sectors of the U.S. economy: buildings, transportation, manufacturing, energy supply, forestry, and food. The potential for emissions reduction in each sector is quantified. A selection of policy options that appear to offer the most promise for achieving these reductions are presented. Author

N91-26600# Geological Survey, Denver, CO.
TRANSPORT AND FATE OF ACETONE IN AN OUTDOOR MODEL STREAM, STENNIS SPACE CENTER NEAR BAY ST. LOUIS, MISSISSIPPI
R. E. Rathbun, D. J. Shultz, D. W. Stephens, and D. Y. Tai 1991 116 p
(PB91-154674; USGS/WRI-89-4141) Avail: NTIS HC/MF A06 CSCL 13B

Organic substances discharged into streams and rivers as components of waste water affect water quality in various ways. The results are presented of the study of the transport and fate of acetone in an outdoor model stream located at the Stennis Space Center near Bay St. Louis, Mississippi. The principal element of the experimental design was a 32-day injection of acetone into the model stream. Other elements of the design included injection of glucose for 3 days and injection of a bacteria-nutrient mixture for 1 day in an attempt to stimulate bacterial growth and degradation of the acetone. Rhodamine-WT dye was injected for 1.5 days at the beginning of the test period and for 1.0 day at the end of the test period to determine the overall stream dispersion and traveltime characteristics. T-Butyl alcohol (TBA) was injected for 0.5 days to determine the volatilization characteristics of the stream. Author

N91-26601# Environmental Research Lab., Athens, GA.
MULTISPECTRAL IDENTIFICATION OF POTENTIALLY HAZARDOUS BYPRODUCTS OF OZONATION AND CHLORINATION. PART 1: STUDIES OF CHROMATOGRAPHIC AND SPECTROSCOPIC PROPERTIES OF MX
T. W. Collette, R. F. Christman, J. M. McGuire, and C. Trusty Mar. 1991 72 p Prepared in cooperation with North Carolina Univ., Chapel Hill
(PB91-161703; EPA/600/4-91/004) Avail: NTIS HC/MF A04 CSCL 13B

The gas chromatographic (GC) and Fourier transform infrared and mass spectroscopic (FT-IR and MS, respectively) properties of (Z)-2-chloro-3-dichloromethyl-4-oxobutenoic acid (MX) (a highly mutagenic byproduct of drinking water chlorination) and several related compounds were studied. Specifically, MX, the methyl ester of MX (MX-OMe), and three MX-model compounds were analyzed on the GC/FT-IR and GC/MS systems. Additionally, several extracts of chlorinations of dissolved organic materials were analyzed. Author

N91-26602# Environmental Research Lab., Athens, GA.
PRELIMINARY TESTING, EVALUATION AND SENSITIVITY ANALYSIS FOR THE TERRESTRIAL ECOSYSTEM EXPOSURE ASSESSMENT MODEL (TEEAM)
S. L. Bird, J. M. Cheplick, and D. S. Brown Mar. 1991 123 p Prepared in cooperation with Computer Sciences Corp., Athens, GA

(PB91-161711; EPA/600/3-91/019) Avail: NTIS HC/MF A06 CSCL 13B

An initial testing and sensitivity analysis of the Terrestrial Ecosystem Exposure Assessment Model (TEEAM) is documented. TEEAM calculates the exposure concentrations of contaminants in plants and animals in terrestrial ecosystems. The project was performed in two phases. First, a sensitivity analysis was performed using a simple system - an American robin inhabiting a typical peanut field in Georgia that had been treated with diazinon. The primary food source for the robin was the earth-worms living in the pesticide-contaminated soil. Second, an intensive model testing and evaluation effort was undertaken to examine each major model component. Results of the testing suggest that continued model development should focus on better simulation of surface ponding, plant transport, and uptake by soil dweller and above ground insect populations. GRA

N91-26603# Virginia Polytechnic Inst. and State Univ., Blacksburg. Center for Environmental/Hazardous Material.

ADAPTATION AND RESISTANCE OF ECOSYSTEMS TO STRESS Final Report, 1 Aug. 1989 - 31 Jan. 1991

John Cairns, Jr. and B. R. Niederlehner 31 Mar. 1991 70 p

(Grant AF-AFOSR-0263-88; AF Proj. 2312)

(AD-A234576; AFOSR-91-0377TR) Avail: NTIS HC/MF A04 CSCL 13/2

This report summarizes results of grant AFOSR-88-0263 entitled Adaptation and Resistance of Ecosystems to Stress. A series of laboratory toxicity tests were conducted examining structural and functional responses of microbial communities to the cumulative impact of a sequence of stresses. Results suggest that acclimated communities sometimes change less in response to a subsequent stress than did unacclimated communities, but acclimated communities were rarely better off in absolute terms. The cumulative impact of a chronic and then an acute stress in the acclimated communities frequently resulted in communities that were less taxonomically rich, had less total and biomass, less net production, and less productivity and respiration than did control communities dealing with only a single stress. GRA

N91-26604# Department of Energy, Washington, DC. Assistant Secretary for Fossil Energy.

GLOBAL CLIMATE CHANGE: A DISCUSSION OF MAJOR UNCERTAINTIES

R. L. Kane, M. E. Fernau, and D. W. South (Argonne National Lab., IL.) 1991 7 p Presented at the 53rd Annual Meeting and Exhibit of the American Power Conference, Chicago, 20 Apr. - 1 May 1991

(Contract W-31-109-eng-38)

(DE91-011746; ANL/CP-72859; CONF-9104106-5) Avail: NTIS HC/MF A02

The substantial uncertainties that exist regarding the scientific aspects and modeling of potential greenhouse gas-induced climate change are addressed. Uncertainties in the identification of temperature trends in the historical record, the quantification of future emissions and concentrations, and the prediction of potential climate change are examined. These uncertainties make it impossible at this time to produce reliable predictions of future climate change are examined. These uncertainties make it impossible at this time to produce reliable predictions of future climate change, due to increased greenhouse gas emissions, for use in developing policy options and response strategies. DOE

N91-26605# Brookhaven National Lab., Upton, NY.

AN ASSESSMENT OF CO2 GREENHOUSE GAS MITIGATION TECHNOLOGIES

M. Steinberg, J. Lee, and S. Morris Mar. 1991 149 p

(Contract DE-AC02-76CH-00016)

(DE91-011972; BNL-46045) Avail: NTIS HC/MF A07

Over the past decade there has become an increasing worldwide concern about the CO2 Global Greenhouse Effect. Most of the work on this subject has gone into studying the science of the concentration buildup of CO2 in the atmosphere which includes development and utilization of sophisticated global climate change models for purposes of predicting global temperature changes. However, large uncertainties still exist in attempting to predict the global and regional effects of CO2 concentration increase in the atmosphere. Until recently, little effort has gone into CO2 mitigation technologies. This report makes an attempt to review and assess suggested CO2 mitigation technologies primarily with a view towards reducing CO2 emissions from the utilization of fossil fuel. A categorization and a technical and economical evaluation of known and advanced CO2 mitigation technologies are presented. The study is divided into two parts. The first, part A, reviews the mitigation technologies, critiques the status of the technologies and presents economic case studies and comparative evaluations. The second, part B, uses the MARKAL linear energy programming model to determine the least cost mix of technologies to meet the U.S. schedule of energy demands under different levels of CO2 emissions restrictions. The new CO2 mitigation technologies were added to the more than 200 energy technologies already in the Markal data base in making this assessment. DOE

N91-26606# Lawrence Livermore National Lab., CA.

SIMULATION OF PRECIPITATION SCAVENGING IN A THREE-DIMENSIONAL GLOBAL MODEL

K. R. Sperber, J. E. Penner, J. J. Walton, and S. Hameed (State Univ. of New York, Stony Brook.) Mar. 1991 17 p Presented at the 5th International Conference on Precipitation Scavenging and Atmosphere Surface Exchange Process, Richland, 15-19 Jul. 1991

(Contract W-7405-eng-48)

(DE91-011531; UCRL-JC-106107; CONF-9107104-1) Avail: NTIS HC/MF A03

The wet deposition is studied of nitrate in a 3-D model of the reactive nitrogen cycle using the Lagrangian transport scheme of Walton et al., (1988). Known sources of reactive nitrogen are included and meteorological fields from the Lawrence Livermore version of the NCAR CCM are input to the Lagrangian transport model for January and July simulations. Two scavenging rate parameterizations are used, one in which removal depends upon the simulated precipitation rates, and an alternate Monte Carlo scheme which reproduces the frequency distribution of observed removal rates (Sperber and Hameed 1986a). The precipitation rate dependent scheme results in a substantial underestimate of nitrate deposition in regions where observations are available. The Monte Carlo scheme generally results in deposition which is more comparable to observations. The more effective removal results in lower surface air NO(x) concentrations. In July, this scheme overestimates deposition over the United States and western Europe. However it is believed that the overestimate is related to inadequate sampling of precipitation duration statistics due to the overestimate is related to inadequate sampling of precipitation duration statistics due to the the twelve hour timestep at which precipitation is updated. Simulations to investigate this hypothesis are currently being planned. DOE

N91-26607# Brookhaven National Lab., Upton, NY.

RELATIONSHIPS BETWEEN PAN AND OZONE AT SITES IN EASTERN NORTH AMERICA

J. M. Roberts, L. Newman, R. L. Tanner, V. C. Bowersox, and N. W. Reid (Ontario Ministry of the Environment, Toronto.) Aug. 1990 33 p

(Contract DE-AC02-76CH-00016)

(DE91-011728; BNL-45884) Avail: NTIS HC/MF A03

Measurements of Ozone and PAN (peroxyacetic nitric anhydride) were made at five sites in Eastern North America; Bondville, Ill., Dorset, Ont., Egbert, Ont., Scotia, Pa., and Whitetop Mtn., Va., in July and August of 1988 as part of the North American Cooperative Network of Enhanced Measurement Sites (NACNEMS) study. The concentrations of PAN ranged from less than 0.010 to 9.2 ppbv and those of O3 ranged from less than 2 to 139 ppbv. Diurnal concentration profiles showed PAN and O3 to be removed within nocturnal boundary layers, especially if nitric oxide was present, and that O3 was more rapidly removed than PAN. The only mountain top site at which PAN was measured showed distinctly different diurnal profiles in which O3 was actually higher

at night, suggesting that convective flow driven by surface cooling served to transport air from higher in the mixed layer down to the site at night. The afternoon production of PAN and O3 was also apparent and lead to an overall linear correlation of O3 and PAN between the hours of 1300 and 1800. The comparison of this result with other measurements and model calculations indicates that there is a wide disparity in model descriptions of PAN production, and confirms the nonlinear dependence of O3 production on NO(x). DOE

N91-26608# Argonne National Lab., IL.
AQUIS: AN AIR QUALITY AND PERMIT INFORMATION MANAGEMENT SYSTEM
A. E. Smith, C. C. Huber, J. Tschanz, and S. J. Ryckman, Jr. (Air Force Logistics Command, Wright-Patterson AFB, OH.) 1991 16 p Presented at the 84th Annual Meeting and Exhibition of the Air and Waste Management Association (AWMA), Vancouver (Canada), 16-21 Jun. 1991
(Contract W-31-109-eng-38)
(DE91-011750; ANL/CP-71726; CONF-910659-13) Avail: NTIS HC/MF A03

The Air Quality Utility Information System (AQUIS) is a data base management system that operates on a dedicated, IBM-compatible personal computer using dBASE IV. AQUIS is in operation at six of the seven U.S. Air Force Logistics Command (AFLC) bases to assist with the management of the source inventory, permit tracking, and the estimating and tracking of emissions. The system also provides environmental management personnel with information on regulatory requirements and other compliance information. An AFLC base can have over 500 regulated or unregulated emission sources, and the task of tracking and correlating emissions, sources, and permits is substantial. AQUIS is a comprehensive management tool that provides a single system for storing and accessing information previously available only in multiple, uncorrelated files. The development is discussed of the system and an overview is provided of the system structure and the relationship of that structure to sources in the field. Certain features such as the linking capability and compound-specific emissions are highlighted. The experience of environmental managers, the ultimate system users, is discussed, including specific ways in which AQUIS has proven useful in responding to managers' needs for air quality information. DOE

N91-26609# Brookhaven National Lab., Upton, NY.
FREE-AIR CARBON DIOXIDE ENRICHMENT: A NEW APPROACH TO RESEARCH ON CARBON EXCHANGE PROCESSES
G. R. Hendrey, F. W. Lipfert, K. F. Lewin, and J. Nagy Apr. 1991 17 p Presented at the 84th Annual Meeting and Exhibition of the Air and Waste Management Association (AWMA), Vancouver (Canada), 16-21 Jun. 1991
(Contract DE-AC02-76CH-00016)
(DE91-012074; BNL-46062; CONF-910659-17) Avail: NTIS HC/MF A03

Terrestrial-atmospheric carbon balances are currently poorly understood and are vital for predicting future trends in the global carbon budget. Uncertainties in C exchange rates can best be reduced by realistic experiments to determine flux rates in managed and natural ecosystems. Such experiments must minimize any artificiality imposed by the apparatus and should be capable of economical and reliable operation over entire growing seasons or longer. Brookhaven National Laboratory (BNL) has developed a system for exposing field-grown plants to controlled elevated concentrations of atmospheric gases, including CO2, without use of confining chambers that alter important atmospheric exchange processes. This system, called FACE for Free Air CO2 Enrichment, has been proven in over 15000 hours of testing at three locations. FACE uses a 15 to 27 m. diameter array of vertical ventpipes and offers significant improvements over previous attempts at chamber-free fumigation. BNL's FACE arrays have demonstrated these capabilities in experiment on field-grown cotton. This paper reviews the design concepts of FACE and presents operational results from several recent field campaigns involving seasonal fumigation of field-grown cotton with CO2 at concentrations ranging from 500 to 700 ppm. The use of chamber-free experiments in conjunction with mathematical models of plant growth is discussed as a paradigm for assessing climate change effects on vegetation. DOE

N91-26610# Brookhaven National Lab., Upton, NY.
THE IMPACT OF ATMOSPHERIC DAMAGE TO MATERIALS ON CONSUMERS: NEWS YOU CAN USE
F. W. Lipfert Apr. 1991 9 p Presented at the 84th Annual Meeting and Exhibition of the Air and Waste Management Association (AWMA), Vancouver (Canada), 16-21 Jun. 1991
(Contract DE-AC02-76CH-00016)
(DE91-012075; BNL-46065; CONF-910659-18) Avail: NTIS HC/MF A02

Recent research on the mechanisms and rates of atmospheric damage to materials, sponsored by the National Acid Precipitation Assessment Program (NAPAP) and the U.S. Environmental Protection Agency, has provided some new insights into the relative roles of wet and dry deposition of air pollutants on the useful lifetimes of objects normally exposed to outdoor weathering. While NAPAP was unable to carry out an economic assessment per se for materials damage, much of the information developed from this research is of direct use to consumers. This paper is intended to provide this information. The discussion is centered on common construction materials. The concept of substitute materials is stressed, so that consumers may become aware of the risks of accelerated weathering that may result from uninformed selections of materials. The categories of materials discussed include paints (architectural and automotive), metals, and masonry. DOE

N91-26574*# Ohio State Univ., Columbus. Byrd Polar Research Center.
A REVIEW OF PRECIPITATION-RELATED ASPECTS OF WEST ANTARCTIC METEOROLOGY
David H. Bromwich, Andrew M. Carleton, and Thomas R. Parish (Wyoming Univ., Laramie.) *In* NASA. Goddard Space Flight Center, West Antarctic Ice Sheet Initiative. Volume 2: Discipline Reviews May 1991 p 1-22 (For primary document see N91-26573 18-42)
Avail: NTIS HC/MF A07 CSCL 13B

46 GEOPHYSICS

Includes aeronomy; upper and lower atmosphere studies; ionospheric and magnetospheric physics; and geomagnetism.

For space radiation see *93 Space Radiation.*

N91-26611 Nevada Univ., Reno.
GROWTH, EVAPORATION AND MELTING OF ICE CRYSTALS: IMPLICATIONS FOR RADIATION, ATMOSPHERIC DYNAMICS AND PARTICLE SCAVENGING Ph.D. Thesis
Riza Gurcan Oraltay 1990 126 p
Avail: Univ. Microfilms Order No. DA9110599

Ice crystals were grown, evaporated, and melted in the lab under controlled conditions. Morphological changes during growth, evaporation, and melting of ice crystals were studied under controlled saturation, temperature, and air flow velocity. Temperatures ranged between +5 and -25 C, relative humidity between 45 and 95 pct (with respect to ice), with air flow approx. = to the terminal fall velocity of the particle. Melting and evaporation of ice crystals near 0 C and evaporation approaching cirrus temperatures (-25 C) were studied. Ice breakup was observed during evaporation occurring more frequently at low relative humidity (less than 80 pct). The results show more rapid initiation of downbursts by evaporative cooling of breaking particles. Aircraft data from two field studies were analyzed and combined with lab results and were shown to be consistent with a model of radar bright band incorporating aggregation and ice breakup during evaporation. Ice crystals were also grown, evaporated, or kept at ice saturation in the presence of aerosol particles. The effect of

the state of ice crystal on the scavenging of latex spheres and polydisperse and submicron soot particles was studied.
Dissert. Abstr.

N91-26612# Lawrence Livermore National Lab., CA.
PLATE MOTION AND DEFORMATION
B. Minster, W. Prescott, and L. Royden Feb. 1991 44 p Presented at the Conference on Future of the NASA Geodynamics Program, Coolfront, 22-28 Jul. 1989
(Contract W-7405-eng-48)
(DE91-010466; UCRL-JC-106677; CONF-8907240-1) Avail: NTIS HC/MF A03

Our goal is to understand the motions of the plates, the deformation along their boundaries and within their interiors, and the processes that control these tectonic phenomena. In the broadest terms, we must strive to understand the relationships of regional and local deformation to flow in the upper mantle and the rheological, thermal and density structure of the lithosphere. The essential data sets which we require to reach our goal consist of maps of current strain rates at the earth's surface and the distribution of integrated deformation through time as recorded in the geologic record. Our success will depend on the effective synthesis of crustal kinematics with a variety of other geological and geophysical data, within a quantitative theoretical framework describing processes in the earth's interior. Only in this way can we relate the snapshot of current motions and earth structure provided by geodetic and geophysical data with long-term processes operating on the time scales relevant to most geological processes. The wide-spread use of space-based techniques, coupled with traditional geological and geophysical data, promises a revolution in our understanding of the kinematics and dynamics of plate motions over a broad range of spatial and temporal scales and in a variety of geologic settings. The space-based techniques that best address problems in plate motion and deformation are precise space-geodetic positioning -- on land and on the seafloor -- and satellite acquisition of detailed altimetric and remote sensing data in oceanic and continental areas. The overall science objectives for the NASA Solid Earth Science plan for the 1990's, are to understand the motion and deformation of the lithosphere within and across plate boundaries, and to understand the dynamics of the mantle, the structure and evolution of the lithosphere, and the landforms that result from local and regional deformation.
DOE

N91-26613*# International Council of Scientific Unions, Kyoto (Japan). Scientific Committee on Solar-Terrestrial Physics.
MIDDLE ATMOSPHERE PROGRAM. HANDBOOK FOR MAP. VOLUME 30: INTERNATIONAL SCHOOL ON ATMOSPHERIC RADAR
Shoichiro Fukao, ed. Urbana, IL Oct. 1989 371 p School held in Kyoto, Japan, 24-28 Nov. 1988 Sponsored by NASA and UNESCO
(Contract MAP-Handbook-30)
(NASA-CR-188623; NAS 1.26:188623) Avail: NTIS HC/MF A16; also available from SCOSTEP Secretariat, Illinois Univ., 1406 Green Street, Urbana, IL 61801 CSCL 04A

Broad, tutorial coverage is given to the technical and scientific aspects of mesosphere stratosphere troposphere (MST) meteorological radar systems. Control issues, signal processing, atmospheric waves, the historical aspects of radar atmospheric dynamics, incoherent scatter radars, radar echoes, radar targets, and gravity waves are among the topics covered. For individual titles, see N91-26614 through N91-26623.

N91-26614*# Kyoto Univ. (Japan). Radio Atmospheric Science Center.
HISTORICAL ASPECTS OF RADAR ATMOSPHERIC DYNAMICS
Susumu Kato *In* International Council of Scientific Unions, Kyoto Middle Atmosphere Program. Handbook for MAP. Volume 30: International School on Atmospheric Radar Oct. 1989 p 1-18 (For primary document see N91-26613 18-46)
Avail: NTIS HC/MF A16; also available from SCOSTEP Secretariat, Illinois Univ., 1406 Green Street, Urbana, IL 61801 CSCL 04A

A review of the history of radar techniques which have been applied to atmospheric observation is given. The author starts with ionosphere observation with the ionosonde, symbolizing as it does the earliest history of radar observation, and proceeds to later developments in radar observation such as the use of partial reflection, meteor, and incoherent scatter radars. Mesosphere stratosphere troposphere (MST) radars are discussed in terms of lower atmosphere observation.
Author

N91-26615*# Kyoto Univ. (Japan). Radio Atmospheric Science Center.
RADAR PRINCIPLES **c32**
Toru Sato *In* International Council of Scientific Unions, Kyoto Middle Atmosphere Program. Handbook for MAP. Volume 30: International School on Atmospheric Radar Oct. 1989 p 19-53 (For primary document see N91-26613 18-46)
Avail: NTIS HC/MF A16; also available from SCOSTEP Secretariat, Illinois Univ., 1406 Green Street, Urbana, IL 61801 CSCL 17I

Discussed here is a kind of radar called atmospheric radar, which has as its target clear air echoes from the earth's atmosphere produced by fluctuations of the atmospheric index of refraction. Topics reviewed include the vertical structure of the atmosphere, the radio refractive index and its fluctuations, the radar equation (a relation between transmitted and received power), radar equations for distributed targets and spectral echoes, near field correction, pulsed waveforms, the Doppler principle, and velocity field measurements.
Author

N91-26616*# EISCAT Scientific Association, Kiruna (Sweden).
THE INSTRUMENTAL PRINCIPLES OF MST RADARS AND INCOHERENT SCATTER RADARS AND THE CONFIGURATION OF RADAR SYSTEM HARDWARE **c32**
Juergen Roettger (Max-Planck-Inst. fuer Aeronomie, Katlenburg-Lindau, Germany, F.R.) *In* International Council of Scientific Unions, Kyoto Middle Atmosphere Program. Handbook for MAP. Volume 30: International School on Atmospheric Radar Oct. 1989 p 54-113 (For primary document see N91-26613 18-46)
Avail: NTIS HC/MF A16; also available from SCOSTEP Secretariat, Illinois Univ., 1406 Green Street, Urbana, IL 61801 CSCL 17I

The principle of pulse modulation used in the case of coherent scatter radars (MST radars) is discussed. Coherent detection and the corresponding system configuration is delineated. Antenna requirements and design are outlined and the phase-coherent transmitter/receiver system is described. Transmit/receive duplexers, transmitters, receivers, and quadrature detectors are explained. The radar controller, integrator, decoder and correlator design as well as the data transfer and the control and monitoring by the host computer are delineated. Typical operation parameters of some well-known radars are summarized.
Author

N91-26617*# Instituto Geofisico del Peru, Lima. Jicamarca Radio Observatory.
STATISTICAL CHARACTERISTICS OF MST RADAR ECHOES AND ITS INTERPRETATION **c32**
Ronald F. Woodman *In* International Council of Scientific Unions, Kyoto Middle Atmosphere Program. Handbook for MAP. Volume 30: International School on Atmospheric Radar Oct. 1989 p 114-150 (For primary document see N91-26613 18-46)
Avail: NTIS HC/MF A16; also available from SCOSTEP Secretariat, Illinois Univ., 1406 Green Street, Urbana, IL 61801 CSCL 17I

Two concepts of fundamental importance are reviewed: the autocorrelation function and the frequency power spectrum. In addition, some turbulence concepts, the relationship between radar signals and atmospheric medium statistics, partial reflection, and the characteristics of noise and clutter interference are discussed.
Author

N91-26618*# Kyoto Univ. (Japan). Radio Atmospheric Science Center.

DATA ACQUISITION AND PROCESSING **c32**

Toshitaka Tsuda *In* International Council of Scientific Unions, Kyoto Middle Atmosphere Program. Handbook for MAP. Volume 30: International School on Atmospheric Radar Oct. 1989 p 151-183 (For primary document see N91-26613 18-46)

Avail: NTIS HC/MF A16; also available from SCOSTEP Secretariat, Illinois Univ., 1406 Green Street, Urbana, IL 61801 CSCL 17I

Fundamental methods of signal processing used in normal mesosphere stratosphere troposphere (MST) radar observations are described. Complex time series of received signals obtained in each range gate are converted into Doppler spectra, from which the mean Doppler shift, spectral width and signal-to-noise ratio (SNR) are estimated. These spectral parameters are further utilized to study characteristics of scatterers and atmospheric motions. Author

N91-26619*# Case Western Reserve Univ., Cleveland, OH. Dept. of Electrical Engineering and Applied Physics.

SPECTRAL AND CORRELATION ANALYSIS WITH APPLICATIONS TO MIDDLE-ATMOSPHERE RADARS **c32**

Prabhat K. Rastogi *In* International Council of Scientific Unions, Kyoto Middle Atmosphere Program. Handbook for MAP. Volume 30: International School on Atmospheric Radar Oct. 1989 p 184-227 (For primary document see N91-26613 18-46)

Avail: NTIS HC/MF A16; also available from SCOSTEP Secretariat, Illinois Univ., 1406 Green Street, Urbana, IL 61801 CSCL 17I

The correlation and spectral analysis methods for uniformly sampled stationary random signals, estimation of their spectral moments, and problems arising due to nonstationary are reviewed. Some of these methods are already in routine use in atmospheric radar experiments. Other methods based on the maximum entropy principle and time series models have been used in analyzing data, but are just beginning to receive attention in the analysis of radar signals. These methods are also briefly discussed. Author

N91-26620*# Kyoto Univ. (Japan). Radio Atmospheric Science Center.

TARGET PARAMETER ESTIMATION **c32**

W. K. Hocking (Adelaide Univ., Australia) *In* International Council of Scientific Unions, Kyoto Middle Atmosphere Program. Handbook for MAP. Volume 30: International School on Atmospheric Radar Oct. 1989 p 228-268 (For primary document see N91-26613 18-46)

Avail: NTIS HC/MF A16; also available from SCOSTEP Secretariat, Illinois Univ., 1406 Green Street, Urbana, IL 61801 CSCL 17I

The objective of any radar experiment is to determine as much as possible about the entities which scatter the radiation. This review discusses many of the various parameters which can be deduced in a radar experiment, and also critically examines the procedures used to deduce them. Methods for determining the mean wind velocity, the RMS fluctuating velocities, turbulence parameters, and the shapes of the scatterers are considered. Complications with these determinations are discussed. It is seen throughout that a detailed understanding of the shape and cause of the scatterers is important in order to make better determinations of these various quantities. Finally, some other parameters, which are less easily acquired, are considered. For example, it is noted that momentum fluxes due to buoyancy waves and turbulence can be determined, and on occasions radars can be used to determine stratospheric diffusion coefficients and even temperature profiles in the atmosphere. Author

N91-26621*# Max-Planck-Inst. fuer Aeronomie, Katlenburg-Lindau (Germany, F.R.).

GRAVITY WAVES AND INSTABILITIES IN THE LOWER AND MIDDLE ATMOSPHERE **c48**

Juergen Klostermeyer *In* International Council of Scientific Unions, Kyoto Middle Atmosphere Program. Handbook for MAP. Volume 30: International School on Atmospheric Radar Oct. 1989 p 269-298 (For primary document see N91-26613 18-46)

Avail: NTIS HC/MF A16; also available from SCOSTEP Secretariat, Illinois Univ., 1406 Green Street, Urbana, IL 61801 CSCL 04A

Some basic aspects of mesoscale and small-scale gravity waves and instability mechanisms are discussed. Internal gravity waves with wavelengths between ten and less than one kilometer and periods between several hours and several minutes appear to play a central role in atmospheric wavenumber and frequency spectra. Therefore, the author discusses the propagation of gravity waves in simplified atmospheric models. Their interaction with the wind as well as their mutual interaction and stability mechanisms based on these processes are discussed. Mesosphere stratosphere troposphere radar observations showing the relevant hydrodynamic processes are stressed. Author

N91-26622*# Clemson Univ., SC. Dept. of Physics and Astronomy.

APPLICATIONS OF MST RADARS: METEOROLOGICAL APPLICATIONS **c47**

M. F. Larsen *In* International Council of Scientific Unions, Kyoto Middle Atmosphere Program. Handbook for MAP. Volume 30: International School on Atmospheric Radar Oct. 1989 p 299-332 (For primary document see N91-26613 18-46)

Avail: NTIS HC/MF A16; also available from SCOSTEP Secretariat, Illinois Univ., 1406 Green Street, Urbana, IL 61801 CSCL 04B

Applications of mesosphere stratosphere troposphere radar to mesoscale meteorology are discussed. The applications include using the radar either as a research tool to improve our understanding of certain dynamical systems or as part of a network used to provide input data for weather forecasting. The workhorse of the operational observing network is the radiosonde balloon which provides measurements of pressure, temperature, humidity, and winds up to heights of 16 to 20 km. Horizontal and vertical measurement capabilities, reflectivity data, derivable quantities and parameters, and special operational requirements are surveyed. Author

N91-26623*# Cornell Univ., Ithaca, NY. National Astronomy and Ionosphere Center.

INCOHERENT SCATTER RADAR OBSERVATIONS OF THE IONOSPHERE

Tor Hagfors *In* International Council of Scientific Unions, Kyoto Middle Atmosphere Program. Handbook for MAP. Volume 30: International School on Atmospheric Radar Oct. 1989 p 333-364 (For primary document see N91-26613 18-46)

Avail: NTIS HC/MF A16; also available from SCOSTEP Secretariat, Illinois Univ., 1406 Green Street, Urbana, IL 61801 CSCL 04A

Incoherent scatter radar (ISR) has become the most powerful means of studying the ionosphere from the ground. Many of the ideas and methods underlying the troposphere and stratosphere (ST) radars have been taken over from ISR. Whereas the theory of refractive index fluctuations in the lower atmosphere, depending as it does on turbulence, is poorly understood, the theory of the refractivity fluctuations in the ionosphere, which depend on thermal fluctuations, is known in great detail. The underlying theory is one of the most successful theories in plasma physics, and allows for many detailed investigations of a number of parameters such as electron density, electron temperature, ion temperature, electron mean velocity, and ion mean velocity as well as parameters pertaining to composition, neutral density and others. Here, the author reviews the fundamental processes involved in the scattering from a plasma undergoing thermal or near thermal fluctuations in density. The fundamental scattering properties of the plasma to the physical parameters characterizing them from first principles. He does not discuss the observation process itself, as the observational principles are quite similar whether they are applied to a neutral gas or a fluctuating plasma. Author

N91-26624*# Jet Propulsion Lab., California Inst. of Tech., Pasadena.
ATMOSPHERIC INFRARED SOUNDER (AIRS): SCIENCE AND MEASUREMENT REQUIREMENTS
17 Sep. 1990 36 p
(NASA-TM-104977; JPL-D-6665; NAS 1.15:104977; PB91-156224) Avail: NTIS HC/MF A03 CSCL 04A

The Atmospheric Infrared Sounder (AIRS) is a high spectral resolution sounder selected as a facility instrument on the Earth Observing System (EOS). The complete infrared coverage of AIRS from 3.3 micrometers to 15.4 micrometers, together with the capabilities of the Advanced Microwave Sounding Unit (AMSU), will provide an all-weather observational capability for a large number of atmospheric and surface parameters. Measurements from AIRS will satisfy the requirements of general circulation modeling in accuracy, resolution, and coverage. It will provide day and night global coverage of the Earth twice a day with a footprint of 13.5 km (1.1 deg) at nadir from the 705 km orbital altitude of Eos. Measurement requirements, AIRS measurement specifications, the hardware implementation concept, and the AIRS ground-based data analysis concept are presented. Author

N91-26625# Naval Ocean Systems Center, San Diego, CA.
EVALUATION OF THE NAVY OCEANIC VERTICAL AEROSOL MODEL USING LIDAR AND PMS PARTICLE-SIZE SPECTROMETERS Final Report, Mar. 1989 - Apr. 1990
D. R. Jensen Dec. 1990 16 p
(AD-A233653; NOSC/TR-1391) Avail: NTIS HC/MF A03 CSCL 04/2

The Navy Oceanic Vertical Aerosol Model (NOVAM) was evaluated by making nearly simultaneous measurements of atmospheric structure with an airborne lidar and Particle Measuring Systems, Inc., aerosol spectrometers. Profiles of measured aerosol-size distributions were scaled to the lidar returns, and the calculated extinction coefficients were compared with the NOVAM predictions. NOVAM predicted extinction coefficient profiles have similar structure to the aircraft-measured profiles but underestimate the absolute value. When scaled to visibility, good agreement exists between the measured and predicted profiles. Agreement between the predicted and measured extinction coefficients is strongly dependent on air mass factor. GRA

N91-26626# Air Force Geophysics Lab., Hanscom AFB, MA.
SOUNDING ROCKET FLIGHT DATA SUMMARY Special Report, 1977 - Oct 1990
Edward McKenna 26 Oct. 1990 27 p
(AF Proj. 7659)
(AD-A233656; GL-TR-90-0288; GL-SR-264) Avail: NTIS HC/MF A03 CSCL 19/7

This report is a summary listing of all Geophysics Laboratory sounding rockets launched from 1977 to October 1990. Listed data includes launch date, rocket type, launch location, principal scientist, payload weight, payload diameter, apogee information, system performance, and experiment description. GRA

N91-26627# Lowell Univ., MA. Center for Atmospheric Research.
TECHNIQUE FOR MEASURING IONOSPHERIC IRREGULARITIES GENERATED BY HIGH POWER OBLIQUE HF HEATING OF THE F-REGION
Gary S. Sales, Bodo W. Reinisch, and John A. Ralls Aug. 1990 36 p
(Contract F29638-87-K-0012)
(AD-A233883; ULRF-458/CAR; GL-TR-90-0206) Avail: NTIS HC/MF A03 CSCL 04/1

A new technique for investigating the changes in the small to medium scale structure of the F-layer of the ionosphere is developed using the existing capabilities of the University of Lowell Center for Atmospheric Research Digisonde 256 vertical ionospheric sounder. When the ionosphere is heated by a high power HF transmitter operating in an oblique radar or communications mode the formation of irregularities has been observed. The development of these irregularities is described in terms of an index of ionospheric roughness which is shown to correlate very well with the natural formation of spread-F. These measurements are relatively simple and can be carried out from a site directly below the heated region. GRA

N91-26628# Washington Univ., Seattle. Quaternary Research Center.
PROCESS STUDY OF SORTED PATTERNS ON ARCTIC SOILS Final Report, 1987 - 1990
Bernard Hallet and Edwin Waddington 1 Mar. 1991 22 p
(Contract DAAL03-87-K-0058)
(AD-A234089; ARO-24376.4-GS) Avail: NTIS HC/MF A03 CSCL 08/12

Patterned ground is ubiquitous in Arctic and alpine areas. To improve understanding of this phenomenon, extensive field instrumentation was developed that has been recording principal soil properties over the past four years. The resulting data constitute the first quantitative year round records of important seasonal process such as freezing, thawing, frost heaving, and settling in the active layer in a sorted circle area. The data provide unprecedented insight into the long term dynamics of active sorted soil patterns. The field research was completed with analytical and numerical studies of sorted pattern formation. Deterministic and stochastic analyses of pattern development in the absence of significant soil deformation reveal strong textural instabilities; stones initially distributed at random through the soil tend to migrate quickly toward domains slightly richer in stones, which eventually leads to the distinct sorting characteristic of diverse forms of patterned ground. The numerical model of sorted stripe formation successfully simulates stripe development, and sheds considerable light on formative process. A novel model was also developed to assess buoyancy forces that arise in the thaw process, and may be responsible for the long term circulatory soil motion documented in sorted circles in Spitsbergen. GRA

N91-26629# Naval Postgraduate School, Monterey, CA. Dept. of Physics.
ATMOSPHERIC OPTICAL TURBULENCE MEASUREMENTS TAKEN AT ANDERSON MESA, FLAGSTAFF, ARIZONA BETWEEN 10-19 JULY 1990
Gail T. Vaucher, Christopher A. Vaucher, and Donald L. Walters 15 Feb. 1991 87 p
(AD-A234190; NPS-PH-91-007) Avail: NTIS HC/MF A05 CSCL 20/6

From 10 to 19 July 1990, the Naval Postgraduate School Atmospheric Optics Group acquired atmospheric optical turbulence measurements at the 13 inch Lowell Observatory astrographic telescope dome on Anderson Mesa, 16 km southeast of Flagstaff, Arizona. This collection of transverse coherence lengths and isoplanatic angles was the last in a three part Anderson Mesa site-survey measurement set for a large-scale, ground-based, synthetic aperture system (100 to 300 m baseline stellar interferometer). The intent of this report is to compile, analyze and summarize the acquired optical data, as well as correlate the meteorological and optical conditions present during the data acquisitions. GRA

N91-26630# ARCO Power Technologies, Inc., Washington, DC.
SYSTEM CONCEPT AND ANALYSIS OF AN ARTIFICIAL IONOSPHERIC MIRROR (AIM) RADAR Report, 31 Aug. 1989 - 31 Aug. 1990
Robert D. Short, Clayton V. Stewart, Tom Wallace, Pierre Lallement, and Peter Koert 31 Aug. 1990 51 p
(Contract F19628-89-C-0174)
(AD-A234289; APTI-5005; GL-TR-90-0267; SR-1) Avail: NTIS HC/MF A04 CSCL 04/1

Recognition of performance limitations associated with traditional skywave over-the-horizon (OTH) high frequency (HF) radars has led a number of investigators to propose the creation of an Artificial Ionospheric Mirror (AIM) in the upper atmosphere, in order to reflect ground-based radar signals for OTH surveillance. The AIM is produced by beaming sufficient electromagnetic power to the lower ionosphere (around 70 km) to enhance the in situ

ionization level to 10(exp 7) to 10(exp 8) electrons/cu cm, thereby providing an ionized layer capable of reflecting radar frequencies of 30 to 90 MHz. This paper presents a baseline AIM system concept and an associated performance evaluation, based upon the relevant ionization and propagation physics and in the context of air surveillance for the cruise missile threat. Results of the subject study indicate that a system using this concept would both complement and enhance the performance of the existing skywave OTH radars. GRA

N91-26631# Michigan Univ., Ann Arbor. Space Physics Research Lab.

DEVELOPMENT OF A VECTOR SPHERICAL HARMONIC (VSH) MODEL OF THE NEUTRAL THERMOSPHERE

Timothy L. Killeen and Raymond G. Roble Mar. 1990 161 p
(Contract F19628-89-K-0026)
(AD-A234744; GL-TR-90-0145; SR-1) Avail: NTIS HC/MF A08

The Air Force has requirements for accurate knowledge and specifications of the state variables of the Earth's thermosphere. Work done under this contract will lead to a new model of global thermospheric density that can be used to specify and forecast neutral densities, temperatures, and winds for a wide range of solar and geomagnetic activity. The model will be based on simulations made with the National Center for Atmospheric Research (NCAR) Thermosphere/Ionosphere General Circulation Model (TIGCM) and on data. It will be capable of using real-time geophysical indices or data from ground-based and satellite inputs and will provide neutral variables at specified locations and times in the altitude range 90 to 1500 km. This hybrid theoretical and semi-empirical model will be based on a new Vector Spherical Harmonic (VSH) analysis technique developed at the University of Michigan that permits the incorporation of the TIGCM outputs and data into the model. The VSH model will be provided for use by the Air Force in an additional setting and will be a more accurate version of existing models of the neutral upper atmosphere. This technical report describes the progress in the development of the hybrid model. GRA

N91-26632# Boston Univ., MA. Center for Space Physics.

THE EFFECTS OF MAGNETIC STORM PHASES ON F-LAYER IRREGULARITIES FROM AURORAL TO EQUATORIAL LATITUDES Quarterly Report, 1 Jan. - 31 Mar. 1991

Jules Aarons and Michael Mendillo 31 Mar. 1991 3 p
(Contract N00014-89-J-1754)
(AD-A235170) Avail: NTIS HC/MF A01 CSCL 08/4

The irregularities in the ionosphere at F-layer heights produce clutter on Over-the-Horizon Radars, amplitude and phase fluctuations on satellite to ground signals, and fading on HF communications. The morphology of F-layer irregularities at polar, auroral, and sub-auroral latitudes is in hand and it is possible to forecast for the system developer what to expect at auroral and polar latitudes as a function of sunspot number and magnetic index. However system operators must evaluate the duration and severity of the effects for particular locations. Magnetic storms have an immediate effect on the development of irregularities at auroral and sub-auroral latitudes. Forecasting the dynamics will allow the use of real time warning and possible use of other means of detection or communication. The time development of irregularities during various phases of magnetic storms is discussed. GRA

N91-26633# Lowell Univ., MA. Center for Atmospheric Research.

ARTIST TAPE OUTPUT FORMATS

Jane Tang, Claude G. Dozois, and Robert R. Gamache Jul. 1990 40 p
(Contract F19628-90-K-0029)
(AD-A235173; ULRF-457/CAR; GL-TR-90-0190) Avail: NTIS HC/MF A03 CSCL 14/3

The format of the ARTIST data and raw data records written to magnetic tape are described. The contents of each record type are fully explained making possible an unpacking of the data for subsequent analysis. A new generation of modern ionosondes is now being deployed world wide. These are the University of Lowell Center for Atmospheric Research (ULCAR) Digisonde 256 and AN/FMQ-12 DISS systems. The Digisonde 256 network will provide a consistent data set of ionospheric parameters that are automatically scaled in real time. The automated stations output the standard ionospheric parameters, the h'N(f) traces with amplitudes and Doppler frequencies, and the electron density profiles. There are currently 32 systems in operation or are close to being installed. The global station distribution is very uneven, the majority of sites lying in the northern hemisphere, and there are no equatorial stations. Nevertheless this network provides an extensive data base of ionospheric parameters in digital form, making it easy to process and analyze the data in terms of average diurnal variations, storms, and irregularities. This data base will be invaluable for the testing of global ionosphere models. GRA

N91-26634# Lamont-Doherty Geological Observatory, Palisades, NY.

A MULTICHANNEL SEISMIC INVESTIGATION OF VARIATIONS IN CRUSTAL STRUCTURE IN THE WESTERN NORTH ATLANTIC Final Report

John C. Mutter, Peter Buhl, and Robert S. Detrick 15 Mar. 1991 10 p
(Contract N00014-87-K-0074)
(AD-A235245) Avail: NTIS HC/MF A02 CSCL 08/7

A seismic characterization is provided of the Mesozoic-aged oceanic crust in a region of the western North Atlantic adjacent to the Blake Spur Fracture zone, using single and two-ship reflection methods, and two-ship wide-angle refraction methods. The observation of dipping reflectors on a previous seismic reflection line through the area led to the proposal of the current work. This same line also showed an apparent thinning of the crust as it obliquely crosses the Blake Spur Fracture Zone. GRA

N91-26635# Oregon State Univ., Corvallis. Dept. of Atmospheric Sciences.

BOUNDARY LAYER PARAMETERIZATION FOR A GLOBAL SPECTRAL MODEL Final Report, 1 Oct. 1987 - 30 Sep. 1990

L. Mahrt, M. Ek, J. Kim, and A. A. Holtslag 27 Jan. 1991 216 p
(Contract F19628-88-K-0001)
(AD-A235310; PL-TR-91-2031) Avail: NTIS HC/MF A10 CSCL 04/1

Work is described on the AFGL atmospheric boundary layer model which was developed to provide turbulence parameterization schemes for a global spectral model. The research has led to new boundary layer model developments, such as formulations for transport by clear air turbulence and transport due to topographically forced gravity waves. The study of boundary layer moisture regimes finds two asymptotic classes, drying and moistening, with the development of clouds found to be quite different for each class. A formulation for boundary layer cloud cover is developed that includes important influences of turbulent scale and subgrid-mesoscale variations of relative humidity. The new surface roughness formulation allows the roughness length for momentum to be significantly larger than that for heat, accommodating recent observational evidence. An additional study examines the daytime evolution of the boundary layer relative humidity and illustrates the complex interactions of the boundary layer, large scale vertical motion and soil moisture. GRA

N91-26636 Tel-Aviv Univ. (Israel). Dept. of Interdisciplinary Studies.

UV AURORA MAPPING IN CORRECTED GEOMAGNETIC COORDINATES M.S. Thesis

Arnoldo Rabitz Oct. 1989 127 p In HEBREW; ENGLISH summary
(ITN-91-85106) Copyright Avail: Tel-Aviv Univ., Exact Sciences Library, Ramat Aviv 69978, Israel

Ultraviolet images obtained by the USAF Geophysics Lab's Polar Bear satellite were subjected to geometric and photometric correction and used to map the UV aurora intensity in the north polar region. Radiation was measured at 135.6 and 159.6

nanometers. The work mainly comprised statistical processing of the aurora data, mapped on the corrected geomagnetic coordinate system, with a fixed direction relative to the sun. This enabled about 40 pictures to be processed in a common coordinate system. The statistical processing included computation of the mean aurora intensity and frequency of appearance. The images were separated into 5 groups according to the level of geomagnetic disturbance prevailing at the time of image reception. The final result was a statistical mapping of the UV aurora as a function of the geomagnetic disturbance level. The main conclusions are: (1) the UV aurora is distributed in an oval shape about the geomagnetic pole; (2) the radiation intensity and spatial distribution depend on the geomagnetic disturbance level, the dependence resembles that of the visible aurora; and (3) there is a general correspondence to the Feldstein ovals. The most important deviation detected was 5-degree poleward on the day side. ISA

N91-26637*# Alabama Univ., Huntsville. Dept. of Physics.
THEORETICAL AND EXPERIMENTAL STUDIES RELEVANT TO INTERPRETATION OF AURORAL EMISSIONS Annual Report
Charles E. Keffer 24 Jun. 1991 623 p
(Grant NAG8-834)
(NASA-CR-188491; NAS 1.26:188491) Avail: NTIS HC/MF A99 CSCL 04A

The accomplishments achieved over the past year are detailed with emphasis on the interpretation or auroral emissions and studies of potential spacecraft-induced contamination effects. Accordingly, the research was divided into two tasks. The first task is designed to add to the understanding of space vehicle induced external contamination. An experimental facility for simulation of the external environment for a spacecraft in low earth orbit was developed. The facility was used to make laboratory measurements of important phenomena required for improving the understanding of the space vehicle induced external environment and its effect on measurement of auroral emissions from space-based platforms. A workshop was sponsored to provide a forum for presentation of the latest research by nationally recognized experts on space vehicle contamination and to discuss the impact of this research on future missions involving space-based platforms. The second task is to add an ab initio auroral calculation to the extant ionospheric/thermospheric global modeling capabilities. Once the addition of the code was complete, the combined model was to be used to compare the relative intensities and behavior of various emission sources (dayglow, aurora, etc.). Such studies are essential to an understanding of the types of vacuum ultraviolet (VUV) auroral images which are expected to be available within two years with the successful deployment of the Ultraviolet Imager (UVI) on the ISTP POLAR spacecraft. In anticipation of this, the second task includes support for meetings of the science working group for the UVI to discuss operational and data analysis needs. Taken together, the proposed tasks outline a course of study designed to make significant contributions to the field of space-based auroral imaging. Author

N91-26151*# National Aeronautics and Space Administration. Langley Research Center, Hampton, VA.
MEASUREMENT OF ATMOSPHERIC TURBULENCE
Harold N. Murrow *In* AGARD, Manual on the Flight of Flexible Aircraft in Turbulence May 1991 p 1-30 (For primary document see N91-26150 18-08)
Copyright Avail: NTIS HC/MF A08; Non-NATO Nationals requests available only from AGARD/Scientific Publications Executive CSCL 04A

N91-26171# Joint Publications Research Service, Arlington, VA.
MEASUREMENTS OF THE LONGITUDINAL MOVEMENTS OF O(+) IONS IN THE SUBAURORAL UPPER ATMOSPHERE FROM THE AUREOL 3 SATELLITE Abstract Only
L. V. Zinin, V. S. Solovyev, Yu. I. Galperin, V. A. Gladyshev, and S. A. Grigoryev *In its* JPRS Report: Science and Technology. USSR: Space 16 Apr. 1991 p 35 Transl. into ENGLISH from Kosmicheskiye Issledovaniya (Moscow, USSR), v. 28, no. 6, Nov.-Dec. 1990 p 886-889 (For primary document see N91-26162 18-12)
Avail: NTIS HC/MF A06

N91-26576*# Wisconsin Univ., Madison. Geophysical and Polar Research Center.
TERRESTRIAL GEOPHYSICS IN THE SEARISE PROJECT
C. R. Bentley *In* NASA. Goddard Space Flight Center, West Antarctic Ice Sheet Initiative. Volume 2: Discipline Reviews May 1991 p 49-54 (For primary document see N91-26573 18-42)
Avail: NTIS HC/MF A07 CSCL 08G

N91-26577*# Maine Univ., Orono. Dept. of Geological Sciences.
LATE WISCONSIN AND EARLY HOLOCENE GLACIAL HISTORY, INNER ROSS EMBAYMENT, ANTARCTICA
George H. Denton, James G. Bockheim, Scott C. Wilson, and Minze Stuiver (Washington Univ., Seattle.) *In* NASA. Goddard Space Flight Center, West Antarctic Ice Sheet Initiative. Volume 2: Discipline Reviews May 1991 p 55-86 Sponsored in part by NSF and Navy (For primary document see N91-26573 18-42)
Avail: NTIS HC/MF A07 CSCL 08G

N91-26580*# Ohio State Univ., Columbus. Byrd Polar Research Center.
GLACIAL DYNAMICS (GLACIOLOGY)
Ian Whillans *In* NASA. Goddard Space Flight Center, West Antarctic Ice Sheet Initiative. Volume 2: Discipline Reviews May 1991 p 131-143 (For primary document see N91-26573 18-42)
Avail: NTIS HC/MF A07 CSCL 08G

N91-26584# Joint Publications Research Service, Arlington, VA.
EFFECT OF TURBULENCE ON IMPURITY OBSERVATION IN UPPER ATMOSPHERE USING LIDAR METHOD
M. F. Lagutin, D. M. Smagin, and A. D. Pivnenko *In its* JPRS Report: Science and Technology. USSR: Earth Sciences 12 Apr. 1991 p 24-29 Transl. into ENGLISH from Izvestiya Akademii Nauk Turkmenskoy SSR: Seriya Fiziko-Tekhnicheskikh, Khimicheskikh i Geologicheskikh Nauk (Ashkhabad, USSR), no. 5, Sep.-Oct. 1990 p 18-22 (For primary document see N91-26582 18-42)
Avail: NTIS HC/MF A03

47 METEOROLOGY AND CLIMATOLOGY

Includes weather forecasting and modification.

N91-26638 Royal Netherlands Meteorological Inst., De Bilt.
DESCRIPTION OF THE RIVM/KNMI PUFF DISPERSION MODEL
G. H. L. Verver, F. A. A. M. deLeeuw, and H. J. vanRheineck-Leyssius (Rijksinstituut voor Volksgezondheid en Milieuhygieene, Bilthoven, Netherlands) 1990 55 p
(KNMI-177; RIVM-222501001; ETN-91-99100) Copyright Avail: Royal Netherlands Meteorological Inst., P.O. Box 201, 3730 AE De Bilt, Wilhelminalaan 10, Netherlands

The model is intended for operational use in case of an accidental release of (toxic or radioactive) gases or particles into the atmosphere. The area covered by the model is restricted by the meteorological input that is available; the operational version will cover most of Europe. The main processes accounted for by the model are: relative diffusion by wind shear and turbulence, advection as a function of space and time, the diurnal cycle of boundary layer height and stability, dry and wet deposition and linear chemical transformation or radioactive decay. Input fields for the model are: horizontal wind (every 3 or 6 hours, on 2 or 3 levels), precipitation data (every 3 hours; optional) and height of the boundary layer (or mixed layer; every 3 hours; optimal). The meteorological data used may be either analyses or prognostics fields. The source is defined by an effective emission height and the source strength as a function of time. The model calculates

fields of concentrations near the surface and dry and wet depositions as a function of time. The puff model is tested on the Cs-137 and iodine-131 dispersion over Europe during the Chernobyl episode (April and May 1986). A ten day period is simulated and results are compared with measurements. Arrival times of the material are simulated well, in most cases within 6 hours accuracy. The observed air concentrations and model outcome show a reasonable agreement, but may differ an order of magnitude.
ESA

N91-26639# Reading Univ. (England).
COORDINATION OF MESOSCALE METEOROLOGICAL RESEARCH BETWEEN ASL AND EUROPEAN GROUPS Interim Report, No. 3, 1 Aug. 1990 - 31 Jan. 1991
R. P. Pearce 31 Jan. 1991 22 p
(Contract DAJA45-90-C-0009)
(AD-A233586; R/D-6323-EN-01) Avail: NTIS HC/MF A03 CSCL 04/2

The purposes of the meeting were to: (1) update the panel on recent developments at ASL; (2) plan the Mesomet Modelling Workshop, proposed at the previous (17th) panel meeting; and (3) produce evaluation criteria for the workshop. The topics presented include the following: developments at ASL since April, 1990; plans for the 1992 Mesoscale Modelling Workshop at ASL; workshop evaluation procedures; and future activities of the panel.
Author

N91-26640 Iowa State Univ. of Science and Technology, Ames.
A NUMERICAL STUDY OF BLOCKING Ph.D. Thesis
Ren-Yow Tzeng 1990 175 p
Avail: Univ. Microfilms Order No. DA9110574

A linear transient nine-level primitive equation model was developed to test three hypothesized mechanisms (residual, transient, and remote forcing) by which the blocking is initiated and maintained. Residual forcing consists of the time-average of the product of perturbations and diabatic heating anomaly. Transient forcing is represented by the time-average of the divergence of the vorticity flux with only synoptic-synoptic wave interactions. Remote forcing is derived from outgoing longwave radiation (OLR) using a vertical distribution of parameter. The model forcing is based on blocking anomalies, which is the difference between the blocking and nonblocking composites. The standing mode of the model is the nonblocking composite flow and the transient mode is the blocking anomaly flow.
Author

N91-26641# National Oceanic and Atmospheric Administration, Miami, FL. Hurricane Research Div.
HURRICANE RESEARCH DIVISION FISCAL YEAR 1990 PROGRAMS-FISCAL YEAR 1991 PROJECTIONS
Jan. 1991 67 p
(PB91-153452) Avail: NTIS HC/MF A04 CSCL 04B

Several topics in hurricane research are discussed. Topics covered include spectral modeling of a hurricane, development of a nested spectral barotropic hurricane track prediction model, initialization of tropical cyclone models, asymmetric evolution of the hurricane, tropical cyclone awareness research, observational studies of the South Florida sea breeze, and ground truth for spaceborne rainfall estimates.
Author

N91-26642# Florida Univ., Gainesville. Dept. of Electrical Engineering.
COMPARISON OF THE RF FREQUENCY SPECTRA OF HEMP AND LIGHTNING Technical Report, 22 Sep. 1987 - 10 Jul. 1990
Martin A. Uman 1 Mar. 1991 47 p
(Contract DNA001-87-C-0180)
(AD-A234306; DNA-TR-90-101) Avail: NTIS HC/MF A03 CSCL 20/15

Cloud pulses are much more common than these earlier studies indicate. Our spectra of the largest overhead cloud pulses are nearly parallel to but significantly below the HEMP spectrum from 1 MHz to 50 MHz, while obtained from lightning that was tens of kilometer offshore over salt water show faster relative decay with increasing frequency, are significantly below ours between 10 and 50 MHz, and are about equal to ours between 3 and 10 MHz. The shortest rise time to initial peak value of overhead lightning pulses are of the order of 0.3 micro sec. A broader bandwidth system than that used would allow measurement of the rapid field variation occurring throughout the cloud pulses associated with frequencies above about 50 MHz but would observe essentially the same risetime to initial peak. That is, the higher frequency content of the cloud pulses is contained in the rapid field variation throughout the overall waveforms and not in the initial rise to peak value.
GRA

N91-26643# Utah Univ., Salt Lake City. Center for Atmospheric and Remote Sounding Studies.
DEVELOPMENT AND VERIFICATION OF A PHYSICAL CLOUD-MOISTURE MODEL FOR USE IN GENERAL CIRCULATION MODELS Final Report, 1 Jul. 1987 - 31 Oct. 1990
J. L. Lee, K. N. Liou, and S. C. Ou 31 Jan. 1991 161 p
(Grant AF-AFOSR-0294-87; AF Proj. 2310)
(AD-A234751; AFOSR-91-0267TR) Avail: NTIS HC/MF A08 CSCL 04/2

A time dependent, three dimensional, large-scale cloud moisture model has been developed for the prediction of cloud cover, cloud liquid/ice water content (LWC/IWC), precipitation, specific humidity and temperature. Partial cloudiness is allowed to form when large-scale relative humidity is less than 100 pct. In the vertical, a 16-layer z-coordinate is adopted. The horizontal resolution is described by 48 equally-spaced longitudinal points and 38 Gaussian latitudes. The wind field is prescribed using the results from a general circulation model (GCM). Both liquid and ice phases are included in the model. The liquid phase processes consist of evaporation, condensation, auto conversion, and precipitation. The ice phase processes include heterogeneous nucleation to generate ice crystals, depositional growth to simulate Bergeron-Findeison's processes, sublimation to deplete ice crystals, and gravitational settling of ice crystals. The radiative transfer parameterization program is based on a broadband method and involves the transfer of infrared and solar radiation in clear and cloudy regions.
GRA

N91-26644# Army Cold Regions Research and Engineering Lab., Hanover, NH.
ROTATING MULTICYLINDER METHOD FOR THE MEASUREMENT OF CLOUD LIQUID-WATER CONTENT AND DROPLET SIZE
John B. Howe Jan. 1991 22 p
(DA Proj. 4A1-61102-AT-24)
(AD-A234780; CRREL-91-2) Avail: NTIS HC/MF A03 CSCL 04/2

Since its development at the Mt. Washington Observatory in the 1940s the rotating multicylinder (RMC) method has been the simplest, most reliable, and usually the most accurate means of measuring the liquid-water content and droplet size in clouds and fog. The development history of the method is reviewed in this report. Fabrication of the instrument, exposure and data-reduction techniques, and the underlying theory of the method are described in detail. Accuracy of the RMC method is discussed and comparison tests with other instruments are briefly reviewed.
GRA

N91-26645# Weather Wing (1st), Hickam AFB, HI.
AN OVERVIEW OF TROPICAL CIRCULATION
Frank Sornatale Jul. 1990 34 p
(AD-A234984; Rept-1WW/TN-90/001) Avail: NTIS HC/MF A03 CSCL 04/1

This report on atmospheric circulation in tropical regions discusses its role in supporting the larger general circulation system. The historical presentation of general circulation theory, the influence of tropical circulation on heat and momentum budgets, and localized circulation patterns are discussed.
GRA

N91-26646# Air Force Environmental Technical Applications Center, Scott AFB, IL.
SURFACE OBSERVATION CLIMATIC SUMMARIES (SOCS) FOR KODIAK, ALASKA Data Summary Report, Jan. 1949 - Dec. 1989
Sep. 1990 375 p
(AD-A235182; USAFETAC/DS-90/231) Avail: NTIS HC/MF A16 CSCL 04/2

The following subject areas are covered: atmospheric phenomena summaries; precipitation snowfall and snow depth; surface wind; ceiling, visibility, and sky cover; temperature and relative humidity; pressure (from hourly obs); crosswind summaries (from hourly obs); and degree day summaries (from hourly obs). GRA

N91-26647# Air Force Environmental Technical Applications Center, Scott AFB, IL.
SURFACE OBSERVATION CLIMATIC SUMMARIES FOR NORTON AFB, CALIFORNIA
Nov. 1990 363 p
(AD-A235227; USAFETAC/DS-90/234) Avail: NTIS HC/MF A16 CSCL 04/2

Surface observation climatic summaries (SOCS) provide statistical climatic summaries of surface weather observations taken and recorded at specified USAF, civilian, and foreign observing stations. Hourly observations are summarized from a ten year period of record (POR). Summary of day (SOD) information is summarized from all available data in the OL-A, USAFETAC climatic database. GRA

N91-26648# Air Force Environmental Technical Applications Center, Scott AFB, IL.
SURFACE OBSERVATION CLIMATIC SUMMARIES FOR TONOPAH TEST RANGE, NEVADA
Oct. 1990 347 p
(AD-A235228; USAFETAC/DS-90/232) Avail: NTIS HC/MF A15 CSCL 04/2

Surface observation climatic summaries (SOCS) provide statistical climatic summaries of surface weather observations taken and recorded at specified USAF, civilian, and foreign observing stations. Hourly observations are summarized from a ten year period of record (POR). Summary of day (SOR) information is summarized from all available data in the OL-A, USAFETAC climatic database. GRA

N91-26649# Air Force Global Weather Central, Offutt AFB, NE.
IMPROVED POINT ANALYSIS MODEL (IPAM) (USERS GUIDE)
Feb. 1991 201 p
(AD-A235305; AFGWC/TN-91/001) Avail: NTIS HC/MF A10 CSCL 04/2

The Air Force Global Weather Central (AFGWC) and the USAF Environmental Technical Applications Center (USAFETAC) have provided vertical meteorological profiles to military organizations, government agencies, and DoD contractors for a number of years. These products are called Point Analyses, or PAs. The contents of a PA let customers use applicable meteorological information to assess and evaluate their own data with respect to the state of the atmosphere at a specific place and time. The capabilities of the PA have recently been improved to accommodate new meteorological databases, new data sources, updated or new climatological data fields and models, and sophisticated mathematical techniques that enhance the accuracy and reliability of the data profile. The improved product is known as the Improved Point Analysis Model, or IPAM. This users guide describes the IPAM in detail, explaining its capabilities and limitations in sufficient depth to allow customers to use and apply the data to their own purposes. GRA

N91-26650# Mesoscale Environmental Simulations and Operations, Inc., Troy, NY.
THE DEVELOPMENT OF AN IMPROVED CONVECTIVE INITIATION SCHEME FOR MESOSCALE NUMERICAL WEATHER PREDICTION MODELS, PHASE 1 Final Report, 1 Sep. 1990 - 28 Feb. 1991
Kenneth T. Waight, III and Pamela E. Price 29 Apr. 1991 53 p
(Contract F49620-90-C-0057)
(AD-A235417; Rept-28-3-Phase-1; AFOSR-91-0493TR-Phase-1)
Avail: NTIS HC/MF A04 CSCL 04/2

A three-dimensional nonhydrostatic cloud model, the Terminal Area Simulation System (TASS), is used to investigate the convective initiation process for an idealized case over central Florida where the forcing is provided by differential surface heating. The surface heating pattern is generated from high resolution land use data by making simple assumptions relating surface characteristics to particular land use types. The cloud model simulation produces a complicated field of both shallow and precipitating cumulus clouds. Current mesoscale parameterization schemes are evaluated for their ability to predict convective initiation. Analysis of the results show that in the first half of the run, localized differential surface sensible heating produces small areas of deep convection associated with surface features. In the latter half of the simulation, mesoscale convergence develops due to the lateral boundary conditions and provides a mesoscale organization which is well resolved by a conventional measure of mesoscale moisture convergence. Subgrid scale convergence is very well correlated with convective activity. Results suggest that the cloud model is a valuable tool for the investigation of realistic convective initiation and evolution, and that a combination of mesoscale and subgrid scale properties are necessary for successful mesoscale modeling of cumulus convection. GRA

N91-26651*# National Aeronautics and Space Administration. Goddard Space Flight Center, Greenbelt, MD.
NIMBUS-7 TOMS ANTARCTIC OZONE ATLAS: AUGUST - DECEMBER 1990
Arlin J. Krueger, Lanning M. Penn, Patricia T. Guimaraes, Courtney J. Scott, David E. Larko, and Scott D. Doiron (ST Systems Corp., Vienna, VA.) Washington Jun. 1991 216 p
(Contract NAS5-29373)
(NASA-RP-1264; Rept-91B00103; NAS 1.61:1264) Avail: NTIS HC/MF A10 CSCL 04B

Because of the great environmental significance of ozone and to support continuing research at the Antarctic and other Southern Hemisphere stations, the development of the 1990 ozone hole was monitored using data from the Nimbus-7 Total Ozone Mapping Spectrometer (TOMS) instrument, produced in near-real-time. This Atlas provides a complete set of daily polar orthographic projections of the TOMS total ozone measurements over the Southern Hemisphere for the period 1 Aug. through 31 Dec. 1990. The 1990 ozone hole developed in a manner similar to that of 1987 and 1989, reaching a comparable depth in early October. This was in sharp contrast to the much weaker hold of 1988. The 1990 ozone hole remained at polar latitudes as it filled in Nov., in contrast to other recent years when the hold drifted to mid-latitudes before disappearing. Daily ozone values above selected Southern Hemisphere stations are presented, along with comparisons of the 1990 ozone distribution to that of other years. A new calibration scheme (Version 6) was used to process 1990 ozone values, as well as to reprocess those of previous years. Author

N91-26652 Tel-Aviv Univ. (Israel). Dept. of Geophysics and Planetary Sciences.
ON THE EVOLUTION OF RAINDROP SPECTRA AND THEIR EFFECT ON THE ATMOSPHERE BELOW CLOUD BASE: NUMERICAL MODELS AND COMPARISONS WITH OBSERVATIONS Ph.D. Thesis
Graham Feingold Sep. 1989 175 p
(ITN-91-85113) Copyright Avail: Tel-Aviv Univ., Exact Sciences Library, Ramat Aviv 69978, Israel

In studying the evolution of raindrop spectra below cloud base, the method of moments facilitates solution of the equations for 2

or more moments of the drop spectrum, and may be applicable to the mass transfer equations involved in cloud physics. Moment-conserving solutions to all the warm microphysical processes are presented. In each case the results obtained by this method are compared with analytic solutions and those obtained by one-moment methods. A vertical rainshaft describing the evolution of the raindrop spectrum and its moments is presented in both saturated and non-saturated environments, for steady and non-steady sources. Calculated radar reflectivity and scavenging coefficient profiles are presented. The microphysical processes are included in a cylindrical, axisymmetrical dynamic model, which facilitates tracing drop-spectrum evolution and rain-induced changes in the sub-cloud environment. The model is applied to a simulation of intense evaporatively driven downdraughts (microbursts), and it is shown that, owing to the sensitivity of evaporation to drop size, changes in drop spectrum induced by collection and breakup cannot be neglected. The dynamic model is used to compare the calculated spectral evolution with observed spectra at different elevations in the Swiss Alps, although the comparison is not fully justified, since the model does not include topography. The model was found to predict accurately the loss of rainrate with fall distance. The rainshaft model can be applied to a wide range of practical problems; the accuracy of the microphysical treatment of the drop spectrum should make the model especially useful in calculating the evaporation of rain below cloud base in arid regions, and the scavenging of aerosols by raindrops. ISA

N91-26653# Sandia National Labs., Albuquerque, NM.
THE 1990 SANDIA ROCKET-TRIGGERED LIGHTNING FIELD TESTS AT KENNEDY SPACE CENTER, FLORIDA
R. J. Fisher and G. H. Schnetzer Mar. 1991 97 p
(Contract DE-AC04-76DP-00789)
(DE91-011263; SAND-90-2926) Avail: NTIS HC/MF A05

During 1990, the Sandia Transportable Triggered Lightning Instrumentation Facility (SATTLIF) was designed, fabricated, and fielded at the Kentucky Space Center (KSC) rocket-triggered lighting test range in Florida. In preparation for lighting tests of a specially fitted munitions storage bunker during 1991, instrumentation for directly measuring lightning channel currents and response currents in structures was evaluated and demonstrated to function well. A set of 77-mm-thick 2024-T3 aluminum and 35-mm-thick 4130 steel metallic samples was exposed to measured triggered lighting flash currents. The resultant damage spots on these specimens represent the first such data points produced by known lighting currents. They are intended for use as benchmarks against which to improve and quantify the fidelity of laboratory simulations of lightning penetration. Two particularly significant results were obtained. In the first, a damage spot of approximately 0.3-inch diameter and greater than 0.01-inch depth was produced by a continuing current of well less than median-level severity that transferred less than 13.6 coulombs of charge. In the second case, one of the steel samples was virtually burned through under a return-stroke/continuing current combination transferring an eightieth percentile charge of approximately 49 coulombs. Photographic evidence of upward-going streamers preceding return strokes initiated by dart leaders was also obtained and is presented. DOE

N91-26654*# National Aeronautics and Space Administration. Marshall Space Flight Center, Huntsville, AL.
THE NASA/MSFC GLOBAL REFERENCE ATMOSPHERIC MODEL: 1990 VERSION (GRAM-90). PART 1: TECHNICAL/USERS MANUAL
C. G. Justus, F. N. Alyea, D. M. Cunnold, W. R. Jeffries, III (New Technology, Inc., Huntsville, AL.), and D. L. Johnson Washington Apr. 1991 88 p
(Grant NAG8-078)
(NASA-TM-4268; M-657; NAS 1.15:4268) Avail: NTIS HC/MF A05 CSCL 04B

A technical description of the NASA/MSFC Global Reference Atmospheric Model 1990 version (GRAM-90) is presented with emphasis on the additions and new user's manual descriptions of the program operation aspects of the revised model. Some sample results for the new middle atmosphere section and comparisons with results from a three dimensional circulation model are provided. A programmer's manual with more details for those wishing to make their own GRAM program adaptations is also presented. Author

N91-26655*# Georgia Tech Research Inst., Atlanta.
ADVANCED MICROWAVE PRECIPITATION RADIOMETER (AMPR) FOR REMOTE OBSERVATION OF PRECIPITATION Final Technical Report, 31 Dec. 1987 - 31 Dec. 1990
J. A. Galliano and R. H. Platt 31 Dec. 1990 124 p
(Contract NAS8-37142; GTRI Proj. A-8013)
(NASA-CR-184165; NAS 1.26:184165) Avail: NTIS HC/MF A06 CSCL 04B

The design, development, and tests of the Advanced Microwave Precipitation Radiometer (AMPR) operating in the 10 to 85 GHz range specifically for precipitation retrieval and mesoscale storm system studies from a high altitude aircraft platform (i.e., ER-2) are described. The primary goals of AMPR are the exploitation of the scattering signal of precipitation at frequencies near 10, 19, 37, and 85 GHz together to unambiguously retrieve precipitation and storm structure and intensity information in support of proposed and planned space sensors in geostationary and low earth orbit, as well as storm-related field experiments. The development of AMPR will have an important impact on the interpretation of microwave radiances for rain retrievals over both land and ocean for the following reasons: (1) A scanning instrument, such as AMPR, will allow the unambiguous detection and analysis of features in two dimensional space, allowing an improved interpretation of signals in terms of cloud features, and microphysical and radiative processes; (2) AMPR will offer more accurate comparisons with ground-based radar data by feature matching since the navigation of the ER-2 platform can be expected to drift 3 to 4 km per hour of flight time; and (3) AMPR will allow underflights of the SSM/I satellite instrument with enough spatial coverage at the same frequencies to make meaningful comparisons of the data for precipitation studies. Author

N91-26656# Oak Ridge National Lab., TN.
CHARACTERIZATION OF VERTICAL ELECTRIC FIELDS AND ASSOCIATED VOLTAGES INDUCED ON AN OVERHEAD POWER LINE FROM CLOSE ARTIFICIALLY INITIATED LIGHTNING
M. Rubinstein, Martin A. Uman, E. M. Thomson, and P. J. Medelius (Florida Univ., Gainesville.) 16 Apr. 1991 11 p Presented at the 1991 International Conference on Lightning and Static Electricity, Cocoa Beach, 16-19 Apr. 1991
(Contract DE-AC05-84OR-21400)
(DE91-010781; CONF-9104163-6) Avail: NTIS HC/MF A03

Measurements were characterized of simultaneous vertical electric fields and voltages induced at both ends of a 448 m overhead power line by artificially initiated lightning return strokes. The lightning discharges struck ground about 20 m from one end of the line. The measured line voltages could be grouped into two categories: (1) those in which multiple, similarly shaped, evenly spaced pulses were observed, which are called oscillatory; and (2) those dominated by a principal pulse with subsidiary oscillations of much smaller amplitude, which are called impulsive. Observed voltage amplitudes range from tens of kilovolts for oscillatory voltages to hundreds of kilovolts for impulsive voltages. DOE

N91-26622*# Clemson Univ., SC. Dept. of Physics and Astronomy.
APPLICATIONS OF MST RADARS: METEOROLOGICAL APPLICATIONS
M. F. Larsen *In* International Council of Scientific Unions, Kyoto Middle Atmosphere Program. Handbook for MAP. Volume 30: International School on Atmospheric Radar Oct. 1989 p 299-332 (For primary document see N91-26613 18-46)
Avail: NTIS HC/MF A16; also available from SCOSTEP Secretariat, Illinois Univ., 1406 Green Street, Urbana, IL 61801 CSCL 04B

48 OCEANOGRAPHY

Includes biological, dynamic, and physical oceanography; and marine resources.

For related information see also *43 Earth Resources and Remote Sensing.*

N91-26657 Delaware Univ., Newark.
THE TROPICAL PACIFIC OCEAN'S HEAT BUDGET DURING A COLD EVENT, FROM A NUMERICAL MODEL Ph.D. Thesis
Thomas Michael Smith 1990 165 p
Avail: Univ. Microfilms Order No. DA9109939

Output from a high-resolution numerical model of the tropical Pacific Ocean was studied to determine the model ocean's heat budget and investigate dynamics associated with interannual variability. The model output spans the period from February 1985 to April 1989. The heat budget over that period experienced interannual variability associated with warming of east-equatorial Pacific sea-surface temperature (SST), from mid 1986 through 1987 (El Nino). Abrupt cooling of the east-equatorial Pacific SST (La Nina) began in early 1988 and lasted through the year. Mechanisms associated with the cooling, which has received relatively little study in the past, are of particular interest. This study gives a detailed examination of the mechanisms which cause the ocean model's La Nina. The primary cause of the model's cooling was enhanced northward heat transports out of the equatorial ocean in late 1987 and early 1988, causing a strong meridional heat divergence. From the summer of 1987 to the winter of 1988, the meridional heat divergence from between 10 degrees N and 10 degrees S was more than 10(exp 15) W above the average seasonal divergence, averages computed from the 1985 to 1988 record. The divergence anomaly was sufficient to cool the eastern-equatorial Pacific SST more than 0.7 C/month. The enhanced northward heat transport was caused by much stronger than normal easterly wind stress near 10 degrees N. The stress was especially strong during the 1987 to 1988 boreal winter. Westward advection at the equator enhanced and prolonged the La Nina. The La Nina ended during the boreal spring of 1989, when relatively warm waters were transported eastward along the equator. Dissert. Abstr.

N91-26658# Planning Systems, Inc., McLean, VA.
PROGRESS WITH NEURAL NETWORK GULF STREAMS Final Technical Report
Eugene Molinelli, Gregory Muncill, and Kevin Pepe 31 Dec. 1990 52 p
(Contract N00014-90-C-6007)
(AD-A233810; PSI-TR-545445; NOARL-CR-019; Rept-91) Avail: NTIS HC/MF A04 CSCL 08/3

An expert human analyst is capable of examining an infrared image of sea surface temperature in the western North Atlantic Ocean offshore of Cape Hatteras, and identifying a Gulf Stream north wall where the sea surface is not obscured by clouds. The north wall of the Gulf Stream is a spatially continuous but temporally meandering narrow boundary between warm waters carried swiftly from the south and cold waters indigenous to the continental slope regime off the east coast of the United States. The north wall is closely related to a boundary between two ocean regions in which acoustic propagation conditions are dramatically different. The position of the north wall of the Gulf Stream is therefore important to acoustic antisubmarine warfare (ASW) tactics and hence is important to Navy operations. The current analyses are time consuming, tedious, qualitative, and subjective, i.e., dependent on the person performing the analysis. Researchers at NAVOCEANO and at NOARL are developing more objective, numerical procedures that can be implemented on modern computer systems and that can, at least, assist the analyses performed by humans. This article reports on the progress in NOARL sponsored efforts to utilize the emerging technology of neural networks to automatically interpret infrared imagery to detect Gulf Stream north wall positions. GRA

N91-26659# Michigan Univ., Ann Arbor. Communiucations and Signal Processing Lab.
OCEAN ACOUSTIC TOMOGRAPHY AND TELEMETRY Final Report, 7 Mar. 1984 - 7 Jul. 1987
Theodore G. Birdsall 17 Mar. 1991 11 p
(Contract N00014-84-K-0017)
(AD-A233826; Rept-021535-1-F) Avail: NTIS HC/MF A03 CSCL 20/1

The purpose of ocean tomography is to measure the (time-varying) speed of sound c(x,y,z;t) and ocean currents u(x,y,z;t) in three dimensions. The oceanographers can further transform these, with other information, into three-dimensional temperature and heat-flux fields. The method of Ocean Acoustic Tomography is to send acoustic timing signals, from each of a number of transmitters to a number of receivers these being spaced perhaps 250 to 1250 km apart. At such range the sound from any specified transmitter to any specified receiver will travel over several distinctly different identified raypaths, perhaps 5 to 25. As the ocean propagation conditions change, the pattern of changes in the travel times along all the identified raypaths from all transmitters to all receivers can be mathematically 'inverted' to estimate the three dimensional sound speed c(x,y,z;t). GRA

N91-26660# David Taylor Research Center, Bethesda, MD.
ANALYSIS OF WAVE CHARACTERISTICS IN EXTREME SEAS Final Report
William H. Buckley 1991 189 p
(AD-A234538; DTRC-SR-1309; SSC-353) Avail: NTIS HC/MF A09 CSCL 08/3

Results from three studies concerning identification and characterization of extreme waves in storm driven seaways are presented. Methods and results using time-series wave height data from hurricane Camille are illustrated. Task one demonstrated the utility of the half-cycle matrix (HAYCM) method in analyzing nonlinear time-series data. Task two involved wave making experiments where the Camille nonlinear wave spectrum was replicated. Task three, using second order wave-wave interaction theory, provided a nonlinear time domain wave height model conforming to the Camille nonlinear wave spectrum. In Task one, the HAYCM analysis of input and output realizations from Dalzell's nonlinear simulation model showed that this analysis method provides a clear indication of the nonlinearity of a time series random variable. In Task two, the nonlinearity of waves generated in two different towing tanks approached that of the original Camille seaway when the wave spectrum was approximated by mechanically generated waves. In Task three, while numerically modeled hurricane Camille time series showed somewhat less nonlinearity than the original time series data, the flattening of wave troughs and elevations of crests due to nonlinear wave-wave interaction was realistic. GRA

N91-26661# Coastal Engineering Research Center, Vicksburg, MS.
DIRECTIONAL CHARACTERISTICS OF WAVES IN SHALLOW WATER Final Report
Charles E. Long and Joan M. Oltman-Shay Mar. 1991 155 p
Sponsored by Corps of Engineers, Washington, DC
(AD-A234568; CERC-TR-91-1) Avail: NTIS HC/MF A08 CSCL 08/3

Proper coastal engineering design relies ultimately on a complete description of sea states to which natural or man-made structures are exposed. The character of directionally distributed wind wave energy is an intuitively and demonstrably important aspect of sea state definition, yet no long-term high-resolution coastal observations exist upon which to base engineering guidance. To remedy this, a multi-year series of wind direction and swell measurements has been undertaken. This report contains a preliminary analysis of 1,046 directional observations obtained during the first year of data collection. The climate during this year was typical of this site based on longer time series observations of winds, waves, and currents at the FRF. GRA

N91-26662# Rhode Island Univ., Narragansett. Graduate School of Oceanography.
THE SYNOP EXPERIMENT: INVERTED ECHO SOUNDER DATA REPORT FOR JUNE 1989 TO SEPTEMBER 1990 Summary Report, May 1989 - Sep. 1990
Erik Fields and D. R. Watts Mar. 1991 256 p
(Contracts N00014-90-J-1568; N00014-90-J-1548)
(AD-A234625; URI/GSO-TR-91-2) Avail: NTIS HC/MF A12 CSCL 08/3

The SYNoptic Ocean Prediction experiment (SYNOP) was undertaken with the goal that increased observations could be integrated with numerical models, including predictive models of the Gulf Stream. Our moored experiment, which began in the fall of 1987, consisted of two separate arrays in the Gulf Stream as part of the SYNOP program. The Inlet array of inverted echo sounders (IES) and deep current meters measured key parameters that describe the variability of the Gulf Stream and deep western boundary current (DWBC) near Cape Hatteras. In this region the Gulf Stream first flows into deeper water and crosses over the DWBC. The Central array of IESs, in a 350 km square centered on the Gulf Stream near 68 deg W, monitored the thermocline structure of the Gulf Stream in the region of large meanders and frequent interactions with rings. This report documents IES data recovered during the summer of 1990, from the Year 3 deployment period. The plots are time series of measured travel time, pressure, temperature; the residual pressure; and low-pass filtered records of residual pressure, thermocline depth, and temperature. A brief description of the experiment is given; the standard steps of data processing are discussed along with special processing for several IES records that had different problems. GRA

N91-26663# Woods Hole Oceanographic Inst., MA.
THE HIGH RESOLUTION PROFILER (HRP): USER'S GUIDE AND SOFTWARE MODIFICATIONS DOCUMENTATION
Ellyn T. Montgomery Jan. 1991 36 p
(Contract N00014-89-J-1073)
(AD-A234640; WHOI-91-01) Avail: NTIS HC/MF A03 CSCL 12/5

This report provides a User's Guide for operation of the High Resolution Profiler (HRP) and documentation of the software structure and recent modifications. The HRP is a free fall microstructure measurement instrument that acquires and stores up to 16 types of physical oceanographic data. A profile is logged as the HRP falls through the water column during each deployment. It controls its dives based on user-specified trigger levels input during a pre-cast setup. Communications, the setup process, and how to check out and run the profiler are described fully. Also included are the current sensor configuration and summaries of assembly, mechanical preparation, tracking, data transfer and processing. During 1990, the software controlling the HRP was almost completely reworked in order to port VRTX (Versatile Real Time Executive) to the HRP. This was accomplished to facilitate use of a fast data link that was being developed. Other modifications were made to the software to improve the user interface, to allow use of up to 16 Mbytes of Random Access Memory, to speed up the serial interface, and to fix previously undetected problems. In addition, the use of an altimeter to determine height above bottom was added to the dive control logic of the profiler. GRA

N91-26664# California Univ., Los Angeles.
LABORATORY MODELLING OF THE DYNAMICS OF COASTAL UPWELLING Report, 1 Sep. 1987 - 28 Feb. 1991
T. Maxworthy and S. Narimousa 28 Feb. 1991 122 p LIMITED REPRODUCIBILITY: Availability: Document partially illegible
(Contract N00014-87-K-0809)
(AD-A234987) Avail: NTIS HC/MF A06 CSCL 08/3

The aim of this research was to study and understand the dynamics of the filamentary structures that have been repeatedly observed by satellite (IR) images taken from the West Coast of the USA, during coastal upwelling episodes. We have simulated such episodes in our laboratory model and generated coastal upwelling fronts and associated jets and eddies. When the experimental model was free of coastal irregularities (capes, ridges, canyons, etc.), the upwelled front was uniform and a train of cyclonic-anticyclonic eddies were formed. Under some circumstances, many of these eddies pinched off and moved offshore into the fluid interior. We investigated the structure of such an eddy system and show that its structure falls within the category of two-dimensional and/or geostrophic turbulence. This in turn suggests that the eddy field contains many turbulent jets or rivers that are responsible for the transport of the passive material and cold, upwelled fluid across the eddy field. To demonstrate this, we released a passive marker near the front and noted that it was immediately transported offshore by the turbulent jets, and filamentary structures, similar to those seen in the satellite images, have evolved. When coastal irregularities were included into the system, many more eddies were generated and injected into the eddy system. GRA

N91-26665# Consultants Choice, Inc., Atlanta, GA.
OSIRRUS: OCEANIC SYMBOLIC IMAGE REPRESENTATION, RECOGNITION AND UNDERSTANDING SOFTWARE Final Report, Aug. 1980 - Nov. 1990
Lee A. Atkinson Dec. 1990 57 p
(Contract N00014-89-C-6027)
(AD-A235112; CCI-G89-0056-01) Avail: NTIS HC/MF A04 CSCL 08/3

Symbolic contours representing isotherms are used for shape and feature analysis of infrared oceanic satellite imagery. Techniques for detecting and analyzing oceanic thermal structures are presented. An effective image-processing technique called Image Modulation expedites time-consuming symbolic processing. Eddy-rings are successfully shape-recognized and false alarms are rule-discriminated. Verified eddy-rings are provided with a feature suite analysis useful for an automated image analysis work-station. Potential applications include Gulf Stream detection, symbolic image classification, image repair, and signal protection. GRA

N91-26666# Colorado Univ., Boulder. Cooperative Inst. for Research in Environmental Science.
LEAD DETECTION AND MAPPING WITH REFERENCE TO RELATIONSHIPS BETWEEN SCALE, SENSOR CHARACTERISTICS, SURFACE CONDITIONS AND ATMOSPHERIC PROPERTIES Annual Report, 15 Apr. 1990 - 14 Apr. 1991
J. Key, J. A. Maslanik, R. S. Stone, and A. S. McLaren 14 Apr. 1991 94 p
(Contract N00014-90-J-1840)
(AD-A235121) Avail: NTIS HC/MF A05 CSCL 08/12

Empirical studies of scale relationships in retrieval of sea ice lead statistics have been undertaken, as have modeling investigations of atmospheric influences on the satellite signal. Statistical models that describe the scaling properties of leads were being developed. The empirical studies have been based primarily on comparisons within and between LANDSAT and AVHRR imagery, while the atmospheric models have been specific to the AVHRR. Submarine sonar data have been used in the statistical model development. Accomplishments include: Parameterizations of clouds, haze, and atmospheric chemical constituents in the LOWTRAN 7 radiative transfer model, were reviewed. Atmospheric temperature and humidity profiles for the Arctic have been constructed from Soviet ice island data and are being used in the model. Resampling methods have been tested on synthetic, AVHRR, and LANDSAT images, as have the effects of digital enhancements. Procedures for retrieval of lead statistics were developed and applied to LANDSAT imagery successively degraded to coarser resolutions. The relationship between apparent lead widths measured along a transect (e.g., from submarine sonar or as a sampling method for satellite imagery) and the true lead width distribution may be obtained from the other. The effect of a limited number of atmosphere/surface conditions of the AVHRR-measured radiance in the thermal channel was examined. GRA

N91-26667# Brookhaven National Lab., Upton, NY.
INORGANIC CARBON SURVEYS OF OCEANIC BASINS
R. J. Wilke 25 Apr. 1991 6 p
(Contract DE-AC02-76CH-00016)
(DE91-011132; BNL-44234) Avail: NTIS HC/MF A02

Measurements were made aboard the F. S. Meteor, along the 19 degree South cruise track of the following chemical parameters: total dissolved inorganic carbon, pH, pCO2, CFC-12, CFC-11, CFC-113, CC14. This was the first cruise of OASD's newly formed CO2 group. The purpose was to survey World Ocean Circulation Experiment (WOCE) line A9 for inorganic carbon for the Department of Energy's Office of CO2 Research. DOE

N91-26668# Brookhaven National Lab., Upton, NY.
SEEP 2 ZOOPLANKTON DATA REPORT: WINTER, SPRING AND SUMMER COLLECTIONS AT MOORING 3 DURING 1988
P. V. Z. Lane, S. L. Smith, C. N. Flagg, and E. M. Schwarting Mar. 1991 106 p
(Contract DE-AC02-76CH-00016)
(DE91-012077; BNL-45968) Avail: NTIS HC/MF A06

The second Shelf Edge Exchange Processes (SEEP 2) experiment was designed as an extension of SEEP 1 work and was a multidisciplinary effort to describe the transport of carbon along and across the shelf and slope of the middle Atlantic Bight. A significant portion of the zooplankton work conducted during this project was devoted to repeated net sampling in close proximity to a moored acoustic Doppler current profiler (ADCP) in order to establish the calibration of the backscatter amplitude with respect to biomass in the water column. The Brookhaven ADCP was deployed at mooring site M-3 of the SEEP 2 study region. We used a multiple opening/closing net and environmental sensing system to collect stratified samples of zooplankton as close to the ADCP as towing conditions would allow. In addition, when MOCNESS tows were not feasible due to time constraints, Bongo nets were towed vertically in close proximity to the ADCP. The data in this report are the quantitative taxonomic analyses of the samples collected for ADCP calibration in 1988. DOE

N91-26575*# Lamont-Doherty Geological Observatory, Palisades, NY.
SEA-LEVEL RESPONSE TO ICE SHEET EVOLUTION: AN OCEAN PERSPECTIVE
Stanley S. Jacobs *In* NASA. Goddard Space Flight Center, West Antarctic Ice Sheet Initiative. Volume 2: Discipline Reviews May 1991 p 23-47 (For primary document see N91-26573 18-42)
Avail: NTIS HC/MF A07 CSCL 08C

N91-26578*# Rice Univ., Houston, TX. Dept. of Geology and Geophysics.
MARINE RECORD OF LATE QUATERNARY GLACIAL-INTERGLACIAL FLUCTUATIONS IN THE ROSS SEA AND EVIDENCE FOR RAPID, EPISODIC SEA LEVEL CHANGE DUE TO MARINE ICE SHEET COLLAPSE
John B. Anderson *In* NASA. Goddard Space Flight Center, West Antarctic Ice Sheet Initiative. Volume 2: Discipline Reviews May 1991 p 87-110 (For primary document see N91-26573 18-42)
Avail: NTIS HC/MF A07 CSCL 08C

N91-26579*# Pennsylvania State Univ., University Park. Dept. of Geosciences.
ICE CORES AND SEARISE: WHAT WE DO (AND DON'T) KNOW
Richard B. Alley *In* NASA. Goddard Space Flight Center, West Antarctic Ice Sheet Initiative. Volume 2: Discipline Reviews May 1991 p 111-130 Sponsored in part by NSF (For primary document see N91-26573 18-42)
Avail: NTIS HC/MF A07 CSCL 08C

N91-26583# Joint Publications Research Service, Arlington, VA.
IN THE ENERGY ACTIVE REGION OF THE OCEAN
R. V. Ozmidov *In its* JPRS Report: Science and Technology. USSR: Earth Sciences 12 Apr. 1991 p 16-23 Transl. into ENGLISH from Zemlya i Vselennaya (Moscow, USSR), no. 4, Jul.-Aug. 1990 p 59-64 (For primary document see N91-26582 18-42)
Avail: NTIS HC/MF A03

N91-26621*# Max-Planck-Inst. fuer Aeronomie, Katlenburg-Lindau (Germany, F.R.).
GRAVITY WAVES AND INSTABILITIES IN THE LOWER AND MIDDLE ATMOSPHERE
Juergen Klostermeyer *In* International Council of Scientific Unions, Kyoto Middle Atmosphere Program. Handbook for MAP. Volume 30: International School on Atmospheric Radar Oct. 1989 p 269-298 (For primary document see N91-26613 18-46)
Avail: NTIS HC/MF A16; also available from SCOSTEP Secretariat, Illinois Univ., 1406 Green Street, Urbana, IL 61801 CSCL 04A

51 LIFE SCIENCES (GENERAL)

N91-26669* Lockheed Engineering and Sciences Co., Washington, DC.
USSR SPACE LIFE SCIENCES DIGEST, ISSUE 29
Lydia Razran Stone, ed., Ronald Teeter, ed., and Joseph Rowe, ed. (Library of Congress, Washington, DC.) Washington NASA Mar. 1991 156 p
(Contract NASw-4292)
(NASA-CR-3922(34); NAS 1.26:3922(34)) Avail: NTIS HC/MF A08 CSCL 06E

This is the twenty-ninth issue of NASA's Space Life Sciences Digest. It is a double issue covering two issues of the Soviet Space Biology and Aerospace Medicine Journal. Issue 29 contains abstracts of 60 journal papers or book chapters published in Russian and of three Soviet monographs. Selected abstracts are illustrated with figures and tables from the original. A review of a book on environmental hygiene and a list of papers presented at a Soviet conference on space biology and medicine are also included. The materials in this issue were identified as relevant to 28 areas of space biology and medicine. The areas are: adaptation, aviation medicine, biological rhythms, body fluids, botany, cardiovascular and respiratory systems, developmental biology, digestive system, endocrinology, equipment and instrumentation, genetics, habitability and environment effects, hematology, human performance, immunology, life support systems, mathematical modeling, metabolism, musculoskeletal system, neurophysiology, nutrition, personnel selection, psychology, radiobiology, reproductive system, space biology and medicine, and the economics of space flight. Author

N91-26670* Lockheed Engineering and Sciences Co., Washington, DC.
USSR SPACE LIFE SCIENCES DIGEST, ISSUE 30
Lydia Razran Stone, ed., Ronald Teeter, ed., and Joseph Rowe, ed. (Library of Congress, Washington, DC.) Washington NASA May 1991 112 p
(Contract NASw-4292)
(NASA-CR-3922(36); NAS 1.26:3922(36)) Avail: NTIS HC/MF A06 CSCL 06E

This is the thirtieth issue of NASA's Space Life Sciences Digest. It contains abstracts of 47 journal papers or book chapters published in Russian and of three Soviet monographs. Selected abstracts are illustrated with figures and tables from the original. The abstracts in this issue have been identified as relevant to 20 areas of space biology and medicine. These areas include: adaptation, biospheric research, cardiovascular and respiratory systems, endocrinology, equipment and instrumentation, gastrointestinal system, group dynamics, habitability and environmental effects, hematology, human performance, immunology, life support systems, mathematical modeling,

metabolism, musculoskeletal system, neurophysiology, nutrition, psychology, radiobiology, and space biology and medicine.
Author

N91-26671# Army Biomedical Research and Development Lab., Fort Detrick, MD.
US ARMY BIOMEDICAL RESEARCH AND DEVELOPMENT LABORATORY Annual Progress Report, 1 Oct. 1989 - 30 Sep. 1990
Stephen C. Hembree 1 Jan. 1991 270 p
(DA Proj. 4E1-61102-BS-04; DA Proj. 3M1-61102-BS-15)
(AD-A233664) Avail: NTIS HC/MF A12 CSCL 15/6

The Annual Progress Report, Fiscal Year 1990, summarizes the research performed by the U.S. Army Biomedical Research and Development Laboratory in projects authorized by the U.S. Army Surgeon General and the Commander, U.S. Army Medical Research and Development Command. This research was supported by RDTE funds from the U.S. Army corps of Engineers, and from several additional sources. GRA

N91-26672# Nova Univ., Fort Lauderdale, FL.
PHYTOPLANKTON ABUNDANCE IN RELATION TO LAGRANGIAN PATHS Final Project Report, 1 Nov. 1988 - 31 Oct. 1990
Gary Hitchcock 1990 3 p
(Contract N00014-87-K-0040)
(AD-A233728) Avail: NTIS HC/MF A01 CSCL 08/1

The main objective of this effort was to examine the near-surface distribution of phytoplankton pigment, specifically chlorophyll a, in Gulf Stream meanders. This was accomplished by surveys of anticyclonic (crests) and cyclonic (troughs) meanders features during cruises in September, 1988 and April, 1989. This research program was part of the BioSYNOP Program, and our effort was conducted in conjunction with an NSF-sponsored physical oceanographic field effort supervised by Dr. Tom Rossby, University of Rhode Island. The hypothesis which was initially posed to the Office of Naval Research was that if our present understanding of the dynamics of meanders is correct, then upwelling of nutrient-rich, cool water along the leading edge of meander crests (that is, anticyclonic meanders), should result in enhanced standing stocks of phytoplankton biomass in these features. GRA

N91-26673# Naval Medical Research Inst., Bethesda, MD.
THE TRENDELENBURG POSITION AFTER CEREBRAL AIR EMBOLISM IN DOGS: EFFECTS ON THE SOMATOSENSORY EVOKED POTENTIAL, INTRACRANIAL PRESSURE, AND BLOOD-BRAIN BARRIER Technical Report, Sep. 1988 - Sep. 1989
Andrew J. Dutka, John E. Polychronidis, Richard B. Mink, and John M. Hallenbeck Nov. 1990 41 p
(AD-A233809; NMRI-90-116) Avail: NTIS HC/MF A03 CSCL 06/5

Medical personnel routinely recommend placing the victim of dysbaric or nosocomial cerebral air embolism in the Trendelenburg position. This maneuver is expected to reduce the chance of subsequent cerebral air emboli and to hasten clearance of bubbles trapped in the cerebral circulation. The Trendelenburg position will also increase intracranial pressure and reduce cerebral perfusion pressure; this may have an adverse effect on recovery of the injured brain. We placed 8 dogs in the left lateral decubitus, 45 deg. Trendelenburg position for 1 h following cerebral air embolism and transient hypertension, then treated the animals with compression on a modified U.S. Navy Treatment Table 6A (head-down or HD group). We compared somatosensory evoked potentials (SSEP), intracranial pressure and pressure-volume index (PVI), brain water, and blood-brain barrier function assessed by extravasation of Evans Blue to these variables in nine embolized and hypertensive dogs maintained in a head-up (sphinx) position as controls (horizontal or HZ group). GRA

N91-26674# Naval Biodynamics Lab., New Orleans, LA.
A STATISTICAL ANALYSIS OF -X RHESUS HEAD KINEMATICS Research Report, 1985 - 1987
Salvadore J. Guccione, Jr. 1 Oct. 1990 113 p
(AD-A233977; NBDL-89R006) Avail: NTIS HC/MF A06 CSCL 06/5

The use of the rhesus as a human surrogate in studying head-neck injury due to impact acceleration depends of the similarity of human and rhesus head-neck kinematic and dynamic responses. This report addresses the question of -X rhesus head-neck kinematics. The dependence of the first major peaks of head linear and angular accelerations, velocities and displacements on sled acceleration parameters and initial head position is statistically analyzed. The effects of anesthetic state, repeated exposures and out-of-plane response on these key kinematics outputs are assessed. Various graphical and statistical comparisons indicate that: (1) human and rhesus -X head kinematics are not only similar in shape but, more importantly, depend on the same sled and head initial position parameters; (2) anesthetic state has no significant statistical effect on rhesus kinematic output; and (3) the effects of repeated tests and out-of-plane response can be reasonably explained. These results justify a fullscale attempt to fit key human and rhesus kinematics and dynamic responses and develop appropriate scaling procedures. Recommendations concerning the structuring of future human and rhesus experiments to facilitate the necessary statistical comparisons are also given. GRA

N91-26675# California Univ., Los Angeles. Mental Retardation Research Center.
INTRACELLULAR PHYSIOLOGY OF THE RAT SUPRACHIASMATIC NUCLEUS: ELECTRICAL PROPERTIES, NEUROTRANSMISSION, AND EFFECTS OF NEUROMODULATORS Annual Report, 1 Nov. 1989 - 31 Oct. 1990
F. E. Dudek 28 Mar. 1991 7 p
(Contract AF-AFOSR-0056-90; AF Proj. 2312)
(AD-A234442; AFOSR-91-0376TR) Avail: NTIS HC/MF A02 CSCL 06/5

The primary goal of this research has been to determine the electrophysiological properties of neurons in the suprachiasmatic nucleus (SCN), with particular emphasis on the mechanisms underlying synaptic transmission and neuromodulation. We have focused on the role of excitatory amino acids (i.e., glutamate) in synaptic transmission from the retina to the SCN. Our recent data indicate that non-NMDA receptors mediate transmission at low levels of activity, but NMDA receptors are likely important when the cells are depolarized. Our studies of synaptic inhibition in the SCN indicate that gamma amino-butyric acid (GABA) mediates fast inhibitory postsynaptic potentials. Ongoing experiments are aimed at examining the role of glutamate and GABA in expression of the circadian rhythm of electrical activity in the SCN. Finally, a series of experiments partially supported by this grant has been undertaken in the paraventricular nucleus and preoptic area of the hypothalamus. GRA

N91-26676# Utah Univ., Salt Lake City. Dept. of Chemistry.
IMAGING OF FLUORESCENT AND CHEMILUMINESCENT DNA HYBRIDS USING A 2-D CCD CAMERA Technical Report, Jun. 1990 - May 1991
A. Karger, J. T. Ives, R. B. Weiss, J. M. Harris, and R. F. Gesteland 22 Apr. 1991 14 p
(Contract N00014-89-J-1412)
(AD-A234641; TR-26-ONR) Avail: NTIS HC/MF A03 CSCL 06/1

Fluorescent and chemiluminescent detection of DNA hybrids on polymer membranes has been investigated using a cryogenically cooled, slow readout, two dimensional CCD camera in an imaging mode. The fluorescent background characteristics of commercially available nylon blotting membranes and a polypropylene membrane modified to bind DNA have been studied. The polypropylene membrane exhibits a 15-fold increase in DNA binding, 3-fold less background fluorescence and less background noise than nylon blotting membranes. However the detection limits determined from vacuum slot blots of crosslinked fluorescein-labelled oligonucleotides show that the improved qualities of the

polypropylene support do not result in a lower detection limit. This is mainly due to background noise arising from sources other than the membrane itself during the blotting/washing procedure and to a low signal-to-amount of DNA ratio with the polypropylene membrane. The lowest amount of fluorescein-labelled oligonucleotide detectable is 1.4 femtomol, with a typical exposure time of 10 minutes to image a 6x9 cm area of the membrane. The detection of chemiluminescence was done using a biotin-avidin complex in combination with an enzymatic assay. GRA

N91-26677# Texas Univ., San Antonio. Health Science Center.
INTERACTION OF IONIZING RADIATION, GENETICALLY ACTIVE CHEMICALS, AND RADIOFREQUENCY RADIATION IN HUMAN AND RODENT CELLS Final Report, 1 Oct. 1987 - 30 Sep. 1989
Martin L. Meltz, Patricia K. Holahan, Steven T. Smith, James J. Kerbacher, and Victor Ciaravino Dec. 1990 79 p
(Contract F33615-87-C-0610)
(AD-A234747; USAFSAM-TR-90-18) Avail: NTIS HC/MF A05 CSCL 06/5

The purpose of this project was to investigate the possible interaction between radiofrequency radiation (RFR) and agents which are known to damage DNA. Experiments were performed using exposures of CHO cells to 350, 850, 1200, and 2450 MHz RFR at up to 40 W/kg and temperatures ranging from 37 to 40 C. No genotoxic effect was observed by sister chromotid exchange induction, chromosome aberration induction, or gene mutation (at the thymidine kinase locus). At levels at or below 10 mW/sq cm and specific absorption rates (SARs) at or below 4 W/kg, there was no evidence that DNA repair was induced or repair of preexisting DNA damage was inhibited. Adriamycin but not mitomycin C caused a statistically significant increase in the frequency of aberrant cells at 40 C with or without RFR. These observations support thermal mechanisms of RFR interaction. GRA

N91-26678# General Electric Co., Schenectady, NY. Biological Sciences Div.
BIOLOGICAL SYNTHESIS OF SUBSTITUTED O-AMINOPHENOLS Final Report, 1 Nov. 1987 - 13 Dec. 1990
Terry K. Leib Feb. 1991 86 p
(Contract F49620-88-C-0016)
(AD-A234910; Rept-91SRD001; AFOSR-91-0236TR) Avail: NTIS HC/MF A05 CSCL 06/5

Polybenzoxazoles are thermally stable, high modulus polymers made by the condensation of carboxylic acids with o-aminophenols. This report summarizes research to develop methods for the biosynthesis of substituted o-aminophenols from less expensive precursors such as substituted anilines, benzidine, and o-nitrophenols. One approach has been to exploit isolated enzymes to catalyze the desired reactions. Of the four enzymes we have studied for this purpose, tyrosinase shows the most promise. This enzyme has the desired catalytic activity, catalyzing the ortho hydroxylation of several anilines and benzidines, but the reaction rate is 100-fold slower than with phenols and an exogenous reductant must be added to the reaction to inhibit the enzyme-catalyzed oxidation of the desired o-aminophenol. As an alternative to this approach, we investigated the biosynthesis of o-aminophenols via bacterial reduction of o-nitrophenols. Bacterial strain PI1, a GE isolate, catalyzes the reduction of nitroaromatic compounds. This bacterium, identified as a Group D Streptococci, has broad substrate specificity for this nitro-reductase activity and good viability under high product and substrate concentrations. GRA

N91-26679# Ames Lab., IA.
ELECTRONIC EXCITATION TRANSPORT IN PHOTOSYNTHESIS AND CRYSTAL AND MOLECULAR STRUCTURES OF PORPHYRIN COMPOUNDS Ph.D. Thesis
Shumei Yang 22 Apr. 1991 276 p
(Contract W-7405-eng-82)
(DE91-012024; IS-T-1513) Avail: NTIS HC/MF A13

The excitation energy transfer in three photosynthetic organism samples, Bacteriochlorophyll a-protein from Prosthecochloris aestuarii, and enriched photosystem 1 particles from spinach chloroplasts, have been investigated by pump-probe ultrafast spectroscopy. The isotropic photobleaching profiles were best described by two exponential decay components in one Bchl a-protein complex, and three exponential decay components in another. The experimental results from the three samples show that nonrandom chromophore orientations exist and Sauer's pebble mosaic model is an appropriate one for excitation transfer in these samples. The polarized pump-probe transients have been analyzed in terms of an exciton hopping model that incorporates the known geometry of the Bchl a-protein. The crystal and molecular structures of four metalloporphyrins have been determined by x ray diffraction and molecular mechanics. DOE

N91-26680# Oak Ridge National Lab., TN.
INTRODUCTION TO SESSION 2: APPLIED BIOLOGICAL RESEARCH
G. W. Strandberg and A. L. Demain (Massachusetts Inst. of Tech., Cambridge.) 1991 2 p Presented at the 13th Symposium on Biotechnology for Fuels and Chemicals, Colorado Springs, 6-10 May 1991
(Contract DE-AC05-84OR-21400)
(DE91-012067; CONF-910550-1-Extd-Abst) Avail: NTIS HC/MF A01

The papers in this session continue in the tradition of presenting excellent research directed at the development of new and enhanced biological process through applied biological research. The majority of the research discussed entails the use of newer, molecular biological approaches which have added significantly to our abilities to understand and control microbial activities. DOE

N91-26681# California Univ., Berkeley. Lawrence Berkeley Lab.
FLUORESCENCE SPECTROSCOPY OF EXCITATION TRANSFER IN PHOTOSYSTEM 1 Ph.D. Thesis
I. Mukerji Dec. 1990 140 p
(Contract DE-AC03-76SF-00098)
(DE91-011867; LBL-30136) Avail: NTIS HC/MF A07

A study is presented of excitation transfer in a photosynthetic antenna array. The spectroscopic properties of two pigment-protein complexes were investigated. These complexes, isolated from higher plants, display an unusual temperature dependent fluorescence behavior. This fluorescence behavior was studied with respect to energy transfer to the reaction center and in an isolated intact antenna preparation. A Photosystem 1 complex, PSI-200, was isolated from spinach. This system was characterized by both steady state and time resolved fluorescence spectroscopy. Fluorescence polarization measurements indicate that this emission arises from pigments which absorb in the long wavelength region of the spectrum and comprise a relatively small portion of the antenna population. Comparison of spectral characteristics were made with a PSI complex isolated from the thermophilic cyanobacterium, Synechococcus, sp. To address the role of Chl b in stimulating long wavelength fluorescence and the temperature dependence of the system, the energy transfer dynamics were studied in an antenna complex, LHC-I isolated from PSI-200. Kinetic measurements indicate that initially absorbed excitation is rapidly redistributed to longer wavelength emitting pigments within 40 ps. The temperature dependence of F685 results from increased back transfer from long wavelength emitters to F685. It is suggested that changes in excitation transfer between the various emitting species and a non-radiative fluorescence quenching mechanism account for the temperature dependence of the system. DOE

N91-26682# Arizona Univ., Tucson. Dept. of Biochemistry.
PHOTOCHEMICAL ENERGY CONVERSION BY MEMBRANE-BOUND PHOTOREDOX SYSTEMS
G. Tollin 1991 5 p
(Contract DE-FG02-86ER-13631)
(DE91-012171; DOE/ER-13631/T1) Avail: NTIS HC/MF A01

We have developed a system for carrying out chlorophyll (chl)-photosensitized vectorial transbilayer electron transfer from

reduced cytochrome c (cyt) in the inner aqueous compartment of negatively charged unilamellar lipid bilayer vesicles to oxidized ferridoxin (fd) in the outer aqueous phase, with the viologen analog propylene diquat in the outer phase as a mediator. This was investigated using both laser flash and steady state photolysis techniques. The results demonstrate that triplet chl is initially quenched by viologen at the outer membrane surface to form chl cation radical and viologen radical, followed by a biphasic recombination. The slow phase represents reverse electron transfer and could be suppressed by reduction of the chl radical by reduced cyt at the inner vesicle surface, following transbilayer electron transfer, and by electron transfer from viologen radical to oxidized fd. These reactions lead to charge separation across the vesicular membrane. The yields are limited by the formation of the transmembrane potential and accumulation of oxidized cyt in the lumen of the vesicle. Addition of the ionophore valinomycin will diminish the membrane potential, and double the reaction yield. It is important to note that this system mimics one of the key events in photosynthesis (Photosystem 1) and results in appreciable energy storage in the reaction products (about 0.7 V). Reduction of cyt has been investigated at a Pt electrode modified with a lipid bilayer membrane with immobilized vinyl ferrocene as a mediator. The current-voltage curves show that the direct reduction of cyt at the electrode occurs quite efficiently, allowing us to calculate an absorption equilibrium constant and an electron transfer rate constant. These results suggest that biomembrane-like electrode surfaces have potential for metalloprotein electrochemistry, as well as the development of biosensors.

DOE

N91-26703# Joint Publications Research Service, Arlington, VA.
EFFECTS OF 13 DAY SPACE FLIGHT ON SKELETAL MUSCLES AND NEUROMUSCULAR JUNCTIONS IN RATS Abstract Only

O. M. Pozdnyakov, L. L. Babakova, M. S. Demorzhi, and Ye. I. Ilyina-Kakuyeva *In its* JPRS Report: Science and Technology. USSR: Life Sciences 20 May 1991 p 2 Transl. into ENGLISH from Kosmicheskaya Biologiya i Aviakosmicheskaya Meditsina (Moscow, USSR), v. 24, no. 5, Sep. - Oct. 1990 p 38-42 (For primary document see N91-26696 18-52)
Avail: NTIS HC/MF A03

N91-26704# Joint Publications Research Service, Arlington, VA.
EFFECT OF 7 DAY ANTIORTHOSTATIC HYPOKINESIA ON CARDIAC PUMPING ACTION IN MONKEYS Abstract Only

G. T. Kazakov and V. P. Krotov *In its* JPRS Report: Science and Technology. USSR: Life Sciences 20 May 1991 p 2-3 Transl. into ENGLISH from Kosmicheskaya Biologiya i Aviakosmicheskaya Meditsina (Moscow, USSR), v. 24, no. 5, Sep. - Oct. 1990 p 56-57 (For primary document see N91-26696 18-52)
Avail: NTIS HC/MF A03

52 AEROSPACE MEDICINE

Includes physiological factors; biological effects of radiation; and effects of weightlessness on man and animals.

N91-26683# Joint Publications Research Service, Arlington, VA.
JPRS REPORT: SCIENCE AND TECHNOLOGY. USSR: LIFE SCIENCES

6 May 1991 86 p Transl. into ENGLISH of various Russian articles
(JPRS-ULS-91-010) Copyright Avail: NTIS HC/MF A05

Abstracts of Soviet literature in various areas of the life sciences are compiled. The following subject areas are covered: aerospace medicine, biochemistry, biotechnology, epidemiology, medicine, microbiology, physiology, public health, radiobiology, and virology. For individual titles, see N91-26684 through N91-26687.

N91-26684# Joint Publications Research Service, Arlington, VA.
PHARMACOLOGICAL CORRECTION OF FUNCTIONAL CONDITION OF ARMY AIR FORCE FLYERS IN HOT CLIMATE WITH ASPARKAM Abstract Only

A. A. Bochenkov and V. A. Chvyakin *In its* JPRS Report: Science and Technology. USSR: Life Sciences 6 May 1991 p 1-2 Transl. into ENGLISH from Voyenno-Meditsinskiy Zhurnal (Moscow, USSR), no. 7, Jul. 1990 p 62-63 (For primary document see N91-26683 18-52)
Copyright Avail: NTIS HC/MF A05

Unfavorable conditions for flight personnel arise when crews fly modern aircrafts in a regions with a hot climate. The complex of climatic and geographical factors in such zones has a pronounced influence on the mechanisms of thermoregulation and the activity of systems such as cardiovascular system. Increasingly, a determination of the activity of succinate dehydrogenase (SDH) of the lymphocytes, a key enzyme of tissue respiration, was used to characterize the functional condition of the body. The drug Asparkam was used to adjust the functional condition of the flyer's body, in a dosage of one tablet three times per day for one month. The influence of the drug Asparkam in the flyer's body consisted of a positive trend in metabolic shifts and improved functional conditions of the body. Author

N91-26685# Joint Publications Research Service, Arlington, VA.
RISK FACTORS AND PREDICTION OF SYNCOPIC STATES IN FLYERS Abstract Only

B. Kh. Semenov *In its* JPRS Report: Science and Technology. USSR: Life Sciences 6 May 1991 p 2 Transl. into ENGLISH from Voyenno-Meditsinskiy Zhurnal (Moscow, USSR), no. 7, Jul. 1990 p 63 (For primary document see N91-26683 18-52)
Copyright Avail: NTIS HC/MF A05

On the basis of many years of investigation and clinical observation by specialists of civil aviation, risk factors were identified for the development of syncope in flyers - vascular and cardiac factors, the composition of the blood, autonomic tonus, factors which weaken the body, etc. The clinical data of 120 flight personnel were studied. On the basis of the findings of a correlation analysis, significant factors were discerned and given a rating on a point scale in accordance with the degree of closeness of the correlation curve. Author

N91-26686# Joint Publications Research Service, Arlington, VA.
SURVEY OF THE PRINCIPAL RESULTS OF MEDICAL RESEARCH IN THE FLIGHT PROGRAM OF THE SECOND MAIN EXPEDITION ABOARD THE MIR ORBITING COMPLEX Abstract Only

O. G. Gazenko, A. I. Grigoryev, S. A. Bugrov, A. D. Yegorov, V. V. Bogomolov, I. B. Kozlovskaya, and I. K. Tarasov *In its* JPRS Report: Science and Technology. USSR: Life Sciences 6 May 1991 p 2-3 Transl. into ENGLISH from Kosmicheskaya Biologiya and Aviakosmicheskaya Meditsina (Moscow, USSR), v. 24, no. 4, Jul. - Aug. 1990 p 3-11 (For primary document see N91-26683 18-52)
Copyright Avail: NTIS HC/MF A05

The mission of the second main expedition aboard the Mir/Soyuz-TM/Kvant/Progress orbiting complex is described. The scientific flight program included continuing study of Earth resources and conduct of meteorological, astrophysical, geophysical, biomedical, and other research. The scientific medical program consisted primarily in continuing and expanding research on the phenomenology and mechanisms of change in the conditions of the principal body systems in the various stages of a long flight and after the flight is over. Author

N91-26687# Joint Publications Research Service, Arlington, VA.
STATE-OF-THE-ART AUTOMATED EVALUATION OF FUNCTIONAL STATE OF THE BODY IN THE SPACE PROGRAM AND PREVENTIVE MEDICINE Abstract Only

B. A. Adamovich, R. M. Bayevskiy, A. P. Berseneva, and I. I. Funtova *In its* JPRS Report: Science and Technology. USSR: Life Sciences 6 May 1991 p 11-18 Transl. into ENGLISH from Kosmicheskaya Biologiya and Aviakosmicheskaya Meditsina

(Moscow, USSR), v. 24, no. 4, Jul. - Aug. 1990 p 11-18 (For primary document see N91-26683 18-52)
Copyright Avail: NTIS HC/MF A05

A scale consisting of four gradations of functional capacity was developed to evaluate adaptational potential (level of health): (1) high or adequate functional capacities of the body, satisfactory adaptation to environmental conditions; (2) a state of exertion of adaptive mechanisms that ensure sufficient functional capacities through the mobilization of additional functional reserves; (3) lowered functional capacities of the body, unsatisfactory adaptation to environmental conditions; and (4) low or minimal functional capacities of the body, failure of adaptation. The development of automated information analysis systems is discussed. One of the important objectives is the standardization and automation of the evaluation of the results of medical monitoring, which considerably raises the objectivity of medical conclusions concerning the body's functional capacities. Author

N91-26688# Joint Publications Research Service, Arlington, VA.
JPRS REPORT: SCIENCE AND TECHNOLOGY. USSR: LIFE SCIENCES
18 Apr. 1991 88 p Transl. into ENGLISH of various Russian articles
(JPRS-ULS-91-009) Avail: NTIS HC/MF A05

Abstracts and brief reports on a number of topics relative to life sciences research in the U.S.S.R are given. Topics covered include aerospace medicine, insecticides, biochemistry, biophysic, epidemiology, genetics, human factors engineering, radiation effects, toxicology, pharmacology, physiology, public health, radiation biology, and virology. For individual titles, see N91-26689 through N91-26695.

N91-26689# Joint Publications Research Service, Arlington, VA.
HORMONAL REGULATORS OF CALCIUM METABOLISM FOLLOWING SPACE FLIGHTS OF VARIOUS DURATIONS Abstract Only
L. G. Pozharskaya and V. B. Noskov *In its* JPRS Report: Science and Technology. USSR: Life Sciences 18 Apr. 1991 p 1 Transl. into ENGLISH from Kosmicheskaya Biologiya and Aviakosmicheskaya Meditsina (Moscow, USSR), v. 24, no. 4, Jul. - Aug. 1990 p 18-20 (For primary document see N91-26688 18-52)
Avail: NTIS HC/MF A05

The degree of parathormone, calcitonin, and gastrin system activity depending in the duration of weightlessness conditions was compared in 19 cosmonauts, 12 of which had seven-day flights, and 7 of which had flights lasting from 150 to 237 days. Blood samples were drawn 30 days before departure and 1, 7, and more days following arrival with the parathormone, calcitonin, and gastrin concentrations calculated using standard commercial test kits. Members of the short-term flight group exhibited a 45 percent average elevation in calcitonin, and a 44 percent gastrin content increase, while parathormone levels remained essentially unchanged. In members of the long-term flight group, parathormone levels were quite elevated and did not return to normal until 45 days after landing. Calcitonin levels were substantially depressed and in some subjects did not return to baseline levels by the end of the research period (45 days after landing). Gastrin levels were 3.3 times higher than pre-flight concentrations, and normalized within 45 days after returning to earth. The results demonstrated that parathormone and calcitonin help maintain calcium homeostasis by their opposite effects on calcium transport in the intestines and kidneys. The findings suggest that one of the reasons for hypergastrinemia following space flight may be the elevated parathormone level and abrupt decrease in calcitonin production. Furthermore, it is probable that components of the system maintaining calcium homeostasis vary depending on the duration of weightless and functional activity of the related regulatory systems. Author

N91-26690# Joint Publications Research Service, Arlington, VA.
COMPUTER TOMOGRAPHY MEASUREMENT OF VERTEBRAL BONES AND MUSCLES AFTER EXTENDED MANNED SPACE FLIGHTS Abstract Only
V. S. Oganov, K. Kann, A. S. Rakhmanov, and S. K. Ternovoy *In its* JPRS Report: Science and Technology. USSR: Life Sciences 18 Apr. 1991 p 1 Transl. into ENGLISH from Kosmicheskaya Biologiya and Aviakosmicheskaya Meditsina (Moscow, USSR), v. 24, no. 4, Jul. - Aug. 1990 p 20-21 (For primary document see N91-26688 18-52)
Avail: NTIS HC/MF A05

Computer tomography was employed to measure the mineral density of lumbar vertebrae spongy tissue and lumbar muscle mineral volume and density in four cosmonauts 1 to 3 months prior to and 20 to 27 days following extended space flights (5 and 7 months). The results demonstrated a 7.8 percent decrease in calcium density in the posterior vertebral bodies and a 4.4 percent decrease in spinal muscle volume. Studies on volunteers on earth demonstrated a decrease in mineral density in only 10 percent of the subjects. The lack of changes in some of the subjects in both groups was attributed to the effectiveness of preventive measures and defense mechanisms of the muscles and bones. The results demonstrated that the changes in bones and muscles were not dependent on the length of flight and that physical exercise did not completely prevent unfavorable changes. These data are of interest in assessing the risk of developing osteoporosis and the potential the skeleton has of losing its strength in conditions of weightlessness. Suggestions are also made for further studies on bone metabolism during space flights. Author

N91-26691# Joint Publications Research Service, Arlington, VA.
FUNCTIONAL ACTIVITY OF HYPOPHYSEAL-THYROID SYSTEM DURING 370-DAY ANTIORTHOSTATIC HYPOKINESIA Abstract Only
Ye. N. Kabitskiy *In its* JPRS Report: Science and Technology. USSR: Life Sciences 18 Apr. 1991 p 1-2 Transl. into ENGLISH from Kosmicheskaya Biologiya and Aviakosmicheskaya Meditsina (Moscow, USSR), v. 24, no. 4, Jul. - Aug. 1990 p 28-30 (For primary document see N91-26688 18-52)
Avail: NTIS HC/MF A05

Biochemical investigations of the hypophyseal-thyroid system were conducted on 10 healthy male volunteers at -5 degrees antiorthostic hypokinesia. The principal means of preventing tissue degeneration was physical exercise while lying down. Group A began exercising on day 20 of the experiment, while group B began 100 days later. The 11 blood samples taken throughout the experiment were used to calculate the concentrations of thyrotropic hormone of the adenohypophysis, free thyroxin (FT sub 4) bound with thyroxin (T sub 4), and triiodothreonine (T sub 3). Radioimmunologic assay data detected no change in (T sub 4) concentrations and only a partial decrease in thyrotropic hormone. The data on (FT sub 4) suggest that inhibitory dissociation of the protein-hormone bond occurs during antiorthostatic hypokinesia. The results demonstrated that the decreased concentrations of T3 observed during antiorthostatic hypokinesia may reflect a decrease in plastic metabolism. The data also indicate that depression of (T sub 3) and (F sib 4) levels is due to enhance rates of utilization of these hormones by tissues in connection with increased motor activity and anaerobic processes. These findings suggest that exercise in conjunction with antiorthistic hypokinesia decreases the role of the humoral factor in activation of the thyroid by the adenohypophysis. This leads to a slight decrease in thyroid activity which is manifest as a decrease in (FT sub 4) and (T sub 3) concentrations in the blood. Furthermore, these findings also demonstrated that exercise had no substantial effect on the functional activity of the hypophysis and thyroid. Author

N91-26692# Joint Publications Research Service, Arlington, VA.
CHANGES IN RHEOLOGIC INDICES OF BLOOD AND HEMODYNAMICS DURING 14-DAY ANTIORTHOSTATIC HYPOKINESIA Abstract Only

A. P. Ivanov, I. B. Goncharov, and L. G. Repenkova *In its* JPRS Report: Science and Technology. USSR: Life Sciences 18 Apr. 1991 p 2 Transl. into ENGLISH from Kosmicheskaya Biologiya and Aviakosmicheskaya Meditsina (Moscow, USSR), v. 24, no. 4, Jul. - Aug. 1990 p 30-32 (For primary document see N91-26688 18-52)
Avail: NTIS HC/MF A05

Rheologic indicies of the blood and hemodynamics were compared in nine essentially healthy men aged 25 - 42 years during various stages of 14-day antiorthostatic hypokinesia at -8 degrees. Blood was drawn from the cubital vein on days 3, 7, and 14 of antiorthostatic hypokinesia and exhibited a 124.4 percent increase in Cassion blood viscosity, a 25.9 percent decrease in stroke volume, a 25.5 percent decrease in minute circulating volume, and a 23.6 percent increase in total peripheral resistance. These data suggest that there is a close relationship between central hemodynamic and rheologic parameter indices in antiorthostatic hypokinesia. The negative correlation relationship between total peripheral resistance and the dynamic viscosity of the blood is apparently associated with an increases in total peripheral resistance and blood viscosity as a result of slower circulation. Stases develop in the venous and capillary sections of the peripheral vascular system, and some of the formed elements of the blood are excluded from active circulation. All of these effects result in the additional opening of arteriovenous anastomoses in order to support adequate stroke and minute volumes. It is hoped that these studies will contribute to an understanding of how to control high blood viscosity, one of the risk factors of developing ischemic heart disease. Author

N91-26693# Joint Publications Research Service, Arlington, VA.
HIGHER PLANTS AS PART OF BIOLOGICAL HUMAN LIFE SUPPORT SYSTEM Abstract Only **c54**
I. Ye. Ivanova, T. A. Derendyayeva, T. P. Alekhina, and Yu. I. Shaydorov *In its* JPRS Report: Science and Technology. USSR: Life Sciences 18 Apr. 1991 p 2 Transl. into ENGLISH from Kosmicheskaya Biologiya and Aviakosmicheskaya Meditsina (Moscow, USSR), v. 24, no. 4, Jul. - Aug. 1990 p 40-43 (For primary document see N91-26688 18-52)
Avail: NTIS HC/MF A05

The functional characteristics of a man-plant-mineralization system were studied using higher plants that perform a photoautotropic role with Chlorella in a biological life support system. Wheat, peas, carrots, beets, cabbage, etc., were hydroponically cultivated in a winter garden and periodically given nutrients. The plants were cultivated for 6 months at 22 - 25 C, 55 -70 percent relative humidity, with 24-hour per day lighting of 60 - 80 W/sq m for the vegetables and 125 - 185 W/ sq m for the wheat. The plants demonstrated maximum productivity during days 70 - 100 of the experimental period, when mineralization products, dying of organic waste, and human and algal waste products all acted on the plants. The increase in the edible biomass of all the vegetables except the carrots was less than in the control group. Calculations of the vegetable contents of sugars, cellulose, ascorbic acid, and carotene (carrots only) demonstrated a 2.5-fold increase in vitamin C content in carrots, and a 2.2-fold increase in vitamin C and fructose in beets, with a 2-fold decrease in glucose and sucrose in the latter. The cellulose content of the peas also decreased by 13 percent. These results demonstrated that higher plants and Chlorella are compatible in a common atmosphere. It was also shown that the nutritive solutions given to the plants did not increase plant productivity. The reasons for the low productivity of the plants in a closed system remain inexplicable and thus require further study. Author

N91-26694# Joint Publications Research Service, Arlington, VA.
BIOCHEMICAL ASPECTS OF HUMAN ADAPTATION TO COMBINED EFFECT OF ANTIORTHOSTASIS, DECREASED BAROMETRIC PRESSURE, AND INCREASED OXYGEN CONTENT Abstract Only
T. N. Balandina, Ye. I. Nikitin, Ye. A. Kovalenko, and V. P. Savina *In its* JPRS Report: Science and Technology. USSR: Life Sciences 18 Apr. 1991 p 2-3 Transl. into ENGLISH from Kosmicheskaya Biologiya and Aviakosmicheskaya Meditsina (Moscow, USSR), v. 24, no. 4, Jul. - Aug. 1990 p 56-57 (For primary document see N91-26688 18-52)
Avail: NTIS HC/MF A05

The effects of relatively slight hyperoxia (pO2 of 300 mm Hg) for 5 h and -8 degrees antiorthostasis were assessed on seven men aged 25 - 35 years in an altitude chamber set at 7,100 m. The test subjects were also exposed to thermal (37 C) and physical stress (600 kg/m/min) for 5 min in the first, third, and fifth hours in the chamber and for 25 min also during the fifth hour. Venous blood was drawn before and after each trial for purposes of calculating malonic dialdehyde and self-induced lipid peroxidation levels. The results demonstrated that during the five-hour antiorthostatic period without exertion, erythrocytic catalase activity activated the protection antioxidant system, while the formation of self-induced lipid peroxidation with exertion, the opposite was observed, i.e., normalization of metbolism. The results of the biochemical investigations as a whole suggest that in 5 h of antiorthostasis at -8 degrees without exertion and with a pO2 of 300 mm Hg there is an aspect of stressing erythrocyte metabolism and compensating reactions. It was established that physical exercise in both regimens stabilizes the metabolic equilibrium that was distributed in the cells, which is reflected in retention of the structural integrity of the erythrocyte membrane. In addition, considering the degree of expression of the changes observed and signs of reparations of the erythrocyte membrane, these manifestations are judged to be functionally somewhat reversible, structural changes. Author

N91-26695# Joint Publications Research Service, Arlington, VA.
INDIVIDUAL STEREOTYPES OF HUMAN NEUROPSYCHIC PROGNOSTIC ACTIVITY IN PROBLEM SITUATIONS WITH DIFFERENT PROBABILITY STRUCTURES **c53**
A. Krauklis and I. Kazanovskaya *In its* JPRS Report: Science and Technology. USSR: Life Sciences 18 Apr. 1991 p 19-25 Transl. into ENGLISH from Izvestiya Latviyskoy Akademii Nauk (Riga, USSR), no. 9, Sep. 1990 p 86-96 (For primary document see N91-26688 18-52)
Avail: NTIS HC/MF A05

The formation of man's adaptive psychophysiological reactions, their individual variants and different degrees of adaptive effectiveness in problem situations were studied by a decision-making model. It was established that the form of manifestation depends in the probability structure of the problem situation. Every subject displayed substantial difference in individual speed in forming an adequate pattern of action after a stereotype signal sequence, with motor automation preceding detection of the stereotype signal sequence. On the basis of the time required by the subjects to detect the stereotype presentation of signals, the dynamics of the problem-solving time and the intensity of effector reactions, individual variants of neuropsychic self-regulation stereotypes characterized by differing adaptive effectiveness were revealed. Author

N91-26696# Joint Publications Research Service, Arlington, VA.
JPRS REPORT: SCIENCE AND TECHNOLOGY. USSR: LIFE SCIENCES
20 May 1991 27 p Transl. into ENGLISH of various Russian articles
(JPRS-ULS-91-011) Avail: NTIS HC/MF A03

Topics addressed include: aerospace medicine; biochemistry; environment; genetics; immunology; laser bioeffects; and clinical medicine. For individual titles, see N91-26697 through N91-26707.

N91-26697# Joint Publications Research Service, Arlington, VA.
VISUAL ACCOMMODATION IN COSMONAUTS Abstract Only
I. A. Skiba, V. K. Tkachenko, and I. A. Plyasova-Bakunina *In its* JPRS Report: Science and Technology. USSR: Life Sciences 20 May 1991 p 1 Transl. into ENGLISH from Kosmicheskaya Biologiya i Aviakosmicheskaya Meditsina (Moscow, USSR), v. 24, no. 5, Sep. - Oct. 1990 p 14-16 (For primary document see N91-26696 18-52)
Avail: NTIS HC/MF A03

Ophthalmoergographic studies were conducted on three cosmonauts before, during, and after space flight to assess visual accommodation. The results revealed various degrees of deterioration in visual accommodation due to peripheral and central fatigue as a result of overload on the visual analyzer. The findings point to the need for improving illumination aboard spacecraft and mitigation of close-up work to the extent possible. Additional measures will have to include prophylactic measures as well as to render the visual system more tolerant of prolonged stress.

Author

N91-26698# Joint Publications Research Service, Arlington, VA.
VESTIBULAR REACTIONS AND INTERSENSORY INTERACTIONS IN WEIGHTLESSNESS: RESULTS OF OPTOKINEZ EXPERIMENT Abstract Only

L. N. Kornilova, G. Bodo, I. K. Tarasov, and V. N. Alekseyev *In its* JPRS Report: Science and Technology. USSR: Life Sciences 20 May 1991 p 1 Transl. into ENGLISH from Kosmicheskaya Biologiya i Aviakosmicheskaya Meditsina (Moscow, USSR), v. 24, no. 5, Sep. - Oct. 1990 p 16-20 (For primary document see N91-26696 18-52)

Avail: NTIS HC/MF A03

The responsiveness of opto- and vestibulooculomotor systems was analyzed in the course of Optokinez experiment performed in 1984 on cosmonauts involved in a joint 7-day Soviet-Indian space flight, and during a 237-day mission aboard Salyut-7 space station. Although the subjects did not complain of motion sickness, the resultant data demonstrated that weightlessness enhanced spontaneous eye movements (including nystagmus in one crew member), and led to deterioration of saccadic tracking, diminished the amplitude of saccadic movements and incidence of corrective microsaccades in fixation events. Compensatory counter-movement of the eyes during sidewise head movements was diminished while wearing dark glasses, but did not disappear and was accompanied by low amplitude nystagmus. The findings were interpreted as a reflection of enhanced dynamic excitability of visual and vestibular afferent pathways and diminished static vestibular excitability. The diminished sensory response thresholds were attributed to the interplay of diminished proprioceptive inflow and abatement of corticofugal outflow, a combination which attenuates inhibition of subcortical formations by cortical regions. A more comprehensive assessment of the intersensory interactions would need to consider the effects of weightlessness on fluid displacement in the vestibular apparatus and its effects on brain function.

Author

N91-26699# Joint Publications Research Service, Arlington, VA.
EFFECT OF EXCESS RESPIRATORY RESISTANCE ON PHYSICAL PERFORMANCE AND CARDIORESPIRATORY FUNCTION Abstract Only

A. S. Barer, I. S. Breslav, G. G. Isayev, and Ye. A. Sokol *In its* JPRS Report: Science and Technology. USSR: Life Sciences 20 May 1991 p 1 Transl. into ENGLISH from Kosmicheskaya Biologiya i Aviakosmicheskaya Meditsina (Moscow, USSR), v. 24, no. 5, Sep. - Oct. 1990 p 20-22 (For primary document see N91-26696 18-52)

Avail: NTIS HC/MF A03

An analysis was conducted on the effects of increased respiratory resistance on physical performance and cardio-respiratory function. The study involved 13 healthy males, 22 to 47 years old, subjected to an increasing physical load on an exercise bicycle at a rate of 30 W every 3 min in conjunction with respiratory (inhalatory and expiratory) resistance of 12, 16, 20 or 40 cm H2/L x sec. The results showed that the maximum physical load tolerated under these conditions was inversely related to the square root of the increase in respiratory resistance multiplied by 1.5.

Author

N91-26700# Joint Publications Research Service, Arlington, VA.
EFFECT OF SHIFT WORK OF AIR TRAFFIC CONTROLLERS ON SYMPATHETIC NERVOUS SYSTEM Abstract Only **c53**

Ye. L. Kan and V. A. Kupriyanov *In its* JPRS Report: Science and Technology. USSR: Life Sciences 20 May 1991 p 1-2 Transl. into ENGLISH from Kosmicheskaya Biologiya i Aviakosmicheskaya Meditsina (Moscow, USSR), v. 24, no. 5, Sep. - Oct. 1990 p 22-25 (For primary document see N91-26696 18-52)

Avail: NTIS HC/MF A03

A comprehensive analysis was conducted on humoral factors reflective of the sympathetic nervous system (SNS) in 21 male air traffic controllers, 25 to 35 years old. Urinary monitoring demonstrated that night shift represented the most stressful job situation despite the relatively light work load and was attended by highest excretion of norepinephrine. In addition, individuals were identified during every shift (early morning, day, night) who presented with diminished catecholamine excretion, indicative of adaptive failure and depletion of the functional reserves of the SNS. Correlation of norepinephrine excretion with epinephrine concentrations demonstrated synchronization between neural and endocrine mechanisms in adaptation to working conditions. However, negative correlation coefficients between norepinephrine and DOPA and dopamine, especially during night work, provided further evidence of SNS exhaustion.

Author

N91-26701# Joint Publications Research Service, Arlington, VA.
PHYSICAL AND PSYCHOGENIC SEQUELAE OF IMPACT ACCELERATION ON TRACKING PERFORMANCE OF OPERATORS Abstract Only

A. K. Yepishkin *In its* JPRS Report: Science and Technology. USSR: Life Sciences 20 May 1991 p 2 Transl. into ENGLISH from Kosmicheskaya Biologiya i Aviakosmicheskaya Meditsina (Moscow, USSR), v. 24, no. 5, Sep. - Oct. 1990 p 28-30 (For primary document see N91-26696 18-52)

Avail: NTIS HC/MF A03

An analysis was conducted on the psychogenic and physical factors of impact acceleration (10 to 16 Gs) as they affect tracking performance. The study was performed on nine healthy males, 18 to 20 years of age, subjected to six impact acceleration events in the head-pelvis projection (1 to 2 experiments/day at 2 to 4 day intervals). Tracking and heart rate were monitored before and after the impact. The results demonstrated that impact acceleration increased both the error rate and the response time to changes in signal frequency. In addition, psychogenic factors, as deduced from the heart rate, were of major importance in determining the error rate. Accordingly, the mental stress represented by anticipation of the impact acted synergestically with physical stress on sensorimotor performance. Nevertheless, with repetition the degree of sensorimotor disturbances abated after successive impacts, and tracking performance improved. Consequently, emotional factors were shown to have positive and negative components, suggesting that a proper training and preparation may be employed in averting deterioration of sensorimotor performance due to physical stress.

Author

N91-26702# Joint Publications Research Service, Arlington, VA.
REACTION OF HUMAN SKELETAL MUSCLE FIBERS TO 370 DAY ANTIORTHOSTATIC HYPOKINESIA COMBINED WITH PHYSICAL EXERTION Abstract Only

S. L. Kuznetsov and V. V. Stepanov *In its* JPRS Report: Science and Technology. USSR: Life Sciences 20 May 1991 p 2 Transl. into ENGLISH from Kosmicheskaya Biologiya i Aviakosmicheskaya Meditsina (Moscow, USSR), v. 24, no. 5, Sep. - Oct. 1990 p 34-38 (For primary document see N91-26696 18-52)

Avail: NTIS HC/MF A03

Ten healthy males, 27 to 44 years old, were subjected to a 370 antiorthostatic (-8 degrees head inclination) hypokinesia to assess the effects of various schedules of physical activity on skeletal muscles at the ultrastructural level. Examination of biopsies obtained from the gastrocnemius muscle showed that prolonged antiorthostatic hypokinesia led to astrophobic changes and attenuation of metabolic processes. Regular periods of exercise had beneficial effects on averting adverse changes, with the benefits showing a direct correlation with intensity and early institution. The exercise program was far less effective when delayed to the 120th day of bedrest. In general, examination of

the myofibrils demonstrated that exercise-promoted recovery was favored by retention of normal structural relationships between actin and myosin. Author

N91-26703# Joint Publications Research Service, Arlington, VA.
EFFECTS OF 13 DAY SPACE FLIGHT ON SKELETAL MUSCLES AND NEUROMUSCULAR JUNCTIONS IN RATS Abstract Only **c51**
O. M. Pozdnyakov, L. L. Babakova, M. S. Demorzhi, and Ye. I. Ilyina-Kakuyeva *In its* JPRS Report: Science and Technology. USSR: Life Sciences 20 May 1991 p 2 Transl. into ENGLISH from Kosmicheskaya Biologiya i Aviakosmicheskaya Meditsina (Moscow, USSR), v. 24, no. 5, Sep. - Oct. 1990 p 38-42 (For primary document see N91-26696 18-52)
Avail: NTIS HC/MF A03

Ultrastructural studies were performed on the soleus, gastrocnemius, and diaphragmatic muscles of 334 g Wistar rats to assess the effect on a 13 day space flight aboard a Cosmos biosatellite. The study was designed to assess changes occurring in skeletal muscles differing in normal physiological requirements for contraction. Accordingly, minimal adverse changes of a readily reversible nature were evident in the diaphragm. The atrophic changes were more pronounced in the gastrocnemius muscles than in the soleus, again confirming the fact that baseline activity was a key factor in tolerating the adverse effects of weightlessness. Assessment of neuromuscular junctions paralleled the results obtained with the muscles. Fragmentation of the junctions was most pronounced in the gastrocnemius and was compounded by macrophage invasion. Author

N91-26704# Joint Publications Research Service, Arlington, VA.
EFFECT OF 7 DAY ANTIORTHOSTATIC HYPOKINESIA ON CARDIAC PUMPING ACTION IN MONKEYS Abstract Only **c51**
G. T. Kazakov and V. P. Krotov *In its* JPRS Report: Science and Technology. USSR: Life Sciences 20 May 1991 p 2-3 Transl. into ENGLISH from Kosmicheskaya Biologiya i Aviakosmicheskaya Meditsina (Moscow, USSR), v. 24, no. 5, Sep. - Oct. 1990 p 56-57 (For primary document see N91-26696 18-52)
Avail: NTIS HC/MF A03

The effects of a 7 day antiorthostatic, hypokinetic regimen on the pumping and contractile activity of the left ventricle were studied in three rheses monkeys, weighing 4.9 kg. The results showed that a -20 degree inclination resulted in a significant decrease in the end diastolic volume (12 percent), as well as a reduction in the stroke index (7 percent), end systolic volume (6 percent), ejection fraction (4 percent) and delta S (7 percent). The heart rate and cardiac index were increased by 15 and 11 percent, respectively. The changes became even more pronounced after seven days when the animals were returned to the horizontal position, with the exception of the ejection fraction and delta S which remained unaltered. Consequently, the sequelae of seven days of antiorthostatic hypokinesia consisted of diminished venous return and only moderate abatement of left ventricular contractility. Author

N91-26705# Joint Publications Research Service, Arlington, VA.
DIAGNOSTIC UTILITY OF CONTINUOUS NONINVASIVE BLOOD PRESSURE MONITORING (PENAZ METHOD) IN GRAVITY-INDUCED BLOOD REDISTRIBUTION Abstract Only
V. Yu. Lukyanyuk, A. R. Kotovskaya, I. F. Vil-Vilyams, L. Novak, Ya. Penyaz, V. M. Mikhaylov, Yu. D. Pometov, V. S. Georgiyevskiy, G. F. Nikolashin, and V. I. Kuzina *In its* JPRS Report: Science and Technology. USSR: Life Sciences 20 May 1991 p 3-4 Transl. into ENGLISH from Kosmicheskaya Biologiya i Aviakosmicheskaya Meditsina (Moscow, USSR), v. 24, no. 5, Sep. - Oct. 1990 p 30-34 (For primary document see N91-26696 18-52)
Avail: NTIS HC/MF A03

The Penaz method of continuous, noninvasive monitoring of arterial blood pressure (BP) was assessed for its diagnostic utility vis-a-vis syncope resulting from redistribution of blood volume. The method is based on measuring BP in a finger, with the palm maintained at heart level. The study was conducted on 25 to 45 year old subjects after 240 days of simulated weightlessness (antiorthostasis at -8 degrees), and involved passive antiorthostatis at 75 degrees for 20 min or negative pressure suits (-25 to -60 mm Hg) on the lower half of the trunk for 25 min. The results demonstrated that incipient syncope was preceded by onset of second and third order BP waves on servotonograms. In addition, appearance of these wave patterns was accompanied by a sharp fall in pulse pressure to critical levels due to reduction in the stroke volume and diminished venous return. The Penaz method was demonstrated to provide an earlier indication of such events than the use of discrete methods for BP monitoring. Author

N91-26706# Joint Publications Research Service, Arlington, VA.
STATE AND FORMS OF ADAPTATION OF VESTIBULAR FUNCTION AFTER SPACE FLIGHTS Abstract Only
L. N. Kornilova and I. K. Tarasov *In its* JPRS Report: Science and Technology. USSR: Life Sciences 20 May 1991 p 4 Transl. into ENGLISH from Vestnik Otorinolaringologii (Moscow, USSR), no. 6, Nov. - Dec. 1990 p 22-27 (For primary document see N91-26696 18-52)
Avail: NTIS HC/MF A03

Electrooculographic studies revealed the state of vestibular function and the sensory systems interacting with it 30 days before a flight and on 0-1, 2-3, 5-6, 8-10 and, sometimes, 14-15 and 75 days after the flight. The study assessed the characteristics of spontaneous nystagmus and positional nystagmus after passive (on a tilt-table) changes of body position and during vestibular, oculovestibular, proprioceptive stimulation and during cerebellar tests in the sitting position, clinostatic, antiorthostatic and orthostatic positions. All cosmonauts (except some crew commanders) displayed signs of vestibular dysfinction with differing degrees of pronouncement of illusory, motor and autonomic reactions. The dysfunction was transitory and reflected normally proceeding adaptation to a new sensory environment. The procedure employed permitted differentiation of mechanisms of vestibular dysfunction revealed after the flight. Some cosmonauts showed nystagmoid responses only in tilt-table tests while others displayed them as a result of additional proprioceptive and oculovestibular stimulation and in cerebellar coordination tests. The study made it possible to differentiate pathogenesis of vestibular dysfunctions and to study ways and forms of adaptation of vestibular function to gravitation. Author

N91-26707# Joint Publications Research Service, Arlington, VA.
COMBINED EFFECT OF NOISE AND VIBRATION ON CELLS OF AUDITORY AND VESTIBULAR APPARATUS Abstract Only
A. S. Nekhoroshev and A. N. Ignatyuk *In its* JPRS Report: Science and Technology. USSR: Life Sciences 20 May 1991 p 4 Transl. into ENGLISH from Vestnik Otorinolaringologii (Moscow, USSR), no. 6, Nov. - Dec. 1990 p 27-30 (For primary document see N91-26696 18-52)
Avail: NTIS HC/MF A03

A study of the effect of whole-body vertical vibrational acceleration with a peak at mean geometric frequencies of 31.5 and 60 Hz octave bands, equalling 66 and 76 dB respectively and constant wide-band noise with sound pressure of 85 DBa and 90 dBLin on the membranous labyrinth of the cochlea and receptor cells of the semicircular canals was described and discussed. Male guinea pigs (90) underwent the effect of these factors for 1, 5, 10, 15, 20, 60, and 90 days for 3 hours daily. After the experiments, the guinea pigs were decapitated and histological sections were studied by electron microscopy. The combined effect of the noise and vibration injured the receptor cells of the auditory analyzer and affected the spiral organ especially. Changes observed appeared as rhythmic functional pulsation of the nuclei with deformation of the cellular nuclei in some cases. The phenomena increased with an increase of the duration of effect and embraced almost all sensitive cells of the spiral organ. Electron microscopy data showed changes not only of the nuclei of the injured sensitive cells but also of the endoplasmic reticulum of the cytoplasm, especially with changes

of the mitochondria and simultaneous changes of the endoplasmic reticulum membranes. These changes were reversibly for up to 20 days. After longer exposure (60 and 90 days) changes in hair cells of the spiral organ involving deformation and disintegration of chromatin, mitochondria, and endoplasmic reticulum membranes were irreversible and caused decay of the injured cells. Author

N91-26708# California Univ., Los Angeles.
PEPTIDE TRANSPORT THROUGH THE BLOOD-BRAIN BARRIER Final Report, 1 Jul. 1987 - 31 Dec. 1990
William M. Partridge 15 Jan. 1991 15 p
(Contract DAMD17-87-C-7137; DA Proj. 3M1-61102-BS-12)
(AD-A233753) Avail: NTIS HC/MF A03 CSCL 06/1

Most neuropeptides are incapable of entering the brain from blood owing to the presence of unique anatomical structures in the brain capillary wall, which makes up the blood-brain barrier (BBB). Such neuropeptides could be introduced into the bloodstream by intranasal insufflation and, thus, could have powerful medicinal properties (e.g., Beta-endorphin for the treatment of pain, vasopressin analogues for treatment of memory, ACTH analogues for treatment of post-traumatic epilepsy), should these peptides be capable of traversing the BBB. One such strategy for peptide delivery through the BBB is the development of chimeric peptides, which is the basis of the present contract. The production of chimeric peptides involves the covalent coupling of a nontransportable peptide (e.g., Beta-endorphin, vasopressin) to a transportable vector peptide (e.g., insulin, transferrin, cationized albumin, histone). The transportable peptide is capable of penetrating the BBB via receptor-mediated or absorptive-mediated transcytosis. Therefore, the introduction of chimeric peptides allows the nontransportable peptide to traverse the BBB via a physiologic piggy back mechanism. GRA

N91-26709# Naval Medical Research Inst., Bethesda, MD.
YOUNG AND OLDER OBSERVERS SHOW SIMILAR PERCEIVED CONTRAST FUNCTIONS FOR ISOLUMINANT STIMULI Technical Report, Oct. 1984 - Sep. 1990
Karl F. VanOrden and Joseph F. Sturr Jan. 1991 28 p
(DA Proj. 3M4-63764-B-995)
(AD-A233766; NMRI-91-09) Avail: NTIS HC/MF A03 CSCL 06/4

Previous research from our laboratory has demonstrated an age-related difference in the perceived brightness of brief, low intensity flashes of light. The purpose of this experiment was to determine if the age-related brightness differences would generalize to isoluminant conditions. Thus, the effect of age on visual system contrast gain was examined by use of sinusoidal grating stimuli with the method of contrast estimation. Ten young and 10 older males (mean ages 20 and 64.5 yrs) viewed counterphase flickered gratings of 0.6 and 6.0 c/deg ranging in contrast from 1 to 50 percent. The resulting linear functions of log perceived contrast as a function of log stimulus contrast showed no age-related differences and suggest equivalent contrast gain with age. These results, placed within the context of previous research, suggest that the largest age-related differences in visual performance are found when subjects must perform a detection/recognition task that is embedded in a flashing background. GRA

N91-26710# Naval Medical Research Inst., Bethesda, MD.
COLDEX-86: PHYSICAL WORK CAPACITY DURING PROLONGED COLD WATER IMMERSION AT 6.1 msw Technical Report, May - Sep. 1986
T. J. Doubt and D. J. Smith Dec. 1990 33 p
(AD-A233767; NMRI-90-135) Avail: NTIS HC/MF A03 CSCL 06/5

Response to submaximal leg exercise was quantified in 16 U.S. Navy divers who performed whole body immersions in 5 C water for periods of up to 6 h. Diverse wore passive dry suit thermal protection. Immersions were done during the course of 5-day air saturation dives at a depth of 6.1 msw (20 fsw). Each diver participated in 2 saturation dives. Two immersions were conducted per dive, one beginning at 1000 h, and one beginning at 2200 h; there was a period of 54 h between immersions. During the second saturation dive the presentation of immersion times was reversed. The subjects performed leg exercise on a cycle ergometer for 3 min each at workloads of 50, 70, and 90 watts (W). Heart rate (HR) and O2 consumption (VO2) were measured during the last minute at each workload. The study was divided into 2 series. GRA

N91-26711# Naval Medical Research Inst., Bethesda, MD.
COLDEX-86: FLUID AND ELECTROLYTE CHANGES DURING PROLONGED COLD WATER IMMERSION Technical Report, May 1986 - Aug. 1987
P. A. Deuster, D. J. Smith, B. L. Smoak, L. C. Montgomery, and T. J. Doubt Dec. 1990 56 p
(AD-A233768; NMRI-90-133) Avail: NTIS HC/MF A04 CSCL 07/4

Dehydration and hypothermia are major inhibitors of diver performance in cold water. To characterize the dehydration that accompanies cold water immersion, 16 U.S. Navy divers participated in two 5-day air saturation dives (ASD) at a depth of 6.1 meters sea water (msw). During each ASD, divers completed two immersions in 5 C water: one began at 1000 h (AM) and the other at 2200 h (PM); a period of 54 h separated the immersions. Divers wore dry suits for thermal protection, and full face masks during immersions that lasted 3-6 h. All divers consumed identical diets. Blood samples were collected before and after each immersion, and urine was collected for 24 h in three separate periods on immersion days: for 12 h prior to immersion, during immersion, and after immersion until the end of the 24 h period. Plasma volume decreased significantly by approximately 17 percent during both AM and PM immersions. GRA

N91-26712# Rockefeller Univ., New York, NY.
CARBOXYALKYLATED HEMOGLOBIN AS A POTENTIAL BLOOD SUBSTITUTE Annual Report, 1 Sep. 1989 - 31 Aug. 1990
James M. Manning 25 Sep. 1990 29 p
(Contract DAMD17-88-C-81699)
(AD-A233822) Avail: NTIS HC/MF A03 CSCL 06/1

A new crosslinking agent for hemoglobin, a diisothiocyanobenzene sulfonate derivative, has been explored this past year. The yield of crosslinked products (5 to 6) is high (about 75 percent) and all the crosslinking is within the tetramer to produce 64,000 molecular weight species, which do not dissociate. The major crosslinked component was purified and the position of the crosslink was established by a combination of amino acid analysis, protein sequencing and mass spectral analysis. Its single crosslink was found to be between the NH2-terminal residues of the alpha-chains. In a collaborative effort, the material was supplied to the Letterman Army Institute of Research. That investigation found that the plasma retention time of this species in rats was prolonged almost 4-fold to an average of 3.1 hrs, compared to 0.7 hrs for uncrosslinked, carboxymethylated hemoglobin. Therefore, the plasma retention time is related to the crosslinking hemoglobin but not to its oxygen affinity. GRA

N91-26713# Louisiana State Univ., New Orleans.
METABOLIC CHANGES AND HEMODYNAMIC DYSFUNCTION FOLLOWING HYPOTHERMIC SHOCK Status Report, 1 Oct. 1990 - 31 Jan. 1991
Harvey I. Miller 1 Oct. 1990 10 p
(Contract N00014-89-J-3124)
(AD-A233942) Avail: NTIS HC/MF A02 CSCL 06/10

Shock, which is the result of acute and severe accidental hypothermia, can produce subtle injuries to several organs. The manifestations of these injuries are difficult to observe because of compensatory mechanisms; however, they can persist many hours past the return to normal body temperature. The severity of these organ dysfunctions is not always great but coupled with other changes can jeopardize the survival of the victim. The purpose of these investigations is to uncover the mechanisms which produce the dysfunctions and determine proper therapeutic procedures to stop and reverse this pathological process. One of the therapeutic interventions which is being studied is fluid resuscitation, which is

applied during the short rewarm period. We have shown that following hypothermia and rewarm a cardiac dysfunction persists over 48 hours. This dysfunction is hidden in the whole intact animal because of the cardiovascular compensatory mechanism. GRA

N91-26714# City of Hope Medical Center, Duarte, CA.
EVALUATION OF LIPOSOME-ENCAPSULATED HEMOGLOBIN/LR16 FORMULATION AS A POTENTIAL BLOOD SUBSTITUTE
Thomas G. Burke 15 Mar. 1991 6 p
(Contract N00014-90-J-1648)
(AD-A233973; Rept-1) Avail: NTIS HC/MF A02 CSCL 06/5

During the last four months of our project entitled, Evaluation of Liposome-Encapsulated Hemoglobin/LR16 Formulation as a Potential Blood Substitute, efforts have been made in the following four areas: (1) the resynthesis of LR16; (2) physical characterization of LEH/LR16 formulations; (3) design and development of membrane-impermeable LR16 analogues; and (4) preparations for small animal testing of surrogate blood preparations. The work completed in each of these areas is outlined below. GRA

N91-26715# Naval Medical Research Inst., Bethesda, MD.
COLDEX-86: SUMMARY OF THE EXPERIMENTAL PROTOCOL AND GENERAL RESULTS Technical Report, May - Sep. 1986
T. J. Doubt, R. P. .Weinberg, D. J. Smith, P. A. Deuster, and A. J. Dutka Dec. 1990 28 p
(AD-A234031; NMRI-90-132) Avail: NTIS HC/MF A03 CSCL 13/10

Aspects of temperature regulation, exercise capacity, and passive rewarming were evaluated during planned 6 h immersions in 5 deg C (41 deg F) water. A total of 16 divers (12 First Class divers, 4 SEALs) performed 63 manned immersions. Each diver wore a full face mask (modified AGA mask) and breathed compressed air at 6.1 msw (20 fsw). A butyl-nylon dry suit with M-600 Thinsulate thermal protection undergarments was worn. Hands were protected with a M-200 Thinsulate glove worn beneath a water tight latex glove; a neoprene outer gauntlet mitt was worn over the latex glove. The divers completed two 5 day air saturation dives at 6.1 msw, with a week separating dives. Each diver made two immersions during the dives, with 54 hours between immersions. One immersion began at 1000 hours (AM dive) and the other at 2200 hours (PM dive). The order of presentation of AM and PM dives was varied among the subjects. During one saturation dive the divers were fed a high carbohydrate diet, while during the second dive the drivers were fed a standard American mixed diet. Both diets provided 3000 kcal per day. Urine and venous blood samples were obtained before and after each immersion. Urine was also collected during the immersion. Body temperatures, regional heat fluxes, oxygen consumption, and EKG recordings were obtained throughout the immersion. GRA

N91-26716# Illinois Univ., Chicago.
ATTENTION SPAN, ANXIETY, AND BENZODIAZEPINE RECEPTORS Final Report, 1 Jul. 1987 - 30 Dec. 1990
Thaddeus J. Marczynski 26 Feb. 1991 60 p
(Grant AF-AFOSR-0364-87; AF Proj. 2312)
(AD-A234549; AFOSR-91-0283TR) Avail: NTIS HC/MF A04 CSCL 15/6

The specific (H-3) flunitrazepam binding to neocortical and hippocampal membranes was measured following a two week treatment of rats with the benzodiazepine receptor antagonist flumazenil (FL; Ro 15-1788; 2.7 or 4 mg/kg/day in drinking water). The binding sites showed a gradually increasing density, which remained elevated for up to 24 and 72 hours after drug withdrawal. The dissociation constants (Kd) for the ligand remained largely unchanged. Most importantly, a strong coupling between the GABA and the benzodiazepine recognition sites was found in the cortex but not in the hippocampus, as measured by reduction in GABA enhanced (H-3) flunitrazepam bindings to neuronal membranes from FL- treated animals killed 72 hours after drug withdrawal. The behavioral correlates of chronic exposure of adult rats to FL are presented. GRA

N91-26717# Naval Health Research Center, San Diego, CA.
SMOKING, EXERCISE, AND PHYSICAL FITNESS Interim Report
Terry L. Conway and Terry A. Cronan 30 Nov. 1990 22 p
(AD-A234658; NHRC-90-43) Avail: NTIS HC/MF A03 CSCL 06/5

Research on smoking and physical activity provides strong evidence of smoking's negative impact and physical activity's positive impact on long-term health. However, evidence is lacking on the association between smoking and spontaneous exercise activity and the independent effects of these factors on physical fitness. These factors were studied in 3,045 Navy personnel. Smoking was clearly associated with lower exercise levels and lower physical endurance (cardiorespiratory and muscular) even after controlling for exercise. Smoking was not related to overall body strength (lean body mass) nor percent body fat after controlling for exercise. These findings suggests that both the direct and indirect links among smoking, exercise, and physical fitness should be explored in model's examining health. GRA

N91-26718# Naval Health Research Center, San Diego, CA.
METHYLPHENIDATE AND PEMOLINE: EFFECTS ON SLEEPINESS AND MOOD DURING SLEEP DEPRIVATION Interim Report
4 Mar. 1991 16 p
(AD-A234659; NHRC-90-41) Avail: NTIS HC/MF A03 CSCL 06/10

Thirty-six male subjects (mean age = 20.94) participated in a study of the effects of methylphenidate (10 mg every 6 hours; 8 doses) or pemoline (37.5 mg every 12 hours; 4 doses) in maintaining alertness during 64 hours of sleep deprivation. Subjective sleepiness was measured by a Visual Analog Scale (VAS), objective sleepiness by the number of lapses (intertap interval 3 seconds) on a 10 minute tapping task, and mood by the Profile of Mood States (POMs). Results indicate that 37.5 mg pemoline administered every 12 hours significantly reduced both subjective and objective sleepiness in sleep deprived subjects. Primarily during the circadian throughs periods which occur during the early morning and early afternoon hours, but has little effect on self ratings of mood; while 10 mg of methylphenidate administered every 6 hours has no significant effect on these measures. GRA

N91-26719# Chicago Univ., IL. Dept. of Medicine.
DEVELOPMENT OF ADVANCED METHODS BASED ON STABLE ISOTOPE TECHNOLOGY FOR STUDIES OF EXERCISE IN HEAT Final Report, 28 Sep. 1987 - 27 Sep. 1990
Morteza Janghorbani 20 Oct. 1990 30 p
(Contract DAMD17-87-C-7235; DA Proj. 3M1-61102-BS-15)
(AD-A234670) Avail: NTIS HC/MF A03 CSCL 18/2

Stable isotope methods were developed for studies of dynamics of turnover of total body water, extracellular and intracellular fluid volume, total body potassium and magnesium. The methods were based on the new technique of inductively coupled plasma mass spectrometry. These methods were then applied for studies of distribution of body water in micro swine, studies of total body potassium and magnesium in the rat, and study of turnover of endogenous body potassium and magnesium in the mouse. It was shown that these methods permit detailed investigation of dynamics of electrolyte turnover. Compartmentation of body magnesium was studied under the conditions of dietary magnesium restriction. It was found that important shifts occurred in terms of exchangeability of organ magnesium under these conditions. GRA

N91-26720# California Univ., San Francisco.
[THE EFFECT OF CATECHOLAMINES ON ARTERIAL BLOOD PRESSURE AND HEART RATE] Final Report
Mary F. Dallman and Daniel N. Darlington 1 Oct. 1990 33 p
(Contract N00014-88-K-0059)
(AD-A234755) Avail: NTIS HC/MF A03 CSCL 06/5

There is an abundant amount of evidence suggesting that catecholamines administered centrally can regulate adreno-corticotropin (ACTH) and vasopressin (AVP) release. Because there is a heavy catecholaminergic projection from the brain-

stem innervating the para-ventricular nucleus (PVN) of the hypothalamus, the nuclear region that regulates AVP and ACTH release from the pituitary it has been suggested that catecholaminergic regulation of ACTH and AVP may occur directly at this site. Also, these catecholaminergic cell groups are located in regions involved in the regulation of baroreflexes and the regulation of arterial blood pressure and heart rate during hemorrhage. GRA

N91-26721# Federal Aviation Administration, Washington, DC. Office of Aviation Medicine.

UTILIZATION OF EMERGENCY MEDICAL KITS BY AIR CARRIERS

J. R. Hordinsky and M. H. George Mar. 1991 7 p
(AD-A234784; DOT/FAA/AM-91/2) Avail: NTIS HC/MF A02 CSCL 06/5

The Department of Transportation Emergency Medical Equipment Requirements Rule of January 9, 1986, mandated a period of 24 months (August 1986-July 1988) during which all air carriers flying under Federal Aviation Regulation, Part 121, would monitor medical emergencies and use of the prescribed medical kits. The reporting airlines were to provide descriptions of how the medical kits were used, by whom, and the outcome of the medical emergency. During the two year monitoring period, a total of 2,322 reports of medical emergencies were documented; these included 33 inflight deaths, with only one of these representing a crew member (secondary to aircraft structural failure and resultant physical trauma). In the 2,293 actual uses of the medical kit, a physician was the provider in over 85% of the cases. The most common presenting symptom was pain, with unconsciousness, impaired breathing, nausea and/or vomiting, and various myocardial diagnose the most common presenting sign (in descending order of frequency). High frequency recurrent complaints about kit adequacy were not noted during the two year monitoring period; there were scattered references about the poor technical quality of the most frequently employed equipment; the medical kit content might selectively be expanded to include analgesics, antiarrhythmics, antiemetics, and bronchodilators. GRA

N91-26722# Army Natick Labs., MA.

PHYSIOLOGICAL AND PERCEPTUAL RESPONSES TO LOAD CARRYING IN FEMALE SUBJECTS USING INTERNAL AND EXTERNAL FRAME BACKPACKS Final Report, Jan. - Oct. 1990

John Kirk and Donald A. Schneider Apr. 1991 82 p
(AD-A234941; NATICK/TR-91/023) Avail: NTIS HC/MF A05 CSCL 06/10

Eleven female subjects (ages 18-33) walked on a motor driven treadmill at 3.2 mph for one hour carrying 33 percent of their body weight. The grade of the treadmill alternated every 15 minutes from 0 to 3 percent. Each subject carried an internal frame backpack for one trial and an external frame backpack for another trial on a separate day. The variables measured during the two load-carrying experiments included oxygen consumption (VO2), heart rate (HR), respiratory exchange ratio (R), minute ventilation (VE), and the ratings of perceived exertion for the chest (RPE-chest), shoulders (RPE-shoulders), and legs (RPE-legs). There were no statistically significant differences found between the two packs for any of the metabolic, cardiorespiratory, or perceptual variables measured. The grade of the treadmill had a significant effect on VO2, R, VE, and HR regardless of the type of pack carried. Minute ventilation was the only physiological response to load carrying that was significantly influenced by exercise time. The values for RPE-chest, RPE-shoulders, and RPE-legs were significantly increased by exercise time and treadmill slope, regardless of the type of pack frame carried. It was concluded that when a load is carried on the back, differences in backpack frame designs are not great enough to produce significant differences in the energy cost or perception of carrying a moderately heavy load. GRA

N91-26723# Johns Hopkins Univ., Baltimore, MD.

STUDIES OF MUTANT HEMOGLOBINS TO DEFINE TYPES OF MODIFICATIONS USEFUL IN THE DESIGN OF BLOOD SUBSTITUTES Final Report, 16 Jun. 1988 - 31 Dec. 1989

Gary K. Ackers 25 Mar. 1991 140 p
(Contract DAMD17-88-C-8014; DA Proj. 3M1-62772-A-874)
(AD-A234997) Avail: NTIS HC/MF A07 CSCL 06/5

Studies were carried out with mutant and chemically-modified human hemoglobins to determine structure-function characteristics that may be useful in the design of a blood substitute (i.e., by eventual combination of cross-linking and amino acid residue modifications). The results from 57 hemoglobins provide an unprecedented data base regarding the responses of oxygen binding cooperativity to single site modifications. These data define the structural location of and the nature of the driving forces for cooperativity. They provide the first systematic assessment of the relationship between structural location and chemical nature of the modified residue site in altering cooperativity. The results provide an optimistic initial baseline from which to anticipate the eventual rational design of hemoglobins with desired functional and regulatory properties. GRA

N91-26724# Texas Univ., Galveston. Medical Branch.

PHARMACOLOGICAL SPARING OF PROTEIN IN BURN INJURY Final Annual Report, 15 Mar. 1987 - 14 Mar. 1990

Robert R. Wolfe 1 Nov. 1990 101 p
(Contract DAMD17-87-C-7030; DA Proj. 3S1-62772-A-874)
(AD-A235026) Avail: NTIS HC/MF A06 CSCL 06/5

The primary goal of the research studies sponsored by this project was to assess the effect of sepsis and/or severe burn injury on the normal anabolic effect of insulin on protein metabolism. All studies were performed in human patients and normal volunteers using stable isotopic tracers and mass spectrometry analysis to quantify various metabolic factors. The first protocol involved the assessment of the effect of seven days bedrest in normal volunteers on glucose and protein responsiveness to insulin. The results following bedrest served as control values for subsequent studies in patients. The most striking aspect of these studies was the modest effect of bedrest, per se, as compared to the responses observed in bedrested patients following severe burn injury or during sepsis. Severe burn injury without systemic sepsis induced only a moderate resistance to the action of insulin on glucose uptake and potassium uptake, when compared to the bedrested controls. Sepsis halved the normal stimulatory effect of insulin on glucose uptake. Potassium uptake remained normally responsive to insulin in septic patients. Further studies are required to delineate a specific dose-response curve between insulin concentration, suppression of protein breakdown, and fat balance in the liver in order to formulate optimal treatment protocols incorporating the administration of insulin as an anabolic agent. GRA

N91-26725# Navy Personnel Research and Development Center, San Diego, CA.

THE P300 COMPONENT OF THE AUDITORY EVENT-RELATED POTENTIAL: INTERLABORATORY CONSISTENCY AND TEST-RETEST RELIABILITY Final Report, Oct. 1988 - Sep. 1989

Leonard J. Trejo, Mark Inlow, Robert R. Stanny, William A. Morey, and Scott Makeig Mar. 1991 47 p
(AD-A235114; NPRDC-TR-91-6) Avail: NTIS HC/MF A03 CSCL 06/4

The auditory evoked potential in a signal classification task using rare and frequent tones was measured by four independent laboratories, to assess the test-retest reliability and interlaboratory consistency of the P300 component. Across laboratories, 61 male subjects (three samples of military subjects, n=25, n=18, and n=8; one sample of college students, n=10), ranging between 18 and 49 years of age were tested. With few exceptions, all experimental and subject factors were controlled. At each of three electrode sites (Fz, Cz, Pz), peak amplitude, peak latency, and root-mean-square amplitude (RMS), of the P300 were computed for each subject in test and retest conditions. Statistical analyses of the data supported three strong inferences: (1) test-retest

reliability and interlaboratory consistency of P300 measures is high for RMS amplitude, lower for peak amplitude, and lowest for peak latency; (2) recordings from size Pz provide higher reliability and consistency than sites Fz or Cz; and (3) the RMS amplitude of P300 is negatively correlated with reaction time to correctly classify rare tones. The data support the notion that (Event Related Potential) components, such as P300, can be reliably measured by different laboratories, with a test-retest correlation coefficient of 0.8 or higher. GRA

N91-26726# Texas A&M Univ., College Station.
PROTON ARC DOSES TO THE PRIMATE HEAD Final Report, 30 Nov. 1989 - 30 Sep. 1990
Dennis D. Leavitt Dec. 1990 21 p
(Contract F33615-87-D-0627)
(AD-A235134; USAFSAM-TP-90-24) Avail: NTIS HC/MF A03 CSCL 06/7

The radiation dose distributions to the primate head are calculated for 10, 32, 55, and 110 MeV protons incident in the primate. Rotation of the primate in the fields is simulated by summing a 360 degree arc in 1/2 degree increments. Representative anatomy is determined by computerized tomography scans of a primate head phantom. Dose-volume histograms are used to compare the dose to the brain for each of the four irradiation techniques. Surface dose and depth dose calculations are made to evaluate the dosimetric effects to the primate eye. Estimates are made of the effects of irradiation with the primate eyes open versus closed. A focusing effect is described to explain the localized high doses seen with 32 and 55 MeV proton exposures. Doses to the eye are calculated and tabulated by animal identification key for a series of irradiated primates. These calculations demonstrate significant departures from the dose predictions based on simple cylindrical phantoms, suggesting that careful review of the primate dosimetry must accompany any evaluation of radiation effects on these animals. GRA

N91-26727# School of Aerospace Medicine, Brooks AFB, TX.
ADMINISTRATIVE GUIDE FOR THE FLIGHT SURGEON AND THE AEROMEDICAL TECHNICIAN: PERFORMING MEDICAL EXAMINATIONS Final Report, Aug. - Oct. 1990
John C. Hausmann, Jr. Dec. 1990 63 p
(AD-A235178; USAFSAM-SR-90-5) Avail: NTIS HC/MF A04 CSCL 06/5

This handout consolidates information taught in the Aerospace Medicine Primary, Aerospace Medicine Specialist, and Advanced Medical Standards courses, as well as guidance presented in Air Force Regulations and Pamphlets. This information is used on a daily basis in the Flight Surgeon's Office and Physical Examinations and Standards Sections. It is now being presented in a single, consolidated reference source. GRA

N91-26728# Army Research Inst. of Environmental Medicine, Natick, MA.
LEVEL OF DIETARY FAT DOES NOT AFFECT FUEL OXIDATION OR ENDURANCE EXERCISE PERFORMANCE OF SOLDIERS Final Report
R. W. Hoyt, T. E. Jones, M. S. Rose, V. A. Forte, Jr., and M. J. Durkot 15 Mar. 1991 84 p
(AD-A235194) Avail: NTIS HC/MF A05 CSCL 06/8

The objective was to determine whether additional dietary fat calories influenced the physiology or endurance exercise performance of physically active soldiers. Eight male soldiers (age 22 +/- 2 yrs, X +/- SEM) participated in two five-day test cycles while eating either a basal diet (2300 kcal; 40 percent fat calories) alone or with additional fat calories (3300 kcal and 57 percent fat calories). Carbohydrate (300 g/day) and protein (70 g/day) levels were kept constant. A four-day exercise program (total daily energy expenditure equal to 4645 +/- 237 kcal/day), was followed by a progressive treadmill test to exhaustion on day five. The exercise endurance times did not differ between the basil diet alone (106.1 +/- 11.2 min) or with additional fat calories (106.5 +/- 7.6 min). There were no significant physiologic differences between the groups at rest or during exercise. However, changes in resting blood chemistry and gas exchange indicated that fat metabolism predominated regardless of diet. In conclusion, (1) the fat content of rations has little short-term effect on either physiologic responses or physical performance of active soldiers, (2) short-term fat requirements can be met by using body fat stores, and (3) a dietary carbohydrate intake of 300 g/day is insufficient to prevent a transition from a carbohydrate- to a fat-predominant metabolism during four days of moderate exercise. GRA

N91-26729# Texas Univ., San Antonio.
ANALYSIS OF VISUAL LOSS FROM RETINAL LESIONS Annual Technical Report, 1 Sep. - 30 Nov. 1990
Harold Longbotham 12 Jul. 1990 5 p
(Grant AF-AFOSR-0490-89; AF Proj. 2304)
(AD-A235268; AFOSR-91-0501TR) Avail: NTIS HC/MF A01 CSCL 06/4

Papers 1, 2, and 3 deal with the theory of Order Statistic filters. These nonlinear filter have proven useful for filtering impulsive, bursty, and additive i.i.d. noise. They are being used to analyze VEP (visual evoked potential) data here at USAFSAM/RZV. Paper 4 outlines their usefulness in the case of any periodic signal and as an example, their usage on VEP data taken here at USAFSAM/RZV. Papers 5 and 6 are our first efforts in the hexagonal sampling scheme. Paper 5 deals with the recording, manipulation and storage of hexagonally sampled data. Many other authors have worked on hexagonally sampled data. Many other authors have worked on hexagonally sampled data for various optimality reasons. In paper 6 we were able to show that ANN's for pattern classification were more easily trained (they were trained more quickly and would recognize more patterns) when sampled hexagonally. Paper 7 is the only paper that is not directly related to my research at BAFB. I decided I had to go back and present my work (masters thesis) in Quasi-Perfect codes due to the recent interest shown at IBM in double error correcting codes. GRA

N91-26730# Sloan-Kettering Inst. for Cancer Research, New York, NY.
WOUND HEALING BY CULTURED SKIN CELLS AND GROWTH FACTORS Report, 16 May 1988 - 15 Nov. 1989
Magdalena Eisinger 28 Aug. 1990 50 p
(Contract DAMD17-88-C-8105; DA Proj. 3M1-62787-A-874)
(AD-A235300) Avail: NTIS HC/MF A03 CSCL 06/1

The studies described in this report were aimed at the biochemical characterization and purification of a wound healing growth factor, named Epidermal Cell derived Factor (EDF). The biological activity of EDF was found to embody enhancement of epidermal regeneration and regulation of dermal repair in skin wounds. We have accomplished the following: A tissue culture bioassay that is based on the capability of fibroblasts to contract collagen gels was shown to reflect in vivo effects of EDF on dermal cells and was adopted for examination of large numbers of samples during biochemical purification steps. Supernatant fluids of epidermal cell cultures and cell extracts of epidermal cells grown in tissue culture were tested as possible sources for purification of the factor, but substituted by epidermal cells obtained from animals following a superficial wounding. Cell extracts prepared from such regenerating epidermal cells have been found to be the richest source from all tissues tested. GRA

N91-26731# Uniformed Services Univ. of the Health Sciences, Bethesda, MD.
MOLECULAR STUDIES OF CYTOKINE INDUCTION Annual Report No. 1, Feb. - Nov. 1989
Carl W. Dieffenbach 8 Apr. 1991 20 p
(Contract N00014-90-J-1311; NR Proj. RR0-4108)
(AD-A235326) Avail: NTIS HC/MF A03 CSCL 06/5

The immune system has evolved to respond to certain microbial products with a sequence of physiological events, termed the acute phase response, that appears to be adaptive. The molecular triggers for the acute phase response appear to be cell wall products such as endotoxin, in the case of bacteria and double stranded RNA, in the case of viruses. Both endotoxin and double stranded RNA induce a class of hormone like substances,

cytokines, that drive the acute phase response. It is not known if bacterial and viral products induce overlapping sets of cytokines or if the virus response is completely dependent on interferon. Until now there has been no convenient way of assaying either serum for multiple cytokine activity, or detection of cytokine RNA's. To circumvent this problem, I have developed a polymerase chain reaction method (RNAPCR) for the detection and semi-quantitation of specific mRNA species. This method will detect mRNA in a range of 10-4 to 10-5 copies per cell allowing for a systematic analysis for multiple cytokines simultaneously. Data on the double stranded RNA induced production of cytokine mRNA's by the mouse macrophage line RAW is shown. Because the RNAPCR is strand specific, the methodology can be used to monitor the production of double stranded RNA in infected tissues. The power of this technique is just beginning to be exploited. GRA

N91-26732# Aerojet Electrosystems Co., Azusa, CA.
PROCEEDINGS OF THE 12TH ANNUAL MEETING OF THE UIPS COMMISSION ON GRAVITATIONAL PHYSIOLOGY Final Report, 1 Sep. 1990 - 31 Aug. 1991
N. Pace 16 Apr. 1991 252 p Meeting held in Leningrad, USSR, 14-18 Oct. 1990
(Grant AF-AFOSR-0320-90; AF Proj. 2312)
(AD-A235337; AFOSR-91-0442TR) Avail: NTIS HC/MF A12 CSCL 06/10

Papers presented at the 12th Annual Meeting of the UIPS Commission on Gravitational Physiology are compiled. The gravitational effects on the physiological systems of humans, animals and plants are discussed. The effects of weightlessness during space flights, acute and chronic acceleration, vibration, and the various forms of simulated weightlessness are included, as well as consideration of the evolutionary consequences of gravity and the role of gravity in the manifestation of scale effects in animals and plants. Author

N91-26178# Joint Publications Research Service, Arlington, VA.
REVIEW OF PRIMARY MEDICAL RESULTS OF YEAR-LONG FLIGHT ON MIR STATION
A. I. Grigoryev, S. A. Bugrov, V. V. Bogomolov, A. D. Yegorov, I. B. Kozlovskaya, I. D. Pestov, and I. K. Tarasov *In its* JPRS Report: Science and Technology. USSR: Space 16 Apr. 1991 p 42-49 Transl. into ENGLISH from Kosmicheskaya Biologiya i Aviakosmicheskaya Meditsina (USSR), v. 24, no. 5, Sep.-Oct. 1990 p 3-10 (For primary document see N91-26162 18-12)
Avail: NTIS HC/MF A06

N91-27091*# Alabama Univ., Tuscaloosa. Health and Human Performance Studies.
TECHNIQUES FOR DETERMINING TOTAL BODY WATER USING DEUTERIUM OXIDE Final Report
Phillip A. Bishop *In* Houston Univ., NASA/ASEE Summer Faculty Fellowship Program, 1990, Volume 1 Dec. 1990 13 p (For primary document see N91-27088 18-99)
(Grant NGT-44-005-803)
Avail: NTIS HC/MF A10 CSCL 06P

N91-27095*# Houston Baptist Univ., TX. Dept. of Biology.
NONLINEAR SYSTEMS DYNAMICS IN CARDIOVASCULAR PHYSIOLOGY: THE HEART RATE DELAY MAP AND LOWER BODY NEGATIVE PRESSURE Final Report
John C. Hooker *In* Houston Univ., NASA/ASEE Summer Faculty Fellowship Program, 1990, Volume 1 Dec. 1990 12 p (For primary document see N91-27088 18-99)
(Grant NGT-44-005-803)
Avail: NTIS HC/MF A10 CSCL 06P

N91-27101*# Fordham Univ., New York, NY. Div. of Science and Mathematics.
A STUDY OF MURINE BONE MARROW CELLS CULTURED IN BIOREACTORS WHICH CREATE AN ENVIRONMENT WHICH SIMULATED MICROGRAVITY Final Report
Brother DeSales Lawless *In* Houston Univ., NASA/ASEE Summer Faculty Fellowship Program, 1990, Volume 1 Dec. 1990 15 p (For primary document see N91-27088 18-99)
(Grant NGT-44-005-803)
Avail: NTIS HC/MF A10 CSCL 06P

N91-27102*# Kansas State Univ., Manhattan. Dept. of Kinesiology.
THE EFFECTS OF DEUTERIUM ON STATIC POSTURE CONTROL Final Report
Charles S. Layne *In* Houston Univ., NASA/ASEE Summer Faculty Fellowship Program, 1990, Volume 1 Dec. 1990 12 p (For primary document see N91-27088 18-99)
(Grant NGT-44-005-803)
Avail: NTIS HC/MF A10 CSCL 06P

N91-27112*# Texas Lutheran Coll., Seguin. Dept. of Biology.
MECHANICS, IMPACT LOADS AND EMG ON THE SPACE SHUTTLE TREADMILL Final Report
William G. Squires *In* Houston Univ., NASA/ASEE Summer Faculty Fellowship Program, 1990, Volume 2 Dec. 1990 3 p (For primary document see N91-27103 18-99)
(Grant NGT-44-005-803)
Avail: NTIS HC/MF A09 CSCL 06E

N91-27114*# Philadelphia Coll. of Pharmacy and Science, PA. Dept. of Pharmacy Practice/Pharmacy Administration.
ASSESSMENT OF THE PHARMACODYNAMICS OF INTRANASAL, INTRAVENOUS AND ORAL SCOPOLAMINE Final Report
Karen J. Tietze *In* Houston Univ., NASA/ASEE Summer Faculty Fellowship Program, 1990, Volume 2 Dec. 1990 14 p (For primary document see N91-27103 18-99)
(Grant NGT-44-005-803)
Avail: NTIS HC/MF A09 CSCL 06E

53 BEHAVIORAL SCIENCES

Includes psychological factors; individual and group behavior; crew training and evaluation; and psychiatric research.

N91-26733# Office of Naval Research, Arlington, VA.
COGNITIVE AND NEURAL SCIENCES DIVISION 1990 PROGRAMS Summary Report, 1 Oct. 1989 - 30 Sep. 1990
Williard S. Vaughan Aug. 1990 252 p
(AD-A233773; OCNR-114290-17) Avail: NTIS HC/MF A12 CSCL 05/8

Cognitive and Neural Sciences Division programs are carried out under contracts and grants awarded on the basis of proposals received in response to a broad agency announcement in the Commerce Business Daily. They are evaluated on the scientific merit of the proposed research, the facilities available for its conduct, the competence of the principal investigators, and relevance to Navy needs. The elements that shape our research program are scientific gaps and opportunities, and operational needs identified in Navy planning documents. Our overall aim is to support quality science for the good of the Navy and the nation. GRA

N91-26734# California Univ., Irvine. Center for the Neurobiology of Learning and Memory.
MECHANISMS OF ADAPTIVE INFORMATION PROCESSING Final Report, 1 Jun. - 30 Sep. 1990
Norman M. Weinberger 30 Sep. 1990 7 p
(Contract N00014-90-J-1815)
(AD-A234435) Avail: NTIS HC/MF A02 CSCL 06/3

It has long been known that associative processes rapidly induce increased responses to acoustic signals in the auditory cortex. This facilitation could be due either to a general increase in responsivity to acoustic (or even all sensory) stimulation, or to a specific change in the way that information is processed, represented and stored, i.e., it could reflect adaptive information processing. Our previous studies have resolved that issue by determining the effects of classical conditioning on the frequency

receptive fields of neurons in the auditory cortex. They provided unequivocal support that learning involves adaptive information processing (Diamond and Weinberger, 1986; 1989). Thus, responses to the CS frequency were specifically increased whereas responses to other frequencies, including the pre-training best frequency, were reduced. This pattern of change was often large enough to produce a strong retuning of cells such that the frequency of the CS became the best frequency (Bakin and Weinberger, 1990). This project tests a model of such adaptive information processing. GRA

N91-26735# Stanford Univ., CA. Dept. of Psychology.
INDUCED PICTORIAL REPRESENTATIONS Final Technical Report, 1 Dec. 1989 - 31 Jan. 1991
Barbara Tversky 15 Feb. 1991 77 p
(Grant AF-AFOSR-0076-89; AF Proj. 2313)
(AD-A234548; AFOSR-91-0284TR) Avail: NTIS HC/MF A05 CSCL 05/8

When understanding discourse, people form mental representations at many levels, including a model of the situation. This report describes two projects investigating spatial mental models induced by text. The first explored characteristics of static mental models of environments established from survey or route descriptions. Memory measures indicated that descriptions from both perspectives appear to induce the same perspective-free mental models. Like structural descriptions, these mental models incorporate spatial relations among landmarks, and allow the taking of many specific perspectives. In the second project, narratives described a common situation, an observer surrounded by objects. Narratives periodically reoriented observers, and subjects were probed for objects at various directions from the body of the observer. The pattern of reaction times suggested that people form mental spatial frameworks to keep track of the positions of objects relative to the observer. Spatial frameworks are not image - or perception-like, but rather reflect people's conceptions of space based on typical interactions with space. GRA

N91-26736# Army Health Care Studies and Clinical Investigation Activity, Fort Sam Houston, TX.
PROCEEDINGS OF THE 7TH USER'S STRESS WORKSHOP Final Report, Dec. 1989 - Dec. 1990
A. D. Mangelsdorff Dec. 1990 246 p Workshop held in San Antonio, TX, 10-15 Dec. 1989
(AD-A234583; HCSCIA-CR91-001) Avail: NTIS HC/MF A11 CSCL 06/5

The proceedings document the presentations at a workshop conducted in December 1989 on the training programs designed for managing psychological trauma and stress. The interaction between local, national, and international efforts was examined. The program was designed to provide up to date information and skills to health and emergency service providers on how to recognize, treat, and manage victims of psychic trauma. The program was presented in lecture, discussion, practical exercises, and role playing situations. GRA

N91-26737# Oregon State Univ., Newport. Marine Science Center.
PARALLEL PROCESSING AND LEARNING: VARIABILITY AND CHAOS IN SELF-ORGANIZATION OF ACTIVITY IN GROUPS OF NEURONS Annual Report, 14 Jan. 1990 - 13 Jan. 1991
George J. Mpitsos 8 Mar. 1991 9 p
(Grant AF-AFOSR-0262-89; AF Proj. 2312)
(AD-A234589; AFOSR-91-0243TR) Avail: NTIS HC/MF A02 CSCL 06/5

We have examined the immunohistochemical localization of over 12 different neurotransmitters in all of the nervous system components of two different marine molluscs, Aplysia and Pleurobranchaea. To do this for each neurotransmitter, we made complete serial histological sections of all major ganglia in each nervous system. Localizations were performed using immunohistochemistry and fluorescence microscopy. Since many of the commercially available antisera proved to be nonspecific, we generated 11 antisera in our laboratory. One of the major achievements occurred in our work on acetylcholine, which our previous AFOSR-funded work implicated as having an important role in associative learning in Pleurobranchaea through muscarinic receptors. GRA

N91-26738# Systems Research Labs., Inc., Dayton, OH.
AIRCREW EVALUATION SUSTAINED OPERATIONS PERFORMANCE (AESOP): A TRISERVICE FACILITY FOR TECHNOLOGY TRANSITION Interim Report, Sep. 1987 - Sep. 1990
Samual E. Schiflett, David R. Strome, Douglas R. Eddy, and Mathieu A. Dalrymple Dec. 1990 32 p Prepared in cooperation with NTI, Inc., Dayton, OH
(Contract F33615-87-D-0601)
(AD-A234626; USAFSAM-TP-90-26) Avail: NTIS HC/MF A03 CSCL 06/10

A primary mission of the Sustained Operations Branch, Crew Technology Div., Armstrong Lab. (AFSC), is to develop procedures and provide guidance to operational commands on maintaining and extending crew performance during sustained operations and continuous duty. The Crew Technology Div. developed the AESOP facility to meet the triservice research and mission requirements for team performance metrics. The AESOP facility evaluates the interactive effects of fatigue, stress, and medications on AWACS aircrew performance so effective countermeasures can be transitioned from the laboratory to field test environments to actual operations. The basic design of the facility allows the flexibility and experimental control to either assess performance decrements or develop performance enhancement techniques in a realistic operational environment. The simulation integrates hardware and software resources, data collection and analysis systems, verbal communication networks, command/control scenarios, and performances measures. Examples of individual and team performance on complex decision making are illustrated. Emphasis is placed on flexibility of measurement, hierarchical organization of measurement levels, and data collection from multiple perspectives. Future research opportunities for the development and evaluation of candidate models to describe and predict team decision making under stress from the perspective of operational performance-based criteria are identified. GRA

N91-26739# Massachusetts Univ., Amherst. Dept. of Psychology.
A CONFERENCE ON EYE MOVEMENTS AND VISUAL COGNITION Final Technical Report, 1 Jan. - 31 Dec. 1990
Keith Rayner 4 Mar. 1991 31 p Conference held in Amherst, MA, Aug. 1990
(Grant AF-AFOSR-0073-90; AF Proj. 2313)
(AD-A234754; AFOSR-91-0255TR) Avail: NTIS HC/MF A03 CSCL 06/4

This report summarizes a conference held in Amherst, MA in August 1990. The conference brought together investigators interested in a number of topics relevant to eye movements and visual cognition. Papers were presented on the following topics: (1) Programming saccades, (2) Visual Search and Integration, (3) Scene Perception, (4) Reading, and (5) Reading and Pictures. The conference was very stimulating, the talks were excellent, and the participants agreed that the meeting was very worthwhile. An edited volume will appear in 1992 with the conference papers. GRA

N91-26740# York Univ., Downsview (Ontario).
VISUAL SENSITIVITIES AND DISCRIMINATIONS AND THEIR ROLE IN AVIATION Final Report, 1 Nov. 1989 - 31 Oct. 1990
David Regan 20 Feb. 1991 81 p
(Contract F49620-88-C-0002)
(AD-A234866; AFOSR-91-0237TR) Avail: NTIS HC/MF A05 CSCL 01/3

Selective blindness to approaching or receding motion in depth exists and seems to be not uncommon in normally-sighted individuals. Of 16 subjects, 8 had visual field defects for either approaching or receding motion. Of 21 subjects, only 6 had full symmetrical fields for oscillatory motion in depth. Visual sensitivity

to sideways motion was normal in stereomotion-blind areas. The possible relevance to aviation is pointed out. A perfectly camouflaged bar within a random dot pattern was rendered visible by moving dots within the bar and outside the bar with equal and opposite velocities (motion parallax). The bar's orientation could be judged with equal precision (0.5 deg) to that of an uncamouflaged dotted bar made visible by brightness contrast providing that dot speed and contrast were high. But when contrast was reduced, discrimination collapsed for the camouflaged bar. Shape discrimination was compared for motion-defined and contrast-defined dotted rectangles. At high dot speeds and contrasts aspect ratio discrimination equal for the two kinds of rectangle and, at 2 to 3 percent, corresponded to a change of side length of only 24 arc sec. GRA

N91-26741# Chicago Univ., IL. Dept. of Psychology.
CATEGORIES AND PARTICULARS: PROTOTYPE EFFECTS IN ESTIMATING SPATIAL LOCATION Annual Report, 1 Mar. 1990 - 28 Feb. 1991
Janellen Huttenlocher, L. V. Hedges, and S. Duncan 12 Mar. 1991 80 p
(Grant AF-AFOSR-0218-90; AF Proj. 2313)
(AD-A234955; AFOSR-91-0245TR) Avail: NTIS HC/MF A05 CSCL 05/8

A final version was completed of a paper describing a model of spatial estimation based on hierarchical representation in memory. In the paper, the model to the representation of spatial location was applied, and results were reported on four experiments on coding the location of a dot in a circle. In addition, four other studies of ways people hierarchically organize other shapes and of the consequent effects of spatial estimation were carried out. The later studies raise various issues which have led to greater refinement in modeling people's reports of location under conditions of uncertainty. GRA

N91-26742# Johns Hopkins Univ., Baltimore, MD. Dept. of Psychology.
NEURAL MECHANISMS OF ATTENTION Annual Report, 1 Aug. 1989 - 31 Jul. 1990
David Olton and Howard Egeth Sep. 1990 9 p
(Grant AF-AFOSR-0481-89; AF Proj. 2313)
(AD-A235003; AFOSR-91-0242TR) Avail: NTIS HC/MF A02 CSCL 05/8

Assessment of attention in animals provides information about the neural mechanisms involved in attention, which can help develop computational and cognitive models that describe in detail the systematic steps mediating different types of attention. In order to increase the applicability of the results from these experiments to those of humans, the behavioral testing procedures have been designed to be as similar as possible to those used for humans. The initial behavioral experiments indicate strong operational and psychological validity of these tests of attention, providing the opportunity to pursue the neural mechanisms in the subsequent funding period. GRA

N91-26743# Human Engineering Labs., Aberdeen Proving Ground, MD.
THE EFFECTS OF DISPLAY FAILURES AND SYMBOL ROTATION ON VISUAL SEARCH AND RECOGNITION PERFORMANCE
Jennie J. Decker, Craig J. Dye, Charles J. Lloyd, and Harry L. Snyder Feb. 1991 42 p
(DA Proj. 1L1-62716-AH-70)
(AD-A235035; HEL-TM-4-91) Avail: NTIS HC/MF A03 CSCL 23/2

This study was conducted to investigate the effects of display failures and rotation of dot-matrix symbols on visual search and recognition performance. The type of display failure (cell, horizontal line, vertical line), failure mode (On, failures matched the symbols; Off, failures matched the background), percentage of cells failed (0, 1, 2, 3, 4 percent), and rotation angle (0, 70, 105 deg) were the variables examined. Results showed that displays that exhibit On cell failures greater than 1 percent significantly affect search time performance. Cell failures degrade performance more than line failures. Search time and accuracy are best when symbols are oriented upright. The effects of display failures and rotation angle on search time were found to be independent. Implications for display design and suggestions for quantifying the distortion caused by rotation are discussed. GRA

N91-26744# University of Southern California, Los Angeles. Dept. of Psychology.
INTEGRATION OF NEUROBIOLOGICAL AND COMPUTATIONAL ANALYSES OF THE NEURAL NETWORK ESSENTIALS FOR CONDITIONED TASTE AVERSION Final Progress Report, 15 Dec. 1988 - 14 Mar. 1991
Kathleen C. Chambers 29 Apr. 1991 15 p
(Contract N00014-89-J-1296)
(AD-A235164) Avail: NTIS HC/MF A03 CSCL 05/8

The general goal of this project was to determine the neural basis of learning and memory, that is, how the brain stores and retrieves memory. The special form of learning which was the focus of this project was conditioned taste aversions, learned aversions to the taste of food or fluid when consumption of that substance is followed by illness. Studies were made of the illness pathway and illness-taste integration pathway. Conditions under which endogenous substances act as illness-inducing agents were determined, techniques to study neural substrates for those substances as well as exogenous toxins were developed and evidence refuting hypotheses regarding the role of particular brain areas as substrates for illness-integration was obtained. Endogenous factors that modulate the acquisition and extinction of conditioned taste aversions were also identified. Variations in endogenous hormone levels, availability of water, and age alter the facility with which an aversion is learned and unlearned. Finally, a neural model encompassing the illness pathway, the taste pathway, the behavioral pathways, and the modulatory pathways was developed. GRA

N91-26695# Joint Publications Research Service, Arlington, VA.
INDIVIDUAL STEREOTYPES OF HUMAN NEUROPSYCHIC PROGNOSTIC ACTIVITY IN PROBLEM SITUATIONS WITH DIFFERENT PROBABILITY STRUCTURES
A. Krauklis and I. Kazanovskaya *In its* JPRS Report: Science and Technology. USSR: Life Sciences 18 Apr. 1991 p 19-25 Transl. into ENGLISH from Izvestiya Latviyskoy Akademii Nauk (Riga, USSR), no. 9, Sep. 1990 p 86-96 (For primary document see N91-26688 18-52)
Avail: NTIS HC/MF A05

N91-26700# Joint Publications Research Service, Arlington, VA.
EFFECT OF SHIFT WORK OF AIR TRAFFIC CONTROLLERS ON SYMPATHETIC NERVOUS SYSTEM Abstract Only
Ye. L. Kan and V. A. Kupriyanov *In its* JPRS Report: Science and Technology. USSR: Life Sciences 20 May 1991 p 1-2 Transl. into ENGLISH from Kosmicheskaya Biologiya i Aviakosmicheskaya Meditsina (Moscow, USSR), v. 24, no. 5, Sep. - Oct. 1990 p 22-25 (For primary document see N91-26696 18-52)
Avail: NTIS HC/MF A03

N91-27097*# Houston Univ., TX. Dept. of Psychology.
TRAINING EFFECTIVENESS OF AN INTELLIGENT TUTORING SYSTEM FOR A PROPULSION CONSOLE TRAINER Final Report
Debra Steele Johnson *In its* NASA/ASEE Summer Faculty Fellowship Program, 1990, Volume 1 Dec. 1990 15 p (For primary document see N91-27088 18-99)
(Grant NGT-44-005-803)
Avail: NTIS HC/MF A10 CSCL 05I

54 MAN/SYSTEM TECHNOLOGY AND LIFE SUPPORT

Includes human engineering; biotechnology; and space suits and protective clothing.

For related information see also *16 Space Transportation.*

N91-26745# National Inst. for Occupational Safety and Health, Cincinnati, OH.

PHYSIOLOGICAL RESPONSES TO THE WEARING OF PROTECTIVE EQUIPMENT AND RESPIRATORS: EFFECTS OF HOT, HUMID INSPIRED AIR ON WORK OF BREATHING Final Report

N. L. Turner 1990 39 p

(PB91-152884) Avail: NTIS HC/MF A03 CSCL 05H

The physiological effects of breathing cool/dry, cool/humid, hot/dry, and hot/humid air were observed during rest, and during light and moderate intensity exercise on a cycle ergometer. Nine male volunteers, 18 to 35 years old, took part in four 50-minute submaximal exercise tests under the four different inspired air conditions. The results demonstrated several positive effects of hot air breathing on lung mechanics. Dynamic lung compliance was increased with both hot/dry and hot/humid air breathing during rest and exercise. These increases in compliance implied a decrease in the inspiratory work of breathing, although no statistically significant decreases were demonstrated. Frequency of breathing was decreased and tidal volume increased with hot air, allowing a more efficient breathing pattern. These results lent support to the current inspired air temperature criteria for SCBA certification, as set for in 30 CFR, Part 11 and proposed 42 CFR, Part 84. The study suggests that future research in the area include a study in which both inspired air and ambient air temperature are varied. The possibility of interactions between hot inspired air and hot ambient air should be explored as closed circuit respirators used in both fire fighting and hazardous waste operations may be used under hot ambient conditions. Author

N91-26746# GEOMET Technologies, Inc., Germantown, MD.

AIRLINER CABIN ENVIRONMENT: CONTAMINANT MEASUREMENTS, HEALTH RISKS, AND MITIGATION OPTIONS Final Report, Dec. 1988 - Dec. 1989

N. L. Nagda, R. C. Fortmann, M. D. Koontz, S. R. Baker, and M. E. Ginevan Dec. 1989 310 p

(Contract DOTS59-89-C-00082)

(PB91-159384; GEOMET-IE-2096; DOT-P-15-89-5) Avail: NTIS HC/MF A14; also available SOD HC $19.00 as 050-000-00531-3 CSCL 06K

The purpose of the study was to develop information to be used for determining health risks from exposure to environmental tobacco smoke (ETS) and other pollutants for airliner occupants. Selected ETS contaminants (nicotine, respirable suspended particles, and carbon monoxide) as well as ozone, microbial aerosols, carbon dioxide, and the other environmental variables were measured in different parts of airliner cabins for 92 randomly selected smoking and nonsmoking flights. In assessing mitigation strategies, a total or partial ban on smoking provided the greatest benefit at least cost. Exposure management was the only viable option for reducing risks due to cosmic radiation. For removal of CO2, sorption on solid, regenerative absorbent beds was considered to be a method with potential benefits. Author

N91-26747* National Aeronautics and Space Administration. Lyndon B. Johnson Space Center, Houston, TX.

METHOD AND APPARATUS FOR WASTE COLLECTION AND STORAGE Patent

William E. Thornton, Jr., inventor (to NASA) and Henry B. Whitemore, inventor (to NASA) 9 Apr. 1991 15 p Filed 10 Aug. 1989 Division of US-Patent-Appl-SN-035401, filed 7 Apr. 1987

(NASA-Case-MSC-21025-3; US-Patent-5,005,457; US-Patent-Appl-SN-392174; US-Patent-Appl-SN-035401; US-Patent-Class-83-206; US-Patent-Class-83-203; US-Patent-Class-83-277; US-Patent-Class-83-282; US-Patent-Class-83-614; US-Patent-Class-83-649) Avail: US Patent and Trademark Office CSCL 06K

A method and apparatus are disclosed for collection of fecal matter designed to operate efficiently in zero gravity environment. The system comprises a waste collection area within a body having a seat opening. Low pressure within a waste collection area directs fecal matter away from the user's buttocks and prevents the escape of undesirable gases. The user actuates a piston covered with an absorbent pad that sweeps through the waste collection area, press the waste against an end of the waste collection area and retracts, leaving the used pad. Multiple pads are provided on the piston to accommodate multiple uses of the system. Also a valve allows air to be drawn through the body, which valve will not be plugged with fecal matter. A sheet feeder feeds fresh sheets of absorbent pad to a face of the piston with each actuation. Author

N91-26748# Aerospace Medical Research Labs., Wright-Patterson AFB, OH.

AN ADVANCED KNOWLEDGE AND DESIGN ACQUISITION METHODOLOGY: APPLICATION FOR THE PILOT'S ASSOCIATE Final Report, Feb. - Oct. 1990

Michael D. McNeese, Brian S. Zaff, Karen J. Peio, Daniel E. Snyder, and John C. Duncan Dec. 1990 234 p

(AF Proj. 7184)

(AD-A233700; AAMRL-TR-90-060) Avail: NTIS HC/MF A11 CSCL 12/7

This report documents the creation, development, and evaluation of an advanced knowledge and design acquisition methodology. The methodology develops user requirements along three separate yet integrated perspectives: (1) intuitive/experiential knowledge, (2) structural/functional models, and (3) knowledge as design. Three specific tools to implement perspectives; concept mapping, IDEF modeling, and design storyboarding are discussed. An integrative structure is proposed as an interactive way to let users and other design team members assimilate, deepen, and combine knowledge for the purpose of developing intelligent systems and human machine interface designs. Hence, system designs are directly derived from user engineering and from user conceptualization and participation. The project applies this methodology to the Pilot's Associate program which resolves complex knowledge acquisition/representation requirements. Results indicate that pilots could successfully reveal their own comprehension of an air to ground mission and transform this conceptual knowledge into actual designs for an intelligent pilot vehicle interface. The ability of this methodology to elicit multiple knowledge perspectives and to preserve them in an integrated form (which facilitates interaction with new domain experts in the future) creates an effective means for all phases of the system design. GRA

N91-26749# California Univ., Los Angeles.

EXPERT SYSTEM EXPLANATION: THE USER PERSPECTIVE Research Report, 1 Jun. - 31 Oct. 1990

Anat Jacoby Oct. 1990 37 p

(Contract N00014-86-K-0395; NR Proj. RR0-4206)

(AD-A233739) Avail: NTIS HC/MF A03 CSCL 12/5

To understand how to tailor expert system explanation to users, a study was conducted that examined the relationship of goals and explanations to two types of task performance. It was predicted that students receiving goals, explanations, and tasks with highest congruence, would perform best. Fifty-three high school students were randomly assigned to one of two explanation groups or a control group. All groups received the same goal of replicating a scheduling task. All groups received a sampled schedule, and the explanation groups received, in addition, one of two explanations, a retrospective-trace explanation or a reconstructive-justification explanation. The retrospective-trace explanation provided the detailed steps of how to construct a schedule; the reconstructive-justification explanation provided justification of a given schedule. All groups received two tasks,

given in random order: a replication task of producing a schedule and a verification task of verifying the correctness of a schedule. GRA

N91-26750# Army Aeromedical Research Lab., Fort Rucker, AL.
SPH-4 AIRCREW HELMET IMPACT PROTECTION IMPROVEMENTS 1970-1990 Final Report
Ronald W. Palmer Feb. 1991 43 p
(AD-A233784; USAARL-91-11) Avail: NTIS HC/MF A03
CSCL 05/8

The Sound Protective Helmet-4 (SPH-4), a derivative of the Navy SPH-3, has been used by the Army since 1970. As the knowledge of crash environments and human impact tolerance has increased through analyses of aircraft accidents and laboratory research, the performance of the standard SPH-4 helmet has been continuously reappraised, and the helmet's shell, liner, retention, earcups, and suspension have been upgraded to provide more impact protection. This report includes a discussion of improvements made in the SPH-4 helmet and the effects these improvements have had on its performance. The SPH-4, SPH-4B, and HGU-56/P are compared in terms of major design features, impact protection, and retention capabilities. The development of helmet impact testing methodology used at the U.S. Army Aeromedical Research Laboratory, Fort Rucker, Alabama, also is discussed. GRA

N91-26751# Analysis and Technology, Inc., New London, CT.
EVALUATION OF NIGHT VISION GOGGLES FOR MARITIME SEARCH AND RESCUE Interim Report, Mar. 1989 - Sep. 1990
W. H. Reynolds, R. Q. Robe, G. L. Hover, and J. V. Plourde Aug. 1990 112 p
(Contract DTCG39-89-C-E10G56)
(AD-A233798; USCG-D-01-91) Avail: NTIS HC/MF A06 CSCL 17/5

Experiments were conducted to evaluate night vision goggles (NVGs) for their effectiveness in detecting small targets at night. Three types of NVGs were evaluated: the AN/AVS-6 Aviators Night Vision Imaging System (ANVIS) NVG was tested onboard Coast Guard HH-3 and CH-3 helicopters, and the AN/PVS-5C and AN/PVS-7A NVGs were tested onboard 41-foot Coast Guard utility boats. During the spring 1990 experiments, simulated persons in the water wearing orange personal floatation devices, retroreflective tape, and either a green personnel marker light or a red safety light; 4- and 6-person life rafts with and without retroreflective tape; and 18- and 21-foot white boats were employed as targets during realistically-simulated search missions. A total of 1355 target detection opportunities were generated for the above-mentioned target types during four experiments. These data were analyzed to determine which of 25 search parameters of interest exerted a statistically-significant influence on target detection probability. Lateral range curves and sweep width estimates are developed for each search unit/target type combination. Human factors data are presented and discussed. Recommendations for conducting NVG searches for small targets are provided. GRA

N91-26752# Army Natick Research and Development Command, MA.
NOTIONAL HELMET CONCEPTS: A SURVEY OF NEAR-TERM AND FUTURE TECHNOLOGIES Final Report, Oct. 1989 - Sep. 1990
Henry Girolamo Mar. 1991 60 p
(AD-A234475; NATICK/TR-91/017) Avail: NTIS HC/MF A04
CSCL 14/2

This research identified, explored, and evaluated near-term and future technologies having potential applications in developing a future helmet-mounted display and an integrated battlefield communication/information management system that will enhance the dismounted soldier's performance. This report was written with the combat developer in mind and is intended to serve as a technology guide. Helmet-mounted displays would have a multi-purpose full-face shield capable of displaying alphanumeric data and graphics. It would need a polycarbonate resin that would provide protection against ballistic fragmentation and directed energy hazards. The display would include night vision enhancement capabilities and electro-optical weapon sights for remote weapon sighting; sensors to medically monitor the soldiers physiological functions; and sensors that would warn soldiers of chemical and biological agents, radiation, and other hazardous atmospheric conditions. GRA

N91-26753# Department of the Navy, Washington, DC.
REGENERATION OF WHETLERITE FOR ADSORBING TOXIC POLLUTANTS FROM AIR Patent Application
Victor R. Deitz, inventor (to Navy) 13 Dec. 1990 12 p
(AD-D014859; US-Patent-Appl-SN-627163) Avail: NTIS HC/MF A03 CSCL 24/1

This invention relates to a method of regenerating adsorbents for removing toxic pollutants from air. More specifically, it relates to a method of restoring the ability of metal oxide-impregnated activated carbon referred to as whetlerite to remove cyanogen chloride from air. Whetlerites are activated carbon-based composites impregnated with ammoniacal solutions of divalent copper and monovalent silver, with or without hexavalent chromium, in various concentrations. Optionally, triethylenediamine (TEDA) is added to prolong the service life of the absorbent and resist the adverse effects of humid environments. Whetlerites adsorb a wide variety of toxic air pollutants, in particular cyanogen chloride, cyanogen, and hydrogen cyanide. GRA

N91-26754# Army Aeromedical Research Lab., Fort Rucker, AL.
VISUAL AND FIELD-OF-VIEW EVALUATION OF THE M-43 PROTECTIVE MASK WITH PRESCRIPTION EYEPIECES Final Report
John K. Crosley, Clarence E. Rash, and Richard R. Levine Mar. 1991 37 p
(AD-A234592; USAARL-91-13) Avail: NTIS HC/MF A03
CSCL 23/2

The U.S. Army Aeromedical Research Laboratory was requested by the proponent of the 43 aviator protective mask to conduct a laboratory study of the visual performance of flight AH-64 Apache helicopter pilots wearing masks with 'glue-on' prescription lenses. In response, several visual functions tests were conducted including: high and low contrast visual acuity, heterophoria, fixation disparity, and stereopsis at both near and far. In addition, visual field losses of the integrated helmet and display sighting system were examined. Performance in the corrective mask was compared to that with habitual correction, either spectacles or contact lenses. The results of the visual functions tests indicated acceptable performance on all the measures except fixation disparity. The high degree of variability found on this test suggested problems associated with the prescription lens optical design, namely its high radius of curvature and its additional thickness. Field-of-view results indicated losses in visual field above those obtained with spectacle correction, but comparable to that found with the plano mask. GRA

N91-26755# Naval Health Research Center, San Diego, CA.
EFFECT OF A PASSIVE COOLING VEST ON TENSION/ANXIETY AND FATIGUE IN A HIGH HEAT AND HIGH HUMIDITY NAVAL ENVIRONMENT Interim Report, Jun. - Oct. 1989
Ralph G. Burr, Guy R. Banta, J. T. Coyne, James A. Hodgdon, and Charles V. Chesson, II 16 Oct. 1990 27 p
(AD-A234657; NHRC-90-23) Avail: NTIS HC/MF A03 CSCL 06/10

Crewmembers aboard U.S. Navy ships in the Persian Gulf theater of operations are subjected to continuous heat strain. During the months of July and August, it is not unusual for this part of the world to reach ambient temperatures in the range of 120 to 130 F with the relative humidity up to 90 pct. Previous field studies on U.S. Navy ships in the Persian Gulf have shown crewmembers have difficulty falling asleep at lights out, poor quality sleep, falling asleep on the job, physical and psychological fatigue, and feelings

of confusion and tension/anxiety. Exposure to heat has also been shown to affect performance capabilities during sustained work. Grether (1973) reported that human performance of such tasks as time estimation, reaction time, vigilance, tracking, and other skilled cognitive operations, show performance decrement in ambient temperatures above 85 F. GRA

N91-26756# Systems Research Labs., Inc., Dayton, OH.
ADVANCED DYNAMIC ANTHROPOMORPHIC MANIKIN (ADAM) DESIGN REPORT Final Report, Feb. 1985 - Jun. 1989
Aileen M. Bartol, Vernon L. Hazen, Joseph F. Kowalski, Brian P. Murphy, and Richard P. White, Jr. Mar. 1990 672 p
(Contract F33615-85-C-0535)
(AD-A234761; AAMRL-TR-90-023) Avail: NTIS HC/MF A99 CSCL 05/8

The USAF has embarked on a new effort to design and develop an Advanced Dynamic Anthropomorphic Manikin (ADAM) with improved biofidelity and instrumentation over currently available escape system test manikins. This report described the design of three prototypes (one small, one mid-size, and one large) instrumentated, anthropomorphic manikins for testing, evaluating, and qualifying high-performance aircraft escape systems, including restraint and harness systems. Among the required responses are that it provide a human-like reactive live load into the ejection sear and possess realistic dynamics and kinematics due to windblast, impact vibration, and acceleration forces representative of those encountered during ejection from an aircraft. In addition to improved biomechanical response properties, the manikin has instrumentation and an on-board data acquisition system to measure, store, and transmit its responses and the data form the escape system. Two prototype manikins, a small and a large, will be fabricated and tested at Wright-Patterson AFB, OH. GRA

N91-26757# Anacapa Sciences, Inc., Fort Rucker, AL.
TASK ANALYSIS AND WORKLOAD PREDICTION FOR THE MH-47E MISSION AND A COMPARISON WITH CH-47D WORKLOAD PREDICTIONS. VOLUME 2: APPENDIXES A THROUGH N Final Report, Dec. 1988 - Aug. 1990
Carl R. Bierbaum and David B. Hamilton Mar. 1991 450 p
(Contract MDA903-87-C-0523; DA Proj. 2Q2-63007-A-793)
(AD-A235249; ASI690-329-90-II-Vol-2; ARI-RN-91-35-Vol-2)
Avail: NTIS HC/MF A19 CSCL 05/9

For this research, a mission scenario was used to conduct a comprehensive task analysis for MH-47E operations. The analysis used a top-down approach to identify the phases, functions, and tasks for the mission and identified 5 phases, 15 segments, 73 functions, and 239 tasks. The crew member performing each task was identified, and estimates of the sensory, cognitive, and psychomotor workload associated with the tasks were derived. Estimates of the task durations also were derived. The mission/task/workload analysis data were used to develop a computer model of workload for MH-47E crew members. The model used a bottom-up approach to build mission functions from tasks and mission segments from functions. Decision rules were written to specify the procedure for combining the tasks into functions and the functions into segments. The model permitted an analysis of total workload experienced by the pilot and copilot in the performance of both sequential and concurrent tasks. The predicted workload for the MH-47E pilot and copilot was compared to the CH-47D baseline workload prediction to determine the impact of the advanced technology on the MH-47E. The comparison indicated little difference in the predicted workload for the pilot and indicated a lower predicted workload for the copilot in the MH-47E. Volume 1 of the report describes the methodology and summarizes the results of the research. This volume contains the appendixes, which present the workload predictions of the CH-47D. GRA

N91-26758# Defence and Civil Inst. of Environmental Medicine, Downsview (Ontario).
EFFECTIVENESS OF ICE-VEST COOLING IN PROLONGING WORK TOLERANCE TIME DURING HEAVY EXERCISE IN THE HEAT FOR PERSONNEL WEARING CANADIAN FORCES CHEMICAL DEFENCE ENSEMBLES
B. Bain Jan. 1991 11 p
(AD-A235273; DCIEM-91-06) Avail: NTIS HC/MF A03 CSCL 05/8

Effectiveness of a portable, ice-pack cooling vest (Steelevest) in prolonging work tolerance time in chemical defense clothing in the heat (33 C dry bulb, 33 percent relative humidity or 25 C WBGT) was evaluated while subjects exercised at a metabolic rate of approximately 700 watts. Subjects were six male volunteers. The protocol consisted of a 20 minute treadmill walk at 1.33 m/s and 7.5 percent grade, followed by 15 minutes of a lifting task, 5 minutes rest, then another 20 minutes of lifting task for a total of one hour. The lifting task consisted of lifting a 20 kg box, carrying task for a total of one hour. The lifting task consisted of lifting a 20 kg box, carrying it 3 metres and setting it down. This was followed by a 6 m walk (3m back to the start point and 3 m back to the box) in 15 sec after which the lifting cycle began again. The work was classified as heavy as previously defined. This protocol was repeated until the subjects were unable to continue or they reached a physiological endpoint. Time to voluntary cessation or physiological endpoint was called the work tolerance time. Physiological endpoints were rectal temperature of 39 C, heart rate exceeding 95 percent of maximum for two consecutive minutes of visible loss of motor control or nausea. The cooling vest had no effect on work tolerance time, rate of rise of rectal temperature or sweat loss. It was concluded that the Steelevest ice-vest is ineffective in prolonging work tolerance time and preventing increases in rectal temperature GRA

N91-26759*# National Aeronautics and Space Administration. John F. Kennedy Space Center, Cocoa Beach, FL.
INVESTIGATING COMBUSTION AS A METHOD OF PROCESSING INEDIBLE BIOMASS PRODUCED IN NASA'S BIOMASS PRODUCTION CHAMBER
T. W. Dreschel, R. M. Wheeler, C. R. Hinkle, J. C. Sager, and W. M. Knott May 1991 21 p Prepared in cooperation with Bionetics Corp., Cocoa Beach, FL
(Contract NAS10-11624)
(NASA-TM-103821; NAS 1.15:103821) Avail: NTIS HC/MF A03 CSCL 06K

The Controlled Ecological Life Support System (CELSS) Breadboard Project at the John F. Kennedy Space Center is a research program to integrate and evaluate biological processes to provide air, water, and food for humans in closed environments for space habitation. This project focuses on the use of conventional crop plants as grown in the Biomass Production Chamber (BPC) for the production and recycling of oxygen, food, and water. The inedible portion of these crops has the potential to be converted to edible biomass or directly to the elemental constituents for direct recycling. Converting inedible biomass directly, by combustion, to carbon dioxide, water, and minerals could provide a baseline for estimating partitioning of the mass balance during recycling in a CELSS. Converting the inedible biomass to carbon dioxide and water requires the same amount of oxygen that was produced by photosynthesis. The oxygen produced during crop growth is just equal to the oxygen required to oxidize all the biomass produced during growth. Thus, the amount of oxygen produced that is available for human consumption is in proportion to the amount of biomass actually utilized by humans. The remaining oxygen must be available to oxidize the rest of the biomass back to carbon dioxide and water or the system will not be a regenerative one. Author

N91-26760 Tel-Aviv Univ. (Israel). Dept. of Interdisciplinary Studies.
SITTING POSTURE ANALYSIS. AN EXPERIMENTAL OPTIMISATION APPROACH M.S. Thesis
Ram Barnea Apr. 1989 88 p In HEBREW; ENGLISH summary
(ITN-91-85114) Copyright Avail: Tel-Aviv Univ., Exact Sciences Library, Ramat Aviv 69978, Israel

An instrumented chair was developed and used for the automated acquisition and processing of data on contact pressure distribution and its variation with posture. A pressure distribution

coefficient was defined which facilitated the evaluation of the effect on contact pressure distribution of variations in sitting plane inclination, back rest inclination and vertical height of the sitting plane. The sitting plane and back rest inclinations ranged from 0 to 12 degs to the horizontal and vertical, respectively, and the sitting plane height varied from 38 to 44 cm above the footrest. Measurements involving 6 subjects indicated that the optimum pressure distribution was obtained for sitting and back plane angles of 0 and 12 degs, respectively, and seat height of 44 cm. The maximum local contact pressure, of 240,000 pascal, was obtained for both angles of 0 degs and seat height of 38 cm. The data analysis techniques developed could be applied to seat design and to clinical diagnosis and treatment of sitting posture disorders. ISA

N91-26693# Joint Publications Research Service, Arlington, VA.
HIGHER PLANTS AS PART OF BIOLOGICAL HUMAN LIFE SUPPORT SYSTEM Abstract Only
I. Ye. Ivanova, T. A. Derendyayeva, T. P. Alekhina, and Yu. I. Shaydorov *In its* JPRS Report: Science and Technology. USSR: Life Sciences 18 Apr. 1991 p 2 Transl. into ENGLISH from Kosmicheskaya Biologiya and Aviakosmicheskaya Meditsina (Moscow, USSR), v. 24, no. 4, Jul. - Aug. 1990 p 40-43 (For primary document see N91-26688 18-52)
Avail: NTIS HC/MF A05

N91-27093*# Mary Hardin-Baylor Univ., Belton, TX. Dept. of Mathematics and Physics.
AN AIR REVITALIZATION MODEL (ARM) FOR REGENERATIVE LIFE SUPPORT SYSTEMS (RLSS) Final Report
Maxwell M. Hart *In* Houston Univ., NASA/ASEE Summer Faculty Fellowship Program, 1990, Volume 1 Dec. 1990 15 p (For primary document see N91-27088 18-99)
(Grant NGT-44-005-803)
Avail: NTIS HC/MF A10 CSCL 06K

N91-27096*# South Carolina Univ., Columbia. Dept. of Computer Science.
INCORPORATION OF SHUTTLE CCT PARAMETERS IN COMPUTER SIMULATION MODELS Final Report
Terry Huntsberger *In* Houston Univ., NASA/ASEE Summer Faculty Fellowship Program, 1990, Volume 1 Dec. 1990 12 p (For primary document see N91-27088 18-99)
(Grant NGT-44-005-803)
Avail: NTIS HC/MF A10 CSCL 05H

55 SPACE BIOLOGY

Includes exobiology; planetary biology; and extraterrestrial life.

No abstracts in this category.

59 MATHEMATICAL AND COMPUTER SCIENCES (GENERAL)

No abstracts in this category.

60 COMPUTER OPERATIONS AND HARDWARE

Includes hardware for computer graphics, firmware, and data processing.

For components see *33 Electronics and Electrical Engineering.*

N91-26761# Naval Research Lab., Washington, DC.
TESTING THE ONE-PORT RANDOM ACCESS MEMORY (1PRAM) MODULE OF TRW'S CPUAX SIGNAL PROCESSING SUPERCHIP Final Report
Gregory C. Tavik 16 Apr. 1991 51 p
(AD-A234127; NRL-MR-6775) Avail: NTIS HC/MF A04 CSCL 12/5

The CPUAX Signal Processing Superchip has been developed by TRW under the VHSIC Phase 2 program. The chip utilizes a 0.5 micron Complementary Metal Oxide Semiconductor process and achieves a maximum throughput of 200 Mflops. The chip consists of 61 active macrocells, including 2 floating point arithmetic logic units (ALUs), 2 multiply accumulators (MACs), read and write address generators, 6 storage elements, read and write memory interfaces, and 39 identical 4Kx1-bit one port random access memory (1PRAM) modules. Each macrocell is provided with a chip specification and an IEEE 1076 VHSIC Hardware Description Language (VHDL) functional model. This report describes the testing of the functional performance and VHDL model of the 1PRAM macrocell by NRL. Testing was performed for two reasons: to verify that the macrocell behaves as specified and to validate the VHDL model. Three 1PRAM macrocells were received, each mounted on a 28-pin DIP test chip. All testing described herein was carried out on a Daisy Megalogician connected to a Physical Modeling Extension (PMX) using the 5.03 version of the Daisy DNIX operating system. This report describes the testing procedures, the problems encountered, and the ramifications of these. An algorithm is also included for future testing of similar devices on the Daisy CAD system with use of the PMX. It is shown that the 1PRAM functioned as TRW described in this design publications, which can be found in the References. GRA

N91-26762# IIT Research Inst., Lanham, MD.
REQUIREMENTS FOR DEVELOPING EMBEDDED REAL-TIME TRUSTED COMPUTER SYSTEM (ERT-TCSS) Final Report
31 Jul. 1990 172 p
(AD-A234325) Avail: NTIS HC/MF A08 CSCL 12/8

This paper documents the results of a research effort that attempts to define and categorize the requirements for secure embedded realtime systems. The recognition that security environments and requirements change during the life cycle of these systems is of major importance. Thus, this paper defines separate requirements for the development, operations, and maintenance environments for secure embedded real time systems. GRA

N91-26763# Syracuse Univ., NY.
CONTENT ADDRESSABLE MEMORY PROJECT Final Report, Sep. 1988 - Jan. 1990
Saul Y. Levy, J. S. Hall, and Donald E. Smith Nov. 1990 114 p Prepared in cooperation with Rutgers Univ., New Brunswick, NJ
(Contract F30602-88-D-0027)
(AD-A234524; RADC-TR-90-290) Avail: NTIS HC/MF A06 CSCL 12/5

The Content Addressable Memory Project Consists of the development of several experimental software systems on an AMT Distributed Array Processor (DAP) for evaluation and research purposes. The resulting determinations of the strengths and weaknesses of the DAP are discussed. Two new machine architectures were developed in an attempt to consolidate the strengths and overcome the weaknesses. The effort led to the analysis of certain parallel algorithms from a new point of view, and thus to a new class of parallel algorithms, the semiserial algorithms. GRA

N91-26764# Massachusetts Inst. of Tech., Cambridge. Lab. for Computer Science.
WAITING ALGORITHMS FOR SYNCHRONIZATION IN LARGE-SCALE MULTIPROCESSORS M.S. Thesis
Beng-Hong Lim Feb. 1991 106 p
(Contract N00014-87-K-0825)
(AD-A234985; MIT/LCS/TR-498) Avail: NTIS HC/MF A06 CSCL 12/5

A program running on a parallel machine consists of multiple asynchronous threads that have to synchronize at various points to ensure program correctness. At a synchronization point, a thread may be forced to wait until the synchronization condition is satisfied. Waiting incurs a cost. This thesis investigates various types of synchronization mechanisms and techniques to minimize wasted processor cycles while waiting algorithms and multithreading are used to reduce the cost of waiting. The utility of these methods are analyzed with mathematical models and demonstrated through simulations. Two-phase waiting algorithms that rely on efficient waiting mechanisms provided by multithreaded processors are shown to be very robust under most operating circumstances. GRA

N91-26765# Duke Univ., Durham, NC. Dept. of Computer Science.
COMPUTATIONAL COMPLEXITY AND EFFICIENCY IN ELECTRO-OPTICAL COMPUTING SYSTEM Final Report, 1 Sep. 1987 - 30 Sep. 1990
John Reif Feb. 1991 40 p
(Grant AF-AFOSR-0386-87; AF Proj. 2305)
(AD-A235013; AFOSR-91-0397TR) Avail: NTIS HC/MF A03 CSCL 09/5

The goals were (1) To develop robust theoretical model for a wide class of electro optical computing systems; (2) To extend the known capabilities, by design of new, more efficient algorithms for electro optical computing using less time, volume and energy. In particular, to develop efficient algorithms that use optimal combinations of time, volume and energy on electro optical computing systems; (3) To determine the fundamental theoretical limitations and capabilities of electro optical computing systems; In particular to determine lower bounds on tradeoffs between volume, time, and other resources (such as energy) of any electro optical computing system to solve fundamental problems. GRA

61 COMPUTER PROGRAMMING AND SOFTWARE

Includes computer programs, routines, alogorithms, and specific applications, e.g., CAD/CAM.

N91-26766*# Houston Univ., Clear Lake, TX. Software Engineering Professional Education Center.
OBJECT-ORIENTED REQUIREMENTS ANALYSIS: A QUICK TOUR
Edward V. Berard 1990 97 p Presented at the RICIS Software Engineering Symposium, Houston, TX
(Contract NCC9-16)
(NASA-CR-187919; NAS 1.26:187919) Avail: NTIS HC/MF A05 CSCL 09B

Of all the approaches to software development, an object-oriented approach appears to be both the most beneficial and the most popular. The description of the object-oriented approach is presented in the form of the view graphs. Author

N91-26767*# Institute for Computer Applications in Science and Engineering, Hampton, VA.
A PARALLEL RENDERING ALGORITHM FOR MIMD ARCHITECTURES Final Report
Thomas W. Crockett and Tobias Orloff (Great Northwestern Graphics, Minneapolis, MN.) Jun. 1991 26 p Submitted for publication
(Contract NAS1-18605)
(NASA-CR-187571; NAS 1.26:187571; ICASE-IR-91-3) Avail: NTIS HC/MF A03 CSCL 09B

Applications such as animation and scientific visualization demand high performance rendering of complex three dimensional scenes. To deliver the necessary rendering rates, highly parallel hardware architectures are required. The challenge is then to design algorithms and software which effectively use the hardware parallelism. A rendering algorithm targeted to distributed memory MIMD architectures is described. For maximum performance, the algorithm exploits both object-level and pixel-level parallelism. The behavior of the algorithm is examined both analytically and experimentally. Its performance for large numbers of processors is found to be limited primarily by communication overheads. An experimental implementation for the Intel iPSC/860 shows increasing performance from 1 to 128 processors across a wide range of scene complexities. It is shown that minimal modifications to the algorithm will adapt it for use on shared memory architectures as well. Author

N91-26768# Center for Mathematics and Computer Science, Amsterdam (Netherlands). Dept. of Numerical Mathematics.
NUMVEC FORTRAN LIBRARY MANUAL. CHAPTER: PARTIAL DIFFERENTIAL EQUATIONS. ROUTINE: ICGG3D
H. A. vanderVorst and J. J. F. M. Schlichting (Utrecht State Univ., Netherlands) Oct. 1990 15 p Sponsored by Netherlands Organization for the Advancement of Research
(CWI-NM-R9018; ETN-91-99411) Copyright Avail: NTIS HC/MF A03

The NUMVEC FORTRAN library routine ICCG3D for the solution of seven diagonal symmetrical linear systems, that arise from the seven point discretization of a partial differential equation over a three dimensional domain is described. Use is made of the so called MICCG hyperplane method with scaled initial diagonal, Eisenstat's trick and cyber 205 sparse vector instructions. An example shows a performance of nearly 85 MFLOPS for this routine. ESA

N91-26769# Naval Ocean Systems Center, San Diego, CA.
ITERATED TRANSFORM IMAGE COMPRESSION Final Report, Sep. 1989 - Oct. 1990
Y. Fisher, E. W. Jacobs, and R. D. Boss Apr. 1991 28 p
(NR Proj. RV3-6121)
(AD-A233655; NOSC/TR-1408) Avail: NTIS HC/MF A03 CSCL 12/9

The objectives of this research were to present in a clear manner an algorithm based on iterated transforms that can be used to compress grayscale images and demonstrate the algorithm and present results for various images. The theoretical framework for iterated transform image compression has been generalized to include noncontractive transforms. The method has been used to encode the 512 x 512 8-bpp image of Lena at a compression of 15.9:1 with the decode image having a root mean square error of 6.33 (32.1 dB). Other images have been encoded at various encoding conditions with the resulting compressions ranging from 10:1 to 63:1. It was shown that the relaxation of the contractivity constraint can lead to improvement in the fidelity of decoded images. GRA

N91-26770# Institute for Defense Analyses, Alexandria, VA.
AN APPROACH FOR CONSTRUCTING REUSABLE SOFTWARE COMPONENTS IN Ada Final Report
Stephen Edwards Sep. 1990 203 p
(Contract MDA903-89-C-0003)
(AD-A233662; IDA-P-2378; IDA/HQ-90-035362; AD-E501362)
Avail: NTIS HC/MF A10 CSCL 12/5

This paper discusses the topic of software reuse and is aimed at the software engineer who may actually be designing reusable software. The paper concentrates on many of the technical problems encountered when constructing reusable software components today. This paper does not, however, focus on the general problem of reusable software design. Instead, it focuses on the Ada programming language, and the problems software

engineers may encounter when designing components in this language. This paper is intended to be a companion to IDA Paper P-2494, Strategy and Mechanisms for Encouraging Reuse in the Acquisition of SDI Software. P-2494 discusses the managerial and legal issues involved with software reuse. GRA

N91-26771# Information Systems and Technology Center, Wright-Patterson AFB, OH. Validat Ion Facility.
Ada COMPILER VALIDATION SUMMARY REPORT: CERTIFICATION NUMBER: 9000703W1.11014, SILICON GRAPHICS 4D ADA IRIS-4D/380 (HOST) IRIS-4D/380 (TARGET) Final Report
7 Feb. 1991 33 p Sponsored by DOD
(AD-A233714; AVF-VSR-383.0291) Avail: NTIS HC/MF A03 CSCL 12/5

The following Ada implementation was tested and determined to pass ACVC 1.11. Testing was completed on 3 July 1990. Compiler name and version: 4D Ada 3.0; Host computer system: Iris-4D/380, IRIX Release 4D-3.3; Target computer system: Iris-4D/380, IRIX Release 4D-3.3; and Customer agreement number: 90-against the Ada Standard Ada83-03-16-SIL. The Ada implementation described above was tested according to the Ada Validation Procedures Pro90 using the current Ada Compiler Validation Capability (ACVC). This validation summary report gives an account of the testing of this Ada implementation. GRA

N91-26772# Stanford Univ., CA. Center for Large Scale Scientific Computation.
A SYSTEM AND LANGUAGE ENVIRONMENT FOR SCIENTIFIC COMPUTING Interim Report, Jul. 1989 - Mar. 1991
Joseph Oliger Mar. 1991 11 p
(Contracts N00014-89-J-1815; N00014-90-J-1344)
(AD-A233747; SU-CLASSIC-MANUSCRIPT-91-27) Avail: NTIS HC/MF A03 CSCL 12/5

We discuss the use of component adaptive methods for the solution of time dependent partial differential equations. After a brief discussion of the methods we identify several deficiencies of commonly used languages of scientific computing and introduce a graphical editor, VOUS, and a language, Vorpal, to solve these problems. We also discuss the interaction of the various components of our system and their interfaces. GRA

N91-26773# Institute for Defense Analyses, Alexandria, VA.
Ada SOFTWARE PORTABILITY AND LEVEL 2 SYSTEM SIMULATOR INTEGRATION ISSUES Final Report
Audrey A. Hook and Catherine W. McDonald Jan. 1991 30 p
(Contract MDA903-89-C-0003)
(AD-A233757; IDA-D-898; IDA/HQ-90-36708) Avail: NTIS HC/MF A03 CSCL 12/5

IDA Document D-898, Ada Software Portability and Level 2 System Simulator Integration Issues, identifies some of the issues that will affect the time and effort required to integrate Ada software developed for the Level 2 System Simulator (L2SS) of the Strategic Defense System (SDS) for the Strategic Defense Initiative Organization (SDIO) program. This document provides guidelines for managing ADA software integration problems that could occur when applications are developed on Ada implementations that are different from the target computer system where they will execute. The Cray 2/4D computer system, located at the National Test Facility, is the example of an Ada implementation that may be used as the platform for simulations. Three other Ada implementations considered typical software development environments were compared with the Cray 2/4D. The differences among these Ada implementations, as documented in Ada Validation Summary Reports, indicated the nature of portability issues that require resolution early in the software development process. Recommendations from this analysis are to (1) conduct portability analyses throughout the software development process, (2) endorse specific programming standards that have been demonstrated to be effective for both portability and performance, and (3) establish a working group to address compatibility and integration in SDI software development. GRA

N91-26774# Stanford Univ., CA. Dept. of Computer Science.
DEDUCTIVE PROGRAMMING SYNTHESIS Final Technical Report, 10 Nov. 1988 - 31 Dec. 1990
Zohar Manna 31 Dec. 1990 11 p
(Contract N00039-84-C-0211; DARPA Order 6177)
(AD-A233770) Avail: NTIS HC/MF A03 CSCL 12/5

Program synthesis is the systematic derivation of a computer program to meet a given specification. The specification is a general description of the purpose of the desired program, while the program is a detailed method for achieving that purpose. The method is based on a deductive approach, in which the problem of deriving a program is regarded as one of proving a mathematical theorem. The theorem expresses the existence of an object meeting the specified conditions. The proof is restricted to be sufficiently constructive to indicate a method for finding the desired output. That method becomes the basis for a program, which is extracted from the proof. The emphasis of the work has been on automating as much as possible of the program derivation process. Theorem-proving methods particularly well-suited to the program synthesis application have been developed. An interactive program-derivation system has been implemented. Applications to database management and planning have been investigated. GRA

N91-26775# Stanford Univ., CA. Center for Large Scale Scientific Computation.
ADAPTIVE COMPONENT METHODS FOR TIME DEPENDENT PDE'S Interim Report, Jul. 1989 - Mar. 1991
Joseph Oliger Mar. 1991 10 p
(Contracts N00014-89-J-1815; N00014-90-J-1344)
(AD-A233776; SU-CLASSIC-MANUSCRIPT-91-26) Avail: NTIS HC/MF A02 CSCL 12/3

Component adaptive grid methods for the solution of time dependent partial differential equations are described. These methods allow one to solve problems in complicated regions efficiently and accurately, to automatically control the accuracy of the results obtained, and provide a simple user interface. The use of a graphical editing system, VOUS, for grid generation and program development and of a language, Vorpal, for the implementation of these methods is discussed. GRA

N91-26776# Information Systems and Technology Center, Wright-Patterson AFB, OH. Ada Validat Ion Facility.
Ada COMPILER VALIDATION SUMMARY REPORT: CERTIFICATE NUMBER 900703W1.11015, SILICON GRAPHICS 4D Ada, IRIS-4D/220S (HOST) IRIS-4D/220S (TARGET) Final Report
7 Feb. 1991 33 p
(AD-A233786; AVF-VSR-384.0291) Avail: NTIS HC/MF A03 CSCL 12/5

The Ada implementation described above was tested according to the Ada Validation Procedures Pro90 against the Ada Standard Ada83 using the current Ada Compiler Validation Capability (ACVC). This Validation Summary Report (VSR) gives an account of the testing of this Ada implementation. GRA

N91-26777# Colorado Univ., Boulder. Dept. of Computer Science.
A THEORETICAL AND EXPERIMENTAL STUDY OF THE SYMMETRIC RANK ONE UPDATE
H. Khalfan, R. H. Byrd, and Robert B. Schnabel 31 Dec. 1990 33 p
(Contract DAAL03-88-K-0086)
(AD-A233965; CU-CS-489-90; ARO-24923.10-MA) Avail: NTIS HC/MF A03 CSCL 12/4

In this paper, we first discuss computational experience using the SR1 update in conventional line search and trust region algorithms for unconstrained optimization. Our experiments show that the SR1 is very competitive with the widely used BFGS method. They also indicate two interesting features: the final Hessian approximations produced by the SR1 method are not generally appreciably better than those produced by the BFGS, and the sequences of steps produced by the SR1 do not usually seem to

have the uniform linear independence property that is assumed in some recent convergence analysis. We present a new analysis that shows that the SR1 method with a line search in n+1 step q-superlinearly convergent without assumption of linearly independent iterates. This analysis assumes that the Hessian approximations are positive definite and bounded asymptotically, which from our computational experience are reasonable assumptions. GRA

N91-26778# Colorado Univ., Boulder. Dept. of Computer Science.
A SOFTWARE PACKAGE FOR UNCONSTRAINED OPTIMIZATION USING TENSOR METHODS
Ta-Tung Chow, Elizabeth Eskow, and Robert B. Schnabel 31 Dec. 1990 21 p
(Contract DAAL03-88-K-0086)
(AD-A233989; CU-CS-491-90; ARO-24923.9-MA) Avail: NTIS HC/MF A03 CSCL 12/5

This paper describes a software package for finding the unconstrained minimizer of a nonlinear function of n variables. The package is intended for problems where n is not too large, say n less than 100, so that the cost of storing one n x n matrix, and factoring it at each iteration, is acceptable. The software allows the user to choose between a recently developed tensor method for unconstrained optimization, and an analogous standard method based upon a quadratic model. The tensor method bases each iteration upon a specially constructed fourth order model of the objective function that is not significantly more expensive to form, store, or solve than the standard quadratic model. In our experience, the tensor method requires significantly fewer iterations and function evaluations to solve most unconstrained optimization problems than standard methods based upon quadratic models, and also solves a somewhat wider range of problems. For these reasons, it may be a useful addition to numerical software libraries. GRA

N91-26779# Naval Research Lab., Washington, DC.
NRL CONNECTION MACHINE FORTRAN LIBRARY Final Report
Michael A. Young 16 Apr. 1991 196 p
(AD-A234121; NRL-MR-6807) Avail: NTIS HC/MF A09 CSCL 12/5

The NRL Connection Machine Fortran Library consists of numerous mathematical routines coded in CM Fortran along with lower level routines written in Paris which manipulate data, plot data, and perform operations unavailable in the context of the CM Fortran language. Users are able to remain entirely within the CM Fortran programming environment while making calls to these library routines. Interfaces to the Framebuffer, a high resolution graphics device, and the DataVault, a high speed I/O channel, are available. A summary and demonstration of each routine is provided. GRA

N91-26780# Massachusetts Inst. of Tech., Cambridge. Lab. for Computer Science.
USING MAPPINGS TO PROVE TIMING PROPERTIES
Nancy A. Lynch and Hagit Attiya Mar. 1991 43 p
(Contracts N00014-85-K-0168; N00014-91-J-1046; N00014-87-K-0825; N00014-89-J-1988; NSF CCR-86-11442; NSF CCR-89-15206)
(AD-A234404; MIT/LCS/TM-412.C) Avail: NTIS HC/MF A03 CSCL 12/5

A new technique for proving timing properties for timing based algorithms is described; it is an extension of the mapping techniques previously used in proofs of safety properties for asynchronous concurrent systems. The key to the method is a way of representing a system with timing constraints as an automaton whose state includes predictive timing information. Timing assumptions and timing requirements for the system are both represented in this way. A multi-valued mapping from the assumptions automaton to the requirements automaton is then used to show that the given system satisfies the requirements. One type of mapping is based on a collection of variant functions providing measures of progress toward timing goals. The technique is illustrated with two examples, a simple resource manager and a two-process race system. GRA

N91-26781# Massachusetts Inst. of Tech., Cambridge. Artificial Intelligence Lab.
THE SHAPE OF SHADING Memorandum Report
Daphna Weinshall Oct. 1990 38 p Prepared in cooperation with Whitaker Coll., MA
(Contracts DACA76-85-C-0010; N00014-85-K-0124; NSF IRI-87-19394)
(AD-A234419; AI-M-1264; CBIP-M-60) Avail: NTIS HC/MF A03 CSCL 12/9

The relationship is discussed between the shape of the shading, the surface whose depth at each point equals the brightness in the image, and the shape of the original surface. The shading is suggested as an initial local approximation to shape, and the scope of this approximation and what it may be good for is discussed. In particular, qualitative surface features, such as the sign of the Gaussian curvature, can be computed in some cases directly from the shading. Finally, a method to compute the direction of the illuminant (assuming a single point light source) from shading on occluding contours is shown. GRA

N91-26782# Massachusetts Inst. of Tech., Cambridge. Artificial Intelligence Lab.
CONTINUOUS STOCHASTIC CELLULAR AUTOMATA THAT HAVE A STATIONARY DISTRIBUTION AND NO DETAILED BALANCE Memorandum Report
Tomaso Poggio and Federico Girosi Dec. 1990 7 p
(Contracts DACA76-85-C-0010; N00014-85-K-0124)
(AD-A234421; AI-M-1168) Avail: NTIS HC/MF A02 CSCL 12/1

Marroquin and Ramirez (1990) have recently discovered a class of discrete stochastic cellular automata with Gibbsian invariant measure that have a non-reversible dynamic behavior. Practical applications include more powerful algorithms than the Metropolis algorithm to compute MRF models. In this paper we describe a large class of stochastic dynamical systems that has a Gibbs asymptotic distribution but does not satisfy reversibility. We characterize sufficient properties of a sub-class of stochastic differential equations of the associated Fokker Planck equation for the existence of an asymptotic probability distribution in the system of coordinates which is given. Practical implications include VLSI analog circuits to compute coupled MRF models. GRA

N91-26783# Unisys Corp., Reston, VA. Tactical Systems Div.
SOFTWARE TECHNOLOGY FOR ADAPTABLE, RELIABLE SYSTEMS (STARS), UR60-IRIS-Ada TOOLSET. USER'S GUIDE (DRAFT)
25 Jan. 1991 12 p
(Contract F19628-88-D-0031)
(AD-A234445; STARS-RC-01310/001/00; GR-7670-1162(NP)) Avail: NTIS HC/MF A03 CSCL 12/5

The STARS Iris-Ada toolset consists of a translator which translates Ada program units into the Iris-Ada representation, a set of library management tools, and the basic components needed to construct other tools which use the Iris-Ada representation. This report describes how to install this toolset from sources and how to use the various tools. GRA

N91-26784# Naval Research Lab., Washington, DC.
BaRT MANUAL VERSION 3.0 Memorandum Report
Naveen Hota, Connie L. Ramsey, and Li W. Chang 14 Feb. 1991 47 p
(AD-A234528; NRL-MR-6778) Avail: NTIS HC/MF A03 CSCL 12/5

BaRT is an inference engine which as been developed to aid in classification problem solving. This inference engine uses Bayesian reasoning and can handle problems associated with incomplete and uncertain evidence. It has successfully been used to perform ship classification. This manual describes how to load

the BaRT computer program and how to use all of the available commands. This manual also provides some theoretical background and some implementation details concerning BaRT. GRA

N91-26785# Army Armament Research, Development and Engineering Center, Picatinny Arsenal, NJ.
APPLICATION OF SOFTWARE TOOLS IN EMBEDDED COMPUTERS WITHIN MILITARY SYSTEMS TO ENHANCE SOFTWARE RELIABILITY, QUALITY ASSURANCE, AND MAINTENANCE
William R. Turoczy Apr. 1991 14 p
(AD-A234555; ARFSD-TR-91007) Avail: NTIS HC/MF A03
CSCL 12/5

This report presents the application of the cyclomatic complexity requirement within a military system to improve reliability, quality assurance, and maintenance for the embedded computers within the 155 mm self-propelled Howitzer Improvement Program (HIP). The cyclomatic complexity requirement was used in HIP based on research and documentation described in: (1) NBS 500-99, Cyclomatic Complexity Metric; and (2) the 1985 Reliability and Maintainability Symposium, The Application of Software Test Tools. Results from the Joint U.S. Army/Israeli Defense Force HIP are impressive and the report highlights significant achievements in the software engineering discipline and applications within embedded computers within military systems. GRA

N91-26786# Boeing Computer Services Co., Seattle, WA. Advanced Technology Center.
ELECTRONIC DESIGN PROCESS Interim Technical Paper, Jan. 1988 - Dec. 1990
Charles T. Kitzmiller and Michael A. Anderson Jan. 1991 245 p
(Contract F33615-87-C-0001)
(AD-A234709; AFHRL-TP-90-34) Avail: NTIS HC/MF A11
CSCL 12/5

The goal of the Reliability, Availability, and Maintainability in Computer-Aided Design (RAMCAD) research effort is to define a design environment that fully supports reliability, maintainability, and supportability (RM and S) issues through the use of computer-aided design/computer-aided engineering (CAD/CAE) workstations. The goal of the Boeing Computer Services contract is to define a computer-aided method to help design engineers optimize designs relative to RM and S issues. To accomplish this goal, Boeing analyzed the electronic design process currently used to design avionics systems for military applications. This paper describes the results of that study and describes the major tasks associated with the design of typical avionics systems from system requirements analysis through to detailed design and evaluation. In addition to providing task description and flow charts of the tasks performed during both system engineering and detailed design, the paper also describes the key packaging and manufacturing considerations that must be taken into account and discusses key problem areas in the current design process. GRA

N91-26787# Bell Communications Research, Inc., Morristown, NJ.
COORDINATION IN LARGE SCALE SOFTWARE DEVELOPMENT
Robert E. Kraut and Lynn A. Streeter 1990 23 p
(AD-A234898) Avail: NTIS HC/MF A03 CSCL 12/5

Successful software development requires tight coordination among subgroups involved in the development process. Coordination is difficult because of the division of labor, interdependence and uncertainty inherent in large software projects. A survey in 65 software development projects reveals that informal communication is necessary for coordination under these circumstances. Results show that software professionals got much of their information from other people. They perceived that interpersonal techniques for getting information from beyond their immediate work group were underused, while more formal procedures for tracking routine information were overused compared to their value. Technically uncertain projects and highly interdependent ones had staffs who were poorly informed and were poorly coordinated. When project members had a large network of personal contacts outside the project, information flow improved, especially when the project was uncertain. The paper concludes with organizational and technological suggestions for increasing the flow of relevant information across functional boundaries in projects. GRA

N91-26788# Stanford Univ., CA. Systems Optimization Lab.
CONVERTING A CONVERGING ALGORITHM INTO A POLYNOMIALLY BOUNDED ALGORITHM
George B. Dantzig Mar. 1991 9 p
(Contract N00014-89-J-1659; NSF DMS-89-13089)
(AD-A234961; SU-SOL-91-5) Avail: NTIS HC/MF A02 CSCL 12/3

This document considers a certain general phase one linear programming problem with a convexity constraint which can be written after some algebraic manipulation in the form: Find x(sub j), sum to n terms from 1 to n of P(sub j)x(sub j), sum to n terms from 1 to n of x(sub j) = 1 where P(sub j) are m-vectors satisfying norm of vector P(sub j) = 1. If feasible, von Neumann's center of gravity algorithm generates a sequence of approximate solutions which converges in the limit as t approaches infinity to a feasible solution to the phase one problem. GRA

N91-26789# Stanford Univ., CA. Systems Optimization Lab.
LARGE-SCALE STOCHASTIC LINEAR PROGRAMS: IMPORTANCE SAMPLING AND BENDERS DECOMPOSITION
George B. Dantzig and Gerd Infanger Mar. 1991 16 p
(Contract N00014-89-J-1659; NSF ECS-89-06260)
(AD-A234962; SU-SOL-91-4) Avail: NTIS HC/MF A03 CSCL 12/4

The paper demonstrates how large-scale stochastic linear programs with recourse can be efficiently solved by using a blending of classical Benders decomposition with a relatively new technique called importance sampling. Numerical results of large-scale problems in the area of expansion planning of power systems and financial planning are presented. GRA

N91-26790# North Carolina State Univ., Raleigh.
PARALLEL ALGORITHMS FOR LEAST SQUARES AND RELATED COMPUTATIONS Final Report, 1 Aug. 1988 - 31 Jan. 1991
Robert J. Plemmons 22 Mar. 1991 18 p
(Grant AF-AFOSR-0285-88; AF Proj. 2304)
(AD-A235018; AFOSR-91-0253TR) Avail: NTIS HC/MF A03
CSCL 12/6

Algorithms for signal processing and image processing have been developed and implemented on a variety of computer architectures including a Cray Y-MP, an Intel iPSC/2, a Connection Machine, and an Alliant FX/40. Research has also been conducted on interactive least squares and related methods with applications to structural analysis. GRA

N91-26791# Massachusetts Inst. of Tech., Cambridge. Artificial Intelligence Lab.
PROGRAM IMPROVEMENT BY AUTOMATIC REDISTRIBUTION OF INTERMEDIATE RESULTS Ph.D. Thesis
Robert J. Hall Dec. 1990 278 p
(Contract N00014-88-K-0487)
(AD-A235086; AI-TR-1251) Avail: NTIS HC/MF A13 CSCL 12/5

The introduction of function sharing, a universal principle of design optimization, allows eliminating costly structure by using other structure to perform the function of the original. This approach is particularly applicable to eliminating the inefficiencies that arise naturally in reusing general software components in specific contexts. In this research, I have studied a restricted form of function sharing, redistribution of intermediate results, which is characterized by the fact that each optimization can be implemented using only introduction of new local variables, additional function arguments, and additional function return values. Examples are given showing that these optimizations can capture

many well-known types of optimizations, such as copy elimination; generalized loop fusion; identical value sharing, and data invariant suspension. I have decomposed the problem into two subproblems: first search for a small set of plausible candidates, then certify the correctness of each candidate. My system solves the search/screening subproblem while leaving certification up to one of a variety of possible external approaches. The system performs search and screening by automatically deriving operational filtering predicates from teleological input information obtainable as a natural by-product of the design process. GRA

N91-26792# Massachusetts Inst. of Tech., Lexington. Lincoln Lab.

USING GENETIC ALGORITHMS TO SELECT AND CREATE FEATURES FOR PATTERN CLASSIFICATION

E. I. Chang and Richard P. Lippmann 11 Mar. 1991 90 p
(Contract F19628-90-C-0002)
(AD-A235165; TR-892; ESD-TR-90-144) Avail: NTIS HC/MF A05 CSCL 12/9

Genetic algorithms were used to select and create features and to select reference exemplar patterns for machine vision and speech pattern classification tasks. On a 15-feature machine-vision inspection task, it was found that genetic algorithms performed no better than conventional approaches to feature selection but required much more computation. For a speech recognition task, genetic algorithms required no more computation time than traditional approaches but reduced the number of features required by a factor of five (from 153 to 33 features). On a difficult artificial machine-vision task, genetic algorithms were able to create new features (polynomial functions of the original features) that reduced classification error rates from 10 to almost 0 percent. Neural net and nearest-neighbor classifiers were unable to provide such low error rates using only the original features. Genetic algorithms were also used to reduce the number of reference exemplar patterns and to select the value of k for a k-nearest-neighbor classifier. On a 338 training pattern vowel recognition problem with 10 classes, genetic algorithms simultaneously reduced the number of stored exemplars from 338 to 63 and selected k without significantly decreasing classification accuracy. In all applications, genetic algorithms were easy to apply and found good solutions in many fewer trials than would be required by an exhaustive search. Run times were long but not unreasonable. These results suggest that genetic algorithms may soon be practical for pattern classification problems as faster serial and parallel computers are developed. GRA

N91-26793# California Univ., Davis. Dept. of Mathematics.

NONLINEAR STOCHASTIC OPTIMIZATION SOLUTION PROCEDURES AND INCOMPLETE INFORMATION Final Report, 1 Sep. 1985 - 30 Nov. 1990

Roger Wets 30 Nov. 1990 7 p
(Grant AF-AFOSR-0272-85; AF Proj. 2304)
(AD-A235242; AFOSR-91-0381TR) Avail: NTIS HC/MF A02 CSCL 12/3

The development of solution procedures for large scale linear and nonlinear stochastic optimization problems (decision making under uncertainty) was examined. The achievements include the publication of a number of reports in scientific journals (by the principal investigators, his students and collaborators), the development and testing of experimental computer programs for such classes of problems. An overall program or research in the solution of dynamic, stochastic optimization programs was completed. A new modelling paradigm for these problems, scenario aggregation, was developed. Solution procedures for parallel computers were designed, and a new algorithm, Lagrangian finite generation, was developed. GRA

N91-26794# Joint Data Systems Support Center, Washington, DC.

SOFTWARE REQUIREMENTS SPECIFICATION FOR THE MAPPING AND GRAPHIC INFORMATION CAPABILITY (MAGIC). VOLUME 4: GEOGRAPHIC MAPPING CSCI

Jeanne L. Muenzen 1 Dec. 1990 41 p
(Contract DCA100-89-C-0015)
(AD-A235275; DCA/JDSSC-SRS-1-90-Vol-4) Avail: NTIS HC/MF A03 CSCL 12/5

This Software Requirements Specifications (SRS) establishes the engineering and qualification requirements for the Geographic Mapping CSCI (CSCI-4). The Geographic Mapping CSCI enables the MAGIC user to create, edit, and display both vector and raster based maps with an optical ability to overlay the user's data on a Unix-based workstation. The DeLorme Mapping System (DMS) is used to provide the map data and the overwhelming bulk of functionality for this CSCI with MAGIC providing a user friendly graphical user interface (GUI) to the underlying commercial off the shelf (COTS) package. Map data is retrieved and displayed in an average of 6 seconds from large digital databases. Once retrieved, any location in the world can be specified within 1 meter and all geographic data in the system may be located precisely in terms of its latitude and longitude or Universal Transverse Mercator (UTM) position. GRA

N91-26795# Massachusetts Inst. of Tech., Lexington. Lincoln Lab.

A COMPARATIVE STUDY OF THE PRACTICAL CHARACTERISTICS OF NEURAL NETWORK AND CONVENTIONAL PATTERN CLASSIFIERS

Kenney Ng and Richard P. Lippmann 19 Mar. 1991 121 p
(Contract F19628-90-C-0002)
(AD-A235345; TR-894; ESD-TR-90-118) Avail: NTIS HC/MF A06 CSCL 12/9

Six pattern classifiers were implemented on a serial computer and compared using artificial and speech recognition tasks. Two neural network classifiers (radial basis function and high-order polynomial GMDH network) and four more conventional classifiers (Gaussian mixture, linear tree, KD-tree, and condensed K nearest neighbor) were investigated. These classifiers were chosen to be representative of different approaches to the task of pattern recognition, and to complement and extend those that were investigated in a previous study. The goal was to analyze and compare the performance and behavior of the classifiers on different tasks in terms of classification error rate, complexity, memory requirements, and training and classification times. Radial basis function classifiers generalized well to high-dimensional spaces, and provided low error rates with training times that were much less than those of back-propagation classifiers. High-order polynomial classifiers provided intermediate error rates, but often required very long training times. In addition, the decision regions formed did not extrapolate well to data-poor regions of the input space. GRA

N91-26796*# National Aeronautics and Space Administration. Ames Research Center, Moffett Field, CA.

PARALLEL PROCESSING AND EXPERT SYSTEMS

Sonie Lau and Jerry C. Yan (Sterling Federal Systems, Inc., Palo Alto, CA.) May 1991 40 p
(NASA-TM-103886; A-91077; NAS 1.15:103886) Avail: NTIS HC/MF A03 CSCL 09B

Whether it be monitoring the thermal subsystem of Space Station Freedom, or controlling the navigation of the autonomous rover on Mars, NASA missions in the 1990s cannot enjoy an increased level of autonomy without the efficient implementation of expert systems. Merely increasing the computational speed of uniprocessors may not be able to guarantee that real-time demands are met for larger systems. Speedup via parallel processing must be pursued alongside the optimization of sequential implementations. Prototypes of parallel expert systems have been built at universities and industrial laboratories in the U.S. and Japan. The state-of-the-art research in progress related to parallel execution of expert systems is surveyed. The survey discusses multiprocessors for expert systems, parallel languages for symbolic computations, and mapping expert systems to multiprocessors. Results to date indicate that the parallelism achieved for these systems is small. The main reasons are (1) the body of knowledge applicable in any given situation and the amount of computation executed by each rule firing are small, (2) dividing the problem

solving process into relatively independent partitions is difficult, and (3) implementation decisions that enable expert systems to be incrementally refined hamper compile-time optimization. In order to obtain greater speedups, data parallelism and application parallelism must be exploited. Author

N91-26797*# Boeing Military Airplane Development, Seattle, WA.
STRUCTURED REPRESENTATION FOR REQUIREMENTS AND SPECIFICATIONS
Gerald C. Cohen, Gene Fisher, Deborah Frincke, and Dave Wolber (California Univ., Davis.) 18 Jul. 1991 93 p
(Contract NAS1-18586)
(NASA-CR-187522; NAS 1.26:187522) Avail: NTIS HC/MF A05 CSCL 09B

This document was generated in support of NASA contract NAS1-18586, Design and Validation of Digital Flight Control Systems suitable for Fly-By-Wire Applications, Task Assignment 2. Task 2 is associated with a formal representation of requirements and specifications. In particular, this document contains results associated with the development of a Wide-Spectrum Requirements Specification Language (WSRSL) that can be used to express system requirements and specifications in both stylized and formal forms. Included with this development are prototype tools to support the specification language. In addition a preliminary requirements specification methodology based on the WSRSL has been developed. Lastly, the methodology has been applied to an Advanced Subsonic Civil Transport Flight Control System. Author

N91-26798# Sandia National Labs., Albuquerque, NM.
QUANTITATIVE ANALYSIS PROCEDURES FOR TASK 8
W. F. Chambers and J. H. Doyle Dec. 1990 39 p
(Contract DE-AC04-76DP-00789)
(DE91-009684; SAND-90-1704) Avail: NTIS HC/MF A03

Quantitative analysis routines based on the Bence-Albee, the ZAF, and the Phi rho Z techniques are available for the TASK8 microprobe operating system. All of the routines are able to be run from within TASK8 or as stand alone programs. For quick analyses, energy dispersive x ray data can be collected and processed by running the Tracor standardless quantitative (SQ) routine from within TASK8. For normal analyses, data are collected via the wavelength spectrometers. The procedures and routines described permit the interactive collection and processing of data via joystick control or the automatic collection and processing of data from up to seven line traces or an essentially unlimited number of preselected points. DOE

N91-27099*# Texas A&M Univ., College Station. Dept. of Aerospace Engineering.
A NONRECURSIVE ORDER N PRECONDITIONED CONJUGATE GRADIENT: RANGE SPACE FORMULATION OF MDOF DYNAMICS Final Report
Andrew J. Kurdila *In* Houston Univ., NASA/ASEE Summer Faculty Fellowship Program, 1990, Volume 1 Dec. 1990 16 p
(For primary document see N91-27088 18-99)
(Grant NGT-44-005-803)
Avail: NTIS HC/MF A10 CSCL 09B

62 COMPUTER SYSTEMS

Includes computer networks and special application computer systems.

N91-26799# Arizona Univ., Tucson. Optical Sciences Center.
PART 1: ULTRAFAST LOGIC AND MULTIPLE-BEAM OPTICAL PARALLEL PROCESSING USING NONLINEAR ETALONS. PART 2: NOVEL DEVICES FOR ALL-OPTICAL COMPUTING. PART 3: NOVEL NONLINEAR SEMICONDUCTOR STRUCTURES FOR SIGNAL PROCESSING AND OPTICAL COMPUTING Report, 15 Aug. 1986 - 30 Sep. 1990
H. Gibbs, N. Peyghambarian, G. I. Stegeman, and D. Sarid Feb. 1991 552 p
(Contract N00014-86-K-0719)
(AD-A233410) Avail: NTIS HC/MF A24 CSCL 09/5

The objective of the investigation on ultrafast logic and multiple-beam optical parallel processing using nonlinear etalons was to examine ultrafast optical switching devices and logic gates for optical signal parallel processing using nonlinear semiconductors. The novel devices for all-optical computing addresses nonlinear direction coupler and nonlinear grating devices in InSb waveguides. The novel nonlinear semiconductor structures for signal processing and optical computing section discusses the subsystems of a laboratory for scanning probe microscopy. GRA

N91-26800*# Worcester Polytechnic Inst., MA.
TRANSLATING EXPERT SYSTEM RULES INTO Ada CODE WITH VALIDATION AND VERIFICATION Final Report, Jan. - Dec. 1989
Lee Becker, R. James Duckworth, Peter Green, Bill Michalson (Raytheon Co., Marlborough, MA.), Dave Gosselin, Krishan Nainani, and Adam Pease Jun. 1991 116 p
(Grant NAG1-964)
(NASA-CR-187505; NAS 1.26:187505) Avail: NTIS HC/MF A06 CSCL 09B

The purpose of this ongoing research and development program is to develop software tools which enable the rapid development, upgrading, and maintenance of embedded real-time artificial intelligence systems. The goals of this phase of the research were to investigate the feasibility of developing software tools which automatically translate expert system rules into Ada code and develop methods for performing validation and verification testing of the resultant expert system. A prototype system was demonstrated which automatically translated rules from an Air Force expert system was demonstrated which detected errors in the execution of the resultant system. The method and prototype tools for converting AI representations into Ada code by converting the rules into Ada code modules and then linking them with an Activation Framework based run-time environment to form an executable load module are discussed. This method is based upon the use of Evidence Flow Graphs which are a data flow representation for intelligent systems. The development of prototype test generation and evaluation software which was used to test the resultant code is discussed. This testing was performed automatically using Monte-Carlo techniques based upon a constraint based description of the required performance for the system. Author

N91-26801# North Carolina State Univ., Raleigh.
STRATEGIES FOR RELIABLE AND REAL TIME EXECUTION ON A HETEROGENEOUS MULTIPROCESSOR Final Report
Dharma P. Agrawal and Jon Mauney 28 Feb. 1991 26 p
(Contract DAAL03-89-K-0142)
(AD-A234114; ARO-26150.3-EL) Avail: NTIS HC/MF A03 CSCL 12/6

Two important optimization methods were considered for private memory multiprocessors: (1) a new static dynamic processor allocation and scheduling strategy; and (2) a message segmentation technique to minimize task completion time. The first strategy finds optimal number of processors required for a program; and the second performs an optimal partition of the messages so as to achieve maximum overlap in communication and computation in private memory systems. GRA

N91-26802# Naval Research Lab., Washington, DC.
AN IMPLEMENTATION OF THE SINGULAR VALUE DECOMPOSITION ON THE CONNECTION MACHINE CM-2
Nhi-Anh Chu 11 Apr. 1991 41 p
(AD-A234124; NRL-9318) Avail: NTIS HC/MF A03 CSCL 12/5

In modern digital signal processing, the singular value decomposition is increasingly recognized as an important mathematical tool. The true measure of usefulness of such a tool is very much dependent on the ability to compute it at 'supercomputer' throughput rates. This report describes an

implementation of the singular value decomposition (SVD) on the Connection Machine CM-2 using parallel Fortran. The algorithm is based on Hestenes's, which is a Jacobi iteration in which pairs of rows are rotated to become orthogonal. The Fortran implementation of this algorithm on a full CM-2 is comparable in execution speed to the Linpack implementation on a Convex C220 processor. GRA

N91-26803# Massachusetts Inst. of Tech., Cambridge. Lab. for Computer Science.
STRUCTURE DRIVEN MULTIPROCESSOR COMPILATION OF NUMERIC PROBLEMS Ph.D. Thesis
G. N. Prasanna Apr. 1991 137 p
(Contract N00014-89-J-1489)
(AD-A234653; MIT/LCS/TR-502) Avail: NTIS HC/MF A07 CSCL 12/6

The optimal automatic compilation of computation intensive numeric problems onto multiprocessors is of great current interest. While optimal compilation is NP-Hard in general, the extensive structure present in many numeric algorithms greatly facilitates their optimal compilation. The application is explored of a hierarchical compilation paradigm for such algorithms. These algorithms can be specified as matrix expressions composed of matrix sums, products, and inverses, FFTs, etc. Good compilations for these algorithms can be derived by composing together good routines for these basic operators, thus yielding a hierarchical compilation strategy. The use is explored of the extensive structure present in matrix operations to derive close to optimal routines for them, thus creating a parallel library. It is shown show that these operator routines vary in a smooth fashion over a space of parameterized architectures. GRA

N91-26804*# Cornell Univ., Ithaca, NY. Dept. of Computer Science.
THE PROCESS GROUP APPROACH TO RELIABLE DISTRIBUTED COMPUTING
Kenneth P. Birman Jul. 1991 37 p Sponsored in part by IBM Corp.; Hewlett Packard Corp.; Siemens; GTE; and Hitachi
(Grant NAG2-593)
(NASA-CR-188498; NAS 1.26:188498; TR-91-1216) Avail: NTIS HC/MF A03 CSCL 09B

The difficulty of developing reliable distributed software is an impediment to applying distributed computing technology in many settings. Experience with the ISIS system suggests that a structured approach based on virtually synchronous process groups yields systems which are substantially easier to develop, fault-tolerance, and self-managing. Six years of research on ISIS are reviewed, describing the model, the types of applications to which ISIS was applied, and some of the reasoning that underlies a recent effort to redesign and reimplement ISIS as a much smaller, lightweight system. Author

N91-26805# Department of Energy, Washington, DC. Office of Energy Research.
LARGE SCALE COMPUTING IN THE ENERGY RESEARCH PROGRAMS
May 1991 80 p
(DE91-012128; DOE/ER-0496P) Avail: NTIS HC/MF A05

The Energy Research Supercomputer Users Group (ERSUG) comprises all investigators using resources of the Department of Energy Office of Energy Research supercomputers. At the December 1989 meeting held at Florida State University (FSU), the ERSUG executive committee determined that the continuing rapid advances in computational sciences and computer technology demanded a reassessment of the role computational science should play in meeting DOE's commitments. Initial studies were to be performed for four subdivisions: (1) Basic Energy Sciences (BES) and Applied Mathematical Sciences (AMS), (2) Fusion Energy, (3) High Energy and Nuclear Physics, and (4) Health and Environmental Research. The first two subgroups produced formal subreports that provided a basis for several sections of this report. Additional information provided in the AMS/BES is included as Appendix C in an abridged form that eliminates most duplication. Additionally, each member of the executive committee was asked to contribute area-specific assessments; these assessments are included in the next section. In the following sections, brief assessments are given for specific areas, a conceptual model is proposed that the entire computational effort for energy research is best viewed as one giant nation-wide computer, and then specific recommendations are made for the appropriate evolution of the system. DOE

63 CYBERNETICS

Includes feedback and control theory, artificial intelligence, robotics and expert systems.

For related information see also *54 Man/System Technology and Life Support.*

N91-26806*# Alabama Univ., Huntsville.
APPLICATIONS OF ARTIFICIAL INTELLIGENCE TO MISSION PLANNING Final Technical Progress Report, period ending 31 Aug. 1990
Donnie R. Ford, Stephen A. Floyd, and John S. Rogers 31 Aug. 1990 272 p
(Grant NAG8-717)
(NASA-CR-187953; NAS 1.26:187953) Avail: NTIS HC/MF A12 CSCL 09B

The following subject areas are covered: object-oriented programming task; rule-based programming task; algorithms for resource allocation; connecting a Symbolics to a VAX; FORTRAN from Lisp; trees and forest task; software data structure conversion; software functionality modifications and enhancements; portability of resource allocation to a TI MicroExplorer; frontier of feasibility software system; and conclusions. Author

N91-26807# California Univ., Los Angeles. Center for the Study of Evaluation.
MEASUREMENT EXPERT SYSTEM EFFECTIVENESS Final Report No. 24, 1 Jul. 1989 - 30 Nov. 1990
Harold F. ONeil, Jr. Nov. 1990 19 p
(Contract N00014-86-K-0395)
(AD-A234359) Avail: NTIS HC/MF A03 CSCL 12/5

Work is documented in the area of expert system effectiveness completed under a subcontract to the Cognitive Science Laboratory of the University of Southern California. Key technical outcomes of research which explored the feasibility of using a human benchmarking methodology to evaluate expert systems are examined. This work was done as part of the development of the Artificial Intelligence Measurement System (AIMS). GRA

N91-26808# California Univ., Los Angeles. Center for the Study of Evaluation.
EVALUATION OF EXPERT SYSTEMS: A REVIEW OF THE LITERATURE Research Project Report No. 23, 1 Jul. 1989 - 31 Dec. 1990
Kathleen M. Swigger, Harold F. ONeil, Jr., Yujing Ni, and Anat Jacoby Oct. 1990 27 p
(AD-A234360) Avail: NTIS HC/MF A03 CSCL 12/5

Current trends and experimental results are reviewed that have immediate application to the evaluation of expert systems. A methodology is offered for assessing expert systems in terms of human performance. In order to improve the performance of expert systems, a wide range of methods were proposed for their evaluation. Some of the major assessment techniques are reviewed and their success rate is reported. Particular emphasis is placed on the applicability of current research in software engineering, human performance measurement, simulation, and machine learning. Some of these techniques should be incorporated into a formal methodology that can be used to assess expert systems. Finally, the usefulness is shown of the approach by applying the methodology to a fully developed expert system named GATES. GRA

N91-26809# Massachusetts Inst. of Tech., Cambridge. Artificial Intelligence Lab.
IMAGINATION AND SITUATED COGNITION Memorandum Report
Lynn A. Stein Feb. 1991 10 p
(Contracts N00014-89-J-3202; N00014-85-K-0124)
(AD-A234420; AI-M-1277) Avail: NTIS HC/MF A02 CSCL 12/9

A subsumption-based mobile robot is extended to perform cognitive tasks. Following directions, the robot navigates directly to previously unexplored goals. This robot exploits a novel architecture based on the idea that cognition uses the underlying machinery of interaction, imagining sensations and actions. GRA

N91-26810# Massachusetts Inst. of Tech., Cambridge. Artificial Intelligence Lab.
EXTENSIONS OF A THEORY OF NETWORKS AND LEARNING: OUTLIERS AND NEGATIVE EXAMPLES Memorandum Report
Tomaso Poffio, Federico Girosi, and Bruno Caprile Jul. 1990 26 p Prepared in cooperation with Whitaker Coll., MA
(Contracts DACA76-85-C-0010; N00014-85-K-0124)
(AD-A234425; AI-M-1220; CBIP-46) Avail: NTIS HC/MF A03 CSCL 12/9

Learning an input output mapping from a set of examples, of the type that many neural networks have been constructed to perform, can be regarded as synthesizing an approximation of a multi dimensional function. From this point of view, this form of learning is closely related to regularization theory. The theory developed in Poggio and Girosi (1989) shows the equivalence between regularization and a class of three-layer networks that we call regularization networks or Hyper Basis Functions. These networks are not only equivalent to generalized splines, but are closely related to the classical Radial Basis Functions used for interpolation tasks and to several pattern recognition and neural network algorithms. In this note, we extend the theory by introducing ways of dealing with two aspects of learning: learning in the presence of unreliable examples and learning from positive and negative examples. These two extensions are interesting also from the point of view of the approximation of multivariate functions. The first extension corresponds to dealing with outliers among the sparse data. The second one corresponds to exploiting information about points or regions in the range of the function that are forbidden. GRA

N91-26811# Calspan-Buffalo Univ. Research Center, NY.
STRATEGIES FOR PARALLEL AI IMPLEMENTATIONS Final Report, Jul. 1989 - Jul. 1990
William B. Day Dec. 1990 62 p Prepared in cooperation with Auburn Univ., AL
(Contract F30602-88-D-0026)
(AD-A234449; RADC-TR-90-415) Avail: NTIS HC/MF A04 CSCL 12/6

This report examines computer architectures that are appropriate for the Parallel Knowledge Based System (PKS). As part of this effort, the PKS (originally simulated in Ada) was rewritten in C and renamed the Distributed Datalog (DDL) interpreter. The DDL runs a network of message passing nodes and is a model for either a multiprocessor executing a DDL program within a distributed memory or a logic program distributed among several nodes. This report describes the DDL architecture, addresses appropriate multiprocessor architectures for the DDL, describes the current DDL implementation and discusses a new memory allocation algorithm for the DDL. GRA

N91-26812# Loyola Univ., Chicago, IL. Dept. of Mathematical Sciences.
VISCOSITY METHODS IN OPTIMAL CONTROL OF DISTRIBUTED SYSTEMS. THE BELLMAN EQUATION Final Technical Report, May 1986 - Dec. 1990
Emmanuel N. Barron 28 Feb. 1991 4 p
(Grant AF-AFOSR-0202-86; AF Proj. 2304)
(AD-A234646; AFOSR-91-0278TR) Avail: NTIS HC/MF A01 CSCL 12/2

This project studied several problems in various areas of optimal control along with their applications. Major accomplishments include: (1) the use of dynamic programming to rigorously derive necessary conditions for distributed systems, (2) the initiation of the study of control with discontinuous, unbounded data, (3) the solution of the minimax problem in control and differential games, (4) the initiation of the concept of total risk aversion in stochastic control, and (5) the solution of the control problem with measure controls resulting in bounded variation trajectories. GRA

N91-26813# Massachusetts Inst. of Tech., Cambridge. Artificial Intelligence Lab.
USING MODULAR NEURAL NETWORKS WITH LOCAL REPRESENTATIONS TO CONTROL DYNAMIC SYSTEMS Annual Report, 1 Sep. 1989 - 30 Sep. 1990
Christopher G. Atkeson 26 Mar. 1991 18 p
(Grant AF-AFOSR-0500-89; AF Proj. 2305)
(AD-A234700; AFOSR-91-0452TR) Avail: NTIS HC/MF A03 CSCL 12/9

The objective is to develop an artificial neural network with very fast learning. Major areas of activity include developing cross validation methods to refine parameters such as the distance metric, developing parallel versions of the learning algorithms which allow implementations to be scaled up by simply adding additional processing hardware, with a negligible penalty in processing time, and performing numerical experiments on simulated data to test the approach. The approach was compared with other neural network approaches, and found that it provides equal or better performance. Versions of this approach were implemented on several computers (standard Sun workstations), digital signal processors (Intel i860), a parallel computer (Connection Machine), and using special purpose circuitry. Training and access can be performed sufficiently quick to allow real time learning. GRA

N91-26814# SRI International Corp., Menlo Park, CA.
ENGINEERING FOR ARTIFICIAL INTELLIGENCE SOFTWARE Final Report
John Rushby, Mark E. Stickel, and Richard J. Waldinger Dec. 1990 64 p
(Contract F30602-87-D-0094)
(AD-A234793; RADC-TR-90-424) Avail: NTIS HC/MF A04 CSCL 12/5

Rule based systems are being applied to tasks of increasing responsibility. This report focuses on techniques for the verification and validation of these systems. Conventional software quality assurance depends on the availability of requirements and specification documents. For rule systems, there are generally none because the capabilities of these systems evolve through a development process that is partly experimental in nature. Conventional testing techniques are considered; however, such techniques do not carry over absence of errors. Methods for proving the consistency of rule systems are examined. These methods require that the rules be viewed declaratively, which may be too much of a simplification. A semantics for rule systems based on term rewriting is developed. Standard tests for confluence of term rewriting systems cannot be converted to rule systems, however, because the firing of rules can depend on the absence, as well as the presence, of elements in working memory. Finally, we consider deductive methods for the validation of rule systems. GRA

N91-26815# Northeast Artificial Intelligence Consortium, Syracuse, NY.
NORTHEAST ARTIFICIAL INTELLIGENCE CONSORTIUM (NAIC). VOLUME 1: EXECUTIVE SUMMARY Final Report, Sep. 1984 - Dec. 1989
Volker Weiss and James F. Brule Dec. 1990 71 p
(Contract F30602-85-C-0008)
(AD-A234880; RADC-TR-90-404-Vol-1) Avail: NTIS HC/MF A04 CSCL 12/9

The Northeast Artificial Intelligence Consortium (NAIC) was created by the Air Force Systems Command, Rome Air Development Center, and the Office of Scientific Research. Its

purpose was to conduct pertinent research in artificial intelligence and to perform activities ancillary to this research. This report describes progress during the existence of the NAIC on the technical research tasks undertaken at the member universities. The topics covered in general are: (1) versatile expert system for equipment maintenance; (2) distributed AI for communications systems control; (3) automatic photointerpretation; (4) time-oriented problem solving; (5) speech understanding systems; (6) knowledge-based reasoning and planning; and (7) a knowledge acquisition, assistance, and explanation system. This volume provides the executive summary of the NAIC. GRA

N91-26816# Northeast Artificial Intelligence Consortium, Syracuse, NY.
NORTHEAST ARTIFICIAL INTELLIGENCE CONSORTIUM (NAIC). VOLUME 2: DISCUSSING, USING, AND RECOGNIZING PLANS Final Report, Sep. 1984 - Dec. 1989
Stuart C. Shapiro and Beverly Woolf Dec. 1990 137 p
(Contract F30602-85-C-0008)
(AD-A234881; RADC-TR-90-404-Vol-2) Avail: NTIS HC/MF A07 CSCL 12/9

The Northeast Artificial Intelligence Consortium (NAIC) was created by the Air Force Systems Command, Rome Air Development Center, and the Office of Scientific Research. Its purpose was to conduct pertinent research in artificial intelligence and to perform activities ancillary to this research. This report describes progress during the existence of the NAIC on the technical research tasks undertaken at the member universities. The topics covered in general are: (1) versatile expert system for equipment maintenance; (2) distributed AI for communications system control; (3) automatic photointerpretation; (4) time-oriented problem solving; (5) speech understanding systems; (6) knowledge base maintenance; (7) hardware architectures for very large systems; (8) knowledge based reasoning and planning; and (9) a knowledge acquisition, assistance, and explanation system. The specific topic for this volume is the recognition of plans expressed in natural language, followed by their discussion and use. GRA

N91-26817# Northeast Artificial Intelligence Consortium, Syracuse, NY.
NORTHEAST ARTIFICIAL INTELLIGENCE CONSORTIUM (NAIC). VOLUME 3: THE VERSATILE MAINTENANCE EXPERT SYSTEM (VMES) Final Report, Sep. 1984 - Dec. 1989
Sargur N. Srihari, Stuart C. Shapiro, and Shambhu J. Upadhyaya Dec. 1990 96 p
(Contract F30602-85-C-0008)
(AD-A234882; RADC-TR-90-404-Vol-3) Avail: NTIS HC/MF A05 CSCL 12/5

The Northeast Artificial Intelligence Consortium (NAIC) was created by the Air Force Systems Command, Rome Air Development Center, and the Office of Scientific Research. Its purpose was to conduct pertinent research in artificial intelligence and to perform activities ancillary to this research. This report describes progress during the existence of the NAIC on the technical research tasks undertaken at the member universities. The topics covered in general are: (1) versatile expert system for equipment maintenance; (2) distributed AI for communications system control; (3) automatic photointerpretation; (4) time-oriented problem solving; (5) speech understanding systems; (6) knowledge base maintenance; (7) hardware architectures for very large systems; (8) knowledge based reasoning and planning; and (9) a knowledge acquisition, assistance, and explanation system. The specific topic for this volume is the exploration of methods for developing a versatile expert system for equipment maintenance. GRA

N91-26818# Northeast Artificial Intelligence Consortium, Syracuse, NY.
NORTHEAST ARTIFICIAL INTELLIGENCE CONSORTIUM (NAIC). VOLUME 4: DISTRIBUTED ARTIFICIAL INTELLIGENCE FOR COMMUNICATIONS NETWORK MANAGEMENT Final Report, Sep. 1984 - Dec. 1989
Robert A. Meyer and Susan E. Conry Dec. 1990 161 p
(Contract F30602-85-C-0008)
(AD-A234883; RADC-TR-90-404-Vol-4) Avail: NTIS HC/MF A08 CSCL 12/7

The Northeast Artificial Intelligence Consortium (NAIC) was created by the Air Force Systems Command, Rome Air Development Center, and the office of Scientific Research. Its purpose was to conduct pertinent research in artificial intelligence and to perform activities ancillary to this research. This report describes progress during the existence of the NAIC on the technical research tasks undertaken at the member universities. The topics covered in general are: (1) versatile expert system for equipment maintenance; (2) distributed AI for communications system control; (3) automatic photointerpretation; (4) time-oriented problem solving; (5) speech understanding systems; (6) knowledge base maintenance; (7) hardware architectures for very large systems; (8) knowledge based reasoning and planning, and (9) a knowledge acquisition, assistance, and explanation system. The specific topic for this volume is the use of knowledge based systems for communications network management and control via an architecture for a diversely distributed multi-agent system. GRA

N91-26819# Northeast Artificial Intelligence Consortium, Syracuse, NY.
NORTHEAST ARTIFICIAL INTELLIGENCE CONSORTIUM (NAIC). VOLUME 5: DISTRIBUTED PLANNING FOR DYNAMIC ENVIRONMENTS IN THE PRESENCE OF TIME CONSTRAINTS Final Report, Sep. 1984 - Dec. 1989
Susan E. Conry, Robert A. Meyer, Paul R. Cohen, and Victor R. Lesser Dec. 1990 34 p
(Contract F30602-85-C-0008)
(AD-A234884; RADC-TR-90-404-Vol-5) Avail: NTIS HC/MF A03 CSCL 12/9

The Northeast Artificial Intelligence Consortium (NAIC) was created to conduct pertinent research in artificial intelligence and to perform activities ancillary to this research. This report describes progress during the existence of the NAIC on the technical research tasks undertaken at the member universities. The topics covered in general are: (1) versatile expert systems for equipment maintenance; (2) distributed AI for communications systems control; (3) automatic photointerpretation; (4) time-oriented problem solving; (5) speech understanding systems; (6) knowledge base maintenance; (7) hardware architectures for very large systems; (8) knowledge based reasoning and planning, and (9) a knowledge acquisition, assistance, and explanation system. The specific topic for this volume is the real-time simulation of a distributed planning simulation in the context of a dynamic environment. GRA

N91-26820# Northeast Artificial Intelligence Consortium, Syracuse, NY.
NORTHEAST ARTIFICIAL INTELLIGENCE CONSORTIUM (NAIC). VOLUME 6: BUILDING AN INTELLIGENT ASSISTANT: THE ACQUISITION, INTEGRATION, AND MAINTENANCE OF COMPLEX DISTRIBUTED TASKS Final Report, Sep. 1984 - Dec. 1989
Victor R. Lesser and W. B. Croft Dec. 1990 127 p
(Contract F30602-85-C-0008)
(AD-A234885; RADC-TR-90-404-Vol-6) Avail: NTIS HC/MF A07 CSCL 23/2

The Northeast Artificial Intelligence Consortium (NAIC) was created by the Air Force Systems Command, Rome Air Development Center, and the Office of Scientific Research. Its purpose was to conduct pertinent research in artificial intelligence and to perform activities ancillary to this research. This report describes progress during the existence of the NAIC on the technical research tasks undertaken at the member universities. The topics covered in general are: (1) versatile expert system for equipment maintenance; (2) distributed AI for communications system control; (3) automatic photointerpretation; (4) time-oriented problem solving; (5) speech understanding systems; (6) knowledge base maintenance; (7) hardware architectures for very large systems; (8) knowledge-based reasoning and planning, and (9) a knowledge acquisition, assistance, and explanation system. The

specific topic for this volume is the development of intelligent interfaces to support cooperating users in their interactions with a computer. GRA

N91-26821# Northeast Artificial Intelligence Consortium, Syracuse, NY.
NORTHEAST ARTIFICIAL INTELLIGENCE CONSORTIUM (NAIC). VOLUME 7: AUTOMATIC PHOTOINTERPRETATION Final Report, Sep. 1984 - Dec. 1989
James Modestino and Arthur Sanderson Dec. 1990 44 p
(Contract F30602-85-C-0008)
(AD-A234886; RADC-TR-90-404-Vol-7) Avail: NTIS HC/MF A03 CSCL 12/9

The Northeast Artificial Intelligence Consortium (NAIC) was created by the Air Force Systems Command, Rome Air Development Center, and the Office of Scientific Research. Its purpose was to conduct pertinent research in artificial intelligence and to perform activities ancillary to this research. This report describes progress during the existence of the NAIC on the technical research tasks undertaken at the member universities. The topics covered in general are: (1) versatile expert system for equipment maintenance; (2) distributed AI for communications system control; (3) automatic photointerpretation; (4) time-oriented problem solving; (5) speech understanding systems; (6) knowledge base maintenance; (7) hardware architectures for very large systems; (8) knowledge-based reasoning and planning, and (9) a knowledge acquisition, assistance, and explanation system. The specific topics for this volume are the use of expert systems for automated photointerpretation and other AI techniques to image segmentation and region identification. GRA

N91-26822# Northeast Artificial Intelligence Consortium, Syracuse, NY.
NORTHEAST ARTIFICIAL INTELLIGENCE CONSORTIUM (NAIC). VOLUME 8: ARTIFICIAL INTELLIGENCE APPLICATIONS TO SPEECH RECOGNITION Final Report, Sep. 1984 - Dec. 1989
Harvey E. Rhody and John Biles Dec. 1990 52 p
(Contract F30602-85-C-0008)
(AD-A234887; RADC-TR-90-404-Vol-8) Avail: NTIS HC/MF A04 CSCL 12/9

The Northeast Artificial Intelligence Consortium (NAIC) was created by the Air Force Systems Command, Rome Air Development Center, and the Office of Scientific Research. Its purpose was to conduct pertinent research in artificial intelligence and to perform activities ancillary to this research. This report describes progress during the existence of the NAIC of the technical research tasks undertaken at the member universities. The topics covered in general are: (1) versatile expert system for equipment maintenance; (2) distributed AI for communications system control; (3) automatic photointerpretation; (4) time-oriented problem solving; (5) speech understanding systems; (6) knowledge based maintenance; (7) hardware architectures for very large systems; (8) knowledge based reasoning and planning; and (9) knowledge acquisition, assistance, and explanation system. The specific topic for this volume is the design and implementation of a knowledge-based system to read speech spectrograms. GRA

N91-26823# Northeast Artificial Intelligence Consortium, Syracuse, NY.
NORTHEAST ARTIFICIAL INTELLIGENCE CONSORTIUM (NAIC). VOLUME 9: A PLANNER SYSTEM FOR THE APPLICATION OF INDICATIONS AND WARNING Final Report, Sep. 1984 - Dec. 1989
Sergei Nirenburg Dec. 1990 96 p
(Contract F30602-85-C-0008)
(AD-A234888; RADC-TR-90-404-Vol-9) Avail: NTIS HC/MF A05 CSCL 12/9

The Northeast Artificial Intelligence Consortium (NAIC) was created by the Air Force Systems Command, Rome Air Development Center, and the Office of Scientific Research. Its purpose was to conduct pertinent research in artificial intelligence and to perform activities ancillary to this research. This report describes progress during the existence of the NAIC on the technical research tasks undertaken at the member universities. The topics covered in general are: (1) versatile expert system for equipment maintenance; (2) distributed AI for communications system control; (3) automatic photointerpretation; (4) time-oriented problem solving; (5) speech understanding systems; (6) knowledge based maintenance, hardware architectures for very large systems; (7) knowledge based reasoning and planning; and (8) a knowledge acquisition, assistance, and explanation system. The specific topic for this volume is the design of a planning system for an indications and warning application. GRA

N91-26824# Northeast Artificial Intelligence Consortium, Syracuse, NY.
NORTHEAST ARTIFICIAL INTELLIGENCE CONSORTIUM (NAIC). VOLUME 10: TIME ORIENTED PROBLEM SOLVING Final Report, Sep. 1984 - Dec. 1989
James F. Allen Dec. 1990 23 p
(Contract F30602-85-C-0008)
(AD-A234889; RADC-TR-90-404-Vol-10) Avail: NTIS HC/MF A03 CSCL 12/9

The Northeast Artificial Intelligence Consortium (NAIC) was created by the Air Force Systems Command, Rome Air Development Center, and the Office of Scientific Research. Its purpose was to conduct pertinent research in artificial intelligence and to perform activities ancillary to this research. This report describes progress during the existence of the NAIC on the technical research tasks undertaken at the member universities. The topics covered in general are: (1) versatile expert system for equipment maintenance; (2) distributed AI for communications system control; (3) automatic photointerpretation; (4) time-oriented problem solving; (5) speech understanding systems; (6) knowledge base maintenance; (7) hardware architectures for very large systems; (8) knowledge-based reasoning and planning; and (9) a knowledge acquisition, assistance, and explanation system. The specific topic for this volume is a model theory and axiomatization of a logic for reasoning about planning in domains of concurrent actions. GRA

N91-26825# Northeast Artificial Intelligence Consortium, Syracuse, NY.
NORTHEAST ARTIFICIAL INTELLIGENCE CONSORTIUM (NAIC). VOLUME 11: KNOWLEDGE BASE MAINTENANCE Final Report, Sep. 1984 - Dec. 1989
Kenneth Bowen Dec. 1990 92 p
(Contract F30602-85-C-0008)
(AD-A234890; RADC-TR-90-404-Vol-11) Avail: NTIS HC/MF A05 CSCL 12/9

The Northeast Artificial Intelligence Consortium (NAIC) was created by the Air Force Systems Command, Rome Air Development Center, and the Office of Scientific Research. Its purpose was to conduct pertinent research in artificial intelligence and to perform activities ancillary to this research. This report describes progress during the existence of the NAIC on the technical research tasks undertaken at the member universities. The topics covered in general are: (1) versatile expert system for equipment maintenance; (2) distributed AI for communications system control; (3) automatic photointerpretation; (4) time-oriented problem solving; (5) speech understanding systems; (6) knowledge based maintenance; (7) hardware architectures for very large systems; (8) knowledge based reasoning and planning; and (9) a knowledge acquisition, assistance, and explanation system. The specific topic for this volume is the use of logic programming methodologies for knowledge base maintenance. GRA

N91-26826# Northeast Artificial Intelligence Consortium, Syracuse, NY.
NORTHEAST ARTIFICIAL INTELLIGENCE CONSORTIUM (NAIC). VOLUME 12: COMPUTER ARCHITECTURE FOR VERY LARGE KNOWLEDGE BASES Final Report, Sep. 1984 - Dec. 1989
P. B. Berra, Arif Ghafoor, Soon M. Chung, Nabil I. Hachem, and Slawomir J. Marcinkowski Dec. 1990 336 p

(Contract F30602-85-C-0008)
(AD-A234891; RADC-TR-90-404-Vol-12) Avail: NTIS HC/MF A15 CSCL 12/6

The Northeast Artificial Intelligence Consortium (NAIC) was created by the Air Force Systems Command, Rome Air Development Center, and the Office of Scientific Research. Its purpose was to conduct pertinent research in artificial intelligence and to perform activities ancillary to this research. This report describes progress during the existence of the NAIC on the technical research tasks undertaken at the member universities. The topics covered in general are: (1) versatile expert system for equipment maintenance; (2) distributed AI for communications systems control; (3) automatic photointerpretation; (4) time-oriented problem solving; (5) speech understanding systems; (6) knowledge of base maintenance; (7) hardware architectures for very large systems; (8) knowledge based reasoning and planning; and (9) a knowledge acquisition, assistance, and explanation system. The specific topic for this volume is the development of architectures for very large knowledge bases, especially in light of real time requests, parallelism, and the advent of optical computing. GRA

N91-26827# Northeast Artificial Intelligence Consortium, Syracuse, NY.
NORTHEAST ARTIFICIAL INTELLIGENCE CONSORTIUM (NAIC). VOLUME 18: A DISTRIBUTED ARTIFICIAL INTELLIGENCE APPROACH TO INFORMATION FUSION AND OBJECT CLASSIFICATION Final Report, Sep. 1984 - Dec. 1989
Pramod K. Varshney and Digvijay I. Sikka Dec. 1990 116 p
(Contract F30602-85-C-0008)
(AD-A234892; RADC-TR-90-404-Vol-18) Avail: NTIS HC/MF A06 CSCL 12/9

The Northeast Artificial Intelligence Consortium (NAIC) was created by the Air Force Systems Command, Rome Air Development Center, and the Office of Scientific Research. Its purpose was to conduct pertinent research in artificial intelligence and to perform activities ancillary to this research. This report describes progress during the existence of the NAIC on the technical research tasks undertaken at the member universities. The topics covered in general are: (1) versatile expert system for equipment maintenance; (2) distributed AI for communication system control; (3) automatic photointerpretation; (4) time-oriented problem solving, speech understanding systems; (5) knowledge base maintenance; (6) hardware architectures for very large systems; (7) speech understanding systems; (8) knowledge based reasoning and planning; and (9) a knowledge acquisition, assistance, and explanation system. The specific topic for this volume is the application of distributed Artificial Intelligence tools to the data fusion and classification problem of modern C3I systems. GRA

N91-26828# Northeast Artificial Intelligence Consortium, Syracuse, NY.
NORTHEAST ARTIFICIAL INTELLIGENCE CONSORTIUM (NAIC). VOLUME 14: KNOWLEDGE BASE RETRIEVAL USING PLAUSIBLE INFERENCE Final Report, Sep. 1984 - Dec. 1989
W. B. Croft and Paul R. Cohen Dec. 1990 66 p
(Contract F30602-85-C-0008)
(AD-A234893; RADC-TR-90-404-Vol-14) Avail: NTIS HC/MF A04 CSCL 12/9

The Northeast Artificial Intelligence Consortium (NAIC) was created by the Air Force Systems Command, Rome Air Development Center, and the Office of Scientific Research. Its purpose was conduct pertinent research artificial intelligence and to perform activities to this research. This report describes progress during the existence of the NAIC on the technical research tasks undertaken at the member universities. The topics covered in general are: (1) versatile expert system for equipment maintenance; (2) distributed AI for communications system control; (3) automatic photointerpretation; (4) time-oriented problem solving; (5) speech understanding systems; (6) knowledge base maintenance; (7) hardware architectures for very large systems; (8) knowledge-based reasoning and planning; and (9) a knowledge acquisition, assistance, and explanation system. The specific topic for this volume is plausible inference as an effective computational framework for the retrieval of complex objects. GRA

N91-26829# Northeast Artificial Intelligence Consortium, Syracuse, NY.
NORTHEAST ARTIFICIAL INTELLIGENCE CONSORTIUM (NAIC). VOLUME 15: STRATEGIES FOR COUPLING SYMBOLIC AND NUMERICAL COMPUTATION IN KNOWLEDGE BASE SYSTEMS Final Report, Sep. 1984 - Dec. 1989
Minsoo Suk Dec. 1990 76 p
(Contract F30602-85-C-0008)
(AD-A234894; RADC-TR-90-404-Vol-15) Avail: NTIS HC/MF A05 CSCL 12/7

The Northeast Artificial Intelligence Consortium (NAIC) was created by the Air Force Systems Command, Rome Air Development Center, and the Office of Scientific Research. Its purpose was to conduct pertinent research in artificial intelligence and to perform activities ancillary to this research. This report describes progress during the existence of the NAIC on the technical research tasks undertaken at the member universities. The topics covered in general are: (1) versatile expert for equipment maintenance; (2) distributed AI for communications system control; (3) automatic photointerpretation; (4) time oriented problem solving; (5) speech understanding systems; (6) knowledge base maintenance; (7) hardware architectures for very large systems; (8) knowledge based reasoning and planning; and (9) a knowledge acquisition, assistance, and explanation system. The specific topic for this volume is coupling symbolic and numerical computation as an effective means of solving problems in Knowledge Base Systems. GRA

N91-26830# Northeast Artificial Intelligence Consortium, Syracuse, NY.
NORTHEAST ARTIFICIAL INTELLIGENCE CONSORTIUM (NAIC). VOLUME 16: INTELLIGENT SIGNAL PROCESSING TECHNIQUES FOR MULTI-SENSOR SURVEILLANCE SYSTEMS Final Report, Sep. 1984 - Dec. 1989
Harvey E. Rhody and Robert T. Gayvert Dec. 1990 57 p
(Contract F30602-85-C-0008)
(AD-A234895; RADC-TR-90-404-Vol-16) Avail: NTIS HC/MF A04 CSCL 12/5

The Northeast Artificial Intelligence Consortium (NAIC) was created by the Air Force Systems Command, Rome Air Development Center, and Office of Scientific Research. Its purpose was to conduct pertinent research in artificial intelligence (AI) and to perform activities ancillary to this research. This report describes progress during the existence of the NAIC on the technical research tasks undertaken at the member universities. The topics covered in general are: versatile expert system for equipment maintenance, distributed AI for communications system control, automatic photointerpretation, time-oriented problem solving, speech understanding systems, knowledge based reasoning and planning, and a knowledge acquisition, assistance, and explanation system. The specific topic for this volume is intelligent signal processing techniques for multi-sensor surveillance systems. GRA

N91-26831# Northeast Artificial Intelligence Consortium, Syracuse, NY.
NORTHEAST ARTIFICIAL INTELLIGENCE CONSORTIUM (NAIC). VOLUME 17: HIGH-LEVEL ADAPTIVE SIGNAL PROCESSING Final Report, Sep. 1984 - Dec. 1989
Hamid Nawab and Victor R. Lesser Dec. 1990 51 p
(Contract F30602-85-C-0008)
(AD-A234896; RADC-TR-90-404-Vol-17) Avail: NTIS HC/MF A04 CSCL 12/9

The Northeast Artificial Intelligence Consortium (NAIC) was created by the Air Force Systems Command, Rome Air Development Center, and the Office of Scientific Research. Its purpose was to conduct pertinent research in artificial intelligence (AI) and to perform activities ancillary to this research. This report describes progress during the existence of the NAIC on the

technical research tasks undertaken at the member universities. The topics covered in general are: versatile expert system for equipment maintenance, distributed AI for communications system control, automatic photointerpretation, time-oriented problem solving, speech understanding systems, knowledge base maintenance, hardware architectures for very large system, knowledge based reasoning and planning, and a knowledge acquisition, assistance, and explanation system. The specific topic for this volume is the integration of Artificial Intelligence and Signal Processing for allocating processing resources and adjusting parameters of low-level processing in accordance with evolving high-level interpretations of the signal generating environment. GRA

N91-26832# Northeast Artificial Intelligence Consortium, Syracuse, NY.
NORTHEAST ARTIFICIAL INTELLIGENCE CONSORTIUM (NAIC). VOLUME 13: IMAGE UNDERSTANDING AND INTELLIGENT PARALLEL SYSTEMS Final Report, Sep. 1984 - Dec. 1989
Christopher M. Brown Dec. 1990 79 p
(Contract F30602-85-C-0008)
(AD-A234897; RADC-TR-90-404-Vol-13) Avail: NTIS HC/MF A05 CSCL 12/9

The Northeast Artificial Intelligence Consortium (NAIC) was created by the Air Force Systems Command, Rome Air Development Center, and the Office of Scientific Research. Its purpose was to conduct pertinent research in artificial intelligence (AI) and to perform activities ancillary to this research. This report describes progress during the existence of the NAIC on the technical research tasks undertaken at the member universities. The topics covered in general are: versatile expert system for equipment maintenance, distributed AI for communications system control, automatic photointerpretation, time-oriented problem solving, speech understanding systems, knowledge base maintenance, hardware architectures for very large systems, knowledge-based reasoning and planning, and a knowledge acquisition, assistance, and explanation system. The specific topics for this volume are various aspects of parallel, structural and optimal techniques in computer vision. GRA

N91-26833# Princeton Univ., NJ. Dept. of Electrical Engineering and Computer Science.
H-INFINITY-OPTIMAL CONTROL FOR DISTRIBUTED PARAMETER SYSTEMS Final Report, 1 Jan. 1989 - 31 Dec. 1990
David S. Flamm, Hong Yang, and Katherine Klipec 28 Feb. 1991 94 p
(Grant AF-AFOSR-0205-89; AF Proj. 2304)
(AD-A234931; AFOSR-91-0358TR) Avail: NTIS HC/MF A05 CSCL 09/1

This report describes progress in the development and application of H-infinity optimal control theory to distributed parameter systems. This research is intended to develop both theory and algorithms capable of providing realistic control systems for physical plants which are appropriately modeled as infinite dimensional linear systems, such as large space structures. In pursuing this program, we have focused on issues motivated by specific models of infinite dimensional systems. We have extended outer factor absorption results to cover certain irrational outer factors. This is in order to justify transformations used in a step for further explicit solution. We have generalized previous results on the single-input/single-output (SISO) mixed sensitivity problem to the case of irrational outer factor and unstable plant. We have solved a multi-input/output mixed sensitivity problem which cannot be treated by previous results. Finally, we developed a technique for numerically computing the optimal value of weighted mixed sensitivity for SISO systems, for the case where explicit symbolic inner/outer factorizations are not possible. GRA

N91-26834# Lawrence Livermore National Lab., CA.
GABOR TRANSFORMS AND NEURAL NETWORKS FOR AUTOMATIC TARGET RECOGNITION
G. A. Clark, J. E. Hernandez, B. S. Lawver, and R. J. Sherwood Dec. 1990 18 p Presented at the Workshop on Neural Networks: Academic/Industrial/NASA/Defense, Auburn, 11-13 Feb. 1991
(Contract W-7405-eng-48)
(DE91-011919; UCRL-JC-105362; CONF-910217-1) Avail: NTIS HC/MF A03

Neural networks are being trained to recognize objects in images. An important part of this task is to make the overall system robust with respect to image variations, including rotation, scale, and translation. Two major issues associated with feature extraction for this problem are addressed: Selection of meaningful features, and data compression. Selection of meaningful features: Even though neural networks are very effective and robust pattern classifiers, they have an important limitation; for any given application, why they succeeded or why they failed cannot always be explained. The black box nature of the neural networks makes it difficult to analyze their internal states. Also, their performance is highly dependent on the training data. The approach, therefore, is to create feature vectors that contain information that is as meaningful as possible. The use is described of Gabor representations to generate feature vectors that are robust to variations in rotation, scaling, and translation. Ways are studied to make the system robust to variations in perspective, occlusion, contrast, noise, and background. Gabor filters when used as the receptive field in a hierarchical scheme for feature extraction, offer properties that make them promising for providing the desired robustness to image variations. Unlike other filters, Gabor filters are optimally localized in both the space domain and the frequency domain, so that their space-bandwidth product is minimum. It was shown that their properties of spatial localization, orientation selectivity, and spatial frequency selectivity make Gabor filters a good model for biological vision. Experiments are described which demonstrate the ability of the overall recognition system to classify objects in simulated scenes, even though they have undergone variations in orientation scale, and position. DOE

64 NUMERICAL ANALYSIS

Includes iteration, difference equations, and numerical approximation.

N91-26835# Center for Mathematics and Computer Science, Amsterdam (Netherlands). Dept. of Numerical Mathematics.
STABILITY OF COLLOCATION-BASED RUNGE-KUTTA-NYSTROEM METHODS
P. J. vanderHouwen, B. P. Sommeijer, and Nguyen huu Cong (Hanoi Univ., Vietnam) Sep. 1990 20 p Sponsored in part by Amsterdam Univ. and Netherlands Organization for the Advancement of Research
(CWI-NM-R9016; ETN-91-99409) Copyright Avail: NTIS HC/MF A03

The attainable order and the stability of Runge-Kutta-Nystrom (RKN) methods are analyzed for special second order initial value problems derived by collocation techniques. Like collocation methods for first order equations, the step point order of s stage methods can be raised to 2s if s is even and to 2s - 1 if s is odd. The attainable stage order is one higher and equals s + 1. However, the stability results derived show that a high price must be paid for the increased stage order. ESA

N91-26836# Stanford Univ., CA. Center for Large Scale Scientific Computation.
SYMBOLIC EXPRESSIONS OF COMPOSITE GRID STRUCTURES Interim Report, 1 Jul. 1989 - 1 Jan. 1991
Ramani Pichumani, Joseph Oliger, and Ramana Venkata Jan. 1991 27 p
(Contracts N00014-89-J-1815; N00014-90-J-1344)
(AD-A233794; CLASSIC-91-25) Avail: NTIS HC/MF A03 CSCL 12/5

In summary, graphs and s-expressions are really different manifestations of the same entities. While graphs are visual, they nonetheless possess dual representations in the textual

s-expression alphabet. As a result, LISP, which is based entirely on s-expressions, is an ideal language for dealing with applications that perform extensive manipulations on graph-based objects. Scientific applications which make extensive use of both graph based objects as well as traditional numerical arrays can benefit by implementating their higher level data and control structures in LISP. Segments of code that are computationally intensive can be written in a static language such as C or FORTRAN and linked in with the higher level code. Such a design strategy could preserve the benefits of static compilation (i.e., faster execution speed) while retaining the power and flexibility needed to manipulate complex data structures. GRA

N91-26837# Naval Postgraduate School, Monterey, CA. Dept. of Physics.
PRIMES: THE FIRST 2400 PRIME NUMBERS Technical Report, Nov. 1989 - Nov. 1990
Gilbert F. Kinney Dec. 1990 55 p
(AD-A233979; NPS-PH-91-003) Avail: NTIS HC/MF A04
CSCL 12/1

These simple and mathematically elegant but practically useless prime number listings could have an appeal for afficionados of elementary number theory. They were prepared using a computer adaptation of the Sieve of Aratosthenes of Alexandria and the computations made on a small personal computer with an 8-bit microprocessor, a 64K random access memory, and a 2-megahertz clock. Computing time for checking 21, 380 integers and identifying the included 2400 prime numbers was about thirty minutes. This computational effort is quite modest compared to others such as two which are reported to have examined the first ten million integers. But the mere 2400 primes reported here, plus related items such as the number of prime twins and the integer gap between successive primes, are presented in tangible form. GRA

N91-26838# Pittsburgh Univ., PA. Inst. for Computational Mathematics and Applications.
ON THE SENSITIVITY OF SOLUTIONS OF PARAMETRIZED EQUATIONS
Werner C. Rheinboldt 22 Mar. 1991 22 p
(Contract N00014-90-J-1025; NSF CCR-89-07654)
(AD-A234265; ICMA-91-158) Avail: NTIS HC/MF A03 CSCL 12/2

The sensitivity of a solution of a parameterized equation F(z, lambda) = 0 with respect to the parameter vector lambda is usually defined as the change of the state z in dependence of lambda. In other words, for any solution expressible in the form (z(lambda), lambda) with some smooth function z = z(lambda) the sensitivity is the derivative Dz(lambda). Typically the solutions form a manifold M in the product of the state-space and the parameter space and this sensitivity is available only at those points of M where the parameters can be used to define a local coordinate system. This paper introduces a general sensitivity concept which applies at all solutions on M and which includes the earlier definition. Some general geometric interpretations of the new measure are presented and it is shown that the sensitivity analysis can be easily integrated into the solution process. The theory also suggest the introduction of a readily computable second-order sensitivity measure reflecting the curvature-behavior of M. Two numerical examples illustrate the discussion. GRA

N91-26839# Vanderbilt Univ., Nashville, TN. Dept. of Mathematics.
MATCHING THEORY. A SAMPLER: FROM DENES KOENIG TO THE PRESENT
Michael D. Plummer 1991 47 p
(Contract N00014-85-K-0488)
(AD-A234321) Avail: NTIS HC/MF A03 CSCL 12/2

It was Koenig who gave the next strong impetus to the study of graph factorization after Petersen's ground breaking work, and it is Koenig with whom we are charged to begin our brief summary of the history of matching theory. Fortunately, matching theory serves well as an historical thread extending from the time of Koenig (and before) up to the present, wending its way through graph theory and intersecting many of the most important new ideas which have sprung forth in our discipline. One sees in particular that after the close of World War II this intertwinning of matching theory with the study of graphs as a whole became ever more inextricable, even as the study of graph theory as a discipline unto itself literally exploded upon the mathematical scene. Although it is jumping the gun somewhat with respect to the organization of this paper, we can mention three major areas which have joined with graph theory to give rise to many new and deep results. These are: (1) linear programming and polyhydral combinatorics; (2) the linking of graphs and probability theory in the area of random graphs; and finally (3) the theory of algorithms and computational complexity. GRA

N91-26840# Naval Postgraduate School, Monterey, CA. Dept. of Mathematics.
COVERING A CLOSED CURVE WITH A GIVEN TOTAL CURVATURE Technical Report, Apr. - Oct. 1990
Mostafa Ghandehari 9 Oct. 1990 18 p
(AD-A234342; NPS-MA-91-003) Avail: NTIS HC/MF A03
CSCL 12/1

It is known that if a closed curve C of class C(exp 2) in R(exp n) is constrained to lie in a ball of radius R, then L(C) is less than or equal to RK(C), where K(C) is the total curvature of C and L(C) denotes the Euclidean length of C. We show that (integral(limits 0 and L) of (the absolute value of kappa(s))(exp p) ds)exp 1/p is greater than or equal to L(exp 1/p)/R, where s is the arc length parameter and kappa denotes Euclidean curvature. Extensions of the above two inequalities to Minkowski spaces are discussed. GRA

N91-26841# Vanderbilt Univ., Nashville, TN. Dept. of Mathematics.
EXTENDING MATCHINGS IN GRAPHS: A SURVEY
Michael D. Plummer 1990 17 p
(Contract N00014-85-K-0488)
(AD-A234392) Avail: NTIS HC/MF A03 CSCL 12/1

This paper surveys a variety of results obtained over the past few years concerning n-extendable graphs. In particular, we will describe how the property of n-extendability interacts with such other graph parameters as genus, toughness, claw-freedom and degree sums and generalized neighborhood conditions. We will also investigate the behavior of matching extendability under the operation of Cartesian product. The study of n-extendability for planar graphs has been and continues to be of particular interest. GRA

N91-26842# Pittsburgh Univ., PA. Inst. for Computational Mathematics and Applications.
NFEARS: A NONLINEAR ADAPTIVE FINITE ELEMENT SOLVER. PART 2: USER'S MANUAL
Charles K. Mesztenyi and Werner C. Rheinboldt Mar. 1991 56 p Prepared in cooperation with Maryland Univ., College Park
(Contracts N00014-90-J-1025; N00014-80-C-9455; N00014-85-K-0169)
(AD-A234416; ICMA-91-157-Pt-2) Avail: NTIS HC/MF A04
CSCL 12/5

This represents the second Part of the report on NFEARS, the Nonlinear Finite Element Adaptive Research Solver developed jointly by the Universities of Maryland and Pittsburgh. This part constitutes the User's Manual for the system version 6. It was intended to describe all necessary aspects for running NFEARS successfully without requiring a detailed knowledge of the mathematical background given in Part 1. However, the reader should be generally familiar with the aims and tasks of the program. GRA

N91-26843# New York Univ., New York. Inst. of Mathematical Sciences.
MATHEMATICAL TOPICS IN THE MODELLING AND IDENTIFICATION OF MULTICOMPONENT CONTINUA Final Report, 1 Mar. 1988 - 31 Dec. 1990

Robert V. Kohn Mar. 1991 12 p
(Contract N00014-88-K-0279)
(AD-A234471) Avail: NTIS HC/MF A03 CSCL 12/2

This grant sponsored work in the following three directions: (1) Determining conductivity by boundary measurements; (2) Variational models of phase transitions; and (3) Mathematical analysis of composite materials. The first is a novel approach to remote sensing, notable for its potential biomedical applications as well as for links to inverse scattering. The second is a new approach to interface motion laws and microstructure formation in continuum problems involving several distinct phases. The third is more classical, but its relevance to structural optimization (the main focus of our effort) is just beginning to be appreciated. Though the applications of these three areas are quite distinct, they are all closely related from the mathematical viewpoint. Each has to do with the Calculus of Variations, and more specifically with nonconvex variational problems whose minima are not necessarily achieved. GRA

N91-26844# Naval Underwater Systems Center, New London, CT.
COMPLEX ENVELOPE PROPERTIES, INTERPRETATION, FILTERING, AND EVALUATION Progress Report
Albert H. Nuttall 1 Feb. 1991 94 p
(AD-A234478; NUSC-TR-8827) Avail: NTIS HC/MF A05 CSCL 20/1

The complex envelope of a narrowband waveform y(t) typically has logarithmic singularities, due to discontinuities in y(t) or its derivatives, which have little physical significance. The complex envelope also has a very slow decay in time, due to the discontinuous spectrum associated with its very definition; this slow decay can mask weak desired features of the complex envelope. In order to suppress these undesired behaviors of the mathematically defined complex envelope, a filtered version is suggested and investigated in terms of its singularity rejection capability and better decay rate. Finally, numerical computation of the complex envelope, as well as its filtered version, by means of a fast Fourier transform (FFT) is investigated and the effects of aliasing are assessed quantitatively. A program for the latter task, using an FFT collapsing procedure, is furnished in BASIC. GRA

N91-26845# Boston Univ., MA.
MATHEMATICAL PROBLEMS CONCERNING RHYTHMIC PROCESSES Final Report, 1 Oct. 1989 - 30 Sep. 1990
N. Kopell 30 Sep. 1990 4 p
(Grant AF-AFOSR-0017-90; AF Proj. 2304)
(AD-A234588; AFOSR-91-0247TR) Avail: NTIS HC/MF A01 CSCL 06/3

Two papers (one mathematical and the other experimental) were completed on forced chains oscillators. These papers were motivated by problems concerning the lamprey CPG for undulatory locomotion. Work continued on interpretation of the experiment, and we are preparing a paper on the significance of the data from split bath experiments. In addition, work on the mathematics of oscillator chains with coupling topology more complicated than the nearest neighbor was initiated. This paper deals with the patterns that form when long inhibitory connections are added to local excitatory connections. The work was motivated by the patterns of movement that emerge in early development of vertebrates. GRA

N91-26846# Northwestern Univ., Evanston, IL.
LYAPUNOV EXPONENTS AND ROTATION NUMBERS OF LINEAR SYSTEMS WITH REAL NOISE Final Report, 1 Jul. 1988 - 31 Dec. 1990
Mark Pinsky and Volker Wihstutz 31 Dec. 1990 13 p
(Grant AF-AFOSR-0256-88; AF Proj. 2304)
(AD-A234729; AFOSR-91-0274TR) Avail: NTIS HC/MF A03 CSCL 12/1

In the joint work with Volker of the University of North Carolina, we have investigated the Lyapunov stability of systems defined by a system of differential equations with a stochastic driving term, which may be either white noise or real noise. In the first case we showed that for nilpotent systems it is possible to compute an arbitrary number of terms in the asymptotic expansion of Lyapunov exponent in fractional powers of the noise coefficient when this tends to zero. This includes the important case of critically damped oscillator, which had not been treated previously. These results were then extended to the case of the same nilpotent system driven by a finite-state Markov noise process. This was obtained by a method of homogenization, using techniques previously established to study the central limit theorem for functions of a centered Markov chain. It is shown, as in the case of white noise, that the Lyapunov exponent admits an expansion in fractional powers of the noise parameter, and that the first term of this expansion agrees exactly with the result obtained in the white noise case. GRA

N91-26847# Illinois Univ., Urbana.
ON MEASURES OF MISCONCEPTION STABILITY Technical Report, 1986 - 1990
Kikumi Tatsuoka and Maurice Tatsuoka Mar. 1991 40 p
(Contract N00014-86-K-0290; NR Proj. RR0-4206)
(AD-A234952) Avail: NTIS HC/MF A03 CSCL 05/8

When learning is taking place, students test their hypotheses, evaluate them, and modify their current theories on the basis of new information. The phenomenon is famous and is called the hypothesis testing view or theory changes. Many students tend to change their rule(s) while they are taking a test. This study discusses slip probabilities that quantify the extent to which a student's score on an item deviates from the pure score of his/her original rules. Algebraic relationships between this new slip random variable and the traditional item-score variable are discussed. Then, the indices to measure the stability of rule application and to compute the probability of having a perfect application of the rule are introduced and illustrated with a 64-item signed number test. GRA

N91-26848# Maryland Univ., College Park. Computer Vision Lab.
UNDERSTANDING OBJECT CLASSES: MODELING AND MATCHING Final Report, 1 Apr. 1986 - 31 Jan. 1991
Azriel Rosenfield 28 Feb. 1991 20 p
(Grant AF-AFOSR-0092-86; AF Proj. 2304)
(AD-A235027; AFOSR-91-0254TR) Avail: NTIS HC/MF A03 CSCL 12/9

A general approach was developed for the problem of characterizing generic classes of objects and recognizing them in images. Only objects composed of simple parts were considered, where the classes are defined by constraints on the properties of and relations among the parts. Object classes are characterized (modeled) in terms of both qualitative part properties and relations. GRA

N91-26849# Carnegie-Mellon Univ., Pittsburgh, PA. Management Sciences Research Group.
THE WEIGHTED UNI-DIMENSIONAL SIMILARITIES PROBLEM WITH LEAST ABSOLUTE VALUE METRIC IS NP-HARD Management Sciences Research Report
Nathan P. Ritchey and Gerald L. Thompson Apr. 1990 10 p
(Contracts N00014-85-K-0198; DE-FG02-85ER-13396)
(AD-A235060; MSRR-560; WP-89-90-11) Avail: NTIS HC/MF A02 CSCL 12/1

The purpose of this paper is to prove that the weighted uni-dimensional similarities problem with least absolute value metric (USPAM) is, in general, NP-Hard. In the first four sections of the paper, the USPAM problem and four lemmas are presented which will be used in Section 6 to prove the main theorem of this paper. It is shown that the simple max cut problem can, in a polynomial number of steps, be converted into a special case of the USPAM problem, which shows that the USPAM problem is NP-Hard. Finally, some special cases of the USPAM problem are described for which polynomial solutions exist. GRA

N91-26850# Rensselaer Polytechnic Inst., Troy, NY. Dept. of Computer Science.
NUMERICAL METHODS FOR SINGULARLY PERTURBED DIFFERENTIAL EQUATIONS WITH APPLICATIONS Final Report, 1 Jun. 1985 - 31 Aug. 1990
Joseph E. Flaherty 31 Aug. 1990 10 p
(Grant AF-AFOSR-0156-85; AF Proj. 2304)
(AD-A235188; AFOSR-91-0265TR) Avail: NTIS HC/MF A02 CSCL 12/1

During the period covered by this grant, we conducted research on the development and application of adaptive numerical methods for singularly perturbed initial-boundary value problems for partial differential equations. We studied both local refinement methods and methods of lines techniques using properly nested and overlapping grids. The geometric modeling capabilities of our procedures were improved through the use of finite quadtree and octree encoding schemes; parallel versions of adaptive procedures on shared-memory computers were developed; and variable-order finite element methods to be used with adaptive p- and hp-refinement were created. GRA

N91-26851# Clemson Univ., SC.
POLYHEDRAL APPROACHES FOR SOLVING 0-1 POLYNOMIAL PROGRAMMING PROBLEMS Annual Technical Report, 1 Mar. - 30 Feb. 1991
Adams Apr. 1991 5 p
(Grant AF-AFOSR-0191-90; AF Proj. 2304)
(AD-A235219; AFOSR-91-0500TR) Avail: NTIS HC/MF A01 CSCL 12/4

The research results include the construction of a new linearization strategy for unconstrained 0-1 polynomial programming problems. The extension of duality results for 0-1 quadzotic programming problems and the design and testing of an algorithm for a special family of 0-1 quadratic programming problems. GRA

N91-26852# Stanford Univ., CA. Dept. of Statistics.
WEIGHTED LEAST SQUARES ESTIMATION FOR AALEN'S ADDITIVE RISK MODEL
Fred W. Huffer and Ian W. McKeague 17 Apr. 1991 29 p
(Contract N00014-89-J-1627)
(AD-A235250; SU-TR-441) Avail: NTIS HC/MF A03 CSCL 12/3

Cox's (1972) proportional hazards model has so far been the most popular model for the regression of analysis censored survival data. However, the additive risk model of Aalen (1980) can provide a useful and biologically more plausible alternative. Aalen's model stipulates that the conditional hazard function for a subject, whose covariates are Y = (Y sub 1,...,Y sub p)', has the form h(t/Y) = Y' alpha (t), where alpha = (alpha sub 1,...,alpha sub p)' is an unknown vector of hazard functions. This paper discusses inference for alpha based on a weighted least squares (WLS) estimator of the vector of cumulative hazard functions. The asymptotic distribution of the WLS estimator is derived and used to obtain confidence intervals and bands for the cumulative hazard functions. Both a grouped data and a continuous data version of the estimator are examined. An extensive simulation study is carried out. The method is applied to grouped data on the incidence of cancer mortality among Japanese atomic bomb survivors. GRA

N91-26853 Tel-Aviv Univ. (Israel). Dept of Applied Mathematics.
SPECTRAL RECOVERY OF DISCONTINUOUS DATA M.S. Thesis
Avital Netzer Jun. 1989 155 p In HEBREW; ENGLISH summary
(ITN-91-85115) Copyright Avail: Tel-Aviv Univ., Exact Sciences Library, Ramat Aviv 69978, Israel

The use of spectral and pseudospectral schemes in the numerical solution of hyperbolic initial value problems is discussed. The main aim was to recover the actual solution from the spectral and pseudospectral approximations, achieving spectral accuracy in the regions where the initial condition is smooth, even though the initial condition has discontinuities in its domain of definition. Sobolev spaces, Fourier series, convolutions and regularization, which were necessary to the work described, are reviewed. Spectral and pseudospectral approximations to 2pi periodic functions and spectral differentiation are presented, and spectral differentiation is discussed and compared with differentiation as approximated by finite differences. In discussion of the case of approximation of a function with discontinuities, it is shown that the pointwise values of the function, in the regions where it is smooth, can be spectrally recovered from the spectral approximations. Spectral and pseudospectral methods were applied to the numerical solution of hyperbolic initial value problems with smooth initial data, and convergence analysis was applied to the spectral and pseudospectral methods showing convergence. In the application of spectral methods to hyperbolic initial value problems with nonsmooth initial conditions, it was shown that the solution can be recovered with spectral accuracy in its smooth regions, by applying a filtering process. Numerical results are presented, obtained by applying the pseudospectral method with filtering to several hyperbolic problems with nonsmooth initial conditions. Results are also presented which were obtained by applying the Spectral Vanishing Viscosity method in the real plane to Burgers' equation. ISA

N91-26854# Oak Ridge National Lab., TN.
A DIVIDE AND CONQUER APPROACH TO THE NONSYMMETRIC EIGENVALUE PROBLEM
E. R. Jessup 1991 7 p Presented at the 13th IMACS World Congress on Computation and Applied Mathematics, Dublin (Ireland), 22-26 Jul. 1991
(Contract DE-AC05-84OR-21400)
(DE91-011085; CONF-910771-2) Avail: NTIS HC/MF A02

Serial computation combined with high communication costs on distributed-memory multiprocessors make parallel implementations of the QR method for the nonsymmetric eigenvalue problem inefficient. This paper introduces an alternative algorithm for the nonsymmetric tridiagonal eigenvalue problem based on rank two tearing and updating of the matrix. The parallelism of this divide and conquer approach stems from independent solution of the updating problems. DOE

N91-26855# Illinois Univ., Urbana.
COMPUTATIONAL METHODS AND SOFTWARE FOR DIFFERENTIAL EQUATIONS AND THEIR APPLICATIONS
1990 12 p
(Contract DE-FG02-87ER-25026)
(DE91-012172; DOE/ER-25026/T3) Avail: NTIS HC/MF A03

Parallel and waveform methods are discussed for ordinary differential equations, differential algebraic equations, Hamiltonian systems, and multilevel methods. DOE

N91-26856# Superconducting Super Collider Lab., Dallas, TX.
NORMALIZATION OF THE PARAMETERIZED COURANT-SNYDER MATRIX
Y. Yan Dec. 1990 18 p
(Contract DE-AC02-89ER-40486)
(DE91-012554; SSCL-302) Avail: NTIS HC/MF A03

An explicit normal form of the parameterized Courant-Snyder matrix is obtained by symplectic factorization. The explicit calculation of the delta- (off-momentum-) dependent tune mu(delta) and Twiss parameters beta(delta), gamma(delta), alpha(delta) may have applications in accelerator lattice design. Furthermore, being able to symplectify a truncated parameterized Courant-Snyder matrix is a key step to fully parameterized map studies in nonlinear dynamics. DOE

65 STATISTICS AND PROBABILITY

Includes data sampling and smoothing; Monte Carlo method; and stochastic processes.

N91-26857# State Univ. of New York, Binghamton. Center for Statistics Quality Control and Design.
THE DISTRIBUTION OF THE SIZE AND NUMBER OF SHADOWS CAST ON A LINE SEGMENT IN A POISSON RANDOM FIELD
S. Zacks and Gang Li 15 Feb. 1991 13 p
(Contract DAAL03-89-K-0129)
(AD-A233697; TR-2; ARO-25347.2-MA) Avail: NTIS HC/MF A03 CSCL 12/3

The present paper presents algorithms for the computation of the distributions of the number and lengths of shadows cast on a line segment by random obscuring elements, when there is one source of light (in the origin), and the obscuring elements are realized according to a Poisson random field. These algorithms have applications in problems of line of sight, target detection, image processing, and others. GRA

N91-26858# Naval Postgraduate School, Monterey, CA. Dept. of Operations Research.
MAXIMIZATION ON MATROIDS WITH RANDOM WEIGHTS
Michael P. Bailey Jan. 1991 29 p
(AD-A233978; NPSOR-91-06) Avail: NTIS HC/MF A03 CSCL 12/1

In this work we develop a method for analyzing maximum weight selections in matroids with random element weights, especially exponentially distributed weights. We use the structure of the matroid dual to transform matroid maximization into an equivalent minimization task. We model sample paths of the greedy minimization scheme using a Markov process, and thus solve the original maximization problem. The distribution of the weight of the optimal basic element and moments are found, as well as the probability that a given basic element is optimal. We also derive criticality indices for each ground set element, giving the probability that an element is a member of the optimal solution. We give examples using spanning trees and scheduling problems, each example being a new result in stochastic combinatorial optimization. GRA

N91-26859# California Univ., Irvine. Dept. of Electrical and Computer Engineering.
STATISTICAL ANALYSIS OF STOCHASTIC GRADIENT BASED ALGORITHMS Final Report, 15 Mar. 1986 - 14 Oct. 1990
Neil J. Bershad 5 Mar. 1991 8 p
(Grant AF-AFOSR-0093-86; AF Proj. 2304)
(AD-A234545; AFOSR-91-0277TR) Avail: NTIS HC/MF A02 CSCL 12/3

The work performed during the period from April 15, 1988 to October 15, 1990 is discussed. The AFOSR has supported research work primarily on: (1) the stochastic behavior of LMS and stochastic gradient related adaptive algorithms; and (2) comparative performance analysis of LMS and recursive least squares (RLS) in nonstationary environments. GRA

N91-26860# North Carolina Univ., Chapel Hill. Center for Stochastic Processes.
RESEARCH IN STOCHASTIC PROCESSES Final Report, 1 Sep. 1985 - 31 Dec. 1990
Stamatis Cambanis, Gopinath Kallianpur, and M. R. Leadbetter 28 Feb. 1991 34 p
(Contract F49620-85-C-0144)
(AD-A234650; AFOSR-91-0239TR) Avail: NTIS HC/MF A03 CSCL 12/3

Research was conducted and directed in the area of stochastic processes and their applications in engineering, biology, physics, seismology and oceanography by the principal investigators. Detailed descriptions of the work were given in each of the five annual reports. A list of the main areas of research activity follows: Sampling designs for time series; Monte Carlo integration; Signal compression and digital waveform coding; Nonstationary harmonizable signals; Gaussian processes; Stable processes; Markov processes; Self similar processes; Random fields; Point processes; Nonlinear filtering and prediction; Signal detection; Diffusion models; Propagation of chaos for interacting stochastic differential systems; Homogenous chaos expansions; Feyman integrals; Stochastic calculus; Stochastic evolution; Extremes of random processes and fields; Exceedance random measures; Slepian models; Peaks over threshold modeling; Central limit theory under mixing; Statistical inference for stochastic processes; Exchangeable random processes. GRA

N91-26861# Carnegie-Mellon Univ., Pittsburgh, PA. Dept. of Mathematics.
SINGULAR AND BANG-BANG STOCHASTIC CONTROL Final Report, 1 Oct. 1988 - 30 Sep. 1990
Steven E. Shreve 30 Sep. 1990 2 p
(Grant AF-AFOSR-0075-89; AF Proj. 2304)
(AD-A234752; AFOSR-91-0262TR) Avail: NTIS HC/MF A01 CSCL 12/3

Research supported by this grant focussed on the regularity of the value function for multi-dimensional singular stochastic control problems. In addition, a multi-dimensional finite-fuel problem has been studied, and known results for one dimensional problems have been extended to higher dimensions. GRA

N91-26862# Illinois Univ., Urbana. Dept. of Statistics.
A PROCEDURE TO DETECT ITEM BIAS PRESENT SIMULTANEOUSLY IN SEVERAL ITEMS Technical Report, 1988 - 1991
Robin Shealy and William Stout 25 Apr. 1991 41 p
(Contract N00014-90-J-1940; NR Proj. RR0-4204)
(AD-A235252; Rept-1991-3) Avail: NTIS HC/MF A03 CSCL 12/3

This paper presents a statistical procedure (denoted by SIB) designed to test for undirectional test bias existing simultaneously in several items of an ability test. It was argued in Shealy and Stout (1991) that in order to model such bias with an IRT model, a multidimensional model is necessary. The proposed procedure, based on this multidimensional IRT modeling approach, statistically tests for bias in one or more items at a time and is corrected for the inflation (or deflation) of the test statistic due to target ability difference, a valid group difference that is conceptually independent of psychological test bias. The correction plays the same role as the practice of including the single studied item in the matching criterion score in the Mantel-Haenszel (MH) procedure adapted for test responses by Holland and Thayer (1988). It is shown through the initial portion of an extensive simulation study underway (Shealy (1991)) that, with the correction in place, the procedure performs as well as the MH procedure in many cases when there is a single biased item, and performs well in the case of multiple item test bias. GRA

N91-26863# Argonne National Lab., IL.
PUMPING SYSTEM FAULT DETECTION AND DIAGNOSIS UTILIZING PATTERN RECOGNITION AND FUZZY INFERENCE TECHNIQUES
R. M. Singer, K. C. Gross, and K. E. Humenik (Maryland Univ., Baltimore.) 1991 12 p Presented at the 4th International Conference on Industrial and Engineering Applications of Artificial Intelligence and Expert Systems, Kauai, 2-5 Jun. 1991
(Contract W-31-109-eng-38)
(DE91-011849; ANL/CP-71255; CONF-910648-2) Avail: NTIS HC/MF A03

An integrated fault detection and diagnostic system with a capability of providing extremely early detection of disturbances in a process through the analysis of the stochastic content of dynamic signals is described. The sequential statistical analysis of the signal noise (a pattern-recognition technique) that is employed has been shown to provide the theoretically shortest sampling time to detect disturbances and thus has the potential of providing incipient fault detection information to operators sufficiently early to avoid forced process shutdowns. This system also provides a diagnosis of the cause of the initiating fault(s) by a physical-model-derived

rule-based expert system in which system and subsystem state uncertainties are handled using fuzzy inference techniques. This system has been initially applied to the monitoring of the operational state of the primary coolant pumping system on the EBR-2 nuclear reactor. Early validation studies have shown that a rapidly developing incipient fault on centrifugal pumps can be detected well in advance of any changes in the nominal process signals. DOE

66 SYSTEMS ANALYSIS

Includes mathematical modeling; network analysis; and operations research.

N91-26864# Army War Coll., Carlisle Barracks, PA.
SPACE SUPPORT FOR AIRLAND BATTLE-FUTURE Individual Study Project
Arthur T. Estrada 14 Mar. 1991 43 p
(AD-A233868) Avail: NTIS HC/MF A03 CSCL 15/6

The use of space systems has become a critical component of military strategic, operational, and tactical capabilities. Space forces are employed by the Army to enhance combat support in the functional areas of communications; reconnaissance, surveillance, and target acquisition; weather and environment; and position location and navigation. AirLand Battle-Future doctrine predicts a deep non-linear battlefield environment which will require extensive access to space assets by operational and tactical commanders. This paper postulates that integration of space forces into Army tactical planning and execution will be doctrinally required. The impact of this integration can be described in the context of AirLand Battle tenets and imperatives. If Army officers are to successfully incorporate space forces into campaign and battle planning they must understand what assets are available and how the physics of space influence their employment. GRA

N91-26865# Ohio State Univ., Columbus. Dept. of Computer and Information Science.
GENERIC TASKS FOR KNOWLEDGE-BASED PROBLEM SOLVING: EXTENSION AND NEW DIRECTIONS Final Report, 19 Dec. 1988 - 18 Dec. 1990
B. Chandrasekaran Feb. 1991 140 p
(Grant AF-AFOSR-0250-89; AF Proj. 2304)
(AD-A234925; AFOSR-91-0252TR) Avail: NTIS HC/MF A07 CSCL 12/9

Research completed during 1989 and 1990 has advanced the basic understanding of the structure of tasks in problem solving and how method selection can occur within knowledge based problem solving systems. The important notion of task-structure, providing a means of characterizing the relation of task, method, and subtask, aids in the construction of large, complex, and versatile systems. The analysis of the design task provides a good illustration of task structure methodology. Complexity analysis complements our understanding of the computational resource requirements of various cases of central solving tasks. GRA

N91-26866# Air War Coll., Maxwell AFB, AL.
SPACE DOCTRINE
Gary A. Chilcott May 1990 61 p
(AD-A234971) Avail: NTIS HC/MF A04 CSCL 15/6

United States military space activities have been guided by policy and technological decisions since the 1950s because little work has been done to develop and articulate coherent space doctrine. In December 1988, the Chief of Staff of the Air Force and the Secretary of the Air Force signed a new Air Force space policy which stated that space power would assume as decisive a role in future combat operations as airpower does today. Since doctrine represents our fundamental beliefs based on our experience, it is essential that the military formulate space doctrine so it may evolve as experience is gained in space operations. This paper looks at several space doctrinal tenets and discusses their applicability. It also points to some of the obstacles that have precluded space doctrinal development. It concludes with ideas for the future in developing a space doctrine. GRA

N91-26867 Tel-Aviv Univ. (Israel). Dept. of Statistics.
A SEQUENTIAL JACKSON NETWORK WITH FEEDBACK M.S. Thesis
Jonathan Brandon Sep. 1989 46 p
(ITN-91-85111) Copyright Avail: Tel-Aviv Univ., Exact Sciences Library, Ramat Aviv 69978, Israel

A serial queueing network with Bernoulli feedback to the end of the queue of the first node is considered. The first moment of total sojourn time in the system is developed using Jackson's and Little's theorems, the sequencing of the nodes so as to minimize sojourn time is discussed, a Laplace transform for the sojourn time is developed, and then the result (concerning the first moment) are verified using Arrivals See Time Averages (ASTA). For a one-node queueing system with Bernoulli feedback, the correlation is examined between the number of customers seen on consecutive visits to the server. Several simple generalizations of the serial queueing model are discussed. Author (ISA)

N91-26868 Tel-Aviv Univ. (Israel). Dept. of Statistics.
QUEUEING SYSTEMS WITH ORBITING CUSTOMERS M.S. Thesis
Moshe Sharvit Nov. 1989 43 p In HEBREW; ENGLISH summary
(ITN-91-85112) Copyright Avail: Tel-Aviv Univ., Exact Sciences Library, Ramat Aviv 69978, Israel

Orbiting customers, who have found a queue full and may make further attempts to join it, are characterized by the distribution of the number of attempts to join the system and by the distribution of the length of the time interval between consecutive attempts. The stationary distribution was computed of a system with Poisson arrivals, a single exponential server and limited queue length. Customers finding the system full will return with probability unity after exponentially distributed time intervals. The above model was generalized to the case of a similar system in which there were several identical exponential servers; the stationary distribution for this system was computed. The effects of imposing a cost structure, including payment for services, the cost of waiting in the queue and the cost of each temporarily rejected customer during the time between his first entry attempt and his eventual admittance, were analyzed. The analysis concerned the relative profitabilities of systems with and without orbiting customers. The model was extended to include the possibility of rejecting customers, even when the queue is not full, and calculating the optimal admission/rejection policy to maximize the average profits. This problem was formulated as a linear program. ISA

N91-26869 Tel-Aviv Univ. (Israel). School of Mathematical Sciences.
CREATION OF UNCERTAINTY IN REPEATED TWO-PERSON NON-ZERO-SUM GAMES M.S. Thesis
Eitan Israeli Oct. 1989 47 p In HEBREW; ENGLISH summary
(ITN-91-85118) Copyright Avail: Tel-Aviv Univ., Exact Sciences Library, Ramat Aviv 69978, Israel

The consequences are examined of allowing either or both players of a repeated non-zero-sum game to introduce uncertainty into the game, by inserting additional possible payoff matrices for himself or themselves, and a probability vector by which his payoff matrix is determined. In the resulting game, the interesting point is the payoffs at equilibrium points, if the payoffs matrices selected are the original ones (for both players). Without the added uncertainty the payoff sets for the original game are given by the Folk THM. The uncertainty introduced may enlarge the minimal payoff for this state. An optimal addition is presented for the case in which only one player may introduce uncertainty. The two-sided case, in which both players add the optimal addition from the one-sided case, is examined. Author (ISA)

N91-26870*# National Aeronautics and Space Administration. Lewis Research Center, Cleveland, OH.
COMPARATIVE SURVEY OF DYNAMIC ANALYSES OF FREE-PISTON STIRLING ENGINES
M. David Kankam and Jeffrey S. Rauch (Sverdrup Technology, Inc., Brook Park, OH.) 1991 8 p Presented at the 26th Intersociety Energy Conversion Engineering Conference, Boston, MA, 4-9 Aug. 1991; sponsored by ANS, SAE, ACS, AIAA, ASME, IEEE, and AIChE
(NASA-TM-104491; E-6348; NAS 1.15:104491) Avail: NTIS HC/MF A02 CSCL 12B

Reported dynamics analyses for evaluating the steady-state response and stability of free-piston Stirling engine (FPSE) systems are compared. Various analytical approaches are discussed to provide guidance on their salient features. Recommendations are made in the recommendations remarks for an approach which captures most of the inherent properties of the engine. Such an approach has the potential for yielding results which will closely match practical FPSE-load systems. Author

N91-26871# Los Alamos National Lab., NM.
BOOST-PHASE KILL VERSUS MIDCOURSE DISCRIMINATION: THE GRAND INQUISITOR'S SOLUTION
G. H. Canavan May 1991 14 p
(Contract W-7405-eng-36)
(DE91-011744; LA-11858-MS) Avail: NTIS HC/MF A03

For few interceptors and many decoys, midcourse defenses must discriminate very well or their costs will be unacceptable. Sensitivity to discrimination is suppressed when the defense has many interceptors, which would generally be the cheapest and preferred solution. Good discrimination is one way to compensate for an inadequate number of boost-phase defenders. In the near term, good discrimination could cover for insufficient boost-phase defenders. In the mid and long terms discrimination sets the balance between boost and midcourse defenses. DOE

67 THEORETICAL MATHEMATICS

Includes topology and number theory.

No abstracts in this category.

70 PHYSICS (GENERAL)

For precision time and time interval (PTTI) see *35 Instrumentation and Photography;* for geophysics, astrophysics or solar physics see *46 Geophysics, 90 Astrophysics,* or *92 Solar Physics.*

N91-26872*# National Aeronautics and Space Administration. Lewis Research Center, Cleveland, OH.
A MODEL FOR THE SCATTERING OF HIGH-FREQUENCY ELECTROMAGNETIC FIELDS FROM DIELECTRICS EXHIBITING THERMALLY-ACTIVATED ELECTRICAL LOSSES
Raiford E. Hann May 1991 13 p
(NASA-TM-104376; E-6040-1; NAS 1.15:104376) Avail: NTIS HC/MF A03 CSCL 20C

An equivalent circuit model (ECM) approach is used to predict the scattering behavior of temperature-activated, electrically lossy dielectric layers. The total electrical response of the dielectric (relaxation + conductive) is given by the ECM and used in combination with transmission line theory to compute reflectance spectra for a Dallenbach layer configuration. The effects of thermally-activated relaxation processes on the scattering properties is discussed. Also, the effect of relaxation and conduction activation energy on the electrical properties of the dielectric is described. Author

N91-26873# Texas A&M Univ., College Station. Dept. of Statistics.
COMPARISON CHANGE ANALYSIS
Emanuel Parzen Feb. 1991 22 p
(Contract DAAL03-90-G-0069)
(AD-A233690; TR-133; ARO-27574.4-MA) Avail: NTIS HC/MF A03 CSCL 12/3

This paper is an introduction to a theory of detection and estimation of change and introduces many new concepts and terminology. It emphasizes the interplay of ideas (analogies between analogies) rather than complete statements of theorems; many of the proofs required fortunately can be assembled from results already in the literature. The concepts presented can provide a statistical technology, useable by consumers, which show that much esoteric theory can be made exoteric (applicable by applied scientists who need not study the theory) and data analytic. Its contents are: (1) Introduction to Change Analysis; (2) Introduction to Brownian Bridge Dynamic Statistics; (3) Phases of Change Analysis; (4) Comparison Analysis and Non-parametric Statistical Inference; (5) Comparison Change Analysis as a Probability Concept; (6) Features of Sample Comparison Change Analysis; and (7) Concepts and terminology list. GRA

N91-26874# Maryland Univ., College Park. Center for Automation Research.
HIGH ORDER DIFFERENTIATION FILTERS THAT WORK
Isaac Weiss Mar. 1991 39 p
(Contract N00014-91-J-1222)
(AD-A234504; CAR-TR-545; CS-TR-2639) Avail: NTIS HC/MF A03 CSCL 20/3

Reliable derivatives of digital images have always been hard to obtain, especially (but not only) at high orders. We present new filters that give more accurate derivatives than the traditional Gaussian ones. We show that the traditional filters give incorrect derivatives even for an analytic, noiseless, infinite image, because they smooth the image too much. For a finite interval, the effects of truncating the filter become intolerable for high derivatives. We derive filters that allow a higher amount of noise suppression with less compromise of accuracy than the Gaussian. The filters are easy to compute at arbitrary size. In addition, a general analytic (non-filter) solution is derived for the regularization problem on a finite interval. GRA

N91-26875# State Univ. of New York, Buffalo. Dept. of Chemistry.
TRIMODAL RANDOM-FIELD ISING SYSTEMS IN A TRANSVERSE FIELD
Yu-quiang Ma, Z. Y. Li, D. L. Lin, and Thomas F. George Apr. 1991 21 p
(Contract N00014-90-J-1193)
(AD-A235038; UBUFFALO/DC/91/TR-48) Avail: NTIS HC/MF A03 CSCL 20/13

The trimodal random-field Ising model with the presence of a transverse field is investigated by introducing a parameter to simulate the fraction of spins not exposed to the external longitudinal magnetic field. Phase diagrams are obtained for different cases, and conditions for the occurrence of tricritical and reentrant phenomena are found. GRA

71 ACOUSTICS

Includes sound generation, transmission and attenuation. For noise pollution see *45 Environmental Pollution.*

N91-26876 Delaware Univ., Newark.
INVERSE SCATTERING PROBLEMS FOR ACOUSTIC WAVES IN AN INHOMOGENEOUS MEDIUM Ph.D. Thesis
Andrzej Wladyslaw Kedzierawski 1990 89 p
Avail: Univ. Microfilms Order No. DA9109938

The inverse scattering problem is considered of determining either the absorption of sound in an inhomogeneous medium or the surface impedance of an obstacle from a knowledge of the

far field patterns of the scattered field corresponding to many incident time-harmonic plane waves. First, the inverse problem is studied in the case when the scattering object is an inhomogeneous medium with complex refractive index having compact support. The approach to this problem is the orthogonal projection method of Colton-Monk (1988). After that, the analogue is proven of Karp's Theorem for the scattering of acoustic waves through an inhomogeneous medium with compact support. Some of these results are then generalized to the case when the inhomogeneous medium is no longer of compact support. If the acoustic wave penetrates the inhomogeneous medium by only a small amount then the inverse medium problem leads to the inverse obstacle problem with an impedance boundary condition. The inverse impedance problem is solved of determining the surface impedance of an obstacle of known shape by using both the methods of Kirsch-Kress and Colton-Monk (1989). Dissert. Abstr.

N91-26877# Naval Research Lab., Washington, DC.
A BOUNDARY SCATTERING STRENGTH EXTRACTION ALGORITHM FOR THE ANALYSIS OF LONG-RANGE REVERBERATION DATA Report, Oct. 1987 - Feb. 1989
Richard Pitre, David M. Fromm, and R. E. Franchi 29 Mar. 1991 13 p
(AD-A233721; NRL-9142; ONT-90-165) Avail: NTIS HC/MF A03 CSCL 20/1

This report describes a method for extracting rough boundary scattering strengths from long range reverberation data generated by scattering from the rough ocean surface and bottom. The method is implemented through modifications and extensions of an existing NRL boundary range-dependent reverberation model, RASP. GRA

N91-26878# Florida State Univ., Tallahassee. Dept. of Mathematics.
COMPUTATION OF BROADBAND MIXING NOISE FROM TURBOMACHINERY Semiannual Progress Report, 1 Sep. 1990 - 28 Feb. 1991
Christopher Tam 28 Feb. 1991 3 p
(Contract N00014-89-J-1836)
(AD-A233991) Avail: NTIS HC/MF A01 CSCL 20/1

This work focuses on the phenomena of dispersion and spurious acoustic radiation in calculating propeller noise using the finite difference method. The same phenomena will also affect computational solutions of turbomachinery noise problems. GRA

N91-26879# Naval Postgraduate School, Monterey, CA.
COMPARISON OF SOUND PRESSURE IN A WEDGE-SHAPED OCEAN AS PREDICTED BY AN IMAGE METHOD AND A PE MODEL M.S. Thesis
Jong R. Kim Dec. 1990 45 p
(AD-A234191) Avail: NTIS HC/MF A03 CSCL 20/1

Three different models of acoustic propagation in an ocean with a sloping bottom were compared and contasted, predicting the pressure field in a wedge-shaped ocean with a pressure release surface and an acoustically fast bottom. One image and two PE (Parabolic Equation) models were selected. The computer model for the image method was written in Basic for use on a PC and in Fortran for use on the NPS IBM 3033 computer main frame. The geometric shape of the wedge for the image calculation consists of a plane, sloping penetrable bottom and a plane, horizontal pressure release upper surface. This shape models a real continental shelf. The shape used in a parabolic equation models is a pressure release plane surface above the conical bottom. Two PE models were studied. One is based on a wide angle parabolic equation and providing a contour plot of TL as a function of position. The other, resident on the NPS computer, is based on an implicit finite difference algorithm. Results show that there is fair agreement among the different models. Comparison of the image method and the second PE model show a 2 to 3 dB difference in transmission loss near the surface and good agreement deeper. The transmission loss predicted by the first PE model differs from both other models by 4 to 5 dB near the surface and at the middle depths. Near the bottom they all agree well. GRA

N91-26880# Washington Univ., Seattle. Applied Physics Lab.
VERTICAL INCIDENCE BACKSCATTER AND SURFACE FORWARD SCATTERING FROM NEAR-SURFACE BUBBLES
S. O. McConnell and P. H. Dahl Feb. 1991 29 p
(Contract N00039-88-C-0054)
(AD-A234432; APL-UW-TR-9022) Avail: NTIS HC/MF A03 CSCL 20/1

This report presents results of acoustic measurements of vertical incidence backscattering and surface forward scattering from near-surface bubbles. Applications of this work are directed toward torpedo guidance control, and countermeasure technologies, such as detection and signal-processing constraints imposed by the near-surface environment. Acoustic measurements of the concentration and vertical extent of near-surface bubbles generated by breaking waves were made in the frequency range 15 to 50 kHz. The vertical incidence measurements, which were interspersed with the surface forward scattering measurements, produced a vertical profile of volume scattering cross section due to bubbles that decreased exponentially with depth. By integrating this profile in depth, a direct estimate of integrated volume scattering strength sigma(sub l) was made, which is a measure of total bubble concentration. The surface forward scattering measurements show a loss for a single interaction. This loss, attributable to bubbles, is referred to as the surface bubble loss (SBL), and an infrared estimate of sigma(sub l) was obtained from the SBL through a transfer function that incorporates the total extinction cross section from bubbles. The vertical incidence backscattering data and the forward scattering data, interpreted in terms of scattering and absorption by resonant bubbles, did not produce comparable trends in frequency and wind speed functional dependence, and differed significantly in overall level. GRA

N91-26881# Krug Life Sciences, Inc., San Antonio, TX.
REVIEW OF AUDITION LITERATURE: SELECTION OF ACOUSTIC SIGNALS FOR USE IN THE SYNTHESIS OF AUDITORY SPACE Final Report, Aug. 1989 - Aug. 1990
Don C. Teas Dec. 1990 38 p
(Contract F33615-89-C-0603)
(AD-A234579; USAFSAM-TR-90-33) Avail: NTIS HC/MF A03 CSCL 20/1

The purpose of this review is to aid pilot orientation. It provides information about topics of current interest in psychoacoustics that seem particularly relevant to the problem of synthesizing auditory space and presenting information within it. Included is a historical background with an orientation toward contemporary psychoacoustic information. Appendix A lists, with descriptors, the journal articles reviewed. Appendix B is a bibliography. GRA

N91-26882# National Inst. of Standards and Technology, Gaithersburg, MD.
PROGRESS IN ULTRASONIC MEASUREMENTS RESEARCH IN 1990: TRANSIENT SOURCES FOR ACOUSTIC EMISSION WORK Annual Report, 1 Oct. 1989 - 30 Sep. 1990
F. R. Breckenridge, T. M. Proctor, N. N. Hsu, S. E. Frick, and D. G. Eitzen 21 Aug. 1990 19 p
(Contract N00014-90-F-0001)
(AD-A234965) Avail: NTIS HC/MF A03 CSCL 20/1

Many techniques have been used by acoustic emission workers to produce rapid transient disturbances in elastic media. Techniques employing transient sources are necessary for characterizing many acoustic emission system components such as receiving transducers, transfer media, and other sources as well. Wave forms from seven types of sources were studied by performing experiments in which the source and a high fidelity receiver were mounted on opposite sides of an aluminum plate. Soundspeeds in the plate had been previously measured to provide information necessary for the calculation of the plate Green's function. In each experiment, a source was triggered and the ensuing output

from the receiver was captured by a transient recorder. The force waveform of the source was calculated by convolving the inverse of the plate Green's function with the captured waveform. GRA

N91-26883# Pennsylvania State Univ., University Park. Applied Research Lab.
HYDROACOUSTICS OF INTERMITTENT BOUNDARY-LAYER FLOW: A REVIEW
G. C. Lauchle 27 Mar. 1991 52 p
(Contract N00039-88-C-0051)
(AD-A235092; TM-91-78) Avail: NTIS HC/MF A04 CSCL 20/1

Intermittent boundary layer flow is present in the laminar to turbulent transition region of surfaces and bodies. The intermittency is a result of a simultaneous mixture of both laminar and turbulent regimes occurring randomly in space and time. The turbulent regimes are known as turbulent spots, they grow rapidly with downstream distance, and they ultimately coalesce to form the beginning of fully-developed turbulent boundary-layer flow. It has been long suspected that such a region of unsteadiness may give rise to local pressure fluctuations and radiated sound that are different from those created by the fully-developed turbulent boundary layer at equivalent Reynolds number. This article reviews the available literature on this subject. The emphasis of this literature is on natural and artificially created transitional boundary layers under mostly incompressible conditions; hence, the world hydroacoustics in the title. The local wall pressure fluctuations created by the passage of turbulent spots are discussed separately from the acoustic emissions, although there is growing evidence that the wall pressure field may be dominated by the acoustics of the flow if adverse pressure gradient and surface curvature effects are present. In essence, the three-dimensional effects present in most real-world flows may be the single most important issue to be addressed in regard to intermittent boundary layer hydroacoustics. GRA

N91-26884# Applied Research Lab., State College, PA.
BOUNDARY LAYER TRANSITION NOISE ART
R. C. Marboe 5 Apr. 1991 17 p Transl. into ENGLISH from J. Acoustique (France)
(Contract N00039-88-C-0051)
(AD-A235093; PSU/ARL-TM-91-81) Avail: NTIS HC/MF A03 CSCL 20/1

Imbedded acoustic arrays under a transitional or turbulent boundary layer are subject to an important contamination by flow noise. The results of a new model adapted to the transition zone are presented. A positive comparison is made with several experimental studies clearly shows the predominance, in numerous cases, of monopolar sources due to the intermittency. Thus validated, this model confirms the importance of the acoustic radiation from the transition zone; it is capable of interacting with the laminar boundary layer upstream. GRA

N91-26885# Illinois Univ., Chicago. Dept. of Mathematics.
UNDERWATER SCATTERING OF SOUND Final Report
Victor Twersky 1991 73 p
(Contract N00014-90-J-1041)
(AD-A235097) Avail: NTIS HC/MF A04 CSCL 20/1

The objective of this study is to further the understanding of volume and surface scattering effects on propagation. This report consists primarily of seven reprints: Their titles are: Multiple scattering by finite regular arrays of resonators; High-frequency reflection and scattering by multicomponent rough surface distributions; Comments on resonant systems of scatters; Moments of the Percus-Yevick hard-sphere correlation function; Coherent propagation of sound in correlated distributions of resonant spherical scatters; Regular polygonal arrays of resonant scatters; and Polydisperse scattering theory and comparison with data for red blood cells. GRA

N91-26886# Pennsylvania State Univ., University Park. Applied Research Lab.
BACKSCATTERING FROM ROUGH INTERFACES AND THE PARABOLIC APPROXIMATION
S. T. McDaniel 12 Apr. 1991 31 p Sponsored by ONR
(AD-A235184; PSU/ARL-TM-91-104) Avail: NTIS HC/MF A03 CSCL 12/1

Iterative solutions of coupled parabolic wave equations are examined to determine the validity of applying this method to predict low frequency ocean acoustic reverberation. Solutions for backscattering from a random rough interface between two media of differing wave number are obtained in the form of an expansion in powers of the rough interface excursion from its mean value. This expansion is found to differ significantly from the corresponding expansion obtained by applying perturbation theory to the full elliptic wave equation. GRA

N91-26887# Pennsylvania State Univ., University Park. Applied Research Lab.
ACOUSTIC RADIATION FROM FLUID-LOADED, RIBBED CYLINDRICAL SHELLS EXCITED BY DIFFERENT TYPES OF CONCENTRATED MECHANICAL DRIVES
C. B. Burroughs and J. E. Hallander 14 Jan. 1991 91 p
(Contract N00039-88-C-0051)
(AD-A235324; PSU-ARL-TM-90-320) Avail: NTIS HC/MF A05 CSCL 20/1

Analytic expressions are derived for the far field acoustic radiation from a fluid-loaded circular cylindrical shell reinforced with two sets of parallel periodic ribs and excited by seven types of mechanical point drives: single radial, in- and out-of-phase double radial, axial moment, circumferential moment, and in- and out-of-phase in-plane double circumferential. The ribs interact with the cylindrical shell only through normal forces. The mathematical model includes the effects of fluid loading, internal damping, and interactions between ribs. Comparisons of predictions for the shell with a large radius are made to published results for unsupported and line-supported flat plates. Measurements of the acoustic radiation from a ribbed cylindrical shell excited by different types of drives are presented. Comparisons between measured and predicted results are made. Mathematical prediction of the acoustic radiation from the unsupported and supported shell with different types of drives are compared. The effects of properties of the shell and types of drives on the acoustic radiation are examined by example, and some physical interpretation of significant features are offered. GRA

N91-26888# Sandia National Labs., Albuquerque, NM.
MULTIPLE-FREQUENCY SAW DEVICES FOR CHEMICAL SENSING AND MATERIALS CHARACTERIZATION
A. J. Ricco and S. J. Martin 1991 5 p Presented at the Transducers 1991 Conference, San Francisco, 23-27 Jun. 1991
(Contract DE-AC04-76DP-00789)
(DE91-010856; SAND-91-0063C; CONF-9106116-3) Avail: NTIS HC/MF A01

The authors have demonstrated the use of multiple-frequency surface acoustic wave (SAW) devices for chemical detection and characterization of thin film properties. A seven-frequencies SAW device was designed and fabricated with nominal Rayleigh wave center frequencies ranging from 25 to 200 MHz in square root of 2 multiples. For this device, transducer periodicity, finger length, and center-to-center transducer separation all scale with the reciprocal of the center frequency. Coating this device with a thin polymer film allows the study of frequency-dependent changes in the viscoelastic properties of the polymer as a function of temperature and of the concentration of various organic solvents, which in turn provides a means for selectively detecting these compounds. Multifrequency devices provide a means to distinguish the many perturbations affecting SAW propagation from one another. DOE

N91-26889*# Duke Univ., Durham, NC. Dept. of Mechanical Engineering and Materials Science.
AIRCRAFT INTERIOR NOISE REDUCTION BY ALTERNATE RESONANCE TUNING Final Progress Report, period ending Dec. 1990
James A. Gottwald and Donald B. Bliss Dec. 1990 215 p
(Grant NAG1-722)
(NASA-CR-185453; NAS 1.26:185453) Avail: NTIS HC/MF A10 CSCL 20A

The focus is on a noise control method which considers aircraft fuselages lined with panels alternately tuned to frequencies above and below the frequency that must be attenuated. An interior noise reduction called alternate resonance tuning (ART) is described both theoretically and experimentally. Problems dealing with tuning single paneled wall structures for optimum noise reduction using the ART methodology are presented, and three theoretical problems are analyzed. The first analysis is a three dimensional, full acoustic solution for tuning a panel wall composed of repeating sections with four different panel tunings within that section, where the panels are modeled as idealized spring-mass-damper systems. The second analysis is a two dimensional, full acoustic solution for a panel geometry influenced by the effect of a propagating external pressure field such as that which might be associated with propeller passage by a fuselage. To reduce the analysis complexity, idealized spring-mass-damper panels are again employed. The final theoretical analysis presents the general four panel problem with real panel sections, where the effect of higher structural modes is discussed. Results from an experimental program highlight real applications of the ART concept and show the effectiveness of the tuning on real structures. Author

72 ATOMIC AND MOLECULAR PHYSICS

Includes atomic structure, electron properties, and molecular spectra.

N91-26890# National Inst. of Standards and Technology, Gaithersburg, MD. Center for Radiation Research.
ABSORBED-DOSE CALIBRATION OF IONIZATION CHAMBERS IN A Co-60 GAMMA-RAY BEAM Final Report
John S. Pruitt Oct. 1990 56 p
(PB91-132290; NIST/SP-250/40) Avail: NTIS HC/MF A04 CSCL 20H

Calibrations were provided for customer-owned ionization chambers so that they may be used to determine absorbed dose to water in Co-60 gamma-ray beams. The calibrations are based on calorimetric measurement of absorbed dose to graphite in a graphite phantom. Transformation of the calibrations to a water phantom is made with a specially-designed graphite ionization chamber, and requires knowledge of photon mass attenuation coefficients and the perturbation of the graphite chamber in the water medium. The determination of these quantities is described in detail, along with the operational techniques normally used to transfer the calibration to customer-owned chambers. Author

N91-26891# Northwestern Univ., Evanston, IL. Dept. of Materials Science and Engineering.
CHEMISTRY ON AN ATOMIC SCALE OF ION-BEAM MODIFIED SURFACES Final Report
David N. Seidman Jan. 1991 26 p
(Contract DAAL03-86-G-0063)
(AD-A233707; ARO-23804.1-MS-F) Avail: NTIS HC/MF A03 CSCL 11/6

A miniature electron-beam evaporator (MEBE) has been fabricated and adapted to our ultrahigh-vacuum atom-probe field-ion microscope (APFIM). The MEBE allows for in situ vapor deposition--under ultrahigh-vacuum conditions of a wide range of elements, on the surface of an atomically clean FIM specimen; the surface is prepared via the field-evaporation process. The deposition rate of an evaporant from the MEBE is calibrated to give an accurate value of this quantity. Examples of the deposition of silicon or titanium on tungsten FIM specimens are presented. And in the case of the Ti/W couple it is demonstrated that the interface between the tungsten substrate and the titanium overlayer is chemically sharp on an atomic scale; the titanium was vapor deposited at a substrate temperature of 77 K. Also a 20 kV electron beam gun was adapted to the APFIM. This gun is useful for in situ electron-beam heating of bilayer couples, or the introduction of point defects in metal oxide or semiconductor overlayers via electronic mechanisms. GRA

N91-26892# Northwestern Univ., Evanston, IL. Dept. of Chemistry.
HIGH ENERGY DENSITY SYSTEMS IN CRYOGENIC MEDIA: THE PRODUCTION AND REACTION OF ATOMS AND RADICALS Final Report, Jul. 1987 - Jul. 1990
Eric Weitz 14 Jan. 1991 48 p
(Contract F33615-87-C-2737)
(AD-A233785; WRDC-TR-90-2112) Avail: NTIS HC/MF A03 CSCL 21/2

The lifetime and reactive behavior of energetic species in low temperature rare gas media have been investigated. A technique for measuring the diffusion coefficient of reactive species has been developed and applied in detail to probe O atoms in Xenon matrices. O atoms have long lifetimes in xenon matrices at 32 K. For initial concentrations on the order of one part in 10,000 approximately half of the initial atoms are unreacted on a timescale of one week. The long timescale for this process is discussed in relationship to the shorter timescales observed for atom and radical diffusion under conditions involving constant photolysis of matrices. The lifetime excited state species are important in understanding the storage and reactivity of energetic species in low temperature cryogenic media. Isolated Binary Collision (IBC) models attempt to predict lifetimes of excited states in condensed media based on the probability of collision deactivation of the species in the gas phase and the local density of the condensed phase media. The predictions of this theory have been tested for a number of systems. While the predictions have been shown to generally be very good for non-polar systems undergoing vibration-translation/rotation relaxation processes, some possible anomalies are noted for the hydrogen halides in heavy rare gases. Possible sources of these anomalies and their ramifications are discussed. GRA

N91-26893# State Univ. Coll. of New York, Buffalo. Dept. of Chemistry.
PROPAGATORS FOR QUANTUM OSCILLATOR CHAINS
V. V. Dodonov, Thomas F. George, Olga V. Manko, Chung-in Um, and Kyu-Hwang Yeon Apr. 1991 20 p
(Contract N00014-90-J-1193)
(AD-A234467; UBUFFALO/DC/91/TR-44) Avail: NTIS HC/MF A03 CSCL 20/10

Two different methods (path integrals and integrals of the motion) are used to calculate exact propagators for two sets of coupling constants between neighboring particles. GRA

N91-26894# State Univ. of New York, Buffalo. Dept. of Chemistry.
RESONANCE FLUORESCENCE SPECTRUM OF AN ATOM NEAR A PHASE CONJUGATOR
Henk F. Arnoldus and Thomas F. George Apr. 1991 30 p
(Contract N00014-90-J-1193)
(AD-A234535; UBUFFALO/DC/91/TR-45) Avail: NTIS HC/MF A03 CSCL 20/5

Resonance fluorescence by an atom near the surface of a phase conjugator is studied. The atom is irradiated by a finite-linewidth laser beam, and the bandwidth is modeled by a randomly fluctuating phase. Expressions for the steady-state atomic density operator and the resonance fluorescence spectrum are obtained. For a small laser linewidth, the spectrum contains two delta peaks: the usual peak at the laser frequency; and its phase conjugate image. In the limit of separated lines, the spectrum consists of the Mollow triplet and its phase-conjugate replica. In the image triplet, the positions of the fluorescence line and the

three-photon line are reversed, as compared to the original triplet. Also, the intensity of the image spectrum is distributed differently over the three lines. GRA

N91-26895# Massachusetts Inst. of Tech., Cambridge. Research Lab. of Electronics.
EXPERIMENTS WITH TRAPPED ATOMS Annual Report, 1 Feb. 1990 - 31 Jan. 1991
David E. Pritchard 10 Apr. 1991 6 p
(Contract N00014-90-J-1642)
(AD-A234580) Avail: NTIS HC/MF A02 CSCL 20/5

Our current objective is to produce an intense slow atom beam and trap it in a magnetic trap. The atoms will be trapped by the forces of an inhomogeneous magnetic field on the magnetic moment of the atom. We have several schemes in mind which will greatly increase the density in the bottom of the trap. Dense samples of atoms cooled to microkelvin temperatures promise to open up new and exciting areas of physics. The lower interaction rate of the atoms due to their reduced thermal motion, together with the possibility of indefinitely long interaction times, make samples of trapped atoms ideal for high resolution spectroscopy and for use as atomic frequency standards PRI86. High density samples of ultra-cold atoms will also make it possible to study interatomic collisions in a new regime characterized by: a long deBroglie wavelength; the importance of weak forces; and collision durations which are longer than radiative lifetimes so that absorption, stimulated, and spontaneous radiative transitions take place during a collision. This opens the possibility of controlling the outcome of collisions by weak laser irradiation. High density samples of atoms at low temperature atoms are well suited in the search for quantum collective phenomena such as Bose-Einstein condensation. GRA

N91-26896# California Univ., Berkeley.
NEUTRAL ATOM DEBROGLIE-WAVE INTERFEROMETRY Quarterly Report No., 1 Jan. - Mar. 1991
John F. Clauser Mar. 1991 4 p
(Contract N00014-90-J-1475)
(AD-A234624) Avail: NTIS HC/MF A01 CSCL 07/2

The optimal species for experiments was earlier chosen as potassium, but this choice was reexamined in light of our current status and experience. The conclusion is that potassium still appears to be the best choice, although lithium may become preferable as laser technology evolves. Potassium's most significant difficulty is in producing cooled diode lasers, but the remaining trade-offs appear to warrant solving this problem. Lithium offers very wide diffraction angles for available grating periods at a lower limit velocity of Sm/sec (to prevent significant gravitational free-fall). Thus its use would allow simple grating fabrication techniques employing optical lithography for either separated - beam or Talbot fringe interferometers. GRA

N91-26897# State Univ. of New York, Buffalo. Research Foundation.
MOLECULAR ENGINEERING DYNAMICS OF ELECTRON TRANSPORT AND NONLINEAR OPTICAL INTERACTION IN LANGMUIR-BLODGETT FILMS OF ORGANIC SEMICONDUCTOR HETEROSTRUCTURE Final Report, Aug. 1987 - Jul. 1990
Paras N. Prasad 12 Mar. 1991 24 p
(Contract F49620-87-C-0097)
(AD-A235001; AFOSR-91-0246TR) Avail: NTIS HC/MF A03 CSCL 20/6

The project was able to develop a very comprehensive research program in the area of photonics. This program covered microscopic theory of optical nonlinearity, design and synthesis of novel structures, materials processing for guided waves, measurements of optical nonlinearities and study of device processes. We made significant accomplishments in each topic as recognized by the number of invitations received to give talks at various international conferences. GRA

N91-26898# California Inst. of Tech., Pasadena.
STUDIES OF RESONANTLY ENHANCED MULTIPHOTON IONIZATION PROCESSES IN MOLECULES Final Report, 1 Nov. 1986 - 31 May 1990
Vincent McKoy Apr. 1991 36 p
(Grant AF-AFOSR-0039-87; AF Proj. 2303)
(AD-A235217; AFOSR-91-0496TR) Avail: NTIS HC/MF A03 CSCL 20/5

Studies were completed of several Resonance Enhanced Multiphoton Ionization (REMPI) processes in molecules. The overall objective of this effort was to provide a robust theoretical analysis and prediction of the key spectral features associated with various experimental and technology applications of this technique including its use for state-specific detection and production of species and for diagnostics in combustion and processing plasmas. Specific achievements of this research included: (1) studies of ion vibrational distributions produced by REMPI with emphasis on anomalous behavior in these distributions in molecules and molecular fragments, e.g., OH and CF; (2) ion rotational distributions that results from REMPI, the underlying dynamics of these processes, and the identification of schemes for enhancing state selectivity in these distributions; (3) use of photoelectron angular distributions produced by REMPI to probe molecular alignment, an important dynamical feature in gas-surface collisions and molecular fragmentation. GRA

N91-26899# Cornell Univ., Ithaca, NY. Lab. of Atomic and Solid State Physics.
CHARGE EXCHANGE IN ION-SURFACE SCATTERING AT HYPERTHERMAL (10-100 eV) AND keV ENERGIES Final Report, 15 Nov. 1987 - 1 Jan. 1991
Barbara H. Cooper 9 Apr. 1991 38 p
(Grant AF-AFOSR-0069-88; AF Proj. 2303)
(AD-A235233; AFOSR-91-0445TR) Avail: NTIS HC/MF A03 CSCL 20/5

Investigated are the interactions of hyperthermal (10 to 100 eV) and keV ions with clean and adsorbate-covered metal surfaces, with particular emphasis on ion-surface charge exchange processes. Nonadiabatic resonant charge transfer to hyperthermal energy K+ scattered from clean and adsorbate-covered Cu(001) and Cu(110) were observed. Very small coverages of alkali adsorbates (less than or equal to 0.05 ML) dramatically increased the charge transfer rate. Classical trajectory calculation was used to determine the scattered K+ velocities, and a numerical solution of the Brako-Newns equations for nonadiabatic resonant electron tunneling to a single K level to determine the ion survival probability. Very good agreement with experiment was obtained, once the adsorbate-induced inhomogeneities in the electrostatic potential were modeled. Both experimental and theoretical capabilities were extended to study more complex charge transfer behavior. The extended model treats systems with several atomic states participating in the charge transfer. A time-of-flight detector for neutral alkalis and a UHV sample preparation chamber were completed. We have observed, for Li+ scattering from low work function surfaces, Li+, Li-, Li(0) and excited state Li in the scattered flux and, for 0+ scattering from Cu, O+ and O- in ratios that vary dramatically with beam energy and scattering geometry. We are measuring branching ratios for these different final states to test our extended model. Studies were begun of charge transfer and dissociation for hyperthermal O2(+) scattered from clean and adsorbate-covered Cu(001). GRA

N91-26900# California Univ., Berkeley. Dept. of Chemistry.
NEGATIVE ION PHOTODETACHMENT AS A PROBE OF THE TRANSITION STATE REGION: THE I + HI REACTION Interim Report, 1-30 Apr. 1991
Daniel M. Neumark 30 Apr. 1991 42 p
(Contract N00014-87-K-0495)
(AD-A235297; TR-7) Avail: NTIS HC/MF A03 CSCL 07/4

The study of the transition state of bimolecular reactions using negative ion photodetachment is described. The I + HI reaction is used as an example of this method. The photoelectron spectrum of IHI(-) shows resolved vibrational features assigned to a

progression in the antisymmetric stretch mode of the neutral IHI complex. Threshold photodetachment studies of this system at higher resolution show additional structure that arises from two sources: (1) resonances supported by the I + IHI potential energy surface, and (2) transitions to nearly free internal rotor states of the IHI complex. The photoelectron spectrum of the cluster anion IDI(-)(N20) is also described. GRA

N91-26901# SRI International Corp., Menlo Park, CA.
AB INITIO MOLECULAR DYNAMICS SIMULATIONS OF SURFACES AND INTERFACES Final Report
Mark VanSchilfgaarde Feb. 1991 48 p
(Contract N00014-89-K-0132)
(AD-A235315) Avail: NTIS HC/MF A03 CSCL 20/12

This work was to develop and apply density-functional methods to semiconductor surfaces and interfaces. The method of Linear Muffin Tin Orbitals (LMTO) was used to make a detailed study of the properties of the ideal metal/GaAs interface. This was the first systematic study of the properties of a Schottky barrier using a first-principles method, and these explicit calculations shed light on some of the many theories which have been advanced to explain its observed pinning behavior. This work was further pursued along two lines. First, some As antisite defects were incorporated in planes near the metal interface to determine to what extent they alter the Schottky barrier pinning position. The early stages of Schottky barrier formation are also studied using the LMTO method. This work confirms the tight-binding picture that the potential of the first layer of GaAs deepens as Al is deposited. We also predict that the Al atom favors the Ga site over the As site; and that the reconstructed free GaAs surface partially (but not completely) dissociates as metal adatoms are deposited. We are hopeful that this approach will quantitatively predict donor and acceptor levels, and pinpoint the evolution of the interfacial dipole and the onset of metallization. GRA

N91-26902# Argonne National Lab., IL.
THEORETICAL STUDIES OF POTENTIAL ENERGY SURFACES AND COMPUTATIONAL METHODS
L. B. Harding, R. J. Harrison, and R. Shepard 1991 4 p Presented at the Department of Energy-Basic Energy Sciences (DOE-BES) Combustion Research Meeting, Lake Geneva, 28-31 May 1991
(Contract W-31-109-eng-38)
(DE91-011126; ANL/CP-70073; CONF-9105162-2) Avail: NTIS HC/MF A01

The goal of this program is to calculate accurate potential energy surfaces (PES) for both reactive and nonreactive systems. To do this the electronic Schroedinger equation must be solved. Our approach to this solution has three elements: (1) the use of multiconfiguration self-consistent field (MCSCF) wave functions; (2) the inclusion of electron correlation via configuration interaction (CI); and (3) the use of basis sets optimized for correlated calculations. With this approach, we are able to provide useful predictions of the energetics for a broad range of systems. More recently, we have begun work on two new families of methods. The first is the coupled-cluster (CC) method which allows the most efficient calculation of electronic excitation energies. The second is full- and selected-CI methods. A full-CI calculation gives the exact wavefunction for the given basis set. The selected-CI method approaches the full-CI by a perturbation treatment of the minor configurations. Complementary to this theoretical effort, a new initiative in the group aims to harness the cost-effectiveness and high peak-performance offered by parallel computers. We are following a dual strategy of porting existing production codes to few processor machines as well as developing tools and algorithms suitable for highly parallel computers. The following is a summary of recent progress and future plans in this program. DOE

N91-26903# Ames Lab., IA.
NONPERTURBATIVE BEHAVIOR OF QUARKS
K. E. Lassila (Ames Lab., IA.) 1990 6 p Presented at the 5th International Conference on Hadronic Mechanics and Nonpotential Interactions, Cedar Falls, 13-17 Aug. 1990
(Contract W-7405-eng-82)
(DE91-011905; IS-M-663; CONF-9008204-1) Avail: NTIS HC/MF A02

Several experiments have established that quarks exhibit different aspects of their interactions depending on their environment when they are probed. The nonlinear behavior found in nuclei is treated by expanding the many quark nuclear state as a series in color singlet multiquark states. The effects found in numerous nuclear target experiments can all be described by including the first two terms in this multiquark expansion. Comparisons with data from deep inelastic scattering by electrons, muons, neutrinos and antineutrinos will be given and also comparisons with dimuon production by protons on nuclei will be examined. Dilepton depletion at small target parton momentum fraction in proton-nucleus collisions will also be discussed as an example of this nonlinear behavior. DOE

N91-26904# California Univ., Berkeley. Lawrence Berkeley Lab.
A STUDY OF SIGNAL GENERATION AND CHARGE COLLECTIONIN a-Si:H DIODES FOR RADIATION IMAGING Ph.D. Thesis
I. Fujieda Oct. 1990 130 p
(Contract DE-AC03-76SF-00098)
(DE91-010243; LBL-30291) Avail: NTIS HC/MF A07

Its high radiation resistivity and large area capability are the expected advantages of this material together with its ability to provide a front-end readout electronics in the vicinity of the sensor element. Electrons and holes created by incoming charged particles, X rays, gamma rays, are drifted by the electric field inside a-Si:H diodes and this carrier movement induces signal charges on electrodes. Charge collection and signal generation process are analyzed in terms of carrier mobilities, lifetimes and electric field. Charge collection in thick a-Si:H diodes is often limited by deep-level trapping of carriers during transit and a finite charge integration time required for single particle counting in some applications and sometimes by volume recombination of carriers for detecting heavily ionizing particles such as alpha particles. The charge collection process is also strongly affected by the nonuniform electric field profiles in a-Si:H diodes caused by the fixed space charges inside the material under reverse bias. Signal generation due to a weak light pulse irradiating each end of a thick diode is measured as a function of a reverse bias and it gives a valuable information about the fixed space charges. Field profiles can be manipulated by either doping, electrode geometry, or combination of both to improve the charge collection process. One can apply a higher reverse bias on a diode with an equivalent thickness by providing buffer layers at each end of the diode and thus suppressing soft breakdown phenomena. X ray detection with a good sensitivity is demonstrated by an a-Si:H photodiode coupled to an evaporated CsI scintillator. The scintillation quality of evaporated CsI layers can be made almost identical to its single crystal counterpart. Fields of a-Si:H radiation detector application include high energy physics, medical imaging, materials science and life science. DOE

N91-26905# Ohio State Univ., Columbus. Dept. of Chemistry.
MOLECULAR ORBITAL STUDIES OF THE BONDING IN HEAVY ELEMENT ORGANOMETALLICS
B. E. Bursten Mar. 1991 11 p
(Contract DE-FG02-86ER-13529)
(DE91-010915; DOE/ER-13529/5) Avail: NTIS HC/MF A03

A number of technological advances have allowed expanded studies of actinide systems in the past year. Expertise was developed in the use and administration of Digital Equipment DECstation 3100 UNIX-based worksystem, purchased with DOE funds. The access to this extremely powerful stand-alone computer, as well as its facility in tying into the Cray supercomputer at the Ohio Supercomputer Center, has allowed the expansion of the computational vistas greatly. The access to more powerful computers has allowed use of more sophisticated, albeit more complex, electronic structure methods in the investigations. These methods include local density functional (LDF) and ab initio

approaches. Several projects were concluded and the program of actinide research was continued. The highlights of these projects are as follows: bonding in Np, Pu, and transplutonium organometallic compounds; application of the DV-X(alpha) (discrete variational X(alpha)) method to actinide chemistry; ad initio calculations on actinide molecules; experimental comparisons of organoactinide and organotransition metal chemistry. DOE

N91-26906# Brookhaven National Lab., Upton, NY.
PHOTONS AND NEUTRONS
G. Shirane Oct. 1990 6 p Presented at the International Collaboration on Advanced Neutron Sources (ICANS), Tsukuba, Japan, 21-26 Oct. 1990
(Contract DE-AC02-76CH-00016)
(DE91-010980; BNL-45993; CONF-9010243-17) Avail: NTIS HC/MF A02

A review is given of two selected topics in current activities of synchrotron x-ray studies; magnetic x-ray scattering and inelastic x-ray scattering. These are the research areas where photons and neutrons directly compete and supplement each other. A great deal of progress has been made in the field of magnetic x-ray scattering with synchrotron radiation. A series of high resolution studies on Ho and other rare earth magnetic structures has revealed many important features of spin arrangements, which escaped clarification by previous neutron diffraction studies. Magnetic x-ray scattering recently entered into its next stage of development when the resonance at the absorption edge was shown to enhance the Ho magnetic cross section by a factor of 50. The second area where x-ray scattering is beginning to overlap with neutron research is direct inelastic x-ray scattering. Because of its favorable energy-wavelength relation, neutron scattering has been the natural tool for the direct observation of elementary excitations in condensed matter. The most commonly used neutrons have 14 meV of energy and a 2.3 A in wavelength. The energy of x-rays with the same wavelength is 5 KeV. In order to attain a sufficient energy resolution for phonon studies, one has to use backscattering from a perfect crystal. This type of experimental arrangement became feasible recently because of the brightness of x-rays emitted by synchrotron and storage rings. DOE

N91-26907# Stanford Linear Accelerator Center, CA.
GAUGE BOSONS AND HEAVY QUARKS: PROCEEDINGS OF SUMMER INSTITUTE ON PARTICLE PHYSICS
J. F. Hawthorne, ed. Jan. 1991 528 p Presented at the 18th SLAC Summer Inst. on Particle Physics: Heavy Quarks and Gauge Bosons, Stanford, 16-27 Jul. 1990
(Contract DE-AC03-76SF-00515)
(DE91-011248; SU-SLAC-378; CONF-900799) Avail: NTIS HC/MF A23

This report contains papers on the following topics: Z decays and tests of the standard model; future possibilities for LEP; studies of the interactions of electroweak gauge bosons; top quark topics; the next linear collider; electroweak processes in hadron colliders; theoretical topics in B-physics; experimental aspects of B-physics; B-factory storage ring design; rare kaon decays; CP violation in K(sup 0) decays at CERN; recent K(sup 0) decay results from Fermilab E-731; results from LEP on heavy quark physics; review of recent results on heavy flavor production; weak matrix elements and the determination of the weak mixing angles; recent results from CLEO I and a glance at CLEO II data; recent results from ARGUS; neutrino lepton physics with the CHARM 2 detector; recent results from the three TRISTAN experiments; baryon number violation at high energy in the standard model: fact or fiction? New particle searches at LEP; review of QCD at LEP; electroweak interactions at LEP; recent results on W physics from the UA2 experiment at the CERN rho(bar rho) collider; B physics at CDF; and review of particle astrophysics. DOE

N91-26908# Oak Ridge National Lab., TN.
CORRELATION IN PHOTODETACHMENT
D. J. Pegg (Oak Ridge National Lab., TN.) 1991 11 p Presented at the 3rd US/Mexico Symposium on Atomic and Molecular Physics, Cocoyoc (Mexico), 13-16 Apr. 1991
(Contract DE-AC05-84OR-21400)
(DE91-011369; CONF-9104242-1) Avail: NTIS HC/MF A03

Electron correlation plays a major role in all aspects of the photodetachment of an electron from a negative ion. Photodetachment measurements are well suited to investigate the relatively short range forces associated with correlation due to the absence of the long range Coulomb interaction. Measurements of electron affinities, asymmetry parameters and cross sections are described to illustrate the influence of correlation on photodetachment. DOE

N91-26909# Oak Ridge National Lab., TN.
NEGATIVE ION FORMATION BY RYDBERG ELECTRON TRANSFER: ISOTOPE-DEPENDENT RATE CONSTANTS
H. S. Carman, Jr., C. E. Klots, and R. N. Compton 1991 14 p Presented at the 201st American Chemical Society (ACS) National Meeting, Atlanta, 14-19 Apr. 1991
(Contract DE-AC05-84OR-21400)
(DE91-012058; CONF-910402-15) Avail: NTIS HC/MF A03

The formation of negative ions during collisions of rubidium atoms in selected ns and nd Rydberg states with carbon disulfide molecules has been studied for a range of effective principal quantum numbers (10 less than n* less than 25). For a narrow range of n* near n* = 17, rate constants for CS2(-) formation are found to depend upon the isotopic composition of the molecule, producing a negative ion isotope ratio (mass 78 to mass 76, amu) up to 10.5 times larger than the natural abundance ratio of CS2 isotopes in the reagent. The isotope ratio is found to depend strongly upon the initial quantum state of the Rydberg atom and perhaps upon the collision energy and CS2 temperature. DOE

N91-26910# Jackson State Univ., MS. Dept. of Chemistry.
INFRARED AND VISIBLE LASER DOUBLE RESONANCE STUDIES OF VIBRATIONAL ENERGY TRANSFER PROCESSES IN POLYATOMIC MOLECULES
R. Bhatnagar 1990 3 p
(Contract DE-FG05-88ER-13925)
(DE91-012162; DOE/ER-13925/2) Avail: NTIS HC/MF A01

We have purchased a new probe laser (Nitrogen laser pumped dye laser) from Laser Photonics for use in this project. The new laser is already installed and tested with several dyes. We have acquired two frequency doubling crystals, KDP and BBO and at this time we are conducting experiments to optimize their performance. The frequency doubling capability will extend the useful range of our dye laser in the ultra-violet region. We intend to use this capability at a later stage to study the reaction dynamics of free radicals generated by the CO2 laser pulse. We have synthesized s-tetrazine in our laboratory and although the yield was poor, we were successful in our attempt. The compound is unstable over a long period of time and due to the cost of chemicals involved, we have postponed further synthesis until all our equipment is ready for an experiment. DOE

N91-26911# Oak Ridge National Lab., TN.
ELECTRON-EXCITED MOLECULE INTERACTIONS
L. G. Christophorou (Oak Ridge National Lab., TN.) 1991 40 p Presented at the 20th International Conference on Phenomena in Ionized Gases, Barga (Italy), 8-12 Jul. 1991
(Contract DE-AC05-84OR-21400)
(DE91-012227; CONF-910711-6) Avail: NTIS HC/MF A03

In this paper the limited but significant knowledge to date on electron scattering from vibrationally/rotationally excited molecules and electron scattering from and electron impact ionization of electronically excited molecules is briefly summarized and discussed. The profound effects of the internal energy content of a molecule on its electron attachment properties are highlighted focusing in particular on electron attachment to vibrationally/rotationally and to electronically excited molecules. The limited knowledge to date on electron-excited molecule interactions clearly shows that the cross sections for certain electron-molecule collision processes can be very different from those involving ground state molecules. For example, optically

enhanced electron attachment studies have shown that electron attachment to electronically excited molecules can occur with cross sections 10(exp 6) to 10(exp 7) times larger compared to ground state molecules. The study of electron-excited molecule interactions offers many experimental and theoretical challenges and opportunities and is both of fundamental and technological significance. DOE

N91-26912# Duke Univ., Durham, NC. Dept. of Physics.
STUDIES OF INTERACTIONS BETWEEN ELEMENTARY PARTICLES AND NUCLEI
L. R. Fortney, A. T. Goshaw, and W. D. Walker Aug. 1990 49 p
(Contract DE-AS05-76ER-03065)
(DE91-012300; DOE/ER-03065/T8) Avail: NTIS HC/MF A03

This report discusses the following research: Particle production in proton-antiproton collision at (radical)s = 1.8 TeV; SSC subsystems R and D; the solenoid detector collaboration particle nucleus collisions; task expenditure statement. Hadroproduction using 300 GeV particle beams Fermilab; hadroproduction of beauty Fermilab; and vector meson photo production. DOE

73 NUCLEAR AND HIGH-ENERGY PHYSICS

Includes elementary and nuclear particles; and reactor theory.

For space radiation see *93 Space Radiation.*

N91-26913# Oesterreichisches Forschungszentrum Seibersdorf G.m.b.H., Vienna. Hauptabt. fuer Strahlenschutz.
A TEST OF THE IAEA CODE OF PRACTICE FOR ABSORBED DOSE DETERMINATION IN PHOTON AND ELECTRON BEAMS
Arnold Leitner, Wilhelm Tiefenboeck, Josef Witzani (Bundesamt fuer Eich- und Vermessungwesen, Vienna, Austria), and Christian Strachotinsky Dec. 1990 24 p
(OEFZS-4565; ETN-91-99496) Copyright Avail: NTIS HC/MF A03

The IAEA (International Atomic Energy Agency) code of practice TRS 277 gives recommendations for absorbed dose determination in high energy photon and electron beams based on the use of ionization chambers calibrated in terms of exposure of air kerma. The scope of the work was to test the code for cobalt 60 gamma radiation and for several radiation qualities at four different types of electron accelerators and to compare the ionization chamber dosimetry with ferrous sulphate dosimetry. The results show agreement between the two methods within about one per cent for all the investigated qualities. In addition the response of the TLD capsules of the IAEA/WHO TL dosimetry service was determined. ESA

N91-26914# Fermi National Accelerator Lab., Batavia, IL.
UNIX (TM) IN HIGH ENERGY PHYSICS: WHAT WE CAN LEARN FROM THE INITIAL EXPERIENCES AT FERMILAB
J. N. Butler Mar. 1991 24 p Presented at the Conference on Computing in High Energy Physics, Tsukuba (Japan), 11-15 Mar. 1991
(Contract DE-AC02-76CH-03000)
(DE91-011976; FNAL/C-91/91; CONF-910373-4) Avail: NTIS HC/MF A03

The reasons why Fermilab decided to support the UNIX operating system are reviewed and placed in the content of an overall model for high energy physics data analysis. The strengths and deficiencies of the UNIX environment for high energy physics are discussed. Fermilab's early experience in dealing with a an open multivendor environment, both for computers and for peripherals, is described. The human resources required to fully exploit the opportunities are clearly growing. The possibility of keeping the development and support efforts within reasonable bounds may depend on the ability to collaborate or at least to share information even more effectively than we have in the past. DOE

N91-26915# Los Alamos National Lab., NM.
AN ACTIVE PARTICLE ACCELERATOR
T. Goldman 1991 16 p Presented at the 1991 Institute of Electrical and Electronics Engineers (IEEE) Particle Accelerator Conference (PAC), San Francisco, 6-9 May 1991
(Contract W-7405-eng-36)
(DE91-011404; LA-UR-91-1287; CONF-910505-12) Avail: NTIS HC/MF A03

Although a static charge is difficult to maintain on macroscopic particles, it is straightforward to construct a small object with a regularly oscillating electric dipole moment. For objects of a given size, one may then construct an accelerator by appropriately matching the frequency and separations of an external array of electrodes to this size. Physically feasible size ranges, an accelerator design, and possible applications of such systems are discussed. DOE

N91-26916# Fermi National Accelerator Lab., Batavia, IL.
PROVIDING A COMPUTING ENVIRONMENT FOR A HIGH ENERGY PHYSICS WORKSHOP
J. Nicholls Mar. 1991 10 p Presented at the Conference on Computing in High Energy Physics, Tsukuba (Japan), 11-15 Mar. 1991
(Contract DE-AC02-76CH-03000)
(DE91-012049; FNAL/C-91/83; CONF-910373-Summ) Avail: NTIS HC/MF A02

Although computing facilities have been provided at conferences and workshops remote from the home institution for some years, the equipment provided has rarely been capable of providing for much more than simple editing and electronic mail over leased lines. This presentation describes the pioneering effort involved by the Computing Department/Division at Fermilab in providing a local computing facility with world-wide networking capability for the Physics at Fermilab in the 1990's workshop held in Breckenridge, Colorado, in August 1989, as well as the enhanced facilities provided for the 1990 Summer Study on High Energy Physics at Snowmass, Colorado, in June/July 1990. Issues discussed include type and sizing of the facilities, advance preparations, shipping, on-site support, as well as an evaluation of the value of the facility to the workshop participants. DOE

N91-26917# Superconducting Super Collider Lab., Dallas, TX.
COHERENT BEAM-BEAM EFFECTS
A. W. Chao Jan. 1991 51 p
(Contract DE-AC02-89ER-40486)
(DE91-012512; SSCL-346) Avail: NTIS HC/MF A04

This report discusses the following about beam-beam interactions: the dynamic-beta model; flip-flop effect; steady-state with nonlinear beam-beam force; dynamics about the steady-state; rigid dipole model; quadrupole modes; quadrupole modes around dynamic-beta; higher order moments; and coherent beam blow-up model. DOE

74 OPTICS

Includes light phenomena; and optical devices.

For lasers see *36 Lasers and Masers.*

N91-26918* National Aeronautics and Space Administration. Pasadena Office, CA.
METHOD AND APPARATUS FOR SECOND-RANK TENSOR GENERATION Patent
Hua-Kuang Liu, inventor (to NASA) (Jet Propulsion Lab., California Inst. of Tech., Pasadena.) 9 Apr. 1991 5 p Filed 16 Feb. 1989 Sponsored by NASA
(NASA-Case-NPO-17512-1-CU; US-Patent-5,005,954; US-Patent-Appl-SN-310992; US-Patent-Class-350-354; US-Patent-Class-350-353; US-Patent-Class-350-358; US-Patent-Class-364-713; US-Patent-Class-364-822; US-Patent-Class-364-837; US-Patent-Class-364-841) Avail: US Patent and Trademark Office CSCL 20F

A method and apparatus are disclosed for generation of

second-rank tensors using a photorefractive crystal to perform the outer-product between two vectors via four-wave mixing, thereby taking 2n input data to a control n squared output data points. Two orthogonal amplitude modulated coherent vector beams x and y are expanded and then parallel sides of the photorefractive crystal in exact opposition. A beamsplitter is used to direct a coherent pumping beam onto the crystal at an appropriate angle so as to produce a conjugate beam that is the matrix product of the vector beam that propagates in the exact opposite direction from the pumping beam. The conjugate beam thus separated is the tensor output xy (sup T). Author

N91-26919# Naval Research Lab., Washington, DC.
ONE-DIMENSIONAL TRANSLATION MEASUREMENT OF SPECKLE FROM ROUGH ROTATING OBJECTS IN ULTRAVIOLET ILLUMINATION Interim Report
Bonnie Light and Gary L. Trusty 31 Dec. 1990 67 p
(AD-A233719; NRL-9293) Avail: NTIS HC/MF A04 CSCL 20/6

The experimental measurement of translation in one dimension from near-field speckle produced by rough rotating objects is considered in this report. Rotation rates about single fixed axis are estimated from measured speckle intensity pattern translation values. The feasibility of translation measurements made by cross-correlation technique in a single dimension is demonstrated. A technique for image enhancement is also demonstrated. The speckle pattern images can be enhanced so that intensity distributions meet near-ideal distributions and contrast values. Speckle is produced experimentally by small (2.5-, 4.0-, 5.0-mm diameter) spherical objects with aluminum paint surfaces in coherent ultraviolet illumination. The measurements are made from imagery taken before and after object angular displacement, rather than from imagery taken from objects revolving in real time. Signal to noise ratios are compared for the direct evaluation of the cross correlation function and for the evaluation of the normalized form of the cross-correlation function as well as for correlation functions for enhanced and unenhanced imagery. GRA

N91-26920# Massachusetts Inst. of Tech., Lexington. Lincoln Lab.
ANALYSIS OF NONLINEAR OPTICAL FREQUENCY CONVERSION Technical Report, 1 Nov. 1988 - 30 Sep. 1989
Norman Menyuk and Paul L. Kelley 8 Jan. 1991 40 p
(Contract F19628-90-C-0002)
(AD-A233726; TR-907; ESD-TR-90-140) Avail: NTIS HC/MF A03 CSCL 20/6

Nonlinear optical techniques have been evaluated for the conversion of out-of-band diode laser radiation into the 2 to 5 micron region. It is concluded that frequency conversion using an optical parametric oscillator is the preferred nonlinear approach and that ZnGeP2 is the most promising nonlinear material. Direct diode or diode array pumping of the nonlinear material may require semiconductor laser operation in the 1.7- to 2.0 micron region and will entail substantial increases in the peak power and beam quality in comparison to that obtainable from present devices. Diode-pumped solid state lasers might provide a reasonable near-term solution to the pump source requirements. GRA

N91-26921# Rochester Univ., NY. Inst. of Optics.
PROCEEDINGS OF THE OPTOELECTRONIC WORKSHOP 25: LIQUID CRYSTAL MATERIALS AND DEVICES FOR OPTO-ELECTRONIC APPLICATIONS
Stephen Jacobs and James Miller 5 Dec. 1990 87 p Workshop held in Rochester, NY, 5 Dec. 1990; sponsored in part by Rochester Univ., and Army
(Contract DAAL03-86-K-0173)
(AD-A233780; ARO-24626.210-PH-UIR) Avail: NTIS HC/MF A05 CSCL 17/5

The workshop was opened by a brief review of the device requirements for an electro-optic element to replace a mechanical chopper for uncooled IR detector arrays. Then the liquid crystal TLSM/IR chopper project was reviewed with recent results. Key highlights presented included the following: (1) A TLSM cell driven by a programmable waveform generator designed and built at UR/LLE was shown to be capable of generating a square-wave optical response with rise and decay times of 500 microsec; (2) A modulation depth of 40 percent in the 8 to 12 micrometer region of the infrared was demonstrated in an FTIR experiment using a prototype TLSM/IR chopper; (3) The design and synthesis of a new ferroelectric liquid crystal with the potential for improved transmission in the 8 to 12 micrometer region was described; and (4) A functional prototype TLSM/IR chopper and programmable waveform generator were delivered to C2NVEO for further characterization and experimentation. GRA

N91-26922# ERG Systems, Inc., Saint James, NY.
FULL SURFACE TESTING OF GRAZING INCIDENCE MIRRORS Quarterly Report, No. 2
John L. Remo 3 Mar. 1991 6 p
(Contract N00014-90-C-0246)
(AD-A234005) Avail: NTIS HC/MF A02 CSCL 20/6

The major goal of the first two quarters of the Full Surface Interferometric Scanner (FSIS) project was the design of the optical, mechanical, and electrical/digital prototype. During this period, procurement, testing and the overall design of the mathematics, systems and algorithms development were also initiated. The prototype design of the FSIS optical, mechanical, and electrical/digital system is complete. GRA

N91-26923# Department of the Navy, Washington, DC.
AN ULTRAVIOLET OPTICAL ISOLATOR UTILIZING THE KDP-ISOMORPHS Patent Application
James L. Dexter, inventor (to Navy), John F. Reintjes, inventor (to Navy), Joseph F. Landry, inventor (to Navy), and David G. Cooper, inventor (to Navy) 17 Oct. 1990 24 p
(AD-D014860; US-Patent-Appl-SN-597847) Avail: NTIS HC/MF A03 CSCL 14/2

This invention relates to optical isolators and particularly to an ultraviolet optical isolator which utilizes a KDP-isomorph for rotating the polarization of ultraviolet radiation in the wavelength range from about 190 to about 350 nanometers. Optical isolators using Faraday rotators have many uses in laser technology, such as for isolating stages of oscillator-amplifier systems and for discriminating against reverse-traveling waves in ring cavities. A Faraday rotator is a device that rotates the angle of polarization of light by using the Faraday effect. The Faraday effect is a magneto-optic effect wherein a magnetic field applied to a Faraday material causes the axis of polarization of the linearly polarized light to rotate. GRA

N91-26924# Department of the Navy, Washington, DC.
IMPROVED INLINE FIBER OPTIC SENSOR ARRAYS Patent Application
Aileen M. Yurek, inventor (to Navy), Anthony Dandridge, inventor (to Navy), and Alan D. Kersey, inventor (to Navy) 16 Jan. 1991 18 p
(AD-D014864; US-Patent-Appl-SN-641843) Avail: NTIS HC/MF A03 CSCL 17/5

An improved inline fiber optic sensor array is achieved by packaging a plurality of fiber optic sensor units such that each fiber optic sensor unit incorporates a complete functional sensor and adjacent fiber optic sensor units are separated by a delay element connected in series between each pair of fiber optic sensor units. Delay elements temporally separate measure and signals received from the individual fiber optic sensor units and permit decoupling of signals produced in response to environmental stress on the non-sensor unit portions of the array. GRA

N91-26925 Department of the Navy, Washington, DC.
DESIGN FOR ELECTRONIC SPECTRALLY TUNABLE INFRARED DETECTOR Patent
Tak-Kin Chu, inventor (to Navy) 26 Feb. 1991 9 p Filed 4 Feb. 83
(AD-D014877; US-Patent-4,996,579; US-Patent-Appl-SN-464100; US-Patent-Class-357-30) Avail: US Patent and Trademark Office CSCL 17/5

The invention is a single element infrared detector consisting of multiple layers of successive epilayers of lead chalcogenides or their alloys with tin or cadmium to form two or more adjacent contiguous surfaces whereupon each surface is deposited with an ohmic contact. The multiple adjacent semiconductor surfaces are also each fitted or equipped with an non-ohmic contact that yields novel applications in term of broad band and narrow scanning. This is particularly the case when the epilayers are geometrically arranged to selectively allow the transmission of radiation to yield both broad band and narrow band responses concurrently so as to obtain a separate electrical signal from each adjacent contiguous semiconducting epilayer surface. GRA

N91-26926# Institute of Electrical and Electronics Engineers, New York, NY.
THE FIRST NONLINEAR OPTICS: MATERIALS, PHENOMENA, AND DEVICES CONFERENCE Final Report, 1 Apr. - 31 Dec. 1990
Robert T. Wangemann, Hyatt M. Gibbs, Juan F. Lam, Duncan G. Steel, and Pochi Yeh 13 Mar. 1991 363 p Conference held in Kauai, HI, 16-20 Jul. 1990
(Grant AF-AFOSR-0197-90; AF Proj. 2301)
(AD-A234733; AFOSR-91-0273TR) Avail: NTIS HC/MF A16 CSCL 20/6

Papers presented at the first International Meeting on Nonlinear Optics are compiled. The following subject areas are covered: fundamental phenomena, laser spectroscopy, liquid crystals, organics, fibers, waveguides/couplers, phase conjugation, applications of nonlinear semiconductor, photorefractives, semiconductors, organic NLO and devices, photorefractive applications, and semiconductor lasers and interfaces. GRA

N91-26927# Syracuse Univ., NY. Dept. of Chemistry.
DESIGN AND CONSTRUCTION OF APPARATUS FOR OPTICAL SWITCH EVALUATION Final Technical Report, May 1989 - Jun. 1990
Joseph Chaiken Dec. 1990 27 p
(Contract F30602-88-D-0027)
(AD-A234765; RADC-TR-90-417) Avail: NTIS HC/MF A03 CSCL 20/6

The goal of this effort was to develop apparatus for evaluation of optical switches relevant to digital optical computing. We state the basic aspects of optical switch evaluation (OSE) and describe appropriate general apparatus and procedures we have developed, which retains adequate flexibility to accommodate a wide variety of switches. We anticipated that such flexibility would be essential because existing switches, and ones under development, have widely varying characteristics. Our concept of the general characteristics of OSE has led us to develop an apparatus which will allow us to evaluate such switches. This report first describes the general concepts of optical switch evaluation together with the characteristics of an apparatus appropriate to implementing discrete components of such an apparatus, and progress in switch development. GRA

N91-26928# Air Force Inst. of Tech., Wright-Patterson AFB, OH. Foreign Technology Div.
OPTICAL METHODS OF MEASURING THE ROUGHNESS OF THE SURFACES OF HIGH PRECISION STEEL BALLS
Shen Yan and E. Zhang 21 Mar. 1991 12 p Transl. into ENGLISH from Jiliang Jishu (China), v. 10, no. 182, 1989 p 13-15
(AD-A234796; FTD-ID(RS)T-1272-90) Avail: NTIS HC/MF A03 CSCL 11/6

This article introduces a type of lens reflection section which makes use of laser light in connection with rough surface scattering to carry out methods for measuring the degree of roughness of high precision ball surfaces. The principles in this type of method are reliable. The design of the instruments is simple. Production costs are low. The environmental requirements are not high. Along with this, it is possible, on the presuposition that light path adjustments are not carried out, to carry out measurements on steel balls with different radii. It is suitable for checks at the production site. On the basis of the theory of light scattering, when a one beam unit strength straight laser beam is fired into a rough surface, the scattered light scatters into space toward various individual directions. GRA

N91-26929# University of Southern California, Los Angeles.
STUDIES OF OPTICAL BEAM PHASE-CONJUGATION AND ELECTROMAGNETIC SCATTERING PROCESS Final Technical Report, 1 Dec. 1987 - 30 Nov. 1990
Robert W. Hellwarth 6 Mar. 1991 23 p
(Contract F49620-88-C-0027)
(AD-A234830; AFOSR-91-0231TR) Avail: NTIS HC/MF A03 CSCL 20/6

This project performed both experimental and theoretical studies of optical beam phase-conjugation and of electromagnetic scattering and propagation with intense optical fields. We have: (1) made the first determination of the nonlinear optical index of air and of common gases throughout the visible spectrum; (2) established the threshold beam intensities required to produce nonlinear effects in plasma; (3) measured the linear and nonlinear refractive indices of many new optical polymers; (4) made the first measurements of the fidelity of optical beam phase conjugation in photorefractive materials; (5) built a cellular automaton to simulate optical computation; (6) made comparative optical measurements characterizing photorefractive crystals; (7) made comparative photoconductivity measurements on various insulating crystals; (8) studied anomalous acoustic damping in polymers and crystals by picosecond optical techniques; and (9) verified the existence of predicted resonant two-photon absorption in Cr-pthalocyanine molecules. GRA

N91-26930# Naval Ocean Systems Center, San Diego, CA.
THICKNESS MEASUREMENTS OF SILICON FILMS USING PARTIAL COHERENCE INTERFEROMETRY Final Technical Report, Oct. 1988 - Sep. 1989
M. N. McLandrich and D. J. Albares Feb. 1991 28 p
(AD-A235211; NOSC-TR-1372) Avail: NTIS HC/MF A03 CSCL 20/6

An optical system composed of a Michelson interferometer, a short coherence length edge-emitting diode (ELED), and a fiber-optic-coupler probe has been described and used to measure the thickness of thin silicon charge-coupled device (CCD) films. The measurement precision for samples with a thickness of the order of 10 micrometers is better than 0.1 micrometers and the range of thickness that can be measured can be from a few micrometers to hundreds of micrometers if a suitable source is used. The fiber probe assembly is adaptable for remote in situ measurements of samples within an etching chamber, and the measurement results can be used to control the sample etching process. The fiber probe also allows for localized measurements at selected positions across the area of the sample, and these results can be used for control of thickness uniformity. GRA

N91-26931# University of Southern California, Los Angeles. Dept. of Electrical Engineering and Electrophysics.
CENTER FOR THE INTEGRATION OF OPTICAL C Annual Technical Report, 15 Feb. 1990 - 14 Feb. 1991
Alexander A. Sawchuk and W. H. Steier 15 Mar. 1991 55 p
(Grant AF-AFOSR-0133-90; AF Proj. 3484)
(AD-A235277) Avail: NTIS HC/MF A04 CSCL 09/5

Topics reviewed include: Optical interconnections, Lenslet array processors, Generalizable neural networks, Spatial light modulators, MBE growth of Quantum well structures, Ultralow threshold laser arrays, Charge transport optical nonlinearities, Neural computation of vision algorithms, Wave mixing at the band edge in III-V semiconductors, and Photorefractive optical interconnections. GRA

N91-26932# University of Southern California, Los Angeles. Signal and Image Processing Inst.
RESEARCH INSTRUMENTATION FOR OPTICAL COMPUTING Final Report, 1 Dec. 1988 - 30 Jun. 1990
Alexander A. Sawchuk 30 Jun. 1990 19 p

(Grant AF-AFOSR-0175-89; AF Proj. 3482)
(AD-A235335; AFOSR-91-0199TR) Avail: NTIS HC/MF A03 CSCL 09/5

During the period 1 December 88 to 30 June 90 several pieces of equipment which are key to the continued research on optical computing at USC were purchased under Grant AFOSR-89-0175. These include: E-beam deposition system; Argon ion laser; Liquid crystal spatial light modulator; CCD video camera; and Digital optical power meter. This instrumentation has led a wide impact on the research in optical computing which is funded by several government agencies. GRA

N91-26933# Massachusetts Inst. of Tech., Lexington. Lincoln Lab.
BINARY OPTICS TECHNOLOGY: THEORETICAL LIMITS ON THE DIFFRACTION EFFICIENCY OF MULTILEVEL DIFFRACTIVE OPTICAL ELEMENTS
Gary J. Swanson 1 Mar. 1991 32 p
(Contract F19628-90-C-0002)
(AD-A235404; TR-914; ESD-TR-90-188) Avail: NTIS HC/MF A03 CSCL 20/6

Diffractive optical elements are being considered as potential solutions to a number of optical design problems that are difficult or impossible to solve with conventional refractive and reflective elements. Two unique characteristics of diffractive elements can be exploited; the first is the dispersion property. Diffractive structures bend light rays of longer wavelengths more than those of shorter wavelengths, which is the reverse of refractive materials; therefore, diffractive structures minimize or eliminate the dispersive effects of refractive materials. The second unique characteristic is the relative ease with which arbitrary phase profiles can be implemented. Advances in both diamond turning technology and the use of semiconductor fabrication equipment have made possible the construction of a variety of diffractive elements. Diamond turning technology allows fabricating diffractive surfaces over large areas in a relatively short period of time. However, there are limitations: the phase profile has to be circularly symmetric, and the accuracy with which a diffractive profile can be made is dependent on the tip size of the diamond turning tool. Using semiconductor fabrication equipment to make diffractive elements has become a powerful technique. This particular approach produces a stepped approximation, referred to as a multilevel structure, to the ideal profile. GRA

N91-26934# Geltech, Inc., Alachua, FL.
TRANSPIRATION COOLED ULTRAVIOLET SOL-GEL SILICA OPTICS Final Report, 15 Aug. 1990 - 15 Mar. 1991
Vinay K. Seth and Jean-Luc Noques 1 Apr. 1991 94 p
(Contract F49620-90-C-0055)
(AD-A235426; AFOSR-91-0495TR) Avail: NTIS HC/MF A05 CSCL 19/7

All rocket guidance systems essentially require broadband optical transmission windows. These windows must also be temperature insensitive to transmission, thermal shock resistant, thermally stable, reasonably strong, and impact resistant. At hypersonic velocity, convective cooling is preferred to radiative cooling. Transpiration cooling is a novel and effective mode of convective cooling. Porous silica windows offer excellent rocket windows for transpiration cooling at a relatively inexpensive price. Sol-gel technology is an enabling technology which facilitates the fabrication of these rocket windows. This research used sol-gel technology to demonstrate the concept of transpiration-cooled porous silica windows. These windows were fabricated with various pore sizes and characterized with respect to gas diffusion, transpiration, high temperature transmission, thermal stability and shock resistance, hardness, impact resistance, and strength. The manufacturability aspect was also addressed. The diffusion of various gases through porous silica windows was studied and their permeabilities measured. In the experimental range, Knusden diffusion seemed to be the predominant mass transport mechanism. At a low transpiration velocity of 0.52 cm/s of helium, a 44 C temperature drop was observed showing the promise of this material for rocket window application. High temperature spectroscopy showed improved performance. The porous silica windows had thermal stability and thermal shock resistance and reasonable mechanical properties. GRA

N91-26935 Tel-Aviv Univ. (Israel). Dept. of Interdisciplinary Studies.
TEMPORAL AND SPATIAL CORRELATIONS IN IMAGES DISTORTED BY A RANDOM MEDIUM M.S. Thesis
Michael Wasserstein Sep. 1989 81 p In HEBREW; ENGLISH summary
(ITN-91-85107) Copyright Avail: Tel-Aviv Univ., Exact Sciences Library, Ramat Aviv 69978, Israel

Following the suggestion that there is always a finite chance to obtain near-diffraction-limited resolution over a small field of view, in a series of exposures through a turbulent atmosphere, this work involved the study of temporal and spatial correlations in short-exposure images. The images were made through a laboratory-simulated random medium and studied as a function of the imaging aperture and the strength of the refractive index fluctuations. A 1.5x1.0x0.6-m simulation tank was filled with demineralized water and subjected to an unstable vertical temperature gradient. The object was a narrow vertical slit, viewed via the tank by a TV camera coupled to a video recorder. The heat supply to the tank was varied between 0.4 W and 4.6 kW, and the aperture of the viewing lens ranged from 2.5-109 mm. By digitizing one horizontal cut across the image, from each successive frame, the temporal correlations of the slit-width fluctuations were calculated as functions of the turbulence strength and the aperture diameter. The results indicate that, for a given turbulence strength, the correlation increases with increasing aperture. The averaging action of a large aperture serves to smooth fast variations between consecutive frames. Once the conditions to obtain a sufficiently narrow cut had been established, it was very important to assess the height of the region around the cut whose width remained narrow, i.e., the size of the isoplanatic patch had to be determined. This was achieved by studying the vertical width correlation in fully digitized frames. ISA

N91-26936# Sandia National Labs., Albuquerque, NM.
AUTOMATIC TARGET RECOGNITION USING ACOUSTO-OPTIC IMAGE CORRELATOR
P. A. Molley and B. A. Kast 1991 9 p Presented at the SPIE International Symposium on Optical Engineering and Photonics in Aerospace Sensing, Orlando, 1-5 Apr. 1991
(Contract DE-AC04-76DP-00789)
(DE91-011499; SAND-90-2331C; CONF-910450-8) Avail: NTIS HC/MF A02

A hybrid electro-optic image processor was developed for automatic target recognition using an acousto-optic correlator and digital electronics. The optical system performs the computationally intensive correlation operation on the large 2-D input scenes. The electronics provide the decision making capability and also performs part of the normalization needed for increasing the peak-to-sidelobe ratio in cluttered scenes. The system is able to analyze each correlation plane and apply a real time template selection algorithm to accommodate scale or rotation changes of the target. A demonstration of the current system capabilities is presented using a terrain board with several different types of stationary and moving model vehicles. DOE

N91-27115*# Stevens Inst. of Tech., Hoboken, NJ. Dept. of Electrical Engineering and Computer Science.
HIGH ACCURACY OPTICAL RATE SENSOR Final Report
J. Uhde-Lacovara *In* Houston Univ., NASA/ASEE Summer Faculty Fellowship Program, 1990, Volume 2 Dec. 1990 13 p (For primary document see N91-27103 18-99)
(Grant NGT-44-005-803)
Avail: NTIS HC/MF A09 CSCL 20F

75 PLASMA PHYSICS

Includes magnetohydrodynamics and plasma fusion.

For ionospheric plasmas see *46 Geophysics*. For space plasmas see *90 Astrophysics*.

N91-26937# National Inst. for Fusion Science, Nagoya (Japan).
DESIGN AND FABRICATION OF FORCED-FLOW COILS AS AN R/D PROGRAM FOR LARGE HELICAL DEVICE
K. Takahata, N. Yanagi, T. Mito, O. Motojima, J. Yamamoto, K. Nakamoto, S. Mizukami, K. Kitamura, Y. Wachi, and H. Shinohara (Toshiba Corp., Yokohama, Japan) et al Mar. 1991 16 p
(NIFS-81; ISSN-0915-633X) Avail: NTIS HC/MF A03

As research and development of helical field coil and poloidal field coil for large helical device (LHD), two forced-flow cooled NbTi superconducting coils (TOKI-TF, PF) were designed and fabricated. The helical coil (TOKI-TF) is a 1/4 scale model of LHD. It has the major radius of 0.9 m, the minor radius of 0.25 m and pitch number of 4. Nominal current and maximum field were designed to be 8 kA and 2.8 T, respectively. Another coil (TOKI-PF) was fabricated for the demonstration of LHD poloidal field coils. It consists of two double-pancakes with the inner radius of 0.6 m and the outer radius of 0.82 m. Nominal current of 25 kA simulates that of LHD poloidal field coils. Cable-in-conduit type conductors were used for both coils. The test facility was also constructed with a vacuum vessel, liquid nitrogen shield, 30 kA power leads, a heat exchanger, cryogenic supports, and others. In this paper, design concepts and details are presented. Author

N91-26938# General Atomic Co., San Diego, CA.
COMPARISON OF DIMENSIONALLY SIMILAR DISCHARGES WITH SIMILAR HEAT DEPOSITION DISCHARGES
J. C. DeBoo, R. E. Waltz, and T. Osborne Apr. 1991 7 p Presented at the 18th European Conference on Controlled Fusion and Plasma Physics, Berlin, Federal Rep. of Germany, 3-7 Jun. 1991
(Contract DE-AC03-89ER-51114)
(DE91-011740; GA-A-20466; CONF-910609-13) Avail: NTIS HC/MF A02

Dimensionally similar scaling is a technique to scale existing tokamak discharges to larger size, A, or larger magnetic field, B, by fixing dimensionless parameters such as the plasma beta and collisionality as well as safety factor q, elongation, and aspect ratio while varying the normalized gyroradius, rho(sub *) = rho/alpha. Diffusion mechanisms can be classified by their dependence on rho(sub *). The confinement time scales as tau proportional to omega(sup -1) rho(sub *)(sup -3) proportional to Ba(sup 5/2) or gyroBohm-like mechanisms or tau proportional to omega(sup -1) rho(sub *)(sup -2) proportional to B(sup 1/3)a(sup 5/3) for Bohm-like mechanisms. Establishing that either mechanism dominates transport allows one to predict performance for next generation devices with reasonable confidence without knowledge of the complex and likely coupled transport mechanisms governing confinement. Statistical studies of global confinement time have consistently shown that the standard L-mode scaling is close to or worse than Bohm-like whereas the majority of theories suggest a gyroBohm-like local diffusion process. During the past year, experiments to resolve this difference were performed on DIII-D and subsequently on TFTR. The results of these experiments are discussed. DOE

N91-26939# General Atomic Co., San Diego, CA.
STATISTICAL PROPERTIES OF INTRINSIC TOPOLOGICAL NOISE IN TOKAMAKS
T. E. Evans Apr. 1991 7 p Presented at the 18th European Conference on Controlled Fusion and Plasma Physics, Berlin, Federal Rep. of Germany, 3-7 Jun. 1991
(Contract DE-AC03-89ER-51114)
(DE91-011741; GA-A-20448; CONF-910609-14) Avail: NTIS HC/MF A02

The analysis presented in this paper is based on a model which generally predicts the existence of stationary intrinsic magnetic islands and stochasticity in all toroidal confinement devices. In tokamaks, these intrinsic islands could be responsible for MHD mode locking and may provide a unifying link between a broad number of standard but poorly understood discharge phenomenology. In addition, the intrinsic island model is generally in agreement with the critical temperature gradient idea of anomalous electron heat transport and may provide a simple physical mechanism for the production of ergodicity in the anomalous zone. Intrinsic islands were first observed during resonant helical divertor experiments and are thought to be responsible for discharge asymmetries which modify the spatial energy loading distributions on the target plates of poloidally diverted tokamaks. These observations imply that delta b(sub r) contributions due to random toroidal field (TF) coil positions dominate S(sub tn). In general, each TF coil has seven degrees of freedom, including shape variations, which are subject to random perturbations. Nevertheless, a restricted (single degree of freedom (sdf)) analysis, in which small random perturbations delta R(sub o,j) are applied to the axial positions of all j = 1, 2, ..., N(sub TF) TF coils, is of interest for establishing the basic statistical properties of S(sub tn) and for demonstrating its overall sensitivity to small perturbations. The object of this paper is to estimate statistical upper limit bounds on the spectral amplitudes of n = 1 (m less than or equal to 5) topological noise components with sdf TF coil perturbations and a set of generalized structural parameters which are easily modified to fit most currently operating or future ignition scale tokamaks. Plasma effects are not included in this stage of the analysis. DOE

N91-26940# Brandeis Univ., Waltham, MA. Dept. of Chemistry.
THE CHEMICAL MODIFICATION OF PLASMAS Final Report, Dec. 1988 - Sep. 1989
Michael Henchman Dec. 1990 65 p
(Contract F30602-88-D-0025)
(AD-A234448; RADC-TR-90-342) Avail: NTIS HC/MF A04
CSCL 20/9

This report presents results of a study to analyze available data on electron affinities, and thermochemical properties of species of interest in the chemical modification of plasmas. Using these data, together with related information on chemical and physical properties, candidate species are identified for tests on modification of free electron densities in plasmas. GRA

N91-26941# Phillips Lab., Edwards AFB, CA.
PARAMETRIC STUDIES OF DENSE PLASMA FOCUS FOR FUSION SPACE PROPULSION WITH D-He3 Special Report, May - Aug. 1990
C. L. Leakeas Mar. 1991 50 p
(AF Proj. 3058)
(AD-A234578; PL-TR-91-3014) Avail: NTIS HC/MF A03
CSCL 21/6

A coaxial electrode system known as the dense plasma focus (DPF) is investigated as a possible space propulsion concept. A large potential difference between the electrodes ionizes the gaseous fusion fuel and forms an annular plasma sheath. This sheath then propagates down the length of the anode entraining additional fuel along the way. The rundown phase is analyzed by solving the momentum equation using this snowplow model. At the end of the anode, MHD instabilities cause the sheath to collapse into a hot, high density plasma where fusion events occur. Fusion reaction products as well as unreacted fuel can then be used to produce thrust. It is also possible to use the reaction products to heat hydrogen propellant in order to produce more thrust. An open-ended coolant cycle may be used in order to avoid the necessity for large radiators. In this way, the heated coolant can be used to drive a turbogenerator to produce electricity before it is exhausted as propellant. A model of the DPF is developed, various operating regimes are identified, and key parameters varied to define optimum operating ranges. Computations were made with the FORTRAN code found in the appendix. Operation with no hydrogen propellant allows high specific impulse values, about 1 million s, possible at thrusts of about 44.5 N (10 lbf). High specific impulse make larger mission V's possible and can decrease trip time and reduce exposure of astronauts to cosmic radiation. GRA

N91-26942# Varian Associates, Palo Alto, CA. Microwave Power Tube Products.
DEVELOPMENT OF A TACTICAL HIGH-POWER MICROWAVE SOURCE USING THE PLASMA ELECTRON MICROWAVE SOURCE (PEMS) CONCEPT Final Report, 1 Aug. 1988 - 30 Sep. 1990
R. A. Dandl, G. E. Guest, and H. R. Jory Dec. 1990 63 p Prepared in cooperation with Applied Microwave Plasma Concepts, Carlsbad, CA
(Contract F49620-88-C-0102)
(AD-A234967; AFOSR-91-0240TR) Avail: NTIS HC/MF A04 CSCL 20/15

The AMPHED facility was used to perform feasibility experiments to explore the generation of high-power microwave pulses from energy stored in a magnetic mirror plasma. The facility uses an open-ended magnetic mirror driven by pulsed or cw c- and x-band sources. Microwave horns were constructed to couple in the frequency range of 2.4 to 4 GHz to whistler waves in the plasma. Spontaneous bursts of microwave radiation in the range of 3 to 5 GHz were observed in the experiments. But the power levels were lower than expected for the whistler wave interaction. It is probable that the hot-electron energy densities achieved were not high enough to approach the threshold of the desired interaction.
GRA

N91-26943# Lawrence Livermore National Lab., CA.
PLANAR INDIRECT-DRIVE RAYLEIGH-TAYLOR EXPERIMENTS ON NOVA
B. A. Remington, S. W. Hann, S. G. Glendinning, J. D. Kilkenny, and R. J. Wallace Apr. 1991 32 p Presented at the 21st Annual Anomalous Absorption Conference, Banff (Canada), 15-19 Apr. 1991
(Contract W-7405-eng-48)
(DE91-011967; UCRL-JC-106652; CONF-9104241-1) Avail: NTIS HC/MF A03

A critical issue for laser-driven fusion is the extent to which surface perturbations grow during acceleration in high-gain implosion designs. To address this issue, an experimental and theoretical effort was initiated at the Nova Laser Facility to study perturbation growth due to the Rayleigh-Taylor instability on planar foils accelerated radiatively by a shaped drive. The growth of single-mode sinusoidal perturbations was measured in a set of experiments that varied separately the perturbation amplitude, wavelength, and foil thickness. To investigate mode coupling, foils were accelerated with two modes (wavelengths lambda(sub 1,2) = 50 micron, 75 micron) superposed on the surface. As a first attempt at determining the effect of a broad spectrum of modes, foils were recently accelerated whose surface perturbation is the superposition of eight modes (lambda(sub 1-8) = 22.5 to 180 micron) with random amplitudes. The experimental results and comparisons with 2-dimensional computer simulations will be presented.
DOE

N91-26944*# Texas Univ., Austin. Dept. of Electrical and Computer Engineering.
NEAR FIELD INTERACTION OF MICROWAVE SIGNALS WITH A BOUNDED PLASMA PLUME Final Report, 20 Jan. 1989 - 19 Jan. 1991
Hao Ling, Gary A. Hallock, Hyeongdong Kim, and Bjorn Birkner Jan. 1991 134 p
(Contract NCC3-127)
(NASA-CR-185358; NAS 1.26:185358) Avail: NTIS HC/MF A07 CSCL 20I

The objective was to study the effect of the arcjet thruster plume on the performance of an onboard satellite reflector antenna. A project summary is presented along with sections on plasma and electromagnetic modeling. The plasma modeling section includes the following topics: wave propagation; plasma analysis; plume electron density model; and the proposed experimental program. The section on electromagnetic modeling includes new developments in ray modeling and the validation of three dimensional ray results.
K.S.

N91-26945# Pittsburgh Energy Technology Center, PA.
MHD CONTRACTORS' REVIEW MEETING
1991 314 p Presented at the Magnetohydrodynamic (MHD) Contractors Review Meeting, Pittsburgh, 19-21 Feb. 1991
(DE91-011295; CONF-9102112-Absts) Avail: NTIS HC/MF A14

The following research programs on magnetohydrodynamic conversion were described at the contractors' review meeting: MHD integrated topping cycle project; Activity summary for DOE's component development and integration facility; MHD bottoming cycle component testing at the coal fired flow facility; MHD heat recovery seed recovery system development; Diagnostic development and support of MHD test facilities; Heat and seed recovery technology project; TRW Econoseed process for MHD seed recovery and regeneration; and MIT magnet. Papers describe the objectives, the work to date, and results obtained. Papers have been processed separately for inclusion on the data base.
DOE

N91-26946# Argonne National Lab., IL.
MULTI-DIMENSIONAL COMPUTER SIMULATION OF MHD COMBUSTOR HYDRODYNAMICS
G. F. Berry, S. L. Chang, S. A. Lottes, and W. A. Rimkus Apr. 1991 15 p Presented at the 10th AIAA Computational Fluid Dynamics Conference in Conjunction with the 22nd AIAA Fluid Dynamics, Plasma Dynamics, and Lasers Conference and the 26th AIIA Thermophysics Conference, Honolulu, 24-26 Jun. 1991
(Contract W-31-109-eng-38)
(DE91-011851; ANL/CP-72897; CONF-910651-8) Avail: NTIS HC/MF A03

Argonne National Laboratory is investigating the nonreacting jet gas mixing patterns in an MHD second stage combustor by using a 2-D multiphase hydrodynamics computer program and a 3-D single phase hydrodynamics computer program. The computer simulations are intended to enhance the understanding of flow and mixing patterns in the combustor, which in turn may lead to improvement of the downstream MHD channel performance. A 2-D steady state computer model, based on mass and momentum conservation laws for multiple gas species, is used to simulate the hydrodynamics of the combustor in which a jet of oxidizer is injected into an unconfined cross stream gas flow. A 3-D code is used to examine the effects of the side walls and the distributed jet flows on the non-reacting jet gas mixing patterns. The code solves the conservation equations of mass, momentum, and energy, and a transport equation of a turbulence parameter and allows permeable surfaces to be specified for any computational cell.
DOE

N91-26947# Lawrence Livermore National Lab., CA.
HYLIFE-2 INERTIAL CONFINEMENT: FUSION POWER PLANT DESIGN
R. W. Moir 14 Dec. 1990 26 p Presented at the International Symposium on Heavy Ion Inertial Fusion, Monterey, 3-6 Dec. 1990
(Contract W-7405-eng-48)
(DE91-012089; UCRL-JC-105102; CONF-901219-14) Avail: NTIS HC/MF A03

The HYLIFE-2 inertial fusion power plant design study uses a liquid fall, in the form of jets to protect the first structural wall from neutron damage, x rays, and blast to provide a 30-y lifetime. HYLIFE-1 used liquid lithium. HYLIFE 2 avoids the fire hazard of lithium by using a molten salt composed of fluorine, lithium, and beryllium (Li2BeF4) called Flibe. Access for heavy-ion beams is provided. Calculations for assumed heavy-ion beam performance show a nominal gain of 70 at 5 MJ producing 350 MJ, about 5.2 times less yield than the 1.8 GJ from a driver energy of 4.5 MJ with gain of 400 for HYLIFE-1. The nominal 1 GWe of power can be maintained by increasing the repetition rate by a factor of about 5.2, from 1.5 to 8 Hz. A higher repetition rate requires faster re-establishment of the jets after a shot, which can be accomplished in part by decreasing the jet fall height and increasing the jet flow velocity. Multiple chambers may be required. In addition, although not considered for HYLIFE-1, there is undoubtedly liquid splash that must be forcibly cleared because gravity is too slow,

especially at high repetition rates. Splash removal can be accomplished by either pulsed or oscillating jet flows. The cost of electricity is estimated to be 0.09 $/kW x h in constant 1988 dollars, about twice that of future coal and light water reactor nuclear power. The driver beam cost is about one-half the total cost. DOE

76 SOLID-STATE PHYSICS

Includes superconductivity.

For related information, see also *33 Electronics and Electrical Engineering* and *36 Lasers and Masers.*

N91-26948*# Clemson Univ., SC. Dept. of Ceramic Engineering.
DEVELOPMENT OF HIGH Tc (GREATER THAN 110K) Bi, Tl AND Y-BASED MATERIALS AS SUPERCONDUCTING CIRCUIT ELEMENTS Annual Report, 7 Mar. 1990 - 21 Feb. 1991
Gene H. Haertling, Burtrand Lee, Gregory Grabert, and Phillip Gilmour 28 Jun. 1991 110 p
(Grant NAG1-1108)
(NASA-CR-188581; NAS 1.26:188581) Avail: NTIS HC/MF A06 CSCL 20L

This report is presented in two parts. Part 1 deals primarily with Bi-based materials and a small amount of work on a Y-based composition while Part 2 covers work on Tl-based materials. In Part 1, a reliable and reproducible process for producing bulk bismuth-based superconductors has been developed. It is noted however, that a percentage of the tapecast material experiences curling and fracturing after a 30 hour sintering period and is thus in need of further examination. The Bi-Sr-Ca-Cu-O (BSCCO) material has been characterized by critical temperature data, X-ray diffraction data, and surface morphology. In the case of T sub c, it is not critical to anneal the material. It appears that the BSCCO material has the possibility of producing a better grounding strap than that of the 123 material. Attempts to reproduce near room temperature superconductors in the Y-Ba-Cu-O system were unsuccessful. In Part 2, several methods of processing the high temperature superconductor Tl2Ba2Ca2Cu3O10 were investigated; i.e., different precursor compositions were sintered at various sintering times and temperatures. The highest superconductig temperature was found to be 117.8K when fired at 900 C for three hours. Higher sintering temperatures produced a melted sample which was nonsuperconducting at liquid nitrogen temperature. Also, a preliminary study found Li2O substitutions for copper appeared to increase the transition temperature and create fluxing action upon sintering. It was suggested that lower sintering temperatures might be obtained with lithium additions to produce reliable Tl2Ba2Ca2Cu3O10 processing methods. L.K.S.

N91-26949# Duke Univ., Durham, NC. Dept. of Chemistry.
PREPARATION OF A NOVEL GALLIUM ARSENIDE SINGLE-SOURCE PRECURSOR HAVING THE EMPIRICAL FORMULA AsCl3Ga2
R. L. Wells, R. B. Hallock, A. T. McPhail, Colin G. Pitt, and J. D. Johansen 27 Mar. 1991 8 p
(Contract N00014-89-J-1545)
(AD-A233704; DU/DC/TR-19) Avail: NTIS HC/MF A02 CSCL 07/2

Properly sized clusters/crystallites of the semiconductor gallium arsenide (GaAs) are expected to exhibit a range of interesting and useful properties, among them being superior nonlinear optical qualities. The reaction of GaCl3 and (Me3Si)3As in a 2:1 mole ratio at room temperature to yield a moderately stable yellow substance, empirical formula AsCl3Ga2, is discussed. When heated, this new single-source precursor eliminates GaCl3 to give microcrystalline gallium arsenide. GRA

N91-26950# Naval Ocean Systems Center, San Diego, CA.
OHMIC CONTACTS TO SEMICONDUCTING DIAMOND Final Report, Oct. 1989 - Sep. 1990
James R. Zeidler, M. J. Taylor, Carl R. Zeisse, C. A. Hewett, and Paul R. DeLaHoussaye Oct. 1990 48 p
(AD-A234130; NOSC/TD-2055) Avail: NTIS HC/MF A03 CSCL 20/12

Work was carried out to improve the electron beam evaporation system in order to achieve better deposited films. The basic system is an ion pumped vacuum chamber, with a three-hearth, single-gun e-beam evaporator. Four improvements were made to the system. The system was thoroughly cleaned and new ion pump elements, an e-gun beam adjust unit, and a more accurate crystal monitor were installed. The system now has a base pressure of 3 X 10(exp -9) Torr, and can easily deposit high-melting-temperature metals such as Ta with an accurately controlled thickness. Improved shadow masks were also fabricated for better alignment and control of corner contacts for electrical transport measurements. Appendices include: A Thermally Activated Solid State Reaction Process for Fabricating Ohmic Contacts to Semiconducting Diamond; Tantalum Ohmic Contacts to Diamond by a Solid State Reaction Process; Metallization of Semiconducting Diamond: Mo, Mo/Au, and Mo/Ni/Au; Specific Contact Resistance Measurements of Ohmic Contracts to Diamond; and Electrical Activation of Boron Implanted into Diamond. GRA

N91-26951# North Carolina Univ., Chapel Hill. Dept. of Chemistry.
STRONG EXCHANGE COUPLING IN LANTHANIDE BIS(PHTHALOCYANINATO) SANDWICH COMPOUNDS
Kathleen L. Trojan, William E. Hatfield, Keith D. Kepler, and Martin L. Kirk 29 Mar. 1991 16 p
(Contract N00014-89-J-1734)
(AD-A234466) Avail: NTIS HC/MF A03 CSCL 07/2

Bis (phthalocyaninato) lanthanide sandwich compounds, which have the formula Pc2-LnPc1-, have been synthesized for Ln = terbium, homium and lutecium. Low temperature magnetic susceptibility data for Ho (Pc)2 and Tb (Pc)2 show a reduction in moment from that which is expected for the lanthanide free ion value, which correlates with an antiferromagnetic exchange between the lanthanide f-electrons and the phthalocyaninato ligand radical electron. The g-factors determined from least squares fitting of the Curie-Weiss Law to the magnetic data show excellent agreement to the g-factors calculated for the strongly coupled state. Magnetic moments calculated from the experimentally determined Curie constants are also in good agreement with those expected for the strongly coupled state. GRA

N91-26952# State Univ. of New York, Stony Brook. Dept. of Physics.
STUDY OF JOSEPHSON EFFECT ARRAYS AS SOURCES AT 1 THz Final Report, Aug. 1986 - Jan. 1990
James Lukens Oct. 1990 62 p
(Contract F19628-86-K-0039)
(AD-A234526; RADC-TR-90-220) Avail: NTIS HC/MF A04 CSCL 20/10

Techniques have been developed and tested for coupling 40 junction arrays of Josephson effect oscillators to achieve coherent operation in the submillimeter wave range. Arrays have been fabricated using both lead alloy and niobium trilayer technology. Coherent operation has been demonstrated between 150 and 500 GHz. The maximum power was developed at 400 GHz where 7 microwatts was delivered to a 20 Ohm on-chip load. GRA

N91-26953# General Atomic Co., San Diego, CA.
HIGH-TEMPERATURE CERAMIC SUPERCONDUCTORS Report, 1 Oct. 1990 - 31 Mar. 1991
K. S. Mazdiyasni, K. C. Chen, M. B. Maple, L. Paulius, and P. K. Tsai Mar. 1991 24 p
(Contract N00014-88-C-0714)
(AD-A234620; GA-C19466) Avail: NTIS HC/MF A03 CSCL 11/2

The principal objectives of this program are (1) to demonstrate fabrication of high-temperature ceramic superconductors that can operate at or above 90 K with appropriate current density, Jc, in forms useful for application in resonant cavities, magnets, motors,

sensors, computers, and other devices; and (2) to fabricate and demonstrate selected components made of these materials, including microwave cavities and magnetic shields. GRA

N91-26954# Wisconsin Univ., Milwaukee. Dept. of Physics.
BULK WAVE CHARACTERIZATION OF HIGH T(SUB c) SUPERCONDUCTORS Final Report, 1 Apr. 1988 - 31 Dec. 1990
Moises Levy and Bimal Sarma 22 Apr. 1991 23 p Sponsored by ONR
(AD-A234649) Avail: NTIS HC/MF A03 CSCL 20/3

The objective of this research project were to characterize high Tc superconductors and heavy Fermion superconductors with longitudinal and transverse ultrasonic waves and with surface acoustic waves. Sound attenuation measurements in sintered and sinter forged Y1Ba2Cu3O7 exhibited three maxima which appear to be produced by relaxation processes with activation energies in the range of 450, 1100, and 650 K. The high activation energy is associated with the middle attenuation maximum which appears to be isotropic and is the only one present in another 123 isomorph Er1Ba2Cu3O7. This is the energy of the virtual excitations proposed in some theoretical models that is required for the appearance of high Tc superconductivity. Sound measurements in a Tl based superconducting compound exhibited a frequency independent maximum at the superconducting transition. This appears to be the first attenuation effect that is directly produced by the superconducting transition itself. Such a peak was also observed in Y1Ba2Cu3O7 after careful analysis of the data. These may be produced by interactions with superconducting fluctuations, enhanced by the two dimensional nature of the systems. GRA

N91-26955# Massachusetts Inst. of Tech., Cambridge. Materials Processing Center.
ELECTROCHEMICALLY MODULATED SUPERCONDUCTIVITY Final Report, 1 Nov. 1988 - 31 May 1990
Donald Sadoway 26 Feb. 1991 12 p
(Grant AF-AFOSR-0009-89; AF Proj. 2306)
(AD-A234703; AFOSR-91-0281TR) Avail: NTIS HC/MF A03 CSCL 20/3

The goal of the project is to test the feasibility of electrochemically modulated superconductivity in the cuprate superconductors. Such a test is possible because the new high temperature superconductors are ionic solids that are extremely sensitive to oxygen potential. Passive optimization of the latter is impossible, not only because of materials processing limitations but also due to thermodynamic and structural instabilities. Our approach is active intervention by electrochemical means, in other words, electrochemical polarization while the material is actually or potentially in the superconducting state. This is possible only by the use of electrolytes that are functional at cryogenic temperatures. Several years ago we discovered cryogenic electrolysis and demonstrated the existence of such electrolytes. Success in this effort would make possible a new class of electronic and photonic devices that exploit the capability to control actively the transition into and out of the superconducting state while the material is in service. GRA

N91-26956# National Inst. of Standards and Technology, Gaithersburg, MD.
TRANSMISSION ELECTRON MICROSCOPY OF THE CVD DIAMOND FILM/SUBSTRATE INTERFACE Interim Report
Dan Shechtman 15 Mar. 1991 28 p
(Contract N00014-90-F-0011)
(AD-A234790) Avail: NTIS HC/MF A03 CSCL 07/2

Progress has been made in understanding growth patterns of thin fine grain diamond CVD films. In the study which was performed by high resolution electron microscopy, attention was focused on the fault structure as a function of the position in the grain as well as on the formation of mismatch boundaries within the growing diamond crystal. These boundaries are formed due to mismatch between certain twins within the growing crystal. It was found that these boundaries can serve as precise indicators for the local growth direction of the crystal; thus, leading back to the nucleation point in a given TEM cross section. In an example, the local nucleation point is traced back to a 5-fold twin site. GRA

N91-26957# North Carolina State Univ., Raleigh.
SYMPOSIUM E: PROPERTIES OF 2-6 SEMICONDUCTORS. BULK CRYSTALS, EPITAXIAL FILMS, QUANTUM WELL STRUCTURES Final Report, 15 Nov. 1989 - 31 Oct. 1990
J. F. Schetzina 1 Mar. 1991 4 p
(Contract N00014-90-C-1278)
(AD-A234835) Avail: NTIS HC/MF A01 CSCL 20/12

The focus is on recent developments in II-VI semiconductors. The meeting covered a wide variety of topics including synthesis of II-VI materials (bulk crystals, thin films, and layered structures), properties studies (electrical, optical, photoelectric, structural, mechanical), defects (theory and measurement), controlled substitutional doping, and applications of II-VI semiconductors. The II-VI compound semiconductors possess characteristics which, as a group, are unique. Among the most active areas of investigation in these materials today are blue light emitters based on ZnSe, infrared detectors based on mercury-containing compounds such as HgCdTe, and the properties of dilute magnetic semiconductors. GRA

N91-26958# Massachusetts Inst. of Tech., Lexington.
SOLID STATE RESEARCH Quarterly Technical Report, 1 May - 31 Jul. 1990
Alan L. McWhorter 15 Aug. 1990 90 p
(Contract F19628-90-C-0002)
(AD-A234836; Rept-1990; Rept-3; ESD-TR-90-119) Avail: NTIS HC/MF A05 CSCL 20/3

This report covers in detail the research work of the Solid State Division at Lincoln Laboratory for the period May 1 though July 31, 1990. The topics covered include the following: (1) electrooptical devices; (2) quantum electronics; (3) materials research; (4) submicrometer technology; (5) microelectronics; and (6) analog device technology. GRA

N91-26959# Honeywell, Inc., Bloomington, MN. Sensor and System Development Center.
MONOLITHIC INTEGRATION SEMICONDUCTOR AND SUPERCONDUCTOR COMPONENTS Report, 1 Jan. - 31 Mar. 1991
Burgess Johnson 31 Mar. 1991 6 p
(Contract N00014-90-C-0226)
(AD-A234986) Avail: NTIS HC/MF A02 CSCL 20/3

The goal of the program is to develop transistor technology compatible with high transition temperature superconductor technology so that transistor pixel switches can be integrated with YBaCuO superconducting microbolometers in the same silicon substrate. A 4x4 matrix-addressable superconducting microbolometer array will be delivered at the completion of the program. GRA

N91-26960# Johns Hopkins Univ., Baltimore, MD. Dept. of Electrical and Computer Engineering.
MATERIAL ENGINEERING OF NOVEL SEMICONDUCTOR STRUCTURES Final Report, 1 Jun. 1989 - 30 Nov. 1990
J. Khurgin 30 Nov. 1990 21 p
(Grant AF-AFOSR-0379-89; AF Proj. 2305)
(AD-A235014; AFOSR-91-0396TR) Avail: NTIS HC/MF A03 CSCL 20/6

The first experiments were done in the visible region of the spectrum, using familiar nonlinear material ZnSe in order to acquire experience in nonlinear spectroscopy. Highly sensitive measurements of the spectrum of nonlinear refractive index of ZnSe were done using the method of self-bending. This method, has shown significant advantage over conventional Kramers-Kronig method. The results of the measurements were somewhat unexpected, since the nonlinear index of refraction, n2 measured by us turned out to be quite large (10 to the -8th power sq cm/W) and hard to explain using conventional wisdom of the thermally-induced bandgap shrinking. Therefore, we conducted an

additional set of measurements that gave the proof of the excitonic origin of the nonlinearity. After the near-infrared laser became fully operational, the main thrust was in the direction of investigation of nonlinear optical and electro-optical properties of the asymmetric coupled quantum wells (QW). Efforts to locate reliable sources of MBE-grown QW material had finally succeeded. First experiments on photoluminescence and photoconductivity spectroscopy of asymmetric coupled QW's started. The samples used had 25 coupled QW periods each consisting of two Al 0.357 Ga 0.65 As QW's, with thickness of 18A and 32A separated by 15A GaAs barrier. Thicker 100 A barriers separated the coupled QW's from each other. The entire undoped multiple QW structure was sandwiched between n and p Al 0.35 Ga 0.65 As layers. GRA

N91-26961# Massachusetts Inst. of Tech., Cambridge. Dept. of Materials Science and Engineering.
LUMINESCENCE AND LASING IN II-VI SEMICONDUCTORS Final Report, 11 Dec. 1987 - 31 Aug. 1990
August Witt 31 Aug. 1990 28 p
(Contract F49620-88-C-0035; ARPA Order 9520)
(AD-A235019; AFOSR-91-0388TR) Avail: NTIS HC/MF A03 CSCL 20/6

The objective of this contract was to develop a method for growth of bulk semiconducting material, suitable for monolithic infrared focal plane detectors, light emitting diodes, and laser structures. The project focused on narrow band gap HgMnTe alloys, semimagnetic semiconductors. HgMnTe is an infrared detector material with properties similar to those of HgCdTe in particular, HgMnTe electroluminescence more efficiently than HgCdTe, and p-type HgMnTe has higher conductivity than comparable p-HgCdTe; both features are advantageous in device applications. GRA

N91-26962# Hypress, Inc., Elmsford, NY.
SUPERCONDUCTING HIGH T(SUB c) THIN FILM VORTEX-FLOW TRANSISTOR, PHASE 1 Final Report, 1 Aug. 1990 - 31 Mar. 1991
G. K. Hohenwarter 28 Mar. 1991 29 p
(Contract F49620-90-C-0054)
(AD-A235025; AFOSR-91-0390TR-Phase-1) Avail: NTIS HC/MF A03 CSCL 20/3

A device is investigated based on vortex-flow in a superconducting thin-film. This transistor-like device is referred to as a superconducting flux-flow transistor (SFFT). Alongside step edge and grain boundary tunneling junctions the SFFT appears to be a promising candidate for active high temperature circuits. SFFT operation relies on the control of electrical characteristics at the output terminals by a magnetic field at the device boundaries. This field can be provided by the flow of a current in a control line; the device's input resistance hence will be very low. Substantial power grain can result. The low input resistance, yet moderate output resistant of the device appears beneficial for interfacing digital Josephson junction electronics with semiconductor circuits. This was proven in an experiment where Josephson junction was connected to a SFFT. GRA

N91-26963# State Univ. of New York, Buffalo. Dept. of Chemistry.
POLARON GROUND STATE IN A DOUBLE HETEROSTRUCTURE OF POLAR CRYSTALS
D. L. Lin, R. Chen, and Thomas F. George Apr. 1991 29 p
(Contract N00014-90-J-1193)
(AD-A235037; UBUFFALO/DC/91/TR-49) Avail: NTIS HC/MF A03 CSCL 20/12

The ground-state energy and effective mass of a polaron in the GaAs well of a GaAs/AlAs double heterostructure are calculated as functions of the well width. In considering electron-phonon interactions, both the confined LO were included as well as the interface phonon modes. The results differ qualitatively from what can be found in the literature, demonstrating the importance of interface modes as well as the confinement of LO modes. GRA

N91-26964# Case Western Reserve Univ., Cleveland, OH. Dept. of Macromolecular Science.
AN INDUCTION TIME APPROACH TO SURFACE INDUCED CRYSTALLIZATION IN POLYETHYLENE/POLY (E-CAPROLACTONE) MELT
Hatsuo Ishida and Philippe Bussi Mar. 1991 42 p
(Contract N00014-88-R-0330)
(AD-A235102; CWRU/DMS/TR-38) Avail: NTIS HC/MF A03 CSCL 07/6

The surface induced crystallization of poly (epsilon-caprolactone) (PCL) on an ultra-high modulus polyethylene (PE) fiber was investigated using a new approach based on the induction time + subi. This approach allows to estimate the value of the free energy difference function Delta(sigma) as it appears in the theory of heterogeneous nucleation. The classical approach based on the rate of heterogeneous nucleation I is not applicable to transcrystallization because the nucleation density at the fiber surface cannot be measured. A relationship between I and t(subi) is proposed and a theoretical justification is presented. Good agreement between the two approaches is obtained for a verification case where both I and t(subi) can be determined. A transcrystalline growth rate study yields an estimate of parameter sigma (signa) sub e for PCL. The maximum growth rate g is also obtained. The results obtained allow us to clarify the influence of certain parameters in the appearance of transcrystallinity. It is also shown how the interfacial mornphology can be controlled by the knowledge of the variations of the induction time with temperature. GRA

N91-26965# Stanford Univ., CA. Dept. of Applied Mechanics.
HIGH TEMPERATURE SUPERCONDUCTING FILMS AND CRYSTALS Final Report, 1 Oct. 1987 - 30 Sep. 1990
Theodore H. Geballe and Aharon Kapitulnik 2 Feb. 1991 16 p
(Contract F49620-88-C-0004)
(AD-A235234; AFOSR-91-0443TR) Avail: NTIS HC/MF A03 CSCL 20/3

A new high Tc phase, the compound Y2Ba4Cu8O20-Mx(248) was discovered. Its equilibrium with YBaZCu3O7(123) was studied. The thermal motion of the magnetic vortex lattice when a large macroscopic current is carried under strong magnetic fields was studied. The low temperature heat capacity of single crystals of Bi2Sr2CaCu2O8 and Ti2Ca2Ba2Cu3O10 was studied. The thickness dependence of superconducting properties was studied from 20 to 5000 A. The relaxation of the shielding current-induced magnetic moment was studied in YBaZCu3O7 in-situ grown thin films. Reflectance and spectroellipsometric measurements were performed on a high-quality c-axis oriented La(1.85)Sr(0.15)CuO4 film. X-ray absorption fine structure (EXAFS) measurements probed the local environment of atoms. A new instrument with a sensitivity of a 2 microrad for non-reciprocal phase shifts was developed by modifying a fiber-optic gyroscope. B.G.

N91-26966*# National Aeronautics and Space Administration. Lewis Research Center, Cleveland, OH.
PROCESS FOR THE CONTROLLED GROWTH OF SINGLE-CRYSTAL FILMS OF SILICON CARBIDE POLYTYPES ON SILICON CARBIDE WAFERS Patent Application
J. Anthony Powell, inventor (to NASA) 12 Jun. 1991 20 p
(NASA-Case-LEW-15222-1; NAS 1.71:LEW-15222-1; US-Patent-Appl-SN-718315) Avail: NTIS HC/MF A03 CSCL 20K

This invention is a method for the controlled growth of single-crystal semiconductor device quality films of SiC polytypes on vicinal (0001) SiC wafers with low tilt angles. Both homoepitaxial and heteroepitaxial SiC films can be produced on the same wafer. In particular, 3C-SiC and 6H-SiC films can be produced within selected areas of the same 6H-SiC wafer. NASA

N91-26967*# National Aeronautics and Space Administration. Lewis Research Center, Cleveland, OH.
PROCESS FOR THE HOMOEPITAXIAL GROWTH OF SINGLE-CRYSTAL SILICON CARBIDE FILMS ON SILICON CARBIDE WAFERS Patent Application

J. Anthony Powell, inventor (to NASA) 12 Jun. 1991 15 p
(NASA-Case-LEW-15223-1; NAS 1.71:LEW-15223-1;
US-Patent-Appl-SN-718314) Avail: NTIS HC/MF A03 CSCL 20L

The invention is a method for growing homoepitaxial films of SiC on low tilt angle vicinal (0001) SiC wafers. The invention proposes and teaches a new theoretical model for the homoepitaxial growth of SiC films on (0001) SiC substrates. The inventive method consists of (1) preparing the growth surface of SiC wafers slightly off-axis (from less the 0.1 to 6 deg) from the (0001) plane, (2) subjecting the growth surface to a suitable etch, and then (3) growing the homoepitaxial film using conventional SiC growth techniques. NASA

N91-26968*# National Aeronautics and Space Administration. Marshall Space Flight Center, Huntsville, AL.
CRYSTAL GROWTH IN A MICROGRAVITY ENVIRONMENT Patent Application
Roger L. Kroes, inventor (to NASA), Donald A. Reiss, inventor (to NASA), and Sandor L. Lehoczky, inventor (to NASA) 19 Jun. 1991 15 p
(NASA-Case-MFS-28473-1; NAS 1.71:MFS-28473-1;
US-Patent-Appl-SN-717447) Avail: NTIS HC/MF A03 CSCL 20B

Gravitational phenomena, including convection, sedimentation, and interactions of materials with their containers all affect the crystal growth process. If they are not taken into consideration they can have adverse effects on the quantity and quality of crystals produced. As a practical matter, convection, and sedimentation can be completely eliminated only under conditions of low gravity attained during orbital flight. There is, then, an advantage to effecting crystallization in space. In the absence of convection in a microgravity environment cooling proceeds by thermal diffusion from the walls to the center of the solution chamber. This renders control of nucleation difficult. Accordingly, there is a need for a new improved nucleation process in space. Crystals are nucleated by creating a small localized region of high relative supersaturation in a host solution at a lower degree of supersaturation. NASA

N91-26969 Tel-Aviv Univ. (Israel). Dept. of Physics and Astronomy.
CRYSTALLIZATION OF THIN FILMS OF AMORPHOUS GERMANIUM ALLOYS Ph.D. Thesis
Yossi Lereah May 1989 119 p In HEBREW; ENGLISH summary
(ITN-91-85110) Copyright Avail: Tel-Aviv Univ., Exact Sciences Library, Ramat Aviv 69978, Israel

Films of amorphous germanium alloys were crystallized by heating them in an electron microscope, so that the crystallization process could be observed in situ. The main emphasis was on the morphologies evolved in the crystallization of germanium-aluminum (Ge:Al) films. Amorphous Ge:Al films were found to crystallize by nucleation and growth of colonies, tens of micrometers in size, containing Ge and Al crystals, hundreds to thousands of angstroms in size. An example of dense branching morphology was observed and the influence of crystallization temperature on the colony's growth rate and characteristic length scale was studied. The influence on morphology of film preparation and heating conditions was studied. Aluminum-rich films were found to contain aluminum crystals in an amorphous matrix. Crystallization of these films also yielded dense branching morphology, with very frequent nucleation of colonies. These films provided an opportunity to study the nucleation process under high magnification, since there was high probability of a nucleation event occurring in the field under observation. Results obtained with germanium-lead and germanium-tin alloys are briefly summarized. ISA

N91-26970# Institute of Gas Technology, Chicago, IL.
SOLID-STATE PROTON CONDUCTORS
J. R. Jewulski, T. L. Osif, and R. J. Remick Dec. 1990 107 p
(Contract DE-AC21-88MC-24218)
(DE91-002050; DOE/MC-24218/2957) Avail: NTIS HC/MF A06

The purpose of this program was to survey the field of solid-state proton conductors (SSPC), identify conductors that could be used to develop solid-state fuel cells suitable for use with coal derived fuel gases, and begin the experimental research required for the development of these fuel cells. This document covers the following topics: the history of developments and current status of the SSPC, including a review of proton conducting electrolyte structures, the current status of the medium temperature SSPC development, electrodes for moderate temperature (SSPC) fuel cell, basic material and measurement techniques applicable for SSPC development, modeling, and optimization studies. Correlation and optimization studies are described which include correlation studies on proton conduction and oxide cathode optimization for the SSPC fuel cell. Experiments with the SSPC fuel cells are presented which include the fabrication of the electrolyte disks, apparatus for conducting measurements, the strontium-cerium based electrolyte, the barium-cerium based electrolyte with solid foil electrodes, the barium-cerium based electrolyte with porous electrodes, and conduction mechanisms. DOE

N91-26971# Argonne National Lab., IL.
FORMATION OF INTERMEDIATE COMPOUNDS DURING REDUCED PRESSURE CALCINATION OF Y-Ba-Cu-O PRECURSOR
U. Balachandran, S. L. Morissette, R. A. Russell, S. E. Dorris, and R. B. Poeppel Jan. 1991 18 p Presented at the Annual Meeting and Exhibition of the Minerals, Metals and Materials Society (TMS), New Orleans, 17-21 Feb. 1991
(Contract W-31-109-eng-38)
(DE91-011179; ANL/CP-71092; CONF-910202-12) Avail: NTIS HC/MF A03

Reaction of Y2O3, BaCO3, and CuO for 4 h at 800 C in flowing O2 with a total pressure of about 2 mm Hg, followed by cooling in O2 at ambient pressure, has produced phase-pure orthorhombic YBa2Cu3O(x) (123). During calcination, BaCO3 first decomposes and then reacts to form intermediate compounds. Reactions among the intermediate compounds result in formation of the 123 superconductor. Formation of intermediate compounds during calcination was monitored by x-ray diffraction, scanning electron microscopy, and thermal analyses of precursor powders heated to various temperatures up to 800 C. The reaction passes through the formation of BaCuO2, BaCO3, Y2Cu2O5, and Y2BaCuO5. The 123 phase begins to form at temperatures as low as 725 C in a pressure of about 2 mm Hg of oxygen. DOE

N91-26972# Sandia National Labs., Albuquerque, NM.
A TEMPERATURE DEPENDENT SPICE MACRO-MODEL FOR POWER MOSFETS
D. G. Pierce 1991 6 p Presented at the 34th Midwest Symposium on Circuits and Systems, Monterey, 14-17 May 1991
(Contract DE-AC04-76DP-00789)
(DE91-011737; SAND-91-0422C; CONF-9105169-1) Avail: NTIS HC/MF A02

The power MOSFET SPICE Macro-Model has been developed suitable for use over the temperature range -55 to 125 C. The model is comprised of a single parameter set with temperature dependence accessed through the SPICE .TEMP card. SPICE parameter extraction techniques for the model and model predictive accuracy are discussed. DOE

N91-26973# California Univ., Berkeley. Lawrence Berkeley Lab.
QUANTUM LIMITED QUASIPARTICLE MIXERS AT 100 GHz
C. A. Mears, Qing Hu, P. L. Richards, A. H. Worsham, D. E. Prober, and A. V. Raeisaenen (Helsinki Univ. of Technology, Espoo, Finland) Sep. 1990 10 p Presented at the Applied Superconductivity Conference, Aspen, 24-28 Sep. 1990
(Contract DE-AC03-76SF-00098)
(DE91-011894; LBL-28991; CONF-900944-43) Avail: NTIS HC/MF A02

We have made accurate measurements of the noise and gain of superconducting-insulating-superconducting (SIS) mixers employing small area (1sq micron) Ta/Ta2O5/Pb(0.9)Bi(0.1) tunnel junctions. We have measured an added mixer noise of 0.61 +/-

0.31 quanta at 95.0 GHz, which is within 25 percent of the quantum limit of 0.5 quanta. We have carried out a detailed comparison between theoretical predictions of the quantum theory of mixing and experimentally measured noise and gain. We used the shapes of I-V curves pumped at the upper and lower sideband frequencies to deduce values of the embedding admittances at these frequencies. Using these admittances, the mixer noise and gain predicted by quantum theory are in excellent agreement with experiment. DOE

N91-26974# California Univ., Berkeley. Lawrence Berkeley Lab.
STUDY OF THE EFFECT OF REACTIVE ELEMENT ADDITION BY IMPLANTING METAL IONS IN A PRE-FORMED OXIDE LAYER
P. Y. Hou, I. G. Brown, and J. Stringer (Electric Power Research Inst., Palo Alto, CA.) Sep. 1990 16 p Presented at the 7th International Conference on Ion Beam Modification of Materials, Knoxville, 9-14 Sep. 1990
(Contract DE-AC03-76SF-00098)
(DE91-011916; LBL-29522; CONF-900936-28) Avail: NTIS HC/MF A03

The influence of ion-implanted Y, Hf, Zr and Cr on the oxidation behavior of a Ni-25 wt percent CR alloy at 1000 C has been investigated. The implantation dosage was 5 x 10(exp 16) ions/sq cm. Two methods of implantation have been used. One was to implant ions directly into a clean alloy surface; the other was to implant into an approximately 0.6 micron thick Cr2O3 layer formed at 1000 C on the alloy. In neither case did the Cr implantation show any beneficial effects. Implantations of Y, Hf, and Zr produced all the reactive element effects, i.e., reduction in oxidation rate, elimination of base metal oxide formation, and improvement in scale adhesion, only if the ions were initially implanted in the alloy. When the ions were implanted in a preformed oxide, the subsequent oxidation process was altered to the same degree as before, but the scale adhesion was not affected. Implications of these results to the mechanism of the reactive element effect are discussed. DOE

N91-26975# Lawrence Livermore National Lab., CA.
VACUUM DESIGN FOR A SUPERCONDUCTING MINI-COLLIDER
W. A. Barletta and S. Monteiro (Moorpark Coll., CA.) Apr. 1991 4 p Presented at the 1991 Institute of Electrical and Electronics Engineers (IEEE) Particle Accelerator Conference (PAC), San Francisco, 6-9 May 1991
(Contract W-7405-eng-48)
(DE91-011964; UCRL-JC-105594; CONF-910505-34) Avail: NTIS HC/MF A01

The phi factory (Superconducting Mini-Collider or SMC) proposed for construction at UCLA is a single storage ring with circulating currents of 2 A each of electrons and positrons. The small circumference exacerbates the difficulties of handling the gas load due to photo-desorption from the chamber walls. The vacuum system for the phi factory was analyzed to specify design choices. DOE

N91-26976*# Case Western Reserve Univ., Cleveland, OH. Dept. of Physics.
MICROWAVE PROPERTIES OF HIGH TRANSITION TEMPERATURE SUPERCONDUCTING THIN FILMS Final Technical Report
W. L. Gordon 21 Jun. 1991 19 p
(Contract NCC3-40)
(NASA-CR-185842; NAS 1.26:185842) Avail: NTIS HC/MF A03 CSCL 20L

Extensive studies of the interaction of microwaves with YBa2Cu3O(7-delta), Bi-based, and Tl-based superconducting thin films deposited in several microwave substrates were performed. The data were obtained by measuring the microwave power transmitted through the film in the normal and the superconducting state and by resonant cavity techniques. The main motives were to qualify and understand the physical parameters such as the magnetic penetration depth, the complex conductivity, and the surface impedance, of high temperature superconducting (HTS) materials at microwave frequencies. Based on these parameters, the suitability of these HTS thin films is discussed for microwave applications. B.G.

N91-26977# Lawrence Livermore National Lab., CA.
THE ELECTRONIC STRUCTURE OF THE IONIC INSULATOR SODIUM NITRITE
R. F. Gallup and C. Y. Fong (California Univ., Davis.) Feb. 1991 23 p
(Contract W-7405-eng-48)
(DE91-009766; UCRL-CR-106691) Avail: NTIS HC/MF A03

The electronic properties of the ionic insulator sodium nitrite (NaNO2) were studied using the self-consistent, ab-initio pseudopotential density functional method. The Kohn-Sham equations of density functional theory were solved for the electronic wavefunctions and energies using a modified Car-Parrinello molecular dynamics density functional technique. The correspondence between certain Bloch states in the NaNO2 crystal and the pi-molecular orbitals on the free NO2(-) ion was demonstrated. In addition, the ordering of these Bloch state energies and their electronic occupations in the ground state of NaNO2 was shown to resemble the energy ordering and electronic occupations of the pi-orbitals in the free ion. The NO2(-) ion therefore retains elements of its free identity in the NaNO2 crystal. The long term goal of the present investigation is to determine the contribution of the pi-molecular orbitals on the NO2(-) ion to the second-harmonic response (SHR) of NaNO2. DOE

N91-26978# Argonne National Lab., IL.
ON THE NATURE OF GRAIN BOUNDARY STRUCTURES IN NANOPHASE MATERIALS
R. W. Siegel and G. J. Thomas (Sandia National Labs., Albuquerque, NM.) Feb. 1991 13 p Presented at the Fall Meeting of the Materials Research Society (MRS), Boston, 24 Nov. - 1 Dec. 1990
(Contracts W-31-109-eng-38; DE-AC04-76DR-00789)
(DE91-010285; ANL/CP-70929; CONF-901105-115) Avail: NTIS HC/MF A03

A significant fraction of the atoms in nanophase materials are associated with grain boundaries. Hence, the nature of the grain boundary structures in these materials is interesting in its own right as well as ultimately important to the properties of nanophase materials. Considerable uncertainty has surrounded the atomic structure of nanophase boundaries, but recent experiments have shed some light on these interesting structures. These investigations have included direct HREM observations combined with image simulations, as well as Raman spectroscopy and SANS. The emerging picture is one of nanophase boundaries that are not dissimilar in structure to those normally encountered in conventional polycrystals. The connections between this picture, of nanophase materials as ultrafine grained polycrystals, and experimental observations on these materials are discussed. DOE

N91-26979# Argonne National Lab., IL.
DEFECTS IN DECOMPOSED YBa2Cu4O8 (124) SUPERCONDUCTOR AFTER RAPID ANNEALING
Y. Li, Y. Gao, K. L. Merkle, H. Shi, and U. Balachandran 1990 7 p Presented at the Fall Meeting of the Materials Research Society (MRS), Boston, 24 Nov. - 1 Dec. 1990
(Contract W-31-109-eng-38)
(DE91-010597; ANL/CP-71156; CONF-901105-116) Avail: NTIS HC/MF A02

Decomposition of 124 into 123 was studied after rapid annealing at temperatures from 800 to 1000 C. It was found that the superconducting transition temperature (Tc) depended on the annealing temperature and atmosphere. For decomposed samples, fine-scale defects with strong strain contrast are observed in the 123 matrix. High resolution electron microscopy studies show that the defects are parallel to the (001) planes of the 123 matrix. The length of the defects varies and ranges from 5 nm to 50 nm

in the direction parallel to the (001) planes. The defects were interpreted to be copper oxides, which could be flux pinning centers in these materials. DOE

N91-26980# Argonne National Lab., IL.
EFFICIENT PHOTOINDUCED CHARGE SEPARATION AND STORAGE IN THE SOLID STATE, RATES, ENERGETICS, AND SPIN-POLARIZATION
M. R. Wasielewski, G. L. Gaines, M. P. ONeil, W. A. Svec, and M. P. Niemczyk 1991 2 p Presented at the Energy Conversion Sciences Conference, Tokyo, Japan, 17-21 Feb. 1991
(Contract W-31-109-eng-38)
(DE91-010727; ANL/CP-72194; CONF-9102104-1) Avail: NTIS HC/MF A01

Rates of photoinduced charge separation proceeding from the lowest excited singlet state in 14 fixed distance porphyrin triptycene acceptor molecules were measured in 2-methyl tetrahydrofuran glass at 77 K. Analysis of the rate data as a function of free energy of reaction reveals that the ion-pair state of the oxidized donor and reduced acceptor is destabilized in a rigid glass medium by 0.8 eV relative to the ion-pair state energy determined from the sum of the one-electron redox potentials for the donor and acceptor in polar liquids. The measured value of this destabilization energy agrees remarkably well with predictions based on the dielectric continuum model of the solvent. From the maximum of the rate vs free energy profile for photoinduced charge separation, the total reorganization energy of the reaction is 0.6 eV. Analysis of this data shows that the solvent reorganization energy is 0.3 eV, while the internal nuclear reorganization energy of the donor-acceptor molecules is 0.3 eV. This data was used to optimize the efficiency of photoinduced charge separation for donor-acceptor molecules in the solid state. DOE

N91-26981# California Univ., Berkeley. Lawrence Berkeley Lab.
HIGH-T(SUB c) THIN-FILM MAGNETOMETER
A. H. Miklich, F. C. Wellstood, J. J. Kingston, J. Clarke, M. S. Colclough, A. H. Cardona, L. C. Bourne, W. L. Olson, and M. M. Eddy (Superconductor Technologies, Inc., Santa Barbara, CA.) Sep. 1990 5 p Presented at the Applied Superconductivity Conference, Aspen, 24-28 Sep. 1990
(Contract DE-AC03-76SF-00098)
(DE91-011828; LBL-28892; CONF-900944-42) Avail: NTIS HC/MF A01

High Tc magnetometers were constructed and tested by coupling a high Tc thin film Superconducting QUantum Interference Device (SQUID) to two different high Tc thin film flux transformers. The SQUID was made from Tl2CaBa2Cu2O(8+y) films grown on MgO, with junctions consisting of native grain boundaries. The flux transformers were made from YBa2Cu3O(7-x), and each had 10-turn input coils and a single turn pickup loop. The first transformer, which was patterned with a combination of shadow masks and photolithography, yielded a magnetic field gain of about -7.5, functioned up to 79 K, and gave a magnetic field sensitivity B(N) (10 Hz) approx. 3.1 pT Hz(exp -1/2) at 38 K. The second transformer, which was patterned entirely by photolithography, yielded a gain of about -8.7, functioned up to 25 K, and had a sensitivity B(N) (10 Hz) approx. 3.5 pT Hz(exp -1/2) at 4.2 K. In both cases, the limiting noise arose in the SQUID. DOE

N91-26982# Argonne National Lab., IL.
CRITICAL CURRENTS IN PROTON IRRADIATED YBa2Cu3O(7-DELTA) CRYSTALS
L. Civale, M. W. McElfresh, A. D. Marwick, T. K. Worthington, A. P. Malozemoff, F. Holtzberg, C. Feild (International Business Machines Corp., Yorktown Heights, NY.), J. R. Thompson, and D. Christen Apr. 1991 20 p Presented at the 12th Winter Meeting on Low Temperature Physics, Cuernavaca (Mexico), 13-16 Jan. 1991
(Contracts W-31-109-eng-38; DE-AC05-84OR-21400)
(DE91-011835; ANL/CP-72968; CONF-910192-1) Avail: NTIS HC/MF A03

A large enhancement in the critical current of YBaCuO crystals in magnetic field is observed after irradiation with 3 MeV protons. Critical current densities with values up to 2 x 10(exp 5) A/sq cm at 77 K and 1 T are observed. TEM studies show the presence of isolated clusters of defects after irradiation; however, an analysis of the critical current scaling indicates that these clusters are not the dominant pinning sites. The dose dependence of the current density suggests that the pinning is dominated by the randomly distributed point defects generated by the protons and can be described by a collective pinning model in the amorphous limit. DOE

N91-26983# Oak Ridge National Lab., TN.
EFFECT OF BORON ADDITION ON RECRYSTALLIZATION AND GRAIN GROWTH IN Ni3Al POLYCRYSTALS
B. Zhou, S. L. Yu, Y. T. Chou (Lehigh Univ., Bethlehem, PA.), and C. T. Liu 1991 5 p Presented at the 6th Japan Institute of Metals (JIM) International Symposium on Intermetallic Compounds: Structure and Mechanical Properties, Sendai (Japan), 17-20 Jun. 1991
(Contracts DE-AC05-84OR-21400; DE-FG02-86ER-45256)
(DE91-011966; CONF-9106146-4) Avail: NTIS HC/MF A01

The recrystallization and grain growth kinetics in pure and boron-doped Ni3Al polycrystals were investigated in the temperature range from 850 to 1000 C. At 16.7 pct. deformation, the recrystallization processes of the two sets of alloys were found to be similar in characteristics and magnitudes. Both alloys obey the classical Avrami equation. The activation energy of recrystallization for the boron-doped alloy was found to be 488 kJ/mol, which is slightly greater than the activation energy for the boron-free alloy, 476 kJ/mol. The grain growth kinetics obey the power relation with the time exponent less than 0.5, indicating a sluggish growth due to long range ordering. DOE

N91-26984# Ames Lab., IA.
MAGNETIC RELAXATION, FLUX PINNING AND, CRITICAL CURRENTS IN SUPERCONDUCTORS Ph.D. Thesis
K. S. Lichtenberger 2 May 1991 154 p
(Contract W-7405-eng-82)
(DE91-012022; IS-T-1543) Avail: NTIS HC/MF A08

A systematic study of the magnetic flux pinning properties in superconductors has been undertaken in an attempt to understand the differences between the flux creep behavior of classical superconductors and high-temperature superconductors (HTSC's). In HTSC's, the ratio of the effective flux pinning energy to the thermal energy, U(sub 0)/kT, is much smaller than that of conventional superconductors, often approaching unity. This results in much larger creep rates in HTSC's than in conventional superconductors. It is necessary to find suitable models that describe flux creep in both classical superconductors and HTSC's. Results show that while these two classes of materials are quantitatively very different, a single pinning barrier mode adequately describes both, within the proper region of the H-T plane. The model is applied to a variety of superconductors and the results are contrasted. Although the H-T plane appears to be very different HTSC's than for conventional superconductors, qualitatively the same physics describes both. In HTSC's, near the upper critical field there exists a relatively wide region of superconducting fluctuations, followed successively by regions of thermodynamic reversibility, thermally assisted flux, flux creep, and finally rigid flux lattice where little, if any, motion of the flux lattice occurs. All of these regions are also present in conventional superconductors, but often much more difficult, especially the irreversibility transition and the fluctuation region. The central finding of the flux creep analysis is that the region of flux creep is defined as a band in the H-T plane in which 2 (le) U(sub 0)/kT (le) 100, and that the flux creep model applies best within this band. DOE

N91-26985# California Univ., Berkeley. Lawrence Berkeley Lab.
THIN FILM ALLOYS ON SEMICONDUCTOR SUBSTRATES
D. A. Olson, K. M. Yu, J. Washburn, and T. Sands (Bell Communications Research, Inc., Red Bank, NJ.) Nov. 1990

7 p Presented at the Fall Meeting of the Materials Research Society (MRS), Boston, 24 Nov. - 1 Dec. 1990
(Contract DE-AC03-76SF-00098)
(DE91-012355; LBL-29862; CONF-901105-123) Avail: NTIS HC/MF A02

The interactions between Pt thin films and In(0.53)Ga(0.47)As have been studied. An important result is that the reaction kinetics deviate from those of other metal/compound semiconductor reactions. The kinetics can be divided into two stages, where the reaction slows by a factor of 5 after approximately 60 minutes of annealing at 400 C. In addition, Auger depth-profiling indicates that an In-rich layer develops at the reacted layer/substrate interface. DOE

N91-26986# Argonne National Lab., IL.
HREM STUDY OF HETEROEPITAXIAL INTERFACES IN THE TiO2/Al2O3 SYSTEM
Y. Gao, K. L. Merkle, H. L. M. Chang, T. J. Zhang, and D. J. Lam Apr. 1991 7 p Presented at the Spring Meeting of the Materials Research Society (MRS), Anaheim, 29 Apr. - 3 May 1991
(Contract W-31-109-eng-38)
(DE91-012473; ANL/CP-71865; CONF-910406-9) Avail: NTIS HC/MF A02

TiO2 thin films were grown epitaxially on (112'0) sapphire (alpha-Al2O3) at 800 C by the metal-organic vapor deposition (MOCVD) method. The TiO2 films and TiO2/Al2O3 interfaces were characterized by transmission electron microscopy (TEM) and high-resolution electron microscopy (HREM). The observations indicate that the TiO2 films are single crystalline and have the rutile structure. A majority of the films has the epitaxial orientation relationship between the TiO2 rutile films (R) and the alpha-Al2O3 substrates (S): (101) zone axes(010)(sub R) parallel (112'0) zone axes(0001)(sub S), while the epitaxial relationship of (100) zone axes(010)(sub R) parallel (112'0) zone axes(0001)(sub S) has also been observed for one film. HREM studies show that the (100) film was grown on an off-cut substrate, vicinal to (112'0). Detailed atomic structures of the interfaces will be presented and discussed in terms of the growth mechanism and misfit dislocation structure. DOE

77 THERMODYNAMICS AND STATISTICAL PHYSICS

Includes quantum mechanics; theoretical physics; and Bose and Fermi statistics.

For related information see also *25 Inorganic and Physical Chemistry* and *34 Fluid Mechanics and Heat Transfer.*

N91-26987 Boston Univ., MA.
GENERAL RELATIVISTIC CONTINUUM MECHANICS AND THE POST-NEWTONIAN EQUATIONS OF MOTION Ph.D. Thesis
Thomas H. Morrill 1991 137 p
Avail: Univ. Microfilms Order No. DA9110831

Aspects are examined of general relativistic continuum mechanics. Perfectly elastic materials are dealt with but not exclusively. The derivation of their equations of motion is emphasized, in the post-Newtonian approximation. A reformulation is presented based on the tetrad formalism, of Carter and Quintana's theory of general relativistic elastic continua. A field Lagrangian is derived describing perfect material media; show that the usual covariant conservations law for perfectly elastic media is fully equivalent to the Euler-Lagrange equations describing these same media; and further show that the equations of motion for such materials follow directly from Einstein's field equations. In addition, a version of this principle shows that the local mass density in curved space-time partially depends on the amount and distribution of mass energy in the entire universe and is related to the mass density that would occur if space-time were flat. The total Lagrangian was also expanded in an EIH (Einstein, Infeld, Hoffmann) series to obtain a total post-Newtonian Lagrangian. The results agree with those found by solving Einstein's equations for the metric coefficients and by deriving the post-Newtonian equations of motion from the covariant conservation law.
Dissert. Abstr.

N91-26988# Ballistic Research Labs., Aberdeen Proving Ground, MD.
AN ANALYSIS ON THE STABILITY OF THE MIE-GRUNEISEN EQUATION OF STATE FOR DESCRIBING THE BEHAVIOR OF SHOCK-LOADED MATERIALS Final Report, Jun. 1989 - Sep. 1990
Steven B. Segletes Mar. 1991 56 p
(DA Proj. 1L1-62618-AH-80)
(AD-A233827; BRL-TR-3214) Avail: NTIS HC/MF A04 CSCL 20/13

A review of fundamental shock-transition theory is presented. The equation of state (EOS) is introduced as an analytical vehicle to express material pressure as a function of density and temperature (or internal energy in the case of adiabatic transition). Starting from the fundamental laws of thermodynamics, three criteria are developed to measure the stability of equations of state and are applied specifically to the Mie-Gruneisen EOS, with Hugoniot reference, to investigate the stability characteristics thereof. This EOS is singled out for study because of its relative importance in the computational modeling of shock transition. Results indicate numerous possibilities of instability under various circumstances. Various remedies are proposed to correct the observed instabilities and compared with existing models. GRA

N91-26989# Scientific Research Associates, Inc., Glastonbury, CT.
QUANTUM DEVICES AND STRUCTURES Final Report, 25 Jul. 1990 - 24 Jan. 1991
H. L. Grubin and T. R. Govindan 26 Mar. 1991 35 p
(Contract F49620-90-C-0061)
(AD-A235298; SRA-R91-910032-F; AFOSR-91-0389TR) Avail: NTIS HC/MF A03 CSCL 20/10

All devices constructed from quantum mechanical resonant tunneling structures are dependent upon their ability to move charge in and out of the quantum well. The ability to effectively modulate this charge is dependent upon the device structure; which in turn depends upon an understanding of quantum device physics; which in turn depends upon device theory, simulation, and experiment. In the present study, Scientific Research Associates, Inc. implemented its time-dependent quantum Liouville equation algorithm for obtaining the density matrix in the coordinate representation. Switching times as well as response times to ac signals were determined for tunneling structures with variable charge densities. A recommended future program involves implementing the algorithm for designing three proto-typical tunneling devices, and determining the limits of operation. These devices are: (1) a resonant tunneling self-excited, high-frequency local oscillator, (2) a resonant tunneling high-speed photo-induced two-terminal electrical switching element, and (3) a permeable base like resonant tunneling high current-level three terminal switching transistor. GRA

N91-26990# Brookhaven National Lab., Upton, NY.
THERMOLUMINESCENCE KINETICS OF PYRITE (FeS2)
A. N. Silverman, P. W. Levy, and J. A. Kierstead 1990 30 p Presented at the 6th International Specialist Seminar on Thermoluminescence (TL) and Electron Spin Resonance (ESR) Dating, Clermont (France), Jul. 1990
(Contract DE-AC02-76CH-00016)
(DE91-011710; BNL-46067; CONF-9007188-2) Avail: NTIS HC/MF A03

Thermoluminescence of pyrite (FeS2) was investigated to study the kinetics of single peak glow curves. The material used normally exhibits one large and four small peaks. However a glow curve can be obtained with only the large single peak that is suitable for testing thermoluminescence kinetics. Glow curves from aliquots of a single natural pyrite crystal studied in detail contain two low intensity thermoluminescence (TL) peaks at approximately 90 and 250 C, and two chemiluminescence (CL) peaks at approximately

350 and 430 C. The CL peaks are largely removable by initially heating the sample chamber under vacuum, pumping through liquid nitrogen traps, and recording glow curves immediately after helium is introduced, procedures which reduce system contaminants that react with pyrite. The shape, the variation of the temperature of the peak maximum (T(sub max)) with dose, and the retrapping to recombination cross section ratio (sigma) of the large 250 C peak are better described by the general one trap (GOT) kinetic equation, the basic equation from which the 1st and 2nd order kinetic equations are obtained as special cases, than by the 1st and 2nd order equations. DOE

N91-26991# California Univ., Berkeley. Lawrence Berkeley Lab.
QUANTUM LIMITED QUASIPARTICLE MIXERS AT 100 GHz
C. A. Mears, Qing Hu, P. L. Richards, A. H. Worsham, D. E. Prober, and A. V. Raeisaenen (Helsinki Univ. of Technology, Espoo, Finland) Apr. 1991 16 p Presented at the Superconductivity Applications for Infrared and Microwave Devices 2 Conference, Orlando, 1-5 Apr. 1991
(Contract DE-AC03-76SF-00098)
(DE91-011826; LBL-29546; CONF-9104234-2) Avail: NTIS HC/MF A03

Accurate measurements were made of the noise and gain of superconducting-insulating-superconducting (SIS) mixers employing small area (1 sq micron) Ta/Ta2O5/Pb(0.9)Bi(0.1) tunnel junctions. An added mixer noise of 0.61 + or - 0.31 quanta at 95.0 GHz, which is within 25 percent of the quantum limit of 0.5 quanta was measured. A detailed comparison between theoretical predictions of the quantum theory of mixing and experimentally measured noise and gain was performed. The shapes of I-V curves pumped at the upper and lower sideband frequencies were used to deduce values of the embedding admittances at these frequencies. Using these admittances, the mixer noise and gain predicted by quantum theory are in excellent agreement with experiment. DOE

N91-26992# California Univ., Berkeley. Lawrence Berkeley Lab.
SUPERSYMMETRY BREAKING FROM SUPERSTRINGS AND THE GAUGE HIERARCHY
M. K. Gaillard 11 Jul. 1990 11 p Presented at the 30th Cracow Summer School, Zakopane (Poland), 3-16 Jun. 1990
(Contract DE-AC03-76SF-00098)
(DE91-011899; LBL-29313; CONF-9006343-1; UCB-PTH-90/30) Avail: NTIS HC/MF A03

The gauge hierarchy problem is reviewed and a class of effective field theories obtained from superstrings is described. These are characterized by a classical symmetry, related to the space-time duality of string theory, that is responsible for the suppression of observable supersymmetry breaking effects. At the quantum level, the symmetry is broken by anomalies that provide the seed of observable supersymmetry breaking, and an acceptably large gauge hierarchy may be generated. DOE

80 SOCIAL SCIENCES (GENERAL)

Includes educational matters.

No abstracts in this category.

81 ADMINISTRATION AND MANAGEMENT

Includes management planning and research.

N91-26993# Air Force Systems Command, Griffiss AFB, NY.
A ROME LABORATORY GUIDE TO BASIC TRAINING IN TQM ANALYSIS TECHNIQUES
Anthony Coppola Mar. 1991 57 p
(AF Proj. 9993)
(AD-A233855; RL-TR-91-29) Avail: NTIS HC/MF A04 CSCL 05/1

Total Quality Management (TQM) is a DoD initiative for continuously improving performance at every level, in every area of DoD responsibility. Implementing this philosophy will require a cultured change in the defense community. It will also require the intelligent use of appropriate analysis techniques. This report describes the basic analytical tools used in TQM: Process flow charts, Ishikawa charts, Statistical process control, Histograms, Pareto diagrams, Scattergrams and the Shewhart cycle. For easier comprehension, a mythical scenario is used in which the tools are introduced to a willing, but untrained, manager (and to the reader) by a TQM specialist. GRA

N91-26994# Rome Air Development Center, Griffiss AFB, NY.
MEASURING THE QUALITY OF KNOWLEDGE WORK
Anthony Coppola Apr. 1991 25 p
(AF Proj. 2338)
(AD-A235354; RL-TR-91-48) Avail: NTIS HC/MF A03 CSCL 05/1

There are a variety of ways in which the quality of knowledge work can be measured, depending on the definition of quality and the intended use of the measure. This report summarizes these for the guidance of the managers of knowledge workers, such as the engineers and scientists of Government laboratories. GRA

N91-26995# Aeronautical Systems Div., Wright-Patterson AFB, OH.
RESULTS OF THE AERONAUTICAL SYSTEMS DIVISION CRITICAL PROCESS TEAM ON INTEGRATED PRODUCT DEVELOPMENT Final Report
Lavern J. Menker Nov. 1990 49 p
(AD-A235419; ASD-TR-90-5014) Avail: NTIS HC/MF A03 CSCL 12/6

This report provides a vision of the Integrated Product Development (IPD) Process as it could be implemented within the Aeronautical Systems Division (ASD). It captures the results of the ASD Critical Process Team on IPD and recent efforts to refine guidance for its implementation. The primary purpose of this document is to provide a conceptual framework to provoke dialogue that will lead to incremental improvements in the acquisition process. IPD is an efficient process of bringing a product from user's needs to field operation. The basic principle is to iterate and integrate the design of a product and the design of its manufacturing, operation, support and training processes with specific focus on achieving low-cost development, production, operations and support within the shortest schedule while achieving robust quality of products and services. GRA

N91-26996 Tel-Aviv Univ. (Israel). Dept. of Statistics.
HEURISTICS FOR A FLOW-SHOP MODEL WITH PARALLEL MACHINES AND SETUP TIMES M.S. Thesis
David Nir Apr. 1989 41 p In HEBREW; ENGLISH summary
(ITN-91-85117) Copyright Avail: Tel-Aviv Univ., Exact Sciences Library, Ramat Aviv 69978, Israel

The problem involved n jobs with m stages to be completed in the same order, in a flow-shop model representing a plant. For each stage there are several machines with different processing speeds; each machine can process no more than one job during one processing period. The aim was to compare methods of sequencing jobs so as to minimize the total weighted completion delays. The problem was defined in integer programming form, with a heuristic defined for each subproblem. Each heuristic includes parameters which enable it to generate several solutions and choose the best one, if there is sufficient computer time. Heuristics are described which calculate the values of assigning jobs to sets of machines, and organize the assignments so as to maximize the total value, and which assign priorities to jobs according to their remaining allowed completion time. The solutions found by the above heuristics were compared with those obtained by random search. All the heuristics yielded better solutions than

random search, the best being that which calculated assignment values. This heuristic is flexible and easily adjustable to other flow shop models. A FORTRAN program of about 2000 lines was written, to compare the heuristics. ISA

82 DOCUMENTATION AND INFORMATION SCIENCE

Includes information management; information storage and retrieval technology; technical writing; graphic arts; and micrography.

For computer documentation see *61 Computer Programming and Software.*

N91-26997# EnviroSystems Supply, Inc., Fort Myers, FL.
NATIONAL BUREAU OF STANDARDS PUBLICATIONS 1977-1987. VOLUME 2: INDEXES Final Report, 1977-1987
R. Pardee, E. Gladden, and D. Harris Aug. 1990 1442 p
(PB91-136515; NIST/SP-790-Vol-2) Avail: NTIS HC/MF A99 CSCL 05B

Volume 1 contains full bibliographic citations, key words, and abstracts for 15,746 National Bureau of Standards (NBS) (as of August 23, 1988 the National Institute of Standards and Technology (NIST)) papers published and entered into the National Technical Information Service (NTIS) collection between 1977 and 1987. Also included are several papers published prior to 1977 but not entered into the NTIS collection until 1977. The volume, Volume 2, contains four indexes to allow the user to identify papers by personal author, key words, title, and NTIS order/report number. Author

N91-26998# Executive Office of the President, Washington, DC. Office of Administration.
PUBLICATIONS OF THE EXECUTIVE OFFICE OF THE PRESIDENT, JANUARY 20, 1989 TO DECEMBER 31, 1990
1991 9 p
(PB91-127423) Avail: NTIS HC/MF A02 CSCL 05B

The document lists the publication of the Executive Office of the President issued by the Bush Administration from January 20, 1989 through December 31, 1990. The following publications are included: Council of Economic Advisers (CEA), Council on Environmental Quality (CEQ), Office of Management and Budget (OMB), Office of National Drug Control Policy (ONDCP), Office of Science and Technology Policies (OSTP), Office of the United States Trade Representative (USTR), and White House Office (WHO). Author

N91-26999# Air Force Historical Research Center, Maxwell AFB, AL.
PERSONAL PAPERS IN THE UNITED STATES AIR FORCE HISTORICAL RESEARCH CENTER, 5TH EDITION
R. E. Morse, L. O. Gamma, L. N. Romesburg, and G. L. McDaniel 1990 232 p
(PB91-156380) Avail: NTIS HC/MF A11 CSCL 05B

The present work describes 381 collections. The material covers the entire range of American military aviation from the Air Force Historical Research Center. Not surprisingly, the papers of significant Air Force leaders and policymakers predominate. Yet a sizable fraction of the documents includes the personal collection of aircraft designers, explorers, authors, journalists, and public officials, whose fundamental contributions are an indispensable part of the history of military aviation. Entries are listed in alphabetical order under the principal's name. Immediately thereafter is the colleciton's chronological range, the volume (in cubic feet) of material, as well as the file number and the finding number of the automated retrieval system IRIS, a selective biographical entry of the principal: a brief description of the collection's contents, and any administrative or security restrictions, as well as the existence of related material in the Center and/or elsewhere. GRA

N91-27000# National Inst. of Standards and Technology, Gaithersburg, MD.
PROCEEDINGS OF THE OBJECT-ORIENTED DATABASE TASK GROUP WORKSHOP
E. N. Fong Jan. 1991 150 p Workshop held in Ottawa, Ontario, 23 Oct. 1990
(PB91-157198; NISTIR-4488) Avail: NTIS HC/MF A07 CSCL 05B

The report constitutes the proceedings of a one-day workshop on standardization of object database systems. The workshop was the second attempt to solicit public input to identify what aspects of object database systems may be candidates for consensus that can lead to standards. The workshop goals focused on concrete proposals for languages or module interfaces, exchange mechanisms, abstract specifications, common libraries, or benchmarks. The workshop announcement also solicited papers on relationships of object database systems capabilities to existing standards, including assertions that question the wisdom of standardization. The proceedings consist of 13 position papers covering various aspects where standardization on object database systems may be possible. Author

N91-27001# Naval Research Lab., Washington, DC.
MATERIALS SCIENCE AND ENGINEERING, 1989 PUBLICATIONS
29 Mar. 1991 64 p
(AD-A234087; NRL-PUB-195-6000) Avail: NTIS HC/MF A04 CSCL 05/2

Listed is the 1989 open-literature publications in materials science and engineering from NRL. E.R.

N91-27002# Pennsylvania Univ., Philadelphia. Dept. of Chemistry.
PHOTOINDUCED ABSORPTION AND ERASABLE OPTICAL INFORMATION STORAGE IN POLYANILINES
R. P. McCall, J. M. Ginder, J. M. Leng, K. A. Coplin, and H. J. Ye 18 Mar. 1991 6 p
(Contract N00014-90-J-1559)
(AD-A234108; TR-1990-17) Avail: NTIS HC/MF A02 CSCL 05/2

Photoinduced absorption spectroscopy has been used to study a variety of forms of polyaniline. Experiments on emeraldine base and leucoemeraldine base have led to a picture of the photoproduction and decay of massive, long-lived defect states that can be described in terms of conformational changes involving rotations of the C6H4 rings. Photoexcitation spectra of other polyanilines, such as pernigraniline base and poly(o-toluidine), exhibit similar features including relatively weak photoinduced infrared vibrations and a relatively strong photoinduced absorption peak near 1.4-1.5 eV. In several of these materials, the photoinduced changes are very long-lived, leading to an investigation of the polyanilines as media for erasable optical information storage. GRA

N91-27003# California Univ., San Diego, La Jolla. Dept. of Electrical Engineering and Computer Sciences.
PROCEEDINGS OF THE FIRST WORKSHOP ON 3-D OPTICAL MEMORIES Final Report, 1 Mar. 1990 - 20 Nov. 1990
Sadik Esener and Alan Craig Mar. 1990 136 p Workshop held in Snowbird, UT, 12-13 Mar. 1990
(Grant AF-AFOSR-0178-90; AF Proj. 2305)
(AD-A234732; AFOSR-91-0271TR) Avail: NTIS HC/MF A07 CSCL 05/2

The first workshop on 3-D memories was held March 12-13, 1990 in Snowbird, Utah. The intent of the workshop was to bring together members of the optical storage and materials, computer architectures, and optoelectronic device communities to discuss issues associated with 3-D storage systems for various high-performance computers. The common concern among the diverse set of about 25 workshop participants was that storage is becoming a major limitation in terms of input/output bandwidth and capacity to achieving higher system performance, and will

impede the future development of high performance computer system. The question was if and how 3-D memories can provide better storage devices. GRA

N91-27004# Naval Ocean Systems Center, San Diego, CA.
ON-LINE MAGNETIC TAPE LIBRARY INVENTORY TRACKING AND REPORTING (LITAR) SYSTEM Final Report, FY 1990 - FY 1991
M. G. Ceruti, R. A. Auclair, J. P. Schill, and K. Yarnell Mar. 1991 18 p
(AD-A234934; NOSC/TD-2057) Avail: NTIS HC/MF A03 CSCL 12/7

The design and operation of the On Line Magnetic Tape Library Inventory Tracking and Reporting (LITAR) System is summarized. The system was developed by NOSC personnel to access efficiently administrative and content information about the magnetic tapes used for supporting database development in the NOSC Information Management Engineering (IME) Laboratory. This user interface was originally developed for tapes classified Secret or below, using ORACLE Relational Database Management System's SQL*FORMS on a VAX 8550. However, the interface has more general applications outside of this environment. Examples of user-input screens are also presented. GRA

N91-27005# Educational Testing Service, Princeton, NJ.
RESPONSE LATENCY MEASURES FOR BIOGRAPHICAL INVENTORIES Final Report, 31 Mar. 1989 - 31 Dec. 1990
Lawrence J. Stricker and David L. Alderton Feb. 1991 15 p
(Contract N00014-89-K-0072)
(AD-A235010) Avail: NTIS HC/MF A03 CSCL 05/9

This is the final report of the project, Response Latency Measures for Biographical Inventories. The purpose of this research was to determine whether recent findings about the connection between response latencies on personality inventory items and item instability can be used to increase an inventory's validity. A study was carried out, using latency-weighted scores and measures of deviant latencies for the Armed Services Applicant Profile, a biographical inventory, to predict the retention of Navy recruits. The latency data did not improve the ASAP's validity directly, but there were indications that employing these data in developing an inventory may enhance validity indirectly. The technical report for this project is summarized, the staff is listed, and directions for future research are outlined. GRA

N91-27006# Massachusetts Univ., Amherst. Dept. of Computer and Information Science.
RETRIEVAL USING PLAUSIBLE INFERENCE Final Report, 1 Jan. - 31 Dec. 1990
W. B. Croft 4 Apr. 1991 13 p
(Grant AF-AFOSR-0110-90; AF Proj. 2304)
(AD-A235015; AFOSR-91-0395TR) Avail: NTIS HC/MF A03 CSCL 05/2

Retrieval is a crucial function in information systems, but the algorithms used in many systems are not effective in locating the required information. For example, text-based systems are an important class of information system where both the query specification and the stored information will be incomplete and uncertain. In this situation, simple models of retrieval based on deductive inference are not adequate. We have proposed a new computational framework that views retrieval as a process of combining multiple sources of evidence, and have carried out a number of experiments in the domain of text retrieval. The experiments show that significant retrieval effectiveness improvements are possible. We have also made progress in the area of text representation using natural language processing, which provides additional evidence for the retrieval model. GRA

N91-27007# Human Engineering Labs., Aberdeen Proving Ground, MD.
THE EFFECTS OF CHARACTER SIZE, MODULATION, POLARITY, AND FONT ON READING AND SEARCH PERFORMANCE IN MATRIX-ADDRESSABLE DISPLAYS
Jennie J. Decker, Pattie L. Kelly, Ko Kurokawa, and Harry L. Snyder Feb. 1991 66 p
(DA Proj. 1L1-62716-AH-70)
(AD-A235033; HEL-TM-6-91) Avail: NTIS HC/MF A04 CSCL 05/2

This research is the second in a series of experiments undertaken to develop optimum design criteria for matrix-addressable displays. This study examined the effects of character size, luminance modulation, font, and polarity on both contextual task (reading) performance and performance in a random search task. The random search task consisted of locating a target letter or numerical within one of nine sectors on the display. Only upper case alphabetic characters and the numerals 0 through 9 were used. Using a font (3) by modulation (3) by polarity (2) by character size (3) within-subjects factorial design, only the main effects of character size, font, and polarity were found to be significant. There were no significant interactions. Post hoc analyses indicated that response speed increased as character size increased from a 7 x 9 matrix, to a 9 x 11 matrix, to an 11 x 15 matrix. Post hoc analyses revealed that response times were longest with the maximum dot font, but did not significantly differ between the Huddleston and Lincoln/MITRE fonts. Additional post hoc comparisons indicated that negative contrast (dark characters on a light background) produced significantly faster response times than did positive contrast (light characters on a dark background). GRA

N91-27008# Human Engineering Labs., Aberdeen Proving Ground, MD.
THE EFFECT OF ROTATION ON LEGIBILITY OF DOT-MATRIX CHARACTERS
Ko Kurokawa, Jennie J. Decker, and Harry L. Snyder Feb. 1991 62 p
(DA Proj. 1L1-62716-AH-70)
(AD-A235034; HEL-TM-5-91) Avail: NTIS HC/MF A04 CSCL 05/2

When dot-matrix characters are rotated, as may be in a moving map display, their dot-matrix patterns are distorted and their legibility is thus affected. In this experiment, 16 subjects performed a random search task in which they were asked to look for a target in a random character pattern. The independent variables were (1) the direction (clockwise or counterclockwise), (2) the angle of stimulus image rotation, and (3) the target character's distance from the center of the screen, which was also the center of rotation. The dependent variables were response time and response correctness. Significant effects were found for the angle of rotation, the target character's distance from the center, and the target character. The results indicate that (1) no angle-dependent mechanism is involved in performing this task and the angle of rotation influences recognition mainly through the distortion of dot-matrix patterns; (2) the target character's radial distance from the center of the screen is the determining factor for search time, while the x and y coordinates of the target contributed to dot-matrix pattern distortion; and (3) the target characters interacted differently with the angle and distance factors to determine the extent of distortion and their legibility. Means to quantify the extent of distortion are discussed and the direction for future research is suggested. GRA

N91-27009*# National Aeronautics and Space Administration. Goddard Space Flight Center, Greenbelt, MD.
PROCEEDINGS OF THE SECOND ANNUAL NASA SCIENCE INTERNET USER WORKING GROUP CONFERENCE
Lenore A. Jackson, ed. (ST Systems Corp., Lanham, MD.) and J. Patrick Gary, ed. Washington May 1991 429 p Conference held in San Mateo, CA, 11-14 Feb. 1991
(NASA-CP-3117; Rept-91B00089; NAS 1.55:3117) Avail: NTIS HC/MF A19 CSCL 05B

Copies of the agenda, list of attendees, meeting summaries, and all presentations and exhibit material are contained. Included are plenary sessions, exhibits of advanced networking applications, and user subgroup meetings on NASA Science Internet policy, networking, security, and user services and applications topics. For individual titles, see N91-27010 through N91-27042.

N91-27010*# National Aeronautics and Space Administration. Ames Research Center, Moffett Field, CA.
NSIUWG: SCIENCE NETWORKING RETREAT
Jim Hart *In* NASA. Goddard Space Flight Center, Proceedings of the Second Annual NASA Science Internet User Working Group Conference May 1991 p 51-67 (For primary document see N91-27009 18-82)
Avail: NTIS HC/MF A19 CSCL 05B

The purpose of this session was to study and identify alternatives to be recommended for the science networking areas of vision; roles and responsibilities; and technical approach and transition. This presentation is represented by charts and viewgraphs only. B.G.

N91-27011*# National Aeronautics and Space Administration. Ames Research Center, Moffett Field, CA.
NSI ORGANIZATION AND HIGHLIGHTS
Fred Rounds *In* NASA. Goddard Space Flight Center, Proceedings of the Second Annual NASA Science Internet User Working Group Conference May 1991 p 69-72 (For primary document see N91-27009 18-82)
Avail: NTIS HC/MF A19 CSCL 05B

The agenda of the NASA Science Internet (NSI) Users Working Group is given. The NSI project organization is laid out in view graph format. Also given are NSI highlights which are divided into three areas: administration, engineering, and operations. E.R.

N91-27012*# National Aeronautics and Space Administration. Ames Research Center, Moffett Field, CA.
CUSTOMER REQUIREMENTS PROCESS
Yvonne Russell and Christine M. Falsetti *In* NASA. Goddard Space Flight Center, Proceedings of the Second Annual NASA Science Internet User Working Group Conference May 1991 p 73-76 (For primary document see N91-27009 18-82)
Avail: NTIS HC/MF A19 CSCL 05B

Customer requirements are presented through three viewgraphs. One graph presents the range of services, which include requirements management, network engineering, operations, and applications support. Another viewgraph presents the project planning process. The third viewgraph presents the programs and/or projects actively supported including life sciences, earth science and applications, solar system exploration, shuttle flight engineering, microgravity science, space physics, and astrophysics. E.R.

N91-27013*# National Aeronautics and Space Administration. Ames Research Center, Moffett Field, CA.
NSI ENGINEERING REVIEW
Mark Leon *In* NASA. Goddard Space Flight Center, Proceedings of the Second Annual NASA Science Internet User Working Group Conference May 1991 p 77-82 (For primary document see N91-27009 18-82)
Avail: NTIS HC/MF A19 CSCL 05B

An engineering review is given of NASA Science Internet (NSI). An outline of the review is presented along with a list of new connections. A map is illustrated of NSI installations. And a listing is given of upgrade scheduling for 1991, 1992, and 1993. E.R.

N91-27014*# National Aeronautics and Space Administration. Ames Research Center, Moffett Field, CA.
BACKBONE UPGRADES AND DEC EQUIPMENT REPLACEMENT
Warren VanCamp *In* NASA. Goddard Space Flight Center, Proceedings of the Second Annual NASA Science Internet User Working Group Conference May 1991 p 83-87 (For primary document see N91-27009 18-82)
Avail: NTIS HC/MF A19 CSCL 05B

The NASA Science Internet (NSI) dual protocol backbone is outlined. It includes DECnet link upgrades to match TCP/IP link performance. It also includes the integration of backbone resources and central management. The phase 1 transition process is outlined. E.R.

N91-27015*# National Aeronautics and Space Administration. Goddard Space Flight Center, Greenbelt, MD.
USER SUPPORT SERVICES AND NETWORK APPLICATION DEVELOPMENT: AN OVERVIEW
J. Patrick Gary *In its* Proceedings of the Second Annual NASA Science Internet User Working Group Conference May 1991 p 89-10 (For primary document see N91-27009 18-82)
Avail: NTIS HC/MF A19 CSCL 05B

An overview is given of the user support services and network application development. The overview consists of the background, elements of NASA Science Internet (NSI) with GSFC responsibility, GSFC element objectives, and a summary of current status and plans. A conclusion of the overview is that refinement to the objectives and plans of the NSI elements under GSFC responsibility is ongoing and will continue to be influenced by user input/feedback through meetings with NSIUWG and user discipline programs, etc. E.R.

N91-27016*# National Aeronautics and Space Administration. Goddard Space Flight Center, Greenbelt, MD.
NSI SECURITY TASK: OVERVIEW
Ron Tencati *In its* Proceedings of the Second Annual NASA Science Internet User Working Group Conference May 1991 p 105-114 (For primary document see N91-27009 18-82)
Avail: NTIS HC/MF A19 CSCL 05B

An overview is presented of the NASA Science Internet (NSI) security task. The task includes the following: policies and security documentation; risk analysis and management; computer emergency response team; incident handling; toolkit development; user consulting; and working groups, conferences, and committees. E.R.

N91-27017*# National Aeronautics and Space Administration, Washington, DC.
NATIONAL RESEARCH AND EDUCATION NETWORK
Tony Villasenor *In* NASA. Goddard Space Flight Center, Proceedings of the Second Annual NASA Science Internet User Working Group Conference May 1991 p 115-133 (For primary document see N91-27009 18-82)
Avail: NTIS HC/MF A19 CSCL 05B

Some goals of this network are as follows: Extend U.S. technological leadership in high performance computing and computer communications; Provide wide dissemination and application of the technologies both to the speed and the pace of innovation and to serve the national economy, national security, education, and the global environment; and Spur gains in the U.S. productivity and industrial competitiveness by making high performance computing and networking technologies an integral part of the design and production process. Strategies for achieving these goals are as follows: Support solutions to important scientific and technical challenges through a vigorous R and D effort; Reduce the uncertainties to industry for R and D and use of this technology through increased cooperation between government, industry, and universities and by the continued use of government and government funded facilities as a prototype user for early commercial HPCC products; and Support underlying research, network, and computational infrastructures on which U.S. high performance computing technology is based. Author

N91-27018*# National Aeronautics and Space Administration. Marshall Space Flight Center, Huntsville, AL.
NASA'S USE OF FTS2000 SERVICES
Dan Scott *In* NASA. Goddard Space Flight Center, Proceedings of the Second Annual NASA Science Internet User Working Group Conference May 1991 p 137-143 (For primary document see N91-27009 18-82)
Avail: NTIS HC/MF A19 CSCL 05B

NASA's use of FTS2000 services are outlined. First, an overview of the services is given. Next, the role of program support communications (PSC) is listed. Then, the status of transition to FTS2000 services is reviewed. Finally, a list of issues of concern to NASA is provided. E.R.

N91-27019*# American Telephone and Telegraph Co., New York, NY.
FTS2000 NETWORK ARCHITECTURE
John Klenart *In* NASA. Goddard Space Flight Center, Proceedings of the Second Annual NASA Science Internet User Working Group Conference May 1991 p 145-152 (For primary document see N91-27009 18-82)
Avail: NTIS HC/MF A19 CSCL 05B

The network architecture of FTS2000 is graphically depicted. A map of network A topology is provided, with interservice nodes. Next, the four basic element of the architecture is laid out. Then, the FTS2000 time line is reproduced. A list of equipment supporting FTS2000 dedicated transmissions is given. Finally, access alternatives are shown. E.R.

N91-27020*# TGV, Inc., Santa Cruz, CA.
MULTINET TCP/P/IP FOR VAX/VMS UPDATE
L. Stuart Vance *In* NASA. Goddard Space Flight Center, Proceedings of the Second Annual NASA Science Internet User Working Group Conference May 1991 p 153-174 (For primary document see N91-27009 18-82)
Avail: NTIS HC/MF A19 CSCL 05B

Outlines of device support; DECnet interoperability; installation; MultiNet services; domain name server; Telnet; FTP; SMTP; DECwindows over TCP/IP; BSD r services; remote printing; RPC services and NFS server; NFS client; netcontrol; diagnostics; programming support; and MultiNet features are presented in viewgraph format. B.G.

N91-27021*# California Univ., Los Angeles. User Service Subgroup.
SCIENCE NETWORK RESOURCES: DISTRIBUTED SYSTEMS
Neal Cline *In* NASA. Goddard Space Flight Center, Proceedings of the Second Annual NASA Science Internet User Working Group Conference May 1991 p 177-189 (For primary document see N91-27009 18-82)
Avail: NTIS HC/MF A19 CSCL 05B

The Master Directory, which is overview information about whole data sets, is outlined. The data system environment is depicted. The question is explored of what is a prototype international directory including purpose and features. Advantages of on-line directories are listed. Interconnected directory assumptions are given. A description of given of DIF (Directory Interchange Format), which is an exchange file for directory information, along with information content of DIF and directories. The directory population status is given in a percentage viewgraph. The present and future directory interconnections status at GSFC is also listed. E.R.

N91-27022*# California Inst. of Tech., Pasadena.
OVERVIEW OF THE NASA ASTROPHYSICS DATA SYSTEM
Rick B. Pomphrey *In* NASA. Goddard Space Flight Center, Proceedings of the Second Annual NASA Science Internet User Working Group Conference May 1991 p 191-224 (For primary document see N91-27009 18-82)
Avail: NTIS HC/MF A19 CSCL 05B

Overview of the NASA Astrophysics Data Systems (ADS) is presented in the form of view graphs. The following subject areas are covered: The problem; the ADS project; architectural approach; elements of the solution; status of the effort; and the future plans. Author

N91-27023*# Space Telescope Science Inst., Baltimore, MD.
USING HST: FROM PROPOSAL TO SCIENCE
P. Shames *In* NASA. Goddard Space Flight Center, Proceedings of the Second Annual NASA Science Internet User Working Group Conference May 1991 p 225-232 (For primary document see N91-27009 18-82)
Avail: NTIS HC/MF A19 CSCL 05B

The following subject areas are covered: a short history; uses of network STSCII (general communication, science collaboration, functional activities, internal data management, and external data access); proposal/observation handling; DMF access; and future uses and requirements. Author

N91-27024*# Jet Propulsion Lab., California Inst. of Tech., Pasadena.
GALILEO: THE EARTH ENCOUNTER
Theodore C. Clarke *In* NASA. Goddard Space Flight Center, Proceedings of the Second Annual NASA Science Internet User Working Group Conference May 1991 p 233-256 (For primary document see N91-27009 18-82)
Avail: NTIS HC/MF A19 CSCL 05B

The following subject areas are covered: Galileo Veega trajectory to Jupiter; lunar science objectives; Earth science objectives; Santa 2 data flow; Galileo - the U.S./Canada connections and European connections; UV spectrometer observations during close encounter periods; phase angle and cone angle of the Earth during the Earth encounters; Lunar orbit traverse at EGA1; Moon imaging - EGA1; Galileo imaging Earth after EGA1; and Earth 1 flyby geometry. Author

N91-27025*# National Aeronautics and Space Administration. Marshall Space Flight Center, Huntsville, AL.
NASA/SPAN AND DOE/ESNET-DECNET TRANSITION STRATEGY FOR DECNET OSI/PHASE 5
Linda Porter and Phil DeMar (Fermi National Accelerator Lab., Batavia, IL.) *In* NASA. Goddard Space Flight Center, Proceedings of the Second Annual NASA Science Internet User Working Group Conference May 1991 p 259-279 (For primary document see N91-27009 18-82)
Avail: NTIS HC/MF A19 CSCL 05B

The technical issues are examined involved with the transition of very large DECnet networks from DECnet phase IV protocols to DECnet OSI/Phase V protocols. The networks involved are the NASA's Science Internet (NSI-DECnet) and the DOE's Energy Science network (ESnet-DECnet). These networks, along with the many universities and research institutions connected to them, combine to form a single DECnet network containing more than 20,000 transitions and crossing numerous organizational boundaries. Discussion of transition planning, including decisions about Phase V naming, addressing, and routing are presented. Also discussed are transition issues related to the use of non-DEC routers in the network. Author

N91-27026*# National Aeronautics and Space Administration. Goddard Space Flight Center, Greenbelt, MD.
NSIUWG SECURITY SUB-GROUP
In its Proceedings of the Second Annual NASA Science Internet User Working Group Conference May 1991 p 283-287 (For primary document see N91-27009 18-82)
Avail: NTIS HC/MF A19 CSCL 05B

The following subject areas are covered: toolkits for NSI security; security policies and documentation; and risk analysis and management. Author

N91-27027*# Sterling Software, Moffett Field, CA.
REQUIREMENTS MANAGEMENT: A CSR'S PERSPECTIVE
Joanie Thompson *In* NASA. Goddard Space Flight Center, Proceedings of the Second Annual NASA Science Internet User Working Group Conference May 1991 p 291-328 (For primary document see N91-27009 18-82)
Avail: NTIS HC/MF A19 CSCL 05B

The following subject areas are covered: customer service overview of network service request processing; Customer Service Representative (CSR) responsibility matrix; extract from a sample Memorandum of Understanding; Network Service Request Form and its instructions sample notification of receipt; and requirements management in the NASA Science Internet. Author

N91-27028*# National Aeronautics and Space Administration. Goddard Space Flight Center, Greenbelt, MD.
OVERVIEW OF THE NSI USER SUPPORT OFFICE (NSI USO)
Lenore A. Jackson *In its* Proceedings of the Second Annual NASA Science Internet User Working Group Conference May 1991 p 329-335 (For primary document see N91-27009 18-82)
Avail: NTIS HC/MF A19 CSCL 05B

Overview of the NSI User Support Office is presented in the form of view graphs. The following subject areas are covered: hot line for user questions; NSI data base updates; on-line services via NSI NIC; and toolkit distribution. Author

N91-27029*# National Aeronautics and Space Administration. Goddard Space Flight Center, Greenbelt, MD.
THE NSINIC ON-LINE SYSTEM
Brian Lev *In its* Proceedings of the Second Annual NASA Science Internet User Working Group Conference May 1991 p 337-352 (For primary document see N91-27009 18-82)
Avail: NTIS HC/MF A19 CSCL 05B

The NSI NIC on-line system is described in the form of view graphs. The following subject areas are covered: NSI history; the ADFTO's other on-line services; the current system; and the next generation of NSI NIC. Author

N91-27030*# National Aeronautics and Space Administration. Goddard Space Flight Center, Greenbelt, MD.
THE INTERNET RESOURCES GUIDE AND THE AUTOMATIC LOGIN EXECUTOR (ALEX)
J. Patrick Gary *In its* Proceedings of the Second Annual NASA Science Internet User Working Group Conference May 1991 p 353-366 (For primary document see N91-27009 18-82)
Avail: NTIS HC/MF A19 CSCL 05B

The following subject areas are covered: computational resources; library catalogs; archives; white pages; networks; and network information centers. Author

N91-27031*# Sterling Software, Moffett Field, CA.
NSI CONFERENCE SUPPORT
Susan Aaron *In* NASA. Goddard Space Flight Center, Proceedings of the Second Annual NASA Science Internet User Working Group Conference May 1991 p 367-375 (For primary document see N91-27009 18-82)
Avail: NTIS HC/MF A19 CSCL 05B

One of the many services NSI provides as an extension of customer/user support is to attend major scientific conferences. The conference effort provides NASA/OSSA scientists with many benefits: (1) scientist get to see NSI in action; they utilize the network to read email, and have recently begun to demonstrate their scientific research to their colleagues; (2) scientist get an opportunity to meet and interact with NSI Staff, which gives scientists a chance to get status on their requirements, ask about network status, get acquainted with our procedures, and learn about services; and (3) scientists are exposed to networking in a larger sense; particularly by knowing about other NASA groups who provide valuable scientific resources over the Internet. Author

N91-27032*# National Aeronautics and Space Administration. Goddard Space Flight Center, Greenbelt, MD.
CRUSH: THE NSI DATA COMPRESSION UTILITY
Ed Seiler *In its* Proceedings of the Second Annual NASA Science Internet User Working Group Conference May 1991 p 377-382 (For primary document see N91-27009 18-82)
Avail: NTIS HC/MF A19 CSCL 05B

CRUSH is a data compression utility that provides the user with several lossless compression techniques available in a single application. It is intended that the future development of CRUSH will depend upon feedback from the user community to identify new features and capabilities desired by the users. CRUSH provides an extension to the UNIX Compress program and the various VMS implementations of Compress that many users are familiar with. An important capability added by CRUSH is the addition of additional compression techniques and the option of automatically determining the best technique for a given data file. The CRUSH software is written in C and is designed to run on both VMS and UNIX systems. VMS files that are compressed will regain their full file characteristics upon decompression. To the extent possible, compressed files can be transferred between VMS and UNIX systems, and thus be decompressed on a different system than they were compressed on. Version 1 of CRUSH is currently available. This version is a VAX VMS implementation. Version 2, which has the full range of capabilities for both VMS and UNIX implementations, will be available shortly. Author

N91-27033*# Georgia Univ., Athens.
ELECTRONIC SOFTWARE SUBMITTAL/DISTRIBUTION
L. Scott Clark *In* NASA. Goddard Space Flight Center, Proceedings of the Second Annual NASA Science Internet User Working Group Conference May 1991 p 383-389 (For primary document see N91-27009 18-82)
Avail: NTIS HC/MF A19 CSCL 05B

Information on electronic software submittal and distribution is given in viewgraph form. A COSMIC program overview, and submittal/distribution issues of connectivity, software distribution, and solicitation of input/feedback are covered. Author

N91-27034*# National Aeronautics and Space Administration. Goddard Space Flight Center, Greenbelt, MD.
THE NASA MASTER DIRECTORY QUICK REFERENCE GUIDE
In its Proceedings of the Second Annual NASA Science Internet User Working Group Conference May 1991 p 394-400 (For primary document see N91-27009 18-82)
Avail: NTIS HC/MF A19 CSCL 05B

The NASA Master Directory (MD) is a free, online, multidisciplinary directory of space and Earth science data sets (NASA and non-NASA data) that are of potential interest to the NASA-sponsored research community. The MD contains high-level descriptions of data sets, other data systems and archives, and campaigns and projects. It provides mechanisms for searching for data sets by important criteria such as geophysical parameters, time, and spatial coverage. The MD also provides information on ordering the data. In order to simplify the process of finding more detailed information or accessing online data, the MD provides automatic connections to a number of data systems such as the NASA Climate Data System, the Planetary Data System, the NASA Ocean Data System, the Pilot Land Data System, and others. The MD also provides general information about many data systems, data centers, and coordinated data analysis projects. It represents the first major step in the Catalog Interoperability project, whose objective is to enable researchers to quickly and efficiently identity, obtain information about, and get access to space and Earth science data. Author

N91-27035*# National Aeronautics and Space Administration. Goddard Space Flight Center, Greenbelt, MD.
A GUIDE TO NASA'S PILOT LAND DATA SYSTEM (PLDS)
In its Proceedings of the Second Annual NASA Science Internet User Working Group Conference May 1991 p 403-404 (For primary document see N91-27009 18-82)
Avail: NTIS HC/MF A19 CSCL 05B

NASA's Pilot Land Data System (PLDS) is a distributed information management system designed to support NASA's land science community. The PLDS provides a wide range of services including management of information about scientific data, access to a library of scientific data, a data ordering capability, communications, connection to data analysis facilities, and electronic mail. The PLDS provides these services by offering the scientist the capability to search for and order data, and to communicate electronically with other scientists and computers. Three functions enable scientists to find what data are available and where they reside. The first two, Find data summaries and Read detailed descriptions give summary and detailed descriptions about data sets or groups of related data sets, science, projects, and institutions which archive land data. The third, gives information about specific pieces of data. This last function has two components, Search systemwide inventory and Search local inventory. The first component enables the user to find data elements (images, geological samples, transects, maps, etc.) that exist anywhere in the PLDS while the second has only information about data at the local site. The first enables the user to find pieces of data from several different data sets with the same temporal and spatial coverage and other elements common to most data sets, while the second allows the user to select a data

set based on these descriptors and on those that are unique to a data set. The PLDS provides capabilities that enable electronic file transfers, intercomputer connection, and electronic mail. Both TCP/IP and DECnet protocols are supported via the NASA Science Internet (NIS). Access is also available through Telenet. Author

N91-27036*# Georgia Univ., Athens.
COSMIC: SOFTWARE CATALOG 1991 EDITION DISKETTE FORMAT
In NASA. Goddard Space Flight Center, Proceedings of the Second Annual NASA Science Internet User Working Group Conference May 1991 p 406-410 (For primary document see N91-27009 18-82)
Avail: NTIS HC/MF A19 CSCL 05B

This PC edition of the annual COSMIC Software contains descriptions of the over 1,200 computer programs available for use within the United States as of January 1, 1991. By using the PC version of the catalog, it is possible to conduct extensive searches of the software inventory for programs that meet specific criteria. Elements such as program keywords, hardware specifications, source code languages, and title acronyms can be used for the basis of such searches. After isolating those programs that might be of best interest to the user, it is then possible to either view at the monitor, or generate a hardcopy listing of all information on those packages. In addition to the program elements that the user can search on, information such as total program size, distribution media, and program price, as well as extensive abstracts on the program, are also available to the user at this time. Another useful feature of the catalog allows for the retention of programs that meet certain search criteria between individual sessions of using the catalog. This allows users to save the information on those programs that are of interest to them in different areas of application. They can then recall a specific collection of programs for information retrieval or further search reduction if desired. In addition, this version of the catalog is adaptable to a network/shared resource environment, allowing multiple users access to a single copy of the catalog database simultaneously. Author

N91-27037*# TGV, Inc., Santa Cruz, CA.
SOFTWARE PRODUCT DESCRIPTION
In NASA. Goddard Space Flight Center, Proceedings of the Second Annual NASA Science Internet User Working Group Conference May 1991 p 413-425 (For primary document see N91-27009 18-82)
Avail: NTIS HC/MF A19 CSCL 05B

An overview of the MultiNet system is presented. Services, supported configurations, remote printer services, netstat, netcontrol, DECnet interoperability services, and programming libraries are briefly described. B.G.

N91-27038*# Sterling Federal Systems, Inc., Moffett Field, CA.
NSI OPERATIONS CENTER
Nancy L. Zanley *In* NASA. Goddard Space Flight Center, Proceedings of the Second Annual NASA Science Internet User Working Group Conference May 1991 p 429-435 (For primary document see N91-27009 18-82)
Avail: NTIS HC/MF A19 CSCL 05B

The NASA Science Internet (NSI) Network Operations Staff is responsible for providing reliable communication connectivity for the NASA science community. As the NSI user community expands, so does the demand for greater interoperability with users and resources on other networks (e.g., NSFnet, ESnet), both nationally and internationally. Coupled with the science community's demand for greater access to other resources is the demand for more reliable communication connectivity. Recognizing this, the NASA Science Internet Project Office (NSIPO) expands its Operations activities. By January 1990, Network Operations was equipped with a telephone hotline, and its staff was expanded to six Network Operations Analysts. These six analysts provide 24-hour-a-day, 7-day-a-week coverage to assist site managers with problem determination and resolution. The NSI Operations staff monitors network circuits and their associated routers. In most instances, NSI Operations diagnoses and reports problems before users realize a problem exists. Monitoring of the NSI TCP/IP Network is currently being done with Proteon's Overview monitoring system. The Overview monitoring system displays a map of the NSI network utilizing various colors to indicate the conditions of the components being monitored. Each node or site is polled via the Simple Network Monitoring Protocol (SNMP). If a circuit goes down, Overview alerts the Network Operations staff with an audible alarm and changes the color of the component. When an alert is received, Network Operations personnel immediately verify and diagnose the problem, coordinate repair with other networking service groups, track problems, and document problem and resolution into a trouble ticket data base. NSI Operations offers the NSI science community reliable connectivity by exercising prompt assessment and resolution of network problems. Author

N91-27039*# National Aeronautics and Space Administration. Ames Research Center, Moffett Field, CA.
NSI WHITE PAGES PROJECT: X.500 DIRECTORY SERVICE
John Yin *In* NASA. Goddard Space Flight Center, Proceedings of the Second Annual NASA Science Internet User Working Group Conference May 1991 p 438-441 (For primary document see N91-27009 18-82)
Avail: NTIS HC/MF A19 CSCL 05B

Information is given on the X.500 Directory Service in viewgraph form. The X.500 is an international standard for a globally distributed directory that provides basic addressing information, detailed information on countries, organizations, people, and resources. The present pilot project is able to access information in 14 countries. Author

N91-27040*# National Aeronautics and Space Administration. Ames Research Center, Moffett Field, CA.
NSI CUSTOMER SERVICE REPRESENTATIVES AND USER SUPPORT OFFICE: NASA SCIENCE INTERNET
In NASA. Goddard Space Flight Center, Proceedings of the Second Annual NASA Science Internet User Working Group Conference May 1991 p 444-447 (For primary document see N91-27009 18-82)
Avail: NTIS HC/MF A19 CSCL 05B

The NASA Science Internet, (NSI) was established in 1987 to provide NASA's Offices of Space Science and Applications (OSSA) missions with transparent wide-area data connectivity to NASA's researchers, computational resources, and databases. The NSI Office at NASA/Ames Research Center has the lead responsibility for implementing a total, open networking program to serve the OSSA community. NSI is a full-service communications provider whose services include science network planning, network engineering, applications development, network operations, and network information center/user support services. NSI's mission is to provide reliable high-speed communications to the NASA science community. To this end, the NSI Office manages and operates the NASA Science Internet, a multiprotocol network currently supporting both DECnet and TCP/IP protocols. NSI utilizes state-of-the-art network technology to meet its customers' requirements. THe NASA Science Internet interconnects with other national networks including the National Science Foundation's NSFNET, the Department of Energy's ESnet, and the Department of Defense's MILNET. NSI also has international connections to Japan, Australia, New Zealand, Chile, and several European countries. NSI cooperates with other government agencies as well as academic and commercial organizations to implement networking technologies which foster interoperability, improve reliability and performance, increase security and control, and expedite migration to the OSI protocols. Author

N91-27041*# National Aeronautics and Space Administration. Ames Research Center, Moffett Field, CA.
THE NASA SCIENCE INTERNET: AN INTEGRATED APPROACH TO NETWORKING
Fred Rounds *In* NASA. Goddard Space Flight Center, Proceedings of the Second Annual NASA Science Internet User Working Group

Conference May 1991 p 448 (For primary document see N91-27009 18-82)
Avail: NTIS HC/MF A19 CSCL 05B

An integrated approach to building a networking infrastructure is an absolute necessity for meeting the multidisciplinary science networking requirements of the Office of Space Science and Applications (OSSA) science community. These networking requirements include communication connectivity between computational resources, databases, and library systems, as well as to other scientists and researchers around the world. A consolidated networking approach allows strategic use of the existing science networking within the Federal government, and it provides networking capability that takes into consideration national and international trends towards multivendor and multiprotocol service. It also offers a practical vehicle for optimizing costs and maximizing performance. Finally, and perhaps most important to the development of high speed computing is that an integrated network constitutes a focus for phasing to the National Research and Education Network (NREN). The NASA Science Internet (NSI) program, established in mid 1988, is structured to provide just such an integrated network. A description of the NSI is presented. Author

N91-27042*# National Aeronautics and Space Administration. Ames Research Center, Moffett Field, CA.
NSI DIRECTED TO CONTINUE SPAN'S FUNCTIONS
Fred Rounds *In* NASA. Goddard Space Flight Center, Proceedings of the Second Annual NASA Science Internet User Working Group Conference May 1991 p 449 (For primary document see N91-27009 18-82)
Avail: NTIS HC/MF A19 CSCL 05B

During a series of network management retreats in June and July 1990, representatives from NASA Headquarters Codes O and S agreed on networking roles and responsibilities for their respective organizations. The representatives decided that NASA Science Internet (NSI) will assume management of both the Space Physics Analysis Network (SPAN) and the NASA Science Network (NSN). SPAN is now known as the NSI/DECnet, and NSN is now known as the NSI/IP. Some management functions will be distributed between Ames Research Center (ARC) and Goddard Space Flight Center (GSFC). NSI at ARC has the lead role for requirements generation and networking engineering. Advanced Applications and the Network Information Center is being developed at GSFC. GSFC will lead the NSI User Services, but NSI at Ames will continue to provide the User Services during the transition. The transition will be made as transparent as possible for the users. DECnet service will continue, but is now directly managed by NSI at Ames. NSI will continue to work closely with routing center managers at other NASA centers, and has formed a transition team to address the change in management. An NSI/DECnet working group had also been formed as a separate engineering group within NSI to plan the transition to Phase 5, DECnet's approach to Open System Integration (OSI). Transition is not expected for a year or more due to delays in produce releases. Plans to upgrade speeds in tail circuits and the backbone are underway. The proposed baseline service for new connections is up to 56 Kbps; 9.6 Kbps lines will gradually be upgraded as requirements dictate. NSI is in the process of consolidating protocol traffic, tail circuits, and the backbone. Currently NSI's backbone is fractional T1; NSI will go to full T1 service as soon as it is feasible. Author

N91-27043# Oak Ridge National Lab., TN.
CATALOG OF DATA BASES AND REPORTS
Feb. 1991 122 p
(Contract DE-AC05-84OR-21400)
(DE91-011516; ORNL/CDIAC-34/R1) Avail: NTIS HC/MF A06

This booklet provides information about the many reports and other materials made available by the U.S. Department of Energy's Carbon Dioxide Research Program (CDRP). It is divided into six sections plus an author and a title index. The reports in Section A provide information about the scope, activities, and direction of the CDRP. Sections B, C, and D contain information about research, workshops, symposia, and reviews that have been sponsored by CDRP. Section E describes reports about research in the joint program of the U.S. Department of Agriculture and CDRP. The computer model packages (CMPs) and numeric data packages (NDPs) (described in Section F) have been compiled by CDRP's Carbon Dioxide Information Analysis Center (CDIAC). CMPs and NDPs include documents and magnetic tapes or floppy diskettes. The documentation provides complete descriptions of the data set, describes limitations and restrictions of the data, suggests data applications, provides tabular listings and graphical displays of the data, and includes reprints of pertinent literature. DOE

N91-27044# Fermi National Accelerator Lab., Batavia, IL.
INTEGRATING UNIX WORKSTATION INTO EXISTING ONLINE DATA ACQUISITION SYSTEMS FOR FERMILAB EXPERIMENTS
G. Oleynik Mar. 1991 13 p Presented at the Conference on Computing in High Energy Physics, Tsukuba (Japan), 11-15 Mar. 1991
(Contract DE-AC02-76CH-03000)
(DE91-011974; FNAL/C-91/86; CONF-910373-6) Avail: NTIS HC/MF A03

With the availability of cost effective computing prior from multiple vendors of UNIX workstations, experiments at Fermilab are adding such computers to their VMS based online data acquisition systems. In anticipation of this trend, the software products available in the widely used VAXONLINE and PANDA data acquisition software systems were extended to provide support for integrating these workstations into existing distributed online systems. The software packages provided pave the way for the smooth migration of applications from the current Data Acquisition Host and Monitoring computers running the VMS operating systems, to UNIX based computers of various flavors. Software is provided for Online Event Distribution from VAXONLINE and PANDA, integration of Message Reporting Facilities, and a framework under UNIX for experiments to monitor and view the raw event data produced at any level in their DA system. Software was developed that allows host UNIX computers to communicate with intelligent front-end embedded read-out controllers and processor boards running the pSOS operating system. Both RS-232 and Ethernet control paths are supported. This enables calibration and hardware monitoring applications to be migrated to these platforms. DOE

N91-27045# Lawrence Livermore National Lab., CA.
A SYSTEM FOR UNIX COMMAND RETRIEVAL USING A MULTILAYERED NEURAL NETWORK Ph.D. Thesis
D. R. Preston Apr. 1991 72 p
(Contract W-7405-eng-48)
(DE91-012105; UCRL-LR-107023) Avail: NTIS HC/MF A04

This project developed a system that allows a user to access information on UNIX commands by entering a natural language description of the function the user wishes to have performed. The user is not constrained by having to phrase the query in Boolean notation, and the system does not use strict and-ing and or-ing to retrieve the information. This was done in two parts: first, the UNIX man pages were indexed using statistically-based automatic indexing techniques. This process resulted in a list of the terms contained in a man page document that are most useful for recalling the command described in that man page. Second, a multilayer neural network was defined that associated the extracted terms with their commands. The multilayer neural network allows a retrieval paradigm that falls between and-ing the query terms and or-ing the query terms, and allows the user to control the broadness of the results. DOE

83 ECONOMICS AND COST ANALYSIS

Includes cost effectiveness studies.

N91-27116*# Mississippi Valley State Univ., Itta Bena. Dept. of Computer Science and Mathematics.
PLANETARY SPACECRAFT COST MODELING UTILIZING LABOR ESTIMATING RELATIONSHIPS Final Report
Raymond Williams *In* Houston Univ., NASA/ASEE Summer Faculty Fellowship Program, 1990, Volume 2 Dec. 1990 6 p
(For primary document see N91-27103 18-99)
(Grant NGT-44-005-803)
Avail: NTIS HC/MF A09 CSCL 05C

84 LAW, POLITICAL SCIENCE AND SPACE POLICY

Includes NASA appropriation hearings; aviation law; space law and policy; international law; international cooperation; and patent policy.

N91-27046# Committee on Science, Space and Technology (U.S. House).
NATIONAL AERONAUTICS AND SPACE ADMINISTRATION MULTIYEAR AUTHORIZATION ACT OF 1991
George E. Brown, Jr., Ralph M. Hall, Tom Lewis, F. James Sensenbrenner, Jr., and Tim Valentine Washington GPO 23 Apr. 1991 22 p A bill on H.R. 1988 referred to the Committee on Science, Space and Technology, 102d Congress, 1st Session, 23 Apr. 1991
Avail: Document Room, House of Representatives, Washington, DC 20515 HC free

Presented here is the text for a bill to authorize appropriations to the National Aeronautics and Space Administration (NASA) for research and development, space flight, control, data communications, construction of facilities, research and program management, and the Inspector General, as well as for other purposes. Author

85 URBAN TECHNOLOGY AND TRANSPORTATION

Includes applications of space technology to urban problems; technology transfer; technology assessment; and surface and mass transportation.

For related information see also *03 Air Transportation and Safety, 16 Space Transportation,* and *44 Energy Production and Conversion.*

No abstracts in this category.

88 SPACE SCIENCES (GENERAL)

No abstracts in this category.

89 ASTRONOMY

Includes radio, gamma-ray, and infrared astronomy, and astrometry.

N91-27047 Florida Univ., Gainesville. Dept. of Astronomy.
A CATALOG OF HIGH RESOLUTION JOVIAN DECAMETRIC RADIO NOISE BURST SPECTRA, VOLUME 1
R. S. Flagg, W. B. Greenman, F. Reyes, and T. D. Carr 1991 194 p
(Grant NSF AST-89-20861)
Copyright Avail: Issuing Activity

The probability of receiving radio emissions depends on the observing frequency, as well as the Central Meridian Longitude (CML) of Jupiter and the orbital location of the volcanic moon Io. The two main portions of this catalog are the classification and the storm sections. In the classification section, spectra typical of the many and varied burst types which were observed, were recorded. In the storm section, spectral records from 22 Jupiter storms recorded over a 17 year period are shown along with measurements of such burst parameters as drift rate, separation, and intensity. B.G.

N91-27048# Mission Research Corp., Nashua, NH.
CBSD VERSION 2 COMPONENT MODELS OF THE IR CELESTIAL BACKGROUND
John P. Kennealy and Gene A. Glaudell 7 Dec. 1990 129 p
(Contract F19628-88-C-0014)
(AD-A235372; GL-TR-90-0328; SR-1) Avail: NTIS HC/MF A07 CSCL 03/1

CBSD Version 2 addresses the development of algorithms and software which implement realistic models of all the primary celestial background phenomenologies, including solar system, galactic, and extra-galactic features. During 1990, the CBSD program developed and refined IR scene generation models for the zodiacal emission, thermal emission from asteroids and planets, and the galactic point source background. Chapters in this report are devoted to each of those areas. Ongoing extensions to the point source module for extended source descriptions of nebulae and HII regions are briefly discussed. Treatment of small galaxies will also be a natural extension of the current CBSD point source module. Although no CBSD module yet exists for inter-stellar IR cirrus, MRC has been working closely with the Royal Aerospace Establishment in England to achieve a data-base understanding of cirrus fractal characteristics. The CBSD modules discussed in Chapters 2, 3, and 4 are all now operational and have been employed to generate a significant variety of scenes. CBSD scene generation capability has been well accepted by both the IR astronomy community and the DoD user community and directly supports the SDIO SSGM program. GRA

N91-27049 Tel-Aviv Univ. (Israel). Dept. of Physics and Astronomy.
THE LIGHT CURVE OF THE MAGNETIC STAR AM - HERCULIS M.S. Thesis
Addie Ney Jul. 1990 80 p In HEBREW; ENGLISH summary
(ITN-91-85108) Copyright Avail: Tel-Aviv Univ., Exact Sciences Library, Ramat Aviv 69978, Israel

AM - Herculis is a cataclysmic variable binary system, containing a strongly magnetic white-dwarf primary, accreting matter from a red, low-mass secondary. Since its discovery, 14 years ago, this system, and others of the same type which were discovered since then, have been the object of much interest, thought and studies. In this work the optical light curve of the system is studied, in order to search for modulations of the observed primary minimum time, and to construct a geometrical model for the system that will simulate its observed light curve. Modulations of the primary minimum times, if found, may be caused by modulations of the system's period, implying the existence of physical processes. Within the framework of this study, observations of the system were carried out at the Wise Observatory in Mitzpe Ramon. The search for primary minimum time modulations was based on these observations, and on earlier observational results. The system's optical light curve is quite unstable; its intensity and shape vary

within short periods of time. A simulation of the light curve using a simple geometrical model, and some simple basic assumptions, and without considering complicated physical processes, implies that most of the features of the system's light curve are accounted for by the geometrical structure of the system, and changes in a few parameters in the model can account for the variations in the light curve from one observation to another. Author (ISA)

N91-27050# California Univ., Berkeley. Lawrence Berkeley Lab.
PRELIMINARY ESTIMATES OF CORE-COLLAPSE SUPERNOVA RATES FROM THE BERKELEY AUTOMATED SUPERNOVA SEARCH
C. Pennypacker, S. Perlmutter, R. A. Muller, N. Hamilton, C. Smith, T. Sasseen, S. Carlson, H. Marvin, Li-Ping Wang, and F. Crawford et al Nov. 1990 8 p Presented at the Supernova Watch Workshop, Los Angeles, 26 Nov. - 1 Dec. 1990
(Contract DE-AC03-76SF-00098)
(DE91-011824; LBL-30590; CONF-9011198-1) Avail: NTIS HC/MF A02

Over the last few years, the Berkeley Automated Supernova Search has discovered 19 supernova. Preliminary measurements of supernova rates are presented from a subset of these supernovae, which were found from a sample of well-monitored galaxies. Two effects are apparent: a surprising number of the supernovae are Type Ic supernovae, and most (17 out of 19) of the supernovae are in late spiral galaxies. Less luminous supernovae may still be escaping attention. If the Milky Way galaxy is a late spiral, the core-collapse supernova rate (i.e., for supernovae of types II, Ib, and Ic) should be at least one supernova every 44 + or - 9 years (assuming H = 75 km/sec/Mpc). A crude estimate of the core collapse supernova rate in Sc and Sbc galaxies within 5 Mpc would be one supernova every 7 years. These rates have important implications for the design of supernova neutrino, gamma-ray, and gravity-wave detectors. Plans were developed to extend the search to a better site with more sensitivity to understand the true core-collapse supernova rate in nearby galaxies. DOE

N91-27051# California Univ., Berkeley. Lawrence Berkeley Lab.
THE BERKELEY/ANGLO-AUSTRALIAN OBSERVATORY HIGH-REDSHIFT SUPERNOVA SEARCH Progress Report
G. Goldhaber, S. Perlmutter, C. Pennypacker, H. Marvin, R. A. Muller, W. Couch, and Brian Boyle (Cambridge Univ., England) Nov. 1990 23 p Presented at the Supernova Watch Workshop, Los Angeles, 26 Nov. - 1 Dec. 1990
(Contract DE-AC03-76SF-00098)
(DE91-012348; LBL-30591; CONF-9011198-3) Avail: NTIS HC/MF A03

There are two main efforts related to supernovae in progress at Berkeley. The first is an automated supernova search for nearby supernovae, which was already discussed by Carl Pennypacker at this conference. The second is a search for distant supernovae, in the z = 0.3 to 0.5 region, aimed at measuring Omega. It is the latter that I want to discuss in this paper. DOE

90 ASTROPHYSICS

Includes cosmology; celestial mechanics; space plasmas; and interstellar and interplanetary gases and dust.
For related information see also *75 Plasma Physics.*

N91-27052# Lawrence Livermore National Lab., CA.
WEAK INTERACTIONS AND PRESUPERNOVA EVOLUTION
M. B. Aufderheide (Lawrence Livermore National Lab., CA.) 19 Feb. 1991 12 p Presented at the Workshop on Strong, Weak, and Electromagnetic Interactions in Nuclei and Astrophysics, Livermore, 3-4 Jan. 1991
(Contracts W-7405-eng-48; DE-FG02-88ER-40388)
(DE91-011543; UCRL-JC-106597; CONF-9101100-1) Avail: NTIS HC/MF A03

The role of weak interactions, particularly electron capture and Beta(-) decay, in presupernova evolution is discussed. The present uncertainty in these rates is examined and the possibility of improving the situation is addressed. DOE

N91-27053# Sandia National Labs., Albuquerque, NM.
INVESTIGATION OF PLESSITE IN IRON METERORITES AND LABORATORY Fe-Ni(P) ALLOYS
J. Zhang, D. B. Williams, and J. I. Goldstein (Lehigh Univ., Bethlehem, PA.) 1991 3 p Presented at the Lunar and Planetary Science Conference, Houston, 18-22 Mar. 1991
(Contract DE-AC04-76DP-00789)
(DE91-010858; SAND-91-0563C; CONF-9103134-3) Avail: NTIS HC/MF A01

Plessite in iron meteorites is a two phase structure with an fcc precipitate phase in a bcc matrix. After Fe-Ni martensite forms during slow cooling, the martensite decomposition occurs at different temperatures. The morphology of the precipitates and the Ni content of both precipitate and matrix vary with the local average Ni composition of the plessite. The plessite structure of two octahedrites, Carlton and Grant, was characterized using the analytical electron microscope (AEM). The composition of the taenite precipitates in various regions of plessite which have 9 to 13 wt pct. and 15 to 20 wt pct. Ni composition were measured using an x ray energy dispersive spectrometer (EDS) in the AEM. To understand the phase transformation processes which occurred during the plessite formation, an experimental set of Fe-Ni binary and Fe-Ni-P ternary alloys were made and analyzed also using the AEM. The alloys, which have 15 to 30 wt pct. Ni (0.2 to 0.3 wt pct. P for ternary alloys), were first homogenized at 1200 C and quenched to liquid nitrogen temperature to form martensite. They were then isothermally heat treated for 60 to 400 days in the temperature range from 450 to 300 C. Two phase structures, which are similar to those of plessite, were formed in these alloys. The Fe-Ni phase equilibria measured in the decomposed martensite alloys can be used to explain the difference in Ni composition between precipitates in the high Ni and low Ni plessite regions. DOE

N91-27113*# Alma Coll., MI. Dept. of Chemistry.
SOLUTIONS TO PROBLEMS OF WEATHERING IN ANTARCTIC EUCRITES Final Report
Melissa M. Strait *In* Houston Univ., NASA/ASEE Summer Faculty Fellowship Program, 1990, Volume 2 Dec. 1990 13 p (For primary document see N91-27103 18-99)
(Grant NGT-44-005-803)
Avail: NTIS HC/MF A09 CSCL 03B

91 LUNAR AND PLANETARY EXPLORATION

Includes planetology; and manned and unmanned flights.
For spacecraft design or space stations see *18 Spacecraft Design, Testing and Performance.*

N91-27054 Cincinnati Univ., OH.
A GRAVITATIONALLY CONSISTENT SECOND-ORDER ANALYTIC SECULAR SOLUTION FOR THE POINT-MASS MOTION OF THE EIGHT PRINCIPAL PLANETS Ph.D. Thesis
Thomas Jerome Kelly 1990 153 p
Avail: Univ. Microfilms Order No. DA9108682

A first-order gravitationally consistent analytic planetary theory and through second order a semi-analytic solution for the point-mass motion of the eight principal planets were developed. In place of the Earth the motion of the Earth-Moon barycenter is determined. The Einstein, Infeld and Hoffman (EIH) N-body relativistic equations serves as the basis in which the solar-system dynamics are modeled mathematically. A Hamiltonian is constructed for the system described by the EIH equations. Within the context of Deprit's perturbation method, two subsequent canonical Lie transformations are constructed which completely normalize an appropriately reduced form of the EIH Hamiltonian

through first order in the masses. Implicit variables are used throughout the analytic developments to avoid expansions in the mean anomaly and eccentricity. Author

N91-27055*# National Aeronautics and Space Administration, Washington, DC.
REPORT OF THE 90-DAY STUDY ON HUMAN EXPLORATION OF THE MOON AND MARS
Nov. 1989 159 p
(NASA-TM-102999; NAS 1.15:102999) Avail: NTIS HC/MF A08 CSCL 03B

The basic mission sequence to achieve the President's goal is clear: begin with Space Station Freedom in the 1990's, return to the Moon to stay early in the Next century, and then journey to Mars. Five reference approaches are modeled building on past programs and recent studies to reflect wide-ranging strategies that incorporate varied program objectives, schedules, technologies, and resource availabilities. The reference approaches are (1) balance and speed; (2) the earliest possible landing on Mars; (3) reduce logistics from Earth; (4) schedule adapted to Space Station Freedom; and (5) reduced scales. The study and programmatic assessment have shown that the Human Exploration Initiative is indeed a feasible approach to achieving the President's goals. Several reasonable alternatives exist, but a long-range commitment and significant resources will be required. However, the value of the program and the benefits to the Nation are immeasurable.
B.G.

N91-27056*# Arizona State Univ., Tempe. Dept. of Geology.
RADAR-AEOLIAN ROUGHNESS PROJECT
Ronald Greeley, A. Dobrovolskis, L. Gaddis, J. D. Iversen, N. Lancaster, Rodman N. Leach, K. Rasnussen, S. Saunders, J. VanZyl, and S. Wall (Jet Propulsion Lab., California Inst. of Tech., Pasadena.) et al Washington NASA Jun. 1991 128 p
(Grant NsG-7415)
(NASA-CR-4378; NAS 1.26:4378) Avail: NTIS HC/MF A07 CSCL 03B

The objective is to establish an empirical relationship between measurements of radar, aeolian, and surface roughness on a variety of natural surfaces and to understand the underlying physical causes. This relationship will form the basis for developing a predictive equation to derive aeolian roughness from radar backscatter. Results are given from investigations carried out in 1989 on the principal elements of the project, with separate sections on field studies, radar data analysis, laboratory simulations, and development of theory for planetary applications. Author

N91-27057*# National Aeronautics and Space Administration. Ames Research Center, Moffett Field, CA.
SAND AND DUST ON MARS
Ronald Greeley (Arizona State Univ., Tempe.) and Robert M. Haberle May 1991 65 p Workshop held in Tempe, AZ, 4-5 Feb. 1991
(Contract NCC2-346)
(NASA-CP-10074; A-91130; NAS 1.55:10074) Avail: NTIS HC/MF A04 CSCL 03B

Mars is a planet of high scientific interest. Various studies are currently being made that involve vehicles that have landed on Mars. Because Mars is known to experience frequent wind storms, mission planners and engineers require knowledge of the physical and chemical properties of Martian windblown sand and dust, and the processes involved in the origin and evolution of sand and dust storms. For individual titles, see N91-27058 through N91-27082.

N91-27058*# National Aeronautics and Space Administration. Ames Research Center, Moffett Field, CA.
THE CHEMISTRY AND MINERALOGY OF MARS SOIL AND DUST
A. Banin (Hebrew Univ. of Jerusalem, Rehovot, Israel) *In its* Sand and Dust on Mars May 1991 p 11-12 (For primary document see N91-27057 18-91)
Avail: NTIS HC/MF A04 CSCL 03B

A single geological unit consisting of fine, apparently weathered soil material is covering large portions of the surface of Mars. This soil material has been thoroughly homogenized by global dust storms and it is plausible to assume that Mars dust is strongly correlated with it. The chemical-elemental composition of the soil was directly measured by the Viking Landers. Positive detection of Si, Al, Fe, Mg, Ca, Ti, S, Cl, and Br was achieved. Analyses of the SNC meteorites, a group of meteorites that has been suggested to be ejected Martian rocks, supply additional elemental-concentration data, broadening considerably the chemical data-base on the surface materials. A composition model for Mars soil, giving selected average elemental concentrations of major and trace elements, was recently suggested. It was constructed by combining the Viking Lander data, the SNC meteorite analyses, and other analyses. The mineralogy of the surface materials on Mars has not been directly measured yet. By use of various indirect approaches, including chemical correspondence to the surface analyses, spectral analogies, simulations of Viking Lander experiments, analyses of the SNC meteorites and various modeling efforts, the mineralogical composition was constrained to some extent. No direct analyses of soil reactivity have been done yet. Indirect evidence, mostly from the Viking biology experimental results, suggests that the soil probably has a slightly acidic reaction and is generally oxidized. Unambiguous identification of the Mars soil minerals by direct mineralogical analyses, and non-disturbed or in-situ measurements of the soil's reactivity, are of primary importance in future Mars research. Author

N91-27059*# Arizona State Univ., Tempe. Dept. of Geology.
THE DISTRIBUTION OF PARTICULATE MATERIAL ON MARS
Philip R. Christensen *In* NASA. Ames Research Center, Sand and Dust on Mars May 1991 p 13-15 (For primary document see N91-27057 18-91)
Avail: NTIS HC/MF A04 CSCL 03B

The surface materials on Mars were extensively studied using a variety of spacecraft and Earth-based remote sensing observations. These measurements include: (1) diurnal thermal measurements, used to determine average particle size, rock abundance, and the presence of crusts; (2) radar observations, used to estimate the surface slope distributions, wavelength scale roughness, and density; (3) radio emission observations, used to estimate subsurface density; (4) broadband albedo measurements, used to study the time variation of surface brightness and dust deposition and removal; and (5) color observations, used to infer composition, mixing, and the presence of crusts. Remote sensing observations generally require some degree of modeling to interpret, making them more difficult to interpret than direct observations from the surface. They do, however, provide a means for examining the surface properties over the entire planet and a means of sampling varying depths within the regolith. Albedo and color observations only indicate the properties of the upper-most few microns, but are very sensitive to thin, sometimes emphemeral dust coatings. Thermal observations sample the upper skin depth, generally 2 to 10 cm. Rock abundance measurements give an indirect indication of surface mantling, where the absence of rocks suggests mantles of several meters. Finally, radar and radio emission data can penetrate several meters into the surface, providing an estimate of subsurface density and roughness.
Author

N91-27060*# Colorado Univ., Boulder.
RECENT STUDIES OF THE OPTICAL PROPERTIES OF DUST AND CLOUD PARTICLES IN THE MARS ATMOSPHERE AND THE INTERANNUAL FREQUENCY OF GLOBAL DUST STORMS
R. T. Clancy, S. W. Lee, and D. O. Muhleman (California Inst. of Tech., Pasadena.) *In* NASA. Ames Research Center, Sand and Dust on Mars May 1991 p 16-17 (For primary document see N91-27057 18-91)
Avail: NTIS HC/MF A04 CSCL 03B

The results of research with two distinctly separate sets of observations yield new information on the optical properties of

particulate scatterers in the Mars atmosphere, and on the interannual variability of the abundance of such scatterers in the Mars atmosphere. The first set of observations were taken by the IRTM (Infrared Thermal Mapper) instrument onboard the Viking Orbiters, during the period 1976 to 1980. Several hundred emission phase function (EPF) sequences were obtained over the Viking mission, in which the IRTM visual brightness channel observed the same area of surface/atmosphere as the spacecraft passed overhead. The 1 to 2 percent accuracy of calibration and the phase-angle coverage that characterizes these data make them ideally suited to determining both the optical depths and optical properties of dust and cloud scatterers in the Mars atmosphere versus latitude, longitude, seasons (L sub s), and surface elevation over the extended period of Viking observations. The EPF data were analyzed with a multiple scattering radiative transfer code to determine dust single scattering albedos which are distinctly higher than indicated by the Viking Lander observations. The second set of observations regard ground-based observations of the 1.3 to 2.6 mm rotational transitions of CO in the Martian atmosphere. The low-to-mid latitude average of the atmospheric temperature profile (0 to 70 km altitude) were derived from a number of such observations over the 1980 to 1990 period. Author

N91-27061*# National Aeronautics and Space Administration. Lewis Research Center, Cleveland, OH.
EFFECTS OF MARTIAN DUST ON POWER SYSTEM COMPONENTS
J. R. Gaier and M. E. Perez-Davis *In* NASA. Ames Research Center, Sand and Dust on Mars May 1991 p 18-19 (For primary document see N91-27057 18-91)
Avail: NTIS HC/MF A04 CSCL 03B

Before large power systems for manned exploration of the Martian surface can be put into place, it must be determined how their performance will be affected by the Martian environment. A program was started to assess the impact of these environmental factors on power system performance, and to find ways to mitigate the degradative effects. The effects of blowing dust on photovoltaic (PV) and radiator surfaces is studied. Extensive use was made of the Martian Surface Wind Tunnel (MARSWIT) located at NASA-Ames to simulate Martian winds. Two basic types of experiment sets were run. In the first, the threshold clearing velocity of dust deposited on PV coverslip material and high emissivity radiator materials in clear Martian-like winds was examined. In the second, dust was dropped near the inlet of the wind tunnel and the winds were allowed to carry the dust past the samples, simulating a dust storm. A summary of results is given. Author

N91-27062*# Jet Propulsion Lab., California Inst. of Tech., Pasadena.
HAVE GRABEN WALL SCARPS ACCUMULATED SAND AND DUST ON MARS?
M. P. Golombek and P. A. Davis (Geological Survey, Flagstaff, AZ.) *In* NASA. Ames Research Center, Sand and Dust on Mars May 1991 p 20 (For primary document see N91-27057 18-91)
Avail: NTIS HC/MF A04 CSCL 03B

Grabens are linear fault bounded troughs that are extremely abundant on Mars (about 7000 cover the Western Hemisphere). Analysis of lunar and Martian grabens as well as analogous structures on Earth indicates that grabens form under extension when the crust is pulled apart. On Mars, topographic maps are not of sufficient resolution to measure graben wall slopes. Seismic shaking on Mars might be capable of reducing 60 deg fault scarps to an angle of repose. Some other process must be responsible for further reducing graben wall slopes. If the deposition of sand and dust along graben walls is responsible for their extremely low slopes, then a variety of implications are possible. Sand and/or dust movement and deposition is ubiquitous in grabens over most of Mars, as similar looking grabens are found over the entire Western Hemisphere and this requires a plentiful supply of sand or dust. If the material that accumulates is of low density and cohesion, attempts to traverse graben walls might be difficult. Rimless shallow depressions could be more effective sinks for sand and dust on Mars than has been realized. Author

N91-27063*# National Aeronautics and Space Administration. Lyndon B. Johnson Space Center, Houston, TX.
CHEMISTRY AND MINERALOGY OF MARTIAN DUST: AN EXPLORER'S PRIMER
James L. Gooding *In* NASA. Ames Research Center, Sand and Dust on Mars May 1991 p 21-22 (For primary document see N91-27057 18-91)
Avail: NTIS HC/MF A04 CSCL 03B

A summary of chemical and mineralogical properties of Martian surface dust is offered for the benefit of engineers or mission planners who are designing hardware or strategies for Mars surface exploration. For technical details and specialized explanations, references should be made to literature cited. Four sources used for information about Martian dust composition: (1) Experiments performed on the Mars surface by the Viking Landers 1 and 2 and Earth-based lab experiments attempting to duplicate these results; (2) Infrared spectrophotometry remotely performed from Mars orbit, mostly by Mariner 9; (3) Visible and infrared spectrophotometry remotely performed from Earth; and (4) Lab studies of the shergottite nakhlite chassignite (SNC) clan of meteorites, for which compelling evidence suggests origin on Mars. Source 1 is limited to fine grained sediments at the surface whereas 2 and 3 contain mixed information about surface dust (and associated rock) and atmospheric dust. Source 4 has provided surprisingly detailed information but investigations are still incomplete. Author

N91-27064*# Arizona State Univ., Tempe. Dept. of Geology.
WIND ABRASION ON MARS
Ronald Greeley *In* NASA. Ames Research Center, Sand and Dust on Mars May 1991 p 23 (For primary document see N91-27057 18-91)
Avail: NTIS HC/MF A04 CSCL 03B

Aeolian activity was predicted for Mars from earth based observations of changing surface patterns that were interpreted as dust storms. Mariner 9 images showed conclusive evidence for aeolian processes in the form of active dust storms and various aeolian landforms including dunes and yardangs. Windspeeds to initiate particle movement are an order of magnitude higher on Mars than on Earth because of the low atmospheric density on Mars. In order to determine rates of abrasion by wind blown particles, knowledge of three factors is required: (1) particle parameters such as numbers and velocities of windblown grains as functions of windspeeds at various heights above the surface; (2) the susceptibility to abrasion of various rocks and minerals; and (3) wind frequencies and speeds. For estimates appropriate to Mars, data for the first two parameters can be determined through lab and wind tunnel tests; data for the last two factors are available directly from the Viking Lander meteorology experiments for the two landing sites. Author

N91-27065*# Iowa State Univ. of Science and Technology, Ames. Dept. of Aerospace Engineering.
THE AEOLIAN WIND TUNNEL **c09**
J. D. Iversen *In* NASA. Ames Research Center, Sand and Dust on Mars May 1991 p 24-25 (For primary document see N91-27057 18-91)
Avail: NTIS HC/MF A04 CSCL 14B

The aeolian wind tunnel is a special case of a larger subset of the wind tunnel family which is designed to simulate the atmospheric surface layer winds to small scale (a member of this larger subset is usually called an atmospheric boundary layer wind tunnel or environmental wind tunnel). The atmospheric boundary layer wind tunnel is designed to simulate, as closely as possible, the mean velocity and turbulence that occur naturally in the atmospheric boundary layer (defined as the lowest portion of the atmosphere, of the order of 500 m, in which the winds are most greatly affected by surface roughness and topography). The aeolian wind tunnel is used for two purposes: to simulate the physics of the saltation process and to model at small scale the erosional

and depositional processes associated with topographic surface features. For purposes of studying aeolian effects on the surface of Mars and Venus as well as on Earth, the aeolian wind tunnel continues to prove to be a useful tool for estimating wind speeds necessary to move small particles on the three planets as well as to determine the effects of topography on the evolution of aeolian features such as wind streaks and dune patterns. Author

N91-27066*# Colorado Univ., Boulder. Lab. for Atmospheric and Space Physics.
MEASUREMENTS OF DUST ON MARS TO BE OBTAINED FROM UPCOMING MISSIONS
Bruce M. Jakosky *In* NASA. Ames Research Center, Sand and Dust on Mars May 1991 p 26-32 (For primary document see N91-27057 18-91)
Avail: NTIS HC/MF A04 CSCL 03B

Measurements of dust on the Mars surface and in its atmosphere will be made from several upcoming missions. The best defined missions are Mars Observer, the Soviet Mars 94 mission, and the Mars Environment Survey (MESUR) mission. A discussion is presented of what measurements pertaining to airborne or surface dust will be made and what properties can be inferred from them. The payloads for the latter two missions are not yet determined. In all cases, only that information which pertains to dust is included; each mission contains additional instruments that provide no information on this topic. Following the discussion of individual instruments is a summary of the types of measurements and observations that will be made from the ensemble collection of instruments and missions, and a brief discussion of the types of measurements of dust which will not be made. Author

N91-27067*# National Aeronautics and Space Administration. Lyndon B. Johnson Space Center, Houston, TX.
ENGINEERING KNOWLEDGE REQUIREMENTS FOR SAND AND DUST ON MARS
D. I. Kaplan *In* NASA. Ames Research Center, Sand and Dust on Mars May 1991 p 33 (For primary document see N91-27057 18-91)
Avail: NTIS HC/MF A04 CSCL 03B

The successful landing of human beings on Mars and the establishment of a permanent outpost there will require an understanding of the Martian environment by the engineers. A key feature of the Martian environment is the nearly ubiquitous presence of sand and dust. The process which the engineering community will undertake to determine the sensitivities of their designs to the current level of knowledge about Mars sand and dust is emphasized. The interaction of the engineering community with the space exploration initiative (SEI) mission planners and management is described. Author

N91-27068*# National Aeronautics and Space Administration. Lewis Research Center, Cleveland, OH.
ELECTRICAL SYSTEM/ENVIRONMENT INTERACTIONS ON THE PLANET MARS
J. C. Kolecki, G. B. Hillard, and D. C. Ferguson *In* NASA. Ames Research Center, Sand and Dust on Mars May 1991 p 34-35 (For primary document see N91-27057 18-91)
Avail: NTIS HC/MF A04 CSCL 03B

The Martian environment is a diverse environment with which systems will interact in numerous ways. Preliminary thoughts on electrical system/environment interactions which might be of interest to system designers at all stages of system design are presented. These interactions are primarily related to electrical charging, contamination, and Martian surface sand and dust. Author

N91-27069*# Arizona State Univ., Tempe.
EFFECT OF PRESSURE ON ELECTROSTATIC PROCESSES ON MARS
Rodman N. Leach *In* NASA. Ames Research Center, Sand and Dust on Mars May 1991 p 36 (For primary document see N91-27057 18-91)
Avail: NTIS HC/MF A04 CSCL 03B

Paschen's Law as illustrated by Paschen curves for various gases shows that the minimum breakdown voltage for gases for breakdown distances of interest, i.e., 1 to 1000 mm is at or near the surface pressure on Mars. This means that the physics of many electrostatic processes is markedly different on Mars than on Earth. The primary effect is that voltage potentials above 100 volts are subject to breakdown in the Martian atmosphere. Sharp electrodes, dusty atmospheric conditions, or other anomalies modify the breakdown voltage, usually causing lower breakdown voltages. Paschen's curves for most common pure gases were experimentally determined. A very small amount of mixing of different gases radically changes the curve as shown in the curve for neon plus 0.1 percent argon compared to either neon or argon. Paschen's curve for the exact composition of gases for Mars was not determined; thus, the breakdown voltages are not known. A second important effect is that the breakdown for most Martian cases is a glow discharge rather than a spark discharge. It would seem that simple measurements of breakdown manner and voltage should be included on a Mars lander vehicle. Author

N91-27070*# Arizona State Univ., Tempe.
SALTATION THRESHOLD DETECTION IN A WIND TUNNEL BY THE MEASUREMENT OF THE NET ELECTROSTATIC CHARGE
Rodman N. Leach *In* NASA. Ames Research Center, Sand and Dust on Mars May 1991 p 37 (For primary document see N91-27057 18-91)
Avail: NTIS HC/MF A04 CSCL 03B

The Mars surface wind tunnel (MARSWIT) is an open circuit wind tunnel used for aeolian studies and is located inside a large vacuum chamber allowing testing at Martian surface atmospheric pressure. Since direct access is not available to the tunnel during operation at low pressure, a remote method of saltation detection is needed. The bed is observed by means of closed circuit video, but it is often difficult to determine the initiation of threshold. The measurement by means of an electrometer of the net electric charge produced by the saltating particles has provided a reliable means of saltation threshold detection. Saltating particles become charged several ways, both in wind tunnels and in a natural environment. The most significant of these methods are tribo-charging and contact charging, which always occur. Fracture charging may also occur under the high velocities associated with particle transport on Mars or under simulated Martian conditions. Detection in MARSWIT is achieved by allowing the saltating particles to impinge on a planar conducting surface normal to the flow that is connected to ground through a Keithly electrometer. The signal from the electrometer is connected to a strip chart recorder along with the analog signal from the pitot tube transducer that is used to determine the wind velocity in the tunnel. Thus, a record of wind velocity and the initiation of particle saltation is conveniently displayed together. While both positive and negative charges are produced during saltation, this method measures only the net charge; thus the charge may be either positive or negative depending upon the particles being tested, the size and size distribution of the test material, and the wind velocity. This has proven to be a very trustworthy and sensitive method of saltation threshold detection, being especially useful with the smaller sized particles which are the most difficult to observe visually. Author

N91-27071*# Arizona State Univ., Tempe. Dept. of Geology.
SALTATION THRESHOLD REDUCTION DUE TO THE ELECTROSTATIC AGGLOMERATION OF FINE PARTICLES **c34**
Rodman N. Leach and Ronald Greeley *In* NASA. Ames Research Center, Sand and Dust on Mars May 1991 p 38 (For primary document see N91-27057 18-91)
Avail: NTIS HC/MF A04 CSCL 20D

Particles between 80 and 110 microns in diameter are the most easily moved by the wind. As the particle size decreases below 60 microns, they are increasingly more difficult to move by surface winds, and a number of experiments were performed in

an attempt to reduce the required wind velocity. These include: (1) the bombardment of a bed of fine particles by particles near the optimum size, the larger particles kicking the fine particles into the windstream where they are entrained; and (2) the electrostatic agglomeration of fine particles into sizes more easily saltated. The results of these experiments are discussed. Author

N91-27072*# Colorado Univ., Boulder. Lab. for Atmospheric and Space Physics.
THE EFFECTS OF ATMOSPHERIC DUST ON OBSERVATIONS OF MARTIAN SURFACE ALBEDO
S. W. Lee and R. T. Clancy *In* NASA. Ames Research Center, Sand and Dust on Mars May 1991 p 39-40 (For primary document see N91-27057 18-91)
(Grant NAGw-1378)
Avail: NTIS HC/MF A04 CSCL 03B

The Mariner 9 and Viking missions provided abundant evidence that aeolian processes are active over much of surface of Mars. A radiative transfer model was developed which allows the effects of atmospheric dust loading and variable surface albedo to be investigated. This model incorporated atmospheric dust opacity, the single scattering albedo, and particle phase function of atmospheric dust, the bidirectional; reflectance of the surface, and variable lighting and viewing geometry. The Cerberus albedo feature was examined in detail using this technique. Author

N91-27073*# Geological Survey, Menlo Park, CA.
MARTIAN SURFACE MATERIALS
H. J. Moore *In* NASA. Ames Research Center, Sand and Dust on Mars May 1991 p 41-43 (For primary document see N91-27057 18-91)
Avail: NTIS HC/MF A04 CSCL 03B

A semiquantitative appreciation for the physical properties of the Mars surface materials and their global variations can be gained from the Viking Lander and remote sensing observations. Analyses of Lander data yields estimates of the mechanical properties of the soil-like surface materials and best guess estimates can be made for the remote sensing signatures of the soil-like materials at the landing sites. Results show that significant thickness of powderlike surface materials with physical properties similar to drift material are present on Mars and probably pervasive in the Tharsis region. It also appears likely that soil-like materials similar to crusty to cloddy material are typical for Mars, and that soil-like material similar to blocky material are common on Mars. Author

N91-27074*# Geological Survey, Denver, CO.
MAGNETIC AND ELECTRICAL PROPERTIES OF MARTIAN PARTICLES
G. R. Olhoeft *In* NASA. Ames Research Center, Sand and Dust on Mars May 1991 p 44-46 (For primary document see N91-27057 18-91)
Avail: NTIS HC/MF A04 CSCL 03B

The only determinations of the magnetic properties of Martian materials come from experiments on the two Viking Landers. The results suggest Martian soil containing 1 to 10 percent of a highly magnetic phase. Though the magnetic phase mineral was not conclusively identified, the predominate interpretation is that the magnetic phase is probably maghemite. The electrical properties of the surface of Mars were only measured remotely by observations with Earth based radar, microwave radiometry, and inference from radio-occultation of Mars orbiting spacecraft. No direct measurements of electrical properties on Martian materials have been performed. Author

N91-27075*# San Francisco State Univ., CA.
REFLECTANCE SPECTROSCOPY OF PALAGONITE AND IRON-RICH MONTMORILLONITE CLAY MIXTURES: IMPLICATIONS FOR THE SURFACE COMPOSITION OF MARS
J. B. Orenberg and J. Handy *In* NASA. Ames Research Center, Sand and Dust on Mars May 1991 p 47-48 (For primary document see N91-27057 18-91)
Avail: NTIS HC/MF A04 CSCL 03B

Because of the power of remote sensing reflectance spectroscopy in determining mineralogy, it was used as the major method of identifying possible mineral analogs of the Martian surface. A summary of proposed Martian surface compositions from reflectance spectroscopy before 1979 was presented. Since that time, iron-rich montmorillonite clay, nanocrystalline or nanophase hematite, and palagonite were suggested as Mars soil analog materials. Author

N91-27076*# California Univ., Los Angeles. Dept. of Earth and Space Sciences.
THERMAL AND ALBEDO MAPPING OF THE NORTH AND SOUTH POLAR REGIONS OF MARS
D. A. Paige and K. D. Keegan *In* NASA. Ames Research Center, Sand and Dust on Mars May 1991 p 49-50 (For primary document see N91-27057 18-91)
Avail: NTIS HC/MF A04 CSCL 03B

The first maps are presented of the north and south polar regions of Mars. The thermal properties of the midlatitude regions from -60 deg to +60 deg latitude were mapped in previous studies. The presented maps complete the mapping of entire planet. The maps for the north and south polar regions were derived from Viking Infrared Thermal Mapper (IRTM) observations. Best fit thermal inertias were determined by comparing the available IRTM 20 micron channel brightness within a given region to surface temperatures computed by a diurnal and seasonal thermal model. The model assumes no atmospheric contributions to the surface heat balance. The resulting maps of apparent thermal inertia and average IRTM measured solar channel lambert albedo for the north and south polar regions from the poles to +/- 60 deg latitude. Author

N91-27077*# National Aeronautics and Space Administration. Ames Research Center, Moffett Field, CA.
DERIVATION OF MID-INFRARED (5-25 MICRONS) OPTICAL CONSTANTS OF SOME SILICATES AND PALAGONITE
T. L. Roush, J. B. Pollack, and J. B. Orenberg (San Francisco State Univ., CA.) *In its* Sand and Dust on Mars May 1991 p 51-52 (For primary document see N91-27057 18-91)
Avail: NTIS HC/MF A04 CSCL 03B

Recent reports concerning the mid-infrared reflectance properties of silicates coupled with recent observations of the Earth and other planets in the mid-infrared and the planned Thermal Emission Spectrometer scheduled as an instrument to be included on the Mars Observer all illustrate the increasing interest in the optical properties of materials in the mid-infrared and their direct application to remote sensing observations of other planetary surfaces. As the laboratory and observational data increase they will ultimately be modeled to aid in the understanding of the composition mineralogy, and distribution of the surface and atmospheric constituents on these bodies. In order to facilitate such quantitative analyses, knowledge regarding the optical constants (real (n) and imaginary (k) indices of refraction) of a wide variety of pertinent materials is required. Examples of the application of such quantitative analyses to the interpretation of Martian surface and atmospheric constituents, based on the optical constants of minerals, are presented. This study was initially conceived in order to aid in the interpretation of Martian surface and atmospheric aerosol mineralogy. As a result, the minerals included are biased toward samples which represent hydrated and hydroxylated silicates. These include the Al and Mg end members of the 1:1 layer lattice silicates, kaolinite and serpentine, respectively; an Al-bearing 2:1 layer lattice silicate, pyrophyllite; the Mg and Al smectite clays saponite and montmorillonite, respectively; and a palagonite, typically a poorly characterized alteration product of basaltic glass. The reflectivities of all samples were determined by placing them at the focus of a near-normal reflective attachment located in a Fourier transform spectrometer. To derive the optical constants of a material as a function of wavelength, researchers used the commonly employed technique of dispersion analysis. Author

N91-27078*# California Univ., Los Angeles. Inst. of Geophysics and Planetary Physics.

ELECTROSTATIC FIELDS IN A DUSTY MARTIAN ENVIRONMENT

D. D. Sentman *In* NASA. Ames Research Center, Sand and Dust on Mars May 1991 p 53 (For primary document see N91-27057 18-91)

Avail: NTIS HC/MF A04 CSCL 03B

While there have been several studies suggesting the possibility of electrical activity on Mars, to date there have been no measurements to search for evidence of such activity. In the absence of widespread water clouds and convective storm systems similar to those on the Earth and Jupiter, the most likely candidate for the creation of electrostatic charges and fields is triboelectric charging of dust, i.e., the friction between blown dust and the ground, and of dust particles with each other. Terrestrial experience demonstrates that electric fields 5 to 15 kV-m(exp -1) are not uncommon in dust storms and dust devils in desert regions, where the polarity varies according to the chemical composition and grain size. Simple laboratory experiments have demonstrated that modest electrostatic fields of roughly 5,000 V-m(exp -1) may be produced, along with electrical spark discharges and glow discharges, in a simulation of a dusty, turbulent Martian surface environment. While the Viking landers operated for several years with no apparent deleterious effects from electrostatic charging, this may have been at least partly due to good engineering design utilizing pre-1976 electronic circuitry to minimize the possibility of differential charging among the various system components. However, free roaming rovers, astronauts, and airborne probes may conceivably encounter an environment where electrostatic charging is a frequent occurrence, either by way of induction from a static electric field or friction with the dusty surface and atmosphere. This raises the possibility of spark discharges or current surges when subsequent contact is made with other pieces of electrical equipment, and the possibility of damage to modern microelectronic circuitry. Measurements of electrostatic fields on the surface of Mars could therefore be valuable for assessing this danger. Electric field measurements could also be useful for detecting natural discharges that originate in dust storms. This detection could be performed at distances ranging from 10s of km in the case of J-charge-like discharge signatures, to planetary distances if there exists a global electrical circuit or Schumann resonance spectrum. Author

N91-27079*# Lockheed Corp., Houston, TX. Life Support Development Lab.

IMPACT OF MARS SAND ON DUST ON THE DESIGN OF SPACE SUITS AND LIFE SUPPORT EQUIPMENT: A TECHNOLOGY ASSESSMENT

Charles H. Simonds *In* NASA. Ames Research Center, Sand and Dust on Mars May 1991 p 54-55 (For primary document see N91-27057 18-91)

Avail: NTIS HC/MF A04 CSCL 03B

Space suits and life support equipment will come in intimate contact with Martian soil as aerosols, wind blown particles and material thrown up by men and equipment on the Martian surface. For purposes of this discussion the soil is assumed to consist of a mixture of cominuted feldspar, pyroxene, olivine, quartz, titanomagnetite and other anhydrous and hydrous iron bearing oxides, clay minerals, scapolite and water soluble chlorides and sulfates. The soil may have photoactivated surfaces that acts as a strong oxidizer with behavior similar to hydrogen peroxide. The existing data about the Mars soil suggests that the dust and sand will require designs analogous to those uses on equipment exposed to salty air and blowing sand and dust. The major design challenges are in developing high performance radiators which can be cleaned after each EVA without degradation, designing seals that are readily cleaned and possibly in selecting materials which will not be degraded by any strong oxidants in the soil. The magnitude of the dust filtration challenge needs careful evaluation in terms of the trade off between fine-particle dust filters with low pressure drop that are either physically large and heavy, like filter baghouses require frequent replacement of filter elements, of low volume high pressure thus power consumption approaches, or washable filters. In the latter, filter elements are cleaned with water, as could the outsides of the space suits in the airlock. Author

N91-27080*# National Aeronautics and Space Administration. Ames Research Center, Moffett Field, CA.

SAND AND DUST ISSUES FOR THE MESUR MISSION

P. F. Wercinski and G. S. Hubbard *In its* Sand and Dust on Mars May 1991 p 56-57 (For primary document see N91-27057 18-91)

Avail: NTIS HC/MF A04 CSCL 03B

The presence of particles in the Martian atmosphere increases the rate of erosion of the heat shield during the entry phase of the MESUR mission. Preliminary analysis has shown that under certain conditions particles will penetrate the bow shock of the entry vehicle, impact and erode the heat shield, above the anticipated rate from the ablation process. Knowledge of the distribution, sizes, and composition of particles suspended in the atmosphere will permit the estimation of the heat shield recession both for a nominal Mars atmosphere and in dust storm conditions. On the surface of Mars, sand and dust can effect the operations and design of the science instruments (i.e., imaging) and lander subsystems (i.e., solar arrays). Distribution and deposition of sand and dust on the planet's surface will dictate the feasibility of using solar arrays as a power source for the lander. Furthermore, the potential abrasive nature of blowing particles must be understood in order to properly select suitable materials for lander structure and any components exposed to the environment. The selection of lander material may also be dictated by corrosive and chemically active properties of particles at a potential landing site. Some key interests concerning sand and dust on the surface and in the atmosphere are summarized in a number of questions that are included. Author

N91-27081*# California Univ., Davis. Dept. of Mechanical Engineering.

MARTIAN DUST THRESHOLD MEASUREMENTS: SIMULATIONS UNDER HEATED SURFACE CONDITIONS

Bruce R. White, Ronald Greeley, and Rodman N. Leach (Arizona State Univ., Tempe.) *In* NASA. Ames Research Center, Sand and Dust on Mars May 1991 p 58-59 (For primary document see N91-27057 18-91)

Avail: NTIS HC/MF A04 CSCL 03B

Diurnal changes in solar radiation on Mars set up a cycle of cooling and heating of the planetary boundary layer, this effect strongly influences the wind field. The stratification of the air layer is stable in early morning since the ground is cooler than the air above it. When the ground is heated and becomes warmer than the air its heat is transferred to the air above it. The heated parcels of air near the surface will, in effect, increase the near surface wind speed or increase the aeolian surface stress the wind has upon the surface when compared to an unheated or cooled surface. This means that for the same wind speed at a fixed height above the surface, ground-level shear stress will be greater for the heated surface than an unheated surface. Thus, it is possible to obtain saltation threshold conditions at lower mean wind speeds when the surface is heated. Even though the mean wind speed is less when the surface is heated, the surface shear stress required to initiate particle movement remains the same in both cases. To investigate this phenomenon, low-density surface dust aeolian threshold measurements have been made in the MARSWIT wind tunnel located at NASA Ames Research Center, Moffett Field, California. The first series of tests examined threshold values of the 100 micron sand material. At 13 mb surface pressure the unheated surface had a threshold friction speed of 2.93 m/s (and approximately corresponded to a velocity of 41.4 m/s at a height of 1 meter) while the heated surface equivalent bulk Richardson number of -0.02, yielded a threshold friction speed of 2.67 m/s (and approximately corresponded to a velocity of 38.0 m/s at a height of 1 meter). This change represents an 8.8 percent decrease in threshold conditions for the heated case. The values of velocities are well within the threshold range as observed by Arvidson et al., 1983. As the surface was heated the threshold

decreased. At a value of bulk Richardson number equal to -0.02 the threshold friction speed and threshold wind speed appears to level-off to a constant value. This trend also was observed in the MARSWIT experiments involving the 11 micron sized-silt material.
Author

N91-27082*# National Aeronautics and Space Administration. Ames Research Center, Moffett Field, CA.
DUST IN THE MARS ATMOSPHERE
R. W. Zurek and Robert M. Haberle *In its* Sand and Dust on Mars May 1991 p 60-61 Prepared in cooperation with Jet Propulsion Lab., California Inst. of Tech., Pasadena (For primary document see N91-27057 18-91)
Avail: NTIS HC/MF A04 CSCL 03B

The amount of dust suspended in the Martian atmosphere is highly variable with location and with time. The opacity of the sky is best known at the two Viking Lander sites, where visual, vertical-column optical depth never fell below a value of a few tenths during the 1.25 Mars years of observations and yet exceeded 2 to 3 during two great dust storms in 1977. Elsewhere on the planet, optical depths have been estimated from orbiter visible imaging of surface contrasts and from mapping of infrared emission from the surface and the overlying (dusty) atmosphere. In many cases these opacities (and thus dust amounts) may be uncertain by as much as a factor of two. Viking Lander observations of twilight indicate that the background dust haze is more or less uniformly mixed with altitude in the lower atmosphere. Observations from spacecraft indicate that there may be come seasonal variations to the height of these dust hazes, which sometimes extend above 30 km. (Ice haze layers may occur as high as 80 km.) The existing observations do not constrain the composition or the size distribution of the suspended dust particles very well. Remote sensing observations depend principally upon the product of the number of particles, the geometric cross-sections (and so particle size and shape), and the extinction efficiency of the particles (and so the particle composition), as integrated over the particle size distribution and along the line of sight. While the observed variation of dust opacity with wavelength constrains these quantities, it does not often permit the unique determination of the individual properties of the suspended dust. A size distribution having a cross-section weighted mean particle radius of 2.5 microns was deduced from a synthesis of the IR thermal emission spectra observed in the Southern Hemisphere by Mariner 9 during the 1971 global dust storm. Although the IR thermal emission is relatively insensitive to the sub-micron sized particles which tend to dominate visible opacity, this same size distribution was consistent with modeling of the sky brightness variation near the sun, as seen through the background haze above the Viking lander sites in the Northern Hemisphere. Author

N91-26174# Joint Publications Research Service, Arlington, VA.
TURBULENT PROCESSES OF MASS-LOADING OF NEW IONS ON VENUS AND MARS AND THE PROBLEMS OF NUMERICAL MODELS OF THE INTERACTION OF SOLAR WIND WITH THESE PLANETS. 1: CHARACTERISTICS OF THE FLOW OF SOLAR WIND AROUND THE PLANETS Abstract Only
T. K. Breus and A. M. Krymskiy *In its* JPRS Report: Science and Technology. USSR: Space 16 Apr. 1991 p 40 Transl. into ENGLISH from Kosmicheskiye Issledovaniya (Moscow, USSR), v. 28, no. 6, Nov.-Dec. 1990 p 923-935 (For primary document see N91-26162 18-12)
Avail: NTIS HC/MF A06

N91-26175# Joint Publications Research Service, Arlington, VA.
CHARACTERISTICS OF AEROSOL IN THE ATMOSPHERE OF MARS ACCORDING TO DATA FROM THE KRFM EXPERIMENT Abstract Only
V. I. Moroz, Ye. V. Petrova, L. V. Ksanformaliti, L. Esposito, J. P. Bibring, M. Combes, A. Soufflot, O. F. Ganpantserova, N. V. Goroshkova, and A. V. Zharkov et al *In its* JPRS Report: Science and Technology. USSR: Space 16 Apr. 1991 p 40 Transl. into ENGLISH from Kosmicheskiye Issledovaniya (Moscow, USSR), v. 28, no. 6, Nov.-Dec. 1990 p 936-942 (For primary document see N91-26162 18-12)
Avail: NTIS HC/MF A06

N91-26176# Joint Publications Research Service, Arlington, VA.
RESULTS OF MORPHOMETRIC ANALYSIS OF THE TESSERAE SURFACE OF VENUS ACCORDING TO VENERA-15 AND -16 DATA Abstract Only
M. A. Ivanov *In its* JPRS Report: Science and Technology. USSR: Space 16 Apr. 1991 p 40 Transl. into ENGLISH from Astronomicheskiy Vestnik (Moscow, USSR), v. 24, no. 4, Oct.-Dec. 1990 p 288-295 (For primary document see N91-26162 18-12)
Avail: NTIS HC/MF A06

N91-27104*# University of Northern Arizona, Flagstaff. Dept. of Geology.
EVALUATION OF GEOPHYSICAL PROPERTIES OF THE LUNAR REGOLITH FOR THE DESIGN OF PRECURSOR SCIENTIFIC MISSIONS FOR THE SPACE EXPLORATION INITIATIVE Final Report
Paul Morgan *In* Houston Univ., NASA/ASEE Summer Faculty Fellowship Program, 1990, Volume 2 Dec. 1990 13 p (For primary document see N91-27103 18-99)
(Grant NGT-44-005-803)
Avail: NTIS HC/MF A09 CSCL 03B

92 SOLAR PHYSICS

Includes solar activity, solar flares, solar radiation and sunspots.

For related information see *93 Space Radiation.*

N91-27083# National Geophysical Data Center, Boulder, CO.
SOLAR-GEOPHYSICAL DATA NUMBER 556, DECEMBER 1990. PART 1: (PROMPT REPORTS). DATA FOR NOVEMBER, OCTOBER 1990, AND LATE DATA
H. E. Coffey Dec. 1990 159 p
(PB91-152140; SGD-556-Pt-1) Avail: NTIS HC/MF A08 CSCL 03B

The following subject areas are covered: detailed index for 1990; data for November 1990 (solar-terrestrial environment, IUWDS alert periods, solar activity indices, solar flares, solar radio emission, Stanford mean solar magnetic field); data for October 1990 (solar activity regions, sudden ionospheric disturbances, solar radio spectral observations, cosmic ray measurements by neutron monitor, and geomagnetic indices); and late data (cosmic rays Huancayo August 1990, geomagnetic activity indices September 1990, and International Geophysical Calendar 1991 with recommended scientific programs). Author

N91-27084# National Geophysical Data Center, Boulder, CO.
SOLAR-GEOPHYSICAL DATA NUMBER 556, DECEMBER 1990. PART 2: (COMPREHENSIVE REPORTS). DATA FOR JUNE 1990 AND MISCELLANEOUS
H. E. Coffey Dec. 1990 90 p
(PB91-152157; SGD-556-Pt-2) Avail: NTIS HC/MF A05 CSCL 03B

Data from June 1990 is given in tabular form on solar flares, solar radio bursts at fixed frequencies, interplanetary solar particles and plasma, solar x-ray radiation from GOES satellite graphs, mass ejections from the Sun, and active solar prominences and filaments. Author

N91-27085# National Geophysical Data Center, Boulder, CO.
SOLAR GEOPHYSICAL DATA NUMBER 551, JULY 1990. PART 1: (PROMPT REPORTS). DATA FOR JUNE, MAY 1990 AND LATE DATA
H. E. Coffey Jul. 1990 148 p
(PB91-160713; SGD-551-Pt-1) Avail: NTIS HC/MF A07 CSCL 03B

Data from June 1990 are given in tabular form on solar flares, solar radio emission, and mean solar magnetic field. Data from May 1990 are given on solar active regions, sudden ionospheric

disturbances, solar radio spectral observations, cosmic ray measurements by a neutron monitor, and geomagnetic indices. Data from February to April 1990 are given on sudden commencements/solar flare effects. Author

N91-27086# National Geophysical Data Center, Boulder, CO.
SOLAR-GEOPHYSICAL DATA NUMBER 551, JULY 1990. PART 2: (COMPREHENSIVE REPORTS). DATA FOR JANUARY 1990 AND MISCELLANEOUS
H. E. Coffey Jul. 1990 83 p
(PB91-160721; SGD-551-Pt-2) Avail: NTIS HC/MF A05 CSCL 03B

Data from January 1990 is given in tabular form on solar flares, solar radio bursts at fixed frequencies, solar wind, solar x-ray radiation from GOES satellite graphs, mass ejections from the Sun, and active solar prominences and filaments. Author

N91-27087*# National Aeronautics and Space Administration. Goddard Space Flight Center, Greenbelt, MD.
THE 1980 SOLAR MAXIMUM MISSION EVENT LISTING
D. M. Speich, J. J. Nelson, J. P. Licata, and A. K. Tolbert Jun. 1991 435 p Prepared in cooperation with ST Systems Corp., Lanham, MD
(NASA-TM-4287; Rept-91B00095; NAS 1.15:4287) Avail: NTIS HC/MF A19 CSCL 03B

Information is contained on solar burst and transient activity observed by the Solar Maximum Mission (SMM) during 1980 pointed observations. Data from the following SMM experiments are included: (1) Gamma Ray Spectrometer, (2) Hard X-Ray Burst Spectrometer, (3) Hard X-Ray Imaging Spectrometer, (4) Flat Crystal Spectrometer, (5) Bent Crystal Spectrometer, (6) Ultraviolet Spectrometer and Polarimeter, and (7) Coronagraph/Polarimeter. Correlative optical, radio, and Geostationary Operational Environmental Satellite (GOES) x ray data are also presented. Where possible, bursts or transients observed in the various wavelengths were grouped into discrete flare events identified by unique event numbers. Each event carries a qualifier denoting the quality or completeness of the observations. Spacecraft pointing coordinates and flare site angular displacement values from Sun center are also included. Author

N91-26172# Joint Publications Research Service, Arlington, VA.
DYNAMICS OF EQUATORIAL AND POLAR BOUNDARIES OF PENETRATION OF SOLAR PROTONS WITH ENERGY ABOUT 1 MeV INTO MAGNETOSPHERE DURING STRONG MAGNETIC STORM Abstract Only
L. A. Darchiyeva, T. A. Ivanova, E. N. Sosnovets, and L. V. Tverskaya *In its* JPRS Report: Science and Technology. USSR: Space 16 Apr. 1991 p 37-38 Transl. into ENGLISH from Geomagnetizm i Aeronomiya (Moscow, USSR), v. 30, no. 5, Sep.-Oct. 1990 p 856-858 (For primary document see N91-26162 18-12)
Avail: NTIS HC/MF A06

93 SPACE RADIATION

Includes cosmic radiation; and inner and outer earth's radiation belts.

For biological effects of radiation see *52 Aerospace Medicine*. For theory see *73 Nuclear and High-Energy Physics*.

N91-26173# Joint Publications Research Service, Arlington, VA.
MODELLING THE DYNAMICS OF FLUXES OF ELECTRONS WITH ENERGIES 30-300 keV IN GEOSTATIONARY ORBIT Abstract Only
V. I. Degtyarev, G. V. Popov, and S. S. Sheshukov *In its* JPRS Report: Science and Technology. USSR: Space 16 Apr. 1991 p 38 Transl. into ENGLISH from Geomagnetizm i Aeronomiya (Moscow, USSR), v. 30, no. 5, Sep.-Oct. 1990 p 866-868 (For primary document see N91-26162 18-12)
Avail: NTIS HC/MF A06

99 GENERAL

N91-27088*# Houston Univ., TX.
NASA/ASEE SUMMER FACULTY FELLOWSHIP PROGRAM, 1990, VOLUME 1
Richard B. Bannerot, ed. and Stanley H. Goldstein, ed. (National Aeronautics and Space Administration. Lyndon B. Johnson Space Center, Houston, TX.) Dec. 1990 207 p Program held in Houston, TX, 1990
(Grant NGT-44-005-803)
(NASA-CR-185637-Vol-1; NAS 1.26:185637-Vol-1) Avail: NTIS HC/MF A10 CSCL 05B

The 1990 Johnson Space Center (JSC) NASA/American Society for Engineering Education (ASEE) Summer Faculty Fellowship Program was conducted by the University of Houston-University Park and JSC. A compilation of the final reports on the research projects are presented. The topics covered include: the Space Station; the Space Shuttle; exobiology; cell biology; culture techniques; control systems design; laser induced fluorescence; spacecraft reliability analysis; reduced gravity; biotechnology; microgravity applications; regenerative life support systems; imaging techniques; cardiovascular system; physiological effects; extravehicular mobility units; mathematical models; bioreactors; computerized simulation; microgravity simulation; and dynamic structural analysis. For individual titles, see N91-27089 through N91-27102.

N91-27089*# Xavier Univ. of Louisiana, New Orleans. Dept. of Physics.
LIF AND EMISSION STUDIES OF COPPER AND NITROGEN Final Report **c26**
Murty A. Akundi *In* Houston Univ., NASA/ASEE Summer Faculty Fellowship Program, 1990, Volume 1 Dec. 1990 16 p (For primary document see N91-27088 18-99)
(Grant NGT-44-005-803)
Avail: NTIS HC/MF A10 CSCL 11F

A technique is developed to determine the rotational temperature of nitrogen molecular ion, N2(+), from the emission spectra of B-X transition, when P and R branches are not resolved. Its validity is tested on simulated spectra of the 0-1 band of N2(+) produced under low resolution. The method is applied to experimental spectra of N2(+) taken in the shock layer of a blunt body at distances of 1.91, 2.54, and 3.18 cm from the body. The laser induced fluorescence (LIF) spectra of copper atoms is analyzed to obtain the free stream velocities and temperatures. The only broadening mechanism considered is Doppler broadening. The temperatures are obtained by manual curve fitting, and the results are compared with least square fits. The agreement on the average is within 10 percent. Author

N91-27090*# Houston Univ., TX. Dept. of Applied Mathematical Sciences.
COMPOUND ESTIMATION PROCEDURES IN RELIABILITY Final Report **c38**
Ron Barnes *In its* NASA/ASEE Summer Faculty Fellowship Program, 1990, Volume 1 Dec. 1990 16 p (For primary document see N91-27088 18-99)
(Grant NGT-44-005-803)
Avail: NTIS HC/MF A10 CSCL 14D

At NASA, components and subsystems of components in the Space Shuttle and Space Station generally go through a number of redesign stages. While data on failures for various design stages are sometimes available, the classical procedures for evaluating reliability only utilize the failure data on the present design stage of the component or subsystem. Often, few or no failures have been recorded on the present design stage. Previously, Bayesian estimators for the reliability of a single component, conditioned on the failure data for the present design, were developed. These new estimators permit NASA to evaluate the reliability, even when few or no failures have been recorded. Point estimates for the latter evaluation were not possible with the classical procedures. Since different design stages of a component (or subsystem)

generally have a good deal in common, the development of new statistical procedures for evaluating the reliability, which consider the entire failure record for all design stages, has great intuitive appeal. A typical subsystem consists of a number of different components and each component has evolved through a number of redesign stages. The present investigations considered compound estimation procedures and related models. Such models permit the statistical consideration of all design stages of each component and thus incorporate all the available failure data to obtain estimates for the reliability of the present version of the component (or subsystem). A number of models were considered to estimate the reliability of a component conditioned on its total failure history from two design stages. It was determined that reliability estimators for the present design stage, conditioned on the complete failure history for two design stages have lower risk than the corresponding estimators conditioned only on the most recent design failure data. Several models were explored and preliminary models involving bivariate Poisson distribution and the Consael Process (a bivariate Poisson process) were developed. Possible short comings of the models are noted. An example is given to illustrate the procedures. These investigations are ongoing with the aim of developing estimators that extend to components (and subsystems) with three or more design stages. Author

N91-27091*# Alabama Univ., Tuscaloosa. Health and Human Performance Studies.

TECHNIQUES FOR DETERMINING TOTAL BODY WATER USING DEUTERIUM OXIDE Final Report **c52**

Phillip A. Bishop *In* Houston Univ., NASA/ASEE Summer Faculty Fellowship Program, 1990, Volume 1 Dec. 1990 13 p (For primary document see N91-27088 18-99)
(Grant NGT-44-005-803)
Avail: NTIS HC/MF A10 CSCL 06P

The measurement of total body water (TBW) is fundamental to the study of body fluid changes consequent to microgravity exposure or treatment with microgravity countermeasures. Often, the use of radioactive isotopes is prohibited for safety or other reasons. It was selected and implemented for use by some Johnson Space Center (JCS) laboratories, which permitted serial measurements over a 14 day period which was accurate enough to serve as a criterion method for validating new techniques. These requirements resulted in the selection of deuterium oxide dilution as the method of choice for TBW measurement. The development of this technique at JSC is reviewed. The recommended dosage, body fluid sampling techniques, and deuterium assay options are described. Author

N91-27092*# Mankato State Coll., MN. Dept. of Mathematics, Astronomy and Statistics.

MATHEMATICAL MODELING OF THE FLOW FIELD AND PARTICLE MOTION IN A ROTATING BIOREACTOR AT UNIT GRAVITY AND MICROGRAVITY Final Report **c29**

Ernest J. Boyd *In* Houston Univ., NASA/ASEE Summer Faculty Fellowship Program, 1990, Volume 1 Dec. 1990 17 p (For primary document see N91-27088 18-99)
(Grant NGT-44-005-803)
Avail: NTIS HC/MF A10 CSCL 12A

The biotechnology group at NASA Johnson Space Center is developing systems for culturing mammalian cells that stimulate some aspect of microgravity and provide a low shear environment for microgravity-based studies on suspension and anchorage dependent cells. The design of these vessels for culturing cells is based on the need to suspend cells and aggregates of cells and microcarrier beads continually in the culturing medium. The design must also provide sufficient circulation for adequate mass transfer of nutrients to the cells and minimize the total force on the cells. Forces, resulting from sources such as hydrodynamic fluid shear and collisions of cells and walls of the vessels, may damage delicate cells and degrade the formation of three dimensional structures. This study examines one particular design in both unit gravity and microgravity based on two concentric cylinders rotating in the same direction at different speeds to create a Couette flow between them. A numerical simulation for the flow field and the trajectories of particles in the vessel. The flow field for the circulation of the culturing medium is modeled by the Navier-Stokes equations. The forces on a particle are assumed to be drag from the fluid's circulation, buoyancy from the gravitational force and centrifugal force from the rotation of the vessel. The problem requires first solving the system of partial differential equations for the fluid flow by a finite difference method and then solving the system of ordinary differential equations for the trajectories by Gear's stiff method. Results of the study indicate that the trajectories in unit gravity and microgravity are very similar except for small spatial deviations on the fast time scale in unit gravity. The total force per unit cross sectional area on a particle in microgravity, however, is significantly smaller than the corresponding value in unit gravity, which is also smaller than anticipated. Hence, this study indicates that this design for a bioreactor with optimal rates of rotation can provide a good environment for culturing cells in microgravity with adequate circulation and minimal force on the cells. Author

N91-27093*# Mary Hardin-Baylor Univ., Belton, TX. Dept. of Mathematics and Physics.

AN AIR REVITALIZATION MODEL (ARM) FOR REGENERATIVE LIFE SUPPORT SYSTEMS (RLSS) Final Report **c54**

Maxwell M. Hart *In* Houston Univ., NASA/ASEE Summer Faculty Fellowship Program, 1990, Volume 1 Dec. 1990 15 p (For primary document see N91-27088 18-99)
(Grant NGT-44-005-803)
Avail: NTIS HC/MF A10 CSCL 06K

The primary objective of the air revitalization model (ARM) is to determine the minimum buffer capacities that would be necessary for long duration space missions. Several observations are supported by the current configuration sizes: the baseline values for each gas and the day to day or month to month fluctuations that are allowed. The baseline values depend on the minimum safety tolerances and the quantities of life support consumables necessary to survive the worst case scenarios within those tolerances. Most, it not all, of these quantities can easily be determined by ARM once these tolerances are set. The day to day fluctuations also require a command decision. It is already apparent from the current configuration of ARM that the tighter these fluctuations are controlled, the more energy used, the more nonregenerable hydrazine consumed, and the larger the required capacities for the various gas generators. All of these relationships could clearly be quantified by one operational ARM. Author

N91-27094*# Texas A&M Univ., Galveston. Dept. of Marine Science.

PHOTOGRAPHIC IMAGE ENHANCEMENT Final Report **c35**

Gerald E. Hite *In* Houston Univ., NASA/ASEE Summer Faculty Fellowship Program, 1990, Volume 1 Dec. 1990 14 p (For primary document see N91-27088 18-99)
(Grant NGT-44-005-803)
Avail: NTIS HC/MF A10 CSCL 14E

Deblurring capabilities would significantly improve the scientific return from Space Shuttle crew-acquired images of the Earth and the safety of Space Shuttle missions. Deblurring techniques were developed and demonstrated on two digitized images that were blurred in different ways. The first was blurred by a Gaussian blurring function analogous to that caused by atmospheric turbulence, while the second was blurred by improper focussing. It was demonstrated, in both cases, that the nature of the blurring (Gaussian and Airy) and the appropriate parameters could be obtained from the Fourier transformation of their images. The difficulties posed by the presence of noise necessitated special consideration. It was demonstrated that a modified Wiener frequency filter judiciously constructed to avoid over emphasis of frequency regions dominated by noise resulted in substantially improved images. Several important areas of future research were identified. Two areas of particular promise are the extraction of blurring information directly from the spatial images and improved noise abatement form investigations of select spatial regions and the elimination of spike noise. Author

N91-27095*# Houston Baptist Univ., TX. Dept. of Biology.
NONLINEAR SYSTEMS DYNAMICS IN CARDIOVASCULAR PHYSIOLOGY: THE HEART RATE DELAY MAP AND LOWER BODY NEGATIVE PRESSURE Final Report **c52**
John C. Hooker *In* Houston Univ., NASA/ASEE Summer Faculty Fellowship Program, 1990, Volume 1 Dec. 1990 12 p (For primary document see N91-27088 18-99)
(Grant NGT-44-005-803)
Avail: NTIS HC/MF A10 CSCL 06P

A preliminary study of the applicability of nonlinear dynamic systems analysis techniques to low body negative pressure (LBNP) studies. In particular, the applicability of the heart rate delay map is investigated. It is suggested that the heart rate delay map has potential as a supplemental tool in the assessment of subject performance in LBNP tests and possibly in the determination of susceptibility to cardiovascular deconditioning with spaceflight.
Author

N91-27096*# South Carolina Univ., Columbia. Dept. of Computer Science.
INCORPORATION OF SHUTTLE CCT PARAMETERS IN COMPUTER SIMULATION MODELS Final Report **c54**
Terry Huntsberger *In* Houston Univ., NASA/ASEE Summer Faculty Fellowship Program, 1990, Volume 1 Dec. 1990 12 p (For primary document see N91-27088 18-99)
(Grant NGT-44-005-803)
Avail: NTIS HC/MF A10 CSCL 05H

Computer simulations of shuttle missions have become increasingly important during recent years. The complexity of mission planning for satellite launch and repair operations which usually involve EVA has led to the need for accurate visibility and access studies. The PLAID modeling package used in the Man-Systems Division at Johnson currently has the necessary capabilities for such studies. In addition, the modeling package is used for spatial location and orientation of shuttle components for film overlay studies such as the current investigation of the hydrogen leaks found in the shuttle flight. However, there are a number of differences between the simulation studies and actual mission viewing. These include image blur caused by the finite resolution of the CCT monitors in the shuttle and signal noise from the video tubes of the cameras. During the course of this investigation the shuttle CCT camera and monitor parameters are incorporated into the existing PLAID framework. These parameters are specific for certain camera/lens combinations and the SNR characteristics of these combinations are included in the noise models. The monitor resolution is incorporated using a Gaussian spread function such as that found in the screen phosphors in the shuttle monitors. Another difference between the traditional PLAID generated images and actual mission viewing lies in the lack of shadows and reflections of light from surfaces. Ray tracing of the scene explicitly includes the lighting and material characteristics of surfaces. The results of some preliminary studies using ray tracing techniques for the image generation process combined with the camera and monitor effects are also reported.
Author

N91-27097*# Houston Univ., TX. Dept. of Psychology.
TRAINING EFFECTIVENESS OF AN INTELLIGENT TUTORING SYSTEM FOR A PROPULSION CONSOLE TRAINER Final Report **c53**
Debra Steele Johnson *In its* NASA/ASEE Summer Faculty Fellowship Program, 1990, Volume 1 Dec. 1990 15 p (For primary document see N91-27088 18-99)
(Grant NGT-44-005-803)
Avail: NTIS HC/MF A10 CSCL 05I

A formative evaluation was conducted on an Intelligent Tutoring System (ITS) developed for tasks performed on the Propulsion Console. The ITS, which was developed primarily as a research tool, provides training on use of the Manual Select Keyboard (MSK). Three subjects completed three phases of training using the ITS: declarative, speed, and automaticity training. Data were collected on several performance dimensions, including training time, number of trials performed in each training phase, and number of errors. Information was also collected regarding the user interface and content of training. Suggestions for refining the ITS are discussed. Further, future potential uses and limitations of the ITS are discussed. The results provide an initial demonstration of the effectiveness of the Propulsion Console ITS and indicate the potential benefits of this form of training tool for related tasks.
Author

N91-27098*# Texas Univ., San Antonio. Div. of Engineering.
REEXAMINATION OF METMAN, RECOMMENDATIONS ON ENHANCEMENT OF LCVG, AND DEVELOPMENT OF NEW CONCEPTS FOR EMU HEAT SINK Final Report **c34**
Amir Karimi *In* Houston Univ., NASA/ASEE Summer Faculty Fellowship Program, 1990, Volume 1 Dec. 1990 16 p (For primary document see N91-27088 18-99)
(Grant NGT-44-005-803)
Avail: NTIS HC/MF A10 CSCL 20D

METMAN is a 41-node transient metabolic computer code developed in 1970 and revised in 1989 by Lockheed Engineering and Sciences, Inc. This program relies on a mathematical model to predict the transient temperature distribution in a body influenced by metabolic heat generation and thermal interaction with the environment. A more complex 315-node model is also available that not only simulates the thermal response of a body exposed to a warm environment, but is also capable of describing the thermal response resulting from exposure to a cold environment. It is important to compare the two models for the prediction of the body's thermal response to metabolic heat generation and exposure to various environmental conditions. Discrepancies between the twi models may warrant an investigation of METMAN to ensure its validity for describing the body's thermal response in space environment. The Liquid Cooling and Ventilation Garment is a subsystem of the Extravehicular Mobility Unit (EMU). This garment, worn under the pressure suit, contains the liquid cooling tubing and gas ventilation manifolds; its purpose is to alleviate or reduce thermal stress resulting from metabolic heat generation. There is renewed interest in modifying this garment through identification of the locus of maximum heat transfer at body-liquid cooled tubing interface. The sublimator is a vital component of the Primary Life Support System (PLSS) in the EMU. It acts as a heat sink to remove heat and humidity from the gas ventilating circuit and the liquid cooling loop of the LCVG. The deficiency of the sublimator is that the ice, used as the heat sink, sublimates into space. There is an effort to minimize water losses in the feedwater circuit of the EMU. This requires developing new concepts to design an alternative heat sink system. Efforts are directed to review and verify the heat transfer formulation of the analytical model employed by METMAN. A conceptual investigation of regenerative non-venting heat-sink subsystem for the EMU is recommended.
Author

N91-27099*# Texas A&M Univ., College Station. Dept. of Aerospace Engineering.
A NONRECURSIVE ORDER N PRECONDITIONED CONJUGATE GRADIENT: RANGE SPACE FORMULATION OF MDOF DYNAMICS Final Report **c61**
Andrew J. Kurdila *In* Houston Univ., NASA/ASEE Summer Faculty Fellowship Program, 1990, Volume 1 Dec. 1990 16 p (For primary document see N91-27088 18-99)
(Grant NGT-44-005-803)
Avail: NTIS HC/MF A10 CSCL 09B

While excellent progress has been made in deriving algorithms that are efficient for certain combinations of system topologies and concurrent multiprocessing hardware, several issues must be resolved to incorporate transient simulation in the control design process for large space structures. Specifically, strategies must be developed that are applicable to systems with numerous degrees of freedom. In addition, the algorithms must have a growth potential in that they must also be amenable to implementation on forthcoming parallel system architectures. For mechanical system simulation, this fact implies that algorithms are required that induce parallelism on a fine scale, suitable for the emerging class of highly parallel processors; and transient simulation methods must

be automatically load balancing for a wider collection of system topologies and hardware configurations. These problems are addressed by employing a combination range space/preconditioned conjugate gradient formulation of multi-degree-of-freedom dynamics. The method described has several advantages. In a sequential computing environment, the method has the features that: by employing regular ordering of the system connectivity graph, an extremely efficient preconditioner can be derived from the 'range space metric', as opposed to the system coefficient matrix; because of the effectiveness of the preconditioner, preliminary studies indicate that the method can achieve performance rates that depend linearly upon the number of substructures, hence the title 'Order N'; and the method is non-assembling. Furthermore, the approach is promising as a potential parallel processing algorithm in that the method exhibits a fine parallel granularity suitable for a wide collection of combinations of physical system topologies/computer architectures; and the method is easily load balanced among processors, and does not rely upon system topology to induce parallelism. Author

N91-27100*# Stevens Inst. of Tech., Hoboken, NJ. Dept. of Electrical Engineering.

APPLICATIONS OF FORMAL SIMULATION LANGUAGES IN THE CONTROL AND MONITORING SUBSYSTEMS OF SPACE STATION FREEDOM Final Report **c32**

R. C. Lacovara *In* Houston Univ., NASA/ASEE Summer Faculty Fellowship Program, 1990, Volume 1 Dec. 1990 13 p (For primary document see N91-27088 18-99)
(Grant NGT-44-005-803)
Avail: NTIS HC/MF A10 CSCL 17B

The notions, benefits, and drawbacks of numeric simulation are introduced. Two formal simulation languages, Simpscript and Modsim are introduced. The capabilities of each are discussed briefly, and then the two programs are compared. The use of simulation in the process of design engineering for the Control and Monitoring System (CMS) for Space Station Freedom is discussed. The application of the formal simulation language to the CMS design is presented, and recommendations are made as to their use. Author

N91-27101*# Fordham Univ., New York, NY. Div. of Science and Mathematics.

A STUDY OF MURINE BONE MARROW CELLS CULTURED IN BIOREACTORS WHICH CREATE AN ENVIRONMENT WHICH SIMULATED MICROGRAVITY Final Report **c52**

Brother DeSales Lawless *In* Houston Univ., NASA/ASEE Summer Faculty Fellowship Program, 1990, Volume 1 Dec. 1990 15 p (For primary document see N91-27088 18-99)
(Grant NGT-44-005-803)
Avail: NTIS HC/MF A10 CSCL 06P

Previous research indicated that mouse bone marrow cells could be grown in conditions of simulated microgravity. This environment was created in rotating bioreactor vessels. On three attempts mouse cells were grown successfully in the vessels. The cells reached a stage where the concentrations were doubling daily. Phenotypic analysis using a panel of monoclonal antibodies indicated that the cell were hematopoietic pluripotent stem cells. One unsuccessful attempt was made to reestablish the immune system in immunocompromised mice using these cells. Since last summer, several unsuccessful attempts were made to duplicate these results. It was determined by electron microscopy that the cells successfully grown in 1989 contained virus particles. It was suggested that these virally parasitized cells had been immortalized. The work of this summer is a continuation of efforts to grow mouse bone marrow in these vessels. A number of variations of the protocol were introduced. Certified pathogen free mice were used in the repeat experiments. In some attempts the medium of last summer was used; in others Dexture Culture Medium containing Iscove's Medium supplemented with 20 percent horse serum and 10-6 M hydrocortisone. Efforts this summer were directed solely to repeating the work of last summer. Plans were made for investigations if stem cells were isolated. Immortalization of the undifferentiated stem cell would be attempted by transfection with an oncogenic vector. Selective differentiation would be induced in the stem cell line by growing it with known growth factors and immune response modulators. Interest is in identifying any surface antigens unique to stem cells that would help in their characterization. Another goal was to search for markers on stem cells that would distinguish them from stem cells committed to a particular lineage. If the undifferentiated hematopoietic stem cell was obtained, the pathways that would terminally convert it to myeloid, lyphoid, erythroid, or other cell lines would be studied. Transfection with a known gene would be attempted and then conversion to a terminally identifiable cell. Author

N91-27102*# Kansas State Univ., Manhattan. Dept. of Kinesiology.

THE EFFECTS OF DEUTERIUM ON STATIC POSTURE CONTROL Final Report **c52**

Charles S. Layne *In* Houston Univ., NASA/ASEE Summer Faculty Fellowship Program, 1990, Volume 1 Dec. 1990 12 p (For primary document see N91-27088 18-99)
(Grant NGT-44-005-803)
Avail: NTIS HC/MF A10 CSCL 06P

A significant operational problem impacting upon the Space Shuttle program involves the astronaut's ability to safely egress from the Orbiter during an emergency situation. Following space flight, astronauts display significant movement problems. One variable which may contribute to increased movement ataxia is deuterium (D2O). Deuterium is present in low levels within the Orbiter's water supply but may accumulate to significant physiological levels during lengthy missions. Deuterium was linked to a number of negative physiological responses, including motion sickness, decreased metabolism, and slowing of neural conduction velocity. The effects of D2O on static postural control in response to a range of dosage levels were investigated. Nine sugjects were divided into three groups of three subjects each. The groups were divided into a low, medium, and a high D2O dosage group. The subjects static posture was assessed with the use of the EquiTest systems, a commercially available postural control evaluation system featuring movable force plates and a visual surround that can be servoed to the subject's sway. In addition to the force plate information, data about the degree of subject sway about the hips and shoulders was obtained. Additionally, surface electromyographic (EMG) data from the selected lower limb muscles were collected along with saliva samples used to determine the amount of deuterium enrichment following D2O ingestion. Two baseline testing sessions were performed using the EquiTest testing protocol prior to ingestion of the D2O. Thirty minutes after dosing, subjects again performed the tests. Two more post-dosing tests were run with an interest interval of one hour. Preliminary data anlaysis indicates that only subjects in the igh dose group displayed any significant static postural problems. Future analyses of the sway and EMG is expected to reveal significant variations in the subject's postural control strategy following D2O dosing. While functionally significant static postural problems were not commonly observed, subjects in both the medium and high dosage groups displayed significant, and in some cases, severe voluntary movement problems. Author

N91-27103*# Houston Univ., TX.

NASA/ASEE SUMMER FACULTY FELLOWSHIP PROGRAM, 1990, VOLUME 2

Richard B. Bannerot, ed. and Stanley H. Goldstein, ed. (National Aeronautics and Space Administration. Lyndon B. Johnson Space Center, Houston, TX.) Dec. 1990 177 p Program held in Houston, TX, 1990
(Grant NGT-44-005-803)
(NASA-CR-185637-Vol-2; NAS 1.26:185637-Vol-2) Avail: NTIS HC/MF A09 CSCL 05B

The 1990 Johnson Space Center (JSC) National Aeronautics and Space Administration (NASA)/American Society for Engineering Education (ASEE) Summer Faculty Fellowship Program was conducted by the University of Houston-University Park and Johnson Space Centers (JSC). A compilation of the final reports

on the research projects is presented. The following topics are covered: the Space Shuttle; the Space Station; lunar exploration; mars exploration; spacecraft power supplies; mars rover vehicle; mission planning for the Space Exploration Initiative; instrument calibration standards; a lunar oxygen production plant; optical filters for a hybrid vision system; dynamic structural analysis; lunar bases; pharmacodynamics of scopolamine; planetary spacecraft cost modeling; and others. For individual titles, see N91-27104 through N91-27117.

N91-27104*# University of Northern Arizona, Flagstaff. Dept. of Geology.

EVALUATION OF GEOPHYSICAL PROPERTIES OF THE LUNAR REGOLITH FOR THE DESIGN OF PRECURSOR SCIENTIFIC MISSIONS FOR THE SPACE EXPLORATION INITIATIVE Final Report **c91**

Paul Morgan *In* Houston Univ., NASA/ASEE Summer Faculty Fellowship Program, 1990, Volume 2 Dec. 1990 13 p (For primary document see N91-27103 18-99)
(Grant NGT-44-005-803)
Avail: NTIS HC/MF A09 CSCL 03B

The following topics are addressed: (1) the frequency of encountering boulders that represent hazards to lunar operations; (2) the ease of lunar soil excavation; (3) the use of explosives in excavation operation; (4) the trafficability of the regolith; (5) problems encountered in mining (probably strip mining) of the regolith; (6) the stable angle(s) of repose in excavation of the regolith; (7) the layering to be encountered in the subsurface; (8) knowledge of the regolith site and the possibility of its general application to any site on the lunar surface; (9) the data needed to characterize a site for a lunar base; (10) the influence of regolith properties on the design of geophysical experiments from the lunar base; and (11) terrestrial analogues for the geophysical properties of the lunar regolith. Author

N91-27105*# Florida Inst. of Tech., Melbourne. Dept. of Computer Science.

A DESIGN FOR AN INTELLIGENT MONITOR AND CONTROLLER FOR SPACE STATION ELECTRICAL POWER USING PARALLEL DISTRIBUTED PROBLEM SOLVING Final Report **c33**

Robert A. Morris *In* Houston Univ., NASA/ASEE Summer Faculty Fellowship Program, 1990, Volume 2 Dec. 1990 15 p (For primary document see N91-27103 18-99)
(Grant NGT-44-005-803)
Avail: NTIS HC/MF A09 CSCL 09C

The emphasis is on defining a set of communicating processes for intelligent spacecraft secondary power distribution and control. The computer hardware and software implementation platform for this work is that of the ADEPTS project at the Johnson Space Center (JSC). The electrical power system design which was used as the basis for this research is that of Space Station Freedom, although the functionality of the processes defined here generalize to any permanent manned space power control application. First, the Space Station Electrical Power Subsystem (EPS) hardware to be monitored is described, followed by a set of scenarios describing typical monitor and control activity. Then, the parallel distributed problem solving approach to knowledge engineering is introduced. There follows a two-step presentation of the intelligent software design for secondary power control. The first step decomposes the problem of monitoring and control into three primary functions. Each of the primary functions is described in detail. Suggestions for refinements and embelishments in design specifications are given. Author

N91-27106*# Houston Univ., TX. Dept. of Applied Math. Sciences.

FUZZY LOGIC CONTROL SYSTEM TO PROVIDE AUTONOMOUS COLLISION AVOIDANCE FOR MARS ROVER VEHICLE Final Report **c37**

Michael G. Murphy *In its* NASA/ASEE Summer Faculty Fellowship Program, 1990, Volume 2 Dec. 1990 13 p (For primary document see N91-27103 18-99)
(Grant NGT-44-005-803)
Avail: NTIS HC/MF A09 CSCL 13F

NASA is currently involved with planning unmanned missions to Mars to investigate the terrain and process soil samples in advance of a manned mission. A key issue involved in unmanned surface exploration on Mars is that of supporting autonomous maneuvering since radio communication involves lengthy delays. It is anticipated that specific target locations will be designated for sample gathering. In maneuvering autonomously from a starting position to a target position, the rover will need to avoid a variety of obstacles such as boulders or troughs that may block the shortest path to the target. The physical integrity of the rover needs to be maintained while minimizing the time and distance required to attain the target position. Fuzzy logic lends itself well to building reliable control systems that function in the presence of uncertainty or ambiguity. The following major issues are discussed: (1) the nature of fuzzy logic control systems and software tools to implement them; (2) collision avoidance in the presence of fuzzy parameters; and (3) techniques for adaptation in fuzzy logic control systems. Author

N91-27107*# Virginia Commonwealth Univ., Richmond. Dept. of Mathematical Sciences.

EVALUATING THE EFFECT OF ACCURACY RATIOS ON THE PERCENT OF CALIBRATIONS WHICH ARE OUT OF TOLERANCE Final Report **c38**

Sharon E. Navard *In* Houston Univ., NASA/ASEE Summer Faculty Fellowship Program, 1990, Volume 2 Dec. 1990 15 p (For primary document see N91-27103 18-99)
(Grant NGT-44-005-803)
Avail: NTIS HC/MF A09 CSCL 14D

The standard practice in calibration laboratories across the country, including the Measurement Standards and Calibration Laboratory (MSCL) at the Johnson Space Center, is to use accuracy ratios to determine if instruments are in-tolerance rather than computing the actual uncertainty associated with the instruments. In the past, the accepted practice was to use an accuracy ratio of 10:1, but then state of the art advanced to the point where the 10:1 ratio could no longer be maintained, and the ratio was arbitrarily lowered to 4:1. It is now becoming increasingly difficult to maintain the 4:1 accuracy ratio, and in some cases 1:1 is the best that can be achieved. However, the effect of using these small accuracy ratios on the number of mistakes made in classifying instruments as in or out of tolerance is completely unknown. In order to assess the effect of using accuracy ratios in calibration, a simulation program was written to compute the proportion of instruments determined to be out of tolerance which were actually in, denoted by alpha, and the proportion of instruments determined to be in-tolerance which were actually out, denoted by beta. This was done for accuracy ratios of 1:1 and 10:1, for one to five progressive calibrations, under varying standard and instrument conditions. Selected results are presented and explained. Author

N91-27108*# Houston Univ., TX. Coll. of Architecture.

DEVELOPING A TAXONOMY FOR MISSION ARCHITECTURE DEFINITION Final Report **c12**

Deborah J. Neubek *In its* NASA/ASEE Summer Faculty Fellowship Program, 1990, Volume 2 Dec. 1990 9 p (For primary document see N91-27103 18-99)
(Grant NGT-44-005-803)
Avail: NTIS HC/MF A09 CSCL 22A

The Lunar and Mars Exploration Program Office (LMEPO) was tasked to define candidate architectures for the Space Exploration Initiative to submit to NASA senior management and an externally constituted Outreach Synthesis Group. A systematic, structured process for developing, characterizing, and describing the alternate mission architectures, and applying this process to future studies was developed. The work was done in two phases: (1) national needs were identified and categorized into objectives achievable by the Space Exploration Initiative; and (2) a program development process was created which both hierarchically and iteratively describes the program planning process. Author

N91-27109*# Prairie View Agricultural and Mechanical Coll., TX. Dept. of Civil Engineering.
DESIGN OF A LUNAR OXYGEN PRODUCTION PLANT Final Report **c31**
Ramalingam Radhakrishnan *In* Houston Univ., NASA/ASEE Summer Faculty Fellowship Program, 1990, Volume 2 Dec. 1990 12 p (For primary document see N91-27103 18-99)
(Grant NGT-44-005-803)
Avail: NTIS HC/MF A09 CSCL 13B

To achieve permanent human presence and activity on the moon, oxygen is required for both life support and propulsion. Lunar oxygen production using resources existing on the moon will reduce or eliminate the need to transport liquid oxygen from earth. In addition, the co-products of oxygen production will provide metals, structural ceramics, and other volatile compounds. This will enable development of even greater self-sufficiency as the lunar outpost evolves. Ilmenite is the most abundant metal-oxide mineral in the lunar regolith. A process involving the reaction of ilmenite with hydrogen at 1000 C to produce water, followed by the electrolysis of this water to provide oxygen and recycle the hydrogen has been explored. The objective of this 1990 Summer Faculty Project was to design a lunar oxygen-production plant to provide 5 metric tons of liquid oxygen per year from lunar soil. The results of this study describe the size and mass of the equipment, the power needs, feedstock quantity and the engineering details of the plant. Author

N91-27110*# Tennessee Technological Univ., Cookeville. Dept. of Electrical Engineering.
DESIGN OF OPTIMAL CORRELATION FILTERS FOR HYBRID VISION SYSTEMS Final Report **c33**
Periasamy K. Rajan *In* Houston Univ., NASA/ASEE Summer Faculty Fellowship Program, 1990, Volume 2 Dec. 1990 15 p (For primary document see N91-27103 18-99)
(Grant NGT-44-005-803)
Avail: NTIS HC/MF A09 CSCL 09C

Research is underway at the NASA Johnson Space Center on the development of vision systems that recognize objects and estimate their position by processing their images. This is a crucial task in many space applications such as autonomous landing on Mars sites, satellite inspection and repair, and docking of space shuttle and space station. Currently available algorithms and hardware are too slow to be suitable for these tasks. Electronic digital hardware exhibits superior performance in computing and control; however, they take too much time to carry out important signal processing operations such as Fourier transformation of image data and calculation of correlation between two images. Fortunately, because of the inherent parallelism, optical devices can carry out these operations very fast, although they are not quite suitable for computation and control type operations. Hence, investigations are currently being conducted on the development of hybrid vision systems that utilize both optical techniques and digital processing jointly to carry out the object recognition tasks in real time. Algorithms for the design of optimal filters for use in hybrid vision systems were developed. Specifically, an algorithm was developed for the design of real-valued frequency plane correlation filters. Furthermore, research was also conducted on designing correlation filters optimal in the sense of providing maximum signal-to-nose ratio when noise is present in the detectors in the correlation plane. Algorithms were developed for the design of different types of optimal filters: complex filters, real-value filters, phase-only filters, ternary-valued filters, coupled filters. This report presents some of these algorithms in detail along with their derivations. Author

N91-27111*# California Univ., San Diego, La Jolla. Dept. of AMES.
DEVELOPMENT OF LOAD-DEPENDENT RITZ VECTOR METHOD FOR STRUCTURAL DYNAMIC ANALYSIS OF LARGE SPACE STRUCTURES Final Report **c39**
James M. Ricles *In* Houston Univ., NASA/ASEE Summer Faculty Fellowship Program, 1990, Volume 2 Dec. 1990 16 p (For primary document see N91-27103 18-99)
(Grant NGT-44-005-803)
Avail: NTIS HC/MF A09 CSCL 20K

The development and preliminary assessment of a method for dynamic structural analysis based on load-dependent Ritz vectors are presented. The vector basis is orthogonalized with respect to the mass and structural stiffness in order that the equations of motion can be uncoupled and efficient analysis of large space structure performed. A series of computer programs was developed based on the algorithm for generating the orthogonal load-dependent Ritz vectors. Transient dynamic analysis performed on the Space Station Freedom using the software was found to provide solutions that require a smaller number of vectors than the modal analysis method. Error norm based on the participation of the mass distribution of the structure and spatial distribution of structural loading, respectively, were developed in order to provide an indication of vector truncation. These norms are computed before the transient analysis is performed. An assessment of these norms through a convergence study of the structural response was performed. The results from this assessment indicate that the error norms can provide a means of judging the quality of the vector basis and accuracy of the transient dynamic solution. Author

N91-27112*# Texas Lutheran Coll., Seguin. Dept. of Biology.
MECHANICS, IMPACT LOADS AND EMG ON THE SPACE SHUTTLE TREADMILL Final Report **c52**
William G. Squires *In* Houston Univ., NASA/ASEE Summer Faculty Fellowship Program, 1990, Volume 2 Dec. 1990 3 p (For primary document see N91-27103 18-99)
(Grant NGT-44-005-803)
Avail: NTIS HC/MF A09 CSCL 06E

The ability of astronauts to egress the Shuttle, particularly during emergency conditions, is likely to be reduced following physiological adaptation in space. It is well established that effective application of exercise counter measures requires the exercise to be applied specifically. The problem is that objective scientific evidence is not available to validate the Space Shuttle treadmill with respect to in its role in diminishing the deleterious effects of a prolonged exposure to the microgravity environment. Author

N91-27113*# Alma Coll., MI. Dept. of Chemistry.
SOLUTIONS TO PROBLEMS OF WEATHERING IN ANTARCTIC EUCRITES Final Report **c90**
Melissa M. Strait *In* Houston Univ., NASA/ASEE Summer Faculty Fellowship Program, 1990, Volume 2 Dec. 1990 13 p (For primary document see N91-27103 18-99)
(Grant NGT-44-005-803)
Avail: NTIS HC/MF A09 CSCL 03B

Neutron activation analysis was performed for major and trace elements on a suite of eucrites from both Antarctic and non-Antarctic sources. The chemistry was examined to see if there was an easy way to distinguish Antarctic eucrites that had been disturbed in their trace elements systematics from those that had normal abundances relative to non-Antarctic eucrites. There was no simple correlation found, and identifying the disturbed meteorites still remains a problem. In addition, a set of mineral separates from an eucrite were analyzed. The results showed no abnormalities in the chemistry and provides a possible way to use Antarctic eucrites that were disturbed in modelling of the eucrite parent body. Author

N91-27114*# Philadelphia Coll. of Pharmacy and Science, PA. Dept. of Pharmacy Practice/Pharmacy Administration.
ASSESSMENT OF THE PHARMACODYNAMICS OF INTRANASAL, INTRAVENOUS AND ORAL SCOPOLAMINE Final Report **c52**
Karen J. Tietze *In* Houston Univ., NASA/ASEE Summer Faculty Fellowship Program, 1990, Volume 2 Dec. 1990 14 p (For primary document see N91-27103 18-99)
(Grant NGT-44-005-803)
Avail: NTIS HC/MF A09 CSCL 06E

Space motion sickness is an important issue in the space

medical sciences program. One of the objectives of the ongoing clinical experimental protocol Pharmacokinetics of Intranasal Scopolamine in Normal Subjects is to evaluate the pharmacodynamics of scopolamine using salivary flow rate and pH profiles and cognitive performance tests as pharmacodynamic parameters. Normal volunteers collected saliva and performed the NTI Multiresource Performance Battery tests at designed time intervals to establish control saliva flow rates, salivary pH profiles, and the characteristics of the learning curve for the performance program under normal conditions. In the clinical part of the study, saliva samples and performance test scores are collected from healthy nonsmoking subjects after receiving a single 0.4 mg dose of either intranasal, intravenous, or oral scopolamine. Author

N91-27115*# Stevens Inst. of Tech., Hoboken, NJ. Dept. of Electrical Engineering and Computer Science.
HIGH ACCURACY OPTICAL RATE SENSOR Final Report c74
J. Uhde-Lacovara *In* Houston Univ., NASA/ASEE Summer Faculty Fellowship Program, 1990, Volume 2 Dec. 1990 13 p (For primary document see N91-27103 18-99)
(Grant NGT-44-005-803)
Avail: NTIS HC/MF A09 CSCL 20F

Optical rate sensors, in particular CCD arrays, will be used on Space Station Freedom to track stars in order to provide inertial attitude reference. An algorithm to provide attitude rate information by directly manipulating the sensor pixel intensity output is presented. The star image produced by a sensor in the laboratory is modeled. Simulated, moving star images are generated, and the algorithm is applied to this data for a star moving at a constant rate. The algorithm produces accurate derived rate of the above data. A step rate change requires two frames for the output of the algorithm to accurately reflect the new rate. When zero mean Gaussian noise with a standard deviation of 5 is added to the simulated data of a star image moving at a constant rate, the algorithm derives the rate with an error of 1.9 percent at a rate of 1.28 pixels per frame. Author

N91-27116*# Mississippi Valley State Univ., Itta Bena. Dept. of Computer Science and Mathematics.
PLANETARY SPACECRAFT COST MODELING UTILIZING LABOR ESTIMATING RELATIONSHIPS Final Report c83
Raymond Williams *In* Houston Univ., NASA/ASEE Summer Faculty Fellowship Program, 1990, Volume 2 Dec. 1990 6 p (For primary document see N91-27103 18-99)
(Grant NGT-44-005-803)
Avail: NTIS HC/MF A09 CSCL 05C

A basic computerized technology is presented for estimating labor hours and cost of unmanned planetary and lunar programs. The user friendly methodology designated Labor Estimating Relationship/Cost Estimating Relationship (LERCER) organizes the forecasting process according to vehicle subsystem levels. The level of input variables required by the model in predicting cost is consistent with pre-Phase A type mission analysis. Twenty one program categories were used in the modeling. To develop the model, numerous LER and CER studies were surveyed and modified when required. The result of the research along with components of the LERCER program are reported. Author

N91-27117*# Coast Guard Academy, New London, CT. Dept. of Engineering.
STRUCTURAL CONCEPT STUDIES FOR A HORIZONTAL CYLINDRICAL LUNAR HABITAT AND A LUNAR GUYED TOWER Final Report c39
Paul K. Yin *In* Houston Univ., NASA/ASEE Summer Faculty Fellowship Program, 1990, Volume 2 Dec. 1990 15 p (For primary document see N91-27103 18-99)
(Grant NGT-44-005-803)
Avail: NTIS HC/MF A09 CSCL 20K

A conceptual structural design of a horizontal cylindrical lunar habitat is presented. The design includes the interior floor framing, the exterior support structure, the foundation mat, and the radiation shielding. Particular attention was given on its efficiency in shipping and field erection, and on selection of structural materials. Presented also is a conceptual design of a 2000-foot lunar guyed tower. A special field erection scheme is implemented in the design. In order to analyze the over-all column buckling of the mast, where its axial compression includes its own body weight, a simple numerical procedure is formulated in a form ready for coding in FORTRAN. Selection of structural materials, effect of temperature variations, dynamic response of the tower to moonquake, and guy anchoring system are discussed. Proposed field erection concepts for the habitat and for the guyed tower are described. Author

N91-27118# Naval Academy, Annapolis, MD.
SUMMARY OF RESEARCH ACADEMIC DEPARTMENTS, OCTOBER 1990 Annual Report, Jul. 1989 - Jun. 1990
Fred Fetrow Oct. 1990 321 p
(AD-A234353; USNA-3910-3; Rept-15) Avail: NTIS HC/MF A14 CSCL 05/2

The research work of the Naval Academy faculty and midshipmen is summarized. Sponsored and independent research projects are listed by title, followed by the names of the investigators and an abstract. A list of publications and their abstracts are included as well as presentations at professional meetings, conferences, and seminars. GRA

N91-27119*# National Aeronautics and Space Administration, Washington, DC.
NASA INFORMATION SCIENCES AND HUMAN FACTORS PROGRAM Annual Report, 1990
Lee Holcomb, Ray Hood, Melvin Montemerlo, James Jenkins, Paul Smith, John DiBattista, Ramon DePaula, Paul Hunter, and David Lavery May 1991 226 p
(NASA-TM-4291; NAS 1.15:4291) Avail: NTIS HC/MF A11 CSCL 05H

The FY-90 descriptions of technical accomplishments are contained in seven sections: Automation and Robotics, Communications, Computer Sciences, Controls and Guidance, Data Systems, Human Factors, and Sensor Technology. Author

Typical Subject Index Listing

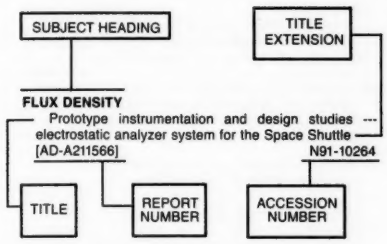

The subject heading is a key to the subject content of the document. Titles, report numbers, and accession numbers of pertinent documents are provided under each subject heading. When the title is insufficiently descriptive of the document content, a title extension has been added, separated from the title by three hyphens. The report number helps to indicate the type of document cited (e.g., NASA report, NASA translation, NASA contractor report). The accession number is the number by which the document abstracts are arranged in this journal and by which the document is sold or requested. The titles, with title extensions if present, are arranged under each subject heading in ascending accession number order. The subject headings have been selected from the latest revision of the *NASA Thesaurus* (NASA SP-7064).

A

ABILITIES
A procedure to detect item bias present simultaneously in several items
[AD-A235252] N91-26862

ABLATION
Size dependence of gaseous cluster reactivity and evaporation dynamics as a mechanistic probe
[AD-A233811] N91-26249
Diagnostic studies of YBa2Cu3O(7-delta) laser ablation
[DE91-011382] N91-26515
In-situ monitoring of laser ablation of superconductors
[DE91-012057] N91-26524
Sand and dust issues for the MESUR mission
N91-27080

ABRASION
Abrasive-waterjet machining of isogrid structures
[AD-A234628] N91-26405
Wind abrasion on Mars N91-27064

ABRASION RESISTANCE
Performance evaluation of a novel erosion-resistant pump design
[DE91-008201] N91-26528

ABRASIVES
Numerical simulations of the indentation of glass with implications to ductile grinding
[DE91-011512] N91-26381
Sand and dust issues for the MESUR mission
N91-27080

ABSORPTION SPECTRA
Photoexcitation spectroscopy of pernigraniline
[AD-A233841] N91-26250
Tetra neopentoxy phthalo cyanine Langmuir-Blodgett films: Spectroscopy at the air/water interface
[AD-A234603] N91-26261

ABSORPTION SPECTROSCOPY
Elementary reaction rate measurements at high temperatures by tunable-laser flash-absorption
[DE91-011850] N91-26516
Infrared and visible laser double resonance studies of vibrational energy transfer processes in polyatomic molecules
[DE91-012162] N91-26910
Photoinduced absorption and erasable optical information storage in polyanilines
[AD-A234108] N91-27002

ABSTRACTS
JPRS report: Science and technology. USSR: Life sciences
[JPRS-ULS-91-010] N91-26683
Cognitive and neural sciences division 1990 programs
[AD-A233773] N91-26733
Materials Science and Engineering, 1989 publications
[AD-A234087] N91-27001
Summary of research academic departments, October 1990
[AD-A234353] N91-27118

ABUNDANCE
Phytoplankton abundance in relation to Lagrangian paths
[AD-A233728] N91-26672
The distribution of particulate material on Mars
N91-27059

ACCELERATED LIFE TESTS
Lifetimes and failure mechanisms of W/Re hairpin filaments
[AD-A235199] N91-26305
Long-term prediction test procedure for most ICs, based on linear response theory
[NASA-CR-185843] N91-26462
Performance evaluation of a novel erosion-resistant pump design
[DE91-008201] N91-26528

ACCELERATION (PHYSICS)
Acceleration insensitive resonators
[AD-A235400] N91-26458

ACCELERATION PROTECTION
Liquid film cooling in rocket engines
[AD-A234288] N91-26197

ACCIDENTS
Minutes of the 24th Explosives Safety Seminar, volume 2
[AD-A235006] N91-26396

ACCUMULATORS
Depressed collector experiments on a quasioptical gyrotron
[AD-A234559] N91-26492

ACCURACY
Calculation of the pointing accuracy of spacecraft equipment using autonomous measurements of the angular position of the object of investigation
N91-26167
The effects of display failures and symbol rotation on visual search and recognition performance
[AD-A235035] N91-26743

ACETATES
Surface characterization of electrically conducting nickel tetrathiooxalate/poly(vinyl alcohol) composites
[AD-A234598] N91-26353

ACETONE
Transport and fate of acetone in an outdoor model stream, Stennis Space Center near Bay St. Louis, Mississippi
[PB91-154674] N91-26600

ACETONITRILE
Raman spectroscopy study of solvation structure in acetonitrile/water mixtures
[AD-A234921] N91-26271

ACETYLENE
Adsorption and decomposition of acetylene on Si(100)-(2x1)
[AD-A233808] N91-26248
Synthesis, polymerization and thermal properties of a new acetylene-terminated Schiff base
[AD-A233806] N91-26328

ACID RAIN
Acid rain in Asia
[DE91-011160] N91-26595
Simulation of precipitation scavenging in a three-dimensional global model
[DE91-011531] N91-26606
The impact of atmospheric damage to materials on consumers: News you can use
[DE91-012075] N91-26610

ACOUSTIC EMISSION
The hysteresis and incremental collapse of complex structures: A paradigm for the fatigue failure of materials
[AD-A234831] N91-26563
Progress in ultrasonic measurements research in 1990: Transient sources for acoustic emission work
[AD-A234965] N91-26882
Hydroacoustics of intermittent boundary-layer flow: A review
[AD-A235092] N91-26883

ACOUSTIC IMPEDANCE
Inverse scattering problems for acoustic waves in an inhomogeneous medium N91-26876

ACOUSTIC MEASUREMENT
Methods for determining crack depth
[AD-A234799] N91-26562
The hysteresis and incremental collapse of complex structures: A paradigm for the fatigue failure of materials
[AD-A234831] N91-26563
Vertical incidence backscatter and surface forward scattering from near-surface bubbles
[AD-A234432] N91-26880
Progress in ultrasonic measurements research in 1990: Transient sources for acoustic emission work
[AD-A234965] N91-26882
Multiple-frequency SAW devices for chemical sensing and materials characterization
[DE91-010856] N91-26888

ACOUSTIC PROPAGATION
Reflection of incident pressure waves by ribbed panels
[AD-A233671] N91-26469

ACOUSTIC PROPERTIES
Lead detection and mapping with reference to relationships between scale, sensor characteristics, surface conditions and atmospheric properties
[AD-A235121] N91-26666

ACOUSTIC SCATTERING
Inverse scattering problems for acoustic waves in an inhomogeneous medium N91-26876
A boundary scattering strength extraction algorithm for the analysis of long-range reverberation data
[AD-A233721] N91-26877
Underwater scattering of sound
[AD-A235097] N91-26885

ACOUSTICS
Control of an axisymmetric turbulent jet by multi-modal excitation
[NASA-TM-104483] N91-26121
Progress with neural network gulf streams
[AD-A233810] N91-26658
Ocean acoustic tomography and telemetry
[AD-A233826] N91-26659
Boundary layer transition noise art
[AD-A235093] N91-26884

ACOUSTO-OPTICS
Automatic target recognition using acousto-optic image correlator
[DE91-011499] N91-26936

ACRYLATES
Laser ionic multiphoton dissociation of some acrylate clusters
[AD-A233801] N91-26247

ACRYLIC RESINS
High pulse-energy flashlamp-pumpable laser dyes
[AD-A233837] N91-26499

ACTINIDE SERIES
Molecular orbital studies of the bonding in heavy element organometallics
[DE91-010915] N91-26905

ACTIVATION
Adsorption and thermal behavior of ethylene on Si(100)-(2x1)
[AD-A234098] N91-26252
ACTIVATION ENERGY
A model for the scattering of high-frequency electromagnetic fields from dielectrics exhibiting thermally-activated electrical losses
[NASA-TM-104376] N91-26872
Bulk wave characterization of high T(sub c) superconductors
[AD-A234649] N91-26954
ACTIVE CONTROL
Improved reduction of gust loads data for gust intensity N91-26153
Nonlinear dynamics and control of flexible structures
[AD-A235186] N91-26191
The delay of turbulent boundary layer separation by oscillatory active control
[ITN-91-85104] N91-26482
ACTIVITY (BIOLOGY)
Individual stereotypes of human neuropsychic prognostic activity in problem situations with different probability structures N91-26695
ACTS
Advanced Satellite Research Project: SCAR Research Database. Bibliographic analysis
[NASA-CR-186086] N91-26182
ADA (PROGRAMMING LANGUAGE)
An approach for constructing reusable software components in Ada
[AD-A233662] N91-26770
Ada compiler validation summary report: Certification number: 9000703W1.11014, Silicon Graphics 4D ADA Iris-4D/380 (host) Iris-4D/380 (target)
[AD-A233714] N91-26771
Ada software portability and level 2 system simulator integration issues
[AD-A233757] N91-26773
Ada compiler validation summary report: Certificate number 900703W1.11015, Silicon Graphics 4D Ada, Iris-4D/220S (host) Iris-4D/220S (target)
[AD-A233786] N91-26776
Software Technology for Adaptable, Reliable Systems (STARS), UR60-IRIS-Ada toolset. User's guide (draft)
[AD-A234445] N91-26783
Translating expert system rules into Ada code with validation and verification
[NASA-CR-187505] N91-26800
Strategies for parallel AI implementations
[AD-A234449] N91-26811
ADAPTATION
Adaptation and resistance of ecosystems to stress
[AD-A234576] N91-26603
JPRS Report: Science and technology. USSR: Life sciences
[JPRS-ULS-91-009] N91-26688
Biochemical aspects of human adaptation to combined effect of antiorthostasis, decreased barometric pressure, and increased oxygen content N91-26694
Individual stereotypes of human neuropsychic prognostic activity in problem situations with different probability structures N91-26695
Visual accommodation in cosmonauts N91-26697
State and forms of adaptation of vestibular function after space flights N91-26706
ADAPTIVE CONTROL
Adaptive control of direct drive dexterous robotic hand with bilateral tactile sensing
[AD-A233980] N91-26532
ROBOT: A journal of Chinese Society of Automation
[AD-A234808] N91-26538
ADAPTIVE OPTICS
Scaling CW electron beam pumped rare gas lasers to ultra-high average power
[AD-A235120] N91-26513
ADDITIVES
New developments in the synthesis and doping of polyacetylene and polyaniline
[AD-A233702] N91-26244
Synthetic metals: A novel role for organic polymers
[AD-A233862] N91-26334
Impedance profiling: A convenient technique for determining the redox or protonic acid doping characteristics of conducting polymers
[AD-A233941] N91-26337
Additives for high temperature liquid lubricants
[DE91-011018] N91-26386
ADHESION
Characterization studies of fluorinated epoxy resins: Naval experimental resin C8/1SA as a structural material and for use in blends and composites
[AD-A234186] N91-26338
ADHESIVE BONDING
The development of piezoelectric poly(vinylidene fluoride) sensors for measuring peel stresses in adhesive joints
[AD-A233880] N91-26559
ADIABATIC EQUATIONS
An analysis on the stability of the Mie-Gruneisen equation of state for describing the behavior of shock-loaded materials
[AD-A233827] N91-26988
ADSORBENTS
Regeneration of whetlerite for adsorbing toxic pollutants from air
[AD-D014859] N91-26753
ADSORPTION
Adsorption and thermal behavior of ethylene on Si(100)-(2x1)
[AD-A234098] N91-26252
Adsorption and decomposition of diethylsilane on silicon surfaces
[AD-A234639] N91-26267
Surface diffusion at the liquid-solid interface: Quenching of fluorescence from pyrene covalently bound to methylated silica
[AD-A234645] N91-26268
The stepwise dissociation of NH3 on the Si(111)-(7x7) surface: Low temperature dissociative adsorption and thermal effects
[AD-A235009] N91-26274
Adsorption of ammonia on iron clusters
[DE91-011125] N91-26308
Epitaxy of metal atoms on metal surfaces: Deposition and diffusion
[DE91-011142] N91-26309
ADVANCED LAUNCH SYSTEM (STS)
ALS liquid hydrogen turbopump: Advanced Development Program
[NASA-CR-183730] N91-26196
AEOLIAN TONES
Radar-aeolian roughness project
[NASA-CR-4378] N91-27056
The aeolian wind tunnel N91-27065
AERIAL EXPLOSIONS
Minutes of the 24th Explosives Safety Seminar, volume 2
[AD-A235006] N91-26396
AERODYNAMIC CHARACTERISTICS
Aerodynamics of a 0.60 caliber electromagnetic projectile
[AD-A234660] N91-26116
The effect of sabot wheelbase and position on the launch dynamics of fin-stabilized kinetic energy ammunition
[AD-A234945] N91-26118
Performance optimization of helicopter rotor blades
[NASA-TM-104054] N91-26137
Size dependence of gaseous cluster reactivity and evaporation dynamics as a mechanistic probe
[AD-A233811] N91-26249
An experimental investigation of structure, mixing, and combustion in compressible turbulent shear layers
[AD-A235278] N91-26281
AERODYNAMIC DRAG
Viscous flow simulations of internal store carriage and separation
[NASA-CR-185343] N91-26123
Oscillations of a small-mass satellite probe caused by aerodynamic and gravitational forces N91-26165
AERODYNAMIC FORCES
Aerodynamics of a 0.60 caliber electromagnetic projectile
[AD-A234660] N91-26116
Viscous flow simulations of internal store carriage and separation
[NASA-CR-185343] N91-26123
AERODYNAMIC INTERFERENCE
Viscous flow simulations of internal store carriage and separation
[NASA-CR-185343] N91-26123
AERODYNAMIC LOADS
Manual on the flight of flexible aircraft in turbulence
[AGARD-AG-317] N91-26150
AERODYNAMIC STABILITY
The effect of sabot wheelbase and position on the launch dynamics of fin-stabilized kinetic energy ammunition
[AD-A234945] N91-26118
Dynamics of elastic bending and torsion of hingeless rotors with dynamic stall
[AD-A234775] N91-26134
AERODYNAMIC STALLING
Dynamics of elastic bending and torsion of hingeless rotors with dynamic stall
[AD-A234775] N91-26134
AERODYNAMICS
Calculated aerodynamics of wings in severe maneuver
[AD-A235241] N91-26120
Experimental techniques in the field of low density aerodynamics
[AGARD-AG-318(E)] N91-26124
JPRS report: Science and technology. USSR: Space
[JPRS-USP-91-002] N91-26162
Vehicle steering device
[AD-D014861] N91-26537
AEROELASTICITY
Development of an integrated aeroservoelastic analysis program and correlation with test data
[NASA-TP-3120] N91-26113
State space models for aeroelastic and viscoelastic systems
[AD-A234730] N91-26117
AEROEMBOLISM
The Trendelenburg position after cerebral air embolism in dogs: Effects on the somatosensory evoked potential, intracranial pressure, and blood-brain barrier
[AD-A233809] N91-26673
AERONAUTICAL ENGINEERING
Results of the aeronautical systems division critical process team on integrated product development
[AD-A235419] N91-26995
AEROSOLS
Characteristics of aerosol in the atmosphere of Mars according to data from the KRFM experiment N91-26175
Atmospheric propagation of laser beams
[AD-A234314] N91-26501
Effect of aerosols on laser-induced breakdown
[AD-A234324] N91-26502
Modal aerosol dynamics modeling
[PB91-161729] N91-26598
Growth, evaporation and melting of ice crystals: Implications for radiation, atmospheric dynamics and particle scavenging N91-26611
Evaluation of the Navy oceanic vertical aerosol model using lidar and PMS particle-size spectrometers
[AD-A233653] N91-26625
Airliner cabin environment: Contaminant measurements, health risks, and mitigation options
[PB91-159384] N91-26746
AEROSPACE ENGINEERING
JPRS report: Science and technology. USSR: Space
[JPRS-USP-91-002] N91-26162
Prime Minister Li Peng talks with representatives to a discussion meeting on satellite applications and applied satellite technology about the development of our country's activities in space
[AD-A234801] N91-26181
LaRC-ITPI/arylene ether copolymers
[NASA-TM-104099] N91-26378
AEROSPACE ENVIRONMENTS
Reexamination of METMAN, recommendations on enhancement of LCVG, and development of new concepts for EMU heat sink N91-27098
AEROSPACE MEDICINE
USSR Space Life Sciences Digest, issue 29
[NASA-CR-3922(34)] N91-26669
USSR Space Life Sciences Digest, issue 30
[NASA-CR-3922(36)] N91-26670
Risk factors and prediction of syncopic states in flyers N91-26685
Survey of the principal results of medical research in the flight program of the second main expedition aboard the Mir orbiting complex N91-26686
JPRS Report: Science and technology. USSR: Life sciences
[JPRS-ULS-91-009] N91-26688
JPRS report: Science and technology. USSR: Life sciences
[JPRS-ULS-91-011] N91-26696
Utilization of emergency medical kits by air carriers
[AD-A234784] N91-26721
SPH-4 aircrew helmet impact protection improvements 1970-1990
[AD-A233784] N91-26750
AEROSPACE SYSTEMS
State space models for aeroelastic and viscoelastic systems
[AD-A234730] N91-26117
Studies in modeling, dynamics, and control of space structures
[AD-A235059] N91-26190
Space support for airland battle-future
[AD-A233868] N91-26864
Results of the aeronautical systems division critical process team on integrated product development
[AD-A235419] N91-26995
AEROSPACE VEHICLES
Aerospace plane technology: Research and development efforts in Europe. Report to the Chairman, Committee on Science, Space, and Technology, House of Representatives
[GAO/NSIAD-91-194] N91-26141

AFFINITY
The chemical modification of plasmas
[AD-A234448] N91-26940
AFTERBODIES
Navier-Stokes calculations of scramjet-nozzle-afterbody flowfields
[NASA-CR-185356] N91-26488
AFTERBURNING
Turbulent premixed hydrogen/air flames
[AD-A235109] N91-26278
AGE FACTOR
Young and older observers show similar perceived contrast functions for isoluminant stimuli
[AD-A233766] N91-26709
AGGLOMERATION
Saltation threshold reduction due to the electrostatic agglomeration of fine particles N91-27071
AGGREGATES
Molecular orientation of the silver tetra neopentoxy phthalo cyanine and stearic acid mixed Langmuir-Blodgett film and its chemical and electrochemical behaviour
[AD-A234601] N91-26206
AGING (BIOLOGY)
Young and older observers show similar perceived contrast functions for isoluminant stimuli
[AD-A233766] N91-26709
AGING (MATERIALS)
Evaluation of environmentally aged polymer/composite material by ultrasonic inspection
[AD-A235343] N91-26231
AH-64 HELICOPTER
Visual and field-of-view evaluation of the M-43 protective mask with prescription eyepieces
[AD-A234592] N91-26754
AIR
Refurbishing AV-8 on-board oxygen generation system beds
[AD-A235083] N91-26136
AIR BREATHING ENGINES
Turbulent premixed hydrogen/air flames
[AD-A235109] N91-26278
AIR DEFENSE
Space doctrine
[AD-A234971] N91-26866
AIR LOCKS
Impact of Mars sand on dust on the design of space suits and life support equipment: A technology assessment N91-27079
AIR NAVIGATION
Autonomous aircraft initiative study
[NASA-CR-186013] N91-26140
AIR POLLUTION
JPRS report: Science and technology. USSR: Earth sciences
[JPRS-UES-91-003] N91-26582
Ecological exposure and effects of airborne toxic chemicals: An overview
[PB91-148460] N91-26594
Acid rain in Asia
[DE91-011160] N91-26595
An assessment of CO2 greenhouse gas mitigation technologies
[DE91-011972] N91-26605
Relationships between PAN and ozone at sites in eastern North America
[DE91-011728] N91-26607
AQUIS: An air quality and permit information management system
[DE91-011750] N91-26608
Free-air carbon dioxide enrichment: A new approach to research on carbon exchange processes
[DE91-012074] N91-26609
The impact of atmospheric damage to materials on consumers: News you can use
[DE91-012075] N91-26610
Description of the RIVM/KNMI puff dispersion model
[KNMI-177] N91-26638
Regeneration of whetlerite for adsorbing toxic pollutants from air
[AD-D014859] N91-26753
AIR PURIFICATION
An Air Revitalization Model (ARM) for Regenerative Life Support Systems (RLSS) N91-27093
AIR QUALITY
AQUIS: An air quality and permit information management system
[DE91-011750] N91-26608
Adaptive component methods for time dependent PDE's
[AD-A233776] N91-26775
AIR SEA ICE INTERACTIONS
Ice cores and SeaRISE: What we do (and don't) know N91-26579
AIR TO SURFACE MISSILES
Apparatus for guiding a missile
[AD-D014866] N91-26147
AIR TRAFFIC
Civil tiltrotor missions and applications. Phase 2: The commercial passenger market
[NASA-CR-177576] N91-26126
Format and basic geometry of a perspective display of air traffic for the cockpit
[NASA-TM-86680] N91-26142
AIR TRAFFIC CONTROL
Functional baseline specification for ATC data link service implementation in the host computer system
[DOT/FAA/CT-91/12] N91-26433
AIR TRAFFIC CONTROLLERS (PERSONNEL)
Effect of shift work of air traffic controllers on sympathetic nervous system N91-26700
AIR TRANSPORTATION
Civil tiltrotor missions and applications. Phase 2: The commercial passenger market
[NASA-CR-177576] N91-26126
AIR WATER INTERACTIONS
Tetra neopentoxy phthalo cyanine Langmuir-Blodgett films: Spectroscopy at the air/water interface
[AD-A234603] N91-26261
JPRS report: Science and technology. USSR: Earth sciences
[JPRS-UES-91-003] N91-26582
In the energy active region of the ocean N91-26583
Directional characteristics of waves in shallow water
[AD-A234568] N91-26661
Laboratory modelling of the dynamics of coastal upwelling
[AD-A234987] N91-26664
Inorganic carbon surveys of oceanic basins
[DE91-011132] N91-26667
AIRCRAFT BRAKES
A look at digital nose wheel steering
[AD-A233944] N91-26131
AIRCRAFT COMPARTMENTS
Airliner cabin environment: Contaminant measurements, health risks, and mitigation options
[PB91-159384] N91-26746
Aircraft interior noise reduction by alternate resonance tuning
[NASA-CR-185453] N91-26889
AIRCRAFT CONFIGURATIONS
Technology needs for high-speed rotorcraft, volume 1
[NASA-CR-177585] N91-26139
AIRCRAFT CONSTRUCTION MATERIALS
Composite fiber hazards
[AD-A233924] N91-26211
AIRCRAFT CONTROL
Flight control law synthesis using neural network theory
[AD-A234990] N91-26149
AIRCRAFT DESIGN
Manual on the flight of flexible aircraft in turbulence
[AGARD-AG-317] N91-26150
Measurement of atmospheric turbulence N91-26151
Certification procedures and requirements N91-26154
AIRCRAFT ENGINES
Survey of current aircraft engine conditions
[AD-A235143] N91-26144
Titanium alloy integrated centrifugal impeller 5 coordinate computer assisted manufacturing technology
[AD-A234797] N91-26300
AIRCRAFT MANEUVERS
Calculated aerodynamics of wings in severe maneuver
[AD-A235241] N91-26120
AIRCRAFT NOISE
Aircraft interior noise reduction by alternate resonance tuning
[NASA-CR-185453] N91-26889
AIRCRAFT PERFORMANCE
Acquisition of statistical gust load data by commercial airplanes N91-26152
Advanced Dynamic Anthropomorphic Manikin (ADAM) design report
[AD-A234761] N91-26756
AIRCRAFT RELIABILITY
Gust design procedures N91-26155
AIRCRAFT STRUCTURES
Analysis by the statistical discrete gust method N91-26156
Composite fiber hazards
[AD-A233924] N91-26211
AIRFOIL OSCILLATIONS
Theoretical studies of the kinematics, dynamics, stability, and control of unsteady/vortical flows
[AD-A235190] N91-26477
AIRFRAMES
Survey of current aircraft engine conditions
[AD-A235143] N91-26144
AIRGLOW
UV aurora mapping in corrected geomagnetic coordinates
[ITN-91-85106] N91-26636
AIRLINE OPERATIONS
Civil tiltrotor missions and applications. Phase 2: The commercial passenger market
[NASA-CR-177576] N91-26126
Utilization of emergency medical kits by air carriers
[AD-A234784] N91-26721
AIRPORT PLANNING
Guidelines for design, construction, and evaluation of airport pavement drainage
[DOT/FAA/RD-90/31] N91-26161
AIRPORTS
Guidelines for design, construction, and evaluation of airport pavement drainage
[DOT/FAA/RD-90/31] N91-26161
AIRSPEED
Vehicle steering device
[AD-D014861] N91-26537
ALBEDO
Recent studies of the optical properties of dust and cloud particles in the Mars atmosphere and the interannual frequency of global dust storms N91-27060
The effects of atmospheric dust on observations of Martian surface albedo N91-27072
Thermal and albedo mapping of the north and south polar regions of Mars N91-27076
ALERTNESS
Methylphenidate and pemoline: Effects on sleepiness and mood during sleep deprivation
[AD-A234659] N91-26718
ALGORITHMS
Analytical algorithms to solve an inverse navigation problem for a system of satellites N91-26168
Geometry, dynamics and control of coupled systems N91-26401
Active devices for monolithic millimeter-wave integrated circuits
[AD-A234033] N91-26440
Use of a zone model for validation of a horizontal ceiling/floor vent algorithm
[AD-A234553] N91-26474
Improved algorithms for transient and steady-state fluid-structure interaction
[AD-A235172] N91-26476
Backplane bus distributed realtime clock synchronization
[AD-A234476] N91-26491
Application of thematic mapper images to determine regional evaporation from the playas in the western desert of Egypt
[REPT-31] N91-26585
Testing the One-Port Random Access Memory (1PRAM) module of TRW's CPUAX signal processing superchip
[AD-A234127] N91-26761
Content addressable memory project
[AD-A234524] N91-26763
Waiting algorithms for synchronization in large-scale multiprocessors
[AD-A234985] N91-26764
A parallel rendering algorithm for MIMD architectures
[NASA-CR-187571] N91-26767
Iterated transform image compression
[AD-A233655] N91-26769
Using mappings to prove timing properties
[AD-A234404] N91-26780
Continuous stochastic cellular automata that have a stationary distribution and no detailed balance
[AD-A234421] N91-26782
Converting a converging algorithm into a polynomially bounded algorithm
[AD-A234961] N91-26788
Parallel algorithms for least squares and related computations
[AD-A235018] N91-26790
Using genetic algorithms to select and create features for pattern classification
[AD-A235165] N91-26792
Nonlinear stochastic optimization solution procedures and incomplete information
[AD-A235242] N91-26793
An implementation of the singular value decomposition on the connection machine CM-2
[AD-A234124] N91-26802
Structure driven multiprocessor compilation of numeric problems
[AD-A234653] N91-26803
Applications of artificial intelligence to mission planning
[NASA-CR-187953] N91-26806
Extensions of a theory of networks and learning: Outliers and negative examples
[AD-A234425] N91-26810
Using modular neural networks with local representations to control dynamic systems
[AD-A234700] N91-26813

H-infinity-optimal control for distributed parameter systems
[AD-A234931] N91-26833
Polyhedral approaches for solving 0-1 polynomial programming problems
[AD-A235219] N91-26851
The distribution of the size and number of shadows cast on a line segment in a Poisson random field
[AD-A233697] N91-26857
Statistical analysis of stochastic gradient based algorithms
[AD-A234545] N91-26859
A boundary scattering strength extraction algorithm for the analysis of long-range reverberation data
[AD-A233721] N91-26877
Quantum devices and structures
[AD-A235298] N91-26989
A nonrecursive order N preconditioned conjugate gradient: Range space formulation of MDOF dynamics
N91-27099
Design of optimal correlation filters for hybrid vision systems N91-27110
Development of load-dependent Ritz vector method for structural dynamic analysis of large space structures
N91-27111

ALIGNMENT
Magnetostrictive angular positioning motor
[AD-D014858] N91-26536

ALKALI METAL COMPOUNDS
Charge exchange in ion-surface scattering at hyperthermal (10-100 eV) and keV energies
[AD-A235233] N91-26899

ALKANES
Partial oxidation of light alkanes in transition-metal ion containing zeolites
[DE91-008202] N91-26243
The reduction by deuterium on platinum black of exo-2-norbornyl and endo-2-norbornyl to norbornane-2-d occurs with predominant retention of configuration
[AD-A235057] N91-26277

ALKYLATES
Structure of alkylated silica surfaces: Quenching of fluorescence from covalently bound pyrene
[AD-A234642] N91-26207

ALLOYS
Luminescence and lasing in II-VI semiconductors
[AD-A235019] N91-26961
Thin film alloys on semiconductor substrates
[DE91-012355] N91-26985

ALTERNATING CURRENT
Quantum devices and structures
[AD-A235298] N91-26989

ALTIMETERS
Evaluation of the C/EC/KC-135 Ground Collision Avoidance System (GCAS), study 1
[AD-A235301] N91-26130
The High Resolution Profiler (HRP): User's guide and software modifications documentation
[AD-A234640] N91-26663

ALTITUDE CONTROL
Vehicle steering device
[AD-D014861] N91-26537

ALTITUDE SIMULATION
Biochemical aspects of human adaptation to combined effect of antiorthostasis, decreased barometric pressure, and increased oxygen content N91-26694

ALUMINIDES
Fundamentals of mechanical behavior in intermetallic compounds
[AD-A235016] N91-26301
Microstructure, plastic deformation and mechanical properties of mechanically alloyed NiAl and NiAl based alloys
[AD-A235135] N91-26303
The role of electronic structure in the mechanical behavior of aluminides
[DE91-012508] N91-26325

ALUMINUM
Corrosion of graphite aluminum metal matrix composites
[AD-A234322] N91-26220
Dynamic energy absorption of sandwich structures by inelastic deformation
[AD-A234903] N91-26564

ALUMINUM ALLOYS
Materials/microstructures characterization
[AD-A233751] N91-26295
Cyclic deformation, damage, and effects of environment in the Ni3Al ordered alloy at elevated temperature
[AD-A235168] N91-26304
Mechanical properties of spray atomized SiC particle reinforced aluminum-titanium alloys
[AD-A235231] N91-26306
Grain boundary cavitation processes in a Ni3Al alloy at elevated temperatures
[AD-A235279] N91-26307
The cryogenic mechanical properties of Vintage 3 Al-Li-Zr alloy 2090-T81
[DE91-011897] N91-26311
The corrosion protection of 2219-T87 aluminum by anodizing
[NASA-TM-103540] N91-26312
US and foreign alloy cross-reference database
[NASA-CR-184166] N91-26313
Strain enhanced microstructural evolution
[DE91-011921] N91-26318
Grain boundary chemistry in Al-Cu metallizations as determined by analytical electron microscopy
[DE91-012007] N91-26319
Metastable pitting corrosion of aluminum, Al-Cu, and Al-Si thin films in dilute HF solutions and its relevancy to the processing of integrated circuit interconnections
[DE91-012014] N91-26320
Environmental embrittlement of ordered intermetallic alloys at room temperature in moist atmospheres
[DE91-012051] N91-26321
TEM in-situ straining of B2 compounds
[DE91-012062] N91-26322
Microstructure and hardness of NiAl/Ni2AlX two-phase ordered intermetallic alloys
[DE91-012068] N91-26323
The 1990 Sandia rocket-triggered lightning field tests at Kennedy Space Center, Florida
[DE91-011263] N91-26653
Crystallization of thin films of amorphous germanium alloys
[ITN-91-85110] N91-26969
Effect of boron addition on recrystallization and grain growth in Ni3Al polycrystals
[DE91-011966] N91-26983

ALUMINUM FLUORIDES
Development of a subpicosecond, tunable LiCAF (Cr:LiCaAlF6) laser
[DE91-012082] N91-26526

ALUMINUM OXIDES
Corrosion of graphite aluminum metal matrix composites
[AD-A234322] N91-26220
Dynamic fracture responses of Al2O3, Si3N4, and SiC(w)/Al2O3
[AD-A235286] N91-26229
Microstructure, porosity, and mechanical property relationships of calcium-silicate-hydrate
[AD-A235191] N91-26279
Current distribution modeling for novel alumina electrolysis
[DE91-010060] N91-26315
Transformation toughening of ceramics
[AD-A234926] N91-26359
HREM study of heteroepitaxial interfaces in the TiO2/Al2O3 system
[DE91-012473] N91-26986

AMINES
Molecular mechanics calculations for nitro and amino substituted conjugated systems containing oxygen and nitrogen
[AD-A233928] N91-26389

AMINO ACIDS
Intracellular physiology of the rat suprachiasmatic nucleus: Electrical properties, neurotransmission, and effects of neuromodulators
[AD-A234442] N91-26675
Studies of mutant hemoglobins to define types of modifications useful in the design of blood substitutes
[AD-A234997] N91-26723

AMMONIA
Arcjet endurance test program
[AD-A235232] N91-26198
FTIR studies of water and ammonia decomposition on silicon surfaces
[AD-A234637] N91-26265
The stepwise dissociation of NH3 on the Si(111)-(7x7) surface: Low temperature dissociative adsorption and thermal effects
[AD-A235009] N91-26274
Electrocatalytic study of ammonia synthesis and methane dimerization in high temperature solid electrolyte cells
[DE91-009797] N91-26289
Adsorption of ammonia on iron clusters
[DE91-011125] N91-26308

AMMONIUM COMPOUNDS
Gel solidified microinterface between two immiscible electrolytes applied to amperometric detection of picrate and tetramethylammonium
[AD-A235260] N91-26280

AMMUNITION
Minutes of the 24th Explosives Safety Seminar, volume 1
[AD-A235005] N91-26395

AMORPHOUS MATERIALS
A tribological investigation of the graphite-to-diamond-like behavior of amorphous carbon films ion-beam-deposited on ceramic substrates
[DE91-010816] N91-26379
Crystallization of thin films of amorphous germanium alloys
[ITN-91-85110] N91-26969

AMORPHOUS SILICON
Research on stable, high-efficiency amorphous silicon multijunction modules
[DE91-002159] N91-26591
A study of signal generation and charge collectionin a-Si:H diodes for radiation imaging
[DE91-010243] N91-26904

AMPLIFICATION
X ray laser program
[AD-A234390] N91-26504

AMPLIFIERS
High power klystron amplifier
[AD-D014862] N91-26448

AMPLITUDE MODULATION
Control circuitry using electronic emulation of a synchro signal for accurate control of position and rate of rotation for shafts
[NASA-CASE-MFS-28458-1] N91-26459
Complex envelope properties, interpretation, filtering, and evaluation
[AD-A234478] N91-26844
Method and apparatus for second-rank tensor generation
[NASA-CASE-NPO-17512-1-CU] N91-26918

ANALOG CIRCUITS
Control circuitry using electronic emulation of a synchro signal for accurate control of position and rate of rotation for shafts
[NASA-CASE-MFS-28458-1] N91-26459
Solid state research
[AD-A234836] N91-26958

ANALOG TO DIGITAL CONVERTERS
X ray-computed tomography for inspecting industrial parts
[DE91-011390] N91-26554

ANALOGIES
The weighted uni-dimensional similarities problem with least absolute value metric is NP-Hard
[AD-A235060] N91-26849

ANATOMY
Peptide transport through the blood-brain barrier
[AD-A233753] N91-26708

ANGULAR ACCELERATION
Calculation of the pointing accuracy of spacecraft equipment using autonomous measurements of the angular position of the object of investigation
N91-26167

ANILINE
New developments in the synthesis and doping of polyacetylene and polyaniline
[AD-A233702] N91-26244
Polyaniline: Synthesis and properties of pernigraniline
[AD-A233706] N91-26245
Photoexcitation spectroscopy of pernigraniline
[AD-A233841] N91-26250
Polyaniline: Allowed oxidation states
[AD-A233842] N91-26251
Thermal transitions and mechanical properties of the films of chemically prepared polyaniline
[AD-A233807] N91-26329
Polyaniline: Pernigraniline, an isolable intermediate in the conventional chemical synthesis of emeraldine
[AD-A233840] N91-26330
Light induced electron spin resonance in polyaniline
[AD-A233847] N91-26331
X ray structure of polyanilines
[AD-A233848] N91-26332
Thermal stabilities of polyanilines
[AD-A233849] N91-26333
Electron localization in polyaniline and its derivatives
[AD-A233934] N91-26335
Structure, order and the metallic state in polyaniline and its derivatives
[AD-A233935] N91-26336
Novel concepts in electronic polymers: Polyaniline and its derivatives
[AD-A234214] N91-26339
Spectroscopy and photoexcitation spectroscopies of polyaniline: A model system for new phenomena
[AD-A234215] N91-26340
Ring-torsional polarons in polyaniline and polyparaphenylene sulfide
[AD-A234384] N91-26345
Polyaniline: Oriented films and fibers
[AD-A234414] N91-26347
Biological synthesis of substituted o-aminophenols
[AD-A234910] N91-26678

Photoinduced absorption and erasable optical information storage in polyanilines
[AD-A234108] N91-27002

ANISOTROPIC PLATES
An anisotropic laminated damped plate theory
[AD-A234446] N91-26222
Buckling of laminated composite plates
[ITN-91-85101] N91-26232

ANISOTROPY
Investigation of a Hamiltonian with two sources of anisotropy: The Dzyaloshinskii-Moriya and single-size interactions
[DE91-011381] N91-26292
The cryogenic mechanical properties of Vintage 3 Al-Li-Zr alloy 2090-T81
[DE91-011897] N91-26311
The role of electronic structure in the mechanical behavior of aluminides
[DE91-012508] N91-26325

ANNEALING
Microstructure development during microwave annealing of dense silicon nitride
[DE91-012069] N91-26242
Long-term prediction test procedure for most ICs, based on linear response theory
[NASA-CR-185843] N91-26462
Defects in decomposed YBa2Cu4O8 (124) superconductor after rapid annealing
[DE91-010597] N91-26979

ANNUAL VARIATIONS
SEEP 2 zooplankton data report: Winter, spring and summer collections at mooring 3 during 1988
[DE91-012077] N91-26668

ANNULAR FLOW
Investigation of laminar, fully developed flow in annulus by finite difference model
[ITN-91-85116] N91-26483

ANODIZING
The corrosion protection of 2219-T87 aluminum by anodizing
[NASA-TM-103540] N91-26312

ANTARCTIC REGIONS
West Antarctic Ice Sheet Initiative. Volume 2: Discipline Reviews
[NASA-CP-3115-VOL-2] N91-26573
A review of precipitation-related aspects of West Antarctic meteorology N91-26574
Nimbus-7 TOMS Antarctic ozone atlas: August - December 1990
[NASA-RP-1264] N91-26651
Solutions to problems of weathering in Antarctic eucrites N91-27113

ANTENNA ARRAYS
MMIC integration technology investigation
[NASA-CR-188035] N91-26434
Four-to-one power combiner for 20 GHz phased array antenna using RADC MMIC phase shifters N91-26435
Fluorescence spectroscopy of excitation transfer in Photosystem 1
[DE91-011867] N91-26681

ANTENNA DESIGN
Input impedance and gain of monopole elements with disk ground planes on flat earth
[AD-A234284] N91-26421

ANTIFERROMAGNETISM
Strong exchange coupling in lanthanide bis(phthalocyaninato) sandwich compounds
[AD-A234466] N91-26951

ANTIMISSILE DEFENSE
Boost-phase kill versus midcourse discrimination: The grand inquisitor's solution
[DE91-011744] N91-26871

ANTISUBMARINE WARFARE
Progress with neural network gulf streams
[AD-A233810] N91-26658

ANXIETY
Attention span, anxiety, and benzodiazepine receptors
[AD-A234549] N91-26716
Effect of a passive cooling vest on tension/anxiety and fatigue in a high heat and high humidity naval environment
[AD-A234657] N91-26755

APOGEE BOOST MOTORS
Chinese space science and technology (selected articles)
[AD-A234798] N91-26180

APPLICATIONS PROGRAMS (COMPUTERS)
Surface Chemkin (version 3.7): A FORTRAN package for analyzing heterogeneous chemical kinetics at a solid-surface-gas-phase interface
[DE91-010840] N91-26285
Use of a zone model for validation of a horizontal ceiling/floor vent algorithm
[AD-A234553] N91-26474
Quality effectiveness sensing technique release 3.0
[AD-A233651] N91-26545
The NASA/MSFC global reference atmospheric model: 1990 version (GRAM-90). Part 1: Technical/users manual
[NASA-TM-4268] N91-26654
A software package for unconstrained optimization using tensor methods
[AD-A233989] N91-26778
Computational methods and software for differential equations and their applications
[DE91-012172] N91-26855

APPROPRIATIONS
National Aeronautics and Space Administration Multiyear Authorization Act of 1991 N91-27046

APPROXIMATION
Backscattering from rough interfaces and the parabolic approximation
[AD-A235184] N91-26886

ARC JET ENGINES
Arcjet endurance test program
[AD-A235232] N91-26198
Near field interaction of microwave signals with a bounded plasma plume
[NASA-CR-185358] N91-26944

ARCHITECTURE (COMPUTERS)
Architectures for a high performance distributed operating system
[AD-A235333] N91-26429
Object-oriented requirements analysis: A quick tour
[NASA-CR-187919] N91-26766
A parallel rendering algorithm for MIMD architectures
[NASA-CR-187571] N91-26767
Parallel algorithms for least squares and related computations
[AD-A235018] N91-26790
Structure driven multiprocessor compilation of numeric problems
[AD-A234653] N91-26803
Imagination and situated cognition
[AD-A234420] N91-26809
Strategies for parallel AI implementations
[AD-A234449] N91-26811
Engineering for artificial intelligence software
[AD-A234793] N91-26814
Northeast Artificial Intelligence Consortium (NAIC). Volume 4: Distributed artificial intelligence for communications network management
[AD-A234883] N91-26818
Northeast Artificial Intelligence Consortium (NAIC). Volume 12: Computer architecture for very large knowledge bases
[AD-A234891] N91-26826
Northeast Artificial Intelligence Consortium (NAIC). Volume 13: Image understanding and intelligent parallel systems
[AD-A234897] N91-26832
Computational methods and software for differential equations and their applications
[DE91-012172] N91-26855
UNIX (tm) in high energy physics: What we can learn from the initial experiences at Fermilab
[DE91-011976] N91-26914
Automatic target recognition using acousto-optic image correlator
[DE91-011499] N91-26936
Proceedings of the First Workshop on 3-D Optical Memories
[AD-A234732] N91-27003
FTS2000 network architecture N91-27019

ARCTIC REGIONS
JPRS report: Science and technology. USSR: Earth sciences
[JPRS-UES-91-002] N91-26581
Process study of sorted patterns on Arctic soils
[AD-A234089] N91-26628
Lead detection and mapping with reference to relationships between scale, sensor characteristics, surface conditions and atmospheric properties
[AD-A235121] N91-26666

ARIZONA
Atmospheric optical turbulence measurements taken at Anderson Mesa, Flagstaff, Arizona between 10-19 July 1990
[AD-A234190] N91-26629

ARMATURES
Rail circuit augmentation
[AD-A234944] N91-26184

ARMED FORCES (UNITED STATES)
What fuels our future?
[AD-A233674] N91-26387
Air Force stock fund: Hydrazine sales consistent with the Commercial Space Launch Act. Report to the Chairman, Committee on Science, Space and Technology, House of Representatives
[GAO/NSIAD-91-196] N91-26397
Spread spectrum communications emulator design
[AD-A235403] N91-26430
Development of a Vector Spherical Harmonic (VSH) model of the neutral thermosphere
[AD-A234744] N91-26631
US Army Biomedical Research and Development Laboratory
[AD-A233664] N91-26671
Level of dietary fat does not affect fuel oxidation or endurance exercise performance of soldiers
[AD-A235194] N91-26728
SPH-4 aircrew helmet impact protection improvements 1970-1990
[AD-A233784] N91-26750
Space doctrine
[AD-A234971] N91-26866
Personal papers in the United States Air Force Historical Research Center, 5th edition
[PB91-156380] N91-26999

ARMOR
Reaction processing of ceramic particulate and whisker composites
[AD-A234951] N91-26225

ARRAYS
Application of a conjugate gradient method to the synthesis of phase-only planar arrays
[AD-A233756] N91-26415
Array-typed, sealed-off mini tea CO2 laser
[AD-A234804] N91-26511
Underwater scattering of sound
[AD-A235097] N91-26885
Improved inline fiber optic sensor arrays
[AD-D014864] N91-26924
Study of Josephson effect arrays as sources at 1 THz
[AD-A234526] N91-26952

ARTERIES
Diagnostic utility of continuous noninvasive blood pressure monitoring (Penaz method) in gravity-induced blood redistribution N91-26705
The effect of catecholamines on arterial blood pressure and heart rate
[AD-A234755] N91-26720

ARTIFICIAL INTELLIGENCE
Autonomous aircraft initiative study
[NASA-CR-186013] N91-26140
Piezoelectric micromotors for microrobots
[AD-A234423] N91-26446
An advanced knowledge and design acquisition methodology: Application for the pilot's associate
[AD-A233700] N91-26748
BaRT manual version 3.0
[AD-A234528] N91-26784
Using genetic algorithms to select and create features for pattern classification
[AD-A235165] N91-26792
Applications of artificial intelligence to mission planning
[NASA-CR-187953] N91-26806
Imagination and situated cognition
[AD-A234420] N91-26809
Extensions of a theory of networks and learning: Outliers and negative examples
[AD-A234425] N91-26810
Using modular neural networks with local representations to control dynamic systems
[AD-A234700] N91-26813
Engineering for artificial intelligence software
[AD-A234793] N91-26814
Northeast Artificial Intelligence Consortium (NAIC). Volume 1: Executive summary
[AD-A234880] N91-26815
Northeast Artificial Intelligence Consortium (NAIC). Volume 2: Discussing, using, and recognizing plans
[AD-A234881] N91-26816
Northeast Artificial Intelligence Consortium (NAIC). Volume 3: The Versatile Maintenance Expert System (VMES)
[AD-A234882] N91-26817
Northeast Artificial Intelligence Consortium (NAIC). Volume 4: Distributed artificial intelligence for communications network management
[AD-A234883] N91-26818
Northeast Artificial Intelligence Consortium (NAIC). Volume 5: Distributed planning for dynamic environments in the presence of time constraints
[AD-A234884] N91-26819
Northeast Artificial Intelligence Consortium (NAIC). Volume 6: Building an intelligent assistant: The acquisition, integration, and maintenance of complex distributed tasks
[AD-A234885] N91-26820
Northeast Artificial Intelligence Consortium (NAIC). Volume 7: Automatic photointerpretation
[AD-A234886] N91-26821
Northeast Artificial Intelligence Consortium (NAIC). Volume 8: Artificial intelligence applications to speech recognition
[AD-A234887] N91-26822

Northeast Artificial Intelligence Consortium (NAIC). Volume 9: A planner system for the application of indications and warning
[AD-A234888] N91-26823
Northeast Artificial Intelligence Consortium (NAIC). Volume 10: Time oriented problem solving
[AD-A234889] N91-26824
Northeast Artificial Intelligence Consortium (NAIC). Volume 11: Knowledge base maintenance
[AD-A234890] N91-26825
Northeast Artificial Intelligence Consortium (NAIC). Volume 12: Computer architecture for very large knowledge bases
[AD-A234891] N91-26826
Northeast Artificial Intelligence Consortium (NAIC). Volume 18: A distributed artificial intelligence approach to information fusion and object classification
[AD-A234892] N91-26827
Northeast Artificial Intelligence Consortium (NAIC). Volume 14: Knowledge base retrieval using plausible inference
[AD-A234893] N91-26828
Northeast Artificial Intelligence Consortium (NAIC). Volume 15: Strategies for coupling symbolic and numerical computation in knowledge base systems
[AD-A234894] N91-26829
Northeast Artificial Intelligence Consortium (NAIC). Volume 16: Intelligent signal processing techniques for multi-sensor surveillance systems
[AD-A234895] N91-26830
Northeast Artificial Intelligence Consortium (NAIC). Volume 17: High-level adaptive signal processing
[AD-A234896] N91-26831
A design for an intelligent monitor and controller for space station electrical power using parallel distributed problem solving N91-27105

ARTIFICIAL SATELLITES
Prime Minister Li Peng talks with representatives to a discussion meeting on satellite applications and applied satellite technology about the development of our country's activities in space
[AD-A234801] N91-26181

ASIA
Acid rain in Asia
[DE91-011160] N91-26595

ASPHALT
International State-of-the-Art Colloquium on Low-Temperature Asphalt Pavement Cracking
[AD-A233663] N91-26402
A basic guide to overlay design using nondestructive testing equipment data
[AD-A234472] N91-26403

ASSAYING
Imaging of fluorescent and chemiluminescent DNA hybrids using a 2-D CCD camera
[AD-A234641] N91-26676

ASTRONAUT PERFORMANCE
The effects of deuterium on static posture control N91-27102

ASTRONAUTS
Mechanics, impact loads and EMG on the space shuttle treadmill N91-27112

ASTRONOMICAL CATALOGS
A catalog of high resolution Jovian decametric radio noise burst spectra, volume 1 N91-27047

ASTRONOMICAL MODELS
CBSD version 2 component models of the IR celestial background
[AD-A235372] N91-27048

ASTROPHYSICS
Overview of the NASA astrophysics data system N91-27022
Using HST: From proposal to science N91-27023

ASYMMETRY
Dynamics of equatorial and polar boundaries of penetration of solar protons with energy about 1 MeV into magnetosphere during strong magnetic storm N91-26172
Modelling the dynamics of fluxes of electrons with energies 30-300 keV in geostationary orbit N91-26173
Hurricane Research Division fiscal year 1990 programs-fiscal year 1991 projections
[PB91-153452] N91-26641
A divide and conquer approach to the nonsymmetric eigenvalue problem
[DE91-011085] N91-26854

ASYMPTOTIC SERIES
Lyapunov exponents and rotation numbers of linear systems with real noise
[AD-A234729] N91-26846
Weighted least squares estimation for Aalen's additive risk model
[AD-A235250] N91-26852

ATAXIA
The effects of deuterium on static posture control N91-27102

ATLANTIC OCEAN
VLF nighttime data analysis
[AD-A234006] N91-26417
Inorganic carbon surveys of oceanic basins
[DE91-011132] N91-26667
SEEP 2 zooplankton data report: Winter, spring and summer collections at mooring 3 during 1988
[DE91-012077] N91-26668

ATMOSPHERIC BOUNDARY LAYER
Boundary layer parameterization for a global spectral model
[AD-A235310] N91-26635
The aeolian wind tunnel N91-27065

ATMOSPHERIC CHEMISTRY
Lead detection and mapping with reference to relationships between scale, sensor characteristics, surface conditions and atmospheric properties
[AD-A235121] N91-26666

ATMOSPHERIC CIRCULATION
Atmospheric optical turbulence measurements taken at Anderson Mesa, Flagstaff, Arizona between 10-19 July 1990
[AD-A234190] N91-26629
A numerical study of blocking N91-26640
An overview of tropical circulation
[AD-A234984] N91-26645
The NASA/MSFC global reference atmospheric model: 1990 version (GRAM-90). Part 1: Technical/users manual
[NASA-TM-4268] N91-26654

ATMOSPHERIC COMPOSITION
Free-air carbon dioxide enrichment: A new approach to research on carbon exchange processes
[DE91-012074] N91-26609
The effects of atmospheric dust on observations of Martian surface albedo N91-27072
Derivation of mid-infrared (5-25 microns) optical constants of some silicates and palagonite N91-27077

ATMOSPHERIC DENSITY
Wind abrasion on Mars N91-27064

ATMOSPHERIC ELECTRICITY
Comparison of the RF frequency spectra of HEMP and lightning
[AD-A234306] N91-26642

ATMOSPHERIC GENERAL CIRCULATION MODELS
Development of a Vector Spherical Harmonic (VSH) model of the neutral thermosphere
[AD-A234744] N91-26631
Development and verification of a physical cloud-moisture model for use in general circulation models
[AD-A234751] N91-26643

ATMOSPHERIC HEATING
A numerical study of blocking N91-26640

ATMOSPHERIC IONIZATION
System concept and analysis of an Artificial Ionospheric Mirror (AIM) radar
[AD-A234289] N91-26630

ATMOSPHERIC MODELS
Certification procedures and requirements N91-26154
Satellite data derived estimates of erosion parameters for reentry vehicles
[AD-A234792] N91-26189
A review of precipitation-related aspects of West Antarctic meteorology N91-26574
Late Wisconsin and early holocene glacial history, inner Ross Embayment, Antarctica N91-26577
Modal aerosol dynamics modeling
[PB91-161729] N91-26598
Simulation of precipitation scavenging in a three-dimensional global model
[DE91-011531] N91-26606
Gravity waves and instabilities in the lower and middle atmosphere N91-26621
Evaluation of the Navy oceanic vertical aerosol model using lidar and PMS particle-size spectrometers
[AD-A233653] N91-26625
ARTIST tape output formats
[AD-A235173] N91-26633
Boundary layer parameterization for a global spectral model
[AD-A235310] N91-26635
Theoretical and experimental studies relevant to interpretation of auroral emissions
[NASA-CR-188491] N91-26637
Description of the RIVM/KNMI puff dispersion model
[KNMI-177] N91-26638
Coordination of mesoscale meteorological research between ASL and European groups
[AD-A233586] N91-26639
A numerical study of blocking N91-26640
Hurricane Research Division fiscal year 1990 programs-fiscal year 1991 projections
[PB91-153452] N91-26641
The development of an improved convective initiation scheme for Mesoscale numerical weather prediction models, phase 1
[AD-A235417] N91-26650
The NASA/MSFC global reference atmospheric model: 1990 version (GRAM-90). Part 1: Technical/users manual
[NASA-TM-4268] N91-26654
Lead detection and mapping with reference to relationships between scale, sensor characteristics, surface conditions and atmospheric properties
[AD-A235121] N91-26666
Adaptive component methods for time dependent PDE's
[AD-A233776] N91-26775

ATMOSPHERIC MOISTURE
Liquid water production from atmospheric sources
[AD-A235090] N91-26406
Sea-level response to ice sheet evolution: An ocean perspective N91-26575
Development and verification of a physical cloud-moisture model for use in general circulation models
[AD-A234751] N91-26643

ATMOSPHERIC PHYSICS
JPRS report: Science and technology. USSR: Earth sciences
[JPRS-UES-91-002] N91-26581
Middle Atmosphere Program. Handbook for MAP. Volume 30: International School on Atmospheric Radar
[NASA-CR-188623] N91-26613
Historical aspects of radar atmospheric dynamics N91-26614
Atmospheric optical turbulence measurements taken at Anderson Mesa, Flagstaff, Arizona between 10-19 July 1990
[AD-A234190] N91-26629

ATMOSPHERIC PRESSURE
Biochemical aspects of human adaptation to combined effect of antiorthostasis, decreased barometric pressure, and increased oxygen content N91-26694
Effect of pressure on electrostatic processes on Mars N91-27069
Saltation threshold detection in a wind tunnel by the measurement of the net electrostatic charge N91-27070

ATMOSPHERIC REFRACTION
Radar principles N91-26615
Temporal and spatial correlations in images distorted by a random medium
[ITN-91-85107] N91-26935

ATMOSPHERIC SCATTERING
Effect of aerosols on laser-induced breakdown
[AD-A234324] N91-26502
Temporal and spatial correlations in images distorted by a random medium
[ITN-91-85107] N91-26935

ATMOSPHERIC TEMPERATURE
Recent studies of the optical properties of dust and cloud particles in the Mars atmosphere and the interannual frequency of global dust storms N91-27060

ATMOSPHERIC TURBULENCE
Manual on the flight of flexible aircraft in turbulence
[AGARD-AG-317] N91-26150
Measurement of atmospheric turbulence N91-26151
Certification procedures and requirements N91-26154
Analysis by the statistical discrete gust method N91-26156
Matching of PSD-design loads N91-26157
Atmospheric optical turbulence measurements taken at Anderson Mesa, Flagstaff, Arizona between 10-19 July 1990
[AD-A234190] N91-26629
Laboratory modelling of the dynamics of coastal upwelling
[AD-A234987] N91-26664
Temporal and spatial correlations in images distorted by a random medium
[ITN-91-85107] N91-26935

ATOMIC BEAMS
Atom wave interferometer
[AD-A234863] N91-26494
Experiments with trapped atoms
[AD-A234580] N91-26895

ATOMIC COLLISIONS
Experiments with trapped atoms
[AD-A234580] N91-26895
Negative ion formation by Rydberg electron transfer: Isotope-dependent rate constants
[DE91-012058] N91-26909

ATOMIC ENERGY LEVELS
Photochemical energy conversion by membrane-bound photoredox systems
[DE91-012171] N91-26682

Charge exchange in ion-surface scattering at hyperthermal (10-100 eV) and keV energies
[AD-A235233] N91-26899

ATOMIC SPECTRA
Resonance fluorescence spectrum of an atom near a phase conjugator
[AD-A234535] N91-26894

ATOMIC STRUCTURE
Molecular orientation of the silver tetra neopentoxy phthalo cyanine and stearic acid mixed Langmuir-Blodgett film and its chemical and electrochemical behaviour
[AD-A234601] N91-26206
Energetics, bonding mechanism and electronic structure of metal/ceramic interfaces
[DE91-009787] N91-26239
Surface chemistry of silicon: The behavior of dangling bonds
[AD-A235011] N91-26275
Fundamental studies of carbenes and hydrocarbon radicals
[DE91-011029] N91-26286
Quantum mechanical approach to understanding microstructural and mechanical properties of intermetallics
[AD-A234702] N91-26298
The role of electronic structure in the mechanical behavior of aluminides
[DE91-012508] N91-26325
Synthesis and structure of small-molecule cyclic phosphazenes bearing ortho-substituted aryloxy and phenoxy substituents
[AD-A234377] N91-26344
Ring-torsional polarons in polyaniline and polyparaphenylene sulfide
[AD-A234384] N91-26345
Scanning tunnelling microscope for boron surface studies
[AD-A234716] N91-26452
Electronic excitation transport in photosynthesis and crystal and molecular structures of porphyrin compounds
[DE91-012024] N91-26679
Chemistry on an atomic scale of ion-beam modified surfaces
[AD-A233707] N91-26891
Theoretical studies of potential energy surfaces and computational methods
[DE91-011126] N91-26902
Molecular orbital studies of the bonding in heavy element organometallics
[DE91-010915] N91-26905
The electronic structure of the ionic insulator sodium nitrite
[DE91-009766] N91-26977
On the nature of grain boundary structures in nanophase materials
[DE91-010285] N91-26978

ATOMIZING
Mechanical properties of spray atomized SiC particle reinforced aluminum-titanium alloys
[AD-A235231] N91-26306

ATOMS
High energy density systems in cryogenic media: The production and reaction of atoms and radicals
[AD-A233785] N91-26892
Experiments with trapped atoms
[AD-A234580] N91-26895

ATTENTION
Neural mechanisms of attention
[AD-A235003] N91-26742
Assessment of the pharmacodynamics of intranasal, intravenous and oral scopolamine N91-27114

ATTITUDE CONTROL
High accuracy optical rate sensor N91-27115

AUDITORY PERCEPTION
Review of audition literature: Selection of acoustic signals for use in the synthesis of auditory space
[AD-A234579] N91-26881

AUDITORY SIGNALS
Mechanisms of adaptive information processing
[AD-A234435] N91-26734

AUGMENTATION
Control of an axisymmetric turbulent jet by multi-modal excitation
[NASA-TM-104483] N91-26121

AURORAL ARCS
The analysis of a rocket tomography measurement of the N2+3914A emission and N2 ionization rates in an auroral arc
[NASA-CR-188622] N91-26596

AURORAL IONIZATION
The analysis of a rocket tomography measurement of the N2+3914A emission and N2 ionization rates in an auroral arc
[NASA-CR-188622] N91-26596

AURORAL ZONES
The effects of magnetic storm phases on F-layer irregularities from auroral to equatorial latitudes
[AD-A235170] N91-26632

AURORAS
UV aurora mapping in corrected geomagnetic coordinates
[ITN-91-85106] N91-26636
Theoretical and experimental studies relevant to interpretation of auroral emissions
[NASA-CR-188491] N91-26637

AUTOCORRELATION
Statistical characteristics of MST radar echoes and its interpretation N91-26617

AUTOMATA THEORY
Benchmark study between FIDAP and a cellular automata code
[DE91-011224] N91-26486
Using mappings to prove timing properties
[AD-A234404] N91-26780
Continuous stochastic cellular automata that have a stationary distribution and no detailed balance
[AD-A234421] N91-26782

AUTOMATIC CONTROL
WPG-30 model microprocessor controlled rotating beryllium mirror scanning camera and its applications
[AD-A234802] N91-26493
Dynamic stability of flexible robot manipulators
[AD-A234297] N91-26533
Deductive programming synthesis
[AD-A233770] N91-26774
Northeast Artificial Intelligence Consortium (NAIC). Volume 7: Automatic photointerpretation
[AD-A234886] N91-26821

AUTOMATIC FLIGHT CONTROL
Application of transformational ideas to automatic flight control design
[AD-A234758] N91-26148

AUTOMATION
ROBOT: A journal of Chinese Society of Automation
[AD-A234808] N91-26538

AUTONOMOUS NAVIGATION
Study of the properties of the autonomous optical navigation of a space probe in a rendezvous with an asteroid N91-26169

AUTONOMY
Autonomous aircraft initiative study
[NASA-CR-186013] N91-26140
Calculation of the pointing accuracy of spacecraft equipment using autonomous measurements of the angular position of the object of investigation N91-26167
Parallel processing and expert systems
[NASA-TM-103886] N91-26796

AUXILIARY POWER SOURCES
A design for an intelligent monitor and controller for space station electrical power using parallel distributed problem solving N91-27105

AVIONICS
Evaluation of the C/EC/KC-135 Ground Collision Avoidance System (GCAS), study 1
[AD-A235301] N91-26130
VHSIC electronics and the cost of Air Force avionics in the 1990s
[RAND-R-3843-AF] N91-26143
Digital signal conditioning for flight test, volume 19
[AGARD-AG-160-VOL-19] N91-26432
Electronic design process
[AD-A234709] N91-26786

AWACS AIRCRAFT
Aircrew Evaluation Sustained Operations Performance (AESOP): A triservice facility for technology transition
[AD-A234626] N91-26738

AXES OF ROTATION
Analysis of necessary and sufficient conditions for the equilibrium stability of a gyrostatic satellite N91-26166

B

BACKGROUND RADIATION
CBSD version 2 component models of the IR celestial background
[AD-A235372] N91-27048

BACKSCATTERING
Backscattering enhancement from rough surfaces
[AD-A234707] N91-26426
Comparisons of backscattering from cylindrical shells described by thin shell and elasticity theories
[AD-A234745] N91-26475
Vertical incidence backscatter and surface forward scattering from near-surface bubbles
[AD-A234432] N91-26880
Backscattering from rough interfaces and the parabolic approximation
[AD-A235184] N91-26886

BACKWARD WAVE TUBES
Work performed experiments: 1989-1990
[AD-A235221] N91-26457

BACTERIA
Effect of bacterial biofilms on carbon steel pit propagation in phosphate containing medium
[DE91-010806] N91-26316
Biological synthesis of substituted o-aminophenols
[AD-A234910] N91-26678
Molecular studies of cytokine induction
[AD-A235326] N91-26731

BAGGAGE
Physiological and perceptual responses to load carrying in female subjects using internal and external frame backpacks
[AD-A234941] N91-26722

BAGS
Physiological and perceptual responses to load carrying in female subjects using internal and external frame backpacks
[AD-A234941] N91-26722

BALLISTICS
The effect of sabot wheelbase and position on the launch dynamics of fin-stabilized kinetic energy ammunition
[AD-A234945] N91-26118
Dynamic energy absorption of sandwich structures by inelastic deformation
[AD-A234903] N91-26564

BANDPASS FILTERS
Complex envelope properties, interpretation, filtering, and evaluation
[AD-A234478] N91-26844

BARIUM OXIDES
Diagnostic studies of YBa2Cu3O(7-delta) laser ablation
[DE91-011382] N91-26515
Formation of intermediate compounds during reduced pressure calcination of Y-Ba-Cu-O precursor
[DE91-011179] N91-26971

BAROTROPISM
Hurricane Research Division fiscal year 1990 programs-fiscal year 1991 projections
[PB91-153452] N91-26641

BARRIER LAYERS
Epitaxy of metal atoms on metal surfaces: Deposition and diffusion
[DE91-011142] N91-26309

BASES (CHEMICAL)
Synthesis, polymerization and thermal properties of a new acetylene-terminated Schiff base
[AD-A233806] N91-26328

BAYES THEOREM
BaRT manual version 3.0
[AD-A234528] N91-26784

BAYS (STRUCTURAL UNITS)
Unmanned aerial vehicles. Medium range system components do not fit
[AD-A234131] N91-26132

BEAM INTERACTIONS
Normalization of the parameterized Courant-Snyder matrix
[DE91-012554] N91-26856
Coherent beam-beam effects
[DE91-012512] N91-26917
Vacuum design for a superconducting mini-collider
[DE91-011964] N91-26975

BEAM SPLITTERS
A narrow-bandwidth unstable resonator laser cavity
[AD-D014865] N91-26505
Method and apparatus for second-rank tensor generation
[NASA-CASE-NPO-17512-1-CU] N91-26918

BEAMS (RADIATION)
Studies of optical beam phase-conjugation and electromagnetic scattering process
[AD-A234830] N91-26929

BEAMS (SUPPORTS)
Nonlinear dynamics and control of flexible structures
[AD-A235186] N91-26191

BED REST
Reaction of human skeletal muscle fibers to 370 day antiorthostatic hypokinesia combined with physical exertion N91-26702

BEDS (PROCESS ENGINEERING)
Refurbishing AV-8 on-board oxygen generation system beds
[AD-A235083] N91-26136

BEHAVIOR
Nonlinear behavior of fiber composite materials and its effect on the postbuckling response of laminated plates
[AD-A234203] N91-26218

BELLMAN THEORY
Viscosity methods in optimal control of distributed systems. The Bellman equation
[AD-A234646] N91-26812

BERNOULLI THEOREM
A sequential Jackson network with feedback
[ITN-91-85111] N91-26867
BERYL
Polyaniline: Pernigraniline, an isolable intermediate in the conventional chemical synthesis of emeraldine
[AD-A233840] N91-26330
X ray structure of polyanilines
[AD-A233848] N91-26332
BERYLLIUM
WPG-30 model microprocessor controlled rotating beryllium mirror scanning camera and its applications
[AD-A234802] N91-26493
BETA PARTICLES
Weak interactions and presupernova evolution
[DE91-011543] N91-27052
BIBLIOGRAPHIES
Advanced Satellite Research Project: SCAR Research Database. Bibliographic analysis
[NASA-CR-186086] N91-26182
Materials Science and Engineering, 1989 publications
[AD-A234087] N91-27001
Summary of research academic departments, October 1990
[AD-A234353] N91-27118
BIDIRECTIONAL REFLECTANCE
Bidirectional reflectance distribution (BRDF) of NASA shuttle tiles
[AD-A235115] N91-26188
BINARY ALLOYS
Chemical phase separation in binary iron-chromium alloys
[DE91-010282] N91-26294
BINARY DATA
Binary optics technology: Theoretical limits on the diffraction efficiency of multilevel diffractive optical elements
[AD-A235404] N91-26933
BINARY STARS
The light curve of the magnetic star AM - Herculis
[ITN-91-85108] N91-27049
BIOASSAY
Wound healing by cultured skin cells and growth factors
[AD-A235300] N91-26730
Techniques for determining total body water using deuterium oxide N91-27091
BIOASTRONAUTICS
USSR Space Life Sciences Digest, issue 29
[NASA-CR-3922(34)] N91-26669
USSR Space Life Sciences Digest, issue 30
[NASA-CR-3922(36)] N91-26670
BIOCHEMISTRY
Introduction to Session 2: Applied biological research
[DE91-012067] N91-26680
JPRS Report: Science and technology. USSR: Life sciences
[JPRS-ULS-91-009] N91-26688
Functional activity of hypophyseal-thyroid system during 370-day antiorthostatic hypokinesia N91-26691
Biochemical aspects of human adaptation to combined effect of antiorthostasis, decreased barometric pressure, and increased oxygen content N91-26694
BIOELECTRIC POTENTIAL
The Trendelenburg position after cerebral air embolism in dogs: Effects on the somatosensory evoked potential, intracranial pressure, and blood-brain barrier
[AD-A233809] N91-26673
BIOELECTRICITY
Mathematical problems concerning rhythmic processes
[AD-A234588] N91-26845
BIOGRAPHY
Response latency measures for biographical inventories
[AD-A235010] N91-27005
BIOLOGICAL EFFECTS
Review of primary medical results of year-long flight on Mir station N91-26178
Intracellular physiology of the rat suprachiasmatic nucleus: Electrical properties, neurotransmission, and effects of neuromodulators
[AD-A234442] N91-26675
JPRS report: Science and technology. USSR: Life sciences
[JPRS-ULS-91-011] N91-26696
State and forms of adaptation of vestibular function after space flights N91-26706
COLDEX-86: Fluid and electrolyte changes during prolonged cold water immersion
[AD-A233768] N91-26711
Proceedings of the 12th Annual Meeting of the UIPS Commission on Gravitational Physiology
[AD-A235337] N91-26732
BIOLOGICAL MODELS (MATHEMATICS)
Categories and particulars: Prototype effects in estimating spatial location
[AD-A234955] N91-26741
BIOMASS
Higher plants as part of biological human life support system N91-26693
Investigating combustion as a method of processing inedible biomass produced in NASA's biomass production chamber
[NASA-TM-103821] N91-26759
BIOPHYSICS
Mathematical problems concerning rhythmic processes
[AD-A234588] N91-26845
BIOREACTORS
Mathematical modeling of the flow field and particle motion in a rotating bioreactor at unit gravity and microgravity N91-27092
A study of murine bone marrow cells cultured in bioreactors which create an environment which simulated microgravity N91-27101
BIPOLAR TRANSISTORS
Monolithic integration semiconductor and superconductor components
[AD-A234986] N91-26959
BISMUTH COMPOUNDS
Development of high Tc (greater than 110K) Bi, Tl and Y-based materials as superconducting circuit elements
[NASA-CR-188581] N91-26948
BLINDNESS
Visual sensitivities and discriminations and their role in aviation
[AD-A234866] N91-26740
BLOCK COPOLYMERS
LaRC-ITPI/arylene ether copolymers
[NASA-TM-104099] N91-26378
BLOCKING
A numerical study of blocking N91-26640
BLOOD
Hormonal regulators of calcium metabolism following space flights of various durations N91-26689
Functional activity of hypophyseal-thyroid system during 370-day antiorthostatic hypokinesia N91-26691
Changes in rheologic indices of blood and hemodynamics during 14-day antiorthostatic hypokinesia N91-26692
Peptide transport through the blood-brain barrier
[AD-A233753] N91-26708
Carboxyalkylated hemoglobin as a potential blood substitute
[AD-A233822] N91-26712
Evaluation of liposome-encapsulated Hemoglobin/LR16 formulation as a potential blood substitute
[AD-A233973] N91-26714
COLDEX-86: Summary of the experimental protocol and general results
[AD-A234031] N91-26715
Studies of mutant hemoglobins to define types of modifications useful in the design of blood substitutes
[AD-A234997] N91-26723
BLOOD PRESSURE
Diagnostic utility of continuous noninvasive blood pressure monitoring (Penaz method) in gravity-induced blood redistribution N91-26705
The effect of catecholamines on arterial blood pressure and heart rate
[AD-A234755] N91-26720
Effect of a passive cooling vest on tension/anxiety and fatigue in a high heat and high humidity naval environment
[AD-A234657] N91-26755
BLOOD-BRAIN BARRIER
The Trendelenburg position after cerebral air embolism in dogs: Effects on the somatosensory evoked potential, intracranial pressure, and blood-brain barrier
[AD-A233809] N91-26673
Peptide transport through the blood-brain barrier
[AD-A233753] N91-26708
BLURRING
Photographic image enhancement N91-27094
BODY COMPOSITION (BIOLOGY)
Techniques for determining total body water using deuterium oxide N91-27091
BODY FLUIDS
COLDEX-86: Fluid and electrolyte changes during prolonged cold water immersion
[AD-A233768] N91-26711
Development of advanced methods based on stable isotope technology for studies of exercise in heat
[AD-A234670] N91-26719
Techniques for determining total body water using deuterium oxide N91-27091
BODY MEASUREMENT (BIOLOGY)
Techniques for determining total body water using deuterium oxide N91-27091
BODY TEMPERATURE
Metabolic changes and hemodynamic dysfunction following hypothermic shock
[AD-A233942] N91-26713
BOLOMETERS
Monolithic integration semiconductor and superconductor components
[AD-A234986] N91-26959
BONDING
Isotropic exchange in the platinum-catalyzed reduction of olefins in protic solvents
[AD-A234828] N91-26208
Surface chemistry of silicon: The behavior of dangling bonds
[AD-A235011] N91-26275
Thermal degradation chemistry of poly(diphenoxy phosphazene)
[AD-A235284] N91-26282
Bonding agent for composite propellants
[AD-D014876] N91-26392
BONE MARROW
A study of murine bone marrow cells cultured in bioreactors which create an environment which simulated microgravity N91-27101
BONES
JPRS Report: Science and technology. USSR: Life sciences
[JPRS-ULS-91-009] N91-26688
BORON
Magnetron sputter deposition of boron and boron carbide
[DE91-011194] N91-26241
Boron combustion model development with kinetic sensitivity analysis and measurement of key chemical rate parameters
[AD-A235309] N91-26283
Scanning tunnelling microscope for boron surface studies
[AD-A234716] N91-26452
BORON ALLOYS
Environmental embrittlement of ordered intermetallic alloys at room temperature in moist atmospheres
[DE91-012051] N91-26321
Effect of boron addition on recrystallization and grain growth in Ni3Al polycrystals
[DE91-011966] N91-26983
BORON CARBIDES
Magnetron sputter deposition of boron and boron carbide
[DE91-011194] N91-26241
BORON FIBERS
Composite fiber hazards
[AD-A233924] N91-26211
BORON OXIDES
Boron combustion model development with kinetic sensitivity analysis and measurement of key chemical rate parameters
[AD-A235309] N91-26283
BORON-EPOXY COMPOSITES
On the finite-strain-invariant failure criterion for composites
[AD-A234493] N91-26223
BOSONS
Gauge bosons and heavy quarks: Proceedings of Summer Institute on Particle Physics
[DE91-011248] N91-26907
BOUNDARIES
Dynamics of equatorial and polar boundaries of penetration of solar protons with energy about 1 MeV into magnetosphere during strong magnetic storm N91-26172
Determination of flow-regime boundaries for cohesive particles
[DE91-010552] N91-26468
Progress with neural network gulf streams
[AD-A233810] N91-26658
Mathematical topics in the modelling and identification of multicomponent continua
[AD-A234471] N91-26843
BOUNDARY CONDITIONS
Backscattering enhancement from rough surfaces
[AD-A234707] N91-26426
BOUNDARY LAYER CONTROL
The delay of turbulent boundary layer separation by oscillatory active control
[ITN-91-85104] N91-26482
BOUNDARY LAYER FLOW
Hydroacoustics of intermittent boundary-layer flow: A review
[AD-A235092] N91-26883
BOUNDARY LAYER SEPARATION
The delay of turbulent boundary layer separation by oscillatory active control
[ITN-91-85104] N91-26482

BOUNDARY LAYER STABILITY
Theoretical studies of the kinematics, dynamics, stability, and control of unsteady/vortical flows
[AD-A235190] N91-26477
BOUNDARY LAYER TRANSITION
Boundary layer transition noise art
[AD-A235093] N91-26884
BOUNDARY LAYERS
Experimental techniques in the field of low density aerodynamics
[AGARD-AG-318(E)] N91-26124
BOUNDARY VALUE PROBLEMS
A model for wet filament winding of composite cylinders with arbitrary thickness
[AD-A234102] N91-26215
Stability of collocation-based Runge-Kutta-Nystroem methods
[CWI-NM-R9016] N91-26835
Numerical methods for singularly perturbed differential equations with applications
[AD-A235188] N91-26850
Spectral recovery of discontinuous data
[ITN-91-85115] N91-26853
BRACKETS
Removable hand hold
[NASA-CASE-LEW-15196-1] N91-26543
BRAIN
Peptide transport through the blood-brain barrier
[AD-A233753] N91-26708
BRANCHING (MATHEMATICS)
Chaotic and bifurcating nonlinear systems driven by noise with applications to laser dynamics
[AD-A234841] N91-26512
BRAZING
Residual stresses in metal/ceramic brazes: Effect of creep on finite element analysis results
[DE91-011233] N91-26570
BREADBOARD MODELS
Investigating combustion as a method of processing inedible biomass produced in NASA's biomass production chamber
[NASA-TM-103821] N91-26759
BRIGHTNESS
The light curve of the magnetic star AM - Herculis
[ITN-91-85108] N91-27049
BRIGHTNESS DISCRIMINATION
Visual sensitivities and discriminations and their role in aviation
[AD-A234866] N91-26740
BRILLOUIN EFFECT
Determination of SBS induced damage limits in large fused silica optics for intense, time varying laser pulses
[DE91-012080] N91-26518
BRITTLE MATERIALS
Fragmentation of brittle materials at high rates of loading N91-26237
BRITTLENESS
Microalloyed steel preforms
[AD-A234039] N91-26296
BROADBAND
Evaluation of the MARISAT satellite UHF wideband channel
[AD-A233666] N91-26408
Wideband heterodyne spatial tracking for optical space communications
[AD-A233722] N91-26410
Computation of broadband mixing noise from turbomachinery
[AD-A233991] N91-26878
Design for electronic spectrally tunable infrared detector
[AD-D014877] N91-26925
BROKEN SYMMETRY
Supersymmetry breaking from superstrings and the gauge hierarchy
[DE91-011899] N91-26992
BROWNIAN MOVEMENTS
Comparison change analysis
[AD-A233690] N91-26873
BRUSHES
Rotordynamic and leakage characteristics of a 4-stage brush seal
[AD-A235336] N91-26541
BUBBLES
Vertical incidence backscatter and surface forward scattering from near-surface bubbles
[AD-A234432] N91-26880
BUCKLING
Nonlinear behavior of fiber composite materials and its effect on the postbuckling response of laminated plates
[AD-A234203] N91-26218
BUNCHING
Queueing systems with orbiting customers
[ITN-91-85112] N91-26868
BUOYANCY
Process study of sorted patterns on Arctic soils
[AD-A234089] N91-26628
BURNING RATE
A new high-progressivity/high-density propulsion concept: Partially cut multiperforated stick propellant
[AD-A234255] N91-26391
BURNOUT
Liquid film cooling in rocket engines
[AD-A234288] N91-26197
BURNS (INJURIES)
Pharmacological sparing of protein in burn injury
[AD-A235026] N91-26724

C

C-135 AIRCRAFT
KC-135 ground collision avoidance system questionnaire
[AD-A234385] N91-26125
Evaluation of the C/EC/KC-135 Ground Collision Avoidance System (GCAS), study 1
[AD-A235301] N91-26130
CABIN ATMOSPHERES
Airliner cabin environment: Contaminant measurements, health risks, and mitigation options
[PB91-159384] N91-26746
CABLES
Follow-on cable coupling lightning test. Volume 2: Appendixes A, B, C, and D
[NASA-CR-184124] N91-26195
CALCIUM METABOLISM
Hormonal regulators of calcium metabolism following space flights of various durations N91-26689
CALCIUM SILICATES
Microstructure, porosity, and mechanical property relationships of calcium-silicate-hydrate
[AD-A235191] N91-26279
CALIBRATING
Applied high-speed imaging for the icing research program at NASA Lewis Research Center
[NASA-TM-104415] N91-26490
Nimbus-7 TOMS Antarctic ozone atlas: August - December 1990
[NASA-RP-1264] N91-26651
Absorbed-dose calibration of ionization chambers in a Co-60 gamma-ray beam
[PB91-132290] N91-26890
Evaluating the effect of accuracy ratios on the percent of calibrations which are out of tolerance N91-27107
CALIFORNIA
Surface observation climatic summaries for Norton AFB, California
[AD-A235227] N91-26647
CALORIC REQUIREMENTS
Level of dietary fat does not affect fuel oxidation or endurance exercise performance of soldiers
[AD-A235194] N91-26728
CAMERAS
Imaging of fluorescent and chemiluminescent DNA hybrids using a 2-D CCD camera
[AD-A234641] N91-26676
Incorporation of shuttle CCT parameters in computer simulation models N91-27096
CANCER
Weighted least squares estimation for Aalen's additive risk model
[AD-A235250] N91-26852
CANTILEVER BEAMS
Effect of initial delamination on Mode 1 and Mode 2 interlaminar fracture toughness and fatigue fracture threshold
[NASA-TM-104079] N91-26569
CANTILEVER PLATES
Nonlinear oscillations of mechanical systems under multifrequency parametric excitation
[AD-A233800] N91-26558
CAPACITORS
Surface etching and roughening in integrated processing of thermal oxides
[AD-A234960] N91-26456
CAPILLARIES (ANATOMY)
Peptide transport through the blood-brain barrier
[AD-A233753] N91-26708
CARBENES
Fundamental studies of carbenes and hydrocarbon radicals
[DE91-011029] N91-26286
CARBON
A tribological investigation of the graphite-to-diamond-like behavior of amorphous carbon films ion-beam-deposited on ceramic substrates
[DE91-010816] N91-26379
Scanning tunnelling microscope for boron surface studies
[AD-A234716] N91-26452
CARBON CYCLE
Free-air carbon dioxide enrichment: A new approach to research on carbon exchange processes
[DE91-012074] N91-26609
Inorganic carbon surveys of oceanic basins
[DE91-011132] N91-26667
CARBON DIOXIDE
Commercializing solar hydrogen production
[DE91-011232] N91-26398
An assessment of CO2 greenhouse gas mitigation technologies
[DE91-011972] N91-26605
Free-air carbon dioxide enrichment: A new approach to research on carbon exchange processes
[DE91-012074] N91-26609
CARBON DIOXIDE CONCENTRATION
Global climate change: A discussion of major uncertainties
[DE91-011746] N91-26604
An assessment of CO2 greenhouse gas mitigation technologies
[DE91-011972] N91-26605
CARBON DIOXIDE LASERS
Array-typed, sealed-off mini tea CO2 laser
[AD-A234804] N91-26511
Infrared and visible laser double resonance studies of vibrational energy transfer processes in polyatomic molecules
[DE91-012162] N91-26910
CARBON FIBERS
Composite fiber hazards
[AD-A233924] N91-26211
CARBON MONOXIDE
The synthesis of methanol by a novel method
[DE91-011131] N91-26291
CARBON STEELS
Effect of bacterial biofilms on carbon steel pit propagation in phosphate containing medium
[DE91-010806] N91-26316
CARBON-CARBON COMPOSITES
Investigation into the effect of heat treatment on the thermal conductivity of 3-D carbon/carbon fiber composites
[DE91-010388] N91-26240
Scanning tunnelling microscope for boron surface studies
[AD-A234716] N91-26452
CARBOXYLIC ACIDS
Biological synthesis of substituted o-aminophenols
[AD-A234910] N91-26678
CARCINOGENS
Composite fiber hazards
[AD-A233924] N91-26211
CARDIOVASCULAR SYSTEM
Pharmacological correction of functional condition of Army Air Force flyers in hot climate with asparkam N91-26684
Risk factors and prediction of syncopic states in flyers N91-26685
Metabolic changes and hemodynamic dysfunction following hypothermic shock
[AD-A233942] N91-26713
The effect of catecholamines on arterial blood pressure and heart rate
[AD-A234755] N91-26720
Nonlinear systems dynamics in cardiovascular physiology: The heart rate delay map and lower body negative pressure N91-27095
CARRIAGES
Viscous flow simulations of internal store carriage and separation
[NASA-CR-185343] N91-26123
CARRIER LIFETIME
A study of signal generation and charge collectionin a-Si:H diodes for radiation imaging
[DE91-010243] N91-26904
CARRIER MOBILITY
A study of signal generation and charge collectionin a-Si:H diodes for radiation imaging
[DE91-010243] N91-26904
CARTESIAN COORDINATES
Extending matchings in graphs: A survey
[AD-A234392] N91-26841
CASUALTIES
Metabolic changes and hemodynamic dysfunction following hypothermic shock
[AD-A233942] N91-26713
CATACLYSMIC VARIABLES
The light curve of the magnetic star AM - Herculis
[ITN-91-85108] N91-27049
CATALOGS
The Internet resources guide and the Automatic Login Executor (ALEX) N91-27030

CATALOGS (PUBLICATIONS)
The NASA master directory quick reference guide N91-27034
COSMIC: Software catalog 1991 edition diskette format N91-27036
Catalog of data bases and reports [DE91-011516] N91-27043
CATALYSIS
Isotropic exchange in the platinum-catalyzed reduction of olefins in protic solvents [AD-A234828] N91-26208
The reduction by deuterium on platinum black of exo-2-norbornyl and endo-2-norbornyl to bornane-2-d occurs with predominant retention of configuration [AD-A235057] N91-26277
Heterogeneous catalysis on platinum and self-assembled monolayers on metal and metal oxide surfaces [AD-A235055] N91-26302
Preparation of inorganic and organometallic polymers with controlled structures [AD-A235359] N91-26371
CATALYSTS
Isotropic exchange in the platinum-catalyzed reduction of olefins in protic solvents [AD-A234828] N91-26208
Surface mediated photocatalysis [AD-A233748] N91-26246
Living ring-opening metathesis polymerization of 7-oxa-2,3-difunctionalized norbornenes and norbornadienes by Mo(CHCMe2R) (N-2,6-C6H3-i-Pr2) (O-t-Bu)2 and Mo(CHCMe2R) (N-2,6-C6H3-i-Pr2) (OCMe2CF3)2 [AD-A235235] N91-26365
Catalysts and initiators as instruments controlling structure of polymers with inorganic backbone [AD-A235350] N91-26368
Biological synthesis of substituted o-aminophenols [AD-A234910] N91-26678
CATALYTIC ACTIVITY
Development of a low temperature catalytic combustor for small gas turbine applications [PB91-161273] N91-26529
CATECHOLAMINE
Effect of shift work of air traffic controllers on sympathetic nervous system N91-26700
The effect of catecholamines on arterial blood pressure and heart rate [AD-A234755] N91-26720
CATHODES
RADC cathode life test facility [AD-A234309] N91-26444
Work performed experiments: 1989-1990 [AD-A235221] N91-26457
CATIONS
Cationic polymerization within van der Waals clusters of the form (CH2=R)n where R=CH2, CF2 and CHCH3 [AD-A234233] N91-26255
CAUCHY PROBLEM
State space models for aeroelastic and viscoelastic systems [AD-A234730] N91-26117
CAVITATION FLOW
Grain boundary cavitation processes in a Ni3Al alloy at elevated temperatures [AD-A235279] N91-26307
CAVITIES
Grain boundary cavitation processes in a Ni3Al alloy at elevated temperatures [AD-A235279] N91-26307
CAVITY RESONATORS
A narrow-bandwidth unstable resonator laser cavity [AD-D014865] N91-26505
High-temperature ceramic superconductors [AD-A234620] N91-26953
CELESTIAL GEODESY
CBSD version 2 component models of the IR celestial background [AD-A235372] N91-27048
CELLS (BIOLOGY)
Intracellular physiology of the rat suprachiasmatic nucleus: Electrical properties, neurotransmission, and effects of neuromodulators [AD-A234442] N91-26675
Interaction of ionizing radiation, genetically active chemicals, and radiofrequency radiation in human and rodent cells [AD-A234747] N91-26677
Photochemical energy conversion by membrane-bound photoredox systems [DE91-012171] N91-26682
Wound healing by cultured skin cells and growth factors [AD-A235300] N91-26730
Mathematical modeling of the flow field and particle motion in a rotating bioreactor at unit gravity and microgravity N91-27092
A study of murine bone marrow cells cultured in bioreactors which create an environment which simulated microgravity N91-27101
CELLULOSE
Higher plants as part of biological human life support system N91-26693
CENTER OF GRAVITY
A gravitationally consistent second-order analytic secular solution for the point-mass motion of the eight principal planets N91-27054
CENTRAL NERVOUS SYSTEM STIMULANTS
Methylphenidate and pemoline: Effects on sleepiness and mood during sleep deprivation [AD-A234659] N91-26718
CENTRIFUGAL COMPRESSORS
Titanium alloy integrated centrifugal impeller 5 coordinate computer assisted manufacturing technology [AD-A234797] N91-26300
CENTRIFUGAL PUMPS
Performance evaluation of a novel erosion-resistant pump design [DE91-008201] N91-26528
CERAMIC COATINGS
India-stabilized zirconia coating for composites [AD-D014857] N91-26224
A tribological investigation of the graphite-to-diamond-like behavior of amorphous carbon films ion-beam-deposited on ceramic substrates [DE91-010816] N91-26379
CERAMIC FIBERS
Investigation of interfacial shear strength in SiC/Si3N4 composites [NASA-TM-103739] N91-26233
Ceramic fiber coating development and demonstration [AD-A234773] N91-26358
Strength of SiC- and Si-N-C-ceramic fibers exposed to high-temperature gaseous environments [DE91-011099] N91-26380
CERAMIC MATRIX COMPOSITES
Investigation of interfacial shear strength in SiC/Si3N4 composites [NASA-TM-103739] N91-26233
Polymeric routes to silicon carbide and silicon oxycarbide CMC [NASA-TM-104372] N91-26234
Characterization of mechanical damage mechanisms in ceramic composite materials [NR-032-553] N91-26235
Response of whisker-reinforced ceramic matrix composites to dynamic compressive loading N91-26236
Pressureless densification of ceramic matrix composites [AD-A235031] N91-26362
CERAMICS
Effect of surface forces on the rheology of particle-liquid systems and the consolidation of ceramic powders [AD-A234375] N91-26221
Reaction processing of ceramic particulate and whisker composites [AD-A234951] N91-26225
Fiber coating by sputtering for high temperature composites [AD-A234994] N91-26226
Dynamic fracture responses of Al2O3, Si3N4, and SiC(w)/Al2O3 [AD-A235286] N91-26229
Characterization of mechanical damage mechanisms in ceramic composite materials [NR-032-553] N91-26235
Microstructure development during microwave annealing of dense silicon nitride [DE91-012069] N91-26242
International collaboration program on innovative chemical processing of superior electronic and optical materials [AD-A235030] N91-26276
An analytical methodology to predict the coating characteristics of plasma-sprayed ceramic powders [DE91-010088] N91-26326
Transformation toughening of ceramics [AD-A234926] N91-26359
Organosilicon polymers incorporating the bicyclo(2.2.2)-octane moiety [AD-A234966] N91-26361
Pressureless densification of ceramic matrix composites [AD-A235031] N91-26362
Strength and microstructure of ceramics [AD-A235424] N91-26374
Method of preparing a thermal barrier coating [NASA-CASE-LEW-14999-2] N91-26376
A tribological investigation of the graphite-to-diamond-like behavior of amorphous carbon films ion-beam-deposited on ceramic substrates [DE91-010816] N91-26379
Sliding wear-testing and data analysis strategies for advanced engineering ceramics [DE91-009524] N91-26383
Ceramic technology for advanced heat engines project [DE91-010451] N91-26384
Laser spectroscopy characterization of materials for frequency agile solid state laser systems [AD-A233916] N91-26500
Long-rod penetration of confined ceramic tiles [AD-A234312] N91-26534
Development of high Tc (greater than 110K) Bi, Tl and Y-based materials as superconducting circuit elements [NASA-CR-188581] N91-26948
High-temperature ceramic superconductors [AD-A234620] N91-26953
CEREBRAL CORTEX
The Trendelenburg position after cerebral air embolism in dogs: Effects on the somatosensory evoked potential, intracranial pressure, and blood-brain barrier [AD-A233809] N91-26673
CERTIFICATION
Certification procedures and requirements N91-26154
Trends in certification procedures and design analysis N91-26158
CH-47 HELICOPTER
Task analysis and workload prediction for the MH-47E mission and a comparison with CH-47D workload predictions. Volume 2: Appendixes A through N [AD-A235249] N91-26757
CHAINS
Novel concepts in electronic polymers: Polyaniline and its derivatives [AD-A234214] N91-26339
Propagators for quantum oscillator chains [AD-A234467] N91-26893
CHANNEL CAPACITY
Evaluation of the MARISAT satellite UHF wideband channel [AD-A233666] N91-26408
CHANNELS
Multigigahertz semiconductor lasers [AD-A234776] N91-26510
CHARACTERIZATION
Characterization of mechanical damage mechanisms in ceramic composite materials [NR-032-553] N91-26235
Materials/microstructures characterization [AD-A233751] N91-26295
Polymer characterization using singlet oxygen phosphorescence as a spectroscopic probe [DE91-011735] N91-26382
CHARGE COUPLED DEVICES
Imaging of fluorescent and chemiluminescent DNA hybrids using a 2-D CCD camera [AD-A234641] N91-26676
Thickness measurements of silicon films using partial coherence interferometry [AD-A235211] N91-26930
High accuracy optical rate sensor N91-27115
CHARGE EFFICIENCY
Improvement in the capacity and safety of lithium/inorganic electrolyte sulfur dioxide rechargeable cells, phase 2 [AD-A235303] N91-26589
CHARGE TRANSFER
Electrochemically induced charge and mass transport in polypyrrole/poly(styrene sulfonate) molecular composites [AD-A234599] N91-26354
Charge exchange in ion-surface scattering at hyperthermal (10-100 eV) and keV energies [AD-A235233] N91-26899
Center for the Integration of Optical C [AD-A235277] N91-26931
CHARTS
The Navy standard compressed aeronautical chart database [AD-A235340] N91-26587
CHECKOUT
The High Resolution Profiler (HRP): User's guide and software modifications documentation [AD-A234640] N91-26663
CHEMICAL ANALYSIS
New developments in the synthesis and doping of polyacetylene and polyaniline [AD-A233702] N91-26244
Flexural plate wave devices for chemical analysis [AD-A234129] N91-26254

Electronic excitation transport in photosynthesis and crystal and molecular structures of porphyrin compounds
[DE91-012024] N91-26679
COLDEX-86: Summary of the experimental protocol and general results
[AD-A234031] N91-26715

CHEMICAL BONDS
Energetics, bonding mechanism and electronic structure of metal/ceramic interfaces
[DE91-009787] N91-26239
Adsorption and decomposition of acetylene on Si(100)-(2x1)
[AD-A233808] N91-26248
Study of the low-lying electronic states of Si2 and Si2(-) using negative ion photodetachment techniques
[AD-A234336] N91-26256
Surface chemistry of silicon: The behavior of dangling bonds
[AD-A235011] N91-26275
Adsorption of ammonia on iron clusters
[DE91-011125] N91-26308
The role of electronic structure in the mechanical behavior of aluminides
[DE91-012508] N91-26325
Processable polymers and copolymers of 3-alkylthiophenes and their blends
[AD-A234596] N91-26351
Anionic ring-opening polymerization of cyclotetrasilanes
[AD-A235360] N91-26372
Scanning tunnelling microscope for boron surface studies
[AD-A234716] N91-26452
Electronic excitation transport in photosynthesis and crystal and molecular structures of porphyrin compounds
[DE91-012024] N91-26679
Molecular orbital studies of the bonding in heavy element organometallics
[DE91-010915] N91-26905

CHEMICAL CLOUDS
Coordination of mesoscale meteorological research between ASL and European groups
[AD-A233586] N91-26639

CHEMICAL COMPOSITION
Mechanical behavior and flow mechanisms in refractory metal composition
[AD-A234701] N91-26297
Precipitation in Alloy 718: A combined AEM and APFIM investigation
[DE91-009918] N91-26314
Investigation of plessite in iron meteorites and laboratory Fe-Ni(P) alloys
[DE91-010858] N91-27053
Chemistry and mineralogy of Martian dust: An explorer's primer N91-27063
Reflectance spectroscopy of palagonite and iron-rich montmorillonite clay mixtures: Implications for the surface composition of Mars N91-27075

CHEMICAL DEFENSE
Effectiveness of ice-vest cooling in prolonging work tolerance time during heavy exercise in the heat for personnel wearing Canadian forces chemical defence ensembles
[AD-A235273] N91-26758

CHEMICAL PROPERTIES
Polysilanes, synthesis, modification, and properties
[AD-A235351] N91-26369
Multiple-frequency SAW devices for chemical sensing and materials characterization
[DE91-010856] N91-26888
The chemical modification of plasmas
[AD-A234448] N91-26940
Sand and Dust on Mars
[NASA-CP-10074] N91-27057

CHEMICAL REACTION CONTROL
Regio- and stereochemical control in substitution reactions of cyclophosphazenes
[AD-A234376] N91-26257

CHEMICAL REACTIONS
Reaction processing of ceramic particulate and whisker composites
[AD-A234951] N91-26225
Size dependence of gaseous cluster reactivity and evaporation dynamics as a mechanistic probe
[AD-A233811] N91-26249
Adsorption and thermal behavior of ethylene on Si(100)-(2x1)
[AD-A234098] N91-26252
Desorption product yields following Cl2 adsorption on Si(111)7x7: Coverage and temperature dependence
[AD-A234635] N91-26264
Diethylsilane decomposition on silicon surfaces studied using transmission FTIR spectroscopy
[AD-A234638] N91-26266
A combined XPS-ISS modulated molecular beam investigation of the reactions of oxygen and fluorine with silicon surfaces
[AD-A234867] N91-26269
Theory and experimental and chemical instabilities
[AD-A234916] N91-26270
Computer modeling of soot formation comparing free radical and ionic mechanisms
[AD-A235007] N91-26273
Surface chemistry of silicon: The behavior of dangling bonds
[AD-A235011] N91-26275
Surface Chemkin (version 3.7): A FORTRAN package for analyzing heterogeneous chemical kinetics at a solid-surface-gas-phase interface
[DE91-010840] N91-26285
The chemistry of sodium with sulfur in flames
[DE91-002060] N91-26288
Chemical phase separation in binary iron-chromium alloys
[DE91-010282] N91-26294
Processable polymers and copolymers of 3-alkylthiophenes and their blends
[AD-A234596] N91-26351
Surface characterization of electrically conducting nickel tetrathiooxalate/poly(vinyl alcohol) composites
[AD-A234598] N91-26353
Organosilicon polymers incorporating the bicyclo(2.2.2)-octane moiety
[AD-A234966] N91-26361
Effect of molecular weight on polyphenylquinoxaline properties
[NASA-TM-104100] N91-26377
A study of the gas phase chemistry of solid propellants using a microprobe mass spectrometer (MPMS) system: Preliminary results for solid fuels (HTPB/Zecorez and BAMO/NMMO), single-base propellant (M10) and an RDX-Based propellant (BLX-9)
[AD-A234840] N91-26394
Thin film alloys on semiconductor substrates
[DE91-012355] N91-26985

CHEMICAL REACTORS
The synthesis of methanol by a novel method
[DE91-011131] N91-26291

CHEMICAL WARFARE
Water solubility of bis(2-ethylhexyl) hydrogen phosphite
[AD-A234561] N91-26259

CHEMILUMINESCENCE
Imaging of fluorescent and chemiluminescent DNA hybrids using a 2-D CCD camera
[AD-A234641] N91-26676
Thermoluminescence kinetics of pyrite (FeS2)
[DE91-011710] N91-26990

CHEMISORPTION
Adsorption and decomposition of acetylene on Si(100)-(2x1)
[AD-A233808] N91-26248
Heterogeneous catalysis on platinum and self-assembled monolayers on metal and metal oxide surfaces
[AD-A235055] N91-26302

CHINESE SPACE PROGRAM
Chinese space science and technology (selected articles)
[AD-A234798] N91-26180
Prime Minister Li Peng talks with representatives to a discussion meeting on satellite applications and applied satellite technology about the development of our country's activities in space
[AD-A234801] N91-26181

CHIPS (ELECTRONICS)
VHSIC electronics and the cost of Air Force avionics in the 1990s
[RAND-R-3843-AF] N91-26143

CHIPS (MEMORY DEVICES)
The role of EEPROM devices in upcoming ISDN applications
[AD-A234837] N91-26454
Testing the One-Port Random Access Memory (1PRAM) module of TRW's CPUAX signal processing superchip
[AD-A234127] N91-26761

CHLORELLA
Higher plants as part of biological human life support system N91-26693

CHLORIDES
Desorption product yields following Cl2 adsorption on Si(111)7x7: Coverage and temperature dependence
[AD-A234635] N91-26264

CHLORINATION
Multispectral identification of potentially hazardous byproducts of ozonation and chlorination. Part 1: Studies of chromatographic and spectroscopic properties of MX
[PB91-161703] N91-26601

CHLOROPHYLLS
Phytoplankton abundance in relation to Lagrangian paths
[AD-A233728] N91-26672
Photochemical energy conversion by membrane-bound photoredox systems
[DE91-012171] N91-26682

CHROMIUM ALLOYS
Chemical phase separation in binary iron-chromium alloys
[DE91-010282] N91-26294
Cyclic deformation, damage, and effects of environment in the Ni3Al ordered alloy at elevated temperature
[AD-A235168] N91-26304

CIRCUITS
Rail circuit augmentation
[AD-A234944] N91-26184
Control circuitry using electronic emulation of a synchro signal for accurate control of position and rate of rotation for shafts
[NASA-CASE-MFS-28458-1] N91-26459
Electrostatic fields in a dusty Martian environment N91-27078

CIRCULAR CYLINDERS
Theoretical studies of the kinematics, dynamics, stability, and control of unsteady/vortical flows
[AD-A235190] N91-26477

CIRCULAR ORBITS
Spatial rotations of a satellite in a circular three-body problem for the case of general resonance N91-26164
Analysis of necessary and sufficient conditions for the equilibrium stability of a gyrostatic satellite N91-26166

CIVIL AVIATION
Risk factors and prediction of syncopic states in flyers N91-26685
Utilization of emergency medical kits by air carriers
[AD-A234784] N91-26721

CLASSIFICATIONS
Minutes of the 24th Explosives Safety Seminar, volume 1
[AD-A235005] N91-26395
OSIRRUS: Oceanic symbolic image representation, recognition and understanding software
[AD-A235112] N91-26665
Using genetic algorithms to select and create features for pattern classification
[AD-A235165] N91-26792
Northeast Artificial Intelligence Consortium (NAIC). Volume 18: A distributed artificial intelligence approach to information fusion and object classification
[AD-A234892] N91-26827
Understanding object classes: Modeling and matching
[AD-A235027] N91-26848
A catalog of high resolution Jovian decametric radio noise burst spectra, volume 1 N91-27047

CLASSIFIERS
A comparative study of the practical characteristics of neural network and conventional pattern classifiers
[AD-A235345] N91-26795

CLAYS
Reflectance spectroscopy of palagonite and iron-rich montmorillonite clay mixtures: Implications for the surface composition of Mars N91-27075

CLEAR AIR TURBULENCE
Boundary layer parameterization for a global spectral model
[AD-A235310] N91-26635

CLIMATE
Global climate change: A discussion of major uncertainties
[DE91-011746] N91-26604
Surface observation climatic summaries for Norton AFB, California
[AD-A235227] N91-26647
Pharmacological correction of functional condition of Army Air Force flyers in hot climate with asparkam N91-26684

CLIMATE CHANGE
Ice cores and SeaRISE: What we do (and don't) know N91-26579
Glacial dynamics (glaciology) N91-26580
Global climate change: A discussion of major uncertainties
[DE91-011746] N91-26604

CLIMATOLOGY
Satellite data derived estimates of erosion parameters for reentry vehicles
[AD-A234792] N91-26189
West Antarctic Ice Sheet Initiative. Volume 2: Discipline Reviews
[NASA-CP-3115-VOL-2] N91-26573
Global climate change: A discussion of major uncertainties
[DE91-011746] N91-26604

Surface Observation Climatic Summaries (SOCS) for Kodiak, Alaska
[AD-A235182] N91-26646
Surface observation climatic summaries for Norton AFB, California
[AD-A235227] N91-26647
Surface observation climatic summaries for Tonopah test range, Nevada
[AD-A235228] N91-26648

CLINICAL MEDICINE
JPRS report: Science and technology. USSR: Life sciences
[JPRS-ULS-91-011] N91-26696

CLOCKS
Backplane bus distributed realtime clock synchronization
[AD-A234476] N91-26491

CLOSED ECOLOGICAL SYSTEMS
Investigating combustion as a method of processing inedible biomass produced in NASA's biomass production chamber
[NASA-TM-103821] N91-26759

CLOUD COVER
Development and verification of a physical cloud-moisture model for use in general circulation models
[AD-A234751] N91-26643

CLOUD DISPERSAL
Coordination of mesoscale meteorological research between ASL and European groups
[AD-A233586] N91-26639

CLOUD PHYSICS
On the evolution of raindrop spectra and their effect on the atmosphere below cloud base: Numerical models and comparisons with observations
[ITN-91-85113] N91-26652
Advanced Microwave Precipitation Radiometer (AMPR) for remote observation of precipitation
[NASA-CR-184165] N91-26655

CLOUDS (METEOROLOGY)
Comparison of the RF frequency spectra of HEMP and lightning
[AD-A234306] N91-26642
Rotating multicylinder method for the measurement of cloud liquid-water content and droplet size
[AD-A234780] N91-26644

CLUMPS
Defect clustering and related properties of oxides
[DE91-011072] N91-26290
Adsorption of ammonia on iron clusters
[DE91-011125] N91-26308

CLUSTER ANALYSIS
Cluster beam analysis via photoionization
[AD-A234111] N91-26253

COAL UTILIZATION
MHD contractors' review meeting
[DE91-011295] N91-26945

COASTAL CURRENTS
Laboratory modelling of the dynamics of coastal upwelling
[AD-A234987] N91-26664

COASTAL WATER
Directional characteristics of waves in shallow water
[AD-A234568] N91-26661
SEEP 2 zooplankton data report: Winter, spring and summer collections at mooring 3 during 1988
[DE91-012077] N91-26668

COASTS
Directional characteristics of waves in shallow water
[AD-A234568] N91-26661

COATING
Ceramic fiber coating development and demonstration
[AD-A234773] N91-26358

COATINGS
Corrosion of graphite aluminum metal matrix composites
[AD-A234322] N91-26220
Fiber coating by sputtering for high temperature composites
[AD-A234994] N91-26226
Damage accumulation in advanced metal matrix composites under thermal cycling
[AD-A235002] N91-26227
Ceramic fiber coating development and demonstration
[AD-A234773] N91-26358
Non-destructive evaluation of residual stresses in thin films via x ray diffraction topography methods
[AD-A235328] N91-26552

COBALT 60
Absorbed-dose calibration of ionization chambers in a Co-60 gamma-ray beam
[PB91-132290] N91-26890

COCHLEA
Combined effect of noise and vibration on cells of auditory and vestibular apparatus N91-26707

COCKPITS
Format and basic geometry of a perspective display of air traffic for the cockpit
[NASA-TM-86680] N91-26142

CODING
Symbolic expressions of composite grid structures
[AD-A233794] N91-26836

COGENERATION
Development of a low temperature catalytic combustor for small gas turbine applications
[PB91-161273] N91-26529

COGNITION
Cognitive and neural sciences division 1990 programs
[AD-A233773] N91-26733
Induced pictorial representations
[AD-A234548] N91-26735
A Conference on Eye Movements and Visual Cognition
[AD-A234754] N91-26739
Neural mechanisms of attention
[AD-A235003] N91-26742
Imagination and situated cognition
[AD-A234420] N91-26809

COGNITIVE PSYCHOLOGY
Cognitive and neural sciences division 1990 programs
[AD-A233773] N91-26733
On measures of misconception stability
[AD-A234952] N91-26847

COHERENT RADAR
The instrumental principles of MST radars and incoherent scatter radars and the configuration of radar system hardware N91-26616

COHESION
Determination of flow-regime boundaries for cohesive particles
[DE91-010552] N91-26468

COLD STRENGTH
Plasticity of single crystalline Al3X intermetallic compounds
[AD-A234699] N91-26356

COLD WATER
COLDEX-86: Physical work capacity during prolonged cold water immersion at 6.1 msw
[AD-A233767] N91-26710
COLDEX-86: Fluid and electrolyte changes during prolonged cold water immersion
[AD-A233768] N91-26711

COLLISION AVOIDANCE
KC-135 ground collision avoidance system questionnaire
[AD-A234385] N91-26125
Evaluation of the C/EC/KC-135 Ground Collision Avoidance System (GCAS), study 1
[AD-A235301] N91-26130
Fuzzy logic control system to provide autonomous collision avoidance for Mars rover vehicle N91-27106

COLLOCATION
Stability of collocation-based Runge-Kutta-Nystroem methods
[CWI-NM-R9016] N91-26835

COMBAT
Space support for airland battle-future
[AD-A233868] N91-26864

COMBINATORIAL ANALYSIS
Maximization on matroids with random weights
[AD-A233978] N91-26858

COMBUSTIBLE FLOW
An experimental investigation of structure, mixing, and combustion in compressible turbulent shear layers
[AD-A235278] N91-26281
Basic studies of microstructure of combusting turbulent flows
[AD-A234222] N91-26471

COMBUSTION
Theory and experimental and chemical instabilities
[AD-A234916] N91-26270
A new high-progressivity/high-density propulsion concept: Partially cut multiperforated stick propellant
[AD-A234255] N91-26391
Investigating combustion as a method of processing inedible biomass produced in NASA's biomass production chamber
[NASA-TM-103821] N91-26759

COMBUSTION CHAMBERS
CFD analysis of jet mixing in low NOx flametube combustors
[NASA-TM-104466] N91-26146
Method of injecting fluid propellants into a rocket combustion chamber
[NASA-CASE-LEW-14846-2] N91-26200
Development of a low temperature catalytic combustor for small gas turbine applications
[PB91-161273] N91-26529
Multi-dimensional computer simulation of MHD combustor hydrodynamics
[DE91-011851] N91-26946

COMBUSTION CHEMISTRY
Surface Chemkin (version 3.7): A FORTRAN package for analyzing heterogeneous chemical kinetics at a solid-surface-gas-phase interface
[DE91-010840] N91-26285
Fundamental studies of carbenes and hydrocarbon radicals
[DE91-011029] N91-26286
A study of the gas phase chemistry of solid propellants using a microprobe mass spectrometer (MPMS) system: Initial development of the MPMS system
[AD-A234839] N91-26393
A study of the gas phase chemistry of solid propellants using a microprobe mass spectrometer (MPMS) system: Preliminary results for solid fuels (HTPB/Zecorez and BAMO/NMMO), single-base propellant (M10) and an RDX-Based propellant (BLX-9)
[AD-A234840] N91-26394
Elementary reaction rate measurements at high temperatures by tunable-laser flash-absorption
[DE91-011850] N91-26516

COMBUSTION EFFICIENCY
Development of a low temperature catalytic combustor for small gas turbine applications
[PB91-161273] N91-26529

COMBUSTION PHYSICS
Boron combustion model development with kinetic sensitivity analysis and measurement of key chemical rate parameters
[AD-A235309] N91-26283

COMFORT
Sitting posture analysis. An experimental optimisation approach
[ITN-91-85114] N91-26760

COMMAND AND CONTROL
Aircrew Evaluation Sustained Operations Performance (AESOP): A triservice facility for technology transition
[AD-A234626] N91-26738
Northeast Artificial Intelligence Consortium (NAIC). Volume 16: Intelligent signal processing techniques for multi-sensor surveillance systems
[AD-A234895] N91-26830
Northeast Artificial Intelligence Consortium (NAIC). Volume 17: High-level adaptive signal processing
[AD-A234896] N91-26831
Northeast Artificial Intelligence Consortium (NAIC). Volume 13: Image understanding and intelligent parallel systems
[AD-A234897] N91-26832

COMMERCIAL AIRCRAFT
Acquisition of statistical gust load data by commercial airplanes N91-26152
Improved reduction of gust loads data for gust intensity N91-26153

COMMUNICATION
Providing a computing environment for a high energy physics workshop
[DE91-012049] N91-26916
NASA information sciences and human factors program
[NASA-TM-4291] N91-27119

COMMUNICATION EQUIPMENT
The role of EEPROM devices in upcoming ISDN applications
[AD-A234837] N91-26454

COMMUNICATION NETWORKS
Omega/VLF signal coverage database development
[AD-A235226] N91-26129
Advanced Satellite Research Project: SCAR Research Database. Bibliographic analysis
[NASA-CR-186086] N91-26182
Spread spectrum communication networks
[AD-A233696] N91-26409
Propagation of RF signals through structured ionization: The general model
[AD-A234051] N91-26418
Adaptive spread spectrum networks
[AD-A234084] N91-26419
Functional baseline specification for ATC data link service implementation in the host computer system
[DOT/FAA/CT-91/12] N91-26433
Aircrew Evaluation Sustained Operations Performance (AESOP): A triservice facility for technology transition
[AD-A234626] N91-26738
Northeast Artificial Intelligence Consortium (NAIC). Volume 4: Distributed artificial intelligence for communications network management
[AD-A234883] N91-26818
The NASA Science Internet: An integrated approach to networking N91-27041

COMMUNITIES
Adaptation and resistance of ecosystems to stress
[AD-A234576] N91-26603

COMPARTMENTS
Use of a zone model for validation of a horizontal ceiling/floor vent algorithm
[AD-A234553] N91-26474
Double face sealing device
[NASA-CASE-MFS-28521-1] N91-26542
COMPETITION
Air Force stock fund: Hydrazine sales consistent with the Commercial Space Launch Act. Report to the Chairman, Committee on Science, Space and Technology, House of Representatives
[GAO/NSIAD-91-196] N91-26397
COMPILERS
Ada compiler validation summary report: Certification number: 9000703W1.11014, Silicon Graphics 4D ADA Iris-4D/380 (host) Iris-4D/380 (target)
[AD-A233714] N91-26771
Ada software portability and level 2 system simulator integration issues
[AD-A233757] N91-26773
Ada compiler validation summary report: Certificate number 900703W1.11015, Silicon Graphics 4D Ada, Iris-4D/220S (host) Iris-4D/220S (target)
[AD-A233786] N91-26776
COMPLEX COMPOUNDS
The control of orbital mixing in ruthenium complexes containing quinone related ligands
[AD-A234602] N91-26260
Cross-linking and modification of cytochrome c with redox-active metal complexes
[DE91-012023] N91-26287
Study of intermediates from transition metal excited-state electron-transfer reactions
[DE91-012182] N91-26324
Electroactive, near infrared absorbing nickel bis(dithiolene) complex polycarbonates and polyurethanes
[AD-A234595] N91-26350
COMPOSITE MATERIALS
Gordon Research Conference on Composites
[AD-A233778] N91-26210
Far- and mid-infrared properties of metal-insulator composite materials
[AD-A234264] N91-26219
Reaction processing of ceramic particulate and whisker composites
[AD-A234951] N91-26225
Dynamic fracture responses of Al2O3, Si3N4, and SiC(w)/Al2O3
[AD-A235286] N91-26229
Composite database interface users manual
[AD-A235327] N91-26230
Ionically and electronically conductive composite polymer membranes
[AD-A234587] N91-26349
Electrochemically induced charge and mass transport in polypyrrole/poly(styrene sulfonate) molecular composites
[AD-A234599] N91-26354
Ceramic fiber coating development and demonstration
[AD-A234773] N91-26358
Sliding wear-testing and data analysis strategies for advanced engineering ceramics
[DE91-009524] N91-26383
NATO advanced research workshop on Measurement of Residual and Applied Stress Using Neutron Diffraction
[AD-A235103] N91-26566
Mathematical topics in the modelling and identification of multicomponent continua
[AD-A234471] N91-26843
COMPOSITE PROPELLANTS
Bonding agent for composite propellants
[AD-D014876] N91-26392
COMPOSITE STRUCTURES
Composite fiber hazards
[AD-A233924] N91-26211
Testing of a composite thermal structure to insulate the drivers of a large scale blast/thermal simulator
[AD-A234014] N91-26213
Interfacial slippage of a unidirectional fiber composite under longitudinal shearing
[AD-A234186] N91-26216
Damage accumulation in advanced metal matrix composites under thermal cycling
[AD-A235002] N91-26227
Ionically and electronically conductive composite polymer membranes
[AD-A234587] N91-26349
Block patterning of the metallization of polyvinylidene fluoride transducers
[AD-D014872] N91-26450
Nonlinear oscillations of mechanical systems under multifrequency parametric excitation
[AD-A233800] N91-26558
Symbolic expressions of composite grid structures
[AD-A233794] N91-26836
COMPRESSED AIR
Variable speed gas engine-driven air compressor system. Phase 1: System analysis
[PB91-159533] N91-26530
COMPRESSIBILITY
The effects of compressibility on a supersonic mixing layer
[AD-A234992] N91-26119
Development of a test system and experimental method for in-plane biaxial compressive deformation and failure of fiber composite materials
[AD-A234062] N91-26214
Static and cyclic compressive fatigue of thermoplastic-matrix composite in ambient and moisture environments
[AD-A234187] N91-26217
Characterization of mechanical damage mechanisms in ceramic composite materials
[NR-032-553] N91-26235
COMPRESSIBLE FLOW
The effects of compressibility on a supersonic mixing layer
[AD-A234992] N91-26119
Direct and large-eddy simulations of three-dimensional compressible Navier-Stokes turbulence
[AD-A233717] N91-26470
COMPRESSIBLE FLUIDS
An experimental investigation of structure, mixing, and combustion in compressible turbulent shear layers
[AD-A235278] N91-26281
COMPRESSING
Research in stochastic processes
[AD-A234650] N91-26860
COMPRESSION LOADS
Response of whisker-reinforced ceramic matrix composites to dynamic compressive loading
N91-26236
Fragmentation of brittle materials at high rates of loading N91-26237
COMPRESSIVE STRENGTH
Development of a test system and experimental method for in-plane biaxial compressive deformation and failure of fiber composite materials
[AD-A234062] N91-26214
Static and cyclic compressive fatigue of thermoplastic-matrix composite in ambient and moisture environments
[AD-A234187] N91-26217
Response of whisker-reinforced ceramic matrix composites to dynamic compressive loading
N91-26236
COMPRESSORS
Variable speed gas engine-driven air compressor system. Phase 1: System analysis
[PB91-159533] N91-26530
Investigation of axial positioning for flexural compressors
[NASA-CR-185711] N91-26544
COMPUTATION
Simulation of pore scale porous media flow using lattice gas methods
[DE91-004829] N91-26484
Implementation of the flow-modulated skew-upwind difference scheme in the COMMIX-1C code: A first assessment
[DE91-011168] N91-26489
Laser-induced desorption of H2 from Si(111)7x7
[AD-A234636] N91-26508
Computational complexity and efficiency in electro-optical computing system
[AD-A235013] N91-26765
A theoretical and experimental study of the symmetric rank one update
[AD-A233965] N91-26777
Parallel algorithms for least squares and related computations
[AD-A235018] N91-26790
The process group approach to reliable distributed computing
[NASA-CR-188498] N91-26804
Matching theory. A sampler: From Denes Koenig to the present
[AD-A234321] N91-26839
Computation of broadband mixing noise from turbomachinery
[AD-A233991] N91-26878
An analysis on the stability of the Mie-Gruneisen equation of state for describing the behavior of shock-loaded materials
[AD-A233827] N91-26988
COMPUTATIONAL FLUID DYNAMICS
Numerical investigations in three-dimensional internal flows
[NASA-CR-188615] N91-26114
Viscous flow simulations of internal store carriage and separation
[NASA-CR-185343] N91-26123
CFD analysis of jet mixing in low NOx flametube combustors
[NASA-TM-104466] N91-26146
Benchmark study between FIDAP and a cellular automata code
[DE91-011224] N91-26486
Navier-Stokes calculations of scramjet-nozzle-afterbody flowfields
[NASA-CR-185356] N91-26488
COMPUTATIONAL GRIDS
Viscous flow simulations of internal store carriage and separation
[NASA-CR-185343] N91-26123
Direct and large-eddy simulations of three-dimensional compressible Navier-Stokes turbulence
[AD-A233717] N91-26470
Adaptive component methods for time dependent PDE's
[AD-A233776] N91-26775
COMPUTER AIDED DESIGN
High performance transparency design
[AD-A234456] N91-26133
Active devices for monolithic millimeter-wave integrated circuits
[AD-A234033] N91-26440
Electronic design process
[AD-A234709] N91-26786
COMPUTER AIDED MANUFACTURING
Titanium alloy integrated centrifugal impeller 5 coordinate computer assisted manufacturing technology
[AD-A234797] N91-26300
Electronic design process
[AD-A234709] N91-26786
COMPUTER AIDED MAPPING
The Navy standard compressed aeronautical chart database
[AD-A235340] N91-26587
Software requirements specification for the Mapping And Graphic Information Capability (MAGIC). Volume 4: Geographic mapping CSCI
[AD-A235275] N91-26794
COMPUTER AIDED TOMOGRAPHY
X ray tomographic inspection of printed wiring assemblies and electrical components
[AD-A234748] N91-26548
X ray-computed tomography for inspecting industrial parts
[DE91-011390] N91-26554
Computer tomography measurement of vertebral bones and muscles after extended manned space flights
N91-26690
Proton arc doses to the primate head
[AD-A235134] N91-26726
COMPUTER ASSISTED INSTRUCTION
Training effectiveness of an intelligent tutoring system for a propulsion console trainer N91-27097
COMPUTER GRAPHICS
Format and basic geometry of a perspective display of air traffic for the cockpit
[NASA-TM-86680] N91-26142
Propulsion stability codes for liquid propellant propulsion systems developed for use on a PC computer
[NASA-CR-184983] N91-26201
A system and language environment for scientific computing
[AD-A233747] N91-26772
Ada compiler validation summary report: Certificate number 900703W1.11015, Silicon Graphics 4D Ada, Iris-4D/220S (host) Iris-4D/220S (target)
[AD-A233786] N91-26776
Software requirements specification for the Mapping And Graphic Information Capability (MAGIC). Volume 4: Geographic mapping CSCI
[AD-A235275] N91-26794
UNIX (tm) in high energy physics: What we can learn from the initial experiences at Fermilab
[DE91-011976] N91-26914
COMPUTER INFORMATION SECURITY
Requirements for developing Embedded Real-Time Trusted Computer System (ERT-TCSs)
[AD-A234325] N91-26762
Proceedings of the Second Annual NASA Science Internet User Working Group Conference
[NASA-CP-3117] N91-27009
NSIUWG: Science networking retreat N91-27010
NSI security task: Overview N91-27016
NSIUWG security sub-group N91-27026
COMPUTER NETWORKS
Research on intelligent fault detection and repair advisory systems
[AD-A235267] N91-26551

Providing a computing environment for a high energy physics workshop
[DE91-012049] N91-26916
Proceedings of the Second Annual NASA Science Internet User Working Group Conference
[NASA-CP-3117] N91-27009
NSIUWG: Science networking retreat N91-27010
NSI organization and highlights N91-27011
Customer requirements process N91-27012
NSI engineering review N91-27013
Backbone upgrades and DEC equipment replacement N91-27014
User support services and network application development: An overview N91-27015
NSI security task: Overview N91-27016
National research and education network N91-27017
NASA's use of FTS2000 services N91-27018
FTS2000 network architecture N91-27019
MultiNet TCP/P/IP for VAX/VMS update N91-27020
Science network resources: Distributed systems N91-27021
NASA/SPAN and DOE/ESnet-DECnet transition strategy for DECnet OSI/phase 5 N91-27025
NSIUWG security sub-group N91-27026
Requirements management: A CSR's perspective N91-27027
Overview of the NSI User Support Office (NSI USO) N91-27028
The NSINIC on-line system N91-27029
The Internet resources guide and the Automatic Login Executor (ALEX) N91-27030
NSI conference support N91-27031
A guide to NASA's Pilot Land Data System (PLDS) N91-27035
Software product description N91-27037
NSI operations center N91-27038
NSI customer service representatives and user support office: NASA Science Internet N91-27040
The NASA Science Internet: An integrated approach to networking N91-27041
NSI directed to continue SPAN's functions N91-27042

COMPUTER PROGRAM INTEGRITY
Application of software tools in embedded computers within military systems to enhance software reliability, quality assurance, and maintenance
[AD-A234555] N91-26785
Engineering for artificial intelligence software
[AD-A234793] N91-26814

COMPUTER PROGRAMMING
Autonomous aircraft initiative study
[NASA-CR-186013] N91-26140
Adsorption and decomposition of diethylsilane on silicon surfaces
[AD-A234639] N91-26267
US and foreign alloy cross-reference database
[NASA-CR-184166] N91-26313
The High Resolution Profiler (HRP): User's guide and software modifications documentation
[AD-A234640] N91-26663
Ada software portability and level 2 system simulator integration issues
[AD-A233757] N91-26773
Deductive programming synthesis
[AD-A233770] N91-26774
NRL connection machine Fortran library
[AD-A234121] N91-26779
Coordination in large scale software development
[AD-A234898] N91-26787
Software requirements specification for the Mapping And Graphic Information Capability (MAGIC). Volume 4: Geographic mapping CSCI
[AD-A235275] N91-26794
Applications of artificial intelligence to mission planning
[NASA-CR-187953] N91-26806
Mathematical topics in the modelling and identification of multicomponent continua
[AD-A234471] N91-26843
Proceedings of the Optoelectronic Workshop 25: Liquid Crystal Materials and Devices for Opto-Electronic Applications
[AD-A233780] N91-26921
Heuristics for a flow-shop model with parallel machines and setup times
[ITN-91-85117] N91-26996

COMPUTER PROGRAMS
Development of an integrated aeroservoelastic analysis program and correlation with test data
[NASA-TP-3120] N91-26113
Omega system Performance Assessment and Coverage Evaluation (PACE) workstation design and implementation, volume 1
[AD-A235225] N91-26128
How low can an unmanned air vehicle fly?
[RAND-P-7680-RGS] N91-26138
Propulsion stability codes for liquid propellant propulsion systems developed for use on a PC computer
[NASA-CR-184983] N91-26201
Composite database interface users manual
[AD-A235327] N91-26230
Numerical simulations of the indentation of glass with implications to ductile grinding
[DE91-011512] N91-26381
Modification of the user friendly thermodynamic code to include the effects of minor species
[AD-A233929] N91-26390
VLF nighttime data analysis
[AD-A234006] N91-26417
Input impedance and gain of monopole elements with disk ground planes on flat earth
[AD-A234284] N91-26421
De-embedding millimeter-wave integrated circuits with TRL
[AD-A234194] N91-26442
An electron-beam dose deposition experiment: TIGER 1-D simulation code versus thermoluminescent dosimetry
[AD-A234507] N91-26447
Dynamics of face and annular seals with two-phase flow
[NASA-CR-4256] N91-26479
Benchmark study between FIDAP and a cellular automata code
[DE91-011224] N91-26486
Implementation of the flow-modulated skew-upwind difference scheme in the COMMIX-1C code: A first assessment
[DE91-011168] N91-26489
AQUIS: An air quality and permit information management system
[DE91-011750] N91-26608
Improved Point Analysis Model (IPAM) (users guide)
[AD-A235305] N91-26649
OSIRRUS: Oceanic symbolic image representation, recognition and understanding software
[AD-A235112] N91-26665
Content addressable memory project
[AD-A234524] N91-26763
A parallel rendering algorithm for MIMD architectures
[NASA-CR-187571] N91-26767
NUMVEC FORTRAN library manual. Chapter: Partial differential equations. Routine: ICGG3D
[CWI-NM-R9018] N91-26768
An approach for constructing reusable software components in Ada
[AD-A233662] N91-26770
Deductive programming synthesis
[AD-A233770] N91-26774
BaRT manual version 3.0
[AD-A234528] N91-26784
Application of software tools in embedded computers within military systems to enhance software reliability, quality assurance, and maintenance
[AD-A234555] N91-26785
Program improvement by automatic redistribution of intermediate results
[AD-A235086] N91-26791
Nonlinear stochastic optimization solution procedures and incomplete information
[AD-A235242] N91-26793
Software requirements specification for the Mapping And Graphic Information Capability (MAGIC). Volume 4: Geographic mapping CSCI
[AD-A235275] N91-26794
Quantitative analysis procedures for Task 8
[DE91-009684] N91-26798
The process group approach to reliable distributed computing
[NASA-CR-188498] N91-26804
Applications of artificial intelligence to mission planning
[NASA-CR-187953] N91-26806
NFEARS: A nonlinear adaptive finite element solver. Part 2: User's manual
[AD-A234416] N91-26842
Theoretical studies of potential energy surfaces and computational methods
[DE91-011126] N91-26902
Multi-dimensional computer simulation of MHD combustor hydrodynamics
[DE91-011851] N91-26946
On-line magnetic tape Library Inventory Tracking And Reporting (LITAR) system
[AD-A234934] N91-27004
Electronic software submittal/distribution N91-27033
COSMIC: Software catalog 1991 edition diskette format N91-27036
NSI directed to continue SPAN's functions N91-27042
CBSD version 2 component models of the IR celestial background
[AD-A235372] N91-27048
Reexamination of METMAN, recommendations on enhancement of LCVG, and development of new concepts for EMU heat sink N91-27098
Development of load-dependent Ritz vector method for structural dynamic analysis of large space structures N91-27111
Assessment of the pharmacodynamics of intranasal, intravenous and oral scopolamine N91-27114

COMPUTER STORAGE DEVICES
Quantitative analysis procedures for Task 8
[DE91-009684] N91-26798
Strategies for reliable and real time execution on a heterogeneous multiprocessor
[AD-A234114] N91-26801

COMPUTER SYSTEMS DESIGN
Architectures for a high performance distributed operating system
[AD-A235333] N91-26429
Large scale computing in the Energy Research Programs
[DE91-012128] N91-26805
Measurement expert system effectiveness
[AD-A234359] N91-26807
Evaluation of expert systems: A review of the literature
[AD-A234360] N91-26808

COMPUTER SYSTEMS PERFORMANCE
Architectures for a high performance distributed operating system
[AD-A235333] N91-26429
Quantitative analysis procedures for Task 8
[DE91-009684] N91-26798
Measurement expert system effectiveness
[AD-A234359] N91-26807
Evaluation of expert systems: A review of the literature
[AD-A234360] N91-26808
Using modular neural networks with local representations to control dynamic systems
[AD-A234700] N91-26813
NFEARS: A nonlinear adaptive finite element solver. Part 2: User's manual
[AD-A234416] N91-26842
Heuristics for a flow-shop model with parallel machines and setup times
[ITN-91-85117] N91-26996
Proceedings of the First Workshop on 3-D Optical Memories
[AD-A234732] N91-27003

COMPUTER SYSTEMS PROGRAMS
Autonomous aircraft initiative study
[NASA-CR-186013] N91-26140
UNIX (tm) in high energy physics: What we can learn from the initial experiences at Fermilab
[DE91-011976] N91-26914
A system for UNIX command retrieval using a multilayered neural network
[DE91-012105] N91-27045

COMPUTER TECHNIQUES
High performance transparency design
[AD-A234456] N91-26133
Opportunities for advanced speech processing in military computer-based systems
[AD-A233724] N91-26412
Advanced material handling equipment controls
[AD-A235091] N91-26540
Applications of artificial intelligence to mission planning
[NASA-CR-187953] N91-26806

COMPUTER VISION
Using genetic algorithms to select and create features for pattern classification
[AD-A235165] N91-26792
Northeast Artificial Intelligence Consortium (NAIC). Volume 13: Image understanding and intelligent parallel systems
[AD-A234897] N91-26832
Design of optimal correlation filters for hybrid vision systems N91-27110

COMPUTERIZED SIMULATION
Viscous flow simulations of internal store carriage and separation
[NASA-CR-185343] N91-26123
Engine cycle analysis for a particle bed reactor nuclear rocket
[AD-A235258] N91-26199
Space platform power system hardware testbed
[NASA-CR-185839] N91-26204
Computer modeling of soot formation comparing free radical and ionic mechanisms
[AD-A235007] N91-26273

Epitaxy of metal atoms on metal surfaces: Deposition and diffusion
[DE91-011142] N91-26309
Numerical simulations of the indentation of glass with implications to ductile grinding
[DE91-011512] N91-26381
Spread spectrum communications emulator design
[AD-A235403] N91-26430
An electron-beam dose deposition experiment: TIGER 1-D simulation code versus thermoluminescent dosimetry
[AD-A234507] N91-26447
Improved algorithms for transient and steady-state fluid-structure interaction
[AD-A235172] N91-26476
Benchmark study between FIDAP and a cellular automata code
[DE91-011224] N91-26486
The development of an improved convective initiation scheme for Mesoscale numerical weather prediction models, phase 1
[AD-A235417] N91-26650
Aircrew Evaluation Sustained Operations Performance (AESOP): A triservice facility for technology transition
[AD-A234626] N91-26738
Task analysis and workload prediction for the MH-47E mission and a comparison with CH-47D workload predictions. Volume 2: Appendixes A through N
[AD-A235249] N91-26757
Ada software portability and level 2 system simulator integration issues
[AD-A233757] N91-26773
Northeast Artificial Intelligence Consortium (NAIC). Volume 5: Distributed planning for dynamic environments in the presence of time constraints
[AD-A234884] N91-26819
Complex envelope properties, interpretation, filtering, and evaluation
[AD-A234478] N91-26844
Comparison of sound pressure in a wedge-shaped ocean as predicted by an image method and a PE model
[AD-A234191] N91-26879
Planar indirect-drive Rayleigh-Taylor experiments on Nova
[DE91-011967] N91-26943
MHD contractors' review meeting
[DE91-011295] N91-26945
Multi-dimensional computer simulation of MHD combustor hydrodynamics
[DE91-011851] N91-26946
A temperature dependent SPICE macro-model for power MOSFETs
[DE91-011737] N91-26972
Incorporation of shuttle CCT parameters in computer simulation models N91-27096
A nonrecursive order N preconditioned conjugate gradient: Range space formulation of MDOF dynamics N91-27099
Applications of formal simulation languages in the control and monitoring subsystems of Space Station Freedom N91-27100
Planetary spacecraft cost modeling utilizing labor estimating relationships N91-27116

COMPUTERS
Visual sensitivities and discriminations and their role in aviation
[AD-A234866] N91-26740
Computational complexity and efficiency in electro-optical computing system
[AD-A235013] N91-26765
NASA information sciences and human factors program
[NASA-TM-4291] N91-27119

CONCENTRATION (COMPOSITION)
Improvement in the capacity and safety of lithium/inorganic electrolyte sulfur dioxide rechargeable cells, phase 2
[AD-A235303] N91-26589

CONCENTRATORS
The effects of space debris on solar propulsion
[AD-A235257] N91-26192

CONCRETES
International State-of-the-Art Colloquium on Low-Temperature Asphalt Pavement Cracking
[AD-A233663] N91-26402
A basic guide to overlay design using nondestructive testing equipment data
[AD-A234472] N91-26403

CONCURRENT PROCESSING
Using mappings to prove timing properties
[AD-A234404] N91-26780
Northeast Artificial Intelligence Consortium (NAIC). Volume 10: Time oriented problem solving
[AD-A234889] N91-26824

CONDUCTING POLYMERS
Synthetic metals: A novel role for organic polymers
[AD-A233862] N91-26334
Structure, order and the metallic state in polyaniline and its derivatives
[AD-A233935] N91-26336
Impedance profiling: A convenient technique for determining the redox or protonic acid doping characteristics of conducting polymers
[AD-A233941] N91-26337
Electronic and ionic transport in processable conducting polymers
[AD-A234597] N91-26352

CONDUCTIVITY
Electronic and ionic transport in processable conducting polymers
[AD-A234597] N91-26352

CONFERENCES
Gordon Research Conference on Composites
[AD-A233778] N91-26210
Minutes of the 24th Explosives Safety Seminar, volume 1
[AD-A235005] N91-26395
Minutes of the 24th Explosives Safety Seminar, volume 2
[AD-A235006] N91-26396
The Effect of the Ionosphere on Radiowave Signals and Systems Performance Based on Ionospheric Effects Symposium
[AD-A233797] N91-26416
Proceedings of the Optoelectronic Workshop 27: Semiconductor Lasers and Their Applications
[AD-A233779] N91-26496
NATO advanced research workshop on Measurement of Residual and Applied Stress Using Neutron Diffraction
[AD-A235103] N91-26566
Introduction to Session 2: Applied biological research
[DE91-012067] N91-26680
Proceedings of the 7th User's Stress Workshop
[AD-A234583] N91-26736
Gauge bosons and heavy quarks: Proceedings of Summer Institute on Particle Physics
[DE91-011248] N91-26907
MHD contractors' review meeting
[DE91-011295] N91-26945
Symposium E: Properties of 2-6 semiconductors. Bulk crystals, epitaxial films, quantum well structures
[AD-A234835] N91-26957
Proceedings of the Object-Oriented Database Task Group Workshop
[PB91-157198] N91-27000
Proceedings of the Second Annual NASA Science Internet User Working Group Conference
[NASA-CP-3117] N91-27009
NSI conference support N91-27031

CONFIDENCE LIMITS
Weighted least squares estimation for Aalen's additive risk model
[AD-A235250] N91-26852

CONGRESSIONAL REPORTS
Aerospace plane technology: Research and development efforts in Europe. Report to the Chairman, Committee on Science, Space, and Technology, House of Representatives
[GAO/NSIAD-91-194] N91-26141
Weather satellites: Action needed to resolve status of the US Geostationary Satellite Program. Report to the Chairman, Committee on Science, Space, and Technology, House of Representatives
[GAO/NSIAD-91-252] N91-26194
Air Force stock fund: Hydrazine sales consistent with the Commercial Space Launch Act. Report to the Chairman, Committee on Science, Space and Technology, House of Representatives
[GAO/NSIAD-91-196] N91-26397

CONICAL NOZZLES
Pressure distribution and induced force field on a conical nozzle due to impingement of a normal jet into the supersonic cross-flow
[AD-A233981] N91-26115

CONJUGATE GRADIENT METHOD
Application of a conjugate gradient method to the synthesis of phase-only planar arrays
[AD-A233756] N91-26415
A nonrecursive order N preconditioned conjugate gradient: Range space formulation of MDOF dynamics N91-27099

CONSISTENCY
The P300 component of the auditory event-related potential: Interlaboratory consistency and test-retest reliability
[AD-A235114] N91-26725

CONSOLES
Training effectiveness of an intelligent tutoring system for a propulsion console trainer N91-27097

CONSOLIDATION
Effect of surface forces on the rheology of particle-liquid systems and the consolidation of ceramic powders
[AD-A234375] N91-26221

CONSTRAINTS
Flexural plate wave devices for chemical analysis
[AD-A234129] N91-26254

CONSTRUCTION
Analysis of knowledge-based expert systems as tools for construction design
[AD-A234473] N91-26404
Design and construction of apparatus for optical switch evaluation
[AD-A234765] N91-26927

CONSTRUCTION MATERIALS
Guidelines for design, construction, and evaluation of airport pavement drainage
[DOT/FAA/RD-90/31] N91-26161
Hypervelocity launch capabilities to over 10.4 km/s
[DE91-010859] N91-26186
Structural concept studies for a horizontal cylindrical lunar habitat and a lunar guyed tower N91-27117

CONSUMERS
The impact of atmospheric damage to materials on consumers: News you can use
[DE91-012075] N91-26610

CONTACT LOADS
Sitting posture analysis. An experimental optimisation approach
[ITN-91-85114] N91-26760

CONTACT RESISTANCE
Ohmic contacts to semiconducting diamond
[AD-A234130] N91-26950

CONTAMINANTS
Preliminary testing, evaluation and sensitivity analysis for the Terrestrial Ecosystem Exposure Assessment Model (TEEAM)
[PB91-161711] N91-26602
Airliner cabin environment: Contaminant measurements, health risks, and mitigation options
[PB91-159384] N91-26746
Regeneration of whetlerite for adsorbing toxic pollutants from air
[AD-D014859] N91-26753

CONTINENTAL SHELVES
Comparison of sound pressure in a wedge-shaped ocean as predicted by an image method and a PE model
[AD-A234191] N91-26879

CONTINUOUS WAVE LASERS
Quasi-CW excimer laser, phase 2
[AD-A234771] N91-26509
Scaling CW electron beam pumped rare gas lasers to ultra-high average power
[AD-A235120] N91-26513

CONTINUUM FLOW
Thermoelastic wave propagation in laminated composites N91-26209

CONTINUUM MECHANICS
General relativistic continuum mechanics and the post-Newtonian equations of motion N91-26987

CONTINUUMS
A model for wet filament winding of composite cylinders with arbitrary thickness
[AD-A234102] N91-26215
Mathematical topics in the modelling and identification of multicomponent continua
[AD-A234471] N91-26843

CONTOURS
Comparison of sound pressure in a wedge-shaped ocean as predicted by an image method and a PE model
[AD-A234191] N91-26879

CONTRACT MANAGEMENT
Quality effectiveness sensing technique release 3.0
[AD-A233651] N91-26545

CONTRAST
Young and older observers show similar perceived contrast functions for isoluminant stimuli
[AD-A233766] N91-26709
Visual sensitivities and discriminations and their role in aviation
[AD-A234866] N91-26740
The effects of character size, modulation, polarity, and font on reading and search performance in matrix-addressable displays
[AD-A235033] N91-27007

CONTROL EQUIPMENT
Interfacial force sensor with force-feedback control
[DE91-004897] N91-26495

CONTROL STABILITY
Propulsion stability codes for liquid propellant propulsion systems developed for use on a PC computer
[NASA-CR-184983] N91-26201
Dynamic stability of flexible robot manipulators
[AD-A234297] N91-26533

CONTROL SURFACES
Navier-Stokes calculations of scramjet-nozzle-afterbody flowfields
[NASA-CR-185356] N91-26488
CONTROL SYSTEMS DESIGN
Control of an axisymmetric turbulent jet by multi-modal excitation
[NASA-TM-104483] N91-26121
Application of transformational ideas to automatic flight control design
[AD-A234758] N91-26148
Flight control law synthesis using neural network theory
[AD-A234990] N91-26149
Development and testing of a source subsystem for the supporting development PMAD DC test bed
[NASA-TM-104510] N91-26202
Space platform power system hardware testbed
[NASA-CR-185839] N91-26204
Geometry, dynamics and control of coupled systems N91-26401
Functional baseline specification for ATC data link service implementation in the host computer system
[DOT/FAA/CT-91/12] N91-26433
Control circuitry using electronic emulation of a synchro signal for accurate control of position and rate of rotation for shafts
[NASA-CASE-MFS-28458-1] N91-26459
Advanced material handling equipment controls
[AD-A235091] N91-26540
Structured representation for requirements and specifications
[NASA-CR-187522] N91-26797
Using modular neural networks with local representations to control dynamic systems
[AD-A234700] N91-26813
H-infinity-optimal control for distributed parameter systems
[AD-A234931] N91-26833
MultiNet TCP/P/IP for VAX/VMS update N91-27020
Software product description N91-27037
Applications of formal simulation languages in the control and monitoring subsystems of Space Station Freedom N91-27100
A design for an intelligent monitor and controller for space station electrical power using parallel distributed problem solving N91-27105
Fuzzy logic control system to provide autonomous collision avoidance for Mars rover vehicle N91-27106
NASA information sciences and human factors program
[NASA-TM-4291] N91-27119
CONTROL THEORY
Application of transformational ideas to automatic flight control design
[AD-A234758] N91-26148
Stabilization and control problems in structural dynamics
[AD-A235189] N91-26567
CONTROLLABILITY
ROBOT: A journal of Chinese Society of Automation
[AD-A234808] N91-26538
CONTROLLED FUSION
Design and fabrication of forced-flow coils as an R/D program for large helical device
[NIFS-81] N91-26937
Comparison of dimensionally similar discharges with similar heat deposition discharges
[DE91-011740] N91-26938
Statistical properties of intrinsic topological noise in tokamaks
[DE91-011741] N91-26939
CONTROLLERS
Method of injecting fluid propellants into a rocket combustion chamber
[NASA-CASE-LEW-14846-2] N91-26200
Catalysts and initiators as instruments controlling structure of polymers with inorganic backbone
[AD-A235350] N91-26368
CONVECTION
The development of an improved convective initiation scheme for Mesoscale numerical weather prediction models, phase 1
[AD-A235417] N91-26650
Crystal growth in a microgravity environment
[NASA-CASE-MFS-28473-1] N91-26968
CONVECTIVE FLOW
An experimental investigation of structure, mixing, and combustion in compressible turbulent shear layers
[AD-A235278] N91-26281
CONVECTIVE HEAT TRANSFER
Liquid film cooling in rocket engines
[AD-A234288] N91-26197
Transpiration cooled ultraviolet sol-gel silica optics
[AD-A235426] N91-26934
CONVERGENCE
A theoretical and experimental study of the symmetric rank one update
[AD-A233965] N91-26777
Converting a converging algorithm into a polynomially bounded algorithm
[AD-A234961] N91-26788
CONVERGENT-DIVERGENT NOZZLES
Optical studies of the flow start-up processes in four convergent-divergent nozzles
[AD-A234552] N91-26473
CONVOLUTION INTEGRALS
Gust design procedures N91-26155
Spectral recovery of discontinuous data
[ITN-91-85115] N91-26853
COOLANTS
Liquid cooled supersonic total temperature probe
[NASA-CASE-LAR-14435-1-CU] N91-26159
COOLING
Effectiveness of ice-vest cooling in prolonging work tolerance time during heavy exercise in the heat for personnel wearing Canadian forces chemical defence ensembles
[AD-A235273] N91-26758
Transpiration cooled ultraviolet sol-gel silica optics
[AD-A235426] N91-26934
Crystal growth in a microgravity environment
[NASA-CASE-MFS-28473-1] N91-26968
COOLING SYSTEMS
Absorption heat pump in heating and cooling systems of buildings
[DE91-752988] N91-26593
Effect of a passive cooling vest on tension/anxiety and fatigue in a high heat and high humidity naval environment
[AD-A234657] N91-26755
COORDINATION
Coordination in large scale software development
[AD-A234898] N91-26787
COPOLYMERIZATION
Polymeric routes to silicon carbide and silicon oxycarbide CMC
[NASA-TM-104372] N91-26234
Synthesis of energetic single phase and multi-phase polymers
[AD-A235104] N91-26363
COPOLYMERS
Polymeric routes to silicon carbide and silicon oxycarbide CMC
[NASA-TM-104372] N91-26234
Processable polymers and copolymers of 3-alkylthiophenes and their blends
[AD-A234596] N91-26351
Electronic and ionic transport in processable conducting polymers
[AD-A234597] N91-26352
Polysilanes, synthesis, modification, and properties
[AD-A235351] N91-26369
Synthesis and characterization of polysilanes
[AD-A235357] N91-26370
COPPER
Mechanical behavior of nanocrystalline Cu, Pd, and Ag samples
[DE91-011747] N91-26310
LIF and emission studies of copper and nitrogen N91-27089
COPPER ALLOYS
Grain boundary chemistry in Al-Cu metallizations as determined by analytical electron microscopy
[DE91-012007] N91-26319
Metastable pitting corrosion of aluminum, Al-Cu, and Al-Si thin films in dilute HF solutions and its relevancy to the processing of integrated circuit interconnections
[DE91-012014] N91-26320
COPPER OXIDES
Diagnostic studies of YBa2Cu3O(7-delta) laser ablation
[DE91-011382] N91-26515
Electrochemically modulated superconductivity
[AD-A234703] N91-26955
Formation of intermediate compounds during reduced pressure calcination of Y-Ba-Cu-O precursor
[DE91-011179] N91-26971
Defects in decomposed YBa2Cu4O8 (124) superconductor after rapid annealing
[DE91-010597] N91-26979
CORE SAMPLING
Ice cores and SeaRISE: What we do (and don't) know N91-26579
CORONAL LOOPS
The 1980 solar maximum mission event listing
[NASA-TM-4287] N91-27087
CORRELATION
Spectral and correlation analysis with applications to middle-atmosphere radars N91-26619
Correlation in photodetachment
[DE91-011369] N91-26908
CORRELATORS
Synchronous demodulator
[NASA-CASE-GSC-13179-1] N91-26438
CORROSION
The impact of atmospheric damage to materials on consumers: News you can use
[DE91-012075] N91-26610
CORROSION PREVENTION
The corrosion protection of 2219-T87 aluminum by anodizing
[NASA-TM-103540] N91-26312
Effect of bacterial biofilms on carbon steel pit propagation in phosphate containing medium
[DE91-010806] N91-26316
The impact of atmospheric damage to materials on consumers: News you can use
[DE91-012075] N91-26610
COSMIC RAYS
Preliminary estimates of core-collapse supernova rates from the Berkeley automated supernova search
[DE91-011824] N91-27050
Solar-geophysical data number 556, December 1990. Part 1: (Prompt reports). Data for November, October 1990, and late data
[PB91-152140] N91-27083
Solar geophysical data number 551, July 1990. Part 1: (Prompt reports). Data for June, May 1990 and late data
[PB91-160713] N91-27085
COSMONAUTS
Limited current capabilities for cosmonaut rescue N91-26179
Hormonal regulators of calcium metabolism following space flights of various durations N91-26689
Computer tomography measurement of vertebral bones and muscles after extended manned space flights N91-26690
Visual accommodation in cosmonauts N91-26697
Vestibular reactions and intersensory interactions in weightlessness: Results of Optokinez experiment N91-26698
State and forms of adaptation of vestibular function after space flights N91-26706
COST ANALYSIS
Absorption heat pump in heating and cooling systems of buildings
[DE91-752988] N91-26593
Planetary spacecraft cost modeling utilizing labor estimating relationships N91-27116
COST ESTIMATES
VHSIC electronics and the cost of Air Force avionics in the 1990s
[RAND-R-3843-AF] N91-26143
HYLIFE-2 inertial confinement: Fusion power plant design
[DE91-012089] N91-26947
COSTS
Commercial use of space: Many grantees making progress, but NASA oversight could be improved. Report to the Chair, Subcommittee on VA, HUD, and Independent Agencies, Committee on Appropriations, U.S. Senate
[GAO/NSIAD-91-142] N91-26400
Queueing systems with orbiting customers
[ITN-91-85112] N91-26868
COULOMB COLLISIONS
Correlation in photodetachment
[DE91-011369] N91-26908
COUNTERMEASURES
Vertical incidence backscatter and surface forward scattering from near-surface bubbles
[AD-A234432] N91-26880
COUPLED MODES
Geometry, dynamics and control of coupled systems N91-26401
Planar indirect-drive Rayleigh-Taylor experiments on Nova
[DE91-011967] N91-26943
COUPLING
An anisotropic laminated damped plate theory
[AD-A234446] N91-26222
CRACK GEOMETRY
Preliminary test results from the HSST shallow-crack fracture toughness program
[DE91-010147] N91-26572
CRACK PROPAGATION
Cyclic deformation, damage, and effects of environment in the Ni3Al ordered alloy at elevated temperature
[AD-A235168] N91-26304
TEM in-situ straining of B2 compounds
[DE91-012062] N91-26322
Fatigue crack tip plastic strain range measurement studies in two titanium alloys
[AD-A234973] N91-26565

CRACK TIPS
Transformation toughening of ceramics
[AD-A234926] N91-26359
Investigations into fracture mechanics failure concepts with thermomechanically rolled steels
[BLL-OA-TRANS-4238-(6196.3)] N91-26556
Fatigue crack tip plastic strain range measurement studies in two titanium alloys
[AD-A234973] N91-26565
CRACKING (FRACTURING)
International State-of-the-Art Colloquium on Low-Temperature Asphalt Pavement Cracking
[AD-A233663] N91-26402
CRACKS
Dynamic fracture responses of Al2O3, Si3N4, and SiC(w)/Al2O3
[AD-A235286] N91-26229
Methods for determining crack depth
[AD-A234799] N91-26562
CRASHES
KC-135 ground collision avoidance system questionnaire
[AD-A234385] N91-26125
CREEP ANALYSIS
Residual stresses in metal/ceramic brazes: Effect of creep on finite element analysis results
[DE91-011233] N91-26570
CREEP PROPERTIES
Fundamentals of mechanical behavior in intermetallic compounds
[AD-A235016] N91-26301
Performance of a 22Cr-20Ni-18Co-Fe alloy for service to 870 C
[DE91-011366] N91-26317
CREEP TESTS
Performance of a 22Cr-20Ni-18Co-Fe alloy for service to 870 C
[DE91-011366] N91-26317
CREWS
Review of primary medical results of year-long flight on Mir station N91-26178
CRITICAL TEMPERATURE
Development of high Tc (greater than 110K) Bi, Tl and Y-based materials as superconducting circuit elements
[NASA-CR-188581] N91-26948
CROSS CORRELATION
One-dimensional translation measurement of speckle from rough rotating objects in ultraviolet illumination
[AD-A233719] N91-26919
CROSS FLOW
Pressure distribution and induced force field on a conical nozzle due to impingement of a normal jet into the supersonic cross-flow
[AD-A233981] N91-26115
CROSSLINKING
Cross-linking and modification of cytochrome c with redox-active metal complexes
[DE91-012023] N91-26287
Carboxyalkylated hemoglobin as a potential blood substitute
[AD-A233822] N91-26712
CRUSTAL FRACTURES
A multichannel seismic investigation of variations in crustal structure in the western North Atlantic
[AD-A235245] N91-26634
CRYOGENIC TEMPERATURE
Experiments with trapped atoms
[AD-A234580] N91-26895
Electrochemically modulated superconductivity
[AD-A234703] N91-26955
CRYOGENICS
The cryogenic mechanical properties of Vintage 3 Al-Li-Zr alloy 2090-T81
[DE91-011897] N91-26311
High energy density systems in cryogenic media: The production and reaction of atoms and radicals
[AD-A233785] N91-26892
CRYSTAL DEFECTS
Defect clustering and related properties of oxides
[DE91-011072] N91-26290
Fundamentals of mechanical behavior in intermetallic compounds
[AD-A235016] N91-26301
TEM in-situ straining of B2 compounds
[DE91-012062] N91-26322
Plasticity of single crystalline Al3X intermetallic compounds
[AD-A234699] N91-26356
Ab initio molecular dynamics simulations of surfaces and interfaces
[AD-A235315] N91-26901
Transmission electron microscopy of the CVD diamond film/substrate interface
[AD-A234790] N91-26956
Defects in decomposed YBa2Cu4O8 (124) superconductor after rapid annealing
[DE91-010597] N91-26979
CRYSTAL DISLOCATIONS
The examination of dislocations in ice
[AD-A233716] N91-26586
CRYSTAL GROWTH
New laser materials for laser diode pumping
[NASA-CR-187786] N91-26521
Growth, evaporation and melting of ice crystals: Implications for radiation, atmospheric dynamics and particle scavenging N91-26611
Transmission electron microscopy of the CVD diamond film/substrate interface
[AD-A234790] N91-26956
An induction time approach to surface induced crystallization in polyethylene/poly (e-caprolactone) melt
[AD-A235102] N91-26964
Process for the controlled growth of single-crystal films of silicon carbide polytypes on silicon carbide wafers
[NASA-CASE-LEW-15222-1] N91-26966
Crystal growth in a microgravity environment
[NASA-CASE-MFS-28473-1] N91-26968
Crystallization of thin films of amorphous germanium alloys
[ITN-91-85110] N91-26969
Study of the effect of reactive element addition by implanting metal ions in a pre-formed oxide layer
[DE91-011916] N91-26974
Effect of boron addition on recrystallization and grain growth in Ni3Al polycrystals
[DE91-011966] N91-26983
CRYSTAL OPTICS
The First Nonlinear Optics: Materials, Phenomena, and Devices Conference
[AD-A234733] N91-26926
CRYSTAL OSCILLATORS
Tactical quartz oscillator development
[AD-A234308] N91-26443
CRYSTAL STRUCTURE
Far- and mid-infrared properties of metal-insulator composite materials
[AD-A234264] N91-26219
Energetics, bonding mechanism and electronic structure of metal/ceramic interfaces
[DE91-009787] N91-26239
Defect clustering and related properties of oxides
[DE91-011072] N91-26290
Quantum mechanical approach to understanding microstructural and mechanical properties of intermetallics
[AD-A234702] N91-26298
Environmental embrittlement of ordered intermetallic alloys at room temperature in moist atmospheres
[DE91-012051] N91-26321
Microstructure and hardness of NiAl/Ni2AlX two-phase ordered intermetallic alloys
[DE91-012068] N91-26323
X ray structure of polyanilines
[AD-A233848] N91-26332
Structure, order and the metallic state in polyaniline and its derivatives
[AD-A233935] N91-26338
Novel concepts in electronic polymers: Polyaniline and its derivatives
[AD-A234214] N91-26339
Scanning tunnelling microscope for boron surface studies
[AD-A234716] N91-26452
The examination of dislocations in ice
[AD-A233716] N91-26586
Electronic excitation transport in photosynthesis and crystal and molecular structures of porphyrin compounds
[DE91-012024] N91-26679
Transmission electron microscopy of the CVD diamond film/substrate interface
[AD-A234790] N91-26956
HREM study of heteroepitaxial interfaces in the TiO2/Al2O3 system
[DE91-012473] N91-26986
CRYSTALLINITY
Microstructure, porosity, and mechanical property relationships of calcium-silicate-hydrate
[AD-A235191] N91-26279
Novel liquid crystalline polymers as nonlinear optical materials
[AD-A235371] N91-26373
CRYSTALLITES
International collaboration program on innovative chemical processing of superior electronic and optical materials
[AD-A235030] N91-26276
CRYSTALLIZATION
International collaboration program on innovative chemical processing of superior electronic and optical materials
[AD-A235030] N91-26276
An induction time approach to surface induced crystallization in polyethylene/poly (e-caprolactone) melt
[AD-A235102] N91-26964
Crystallization of thin films of amorphous germanium alloys
[ITN-91-85110] N91-26969
CRYSTALS
Polyaniline: Oriented films and fibers
[AD-A234414] N91-26347
Acceleration insensitive resonators
[AD-A235400] N91-26458
Laser spectroscopy characterization of materials for frequency agile solid state laser systems
[AD-A233916] N91-26500
Method and apparatus for second-rank tensor generation
[NASA-CASE-NPO-17512-1-CU] N91-26918
Ohmic contacts to semiconducting diamond
[AD-A234130] N91-26950
Symposium E: Properties of 2-6 semiconductors. Bulk crystals, epitaxial films, quantum well structures
[AD-A234835] N91-26957
Polaron ground state in a double heterostructure of polar crystals
[AD-A235037] N91-26963
High temperature superconducting films and crystals
[AD-A235234] N91-26965
Crystal growth in a microgravity environment
[NASA-CASE-MFS-28473-1] N91-26968
CULTURE TECHNIQUES
Mathematical modeling of the flow field and particle motion in a rotating bioreactor at unit gravity and microgravity N91-27092
A study of murine bone marrow cells cultured in bioreactors which create an environment which simulated microgravity N91-27101
CUMULUS CLOUDS
The development of an improved convective initiation scheme for Mesoscale numerical weather prediction models, phase 1
[AD-A235417] N91-26650
CURRENT DENSITY
Performance of hypervelocity armatures with replenished metal vapor plasmas
[DE91-011931] N91-26187
Current distribution modeling for novel alumina electrolysis
[DE91-010060] N91-26315
Critical currents in proton irradiated YBa2Cu3O(7-delta) crystals
[DE91-011835] N91-26982
CURRENT DISTRIBUTION
Current distribution modeling for novel alumina electrolysis
[DE91-010060] N91-26315
CURVATURE
Covering a closed curve with a given total curvature
[AD-A234342] N91-26840
CURVES (GEOMETRY)
Covering a closed curve with a given total curvature
[AD-A234342] N91-26840
CUTTING
Abrasive-waterjet machining of isogrid structures
[AD-A234628] N91-26405
CYANO COMPOUNDS
Strong exchange coupling in lanthanide bis(phthalocyaninato) sandwich compounds
[AD-A234466] N91-26951
CYCLIC COMPOUNDS
Regio- and stereochemical control in substitution reactions of cyclophosphazenes
[AD-A234376] N91-26257
Synthesis and structure of small-molecule cyclic phosphazenes bearing ortho-substituted aryloxy and phenoxy substituents
[AD-A234377] N91-26344
CYCLIC HYDROCARBONS
Fundamental studies of carbenes and hydrocarbon radicals
[DE91-011029] N91-26286
CYCLIC LOADS
Static and cyclic compressive fatigue of thermoplastic-matrix composite in ambient and moisture environments
[AD-A234187] N91-26217
Cyclic deformation, damage, and effects of environment in the Ni3Al ordered alloy at elevated temperature
[AD-A235168] N91-26304
Fatigue crack tip plastic strain range measurement studies in two titanium alloys
[AD-A234973] N91-26565

CYCLONES
Hurricane Research Division fiscal year 1990 programs-fiscal year 1991 projections
[PB91-153452] N91-26641
CYCLOTRON RESONANCE DEVICES
Depressed collector experiments on a quasioptical gyrotron
[AD-A234559] N91-26492
CYLINDRICAL BODIES
Structural concept studies for a horizontal cylindrical lunar habitat and a lunar guyed tower N91-27117
CYLINDRICAL SHELLS
Comparisons of backscattering from cylindrical shells described by thin shell and elasticity theories
[AD-A234745] N91-26475
Acoustic radiation from fluid-loaded, ribbed cylindrical shells excited by different types of concentrated mechanical drives
[AD-A235324] N91-26887
CYTOCHROMES
Cross-linking and modification of cytochrome c with redox-active metal complexes
[DE91-012023] N91-26287
Photochemical energy conversion by membrane-bound photoredox systems
[DE91-012171] N91-26682

D

DAMAGE
Static and cyclic compressive fatigue of thermoplastic-matrix composite in ambient and moisture environments
[AD-A234187] N91-26217
India-stabilized zirconia coating for composites
[AD-D014857] N91-26224
Damage accumulation in advanced metal matrix composites under thermal cycling
[AD-A235002] N91-26227
Determination of SBS induced damage limits in large fused silica optics for intense, time varying laser pulses
[DE91-012080] N91-26518
The impact of atmospheric damage to materials on consumers: News you can use
[DE91-012075] N91-26610
Electrostatic fields in a dusty Martian environment N91-27078
DAMAGE ASSESSMENT
The 1990 Sandia rocket-triggered lightning field tests at Kennedy Space Center, Florida
[DE91-011263] N91-26653
HYLIFE-2 inertial confinement: Fusion power plant design
[DE91-012089] N91-26947
DAMPING
Fluid damping of the oscillations of satellites with a large magnetic moment N91-26170
An anisotropic laminated damped plate theory
[AD-A234446] N91-26222
Rotordynamic and leakage characteristics of a 4-stage brush seal
[AD-A235336] N91-26541
DARKNESS
The effects of character size, modulation, polarity, and font on reading and search performance in matrix-addressable displays
[AD-A235033] N91-27007
DATA ACQUISITION
US and foreign alloy cross-reference database
[NASA-CR-184166] N91-26313
Data acquisition and processing N91-26618
Atmospheric optical turbulence measurements taken at Anderson Mesa, Flagstaff, Arizona between 10-19 July 1990
[AD-A234190] N91-26629
Integrating UNIX workstation into existing online data acquisition systems for Fermilab experiments
[DE91-011974] N91-27044
DATA BASE MANAGEMENT SYSTEMS
AQUIS: An air quality and permit information management system
[DE91-011750] N91-26608
NASA/SPAN and DOE/ESnet-DECnet transition strategy for DECnet OSI/phase 5 N91-27025
DATA BASES
Omega/VLF signal coverage database development
[AD-A235226] N91-26129
Acquisition of statistical gust load data by commercial airplanes N91-26152
Advanced Satellite Research Project: SCAR Research Database. Bibliographic analysis
[NASA-CR-186086] N91-26182
Composite database interface users manual
[AD-A235327] N91-26230
US and foreign alloy cross-reference database
[NASA-CR-184166] N91-26313
VLF nighttime data analysis
[AD-A234006] N91-26417
The Navy standard compressed aeronautical chart database
[AD-A235340] N91-26587
Improved Point Analysis Model (IPAM) (users guide)
[AD-A235305] N91-26649
Symbolic expressions of composite grid structures
[AD-A233794] N91-26836
Proceedings of the Object-Oriented Database Task Group Workshop
[PB91-157198] N91-27000
On-line magnetic tape Library Inventory Tracking And Reporting (LITAR) system
[AD-A234934] N91-27004
COSMIC: Software catalog 1991 edition diskette format N91-27036
NSI operations center N91-27038
NSI customer service representatives and user support office: NASA Science Internet N91-27040
Catalog of data bases and reports
[DE91-011516] N91-27043
The chemistry and mineralogy of Mars soil and dust N91-27058
DATA COMPRESSION
The Navy standard compressed aeronautical chart database
[AD-A235340] N91-26587
Iterated transform image compression
[AD-A233655] N91-26769
Gabor transforms and neural networks for automatic target recognition
[DE91-011919] N91-26834
CRUSH: The NSI data compression utility N91-27032
DATA LINKS
Functional baseline specification for ATC data link service implementation in the host computer system
[DOT/FAA/CT-91/12] N91-26433
DATA MANAGEMENT
NASA/SPAN and DOE/ESnet-DECnet transition strategy for DECnet OSI/phase 5 N91-27025
Overview of the NSI User Support Office (NSI USO) N91-27028
The NSINIC on-line system N91-27029
DATA PROCESSING
VLF nighttime data analysis
[AD-A234006] N91-26417
Data acquisition and processing N91-26618
The chemistry and mineralogy of Mars soil and dust N91-27058
DATA PROCESSING EQUIPMENT
Uncertainty handling at speech/natural language interface, volume 1
[AD-A234310] N91-26422
DATA REDUCTION
Measurement of atmospheric turbulence N91-26151
Improved reduction of gust loads data for gust intensity N91-26153
Quantitative analysis procedures for Task 8
[DE91-009684] N91-26798
The chemistry and mineralogy of Mars soil and dust N91-27058
DATA SYSTEMS
Software requirements specification for the Mapping And Graphic Information Capability (MAGIC). Volume 4: Geographic mapping CSCI
[AD-A235275] N91-26794
Customer requirements process N91-27012
NASA's use of FTS2000 services N91-27018
Science network resources: Distributed systems N91-27021
Overview of the NASA astrophysics data system N91-27022
Using HST: From proposal to science N91-27023
NSI conference support N91-27031
NASA information sciences and human factors program
[NASA-TM-4291] N91-27119
DATA TRANSMISSION
IRIG standard format for Global Positioning System (GPS) data for post-operation interrange exchange
[AD-A234932] N91-26127
Chinese space science and technology (selected articles)
[AD-A234798] N91-26180
HORACE: Presentation-level protocol standard for digital transmission of monochrome television images
[AD-A235276] N91-26428
Digital signal conditioning for flight test, volume 19
[AGARD-AG-160-VOL-19] N91-26432
Backbone upgrades and DEC equipment replacement N91-27014
User support services and network application development: An overview N91-27015
FTS2000 network architecture N91-27019
Science network resources: Distributed systems N91-27021
NASA/SPAN and DOE/ESnet-DECnet transition strategy for DECnet OSI/phase 5 N91-27025
A guide to NASA's Pilot Land Data System (PLDS) N91-27035
DE BROGLIE WAVELENGTHS
Neutral atom deBroglie-wave interferometry
[AD-A234624] N91-26896
DEACTIVATION
High energy density systems in cryogenic media: The production and reaction of atoms and radicals
[AD-A233785] N91-26892
DECAMETRIC WAVES
A catalog of high resolution Jovian decametric radio noise burst spectra, volume 1 N91-27047
DECAY
Weak interactions and presupernova evolution
[DE91-011543] N91-27052
DECISION MAKING
Individual stereotypes of human neuropsychic prognostic activity in problem situations with different probability structures N91-26695
Aircrew Evaluation Sustained Operations Performance (AESOP): A triservice facility for technology transition
[AD-A234626] N91-26738
Nonlinear stochastic optimization solution procedures and incomplete information
[AD-A235242] N91-26793
A comparative study of the practical characteristics of neural network and conventional pattern classifiers
[AD-A235345] N91-26795
DECISION THEORY
Fixed sample and sequential problems with applications in reliability
[AD-A234547] N91-26547
DECOMPOSITION
Laser ionic multiphoton dissociation of some acrylate clusters
[AD-A233801] N91-26247
Adsorption and decomposition of acetylene on Si(100)-(2x1)
[AD-A233808] N91-26248
FTIR studies of water and ammonia decomposition on silicon surfaces
[AD-A234637] N91-26265
Diethylsilane decomposition on silicon surfaces studied using transmission FTIR spectroscopy
[AD-A234638] N91-26266
Adsorption and decomposition of diethylsilane on silicon surfaces
[AD-A234639] N91-26267
Chemical synthesis study of deuterated epoxy resins
[AD-A234666] N91-26355
An implementation of the singular value decomposition on the connection machine CM-2
[AD-A234124] N91-26802
Defects in decomposed YBa2Cu4O8 (124) superconductor after rapid annealing
[DE91-010597] N91-26979
DECONTAMINATION
Water solubility of bis(2-ethylhexyl) hydrogen phosphite
[AD-A234561] N91-26259
DECOUPLING
Improved inline fiber optic sensor arrays
[AD-D014864] N91-26924
DEFECTS
Light induced electron spin resonance in polyaniline
[AD-A233847] N91-26331
Digital logic testing and testability
[AD-A234123] N91-26441
DEFENSE PROGRAM
Northeast Artificial Intelligence Consortium (NAIC). Volume 1: Executive summary
[AD-A234880] N91-26815
DEFORMATION
Spatial rotations of a satellite in a circular three-body problem for the case of general resonance N91-26164
Modelling the dynamics of fluxes of electrons with energies 30-300 keV in geostationary orbit N91-26173
Development of a test system and experimental method for in-plane biaxial compressive deformation and failure of fiber composite materials
[AD-A234062] N91-26214
Static and cyclic compressive fatigue of thermoplastic-matrix composite in ambient and moisture environments
[AD-A234187] N91-26217
Nonlinear behavior of fiber composite materials and its effect on the postbuckling response of laminated plates
[AD-A234203] N91-26218

Characterization of mechanical damage mechanisms in ceramic composite materials
[NR-032-553] N91-26235
Advanced processing and properties of high performance alloys
[AD-A234746] N91-26299
Strain enhanced microstructural evolution
[DE91-011921] N91-26318
Dynamic energy absorption of sandwich structures by inelastic deformation
[AD-A234903] N91-26564
Combined effect of noise and vibration on cells of auditory and vestibular apparatus N91-26707

DEGRADATION
Static and cyclic compressive fatigue of thermoplastic-matrix composite in ambient and moisture environments
[AD-A234187] N91-26217
Surface mediated photocatalysis
[AD-A233748] N91-26246
Characterization studies of fluorinated epoxy resins: Naval experimental resin C8/1SA as a structural material and for use in blends and composites
[AD-A234188] N91-26338

DEHYDRATION
COLDEX-86: Fluid and electrolyte changes during prolonged cold water immersion
[AD-A233768] N91-26711

DEHYDROGENATION
Electrocatalytic study of ammonia synthesis and methane dimerization in high temperature solid electrolyte cells
[DE91-009797] N91-26289
Living ring-opening metathesis polymerization of 7-oxa-2,3-difunctionalized norbornenes and norbornadienes by Mo(CHCMe2R) (N-2,6-C6H3-i-Pr2) (O-t-Bu)2 and Mo(CHCMe2R) (N-2,6-C6H3-i-Pr2) (OCMe2CF3)2
[AD-A235235] N91-26365

DELAMINATING
Nondestructive Evaluation (NDE) of fiberglass marine structures state-of-the art review
[AD-A234785] N91-26550
Effect of initial delamination on Mode 1 and Mode 2 interlaminar fracture toughness and fatigue fracture threshold
[NASA-TM-104079] N91-26569

DELTA WINGS
Methods to enhance the accuracy of finite volume schemes 2
[FFA-147] N91-26466

DEMODULATORS
Synchronous demodulator
[NASA-CASE-GSC-13179-1] N91-26438

DENSE PLASMAS
Parametric studies of dense plasma focus for fusion space propulsion with D-He3
[AD-A234578] N91-26941

DENSITY DISTRIBUTION
The distribution of the size and number of shadows cast on a line segment in a Poisson random field
[AD-A233697] N91-26857

DENSITY MEASUREMENT
Determination of the masses and densities of meteoroids from radar observations from one point N91-26177

DEOXYRIBONUCLEIC ACID
Imaging of fluorescent and chemiluminescent DNA hybrids using a 2-D CCD camera
[AD-A234641] N91-26676
Interaction of ionizing radiation, genetically active chemicals, and radiofrequency radiation in human and rodent cells
[AD-A234747] N91-26677

DEPOSITION
Cluster beam deposition of high temperature materials
[AD-A234358] N91-26343
The impact of atmospheric damage to materials on consumers: News you can use
[DE91-012075] N91-26610

DEPOSITS
Ohmic contacts to semiconducting diamond
[AD-A234130] N91-26950

DEPTH MEASUREMENT
Methods for determining crack depth
[AD-A234799] N91-26562

DERIVATION
High order differentiation filters that work
[AD-A234504] N91-26874

DESICCANTS
Liquid water production from atmospheric sources
[AD-A235090] N91-26406

DESIGN ANALYSIS
Performance optimization of helicopter rotor blades
[NASA-TM-104054] N91-26137
Technology needs for high-speed rotorcraft, volume 1
[NASA-CR-177585] N91-26139
Certification procedures and requirements N91-26154
Matching of PSD-design loads N91-26157
Trends in certification procedures and design analysis N91-26158
Analysis of knowledge-based expert systems as tools for construction design
[AD-A234473] N91-26404
Quality by design using statistically planned experiments
[ITN-91-85119] N91-26553
A reliability and mass perspective of SP-100 Stirling cycle lunar-base powerplant designs
[NASA-TM-103736] N91-26592
Visual and field-of-view evaluation of the M-43 protective mask with prescription eyepieces
[AD-A234592] N91-26754
Electronic design process
[AD-A234709] N91-26786
Program improvement by automatic redistribution of intermediate results
[AD-A235086] N91-26791
Binary optics technology: Theoretical limits on the diffraction efficiency of multilevel diffractive optical elements
[AD-A235404] N91-26933

DESORPTION
Comparison of hydrogen desorption kinetics from Si(111)7x7 and Si(100)2x1
[AD-A234633] N91-26262
Comparison of H2 desorption kinetics from Si(111)7x7 and Si(100)2x1
[AD-A234634] N91-26263
Desorption product yields following Cl2 adsorption on Si(111)7x7: Coverage and temperature dependence
[AD-A234635] N91-26264
Adsorption and decomposition of diethylsilane on silicon surfaces
[AD-A234639] N91-26267
Laser-induced desorption of H2 from Si(111)7x7
[AD-A234636] N91-26508

DESTRUCTION
Minutes of the 24th Explosives Safety Seminar, volume 1
[AD-A235005] N91-26395

DETECTION
Imaging of fluorescent and chemiluminescent DNA hybrids using a 2-D CCD camera
[AD-A234641] N91-26676
Pumping system fault detection and diagnosis utilizing pattern recognition and fuzzy inference techniques
[DE91-011849] N91-26863
Multiple-frequency SAW devices for chemical sensing and materials characterization
[DE91-010856] N91-26888
Preliminary estimates of core-collapse supernova rates from the Berkeley automated supernova search
[DE91-011824] N91-27050

DETERIORATION
India-stabilized zirconia coating for composites
[AD-D014857] N91-26224
Evaluation of environmentally aged polymer/composite material by ultrasonic inspection
[AD-A235343] N91-26231
Visual accommodation in cosmonauts N91-26697

DETONATION
Shock response of Detasheet
[DE91-010923] N91-26399

DEUTERIUM
The effects of deuterium on static posture control N91-27102

DEUTERIUM COMPOUNDS
Chemical synthesis study of deuterated epoxy resins
[AD-A234666] N91-26355

DEUTERIUM PLASMA
Parametric studies of dense plasma focus for fusion space propulsion with D-He3
[AD-A234578] N91-26941

DIAGNOSIS
Proceedings of the 7th User's Stress Workshop
[AD-A234583] N91-26736
Pumping system fault detection and diagnosis utilizing pattern recognition and fuzzy inference techniques
[DE91-011849] N91-26863

DIAMONDS
Binary optics technology: Theoretical limits on the diffraction efficiency of multilevel diffractive optical elements
[AD-A235404] N91-26933
Ohmic contacts to semiconducting diamond
[AD-A234130] N91-26950
Transmission electron microscopy of the CVD diamond film/substrate interface
[AD-A234790] N91-26956

DIASTOLE
Effect of 7 day antiorthostatic hypokinesia on cardiac pumping action in monkeys N91-26704

DIATOMIC GASES
A combined XPS-ISS modulated molecular beam investigation of the reactions of oxygen and fluorine with silicon surfaces
[AD-A234867] N91-26269

DIATOMIC MOLECULES
Study of the low-lying electronic states of Si2 and Si2(-) using negative ion photodetachment techniques
[AD-A234336] N91-26256

DIELECTRICS
Investigation of polybenzocyclobutene resins in multilayer thin films for electronic packaging
[AD-A235223] N91-26228
Radiation, scattering, and guidance of electromagnetic fields by arbitrarily shaped structures embedded in layered dielectric media
[AD-A234434] N91-26423
A model for the scattering of high-frequency electromagnetic fields from dielectrics exhibiting thermally-activated electrical losses
[NASA-TM-104376] N91-26872

DIESEL ENGINES
Ceramic technology for advanced heat engines project
[DE91-010451] N91-26384

DIETS
COLDEX-86: Summary of the experimental protocol and general results
[AD-A234031] N91-26715
Level of dietary fat does not affect fuel oxidation or endurance exercise performance of soldiers
[AD-A235194] N91-26728

DIFFERENCE EQUATIONS
A model for wet filament winding of composite cylinders with arbitrary thickness
[AD-A234102] N91-26215
Implementation of the flow-modulated skew-upwind difference scheme in the COMMIX-1C code: A first assessment
[DE91-011168] N91-26489

DIFFERENTIAL AMPLIFIERS
Synchronous demodulator
[NASA-CASE-GSC-13179-1] N91-26438

DIFFERENTIAL EQUATIONS
Continuous stochastic cellular automata that have a stationary distribution and no detailed balance
[AD-A234421] N91-26782
Computational methods and software for differential equations and their applications
[DE91-012172] N91-26855

DIFFRACTION
Neutral atom deBroglie-wave interferometry
[AD-A234624] N91-26896
Binary optics technology: Theoretical limits on the diffraction efficiency of multilevel diffractive optical elements
[AD-A235404] N91-26933

DIFFRACTION LIMITED CAMERAS
Temporal and spatial correlations in images distorted by a random medium
[ITN-91-85107] N91-26935

DIFFRACTION PATTERNS
Defect clustering and related properties of oxides
[DE91-011072] N91-26290

DIFFUSION
Epitaxy of metal atoms on metal surfaces: Deposition and diffusion
[DE91-011142] N91-26309
Structure, order and the metallic state in polyaniline and its derivatives
[AD-A233935] N91-26336
Energy migration, motion and order in synthetic polymers
[AD-A234403] N91-26346
Effect of turbulence on impurity observation in upper atmosphere using lidar method N91-26584
High energy density systems in cryogenic media: The production and reaction of atoms and radicals
[AD-A233785] N91-26892

DIFFUSION COEFFICIENT
Target parameter estimation N91-26620

DIFFUSION FLAMES
Turbulent premixed hydrogen/air flames
[AD-A235109] N91-26278

DIFFUSION WELDING
Abrasive-waterjet machining of isogrid structures
[AD-A234628] N91-26405

DIFFUSIVITY
Testing of a composite thermal structure to insulate the drivers of a large scale blast/thermal simulator
[AD-A234014] N91-26213

DIGITAL COMPUTERS
Design and construction of apparatus for optical switch evaluation
[AD-A234765] N91-26927
DIGITAL DATA
Chinese space science and technology (selected articles)
[AD-A234798] N91-26180
Photographic image enhancement N91-27094
DIGITAL ELECTRONICS
Control circuitry using electronic emulation of a synchro signal for accurate control of position and rate of rotation for shafts
[NASA-CASE-MFS-28458-1] N91-26459
DIGITAL FILTERS
High order differentiation filters that work
[AD-A234504] N91-26874
DIGITAL SIMULATION
Propagation of RF signals through structured ionization: The general model
[AD-A234051] N91-26418
DIGITAL SYSTEMS
A look at digital nose wheel steering
[AD-A233944] N91-26131
Intelligibility of digital speech masked by noise: Normal hearing and hearing impaired listeners
[AD-A234852] N91-26427
Digital signal conditioning for flight test, volume 19
[AGARD-AG-160-VOL-19] N91-26432
Digital logic testing and testability
[AD-A234123] N91-26441
Forecasting digital microcircuit obsolescence
[AD-A234573] N91-26451
The role of EEPROM devices in upcoming ISDN applications
[AD-A234837] N91-26454
Backplane bus distributed realtime clock synchronization
[AD-A234476] N91-26491
Structured representation for requirements and specifications
[NASA-CR-187522] N91-26797
An implementation of the singular value decomposition on the connection machine CM-2
[AD-A234124] N91-26802
Full surface testing of grazing incidence mirrors
[AD-A234005] N91-26922
Research instrumentation for optical computing
[AD-A235335] N91-26932
DIGITAL TELEVISION
HORACE: Presentation-level protocol standard for digital transmission of monochrome television images
[AD-A235276] N91-26428
DIHEDRAL ANGLE
Ring-torsional polarons in polyaniline and polyparaphenylene sulfide
[AD-A234384] N91-26345
DIMENSIONAL STABILITY
Turbulent premixed hydrogen/air flames
[AD-A235109] N91-26278
DIMERIZATION
Electrocatalytic study of ammonia synthesis and methane dimerization in high temperature solid electrolyte cells
[DE91-009797] N91-26289
DIMERS
Adsorption and decomposition of acetylene on Si(100)-(2x1)
[AD-A233808] N91-26248
Comparison of hydrogen desorption kinetics from Si(111)7x7 and Si(100)2x1
[AD-A234633] N91-26262
DIODES
Development and testing of radiation and electromagnetic pulse hardened silicon carbide based electronics
[AD-A233744] N91-26439
DIPHENYL COMPOUNDS
Thermal degradation chemistry of poly(diphenoxy phosphazene)
[AD-A235284] N91-26282
DIPOLE ANTENNAS
Radiation, scattering, and guidance of electromagnetic fields by arbitrarily shaped structures embedded in layered dielectric media
[AD-A234434] N91-26423
DIPOLE MOMENTS
An active particle accelerator
[DE91-011404] N91-26915
DIRECTORIES
Science network resources: Distributed systems
N91-27021
The NASA master directory quick reference guide
N91-27034
NSI white pages project: X.500 directory service
N91-27039
DISCONTINUITY
Spectral recovery of discontinuous data
[ITN-91-85115] N91-26853
DISCRETE FUNCTIONS
Gust design procedures N91-26155
Matching of PSD-design loads N91-26157
DISCRIMINATION
Boost-phase kill versus midcourse discrimination: The grand inquisitor's solution
[DE91-011744] N91-26871
DISINTEGRATION
Combined effect of noise and vibration on cells of auditory and vestibular apparatus N91-26707
DISPERSIONS
Description of the RIVM/KNMI puff dispersion model
[KNMI-177] N91-26638
DISPLACEMENT
An anisotropic laminated damped plate theory
[AD-A234446] N91-26222
DISPLACEMENT MEASUREMENT
Basic studies of microstructure of combusting turbulent flows
[AD-A234222] N91-26471
DISPLAY DEVICES
Format and basic geometry of a perspective display of air traffic for the cockpit
[NASA-TM-86680] N91-26142
HORACE: Presentation-level protocol standard for digital transmission of monochrome television images
[AD-A235276] N91-26428
The effects of display failures and symbol rotation on visual search and recognition performance
[AD-A235035] N91-26743
The effects of character size, modulation, polarity, and font on reading and search performance in matrix-addressable displays
[AD-A235033] N91-27007
The effect of rotation on legibility of dot-matrix characters
[AD-A235034] N91-27008
DISPOSAL
Minutes of the 24th Explosives Safety Seminar, volume 1
[AD-A235005] N91-26395
DISSIPATION
State space models for aeroelastic and viscoelastic systems
[AD-A234730] N91-26117
DISSOCIATION
The stepwise dissociation of NH3 on the Si(111)-(7x7) surface: Low temperature dissociative adsorption and thermal effects
[AD-A235009] N91-26274
The chemistry of sodium with sulfur in flames
[DE91-002060] N91-26288
DISTANCE
The effect of rotation on legibility of dot-matrix characters
[AD-A235034] N91-27008
DISTORTION
The effects of display failures and symbol rotation on visual search and recognition performance
[AD-A235035] N91-26743
The effect of rotation on legibility of dot-matrix characters
[AD-A235034] N91-27008
DISTRIBUTED PARAMETER SYSTEMS
Stabilization and control problems in structural dynamics
[AD-A235189] N91-26567
H-infinity-optimal control for distributed parameter systems
[AD-A234931] N91-26833
DISTRIBUTED PROCESSING
Architectures for a high performance distributed operating system
[AD-A235333] N91-26429
The process group approach to reliable distributed computing
[NASA-CR-188498] N91-26804
Northeast Artificial Intelligence Consortium (NAIC). Volume 4: Distributed artificial intelligence for communications network management
[AD-A234883] N91-26818
Northeast Artificial Intelligence Consortium (NAIC). Volume 5: Distributed planning for dynamic environments in the presence of time constraints
[AD-A234884] N91-26819
Northeast Artificial Intelligence Consortium (NAIC). Volume 18: A distributed artificial intelligence approach to information fusion and object classification
[AD-A234892] N91-26827
Integrating UNIX workstation into existing online data acquisition systems for Fermilab experiments
[DE91-011974] N91-27044
DISTRIBUTION (PROPERTY)
Sea test development of laser altimeter
[AD-A233824] N91-26498
DISTRIBUTION FUNCTIONS
Bidirectional reflectance distribution (BRDF) of NASA shuttle tiles
[AD-A235115] N91-26188
Queueing systems with orbiting customers
[ITN-91-85112] N91-26868
DIURNAL VARIATIONS
Martian dust threshold measurements: Simulations under heated surface conditions N91-27081
DIVING (UNDERWATER)
COLDEX-86: Physical work capacity during prolonged cold water immersion at 6.1 msw
[AD-A233767] N91-26710
COLDEX-86: Fluid and electrolyte changes during prolonged cold water immersion
[AD-A233768] N91-26711
COLDEX-86: Summary of the experimental protocol and general results
[AD-A234031] N91-26715
DMSP SATELLITES
Satellite data derived estimates of erosion parameters for reentry vehicles
[AD-A234792] N91-26189
DOCUMENTS
National Bureau of Standards Publications 1977-1987. Volume 2: Indexes
[PB91-136515] N91-26997
The Internet resources guide and the Automatic Login Executor (ALEX) N91-27030
DOGS
The Trendelenburg position after cerebral air embolism in dogs: Effects on the somatosensory evoked potential, intracranial pressure, and blood-brain barrier
[AD-A233809] N91-26673
DOPED CRYSTALS
Defect clustering and related properties of oxides
[DE91-011072] N91-26290
DOPPLER EFFECT
Optimal Walsh modulations in the presence of Doppler
[AD-A233723] N91-26411
DOPPLER RADAR
Spectral and correlation analysis with applications to middle-atmosphere radars N91-26619
DOSAGE
Pharmacological sparing of protein in burn injury
[AD-A235026] N91-26724
The effects of deuterium on static posture control
N91-27102
DRAINAGE
Guidelines for design, construction, and evaluation of airport pavement drainage
[DOT/FAA/RD-90/31] N91-26161
DROP SIZE
Rotating multicylinder method for the measurement of cloud liquid-water content and droplet size
[AD-A234780] N91-26644
On the evolution of raindrop spectra and their effect on the atmosphere below cloud base: Numerical models and comparisons with observations
[ITN-91-85113] N91-26652
DRYING
Nondestructive Evaluation (NDE) of fiberglass marine structures state-of-the art review
[AD-A234785] N91-26550
DUCTED FLOW
A study of high speed flows in an aircraft transition duct
[NASA-TM-104449] N91-26122
DUCTILITY
Microalloyed steel preforms
[AD-A234039] N91-26296
Quantum mechanical approach to understanding microstructural and mechanical properties of intermetallics
[AD-A234702] N91-26298
Advanced processing and properties of high performance alloys
[AD-A234746] N91-26299
Strain enhanced microstructural evolution
[DE91-011921] N91-26318
Numerical simulations of the indentation of glass with implications to ductile grinding
[DE91-011512] N91-26381
DUCTS
A study of high speed flows in an aircraft transition duct
[NASA-TM-104449] N91-26122
DUMMIES
Advanced Dynamic Anthropomorphic Manikin (ADAM) design report
[AD-A234761] N91-26756

DUPLEXERS
The instrumental principles of MST radars and incoherent scatter radars and the configuration of radar system hardware N91-26616
DUST
Characteristics of aerosol in the atmosphere of Mars according to data from the KRFM experiment N91-26175
Composite fiber hazards [AD-A233924] N91-26211
Sand and Dust on Mars [NASA-CP-10074] N91-27057
The chemistry and mineralogy of Mars soil and dust N91-27058
Recent studies of the optical properties of dust and cloud particles in the Mars atmosphere and the interannual frequency of global dust storms N91-27060
Effects of Martian dust on power system components N91-27061
Have graben wall scarps accumulated sand and dust on Mars? N91-27062
Chemistry and mineralogy of Martian dust: An explorer's primer N91-27063
Measurements of dust on Mars to be obtained from upcoming missions N91-27066
Engineering knowledge requirements for sand and dust on Mars N91-27067
Electrical system/environment interactions on the planet Mars N91-27068
Saltation threshold reduction due to the electrostatic agglomeration of fine particles N91-27071
The effects of atmospheric dust on observations of Martian surface albedo N91-27072
Electrostatic fields in a dusty Martian environment N91-27078
Impact of Mars sand on dust on the design of space suits and life support equipment: A technology assessment N91-27079
Sand and dust issues for the MESUR mission N91-27080
Martian dust threshold measurements: Simulations under heated surface conditions N91-27081
Dust in the Mars atmosphere N91-27082
DUST COLLECTORS
Impact of Mars sand on dust on the design of space suits and life support equipment: A technology assessment N91-27079
DUST STORMS
Sand and Dust on Mars [NASA-CP-10074] N91-27057
Recent studies of the optical properties of dust and cloud particles in the Mars atmosphere and the interannual frequency of global dust storms N91-27060
Effects of Martian dust on power system components N91-27061
Wind abrasion on Mars N91-27064
Sand and dust issues for the MESUR mission N91-27080
Dust in the Mars atmosphere N91-27082
DYE LASERS
High pulse-energy flashlamp-pumpable laser dyes [AD-A233837] N91-26499
Quasi-CW excimer laser, phase 2 [AD-A234771] N91-26509
Infrared and visible laser double resonance studies of vibrational energy transfer processes in polyatomic molecules [DE91-012162] N91-26910
DYES
High pulse-energy flashlamp-pumpable laser dyes [AD-A233837] N91-26499
DYNAMIC CHARACTERISTICS
Size dependence of gaseous cluster reactivity and evaporation dynamics as a mechanistic probe [AD-A233811] N91-26249
Phytoplankton abundance in relation to Lagrangian paths [AD-A233728] N91-26672
Molecular engineering dynamics of electron transport and nonlinear optical interaction in Langmuir-Blodgett films of organic semiconductor heterostructure [AD-A235001] N91-26897
DYNAMIC CONTROL
Studies in modeling, dynamics, and control of space structures [AD-A235059] N91-26190
Nonlinear dynamics and control of flexible structures [AD-A235186] N91-26191
Theoretical studies of the kinematics, dynamics, stability, and control of unsteady/vortical flows [AD-A235190] N91-26477
WPG-30 model microprocessor controlled rotating beryllium mirror scanning camera and its applications [AD-A234802] N91-26493
DYNAMIC LOADS
Response of whisker-reinforced ceramic matrix composites to dynamic compressive loading N91-26236
Advanced study in solid transport: Rheological behavior of dense suspension [DE91-009428] N91-26467
Load-bearing capacity of large pipes with circumferential defects under tensile stress: Comparison of experiments with calculated estimates [BLL-OA-TRANS-4233-(6196.3)] N91-26557
Dynamic energy absorption of sandwich structures by inelastic deformation [AD-A234903] N91-26564
DYNAMIC MODELS
Gust design procedures N91-26155
Analysis by the statistical discrete gust method N91-26156
Studies in modeling, dynamics, and control of space structures [AD-A235059] N91-26190
High accuracy optical rate sensor N91-27115
DYNAMIC PROGRAMMING
Viscosity methods in optimal control of distributed systems. The Bellman equation [AD-A234646] N91-26812
DYNAMIC RESPONSE
Development of an integrated aeroservoelastic analysis program and correlation with test data [NASA-TP-3120] N91-26112
Analysis by the statistical discrete gust method N91-26156
Studies in modeling, dynamics, and control of space structures [AD-A235059] N91-26190
Performance of a 22Cr-20Ni-18Co-Fe alloy for service to 870 C [DE91-011366] N91-26317
Long-term prediction test procedure for most ICs, based on linear response theory [NASA-CR-185843] N91-26462
Sloshing response in a tank containing two liquids [DE91-011844] N91-26487
Nonlinear oscillations of mechanical systems under multifrequency parametric excitation [AD-A233800] N91-26558
A statistical analysis of -X rhesus head kinematics [AD-A233977] N91-26674
Development of load-dependent Ritz vector method for structural dynamic analysis of large space structures N91-27111
DYNAMIC STABILITY
Dynamic stability of flexible robot manipulators [AD-A234297] N91-26533
DYNAMIC STRUCTURAL ANALYSIS
Development of an integrated aeroservoelastic analysis program and correlation with test data [NASA-TP-3120] N91-26113
Nonlinear dynamics and control of flexible structures [AD-A235186] N91-26191
An anisotropic laminated damped plate theory [AD-A234446] N91-26222
The hysteresis and incremental collapse of complex structures: A paradigm for the fatigue failure of materials [AD-A234831] N91-26563
Stabilization and control problems in structural dynamics [AD-A235189] N91-26567
Development of load-dependent Ritz vector method for structural dynamic analysis of large space structures N91-27111
Structural concept studies for a horizontal cylindrical lunar habitat and a lunar guyed tower N91-27117
DYNAMIC TESTS
Advanced study in solid transport: Rheological behavior of dense suspension [DE91-009428] N91-26467
Investigation of axial positioning for flexural compressors [NASA-CR-185711] N91-26544
DYNAMICAL SYSTEMS
Geometry, dynamics and control of coupled systems N91-26401
Chaotic and bifurcating nonlinear systems driven by noise with applications to laser dynamics [AD-A234841] N91-26512

E

EARTH ATMOSPHERE
Global climate change: A discussion of major uncertainties [DE91-011746] N91-26604
An assessment of CO2 greenhouse gas mitigation technologies [DE91-011972] N91-26605
Free-air carbon dioxide enrichment: A new approach to research on carbon exchange processes [DE91-012074] N91-26609
Radar principles N91-26615
Surface Observation Climatic Summaries (SOCS) for Kodiak, Alaska [AD-A235182] N91-26646
Inorganic carbon surveys of oceanic basins [DE91-011132] N91-26667
EARTH CRUST
Plate motion and deformation [DE91-010466] N91-26612
A multichannel seismic investigation of variations in crustal structure in the western North Atlantic [AD-A235245] N91-26634
EARTH IONOSPHERE
The Effect of the Ionosphere on Radiowave Signals and Systems Performance Based on Ionospheric Effects Symposium [AD-A233797] N91-26416
VLF nighttime data analysis [AD-A234006] N91-26417
Propagation of RF signals through structured ionization: The general model [AD-A234051] N91-26418
Incoherent scatter radar observations of the ionosphere N91-26623
Technique for measuring ionospheric irregularities generated by high power oblique HF heating of the F-region [AD-A233883] N91-26627
ARTIST tape output formats [AD-A235173] N91-26633
UV aurora mapping in corrected geomagnetic coordinates [ITN-91-85106] N91-26636
Theoretical and experimental studies relevant to interpretation of auroral emissions [NASA-CR-188491] N91-26637
EARTH MANTLE
Plate motion and deformation [DE91-010466] N91-26612
EARTH MOVEMENTS
Plate motion and deformation [DE91-010466] N91-26612
EARTH OBSERVING SYSTEM (EOS)
Atmospheric infraRed Sounder (AIRS): Science and measurement requirements [NASA-TM-104977] N91-26624
EARTH ORBITAL ENVIRONMENTS
Theoretical and experimental studies relevant to interpretation of auroral emissions [NASA-CR-188491] N91-26637
EARTH ORBITS
Evolution of some types of Earth satellite orbits N91-26163
EARTH SURFACE
Vehicle steering device [AD-D014861] N91-26537
EATING
Level of dietary fat does not affect fuel oxidation or endurance exercise performance of soldiers [AD-A235194] N91-26728
ECCENTRICITY
Evolution of some types of Earth satellite orbits N91-26163
ECHOES
Radar principles N91-26615
ECOLOGY
JPRS report: Science and technology. USSR: Earth sciences [JPRS-UES-91-002] N91-26581
Adaptation and resistance of ecosystems to stress [AD-A234576] N91-26603
Global climate change: A discussion of major uncertainties [DE91-011746] N91-26604
ECONOMY
Aerospace plane technology: Research and development efforts in Europe. Report to the Chairman, Committee on Science, Space, and Technology, House of Representatives [GAO/NSIAD-91-194] N91-26141
ECOSYSTEMS
Ecological exposure and effects of airborne toxic chemicals: An overview [PB91-148460] N91-26594
Acid rain in Asia [DE91-011160] N91-26595
Preliminary testing, evaluation and sensitivity analysis for the Terrestrial Ecosystem Exposure Assessment Model (TEEAM) [PB91-161711] N91-26602

Adaptation and resistance of ecosystems to stress [AD-A234576] N91-26603
Free-air carbon dioxide enrichment: A new approach to research on carbon exchange processes [DE91-012074] N91-26609
SEEP 2 zooplankton data report: Winter, spring and summer collections at mooring 3 during 1988 [DE91-012077] N91-26668
Investigating combustion as a method of processing inedible biomass produced in NASA's biomass production chamber [NASA-TM-103821] N91-26759

EDITING ROUTINES (COMPUTERS)
A system and language environment for scientific computing [AD-A233747] N91-26772

EDUCATION
National research and education network N91-27017
Training effectiveness of an intelligent tutoring system for a propulsion console trainer N91-27097

EFFICIENCY
Results of the aeronautical systems division critical process team on integrated product development [AD-A235419] N91-26995

EGRESS
Mechanics, impact loads and EMG on the space shuttle treadmill N91-27112

EIGENVALUES
A divide and conquer approach to the nonsymmetric eigenvalue problem [DE91-011085] N91-26854

EJECTION SEATS
Advanced Dynamic Anthropomorphic Manikin (ADAM) design report [AD-A234761] N91-26756

ELASTIC ANISOTROPY
An anisotropic laminated damped plate theory [AD-A234446] N91-26222

ELASTIC BENDING
Dynamics of elastic bending and torsion of hingeless rotors with dynamic stall [AD-A234775] N91-26134

ELASTIC BUCKLING
Buckling of laminated composite plates [ITN-91-85101] N91-26232

ELASTIC CYLINDERS
Comparisons of backscattering from cylindrical shells described by thin shell and elasticity theories [AD-A234745] N91-26475

ELASTIC DEFORMATION
Viscoelastic behavior of elastomeric membranes [AD-A234496] N91-26560

ELASTIC MEDIA
Progress in ultrasonic measurements research in 1990: Transient sources for acoustic emission work [AD-A234965] N91-26882
General relativistic continuum mechanics and the post-Newtonian equations of motion N91-26987

ELASTIC PLATES
An anisotropic laminated damped plate theory [AD-A234446] N91-26222
Dynamic energy absorption of sandwich structures by inelastic deformation [AD-A234903] N91-26564

ELASTIC PROPERTIES
The role of electronic structure in the mechanical behavior of aluminides [DE91-012508] N91-26325
The wavenumber-frequency filtering characteristics of compliant layers [AD-A234768] N91-26561

ELASTIC SCATTERING
Calculation of the conductance of two dimensional narrow wires [ITN-91-85109] N91-26460

ELASTOMERS
Double face sealing device [NASA-CASE-MFS-28521-1] N91-26542
Viscoelastic behavior of elastomeric membranes [AD-A234496] N91-26560

ELASTOPLASTICITY
Preliminary test results from the HSST shallow-crack fracture toughness program [DE91-010147] N91-26572

ELECTRIC BATTERIES
Development and testing of a source subsystem for the supporting development PMAD DC test bed [NASA-TM-104510] N91-26202
Space platform power system hardware testbed [NASA-CR-185839] N91-26204

ELECTRIC CHARGE
Quantum devices and structures [AD-A235298] N91-26989

ELECTRIC CONDUCTORS
Ionically and electronically conductive composite polymer membranes [AD-A234587] N91-26349
Solid-state proton conductors [DE91-002050] N91-26970

ELECTRIC CONNECTORS
Metastable pitting corrosion of aluminum, Al-Cu, and Al-Si thin films in dilute HF solutions and its relevancy to the processing of integrated circuit interconnections [DE91-012014] N91-26320
X ray tomographic inspection of printed wiring assemblies and electrical components [AD-A234748] N91-26548
Center for the Integration of Optical C [AD-A235277] N91-26931

ELECTRIC CONTACTS
Methods of obtaining an electrical contact [AD-A234800] N91-26453
Improvement in the capacity and safety of lithium/inorganic electrolyte sulfur dioxide rechargeable cells, phase 2 [AD-A235303] N91-26589

ELECTRIC CURRENT
Magnetic relaxation, flux pinning and, critical currents in superconductors [DE91-012022] N91-26984

ELECTRIC DIPOLES
An active particle accelerator [DE91-011404] N91-26915

ELECTRIC EQUIPMENT
X ray tomographic inspection of printed wiring assemblies and electrical components [AD-A234748] N91-26548

ELECTRIC FIELDS
Methods of obtaining an electrical contact [AD-A234800] N91-26453
Characterization of vertical electric fields and associated voltages induced on an overhead power line from close artificially initiated lightning [DE91-010781] N91-26656
A study of signal generation and charge collectionin a-Si:H diodes for radiation imaging [DE91-010243] N91-26904
Electrostatic fields in a dusty Martian environment N91-27078

ELECTRIC MOTOR VEHICLES
Proof-of-concept zinc/bromine electric vehicle battery [DE91-011767] N91-26463

ELECTRIC POTENTIAL
High-power converters for space applications [NASA-CR-187116] N91-26461
Characterization of vertical electric fields and associated voltages induced on an overhead power line from close artificially initiated lightning [DE91-010781] N91-26656
Solid-state proton conductors [DE91-002050] N91-26970
Effect of pressure on electrostatic processes on Mars N91-27069

ELECTRIC SPARKS
Electrostatic fields in a dusty Martian environment N91-27078

ELECTRIC WIRE
Follow-on cable coupling lightning test. Volume 2: Appendixes A, B, C, and D [NASA-CR-184124] N91-26195
Design and fabrication of forced-flow coils as an R/D program for large helical device [NIFS-81] N91-26937

ELECTRICAL ENGINEERING
Center for electronics and electrical engineering. Technical progress bulletin covering center programs, July to September 1990, with 1991 CEEE events calendar [PB91-159749] N91-26437

ELECTRICAL FAULTS
Electrical system/environment interactions on the planet Mars N91-27068
Effect of pressure on electrostatic processes on Mars N91-27069

ELECTRICAL IMPEDANCE
The wavenumber-frequency filtering characteristics of compliant layers [AD-A234768] N91-26561

ELECTRICAL MEASUREMENT
Ohmic contacts to semiconducting diamond [AD-A234130] N91-26950
Electrostatic fields in a dusty Martian environment N91-27078

ELECTRICAL PROPERTIES
Scaling CW electron beam pumped rare gas lasers to ultra-high average power [AD-A235120] N91-26513
Intracellular physiology of the rat suprachiasmatic nucleus: Electrical properties, neurotransmission, and effects of neuromodulators [AD-A234442] N91-26675
A model for the scattering of high-frequency electromagnetic fields from dielectrics exhibiting thermally-activated electrical losses [NASA-TM-104376] N91-26872
Superconducting high T(sub c) thin film vortex-flow transistor, phase 1 [AD-A235025] N91-26962
Electrical system/environment interactions on the planet Mars N91-27068
Magnetic and electrical properties of Martian particles N91-27074

ELECTRICAL RESISTANCE
Calculation of the conductance of two dimensional narrow wires [ITN-91-85109] N91-26460

ELECTRICAL RESISTIVITY
New developments in the synthesis and doping of polyacetylene and polyaniline [AD-A233702] N91-26244
Structure, order and the metallic state in polyaniline and its derivatives [AD-A233935] N91-26336
Impedance profiling: A convenient technique for determining the redox or protonic acid doping characteristics of conducting polymers [AD-A233941] N91-26337
Terrestrial geophysics in the SeaRISE project N91-26576

ELECTRO-OPTICS
Proceedings of the Optoelectronic Workshop 27: Semiconductor Lasers and Their Applications [AD-A233779] N91-26496
Computational complexity and efficiency in electro-optical computing system [AD-A235013] N91-26765
Proceedings of the Optoelectronic Workshop 25: Liquid Crystal Materials and Devices for Opto-Electronic Applications [AD-A233780] N91-26921
Solid state research [AD-A234836] N91-26958

ELECTROCHEMICAL CORROSION
Corrosion of graphite aluminum metal matrix composites [AD-A234322] N91-26220

ELECTROCHEMICAL OXIDATION
Molecular orientation of the silver tetra neopentoxy phthalo cyanine and stearic acid mixed Langmuir-Blodgett film and its chemical and electrochemical behaviour [AD-A234601] N91-26206
Interaction of cationic polypeptides with electroactive polypyrrole/poly(styrenesulfonate) and poly(N-methylpyrrole)/poly(styrenesulfonate) films [AD-A234469] N91-26258
Electronic and ionic transport in processable conducting polymers [AD-A234597] N91-26352
Electrochemically induced charge and mass transport in polypyrrole/poly(styrene sulfonate) molecular composites [AD-A234599] N91-26354

ELECTROCHEMISTRY
The control of orbital mixing in ruthenium complexes containing quinone related ligands [AD-A234602] N91-26260
Photochemical energy conversion by membrane-bound photoredox systems [DE91-012171] N91-26682
Electrochemically modulated superconductivity [AD-A234703] N91-26955

ELECTRODES
Corrosion of graphite aluminum metal matrix composites [AD-A234322] N91-26220
Proof-of-concept zinc/bromine electric vehicle battery [DE91-011767] N91-26463
Parametric studies of dense plasma focus for fusion space propulsion with D-He3 [AD-A234578] N91-26941
Solid-state proton conductors [DE91-002050] N91-26970

ELECTROJETS
Dynamics of equatorial and polar boundaries of penetration of solar protons with energy about 1 MeV into magnetosphere during strong magnetic storm N91-26172

ELECTROLYSIS
Current distribution modeling for novel alumina electrolysis [DE91-010060] N91-26315

ELECTROLYTES
Gel solidified microinterface between two immiscible electrolytes applied to amperometric detection of picrate and tetramethylammonium
[AD-A235260] N91-26280
COLDEX-86: Fluid and electrolyte changes during prolonged cold water immersion
[AD-A233768] N91-26711
Solid-state proton conductors
[DE91-002050] N91-26970
ELECTROLYTIC CELLS
Electrocatalytic study of ammonia synthesis and methane dimerization in high temperature solid electrolyte cells
[DE91-009797] N91-26289
Improvement in the capacity and safety of lithium/inorganic electrolyte sulfur dioxide rechargeable cells, phase 2
[AD-A235303] N91-26589
ELECTROMAGNETIC ACCELERATION
Electromagnetic launch technology assessment. Scientific basis and unified treatment: Forces and electromechanical power conversion (analytical and numerical methods)
[AD-A235028] N91-26185
ELECTROMAGNETIC COUPLING
Follow-on cable coupling lightning test. Volume 2: Appendixes A, B, C, and D
[NASA-CR-184124] N91-26195
ELECTROMAGNETIC FIELDS
Radiation, scattering, and guidance of electromagnetic fields by arbitrarily shaped structures embedded in layered dielectric media
[AD-A234434] N91-26423
A model for the scattering of high-frequency electromagnetic fields from dielectrics exhibiting thermally-activated electrical losses
[NASA-TM-104376] N91-26872
ELECTROMAGNETIC NOISE
Theory of radar target discrimination
[AD-A234172] N91-26420
Intelligibility of digital speech masked by noise: Normal hearing and hearing impaired listeners
[AD-A234852] N91-26427
A catalog of high resolution Jovian decametric radio noise burst spectra, volume 1 N91-27047
ELECTROMAGNETIC PROPERTIES
Far- and mid-infrared properties of metal-insulator composite materials
[AD-A234264] N91-26219
Backscattering enhancement from rough surfaces
[AD-A234707] N91-26426
High temperature superconducting planar circuit structures for high frequency applications
[AD-A234335] N91-26445
ELECTROMAGNETIC PROPULSION
Aerodynamics of a 0.60 caliber electromagnetic projectile
[AD-A234660] N91-26116
ELECTROMAGNETIC PULSES
Development and testing of radiation and electromagnetic pulse hardened silicon carbide based electronics
[AD-A233744] N91-26439
An electron-beam dose deposition experiment: TIGER 1-D simulation code versus thermoluminescent dosimetry
[AD-A234507] N91-26447
Comparison of the RF frequency spectra of HEMP and lightning
[AD-A234306] N91-26642
ELECTROMAGNETIC RADIATION
Electromagnetic launch technology assessment. Scientific basis and unified treatment: Forces and electromechanical power conversion (analytical and numerical methods)
[AD-A235028] N91-26185
Studies of optical beam phase-conjugation and electromagnetic scattering process
[AD-A234830] N91-26929
ELECTROMAGNETIC SCATTERING
Studies of optical beam phase-conjugation and electromagnetic scattering process
[AD-A234830] N91-26929
ELECTROMAGNETISM
Magnetic field generator
[AD-D014869] N91-26449
ELECTROMECHANICAL DEVICES
Electromagnetic launch technology assessment. Scientific basis and unified treatment: Forces and electromechanical power conversion (analytical and numerical methods)
[AD-A235028] N91-26185
ELECTROMYOGRAPHY
Mechanics, impact loads and EMG on the space shuttle treadmill N91-27112
ELECTRON ACCELERATION
Laser switched power linac
[AD-A234581] N91-26507
ELECTRON ACCELERATORS
Measurement of the nitrogen total cross section from 0.5 eV to 50 MeV and analysis of the 433-keV resonance
[DE91-012222] N91-26293
ELECTRON BEAMS
An electron-beam dose deposition experiment: TIGER 1-D simulation code versus thermoluminescent dosimetry
[AD-A234507] N91-26447
High power klystron amplifier
[AD-D014862] N91-26448
Depressed collector experiments on a quasioptical gyrotron
[AD-A234559] N91-26492
Scaling CW electron beam pumped rare gas lasers to ultra-high average power
[AD-A235120] N91-26513
Radio frequency and microwave plasma for optical thin film deposition
[DE91-012081] N91-26525
Chemistry on an atomic scale of ion-beam modified surfaces
[AD-A233707] N91-26891
A test of the IAEA code of practice for absorbed dose determination in photon and electron beams
[OEFZS-4565] N91-26913
Ohmic contacts to semiconducting diamond
[AD-A234130] N91-26950
ELECTRON CAPTURE
Weak interactions and presupernova evolution
[DE91-011543] N91-27052
ELECTRON DENSITY (CONCENTRATION)
Measurements of the longitudinal movements of O(+) ions in the subauroral upper atmosphere from the Aureol 3 satellite N91-26171
Propagation of RF signals through structured ionization: The general model
[AD-A234051] N91-26418
Incoherent scatter radar observations of the ionosphere N91-26623
The chemical modification of plasmas
[AD-A234448] N91-26940
ELECTRON DISTRIBUTION
Cationic polymerization within van der Waals clusters of the form (CH2=R)n where R=CH2, CF2 and CHCH3
[AD-A234233] N91-26255
ELECTRON ENERGY
Measurements of the longitudinal movements of O(+) ions in the subauroral upper atmosphere from the Aureol 3 satellite N91-26171
Incoherent scatter radar observations of the ionosphere N91-26623
ELECTRON GUNS
Depressed collector experiments on a quasioptical gyrotron
[AD-A234559] N91-26492
ELECTRON IMPACT
Electron-excited molecule interactions
[DE91-012227] N91-26911
ELECTRON MICROSCOPY
Grain boundary chemistry in Al-Cu metallizations as determined by analytical electron microscopy
[DE91-012007] N91-26319
TEM in-situ straining of B2 compounds
[DE91-012062] N91-26322
ELECTRON MOBILITY
Calculation of the conductance of two dimensional narrow wires
[ITN-91-85109] N91-26460
ELECTRON PARAMAGNETIC RESONANCE
The control of orbital mixing in ruthenium complexes containing quinone related ligands
[AD-A234602] N91-26260
Light induced electron spin resonance in polyaniline
[AD-A233847] N91-26331
ELECTRON PHONON INTERACTIONS
Polaron ground state in a double heterostructure of polar crystals
[AD-A235037] N91-26963
ELECTRON PLASMA
Development of a tactical high-power microwave source using the Plasma Electron Microwave Source (PEMS) concept
[AD-A234967] N91-26942
ELECTRON SCATTERING
Measurement of the nitrogen total cross section from 0.5 eV to 50 MeV and analysis of the 433-keV resonance
[DE91-012222] N91-26293
Electron-excited molecule interactions
[DE91-012227] N91-26911
ELECTRON STATES
Study of the low-lying electronic states of Si2 and Si2(-) using negative ion photodetachment techniques
[AD-A234336] N91-26256
Electronic excitation transport in photosynthesis and crystal and molecular structures of porphyrin compounds
[DE91-012024] N91-26679
Negative ion formation by Rydberg electron transfer: Isotope-dependent rate constants
[DE91-012058] N91-26909
ELECTRON TRANSFER
Cross-linking and modification of cytochrome c with redox-active metal complexes
[DE91-012023] N91-26287
Study of intermediates from transition metal excited-state electron-transfer reactions
[DE91-012182] N91-26324
Photochemical energy conversion by membrane-bound photoredox systems
[DE91-012171] N91-26682
Molecular engineering dynamics of electron transport and nonlinear optical interaction in Langmuir-Blodgett films of organic semiconductor heterostructure
[AD-A235001] N91-26897
Negative ion formation by Rydberg electron transfer: Isotope-dependent rate constants
[DE91-012058] N91-26909
ELECTRON TUNNELING
Quantum limited quasiparticle mixers at 100 GHz
[DE91-011894] N91-26973
Quantum devices and structures
[AD-A235298] N91-26989
ELECTRON-ION RECOMBINATION
Computer modeling of soot formation comparing free radical and ionic mechanisms
[AD-A235007] N91-26273
ELECTRONIC CONTROL
Plasma reflectors for electronic beam steering in radar systems
[AD-A234560] N91-26425
ELECTRONIC EQUIPMENT
Electrical system/environment interactions on the planet Mars N91-27068
ELECTRONIC MAIL
A guide to NASA's Pilot Land Data System (PLDS) N91-27035
ELECTRONIC PACKAGING
Investigation of polybenzocyclobutene resins in multilayer thin films for electronic packaging
[AD-A235223] N91-26228
ELECTRONIC TRANSDUCERS
Block patterning of the metallization of polyvinylidene fluoride transducers
[AD-D014872] N91-26450
X ray tomographic inspection of printed wiring assemblies and electrical components
[AD-A234748] N91-26548
ELECTRONS
Modelling the dynamics of fluxes of electrons with energies 30-300 keV in geostationary orbit N91-26173
Electron localization in polyaniline and its derivatives
[AD-A233934] N91-26335
Correlation in photodetachment
[DE91-011369] N91-26908
ELECTROPHYSIOLOGY
Intracellular physiology of the rat suprachiasmatic nucleus: Electrical properties, neurotransmission, and effects of neuromodulators
[AD-A234442] N91-26675
ELECTROSTATIC CHARGE
Saltation threshold detection in a wind tunnel by the measurement of the net electrostatic charge N91-27070
Electrostatic fields in a dusty Martian environment N91-27078
ELECTROSTATICS
Interaction of cationic polypeptides with electroactive polypyrrole/poly(styrenesulfonate) and poly(N-methylpyrrole)/poly(styrenesulfonate) films
[AD-A234469] N91-26258
Sand and Dust on Mars
[NASA-CP-10074] N91-27057
Effect of pressure on electrostatic processes on Mars N91-27069
Saltation threshold reduction due to the electrostatic agglomeration of fine particles N91-27071
Electrostatic fields in a dusty Martian environment N91-27078
ELEMENTARY EXCITATIONS
Quantum limited quasiparticle mixers at 100 GHz
[DE91-011894] N91-26973
Quantum limited quasiparticle mixers at 100 GHz
[DE91-011826] N91-26991

ELEMENTARY PARTICLES
Studies of interactions between elementary particles and nuclei
[DE91-012300] N91-26912
ELLIPSOIDS
Spatial rotations of a satellite in a circular three-body problem for the case of general resonance N91-26164
EMBEDDED COMPUTER SYSTEMS
Requirements for developing Embedded Real-Time Trusted Computer System (ERT-TCSs)
[AD-A234325] N91-26762
Application of software tools in embedded computers within military systems to enhance software reliability, quality assurance, and maintenance
[AD-A234555] N91-26785
EMBEDDING
Radiation, scattering, and guidance of electromagnetic fields by arbitrarily shaped structures embedded in layered dielectric media
[AD-A234434] N91-26423
EMBRITTLEMENT
Environmental embrittlement of ordered intermetallic alloys at room temperature in moist atmospheres
[DE91-012051] N91-26321
EMERGENCIES
Limited current capabilities for cosmonaut rescue N91-26179
Utilization of emergency medical kits by air carriers
[AD-A234784] N91-26721
Proceedings of the 7th User's Stress Workshop
[AD-A234583] N91-26736
EMISSION SPECTRA
Diagnostic studies of YBa2Cu3O(7-delta) laser ablation
[DE91-011382] N91-26515
Theoretical and experimental studies relevant to interpretation of auroral emissions
[NASA-CR-188491] N91-26637
Dust in the Mars atmosphere N91-27082
LIF and emission studies of copper and nitrogen N91-27089
EMITTANCE
X ray spot motion during 220 ps laser pulses
[DE91-012111] N91-26519
EMOTIONAL FACTORS
Physical and psychogenic sequelae of impact acceleration on tracking performance of operators N91-26701
ENCOUNTERS
Galileo: The Earth encounter N91-27024
END EFFECTORS
Constrained trajectory optimization for kinematically redundant arms
[NASA-CR-183477] N91-26527
Adaptive control of direct drive dexterous robotic hand with bilateral tactile sensing
[AD-A233980] N91-26532
ROBOT: A journal of Chinese Society of Automation
[AD-A234808] N91-26538
Passive and active grasping with a prehensile robot end-effector
[AD-A235085] N91-26539
ENDOCRINOLOGY
Effect of shift work of air traffic controllers on sympathetic nervous system N91-26700
ENDOTOXINS
Molecular studies of cytokine induction
[AD-A235326] N91-26731
ENERGY ABSORPTION
Dynamic energy absorption of sandwich structures by inelastic deformation
[AD-A234903] N91-26564
ENERGY CONSERVATION
Commercializing solar hydrogen production
[DE91-011232] N91-26398
ENERGY CONVERSION
Photochemical energy conversion by membrane-bound photoredox systems
[DE91-012171] N91-26682
Development of a tactical high-power microwave source using the Plasma Electron Microwave Source (PEMS) concept
[AD-A234967] N91-26942
ENERGY CONVERSION EFFICIENCY
Photovoltaics: From the laboratory to the marketplace
[DE91-002151] N91-26588
Research on stable, high-efficiency amorphous silicon multijunction modules
[DE91-002159] N91-26591
ENERGY DISSIPATION
The stepwise dissociation of NH3 on the Si(111)-(7x7) surface: Low temperature dissociative adsorption and thermal effects
[AD-A235009] N91-26274
The relationship of traditional damping measures for materials with high damping capacity
[AD-A235347] N91-26568
ENERGY GAPS (SOLID STATE)
Photoexcitation spectroscopy of pernigraniline
[AD-A233841] N91-26250
Ring-torsional polarons in polyaniline and polyparaphenylene sulfide
[AD-A234384] N91-26345
ENERGY LEVELS
Energy levels and branching ratios of Tm(3)+ in ten garnet laser materials
[AD-A235274] N91-26514
ENERGY METHODS
Theoretical studies of potential energy surfaces and computational methods
[DE91-011126] N91-26902
ENERGY OF FORMATION
Efficient photoinduced charge separation and storage in the solid state, rates, energetics, and spin-polarization
[DE91-010727] N91-26980
ENERGY POLICY
Acid rain in Asia
[DE91-011160] N91-26595
ENERGY STORAGE
Development of a tactical high-power microwave source using the Plasma Electron Microwave Source (PEMS) concept
[AD-A234967] N91-26942
ENERGY TECHNOLOGY
Large scale computing in the Energy Research Programs
[DE91-012128] N91-26805
ENERGY TRANSFER
Testing of a composite thermal structure to insulate the drivers of a large scale blast/thermal simulator
[AD-A234014] N91-26213
The chemistry of sodium with sulfur in flames
[DE91-002060] N91-26288
In the energy active region of the ocean N91-26583
Electronic excitation transport in photosynthesis and crystal and molecular structures of porphyrin compounds
[DE91-012024] N91-26679
Fluorescence spectroscopy of excitation transfer in Photosystem 1
[DE91-011867] N91-26681
ENGINE COOLANTS
Engine cycle analysis for a particle bed reactor nuclear rocket
[AD-A235258] N91-26199
ENGINE PARTS
Development of life prediction capabilities for liquid propellant rocket engines. Post-fire diagnostic system for the SSME system architecture study
[NASA-CR-187112] N91-26205
Ceramic technology for advanced heat engines project
[DE91-010451] N91-26384
ENGINE TESTS
Arcjet endurance test program
[AD-A235232] N91-26198
Technical Evaluation Motor No. 7 (TEM-7)
[NASA-CR-184163] N91-26203
ENVIRONMENT EFFECTS
Absorption heat pump in heating and cooling systems of buildings
[DE91-752988] N91-26593
Ecological exposure and effects of airborne toxic chemicals: An overview
[PB91-148460] N91-26594
Changing by degrees: Steps to reduce greenhouse gases
[PB91-163428] N91-26599
An assessment of CO2 greenhouse gas mitigation technologies
[DE91-011972] N91-26605
ENVIRONMENT MODELS
Preliminary testing, evaluation and sensitivity analysis for the Terrestrial Ecosystem Exposure Assessment Model (TEEAM)
[PB91-161711] N91-26602
ENVIRONMENT POLLUTION
Acid rain in Asia
[DE91-011160] N91-26595
ENVIRONMENT PROTECTION
Ecological exposure and effects of airborne toxic chemicals: An overview
[PB91-148460] N91-26594
Changing by degrees: Steps to reduce greenhouse gases
[PB91-163428] N91-26599
ENVIRONMENTAL SURVEYS
Measurements of dust on Mars to be obtained from upcoming missions N91-27066
ENVIRONMENTAL TESTS
Characterization studies of fluorinated epoxy resins: Naval experimental resin C8/1SA as a structural material and for use in blends and composites
[AD-A234188] N91-26338
ENVIRONMENTS
Regeneration of whetlerite for adsorbing toxic pollutants from air
[AD-D014859] N91-26753
ENZYMES
Biological synthesis of substituted o-aminophenols
[AD-A234910] N91-26678
EPIDERMIS
Wound healing by cultured skin cells and growth factors
[AD-A235300] N91-26730
EPINEPHRINE
Effect of shift work of air traffic controllers on sympathetic nervous system N91-26700
EPITAXY
Epitaxy of metal atoms on metal surfaces: Deposition and diffusion
[DE91-011142] N91-26309
Symposium E: Properties of 2-6 semiconductors. Bulk crystals, epitaxial films, quantum well structures
[AD-A234835] N91-26957
Process for the homoepitaxial growth of single-crystal silicon carbide films on silicon carbide wafers
[NASA-CASE-LEW-15223-1] N91-26967
HREM study of heteroepitaxial interfaces in the TiO2/Al2O3 system
[DE91-012473] N91-26986
EPOXY MATRIX COMPOSITES
Characterization studies of fluorinated epoxy resins: Naval experimental resin C8/1SA as a structural material and for use in blends and composites
[AD-A234188] N91-26338
EPOXY RESINS
Chemical synthesis study of deuterated epoxy resins
[AD-A234666] N91-26355
EQUATIONS OF MOTION
An anisotropic laminated damped plate theory
[AD-A234446] N91-26222
A gravitationally consistent second-order analytic secular solution for the point-mass motion of the eight principal planets N91-27054
EQUATIONS OF STATE
An analysis on the stability of the Mie-Gruneisen equation of state for describing the behavior of shock-loaded materials
[AD-A233827] N91-26988
EQUATORIAL ATMOSPHERE
ARTIST tape output formats
[AD-A235173] N91-26633
EQUATORIAL REGIONS
Characteristics of aerosol in the atmosphere of Mars according to data from the KRFM experiment N91-26175
EQUILIBRIUM
Analysis of necessary and sufficient conditions for the equilibrium stability of a gyrostatic satellite N91-26166
ERGOMETERS
Physiological responses to the wearing of protective equipment and respirators: Effects of hot, humid inspired air on work of breathing
[PB91-152884] N91-26745
EROSION
Satellite data derived estimates of erosion parameters for reentry vehicles
[AD-A234792] N91-26189
Performance evaluation of a novel erosion-resistant pump design
[DE91-008201] N91-26528
Sand and dust issues for the MESUR mission N91-27080
ERROR ANALYSIS
Research on intelligent fault detection and repair advisory systems
[AD-A235267] N91-26551
Evaluating the effect of accuracy ratios on the percent of calibrations which are out of tolerance N91-27107
ERROR CORRECTING CODES
Optimal Walsh modulations in the presence of Doppler
[AD-A233723] N91-26411
Analysis of visual loss from retinal lesions
[AD-A235268] N91-26729
ERRORS
Calculation of the pointing accuracy of spacecraft equipment using autonomous measurements of the angular position of the object of investigation N91-26167
The wild weasel development programs, one run, one hit, one error
[RAND-P-7661-RGS] N91-26431

Physical and psychogenic sequelae of impact acceleration on tracking performance of operators N91-26701
Pumping system fault detection and diagnosis utilizing pattern recognition and fuzzy inference techniques [DE91-011849] N91-26863

ESCAPE SYSTEMS
Advanced Dynamic Anthropomorphic Manikin (ADAM) design report [AD-A234761] N91-26756

ESTIMATES
Preliminary estimates of core-collapse supernova rates from the Berkeley automated supernova search [DE91-011824] N91-27050

ESTIMATING
Results of morphometric analysis of the Tesserae surface of Venus according to Venera-15 and -16 data N91-26176
Improvement of procedures for evaluating photochemical models [PB91-160374] N91-26597
Categories and particulars: Prototype effects in estimating spatial location [AD-A234955] N91-26741
Investigating combustion as a method of processing inedible biomass produced in NASA's biomass production chamber [NASA-TM-103821] N91-26759

ESTIMATORS
Compound estimation procedures in reliability N91-27090

ETALONS
Part 1: Ultrafast logic and multiple-beam optical parallel processing using nonlinear etalons. Part 2: Novel devices for all-optical computing. Part 3: Novel nonlinear semiconductor structures for signal processing and optical computing [AD-A233410] N91-26799

ETCHING
Surface etching and roughening in integrated processing of thermal oxides [AD-A234960] N91-26456
The development of piezoelectric poly(vinylidene fluoride) sensors for measuring peel stresses in adhesive joints [AD-A233880] N91-26559
Process for the homoepitaxial growth of single-crystal silicon carbide films on silicon carbide wafers [NASA-CASE-LEW-15223-1] N91-26967

ETHERS
LaRC-ITPI/arylene ether copolymers [NASA-TM-104099] N91-26378

ETHYL COMPOUNDS
Laser ionic multiphoton dissociation of some acrylate clusters [AD-A233801] N91-26247

ETHYLENE
Adsorption and thermal behavior of ethylene on Si(100)-(2x1) [AD-A234098] N91-26252

ETHYLENEDIAMINE
Regeneration of whetlerite for adsorbing toxic pollutants from air [AD-D014859] N91-26753

EUCLIDEAN GEOMETRY
Covering a closed curve with a given total curvature [AD-A234342] N91-26840

EULER EQUATIONS OF MOTION
Methods to enhance the accuracy of finite volume schemes 2 [FFA-147] N91-26466

EULER-LAGRANGE EQUATION
General relativistic continuum mechanics and the post-Newtonian equations of motion N91-26987

EUROPE
Aerospace plane technology: Research and development efforts in Europe. Report to the Chairman, Committee on Science, Space, and Technology, House of Representatives [GAO/NSIAD-91-194] N91-26141

EUTECTICS
Method of preparing a thermal barrier coating [NASA-CASE-LEW-14999-2] N91-26376

EVALUATION
Technology needs for high-speed rotorcraft, volume 1 [NASA-CR-177585] N91-26139
Evaluation of the Navy oceanic vertical aerosol model using lidar and PMS particle-size spectrometers [AD-A233653] N91-26625

EVAPORATION
Size dependence of gaseous cluster reactivity and evaporation dynamics as a mechanistic probe [AD-A233811] N91-26249
Transport processes and interfacial phenomena in an evaporating meniscus [DE91-005581] N91-26284
Application of thematic mapper images to determine regional evaporation from the playas in the western desert of Egypt [REPT-31] N91-26585
Growth, evaporation and melting of ice crystals: Implications for radiation, atmospheric dynamics and particle scavenging N91-26611
Ohmic contacts to semiconducting diamond [AD-A234130] N91-26950

EVOKED RESPONSE (PSYCHOPHYSIOLOGY)
The Trendelenburg position after cerebral air embolism in dogs: Effects on the somatosensory evoked potential, intracranial pressure, and blood-brain barrier [AD-A233809] N91-26673
Attention span, anxiety, and benzodiazepine receptors [AD-A234549] N91-26716
The P300 component of the auditory event-related potential: Interlaboratory consistency and test-retest reliability [AD-A235114] N91-26725

EXCIMER LASERS
Quasi-CW excimer laser, phase 2 [AD-A234771] N91-26509
Tunable excimer lasers [DE91-011399] N91-26522

EXCIMERS
Tunable excimer lasers [DE91-011399] N91-26522

EXCITATION
Control of an axisymmetric turbulent jet by multi-modal excitation [NASA-TM-104483] N91-26121
Spectroscopy and photoexcitation spectroscopies of polyaniline: A model system for new phenomena [AD-A234215] N91-26340
Laser-induced desorption of H2 from Si(111)7x7 [AD-A234636] N91-26508
Saturation and kinetic issues for optical-field-ionized plasma x ray lasers [DE91-012079] N91-26517
Nonlinear oscillations of mechanical systems under multifrequency parametric excitation [AD-A233800] N91-26558
Electronic excitation transport in photosynthesis and crystal and molecular structures of porphyrin compounds [DE91-012024] N91-26679
Fluorescence spectroscopy of excitation transfer in Photosystem 1 [DE91-011867] N91-26681

EXCRETION
Effect of shift work of air traffic controllers on sympathetic nervous system N91-26700

EXERCISE PHYSIOLOGY
Effect of excess respiratory resistance on physical performance and cardiorespiratory function N91-26699
COLDEX-86: Physical work capacity during prolonged cold water immersion at 6.1 msw [AD-A233767] N91-26710
COLDEX-86: Summary of the experimental protocol and general results [AD-A234031] N91-26715

EXHAUST GASES
Pressure distribution and induced force field on a conical nozzle due to impingement of a normal jet into the supersonic cross-flow [AD-A233981] N91-26115
Navier-Stokes calculations of scramjet-nozzle-afterbody flowfields [NASA-CR-185356] N91-26488

EXHAUSTION
Level of dietary fat does not affect fuel oxidation or endurance exercise performance of soldiers [AD-A235194] N91-26728

EXOBIOLOGY
USSR Space Life Sciences Digest, issue 29 [NASA-CR-3922(34)] N91-26669
USSR Space Life Sciences Digest, issue 30 [NASA-CR-3922(36)] N91-26670
NASA/ASEE Summer Faculty Fellowship Program, 1990, Volume 1 [NASA-CR-185637-VOL-1] N91-27088

EXPERIMENT DESIGN
Unmanned aerial vehicles. Medium range system components do not fit [AD-A234131] N91-26132
Investigation of axial positioning for flexural compressors [NASA-CR-185711] N91-26544
Quality by design using statistically planned experiments [ITN-91-85119] N91-26553
Transport and fate of acetone in an outdoor model stream, Stennis Space Center near Bay St. Louis, Mississippi [PB91-154674] N91-26600

EXPERT SYSTEMS
Analysis of knowledge-based expert systems as tools for construction design [AD-A234473] N91-26404
Expert system explanation: The user perspective [AD-A233739] N91-26749
BaRT manual version 3.0 [AD-A234528] N91-26784
Parallel processing and expert systems [NASA-TM-103886] N91-26796
Translating expert system rules into Ada code with validation and verification [NASA-CR-187505] N91-26800
Measurement expert system effectiveness [AD-A234359] N91-26807
Evaluation of expert systems: A review of the literature [AD-A234360] N91-26808
Strategies for parallel AI implementations [AD-A234449] N91-26811
Engineering for artificial intelligence software [AD-A234793] N91-26814
Northeast Artificial Intelligence Consortium (NAIC). Volume 2: Discussing, using, and recognizing plans [AD-A234881] N91-26816
Northeast Artificial Intelligence Consortium (NAIC). Volume 3: The Versatile Maintenance Expert System (VMES) [AD-A234882] N91-26817
Northeast Artificial Intelligence Consortium (NAIC). Volume 4: Distributed artificial intelligence for communications network management [AD-A234883] N91-26818
Northeast Artificial Intelligence Consortium (NAIC). Volume 5: Distributed planning for dynamic environments in the presence of time constraints [AD-A234884] N91-26819
Northeast Artificial Intelligence Consortium (NAIC). Volume 6: Building an intelligent assistant: The acquisition, integration, and maintenance of complex distributed tasks [AD-A234885] N91-26820
Northeast Artificial Intelligence Consortium (NAIC). Volume 7: Automatic photointerpretation [AD-A234886] N91-26821
Northeast Artificial Intelligence Consortium (NAIC). Volume 9: A planner system for the application of indications and warning [AD-A234888] N91-26823
Northeast Artificial Intelligence Consortium (NAIC). Volume 10: Time oriented problem solving [AD-A234889] N91-26824
Northeast Artificial Intelligence Consortium (NAIC). Volume 11: Knowledge base maintenance [AD-A234890] N91-26825
Northeast Artificial Intelligence Consortium (NAIC). Volume 12: Computer architecture for very large knowledge bases [AD-A234891] N91-26826
Northeast Artificial Intelligence Consortium (NAIC). Volume 18: A distributed artificial intelligence approach to information fusion and object classification [AD-A234892] N91-26827
Northeast Artificial Intelligence Consortium (NAIC). Volume 14: Knowledge base retrieval using plausible inference [AD-A234893] N91-26828
Northeast Artificial Intelligence Consortium (NAIC). Volume 15: Strategies for coupling symbolic and numerical computation in knowledge base systems [AD-A234894] N91-26829
Northeast Artificial Intelligence Consortium (NAIC). Volume 16: Intelligent signal processing techniques for multi-sensor surveillance systems [AD-A234895] N91-26830
Northeast Artificial Intelligence Consortium (NAIC). Volume 17: High-level adaptive signal processing [AD-A234896] N91-26831
Northeast Artificial Intelligence Consortium (NAIC). Volume 13: Image understanding and intelligent parallel systems [AD-A234897] N91-26832
Pumping system fault detection and diagnosis utilizing pattern recognition and fuzzy inference techniques [DE91-011849] N91-26863
Generic tasks for knowledge-based problem solving: Extension and new directions [AD-A234925] N91-26865
Training effectiveness of an intelligent tutoring system for a propulsion console trainer N91-27097
A design for an intelligent monitor and controller for space station electrical power using parallel distributed problem solving N91-27105
Fuzzy logic control system to provide autonomous collision avoidance for Mars rover vehicle N91-27106

EXPLOSIONS
Minutes of the 24th Explosives Safety Seminar, volume 2
[AD-A235006] N91-26396
EXPLOSIVES
Minutes of the 24th Explosives Safety Seminar, volume 1
[AD-A235005] N91-26395
Minutes of the 24th Explosives Safety Seminar, volume 2
[AD-A235006] N91-26396
Shock response of Detasheet
[DE91-010923] N91-26399
EXPONENTS
Lyapunov exponents and rotation numbers of linear systems with real noise
[AD-A234729] N91-26846
EXPOSURE
Review of primary medical results of year-long flight on Mir station N91-26178
India-stabilized zirconia coating for composites
[AD-D014857] N91-26224
Preliminary testing, evaluation and sensitivity analysis for the Terrestrial Ecosystem Exposure Assessment Model (TEEAM)
[PB91-161711] N91-26602
EXTRAVEHICULAR ACTIVITY
Impact of Mars sand on dust on the design of space suits and life support equipment: A technology assessment N91-27079
EXTRAVEHICULAR MOBILITY UNITS
Reexamination of METMAN, recommendations on enhancement of LCVG, and development of new concepts for EMU heat sink N91-27098
EXTRUDING
Mechanical behavior and flow mechanisms in refractory metal composition
[AD-A234701] N91-26297
EYE MOVEMENTS
A Conference on Eye Movements and Visual Cognition
[AD-A234754] N91-26739
EYE PROTECTION
Mechanical properties of polycarbonate-polysulfone and polycarbonate-polyetherimide blends
[AD-A234939] N91-26360
EYEPIECES
Visual and field-of-view evaluation of the M-43 protective mask with prescription eyepieces
[AD-A234592] N91-26754

F

F REGION
Technique for measuring ionospheric irregularities generated by high power oblique HF heating of the F-region
[AD-A233883] N91-26627
The effects of magnetic storm phases on F-layer irregularities from auroral to equatorial latitudes
[AD-A235170] N91-26632
F-4 AIRCRAFT
The wild weasel development programs, one run, one hit, one error
[RAND-P-7661-RGS] N91-26431
F-8 AIRCRAFT
Application of transformational ideas to automatic flight control design
[AD-A234758] N91-26148
FABRICATION
Investigation of polybenzocyclobutene resins in multilayer thin films for electronic packaging
[AD-A235223] N91-26228
Magnetron sputter deposition of boron and boron carbide
[DE91-011194] N91-26241
Method of preparing a thermal barrier coating
[NASA-CASE-LEW-14999-2] N91-26376
Surface etching and roughening in integrated processing of thermal oxides
[AD-A234960] N91-26456
Ohmic contacts to semiconducting diamond
[AD-A234130] N91-26950
FABRY-PEROT INTERFEROMETERS
SUNLITE program. Sub-Hertz relative frequency stabilization of two diode laser pumped Nd:YAG lasers locked to a Fabry-Perot interferometer
[NASA-CR-184957] N91-26520
FACTORIZATION
Normalization of the parameterized Courant-Snyder matrix
[DE91-012554] N91-26856
FAILURE ANALYSIS
Gordon Research Conference on Composites
[AD-A233778] N91-26210
Static and cyclic compressive fatigue of thermoplastic-matrix composite in ambient and moisture environments
[AD-A234187] N91-26217
On the finite-strain-invariant failure criterion for composites
[AD-A234493] N91-26223
Fragmentation of brittle materials at high rates of loading N91-26237
Lifetimes and failure mechanisms of W/Re hairpin filaments
[AD-A235199] N91-26305
A new high-progressivity/high-density propulsion concept: Partially cut multiperforated stick propellant
[AD-A234255] N91-26391
Investigations into fracture mechanics failure concepts with thermomechanically rolled steels
[BLL-OA-TRANS-4238-(6196.3)] N91-26556
The hysteresis and incremental collapse of complex structures: A paradigm for the fatigue failure of materials
[AD-A234831] N91-26563
Fatigue crack tip plastic strain range measurement studies in two titanium alloys
[AD-A234973] N91-26565
Analysis of visual loss from retinal lesions
[AD-A235268] N91-26729
The effects of display failures and symbol rotation on visual search and recognition performance
[AD-A235035] N91-26743
MHD contractors' review meeting
[DE91-011295] N91-26945
Compound estimation procedures in reliability N91-27090
FAR FIELDS
Acoustic radiation from fluid-loaded, ribbed cylindrical shells excited by different types of concentrated mechanical drives
[AD-A235324] N91-26887
FARADAY EFFECT
An ultraviolet optical isolator utilizing the KDP-isomorphs
[AD-D014860] N91-26923
FAST FOURIER TRANSFORMATIONS
Backscattering enhancement from rough surfaces
[AD-A234707] N91-26426
FATIGUE (BIOLOGY)
Visual accommodation in cosmonauts N91-26697
Effect of a passive cooling vest on tension/anxiety and fatigue in a high heat and high humidity naval environment
[AD-A234657] N91-26755
FATIGUE (MATERIALS)
Static and cyclic compressive fatigue of thermoplastic-matrix composite in ambient and moisture environments
[AD-A234187] N91-26217
Sliding wear-testing and data analysis strategies for advanced engineering ceramics
[DE91-009524] N91-26383
The hysteresis and incremental collapse of complex structures: A paradigm for the fatigue failure of materials
[AD-A234831] N91-26563
Fatigue crack tip plastic strain range measurement studies in two titanium alloys
[AD-A234973] N91-26565
NATO advanced research workshop on Measurement of Residual and Applied Stress Using Neutron Diffraction
[AD-A235103] N91-26566
FATIGUE LIFE
Improved reduction of gust loads data for gust intensity N91-26153
FATIGUE TESTS
Cyclic deformation, damage, and effects of environment in the Ni3Al ordered alloy at elevated temperature
[AD-A235168] N91-26304
Performance of a 22Cr-20Ni-18Co-Fe alloy for service to 870 C
[DE91-011366] N91-26317
Strength and microstructure of ceramics
[AD-A235424] N91-26374
Effect of initial delamination on Mode 1 and Mode 2 interlaminar fracture toughness and fatigue fracture threshold
[NASA-TM-104079] N91-26569
FATS
Pharmacological sparing of protein in burn injury
[AD-A235026] N91-26724
FAULT TOLERANCE
Research on intelligent fault detection and repair advisory systems
[AD-A235267] N91-26551
The process group approach to reliable distributed computing
[NASA-CR-188498] N91-26804
FAULT TREES
Pumping system fault detection and diagnosis utilizing pattern recognition and fuzzy inference techniques
[DE91-011849] N91-26863
FEEDBACK
Interfacial force sensor with force-feedback control
[DE91-004897] N91-26495
Adaptive control of direct drive dexterous robotic hand with bilateral tactile sensing
[AD-A233980] N91-26532
A sequential Jackson network with feedback
[ITN-91-85111] N91-26867
FEEDBACK CONTROL
Applied high-speed imaging for the icing research program at NASA Lewis Research Center
[NASA-TM-104415] N91-26490
Interfacial force sensor with force-feedback control
[DE91-004897] N91-26495
Advanced material handling equipment controls
[AD-A235091] N91-26540
The relationship of traditional damping measures for materials with high damping capacity
[AD-A235347] N91-26568
FEEDERS
Method and apparatus for waste collection and storage
[NASA-CASE-MSC-21025-3] N91-26747
FEMALES
Physiological and perceptual responses to load carrying in female subjects using internal and external frame backpacks
[AD-A234941] N91-26722
FERMI SURFACES
Calculation of the conductance of two dimensional narrow wires
[ITN-91-85109] N91-26460
FERROELECTRICITY
Proceedings of the Optoelectronic Workshop 25: Liquid Crystal Materials and Devices for Opto-Electronic Applications
[AD-A233780] N91-26921
FERROMAGNETIC MATERIALS
Methods of obtaining an electrical contact
[AD-A234800] N91-26453
FEYNMAN DIAGRAMS
Propagators for quantum oscillator chains
[AD-A234467] N91-26893
FIBER COMPOSITES
Effect of a viscoelastic interface on the transverse behavior of fiber-reinforced composites
[AD-A233986] N91-26212
Development of a test system and experimental method for in-plane biaxial compressive deformation and failure of fiber composite materials
[AD-A234062] N91-26214
Interfacial slippage of a unidirectional fiber composite under longitudinal shearing
[AD-A234186] N91-26216
Static and cyclic compressive fatigue of thermoplastic-matrix composite in ambient and moisture environments
[AD-A234187] N91-26217
Nonlinear behavior of fiber composite materials and its effect on the postbuckling response of laminated plates
[AD-A234203] N91-26218
Fiber coating by sputtering for high temperature composites
[AD-A234994] N91-26226
Investigation of interfacial shear strength in SiC/Si3N4 composites
[NASA-TM-103739] N91-26233
Characterization of mechanical damage mechanisms in ceramic composite materials
[NR-032-553] N91-26235
Investigation into the effect of heat treatment on the thermal conductivity of 3-D carbon/carbon fiber composites
[DE91-010388] N91-26240
FIBER OPTICS
Improved inline fiber optic sensor arrays
[AD-D014864] N91-26924
The First Nonlinear Optics: Materials, Phenomena, and Devices Conference
[AD-A234733] N91-26926
High temperature superconducting films and crystals
[AD-A235234] N91-26965
FIBERS
Effect of a viscoelastic interface on the transverse behavior of fiber-reinforced composites
[AD-A233986] N91-26212
Polyaniline: Oriented films and fibers
[AD-A234414] N91-26347
An induction time approach to surface induced crystallization in polyethylene/poly (e-caprolactone) melt
[AD-A235102] N91-26964

FIBROBLASTS
Wound healing by cultured skin cells and growth factors
[AD-A235300] N91-26730
FIELD COILS
Design and fabrication of forced-flow coils as an R/D program for large helical device
[NIFS-81] N91-26937
FIELD EFFECT TRANSISTORS
Submicron gate InP power MISFET's with improved output power density at 18 and 20 GHz N91-26436
Active devices for monolithic millimeter-wave integrated circuits
[AD-A234033] N91-26440
A temperature dependent SPICE macro-model for power MOSFETs
[DE91-011737] N91-26972
FIELD OF VIEW
Visual and field-of-view evaluation of the M-43 protective mask with prescription eyepieces
[AD-A234592] N91-26754
FIELD THEORY (PHYSICS)
Gauge bosons and heavy quarks: Proceedings of Summer Institute on Particle Physics
[DE91-011248] N91-26907
Quantum limited quasiparticle mixers at 100 GHz
[DE91-011826] N91-26991
FIGHTER AIRCRAFT
Flight control law synthesis using neural network theory
[AD-A234990] N91-26149
FILAMENT WINDING
A model for wet filament winding of composite cylinders with arbitrary thickness
[AD-A234102] N91-26215
FILLERS
Bonding agent for composite propellants
[AD-D014876] N91-26392
Methods of obtaining an electrical contact
[AD-A234800] N91-26453
FILM COOLING
Investigation of hot streak migration and film cooling effects on the heat transfer in rotor/stator interacting flows
[AD-A235420] N91-26145
Liquid film cooling in rocket engines
[AD-A234288] N91-26197
FILTRATION
A model for wet filament winding of composite cylinders with arbitrary thickness
[AD-A234102] N91-26215
FINE STRUCTURE
High temperature superconducting films and crystals
[AD-A235234] N91-26965
On the nature of grain boundary structures in nanophase materials
[DE91-010285] N91-26978
FINITE DIFFERENCE THEORY
A model for wet filament winding of composite cylinders with arbitrary thickness
[AD-A234102] N91-26215
Investigation of laminar, fully developed flow in annulus by finite difference model
[ITN-91-85116] N91-26483
Implementation of the flow-modulated skew-upwind difference scheme in the COMMIX-1C code: A first assessment
[DE91-011168] N91-26489
Spectral recovery of discontinuous data
[ITN-91-85115] N91-26853
Computation of broadband mixing noise from turbomachinery
[AD-A233991] N91-26878
Comparison of sound pressure in a wedge-shaped ocean as predicted by an image method and a PE model
[AD-A234191] N91-26879
FINITE ELEMENT METHOD
Development of an integrated aeroservoelastic analysis program and correlation with test data
[NASA-TP-3120] N91-26113
Electromagnetic launch technology assessment. Scientific basis and unified treatment: Forces and electromechanical power conversion (analytical and numerical methods)
[AD-A235028] N91-26185
Nonlinear behavior of fiber composite materials and its effect on the postbuckling response of laminated plates
[AD-A234203] N91-26218
On the finite-strain-invariant failure criterion for composites
[AD-A234493] N91-26223
Development and verification of global/local analysis techniques for laminated composites
[NASA-CR-185060] N91-26238
Transformation toughening of ceramics
[AD-A234926] N91-26359
Pressureless densification of ceramic matrix composites
[AD-A235031] N91-26362
Numerical simulations of the indentation of glass with implications to ductile grinding
[DE91-011512] N91-26381
Load-bearing capacity of large pipes with circumferential defects under tensile stress: Comparison of experiments with calculated estimates
[BLL-OA-TRANS-4233-(6196.3)] N91-26557
Residual stresses in metal/ceramic brazes: Effect of creep on finite element analysis results
[DE91-011233] N91-26570
NFEARS: A nonlinear adaptive finite element solver. Part 2: User's manual
[AD-A234416] N91-26842
FINITE VOLUME METHOD
Methods to enhance the accuracy of finite volume schemes 2
[FFA-147] N91-26466
FINNED BODIES
The effect of sabot wheelbase and position on the launch dynamics of fin-stabilized kinetic energy ammunition
[AD-A234945] N91-26118
FINS
Computational model for optimizing longitudinal fin heat transfer in laminar internal flows
[DE91-005070] N91-26485
FIRE CONTROL
Visual sensitivities and discriminations and their role in aviation
[AD-A234866] N91-26740
FIRES
Use of a zone model for validation of a horizontal ceiling/floor vent algorithm
[AD-A234553] N91-26474
HYLIFE-2 inertial confinement: Fusion power plant design
[DE91-012089] N91-26947
FIRST AID
Utilization of emergency medical kits by air carriers
[AD-A234784] N91-26721
FLAME PROPAGATION
Use of a zone model for validation of a horizontal ceiling/floor vent algorithm
[AD-A234553] N91-26474
FLAME STABILITY
Turbulent premixed hydrogen/air flames
[AD-A235109] N91-26278
FLAME TEMPERATURE
Modification of the user friendly thermodynamic code to include the effects of minor species
[AD-A233929] N91-26390
FLAMES
The chemistry of sodium with sulfur in flames
[DE91-002060] N91-26288
FLAPS (CONTROL SURFACES)
The delay of turbulent boundary layer separation by oscillatory active control
[ITN-91-85104] N91-26482
FLASH LAMPS
High pulse-energy flashlamp-pumpable laser dyes
[AD-A233837] N91-26499
FLEXIBLE BODIES
Geogrid reinforced base course for flexible pavements for light aircraft: Literature review and test section design
[DOT/FAA/RD-90/28] N91-26160
Nonlinear dynamics and control of flexible structures
[AD-A235186] N91-26191
FLIGHT CHARACTERISTICS
Performance optimization of helicopter rotor blades
[NASA-TM-104054] N91-26137
Acquisition of statistical gust load data by commercial airplanes N91-26152
FLIGHT CONDITIONS
Experimental techniques in the field of low density aerodynamics
[AGARD-AG-318(E)] N91-26124
FLIGHT CONTROL
Development of an integrated aeroservoelastic analysis program and correlation with test data
[NASA-TP-3120] N91-26113
Establishment of a remotely piloted helicopter test flight program for higher harmonic control research
[AD-A234978] N91-26135
Flight control law synthesis using neural network theory
[AD-A234990] N91-26149
Structured representation for requirements and specifications
[NASA-CR-187522] N91-26797
FLIGHT CREWS
Pharmacological correction of functional condition of Army Air Force flyers in hot climate with asparkam N91-26684
Risk factors and prediction of syncopic states in flyers N91-26685
Utilization of emergency medical kits by air carriers
[AD-A234784] N91-26721
Aircrew Evaluation Sustained Operations Performance (AESOP): A triservice facility for technology transition
[AD-A234626] N91-26738
Task analysis and workload prediction for the MH-47E mission and a comparison with CH-47D workload predictions. Volume 2: Appendixes A through N
[AD-A235249] N91-26757
FLIGHT PATHS
How low can an unmanned air vehicle fly?
[RAND-P-7680-RGS] N91-26138
Apparatus for guiding a missile
[AD-D014866] N91-26147
FLIGHT STRESS (BIOLOGY)
Hormonal regulators of calcium metabolism following space flights of various durations N91-26689
FLIGHT SURGEONS
Administrative guide for the flight surgeon and the aeromedical technician: Performing medical examinations
[AD-A235178] N91-26727
FLIGHT TEST INSTRUMENTS
Digital signal conditioning for flight test, volume 19
[AGARD-AG-160-VOL-19] N91-26432
FLIGHT TEST VEHICLES
Establishment of a remotely piloted helicopter test flight program for higher harmonic control research
[AD-A234978] N91-26135
FLIGHT TESTS
Digital signal conditioning for flight test, volume 19
[AGARD-AG-160-VOL-19] N91-26432
FLIP-FLOPS
Coherent beam-beam effects
[DE91-012512] N91-26917
FLOW CHARACTERISTICS
Experimental techniques in the field of low density aerodynamics
[AGARD-AG-318(E)] N91-26124
FLOW CHARTS
Electronic design process
[AD-A234709] N91-26786
FLOW DISTRIBUTION
Pressure distribution and induced force field on a conical nozzle due to impingement of a normal jet into the supersonic cross-flow
[AD-A233981] N91-26115
The kinematics of turbulent boundary layer structure
[NASA-TM-103859] N91-26465
Basic studies of microstructure of combusting turbulent flows
[AD-A234222] N91-26471
Investigation of laminar, fully developed flow in annulus by finite difference model
[ITN-91-85116] N91-26483
Navier-Stokes calculations of scramjet-nozzle-afterbody flowfields
[NASA-CR-185356] N91-26488
Mathematical modeling of the flow field and particle motion in a rotating bioreactor at unit gravity and microgravity N91-27092
FLOW RESISTANCE
Superconducting high T(sub c) thin film vortex-flow transistor, phase 1
[AD-A235025] N91-26962
FLOW STABILITY
Methods to enhance the accuracy of finite volume schemes 2
[FFA-147] N91-26466
Theoretical studies of the kinematics, dynamics, stability, and control of unsteady/vortical flows
[AD-A235190] N91-26477
FLOW VELOCITY
Computer modeling of soot formation comparing free radical and ionic mechanisms
[AD-A235007] N91-26273
Investigation of laminar, fully developed flow in annulus by finite difference model
[ITN-91-85116] N91-26483
FLUID FILLED SHELLS
Acoustic radiation from fluid-loaded, ribbed cylindrical shells excited by different types of concentrated mechanical drives
[AD-A235324] N91-26887
FLUID FLOW
A study of high speed flows in an aircraft transition duct
[NASA-TM-104449] N91-26122
Simulation of pore scale porous media flow using lattice gas methods
[DE91-004829] N91-26484
Benchm. .κ study between FIDAP and a cellular automata code
[DE91-011224] N91-26486

Modal aerosol dynamics modeling
[PB91-161729] N91-26598
FLUID JETS
CFD analysis of jet mixing in low NOx flametube combustors
[NASA-TM-104466] N91-26146
FLUID MECHANICS
Calculated aerodynamics of wings in severe maneuver
[AD-A235241] N91-26120
Simulation of pore scale porous media flow using lattice gas methods
[DE91-004829] N91-26484
Implementation of the flow-modulated skew-upwind difference scheme in the COMMIX-1C code: A first assessment
[DE91-011168] N91-26489
FLUID-SOLID INTERACTIONS
Improved algorithms for transient and steady-state fluid-structure interaction
[AD-A235172] N91-26476
FLUORESCENCE
Structure of alkylated silica surfaces: Quenching of fluorescence from covalently bound pyrene
[AD-A234642] N91-26207
Surface diffusion at the liquid-solid interface: Quenching of fluorescence from pyrene covalently bound to methylated silica
[AD-A234645] N91-26268
Energy migration, motion and order in synthetic polymers
[AD-A234403] N91-26346
High pulse-energy flashlamp-pumpable laser dyes
[AD-A233837] N91-26499
In-situ monitoring of laser ablation of superconductors
[DE91-012057] N91-26524
Imaging of fluorescent and chemiluminescent DNA hybrids using a 2-D CCD camera
[AD-A234641] N91-26676
Fluorescence spectroscopy of excitation transfer in Photosystem 1
[DE91-011867] N91-26681
FLUORIDES
Block patterning of the metallization of polyvinylidene fluoride transducers
[AD-D014872] N91-26450
The development of piezoelectric poly(vinylidene fluoride) sensors for measuring peel stresses in adhesive joints
[AD-A233880] N91-26559
FLUORINE
A combined XPS-ISS modulated molecular beam investigation of the reactions of oxygen and fluorine with silicon surfaces
[AD-A234867] N91-26269
Chemistry of fluorine in the oxidation of silicon
[AD-A234959] N91-26272
FLUOROPOLYMERS
Characterization studies of fluorinated epoxy resins: Naval experimental resin C8/1SA as a structural material and for use in blends and composites
[AD-A234188] N91-26338
FLUX (RATE)
Modelling the dynamics of fluxes of electrons with energies 30-300 keV in geostationary orbit N91-26173
FLUX DENSITY
Cluster beam analysis via photoionization
[AD-A234111] N91-26253
High energy density systems in cryogenic media: The production and reaction of atoms and radicals
[AD-A233785] N91-26892
FLUX PINNING
Magnetic relaxation, flux pinning and, critical currents in superconductors
[DE91-012022] N91-26984
FLY BY WIRE CONTROL
Structured representation for requirements and specifications
[NASA-CR-187522] N91-26797
FOCAL PLANE DEVICES
Luminescence and lasing in II-VI semiconductors
[AD-A235019] N91-26961
FOILS (MATERIALS)
TEM in-situ straining of B2 compounds
[DE91-012062] N91-26322
Solid-state proton conductors
[DE91-002050] N91-26970
FOKKER-PLANCK EQUATION
Continuous stochastic cellular automata that have a stationary distribution and no detailed balance
[AD-A234421] N91-26782
FORECASTING
Forecasting digital microcircuit obsolescence
[AD-A234573] N91-26451
FORGING
Microalloyed steel preforms
[AD-A234039] N91-26296
FORMAT
IRIG standard format for Global Positioning System (GPS) data for post-operation interrange exchange
[AD-A234932] N91-26127
ARTIST tape output formats
[AD-A235173] N91-26633
FORMING TECHNIQUES
Abrasive-waterjet machining of isogrid structures
[AD-A234628] N91-26405
FORMULATIONS
Studies in modeling, dynamics, and control of space structures
[AD-A235059] N91-26190
Interfacial slippage of a unidirectional fiber composite under longitudinal shearing
[AD-A234186] N91-26216
FORTRAN
Surface Chemkin (version 3.7): A FORTRAN package for analyzing heterogeneous chemical kinetics at a solid-surface-gas-phase interface
[DE91-010840] N91-26285
FORWARD SCATTERING
Vertical incidence backscatter and surface forward scattering from near-surface bubbles
[AD-A234432] N91-26880
FOSSIL FUELS
Acid rain in Asia
[DE91-011160] N91-26595
FOURIER TRANSFORMATION
FTIR studies of water and ammonia decomposition on silicon surfaces
[AD-A234637] N91-26265
Diethylsilane decomposition on silicon surfaces studied using transmission FTIR spectroscopy
[AD-A234638] N91-26266
Adsorption and decomposition of diethylsilane on silicon surfaces
[AD-A234639] N91-26267
Multispectral identification of potentially hazardous byproducts of ozonation and chlorination. Part 1: Studies of chromatographic and spectroscopic properties of MX
[PB91-161703] N91-26601
FRACTALS
Field work and dispersion relations of excitations on fractals
[AD-A234953] N91-26455
FRACTIONATION
Supercritical fluid processing of propellant polymers
[AD-A234285] N91-26341
FRACTURE MECHANICS
Development of a test system and experimental method for in-plane biaxial compressive deformation and failure of fiber composite materials
[AD-A234062] N91-26214
Fiber coating by sputtering for high temperature composites
[AD-A234994] N91-26226
Dynamic fracture responses of Al2O3, Si3N4, and SiC(w)/Al2O3
[AD-A235286] N91-26229
Advanced processing and properties of high performance alloys
[AD-A234746] N91-26299
Strength and microstructure of ceramics
[AD-A235424] N91-26374
Numerical simulations of the indentation of glass with implications to ductile grinding
[DE91-011512] N91-26381
Investigations into fracture mechanics failure concepts with thermomechanically rolled steels
[BLL-OA-TRANS-4238-(6196.3)] N91-26556
Fatigue crack tip plastic strain range measurement studies in two titanium alloys
[AD-A234973] N91-26565
FRACTURE STRENGTH
Advanced processing and properties of high performance alloys
[AD-A234746] N91-26299
Transformation toughening of ceramics
[AD-A234926] N91-26359
Strength and microstructure of ceramics
[AD-A235424] N91-26374
Effect of initial delamination on Mode 1 and Mode 2 interlaminar fracture toughness and fatigue fracture threshold
[NASA-TM-104079] N91-26569
Preliminary test results from the HSST shallow-crack fracture toughness program
[DE91-010147] N91-26572
FRACTURES (MATERIALS)
Determination of SBS induced damage limits in large fused silica optics for intense, time varying laser pulses
[DE91-012080] N91-26518
FRACTURING
Dynamic fracture responses of Al2O3, Si3N4, and SiC(w)/Al2O3
[AD-A235286] N91-26229
Effect of initial delamination on Mode 1 and Mode 2 interlaminar fracture toughness and fatigue fracture threshold
[NASA-TM-104079] N91-26569
FRAGMENTATION
Fragmentation of brittle materials at high rates of loading N91-26237
FRAGMENTS
Fragmentation of brittle materials at high rates of loading N91-26237
FREE CONVECTION
Implementation of the flow-modulated skew-upwind difference scheme in the COMMIX-1C code: A first assessment
[DE91-011168] N91-26489
FREE ELECTRONS
The chemical modification of plasmas
[AD-A234448] N91-26940
FREE FLOW
Liquid film cooling in rocket engines
[AD-A234288] N91-26197
FREE RADICALS
Computer modeling of soot formation comparing free radical and ionic mechanisms
[AD-A235007] N91-26273
FREE-PISTON ENGINES
Comparative survey of dynamic analyses of free-piston Stirling engines
[NASA-TM-104491] N91-26870
FREEZING
Process study of sorted patterns on Arctic soils
[AD-A234089] N91-26628
FREQUENCIES
The P300 component of the auditory event-related potential: Interlaboratory consistency and test-retest reliability
[AD-A235114] N91-26725
FREQUENCY CONVERTERS
Analysis of nonlinear optical frequency conversion
[AD-A233726] N91-26920
FREQUENCY DISTRIBUTION
Statistical characteristics of MST radar echoes and its interpretation N91-26617
FREQUENCY DIVIDERS
Design for electronic spectrally tunable infrared detector
[AD-D014877] N91-26925
FREQUENCY RANGES
Quantum limited quasiparticle mixers at 100 GHz
[DE91-011826] N91-26991
FREQUENCY SHIFT
Frequency upshifting of laser pulses by ionization fronts
[AD-A234354] N91-26503
FREQUENCY STABILITY
SUNLITE program. Sub-Hertz relative frequency stabilization of two diode laser pumped Nd:YAG lasers locked to a Fabry-Perot interferometer
[NASA-CR-184957] N91-26520
FRICTION
Turbulent processes of mass-loading of new ions on Venus and Mars and the problems of numerical models of the interaction of solar wind with these planets. 1: Characteristics of the flow of solar wind around the planets N91-26174
FRICTION REDUCTION
Additives for high temperature liquid lubricants
[DE91-011018] N91-26386
FUEL CELLS
High-power converters for space applications
[NASA-CR-187116] N91-26461
Solid-state proton conductors
[DE91-002050] N91-26970
FUEL COMBUSTION
Use of a zone model for validation of a horizontal ceiling/floor vent algorithm
[AD-A234553] N91-26474
Development of a low temperature catalytic combustor for small gas turbine applications
[PB91-161273] N91-26529
MHD contractors' review meeting
[DE91-011295] N91-26945
FUEL CORROSION
India-stabilized zirconia coating for composites
[AD-D014857] N91-26224
FUEL INJECTION
Method of injecting fluid propellants into a rocket combustion chamber
[NASA-CASE-LEW-14846-2] N91-26200
FUEL SYSTEMS
Survey of current aircraft engine conditions
[AD-A235143] N91-26144

FUEL TESTS
Survey of current aircraft engine conditions
[AD-A235143] N91-26144
FUELS
What fuels our future?
[AD-A233674] N91-26387
FULL SCALE TESTS
Geogrid reinforced base course for flexible pavements for light aircraft: Literature review and test section design
[DOT/FAA/RD-90/28] N91-26160
Technical Evaluation Motor No. 7 (TEM-7)
[NASA-CR-184163] N91-26203
FUNCTIONAL ANALYSIS
Stabilization and control problems in structural dynamics
[AD-A235189] N91-26567
FUNCTIONAL DESIGN SPECIFICATIONS
Functional baseline specification for ATC data link service implementation in the host computer system
[DOT/FAA/CT-91/12] N91-26433
FURANS
Molecular mechanics calculations for nitro and amino substituted conjugated systems containing oxygen and nitrogen
[AD-A233928] N91-26389
FUZZY SETS
Uncertainty handling at speech/natural language interface, volume 1
[AD-A234310] N91-26422
FUZZY SYSTEMS
Fuzzy logic control system to provide autonomous collision avoidance for Mars rover vehicle N91-27106

G

GALACTIC EVOLUTION
Preliminary estimates of core-collapse supernova rates from the Berkeley automated supernova search
[DE91-011824] N91-27050
GALILEO PROJECT
Galileo: The Earth encounter N91-27024
GALILEO SPACECRAFT
Galileo: The Earth encounter N91-27024
GALLIUM ARSENIDES
Ab initio molecular dynamics simulations of surfaces and interfaces
[AD-A235315] N91-26901
Preparation of a novel gallium arsenide single-source precursor having the empirical formula AsCl3Ga2
[AD-A233704] N91-26949
GAME THEORY
Creation of uncertainty in repeated two-person non-zero-sum games
[ITN-91-85118] N91-26869
GAMMA RAY ASTRONOMY
Gamma ray astronomy
[NASA-CR-187774] N91-26407
GAMMA RAY BURSTS
Gamma ray astronomy
[NASA-CR-187774] N91-26407
GAMMA RAY OBSERVATORY
Gamma ray astronomy
[NASA-CR-187774] N91-26407
GAMMA RAYS
Absorbed-dose calibration of ionization chambers in a Co-60 gamma-ray beam
[PB91-132290] N91-26890
GANGLIA
Parallel processing and learning: Variability and chaos in self-organization of activity in groups of neurons
[AD-A234589] N91-26737
GARMENTS
Reexamination of METMAN, recommendations on enhancement of LCVG, and development of new concepts for EMU heat sink N91-27098
GARNETS
Laser spectroscopy characterization of materials for frequency agile solid state laser systems
[AD-A233916] N91-26500
Energy levels and branching ratios of Tm(3)+ in ten garnet laser materials
[AD-A235274] N91-26514
GAS CHROMATOGRAPHY
Multispectral identification of potentially hazardous byproducts of ozonation and chlorination. Part 1: Studies of chromatographic and spectroscopic properties of MX
[PB91-161703] N91-26601
GAS EXPANSION
Pressure distribution and induced force field on a conical nozzle due to impingement of a normal jet into the supersonic cross-flow
[AD-A233981] N91-26115
Testing of a composite thermal structure to insulate the drivers of a large scale blast/thermal simulator
[AD-A234014] N91-26213
Size dependence of gaseous cluster reactivity and evaporation dynamics as a mechanistic probe
[AD-A233811] N91-26249
GAS INJECTION
Simulation of pore scale porous media flow using lattice gas methods
[DE91-004829] N91-26484
GAS JETS
Multi-dimensional computer simulation of MHD combustor hydrodynamics
[DE91-011851] N91-26946
GAS LASERS
Scaling CW electron beam pumped rare gas lasers to ultra-high average power
[AD-A235120] N91-26513
GAS TURBINE ENGINES
Survey of current aircraft engine conditions
[AD-A235143] N91-26144
Ceramic technology for advanced heat engines project
[DE91-010451] N91-26384
GAS TURBINES
CFD analysis of jet mixing in low NOx flametube combustors
[NASA-TM-104466] N91-26146
Development of a low temperature catalytic combustor for small gas turbine applications
[PB91-161273] N91-26529
GASIFICATION
Boron combustion model development with kinetic sensitivity analysis and measurement of key chemical rate parameters
[AD-A235309] N91-26283
GAUGE THEORY
Gauge bosons and heavy quarks: Proceedings of Summer Institute on Particle Physics
[DE91-011248] N91-26907
Supersymmetry breaking from superstrings and the gauge hierarchy
[DE91-011899] N91-26992
GELS
Gel solidified microinterface between two immiscible electrolytes applied to amperometric detection of picrate and tetramethylammonium
[AD-A235260] N91-26280
Electroactive, near infrared absorbing nickel bis(dithiolene) complex polycarbonates and polyurethanes
[AD-A234595] N91-26350
Wound healing by cultured skin cells and growth factors
[AD-A235300] N91-26730
GENERATORS
Magnetic field generator
[AD-D014869] N91-26449
GENETIC ENGINEERING
Introduction to Session 2: Applied biological research
[DE91-012067] N91-26680
GENETICS
JPRS report: Science and technology. USSR: Life sciences
[JPRS-ULS-91-011] N91-26696
GEOCHRONOLOGY
Late Wisconsin and early holocene glacial history, inner Ross Embayment, Antarctica N91-26577
Marine record of late quaternary glacial-interglacial fluctuations in the Ross Sea and evidence for rapid, episodic sea level change due to marine ice sheet collapse N91-26578
GEODYNAMICS
Plate motion and deformation
[DE91-010466] N91-26612
GEOGRAPHY
Software requirements specification for the Mapping And Graphic Information Capability (MAGIC). Volume 4: Geographic mapping CSCI
[AD-A235275] N91-26794
GEOLOGICAL FAULTS
Have graben wall scarps accumulated sand and dust on Mars? N91-27062
GEOLOGICAL SURVEYS
A guide to NASA's Pilot Land Data System (PLDS) N91-27035
GEOLOGY
JPRS report: Science and technology. USSR: Earth sciences
[JPRS-UES-91-002] N91-26581
GEOMAGNETIC LATITUDE
The effects of magnetic storm phases on F-layer irregularities from auroral to equatorial latitudes
[AD-A235170] N91-26632
UV aurora mapping in corrected geomagnetic coordinates
[ITN-91-85106] N91-26636
GEOMAGNETISM
Solar-geophysical data number 556, December 1990. Part 1: (Prompt reports). Data for November, October 1990, and late data
[PB91-152140] N91-27083
GEOPHYSICS
Modelling the dynamics of fluxes of electrons with energies 30-300 keV in geostationary orbit N91-26173
Terrestrial geophysics in the SeaRISE project N91-26576
Sounding rocket flight data summary
[AD-A233656] N91-26626
The NASA master directory quick reference guide N91-27034
Solar-geophysical data number 556, December 1990. Part 1: (Prompt reports). Data for November, October 1990, and late data
[PB91-152140] N91-27083
Evaluation of geophysical properties of the lunar regolith for the design of precursor scientific missions for the space exploration initiative N91-27104
GEOSTROPHIC WIND
Laboratory modelling of the dynamics of coastal upwelling
[AD-A234987] N91-26664
GEOSYNCHRONOUS ORBITS
Modelling the dynamics of fluxes of electrons with energies 30-300 keV in geostationary orbit N91-26173
Weather satellites: Action needed to resolve status of the US Geostationary Satellite Program. Report to the Chairman, Committee on Science, Space, and Technology, House of Representatives
[GAO/NSIAD-91-252] N91-26194
GERMANIUM ALLOYS
Crystallization of thin films of amorphous germanium alloys
[ITN-91-85110] N91-26969
GLACIAL DRIFT
Late Wisconsin and early holocene glacial history, inner Ross Embayment, Antarctica N91-26577
Marine record of late quaternary glacial-interglacial fluctuations in the Ross Sea and evidence for rapid, episodic sea level change due to marine ice sheet collapse N91-26578
Glacial dynamics (glaciology) N91-26580
GLASS
Method of preparing a thermal barrier coating
[NASA-CASE-LEW-14999-2] N91-26376
Laser spectroscopy characterization of materials for frequency agile solid state laser systems
[AD-A233916] N91-26500
Derivation of mid-infrared (5-25 microns) optical constants of some silicates and palagonite N91-27077
GLASS FIBER REINFORCED PLASTICS
Evaluation of environmentally aged polymer/composite material by ultrasonic inspection
[AD-A235343] N91-26231
Nondestructive Evaluation (NDE) of fiberglass marine structures state-of-the art review
[AD-A234785] N91-26550
Effect of initial delamination on Mode 1 and Mode 2 interlaminar fracture toughness and fatigue fracture threshold
[NASA-TM-104079] N91-26569
GLASS FIBERS
Dynamic energy absorption of sandwich structures by inelastic deformation
[AD-A234903] N91-26564
GLASS TRANSITION TEMPERATURE
Thermal transitions and mechanical properties of the films of chemically prepared polyaniline
[AD-A233807] N91-26329
GLOBAL POSITIONING SYSTEM
IRIG standard format for Global Positioning System (GPS) data for post-operation interrange exchange
[AD-A234932] N91-26127
The Effect of the Ionosphere on Radiowave Signals and Systems Performance Based on Ionospheric Effects Symposium
[AD-A233797] N91-26416
GLOW DISCHARGES
Electrostatic fields in a dusty Martian environment N91-27078
GOGGLES
Evaluation of night vision goggles for maritime search and rescue
[AD-A233798] N91-26751
GOVERNMENTS
Measuring the quality of knowledge work
[AD-A235354] N91-26994
Publications of the Executive Office of the President, January 20, 1989 to December 31, 1990
[PB91-127423] N91-26998

GRAIN BOUNDARIES
Microstructure development during microwave annealing of dense silicon nitride
[DE91-012069] N91-26242
Microstructure, plastic deformation and mechanical properties of mechanically alloyed NiAl and NiAl based alloys
[AD-A235135] N91-26303
Grain boundary cavitation processes in a Ni3Al alloy at elevated temperatures
[AD-A235279] N91-26307
Precipitation in Alloy 718: A combined AEM and APFIM investigation
[DE91-009918] N91-26314
Grain boundary chemistry in Al-Cu metallizations as determined by analytical electron microscopy
[DE91-012007] N91-26319
Investigation and characterization of ITO/poly-Si photovoltaic junctions
[ITN-91-85105] N91-26590
On the nature of grain boundary structures in nanophase materials
[DE91-010285] N91-26978
High-T(sub c) thin-film magnetometer
[DE91-011828] N91-26981

GRAIN SIZE
Microstructure, plastic deformation and mechanical properties of mechanically alloyed NiAl and NiAl based alloys
[AD-A235135] N91-26303
On the nature of grain boundary structures in nanophase materials
[DE91-010285] N91-26978

GRANTS
Commercial use of space: Many grantees making progress, but NASA oversight could be improved. Report to the Chair, Subcommittee on VA, HUD, and Independent Agencies, Committee on Appropriations, U.S. Senate
[GAO/NSIAD-91-142] N91-26400

GRAPH THEORY
Matching theory. A sampler: From Denes Koenig to the present
[AD-A234321] N91-26839
Extending matchings in graphs: A survey
[AD-A234392] N91-26841

GRAPHITE
Composite fiber hazards
[AD-A233924] N91-26211
Corrosion of graphite aluminum metal matrix composites
[AD-A234322] N91-26220

GRATINGS (SPECTRA)
Atom wave interferometer
[AD-A234863] N91-26494
Laser spectroscopy characterization of materials for frequency agile solid state laser systems
[AD-A233916] N91-26500

GRAVITATION
Proceedings of the 12th Annual Meeting of the UIPS Commission on Gravitational Physiology
[AD-A235337] N91-26732

GRAVITATION THEORY
A gravitationally consistent second-order analytic secular solution for the point-mass motion of the eight principal planets N91-27054

GRAVITATIONAL EFFECTS
Oscillations of a small-mass satellite probe caused by aerodynamic and gravitational forces N91-26165
Review of primary medical results of year-long flight on Mir station N91-26178
Terrestrial geophysics in the SeaRISE project N91-26576
State and forms of adaptation of vestibular function after space flights N91-26706
Proceedings of the 12th Annual Meeting of the UIPS Commission on Gravitational Physiology
[AD-A235337] N91-26732

GRAVITATIONAL FIELDS
Oscillations of a small-mass satellite probe caused by aerodynamic and gravitational forces N91-26165

GRAVITATIONAL PHYSIOLOGY
Proceedings of the 12th Annual Meeting of the UIPS Commission on Gravitational Physiology
[AD-A235337] N91-26732
The effects of deuterium on static posture control N91-27102

GRAVITY WAVES
Gravity waves and instabilities in the lower and middle atmosphere N91-26621

GRAY SCALE
Iterated transform image compression
[AD-A233655] N91-26769
The shape of shading
[AD-A234419] N91-26781

GRAZING
Full surface testing of grazing incidence mirrors
[AD-A234005] N91-26922

GRAZING INCIDENCE
Full surface testing of grazing incidence mirrors
[AD-A234005] N91-26922

GREEN'S FUNCTIONS
Progress in ultrasonic measurements research in 1990: Transient sources for acoustic emission work
[AD-A234965] N91-26882

GREENHOUSE EFFECT
Changing by degrees: Steps to reduce greenhouse gases
[PB91-163428] N91-26599
Global climate change: A discussion of major uncertainties
[DE91-011746] N91-26604
An assessment of CO2 greenhouse gas mitigation technologies
[DE91-011972] N91-26605

GRID GENERATION (MATHEMATICS)
Adaptive component methods for time dependent PDE's
[AD-A233776] N91-26775

GRINDING (COMMINUTION)
Numerical simulations of the indentation of glass with implications to ductile grinding
[DE91-011512] N91-26381

GROUND STATE
Investigation of a Hamiltonian with two sources of anisotropy: The Dzyaloshinskii-Moriya and single-size interactions
[DE91-011381] N91-26292

GROUND WATER
Application of thematic mapper images to determine regional evaporation from the playas in the western desert of Egypt
[REPT-31] N91-26585

GROUND WIND
Martian dust threshold measurements: Simulations under heated surface conditions N91-27081

GROUND-AIR-GROUND COMMUNICATION
Functional baseline specification for ATC data link service implementation in the host computer system
[DOT/FAA/CT-91/12] N91-26433

GROWTH
Wound healing by cultured skin cells and growth factors
[AD-A235300] N91-26730

GULF STREAM
In the energy active region of the ocean N91-26583
Progress with neural network gulf streams
[AD-A233810] N91-26658
The SYNOP experiment: Inverted echo sounder data report for June 1989 to September 1990
[AD-A234625] N91-26662

GUST ALLEVIATORS
Manual on the flight of flexible aircraft in turbulence
[AGARD-AG-317] N91-26150
Measurement of atmospheric turbulence N91-26151
Trends in certification procedures and design analysis N91-26158

GUST LOADS
Manual on the flight of flexible aircraft in turbulence
[AGARD-AG-317] N91-26150
Acquisition of statistical gust load data by commercial airplanes N91-26152
Improved reduction of gust loads data for gust intensity N91-26153
Gust design procedures N91-26155
Analysis by the statistical discrete gust method N91-26156
Matching of PSD-design loads N91-26157
Trends in certification procedures and design analysis N91-26158

GUSTS
Measurement of atmospheric turbulence N91-26151
Acquisition of statistical gust load data by commercial airplanes N91-26152
Improved reduction of gust loads data for gust intensity N91-26153
Certification procedures and requirements N91-26154
Gust design procedures N91-26155
Analysis by the statistical discrete gust method N91-26156
Matching of PSD-design loads N91-26157

GUY WIRES
Structural concept studies for a horizontal cylindrical lunar habitat and a lunar guyed tower N91-27117

GYROSCOPIC COUPLING
Geometry, dynamics and control of coupled systems N91-26401

H

HAMILTONIAN FUNCTIONS
Investigation of a Hamiltonian with two sources of anisotropy: The Dzyaloshinskii-Moriya and single-size interactions
[DE91-011381] N91-26292

HANDBOOKS
Middle Atmosphere Program. Handbook for MAP. Volume 30: International School on Atmospheric Radar
[NASA-CR-188623] N91-26613

HANDLING EQUIPMENT
Advanced material handling equipment controls
[AD-A235091] N91-26540

HARDENING
Methods of obtaining an electrical contact
[AD-A234800] N91-26453

HARDNESS
Mechanical behavior of nanocrystalline Cu, Pd, and Ag samples
[DE91-011747] N91-26310
Microstructure and hardness of NiAl/Ni2AlX two-phase ordered intermetallic alloys
[DE91-012068] N91-26323

HARDNESS TESTS
Microalloyed steel preforms
[AD-A234039] N91-26296

HARMONIC CONTROL
Establishment of a remotely piloted helicopter test flight program for higher harmonic control research
[AD-A234978] N91-26135

HARMONIC GENERATIONS
Novel liquid crystalline polymers as nonlinear optical materials
[AD-A235371] N91-26373

HARMONIC OSCILLATORS
Propagators for quantum oscillator chains
[AD-A234467] N91-26893

HARRIER AIRCRAFT
Refurbishing AV-8 on-board oxygen generation system beds
[AD-A235083] N91-26136

HATCHES
Double face sealing device
[NASA-CASE-MFS-28521-1] N91-26542

HAZARDS
Composite fiber hazards
[AD-A233924] N91-26211
Minutes of the 24th Explosives Safety Seminar, volume 1
[AD-A235005] N91-26395
Minutes of the 24th Explosives Safety Seminar, volume 2
[AD-A235006] N91-26396

HAZE
Characteristics of aerosol in the atmosphere of Mars according to data from the KRFM experiment N91-26175
Dust in the Mars atmosphere N91-27082

HEAD (ANATOMY)
A statistical analysis of -X rhesus head kinematics
[AD-A233977] N91-26674
Proton arc doses to the primate head
[AD-A235134] N91-26726

HEAD MOVEMENT
A statistical analysis of -X rhesus head kinematics
[AD-A233977] N91-26674
Vestibular reactions and intersensory interactions in weightlessness: Results of Optokinez experiment N91-26698

HEALING
Wound healing by cultured skin cells and growth factors
[AD-A235300] N91-26730

HEALTH
Review of primary medical results of year-long flight on Mir station N91-26178
Composite fiber hazards
[AD-A233924] N91-26211
Ecological exposure and effects of airborne toxic chemicals: An overview
[PB91-148460] N91-26594
State-of-the-art automated evaluation of functional state of the body in the space program and preventive medicine N91-26687
Smoking, exercise, and physical fitness
[AD-A234658] N91-26717
Airliner cabin environment: Contaminant measurements, health risks, and mitigation options
[PB91-159384] N91-26746

HEARING
Intelligibility of digital speech masked by noise: Normal hearing and hearing impaired listeners
[AD-A234852] N91-26427

HEART
Effect of 7 day antiorthostatic hypokinesia on cardiac pumping action in monkeys N91-26704
Diagnostic utility of continuous noninvasive blood pressure monitoring (Penaz method) in gravity-induced blood redistribution N91-26705
Metabolic changes and hemodynamic dysfunction following hypothermic shock
[AD-A233942] N91-26713

HEART DISEASES
Changes in rheologic indices of blood and hemodynamics during 14-day antiorthostatic hypokinesia N91-26692

HEART FUNCTION
Effect of excess respiratory resistance on physical performance and cardiorespiratory function N91-26699

HEART RATE
Physical and psychogenic sequelae of impact acceleration on tracking performance of operators N91-26701
Effect of 7 day antiorthostatic hypokinesia on cardiac pumping action in monkeys N91-26704
COLDEX-86: Physical work capacity during prolonged cold water immersion at 6.1 msw
[AD-A233767] N91-26710
Nonlinear systems dynamics in cardiovascular physiology: The heart rate delay map and lower body negative pressure N91-27095

HEAT AFFECTED ZONE
Investigations into fracture mechanics failure concepts with thermomechanically rolled steels
[BLL-OA-TRANS-4238-(6196.3)] N91-26556

HEAT BALANCE
Thermal and albedo mapping of the north and south polar regions of Mars N91-27076

HEAT BUDGET
The tropical Pacific Ocean's heat budget during a cold event, from a numerical model N91-26657

HEAT GENERATION
Absorption heat pump in heating and cooling systems of buildings
[DE91-752988] N91-26593
Reexamination of METMAN, recommendations on enhancement of LCVG, and development of new concepts for EMU heat sink N91-27098

HEAT OF FORMATION
Boron combustion model development with kinetic sensitivity analysis and measurement of key chemical rate parameters
[AD-A235309] N91-26283

HEAT PUMPS
Absorption heat pump in heating and cooling systems of buildings
[DE91-752988] N91-26593

HEAT RESISTANT ALLOYS
Microalloyed steel preforms
[AD-A234039] N91-26296
Advanced processing and properties of high performance alloys
[AD-A234746] N91-26299
Precipitation in Alloy 718: A combined AEM and APFIM investigation
[DE91-009918] N91-26314
Performance of a 22Cr-20Ni-18Co-Fe alloy for service to 870 C
[DE91-011366] N91-26317

HEAT SHIELDING
Sand and dust issues for the MESUR mission N91-27080

HEAT SINKS
Reexamination of METMAN, recommendations on enhancement of LCVG, and development of new concepts for EMU heat sink N91-27098

HEAT TRANSFER
Investigation of hot streak migration and film cooling effects on the heat transfer in rotor/stator interacting flows
[AD-A235420] N91-26145
Transport processes and interfacial phenomena in an evaporating meniscus
[DE91-005561] N91-26284
MHD contractors' review meeting
[DE91-011295] N91-26945
Reexamination of METMAN, recommendations on enhancement of LCVG, and development of new concepts for EMU heat sink N91-27098

HEAT TRANSFER COEFFICIENTS
Elementary reaction rate measurements at high temperatures by tunable-laser flash-absorption
[DE91-011850] N91-26516

HEAT TRANSMISSION
Basic studies of microstructure of combusting turbulent flows
[AD-A234222] N91-26471

HEAT TREATMENT
Investigation into the effect of heat treatment on the thermal conductivity of 3-D carbon/carbon fiber composites
[DE91-010388] N91-26240
Microalloyed steel preforms
[AD-A234039] N91-26296
Grain boundary chemistry in Al-Cu metallizations as determined by analytical electron microscopy
[DE91-012007] N91-26319

HEATERS
Testing of a composite thermal structure to insulate the drivers of a large scale blast/thermal simulator
[AD-A234014] N91-26213

HEATING
Dynamics of face and annular seals with two-phase flow
[NASA-CR-4256] N91-26479
Technique for measuring ionospheric irregularities generated by high power oblique HF heating of the F-region
[AD-A233883] N91-26627

HEATING EQUIPMENT
Absorption heat pump in heating and cooling systems of buildings
[DE91-752988] N91-26593

HEAVY ELEMENTS
Molecular orbital studies of the bonding in heavy element organometallics
[DE91-010915] N91-26905

HEAVY IONS
Turbulent processes of mass-loading of new ions on Venus and Mars and the problems of numerical models of the interaction of solar wind with these planets. 1: Characteristics of the flow of solar wind around the planets N91-26174

HEAVY WATER
Techniques for determining total body water using deuterium oxide N91-27091

HELICAL WINDINGS
Design and fabrication of forced-flow coils as an R/D program for large helical device
[NIFS-81] N91-26937

HELICOPTER DESIGN
Technology needs for high-speed rotorcraft, volume 1
[NASA-CR-177585] N91-26139

HELICOPTERS
Establishment of a remotely piloted helicopter test flight program for higher harmonic control research
[AD-A234978] N91-26135
Performance optimization of helicopter rotor blades
[NASA-TM-104054] N91-26137

HELIOTRONS
Design and fabrication of forced-flow coils as an R/D program for large helical device
[NIFS-81] N91-26937

HELMET MOUNTED DISPLAYS
Notional helmet concepts: A survey of near-term and future technologies
[AD-A234475] N91-26752

HELMETS
SPH-4 aircrew helmet impact protection improvements 1970-1990
[AD-A233784] N91-26750

HEMODYNAMIC RESPONSES
Changes in rheologic indices of blood and hemodynamics during 14-day antiorthostatic hypokinesia N91-26692
Metabolic changes and hemodynamic dysfunction following hypothermic shock
[AD-A233942] N91-26713

HEMODYNAMICS
Changes in rheologic indices of blood and hemodynamics during 14-day antiorthostatic hypokinesia N91-26692

HEMOGLOBIN
Carboxyalkylated hemoglobin as a potential blood substitute
[AD-A233822] N91-26712
Evaluation of liposome-encapsulated Hemoglobin/LR16 formulation as a potential blood substitute
[AD-A233973] N91-26714

HETEROCYCLIC COMPOUNDS
Molecular orientation of the silver tetra neopentoxy phthalo cyanine and stearic acid mixed Langmuir-Blodgett film and its chemical and electrochemical behaviour
[AD-A234601] N91-26206
Novel concepts in electronic polymers: Polyaniline and its derivatives
[AD-A234214] N91-26339
Processable polymers and copolymers of 3-alkylthiophenes and their blends
[AD-A234596] N91-26351
Electronic and ionic transport in processable conducting polymers
[AD-A234597] N91-26352
Template synthesis of polymeric and metal microtubules
[AD-A235307] N91-26367
Molecular mechanics calculations for nitro and amino substituted conjugated systems containing oxygen and nitrogen
[AD-A233928] N91-26389

HETERODYNING
Quantum limited quasiparticle mixers at 100 GHz
[DE91-011826] N91-26991

HETEROGENEITY
Surface Chemkin (version 3.7): A FORTRAN package for analyzing heterogeneous chemical kinetics at a solid-surface-gas-phase interface
[DE91-010840] N91-26285
Strategies for reliable and real time execution on a heterogeneous multiprocessor
[AD-A234114] N91-26801

HEURISTIC METHODS
Research on intelligent fault detection and repair advisory systems
[AD-A235267] N91-26551

HIERARCHIES
Development and testing of a source subsystem for the supporting development PMAD DC test bed
[NASA-TM-104510] N91-26202
Categories and particulars: Prototype effects in estimating spatial location
[AD-A234955] N91-26741
Supersymmetry breaking from superstrings and the gauge hierarchy
[DE91-011899] N91-26992

HIGH ALTITUDE
Advanced Microwave Precipitation Radiometer (AMPR) for remote observation of precipitation
[NASA-CR-184165] N91-26655

HIGH ENERGY INTERACTIONS
UNIX (tm) in high energy physics: What we can learn from the initial experiences at Fermilab
[DE91-011976] N91-26914
Providing a computing environment for a high energy physics workshop
[DE91-012049] N91-26916

HIGH FREQUENCIES
Technique for measuring ionospheric irregularities generated by high power oblique HF heating of the F-region
[AD-A233883] N91-26627
A model for the scattering of high-frequency electromagnetic fields from dielectrics exhibiting thermally-activated electrical losses
[NASA-TM-104376] N91-26872

HIGH POWER LASERS
High pulse-energy flashlamp-pumpable laser dyes
[AD-A233837] N91-26499
Scaling CW electron beam pumped rare gas lasers to ultra-high average power
[AD-A235120] N91-26513
Precision high-power solid-state laser diagnostics for target-irradiation studies and target-plane irradiation modeling
[DE91-012036] N91-26523

HIGH PRESSURE
Dynamics of face and annular seals with two-phase flow
[NASA-CR-4256] N91-26479

HIGH RESOLUTION
A catalog of high resolution Jovian decametric radio noise burst spectra, volume 1 N91-27047

HIGH SPEED
A study of high speed flows in an aircraft transition duct
[NASA-TM-104449] N91-26122
Technology needs for high-speed rotorcraft, volume 1
[NASA-CR-177585] N91-26139
Applied high-speed imaging for the icing research program at NASA Lewis Research Center
[NASA-TM-104415] N91-26490
Multigigahertz semiconductor lasers
[AD-A234776] N91-26510

HIGH TEMPERATURE
Effect of a passive cooling vest on tension/anxiety and fatigue in a high heat and high humidity naval environment
[AD-A234657] N91-26755
Study of the effect of reactive element addition by implanting metal ions in a pre-formed oxide layer
[DE91-011916] N91-26974

HIGH TEMPERATURE AIR
Physiological responses to the wearing of protective equipment and respirators: Effects of hot, humid inspired air on work of breathing
[PB91-152884] N91-26745

HIGH TEMPERATURE ENVIRONMENTS
Cyclic deformation, damage, and effects of environment in the Ni3Al ordered alloy at elevated temperature
[AD-A235168] N91-26304
Performance of a 22Cr-20Ni-18Co-Fe alloy for service to 870 C
[DE91-011366] N91-26317
Strength of SiC- and Si-N-C-ceramic fibers exposed to high-temperature gaseous environments
[DE91-011099] N91-26380
Physiological responses to the wearing of protective equipment and respirators: Effects of hot, humid inspired air on work of breathing
[PB91-152884] N91-26745
HIGH TEMPERATURE FLUIDS
Supercritical fluid processing of propellant polymers
[AD-A234285] N91-26341
HIGH TEMPERATURE GASES
Testing of a composite thermal structure to insulate the drivers of a large scale blast/thermal simulator
[AD-A234014] N91-26213
Supercritical fluid processing of propellant polymers
[AD-A234285] N91-26341
Strength of SiC- and Si-N-C-ceramic fibers exposed to high-temperature gaseous environments
[DE91-011099] N91-26380
HIGH TEMPERATURE LUBRICANTS
Additives for high temperature liquid lubricants
[DE91-011018] N91-26386
HIGH TEMPERATURE PLASMAS
Parametric studies of dense plasma focus for fusion space propulsion with D-He3
[AD-A234578] N91-26941
Development of a tactical high-power microwave source using the Plasma Electron Microwave Source (PEMS) concept
[AD-A234967] N91-26942
HIGH TEMPERATURE SUPERCONDUCTORS
Defect clustering and related properties of oxides
[DE91-011072] N91-26290
Investigation of a Hamiltonian with two sources of anisotropy: The Dzyaloshinskii-Moriya and single-size interactions
[DE91-011381] N91-26292
High temperature superconducting planar circuit structures for high frequency applications
[AD-A234335] N91-26445
Diagnostic studies of YBa2Cu3O(7-delta) laser ablation
[DE91-011382] N91-26515
Development of high Tc (greater than 110K) Bi, Tl and Y-based materials as superconducting circuit elements
[NASA-CR-188581] N91-26948
High-temperature ceramic superconductors
[AD-A234620] N91-26953
Bulk wave characterization of high T(sub c) superconductors
[AD-A234649] N91-26954
Electrochemically modulated superconductivity
[AD-A234703] N91-26955
Monolithic integration semiconductor and superconductor components
[AD-A234986] N91-26959
Superconducting high T(sub c) thin film vortex-flow transistor, phase 1
[AD-A235025] N91-26962
High temperature superconducting films and crystals
[AD-A235234] N91-26965
Formation of intermediate compounds during reduced pressure calcination of Y-Ba-Cu-O precursor
[DE91-011179] N91-26971
Microwave properties of high transition temperature superconducting thin films
[NASA-CR-185842] N91-26976
Defects in decomposed YBa2Cu4O8 (124) superconductor after rapid annealing
[DE91-010597] N91-26979
High-T(sub c) thin-film magnetometer
[DE91-011828] N91-26981
Critical currents in proton irradiated YBa2Cu3O(7-delta) crystals
[DE91-011835] N91-26982
HIGH VOLTAGES
High-power converters for space applications
[NASA-CR-187116] N91-26461
HISTOCHEMICAL ANALYSIS
Parallel processing and learning: Variability and chaos in self-organization of activity in groups of neurons
[AD-A234589] N91-26737
HISTOGRAMS
A physiologically motivated front end for speech recognition
[AD-A233727] N91-26414
HISTORIES
Historical aspects of radar atmospheric dynamics N91-26614
Personal papers in the United States Air Force Historical Research Center, 5th edition
[PB91-156380] N91-26999
HOLDERS
Removable hand hold
[NASA-CASE-LEW-15196-1] N91-26543
HOLDING
Passive and active grasping with a prehensile robot end-effector
[AD-A235085] N91-26539
HOLE GEOMETRY (MECHANICS)
Development and verification of global/local analysis techniques for laminated composites
[NASA-CR-185060] N91-26238
HOLES (MECHANICS)
Development and verification of global/local analysis techniques for laminated composites
[NASA-CR-185060] N91-26238
HOMEOSTASIS
Hormonal regulators of calcium metabolism following space flights of various durations N91-26689
HOMING DEVICES
The wild weasel development programs, one run, one hit, one error
[RAND-P-7661-RGS] N91-26431
HOMOGENEITY
Microstructure, plastic deformation and mechanical properties of mechanically alloyed NiAl and NiAl based alloys
[AD-A235135] N91-26303
HONEYCOMB STRUCTURES
Dynamic energy absorption of sandwich structures by inelastic deformation
[AD-A234903] N91-26564
HOOPS
Shell hoop prestress generated by welding
[DE91-011892] N91-26571
HOPPERS
The 1990 Sandia rocket-triggered lightning field tests at Kennedy Space Center, Florida
[DE91-011263] N91-26653
HORIZONTAL FLIGHT
Dynamics of elastic bending and torsion of hingeless rotors with dynamic stall
[AD-A234775] N91-26134
Performance optimization of helicopter rotor blades
[NASA-TM-104054] N91-26137
HORMONES
Hormonal regulators of calcium metabolism following space flights of various durations N91-26689
Functional activity of hypophyseal-thyroid system during 370-day antiorthostatic hypokinesia N91-26691
HOT SURFACES
India-stabilized zirconia coating for composites
[AD-D014857] N91-26224
HOUSINGS
Double face sealing device
[NASA-CASE-MFS-28521-1] N91-26542
HOVERING
Dynamics of elastic bending and torsion of hingeless rotors with dynamic stall
[AD-A234775] N91-26134
HOWITZERS
Application of software tools in embedded computers within military systems to enhance software reliability, quality assurance, and maintenance
[AD-A234555] N91-26785
HUBBLE SPACE TELESCOPE
Using HST: From proposal to science N91-27023
HUMAN BEHAVIOR
Neural mechanisms of attention
[AD-A235003] N91-26742
HUMAN BEINGS
A statistical analysis of -X rhesus head kinematics
[AD-A233977] N91-26674
Interaction of ionizing radiation, genetically active chemicals, and radiofrequency radiation in human and rodent cells
[AD-A234747] N91-26677
Biochemical aspects of human adaptation to combined effect of antiorthostasis, decreased barometric pressure, and increased oxygen content N91-26694
SPH-4 aircrew helmet impact protection improvements 1970-1990
[AD-A233784] N91-26750
HUMAN BODY
Advanced Dynamic Anthropomorphic Manikin (ADAM) design report
[AD-A234761] N91-26756
HUMAN FACTORS ENGINEERING
Evaluation of night vision goggles for maritime search and rescue
[AD-A233798] N91-26751
Notional helmet concepts: A survey of near-term and future technologies
[AD-A234475] N91-26752
Sitting posture analysis. An experimental optimisation approach
[ITN-91-85114] N91-26760
NASA information sciences and human factors program
[NASA-TM-4291] N91-27119
HUMAN PERFORMANCE
Expert system explanation: The user perspective
[AD-A233739] N91-26749
Notional helmet concepts: A survey of near-term and future technologies
[AD-A234475] N91-26752
HUMAN REACTIONS
Individual stereotypes of human neuropsychic prognostic activity in problem situations with different probability structures N91-26695
HUMAN TOLERANCES
Biochemical aspects of human adaptation to combined effect of antiorthostasis, decreased barometric pressure, and increased oxygen content N91-26694
HUMIDITY
Regeneration of whetlerite for adsorbing toxic pollutants from air
[AD-D014859] N91-26753
Effect of a passive cooling vest on tension/anxiety and fatigue in a high heat and high humidity naval environment
[AD-A234657] N91-26755
HURRICANES
Hurricane Research Division fiscal year 1990 programs-fiscal year 1991 projections
[PB91-153452] N91-26641
Analysis of wave characteristics in extreme seas
[AD-A234538] N91-26660
HYDRATES
Microstructure, porosity, and mechanical property relationships of calcium-silicate-hydrate
[AD-A235191] N91-26279
Electrochemically induced charge and mass transport in polypyrrole/poly(styrene sulfonate) molecular composites
[AD-A234599] N91-26354
HYDRATION
Microstructure, porosity, and mechanical property relationships of calcium-silicate-hydrate
[AD-A235191] N91-26279
HYDRAULIC FLUIDS
Lubricants at low temperatures
[AD-A234536] N91-26348
HYDRAZINES
Air Force stock fund: Hydrazine sales consistent with the Commercial Space Launch Act. Report to the Chairman, Committee on Science, Space and Technology, House of Representatives
[GAO/NSIAD-91-196] N91-26397
HYDRIDES
Diethylsilane decomposition on silicon surfaces studied using transmission FTIR spectroscopy
[AD-A234638] N91-26266
HYDROCARBONS
Fundamental studies of carbenes and hydrocarbon radicals
[DE91-011029] N91-26286
Commercializing solar hydrogen production
[DE91-011232] N91-26398
HYDRODYNAMIC EQUATIONS
Determination of flow-regime boundaries for cohesive particles
[DE91-010552] N91-26468
HYDRODYNAMICS
Measurements of the longitudinal movements of O(+) ions in the subauroral upper atmosphere from the Aureol 3 satellite N91-26171
Turbulent processes of mass-loading of new ions on Venus and Mars and the problems of numerical models of the interaction of solar wind with these planets. 1: Characteristics of the flow of solar wind around the planets N91-26174
JPRS report: Science and technology. USSR: Earth sciences
[JPRS-UES-91-003] N91-26582
Gravity waves and instabilities in the lower and middle atmosphere N91-26621
HYDROGEN
Comparison of H2 desorption kinetics from Si(111)7x7 and Si(100)2x1
[AD-A234634] N91-26263
The synthesis of methanol by a novel method
[DE91-011131] N91-26291
Laser-induced desorption of H2 from Si(111)7x7
[AD-A234636] N91-26508
HYDROGEN ATOMS
Isotropic exchange in the platinum-catalyzed reduction of olefins in protic solvents
[AD-A234828] N91-26208

Comparison of hydrogen desorption kinetics from Si(111)7x7 and Si(100)2x1
[AD-A234633] N91-26262

HYDROGEN PRODUCTION
Commercializing solar hydrogen production
[DE91-011232] N91-26398
Design of a lunar oxygen production plant N91-27109

HYDROGENATION
The reduction by deuterium on platinum black of exo-2-norbornyl and endo-2-norbornyl to norbornane-2-d occurs with predominant retention of configuration
[AD-A235057] N91-26277
The synthesis of methanol by a novel method
[DE91-011131] N91-26291

HYDROLYSIS
Thermal degradation chemistry of poly(diphenoxy phosphazene)
[AD-A235284] N91-26282

HYDROPONICS
Higher plants as part of biological human life support system N91-26693

HYDROSTATICS
The development of an improved convective initiation scheme for Mesoscale numerical weather prediction models, phase 1
[AD-A235417] N91-26650

HYOSCINE
Assessment of the pharmacodynamics of intranasal, intravenous and oral scopolamine N91-27114

HYPERBOLIC DIFFERENTIAL EQUATIONS
Spectral recovery of discontinuous data
[ITN-91-85115] N91-26853

HYPEROXIA
Biochemical aspects of human adaptation to combined effect of antiorthostasis, decreased barometric pressure, and increased oxygen content N91-26694

HYPERSONIC FLOW
Numerical investigations in three-dimensional internal flows
[NASA-CR-188615] N91-26114

HYPERSONIC VEHICLES
Navier-Stokes calculations of scramjet-nozzle-afterbody flowfields
[NASA-CR-185356] N91-26488

HYPERVELOCITY LAUNCHERS
Electromagnetic launch technology assessment. Scientific basis and unified treatment: Forces and electromechanical power conversion (analytical and numerical methods)
[AD-A235028] N91-26185
Hypervelocity launch capabilities to over 10.4 km/s
[DE91-010859] N91-26186
Performance of hypervelocity armatures with replenished metal vapor plasmas
[DE91-011931] N91-26187

HYPOKINESIA
JPRS Report: Science and technology. USSR: Life sciences
[JPRS-ULS-91-009] N91-26688
Functional activity of hypophyseal-thyroid system during 370-day antiorthostatic hypokinesia N91-26691
Changes in rheologic indices of blood and hemodynamics during 14-day antiorthostatic hypokinesia N91-26692
Reaction of human skeletal muscle fibers to 370 day antiorthostatic hypokinesia combined with physical exertion N91-26702
Effect of 7 day antiorthostatic hypokinesia on cardiac pumping action in monkeys N91-26704

HYPOTHERMIA
COLDEX-86: Fluid and electrolyte changes during prolonged cold water immersion
[AD-A233768] N91-26711
Metabolic changes and hemodynamic dysfunction following hypothermic shock
[AD-A233942] N91-26713

HYPOTHESES
Integration of neurobiological and computational analyses of the neural network essentials for conditioned taste aversion
[AD-A235164] N91-26744
On measures of misconception stability
[AD-A234952] N91-26847

HYSTERESIS
An experimental and numerical study of wavemaker dissipation in the process of direct generation of the resonant sloshing waves in a rectangular tank
[ITN-91-85103] N91-26481
The hysteresis and incremental collapse of complex structures: A paradigm for the fatigue failure of materials
[AD-A234831] N91-26563

I

ICE
Characteristics of aerosol in the atmosphere of Mars according to data from the KRFM experiment N91-26175
West Antarctic Ice Sheet Initiative. Volume 2: Discipline Reviews
[NASA-CP-3115-VOL-2] N91-26573
The examination of dislocations in ice
[AD-A233716] N91-26586
Growth, evaporation and melting of ice crystals: Implications for radiation, atmospheric dynamics and particle scavenging N91-26611
Development and verification of a physical cloud-moisture model for use in general circulation models
[AD-A234751] N91-26643

ICE ENVIRONMENTS
A review of precipitation-related aspects of West Antarctic meteorology N91-26574

ICE FORMATION
Applied high-speed imaging for the icing research program at NASA Lewis Research Center
[NASA-TM-104415] N91-26490
Sea-level response to ice sheet evolution: An ocean perspective N91-26575
Ice cores and SeaRISE: What we do (and don't) know N91-26579

ICE MAPPING
Terrestrial geophysics in the SeaRISE project N91-26576
Glacial dynamics (glaciology) N91-26580

ICEBERGS
Sea-level response to ice sheet evolution: An ocean perspective N91-26575

IDENTIFYING
Proton arc doses to the primate head
[AD-A235134] N91-26726

IGNITION
Laser initiated ignition of liquid propellant
[AD-A233777] N91-26388

ILLUMINANCE
Illuminance and luminance distributions of a prototype ambient illumination system for Space Station Freedom
[NASA-TM-103541] N91-26193

ILLUMINATING
Illuminance and luminance distributions of a prototype ambient illumination system for Space Station Freedom
[NASA-TM-103541] N91-26193
Higher plants as part of biological human life support system N91-26693

ILMENITE
Design of a lunar oxygen production plant N91-27109

IMAGE CONTRAST
The shape of shading
[AD-A234419] N91-26781
Comparison of sound pressure in a wedge-shaped ocean as predicted by an image method and a PE model
[AD-A234191] N91-26879

IMAGE CORRELATORS
Automatic target recognition using acousto-optic image correlator
[DE91-011499] N91-26936
Design of optimal correlation filters for hybrid vision systems N91-27110

IMAGE ENHANCEMENT
One-dimensional translation measurement of speckle from rough rotating objects in ultraviolet illumination
[AD-A233719] N91-26919
Photographic image enhancement N91-27094

IMAGE FILTERS
High order differentiation filters that work
[AD-A234504] N91-26874

IMAGE PROCESSING
Chinese space science and technology (selected articles)
[AD-A234798] N91-26180
Applied high-speed imaging for the icing research program at NASA Lewis Research Center
[NASA-TM-104415] N91-26490
UV aurora mapping in corrected geomagnetic coordinates
[ITN-91-85106] N91-26636
OSIRRUS: Oceanic symbolic image representation, recognition and understanding software
[AD-A235112] N91-26665
Iterated transform image compression
[AD-A233655] N91-26769
The shape of shading
[AD-A234419] N91-26781
Parallel algorithms for least squares and related computations
[AD-A235018] N91-26790
Understanding object classes: Modeling and matching
[AD-A235027] N91-26848
Automatic target recognition using acousto-optic image correlator
[DE91-011499] N91-26936
Photographic image enhancement N91-27094
Design of optimal correlation filters for hybrid vision systems N91-27110
High accuracy optical rate sensor N91-27115

IMAGE RESOLUTION
Temporal and spatial correlations in images distorted by a random medium
[ITN-91-85107] N91-26935

IMAGE ROTATION
The effect of rotation on legibility of dot-matrix characters
[AD-A235034] N91-27008

IMAGES
Imaging of fluorescent and chemiluminescent DNA hybrids using a 2-D CCD camera
[AD-A234641] N91-26676
Photoinduced absorption and erasable optical information storage in polyanilines
[AD-A234108] N91-27002

IMAGING TECHNIQUES
Applied high-speed imaging for the icing research program at NASA Lewis Research Center
[NASA-TM-104415] N91-26490
Imaging of fluorescent and chemiluminescent DNA hybrids using a 2-D CCD camera
[AD-A234641] N91-26676
Iterated transform image compression
[AD-A233655] N91-26769
Northeast Artificial Intelligence Consortium (NAIC). Volume 7: Automatic photointerpretation
[AD-A234886] N91-26821
Temporal and spatial correlations in images distorted by a random medium
[ITN-91-85107] N91-26935
Dust in the Mars atmosphere N91-27082

IMMUNITY
A study of murine bone marrow cells cultured in bioreactors which create an environment which simulated microgravity N91-27101

IMMUNOLOGY
JPRS report: Science and technology. USSR: Life sciences
[JPRS-ULS-91-011] N91-26696
Parallel processing and learning: Variability and chaos in self-organization of activity in groups of neurons
[AD-A234589] N91-26737

IMPACT
KC-135 ground collision avoidance system questionnaire
[AD-A234385] N91-26125
Evaluation of the C/EC/KC-135 Ground Collision Avoidance System (GCAS), study 1
[AD-A235301] N91-26130
Ricochet of sphere off water
[ITN-91-85102] N91-26480
SPH-4 aircrew helmet impact protection improvements 1970-1990
[AD-A233784] N91-26750

IMPACT ACCELERATION
A statistical analysis of -X rhesus head kinematics
[AD-A233977] N91-26674
Physical and psychogenic sequelae of impact acceleration on tracking performance of operators N91-26701
Advanced Dynamic Anthropomorphic Manikin (ADAM) design report
[AD-A234761] N91-26756

IMPACT LOADS
Response of whisker-reinforced ceramic matrix composites to dynamic compressive loading N91-26236
Mechanics, impact loads and EMG on the space shuttle treadmill N91-27112

IMPACT STRENGTH
Microalloyed steel preforms
[AD-A234039] N91-26296

IMPACT TESTS
Mechanical properties of polycarbonate-polysulfone and polycarbonate-polyetherimide blends
[AD-A234939] N91-26360
SPH-4 aircrew helmet impact protection improvements 1970-1990
[AD-A233784] N91-26750

IMPEDANCE
Impedance profiling: A convenient technique for determining the redox or protonic acid doping characteristics of conducting polymers
[AD-A233941] N91-26337
Input impedance and gain of monopole elements with disk ground planes on flat earth
[AD-A234284] N91-26421

IMPELLERS
Titanium alloy integrated centrifugal impeller 5 coordinate computer assisted manufacturing technology
[AD-A234797] N91-26300
IMPLOSIONS
Planar indirect-drive Rayleigh-Taylor experiments on Nova
[DE91-011967] N91-26943
IMPURITIES
Effect of turbulence on impurity observation in upper atmosphere using lidar method N91-26584
INCOHERENT SCATTER RADAR
Middle Atmosphere Program. Handbook for MAP. Volume 30: International School on Atmospheric Radar
[NASA-CR-188623] N91-26613
Incoherent scatter radar observations of the ionosphere N91-26623
INCOMPRESSIBLE BOUNDARY LAYER
Hydroacoustics of intermittent boundary-layer flow: A review
[AD-A235092] N91-26883
INCOMPRESSIBLE FLOW
An experimental investigation of structure, mixing, and combustion in compressible turbulent shear layers
[AD-A235278] N91-26281
INCOMPRESSIBLE FLUIDS
An experimental investigation of structure, mixing, and combustion in compressible turbulent shear layers
[AD-A235278] N91-26281
INCONEL (TRADEMARK)
Precipitation in Alloy 718: A combined AEM and APFIM investigation
[DE91-009918] N91-26314
INDEXES (DOCUMENTATION)
National Bureau of Standards Publications 1977-1987. Volume 2: Indexes
[PB91-136515] N91-26997
INDIUM GALLIUM ARSENIDES
Thin film alloys on semiconductor substrates
[DE91-012355] N91-26985
INDIUM PHOSPHIDES
Submicron gate InP power MISFET's with improved output power density at 18 and 20 GHz N91-26436
INDUSTRIAL PLANTS
Design of a lunar oxygen production plant N91-27109
INDUSTRIAL SAFETY
Composite fiber hazards
[AD-A233924] N91-26211
INELASTIC SCATTERING
Calculation of the conductance of two dimensional narrow wires
[ITN-91-85109] N91-26460
Nonperturbative behavior of quarks
[DE91-011905] N91-26903
Photons and neutrons
[DE91-010980] N91-26906
INEQUALITIES
Covering a closed curve with a given total curvature
[AD-A234342] N91-26840
INERTIAL CONFINEMENT FUSION
Development of a subpicosecond, tunable LiCAF (Cr:LiCaAlF6) laser
[DE91-012082] N91-26526
INFERENCE
BaRT manual version 3.0
[AD-A234528] N91-26784
Northeast Artificial Intelligence Consortium (NAIC). Volume 14: Knowledge base retrieval using plausible inference
[AD-A234893] N91-26828
Retrieval using plausible inference
[AD-A235015] N91-27006
INFLATABLE STRUCTURES
The effects of space debris on solar propulsion
[AD-A235257] N91-26192
INFORMATION
Coordination in large scale software development
[AD-A234898] N91-26787
NSI white pages project: X.500 directory service N91-27039
INFORMATION DISSEMINATION
National Bureau of Standards Publications 1977-1987. Volume 2: Indexes
[PB91-136515] N91-26997
NSI white pages project: X.500 directory service N91-27039
INFORMATION FLOW
Coordination in large scale software development
[AD-A234898] N91-26787
INFORMATION MANAGEMENT
Notional helmet concepts: A survey of near-term and future technologies
[AD-A234475] N91-26752
On-line magnetic tape Library Inventory Tracking And Reporting (LITAR) system
[AD-A234934] N91-27004
A guide to NASA's Pilot Land Data System (PLDS) N91-27035
INFORMATION PROCESSING (BIOLOGY)
Mechanisms of adaptive information processing
[AD-A234435] N91-26734
Parallel processing and learning: Variability and chaos in self-organization of activity in groups of neurons
[AD-A234589] N91-26737
Categories and particulars: Prototype effects in estimating spatial location
[AD-A234955] N91-26741
Integration of neurobiological and computational analyses of the neural network essentials for conditioned taste aversion
[AD-A235164] N91-26744
INFORMATION RETRIEVAL
Advanced Satellite Research Project: SCAR Research Database. Bibliographic analysis
[NASA-CR-186086] N91-26182
Lead detection and mapping with reference to relationships between scale, sensor characteristics, surface conditions and atmospheric properties
[AD-A235121] N91-26666
Northeast Artificial Intelligence Consortium (NAIC). Volume 14: Knowledge base retrieval using plausible inference
[AD-A234893] N91-26828
Retrieval using plausible inference
[AD-A235015] N91-27006
COSMIC: Software catalog 1991 edition diskette format N91-27036
INFORMATION SYSTEMS
AQUIS: An air quality and permit information management system
[DE91-011750] N91-26608
Retrieval using plausible inference
[AD-A235015] N91-27006
The Internet resources guide and the Automatic Login Executor (ALEX) N91-27030
NSI conference support N91-27031
Electronic software submittal/distribution N91-27033
The NASA master directory quick reference guide N91-27034
A guide to NASA's Pilot Land Data System (PLDS) N91-27035
NSI white pages project: X.500 directory service N91-27039
NSI customer service representatives and user support office: NASA Science Internet N91-27040
Catalog of data bases and reports
[DE91-011516] N91-27043
INFORMATION TRANSFER
The High Resolution Profiler (HRP): User's guide and software modifications documentation
[AD-A234640] N91-26663
Electronic software submittal/distribution N91-27033
INFRARED ASTRONOMY
CBSD version 2 component models of the IR celestial background
[AD-A235372] N91-27048
INFRARED DETECTORS
Design for electronic spectrally tunable infrared detector
[AD-D014877] N91-26925
INFRARED IMAGERY
Progress with neural network gulf streams
[AD-A233810] N91-26658
OSIRRUS: Oceanic symbolic image representation, recognition and understanding software
[AD-A235112] N91-26665
INFRARED INSTRUMENTS
Atmospheric InfraRed Sounder (AIRS): Science and measurement requirements
[NASA-TM-104977] N91-26624
INFRARED LASERS
Laser switched power linac
[AD-A234581] N91-26507
Infrared and visible laser double resonance studies of vibrational energy transfer processes in polyatomic molecules
[DE91-012162] N91-26910
INFRARED RADIATION
Far- and mid-infrared properties of metal-insulator composite materials
[AD-A234264] N91-26219
Photoexcitation spectroscopy of pernigraniline
[AD-A233841] N91-26250
Atmospheric InfraRed Sounder (AIRS): Science and measurement requirements
[NASA-TM-104977] N91-26624
CBSD version 2 component models of the IR celestial background
[AD-A235372] N91-27048
Derivation of mid-infrared (5-25 microns) optical constants of some silicates and palagonite N91-27077
Dust in the Mars atmosphere N91-27082
INFRARED REFLECTION
Bidirectional reflectance distribution (BRDF) of NASA shuttle tiles
[AD-A235115] N91-26188
INFRARED SPECTRA
FTIR studies of water and ammonia decomposition on silicon surfaces
[AD-A234637] N91-26265
Process monitoring of polyurethane foam using Fourier transform infrared spectroscopy
[DE91-010578] N91-26385
INFRARED SPECTROSCOPY
Diethylsilane decomposition on silicon surfaces studied using transmission FTIR spectroscopy
[AD-A234638] N91-26266
Multispectral identification of potentially hazardous byproducts of ozonation and chlorination. Part 1: Studies of chromatographic and spectroscopic properties of MX
[PB91-161703] N91-26601
INHOMOGENEITY
Inverse scattering problems for acoustic waves in an inhomogeneous medium N91-26876
Temporal and spatial correlations in images distorted by a random medium
[ITN-91-85107] N91-26935
INITIATORS (EXPLOSIVES)
Shock response of Detasheet
[DE91-010923] N91-26399
INJECTION
Transport and fate of acetone in an outdoor model stream, Stennis Space Center near Bay St. Louis, Mississippi
[PB91-154674] N91-26600
INJECTORS
Method of injecting fluid propellants into a rocket combustion chamber
[NASA-CASE-LEW-14846-2] N91-26200
INJURIES
Proceedings of the 7th User's Stress Workshop
[AD-A234583] N91-26736
INLET FLOW
Numerical investigations in three-dimensional internal flows
[NASA-CR-188615] N91-26114
INORGANIC MATERIALS
Catalysts and initiators as instruments controlling structure of polymers with inorganic backbone
[AD-A235350] N91-26368
INPUT/OUTPUT ROUTINES
Ada software portability and level 2 system simulator integration issues
[AD-A233757] N91-26773
NRL connection machine Fortran library
[AD-A234121] N91-26779
INSERTS
Effect of initial delamination on Mode 1 and Mode 2 interlaminar fracture toughness and fatigue fracture threshold
[NASA-TM-104079] N91-26569
INSPECTION
X ray-computed tomography for inspecting industrial parts
[DE91-011390] N91-26554
INSTRUMENT ERRORS
HORACE: Presentation-level protocol standard for digital transmission of monochrome television images
[AD-A235276] N91-26428
Evaluating the effect of accuracy ratios on the percent of calibrations which are out of tolerance N91-27107
INSULATION
Far- and mid-infrared properties of metal-insulator composite materials
[AD-A234264] N91-26219
INSULATORS
The electronic structure of the ionic insulator sodium nitrite
[DE91-009766] N91-26977
INSULIN
Peptide transport through the blood-brain barrier
[AD-A233753] N91-26708
Pharmacological sparing of protein in burn injury
[AD-A235026] N91-26724
INTEGERS
Primes: The first 2400 prime numbers
[AD-A233979] N91-26837
INTEGRAL CALCULUS
Research in stochastic processes
[AD-A234650] N91-26860
INTEGRAL EQUATIONS
Interfacial slippage of a unidirectional fiber composite under longitudinal shearing
[AD-A234186] N91-26216

Covering a closed curve with a given total curvature
[AD-A234342] N91-26840

INTEGRATED CIRCUITS
Grain boundary chemistry in Al-Cu metallizations as determined by analytical electron microscopy
[DE91-012007] N91-26319
Metastable pitting corrosion of aluminum, Al-Cu, and Al-Si thin films in dilute HF solutions and its relevancy to the processing of integrated circuit interconnections
[DE91-012014] N91-26320
MMIC integration technology investigation
[NASA-CR-188035] N91-26434
Four-to-one power combiner for 20 GHz phased array antenna using RADC MMIC phase shifters N91-26435
Active devices for monolithic millimeter-wave integrated circuits
[AD-A234033] N91-26440
De-embedding millimeter-wave integrated circuits with TRL
[AD-A234194] N91-26442
High temperature superconducting planar circuit structures for high frequency applications
[AD-A234335] N91-26445
An electron-beam dose deposition experiment: TIGER 1-D simulation code versus thermoluminescent dosimetry
[AD-A234507] N91-26447
Long-term prediction test procedure for most ICs, based on linear response theory
[NASA-CR-185843] N91-26462
Testing the One-Port Random Access Memory (1PRAM) module of TRW's CPUAX signal processing superchip
[AD-A234127] N91-26761
Monolithic integration semiconductor and superconductor components
[AD-A234986] N91-26959

INTELLIGIBILITY
Intelligibility of digital speech masked by noise: Normal hearing and hearing impaired listeners
[AD-A234852] N91-26427

INTERCEPTION
Boost-phase kill versus midcourse discrimination: The grand inquisitor's solution
[DE91-011744] N91-26871

INTERFACES
Effect of a viscoelastic interface on the transverse behavior of fiber-reinforced composites
[AD-A233986] N91-26212
Interfacial slippage of a unidirectional fiber composite under longitudinal shearing
[AD-A234186] N91-26216
Interfacial force sensor with force-feedback control
[DE91-004897] N91-26495
The High Resolution Profiler (HRP): User's guide and software modifications documentation
[AD-A234640] N91-26663

INTERFACIAL ENERGY
Polaron ground state in a double heterostructure of polar crystals
[AD-A235037] N91-26963

INTERFACIAL TENSION
Simulation of pore scale porous media flow using lattice gas methods
[DE91-004829] N91-26484

INTERFEROMETERS
Atom wave interferometer
[AD-A234863] N91-26494
Full surface testing of grazing incidence mirrors
[AD-A234005] N91-26922

INTERFEROMETRY
Neutral atom deBroglie-wave interferometry
[AD-A234624] N91-26896
Thickness measurements of silicon films using partial coherence interferometry
[AD-A235211] N91-26930

INTERMETALLICS
Quantum mechanical approach to understanding microstructural and mechanical properties of intermetallics
[AD-A234702] N91-26298
Fundamentals of mechanical behavior in intermetallic compounds
[AD-A235016] N91-26301
Environmental embrittlement of ordered intermetallic alloys at room temperature in moist atmospheres
[DE91-012051] N91-26321
Microstructure and hardness of NiAl/Ni2AlX two-phase ordered intermetallic alloys
[DE91-012068] N91-26323
The role of electronic structure in the mechanical behavior of aluminides
[DE91-012508] N91-26325
Plasticity of single crystalline Al3X intermetallic compounds
[AD-A234699] N91-26356

INTERNAL COMBUSTION ENGINES
Turbulent premixed hydrogen/air flames
[AD-A235109] N91-26278
Variable speed gas engine-driven air compressor system. Phase 1: System analysis
[PB91-159533] N91-26530

INTERNAL WAVES
Gravity waves and instabilities in the lower and middle atmosphere N91-26621

INTERPLANETARY SPACECRAFT
Planetary spacecraft cost modeling utilizing labor estimating relationships N91-27116

INTERPROCESSOR COMMUNICATION
NSI organization and highlights N91-27011
Customer requirements process N91-27012
NSI engineering review N91-27013
Backbone upgrades and DEC equipment replacement N91-27014
User support services and network application development: An overview N91-27015
NSI security task: Overview N91-27016
National research and education network N91-27017
NASA's use of FTS2000 services N91-27018
FTS2000 network architecture N91-27019
Science network resources: Distributed systems N91-27021

INTRACRANIAL PRESSURE
The Trendelenburg position after cerebral air embolism in dogs: Effects on the somatosensory evoked potential, intracranial pressure, and blood-brain barrier
[AD-A233809] N91-26673

INTRUSION
Pressure distribution and induced force field on a conical nozzle due to impingement of a normal jet into the supersonic cross-flow
[AD-A233981] N91-26115

INVENTORIES
On-line magnetic tape Library Inventory Tracking And Reporting (LITAR) system
[AD-A234934] N91-27004
Response latency measures for biographical inventories
[AD-A235010] N91-27005
COSMIC: Software catalog 1991 edition diskette format N91-27036

INVERSE SCATTERING
Inverse scattering problems for acoustic waves in an inhomogeneous medium N91-26876

INVERSIONS
The SYNOP experiment: Inverted echo sounder data report for June 1989 to September 1990
[AD-A234625] N91-26662

IO
A catalog of high resolution Jovian decametric radio noise burst spectra, volume 1 N91-27047

IODINE
Surface diffusion at the liquid-solid interface: Quenching of fluorescence from pyrene covalently bound to methylated silica
[AD-A234645] N91-26268

ION BEAMS
Chemistry on an atomic scale of ion-beam modified surfaces
[AD-A233707] N91-26891

ION DENSITY (CONCENTRATION)
Computer modeling of soot formation comparing free radical and ionic mechanisms
[AD-A235007] N91-26273

ION EMISSION
LIF and emission studies of copper and nitrogen N91-27089

ION EXCHANGING
Partial oxidation of light alkanes in transition-metal ion containing zeolites
[DE91-008202] N91-26243
Ionically and electronically conductive composite polymer membranes
[AD-A234587] N91-26349

ION IMPLANTATION
Investigation and characterization of ITO/poly-Si photovoltaic junctions
[ITN-91-85105] N91-26590
Study of the effect of reactive element addition by implanting metal ions in a pre-formed oxide layer
[DE91-011916] N91-26974

ION PROBES
Studies of resonantly enhanced multiphoton ionization processes in molecules
[AD-A235217] N91-26898
Negative ion photodetachment as a probe of the transition state region: The I + HI reaction
[AD-A235297] N91-26900

ION RECOMBINATION
Computer modeling of soot formation comparing free radical and ionic mechanisms
[AD-A235007] N91-26273

ION SCATTERING
Laser spectroscopy characterization of materials for frequency agile solid state laser systems
[AD-A233916] N91-26500

ION STORAGE
Cluster beam analysis via photoionization
[AD-A234111] N91-26253

ION TEMPERATURE
Measurements of the longitudinal movements of O(+) ions in the subauroral upper atmosphere from the Aureol 3 satellite N91-26171

IONIZATION
Laser ionic multiphoton dissociation of some acrylate clusters
[AD-A233801] N91-26247
Cationic polymerization within van der Waals clusters of the form (CH2=R)n where R=CH2, CF2 and CHCH3
[AD-A234233] N91-26255
Frequency upshifting of laser pulses by ionization fronts
[AD-A234354] N91-26503
Saturation and kinetic issues for optical-field-ionized plasma x ray lasers
[DE91-012079] N91-26517

IONIZATION CHAMBERS
Absorbed-dose calibration of ionization chambers in a Co-60 gamma-ray beam
[PB91-132290] N91-26890
A test of the IAEA code of practice for absorbed dose determination in photon and electron beams
[OEFZS-4565] N91-26913

IONIZATION FREQUENCIES
Propagation of RF signals through structured ionization: The general model
[AD-A234051] N91-26418

IONIZING RADIATION
Interaction of ionizing radiation, genetically active chemicals, and radiofrequency radiation in human and rodent cells
[AD-A234747] N91-26677

IONOPAUSE
Turbulent processes of mass-loading of new ions on Venus and Mars and the problems of numerical models of the interaction of solar wind with these planets. 1: Characteristics of the flow of solar wind around the planets N91-26174

IONOSONDES
Historical aspects of radar atmospheric dynamics N91-26614
ARTIST tape output formats
[AD-A235173] N91-26633

IONOSPHERIC DISTURBANCES
Propagation of RF signals through structured ionization: The general model
[AD-A234051] N91-26418
Technique for measuring ionospheric irregularities generated by high power oblique HF heating of the F-region
[AD-A233883] N91-26627
The effects of magnetic storm phases on F-layer irregularities from auroral to equatorial latitudes
[AD-A235170] N91-26632

IONOSPHERIC PROPAGATION
Propagation of RF signals through structured ionization: The general model
[AD-A234051] N91-26418
System concept and analysis of an Artificial Ionospheric Mirror (AIM) radar
[AD-A234289] N91-26630

IONS
Measurements of the longitudinal movements of O(+) ions in the subauroral upper atmosphere from the Aureol 3 satellite N91-26171
Turbulent processes of mass-loading of new ions on Venus and Mars and the problems of numerical models of the interaction of solar wind with these planets. 1: Characteristics of the flow of solar wind around the planets N91-26174
A room-temperature, flashpumped, 2.09 micron solid state laser
[AD-D014871] N91-26506
Strong exchange coupling in lanthanide bis(phthalocyaninato) sandwich compounds
[AD-A234466] N91-26951

IRON
Adsorption of ammonia on iron clusters
[DE91-011125] N91-26308

IRON ALLOYS
Chemical phase separation in binary iron-chromium alloys
[DE91-010282] N91-26294
US and foreign alloy cross-reference database
[NASA-CR-184166] N91-26313
TEM in-situ straining of B2 compounds
[DE91-012062] N91-26322

Investigation of plessite in iron meterorites and laboratory Fe-Ni(P) alloys
[DE91-010858] N91-27053

IRON METEORITES
Investigation of plessite in iron meterorites and laboratory Fe-Ni(P) alloys
[DE91-010858] N91-27053

IRRADIATION
Precision high-power solid-state laser diagnostics for target-irradiation studies and target-plane irradiation modeling
[DE91-012036] N91-26523
Proton arc doses to the primate head
[AD-A235134] N91-26726
Critical currents in proton irradiated YBa2Cu3O(7-delta) crystals
[DE91-011835] N91-26982

IRREGULAR VARIABLE STARS
The light curve of the magnetic star AM - Herculis
[ITN-91-85108] N91-27049

IRREGULARITIES
The effects of magnetic storm phases on F-layer irregularities from auroral to equatorial latitudes
[AD-A235170] N91-26632

ISING MODEL
Trimodal random-field Ising systems in a transverse field
[AD-A235038] N91-26875

ISOLATORS
An ultraviolet optical isolator utilizing the KDP-isomorphs
[AD-D014860] N91-26923

ISOTOPE EFFECT
Development of advanced methods based on stable isotope technology for studies of exercise in heat
[AD-A234670] N91-26719

ISOTROPIC TURBULENCE
Turbulent premixed hydrogen/air flames
[AD-A235109] N91-26278

ISOTROPISM
Isotropic exchange in the platinum-catalyzed reduction of olefins in protic solvents
[AD-A234828] N91-26208

ISOTROPY
Isotropic exchange in the platinum-catalyzed reduction of olefins in protic solvents
[AD-A234828] N91-26208

ITERATIVE SOLUTION
Iterated transform image compression
[AD-A233655] N91-26769
Backscattering from rough interfaces and the parabolic approximation
[AD-A235184] N91-26886

ITO (SEMICONDUCTORS)
Investigation and characterization of ITO/poly-Si photovoltaic junctions
[ITN-91-85105] N91-26590

J

JAHN-TELLER EFFECT
Partial oxidation of light alkanes in transition-metal ion containing zeolites
[DE91-008202] N91-26243

JET ENGINE FUELS
What fuels our future?
[AD-A233674] N91-26387

JET FLOW
Turbulent premixed hydrogen/air flames
[AD-A235109] N91-26278
Abrasive-waterjet machining of isogrid structures
[AD-A234628] N91-26405

JET IMPINGEMENT
Pressure distribution and induced force field on a conical nozzle due to impingement of a normal jet into the supersonic cross-flow
[AD-A233981] N91-26115

JET MIXING FLOW
CFD analysis of jet mixing in low NOx flametube combustors
[NASA-TM-104466] N91-26146

JOINTS (JUNCTIONS)
The development of piezoelectric poly(vinylidene fluoride) sensors for measuring peel stresses in adhesive joints
[AD-A233880] N91-26559

JOSEPHSON JUNCTIONS
Low frequency noise in resonant Josephson soliton oscillators
[DE91-011911] N91-26464
Study of Josephson effect arrays as sources at 1 THz
[AD-A234526] N91-26952
Quantum limited quasiparticle mixers at 100 GHz
[DE91-011894] N91-26973

JP-8 JET FUEL
What fuels our future?
[AD-A233674] N91-26387

JUPITER (PLANET)
A catalog of high resolution Jovian decametric radio noise burst spectra, volume 1 N91-27047

K

KINEMATICS
The kinematics of turbulent boundary layer structure
[NASA-TM-103859] N91-26465
Theoretical studies of the kinematics, dynamics, stability, and control of unsteady/vortical flows
[AD-A235190] N91-26477
Constrained trajectory optimization for kinematically redundant arms
[NASA-CR-183477] N91-26527
Line kinematics for whole-arm manipulation
[AD-A234422] N91-26535
A statistical analysis of -X rhesus head kinematics
[AD-A233977] N91-26674
Advanced Dynamic Anthropomorphic Manikin (ADAM) design report
[AD-A234761] N91-26756

KINETIC ENERGY
Size dependence of gaseous cluster reactivity and evaporation dynamics as a mechanistic probe
[AD-A233811] N91-26249

KINETIC EQUATIONS
Thermoluminescence kinetics of pyrite (FeS2)
[DE91-011710] N91-26990

KINETIC HEATING
Adsorption and decomposition of diethylsilane on silicon surfaces
[AD-A234639] N91-26267

KINETICS
Grain boundary cavitation processes in a Ni3Al alloy at elevated temperatures
[AD-A235279] N91-26307
Thermoluminescence kinetics of pyrite (FeS2)
[DE91-011710] N91-26990

KLYSTRONS
High power klystron amplifier
[AD-D014862] N91-26448

KNOWLEDGE BASES (ARTIFICIAL INTELLIGENCE)
Analysis of knowledge-based expert systems as tools for construction design
[AD-A234473] N91-26404
Translating expert system rules into Ada code with validation and verification
[NASA-CR-187505] N91-26800
Northeast Artificial Intelligence Consortium (NAIC). Volume 2: Discussing, using, and recognizing plans
[AD-A234881] N91-26816
Northeast Artificial Intelligence Consortium (NAIC). Volume 3: The Versatile Maintenance Expert System (VMES)
[AD-A234882] N91-26817
Northeast Artificial Intelligence Consortium (NAIC). Volume 4: Distributed artificial intelligence for communications network management
[AD-A234883] N91-26818
Northeast Artificial Intelligence Consortium (NAIC). Volume 5: Distributed planning for dynamic environments in the presence of time constraints
[AD-A234884] N91-26819
Northeast Artificial Intelligence Consortium (NAIC). Volume 6: Building an intelligent assistant: The acquisition, integration, and maintenance of complex distributed tasks
[AD-A234885] N91-26820
Northeast Artificial Intelligence Consortium (NAIC). Volume 7: Automatic photointerpretation
[AD-A234886] N91-26821
Northeast Artificial Intelligence Consortium (NAIC). Volume 8: Artificial intelligence applications to speech recognition
[AD-A234887] N91-26822
Northeast Artificial Intelligence Consortium (NAIC). Volume 9: A planner system for the application of indications and warning
[AD-A234888] N91-26823
Northeast Artificial Intelligence Consortium (NAIC). Volume 10: Time oriented problem solving
[AD-A234889] N91-26824
Northeast Artificial Intelligence Consortium (NAIC). Volume 11: Knowledge base maintenance
[AD-A234890] N91-26825
Northeast Artificial Intelligence Consortium (NAIC). Volume 12: Computer architecture for very large knowledge bases
[AD-A234891] N91-26826
Northeast Artificial Intelligence Consortium (NAIC). Volume 18: A distributed artificial intelligence approach to information fusion and object classification
[AD-A234892] N91-26827
Northeast Artificial Intelligence Consortium (NAIC). Volume 14: Knowledge base retrieval using plausible inference
[AD-A234893] N91-26828
Northeast Artificial Intelligence Consortium (NAIC). Volume 15: Strategies for coupling symbolic and numerical computation in knowledge base systems
[AD-A234894] N91-26829
Generic tasks for knowledge-based problem solving: Extension and new directions
[AD-A234925] N91-26865

KNOWLEDGE REPRESENTATION
Research on intelligent fault detection and repair advisory systems
[AD-A235267] N91-26551
An advanced knowledge and design acquisition methodology: Application for the pilot's associate
[AD-A233700] N91-26748
Northeast Artificial Intelligence Consortium (NAIC). Volume 2: Discussing, using, and recognizing plans
[AD-A234881] N91-26816

KRYPTON
X ray laser program
[AD-A234390] N91-26504

KRYPTON FLUORIDE LASERS
Quasi-CW excimer laser, phase 2
[AD-A234771] N91-26509
Tunable excimer lasers
[DE91-011399] N91-26522

L

LABOR
Planetary spacecraft cost modeling utilizing labor estimating relationships N91-27116

LABORATORIES
Sounding rocket flight data summary
[AD-A233656] N91-26626
Measuring the quality of knowledge work
[AD-A235354] N91-26994

LAMINAR BOUNDARY LAYER
Boundary layer transition noise art
[AD-A235093] N91-26884

LAMINAR FLOW
Analytical solution of plane Poiseuille flow of a Johnson-Segalman fluid
[AD-A234313] N91-26472
Investigation of laminar, fully developed flow in annulus by finite difference model
[ITN-91-85116] N91-26483
Computational model for optimizing longitudinal fin heat transfer in laminar internal flows
[DE91-005070] N91-26485

LAMINAR HEAT TRANSFER
Computational model for optimizing longitudinal fin heat transfer in laminar internal flows
[DE91-005070] N91-26485

LAMINAR MIXING
Turbulent premixed hydrogen/air flames
[AD-A235109] N91-26278

LAMINATES
Thermoelastic wave propagation in laminated composites N91-26209
Development of a test system and experimental method for in-plane biaxial compressive deformation and failure of fiber composite materials
[AD-A234062] N91-26214
Nonlinear behavior of fiber composite materials and its effect on the postbuckling response of laminated plates
[AD-A234203] N91-26218
On the finite-strain-invariant failure criterion for composites
[AD-A234493] N91-26223
Buckling of laminated composite plates
[ITN-91-85101] N91-26232
Development and verification of global/local analysis techniques for laminated composites
[NASA-CR-185060] N91-26238
Transformation toughening of ceramics
[AD-A234926] N91-26359

LAND ICE
A review of precipitation-related aspects of West Antarctic meteorology N91-26574
Sea-level response to ice sheet evolution: An ocean perspective N91-26575
Late Wisconsin and early holocene glacial history, inner Ross Embayment, Antarctica N91-26577

LAND MANAGEMENT
A guide to NASA's Pilot Land Data System (PLDS) N91-27035

LANDING SITES
Martian surface materials N91-27073
Sand and dust issues for the MESUR mission N91-27080
LANDING SPEED
Study of the properties of the autonomous optical navigation of a space probe in a rendezvous with an asteroid N91-26169
LANTHANUM COMPOUNDS
Investigation of a Hamiltonian with two sources of anisotropy: The Dzyaloshinskii-Moriya and single-size interactions
[DE91-011381] N91-26292
LARGE SPACE STRUCTURES
Studies in modeling, dynamics, and control of space structures
[AD-A235059] N91-26190
NDE pattern recognition of LSS states via wave propagation
[AD-A234772] N91-26549
H-infinity-optimal control for distributed parameter systems
[AD-A234931] N91-26833
A nonrecursive order N preconditioned conjugate gradient: Range space formulation of MDOF dynamics N91-27099
Development of load-dependent Ritz vector method for structural dynamic analysis of large space structures N91-27111
LASER ALTIMETERS
Sea test development of laser altimeter
[AD-A233824] N91-26498
LASER APPLICATIONS
Laser initiated ignition of liquid propellant
[AD-A233777] N91-26388
Laser applications in machining slab materials
[AD-A233823] N91-26497
Laser spectroscopy characterization of materials for frequency agile solid state laser systems
[AD-A233916] N91-26500
Laser-induced desorption of H2 from Si(111)7x7
[AD-A234636] N91-26508
JPRS report: Science and technology. USSR: Life sciences
[JPRS-ULS-91-011] N91-26696
Neutral atom deBroglie-wave interferometry
[AD-A234624] N91-26896
LASER BEAMS
Atmospheric propagation of laser beams
[AD-A234314] N91-26501
Frequency upshifting of laser pulses by ionization fronts
[AD-A234354] N91-26503
A narrow-bandwidth unstable resonator laser cavity
[AD-D014865] N91-26505
Laser-induced desorption of H2 from Si(111)7x7
[AD-A234636] N91-26508
X ray spot motion during 220 ps laser pulses
[DE91-012111] N91-26519
Optical methods of measuring the roughness of the surfaces of high precision steel balls
[AD-A234796] N91-26928
LASER CAVITIES
A narrow-bandwidth unstable resonator laser cavity
[AD-D014865] N91-26505
A room-temperature, flashpumped, 2.09 micron solid state laser
[AD-D014871] N91-26506
LASER DAMAGE
Radio frequency and microwave plasma for optical thin film deposition
[DE91-012081] N91-26525
LASER FUSION
Tunable excimer lasers
[DE91-011399] N91-26522
Radio frequency and microwave plasma for optical thin film deposition
[DE91-012081] N91-26525
LASER HEATING
Laser-induced desorption of H2 from Si(111)7x7
[AD-A234636] N91-26508
LASER INDUCED FLUORESCENCE
Resonance fluorescence spectrum of an atom near a phase conjugator
[AD-A234535] N91-26894
LIF and emission studies of copper and nitrogen N91-27089
LASER MATERIALS
Energy levels and branching ratios of Tm(3)+ in ten garnet laser materials
[AD-A235274] N91-26514
New laser materials for laser diode pumping
[NASA-CR-187786] N91-26521
Development of a subpicosecond, tunable LiCAF (Cr:LiCaAlF6) laser
[DE91-012082] N91-26526
LASER OUTPUTS
Laser ionic multiphoton dissociation of some acrylate clusters
[AD-A233801] N91-26247
Chaotic and bifurcating nonlinear systems driven by noise with applications to laser dynamics
[AD-A234841] N91-26512
Energy levels and branching ratios of Tm(3)+ in ten garnet laser materials
[AD-A235274] N91-26514
Analysis of nonlinear optical frequency conversion
[AD-A233726] N91-26920
LASER PLASMA INTERACTIONS
X ray laser program
[AD-A234390] N91-26504
LASER PLASMAS
Saturation and kinetic issues for optical-field-ionized plasma x ray lasers
[DE91-012079] N91-26517
Precision high-power solid-state laser diagnostics for target-irradiation studies and target-plane irradiation modeling
[DE91-012036] N91-26523
Planar indirect-drive Rayleigh-Taylor experiments on Nova
[DE91-011967] N91-26943
LASER PUMPING
A room-temperature, flashpumped, 2.09 micron solid state laser
[AD-D014871] N91-26506
SUNLITE program. Sub-Hertz relative frequency stabilization of two diode laser pumped Nd:YAG lasers locked to a Fabry-Perot interferometer
[NASA-CR-184957] N91-26520
New laser materials for laser diode pumping
[NASA-CR-187786] N91-26521
Analysis of nonlinear optical frequency conversion
[AD-A233726] N91-26920
LASER SPECTROSCOPY
Laser spectroscopy characterization of materials for frequency agile solid state laser systems
[AD-A233916] N91-26500
Elementary reaction rate measurements at high temperatures by tunable-laser flash-absorption
[DE91-011850] N91-26516
Material engineering of novel semiconductor structures
[AD-A235014] N91-26960
LASER STABILITY
SUNLITE program. Sub-Hertz relative frequency stabilization of two diode laser pumped Nd:YAG lasers locked to a Fabry-Perot interferometer
[NASA-CR-184957] N91-26520
LASER TARGETS
Cluster beam deposition of high temperature materials
[AD-A234358] N91-26343
Precision high-power solid-state laser diagnostics for target-irradiation studies and target-plane irradiation modeling
[DE91-012036] N91-26523
LASERS
Size dependence of gaseous cluster reactivity and evaporation dynamics as a mechanistic probe
[AD-A233811] N91-26249
Laser applications in machining slab materials
[AD-A233823] N91-26497
Determination of SBS induced damage limits in large fused silica optics for intense, time varying laser pulses
[DE91-012080] N91-26518
In-situ monitoring of laser ablation of superconductors
[DE91-012057] N91-26524
LASING
Saturation and kinetic issues for optical-field-ionized plasma x ray lasers
[DE91-012079] N91-26517
Development of a subpicosecond, tunable LiCAF (Cr:LiCaAlF6) laser
[DE91-012082] N91-26526
Luminescence and lasing in II-VI semiconductors
[AD-A235019] N91-26961
LATENT HEAT
Application of thematic mapper images to determine regional evaporation from the playas in the western desert of Egypt
[REPT-31] N91-26585
LATTICE PARAMETERS
Microstructure and hardness of NiAl/Ni2AlX two-phase ordered intermetallic alloys
[DE91-012068] N91-26323
LAUNCHING
Electromagnetic launch technology assessment. Scientific basis and unified treatment: Forces and electromechanical power conversion (analytical and numerical methods)
[AD-A235028] N91-26185
LEADING EDGES
Calculated aerodynamics of wings in severe maneuver
[AD-A235241] N91-26120
LEAKAGE
Dynamics of face and annular seals with two-phase flow
[NASA-CR-4256] N91-26479
Rotordynamic and leakage characteristics of a 4-stage brush seal
[AD-A235336] N91-26541
LEARNING
Integration of neurobiological and computational analyses of the neural network essentials for conditioned taste aversion
[AD-A235164] N91-26744
Using modular neural networks with local representations to control dynamic systems
[AD-A234700] N91-26813
LEARNING THEORY
On measures of misconception stability
[AD-A234952] N91-26847
LEAST SQUARES METHOD
Parallel algorithms for least squares and related computations
[AD-A235018] N91-26790
Weighted least squares estimation for Aalen's additive risk model
[AD-A235250] N91-26852
Statistical analysis of stochastic gradient based algorithms
[AD-A234545] N91-26859
Strong exchange coupling in lanthanide bis(phthalocyaninato) sandwich compounds
[AD-A234466] N91-26951
LEGIBILITY
The effect of rotation on legibility of dot-matrix characters
[AD-A235034] N91-27008
LENS DESIGN
Visual and field-of-view evaluation of the M-43 protective mask with prescription eyepieces
[AD-A234592] N91-26754
LENSES
Visual and field-of-view evaluation of the M-43 protective mask with prescription eyepieces
[AD-A234592] N91-26754
Optical methods of measuring the roughness of the surfaces of high precision steel balls
[AD-A234796] N91-26928
LESIONS
Analysis of visual loss from retinal lesions
[AD-A235268] N91-26729
LIAPUNOV FUNCTIONS
Lyapunov exponents and rotation numbers of linear systems with real noise
[AD-A234729] N91-26846
LIBRARIES
NUMVEC FORTRAN library manual. Chapter: Partial differential equations. Routine: ICGG3D
[CWI-NM-R9018] N91-26768
On-line magnetic tape Library Inventory Tracking And Reporting (LITAR) system
[AD-A234934] N91-27004
The Internet resources guide and the Automatic Login Executor (ALEX) N91-27030
A guide to NASA's Pilot Land Data System (PLDS) N91-27035
Software product description N91-27037
LIE GROUPS
Geometry, dynamics and control of coupled systems N91-26401
LIFE (DURABILITY)
Development of life prediction capabilities for liquid propellant rocket engines. Post-fire diagnostic system for the SSME system architecture study
[NASA-CR-187112] N91-26205
LIFE CYCLE COSTS
VHSIC electronics and the cost of Air Force avionics in the 1990s
[RAND-R-3843-AF] N91-26143
LIFE SCIENCES
JPRS report: Science and technology. USSR: Space
[JPRS-USP-91-002] N91-26162
Living ring-opening metathesis polymerization of 7-oxa-2,3-difunctionalized norbornenes and norbornadienes by Mo(CHCMe2R) (N-2,6-C6H3-i-Pr2) (O-t-Bu)2 and Mo(CHCMe2R) (N-2,6-C6H3-i-Pr2) (OCMe2CF3)2
[AD-A235235] N91-26365
USSR Space Life Sciences Digest, issue 29
[NASA-CR-3922(34)] N91-26669
USSR Space Life Sciences Digest, issue 30
[NASA-CR-3922(36)] N91-26670
JPRS report: Science and technology. USSR: Life sciences
[JPRS-ULS-91-010] N91-26683

JPRS Report: Science and technology. USSR: Life sciences
[JPRS-ULS-91-009] N91-26688
JPRS report: Science and technology. USSR: Life sciences
[JPRS-ULS-91-011] N91-26696
LIFE SUPPORT SYSTEMS
Higher plants as part of biological human life support system N91-26693
Investigating combustion as a method of processing inedible biomass produced in NASA's biomass production chamber
[NASA-TM-103821] N91-26759
Impact of Mars sand on dust on the design of space suits and life support equipment: A technology assessment N91-27079
An Air Revitalization Model (ARM) for Regenerative Life Support Systems (RLSS) N91-27093
LIGANDS
The control of orbital mixing in ruthenium complexes containing quinone related ligands
[AD-A234602] N91-26260
LIGHT AIRCRAFT
Geogrid reinforced base course for flexible pavements for light aircraft: Literature review and test section design
[DOT/FAA/RD-90/28] N91-26160
LIGHT AMPLIFIERS
An ultraviolet optical isolator utilizing the KDP-isomorphs
[AD-D014860] N91-26923
LIGHT GAS GUNS
Hypervelocity launch capabilities to over 10.4 km/s
[DE91-010859] N91-26186
LIGHT MODULATION
Center for the Integration of Optical C
[AD-A235277] N91-26931
The effects of character size, modulation, polarity, and font on reading and search performance in matrix-addressable displays
[AD-A235033] N91-27007
LIGHT SCATTERING
Effect of aerosols on laser-induced breakdown
[AD-A234324] N91-26502
Optical methods of measuring the roughness of the surfaces of high precision steel balls
[AD-A234796] N91-26928
LIGHT SOURCES
Elementary reaction rate measurements at high temperatures by tunable-laser flash-absorption
[DE91-011850] N91-26516
LIGHTNING
Comparison of the RF frequency spectra of HEMP and lightning
[AD-A234306] N91-26642
The 1990 Sandia rocket-triggered lightning field tests at Kennedy Space Center, Florida
[DE91-011263] N91-26653
Characterization of vertical electric fields and associated voltages induced on an overhead power line from close artificially initiated lightning
[DE91-010781] N91-26656
LIGHTNING SUPPRESSION
Follow-on cable coupling lightning test. Volume 2: Appendixes A, B, C, and D
[NASA-CR-184124] N91-26195
Minutes of the 24th Explosives Safety Seminar, volume 2
[AD-A235006] N91-26396
LINE SPECTRA
Light induced electron spin resonance in polyaniline
[AD-A233847] N91-26331
LINEAR ACCELERATORS
Measurement of the nitrogen total cross section from 0.5 eV to 50 MeV and analysis of the 433-keV resonance
[DE91-012222] N91-26293
Laser switched power linac
[AD-A234581] N91-26507
Gauge bosons and heavy quarks: Proceedings of Summer Institute on Particle Physics
[DE91-011248] N91-26907
LINEAR EQUATIONS
A numerical study of blocking N91-26640
LINEAR PROGRAMMING
Converting a converging algorithm into a polynomially bounded algorithm
[AD-A234961] N91-26788
Large-scale stochastic linear programs: Importance sampling and Benders decomposition
[AD-A234962] N91-26789
Matching theory. A sampler: From Denes Koenig to the present
[AD-A234321] N91-26839
LINEAR SYSTEMS
Long-term prediction test procedure for most ICs, based on linear response theory
[NASA-CR-185843] N91-26462
Lyapunov exponents and rotation numbers of linear systems with real noise
[AD-A234729] N91-26846
LIQUID CHROMATOGRAPHY
Raman spectroscopy study of solvation structure in acetonitrile/water mixtures
[AD-A234921] N91-26271
LIQUID COOLING
Reexamination of METMAN, recommendations on enhancement of LCVG, and development of new concepts for EMU heat sink N91-27098
LIQUID CRYSTALS
Organosilicon polymers incorporating the bicyclo(2.2.2)-octane moiety
[AD-A234966] N91-26361
Novel liquid crystalline polymers as nonlinear optical materials
[AD-A235371] N91-26373
Proceedings of the Optoelectronic Workshop 25: Liquid Crystal Materials and Devices for Opto-Electronic Applications
[AD-A233780] N91-26921
LIQUID HYDROGEN
ALS liquid hydrogen turbopump: Advanced Development Program
[NASA-CR-183730] N91-26196
LIQUID PHASES
The synthesis of methanol by a novel method
[DE91-011131] N91-26291
Ceramic fiber coating development and demonstration
[AD-A234773] N91-26358
LIQUID PROPELLANT ROCKET ENGINES
Propulsion stability codes for liquid propellant propulsion systems developed for use on a PC computer
[NASA-CR-184983] N91-26201
Development of life prediction capabilities for liquid propellant rocket engines. Post-fire diagnostic system for the SSME system architecture study
[NASA-CR-187112] N91-26205
LIQUID ROCKET PROPELLANTS
Laser initiated ignition of liquid propellant
[AD-A233777] N91-26388
LIQUID SLOSHING
An experimental and numerical study of wavemaker dissipation in the process of direct generation of the resonant sloshing waves in a rectangular tank
[ITN-91-85103] N91-26481
Sloshing response in a tank containing two liquids
[DE91-011844] N91-26487
LIQUID SURFACES
Ricochet of sphere off water
[ITN-91-85102] N91-26480
LIQUID-SOLID INTERFACES
Surface diffusion at the liquid-solid interface: Quenching of fluorescence from pyrene covalently bound to methylated silica
[AD-A234645] N91-26268
LIQUID-VAPOR INTERFACES
Liquid film cooling in rocket engines
[AD-A234288] N91-26197
LIQUIDS
Transport processes and interfacial phenomena in an evaporating meniscus
[DE91-005561] N91-26284
Sloshing response in a tank containing two liquids
[DE91-011844] N91-26487
LITERATURE
Advanced Satellite Research Project: SCAR Research Database. Bibliographic analysis
[NASA-CR-186086] N91-26182
LITHIUM ALLOYS
The cryogenic mechanical properties of Vintage 3 Al-Li-Zr alloy 2090-T81
[DE91-011897] N91-26311
LITHIUM SULFUR BATTERIES
Improvement in the capacity and safety of lithium/inorganic electrolyte sulfur dioxide rechargeable cells, phase 2
[AD-A235303] N91-26589
LOAD DISTRIBUTION (FORCES)
Development of load-dependent Ritz vector method for structural dynamic analysis of large space structures N91-27111
LOAD TESTS
Shell hoop prestress generated by welding
[DE91-011892] N91-26571
Physiological and perceptual responses to load carrying in female subjects using internal and external frame backpacks
[AD-A234941] N91-26722
LOADING RATE
Characterization of mechanical damage mechanisms in ceramic composite materials
[NR-032-553] N91-26235
LOADS (FORCES)
Interfacial force sensor with force-feedback control
[DE91-004897] N91-26495
Nonlinear oscillations of mechanical systems under multifrequency parametric excitation
[AD-A233800] N91-26558
LOCKING
Removable hand hold
[NASA-CASE-LEW-15196-1] N91-26543
LOCOMOTION
Mathematical problems concerning rhythmic processes
[AD-A234588] N91-26845
LOFTING
Effectiveness of ice-vest cooling in prolonging work tolerance time during heavy exercise in the heat for personnel wearing Canadian forces chemical defence ensembles
[AD-A235273] N91-26758
LOGARITHMS
Interfacial slippage of a unidirectional fiber composite under longitudinal shearing
[AD-A234186] N91-26216
LOGIC
Northeast Artificial Intelligence Consortium (NAIC). Volume 10: Time oriented problem solving
[AD-A234889] N91-26824
LOGIC CIRCUITS
Digital logic testing and testability
[AD-A234123] N91-26441
Control circuitry using electronic emulation of a synchro signal for accurate control of position and rate of rotation for shafts
[NASA-CASE-MFS-28458-1] N91-26459
LOGIC DESIGN
Fuzzy logic control system to provide autonomous collision avoidance for Mars rover vehicle N91-27106
LOGIC PROGRAMMING
Northeast Artificial Intelligence Consortium (NAIC). Volume 11: Knowledge base maintenance
[AD-A234890] N91-26825
LOGISTICS
Forecasting digital microcircuit obsolescence
[AD-A234573] N91-26451
Report of the 90-day study on human exploration of the Moon and Mars
[NASA-TM-102999] N91-27055
LONG DURATION SPACE FLIGHT
Survey of the principal results of medical research in the flight program of the second main expedition aboard the Mir orbiting complex N91-26686
LOSSES
Molecular orientation of the silver tetra neopentoxy phthalo cyanine and stearic acid mixed Langmuir-Blodgett film and its chemical and electrochemical behaviour
[AD-A234601] N91-26206
LOW ALTITUDE
Sea test development of laser altimeter
[AD-A233824] N91-26498
LOW COST
Results of the aeronautical systems division critical process team on integrated product development
[AD-A235419] N91-26995
LOW PASS FILTERS
Gabor transforms and neural networks for automatic target recognition
[DE91-011919] N91-26834
LOW PRESSURE
A program in the chemistry of electronic materials. Task 1: New organometallic precursors for the low pressure chemical vapor deposition of refractory materials for electronics
[AD-A234315] N91-26342
Method and apparatus for waste collection and storage
[NASA-CASE-MSC-21025-3] N91-26747
LOW SPEED WIND TUNNELS
Applied high-speed imaging for the icing research program at NASA Lewis Research Center
[NASA-TM-104415] N91-26490
LOW TEMPERATURE
International State-of-the-Art Colloquium on Low-Temperature Asphalt Pavement Cracking
[AD-A233663] N91-26402
Development of a low temperature catalytic combustor for small gas turbine applications
[PB91-161273] N91-26529
Progress with neural network gulf streams
[AD-A233810] N91-26658
LOW TEMPERATURE ENVIRONMENTS
Lubricants at low temperatures
[AD-A234536] N91-26348

LOW VOLTAGE
Development and testing of radiation and electromagnetic pulse hardened silicon carbide based electronics
[AD-A233744] N91-26439
LOWER ATMOSPHERE
Historical aspects of radar atmospheric dynamics N91-26614
Gravity waves and instabilities in the lower and middle atmosphere N91-26621
Dust in the Mars atmosphere N91-27082
LOWER BODY NEGATIVE PRESSURE
Nonlinear systems dynamics in cardiovascular physiology: The heart rate delay map and lower body negative pressure N91-27095
LUBRICANTS
Lubricants at low temperatures
[AD-A234536] N91-26348
LUBRICATING OILS
Lubricants at low temperatures
[AD-A234536] N91-26348
LUBRICATION
Additives for high temperature liquid lubricants
[DE91-011018] N91-26386
Improved modeling and performance of squeeze film damper bearings
[AD-A233694] N91-26531
LUMINANCE
The effects of character size, modulation, polarity, and font on reading and search performance in matrix-addressable displays
[AD-A235033] N91-27007
LUMINESCENCE
Luminescence and lasing in II-VI semiconductors
[AD-A235019] N91-26961
LUNAR BASES
Report of the 90-day study on human exploration of the Moon and Mars
[NASA-TM-102999] N91-27055
Evaluation of geophysical properties of the lunar regolith for the design of precursor scientific missions for the space exploration initiative N91-27104
Design of a lunar oxygen production plant N91-27109
Structural concept studies for a horizontal cylindrical lunar habitat and a lunar guyed tower N91-27117
LUNAR EXPLORATION
NASA/ASEE Summer Faculty Fellowship Program, 1990, volume 2
[NASA-CR-185637-VOL-2] N91-27103
Developing a taxonomy for mission architecture definition N91-27108
LUNAR GEOLOGY
Evaluation of geophysical properties of the lunar regolith for the design of precursor scientific missions for the space exploration initiative N91-27104
LUNAR MINING
Evaluation of geophysical properties of the lunar regolith for the design of precursor scientific missions for the space exploration initiative N91-27104
LUNAR ORBITS
Galileo: The Earth encounter N91-27024
LUNAR ROCKS
Evaluation of geophysical properties of the lunar regolith for the design of precursor scientific missions for the space exploration initiative N91-27104
Design of a lunar oxygen production plant N91-27109
LUNAR SURFACE
Evaluation of geophysical properties of the lunar regolith for the design of precursor scientific missions for the space exploration initiative N91-27104

M

MACH NUMBER
The effects of compressibility on a supersonic mixing layer
[AD-A234992] N91-26119
MACHINE LEARNING
Evaluation of expert systems: A review of the literature
[AD-A234360] N91-26808
Extensions of a theory of networks and learning: Outliers and negative examples
[AD-A234425] N91-26810
MACHINING
Abrasive-waterjet machining of isogrid structures
[AD-A234628] N91-26405
Laser applications in machining slab materials
[AD-A233823] N91-26497
MACROPHAGES
Effects of 13 day space flight on skeletal muscles and neuromuscular junctions in rats N91-26703
Molecular studies of cytokine induction
[AD-A235326] N91-26731
MAGNESIUM ALLOYS
Materials/microstructures characterization
[AD-A233751] N91-26295
MAGNESIUM ISOTOPES
Development of advanced methods based on stable isotope technology for studies of exercise in heat
[AD-A234670] N91-26719
MAGNETIC COILS
Magnetic field generator
[AD-D014869] N91-26449
MAGNETIC DIFFUSION
Electromagnetic launch technology assessment. Scientific basis and unified treatment: Forces and electromechanical power conversion (analytical and numerical methods)
[AD-A235028] N91-26185
Electron localization in polyaniline and its derivatives
[AD-A233934] N91-26335
MAGNETIC EFFECTS
Measurements of the longitudinal movements of O(+) ions in the subauroral upper atmosphere from the Aureol 3 satellite N91-26171
MAGNETIC FIELD CONFIGURATIONS
Statistical properties of intrinsic topological noise in tokamaks
[DE91-011741] N91-26939
MAGNETIC FIELDS
Fluid damping of the oscillations of satellites with a large magnetic moment N91-26170
Magnetic field generator
[AD-D014869] N91-26449
Magnetostrictive angular positioning motor
[AD-D014858] N91-26536
Trimodal random-field Ising systems in a transverse field
[AD-A235038] N91-26875
Experiments with trapped atoms
[AD-A234580] N91-26895
An ultraviolet optical isolator utilizing the KDP-isomorphs
[AD-D014860] N91-26923
Comparison of dimensionally similar discharges with similar heat deposition discharges
[DE91-011740] N91-26938
MAGNETIC MATERIALS
Magnetic and electrical properties of Martian particles N91-27074
MAGNETIC MEASUREMENT
Investigation of axial positioning for flexural compressors
[NASA-CR-185711] N91-26544
MAGNETIC MOMENTS
Fluid damping of the oscillations of satellites with a large magnetic moment N91-26170
Experiments with trapped atoms
[AD-A234580] N91-26895
Strong exchange coupling in lanthanide bis(phthalocyaninato) sandwich compounds
[AD-A234466] N91-26951
MAGNETIC PROPERTIES
Investigation of a Hamiltonian with two sources of anisotropy: The Dzyaloshinskii-Moriya and single-size interactions
[DE91-011381] N91-26292
Structure, order and the metallic state in polyaniline and its derivatives
[AD-A233935] N91-26336
Magnetic and electrical properties of Martian particles N91-27074
MAGNETIC RELAXATION
Magnetic relaxation, flux pinning and, critical currents in superconductors
[DE91-012022] N91-26984
MAGNETIC SHIELDING
High-temperature ceramic superconductors
[AD-A234620] N91-26953
MAGNETIC STARS
The light curve of the magnetic star AM - Herculis
[ITN-91-85108] N91-27049
MAGNETIC STORMS
Dynamics of equatorial and polar boundaries of penetration of solar protons with energy about 1 MeV into magnetosphere during strong magnetic storm N91-26172
The effects of magnetic storm phases on F-layer irregularities from auroral to equatorial latitudes
[AD-A235170] N91-26632
MAGNETIC TAPES
ARTIST tape output formats
[AD-A235173] N91-26633
On-line magnetic tape Library Inventory Tracking And Reporting (LITAR) system
[AD-A234934] N91-27004
MAGNETIC VARIATIONS
Modelling the dynamics of fluxes of electrons with energies 30-300 keV in geostationary orbit N91-26173
MAGNETICALLY TRAPPED PARTICLES
Experiments with trapped atoms
[AD-A234580] N91-26895
MAGNETO-OPTICS
An ultraviolet optical isolator utilizing the KDP-isomorphs
[AD-D014860] N91-26923
MAGNETOHYDRODYNAMIC GENERATORS
MHD contractors' review meeting
[DE91-011295] N91-26945
Multi-dimensional computer simulation of MHD combustor hydrodynamics
[DE91-011851] N91-26946
MAGNETOHYDRODYNAMIC STABILITY
Parametric studies of dense plasma focus for fusion space propulsion with D-He3
[AD-A234578] N91-26941
MAGNETOHYDRODYNAMICS
MHD contractors' review meeting
[DE91-011295] N91-26945
MAGNETOMETERS
High-T(sub c) thin-film magnetometer
[DE91-011828] N91-26981
MAGNETOSPHERE-IONOSPHERE COUPLING
Measurements of the longitudinal movements of O(+) ions in the subauroral upper atmosphere from the Aureol 3 satellite N91-26171
MAGNETOSTRICTION
Magnetostrictive angular positioning motor
[AD-D014858] N91-26536
MAGNETRONS
Magnetron sputter deposition of boron and boron carbide
[DE91-011194] N91-26241
MAGNETS
Shell hoop prestress generated by welding
[DE91-011892] N91-26571
MAINTAINABILITY
Statistical aspects of reliability, maintainability, and availability
[AD-A234546] N91-26546
MAINTENANCE
OSIRRUS: Oceanic symbolic image representation, recognition and understanding software
[AD-A235112] N91-26665
Northeast Artificial Intelligence Consortium (NAIC). Volume 3: The Versatile Maintenance Expert System (VMES)
[AD-A234882] N91-26817
Northeast Artificial Intelligence Consortium (NAIC). Volume 11: Knowledge base maintenance
[AD-A234890] N91-26825
MALES
Effect of shift work of air traffic controllers on sympathetic nervous system N91-26700
Physical and psychogenic sequelae of impact acceleration on tracking performance of operators N91-26701
MAMMALS
Mathematical modeling of the flow field and particle motion in a rotating bioreactor at unit gravity and microgravity N91-27092
MAN MACHINE SYSTEMS
An advanced knowledge and design acquisition methodology: Application for the pilot's associate
[AD-A233700] N91-26748
Incorporation of shuttle CCT parameters in computer simulation models N91-27096
MAN-COMPUTER INTERFACE
Format and basic geometry of a perspective display of air traffic for the cockpit
[NASA-TM-86680] N91-26142
Northeast Artificial Intelligence Consortium (NAIC). Volume 6: Building an intelligent assistant: The acquisition, integration, and maintenance of complex distributed tasks
[AD-A234885] N91-26820
MANAGEMENT
A Rome Laboratory guide to basic training in TQM analysis techniques
[AD-A233855] N91-26993
MANAGEMENT METHODS
Quality Assurance Manual
[DE91-012618] N91-26555
Proceedings of the Second Annual NASA Science Internet User Working Group Conference
[NASA-CP-3117] N91-27009
NSIUWG: Science networking retreat N91-27010
MANAGEMENT SYSTEMS
Notional helmet concepts: A survey of near-term and future technologies
[AD-A234475] N91-26752

Northeast Artificial Intelligence Consortium (NAIC). Volume 4: Distributed artificial intelligence for communications network management
[AD-A234883] N91-26818
MANDRELS
A model for wet filament winding of composite cylinders with arbitrary thickness
[AD-A234102] N91-26215
MANIFOLDS (MATHEMATICS)
On the sensitivity of solutions of parametrized equations
[AD-A234265] N91-26838
MANIPULATORS
Dynamic stability of flexible robot manipulators
[AD-A234297] N91-26533
Line kinematics for whole-arm manipulation
[AD-A234422] N91-26535
MANNED SPACE FLIGHT
JPRS report: Science and technology. USSR: Space
[JPRS-USP-91-002] N91-26162
State-of-the-art automated evaluation of functional state of the body in the space program and preventive medicine N91-26687
JPRS Report: Science and technology. USSR: Life sciences
[JPRS-ULS-91-009] N91-26688
Computer tomography measurement of vertebral bones and muscles after extended manned space flights N91-26690
Visual accommodation in cosmonauts N91-26697
MANUALS
Quality Assurance Manual
[DE91-012618] N91-26555
NUMVEC FORTRAN library manual. Chapter: Partial differential equations. Routine: ICGG3D
[CWI-NM-R9018] N91-26768
MANY BODY PROBLEM
Geometry, dynamics and control of coupled systems N91-26401
MAPPING
Using mappings to prove timing properties
[AD-A234404] N91-26780
MAPS
The Navy standard compressed aeronautical chart database
[AD-A235340] N91-26587
The effect of rotation on legibility of dot-matrix characters
[AD-A235034] N91-27008
MARINE BIOLOGY
SEEP 2 zooplankton data report: Winter, spring and summer collections at mooring 3 during 1988
[DE91-012077] N91-26668
MARINE ENVIRONMENTS
VLF nighttime data analysis
[AD-A234006] N91-26417
Sea test development of laser altimeter
[AD-A233824] N91-26498
MARINE TECHNOLOGY
Nondestructive Evaluation (NDE) of fiberglass marine structures state-of-the art review
[AD-A234785] N91-26550
MARINER 9 SPACE PROBE
The effects of atmospheric dust on observations of Martian surface albedo N91-27072
MARISAT SATELLITES
Evaluation of the MARISAT satellite UHF wideband channel
[AD-A233666] N91-26408
MARKET RESEARCH
Civil tiltrotor missions and applications. Phase 2: The commercial passenger market
[NASA-CR-177576] N91-26126
MARKETING
Air Force stock fund: Hydrazine sales consistent with the Commercial Space Launch Act. Report to the Chairman, Committee on Science, Space and Technology, House of Representatives
[GAO/NSIAD-91-196] N91-26397
MARKOV PROCESSES
Spread spectrum communication networks
[AD-A233696] N91-26409
A physiologically motivated front end for speech recognition
[AD-A233727] N91-26414
Lyapunov exponents and rotation numbers of linear systems with real noise
[AD-A234729] N91-26846
Maximization on matroids with random weights
[AD-A233978] N91-26858
MARS (PLANET)
Magnetic and electrical properties of Martian particles N91-27074
Martian dust threshold measurements: Simulations under heated surface conditions N91-27081
NASA/ASEE Summer Faculty Fellowship Program, 1990, volume 2
[NASA-CR-185637-VOL-2] N91-27103
Developing a taxonomy for mission architecture definition N91-27108
MARS ATMOSPHERE
Characteristics of aerosol in the atmosphere of Mars according to data from the KRFM experiment N91-26175
Recent studies of the optical properties of dust and cloud particles in the Mars atmosphere and the interannual frequency of global dust storms N91-27060
Effects of Martian dust on power system components N91-27061
Wind abrasion on Mars N91-27064
Effect of pressure on electrostatic processes on Mars N91-27069
Saltation threshold detection in a wind tunnel by the measurement of the net electrostatic charge N91-27070
The effects of atmospheric dust on observations of Martian surface albedo N91-27072
Sand and dust issues for the MESUR mission N91-27080
Dust in the Mars atmosphere N91-27082
MARS ENVIRONMENT
The chemistry and mineralogy of Mars soil and dust N91-27058
Recent studies of the optical properties of dust and cloud particles in the Mars atmosphere and the interannual frequency of global dust storms N91-27060
Measurements of dust on Mars to be obtained from upcoming missions N91-27066
Engineering knowledge requirements for sand and dust on Mars N91-27067
Electrical system/environment interactions on the planet Mars N91-27068
Saltation threshold reduction due to the electrostatic agglomeration of fine particles N91-27071
Electrostatic fields in a dusty Martian environment N91-27078
MARS LANDING
Report of the 90-day study on human exploration of the Moon and Mars
[NASA-TM-102999] N91-27055
MARS OBSERVER
Derivation of mid-infrared (5-25 microns) optical constants of some silicates and palagonite N91-27077
MARS SAMPLE RETURN MISSIONS
Fuzzy logic control system to provide autonomous collision avoidance for Mars rover vehicle N91-27106
MARS SURFACE
Characteristics of aerosol in the atmosphere of Mars according to data from the KRFM experiment N91-26175
Sand and Dust on Mars
[NASA-CP-10074] N91-27057
The chemistry and mineralogy of Mars soil and dust N91-27058
Recent studies of the optical properties of dust and cloud particles in the Mars atmosphere and the interannual frequency of global dust storms N91-27060
Effects of Martian dust on power system components N91-27061
Have graben wall scarps accumulated sand and dust on Mars? N91-27062
Chemistry and mineralogy of Martian dust: An explorer's primer N91-27063
Measurements of dust on Mars to be obtained from upcoming missions N91-27066
Engineering knowledge requirements for sand and dust on Mars N91-27067
Electrical system/environment interactions on the planet Mars N91-27068
Effect of pressure on electrostatic processes on Mars N91-27069
Saltation threshold detection in a wind tunnel by the measurement of the net electrostatic charge N91-27070
The effects of atmospheric dust on observations of Martian surface albedo N91-27072
Martian surface materials N91-27073
Magnetic and electrical properties of Martian particles N91-27074
Reflectance spectroscopy of palagonite and iron-rich montmorillonite clay mixtures: Implications for the surface composition of Mars N91-27075
Thermal and albedo mapping of the north and south polar regions of Mars N91-27076
Derivation of mid-infrared (5-25 microns) optical constants of some silicates and palagonite N91-27077
Electrostatic fields in a dusty Martian environment N91-27078
Impact of Mars sand on dust on the design of space suits and life support equipment: A technology assessment N91-27079
Sand and dust issues for the MESUR mission N91-27080
Martian dust threshold measurements: Simulations under heated surface conditions N91-27081
Dust in the Mars atmosphere N91-27082
MARS SURFACE SAMPLES
Martian surface materials N91-27073
MASKS
Visual and field-of-view evaluation of the M-43 protective mask with prescription eyepieces
[AD-A234592] N91-26754
Ohmic contacts to semiconducting diamond
[AD-A234130] N91-26950
MASS
Electrochemically induced charge and mass transport in polypyrrole/poly(styrene sulfonate) molecular composites
[AD-A234599] N91-26354
MASS SPECTRA
On the evolution of raindrop spectra and their effect on the atmosphere below cloud base: Numerical models and comparisons with observations
[ITN-91-85113] N91-26652
Negative ion formation by Rydberg electron transfer: Isotope-dependent rate constants
[DE91-012058] N91-26909
MASS SPECTROMETERS
A study of the gas phase chemistry of solid propellants using a microprobe mass spectrometer (MPMS) system: Initial development of the MPMS system
[AD-A234839] N91-26393
MASS SPECTROSCOPY
Multispectral identification of potentially hazardous byproducts of ozonation and chlorination. Part 1: Studies of chromatographic and spectroscopic properties of MX
[PB91-161703] N91-26601
MASS TRANSFER
Isotropic exchange in the platinum-catalyzed reduction of olefins in protic solvents
[AD-A234828] N91-26208
Current distribution modeling for novel alumina electrolysis
[DE91-010060] N91-26315
Electrochemically induced charge and mass transport in polypyrrole/poly(styrene sulfonate) molecular composites
[AD-A234599] N91-26354
Modal aerosol dynamics modeling
[PB91-161729] N91-26598
On the evolution of raindrop spectra and their effect on the atmosphere below cloud base: Numerical models and comparisons with observations
[ITN-91-85113] N91-26652
MASSIVELY PARALLEL PROCESSORS
NRL connection machine Fortran library
[AD-A234121] N91-26779
MATCHING
Matching theory. A sampler: From Denes Koenig to the present
[AD-A234321] N91-26839
Understanding object classes: Modeling and matching
[AD-A235027] N91-26848
MATERIAL BALANCE
Molecular mechanics calculations for nitro and amino substituted conjugated systems containing oxygen and nitrogen
[AD-A233928] N91-26389
MATERIALS HANDLING
Advanced material handling equipment controls
[AD-A235091] N91-26540
MATERIALS SCIENCE
Photovoltaics: From the laboratory to the marketplace
[DE91-002151] N91-26588
Materials Science and Engineering, 1989 publications
[AD-A234087] N91-27001
MATHEMATICAL MODELS
Development of an integrated aeroservoelastic analysis program and correlation with test data
[NASA-TP-3120] N91-26113
State space models for aeroelastic and viscoelastic systems
[AD-A234730] N91-26117
Omega system Performance Assessment and Coverage Evaluation (PACE) workstation design and implementation, volume 1
[AD-A235225] N91-26128
Performance optimization of helicopter rotor blades
[NASA-TM-104054] N91-26137
Certification procedures and requirements N91-26154
Guidelines for design, construction, and evaluation of airport pavement drainage
[DOT/FAA/RD-90/31] N91-26161
Modelling the dynamics of fluxes of electrons with energies 30-300 keV in geostationary orbit N91-26173

Turbulent processes of mass-loading of new ions on Venus and Mars and the problems of numerical models of the interaction of solar wind with these planets. 1: Characteristics of the flow of solar wind around the planets N91-26174
Liquid film cooling in rocket engines
[AD-A234288] N91-26197
An anisotropic laminated damped plate theory
[AD-A234446] N91-26222
Investigation of a Hamiltonian with two sources of anisotropy: The Dzyaloshinskii-Moriya and single-size interactions
[DE91-011381] N91-26292
Current distribution modeling for novel alumina electrolysis
[DE91-010060] N91-26315
Performance of a 22Cr-20Ni-18Co-Fe alloy for service to 870 C
[DE91-011366] N91-26317
Spectroscopy and photoexcitation spectroscopies of polyaniline: A model system for new phenomena
[AD-A234215] N91-26340
Strength and microstructure of ceramics
[AD-A235424] N91-26374
Liquid water production from atmospheric sources
[AD-A235090] N91-26406
Proof-of-concept zinc/bromine electric vehicle battery
[DE91-011767] N91-26463
Determination of flow-regime boundaries for cohesive particles
[DE91-010552] N91-26468
Use of a zone model for validation of a horizontal ceiling/floor vent algorithm
[AD-A234553] N91-26474
Improved algorithms for transient and steady-state fluid-structure interaction
[AD-A235172] N91-26476
Simulation of pore scale porous media flow using lattice gas methods
[DE91-004829] N91-26484
Computational model for optimizing longitudinal fin heat transfer in laminar internal flows
[DE91-005070] N91-26485
Sloshing response in a tank containing two liquids
[DE91-011844] N91-26487
Applied high-speed imaging for the icing research program at NASA Lewis Research Center
[NASA-TM-104415] N91-26490
X ray spot motion during 220 ps laser pulses
[DE91-012111] N91-26519
Improved modeling and performance of squeeze film damper bearings
[AD-A233694] N91-26531
Fatigue crack tip plastic strain range measurement studies in two titanium alloys
[AD-A234973] N91-26565
Stabilization and control problems in structural dynamics
[AD-A235189] N91-26567
Effect of turbulence on impurity observation in upper atmosphere using lidar method N91-26584
Global climate change: A discussion of major uncertainties
[DE91-011746] N91-26604
An assessment of CO2 greenhouse gas mitigation technologies
[DE91-011972] N91-26605
Process study of sorted patterns on Arctic soils
[AD-A234089] N91-26628
The tropical Pacific Ocean's heat budget during a cold event, from a numerical model N91-26657
Ocean acoustic tomography and telemetry
[AD-A233826] N91-26659
The SYNOP experiment: Inverted echo sounder data report for June 1989 to September 1990
[AD-A234625] N91-26662
Lead detection and mapping with reference to relationships between scale, sensor characteristics, surface conditions and atmospheric properties
[AD-A235121] N91-26666
A software package for unconstrained optimization using tensor methods
[AD-A233989] N91-26778
Large-scale stochastic linear programs: Importance sampling and Benders decomposition
[AD-A234962] N91-26789
An implementation of the singular value decomposition on the connection machine CM-2
[AD-A234124] N91-26802
Mathematical topics in the modelling and identification of multicomponent continua
[AD-A234471] N91-26843
Numerical methods for singularly perturbed differential equations with applications
[AD-A235188] N91-26850
Comparative survey of dynamic analyses of free-piston Stirling engines
[NASA-TM-104491] N91-26870
A boundary scattering strength extraction algorithm for the analysis of long-range reverberation data
[AD-A233721] N91-26877
Comparison of sound pressure in a wedge-shaped ocean as predicted by an image method and a PE model
[AD-A234191] N91-26879
MHD contractors' review meeting
[DE91-011295] N91-26945
Multi-dimensional computer simulation of MHD combustor hydrodynamics
[DE91-011851] N91-26946
Process for the homoepitaxial growth of single-crystal silicon carbide films on silicon carbide wafers
[NASA-CASE-LEW-15223-1] N91-26967
A temperature dependent SPICE macro-model for power MOSFETs
[DE91-011737] N91-26972
The electronic structure of the ionic insulator sodium nitrite
[DE91-009766] N91-26977
Critical currents in proton irradiated YBa2Cu3O(7-delta) crystals
[DE91-011835] N91-26982
An analysis on the stability of the Mie-Gruneisen equation of state for describing the behavior of shock-loaded materials
[AD-A233827] N91-26988
Thermal and albedo mapping of the north and south polar regions of Mars N91-27076
Mathematical modeling of the flow field and particle motion in a rotating bioreactor at unit gravity and microgravity N91-27092
An Air Revitalization Model (ARM) for Regenerative Life Support Systems (RLSS) N91-27093
Reexamination of METMAN, recommendations on enhancement of LCVG, and development of new concepts for EMU heat sink N91-27098
Planetary spacecraft cost modeling utilizing labor estimating relationships N91-27116

MATHEMATICAL PROGRAMMING
NRL connection machine Fortran library
[AD-A234121] N91-26779

MATRICES (MATHEMATICS)
Gauge bosons and heavy quarks: Proceedings of Summer Institute on Particle Physics
[DE91-011248] N91-26907
Method and apparatus for second-rank tensor generation
[NASA-CASE-NPO-17512-1-CU] N91-26918

MATRIX MATERIALS
Dynamic fracture responses of Al2O3, Si3N4, and SiC(w)/Al2O3
[AD-A235286] N91-26229
Polymeric routes to silicon carbide and silicon oxycarbide CMC
[NASA-TM-104372] N91-26234

MATRIX METHODS
Analysis of wave characteristics in extreme seas
[AD-A234538] N91-26660

MAXIMUM ENTROPY METHOD
Spectral and correlation analysis with applications to middle-atmosphere radars N91-26619

MEASURING INSTRUMENTS
Research instrumentation for optical computing
[AD-A235335] N91-26932
Evaluating the effect of accuracy ratios on the percent of calibrations which are out of tolerance N91-27107

MECHANICAL DEVICES
Nonlinear oscillations of mechanical systems under multifrequency parametric excitation
[AD-A233800] N91-26558

MECHANICAL DRIVES
Magnetic field generator
[AD-D014869] N91-26449
Magnetostrictive angular positioning motor
[AD-D014858] N91-26536
Acoustic radiation from fluid-loaded, ribbed cylindrical shells excited by different types of concentrated mechanical drives
[AD-A235324] N91-26887

MECHANICAL PROPERTIES
Studies in modeling, dynamics, and control of space structures
[AD-A235059] N91-26190
Nonlinear behavior of fiber composite materials and its effect on the postbuckling response of laminated plates
[AD-A234203] N91-26218
Far- and mid-infrared properties of metal-insulator composite materials
[AD-A234264] N91-26219
Damage accumulation in advanced metal matrix composites under thermal cycling
[AD-A235002] N91-26227
Microstructure, porosity, and mechanical property relationships of calcium-silicate-hydrate
[AD-A235191] N91-26279
Microstructure, plastic deformation and mechanical properties of mechanically alloyed NiAl and NiAl based alloys
[AD-A235135] N91-26303
Mechanical properties of spray atomized SiC particle reinforced aluminum-titanium alloys
[AD-A235231] N91-26306
Mechanical behavior of nanocrystalline Cu, Pd, and Ag samples
[DE91-011747] N91-26310
US and foreign alloy cross-reference database
[NASA-CR-184166] N91-26313
Thermal transitions and mechanical properties of the films of chemically prepared polyaniline
[AD-A233807] N91-26329
Mechanical properties of polycarbonate-polysulfone and polycarbonate-polyetherimide blends
[AD-A234939] N91-26360
LaRC-ITPI/arylene ether copolymers
[NASA-TM-104099] N91-26378
A new high-progressivity/high-density propulsion concept: Partially cut multiperforated stick propellant
[AD-A234255] N91-26391
The development of piezoelectric poly(vinylidene fluoride) sensors for measuring peel stresses in adhesive joints
[AD-A233880] N91-26559
The High Resolution Profiler (HRP): User's guide and software modifications documentation
[AD-A234640] N91-26663
MHD contractors' review meeting
[DE91-011295] N91-26945

MEDICAL EQUIPMENT
Utilization of emergency medical kits by air carriers
[AD-A234784] N91-26721

MEDICAL PERSONNEL
Administrative guide for the flight surgeon and the aeromedical technician: Performing medical examinations
[AD-A235178] N91-26727

MEDICAL SCIENCE
US Army Biomedical Research and Development Laboratory
[AD-A233664] N91-26671

MELTING
Sea-level response to ice sheet evolution: An ocean perspective N91-26575
Late Wisconsin and early holocene glacial history, inner Ross Embayment, Antarctica N91-26577
Marine record of late quaternary glacial-interglacial fluctuations in the Ross Sea and evidence for rapid, episodic sea level change due to marine ice sheet collapse N91-26578
Ice cores and SeaRISE: What we do (and don't) know N91-26579
Growth, evaporation and melting of ice crystals: Implications for radiation, atmospheric dynamics and particle scavenging N91-26611
Process study of sorted patterns on Arctic soils
[AD-A234089] N91-26628

MEMBRANE STRUCTURES
Ionically and electronically conductive composite polymer membranes
[AD-A234587] N91-26349

MEMBRANES
Flexural plate wave devices for chemical analysis
[AD-A234129] N91-26254
Electrochemically induced charge and mass transport in polypyrrole/poly(styrene sulfonate) molecular composites
[AD-A234599] N91-26354
Template synthesis of polymeric and metal microtubules
[AD-A235307] N91-26367
Viscoelastic behavior of elastomeric membranes
[AD-A234496] N91-26560
Photochemical energy conversion by membrane-bound photoredox systems
[DE91-012171] N91-26682

MEMORY
Categories and particulars: Prototype effects in estimating spatial location
[AD-A234955] N91-26741

MEMORY (COMPUTERS)
Content addressable memory project
[AD-A234524] N91-26763
A parallel rendering algorithm for MIMD architectures
[NASA-CR-187571] N91-26767

MENISCI
Transport processes and interfacial phenomena in an evaporating meniscus
[DE91-005561] N91-26284

MENTAL PERFORMANCE
Induced pictorial representations
[AD-A234548] N91-26735
Assessment of the pharmacodynamics of intranasal, intravenous and oral scopolamine N91-27114
MERCATOR PROJECTION
Software requirements specification for the Mapping And Graphic Information Capability (MAGIC). Volume 4: Geographic mapping CSCI
[AD-A235275] N91-26794
MERCURY CADMIUM TELLURIDES
Luminescence and lasing in II-VI semiconductors
[AD-A235019] N91-26961
MESOMETEOROLOGY
Applications of MST radars: Meteorological applications N91-26622
Coordination of mesoscale meteorological research between ASL and European groups
[AD-A233586] N91-26639
The development of an improved convective initiation scheme for Mesoscale numerical weather prediction models, phase 1
[AD-A235417] N91-26650
MESOSCALE PHENOMENA
Gravity waves and instabilities in the lower and middle atmosphere N91-26621
Applications of MST radars: Meteorological applications N91-26622
Coordination of mesoscale meteorological research between ASL and European groups
[AD-A233586] N91-26639
The development of an improved convective initiation scheme for Mesoscale numerical weather prediction models, phase 1
[AD-A235417] N91-26650
Advanced Microwave Precipitation Radiometer (AMPR) for remote observation of precipitation
[NASA-CR-184165] N91-26655
MESOSPHERE
Middle Atmosphere Program. Handbook for MAP. Volume 30: International School on Atmospheric Radar
[NASA-CR-188623] N91-26613
The instrumental principles of MST radars and incoherent scatter radars and the configuration of radar system hardware N91-26616
Statistical characteristics of MST radar echoes and its interpretation N91-26617
Data acquisition and processing N91-26618
Applications of MST radars: Meteorological applications N91-26622
MESSAGE PROCESSING
KC-135 ground collision avoidance system questionnaire
[AD-A234385] N91-26125
Strategies for reliable and real time execution on a heterogeneous multiprocessor
[AD-A234114] N91-26801
The process group approach to reliable distributed computing
[NASA-CR-188498] N91-26804
Strategies for parallel AI implementations
[AD-A234449] N91-26811
METABOLISM
JPRS Report: Science and technology. USSR: Life sciences
[JPRS-ULS-91-009] N91-26688
Computer tomography measurement of vertebral bones and muscles after extended manned space flights N91-26690
Functional activity of hypophyseal-thyroid system during 370-day antiorthostatic hypokinesia N91-26691
Biochemical aspects of human adaptation to combined effect of antiorthostasis, decreased barometric pressure, and increased oxygen content N91-26694
Reaction of human skeletal muscle fibers to 370 day antiorthostatic hypokinesia combined with physical exertion N91-26702
Metabolic changes and hemodynamic dysfunction following hypothermic shock
[AD-A233942] N91-26713
Pharmacological sparing of protein in burn injury
[AD-A235026] N91-26724
Reexamination of METMAN, recommendations on enhancement of LCVG, and development of new concepts for EMU heat sink N91-27098
The effects of deuterium on static posture control N91-27102
METAL COMBUSTION
Turbulent premixed hydrogen/air flames
[AD-A235109] N91-26278
Boron combustion model development with kinetic sensitivity analysis and measurement of key chemical rate parameters
[AD-A235309] N91-26283
METAL FILMS
Metastable pitting corrosion of aluminum, Al-Cu, and Al-Si thin films in dilute HF solutions and its relevancy to the processing of integrated circuit interconnections
[DE91-012014] N91-26320
METAL IONS
Partial oxidation of light alkanes in transition-metal ion containing zeolites
[DE91-008202] N91-26243
Charge exchange in ion-surface scattering at hyperthermal (10-100 eV) and keV energies
[AD-A235233] N91-26899
Study of the effect of reactive element addition by implanting metal ions in a pre-formed oxide layer
[DE91-011916] N91-26974
METAL MATRIX COMPOSITES
Corrosion of graphite aluminum metal matrix composites
[AD-A234322] N91-26220
Fiber coating by sputtering for high temperature composites
[AD-A234994] N91-26226
Damage accumulation in advanced metal matrix composites under thermal cycling
[AD-A235002] N91-26227
Mechanical properties of spray atomized SiC particle reinforced aluminum-titanium alloys
[AD-A235231] N91-26306
Oxidation resistant coatings for titanium alloys and titanium alloy matrix composites
[NASA-CASE-LEW-15155-1] N91-26375
METAL OXIDE SEMICONDUCTORS
Chemistry of fluorine in the oxidation of silicon
[AD-A234959] N91-26272
Surface etching and roughening in integrated processing of thermal oxides
[AD-A234960] N91-26456
A temperature dependent SPICE macro-model for power MOSFETs
[DE91-011737] N91-26972
METAL OXIDES
Defect clustering and related properties of oxides
[DE91-011072] N91-26290
Heterogeneous catalysis on platinum and self-assembled monolayers on metal and metal oxide surfaces
[AD-A235055] N91-26302
METAL PLATES
Dynamic energy absorption of sandwich structures by inelastic deformation
[AD-A234903] N91-26564
METAL SURFACES
Turbulent premixed hydrogen/air flames
[AD-A235109] N91-26278
Epitaxy of metal atoms on metal surfaces: Deposition and diffusion
[DE91-011142] N91-26309
Charge exchange in ion-surface scattering at hyperthermal (10-100 eV) and keV energies
[AD-A235233] N91-26899
Ab initio molecular dynamics simulations of surfaces and interfaces
[AD-A235315] N91-26901
Optical methods of measuring the roughness of the surfaces of high precision steel balls
[AD-A234796] N91-26928
METAL VAPORS
Performance of hypervelocity armatures with replenished metal vapor plasmas
[DE91-011931] N91-26187
METALLIC PLASMAS
Performance of hypervelocity armatures with replenished metal vapor plasmas
[DE91-011931] N91-26187
METALLIZING
Block patterning of the metallization of polyvinylidene fluoride transducers
[AD-D014872] N91-26450
Ohmic contacts to semiconducting diamond
[AD-A234130] N91-26950
METALLOGRAPHY
Investigations into fracture mechanics failure concepts with thermomechanically rolled steels
[BLL-OA-TRANS-4238-(6196.3)] N91-26556
METALS
Epitaxy of metal atoms on metal surfaces: Deposition and diffusion
[DE91-011142] N91-26309
Ohmic contacts to semiconducting diamond
[AD-A234130] N91-26950
METATHESIS
Living ring-opening metathesis polymerization of 7-oxa-2,3-difunctionalized norbornenes and norbornadienes by Mo(CHCMe2R) (N-2,6-C6H3-i-Pr2) (O-t-Bu)2 and Mo(CHCMe2R) (N-2,6-C6H3-i-Pr2) (OCMe2CF3)2
[AD-A235235] N91-26365
METEOR TRAILS
Meteor scatter communication between Thule and Station Nord, Greenland
[AD-A234440] N91-26424
METEORITE COLLISIONS
The effects of space debris on solar propulsion
[AD-A235257] N91-26192
METEORITES
Solutions to problems of weathering in Antarctic eucrites N91-27113
METEORITIC COMPOSITION
Investigation of plessite in iron meterorites and laboratory Fe-Ni(P) alloys
[DE91-010858] N91-27053
Solutions to problems of weathering in Antarctic eucrites N91-27113
METEORITIC DAMAGE
The effects of space debris on solar propulsion
[AD-A235257] N91-26192
METEOROID CONCENTRATION
Determination of the masses and densities of meteoroids from radar observations from one point N91-26177
METEOROIDS
Determination of the masses and densities of meteoroids from radar observations from one point N91-26177
METEOROLOGICAL PARAMETERS
Surface Observation Climatic Summaries (SOCS) for Kodiak, Alaska
[AD-A235182] N91-26646
Surface observation climatic summaries for Norton AFB, California
[AD-A235227] N91-26647
Surface observation climatic summaries for Tonopah test range, Nevada
[AD-A235228] N91-26648
Improved Point Analysis Model (IPAM) (users guide)
[AD-A235305] N91-26649
METEOROLOGICAL RADAR
Middle Atmosphere Program. Handbook for MAP. Volume 30: International School on Atmospheric Radar
[NASA-CR-188623] N91-26613
Historical aspects of radar atmospheric dynamics N91-26614
Radar principles N91-26615
The instrumental principles of MST radars and incoherent scatter radars and the configuration of radar system hardware N91-26616
Statistical characteristics of MST radar echoes and its interpretation N91-26617
Data acquisition and processing N91-26618
Spectral and correlation analysis with applications to middle-atmosphere radars N91-26619
Applications of MST radars: Meteorological applications N91-26622
METEOROLOGICAL SATELLITES
Weather satellites: Action needed to resolve status of the US Geostationary Satellite Program. Report to the Chairman, Committee on Science, Space, and Technology, House of Representatives
[GAO/NSIAD-91-252] N91-26194
METEOROLOGY
JPRS report: Science and technology. USSR: Earth sciences
[JPRS-UES-91-002] N91-26581
Atmospheric optical turbulence measurements taken at Anderson Mesa, Flagstaff, Arizona between 10-19 July 1990
[AD-A234190] N91-26629
Catalog of data bases and reports
[DE91-011516] N91-27043
METHANE
Electrocatalytic study of ammonia synthesis and methane dimerization in high temperature solid electrolyte cells
[DE91-009797] N91-26289
METHYL ALCOHOL
The synthesis of methanol by a novel method
[DE91-011131] N91-26291
METHYL COMPOUNDS
Laser ionic multiphoton dissociation of some acrylate clusters
[AD-A233801] N91-26247
METROLOGY
Center for electronics and electrical engineering. Technical progress bulletin covering center programs, July to September 1990, with 1991 CEEE events calendar
[PB91-159749] N91-26437

MICE
Molecular studies of cytokine induction
[AD-A235326] N91-26731
MICROANALYSIS
Mechanical behavior and flow mechanisms in refractory metal composition
[AD-A234701] N91-26297
A study of the gas phase chemistry of solid propellants using a microprobe mass spectrometer (MPMS) system: Initial development of the MPMS system
[AD-A234839] N91-26393
MICROCOMPUTERS
Modification of the user friendly thermodynamic code to include the effects of minor species
[AD-A233929] N91-26390
MICROCRACKS
Fragmentation of brittle materials at high rates of loading N91-26237
NATO advanced research workshop on Measurement of Residual and Applied Stress Using Neutron Diffraction
[AD-A235103] N91-26566
MICROCRYSTALS
Preparation of a novel gallium arsenide single-source precursor having the empirical formula AsCl3Ga2
[AD-A233704] N91-26949
MICROELECTRONICS
Active devices for monolithic millimeter-wave integrated circuits
[AD-A234033] N91-26440
Forecasting digital microcircuit obsolescence
[AD-A234573] N91-26451
Solid state research
[AD-A234836] N91-26958
Monolithic integration semiconductor and superconductor components
[AD-A234986] N91-26959
Electrostatic fields in a dusty Martian environment N91-27078
MICROMOTORS
Piezoelectric micromotors for microrobots
[AD-A234423] N91-26446
MICROORGANISMS
Adaptation and resistance of ecosystems to stress
[AD-A234576] N91-26603
Introduction to Session 2: Applied biological research
[DE91-012067] N91-26680
Molecular studies of cytokine induction
[AD-A235326] N91-26731
MICROPOROSITY
Template synthesis of polymeric and metal microtubules
[AD-A235307] N91-26367
MICROPROCESSORS
WPG-30 model microprocessor controlled rotating beryllium mirror scanning camera and its applications
[AD-A234802] N91-26493
MICROSTRIP ANTENNAS
Radiation, scattering, and guidance of electromagnetic fields by arbitrarily shaped structures embedded in layered dielectric media
[AD-A234434] N91-26423
MICROSTRUCTURE
Microstructure development during microwave annealing of dense silicon nitride
[DE91-012069] N91-26242
Microstructure, porosity, and mechanical property relationships of calcium-silicate-hydrate
[AD-A235191] N91-26279
Materials/microstructures characterization
[AD-A233751] N91-26295
Mechanical behavior and flow mechanisms in refractory metal composition
[AD-A234701] N91-26297
Quantum mechanical approach to understanding microstructural and mechanical properties of intermetallics
[AD-A234702] N91-26298
Microstructure, plastic deformation and mechanical properties of mechanically alloyed NiAl and NiAl based alloys
[AD-A235135] N91-26303
Mechanical properties of spray atomized SiC particle reinforced aluminum-titanium alloys
[AD-A235231] N91-26306
Mechanical behavior of nanocrystalline Cu, Pd, and Ag samples
[DE91-011747] N91-26310
The cryogenic mechanical properties of Vintage 3 Al-Li-Zr alloy 2090-T81
[DE91-011897] N91-26311
Precipitation in Alloy 718: A combined AEM and APFIM investigation
[DE91-009918] N91-26314
Strain enhanced microstructural evolution
[DE91-011921] N91-26318
Grain boundary chemistry in Al-Cu metallizations as determined by analytical electron microscopy
[DE91-012007] N91-26319
Microstructure and hardness of NiAl/Ni2AlX two-phase ordered intermetallic alloys
[DE91-012068] N91-26323
A program in the chemistry of electronic materials. Task 1: New organometallic precursors for the low pressure chemical vapor deposition of refractory materials for electronics
[AD-A234315] N91-26342
Transformation toughening of ceramics
[AD-A234926] N91-26359
Pressureless densification of ceramic matrix composites
[AD-A235031] N91-26362
Strength and microstructure of ceramics
[AD-A235424] N91-26374
A tribological investigation of the graphite-to-diamond-like behavior of amorphous carbon films ion-beam-deposited on ceramic substrates
[DE91-010816] N91-26379
Basic studies of microstructure of combusting turbulent flows
[AD-A234222] N91-26471
Investigations into fracture mechanics failure concepts with thermomechanically rolled steels
[BLL-OA-TRANS-4238-(6196.3)] N91-26556
MICROWAVE ANTENNAS
MMIC integration technology investigation
[NASA-CR-188035] N91-26434
Four-to-one power combiner for 20 GHz phased array antenna using RADC MMIC phase shifters N91-26435
MICROWAVE CIRCUITS
MMIC integration technology investigation
[NASA-CR-188035] N91-26434
Four-to-one power combiner for 20 GHz phased array antenna using RADC MMIC phase shifters N91-26435
Active devices for monolithic millimeter-wave integrated circuits
[AD-A234033] N91-26440
High temperature superconducting plana circuit structures for high frequency applications
[AD-A234335] N91-26445
MICROWAVE EQUIPMENT
Development of a tactical high-power microwave source using the Plasma Electron Microwave Source (PEMS) concept
[AD-A234967] N91-26942
MICROWAVE FREQUENCIES
Microwave properties of high transition temperature superconducting thin films
[NASA-CR-185842] N91-26976
MICROWAVE IMAGERY
Satellite data derived estimates of erosion parameters for reentry vehicles
[AD-A234792] N91-26189
MICROWAVE OSCILLATORS
Work performed experiments: 1989-1990
[AD-A235221] N91-26457
MICROWAVE RADIOMETERS
Advanced Microwave Precipitation Radiometer (AMPR) for remote observation of precipitation
[NASA-CR-184165] N91-26655
MICROWAVE SOUNDING
Atmospheric InfraRed Sounder (AIRS): Science and measurement requirements
[NASA-TM-104977] N91-26624
MICROWAVES
Microstructure development during microwave annealing of dense silicon nitride
[DE91-012069] N91-26242
Radio frequency and microwave plasma for optical thin film deposition
[DE91-012081] N91-26525
Advanced Microwave Precipitation Radiometer (AMPR) for remote observation of precipitation
[NASA-CR-184165] N91-26655
Development of a tactical high-power microwave source using the Plasma Electron Microwave Source (PEMS) concept
[AD-A234967] N91-26942
Near field interaction of microwave signals with a bounded plasma plume
[NASA-CR-185358] N91-26944
Microwave properties of high transition temperature superconducting thin films
[NASA-CR-185842] N91-26976
MIDCOURSE GUIDANCE
Boost-phase kill versus midcourse discrimination: The grand inquisitor's solution
[DE91-011744] N91-26871
MIDDLE ATMOSPHERE
Middle Atmosphere Program. Handbook for MAP Volume 30: International School on Atmospheric Radar
[NASA-CR-188623] N91-26613
Spectral and correlation analysis with applications to middle-atmosphere radars N91-26619
Gravity waves and instabilities in the lower and middle atmosphere N91-26621
MIE SCATTERING
Effect of aerosols on laser-induced breakdown
[AD-A234324] N91-26502
MIGRATION
Energy migration, motion and order in synthetic polymers
[AD-A234403] N91-26346
MILITARY AIR FACILITIES
Surface observation climatic summaries for Norton AFB, California
[AD-A235227] N91-26647
MILITARY OPERATIONS
Scaling CW electron beam pumped rare gas lasers to ultra-high average power
[AD-A235120] N91-26513
Progress with neural network gulf streams
[AD-A233810] N91-26658
Aircrew Evaluation Sustained Operations Performance (AESOP): A triservice facility for technology transition
[AD-A234626] N91-26738
Space doctrine
[AD-A234971] N91-26866
A Rome Laboratory guide to basic training in TQM analysis techniques
[AD-A233855] N91-26993
Personal papers in the United States Air Force Historical Research Center, 5th edition
[PB91-156380] N91-26999
MILITARY TECHNOLOGY
Liquid water production from atmospheric sources
[AD-A235090] N91-26406
Opportunities for advanced speech processing in military computer-based systems
[AD-A233724] N91-26412
Coordination of mesoscale meteorological research between ASL and European groups
[AD-A233586] N91-26639
Personal papers in the United States Air Force Historical Research Center, 5th edition
[PB91-156380] N91-26999
MILLIMETER WAVES
Active devices for monolithic millimeter-wave integrated circuits
[AD-A234033] N91-26440
De-embedding millimeter-wave integrated circuits with TRL
[AD-A234194] N91-26442
MIMD (COMPUTERS)
A parallel rendering algorithm for MIMD architectures
[NASA-CR-187571] N91-26767
MINERALOGY
Sand and Dust on Mars
[NASA-CP-10074] N91-27057
The chemistry and mineralogy of Mars soil and dust N91-27058
Chemistry and mineralogy of Martian dust: An explorer's primer N91-27063
Reflectance spectroscopy of palagonite and iron-rich montmorillonite clay mixtures: Implications for the surface composition of Mars N91-27075
Derivation of mid-infrared (5-25 microns) optical constants of some silicates and palagonite N91-27077
MINERALS
Characteristics of aerosol in the atmosphere of Mars according to data from the KRFM experiment N91-26175
Reflectance spectroscopy of palagonite and iron-rich montmorillonite clay mixtures: Implications for the surface composition of Mars N91-27075
Impact of Mars sand on dust on the design of space suits and life support equipment: A technology assessment N91-27079
MINIATURIZATION
Tactical quartz oscillator development
[AD-A234308] N91-26443
MINIMAX TECHNIQUE
Viscosity methods in optimal control of distributed systems. The Bellman equation
[AD-A234646] N91-26812
MINKOWSKI SPACE
Covering a closed curve with a given total curvature
[AD-A234342] N91-26840
MIR SPACE STATION
Review of primary medical results of year-long flight on Mir station N91-26178
Survey of the principal results of medical research in the flight program of the second main expedition aboard the Mir orbiting complex N91-26686
MIRRORS
Plasma reflectors for electronic beam steering in radar systems
[AD-A234560] N91-26425

Radio frequency and microwave plasma for optical thin film deposition
[DE91-012081] N91-26525
System concept and analysis of an Artificial Ionospheric Mirror (AIM) radar
[AD-A234269] N91-26630
Full surface testing of grazing incidence mirrors
[AD-A234005] N91-26922

MIS (SEMICONDUCTORS)
Submicron gate InP power MISFET's with improved output power density at 18 and 20 GHz N91-26436

MISSILE COMPONENTS
Transpiration cooled ultraviolet sol-gel silica optics
[AD-A235426] N91-26934

MISSILE CONTROL
Apparatus for guiding a missile
[AD-D014866] N91-26147

MISSION PLANNING
Applications of artificial intelligence to mission planning
[NASA-CR-187953] N91-26806
NASA/ASEE Summer Faculty Fellowship Program, 1990, volume 2
[NASA-CR-185637-VOL-2] N91-27103
Developing a taxonomy for mission architecture definition N91-27108

MIXERS
Quantum limited quasiparticle mixers at 100 GHz
[DE91-011826] N91-26991

MIXING CIRCUITS
Quantum limited quasiparticle mixers at 100 GHz
[DE91-011894] N91-26973

MIXING LAYERS (FLUIDS)
The effects of compressibility on a supersonic mixing layer
[AD-A234992] N91-26119

MIXTURES
Raman spectroscopy study of solvation structure in acetonitrile/water mixtures
[AD-A234921] N91-26271
Processable polymers and copolymers of 3-alkylthiophenes and their blends
[AD-A234596] N91-26351

MODELS
Bidirectional reflectance distribution (BRDF) of NASA shuttle tiles
[AD-A235115] N91-26188
Interfacial slippage of a unidirectional fiber composite under longitudinal shearing
[AD-A234186] N91-26216
Pressureless densification of ceramic matrix composites
[AD-A235031] N91-26362
Integration of neurobiological and computational analyses of the neural network essentials for conditioned taste aversion
[AD-A235164] N91-26744
Testing the One-Port Random Access Memory (1PRAM) module of TRW's CPUAX signal processing superchip
[AD-A234127] N91-26761
Understanding object classes: Modeling and matching
[AD-A235027] N91-26848
Boundary layer transition noise art
[AD-A235093] N91-26884
Incorporation of shuttle CCT parameters in computer simulation models N91-27096

MODULES
Research on stable, high-efficiency amorphous silicon multijunction modules
[DE91-002159] N91-26591

MOISTURE
Environmental embrittlement of ordered intermetallic alloys at room temperature in moist atmospheres
[DE91-012051] N91-26321

MOISTURE CONTENT
Rotating multicylinder method for the measurement of cloud liquid-water content and droplet size
[AD-A234780] N91-26644
Techniques for determining total body water using deuterium oxide N91-27091

MOLECULAR BEAM EPITAXY
Center for the Integration of Optical C
[AD-A235277] N91-26931

MOLECULAR BEAMS
Cluster beam deposition of high temperature materials
[AD-A234358] N91-26343

MOLECULAR BIOLOGY
Introduction to Session 2: Applied biological research
[DE91-012067] N91-26680

MOLECULAR CHAINS
Electronic and ionic transport in processable conducting polymers
[AD-A234597] N91-26352

MOLECULAR COLLISIONS
Studies of resonantly enhanced multiphoton ionization processes in molecules
[AD-A235217] N91-26898
Electron-excited molecule interactions
[DE91-012227] N91-26911

MOLECULAR ELECTRONICS
Energy migration, motion and order in synthetic polymers
[AD-A234403] N91-26346

MOLECULAR ENERGY LEVELS
Theoretical studies of potential energy surfaces and computational methods
[DE91-011126] N91-26902

MOLECULAR EXCITATION
The analysis of a rocket tomography measurement of the N2+3914A emission and N2 ionization rates in an auroral arc
[NASA-CR-188622] N91-26596

MOLECULAR INTERACTIONS
Raman spectroscopy study of solvation structure in acetonitrile/water mixtures
[AD-A234921] N91-26271
Electronic and ionic transport in processable conducting polymers
[AD-A234597] N91-26352
Molecular engineering dynamics of electron transport and nonlinear optical interaction in Langmuir-Blodgett films of organic semiconductor heterostructure
[AD-A235001] N91-26897
Ab initio molecular dynamics simulations of surfaces and interfaces
[AD-A235315] N91-26901

MOLECULAR IONS
Study of the low-lying electronic states of Si2 and Si2(-) using negative ion photodetachment techniques
[AD-A234336] N91-26256
LIF and emission studies of copper and nitrogen N91-27089

MOLECULAR ORBITALS
Molecular orbital studies of the bonding in heavy element organometallics
[DE91-010915] N91-26905
The electronic structure of the ionic insulator sodium nitrite
[DE91-009766] N91-26977

MOLECULAR OSCILLATIONS
Studies of resonantly enhanced multiphoton ionization processes in molecules
[AD-A235217] N91-26898

MOLECULAR ROTATION
LIF and emission studies of copper and nitrogen N91-27089

MOLECULAR STRUCTURE
Energetics, bonding mechanism and electronic structure of metal/ceramic interfaces
[DE91-009787] N91-26239
Synthesis and properties of rigid-rod benzobisazole polymers containing benzothiazole pendent groups
[AD-A234742] N91-26357
Synthesis and characterization of polysilanes
[AD-A235357] N91-26370
Preparation of inorganic and organometallic polymers with controlled structures
[AD-A235359] N91-26371
Electronic excitation transport in photosynthesis and crystal and molecular structures of porphyrin compounds
[DE91-012024] N91-26679
Molecular orbital studies of the bonding in heavy element organometallics
[DE91-010915] N91-26905

MOLECULAR WEIGHT
Supercritical fluid processing of propellant polymers
[AD-A234285] N91-26341
Processable polymers and copolymers of 3-alkylthiophenes and their blends
[AD-A234596] N91-26351
Synthesis of energetic single phase and multi-phase polymers
[AD-A235104] N91-26363
Effect of molecular weight on polyphenylquinoxaline properties
[NASA-TM-104100] N91-26377

MOLECULES
Molecular mechanics calculations for nitro and amino substituted conjugated systems containing oxygen and nitrogen
[AD-A233928] N91-26389
Negative ion photodetachment as a probe of the transition state region: The I + HI reaction
[AD-A235297] N91-26900
Electron-excited molecule interactions
[DE91-012227] N91-26911

MOLTEN SALTS
HYLIFE-2 inertial confinement: Fusion power plant design
[DE91-012089] N91-26947

MOMENTS
Underwater scattering of sound
[AD-A235097] N91-26885

MOMENTS OF INERTIA
Fluid damping of the oscillations of satellites with a large magnetic moment N91-26170

MONITORS
COSMIC: Software catalog 1991 edition diskette format N91-27036
NSI operations center N91-27038
Incorporation of shuttle CCT parameters in computer simulation models N91-27096

MONKEYS
A statistical analysis of -X rhesus head kinematics
[AD-A233977] N91-26674
Effect of 7 day antiorthostatic hypokinesia on cardiac pumping action in monkeys N91-26704

MONOCHROMATIC RADIATION
HORACE: Presentation-level protocol standard for digital transmission of monochrome television images
[AD-A235276] N91-26428

MONOMERS
Synthesis, polymerization and thermal properties of a new acetylene-terminated Schiff base
[AD-A233806] N91-26328
Processable polymers and copolymers of 3-alkylthiophenes and their blends
[AD-A234596] N91-26351
Synthesis and properties of rigid-rod benzobisazole polymers containing benzothiazole pendent groups
[AD-A234742] N91-26357
Effect of molecular weight on polyphenylquinoxaline properties
[NASA-TM-104100] N91-26377
Field work and dispersion relations of excitations on fractals
[AD-A234953] N91-26455

MONOPOLE ANTENNAS
Input impedance and gain of monopole elements with disk ground planes on flat earth
[AD-A234284] N91-26421

MONTE CARLO METHOD
Simulation of precipitation scavenging in a three-dimensional global model
[DE91-011531] N91-26606
Research in stochastic processes
[AD-A234650] N91-26860

MONTMORILLONITE
Reflectance spectroscopy of palagonite and iron-rich montmorillonite clay mixtures: Implications for the surface composition of Mars N91-27075

MOODS
Methylphenidate and pemoline: Effects on sleepiness and mood during sleep deprivation
[AD-A234659] N91-26718

MOON
Galileo: The Earth encounter N91-27024

MORPHOLOGY
Results of morphometric analysis of the Tesserae surface of Venus according to Venera-15 and -16 data N91-26176
Polymeric routes to silicon carbide and silicon oxycarbide CMC
[NASA-TM-104372] N91-26234

MORTALITY
Weighted least squares estimation for Aalen's additive risk model
[AD-A235250] N91-26852

MOTION SICKNESS
Vestibular reactions and intersensory interactions in weightlessness: Results of Optokinez experiment N91-26698
The effects of deuterium on static posture control N91-27102
Assessment of the pharmacodynamics of intranasal, intravenous and oral scopolamine N91-27114

MOTION STABILITY
Nonlinear oscillations of mechanical systems under multifrequency parametric excitation
[AD-A233800] N91-26558

MOUNTING
Double face sealing device
[NASA-CASE-MFS-28521-1] N91-26542
Removable hand hold
[NASA-CASE-LEW-15196-1] N91-26543

MULTIPHOTON ABSORPTION
Studies of resonantly enhanced multiphoton ionization processes in molecules
[AD-A235217] N91-26898

MULTIPLE ACCESS
Spread spectrum communication networks
[AD-A233696] N91-26409

MULTIPROCESSING (COMPUTERS)
Waiting algorithms for synchronization in large-scale multiprocessors
[AD-A234985] N91-26764
A parallel rendering algorithm for MIMD architectures
[NASA-CR-187571] N91-26767
Strategies for reliable and real time execution on a heterogeneous multiprocessor
[AD-A234114] N91-26801
Structure driven multiprocessor compilation of numeric problems
[AD-A234653] N91-26803
A divide and conquer approach to the nonsymmetric eigenvalue problem
[DE91-011085] N91-26854

MULTISENSOR APPLICATIONS
Northeast Artificial Intelligence Consortium (NAIC). Volume 16: Intelligent signal processing techniques for multi-sensor surveillance systems
[AD-A234895] N91-26830

MULTIVARIATE STATISTICAL ANALYSIS
Fixed sample and sequential problems with applications in reliability
[AD-A234547] N91-26547

MUSCLES
Computer tomography measurement of vertebral bones and muscles after extended manned space flights N91-26690
Reaction of human skeletal muscle fibers to 370 day antiorthostatic hypokinesia combined with physical exertion N91-26702
Effects of 13 day space flight on skeletal muscles and neuromuscular junctions in rats N91-26703
The effects of deuterium on static posture control N91-27102

MUTATIONS
Interaction of ionizing radiation, genetically active chemicals, and radiofrequency radiation in human and rodent cells
[AD-A234747] N91-26677
Studies of mutant hemoglobins to define types of modifications useful in the design of blood substitutes
[AD-A234997] N91-26723

N

NARROWBAND
Complex envelope properties, interpretation, filtering, and evaluation
[AD-A234478] N91-26844
Design for electronic spectrally tunable infrared detector
[AD-D014877] N91-26925

NASA PROGRAMS
Weather satellites: Action needed to resolve status of the US Geostationary Satellite Program. Report to the Chairman, Committee on Science, Space, and Technology, House of Representatives
[GAO/NSIAD-91-252] N91-26194
Commercial use of space: Many grantees making progress, but NASA oversight could be improved. Report to the Chair, Subcommittee on VA, HUD, and Independent Agencies, Committee on Appropriations, U.S. Senate
[GAO/NSIAD-91-142] N91-26400
The NASA/MSFC global reference atmospheric model: 1990 version (GRAM-90). Part 1: Technical/users manual
[NASA-TM-4268] N91-26654
Parallel processing and expert systems
[NASA-TM-103886] N91-26796
NSI organization and highlights N91-27011
Overview of the NASA astrophysics data system N91-27022
NSIUWG security sub-group N91-27026
The NASA Science Internet: An integrated approach to networking N91-27041
National Aeronautics and Space Administration Multiyear Authorization Act of 1991 N91-27046
Report of the 90-day study on human exploration of the Moon and Mars
[NASA-TM-102999] N91-27055
NASA/ASEE Summer Faculty Fellowship Program, 1990, Volume 1
[NASA-CR-185637-VOL-1] N91-27088
NASA/ASEE Summer Faculty Fellowship Program, 1990, volume 2
[NASA-CR-185637-VOL-2] N91-27103

NASA SPACE PROGRAMS
Developing a taxonomy for mission architecture definition N91-27108

NASTRAN
Development of load-dependent Ritz vector method for structural dynamic analysis of large space structures N91-27111

NATIONAL AEROSPACE PLANE PROGRAM
Aerospace plane technology: Research and development efforts in Europe. Report to the Chairman, Committee on Science, Space, and Technology, House of Representatives
[GAO/NSIAD-91-194] N91-26141

NATURAL LANGUAGE (COMPUTERS)
Uncertainty handling at speech/natural language interface, volume 1
[AD-A234310] N91-26422
Northeast Artificial Intelligence Consortium (NAIC). Volume 2: Discussing, using, and recognizing plans
[AD-A234881] N91-26816
Retrieval using plausible inference
[AD-A235015] N91-27006

NAVIER-STOKES EQUATION
Direct and large-eddy simulations of three-dimensional compressible Navier-Stokes turbulence
[AD-A233717] N91-26470
Simulation of pore scale porous media flow using lattice gas methods
[DE91-004829] N91-26484
Navier-Stokes calculations of scramjet-nozzle-afterbody flowfields
[NASA-CR-185356] N91-26488

NAVIGATION
Analytical algorithms to solve an inverse navigation problem for a system of satellites N91-26168
Study of the properties of the autonomous optical navigation of a space probe in a rendezvous with an asteroid N91-26169
Space support for airland battle-future
[AD-A233868] N91-26864

NAVIGATION INSTRUMENTS
Autonomous aircraft initiative study
[NASA-CR-186013] N91-26140

NAVY
The Navy standard compressed aeronautical chart database
[AD-A235340] N91-26587
Cognitive and neural sciences division 1990 programs
[AD-A233773] N91-26733

NEAR FIELDS
One-dimensional translation measurement of speckle from rough rotating objects in ultraviolet illumination
[AD-A233719] N91-26919
Near field interaction of microwave signals with a bounded plasma plume
[NASA-CR-185358] N91-26944

NEAR INFRARED RADIATION
Electroactive, near infrared absorbing nickel bis(dithiolene) complex polycarbonates and polyurethanes
[AD-A234595] N91-26350
Material engineering of novel semiconductor structures
[AD-A235014] N91-26960

NEGATIVE IONS
Study of the low-lying electronic states of Si2 and Si2(-) using negative ion photodetachment techniques
[AD-A234336] N91-26256
Anionic ring-opening polymerization of cyclotetrasilanes
[AD-A235360] N91-26372
Negative ion photodetachment as a probe of the transition state region: The I + HI reaction
[AD-A235297] N91-26900
Correlation in photodetachment
[DE91-011369] N91-26908
Negative ion formation by Rydberg electron transfer: Isotope-dependent rate constants
[DE91-012058] N91-26909

NEODYMIUM LASERS
SUNLITE program. Sub-Hertz relative frequency stabilization of two diode laser pumped Nd:YAG lasers locked to a Fabry-Perot interferometer
[NASA-CR-184957] N91-26520
New laser materials for laser diode pumping
[NASA-CR-187786] N91-26521
Precision high-power solid-state laser diagnostics for target-irradiation studies and target-plane irradiation modeling
[DE91-012036] N91-26523

NERVES
A physiologically motivated front end for speech recognition
[AD-A233727] N91-26414
Peptide transport through the blood-brain barrier
[AD-A233753] N91-26708

NERVOUS SYSTEM
Neural mechanisms of attention
[AD-A235003] N91-26742

NETWORK ANALYSIS
A sequential Jackson network with feedback
[ITN-91-85111] N91-26867
NSI directed to continue SPAN's functions N91-27042

NETWORK CONTROL
Northeast Artificial Intelligence Consortium (NAIC). Volume 4: Distributed artificial intelligence for communications network management
[AD-A234883] N91-26818

NETWORK SYNTHESIS
Flight control law synthesis using neural network theory
[AD-A234990] N91-26149
Maximization on matroids with random weights
[AD-A233978] N91-26858

NEURAL NETS
Flight control law synthesis using neural network theory
[AD-A234990] N91-26149
Progress with neural network gulf streams
[AD-A233810] N91-26658
Integration of neurobiological and computational analyses of the neural network essentials for conditioned taste aversion
[AD-A235164] N91-26744
A comparative study of the practical characteristics of neural network and conventional pattern classifiers
[AD-A235345] N91-26795
Extensions of a theory of networks and learning: Outliers and negative examples
[AD-A234425] N91-26810
Using modular neural networks with local representations to control dynamic systems
[AD-A234700] N91-26813
Gabor transforms and neural networks for automatic target recognition
[DE91-011919] N91-26834
Mathematical problems concerning rhythmic processes
[AD-A234588] N91-26845
Center for the Integration of Optical C
[AD-A235277] N91-26931
A system for UNIX command retrieval using a multilayered neural network
[DE91-012105] N91-27045

NEUROLOGY
Cognitive and neural sciences division 1990 programs
[AD-A233773] N91-26733
Integration of neurobiological and computational analyses of the neural network essentials for conditioned taste aversion
[AD-A235164] N91-26744

NEUROMUSCULAR TRANSMISSION
Effects of 13 day space flight on skeletal muscles and neuromuscular junctions in rats N91-26703

NEURONS
Parallel processing and learning: Variability and chaos in self-organization of activity in groups of neurons
[AD-A234589] N91-26737

NEUROPHYSIOLOGY
Intracellular physiology of the rat suprachiasmatic nucleus: Electrical properties, neurotransmission, and effects of neuromodulators
[AD-A234442] N91-26675
Attention span, anxiety, and benzodiazepine receptors
[AD-A234549] N91-26716
Cognitive and neural sciences division 1990 programs
[AD-A233773] N91-26733
Parallel processing and learning: Variability and chaos in self-organization of activity in groups of neurons
[AD-A234589] N91-26737

NEUROTRANSMITTERS
Parallel processing and learning: Variability and chaos in self-organization of activity in groups of neurons
[AD-A234589] N91-26737

NEUTRAL ATMOSPHERES
Development of a Vector Spherical Harmonic (VSH) model of the neutral thermosphere
[AD-A234744] N91-26631

NEUTRAL ATOMS
Neutral atom deBroglie-wave interferometry
[AD-A234624] N91-26896

NEUTRAL GASES
Effect of turbulence on impurity observation in upper atmosphere using lidar method N91-26584

NEUTRALIZERS
Investigation and characterization of ITO/poly-Si photovoltaic junctions
[ITN-91-85105] N91-26590

NEUTRINOS
Preliminary estimates of core-collapse supernova rates from the Berkeley automated supernova search
[DE91-011824] N91-27050

NEUTRON ACTIVATION ANALYSIS
Solutions to problems of weathering in Antarctic eucrites N91-27113

NEUTRON DIFFRACTION
Defect clustering and related properties of oxides
[DE91-011072] N91-26290
NATO advanced research workshop on Measurement of Residual and Applied Stress Using Neutron Diffraction
[AD-A235103] N91-26566
NEUTRON SCATTERING
Chemical phase separation in binary iron-chromium alloys
[DE91-010282] N91-26294
Photons and neutrons
[DE91-010980] N91-26906
NEUTRONS
Photons and neutrons
[DE91-010980] N91-26906
NEVADA
Surface observation climatic summaries for Tonopah test range, Nevada
[AD-A235228] N91-26648
NEWFOUNDLAND
In the energy active region of the ocean N91-26583
NEWTON METHODS
General relativistic continuum mechanics and the post-Newtonian equations of motion N91-26987
NICKEL ALLOYS
Microstructure, plastic deformation and mechanical properties of mechanically alloyed NiAl and NiAl based alloys
[AD-A235135] N91-26303
Cyclic deformation, damage, and effects of environment in the Ni3Al ordered alloy at elevated temperature
[AD-A235168] N91-26304
Grain boundary cavitation processes in a Ni3Al alloy at elevated temperatures
[AD-A235279] N91-26307
TEM in-situ straining of B2 compounds
[DE91-012062] N91-26322
Microstructure and hardness of NiAl/Ni2AlX two-phase ordered intermetallic alloys
[DE91-012068] N91-26323
Effect of boron addition on recrystallization and grain growth in Ni3Al polycrystals
[DE91-011966] N91-26983
NICKEL COMPOUNDS
Electroactive, near infrared absorbing nickel bis(dithiolene) complex polycarbonates and polyurethanes
[AD-A234595] N91-26350
Surface characterization of electrically conducting nickel tetrathiooxalate/poly(vinyl alcohol) composites
[AD-A234598] N91-26353
NICOTINE
Smoking, exercise, and physical fitness
[AD-A234658] N91-26717
NIGHT
VLF nighttime data analysis
[AD-A234006] N91-26417
Effect of shift work of air traffic controllers on sympathetic nervous system N91-26700
NIGHT VISION
Evaluation of night vision goggles for maritime search and rescue
[AD-A233798] N91-26751
NIMBUS 7 SATELLITE
Nimbus-7 TOMS Antarctic ozone atlas: August - December 1990
[NASA-RP-1264] N91-26651
NIOBIUM
Mechanical behavior and flow mechanisms in refractory metal composition
[AD-A234701] N91-26297
NITRIC OXIDE
Relationships between PAN and ozone at sites in eastern North America
[DE91-011728] N91-26607
NITRITES
The electronic structure of the ionic insulator sodium nitrite
[DE91-009766] N91-26977
NITROBENZENES
Gel solidified microinterface between two immiscible electrolytes applied to amperometric detection of picrate and tetramethylammonium
[AD-A235260] N91-26280
NITROGEN
Simulation of precipitation scavenging in a three-dimensional global model
[DE91-011531] N91-26606
NITROGEN ATOMS
The control of orbital mixing in ruthenium complexes containing quinone related ligands
[AD-A234802] N91-26260
NITROGEN COMPOUNDS
Additives for high temperature liquid lubricants
[DE91-011018] N91-26386
Molecular mechanics calculations for nitro and amino substituted conjugated systems containing oxygen and nitrogen
[AD-A233928] N91-26389
Biological synthesis of substituted o-aminophenols
[AD-A234910] N91-26678
NITROGEN IONS
Investigation and characterization of ITO/poly-Si photovoltaic junctions
[ITN-91-85105] N91-26590
LIF and emission studies of copper and nitrogen N91-27089
NITROGEN ISOTOPES
Measurement of the nitrogen total cross section from 0.5 eV to 50 MeV and analysis of the 433-keV resonance
[DE91-012222] N91-26293
NITROGEN LASERS
Infrared and visible laser double resonance studies of vibrational energy transfer processes in polyatomic molecules
[DE91-012162] N91-26910
NITROGEN OXIDES
CFD analysis of jet mixing in low NOx flametube combustors
[NASA-TM-104466] N91-26146
NOISE
Chaotic and bifurcating nonlinear systems driven by noise with applications to laser dynamics
[AD-A234841] N91-26512
Statistical properties of intrinsic topological noise in tokamaks
[DE91-011741] N91-26939
NOISE (SOUND)
Computation of broadband mixing noise from turbomachinery
[AD-A233991] N91-26878
NOISE INTENSITY
Flexural plate wave devices for chemical analysis
[AD-A234129] N91-26254
NOISE PROPAGATION
Chaotic and bifurcating nonlinear systems driven by noise with applications to laser dynamics
[AD-A234841] N91-26512
NOISE REDUCTION
High order differentiation filters that work
[AD-A234504] N91-26874
Aircraft interior noise reduction by alternate resonance tuning
[NASA-CR-185453] N91-26889
NOISE SPECTRA
A catalog of high resolution Jovian decametric radio noise burst spectra, volume 1 N91-27047
NONADIABATIC CONDITIONS
Modelling the dynamics of fluxes of electrons with energies 30-300 keV in geostationary orbit N91-26173
NONAQUEOUS ELECTROLYTES
Impedance profiling: A convenient technique for determining the redox or protonic acid doping characteristics of conducting polymers
[AD-A233941] N91-26337
NONDESTRUCTIVE TESTS
Evaluation of environmentally aged polymer/composite material by ultrasonic inspection
[AD-A235343] N91-26231
A basic guide to overlay design using nondestructive testing equipment data
[AD-A234472] N91-26403
NDE pattern recognition of LSS states via wave propagation
[AD-A234772] N91-26549
Nondestructive Evaluation (NDE) of fiberglass marine structures state-of-the art review
[AD-A234785] N91-26550
Non-destructive evaluation of residual stresses in thin films via x ray diffraction topography methods
[AD-A235328] N91-26552
NONLINEAR FEEDBACK
Theory and experimental and chemical instabilities
[AD-A234916] N91-26270
NONLINEAR FILTERS
Analysis of visual loss from retinal lesions
[AD-A235268] N91-26729
Research in stochastic processes
[AD-A234650] N91-26860
NONLINEAR OPTICS
Design of polymers with semiconductor, NLO, and structural properties
[AD-A235215] N91-26364
Part 1: Ultrafast logic and multiple-beam optical parallel processing using nonlinear etalons. Part 2: Novel devices for all-optical computing. Part 3: Novel nonlinear semiconductor structures for signal processing and optical computing
[AD-A233410] N91-26799
Analysis of nonlinear optical frequency conversion
[AD-A233726] N91-26920
The First Nonlinear Optics: Materials, Phenomena, and Devices Conference
[AD-A234733] N91-26926
Studies of optical beam phase-conjugation and electromagnetic scattering process
[AD-A234830] N91-26929
NONLINEAR SYSTEMS
Application of transformational ideas to automatic flight control design
[AD-A234758] N91-26148
Nonlinear dynamics and control of flexible structures
[AD-A235186] N91-26191
Nonlinear behavior of fiber composite materials and its effect on the postbuckling response of laminated plates
[AD-A234203] N91-26218
Chaotic and bifurcating nonlinear systems driven by noise with applications to laser dynamics
[AD-A234841] N91-26512
Nonlinear oscillations of mechanical systems under multifrequency parametric excitation
[AD-A233800] N91-26558
NFEARS: A nonlinear adaptive finite element solver. Part 2: User's manual
[AD-A234416] N91-26842
Normalization of the parameterized Courant-Snyder matrix
[DE91-012554] N91-26856
Molecular engineering dynamics of electron transport and nonlinear optical interaction in Langmuir-Blodgett films of organic semiconductor heterostructure
[AD-A235001] N91-26897
Nonperturbative behavior of quarks
[DE91-011905] N91-26903
Nonlinear systems dynamics in cardiovascular physiology: The heart rate delay map and lower body negative pressure N91-27095
NONLINEARITY
International collaboration program on innovative chemical processing of superior electronic and optical materials
[AD-A235030] N91-26276
Novel liquid crystalline polymers as nonlinear optical materials
[AD-A235371] N91-26373
Application of a conjugate gradient method to the synthesis of phase-only planar arrays
[AD-A233756] N91-26415
Research in nonlinear water waves
[AD-A235410] N91-26478
Molecular engineering dynamics of electron transport and nonlinear optical interaction in Langmuir-Blodgett films of organic semiconductor heterostructure
[AD-A235001] N91-26897
NONNEWTONIAN FLUIDS
Analytical solution of plane Poiseuille flow of a Johnson-Segalman fluid
[AD-A234313] N91-26472
NOREPINEPHRINE
Effect of shift work of air traffic controllers on sympathetic nervous system N91-26700
NORTHERN HEMISPHERE
ARTIST tape output formats
[AD-A235173] N91-26633
NOSE FINS
Vehicle steering device
[AD-D014861] N91-26537
NOSE WHEELS
A look at digital nose wheel steering
[AD-A233944] N91-26131
NOZZLE FLOW
Optical studies of the flow start-up processes in four convergent-divergent nozzles
[AD-A234552] N91-26473
NUCLEAR EXPLOSIONS
Comparison of the RF frequency spectra of HEMP and lightning
[AD-A234306] N91-26642
NUCLEAR FUSION
Parametric studies of dense plasma focus for fusion space propulsion with D-He3
[AD-A234578] N91-26941
NUCLEAR PHYSICS
Normalization of the parameterized Courant-Snyder matrix
[DE91-012554] N91-26856
NUCLEAR PROPULSION
Engine cycle analysis for a particle bed reactor nuclear rocket
[AD-A235258] N91-26199
NUCLEAR REACTIONS
Measurement of the nitrogen total cross section from 0.5 eV to 50 MeV and analysis of the 433-keV resonance
[DE91-012222] N91-26293

Nonperturbative behavior of quarks
[DE91-011905] N91-26903

NUCLEAR REACTORS
A reliability and mass perspective of SP-100 Stirling cycle lunar-base powerplant designs
[NASA-TM-103736] N91-26592

NUCLEAR RESEARCH
Quality Assurance Manual
[DE91-012618] N91-26555

NUCLEATION
Fragmentation of brittle materials at high rates of loading N91-26237
Transmission electron microscopy of the CVD diamond film/substrate interface
[AD-A234790] N91-26956
An induction time approach to surface induced crystallization in polyethylene/poly (e-caprolactone) melt
[AD-A235102] N91-26964
Crystal growth in a microgravity environment
[NASA-CASE-MFS-28473-1] N91-26968
Crystallization of thin films of amorphous germanium alloys
[ITN-91-85110] N91-26969

NUMBER THEORY
Primes: The first 2400 prime numbers
[AD-A233979] N91-26837

NUMERICAL ANALYSIS
Application of a conjugate gradient method to the synthesis of phase-only planar arrays
[AD-A233756] N91-26415
Backscattering enhancement from rough surfaces
[AD-A234707] N91-26426
Acceleration insensitive resonators
[AD-A235400] N91-26458
A software package for unconstrained optimization using tensor methods
[AD-A233989] N91-26778
Symbolic expressions of composite grid structures
[AD-A233794] N91-26836
Numerical methods for singularly perturbed differential equations with applications
[AD-A235188] N91-26850
A gravitationally consistent second-order analytic secular solution for the point-mass motion of the eight principal planets N91-27054

NUMERICAL CONTROL
De-embedding millimeter-wave integrated circuits with TRL
[AD-A234194] N91-26442
WPG-30 model microprocessor controlled rotating beryllium mirror scanning camera and its applications
[AD-A234802] N91-26493
Advanced material handling equipment controls
[AD-A235091] N91-26540

NUMERICAL STABILITY
Stability of collocation-based Runge-Kutta-Nystroem methods
[CWI-NM-R9016] N91-26835

NUMERICAL WEATHER FORECASTING
The development of an improved convective initiation scheme for Mesoscale numerical weather prediction models, phase 1
[AD-A235417] N91-26650

NUTRITION
Level of dietary fat does not affect fuel oxidation or endurance exercise performance of soldiers
[AD-A235194] N91-26728

NYQUIST DIAGRAM
Propulsion stability codes for liquid propellant propulsion systems developed for use on a PC computer
[NASA-CR-184983] N91-26201

NYSTAGMUS
State and forms of adaptation of vestibular function after space flights N91-26706

O

OBJECT PROGRAMS
Object-oriented requirements analysis: A quick tour
[NASA-CR-187919] N91-26766

OBSERVATION
Surface Observation Climatic Summaries (SOCS) for Kodiak, Alaska
[AD-A235182] N91-26646

OBSERVATORIES
The Berkeley/Anglo-Australian Observatory high-redshift supernova search
[DE91-012348] N91-27051

OCEAN CURRENTS
The SYNOP experiment: Inverted echo sounder data report for June 1989 to September 1990
[AD-A234625] N91-26662
Phytoplankton abundance in relation to Lagrangian paths
[AD-A233728] N91-26672

OCEAN DATA ACQUISITIONS SYSTEMS
The NASA master directory quick reference guide N91-27034

OCEAN DYNAMICS
The tropical Pacific Ocean's heat budget during a cold event, from a numerical model N91-26657

OCEAN MODELS
The tropical Pacific Ocean's heat budget during a cold event, from a numerical model N91-26657
Analysis of wave characteristics in extreme seas
[AD-A234538] N91-26660
Laboratory modelling of the dynamics of coastal upwelling
[AD-A234987] N91-26664
Comparison of sound pressure in a wedge-shaped ocean as predicted by an image method and a PE model
[AD-A234191] N91-26879

OCEAN SURFACE
Progress with neural network gulf streams
[AD-A233810] N91-26658
Analysis of wave characteristics in extreme seas
[AD-A234538] N91-26660
A boundary scattering strength extraction algorithm for the analysis of long-range reverberation data
[AD-A233721] N91-26877

OCEANOGRAPHY
JPRS report: Science and technology. USSR: Earth sciences
[JPRS-UES-91-002] N91-26581
Ocean acoustic tomography and telemetry
[AD-A233826] N91-26659
Research in stochastic processes
[AD-A234650] N91-26860

OCEANS
Sea-level response to ice sheet evolution: An ocean perspective N91-26575
In the energy active region of the ocean N91-26583
Ocean acoustic tomography and telemetry
[AD-A233826] N91-26659
Phytoplankton abundance in relation to Lagrangian paths
[AD-A233728] N91-26672
Backscattering from rough interfaces and the parabolic approximation
[AD-A235184] N91-26886

OFF-ON CONTROL
Singular and bang-bang stochastic control
[AD-A234752] N91-26861

OMEGA NAVIGATION SYSTEM
Omega/VLF signal coverage database development
[AD-A235226] N91-26129

ON-LINE SYSTEMS
On-line magnetic tape Library Inventory Tracking And Reporting (LITAR) system
[AD-A234934] N91-27004
Overview of the NSI User Support Office (NSI USO) N91-27028
The NSINIC on-line system N91-27029
Integrating UNIX workstation into existing online data acquisition systems for Fermilab experiments
[DE91-011974] N91-27044

OPACITY
Dust in the Mars atmosphere N91-27082

OPENINGS
Double face sealing device
[NASA-CASE-MFS-28521-1] N91-26542

OPERATING SYSTEMS (COMPUTERS)
The High Resolution Profiler (HRP): User's guide and software modifications documentation
[AD-A234640] N91-26663
NRL connection machine Fortran library
[AD-A234121] N91-26779
The process group approach to reliable distributed computing
[NASA-CR-188498] N91-26804
NSI security task: Overview N91-27016
MultiNet TCP/P/IP for VAX/VMS update N91-27020
NSI directed to continue SPAN's functions N91-27042

OPERATIONS RESEARCH
Creation of uncertainty in repeated two-person non-zero-sum games
[ITN-91-85118] N91-26869

OPERATOR PERFORMANCE
Physical and psychogenic sequelae of impact acceleration on tracking performance of operators N91-26701

OPTICAL COMMUNICATION
Wideband heterodyne spatial tracking for optical space communications
[AD-A233722] N91-26410

OPTICAL COMPUTERS
Part 1: Ultrafast logic and multiple-beam optical parallel processing using nonlinear etalons. Part 2: Novel devices for all-optical computing. Part 3: Novel nonlinear semiconductor structures for signal processing and optical computing
[AD-A233410] N91-26799
Design and construction of apparatus for optical switch evaluation
[AD-A234765] N91-26927
Research instrumentation for optical computing
[AD-A235335] N91-26932

OPTICAL CORRELATORS
Design of optimal correlation filters for hybrid vision systems N91-27110

OPTICAL DATA PROCESSING
Part 1: Ultrafast logic and multiple-beam optical parallel processing using nonlinear etalons. Part 2: Novel devices for all-optical computing. Part 3: Novel nonlinear semiconductor structures for signal processing and optical computing
[AD-A233410] N91-26799
Northeast Artificial Intelligence Consortium (NAIC). Volume 12: Computer architecture for very large knowledge bases
[AD-A234891] N91-26826
Research instrumentation for optical computing
[AD-A235335] N91-26932
Design of optimal correlation filters for hybrid vision systems N91-27110

OPTICAL DATA STORAGE MATERIALS
Proceedings of the First Workshop on 3-D Optical Memories
[AD-A234732] N91-27003

OPTICAL DENSITY
Scaling CW electron beam pumped rare gas lasers to ultra-high average power
[AD-A235120] N91-26513

OPTICAL EQUIPMENT
Array-typed, sealed-off mini tea CO2 laser
[AD-A234804] N91-26511
Computational complexity and efficiency in electro-optical computing system
[AD-A235013] N91-26765
An ultraviolet optical isolator utilizing the KDP-isomorphs
[AD-D014860] N91-26923
The First Nonlinear Optics: Materials, Phenomena, and Devices Conference
[AD-A234733] N91-26926
Thickness measurements of silicon films using partial coherence interferometry
[AD-A235211] N91-26930
Binary optics technology: Theoretical limits on the diffraction efficiency of multilevel diffractive optical elements
[AD-A235404] N91-26933

OPTICAL FIBERS
Improved inline fiber optic sensor arrays
[AD-D014864] N91-26924

OPTICAL FILTERS
Design of optimal correlation filters for hybrid vision systems N91-27110

OPTICAL HETERODYNING
Wideband heterodyne spatial tracking for optical space communications
[AD-A233722] N91-26410

OPTICAL MATERIALS
International collaboration program on innovative chemical processing of superior electronic and optical materials
[AD-A235030] N91-26276
Design of polymers with semiconductor, NLO, and structural properties
[AD-A235215] N91-26364
Novel liquid crystalline polymers as nonlinear optical materials
[AD-A235371] N91-26373
The First Nonlinear Optics: Materials, Phenomena, and Devices Conference
[AD-A234733] N91-26926
Transpiration cooled ultraviolet sol-gel silica optics
[AD-A235426] N91-26934

OPTICAL MEASUREMENT
Laser-induced desorption of H2 from Si(111)7x7
[AD-A234636] N91-26508

OPTICAL MEASURING INSTRUMENTS
High accuracy optical rate sensor N91-27115

OPTICAL MEMORY (DATA STORAGE)
Photoinduced absorption and erasable optical information storage in polyanilines
[AD-A234108] N91-27002
Proceedings of the First Workshop on 3-D Optical Memories
[AD-A234732] N91-27003

OPTICAL PATHS
Center for the Integration of Optical C
[AD-A235277] N91-26931
OPTICAL POLARIZATION
An ultraviolet optical isolator utilizing the KDP-isomorphs
[AD-D014860] N91-26923
OPTICAL PROPERTIES
Far- and mid-infrared properties of metal-insulator composite materials
[AD-A234264] N91-26219
Materials/microstructures characterization
[AD-A233751] N91-26295
Design of polymers with semiconductor, NLO, and structural properties
[AD-A235215] N91-26364
Optical studies of the flow start-up processes in four convergent-divergent nozzles
[AD-A234552] N91-26473
WPG-30 model microprocessor controlled rotating beryllium mirror scanning camera and its applications
[AD-A234802] N91-26493
Laser spectroscopy characterization of materials for frequency agile solid state laser systems
[AD-A233916] N91-26500
Atmospheric propagation of laser beams
[AD-A234314] N91-26501
Neutral atom deBroglie-wave interferometry
[AD-A234624] N91-26896
Molecular engineering dynamics of electron transport and nonlinear optical interaction in Langmuir-Blodgett films of organic semiconductor heterostructure
[AD-A235001] N91-26897
The First Nonlinear Optics: Materials, Phenomena, and Devices Conference
[AD-A234733] N91-26926
Studies of optical beam phase-conjugation and electromagnetic scattering process
[AD-A234830] N91-26929
Center for the Integration of Optical C
[AD-A235277] N91-26931
Recent studies of the optical properties of dust and cloud particles in the Mars atmosphere and the interannual frequency of global dust storms N91-27060
OPTICAL PUMPING
The First Nonlinear Optics: Materials, Phenomena, and Devices Conference
[AD-A234733] N91-26926
OPTICAL RADAR
JPRS report: Science and technology. USSR: Earth sciences
[JPRS-UES-91-003] N91-26582
Effect of turbulence on impurity observation in upper atmosphere using lidar method N91-26584
OPTICAL REFLECTION
Bidirectional reflectance distribution (BRDF) of NASA shuttle tiles
[AD-A235115] N91-26188
OPTICAL RESONANCE
Infrared and visible laser double resonance studies of vibrational energy transfer processes in polyatomic molecules
[DE91-012162] N91-26910
OPTICAL SWITCHING
Design and construction of apparatus for optical switch evaluation
[AD-A234765] N91-26927
OPTICAL THICKNESS
Dust in the Mars atmosphere N91-27082
OPTICAL TRACKING
Wideband heterodyne spatial tracking for optical space communications
[AD-A233722] N91-26410
OPTIMAL CONTROL
High-power converters for space applications
[NASA-CR-187116] N91-26461
ROBOT: A journal of Chinese Society of Automation
[AD-A234808] N91-26538
Aircrew Evaluation Sustained Operations Performance (AESOP): A triservice facility for technology transition
[AD-A234626] N91-26738
Viscosity methods in optimal control of distributed systems. The Bellman equation
[AD-A234646] N91-26812
Northeast Artificial Intelligence Consortium (NAIC). Volume 13: Image understanding and intelligent parallel systems
[AD-A234897] N91-26832
H-infinity-optimal control for distributed parameter systems
[AD-A234931] N91-26833
OPTIMIZATION
Performance optimization of helicopter rotor blades
[NASA-TM-104054] N91-26137
A software package for unconstrained optimization using tensor methods
[AD-A233989] N91-26778
Program improvement by automatic redistribution of intermediate results
[AD-A235086] N91-26791
Nonlinear stochastic optimization solution procedures and incomplete information
[AD-A235242] N91-26793
Maximization on matroids with random weights
[AD-A233978] N91-26858
Heuristics for a flow-shop model with parallel machines and setup times
[ITN-91-85117] N91-26996
The effects of character size, modulation, polarity, and font on reading and search performance in matrix-addressable displays
[AD-A235033] N91-27007
OPTOELECTRONIC DEVICES
Proceedings of the Optoelectronic Workshop 25: Liquid Crystal Materials and Devices for Opto-Electronic Applications
[AD-A233780] N91-26921
ORBIT CALCULATION
TRACE trajectory analysis and orbit determination program. Volume 13: Square root information filtering and smoothing
[AD-A234957] N91-26183
ORBIT TRANSFER VEHICLES
Engine cycle analysis for a particle bed reactor nuclear rocket
[AD-A235258] N91-26199
ORBITAL ELEMENTS
Evolution of some types of Earth satellite orbits N91-26163
ORBITAL SERVICING
Incorporation of shuttle CCT parameters in computer simulation models N91-27096
ORGANIC MATERIALS
Surface mediated photocatalysis
[AD-A233748] N91-26246
ORGANIC SEMICONDUCTORS
Molecular engineering dynamics of electron transport and nonlinear optical interaction in Langmuir-Blodgett films of organic semiconductor heterostructure
[AD-A235001] N91-26897
ORGANIC SILICON COMPOUNDS
Organosilicon polymers incorporating the bicyclo(2.2.2)-octane moiety
[AD-A234966] N91-26361
Second Mini-Conference on Key Problems in Silicon Chemistry
[AD-A235243] N91-26366
ORGANIC SULFUR COMPOUNDS
Processable polymers and copolymers of 3-alkylthiophenes and their blends
[AD-A234596] N91-26351
ORGANIZATIONS
NSI white pages project: X.500 directory service N91-27039
ORGANOMETALLIC COMPOUNDS
A program in the chemistry of electronic materials. Task 1: New organometallic precursors for the low pressure chemical vapor deposition of refractory materials for electronics
[AD-A234315] N91-26342
Molecular orbital studies of the bonding in heavy element organometallics
[DE91-010915] N91-26905
ORGANOMETALLIC POLYMERS
Preparation of inorganic and organometallic polymers with controlled structures
[AD-A235359] N91-26371
ORTHOTROPIC PLATES
Buckling of laminated composite plates
[ITN-91-85101] N91-26232
OSCILLATIONS
Oscillations of a small-mass satellite probe caused by aerodynamic and gravitational forces N91-26165
Fluid damping of the oscillations of satellites with a large magnetic moment N91-26170
Tunable excimer lasers
[DE91-011399] N91-26522
The relationship of traditional damping measures for materials with high damping capacity
[AD-A235347] N91-26568
OSCILLATORS
Low frequency noise in resonant Josephson soliton oscillators
[DE91-011911] N91-26464
An ultraviolet optical isolator utilizing the KDP-isomorphs
[AD-D014860] N91-26923
Study of Josephson effect arrays as sources at 1 THz
[AD-A234526] N91-26952
Quantum devices and structures
[AD-A235298] N91-26989
OVER-THE-HORIZON RADAR
System concept and analysis of an Artificial Ionospheric Mirror (AIM) radar
[AD-A234289] N91-26630
OXIDATION
Partial oxidation of light alkanes in transition-metal ion containing zeolites
[DE91-008202] N91-26243
Polyaniline: Synthesis and properties of pernigraniline
[AD-A233706] N91-26245
Polyaniline: Allowed oxidation states
[AD-A233842] N91-26251
Chemistry of fluorine in the oxidation of silicon
[AD-A234959] N91-26272
Polyaniline: Pernigraniline, an isolable intermediate in the conventional chemical synthesis of emeraldine
[AD-A233840] N91-26330
Polyaniline: Oriented films and fibers
[AD-A234414] N91-26347
Oxidation resistant coatings for titanium alloys and titanium alloy matrix composites
[NASA-CASE-LEW-15155-1] N91-26375
Surface etching and roughening in integrated processing of thermal oxides
[AD-A234960] N91-26456
OXIDATION RESISTANCE
Oxidation resistant coatings for titanium alloys and titanium alloy matrix composites
[NASA-CASE-LEW-15155-1] N91-26375
OXIDATION-REDUCTION REACTIONS
Partial oxidation of light alkanes in transition-metal ion containing zeolites
[DE91-008202] N91-26243
Cross-linking and modification of cytochrome c with redox-active metal complexes
[DE91-012023] N91-26287
Photochemical energy conversion by membrane-bound photoredox systems
[DE91-012171] N91-26682
OXIDES
Study of the effect of reactive element addition by implanting metal ions in a pre-formed oxide layer
[DE91-011916] N91-26974
OXIDIZERS
Bonding agent for composite propellants
[AD-D014876] N91-26392
OXYFLUORIDES
Chemistry of fluorine in the oxidation of silicon
[AD-A234959] N91-26272
OXYGEN
A combined XPS-ISS modulated molecular beam investigation of the reactions of oxygen and fluorine with silicon surfaces
[AD-A234867] N91-26269
Living ring-opening metathesis polymerization of 7-oxa-2,3-difunctionalized norbornenes and norbornadienes by Mo(CHCMe2R) (N-2,6-C6H3-i-Pr2) (O-t-Bu)2 and Mo(CHCMe2R) (N-2,6-C6H3-i-Pr2) (OCMe2CF3)2
[AD-A235235] N91-26365
Strength of SiC- and Si-N-C-ceramic fibers exposed to high-temperature gaseous environments
[DE91-011099] N91-26380
Polymer characterization using singlet oxygen phosphorescence as a spectroscopic probe
[DE91-011735] N91-26382
Molecular mechanics calculations for nitro and amino substituted conjugated systems containing oxygen and nitrogen
[AD-A233928] N91-26389
Electrochemically modulated superconductivity
[AD-A234703] N91-26955
OXYGEN ATOMS
A combined XPS-ISS modulated molecular beam investigation of the reactions of oxygen and fluorine with silicon surfaces
[AD-A234867] N91-26269
OXYGEN PRODUCTION
Refurbishing AV-8 on-board oxygen generation system beds
[AD-A235083] N91-26136
Design of a lunar oxygen production plant N91-27109
OXYGEN SUPPLY EQUIPMENT
An Air Revitalization Model (ARM) for Regenerative Life Support Systems (RLSS) N91-27093
OXYHEMOGLOBIN
Studies of mutant hemoglobins to define types of modifications useful in the design of blood substitutes
[AD-A234997] N91-26723
OZONE
Improvement of procedures for evaluating photochemical models
[PB91-160374] N91-26597

Relationships between PAN and ozone at sites in eastern North America
[DE91-011728] N91-26607
Nimbus-7 TOMS Antarctic ozone atlas: August - December 1990
[NASA-RP-1264] N91-26651

OZONE DEPLETION
Nimbus-7 TOMS Antarctic ozone atlas: August - December 1990
[NASA-RP-1264] N91-26651

P

P-N JUNCTIONS
Development and testing of radiation and electromagnetic pulse hardened silicon carbide based electronics
[AD-A233744] N91-26439

PACIFIC OCEAN
The tropical Pacific Ocean's heat budget during a cold event, from a numerical model N91-26657

PACKAGING
Improved inline fiber optic sensor arrays
[AD-D014864] N91-26924

PAIN
Peptide transport through the blood-brain barrier
[AD-A233753] N91-26708

PAINTS
The impact of atmospheric damage to materials on consumers: News you can use
[DE91-012075] N91-26610

PALLADIUM
Mechanical behavior of nanocrystalline Cu, Pd, and Ag samples
[DE91-011747] N91-26310

PANELS
Reflection of incident pressure waves by ribbed panels
[AD-A233671] N91-26469
Aircraft interior noise reduction by alternate resonance tuning
[NASA-CR-185453] N91-26889

PARALLEL PROCESSING (COMPUTERS)
A parallel rendering algorithm for MIMD architectures
[NASA-CR-187571] N91-26767
Parallel processing and expert systems
[NASA-TM-103886] N91-26796
Part 1: Ultrafast logic and multiple-beam optical parallel processing using nonlinear etalons. Part 2: Novel devices for all-optical computing. Part 3: Novel nonlinear semiconductor structures for signal processing and optical computing
[AD-A233410] N91-26799
Structure driven multiprocessor compilation of numeric problems
[AD-A234653] N91-26803
Strategies for parallel AI implementations
[AD-A234449] N91-26811
Northeast Artificial Intelligence Consortium (NAIC). Volume 12: Computer architecture for very large knowledge bases
[AD-A234891] N91-26826
A divide and conquer approach to the nonsymmetric eigenvalue problem
[DE91-011085] N91-26854
Computational methods and software for differential equations and their applications
[DE91-012172] N91-26855
A nonrecursive order N preconditioned conjugate gradient: Range space formulation of MDOF dynamics N91-27099

PARALLEL PROGRAMMING
A parallel rendering algorithm for MIMD architectures
[NASA-CR-187571] N91-26767

PARAMETERIZATION
Quality by design using statistically planned experiments
[ITN-91-85119] N91-26553
Target parameter estimation N91-26620
Boundary layer parameterization for a global spectral model
[AD-A235310] N91-26635
On the sensitivity of solutions of parametrized equations
[AD-A234265] N91-26838

PARAMETRIC AMPLIFIERS
Analysis of nonlinear optical frequency conversion
[AD-A233726] N91-26920

PARTIAL DIFFERENTIAL EQUATIONS
NUMVEC FORTRAN library manual. Chapter: Partial differential equations. Routine: ICGG3D
[CWI-NM-R9018] N91-26768
A system and language environment for scientific computing
[AD-A233747] N91-26772
Adaptive component methods for time dependent PDE's
[AD-A233776] N91-26775
Numerical methods for singularly perturbed differential equations with applications
[AD-A235188] N91-26850
Spectral recovery of discontinuous data
[ITN-91-85115] N91-26853

PARTICLE ACCELERATOR TARGETS
Magnetron sputter deposition of boron and boron carbide
[DE91-011194] N91-26241
Precision high-power solid-state laser diagnostics for target-irradiation studies and target-plane irradiation modeling
[DE91-012036] N91-26523

PARTICLE ACCELERATORS
Electromagnetic launch technology assessment. Scientific basis and unified treatment: Forces and electromechanical power conversion (analytical and numerical methods)
[AD-A235028] N91-26185
An active particle accelerator
[DE91-011404] N91-26915

PARTICLE BEAMS
Studies of interactions between elementary particles and nuclei
[DE91-012300] N91-26912

PARTICLE COLLISIONS
High energy density systems in cryogenic media: The production and reaction of atoms and radicals
[AD-A233785] N91-26892
Studies of interactions between elementary particles and nuclei
[DE91-012300] N91-26912

PARTICLE DENSITY (CONCENTRATION)
Effect of surface forces on the rheology of particle-liquid systems and the consolidation of ceramic powders
[AD-A234375] N91-26221

PARTICLE INTERACTIONS
Studies of interactions between elementary particles and nuclei
[DE91-012300] N91-26912

PARTICLE MOTION
Wind abrasion on Mars N91-27064
Martian dust threshold measurements: Simulations under heated surface conditions N91-27081
Mathematical modeling of the flow field and particle motion in a rotating bioreactor at unit gravity and microgravity N91-27092

PARTICLE PRODUCTION
Studies of interactions between elementary particles and nuclei
[DE91-012300] N91-26912

PARTICLE SIZE DISTRIBUTION
Characteristics of aerosol in the atmosphere of Mars according to data from the KRFM experiment N91-26175
Modal aerosol dynamics modeling
[PB91-161729] N91-26598
Evaluation of the Navy oceanic vertical aerosol model using lidar and PMS particle-size spectrometers
[AD-A233653] N91-26625
Dust in the Mars atmosphere N91-27082

PARTICLE THEORY
Nonperturbative behavior of quarks
[DE91-011905] N91-26903

PARTICULATES
Gordon Research Conference on Composites
[AD-A233778] N91-26210
Reaction processing of ceramic particulate and whisker composites
[AD-A234951] N91-26225
Mechanical properties of spray atomized SiC particle reinforced aluminum-titanium alloys
[AD-A235231] N91-26306
The distribution of particulate material on Mars N91-27059
Recent studies of the optical properties of dust and cloud particles in the Mars atmosphere and the interannual frequency of global dust storms N91-27060

PASCHEN SERIES
Effect of pressure on electrostatic processes on Mars N91-27069

PASSENGER AIRCRAFT
Civil tiltrotor missions and applications. Phase 2: The commercial passenger market
[NASA-CR-177576] N91-26126

PATHOLOGY
Metabolic changes and hemodynamic dysfunction following hypothermic shock
[AD-A233942] N91-26713

PATIENTS
Pharmacological sparing of protein in burn injury
[AD-A235026] N91-26724

PATTERN RECOGNITION
NDE pattern recognition of LSS states via wave propagation
[AD-A234772] N91-26549
OSIRRUS: Oceanic symbolic image representation, recognition and understanding software
[AD-A235112] N91-26665
Using genetic algorithms to select and create features for pattern classification
[AD-A235165] N91-26792
A comparative study of the practical characteristics of neural network and conventional pattern classifiers
[AD-A235345] N91-26795
Extensions of a theory of networks and learning: Outliers and negative examples
[AD-A234425] N91-26810
Gabor transforms and neural networks for automatic target recognition
[DE91-011919] N91-26834
Pumping system fault detection and diagnosis utilizing pattern recognition and fuzzy inference techniques
[DE91-011849] N91-26863
Automatic target recognition using acousto-optic image correlator
[DE91-011499] N91-26936

PAVEMENTS
Geogrid reinforced base course for flexible pavements for light aircraft: Literature review and test section design
[DOT/FAA/RD-90/28] N91-26160
Guidelines for design, construction, and evaluation of airport pavement drainage
[DOT/FAA/RD-90/31] N91-26161
International State-of-the-Art Colloquium on Low-Temperature Asphalt Pavement Cracking
[AD-A233663] N91-26402
A basic guide to overlay design using nondestructive testing equipment data
[AD-A234472] N91-26403

PAYLOADS
Unmanned aerial vehicles. Medium range system components do not fit
[AD-A234131] N91-26132

PEBBLE BED REACTORS
Engine cycle analysis for a particle bed reactor nuclear rocket
[AD-A235258] N91-26199

PEELING
The development of piezoelectric poly(vinylidene fluoride) sensors for measuring peel stresses in adhesive joints
[AD-A233880] N91-26559

PENETRATION
Dynamics of equatorial and polar boundaries of penetration of solar protons with energy about 1 MeV into magnetosphere during strong magnetic storm N91-26172
Long-rod penetration of confined ceramic tiles
[AD-A234312] N91-26534

PEPTIDES
Interaction of cationic polypeptides with electroactive polypyrrole/poly(styrenesulfonate) and poly(N-methylpyrrole)/poly(styrenesulfonate) films
[AD-A234469] N91-26258
Peptide transport through the blood-brain barrier
[AD-A233753] N91-26708

PERCEPTION
Neural mechanisms of attention
[AD-A235003] N91-26742

PERFORMANCE PREDICTION
Development of life prediction capabilities for liquid propellant rocket engines. Post-fire diagnostic system for the SSME system architecture study
[NASA-CR-187112] N91-26205
Dynamics of face and annular seals with two-phase flow
[NASA-CR-4256] N91-26479

PERFORMANCE TESTS
Omega system Performance Assessment and Coverage Evaluation (PACE) workstation design and implementation, volume 1
[AD-A235225] N91-26128
Guidelines for design, construction, and evaluation of airport pavement drainage
[DOT/FAA/RD-90/31] N91-26161
Development of a test system and experimental method for in-plane biaxial compressive deformation and failure of fiber composite materials
[AD-A234062] N91-26214
Cluster beam analysis via photoionization
[AD-A234111] N91-26253
Evaluation of the MARISAT satellite UHF wideband channel
[AD-A233666] N91-26408

Development and testing of radiation and electromagnetic pulse hardened silicon carbide based electronics
[AD-A233744] N91-26439
Digital logic testing and testability
[AD-A234123] N91-26441
Interfacial force sensor with force-feedback control
[DE91-004897] N91-26495
Performance evaluation of a novel erosion-resistant pump design
[DE91-008201] N91-26528
Rotordynamic and leakage characteristics of a 4-stage brush seal
[AD-A235336] N91-26541
Visual and field-of-view evaluation of the M-43 protective mask with prescription eyepieces
[AD-A234592] N91-26754
Testing the One-Port Random Access Memory (1PRAM) module of TRW's CPUAX signal processing superchip
[AD-A234127] N91-26761
A test of the IAEA code of practice for absorbed dose determination in photon and electron beams
[OEFZS-4565] N91-26913

PEROXIDES
Relationships between PAN and ozone at sites in eastern North America
[DE91-011728] N91-26607

PERSONAL COMPUTERS
Propulsion stability codes for liquid propellant propulsion systems developed for use on a PC computer
[NASA-CR-184983] N91-26201

PERSONALITY TESTS
Response latency measures for biographical inventories
[AD-A235010] N91-27005

PERSONNEL
Evaluation of night vision goggles for maritime search and rescue
[AD-A233798] N91-26751
Notional helmet concepts: A survey of near-term and future technologies
[AD-A234475] N91-26752
Response latency measures for biographical inventories
[AD-A235010] N91-27005

PERTURBATION
Calculation of the pointing accuracy of spacecraft equipment using autonomous measurements of the angular position of the object of investigation
N91-26167
Planar indirect-drive Rayleigh-Taylor experiments on Nova
[DE91-011967] N91-26943

PERTURBATION THEORY
Nonperturbative behavior of quarks
[DE91-011905] N91-26903

PHARMACOLOGY
Pharmacological correction of functional condition of Army Air Force flyers in hot climate with asparkam
N91-26684
Attention span, anxiety, and benzodiazepine receptors
[AD-A234549] N91-26716
Pharmacological sparing of protein in burn injury
[AD-A235026] N91-26724
Assessment of the pharmacodynamics of intranasal, intravenous and oral scopolamine N91-27114

PHASE CHANGE MATERIALS
Supercritical fluid processing of propellant polymers
[AD-A234285] N91-26341

PHASE CONJUGATION
Resonance fluorescence spectrum of an atom near a phase conjugator
[AD-A234535] N91-26894
Studies of optical beam phase-conjugation and electromagnetic scattering process
[AD-A234830] N91-26929

PHASE DIAGRAMS
Trimodal random-field Ising systems in a transverse field
[AD-A235038] N91-26875

PHASE MODULATION
Complex envelope properties, interpretation, filtering, and evaluation
[AD-A234478] N91-26844

PHASE SEPARATION (MATERIALS)
Chemical phase separation in binary iron-chromium alloys
[DE91-010282] N91-26294

PHASE SHIFT CIRCUITS
Four-to-one power combiner for 20 GHz phased array antenna using RADC MMIC phase shifters N91-26435

PHASE SHIFT KEYING
Chinese space science and technology (selected articles)
[AD-A234798] N91-26180
Optimal Walsh modulations in the presence of Doppler
[AD-A233723] N91-26411

PHASE TRANSFORMATIONS
Mechanical behavior and flow mechanisms in refractory metal composition
[AD-A234701] N91-26297
Quantum mechanical approach to understanding microstructural and mechanical properties of intermetallics
[AD-A234702] N91-26298
Investigation of plessite in iron meterorites and laboratory Fe-Ni(P) alloys
[DE91-010858] N91-27053

PHASED ARRAYS
Four-to-one power combiner for 20 GHz phased array antenna using RADC MMIC phase shifters N91-26435

PHENOLS
Method of obtaining phenol-furfural resins
[AD-A233746] N91-26327
Biological synthesis of substituted o-aminophenols
[AD-A234910] N91-26678

PHOSGENE
Synthesis of energetic single phase and multi-phase polymers
[AD-A235104] N91-26363

PHOSPHATES
Effect of bacterial biofilms on carbon steel pit propagation in phosphate containing medium
[DE91-010806] N91-26316

PHOSPHAZENE
Regio- and stereochemical control in substitution reactions of cyclophosphazenes
[AD-A234376] N91-26257
Thermal degradation chemistry of poly(diphenoxy phosphazene)
[AD-A235284] N91-26282
Synthesis and structure of small-molecule cyclic phosphazenes bearing ortho-substituted aryloxy and phenoxy substituents
[AD-A234377] N91-26344

PHOSPHORESCENCE
Polymer characterization using singlet oxygen phosphorescence as a spectroscopic probe
[DE91-011735] N91-26382

PHOSPHORUS COMPOUNDS
Water solubility of bis(2-ethylhexyl) hydrogen phosphite
[AD-A234561] N91-26259

PHOTOCHEMICAL REACTIONS
Polymer characterization using singlet oxygen phosphorescence as a spectroscopic probe
[DE91-011735] N91-26382
Improvement of procedures for evaluating photochemical models
[PB91-160374] N91-26597
Photochemical energy conversion by membrane-bound photoredox systems
[DE91-012171] N91-26682
Efficient photoinduced charge separation and storage in the solid state, rates, energetics, and spin-polarization
[DE91-010727] N91-26980

PHOTOCONDUCTIVITY
Laser switched power linac
[AD-A234581] N91-26507
Material engineering of novel semiconductor structures
[AD-A235014] N91-26960

PHOTODECOMPOSITION
Surface mediated photocatalysis
[AD-A233748] N91-26246

PHOTODETACHMENT
Study of the low-lying electronic states of Si2 and Si2(-) using negative ion photodetachment techniques
[AD-A234336] N91-26256
Negative ion photodetachment as a probe of the transition state region: The I + HI reaction
[AD-A235297] N91-26900
Correlation in photodetachment
[DE91-011369] N91-26908

PHOTOELECTRIC EMISSION
Desorption product yields following Cl2 adsorption on Si(111)7x7: Coverage and temperature dependence
[AD-A234635] N91-26264

PHOTOELECTRONS
Measurements of the longitudinal movements of O(+) ions in the subauroral upper atmosphere from the Aureol 3 satellite N91-26171
Negative ion photodetachment as a probe of the transition state region: The I + HI reaction
[AD-A235297] N91-26900

PHOTOGRAPHIC MEASUREMENT
Sea test development of laser altimeter
[AD-A233824] N91-26498

PHOTOGRAPHS
Photographic image enhancement N91-27094

PHOTOINTERPRETATION
Northeast Artificial Intelligence Consortium (NAIC). Volume 7: Automatic photointerpretation
[AD-A234886] N91-26821
Northeast Artificial Intelligence Consortium (NAIC). Volume 16: Intelligent signal processing techniques for multi-sensor surveillance systems
[AD-A234895] N91-26830

PHOTOIONIZATION
Cluster beam analysis via photoionization
[AD-A234111] N91-26253
X ray laser program
[AD-A234390] N91-26504
Studies of resonantly enhanced multiphoton ionization processes in molecules
[AD-A235217] N91-26898

PHOTOLUMINESCENCE
Material engineering of novel semiconductor structures
[AD-A235014] N91-26960

PHOTON BEAMS
A test of the IAEA code of practice for absorbed dose determination in photon and electron beams
[OEFZS-4565] N91-26913

PHOTONS
Cluster beam analysis via photoionization
[AD-A234111] N91-26253
Photons and neutrons
[DE91-010980] N91-26906

PHOTOOXIDATION
Surface mediated photocatalysis
[AD-A233748] N91-26246

PHOTOPRODUCTION
Photoinduced absorption and erasable optical information storage in polyanilines
[AD-A234108] N91-27002

PHOTOSYNTHESIS
Electronic excitation transport in photosynthesis and crystal and molecular structures of porphyrin compounds
[DE91-012024] N91-26679
Fluorescence spectroscopy of excitation transfer in Photosystem 1
[DE91-011867] N91-26681
Photochemical energy conversion by membrane-bound photoredox systems
[DE91-012171] N91-26682
Investigating combustion as a method of processing inedible biomass produced in NASA's biomass production chamber
[NASA-TM-103821] N91-26759

PHOTOVOLTAIC CONVERSION
Photovoltaics: From the laboratory to the marketplace
[DE91-002151] N91-26588
Investigation and characterization of ITO/poly-Si photovoltaic junctions
[ITN-91-85105] N91-26590
Research on stable, high-efficiency amorphous silicon multijunction modules
[DE91-002159] N91-26591

PHTHALATES
Strong exchange coupling in lanthanide bis(phthalocyaninato) sandwich compounds
[AD-A234466] N91-26951

PHTHALOCYANIN
Tetra neopentoxy phthalo cyanine Langmuir-Blodgett films: Spectroscopy at the air/water interface
[AD-A234603] N91-26261

PHYSICAL EXAMINATIONS
Administrative guide for the flight surgeon and the aeromedical technician: Performing medical examinations
[AD-A235178] N91-26727

PHYSICAL EXERCISE
Functional activity of hypophyseal-thyroid system during 370-day antiorthostatic hypokinesia N91-26691
Biochemical aspects of human adaptation to combined effect of antiorthostasis, decreased barometric pressure, and increased oxygen content N91-26694
Effect of excess respiratory resistance on physical performance and cardiorespiratory function N91-26699
Reaction of human skeletal muscle fibers to 370 day antiorthostatic hypokinesia combined with physical exertion N91-26702
Smoking, exercise, and physical fitness
[AD-A234658] N91-26717
Development of advanced methods based on stable isotope technology for studies of exercise in heat
[AD-A234670] N91-26719
Level of dietary fat does not affect fuel oxidation or endurance exercise performance of soldiers
[AD-A235194] N91-26728
Physiological responses to the wearing of protective equipment and respirators: Effects of hot, humid inspired air on work of breathing
[PB91-152884] N91-26745

Effectiveness of ice-vest cooling in prolonging work tolerance time during heavy exercise in the heat for personnel wearing Canadian forces chemical defence ensembles
[AD-A235273] N91-26758
Mechanics, impact loads and EMG on the space shuttle treadmill N91-27112

PHYSICAL FACTORS
Physical and psychogenic sequelae of impact acceleration on tracking performance of operators N91-26701

PHYSICAL FITNESS
Smoking, exercise, and physical fitness
[AD-A234658] N91-26717
Level of dietary fat does not affect fuel oxidation or endurance exercise performance of soldiers
[AD-A235194] N91-26728

PHYSICAL WORK
Biochemical aspects of human adaptation to combined effect of antiorthostasis, decreased barometric pressure, and increased oxygen content N91-26694
Reaction of human skeletal muscle fibers to 370 day antiorthostatic hypokinesia combined with physical exertion N91-26702
COLDEX-86: Physical work capacity during prolonged cold water immersion at 6.1 msw
[AD-A233767] N91-26710
Physiological and perceptual responses to load carrying in female subjects using internal and external frame backpacks
[AD-A234941] N91-26722

PHYSIOLOGICAL EFFECTS
Pharmacological correction of functional condition of Army Air Force flyers in hot climate with asparkam N91-26684
Risk factors and prediction of syncopic states in flyers N91-26685
State-of-the-art automated evaluation of functional state of the body in the space program and preventive medicine N91-26687
Hormonal regulators of calcium metabolism following space flights of various durations N91-26689
Computer tomography measurement of vertebral bones and muscles after extended manned space flights N91-26690
Biochemical aspects of human adaptation to combined effect of antiorthostasis, decreased barometric pressure, and increased oxygen content N91-26694
Attention span, anxiety, and benzodiazepine receptors
[AD-A234549] N91-26716
Development of advanced methods based on stable isotope technology for studies of exercise in heat
[AD-A234670] N91-26719
Level of dietary fat does not affect fuel oxidation or endurance exercise performance of soldiers
[AD-A235194] N91-26728
Proceedings of the 12th Annual Meeting of the UIPS Commission on Gravitational Physiology
[AD-A235337] N91-26732
Physiological responses to the wearing of protective equipment and respirators: Effects of hot, humid inspired air on work of breathing
[PB91-152884] N91-26745
Effect of a passive cooling vest on tension/anxiety and fatigue in a high heat and high humidity naval environment
[AD-A234657] N91-26755
Nonlinear systems dynamics in cardiovascular physiology: The heart rate delay map and lower body negative pressure N91-27095
Assessment of the pharmacodynamics of intranasal, intravenous and oral scopolamine N91-27114

PHYSIOLOGICAL RESPONSES
Review of primary medical results of year-long flight on Mir station N91-26178
State and forms of adaptation of vestibular function after space flights N91-26706
Physiological and perceptual responses to load carrying in female subjects using internal and external frame backpacks
[AD-A234941] N91-26722
Pharmacological sparing of protein in burn injury
[AD-A235026] N91-26724
Level of dietary fat does not affect fuel oxidation or endurance exercise performance of soldiers
[AD-A235194] N91-26728
Molecular studies of cytokine induction
[AD-A235326] N91-26731
Mechanisms of adaptive information processing
[AD-A234435] N91-26734
Physiological responses to the wearing of protective equipment and respirators: Effects of hot, humid inspired air on work of breathing
[PB91-152884] N91-26745
A study of murine bone marrow cells cultured in bioreactors which create an environment which simulated microgravity N91-27101
The effects of deuterium on static posture control N91-27102

PHYSIOLOGICAL TESTS
Task analysis and workload prediction for the MH-47E mission and a comparison with CH-47D workload predictions. Volume 2: Appendixes A through N
[AD-A235249] N91-26757

PHYTOPLANKTON
Phytoplankton abundance in relation to Lagrangian paths
[AD-A233728] N91-26672

PICOSECOND PULSES
Laser switched power linac
[AD-A234581] N91-26507

PICRATES
Gel solidified microinterface between two immiscible electrolytes applied to amperometric detection of picrate and tetramethylammonium
[AD-A235260] N91-26280

PIEZOELECTRICITY
Piezoelectric micromotors for microrobots
[AD-A234423] N91-26446
The development of piezoelectric poly(vinylidene fluoride) sensors for measuring peel stresses in adhesive joints
[AD-A233880] N91-26559

PILOT PERFORMANCE
Review of audition literature: Selection of acoustic signals for use in the synthesis of auditory space
[AD-A234579] N91-26681

PILOTS (PERSONNEL)
An advanced knowledge and design acquisition methodology: Application for the pilot's associate
[AD-A233700] N91-26748

PIPES (TUBES)
Template synthesis of polymeric and metal microtubules
[AD-A235307] N91-26367
Load-bearing capacity of large pipes with circumferential defects under tensile stress: Comparison of experiments with calculated estimates
[BLL-OA-TRANS-4233-(6196.3)] N91-26557

PISTONS
Method and apparatus for waste collection and storage
[NASA-CASE-MSC-21025-3] N91-26747

PITTING
Effect of bacterial biofilms on carbon steel pit propagation in phosphate containing medium
[DE91-010806] N91-26316
Metastable pitting corrosion of aluminum, Al-Cu, and Al-Si thin films in dilute HF solutions and its relevancy to the processing of integrated circuit interconnections
[DE91-012014] N91-26320

PITUITARY GLAND
Functional activity of hypophyseal-thyroid system during 370-day antiorthostatic hypokinesia N91-26691
The effect of catecholamines on arterial blood pressure and heart rate
[AD-A234755] N91-26720

PITUITARY HORMONES
The effect of catecholamines on arterial blood pressure and heart rate
[AD-A234755] N91-26720

PLANAR STRUCTURES
Application of a conjugate gradient method to the synthesis of phase-only planar arrays
[AD-A233756] N91-26415
High temperature superconducting planar circuit structures for high frequency applications
[AD-A234335] N91-26445

PLANETARY COMPOSITION
Chemistry and mineralogy of Martian dust: An explorer's primer N91-27063

PLANETARY GEOLOGY
The chemistry and mineralogy of Mars soil and dust N91-27058

PLANETARY SURFACES
Derivation of mid-infrared (5-25 microns) optical constants of some silicates and palagonite N91-27077

PLANETS
A gravitationally consistent second-order analytic secular solution for the point-mass motion of the eight principal planets N91-27054

PLANNING
Northeast Artificial Intelligence Consortium (NAIC). Volume 2: Discussing, using, and recognizing plans
[AD-A234881] N91-26816
Northeast Artificial Intelligence Consortium (NAIC). Volume 5: Distributed planning for dynamic environments in the presence of time constraints
[AD-A234884] N91-26819
Northeast Artificial Intelligence Consortium (NAIC). Volume 9: A planner system for the application of indications and warning
[AD-A234888] N91-26823
Northeast Artificial Intelligence Consortium (NAIC). Volume 10: Time oriented problem solving
[AD-A234889] N91-26824
Northeast Artificial Intelligence Consortium (NAIC). Volume 14: Knowledge base retrieval using plausible inference
[AD-A234893] N91-26828
Northeast Artificial Intelligence Consortium (NAIC). Volume 15: Strategies for coupling symbolic and numerical computation in knowledge base systems
[AD-A234894] N91-26829
Space support for airland battle-future
[AD-A233868] N91-26864
Heuristics for a flow-shop model with parallel machines and setup times
[ITN-91-85117] N91-26996

PLANT DESIGN
HYLIFE-2 inertial confinement: Fusion power plant design
[DE91-012089] N91-26947
Design of a lunar oxygen production plant N91-27109

PLANTS (BOTANY)
JPRS Report: Science and technology. USSR: Life sciences
[JPRS-ULS-91-009] N91-26688

PLASMA ANTENNAS
Plasma reflectors for electronic beam steering in radar systems
[AD-A234560] N91-26425

PLASMA CONTROL
Comparison of dimensionally similar discharges with similar heat deposition discharges
[DE91-011740] N91-26938
Statistical properties of intrinsic topological noise in tokamaks
[DE91-011741] N91-26939
Development of a tactical high-power microwave source using the Plasma Electron Microwave Source (PEMS) concept
[AD-A234967] N91-26942

PLASMA DIAGNOSTICS
Precision high-power solid-state laser diagnostics for target-irradiation studies and target-plane irradiation modeling
[DE91-012036] N91-26523

PLASMA DYNAMICS
Studies of resonantly enhanced multiphoton ionization processes in molecules
[AD-A235217] N91-26898

PLASMA FOCUS
Parametric studies of dense plasma focus for fusion space propulsion with D-He3
[AD-A234578] N91-26941

PLASMA FREQUENCIES
Frequency upshifting of laser pulses by ionization fronts
[AD-A234354] N91-26503

PLASMA GENERATORS
Development of a tactical high-power microwave source using the Plasma Electron Microwave Source (PEMS) concept
[AD-A234967] N91-26942

PLASMA HEATING
Comparison of dimensionally similar discharges with similar heat deposition discharges
[DE91-011740] N91-26938

PLASMA INTERACTIONS
Atmospheric propagation of laser beams
[AD-A234314] N91-26501
Frequency upshifting of laser pulses by ionization fronts
[AD-A234354] N91-26503

PLASMA JETS
Laser initiated ignition of liquid propellant
[AD-A233777] N91-26388
Near field interaction of microwave signals with a bounded plasma plume
[NASA-CR-185358] N91-26944

PLASMA PHYSICS
Atmospheric propagation of laser beams
[AD-A234314] N91-26501
Incoherent scatter radar observations of the ionosphere N91-26623

PLASMA PROBES
Studies of resonantly enhanced multiphoton ionization processes in molecules
[AD-A235217] N91-26898

PLASMA SHEATHS
Parametric studies of dense plasma focus for fusion space propulsion with D-He3
[AD-A234578] N91-26941

PLASMA SPRAYING
An analytical methodology to predict the coating characteristics of plasma-sprayed ceramic powders
[DE91-010088] N91-26326
Method of preparing a thermal barrier coating
[NASA-CASE-LEW-14999-2] N91-26376
PLASMA-ELECTROMAGNETIC INTERACTION
Near field interaction of microwave signals with a bounded plasma plume
[NASA-CR-185358] N91-26944
PLASMA-PARTICLE INTERACTIONS
An analytical methodology to predict the coating characteristics of plasma-sprayed ceramic powders
[DE91-010088] N91-26326
PLASMAS (PHYSICS)
Precision high-power solid-state laser diagnostics for target-irradiation studies and target-plane irradiation modeling
[DE91-012036] N91-26523
Radio frequency and microwave plasma for optical thin film deposition
[DE91-012081] N91-26525
Incoherent scatter radar observations of the ionosphere N91-26623
PLASMONS
Field work and dispersion relations of excitations on fractals
[AD-A234953] N91-26455
PLASTIC DEFORMATION
Microstructure, plastic deformation and mechanical properties of mechanically alloyed NiAl and NiAl based alloys
[AD-A235135] N91-26303
TEM in-situ straining of B2 compounds
[DE91-012062] N91-26322
PLASTIC FLOW
Plasticity of single crystalline Al3X intermetallic compounds
[AD-A234699] N91-26356
PLASTIC PROPERTIES
The role of electronic structure in the mechanical behavior of aluminides
[DE91-012508] N91-26325
PLATE THEORY
An anisotropic laminated damped plate theory
[AD-A234446] N91-26222
PLATES
Acceleration insensitive resonators
[AD-A235400] N91-26458
PLATES (STRUCTURAL MEMBERS)
Development and verification of global/local analysis techniques for laminated composites
[NASA-CR-185060] N91-26238
PLATES (TECTONICS)
Plate motion and deformation
[DE91-010466] N91-26612
PLATINUM
Heterogeneous catalysis on platinum and self-assembled monolayers on metal and metal oxide surfaces
[AD-A235055] N91-26302
Thin film alloys on semiconductor substrates
[DE91-012355] N91-26985
PLATINUM BLACK
Isotropic exchange in the platinum-catalyzed reduction of olefins in protic solvents
[AD-A234828] N91-26208
The reduction by deuterium on platinum black of exo-2-norbornyl and endo-2-norbornyl to norbornane-2-d occurs with predominant retention of configuration
[AD-A235057] N91-26277
PLATINUM OXIDES
Heterogeneous catalysis on platinum and self-assembled monolayers on metal and metal oxide surfaces
[AD-A235055] N91-26302
PLAYAS
Application of thematic mapper images to determine regional evaporation from the playas in the western desert of Egypt
[REPT-31] N91-26585
PLOTTING
VLF nighttime data analysis
[AD-A234006] N91-26417
POINT DEFECTS
Critical currents in proton irradiated YBa2Cu3O(7-delta) crystals
[DE91-011835] N91-26982
POISSON DENSITY FUNCTIONS
The distribution of the size and number of shadows cast on a line segment in a Poisson random field
[AD-A233697] N91-26857
POLAR REGIONS
The effects of magnetic storm phases on F-layer irregularities from auroral to equatorial latitudes
[AD-A235170] N91-26632
Thermal and albedo mapping of the north and south polar regions of Mars N91-27076
POLARITY
Structure of alkylated silica surfaces: Quenching of fluorescence from covalently bound pyrene
[AD-A234642] N91-26207
The effects of character size, modulation, polarity, and font on reading and search performance in matrix-addressable displays
[AD-A235033] N91-27007
POLARIZATION (CHARGE SEPARATION)
Electrochemically modulated superconductivity
[AD-A234703] N91-26955
Efficient photoinduced charge separation and storage in the solid state, rates, energetics, and spin-polarization
[DE91-010727] N91-26980
POLARIZATION (WAVES)
Electronic excitation transport in photosynthesis and crystal and molecular structures of porphyrin compounds
[DE91-012024] N91-26679
POLARIZED LIGHT
An ultraviolet optical isolator utilizing the KDP-isomorphs
[AD-D014860] N91-26923
POLARIZED RADIATION
A narrow-bandwidth unstable resonator laser cavity
[AD-D014865] N91-26505
POLARONS
Ring-torsional polarons in polyaniline and polyparaphenylene sulfide
[AD-A234384] N91-26345
Polaron ground state in a double heterostructure of polar crystals
[AD-A235037] N91-26963
POLICIES
Changing by degrees: Steps to reduce greenhouse gases
[PB91-163428] N91-26599
Space doctrine
[AD-A234971] N91-26866
Publications of the Executive Office of the President, January 20, 1989 to December 31, 1990
[PB91-127423] N91-26998
Proceedings of the Second Annual NASA Science Internet User Working Group Conference
[NASA-CP-3117] N91-27009
NSIUWG: Science networking retreat N91-27010
POLLUTION
Global climate change: A discussion of major uncertainties
[DE91-011746] N91-26604
Inorganic carbon surveys of oceanic basins
[DE91-011132] N91-26667
POLLUTION CONTROL
Acid rain in Asia
[DE91-011160] N91-26595
An assessment of CO2 greenhouse gas mitigation technologies
[DE91-011972] N91-26605
POLYACETYLENE
New developments in the synthesis and doping of polyacetylene and polyaniline
[AD-A233702] N91-26244
Synthetic metals: A novel role for organic polymers
[AD-A233862] N91-26334
POLYCARBONATES
Electroactive, near infrared absorbing nickel bis(dithiolene) complex polycarbonates and polyurethanes
[AD-A234595] N91-26350
POLYCRYSTALS
Sliding wear-testing and data analysis strategies for advanced engineering ceramics
[DE91-009524] N91-26383
The examination of dislocations in ice
[AD-A233716] N91-26586
Investigation and characterization of ITO/poly-Si photovoltaic junctions
[ITN-91-85105] N91-26590
Effect of boron addition on recrystallization and grain growth in Ni3Al polycrystals
[DE91-011966] N91-26983
POLYETHYLENES
An induction time approach to surface induced crystallization in polyethylene/poly (e-caprolactone) melt
[AD-A235102] N91-26964
POLYIMIDE RESINS
Investigation of polybenzocyclobutene resins in multilayer thin films for electronic packaging
[AD-A235223] N91-26228
POLYMER BLENDS
Mechanical properties of polycarbonate-polysulfone and polycarbonate-polyetherimide blends
[AD-A234939] N91-26360
POLYMER CHEMISTRY
Thermal degradation chemistry of poly(diphenoxy phosphazene)
[AD-A235284] N91-26282
Synthesis and structure of small-molecule cyclic phosphazenes bearing ortho-substituted aryloxy and phenoxy substituents
[AD-A234377] N91-26344
Ring-torsional polarons in polyaniline and polyparaphenylene sulfide
[AD-A234384] N91-26345
Energy migration, motion and order in synthetic polymers
[AD-A234403] N91-26346
Surface characterization of electrically conducting nickel tetrathiooxalate/poly(vinyl alcohol) composites
[AD-A234598] N91-26353
Organosilicon polymers incorporating the bicyclo(2.2.2)-octane moiety
[AD-A234966] N91-26361
Second Mini-Conference on Key Problems in Silicon Chemistry
[AD-A235243] N91-26366
Effect of molecular weight on polyphenylquinoxaline properties
[NASA-TM-104100] N91-26377
POLYMERIC FILMS
Polyaniline: Synthesis and properties of pernigraniline
[AD-A233706] N91-26245
Flexural plate wave devices for chemical analysis
[AD-A234129] N91-26254
Thermal transitions and mechanical properties of the films of chemically prepared polyaniline
[AD-A233807] N91-26329
Impedance profiling: A convenient technique for determining the redox or protonic acid doping characteristics of conducting polymers
[AD-A233941] N91-26337
Polyaniline: Oriented films and fibers
[AD-A234414] N91-26347
Block patterning of the metallization of polyvinylidene fluoride transducers
[AD-D014872] N91-26450
Methods of obtaining an electrical contact
[AD-A234800] N91-26453
POLYMERIZATION
Polyaniline: Synthesis and properties of pernigraniline
[AD-A233706] N91-26245
Polyaniline: Allowed oxidation states
[AD-A233842] N91-26251
Cationic polymerization within van der Waals clusters of the form (CH2=R)n where R=CH2, CF2 and CHCH3
[AD-A234233] N91-26255
Cross-linking and modification of cytochrome c with redox-active metal complexes
[DE91-012023] N91-26287
Study of intermediates from transition metal excited-state electron-transfer reactions
[DE91-012182] N91-26324
Synthesis, polymerization and thermal properties of a new acetylene-terminated Schiff base
[AD-A233806] N91-26328
Polyaniline: Pernigraniline, an isolable intermediate in the conventional chemical synthesis of emeraldine
[AD-A233840] N91-26330
Light induced electron spin resonance in polyaniline
[AD-A233847] N91-26331
X ray structure of polyanilines
[AD-A233848] N91-26332
Thermal stabilities of polyanilines
[AD-A233849] N91-26333
Novel concepts in electronic polymers: Polyaniline and its derivatives
[AD-A234214] N91-26339
Electroactive, near infrared absorbing nickel bis(dithiolene) complex polycarbonates and polyurethanes
[AD-A234595] N91-26350
Electrochemically induced charge and mass transport in polypyrrole/poly(styrene sulfonate) molecular composites
[AD-A234599] N91-26354
Synthesis and properties of rigid-rod benzobisazole polymers containing benzothiazole pendent groups
[AD-A234742] N91-26357
Living ring-opening metathesis polymerization of 7-oxa-2,3-difunctionalized norbornenes and norbornadienes by Mo(CHCMe2R) (N-2,6-C6H3-i-Pr2) (O-t-Bu)2 and Mo(CHCMe2R) (N-2,6-C6H3-i-Pr2) (OCMe2CF3)2
[AD-A235235] N91-26365
Synthesis and characterization of polysilanes
[AD-A235357] N91-26370
Preparation of inorganic and organometallic polymers with controlled structures
[AD-A235359] N91-26371

Anionic ring-opening polymerization of cyclotetrasilanes
[AD-A235360] N91-26372

POLYMERS
Synthesis, polymerization and thermal properties of a new acetylene-terminated Schiff base
[AD-A233806] N91-26328
Ionically and electronically conductive composite polymer membranes
[AD-A234587] N91-26349
Synthesis and properties of rigid-rod benzobisazole polymers containing benzothiazole pendent groups
[AD-A234742] N91-26357
Organosilicon polymers incorporating the bicyclo(2.2.2)-octane moiety
[AD-A234966] N91-26361
Design of polymers with semiconductor, NLO, and structural properties
[AD-A235215] N91-26364
Catalysts and initiators as instruments controlling structure of polymers with inorganic backbone
[AD-A235350] N91-26368

POLYNOMIALS
Converting a converging algorithm into a polynomially bounded algorithm
[AD-A234961] N91-26788
Polyhedral approaches for solving 0-1 polynomial programming problems
[AD-A235219] N91-26851

POLYPEPTIDES
Interaction of cationic polypeptides with electroactive polypyrrole/poly(styrenesulfonate) and poly(N-methylpyrrole)/poly(styrenesulfonate) films
[AD-A234469] N91-26258

POLYPHENYLS
Ring-torsional polarons in polyaniline and polyparaphenylene sulfide
[AD-A234384] N91-26345
Effect of molecular weight on polyphenylquinoxaline properties
[NASA-TM-104100] N91-26377
High pulse-energy flashlamp-pumpable laser dyes
[AD-A233837] N91-26499

POLYSILANES
Synthesis and characterization of polysilanes
[AD-A235357] N91-26370

POLYSTYRENE
Electroactive, near infrared absorbing nickel bis(dithiolene) complex polycarbonates and polyurethanes
[AD-A234595] N91-26350
Multiple-frequency SAW devices for chemical sensing and materials characterization
[DE91-010856] N91-26888

POLYURETHANE FOAM
Process monitoring of polyurethane foam using Fourier transform infrared spectroscopy
[DE91-010578] N91-26385

POLYURETHANE RESINS
Electroactive, near infrared absorbing nickel bis(dithiolene) complex polycarbonates and polyurethanes
[AD-A234595] N91-26350
Process monitoring of polyurethane foam using Fourier transform infrared spectroscopy
[DE91-010578] N91-26385

POLYVINYL ALCOHOL
Surface characterization of electrically conducting nickel tetrathiooxalate/poly(vinyl alcohol) composites
[AD-A234598] N91-26353

POLYVINYL CHLORIDE
Gel solidified microinterface between two immiscible electrolytes applied to amperometric detection of picrate and tetramethylammonium
[AD-A235260] N91-26280

POPULATION INVERSION
Energy levels and branching ratios of Tm(3)+ in ten garnet laser materials
[AD-A235274] N91-26514

POPULATIONS
SEEP 2 zooplankton data report: Winter, spring and summer collections at mooring 3 during 1988
[DE91-012077] N91-26668

POROSITY
Microstructure, porosity, and mechanical property relationships of calcium-silicate-hydrate
[AD-A235191] N91-26279
Advanced processing and properties of high performance alloys
[AD-A234746] N91-26299
Simulation of pore scale porous media flow using lattice gas methods
[DE91-004829] N91-26484

POROUS MATERIALS
Adsorption and decomposition of diethylsilane on silicon surfaces
[AD-A234639] N91-26267

PORPHYRINS
Efficient photoinduced charge separation and storage in the solid state, rates, energetics, and spin-polarization
[DE91-010727] N91-26980

POSITION (LOCATION)
Determination of the masses and densities of meteoroids from radar observations from one point N91-26177
X ray spot motion during 220 ps laser pulses
[DE91-012111] N91-26519
Vehicle steering device
[AD-D014861] N91-26537
Categories and particulars: Prototype effects in estimating spatial location
[AD-A234955] N91-26741

POSITION ERRORS
Study of the properties of the autonomous optical navigation of a space probe in a rendezvous with an asteroid N91-26169

POSITIONING
Magnetostrictive angular positioning motor
[AD-D014858] N91-26536
Investigation of axial positioning for flexural compressors
[NASA-CR-185711] N91-26544

POSTURE
Sitting posture analysis. An experimental optimisation approach
[ITN-91-85114] N91-26760
The effects of deuterium on static posture control N91-27102

POTABLE WATER
Liquid water production from atmospheric sources
[AD-A235090] N91-26406
Multispectral identification of potentially hazardous byproducts of ozonation and chlorination. Part 1: Studies of chromatographic and spectroscopic properties of MX
[PB91-161703] N91-26601

POTASSIUM
Development of advanced methods based on stable isotope technology for studies of exercise in heat
[AD-A234670] N91-26719

POTENTIAL ENERGY
Theoretical studies of potential energy surfaces and computational methods
[DE91-011126] N91-26902

POWDER (PARTICLES)
Effect of surface forces on the rheology of particle-liquid systems and the consolidation of ceramic powders
[AD-A234375] N91-26221
Polyaniline: Synthesis and properties of pernigraniline
[AD-A233706] N91-26245
An analytical methodology to predict the coating characteristics of plasma-sprayed ceramic powders
[DE91-010088] N91-26326
Determination of flow-regime boundaries for cohesive particles
[DE91-010552] N91-26468
Solid-state proton conductors
[DE91-002050] N91-26970

POWDER METALLURGY
Damage accumulation in advanced metal matrix composites under thermal cycling
[AD-A235002] N91-26227

POWER AMPLIFIERS
High power klystron amplifier
[AD-D014862] N91-26448

POWER EFFICIENCY
Depressed collector experiments on a quasioptical gyrotron
[AD-A234559] N91-26492
Scaling CW electron beam pumped rare gas lasers to ultra-high average power
[AD-A235120] N91-26513

POWER LINES
Characterization of vertical electric fields and associated voltages induced on an overhead power line from close artificially initiated lightning
[DE91-010781] N91-26656

POWER PLANTS
HYLIFE-2 inertial confinement: Fusion power plant design
[DE91-012089] N91-26947

POWER SPECTRA
Measurement of atmospheric turbulence N91-26151
Matching of PSD-design loads N91-26157
Evaluation of the MARISAT satellite UHF wideband channel
[AD-A233666] N91-26408

PRECIPITATION (CHEMISTRY)
Precipitation in Alloy 718: A combined AEM and APFIM investigation
[DE91-009918] N91-26314
Investigation of plessite in iron meteorites and laboratory Fe-Ni(P) alloys
[DE91-010858] N91-27053

PREDICTION ANALYSIS TECHNIQUES
An analytical methodology to predict the coating characteristics of plasma-sprayed ceramic powders
[DE91-010088] N91-26326
Forecasting digital microcircuit obsolescence
[AD-A234573] N91-26451
Long-term prediction test procedure for most ICs, based on linear response theory
[NASA-CR-185843] N91-26462
Determination of flow-regime boundaries for cohesive particles
[DE91-010552] N91-26468
Determination of SBS induced damage limits in large fused silica optics for intense, time varying laser pulses
[DE91-012080] N91-26518
Fatigue crack tip plastic strain range measurement studies in two titanium alloys
[AD-A234973] N91-26565
Comparison of sound pressure in a wedge-shaped ocean as predicted by an image method and a PE model
[AD-A234191] N91-26879
Acoustic radiation from fluid-loaded, ribbed cylindrical shells excited by different types of concentrated mechanical drives
[AD-A235324] N91-26887
Compound estimation procedures in reliability N91-27090

PREDICTION RECORDING
The SYNOP experiment: Inverted echo sounder data report for June 1989 to September 1990
[AD-A234625] N91-26662

PREDICTIONS
In the energy active region of the ocean N91-26583
Improvement of procedures for evaluating photochemical models
[PB91-160374] N91-26597
Radar-aeolian roughness project
[NASA-CR-4378] N91-27056

PREFORMS
Microalloyed steel preforms
[AD-A234039] N91-26296

PREPARATION
Evaluation of liposome-encapsulated Hemoglobin/LR16 formulation as a potential blood substitute
[AD-A233973] N91-26714

PRESIDENTIAL REPORTS
Publications of the Executive Office of the President, January 20, 1989 to December 31, 1990
[PB91-127423] N91-26998

PRESSING (FORMING)
Damage accumulation in advanced metal matrix composites under thermal cycling
[AD-A235002] N91-26227

PRESSURE DISTRIBUTION
Pressure distribution and induced force field on a conical nozzle due to impingement of a normal jet into the supersonic cross-flow
[AD-A233981] N91-26115
Dynamics of face and annular seals with two-phase flow
[NASA-CR-4256] N91-26479
Sitting posture analysis. An experimental optimisation approach
[ITN-91-85114] N91-26760

PRESSURE EFFECTS
Reflection of incident pressure waves by ribbed panels
[AD-A233671] N91-26469
Biochemical aspects of human adaptation to combined effect of antiorthostasis, decreased barometric pressure, and increased oxygen content N91-26694
Effect of pressure on electrostatic processes on Mars N91-27069

PRESSURE GRADIENTS
Analytical solution of plane Poiseuille flow of a Johnson-Segalman fluid
[AD-A234313] N91-26472

PRESSURE OSCILLATIONS
Hydroacoustics of intermittent boundary-layer flow: A review
[AD-A235092] N91-26883

PRESSURE PULSES
Hypervelocity launch capabilities to over 10.4 km/s
[DE91-010859] N91-26186

PRESSURE RATIO
Optical studies of the flow start-up processes in four convergent-divergent nozzles
[AD-A234552] N91-26473

PRESSURE VESSELS
Testing of a composite thermal structure to insulate the drivers of a large scale blast/thermal simulator
[AD-A234014] N91-26213

Preliminary test results from the HSST shallow-crack fracture toughness program
[DE91-010147] N91-26572
PRESTRESSING
Shell hoop prestress generated by welding
[DE91-011892] N91-26571
PRIMATES
Proton arc doses to the primate head
[AD-A235134] N91-26726
PRIMITIVE EQUATIONS
A numerical study of blocking N91-26640
PRINTED CIRCUITS
X ray tomographic inspection of printed wiring assemblies and electrical components
[AD-A234748] N91-26548
PRINTERS
Software product description N91-27037
PRIORITIES
Heuristics for a flow-shop model with parallel machines and setup times
[ITN-91-85117] N91-26996
PROBABILITY DENSITY FUNCTIONS
Continuous stochastic cellular automata that have a stationary distribution and no detailed balance
[AD-A234421] N91-26782
PROBABILITY THEORY
How low can an unmanned air vehicle fly?
[RAND-P-7680-RGS] N91-26138
Calculation of the pointing accuracy of spacecraft equipment using autonomous measurements of the angular position of the object of investigation N91-26167
Spread spectrum communication networks
[AD-A233696] N91-26409
Evaluation of night vision goggles for maritime search and rescue
[AD-A233798] N91-26751
BaRT manual version 3.0
[AD-A234528] N91-26784
Matching theory. A sampler: From Denes Koenig to the present
[AD-A234321] N91-26839
On measures of misconception stability
[AD-A234952] N91-26847
Comparison change analysis
[AD-A233690] N91-26873
PROBLEM SOLVING
Individual stereotypes of human neuropsychic prognostic activity in problem situations with different probability structures N91-26695
A system and language environment for scientific computing
[AD-A233747] N91-26772
Northeast Artificial Intelligence Consortium (NAIC). Volume 2: Discussing, using, and recognizing plans
[AD-A234881] N91-26816
Northeast Artificial Intelligence Consortium (NAIC). Volume 14: Knowledge base retrieval using plausible inference
[AD-A234893] N91-26828
Northeast Artificial Intelligence Consortium (NAIC). Volume 15: Strategies for coupling symbolic and numerical computation in knowledge base systems
[AD-A234894] N91-26829
On measures of misconception stability
[AD-A234952] N91-26847
Understanding object classes: Modeling and matching
[AD-A235027] N91-26848
Generic tasks for knowledge-based problem solving: Extension and new directions
[AD-A234925] N91-26865
NSI operations center N91-27038
PROCEDURES
Air Force stock fund: Hydrazine sales consistent with the Commercial Space Launch Act. Report to the Chairman, Committee on Science, Space and Technology, House of Representatives
[GAO/NSIAD-91-196] N91-26397
PROCESS CONTROL (INDUSTRY)
Method of obtaining phenol-furfural resins
[AD-A233746] N91-26327
Process monitoring of polyurethane foam using Fourier transform infrared spectroscopy
[DE91-010578] N91-26385
PRODUCT DEVELOPMENT
The wild weasel development programs, one run, one hit, one error
[RAND-P-7661-RGS] N91-26431
Tactical quartz oscillator development
[AD-A234308] N91-26443
Results of the aeronautical systems division critical process team on integrated product development
[AD-A235419] N91-26995
PRODUCTION ENGINEERING
Commercializing solar hydrogen production
[DE91-011232] N91-26398
PRODUCTIVITY
Adaptation and resistance of ecosystems to stress
[AD-A234576] N91-26603
Higher plants as part of biological human life support system N91-26693
PROGRAM VERIFICATION (COMPUTERS)
Quality effectiveness sensing technique release 3.0
[AD-A233651] N91-26545
PROGRAMMING LANGUAGES
A system and language environment for scientific computing
[AD-A233747] N91-26772
Proceedings of the Object-Oriented Database Task Group Workshop
[PB91-157198] N91-27000
Applications of formal simulation languages in the control and monitoring subsystems of Space Station Freedom N91-27100
PROGRAMS
Catalog of data bases and reports
[DE91-011516] N91-27043
PROJECT MANAGEMENT
Center for electronics and electrical engineering. Technical progress bulletin covering center programs, July to September 1990, with 1991 CEEE events calendar
[PB91-159749] N91-26437
Coordination in large scale software development
[AD-A234898] N91-26787
NSI organization and highlights N91-27011
Requirements management: A CSR's perspective N91-27027
National Aeronautics and Space Administration Multiyear Authorization Act of 1991 N91-27046
Developing a taxonomy for mission architecture definition N91-27108
PROJECT PLANNING
NSIUWG: Science networking retreat N91-27010
Overview of the NASA astrophysics data system N91-27022
Developing a taxonomy for mission architecture definition N91-27108
PROJECTILES
Aerodynamics of a 0.60 caliber electromagnetic projectile
[AD-A234660] N91-26116
PROPELLANT ADDITIVES
Laser initiated ignition of liquid propellant
[AD-A233777] N91-26388
PROPELLANT CHEMISTRY
A study of the gas phase chemistry of solid propellants using a microprobe mass spectrometer (MPMS) system: Initial development of the MPMS system
[AD-A234839] N91-26393
A study of the gas phase chemistry of solid propellants using a microprobe mass spectrometer (MPMS) system: Preliminary results for solid fuels (HTPB/Zecorez and BAMO/NMMO), single-base propellant (M10) and an RDX-Based propellant (BLX-9)
[AD-A234840] N91-26394
PROPELLANT COMBUSTION
Laser initiated ignition of liquid propellant
[AD-A233777] N91-26388
Modification of the user friendly thermodynamic code to include the effects of minor species
[AD-A233929] N91-26390
A study of the gas phase chemistry of solid propellants using a microprobe mass spectrometer (MPMS) system: Initial development of the MPMS system
[AD-A234839] N91-26393
PROPELLANT DECOMPOSITION
Laser initiated ignition of liquid propellant
[AD-A233777] N91-26388
PROPELLANTS
Method of injecting fluid propellants into a rocket combustion chamber
[NASA-CASE-LEW-14846-2] N91-26200
Supercritical fluid processing of propellant polymers
[AD-A234285] N91-26341
Molecular mechanics calculations for nitro and amino substituted conjugated systems containing oxygen and nitrogen
[AD-A233928] N91-26389
Air Force stock fund: Hydrazine sales consistent with the Commercial Space Launch Act. Report to the Chairman, Committee on Science, Space and Technology, House of Representatives
[GAO/NSIAD-91-196] N91-26397
PROPELLERS
Computation of broadband mixing noise from turbomachinery
[AD-A233991] N91-26878
PROPRIOCEPTION
Vestibular reactions and intersensory interactions in weightlessness: Results of Optokinez experiment N91-26698
State and forms of adaptation of vestibular function after space flights N91-26706
PROPULSION
Training effectiveness of an intelligent tutoring system for a propulsion console trainer N91-27097
PROPULSION SYSTEM CONFIGURATIONS
ALS liquid hydrogen turbopump: Advanced Development Program
[NASA-CR-183730] N91-26196
Propulsion stability codes for liquid propellant propulsion systems developed for use on a PC computer
[NASA-CR-184983] N91-26201
PROPULSION SYSTEM PERFORMANCE
Propulsion stability codes for liquid propellant propulsion systems developed for use on a PC computer
[NASA-CR-184983] N91-26201
PROTECTION
SPH-4 aircrew helmet impact protection improvements 1970-1990
[AD-A233784] N91-26750
PROTECTIVE CLOTHING
Notional helmet concepts: A survey of near-term and future technologies
[AD-A234475] N91-26752
Effectiveness of ice-vest cooling in prolonging work tolerance time during heavy exercise in the heat for personnel wearing Canadian forces chemical defence ensembles
[AD-A235273] N91-26758
PROTECTIVE COATINGS
Engine cycle analysis for a particle bed reactor nuclear rocket
[AD-A235258] N91-26199
India-stabilized zirconia coating for composites
[AD-D014857] N91-26224
Oxidation resistant coatings for titanium alloys and titanium alloy matrix composites
[NASA-CASE-LEW-15155-1] N91-26375
PROTEIN METABOLISM
Pharmacological sparing of protein in burn injury
[AD-A235026] N91-26724
PROTEINS
Carboxyalkylated hemoglobin as a potential blood substitute
[AD-A233822] N91-26712
Pharmacological sparing of protein in burn injury
[AD-A235026] N91-26724
PROTOCOL (COMPUTERS)
HORACE: Presentation-level protocol standard for digital transmission of monochrome television images
[AD-A235276] N91-26428
Architectures for a high performance distributed operating system
[AD-A235333] N91-26429
Backbone upgrades and DEC equipment replacement N91-27014
User support services and network application development: An overview N91-27015
NASA/SPAN and DOE/ESnet-DECnet transition strategy for DECnet OSI/phase 5 N91-27025
NSI operations center N91-27038
NSI customer service representatives and user support office: NASA Science Internet N91-27040
PROTONS
Proton arc doses to the primate head
[AD-A235134] N91-26726
Solid-state proton conductors
[DE91-002050] N91-26970
Critical currents in proton irradiated YBa2Cu3O(7-delta) crystals
[DE91-011835] N91-26982
PROTOTYPES
Advanced Dynamic Anthropomorphic Manikin (ADAM) design report
[AD-A234761] N91-26756
Parallel processing and expert systems
[NASA-TM-103886] N91-26796
Full surface testing of grazing incidence mirrors
[AD-A234005] N91-26922
PROVING
Use of a zone model for validation of a horizontal ceiling/floor vent algorithm
[AD-A234553] N91-26474
Ada compiler validation summary report: Certification number: 9000703W1.11014, Silicon Graphics 4D ADA Iris-4D/380 (host) Iris-4D/380 (target)
[AD-A233714] N91-26771
PSYCHOACOUSTICS
Review of audition literature: Selection of acoustic signals for use in the synthesis of auditory space
[AD-A234579] N91-26881
PSYCHOLOGICAL EFFECTS
Effect of a passive cooling vest on tension/anxiety and fatigue in a high heat and high humidity naval environment
[AD-A234657] N91-26755

PSYCHOLOGICAL TESTS
A procedure to detect item bias present simultaneously in several items
[AD-A235252] N91-26862
PSYCHOLOGY
Proceedings of the 7th User's Stress Workshop
[AD-A234583] N91-26736
Neural mechanisms of attention
[AD-A235003] N91-26742
A procedure to detect item bias present simultaneously in several items
[AD-A235252] N91-26862
PSYCHOMETRICS
On measures of misconception stability
[AD-A234952] N91-26847
PSYCHOMOTOR PERFORMANCE
Task analysis and workload prediction for the MH-47E mission and a comparison with CH-47D workload predictions. Volume 2: Appendixes A through N
[AD-A235249] N91-26757
PSYCHOPHYSIOLOGY
Individual stereotypes of human neuropsychic prognostic activity in problem situations with different probability structures N91-26695
PUBLIC RELATIONS
Requirements management: A CSR's perspective N91-27027
PULSE AMPLITUDE MODULATION
Propagation of RF signals through structured ionization: The general model
[AD-A234051] N91-26418
PULSE COMMUNICATION
Meteor scatter communication between Thule and Station Nord, Greenland
[AD-A234440] N91-26424
PULSE MODULATION
The instrumental principles of MST radars and incoherent scatter radars and the configuration of radar system hardware N91-26616
PULSED LASERS
Frequency upshifting of laser pulses by ionization fronts
[AD-A234354] N91-26503
Quasi-CW excimer laser, phase 2
[AD-A234771] N91-26509
Determination of SBS induced damage limits in large fused silica optics for intense, time varying laser pulses
[DE91-012080] N91-26518
X ray spot motion during 220 ps laser pulses
[DE91-012111] N91-26519
Radio frequency and microwave plasma for optical thin film deposition
[DE91-012081] N91-26525
Development of a subpicosecond, tunable LiCAF (Cr:LiCaAlF6) laser
[DE91-012082] N91-26526
Infrared and visible laser double resonance studies of vibrational energy transfer processes in polyatomic molecules
[DE91-012162] N91-26910
PULSES
Theory of radar target discrimination
[AD-A234172] N91-26420
High pulse-energy flashlamp-pumpable laser dyes
[AD-A233837] N91-26499
PUMP IMPELLERS
Performance evaluation of a novel erosion-resistant pump design
[DE91-008201] N91-26528
PURIFICATION
Wound healing by cultured skin cells and growth factors
[AD-A235300] N91-26730
PYRENES
Structure of alkylated silica surfaces: Quenching of fluorescence from covalently bound pyrene
[AD-A234642] N91-26207
Surface diffusion at the liquid-solid interface: Quenching of fluorescence from pyrene covalently bound to methylated silica
[AD-A234645] N91-26268
PYRITES
Thermoluminescence kinetics of pyrite (FeS2)
[DE91-011710] N91-26990
PYROLYSIS
Polymeric routes to silicon carbide and silicon oxycarbide CMC
[NASA-TM-104372] N91-26234
Fundamental studies of carbenes and hydrocarbon radicals
[DE91-011029] N91-26286
PYROLYTIC MATERIALS
A program in the chemistry of electronic materials. Task 1: New organometallic precursors for the low pressure chemical vapor deposition of refractory materials for electronics
[AD-A234315] N91-26342
PYRROLES
Interaction of cationic polypeptides with electroactive polypyrrole/poly(styrenesulfonate) and poly(N-methylpyrrole)/poly(styrenesulfonate) films
[AD-A234469] N91-26258
Electrochemically induced charge and mass transport in polypyrrole/poly(styrene sulfonate) molecular composites
[AD-A234599] N91-26354

Q

QUADRATIC EQUATIONS
A software package for unconstrained optimization using tensor methods
[AD-A233989] N91-26778
QUADRATIC PROGRAMMING
Polyhedral approaches for solving 0-1 polynomial programming problems
[AD-A235219] N91-26851
QUADRATURES
The instrumental principles of MST radars and incoherent scatter radars and the configuration of radar system hardware N91-26616
QUADRUPOLES
Coherent beam-beam effects
[DE91-012512] N91-26917
QUALITY
HORACE: Presentation-level protocol standard for digital transmission of monochrome television images
[AD-A235276] N91-26428
A Rome Laboratory guide to basic training in TQM analysis techniques
[AD-A233855] N91-26993
QUALITY CONTROL
Quality effectiveness sensing technique release 3.0
[AD-A233651] N91-26545
Quality by design using statistically planned experiments
[ITN-91-85119] N91-26553
Quality Assurance Manual
[DE91-012618] N91-26555
Measuring the quality of knowledge work
[AD-A235354] N91-26994
QUANTITATIVE ANALYSIS
Characteristics of aerosol in the atmosphere of Mars according to data from the KRFM experiment N91-26175
Derivation of mid-infrared (5-25 microns) optical constants of some silicates and palagonite N91-27077
QUANTUM CHROMODYNAMICS
Gauge bosons and heavy quarks: Proceedings of Summer Institute on Particle Physics
[DE91-011248] N91-26907
QUANTUM EFFICIENCY
Saturation and kinetic issues for optical-field-ionized plasma x ray lasers
[DE91-012079] N91-26517
QUANTUM ELECTRONICS
Center for the Integration of Optical C
[AD-A235277] N91-26931
Solid state research
[AD-A234836] N91-26958
Quantum devices and structures
[AD-A235298] N91-26989
QUANTUM MECHANICS
Quantum mechanical approach to understanding microstructural and mechanical properties of intermetallics
[AD-A234702] N91-26298
Propagators for quantum oscillator chains
[AD-A234467] N91-26893
QUANTUM NUMBERS
Gauge bosons and heavy quarks: Proceedings of Summer Institute on Particle Physics
[DE91-011248] N91-26907
QUANTUM THEORY
Calculation of the conductance of two dimensional narrow wires
[ITN-91-85109] N91-26460
High pulse-energy flashlamp-pumpable laser dyes
[AD-A233837] N91-26499
Quantum devices and structures
[AD-A235298] N91-26989
Quantum limited quasiparticle mixers at 100 GHz
[DE91-011826] N91-26991
QUANTUM WELLS
Symposium E: Properties of 2-6 semiconductors. Bulk crystals, epitaxial films, quantum well structures
[AD-A234835] N91-26957
Material engineering of novel semiconductor structures
[AD-A235014] N91-26960
Quantum devices and structures
[AD-A235298] N91-26989
QUARKS
Nonperturbative behavior of quarks
[DE91-011905] N91-26903
Gauge bosons and heavy quarks: Proceedings of Summer Institute on Particle Physics
[DE91-011248] N91-26907
QUARTZ CRYSTALS
Tactical quartz oscillator development
[AD-A234308] N91-26443
QUENCHING
Study of intermediates from transition metal excited-state electron-transfer reactions
[DE91-012182] N91-26324
QUERY LANGUAGES
US and foreign alloy cross-reference database
[NASA-CR-184166] N91-26313
QUEUEING THEORY
A sequential Jackson network with feedback
[ITN-91-85111] N91-26867
Queueing systems with orbiting customers
[ITN-91-85112] N91-26868
QUINOXALINES
Effect of molecular weight on polyphenylquinoxaline properties
[NASA-TM-104100] N91-26377

R

RADAR
Evaluation of the C/EC/KC-135 Ground Collision Avoidance System (GCAS), study 1
[AD-A235301] N91-26130
Propagation of RF signals through structured ionization: The general model
[AD-A234051] N91-26418
Technique for measuring ionospheric irregularities generated by high power oblique HF heating of the F-region
[AD-A233883] N91-26627
RADAR ANTENNAS
Plasma reflectors for electronic beam steering in radar systems
[AD-A234560] N91-26425
RADAR BEAMS
Plasma reflectors for electronic beam steering in radar systems
[AD-A234560] N91-26425
RADAR DATA
Advanced Microwave Precipitation Radiometer (AMPR) for remote observation of precipitation
[NASA-CR-184165] N91-26655
The distribution of particulate material on Mars N91-27059
RADAR DETECTION
The wild weasel development programs, one run, one hit, one error
[RAND-P-7661-RGS] N91-26431
RADAR ECHOES
Theory of radar target discrimination
[AD-A234172] N91-26420
Middle Atmosphere Program. Handbook for MAP. Volume 30: International School on Atmospheric Radar
[NASA-CR-188623] N91-26613
Statistical characteristics of MST radar echoes and its interpretation N91-26617
System concept and analysis of an Artificial Ionospheric Mirror (AIM) radar
[AD-A234289] N91-26630
On the evolution of raindrop spectra and their effect on the atmosphere below cloud base: Numerical models and comparisons with observations
[ITN-91-85113] N91-26652
RADAR IMAGERY
Determination of the masses and densities of meteoroids from radar observations from one point N91-26177
Radar-aeolian roughness project
[NASA-CR-4378] N91-27056
RADAR REFLECTORS
Plasma reflectors for electronic beam steering in radar systems
[AD-A234560] N91-26425
RADAR SCATTERING
Middle Atmosphere Program. Handbook for MAP. Volume 30: International School on Atmospheric Radar
[NASA-CR-188623] N91-26613
Target parameter estimation N91-26620

Incoherent scatter radar observations of the ionosphere N91-26623
RADAR TARGETS
Theory of radar target discrimination [AD-A234172] N91-26420
Middle Atmosphere Program. Handbook for MAP. Volume 30: International School on Atmospheric Radar [NASA-CR-188623] N91-26613
Radar principles N91-26615
Target parameter estimation N91-26620
RADAR TRACKING
Determination of the masses and densities of meteoroids from radar observations from one point N91-26177
Theory of radar target discrimination [AD-A234172] N91-26420
Historical aspects of radar atmospheric dynamics N91-26614
Data acquisition and processing N91-26618
Gravity waves and instabilities in the lower and middle atmosphere N91-26621
Incoherent scatter radar observations of the ionosphere N91-26623
The distribution of particulate material on Mars N91-27059
RADIANCE
Advanced Microwave Precipitation Radiometer (AMPR) for remote observation of precipitation [NASA-CR-184165] N91-26655
RADIATION ABSORPTION
An electron-beam dose deposition experiment: TIGER 1-D simulation code versus thermoluminescent dosimetry [AD-A234507] N91-26447
A test of the IAEA code of practice for absorbed dose determination in photon and electron beams [OEFZS-4565] N91-26913
RADIATION DAMAGE
Adsorption and thermal behavior of ethylene on Si(100)-(2x1) [AD-A234098] N91-26252
Long-term prediction test procedure for most ICs, based on linear response theory [NASA-CR-185843] N91-26462
RADIATION DETECTORS
A study of signal generation and charge collectionin a-Si:H diodes for radiation imaging [DE91-010243] N91-26904
RADIATION DISTRIBUTION
Radiation, scattering, and guidance of electromagnetic fields by arbitrarily shaped structures embedded in layered dielectric media [AD-A234434] N91-26423
RADIATION DOSAGE
An electron-beam dose deposition experiment: TIGER 1-D simulation code versus thermoluminescent dosimetry [AD-A234507] N91-26447
Proton arc doses to the primate head [AD-A235134] N91-26726
Absorbed-dose calibration of ionization chambers in a Co-60 gamma-ray beam [PB91-132290] N91-26890
A test of the IAEA code of practice for absorbed dose determination in photon and electron beams [OEFZS-4565] N91-26913
RADIATION EFFECTS
Interaction of ionizing radiation, genetically active chemicals, and radiofrequency radiation in human and rodent cells [AD-A234747] N91-26677
Proton arc doses to the primate head [AD-A235134] N91-26726
RADIATION HARDENING
Development and testing of radiation and electromagnetic pulse hardened silicon carbide based electronics [AD-A233744] N91-26439
RADIATION HAZARDS
HYLIFE-2 inertial confinement: Fusion power plant design [DE91-012089] N91-26947
RADIATION MEASUREMENT
Absorbed-dose calibration of ionization chambers in a Co-60 gamma-ray beam [PB91-132290] N91-26890
RADIATION SOURCES
Gamma ray astronomy [NASA-CR-187774] N91-26407
RADIATIVE TRANSFER
Recent studies of the optical properties of dust and cloud particles in the Mars atmosphere and the interannual frequency of global dust storms N91-27060
RADICALS
Fundamental studies of carbenes and hydrocarbon radicals [DE91-011029] N91-26286
Electronic and ionic transport in processable conducting polymers [AD-A234597] N91-26352
High energy density systems in cryogenic media: The production and reaction of atoms and radicals [AD-A233785] N91-26892
RADIO COMMUNICATION
Evaluation of the MARISAT satellite UHF wideband channel [AD-A233666] N91-26408
RADIO EMISSION
The distribution of particulate material on Mars N91-27059
RADIO EQUIPMENT
Evaluation of the C/EC/KC-135 Ground Collision Avoidance System (GCAS), study 1 [AD-A235301] N91-26130
RADIO FREQUENCIES
Propagation of RF signals through structured ionization: The general model [AD-A234051] N91-26418
Radio frequency and microwave plasma for optical thin film deposition [DE91-012081] N91-26525
Comparison of the RF frequency spectra of HEMP and lightning [AD-A234306] N91-26642
RADIO METEOROLOGY
Applications of MST radars: Meteorological applications N91-26622
RADIO RECEIVERS
Quantum limited quasiparticle mixers at 100 GHz [DE91-011826] N91-26991
RADIO SIGNALS
A test vector generator for a radar signal processor [AD-A233725] N91-26413
Adaptive spread spectrum networks [AD-A234084] N91-26419
RADIO WAVES
The Effect of the Ionosphere on Radiowave Signals and Systems Performance Based on Ionospheric Effects Symposium [AD-A233797] N91-26416
RADIOACTIVE CONTAMINANTS
Description of the RIVM/KNMI puff dispersion model [KNMI-177] N91-26638
RADIOACTIVE DECAY
Gauge bosons and heavy quarks: Proceedings of Summer Institute on Particle Physics [DE91-011248] N91-26907
RADIOGRAPHY
X ray tomographic inspection of printed wiring assemblies and electrical components [AD-A234748] N91-26548
RADIOSONDES
Applications of MST radars: Meteorological applications N91-26622
RAIL TRANSPORTATION
Geogrid reinforced base course for flexible pavements for light aircraft: Literature review and test section design [DOT/FAA/RD-90/28] N91-26160
RAILGUN ACCELERATORS
Rail circuit augmentation [AD-A234944] N91-26184
Performance of hypervelocity armatures with replenished metal vapor plasmas [DE91-011931] N91-26187
RAILS
Removable hand hold [NASA-CASE-LEW-15196-1] N91-26543
RAIN
On the evolution of raindrop spectra and their effect on the atmosphere below cloud base: Numerical models and comparisons with observations [ITN-91-85113] N91-26652
Advanced Microwave Precipitation Radiometer (AMPR) for remote observation of precipitation [NASA-CR-184165] N91-26655
RAINDROPS
On the evolution of raindrop spectra and their effect on the atmosphere below cloud base: Numerical models and comparisons with observations [ITN-91-85113] N91-26652
RAMAN SPECTRA
Atmospheric propagation of laser beams [AD-A234314] N91-26501
Effect of aerosols on laser-induced breakdown [AD-A234324] N91-26502
RAMAN SPECTROSCOPY
Raman spectroscopy study of solvation structure in acetonitrile/water mixtures [AD-A234921] N91-26271
RANDOM ACCESS MEMORY
Testing the One-Port Random Access Memory (1PRAM) module of TRW's CPUAX signal processing superchip [AD-A234127] N91-26761
RANDOM ERRORS
Evaluating the effect of accuracy ratios on the percent of calibrations which are out of tolerance N91-27107
RANDOM NOISE
Continuous stochastic cellular automata that have a stationary distribution and no detailed balance [AD-A234421] N91-26782
RANDOM PROCESSES
The distribution of the size and number of shadows cast on a line segment in a Poisson random field [AD-A233697] N91-26857
RANDOM VIBRATION
Nonlinear dynamics and control of flexible structures [AD-A235186] N91-26191
RANGEFINDING
Effect of turbulence on impurity observation in upper atmosphere using lidar method N91-26584
RANKING
Technology needs for high-speed rotorcraft, volume 1 [NASA-CR-177585] N91-26139
A theoretical and experimental study of the symmetric rank one update [AD-A233965] N91-26777
RARE EARTH ELEMENTS
Photons and neutrons [DE91-010980] N91-26906
Strong exchange coupling in lanthanide bis(phthalocyaninato) sandwich compounds [AD-A234466] N91-26951
RARE GASES
Scaling CW electron beam pumped rare gas lasers to ultra-high average power [AD-A235120] N91-26513
High energy density systems in cryogenic media: The production and reaction of atoms and radicals [AD-A233785] N91-26892
RAREFIED GAS DYNAMICS
Experimental techniques in the field of low density aerodynamics [AGARD-AG-318(E)] N91-26124
RATES (PER TIME)
Weighted least squares estimation for Aalen's additive risk model [AD-A235250] N91-26852
RATS
Intracellular physiology of the rat suprachiasmatic nucleus: Electrical properties, neurotransmission, and effects of neuromodulators [AD-A234442] N91-26675
Effects of 13 day space flight on skeletal muscles and neuromuscular junctions in rats N91-26703
Attention span, anxiety, and benzodiazepine receptors [AD-A234549] N91-26716
RAY TRACING
Incorporation of shuttle CCT parameters in computer simulation models N91-27096
REACTION KINETICS
Comparison of hydrogen desorption kinetics from Si(111)7x7 and Si(100)2x1 [AD-A234633] N91-26262
Comparison of H2 desorption kinetics from Si(111)7x7 and Si(100)2x1 [AD-A234634] N91-26263
Diethylsilane decomposition on silicon surfaces studied using transmission FTIR spectroscopy [AD-A234638] N91-26266
Theory and experimental and chemical instabilities [AD-A234916] N91-26270
Boron combustion model development with kinetic sensitivity analysis and measurement of key chemical rate parameters [AD-A235309] N91-26283
Surface Chemkin (version 3.7): A FORTRAN package for analyzing heterogeneous chemical kinetics at a solid-surface-gas-phase interface [DE91-010840] N91-26285
Fundamental studies of carbenes and hydrocarbon radicals [DE91-011029] N91-26286
The chemistry of sodium with sulfur in flames [DE91-002060] N91-26288
The synthesis of methanol by a novel method [DE91-011131] N91-26291
Elementary reaction rate measurements at high temperatures by tunable-laser flash-absorption [DE91-011850] N91-26516
Saturation and kinetic issues for optical-field-ionized plasma x ray lasers [DE91-012079] N91-26517
Biological synthesis of substituted o-aminophenols [AD-A234910] N91-26678

Negative ion photodetachment as a probe of the transition state region: The I + HI reaction
[AD-A235297] N91-26900

REACTION PRODUCTS
Study of intermediates from transition metal excited-state electron-transfer reactions
[DE91-012182] N91-26324
Surface characterization of electrically conducting nickel tetrathiooxalate/poly(vinyl alcohol) composites
[AD-A234598] N91-26353
Formation of intermediate compounds during reduced pressure calcination of Y-Ba-Cu-O precursor
[DE91-011179] N91-26971

REACTION TIME
The P300 component of the auditory event-related potential: Interlaboratory consistency and test-retest reliability
[AD-A235114] N91-26725

REACTIVITY
Improvement in the capacity and safety of lithium/inorganic electrolyte sulfur dioxide rechargeable cells, phase 2
[AD-A235303] N91-26589
High energy density systems in cryogenic media: The production and reaction of atoms and radicals
[AD-A233785] N91-26892
Study of the effect of reactive element addition by implanting metal ions in a pre-formed oxide layer
[DE91-011916] N91-26974

REACTOR DESIGN
A reliability and mass perspective of SP-100 Stirling cycle lunar-base powerplant designs
[NASA-TM-103736] N91-26592
Design and fabrication of forced-flow coils as an R/D program for large helical device
[NIFS-81] N91-26937

REACTOR SAFETY
Load-bearing capacity of large pipes with circumferential defects under tensile stress: Comparison of experiments with calculated estimates
[BLL-OA-TRANS-4233-(6196.3)] N91-26557
HYLIFE-2 inertial confinement: Fusion power plant design
[DE91-012089] N91-26947

REACTOR TECHNOLOGY
Computational model for optimizing longitudinal fin heat transfer in laminar internal flows
[DE91-005070] N91-26485

READ-ONLY MEMORY DEVICES
The role of EEPROM devices in upcoming ISDN applications
[AD-A234837] N91-26454

READING
The effects of character size, modulation, polarity, and font on reading and search performance in matrix-addressable displays
[AD-A235033] N91-27007

REAL TIME OPERATION
Backplane bus distributed realtime clock synchronization
[AD-A234476] N91-26491
Development of a Vector Spherical Harmonic (VSH) model of the neutral thermosphere
[AD-A234744] N91-26631
The High Resolution Profiler (HRP): User's guide and software modifications documentation
[AD-A234640] N91-26663
Requirements for developing Embedded Real-Time Trusted Computer System (ERT-TCSs)
[AD-A234325] N91-26762
Parallel processing and expert systems
[NASA-TM-103886] N91-26796
Quantitative analysis procedures for Task 8
[DE91-009684] N91-26798
Translating expert system rules into Ada code with validation and verification
[NASA-CR-187505] N91-26800
Strategies for reliable and real time execution on a heterogeneous multiprocessor
[AD-A234114] N91-26801
Using modular neural networks with local representations to control dynamic systems
[AD-A234700] N91-26813
Northeast Artificial Intelligence Consortium (NAIC). Volume 5: Distributed planning for dynamic environments in the presence of time constraints
[AD-A234884] N91-26819
Northeast Artificial Intelligence Consortium (NAIC). Volume 12: Computer architecture for very large knowledge bases
[AD-A234891] N91-26826
Design of optimal correlation filters for hybrid vision systems N91-27110

RECEIVERS
The instrumental principles of MST radars and incoherent scatter radars and the configuration of radar system hardware N91-26616

RECEPTORS (PHYSIOLOGY)
Parallel processing and learning: Variability and chaos in self-organization of activity in groups of neurons
[AD-A234589] N91-26737

RECHARGING
Improvement in the capacity and safety of lithium/inorganic electrolyte sulfur dioxide rechargeable cells, phase 2
[AD-A235303] N91-26589

RECOGNITION
Young and older observers show similar perceived contrast functions for isoluminant stimuli
[AD-A233766] N91-26709
The effects of display failures and symbol rotation on visual search and recognition performance
[AD-A235035] N91-26743

RECOMBINATION COEFFICIENT
Computer modeling of soot formation comparing free radical and ionic mechanisms
[AD-A235007] N91-26273

RECONNAISSANCE
How low can an unmanned air vehicle fly?
[RAND-P-7680-RGS] N91-26138
Space support for airland battle-future
[AD-A233868] N91-26864

RECRYSTALLIZATION
Residual stresses in metal/ceramic brazes: Effect of creep on finite element analysis results
[DE91-011233] N91-26570
Effect of boron addition on recrystallization and grain growth in Ni3Al polycrystals
[DE91-011966] N91-26983

RECTANGULAR PLATES
Buckling of laminated composite plates
[ITN-91-85101] N91-26232

RECTIFIERS
Development and testing of radiation and electromagnetic pulse hardened silicon carbide based electronics
[AD-A233744] N91-26439

RECURSIVE FUNCTIONS
Statistical analysis of stochastic gradient based algorithms
[AD-A234545] N91-26859

RECYCLING
Investigating combustion as a method of processing inedible biomass produced in NASA's biomass production chamber
[NASA-TM-103821] N91-26759

RED SHIFT
The Berkeley/Anglo-Australian Observatory high-redshift supernova search
[DE91-012348] N91-27051

REDUCED GRAVITY
Crystal growth in a microgravity environment
[NASA-CASE-MFS-28473-1] N91-26968
NASA/ASEE Summer Faculty Fellowship Program, 1990, Volume 1
[NASA-CR-185637-VOL-1] N91-27088
Techniques for determining total body water using deuterium oxide N91-27091
Mathematical modeling of the flow field and particle motion in a rotating bioreactor at unit gravity and microgravity N91-27092
A study of murine bone marrow cells cultured in bioreactors which create an environment which simulated microgravity N91-27101
Mechanics, impact loads and EMG on the space shuttle treadmill N91-27112

REDUCTION (CHEMISTRY)
The reduction by deuterium on platinum black of exo-2-norbornyl and endo-2-norbornyl to norbornane-2-d occurs with predominant retention of configuration
[AD-A235057] N91-26277
Synthesis and characterization of polysilanes
[AD-A235357] N91-26370

REDUNDANCY
Constrained trajectory optimization for kinematically redundant arms
[NASA-CR-183477] N91-26527

REENTRY VEHICLES
Satellite data derived estimates of erosion parameters for reentry vehicles
[AD-A234792] N91-26189

REFLECTANCE
Reflection of incident pressure waves by ribbed panels
[AD-A233671] N91-26469
Sea test development of laser altimeter
[AD-A233824] N91-26498
A room-temperature, flashpumped, 2.09 micron solid state laser
[AD-D014871] N91-26506
A model for the scattering of high-frequency electromagnetic fields from dielectrics exhibiting thermally-activated electrical losses
[NASA-TM-104376] N91-26872
Derivation of mid-infrared (5-25 microns) optical constants of some silicates and palagonite N91-27077

REFLECTED WAVES
Reflection of incident pressure waves by ribbed panels
[AD-A233671] N91-26469

REFLECTOR ANTENNAS
Plasma reflectors for electronic beam steering in radar systems
[AD-A234560] N91-26425
Near field interaction of microwave signals with a bounded plasma plume
[NASA-CR-185358] N91-26944

REFRACTION
Method and apparatus for second-rank tensor generation
[NASA-CASE-NPO-17512-1-CU] N91-26918
Derivation of mid-infrared (5-25 microns) optical constants of some silicates and palagonite N91-27077

REFRACTIVITY
Effect of aerosols on laser-induced breakdown
[AD-A234324] N91-26502
Incoherent scatter radar observations of the ionosphere N91-26623

REFRACTORY MATERIALS
Supercritical fluid processing of propellant polymers
[AD-A234285] N91-26341
Cluster beam deposition of high temperature materials
[AD-A234358] N91-26343

REFRACTORY METALS
Mechanical behavior and flow mechanisms in refractory metal composition
[AD-A234701] N91-26297

REGENERATION (ENGINEERING)
An Air Revitalization Model (ARM) for Regenerative Life Support Systems (RLSS) N91-27093

REGOLITH
Evaluation of geophysical properties of the lunar regolith for the design of precursor scientific missions for the space exploration initiative N91-27104

REGULARITY
Singular and bang-bang stochastic control
[AD-A234752] N91-26861

REGULATIONS
Improved reduction of gust loads data for gust intensity N91-26153
Gust design procedures N91-26155

REGULATORS
Hormonal regulators of calcium metabolism following space flights of various durations N91-26689

REINFORCEMENT (STRUCTURES)
Geogrid reinforced base course for flexible pavements for light aircraft: Literature review and test section design
[DOT/FAA/RD-90/28] N91-26160

REINFORCING FIBERS
Strength of SiC- and Si-N-C-ceramic fibers exposed to high-temperature gaseous environments
[DE91-011099] N91-26380

RELIABILITY
Analytical algorithms to solve an inverse navigation problem for a system of satellites N91-26168
Theory of radar target discrimination
[AD-A234172] N91-26420
The P300 component of the auditory event-related potential: Interlaboratory consistency and test-retest reliability
[AD-A235114] N91-26725

RELIABILITY ANALYSIS
Statistical aspects of reliability, maintainability, and availability
[AD-A234546] N91-26546
Fixed sample and sequential problems with applications in reliability
[AD-A234547] N91-26547
A reliability and mass perspective of SP-100 Stirling cycle lunar-base powerplant designs
[NASA-TM-103736] N91-26592
Electronic design process
[AD-A234709] N91-26786
Compound estimation procedures in reliability N91-27090

RELIABILITY ENGINEERING
Application of software tools in embedded computers within military systems to enhance software reliability, quality assurance, and maintenance
[AD-A234555] N91-26785

REMOTE SENSING
Plate motion and deformation
[DE91-010466] N91-26612
The distribution of particulate material on Mars N91-27059
Martian surface materials N91-27073
Magnetic and electrical properties of Martian particles N91-27074
Derivation of mid-infrared (5-25 microns) optical constants of some silicates and palagonite N91-27077
Dust in the Mars atmosphere N91-27082
REMOTELY PILOTED VEHICLES
Establishment of a remotely piloted helicopter test flight program for higher harmonic control research
[AD-A234978] N91-26135
How low can an unmanned air vehicle fly?
[RAND-P-7680-RGS] N91-26138
REMOVAL
Regeneration of whetlerite for adsorbing toxic pollutants from air
[AD-D014859] N91-26753
RESCUE OPERATIONS
Limited current capabilities for cosmonaut rescue N91-26179
Evaluation of night vision goggles for maritime search and rescue
[AD-A233798] N91-26751
RESEARCH
SPH-4 aircrew helmet impact protection improvements 1970-1990
[AD-A233784] N91-26750
National research and education network N91-27017
Summary of research academic departments, October 1990
[AD-A234353] N91-27118
RESEARCH AIRCRAFT
Acquisition of statistical gust load data by commercial airplanes N91-26152
RESEARCH AND DEVELOPMENT
Aerospace plane technology: Research and development efforts in Europe. Report to the Chairman, Committee on Science, Space, and Technology, House of Representatives
[GAO/NSIAD-91-194] N91-26141
JPRS report: Science and technology. USSR: Space
[JPRS-USP-91-002] N91-26162
Weather satellites: Action needed to resolve status of the US Geostationary Satellite Program. Report to the Chairman, Committee on Science, Space, and Technology, House of Representatives
[GAO/NSIAD-91-252] N91-26194
JPRS report: Science and technology. USSR: Earth sciences
[JPRS-UES-91-002] N91-26581
JPRS report: Science and technology. USSR: Earth sciences
[JPRS-UES-91-003] N91-26582
Photovoltaics: From the laboratory to the marketplace
[DE91-002151] N91-26588
US Army Biomedical Research and Development Laboratory
[AD-A233664] N91-26671
JPRS report: Science and technology. USSR: Life sciences
[JPRS-ULS-91-010] N91-26683
JPRS report: Science and technology. USSR: Life sciences
[JPRS-ULS-91-011] N91-26696
Research instrumentation for optical computing
[AD-A235335] N91-26932
National Aeronautics and Space Administration Multiyear Authorization Act of 1991 N91-27046
RESEARCH FACILITIES
RADC cathode life test facility
[AD-A234309] N91-26444
Providing a computing environment for a high energy physics workshop
[DE91-012049] N91-26916
RESEARCH MANAGEMENT
Large scale computing in the Energy Research Programs
[DE91-012126] N91-26805
Studies of interactions between elementary particles and nuclei
[DE91-012300] N91-26912
Catalog of data bases and reports
[DE91-011516] N91-27043
RESEARCH PROJECTS
Cognitive and neural sciences division 1990 programs
[AD-A233773] N91-26733
Northeast Artificial Intelligence Consortium (NAIC). Volume 1: Executive summary
[AD-A234880] N91-26815
Overview of the NASA astrophysics data system N91-27022
NASA/ASEE Summer Faculty Fellowship Program, 1990, Volume 1
[NASA-CR-185637-VOL-1] N91-27088
RESIDENTIAL AREAS
Absorption heat pump in heating and cooling systems of buildings
[DE91-752988] N91-26593
RESIDUAL STRESS
Magnetostrictive angular positioning motor
[AD-D014858] N91-26536
Non-destructive evaluation of residual stresses in thin films via x ray diffraction topography methods
[AD-A235326] N91-26552
NATO advanced research workshop on Measurement of Residual and Applied Stress Using Neutron Diffraction
[AD-A235103] N91-26566
Residual stresses in metal/ceramic brazes: Effect of creep on finite element analysis results
[DE91-011233] N91-26570
RESINS
Gordon Research Conference on Composites
[AD-A233778] N91-26210
A model for wet filament winding of composite cylinders with arbitrary thickness
[AD-A234102] N91-26215
Method of obtaining phenol-furfural resins
[AD-A233746] N91-26327
RESONANCE
Spatial rotations of a satellite in a circular three-body problem for the case of general resonance N91-26164
Measurement of the nitrogen total cross section from 0.5 eV to 50 MeV and analysis of the 433-keV resonance
[DE91-012222] N91-26293
Underwater scattering of sound
[AD-A235097] N91-26885
Aircraft interior noise reduction by alternate resonance tuning
[NASA-CR-185453] N91-26889
RESONANCE CHARGE EXCHANGE
Charge exchange in ion-surface scattering at hyperthermal (10-100 eV) and keV energies
[AD-A235233] N91-26899
RESONANCE FLUORESCENCE
Resonance fluorescence spectrum of an atom near a phase conjugator
[AD-A234535] N91-26894
RESONANCE SCATTERING
Comparisons of backscattering from cylindrical shells described by thin shell and elasticity theories
[AD-A234745] N91-26475
RESONANT FREQUENCIES
Low frequency noise in resonant Josephson soliton oscillators
[DE91-011911] N91-26464
RESONATORS
Tactical quartz oscillator development
[AD-A234308] N91-26443
Acceleration insensitive resonators
[AD-A235400] N91-26458
RESOURCE ALLOCATION
Applications of artificial intelligence to mission planning
[NASA-CR-187953] N91-26806
RESPIRATION
Effect of excess respiratory resistance on physical performance and cardiorespiratory function N91-26699
Physiological responses to the wearing of protective equipment and respirators: Effects of hot, humid inspired air on work of breathing
[PB91-152884] N91-26745
RESPIRATORY PHYSIOLOGY
Smoking, exercise, and physical fitness
[AD-A234658] N91-26717
RESPONSE BIAS
A procedure to detect item bias present simultaneously in several items
[AD-A235252] N91-26862
RESPONSES
Adaptation and resistance of ecosystems to stress
[AD-A234576] N91-26603
RESUSCITATION
Metabolic changes and hemodynamic dysfunction following hypothermic shock
[AD-A233942] N91-26713
RETINA
Analysis of visual loss from retinal lesions
[AD-A235268] N91-26729
REUSE
An approach for constructing reusable software components in Ada
[AD-A233662] N91-26770
REVERBERATION
A boundary scattering strength extraction algorithm for the analysis of long-range reverberation data
[AD-A233721] N91-26877
RHENIUM ALLOYS
Lifetimes and failure mechanisms of W/Re hairpin filaments
[AD-A235199] N91-26305
RHEOLOGY
Effect of surface forces on the rheology of particle-liquid systems and the consolidation of ceramic powders
[AD-A234375] N91-26221
Polymeric routes to silicon carbide and silicon oxycarbide CMC
[NASA-TM-104372] N91-26234
Advanced study in solid transport: Rheological behavior of dense suspension
[DE91-009428] N91-26467
Improved modeling and performance of squeeze film damper bearings
[AD-A233694] N91-26531
Plate motion and deformation
[DE91-010466] N91-26612
RHYTHM (BIOLOGY)
Mathematical problems concerning rhythmic processes
[AD-A234588] N91-26845
RIBONUCLEIC ACIDS
Molecular studies of cytokine induction
[AD-A235326] N91-26731
RIBS (SUPPORTS)
Reflection of incident pressure waves by ribbed panels
[AD-A233671] N91-26469
Acoustic radiation from fluid-loaded, ribbed cylindrical shells excited by different types of concentrated mechanical drives
[AD-A235324] N91-26887
RIGID ROTORS
Dynamics of elastic bending and torsion of hingeless rotors with dynamic stall
[AD-A234775] N91-26134
RING CURRENTS
The SYNOP experiment: Inverted echo sounder data report for June 1989 to September 1990
[AD-A234625] N91-26662
RING STRUCTURES
Anionic ring-opening polymerization of cyclotetrasilanes
[AD-A235360] N91-26372
RISK
Risk factors and prediction of syncopic states in flyers N91-26685
Creation of uncertainty in repeated two-person non-zero-sum games
[ITN-91-85118] N91-26869
RITZ AVERAGING METHOD
Development of load-dependent Ritz vector method for structural dynamic analysis of large space structures N91-27111
ROASTING
Formation of intermediate compounds during reduced pressure calcination of Y-Ba-Cu-O precursor
[DE91-011179] N91-26971
ROBOT ARMS
Constrained trajectory optimization for kinematically redundant arms
[NASA-CR-183477] N91-26527
Adaptive control of direct drive dexterous robotic hand with bilateral tactile sensing
[AD-A233980] N91-26532
Dynamic stability of flexible robot manipulators
[AD-A234297] N91-26533
Line kinematics for whole-arm manipulation
[AD-A234422] N91-26535
ROBOT: A journal of Chinese Society of Automation
[AD-A234808] N91-26538
ROBOT CONTROL
Constrained trajectory optimization for kinematically redundant arms
[NASA-CR-183477] N91-26527
Dynamic stability of flexible robot manipulators
[AD-A234297] N91-26533
ROBOT DYNAMICS
Piezoelectric micromotors for microrobots
[AD-A234423] N91-26446
Constrained trajectory optimization for kinematically redundant arms
[NASA-CR-183477] N91-26527
Dynamic stability of flexible robot manipulators
[AD-A234297] N91-26533
ROBOTICS
Piezoelectric micromotors for microrobots
[AD-A234423] N91-26446
NASA information sciences and human factors program
[NASA-TM-4291] N91-27119
ROBOTS
Piezoelectric micromotors for microrobots
[AD-A234423] N91-26446

ROBOT: A journal of Chinese Society of Automation
[AD-A234808] N91-26538
Passive and active grasping with a prehensile robot end-effector
[AD-A235085] N91-26539
Imagination and situated cognition
[AD-A234420] N91-26809

ROCKET ENGINE DESIGN
Engine cycle analysis for a particle bed reactor nuclear rocket
[AD-A235258] N91-26199

ROCKET ENGINES
Pressure distribution and induced force field on a conical nozzle due to impingement of a normal jet into the supersonic cross-flow
[AD-A233981] N91-26115
Liquid film cooling in rocket engines
[AD-A234288] N91-26197

ROCKET EXHAUST
Near field interaction of microwave signals with a bounded plasma plume
[NASA-CR-185358] N91-26944

ROCKET LAUNCHING
Sounding rocket flight data summary
[AD-A233656] N91-26626

ROCKETS
The 1990 Sandia rocket-triggered lightning field tests at Kennedy Space Center, Florida
[DE91-011263] N91-26653

RODENTS
Interaction of ionizing radiation, genetically active chemicals, and radiofrequency radiation in human and rodent cells
[AD-A234747] N91-26677

ROOM TEMPERATURE
A room-temperature, flashpumped, 2.09 micron solid state laser
[AD-D014871] N91-26506

ROSS ICE SHELF
Late Wisconsin and early holocene glacial history, inner Ross Embayment, Antarctica N91-26577
Marine record of late quaternary glacial-interglacial fluctuations in the Ross Sea and evidence for rapid, episodic sea level change due to marine ice sheet collapse N91-26578

ROTARY STABILITY
Lyapunov exponents and rotation numbers of linear systems with real noise
[AD-A234729] N91-26846

ROTARY WING AIRCRAFT
Technology needs for high-speed rotorcraft, volume 1
[NASA-CR-177585] N91-26139

ROTARY WINGS
Performance optimization of helicopter rotor blades
[NASA-TM-104054] N91-26137

ROTATING BODIES
One-dimensional translation measurement of speckle from rough rotating objects in ultraviolet illumination
[AD-A233719] N91-26919

ROTATING CYLINDERS
Rotating multicylinder method for the measurement of cloud liquid-water content and droplet size
[AD-A234780] N91-26644

ROTATING FLUIDS
A study of high speed flows in an aircraft transition duct
[NASA-TM-104449] N91-26122

ROTATING MIRRORS
WPG-30 model microprocessor controlled rotating beryllium mirror scanning camera and its applications
[AD-A234802] N91-26493

ROTATING SHAFTS
Control circuitry using electronic emulation of a synchro signal for accurate control of position and rate of rotation for shafts
[NASA-CASE-MFS-28458-1] N91-26459

ROTATION
Spatial rotations of a satellite in a circular three-body problem for the case of general resonance N91-26164
Fluid damping of the oscillations of satellites with a large magnetic moment N91-26170
Control circuitry using electronic emulation of a synchro signal for accurate control of position and rate of rotation for shafts
[NASA-CASE-MFS-28458-1] N91-26459
The effects of display failures and symbol rotation on visual search and recognition performance
[AD-A235035] N91-26743

ROTOR AERODYNAMICS
Dynamics of elastic bending and torsion of hingeless rotors with dynamic stall
[AD-A234775] N91-26134

ROTOR BLADES (TURBOMACHINERY)
Investigation of hot streak migration and film cooling effects on the heat transfer in rotor/stator interacting flows
[AD-A235420] N91-26145

ROTOR DYNAMICS
Improved modeling and performance of squeeze film damper bearings
[AD-A233694] N91-26531
Rotordynamic and leakage characteristics of a 4-stage brush seal
[AD-A235336] N91-26541

ROTOR SPEED
Dynamics of elastic bending and torsion of hingeless rotors with dynamic stall
[AD-A234775] N91-26134

ROUTINES
NUMVEC FORTRAN library manual. Chapter: Partial differential equations. Routine: ICGG3D
[CWI-NM-R9018] N91-26768

ROVING VEHICLES
Fuzzy logic control system to provide autonomous collision avoidance for Mars rover vehicle N91-27106

RULES
Engineering for artificial intelligence software
[AD-A234793] N91-26814

RUN TIME (COMPUTERS)
Using modular neural networks with local representations to control dynamic systems
[AD-A234700] N91-26813

RUNGE-KUTTA METHOD
Stability of collocation-based Runge-Kutta-Nystroem methods
[CWI-NM-R9016] N91-26835

S

S WAVES
Research in nonlinear water waves
[AD-A235410] N91-26478

SABOT PROJECTILES
The effect of sabot wheelbase and position on the launch dynamics of fin-stabilized kinetic energy ammunition
[AD-A234945] N91-26118
Rail circuit augmentation
[AD-A234944] N91-26184

SACCADIC EYE MOVEMENTS
Vestibular reactions and intersensory interactions in weightlessness: Results of Optokinez experiment N91-26698

SAFETY
Limited current capabilities for cosmonaut rescue N91-26179
Minutes of the 24th Explosives Safety Seminar, volume 2
[AD-A235006] N91-26396

SALIVA
Assessment of the pharmacodynamics of intranasal, intravenous and oral scopolamine N91-27114

SALYUT SPACE STATION
Vestibular reactions and intersensory interactions in weightlessness: Results of Optokinez experiment N91-26698

SAMPLERS
Matching theory. A sampler: From Denes Koenig to the present
[AD-A234321] N91-26839

SAMPLING
FTIR studies of water and ammonia decomposition on silicon surfaces
[AD-A234637] N91-26265
The distribution of particulate material on Mars N91-27059

SANDS
Sand and Dust on Mars
[NASA-CP-10074] N91-27057
Have graben wall scarps accumulated sand and dust on Mars? N91-27062
Engineering knowledge requirements for sand and dust on Mars N91-27067
Electrical system/environment interactions on the planet Mars N91-27068
Saltation threshold reduction due to the electrostatic agglomeration of fine particles N91-27071
Impact of Mars sand on dust on the design of space suits and life support equipment: A technology assessment N91-27079
Sand and dust issues for the MESUP mission N91-27080
Martian dust threshold measurements: Simulations under heated surface conditions N91-27081

SANDWICH STRUCTURES
Block patterning of the metallization of polyvinylidene fluoride transducers
[AD-D014872] N91-26450
Nondestructive Evaluation (NDE) of fiberglass marine structures state-of-the art review
[AD-A234785] N91-26550
Dynamic energy absorption of sandwich structures by inelastic deformation
[AD-A234903] N91-26564
Strong exchange coupling in lanthanide bis(phthalocyaninato) sandwich compounds
[AD-A234466] N91-26951

SAPPHIRE
HREM study of heteroepitaxial interfaces in the TiO2/Al2O3 system
[DE91-012473] N91-26986

SATELLITE ANTENNAS
Near field interaction of microwave signals with a bounded plasma plume
[NASA-CR-185358] N91-26944

SATELLITE ATTITUDE CONTROL
Chinese space science and technology (selected articles)
[AD-A234798] N91-26180

SATELLITE COMMUNICATION
Meteor scatter communication between Thule and Station Nord, Greenland
[AD-A234440] N91-26424
Using HST: From proposal to science N91-27023

SATELLITE IMAGERY
Results of morphometric analysis of the Tesserae surface of Venus according to Venera-15 and -16 data N91-26176
Chinese space science and technology (selected articles)
[AD-A234798] N91-26180
Satellite data derived estimates of erosion parameters for reentry vehicles
[AD-A234792] N91-26189
UV aurora mapping in corrected geomagnetic coordinates
[ITN-91-85106] N91-26636
Advanced Microwave Precipitation Radiometer (AMPR) for remote observation of precipitation
[NASA-CR-184165] N91-26655
Lead detection and mapping with reference to relationships between scale, sensor characteristics, surface conditions and atmospheric properties
[AD-A235121] N91-26666

SATELLITE OBSERVATION
Satellite data derived estimates of erosion parameters for reentry vehicles
[AD-A234792] N91-26189
Development of a Vector Spherical Harmonic (VSH) model of the neutral thermosphere
[AD-A234744] N91-26631
Using HST: From proposal to science N91-27023

SATELLITE ORBITS
Evolution of some types of Earth satellite orbits N91-26163
Spatial rotations of a satellite in a circular three-body problem for the case of general resonance N91-26164
Analysis of necessary and sufficient conditions for the equilibrium stability of a gyrostatic satellite N91-26166
Analytical algorithms to solve an inverse navigation problem for a system of satellites N91-26168
Fluid damping of the oscillations of satellites with a large magnetic moment N91-26170
TRACE trajectory analysis and orbit determination program. Volume 13: Square root information filtering and smoothing
[AD-A234957] N91-26183

SATELLITE-BORNE PHOTOGRAPHY
OSIRRUS: Oceanic symbolic image representation, recognition and understanding software
[AD-A235112] N91-26665

SCALE (CORROSION)
Study of the effect of reactive element addition by implanting metal ions in a pre-formed oxide layer
[DE91-011916] N91-26974

SCALING LAWS
Flexural plate wave devices for chemical analysis
[AD-A234129] N91-26254

SCANNERS
X ray-computed tomography for inspecting industrial parts
[DE91-011390] N91-26554

SCANNING TUNNELING MICROSCOPY
Scanning tunnelling microscope for boron surface studies
[AD-A234716] N91-26452

SCATTER PROPAGATION
Meteor scatter communication between Thule and Station Nord, Greenland
[AD-A234440] N91-26424
Underwater scattering of sound
[AD-A235097] N91-26685

Studies of optical beam phase-conjugation and electromagnetic scattering process
[AD-A234830] N91-26929

SCATTERING
Radiation, scattering, and guidance of electromagnetic fields by arbitrarily shaped structures embedded in layered dielectric media
[AD-A234434] N91-26423
A model for the scattering of high-frequency electromagnetic fields from dielectrics exhibiting thermally-activated electrical losses
[NASA-TM-104376] N91-26872
Charge exchange in ion-surface scattering at hyperthermal (10-100 eV) and keV energies
[AD-A235233] N91-26899
Recent studies of the optical properties of dust and cloud particles in the Mars atmosphere and the interannual frequency of global dust storms N91-27060

SCATTERING CROSS SECTIONS
Effect of aerosols on laser-induced breakdown
[AD-A234324] N91-26502
Nonperturbative behavior of quarks
[DE91-011905] N91-26903

SCAVENGING
Simulation of precipitation scavenging in a three-dimensional global model
[DE91-011531] N91-26606

SCHEDULING
Expert system explanation: The user perspective
[AD-A233739] N91-26749

SCHOTTKY DIODES
Ab initio molecular dynamics simulations of surfaces and interfaces
[AD-A235315] N91-26901

SCHROEDINGER EQUATION
Theoretical studies of potential energy surfaces and computational methods
[DE91-011126] N91-26902

SCIENTISTS
Measuring the quality of knowledge work
[AD-A235354] N91-26994

SCINTILLATION
The Effect of the Ionosphere on Radiowave Signals and Systems Performance Based on Ionospheric Effects Symposium
[AD-A233797] N91-26416

SEA ICE
Terrestrial geophysics in the SeaRISE project N91-26576
Ice cores and SeaRISE: What we do (and don't) know N91-26579

SEA LEVEL
West Antarctic Ice Sheet Initiative. Volume 2: Discipline Reviews
[NASA-CP-3115-VOL-2] N91-26573
Marine record of late quaternary glacial-interglacial fluctuations in the Ross Sea and evidence for rapid, episodic sea level change due to marine ice sheet collapse N91-26578

SEA STATES
Analysis of wave characteristics in extreme seas
[AD-A234538] N91-26660
Directional characteristics of waves in shallow water
[AD-A234568] N91-26661

SEA SURFACE TEMPERATURE
The tropical Pacific Ocean's heat budget during a cold event, from a numerical model N91-26657

SEALING
Thermal degradation chemistry of poly(diphenoxy phosphazene)
[AD-A235284] N91-26282
Double face sealing device
[NASA-CASE-MFS-28521-1] N91-26542

SEALS (STOPPERS)
Dynamics of face and annular seals with two-phase flow
[NASA-CR-4256] N91-26479
Rotordynamic and leakage characteristics of a 4-stage brush seal
[AD-A235336] N91-26541

SEARCHING
The effects of display failures and symbol rotation on visual search and recognition performance
[AD-A235035] N91-26743

SEAS
Sea test development of laser altimeter
[AD-A233824] N91-26498

SEATS
Method and apparatus for waste collection and storage
[NASA-CASE-MSC-21025-3] N91-26747

SEDATIVES
Attention span, anxiety, and benzodiazepine receptors
[AD-A234549] N91-26716

SEDIMENT TRANSPORT
Saltation threshold detection in a wind tunnel by the measurement of the net electrostatic charge N91-27070
Saltation threshold reduction due to the electrostatic agglomeration of fine particles N91-27071

SEISMIC WAVES
A multichannel seismic investigation of variations in crustal structure in the western North Atlantic
[AD-A235245] N91-26634

SEISMOLOGY
Terrestrial geophysics in the SeaRISE project N91-26576
Research in stochastic processes
[AD-A234650] N91-26860

SELF CONSISTENT FIELDS
Defect clustering and related properties of oxides
[DE91-011072] N91-26290
Theoretical studies of potential energy surfaces and computational methods
[DE91-011126] N91-26902

SEMICIRCULAR CANALS
Combined effect of noise and vibration on cells of auditory and vestibular apparatus N91-26707

SEMICONDUCTOR DEVICES
The role of EEPROM devices in upcoming ISDN applications
[AD-A234837] N91-26454
Part 1: Ultrafast logic and multiple-beam optical parallel processing using nonlinear etalons. Part 2: Novel devices for all-optical computing. Part 3: Novel nonlinear semiconductor structures for signal processing and optical computing
[AD-A233410] N91-26799
Binary optics technology: Theoretical limits on the diffraction efficiency of multilevel diffractive optical elements
[AD-A235404] N91-26933
Material engineering of novel semiconductor structures
[AD-A235014] N91-26960
Superconducting high T(sub c) thin film vortex-flow transistor, phase 1
[AD-A235025] N91-26962
Process for the controlled growth of single-crystal films of silicon carbide polytypes on silicon carbide wafers
[NASA-CASE-LEW-15222-1] N91-26966

SEMICONDUCTOR DIODES
New laser materials for laser diode pumping
[NASA-CR-187786] N91-26521
A study of signal generation and charge collectionin a-Si:H diodes for radiation imaging
[DE91-010243] N91-26904
Analysis of nonlinear optical frequency conversion
[AD-A233726] N91-26920

SEMICONDUCTOR LASERS
Proceedings of the Optoelectronic Workshop 27: Semiconductor Lasers and Their Applications
[AD-A233779] N91-26496
Multigigahertz semiconductor lasers
[AD-A234776] N91-26510
New laser materials for laser diode pumping
[NASA-CR-187786] N91-26521
Analysis of nonlinear optical frequency conversion
[AD-A233726] N91-26920

SEMICONDUCTORS (MATERIALS)
Surface mediated photocatalysis
[AD-A233748] N91-26246
Comparison of H2 desorption kinetics from Si(111)7x7 and Si(100)2x1
[AD-A234634] N91-26263
Design of polymers with semiconductor, NLO, and structural properties
[AD-A235215] N91-26364
Center for electronics and electrical engineering. Technical progress bulletin covering center programs, July to September 1990, with 1991 CEEE events calendar
[PB91-159749] N91-26437
Ab initio molecular dynamics simulations of surfaces and interfaces
[AD-A235315] N91-26901
The First Nonlinear Optics: Materials, Phenomena, and Devices Conference
[AD-A234733] N91-26926
Center for the Integration of Optical C
[AD-A235277] N91-26931
Preparation of a novel gallium arsenide single-source precursor having the empirical formula AsCl3Ga2
[AD-A233704] N91-26949
Symposium E: Properties of 2-6 semiconductors. Bulk crystals, epitaxial films, quantum well structures
[AD-A234835] N91-26957
Monolithic integration semiconductor and superconductor components
[AD-A234986] N91-26959
Material engineering of novel semiconductor structures
[AD-A235014] N91-26960
Luminescence and lasing in II-VI semiconductors
[AD-A235019] N91-26961
Thin film alloys on semiconductor substrates
[DE91-012355] N91-26985

SENSITIVITY
Acceleration insensitive resonators
[AD-A235400] N91-26458
On the sensitivity of solutions of parametrized equations
[AD-A234265] N91-26838

SENSORIMOTOR PERFORMANCE
Physical and psychogenic sequelae of impact acceleration on tracking performance of operators N91-26701

SENSORY PERCEPTION
The Trendelenburg position after cerebral air embolism in dogs: Effects on the somatosensory evoked potential, intracranial pressure, and blood-brain barrier
[AD-A233809] N91-26673
Physiological and perceptual responses to load carrying in female subjects using internal and external frame backpacks
[AD-A234941] N91-26722

SENSORY STIMULATION
Mechanisms of adaptive information processing
[AD-A234435] N91-26734

SEPARATORS
Proof-of-concept zinc/bromine electric vehicle battery
[DE91-011767] N91-26463

SEQUENCING
Heuristics for a flow-shop model with parallel machines and setup times
[ITN-91-85117] N91-26996

SEQUENTIAL CONTROL
The High Resolution Profiler (HRP): User's guide and software modifications documentation
[AD-A234640] N91-26663

SERVICE LIFE
Lifetimes and failure mechanisms of W/Re hairpin filaments
[AD-A235199] N91-26305
Ceramic technology for advanced heat engines project
[DE91-010451] N91-26384
Forecasting digital microcircuit obsolescence
[AD-A234573] N91-26451
Proof-of-concept zinc/bromine electric vehicle battery
[DE91-011767] N91-26463
Preliminary test results from the HSST shallow-crack fracture toughness program
[DE91-010147] N91-26572
Regeneration of whetlerite for adsorbing toxic pollutants from air
[AD-D014859] N91-26753

SERVICES
Queueing systems with orbiting customers
[ITN-91-85112] N91-26868

SERVOCONTROL
Development of an integrated aeroservoelastic analysis program and correlation with test data
[NASA-TP-3120] N91-26113

SET THEORY
Pumping system fault detection and diagnosis utilizing pattern recognition and fuzzy inference techniques
[DE91-011849] N91-26863

SHADOWS
The distribution of the size and number of shadows cast on a line segment in a Poisson random field
[AD-A233697] N91-26857

SHAFTS (MACHINE ELEMENTS)
Control circuitry using electronic emulation of a synchro signal for accurate control of position and rate of rotation for shafts
[NASA-CASE-MFS-28458-1] N91-26459

SHALLOW WATER
Directional characteristics of waves in shallow water
[AD-A234568] N91-26661

SHAPED CHARGES
Shock response of Detasheet
[DE91-010923] N91-26399

SHAPES
The shape of shading
[AD-A234419] N91-26781

SHEAR LAYERS
Control of an axisymmetric turbulent jet by multi-modal excitation
[NASA-TM-104483] N91-26121
Research in nonlinear water waves
[AD-A235410] N91-26478

SHEAR PROPERTIES
Comparisons of backscattering from cylindrical shells described by thin shell and elasticity theories
[AD-A234745] N91-26475

SHEAR STRENGTH
Investigation of interfacial shear strength in SiC/Si3N4 composites
[NASA-TM-103739] N91-26233
SHEAR STRESS
Advanced study in solid transport: Rheological behavior of dense suspension
[DE91-009428] N91-26467
SHELLS (STRUCTURAL FORMS)
Shell hoop prestress generated by welding
[DE91-011892] N91-26571
SHIPS
VLF nighttime data analysis
[AD-A234006] N91-26417
SHOCK LOADS
An analysis on the stability of the Mie-Gruneisen equation of state for describing the behavior of shock-loaded materials
[AD-A233827] N91-26988
SHOCK SIMULATORS
Optical studies of the flow start-up processes in four convergent-divergent nozzles
[AD-A234552] N91-26473
SHOCK TESTS
Optical studies of the flow start-up processes in four convergent-divergent nozzles
[AD-A234552] N91-26473
SHOCK TUBES
Optical studies of the flow start-up processes in four convergent-divergent nozzles
[AD-A234552] N91-26473
Elementary reaction rate measurements at high temperatures by tunable-laser flash-absorption
[DE91-011850] N91-26516
SHOCK WAVES
Experimental techniques in the field of low density aerodynamics
[AGARD-AG-318(E)] N91-26124
Shock response of Detasheet
[DE91-010923] N91-26399
SIDELOBES
Application of a conjugate gradient method to the synthesis of phase-only planar arrays
[AD-A233756] N91-26415
SIGNAL ANALYZERS
A test vector generator for a radar signal processor
[AD-A233725] N91-26413
SIGNAL DETECTION
OSIRRUS: Oceanic symbolic image representation, recognition and understanding software
[AD-A235112] N91-26665
Research in stochastic processes
[AD-A234650] N91-26860
SIGNAL DETECTORS
Lead detection and mapping with reference to relationships between scale, sensor characteristics, surface conditions and atmospheric properties
[AD-A235121] N91-26666
SIGNAL GENERATORS
A test vector generator for a radar signal processor
[AD-A233725] N91-26413
Northeast Artificial Intelligence Consortium (NAIC). Volume 17: High-level adaptive signal processing
[AD-A234896] N91-26831
A study of signal generation and charge collectionin a-Si:H diodes for radiation imaging
[DE91-010243] N91-26904
SIGNAL PROCESSING
A test vector generator for a radar signal processor
[AD-A233725] N91-26413
The Effect of the Ionosphere on Radiowave Signals and Systems Performance Based on Ionospheric Effects Symposium
[AD-A233797] N91-26416
Theory of radar target discrimination
[AD-A234172] N91-26420
Digital signal conditioning for flight test, volume 19
[AGARD-AG-160-VOL-19] N91-26432
Middle Atmosphere Program. Handbook for MAP. Volume 30: International School on Atmospheric Radar
[NASA-CR-188623] N91-26613
Data acquisition and processing N91-26618
The P300 component of the auditory event-related potential: Interlaboratory consistency and test-retest reliability
[AD-A235114] N91-26725
Testing the One-Port Random Access Memory (1PRAM) module of TRW's CPUAX signal processing superchip
[AD-A234127] N91-26761
Parallel algorithms for least squares and related computations
[AD-A235018] N91-26790
Part 1: Ultrafast logic and multiple-beam optical parallel processing using nonlinear etalons. Part 2: Novel devices for all-optical computing. Part 3: Novel nonlinear semiconductor structures for signal processing and optical computing
[AD-A233410] N91-26799
An implementation of the singular value decomposition on the connection machine CM-2
[AD-A234124] N91-26802
Northeast Artificial Intelligence Consortium (NAIC). Volume 16: Intelligent signal processing techniques for multi-sensor surveillance systems
[AD-A234895] N91-26830
Northeast Artificial Intelligence Consortium (NAIC). Volume 17: High-level adaptive signal processing
[AD-A234896] N91-26831
Vertical incidence backscatter and surface forward scattering from near-surface bubbles
[AD-A234432] N91-26880
SIGNAL RECEPTION
The instrumental principles of MST radars and incoherent scatter radars and the configuration of radar system hardware N91-26616
SIGNAL REFLECTION
System concept and analysis of an Artificial Ionospheric Mirror (AIM) radar
[AD-A234289] N91-26630
SIGNAL TO NOISE RATIOS
Quality by design using statistically planned experiments
[ITN-91-85119] N91-26553
Data acquisition and processing N91-26618
SIGNAL TRANSMISSION
Mechanisms of adaptive information processing
[AD-A234435] N91-26734
Review of audition literature: Selection of acoustic signals for use in the synthesis of auditory space
[AD-A234579] N91-26881
SIGNS AND SYMPTOMS
Utilization of emergency medical kits by air carriers
[AD-A234784] N91-26721
SILANES
Diethylsilane decomposition on silicon surfaces studied using transmission FTIR spectroscopy
[AD-A234638] N91-26266
SILICA GEL
Structure of alkylated silica surfaces: Quenching of fluorescence from covalently bound pyrene
[AD-A234642] N91-26207
Surface diffusion at the liquid-solid interface: Quenching of fluorescence from pyrene covalently bound to methylated silica
[AD-A234645] N91-26268
SILICATES
Derivation of mid-infrared (5-25 microns) optical constants of some silicates and palagonite N91-27077
SILICON
Adsorption and decomposition of acetylene on Si(100)-(2x1)
[AD-A233808] N91-26248
Adsorption and thermal behavior of ethylene on Si(100)-(2x1)
[AD-A234098] N91-26252
Study of the low-lying electronic states of Si2 and Si2(-) using negative ion photodetachment techniques
[AD-A234336] N91-26256
Comparison of hydrogen desorption kinetics from Si(111)7x7 and Si(100)2x1
[AD-A234633] N91-26262
Comparison of H2 desorption kinetics from Si(111)7x7 and Si(100)2x1
[AD-A234634] N91-26263
Desorption product yields following Cl2 adsorption on Si(111)7x7: Coverage and temperature dependence
[AD-A234635] N91-26264
Diethylsilane decomposition on silicon surfaces studied using transmission FTIR spectroscopy
[AD-A234638] N91-26266
Adsorption and decomposition of diethylsilane on silicon surfaces
[AD-A234639] N91-26267
A combined XPS-ISS modulated molecular beam investigation of the reactions of oxygen and fluorine with silicon surfaces
[AD-A234867] N91-26269
Chemistry of fluorine in the oxidation of silicon
[AD-A234959] N91-26272
The stepwise dissociation of NH3 on the Si(111)-(7x7) surface: Low temperature dissociative adsorption and thermal effects
[AD-A235009] N91-26274
Laser-induced desorption of H2 from Si(111)7x7
[AD-A234636] N91-26508
Ada compiler validation summary report: Certificate number 900703W1.11015, Silicon Graphics 4D Ada, Iris-4D/220S (host) Iris-4D/220S (target)
[AD-A233786] N91-26776
Chemistry on an atomic scale of ion-beam modified surfaces
[AD-A233707] N91-26891
SILICON ALLOYS
Mechanical behavior and flow mechanisms in refractory metal composition
[AD-A234701] N91-26297
Metastable pitting corrosion of aluminum, Al-Cu, and Al-Si thin films in dilute HF solutions and its relevancy to the processing of integrated circuit interconnections
[DE91-012014] N91-26320
Environmental embrittlement of ordered intermetallic alloys at room temperature in moist atmospheres
[DE91-012051] N91-26321
SILICON CARBIDES
Dynamic fracture responses of Al2O3, Si3N4, and SiC(w)/Al2O3
[AD-A235286] N91-26229
Investigation of interfacial shear strength in SiC/Si3N4 composites
[NASA-TM-103739] N91-26233
Polymeric routes to silicon carbide and silicon oxycarbide CMC
[NASA-TM-104372] N91-26234
Adsorption and thermal behavior of ethylene on Si(100)-(2x1)
[AD-A234098] N91-26252
Surface chemistry of silicon: The behavior of dangling bonds
[AD-A235011] N91-26275
Mechanical properties of spray atomized SiC particle reinforced aluminum-titanium alloys
[AD-A235231] N91-26306
A tribological investigation of the graphite-to-diamond-like behavior of amorphous carbon films ion-beam-deposited on ceramic substrates
[DE91-010816] N91-26379
Strength of SiC- and Si-N-C-ceramic fibers exposed to high-temperature gaseous environments
[DE91-011099] N91-26380
Development and testing of radiation and electromagnetic pulse hardened silicon carbide based electronics
[AD-A233744] N91-26439
Process for the controlled growth of single-crystal films of silicon carbide polytypes on silicon carbide wafers
[NASA-CASE-LEW-15222-1] N91-26966
Process for the homoepitaxial growth of single-crystal silicon carbide films on silicon carbide wafers
[NASA-CASE-LEW-15223-1] N91-26967
SILICON COMPOUNDS
Anionic ring-opening polymerization of cyclotetrasilanes
[AD-A235360] N91-26372
SILICON DIOXIDE
Structure of alkylated silica surfaces: Quenching of fluorescence from covalently bound pyrene
[AD-A234642] N91-26207
Surface diffusion at the liquid-solid interface: Quenching of fluorescence from pyrene covalently bound to methylated silica
[AD-A234645] N91-26268
Transpiration cooled ultraviolet sol-gel silica optics
[AD-A235426] N91-26934
SILICON FILMS
Thickness measurements of silicon films using partial coherence interferometry
[AD-A235211] N91-26930
SILICON JUNCTIONS
Investigation and characterization of ITO/poly-Si photovoltaic junctions
[ITN-91-85105] N91-26590
SILICON NITRIDES
Dynamic fracture responses of Al2O3, Si3N4, and SiC(w)/Al2O3
[AD-A235286] N91-26229
Investigation of interfacial shear strength in SiC/Si3N4 composites
[NASA-TM-103739] N91-26233
Microstructure development during microwave annealing of dense silicon nitride
[DE91-012069] N91-26242
A tribological investigation of the graphite-to-diamond-like behavior of amorphous carbon films ion-beam-deposited on ceramic substrates
[DE91-010816] N91-26379
Strength of SiC- and Si-N-C-ceramic fibers exposed to high-temperature gaseous environments
[DE91-011099] N91-26380

SILICON OXIDES
Microstructure development during microwave annealing of dense silicon nitride
[DE91-012069] N91-26242
SILICON POLYMERS
Second Mini-Conference on Key Problems in Silicon Chemistry
[AD-A235243] N91-26366
SILOXANES
Organosilicon polymers incorporating the bicyclo(2.2.2)-octane moiety
[AD-A234966] N91-26361
SILVER
Molecular orientation of the silver tetra neopentoxy phthalo cyanine and stearic acid mixed Langmuir-Blodgett film and its chemical and electrochemical behaviour
[AD-A234601] N91-26206
Mechanical behavior of nanocrystalline Cu, Pd, and Ag samples
[DE91-011747] N91-26310
SIMULATION
Water solubility of bis(2-ethylhexyl) hydrogen phosphite
[AD-A234561] N91-26259
Digital logic testing and testability
[AD-A234123] N91-26441
Improvement of procedures for evaluating photochemical models
[PB91-160374] N91-26597
Modal aerosol dynamics modeling
[PB91-161729] N91-26598
Preliminary testing, evaluation and sensitivity analysis for the Terrestrial Ecosystem Exposure Assessment Model (TEEAM)
[PB91-161711] N91-26602
Weighted least squares estimation for Aalen's additive risk model
[AD-A235250] N91-26852
SIMULATORS
Testing of a composite thermal structure to insulate the drivers of a large scale blast/thermal simulator
[AD-A234014] N91-26213
SINGLE CRYSTALS
Plasticity of single crystalline Al3X intermetallic compounds
[AD-A234699] N91-26356
Process for the controlled growth of single-crystal films of silicon carbide polytypes on silicon carbide wafers
[NASA-CASE-LEW-15222-1] N91-26966
Process for the homoepitaxial growth of single-crystal silicon carbide films on silicon carbide wafers
[NASA-CASE-LEW-15223-1] N91-26967
HREM study of heteroepitaxial interfaces in the TiO2/Al2O3 system
[DE91-012473] N91-26986
SINGULARITY (MATHEMATICS)
An implementation of the singular value decomposition on the connection machine CM-2
[AD-A234124] N91-26802
Numerical methods for singularly perturbed differential equations with applications
[AD-A235188] N91-26850
SINTERING
Pressureless densification of ceramic matrix composites
[AD-A235031] N91-26362
SIS (SUPERCONDUCTORS)
Quantum limited quasiparticle mixers at 100 GHz
[DE91-011894] N91-26973
SITTING POSITION
Sitting posture analysis. An experimental optimisation approach
[ITN-91-85114] N91-26760
SIZE DISTRIBUTION
The distribution of the size and number of shadows cast on a line segment in a Poisson random field
[AD-A233697] N91-26857
SKEWNESS
Implementation of the flow-modulated skew-upwind difference scheme in the COMMIX-1C code: A first assessment
[DE91-011166] N91-26489
SKIN (ANATOMY)
Wound healing by cultured skin cells and growth factors
[AD-A235300] N91-26730
SLABS
Laser applications in machining slab materials
[AD-A233823] N91-26497
SLEEP DEPRIVATION
Methylphenidate and pemoline: Effects on sleepiness and mood during sleep deprivation
[AD-A234659] N91-26718
SLIDING
Interfacial slippage of a unidirectional fiber composite under longitudinal shearing
[AD-A234186] N91-26216
SLIDING FRICTION
Sliding wear-testing and data analysis strategies for advanced engineering ceramics
[DE91-009524] N91-26383
SLOPES
Have graben wall scarps accumulated sand and dust on Mars? N91-27062
SLURRIES
Effect of surface forces on the rheology of particle-liquid systems and the consolidation of ceramic powders
[AD-A234375] N91-26221
The synthesis of methanol by a novel method
[DE91-011131] N91-26291
Advanced study in solid transport: Rheological behavior of dense suspension
[DE91-009428] N91-26467
SMOKE
Airliner cabin environment: Contaminant measurements, health risks, and mitigation options
[PB91-159384] N91-26746
SNOW COVER
A review of precipitation-related aspects of West Antarctic meteorology N91-26574
SODIUM
The chemistry of sodium with sulfur in flames
[DE91-002060] N91-26288
Electrochemically induced charge and mass transport in polypyrrole/poly(styrene sulfonate) molecular composites
[AD-A234599] N91-26354
SODIUM COMPOUNDS
The electronic structure of the ionic insulator sodium nitrite
[DE91-009766] N91-26977
SODIUM SULFATES
The chemistry of sodium with sulfur in flames
[DE91-002060] N91-26288
SOFT LANDING
Study of the properties of the autonomous optical navigation of a space probe in a rendezvous with an asteroid N91-26169
SOFTWARE ENGINEERING
Autonomous aircraft initiative study
[NASA-CR-186013] N91-26140
Architectures for a high performance distributed operating system
[AD-A235333] N91-26429
Content addressable memory project
[AD-A234524] N91-26763
Object-oriented requirements analysis: A quick tour
[NASA-CR-187919] N91-26766
An approach for constructing reusable software components in Ada
[AD-A233662] N91-26770
Software Technology for Adaptable, Reliable Systems (STARS), UR60-IRIS-Ada toolset. User's guide (draft)
[AD-A234445] N91-26783
Coordination in large scale software development
[AD-A234898] N91-26787
Program improvement by automatic redistribution of intermediate results
[AD-A235086] N91-26791
Engineering for artificial intelligence software
[AD-A234793] N91-26814
Proceedings of the Second Annual NASA Science Internet User Working Group Conference
[NASA-CP-3117] N91-27009
SOFTWARE TOOLS
Active devices for monolithic millimeter-wave integrated circuits
[AD-A234033] N91-26440
Adaptive component methods for time dependent PDE's
[AD-A233776] N91-26775
Software Technology for Adaptable, Reliable Systems (STARS), UR60-IRIS-Ada toolset. User's guide (draft)
[AD-A234445] N91-26783
Application of software tools in embedded computers within military systems to enhance software reliability, quality assurance, and maintenance
[AD-A234555] N91-26785
Translating expert system rules into Ada code with validation and verification
[NASA-CR-187505] N91-26800
NSIUWG security sub-group N91-27026
Software product description N91-27037
SOIL MECHANICS
Process study of sorted patterns on Arctic soils
[AD-A234089] N91-26628
SOILS
The chemistry and mineralogy of Mars soil and dust N91-27058
SOL-GEL PROCESSES
International collaboration program on innovative chemical processing of superior electronic and optical materials
[AD-A235030] N91-26276
Transpiration cooled ultraviolet sol-gel silica optics
[AD-A235426] N91-26934
SOLAR ACTIVITY
The 1980 solar maximum mission event listing
[NASA-TM-4287] N91-27087
SOLAR ACTIVITY EFFECTS
Turbulent processes of mass-loading of new ions on Venus and Mars and the problems of numerical models of the interaction of solar wind with these planets. 1: Characteristics of the flow of solar wind around the planets N91-26174
SOLAR ARRAYS
Sand and dust issues for the MESUR mission N91-27080
SOLAR CELLS
Investigation and characterization of ITO/poly-Si photovoltaic junctions
[ITN-91-85105] N91-26590
Research on stable, high-efficiency amorphous silicon multijunction modules
[DE91-002159] N91-26591
SOLAR COLLECTORS
Commercializing solar hydrogen production
[DE91-011232] N91-26398
SOLAR ENERGY CONVERSION
Commercializing solar hydrogen production
[DE91-011232] N91-26398
SOLAR FLARES
Solar-geophysical data number 556, December 1990. Part 2: (Comprehensive reports). Data for June 1990 and miscellaneous
[PB91-152157] N91-27084
Solar geophysical data number 551, July 1990. Part 1: (Prompt reports). Data for June, May 1990 and late data
[PB91-160713] N91-27085
Solar-geophysical data number 551, July 1990. Part 2: (Comprehensive reports). Data for January 1990 and miscellaneous
[PB91-160721] N91-27086
The 1980 solar maximum mission event listing
[NASA-TM-4287] N91-27087
SOLAR MAGNETIC FIELD
Solar geophysical data number 551, July 1990. Part 1: (Prompt reports). Data for June, May 1990 and late data
[PB91-160713] N91-27085
SOLAR MAXIMUM MISSION
The 1980 solar maximum mission event listing
[NASA-TM-4287] N91-27087
SOLAR PHYSICS
Solar-geophysical data number 556, December 1990. Part 1: (Prompt reports). Data for November, October 1990, and late data
[PB91-152140] N91-27083
Solar-geophysical data number 556, December 1990. Part 2: (Comprehensive reports). Data for June 1990 and miscellaneous
[PB91-152157] N91-27084
Solar geophysical data number 551, July 1990. Part 1: (Prompt reports). Data for June, May 1990 and late data
[PB91-160713] N91-27085
Solar-geophysical data number 551, July 1990. Part 2: (Comprehensive reports). Data for January 1990 and miscellaneous
[PB91-160721] N91-27086
SOLAR POSITION
Turbulent processes of mass-loading of new ions on Venus and Mars and the problems of numerical models of the interaction of solar wind with these planets. 1: Characteristics of the flow of solar wind around the planets N91-26174
SOLAR PROMINENCES
Solar-geophysical data number 556, December 1990. Part 2: (Comprehensive reports). Data for June 1990 and miscellaneous
[PB91-152157] N91-27084
SOLAR PROPULSION
The effects of space debris on solar propulsion
[AD-A235257] N91-26192
SOLAR PROTONS
Dynamics of equatorial and polar boundaries of penetration of solar protons with energy about 1 MeV into magnetosphere during strong magnetic storm N91-26172
SOLAR RADIATION
Martian dust threshold measurements: Simulations under heated surface conditions N91-27081
SOLAR RADIO BURSTS
Solar-geophysical data number 556, December 1990. Part 2: (Comprehensive reports). Data for June 1990 and miscellaneous
[PB91-152157] N91-27084

Solar-geophysical data number 551, July 1990. Part 2: (Comprehensive reports). Data for January 1990 and miscellaneous
[PB91-160721] N91-27086

SOLAR RADIO EMISSION
Solar geophysical data number 551, July 1990. Part 1: (Prompt reports). Data for June, May 1990 and late data
[PB91-160713] N91-27085

SOLAR SYSTEM
Study of the properties of the autonomous optical navigation of a space probe in a rendezvous with an asteroid N91-26169
CBSD version 2 component models of the IR celestial background
[AD-A235372] N91-27048
A gravitationally consistent second-order analytic secular solution for the point-mass motion of the eight principal planets N91-27054

SOLAR TERRESTRIAL INTERACTIONS
Solar-geophysical data number 556, December 1990. Part 1: (Prompt reports). Data for November, October 1990, and late data
[PB91-152140] N91-27083

SOLAR WIND
Modelling the dynamics of fluxes of electrons with energies 30-300 keV in geostationary orbit N91-26173
Turbulent processes of mass-loading of new ions on Venus and Mars and the problems of numerical models of the interaction of solar wind with these planets. 1: Characteristics of the flow of solar wind around the planets N91-26174
Solar-geophysical data number 551, July 1990. Part 2: (Comprehensive reports). Data for January 1990 and miscellaneous
[PB91-160721] N91-27086

SOLAR X-RAYS
Solar-geophysical data number 556, December 1990. Part 2: (Comprehensive reports). Data for June 1990 and miscellaneous
[PB91-152157] N91-27084

SOLID ELECTROLYTES
Electrocatalytic study of ammonia synthesis and methane dimerization in high temperature solid electrolyte cells
[DE91-009797] N91-26289

SOLID PROPELLANT COMBUSTION
A study of the gas phase chemistry of solid propellants using a microprobe mass spectrometer (MPMS) system: Preliminary results for solid fuels (HTPB/Zecorez and BAMO/NMMO), single-base propellant (M10) and an RDX-Based propellant (BLX-9)
[AD-A234840] N91-26394

SOLID PROPELLANT IGNITION
A study of the gas phase chemistry of solid propellants using a microprobe mass spectrometer (MPMS) system: Initial development of the MPMS system
[AD-A234839] N91-26393
A study of the gas phase chemistry of solid propellants using a microprobe mass spectrometer (MPMS) system: Preliminary results for solid fuels (HTPB/Zecorez and BAMO/NMMO), single-base propellant (M10) and an RDX-Based propellant (BLX-9)
[AD-A234840] N91-26394

SOLID PROPELLANT ROCKET ENGINES
Technical Evaluation Motor No. 7 (TEM-7)
[NASA-CR-184163] N91-26203

SOLID PROPELLANTS
A study of the gas phase chemistry of solid propellants using a microprobe mass spectrometer (MPMS) system: Initial development of the MPMS system
[AD-A234839] N91-26393
A study of the gas phase chemistry of solid propellants using a microprobe mass spectrometer (MPMS) system: Preliminary results for solid fuels (HTPB/Zecorez and BAMO/NMMO), single-base propellant (M10) and an RDX-Based propellant (BLX-9)
[AD-A234840] N91-26394

SOLID ROCKET BINDERS
Bonding agent for composite propellants
[AD-D014876] N91-26392

SOLID ROCKET PROPELLANTS
A new high-progressivity/high-density propulsion concept: Partially cut multiperforated stick propellant
[AD-A234255] N91-26391

SOLID STATE
Solid-state proton conductors
[DE91-002050] N91-26970
Efficient photoinduced charge separation and storage in the solid state, rates, energetics, and spin-polarization
[DE91-010727] N91-26980

SOLID STATE DEVICES
Active devices for monolithic millimeter-wave integrated circuits
[AD-A234033] N91-26440
Solid state research
[AD-A234836] N91-26958

SOLID STATE LASERS
Laser spectroscopy characterization of materials for frequency agile solid state laser systems
[AD-A233916] N91-26500
A room-temperature, flashpumped, 2.09 micron solid state laser
[AD-D014871] N91-26506
New laser materials for laser diode pumping
[NASA-CR-187786] N91-26521
Precision high-power solid-state laser diagnostics for target-irradiation studies and target-plane irradiation modeling
[DE91-012036] N91-26523
Development of a subpicosecond, tunable LiCAF (Cr:LiCaAlF6) laser
[DE91-012082] N91-26526

SOLID-SOLID INTERFACES
Investigation of interfacial shear strength in SiC/Si3N4 composites
[NASA-TM-103739] N91-26233
Energetics, bonding mechanism and electronic structure of metal/ceramic interfaces
[DE91-009787] N91-26239
Scanning tunnelling microscope for boron surface studies
[AD-A234716] N91-26452
Ab initio molecular dynamics simulations of surfaces and interfaces
[AD-A235315] N91-26901

SOLIDIFICATION
Grain boundary cavitation processes in a Ni3Al alloy at elevated temperatures
[AD-A235279] N91-26307

SOLIDS
Advanced study in solid transport: Rheological behavior of dense suspension
[DE91-009428] N91-26467

SOLIDS FLOW
Determination of flow-regime boundaries for cohesive particles
[DE91-010552] N91-26468

SOLITARY WAVES
Low frequency noise in resonant Josephson soliton oscillators
[DE91-011911] N91-26464

SOLUBILITY
Water solubility of bis(2-ethylhexyl) hydrogen phosphite
[AD-A234561] N91-26259
Novel liquid crystalline polymers as nonlinear optical materials
[AD-A235371] N91-26373
Additives for high temperature liquid lubricants
[DE91-011018] N91-26386

SOLUTIONS
The weighted uni-dimensional similarities problem with least absolute value metric is NP-Hard
[AD-A235060] N91-26849

SOLVATION
Raman spectroscopy study of solvation structure in acetonitrile/water mixtures
[AD-A234921] N91-26271

SOLVENTS
Structure of alkylated silica surfaces: Quenching of fluorescence from covalently bound pyrene
[AD-A234642] N91-26207
Raman spectroscopy study of solvation structure in acetonitrile/water mixtures
[AD-A234921] N91-26271
High pulse-energy flashlamp-pumpable laser dyes
[AD-A233837] N91-26499

SONAR
A boundary scattering strength extraction algorithm for the analysis of long-range reverberation data
[AD-A233721] N91-26877

SOOT
Computer modeling of soot formation comparing free radical and ionic mechanisms
[AD-A235007] N91-26273

SORBENTS
Flexural plate wave devices for chemical analysis
[AD-A234129] N91-26254

SORPTION
Method of obtaining phenol-furfural resins
[AD-A233746] N91-26327

SOUND FIELDS
Acoustic radiation from fluid-loaded, ribbed cylindrical shells excited by different types of concentrated mechanical drives
[AD-A235324] N91-26887

SOUND PRESSURE
Combined effect of noise and vibration on cells of auditory and vestibular apparatus N91-26707

SOUND WAVES
Reflection of incident pressure waves by ribbed panels
[AD-A233671] N91-26469
Improved algorithms for transient and steady-state fluid-structure interaction
[AD-A235172] N91-26476
Inverse scattering problems for acoustic waves in an inhomogeneous medium N91-26876
Computation of broadband mixing noise from turbomachinery
[AD-A233991] N91-26878
Boundary layer transition noise art
[AD-A235093] N91-26884
Acoustic radiation from fluid-loaded, ribbed cylindrical shells excited by different types of concentrated mechanical drives
[AD-A235324] N91-26887
Multiple-frequency SAW devices for chemical sensing and materials characterization
[DE91-010856] N91-26888
Bulk wave characterization of high T(sub c) superconductors
[AD-A234649] N91-26954

SOUNDING
Terrestrial geophysics in the SeaRISE project N91-26576
Atmospheric InfraRed Sounder (AIRS): Science and measurement requirements
[NASA-TM-104977] N91-26624
The SYNOP experiment: Inverted echo sounder data report for June 1989 to September 1990
[AD-A234825] N91-26662

SOUNDING ROCKETS
Sounding rocket flight data summary
[AD-A233656] N91-26626

SOVIET SPACECRAFT
JPRS report: Science and technology. USSR: Space
[JPRS-USP-91-002] N91-26162

SOYUZ SPACECRAFT
Survey of the principal results of medical research in the flight program of the second main expedition aboard the Mir orbiting complex N91-26686

SPACE ADAPTATION SYNDROME
Review of primary medical results of year-long flight on Mir station N91-26178
State-of-the-art automated evaluation of functional state of the body in the space program and preventive medicine N91-26687

SPACE BASED RADAR
A test vector generator for a radar signal processor
[AD-A233725] N91-26413

SPACE BASES
Engineering knowledge requirements for sand and dust on Mars N91-27067

SPACE CHARGE
High power klystron amplifier
[AD-D014862] N91-26448

SPACE COMMERCIALIZATION
Air Force stock fund: Hydrazine sales consistent with the Commercial Space Launch Act. Report to the Chairman, Committee on Science, Space and Technology, House of Representatives
[GAO/NSIAD-91-196] N91-26397
Commercial use of space: Many grantees making progress, but NASA oversight could be improved. Report to the Chair, Subcommittee on VA, HUD, and Independent Agencies, Committee on Appropriations, U.S. Senate
[GAO/NSIAD-91-142] N91-26400
National Aeronautics and Space Administration Multiyear Authorization Act of 1991 N91-27046

SPACE COMMUNICATION
Wideband heterodyne spatial tracking for optical space communications
[AD-A233722] N91-26410

SPACE DEBRIS
The effects of space debris on solar propulsion
[AD-A235257] N91-26192

SPACE ENVIRONMENT SIMULATION
Long-term prediction test procedure for most ICs, based on linear response theory
[NASA-CR-185843] N91-26462

SPACE EXPLORATION
Commercial use of space: Many grantees making progress, but NASA oversight could be improved. Report to the Chair, Subcommittee on VA, HUD, and Independent Agencies, Committee on Appropriations, U.S. Senate
[GAO/NSIAD-91-142] N91-26400
National Aeronautics and Space Administration Multiyear Authorization Act of 1991 N91-27046
Report of the 90-day study on human exploration of the Moon and Mars
[NASA-TM-102999] N91-27055
Chemistry and mineralogy of Martian dust: An explorer's primer N91-27063

NASA/ASEE Summer Faculty Fellowship Program, 1990, volume 2
[NASA-CR-185637-VOL-2] N91-27103
Developing a taxonomy for mission architecture definition N91-27108
SPACE FLIGHT STRESS
JPRS Report: Science and technology. USSR: Life sciences
[JPRS-ULS-91-009] N91-26688
SPACE HABITATS
Illuminance and luminance distributions of a prototype ambient illumination system for Space Station Freedom
[NASA-TM-103541] N91-26193
Structural concept studies for a horizontal cylindrical lunar habitat and a lunar guyed tower N91-27117
SPACE MECHANICS
Weak interactions and presupernova evolution
[DE91-011543] N91-27052
SPACE MISSIONS
Planetary spacecraft cost modeling utilizing labor estimating relationships N91-27116
SPACE PERCEPTION
Format and basic geometry of a perspective display of air traffic for the cockpit
[NASA-TM-86680] N91-26142
Induced pictorial representations
[AD-A234548] N91-26735
Review of audition literature: Selection of acoustic signals for use in the synthesis of auditory space
[AD-A234579] N91-26881
SPACE PLATFORMS
Space platform power system hardware testbed
[NASA-CR-185839] N91-26204
Theoretical and experimental studies relevant to interpretation of auroral emissions
[NASA-CR-188491] N91-26637
SPACE POWER REACTORS
A reliability and mass perspective of SP-100 Stirling cycle lunar-base powerplant designs
[NASA-TM-103736] N91-26592
SPACE PROBES
Study of the properties of the autonomous optical navigation of a space probe in a rendezvous with an asteroid N91-26169
SPACE PROGRAMS
Experimental techniques in the field of low density aerodynamics
[AGARD-AG-318(E)] N91-26124
SPACE SHUTTLE BOOSTERS
Follow-on cable coupling lightning test. Volume 2: Appendixes A, B, C, and D
[NASA-CR-184124] N91-26195
SPACE SHUTTLE MAIN ENGINE
Development of life prediction capabilities for liquid propellant rocket engines. Post-fire diagnostic system for the SSME system architecture study
[NASA-CR-187112] N91-26205
Dynamics of face and annular seals with two-phase flow
[NASA-CR-4256] N91-26479
SPACE SHUTTLES
Bidirectional reflectance distribution (BRDF) of NASA shuttle tiles
[AD-A235115] N91-26188
Follow-on cable coupling lightning test. Volume 2: Appendixes A, B, C, and D
[NASA-CR-184124] N91-26195
National Aeronautics and Space Administration Multiyear Authorization Act of 1991 N91-27046
NASA/ASEE Summer Faculty Fellowship Program, 1990, Volume 1
[NASA-CR-185637-VOL-1] N91-27088
Compound estimation procedures in reliability N91-27090
Mechanics, impact loads and EMG on the space shuttle treadmill N91-27112
SPACE STATION POWER SUPPLIES
Development and testing of a source subsystem for the supporting development PMAD DC test bed
[NASA-TM-104510] N91-26202
SPACE STATIONS
Illuminance and luminance distributions of a prototype ambient illumination system for Space Station Freedom
[NASA-TM-103541] N91-26193
Development and testing of a source subsystem for the supporting development PMAD DC test bed
[NASA-TM-104510] N91-26202
Report of the 90-day study on human exploration of the Moon and Mars
[NASA-TM-102999] N91-27055
NASA/ASEE Summer Faculty Fellowship Program, 1990, Volume 1
[NASA-CR-185637-VOL-1] N91-27088
Compound estimation procedures in reliability N91-27090
Applications of formal simulation languages in the control and monitoring subsystems of Space Station Freedom N91-27100
NASA/ASEE Summer Faculty Fellowship Program, 1990, volume 2
[NASA-CR-185637-VOL-2] N91-27103
A design for an intelligent monitor and controller for space station electrical power using parallel distributed problem solving N91-27105
High accuracy optical rate sensor N91-27115
SPACE SUITS
Impact of Mars sand on dust on the design of space suits and life support equipment: A technology assessment N91-27079
SPACE WEAPONS
Space doctrine
[AD-A234971] N91-26866
SPACEBORNE EXPERIMENTS
Oscillations of a small-mass satellite probe caused by aerodynamic and gravitational forces N91-26165
Survey of the principal results of medical research in the flight program of the second main expedition aboard the Mir orbiting complex N91-26686
SPACECRAFT CABIN ATMOSPHERES
An Air Revitalization Model (ARM) for Regenerative Life Support Systems (RLSS) N91-27093
SPACECRAFT CONTAMINATION
Theoretical and experimental studies relevant to interpretation of auroral emissions
[NASA-CR-188491] N91-26637
SPACECRAFT CONTROL
H-infinity-optimal control for distributed parameter systems
[AD-A234931] N91-26833
A design for an intelligent monitor and controller for space station electrical power using parallel distributed problem solving N91-27105
SPACECRAFT DESIGN
ALS liquid hydrogen turbopump: Advanced Development Program
[NASA-CR-183730] N91-26196
SPACECRAFT EQUIPMENT
Calculation of the pointing accuracy of spacecraft equipment using autonomous measurements of the angular position of the object of investigation N91-26167
SPACECRAFT LAUNCHING
Incorporation of shuttle CCT parameters in computer simulation models N91-27096
SPACECRAFT MODELS
H-infinity-optimal control for distributed parameter systems
[AD-A234931] N91-26833
SPACECRAFT POWER SUPPLIES
Space platform power system hardware testbed
[NASA-CR-185839] N91-26204
High-power converters for space applications
[NASA-CR-187116] N91-26461
Effects of Martian dust on power system components N91-27061
A design for an intelligent monitor and controller for space station electrical power using parallel distributed problem solving N91-27105
SPACECRAFT PROPULSION
ALS liquid hydrogen turbopump: Advanced Development Program
[NASA-CR-183730] N91-26196
Parametric studies of dense plasma focus for fusion space propulsion with D-He3
[AD-A234578] N91-26941
SPACECRAFT REENTRY
Experimental techniques in the field of low density aerodynamics
[AGARD-AG-318(E)] N91-26124
SPACECRAFT RELIABILITY
Compound estimation procedures in reliability N91-27090
SPACECRAFT STRUCTURES
Studies in modeling, dynamics, and control of space structures
[AD-A235059] N91-26190
SPACECREWS
Illuminance and luminance distributions of a prototype ambient illumination system for Space Station Freedom
[NASA-TM-103541] N91-26193
SPATIAL DISTRIBUTION
Relationships between PAN and ozone at sites in eastern North America
[DE91-011728] N91-26607
Process study of sorted patterns on Arctic soils
[AD-A234089] N91-26628
Improved Point Analysis Model (IPAM) (users guide)
[AD-A235305] N91-26649
Categories and particulars: Prototype effects in estimating spatial location
[AD-A234955] N91-26741
SPATIAL FILTERING
The wavenumber-frequency filtering characteristics of compliant layers
[AD-A234768] N91-26561
SPECIFICATIONS
Survey of current aircraft engine conditions
[AD-A235143] N91-26144
Atmospheric InfraRed Sounder (AIRS): Science and measurement requirements
[NASA-TM-104977] N91-26624
Structured representation for requirements and specifications
[NASA-CR-187522] N91-26797
SPECKLE PATTERNS
One-dimensional translation measurement of speckle from rough rotating objects in ultraviolet illumination
[AD-A233719] N91-26919
SPECTRA
Data acquisition and processing N91-26618
Gravity waves and instabilities in the lower and middle atmosphere N91-26621
SPECTRAL BANDS
Characteristics of aerosol in the atmosphere of Mars according to data from the KRFM experiment N91-26175
SPECTRAL CORRELATION
Spectral and correlation analysis with applications to middle-atmosphere radars N91-26619
SPECTRAL METHODS
Spectral recovery of discontinuous data
[ITN-91-85115] N91-26853
SPECTRAL RESOLUTION
Atmospheric InfraRed Sounder (AIRS): Science and measurement requirements
[NASA-TM-104977] N91-26624
SPECTRAL THEORY
Boundary layer parameterization for a global spectral model
[AD-A235310] N91-26635
SPECTROGRAMS
Northeast Artificial Intelligence Consortium (NAIC). Volume 8: Artificial intelligence applications to speech recognition
[AD-A234887] N91-26822
SPECTROMETERS
Derivation of mid-infrared (5-25 microns) optical constants of some silicates and palagonite N91-27077
SPECTROSCOPY
Photoexcitation spectroscopy of pernigraniline
[AD-A233841] N91-26250
Tetra neopentoxy phthalo cyanine Langmuir-Blodgett films: Spectroscopy at the air/water interface
[AD-A234603] N91-26261
Chemistry of fluorine in the oxidation of silicon
[AD-A234959] N91-26272
Spectroscopy and photoexcitation spectroscopies of polyaniline: A model system for new phenomena
[AD-A234215] N91-26340
Polymer characterization using singlet oxygen phosphorescence as a spectroscopic probe
[DE91-011735] N91-26382
In-situ monitoring of laser ablation of superconductors
[DE91-012057] N91-26524
Fluorescence spectroscopy of excitation transfer in Photosystem 1
[DE91-011867] N91-26681
SPECTRUM ANALYSIS
Synthesis and properties of rigid-rod benzobisazole polymers containing benzothiazole pendent groups
[AD-A234742] N91-26357
Multispectral identification of potentially hazardous byproducts of ozonation and chlorination. Part 1: Studies of chromatographic and spectroscopic properties of MX
[PB91-161703] N91-26601
Data acquisition and processing N91-26618
Spectral and correlation analysis with applications to middle-atmosphere radars N91-26619
Solar-geophysical data number 556, December 1990. Part 1: (Prompt reports). Data for November, October 1990, and late data
[PB91-152140] N91-27083
SPEECH
A physiologically motivated front end for speech recognition
[AD-A233727] N91-26414
Northeast Artificial Intelligence Consortium (NAIC). Volume 13: Image understanding and intelligent parallel systems
[AD-A234897] N91-26832
SPEECH RECOGNITION
A physiologically motivated front end for speech recognition
[AD-A233727] N91-26414
Uncertainty handling at speech/natural language interface, volume 1
[AD-A234310] N91-26422

Intelligibility of digital speech masked by noise: Normal hearing and hearing impaired listeners
[AD-A234852] N91-26427
Using genetic algorithms to select and create features for pattern classification
[AD-A235165] N91-26792
A comparative study of the practical characteristics of neural network and conventional pattern classifiers
[AD-A235345] N91-26795
Northeast Artificial Intelligence Consortium (NAIC). Volume 8: Artificial intelligence applications to speech recognition
[AD-A234887] N91-26822

SPEED REGULATORS
Advanced material handling equipment controls
[AD-A235091] N91-26540

SPHERES
Ricochet of sphere off water
[ITN-91-85102] N91-26480

SPRAYED COATINGS
An analytical methodology to predict the coating characteristics of plasma-sprayed ceramic powders
[DE91-010088] N91-26326

SPRAYING
Mechanical properties of spray atomized SiC particle reinforced aluminum-titanium alloys
[AD-A235231] N91-26306

SPREAD SPECTRUM TRANSMISSION
Spread spectrum communication networks
[AD-A233696] N91-26409
Adaptive spread spectrum networks
[AD-A234084] N91-26419
Spread spectrum communications emulator design
[AD-A235403] N91-26430

SPUTTERING
Fiber coating by sputtering for high temperature composites
[AD-A234994] N91-26226
Magnetron sputter deposition of boron and boron carbide
[DE91-011194] N91-26241

SQUEEZE FILMS
Improved modeling and performance of squeeze film damper bearings
[AD-A233694] N91-26531

SQUID (DETECTORS)
Low frequency noise in resonant Josephson soliton oscillators
[DE91-011911] N91-26464
High-T(sub c) thin-film magnetometer
[DE91-011828] N91-26981

STABILITY
Analysis of necessary and sufficient conditions for the equilibrium stability of a gyrostatic satellite N91-26166
Theory and experimental and chemical instabilities
[AD-A234916] N91-26270
Research on stable, high-efficiency amorphous silicon multijunction modules
[DE91-002159] N91-26591
Gravity waves and instabilities in the lower and middle atmosphere N91-26621

STABILIZATION
Stabilization and control problems in structural dynamics
[AD-A235189] N91-26567

STABLE OSCILLATIONS
Theoretical studies of the kinematics, dynamics, stability, and control of unsteady/vortical flows
[AD-A235190] N91-26477
Nonlinear oscillations of mechanical systems under multifrequency parametric excitation
[AD-A233800] N91-26558

STACKING FAULT ENERGY
Fundamentals of mechanical behavior in intermetallic compounds
[AD-A235016] N91-26301

STANDARDIZATION
What fuels our future?
[AD-A233674] N91-26387
Proceedings of the Object-Oriented Database Task Group Workshop
[PB91-157198] N91-27000

STANDARDS
IRIG standard format for Global Positioning System (GPS) data for post-operation interrange exchange
[AD-A234932] N91-26127
A test of the IAEA code of practice for absorbed dose determination in photon and electron beams
[OEFZS-4565] N91-26913
National Bureau of Standards Publications 1977-1987. Volume 2: Indexes
[PB91-136515] N91-26997
Evaluating the effect of accuracy ratios on the percent of calibrations which are out of tolerance N91-27107

STANDING WAVES
An experimental and numerical study of wavemaker dissipation in the process of direct generation of the resonant sloshing waves in a rectangular tank
[ITN-91-85103] N91-26481

STAR TRACKERS
Calculation of the pointing accuracy of spacecraft equipment using autonomous measurements of the angular position of the object of investigation N91-26167
High accuracy optical rate sensor N91-27115

STATIC TESTS
Technical Evaluation Motor No. 7 (TEM-7)
[NASA-CR-184163] N91-26203
Investigation of axial positioning for flexural compressors
[NASA-CR-185711] N91-26544

STATICS
Flexural plate wave devices for chemical analysis
[AD-A234129] N91-26254
Symbolic expressions of composite grid structures
[AD-A233794] N91-26836

STATISTICAL ANALYSIS
Manual on the flight of flexible aircraft in turbulence
[AGARD-AG-317] N91-26150
An analytical methodology to predict the coating characteristics of plasma-sprayed ceramic powders
[DE91-010088] N91-26326
Forecasting digital microcircuit obsolescence
[AD-A234573] N91-26451
Advanced study in solid transport: Rheological behavior of dense suspension
[DE91-009428] N91-26467
Statistical aspects of reliability, maintainability, and availability
[AD-A234546] N91-26546
Lead detection and mapping with reference to relationships between scale, sensor characteristics, surface conditions and atmospheric properties
[AD-A235121] N91-26666
A statistical analysis of -X rhesus head kinematics
[AD-A233977] N91-26674
Statistical analysis of stochastic gradient based algorithms
[AD-A234545] N91-26859
Comparison change analysis
[AD-A233690] N91-26873
Compound estimation procedures in reliability N91-27090

STATISTICAL DISTRIBUTIONS
Fixed sample and sequential problems with applications in reliability
[AD-A234547] N91-26547
Statistical properties of intrinsic topological noise in tokamaks
[DE91-011741] N91-26939

STATISTICAL TESTS
Quality effectiveness sensing technique release 3.0
[AD-A233651] N91-26545
Quality by design using statistically planned experiments
[ITN-91-85119] N91-26553

STATOR BLADES
Investigation of hot streak migration and film cooling effects on the heat transfer in rotor/stator interacting flows
[AD-A235420] N91-26145

STEADY STATE
Improved algorithms for transient and steady-state fluid-structure interaction
[AD-A235172] N91-26476
Coherent beam-beam effects
[DE91-012512] N91-26917

STEELS
Microalloyed steel preforms
[AD-A234039] N91-26296
Investigations into fracture mechanics failure concepts with thermomechanically rolled steels
[BLL-OA-TRANS-4238-(6196.3)] N91-26556
Preliminary test results from the HSST shallow-crack fracture toughness program
[DE91-010147] N91-26572
The 1990 Sandia rocket-triggered lightning field tests at Kennedy Space Center, Florida
[DE91-011263] N91-26653

STEERABLE ANTENNAS
Plasma reflectors for electronic beam steering in radar systems
[AD-A234560] N91-26425

STEERING
A look at digital nose wheel steering
[AD-A233944] N91-26131
Vehicle steering device
[AD-D014861] N91-26537

STELLAR EVOLUTION
Weak interactions and presupernova evolution
[DE91-011543] N91-27052

STELLAR LUMINOSITY
The light curve of the magnetic star AM - Herculis
[ITN-91-85108] N91-27049

STELLARATORS
Design and fabrication of forced-flow coils as an R/D program for large helical device
[NIFS-81] N91-26937

STEREOCHEMISTRY
Regio- and stereochemical control in substitution reactions of cyclophosphazenes
[AD-A234376] N91-26257

STIFFNESS
Effect of a viscoelastic interface on the transverse behavior of fiber-reinforced composites
[AD-A233986] N91-26212

STIRLING CYCLE
A reliability and mass perspective of SP-100 Stirling cycle lunar-base powerplant designs
[NASA-TM-103736] N91-26592

STIRLING ENGINES
Comparative survey of dynamic analyses of free-piston Stirling engines
[NASA-TM-104491] N91-26870

STOCHASTIC PROCESSES
Chaotic and bifurcating nonlinear systems driven by noise with applications to laser dynamics
[AD-A234841] N91-26512
Continuous stochastic cellular automata that have a stationary distribution and no detailed balance
[AD-A234421] N91-26782
Large-scale stochastic linear programs: Importance sampling and Benders decomposition
[AD-A234962] N91-26789
Nonlinear stochastic optimization solution procedures and incomplete information
[AD-A235242] N91-26793
Maximization on matroids with random weights
[AD-A233978] N91-26858
Statistical analysis of stochastic gradient based algorithms
[AD-A234545] N91-26859
Research in stochastic processes
[AD-A234650] N91-26860
Singular and bang-bang stochastic control
[AD-A234752] N91-26861
Comparison change analysis
[AD-A233690] N91-26873

STOICHIOMETRY
Isotropic exchange in the platinum-catalyzed reduction of olefins in protic solvents
[AD-A234828] N91-26208
Effect of molecular weight on polyphenylquinoxaline properties
[NASA-TM-104100] N91-26377

STORAGE RINGS (PARTICLE ACCELERATORS)
Photons and neutrons
[DE91-010980] N91-26906
Vacuum design for a superconducting mini-collider
[DE91-011964] N91-26975

STORMS
Dynamics of equatorial and polar boundaries of penetration of solar protons with energy about 1 MeV into magnetosphere during strong magnetic storm N91-26172
In the energy active region of the ocean N91-26583
ARTIST tape output formats
[AD-A235173] N91-26633
Advanced Microwave Precipitation Radiometer (AMPR) for remote observation of precipitation
[NASA-CR-184165] N91-26655
A catalog of high resolution Jovian decametric radio noise burst spectra, volume 1 N91-27047

STRAIN RATE
Fragmentation of brittle materials at high rates of loading N91-26237
Strain enhanced microstructural evolution
[DE91-011921] N91-26318
Analytical solution of plane Poiseuille flow of a Johnson-Segalman fluid
[AD-A234313] N91-26472

STRATEGY
Strategies for reliable and real time execution on a heterogeneous multiprocessor
[AD-A234114] N91-26801
Space doctrine
[AD-A234971] N91-26866

STRATIFICATION
Martian dust threshold measurements: Simulations under heated surface conditions N91-27081

STRATOSPHERE
Middle Atmosphere Program. Handbook for MAP. Volume 30: International School on Atmospheric Radar
[NASA-CR-188623] N91-26613

Data acquisition and processing N91-26618
Target parameter estimation N91-26620
Applications of MST radars: Meteorological applications N91-26622

STRESS (PHYSIOLOGY)
Visual accommodation in cosmonauts N91-26697

STRESS (PSYCHOLOGY)
Physical and psychogenic sequelae of impact acceleration on tracking performance of operators N91-26701
Proceedings of the 7th User's Stress Workshop [AD-A234583] N91-26736

STRESS ANALYSIS
Development of an integrated aeroservoelastic analysis program and correlation with test data [NASA-TP-3120] N91-26113
On the finite-strain-invariant failure criterion for composites [AD-A234493] N91-26223
Advanced study in solid transport: Rheological behavior of dense suspension [DE91-009428] N91-26467
Load-bearing capacity of large pipes with circumferential defects under tensile stress: Comparison of experiments with calculated estimates [BLL-OA-TRANS-4233-(6196.3)] N91-26557

STRESS CYCLES
NATO advanced research workshop on Measurement of Residual and Applied Stress Using Neutron Diffraction [AD-A235103] N91-26566

STRESS DISTRIBUTION
Development and verification of global/local analysis techniques for laminated composites [NASA-CR-185060] N91-26238

STRESS MEASUREMENT
Non-destructive evaluation of residual stresses in thin films via x ray diffraction topography methods [AD-A235328] N91-26552
The development of piezoelectric poly(vinylidene fluoride) sensors for measuring peel stresses in adhesive joints [AD-A233880] N91-26559
NATO advanced research workshop on Measurement of Residual and Applied Stress Using Neutron Diffraction [AD-A235103] N91-26566

STRESS RELAXATION
Effect of a viscoelastic interface on the transverse behavior of fiber-reinforced composites [AD-A233986] N91-26212
Residual stresses in metal/ceramic brazes: Effect of creep on finite element analysis results [DE91-011233] N91-26570

STRESS-STRAIN RELATIONSHIPS
Polymeric routes to silicon carbide and silicon oxycarbide CMC [NASA-TM-104372] N91-26234
Analytical solution of plane Poiseuille flow of a Johnson-Segalman fluid [AD-A234313] N91-26472
The hysteresis and incremental collapse of complex structures: A paradigm for the fatigue failure of materials [AD-A234831] N91-26563

STRESSES
Effect of a viscoelastic interface on the transverse behavior of fiber-reinforced composites [AD-A233986] N91-26212
Development of a test system and experimental method for in-plane biaxial compressive deformation and failure of fiber composite materials [AD-A234062] N91-26214
Fundamentals of mechanical behavior in intermetallic compounds [AD-A235016] N91-26301
Adaptation and resistance of ecosystems to stress [AD-A234576] N91-26603

STRING THEORY
Supersymmetry breaking from superstrings and the gauge hierarchy [DE91-011899] N91-26992

STROKE VOLUME
Changes in rheologic indices of blood and hemodynamics during 14-day antiorthostatic hypokinesia N91-26692
Diagnostic utility of continuous noninvasive blood pressure monitoring (Penaz method) in gravity-induced blood redistribution N91-26705

STRUCTURAL ANALYSIS
Development and verification of global/local analysis techniques for laminated composites [NASA-CR-185060] N91-26238
High temperature superconducting planar circuit structures for high frequency applications [AD-A234335] N91-26445
Comparisons of backscattering from cylindrical shells described by thin shell and elasticity theories [AD-A234745] N91-26475
Improved algorithms for transient and steady-state fluid-structure interaction [AD-A235172] N91-26476

STRUCTURAL BASINS
Inorganic carbon surveys of oceanic basins [DE91-011132] N91-26667

STRUCTURAL DESIGN
Unmanned aerial vehicles. Medium range system components do not fit [AD-A234131] N91-26132
Gust design procedures N91-26155
LaRC-ITPI/arylene ether copolymers [NASA-TM-104099] N91-26378
Analysis of knowledge-based expert systems as tools for construction design [AD-A234473] N91-26404
Synchronous demodulator [NASA-CASE-GSC-13179-1] N91-26438
Passive and active grasping with a prehensile robot end-effector [AD-A235085] N91-26539
NDE pattern recognition of LSS states via wave propagation [AD-A234772] N91-26549
Vacuum design for a superconducting mini-collider [DE91-011964] N91-26975
Structural concept studies for a horizontal cylindrical lunar habitat and a lunar guyed tower N91-27117

STRUCTURAL ENGINEERING
Directional characteristics of waves in shallow water [AD-A234568] N91-26661

STRUCTURAL MEMBERS
High power klystron amplifier [AD-D014862] N91-26448

STRUCTURAL VIBRATION
Nonlinear dynamics and control of flexible structures [AD-A235186] N91-26191
Improved algorithms for transient and steady-state fluid-structure interaction [AD-A235172] N91-26476
The relationship of traditional damping measures for materials with high damping capacity [AD-A235347] N91-26568

STUDENTS
On measures of misconception stability [AD-A234952] N91-26847

SUBMERGING
COLDEX-86: Physical work capacity during prolonged cold water immersion at 6.1 msw [AD-A233767] N91-26710

SUBMILLIMETER WAVES
Study of Josephson effect arrays as sources at 1 THz [AD-A234526] N91-26952

SUBSTITUTES
Carboxyalkylated hemoglobin as a potential blood substitute [AD-A233822] N91-26712
Evaluation of liposome-encapsulated Hemoglobin/LR16 formulation as a potential blood substitute [AD-A233973] N91-26714
Studies of mutant hemoglobins to define types of modifications useful in the design of blood substitutes [AD-A234997] N91-26723

SUBSTRATES
Integration of neurobiological and computational analyses of the neural network essentials for conditioned taste aversion [AD-A235164] N91-26744

SUBSTRUCTURES
A nonrecursive order N preconditioned conjugate gradient: Range space formulation of MDOF dynamics N91-27099

SUDDEN IONOSPHERIC DISTURBANCES
Solar geophysical data number 551, July 1990. Part 1: (Prompt reports). Data for June, May 1990 and late data [PB91-160713] N91-27085

SULFIDES
Ring-torsional polarons in polyaniline and polyparaphenylene sulfide [AD-A234384] N91-26345

SULFONATES
Interaction of cationic polypeptides with electroactive polypyrrole/poly(styrenesulfonate) and poly(N-methylpyrrole)/poly(styrenesulfonate) films [AD-A234469] N91-26258
Method of obtaining phenol-furfural resins [AD-A233746] N91-26327
Carboxyalkylated hemoglobin as a potential blood substitute [AD-A233822] N91-26712

SULFUR
The chemistry of sodium with sulfur in flames [DE91-002060] N91-26288

SULFUR DIOXIDES
Improvement in the capacity and safety of lithium/inorganic electrolyte sulfur dioxide rechargeable cells, phase 2 [AD-A235303] N91-26589

SUMMARIES
Sounding rocket flight data summary [AD-A233656] N91-26626

SUN
Solar-geophysical data number 556, December 1990. Part 2: (Comprehensive reports). Data for June 1990 and miscellaneous [PB91-152157] N91-27084
Solar-geophysical data number 551, July 1990. Part 2: (Comprehensive reports). Data for January 1990 and miscellaneous [PB91-160721] N91-27086

SUPERCOMPUTERS
Large scale computing in the Energy Research Programs [DE91-012128] N91-26805

SUPERCONDUCTING FILMS
In-situ monitoring of laser ablation of superconductors [DE91-012057] N91-26524
Superconducting high T(sub c) thin film vortex-flow transistor, phase 1 [AD-A235025] N91-26962
High temperature superconducting films and crystals [AD-A235234] N91-26965

SUPERCONDUCTIVITY
International collaboration program on innovative chemical processing of superior electronic and optical materials [AD-A235030] N91-26276
Electrochemically modulated superconductivity [AD-A234703] N91-26955
High temperature superconducting films and crystals [AD-A235234] N91-26965
Vacuum design for a superconducting mini-collider [DE91-011964] N91-26975
Microwave properties of high transition temperature superconducting thin films [NASA-CR-185842] N91-26976
Quantum limited quasiparticle mixers at 100 GHz [DE91-011826] N91-26991

SUPERCONDUCTORS
International collaboration program on innovative chemical processing of superior electronic and optical materials [AD-A235030] N91-26276
Design and fabrication of forced-flow coils as an R/D program for large helical device [NIFS-81] N91-26937
Study of Josephson effect arrays as sources at 1 THz [AD-A234526] N91-26952
Vacuum design for a superconducting mini-collider [DE91-011964] N91-26975
Magnetic relaxation, flux pinning and, critical currents in superconductors [DE91-012022] N91-26984

SUPERCRITICAL FLUIDS
Supercritical fluid processing of propellant polymers [AD-A234285] N91-26341

SUPERHIGH FREQUENCIES
Four-to-one power combiner for 20 GHz phased array antenna using RADC MMIC phase shifters N91-26435
Submicron gate InP power MISFET's with improved output power density at 18 and 20 GHz N91-26436

SUPERNOVAE
Preliminary estimates of core-collapse supernova rates from the Berkeley automated supernova search [DE91-011824] N91-27050
The Berkeley/Anglo-Australian Observatory high-redshift supernova search [DE91-012348] N91-27051
Weak interactions and presupernova evolution [DE91-011543] N91-27052

SUPERSATURATION
Crystal growth in a microgravity environment [NASA-CASE-MFS-28473-1] N91-26968

SUPERSONIC COMBUSTION RAMJET ENGINES
Navier-Stokes calculations of scramjet-nozzle-afterbody flowfields [NASA-CR-185356] N91-26488

SUPERSONIC FLOW
Pressure distribution and induced force field on a conical nozzle due to impingement of a normal jet into the supersonic cross-flow [AD-A233981] N91-26115
The effects of compressibility on a supersonic mixing layer [AD-A234992] N91-26119
Liquid cooled supersonic total temperature probe [NASA-CASE-LAR-14435-1-CU] N91-26159

SUPERSONIC SPEED
Aerodynamics of a 0.60 caliber electromagnetic projectile
[AD-A234660] N91-26116
SUPERSYMMETRY
Supersymmetry breaking from superstrings and the gauge hierarchy
[DE91-011899] N91-26992
SUPPORT SYSTEMS
Space support for airland battle-future
[AD-A233868] N91-26864
SURFACE ACOUSTIC WAVE DEVICES
Flexural plate wave devices for chemical analysis
[AD-A234129] N91-26254
Multiple-frequency SAW devices for chemical sensing and materials characterization
[DE91-010856] N91-26888
SURFACE COOLING
Investigation of hot streak migration and film cooling effects on the heat transfer in rotor/stator interacting flows
[AD-A235420] N91-26145
SURFACE DIFFUSION
Surface diffusion at the liquid-solid interface: Quenching of fluorescence from pyrene covalently bound to methylated silica
[AD-A234645] N91-26268
SURFACE DISTORTION
Turbulent premixed hydrogen/air flames
[AD-A235109] N91-26278
SURFACE LAYERS
The aeolian wind tunnel N91-27065
Reflectance spectroscopy of palagonite and iron-rich montmorillonite clay mixtures: Implications for the surface composition of Mars N91-27075
SURFACE PROPERTIES
Surface characterization of electrically conducting nickel tetrathiooxalate/poly(vinyl alcohol) composites
[AD-A234598] N91-26353
Scanning tunnelling microscope for boron surface studies
[AD-A234716] N91-26452
Sea test development of laser altimeter
[AD-A233824] N91-26498
Lead detection and mapping with reference to relationships between scale, sensor characteristics, surface conditions and atmospheric properties
[AD-A235121] N91-26666
Underwater scattering of sound
[AD-A235097] N91-26885
Chemistry on an atomic scale of ion-beam modified surfaces
[AD-A233707] N91-26891
Ab initio molecular dynamics simulations of surfaces and interfaces
[AD-A235315] N91-26901
Microwave properties of high transition temperature superconducting thin films
[NASA-CR-185842] N91-26976
The chemistry and mineralogy of Mars soil and dust N91-27058
The distribution of particulate material on Mars N91-27059
SURFACE REACTIONS
Desorption product yields following Cl2 adsorption on Si(111)7x7: Coverage and temperature dependence
[AD-A234635] N91-26264
A combined XPS-ISS modulated molecular beam investigation of the reactions of oxygen and fluorine with silicon surfaces
[AD-A234867] N91-26269
Surface chemistry of silicon: The behavior of dangling bonds
[AD-A235011] N91-26275
Surface Chemkin (version 3.7): A FORTRAN package for analyzing heterogeneous chemical kinetics at a solid-surface-gas-phase interface
[DE91-010840] N91-26285
SURFACE ROUGHNESS
Backscattering enhancement from rough surfaces
[AD-A234707] N91-26426
Surface etching and roughening in integrated processing of thermal oxides
[AD-A234960] N91-26456
Optical methods of measuring the roughness of the surfaces of high precision steel balls
[AD-A234796] N91-26928
Radar-aeolian roughness project
[NASA-CR-4378] N91-27056
The distribution of particulate material on Mars N91-27059
The aeolian wind tunnel N91-27065
SURFACE ROUGHNESS EFFECTS
Backscattering enhancement from rough surfaces
[AD-A234707] N91-26426
SURFACE TEMPERATURE
The stepwise dissociation of NH3 on the Si(111)-(7x7) surface: Low temperature dissociative adsorption and thermal effects
[AD-A235009] N91-26274
Thermal and albedo mapping of the north and south polar regions of Mars N91-27076
SURFACE TO AIR MISSILES
The wild weasel development programs, one run, one hit, one error
[RAND-P-7661-RGS] N91-26431
SURFACE VEHICLES
Lubricants at low temperatures
[AD-A234536] N91-26348
Adaptive control of direct drive dexterous robotic hand with bilateral tactile sensing
[AD-A233980] N91-26532
SURFACE WAVES
Analysis of wave characteristics in extreme seas
[AD-A234538] N91-26660
SURVEILLANCE
Northeast Artificial Intelligence Consortium (NAIC). Volume 16: Intelligent signal processing techniques for multi-sensor surveillance systems
[AD-A234895] N91-26830
SURVEILLANCE RADAR
System concept and analysis of an Artificial Ionospheric Mirror (AIM) radar
[AD-A234289] N91-26630
SURVEYS
Survey of current aircraft engine conditions
[AD-A235143] N91-26144
Advanced Satellite Research Project: SCAR Research Database. Bibliographic analysis
[NASA-CR-186086] N91-26182
Inorganic carbon surveys of oceanic basins
[DE91-011132] N91-26667
Parallel processing and expert systems
[NASA-TM-103886] N91-26796
Extending matchings in graphs: A survey
[AD-A234392] N91-26841
Comparative survey of dynamic analyses of free-piston Stirling engines
[NASA-TM-104491] N91-26870
SURVIVAL
Metabolic changes and hemodynamic dysfunction following hypothermic shock
[AD-A233942] N91-26713
SWIRLING
A study of high speed flows in an aircraft transition duct
[NASA-TM-104449] N91-26122
SWITCHES
Synchronous demodulator
[NASA-CASE-GSC-13179-1] N91-26438
SWITCHING
Quantum devices and structures
[AD-A235298] N91-26989
SWITCHING CIRCUITS
Laser switched power linac
[AD-A234581] N91-26507
Monolithic integration semiconductor and superconductor components
[AD-A234986] N91-26959
SYMBOLS
The effects of display failures and symbol rotation on visual search and recognition performance
[AD-A235035] N91-26743
Symbolic expressions of composite grid structures
[AD-A233794] N91-26836
The effect of rotation on legibility of dot-matrix characters
[AD-A235034] N91-27008
SYMMETRY
Visual sensitivities and discriminations and their role in aviation
[AD-A234866] N91-26740
A theoretical and experimental study of the symmetric rank one update
[AD-A233965] N91-26777
SYMPATHETIC NERVOUS SYSTEM
Effect of shift work of air traffic controllers on sympathetic nervous system N91-26700
SYNCHRONISM
Backplane bus distributed realtime clock synchronization
[AD-A234476] N91-26491
Magnetostrictive angular positioning motor
[AD-D014858] N91-26536
Waiting algorithms for synchronization in large-scale multiprocessors
[AD-A234985] N91-26764
SYNCHROTRON RADIATION
Photons and neutrons
[DE91-010980] N91-26906
SYNCHROTRONS
Photons and neutrons
[DE91-010980] N91-26906
SYNCOPE
Risk factors and prediction of syncopic states in flyers N91-26685
Diagnostic utility of continuous noninvasive blood pressure monitoring (Penaz method) in gravity-induced blood redistribution N91-26705
SYNOPTIC METEOROLOGY
A numerical study of blocking N91-26640
SYNTHESIS (CHEMISTRY)
Gordon Research Conference on Composites
[AD-A233778] N91-26210
New developments in the synthesis and doping of polyacetylene and polyaniline
[AD-A233702] N91-26244
Polyaniline: Synthesis and properties of pernigraniline
[AD-A233706] N91-26245
The reduction by deuterium on platinum black of exo-2-norbornyl and endo-2-norbornyl to norbornane-2-d occurs with predominant retention of configuration
[AD-A235057] N91-26277
Electrocatalytic study of ammonia synthesis and methane dimerization in high temperature solid electrolyte cells
[DE91-009797] N91-26289
The synthesis of methanol by a novel method
[DE91-011131] N91-26291
Synthesis, polymerization and thermal properties of a new acetylene-terminated Schiff base
[AD-A233806] N91-26328
Polyaniline: Pernigraniline, an isolable intermediate in the conventional chemical synthesis of emeraldine
[AD-A233840] N91-26330
Synthesis and structure of small-molecule cyclic phosphazenes bearing ortho-substituted aryloxy and phenoxy substituents
[AD-A234377] N91-26344
Chemical synthesis study of deuterated epoxy resins
[AD-A234666] N91-26355
Synthesis of energetic single phase and multi-phase polymers
[AD-A235104] N91-26363
Template synthesis of polymeric and metal microtubules
[AD-A235307] N91-26367
Catalysts and initiators as instruments controlling structure of polymers with inorganic backbone
[AD-A235350] N91-26368
Polysilanes, synthesis, modification, and properties
[AD-A235351] N91-26369
Preparation of a novel gallium arsenide single-source precursor having the empirical formula AsCl3Ga2
[AD-A233704] N91-26949
SYNTHETIC METALS
Synthetic metals: A novel role for organic polymers
[AD-A233862] N91-26334
SYSTEM EFFECTIVENESS
Measurement expert system effectiveness
[AD-A234359] N91-26807
SYSTEMS ANALYSIS
Comparative survey of dynamic analyses of free-piston Stirling engines
[NASA-TM-104491] N91-26870
SYSTEMS ENGINEERING
The wild weasel development programs, one run, one hit, one error
[RAND-P-7661-RGS] N91-26431
Precision high-power solid-state laser diagnostics for target-irradiation studies and target-plane irradiation modeling
[DE91-012036] N91-26523
Variable speed gas engine-driven air compressor system. Phase 1: System analysis
[PB91-159533] N91-26530
Results of the aeronautical systems division critical process team on integrated product development
[AD-A235419] N91-26995
NSI engineering review N91-27013
SYSTEMS INTEGRATION
Ada software portability and level 2 system simulator integration issues
[AD-A233757] N91-26773
The NASA Science Internet: An integrated approach to networking N91-27041
NSI directed to continue SPAN's functions N91-27042
Integrating UNIX workstation into existing online data acquisition systems for Fermilab experiments
[DE91-011974] N91-27044

T

TABLES (DATA)
Sounding rocket flight data summary
[AD-A233656] N91-26626
Primes: The first 2400 prime numbers
[AD-A233979] N91-26837
Solar-geophysical data number 556, December 1990. Part 2: (Comprehensive reports). Data for June 1990 and miscellaneous
[PB91-152157] N91-27084
Solar geophysical data number 551, July 1990. Part 1: (Prompt reports). Data for June, May 1990 and late data
[PB91-160713] N91-27085

TACTICS
Space support for airland battle-future
[AD-A233868] N91-26864

TANK GEOMETRY
An experimental and numerical study of wavemaker dissipation in the process of direct generation of the resonant sloshing waves in a rectangular tank
[ITN-91-85103] N91-26481

TANTALUM COMPOUNDS
Quantum limited quasiparticle mixers at 100 GHz
[DE91-011894] N91-26973

TARGET RECOGNITION
Theory of radar target discrimination
[AD-A234172] N91-26420
Evaluation of night vision goggles for maritime search and rescue
[AD-A233798] N91-26751
Gabor transforms and neural networks for automatic target recognition
[DE91-011919] N91-26834
Boost-phase kill versus midcourse discrimination: The grand inquisitor's solution
[DE91-011744] N91-26871
Automatic target recognition using acousto-optic image correlator
[DE91-011499] N91-26936

TARGETS
The effect of rotation on legibility of dot-matrix characters
[AD-A235034] N91-27008

TASKS
Effect of shift work of air traffic controllers on sympathetic nervous system N91-26700
Expert system explanation: The user perspective
[AD-A233739] N91-26749
Generic tasks for knowledge-based problem solving: Extension and new directions
[AD-A234925] N91-26865

TASTE
Integration of neurobiological and computational analyses of the neural network essentials for conditioned taste aversion
[AD-A235164] N91-26744

TAYLOR INSTABILITY
Planar indirect-drive Rayleigh-Taylor experiments on Nova
[DE91-011967] N91-26943

TAYLOR SERIES
Application of a conjugate gradient method to the synthesis of phase-only planar arrays
[AD-A233756] N91-26415

TEA LASERS
Array-typed, sealed-off mini tea CO2 laser
[AD-A234804] N91-26511

TECHNOLOGIES
JPRS report: Science and technology. USSR: Space
[JPRS-USP-91-002] N91-26162
JPRS report: Science and technology. USSR: Earth sciences
[JPRS-UES-91-002] N91-26581
JPRS report: Science and technology. USSR: Earth sciences
[JPRS-UES-91-003] N91-26582
JPRS report: Science and technology. USSR: Life sciences
[JPRS-ULS-91-010] N91-26683
JPRS Report: Science and technology. USSR: Life sciences
[JPRS-ULS-91-009] N91-26688
JPRS report: Science and technology. USSR: Life sciences
[JPRS-ULS-91-011] N91-26696

TECHNOLOGY ASSESSMENT
Electromagnetic launch technology assessment. Scientific basis and unified treatment: Forces and electromechanical power conversion (analytical and numerical methods)
[AD-A235028] N91-26185
Weather satellites: Action needed to resolve status of the US Geostationary Satellite Program. Report to the Chairman, Committee on Science, Space, and Technology, House of Representatives
[GAO/NSIAD-91-252] N91-26194
Commercializing solar hydrogen production
[DE91-011232] N91-26398
MMIC integration technology investigation
[NASA-CR-188035] N91-26434
Basic studies of microstructure of combusting turbulent flows
[AD-A234222] N91-26471
Photovoltaics: From the laboratory to the marketplace
[DE91-002151] N91-26588
An assessment of CO2 greenhouse gas mitigation technologies
[DE91-011972] N91-26805
Impact of Mars sand on dust on the design of space suits and life support equipment: A technology assessment N91-27079

TECHNOLOGY TRANSFER
Ceramic technology for advanced heat engines project
[DE91-010451] N91-26384

TECHNOLOGY UTILIZATION
Nonlinear dynamics and control of flexible structures
[AD-A235186] N91-26191
Opportunities for advanced speech processing in military computer-based systems
[AD-A233724] N91-26412
High-power converters for space applications
[NASA-CR-187116] N91-26461

TECTONICS
Plate motion and deformation
[DE91-010466] N91-26612

TELECOMMUNICATION
Architectures for a high performance distributed operating system
[AD-A235333] N91-26429
Spread spectrum communications emulator design
[AD-A235403] N91-26430
A divide and conquer approach to the nonsymmetric eigenvalue problem
[DE91-011085] N91-26854
Space support for airland battle-future
[AD-A233868] N91-26864

TELEMETRY
Ocean acoustic tomography and telemetry
[AD-A233826] N91-26659

TELEOPERATORS
Adaptive control of direct drive dexterous robotic hand with bilateral tactile sensing
[AD-A233980] N91-26532

TEMPERATURE COMPENSATION
Metabolic changes and hemodynamic dysfunction following hypothermic shock
[AD-A233942] N91-26713

TEMPERATURE DEPENDENCE
Desorption product yields following Cl2 adsorption on Si(111)7x7: Coverage and temperature dependence
[AD-A234635] N91-26264
Plasticity of single crystalline Al3X intermetallic compounds
[AD-A234699] N91-26356
Fluorescence spectroscopy of excitation transfer in Photosystem 1
[DE91-011867] N91-26681
A temperature dependent SPICE macro-model for power MOSFETs
[DE91-011737] N91-26972

TEMPERATURE DISTRIBUTION
Reexamination of METMAN, recommendations on enhancement of LCVG, and development of new concepts for EMU heat sink N91-27098

TEMPERATURE EFFECTS
Investigation into the effect of heat treatment on the thermal conductivity of 3-D carbon/carbon fiber composites
[DE91-010388] N91-26240
The stepwise dissociation of NH3 on the Si(111)-(7x7) surface: Low temperature dissociative adsorption and thermal effects
[AD-A235009] N91-26274
Strain enhanced microstructural evolution
[DE91-011921] N91-26318
Chemical synthesis study of deuterated epoxy resins
[AD-A234666] N91-26355
Development of advanced methods based on stable isotope technology for studies of exercise in heat
[AD-A234670] N91-26719
Effect of a passive cooling vest on tension/anxiety and fatigue in a high heat and high humidity naval environment
[AD-A234657] N91-26755
Development of high Tc (greater than 110K) Bi, Tl and Y-based materials as superconducting circuit elements
[NASA-CR-188581] N91-26948
Efficient photoinduced charge separation and storage in the solid state, rates, energetics, and spin-polarization
[DE91-010727] N91-26980

TEMPERATURE GRADIENTS
Current distribution modeling for novel alumina electrolysis
[DE91-010060] N91-26315

TEMPERATURE MEASUREMENT
LIF and emission studies of copper and nitrogen N91-27089

TEMPERATURE PROBES
Liquid cooled supersonic total temperature probe
[NASA-CASE-LAR-14435-1-CU] N91-26159

TEMPERATURE PROFILES
Recent studies of the optical properties of dust and cloud particles in the Mars atmosphere and the interannual frequency of global dust storms N91-27060

TEMPERING
Microalloyed steel preforms
[AD-A234039] N91-26296

TENSILE DEFORMATION
Cyclic deformation, damage, and effects of environment in the Ni3Al ordered alloy at elevated temperature
[AD-A235168] N91-26304

TENSILE PROPERTIES
Performance of a 22Cr-20Ni-18Co-Fe alloy for service to 870 C
[DE91-011366] N91-26317

TENSILE STRENGTH
Microalloyed steel preforms
[AD-A234039] N91-26296

TENSILE STRESS
Load-bearing capacity of large pipes with circumferential defects under tensile stress: Comparison of experiments with calculated estimates
[BLL-OA-TRANS-4233-(6196.3)] N91-26557

TENSILE TESTS
Damage accumulation in advanced metal matrix composites under thermal cycling
[AD-A235002] N91-26227
Load-bearing capacity of large pipes with circumferential defects under tensile stress: Comparison of experiments with calculated estimates
[BLL-OA-TRANS-4233-(6196.3)] N91-26557

TENSORS
A software package for unconstrained optimization using tensor methods
[AD-A233989] N91-26778
Method and apparatus for second-rank tensor generation
[NASA-CASE-NPO-17512-1-CU] N91-26918

TERMINAL BALLISTICS
The effect of sabot wheelbase and position on the launch dynamics of fin-stabilized kinetic energy ammunition
[AD-A234945] N91-26118
Reaction processing of ceramic particulate and whisker composites
[AD-A234951] N91-26225
Mechanical properties of polycarbonate-polysulfone and polycarbonate-polyetherimide blends
[AD-A234939] N91-26360
Long-rod penetration of confined ceramic tiles
[AD-A234312] N91-26534

TERRAIN
How low can an unmanned air vehicle fly?
[RAND-P-7680-RGS] N91-26138

TEST EQUIPMENT
A basic guide to overlay design using nondestructive testing equipment data
[AD-A234472] N91-26403
A test vector generator for a radar signal processor
[AD-A233725] N91-26413

TEST FACILITIES
RADC cathode life test facility
[AD-A234309] N91-26444

TEST FIRING
Technical Evaluation Motor No. 7 (TEM-7)
[NASA-CR-184163] N91-26203
Development of life prediction capabilities for liquid propellant rocket engines. Post-fire diagnostic system for the SSME system architecture study
[NASA-CR-187112] N91-26205

TEST RANGES
Surface observation climatic summaries for Tonopah test range, Nevada
[AD-A235228] N91-26648

TESTS
On measures of misconception stability
[AD-A234952] N91-26847

TETHERED SATELLITES
Oscillations of a small-mass satellite probe caused by aerodynamic and gravitational forces N91-26165

TETHERING
Oscillations of a small-mass satellite probe caused by aerodynamic and gravitational forces N91-26165
THALLIUM COMPOUNDS
Development of high Tc (greater than 110K) Bi, Tl and Y-based materials as superconducting circuit elements [NASA-CR-188581] N91-26948
THEMATIC MAPPERS (LANDSAT)
Application of thematic mapper images to determine regional evaporation from the playas in the western desert of Egypt [REPT-31] N91-26585
THEOREM PROVING
Deductive programming synthesis [AD-A233770] N91-26774
The weighted uni-dimensional similarities problem with least absolute value metric is NP-Hard [AD-A235060] N91-26849
Comparison change analysis [AD-A233690] N91-26873
THEORETICAL PHYSICS
Field work and dispersion relations of excitations on fractals [AD-A234953] N91-26455
THERMAL ABSORPTION
Absorption heat pump in heating and cooling systems of buildings [DE91-752988] N91-26593
THERMAL ANALYSIS
Comparison of hydrogen desorption kinetics from Si(111)7x7 and Si(100)2x1 [AD-A234633] N91-26262
Thermal transitions and mechanical properties of the films of chemically prepared polyaniline [AD-A233807] N91-26329
Computational model for optimizing longitudinal fin heat transfer in laminar internal flows [DE91-005070] N91-26485
Formation of intermediate compounds during reduced pressure calcination of Y-Ba-Cu-O precursor [DE91-011179] N91-26971
The distribution of particulate material on Mars N91-27059
THERMAL CONDUCTIVITY
Testing of a composite thermal structure to insulate the drivers of a large scale blast/thermal simulator [AD-A234014] N91-26213
Investigation into the effect of heat treatment on the thermal conductivity of 3-D carbon/carbon fiber composites [DE91-010388] N91-26240
THERMAL CONTROL COATINGS
Method of preparing a thermal barrier coating [NASA-CASE-LEW-14999-2] N91-26376
THERMAL CYCLING TESTS
Damage accumulation in advanced metal matrix composites under thermal cycling [AD-A235002] N91-26227
Performance of a 22Cr-20Ni-18Co-Fe alloy for service to 870 C [DE91-011366] N91-26317
THERMAL DEGRADATION
Thermal degradation chemistry of poly(diphenoxy phosphazene) [AD-A235284] N91-26282
Synthesis and properties of rigid-rod benzobisazole polymers containing benzothiazole pendent groups [AD-A234742] N91-26357
THERMAL DIFFUSION
Microstructure development during microwave annealing of dense silicon nitride [DE91-012069] N91-26242
Crystal growth in a microgravity environment [NASA-CASE-MFS-28473-1] N91-26968
THERMAL EMISSION
CBSD version 2 component models of the IR celestial background [AD-A235372] N91-27048
Derivation of mid-infrared (5-25 microns) optical constants of some silicates and palagonite N91-27077
THERMAL ENVIRONMENTS
Adsorption and thermal behavior of ethylene on Si(100)-(2x1) [AD-A234098] N91-26252
THERMAL EXPANSION
Residual stresses in metal/ceramic brazes: Effect of creep on finite element analysis results [DE91-011233] N91-26570
THERMAL MAPPING
The effects of atmospheric dust on observations of Martian surface albedo N91-27072
Thermal and albedo mapping of the north and south polar regions of Mars N91-27076
THERMAL PLASMAS
Desorption product yields following Cl2 adsorption on Si(111)7x7: Coverage and temperature dependence [AD-A234635] N91-26264
An analytical methodology to predict the coating characteristics of plasma-sprayed ceramic powders [DE91-010088] N91-26326
THERMAL PROTECTION
Liquid film cooling in rocket engines [AD-A234288] N91-26197
India-stabilized zirconia coating for composites [AD-D014857] N91-26224
COLDEX-86: Summary of the experimental protocol and general results [AD-A234031] N91-26715
THERMAL RADIATION
Testing of a composite thermal structure to insulate the drivers of a large scale blast/thermal simulator [AD-A234014] N91-26213
India-stabilized zirconia coating for composites [AD-D014857] N91-26224
THERMAL STABILITY
The stepwise dissociation of NH3 on the Si(111)-(7x7) surface: Low temperature dissociative adsorption and thermal effects [AD-A235009] N91-26274
Thermal stabilities of polyanilines [AD-A233849] N91-26333
Chemical synthesis study of deuterated epoxy resins [AD-A234666] N91-26355
THERMOCHEMISTRY
Adsorption and decomposition of acetylene on Si(100)-(2x1) [AD-A233808] N91-26248
Ceramic fiber coating development and demonstration [AD-A234773] N91-26358
Surface etching and roughening in integrated processing of thermal oxides [AD-A234960] N91-26456
THERMOCLINES
The SYNOP experiment: Inverted echo sounder data report for June 1989 to September 1990 [AD-A234625] N91-26662
THERMOCOUPLES
Liquid cooled supersonic total temperature probe [NASA-CASE-LAR-14435-1-CU] N91-26159
THERMODYNAMIC CYCLES
Engine cycle analysis for a particle bed reactor nuclear rocket [AD-A235258] N91-26199
MHD contractors' review meeting [DE91-011295] N91-26945
THERMODYNAMIC PROPERTIES
Damage accumulation in advanced metal matrix composites under thermal cycling [AD-A235002] N91-26227
Adsorption and thermal behavior of ethylene on Si(100)-(2x1) [AD-A234098] N91-26252
The stepwise dissociation of NH3 on the Si(111)-(7x7) surface: Low temperature dissociative adsorption and thermal effects [AD-A235009] N91-26274
Thermal degradation chemistry of poly(diphenoxy phosphazene) [AD-A235284] N91-26282
Transport processes and interfacial phenomena in an evaporating meniscus [DE91-005561] N91-26284
Synthesis, polymerization and thermal properties of a new acetylene-terminated Schiff base [AD-A233806] N91-26328
Scaling CW electron beam pumped rare gas lasers to ultra-high average power [AD-A235120] N91-26513
NATO advanced research workshop on Measurement of Residual and Applied Stress Using Neutron Diffraction [AD-A235103] N91-26566
OSIRRUS: Oceanic symbolic image representation, recognition and understanding software [AD-A235112] N91-26665
THERMODYNAMICS
Modification of the user friendly thermodynamic code to include the effects of minor species [AD-A233929] N91-26390
THERMOELASTICITY
Thermoelastic wave propagation in laminated composites N91-26209
THERMOLUMINESCENCE
Thermoluminescence kinetics of pyrite (FeS2) [DE91-011710] N91-26990
THERMOMECHANICAL TREATMENT
The cryogenic mechanical properties of Vintage 3 Al-Li-Zr alloy 2090-T81 [DE91-011897] N91-26311
THERMOPLASTIC RESINS
Characterization studies of fluorinated epoxy resins: Naval experimental resin C8/1SA as a structural material and for use in blends and composites [AD-A234188] N91-26338
THERMOREGULATION
Pharmacological correction of functional condition of Army Air Force flyers in hot climate with asparkam N91-26684
COLDEX-86: Summary of the experimental protocol and general results [AD-A234031] N91-26715
THERMOSPHERE
Development of a Vector Spherical Harmonic (VSH) model of the neutral thermosphere [AD-A234744] N91-26631
Theoretical and experimental studies relevant to interpretation of auroral emissions [NASA-CR-188491] N91-26637
THICK PLATES
Hypervelocity launch capabilities to over 10.4 km/s [DE91-010859] N91-26186
Nonlinear behavior of fiber composite materials and its effect on the postbuckling response of laminated plates [AD-A234203] N91-26218
THICKNESS
A model for wet filament winding of composite cylinders with arbitrary thickness [AD-A234102] N91-26215
Flexural plate wave devices for chemical analysis [AD-A234129] N91-26254
Effect of initial delamination on Mode 1 and Mode 2 interlaminar fracture toughness and fatigue fracture threshold [NASA-TM-104079] N91-26569
Thickness measurements of silicon films using partial coherence interferometry [AD-A235211] N91-26930
Ohmic contacts to semiconducting diamond [AD-A234130] N91-26950
THIN FILMS
Investigation of polybenzocyclobutene resins in multilayer thin films for electronic packaging [AD-A235223] N91-26228
Adsorption and thermal behavior of ethylene on Si(100)-(2x1) [AD-A234098] N91-26252
Metastable pitting corrosion of aluminum, Al-Cu, and Al-Si thin films in dilute HF solutions and its relevancy to the processing of integrated circuit interconnections [DE91-012014] N91-26320
Thermal transitions and mechanical properties of the films of chemically prepared polyaniline [AD-A233807] N91-26329
A program in the chemistry of electronic materials. Task 1: New organometallic precursors for the low pressure chemical vapor deposition of refractory materials for electronics [AD-A234315] N91-26342
Cluster beam deposition of high temperature materials [AD-A234358] N91-26343
Electronic and ionic transport in processable conducting polymers [AD-A234597] N91-26352
Methods of obtaining an electrical contact [AD-A234800] N91-26453
Diagnostic studies of YBa2Cu3O(7-delta) laser ablation [DE91-011382] N91-26515
Radio frequency and microwave plasma for optical thin film deposition [DE91-012081] N91-26525
Non-destructive evaluation of residual stresses in thin films via x ray diffraction topography methods [AD-A235328] N91-26552
The wavenumber-frequency filtering characteristics of compliant layers [AD-A234768] N91-26561
Photovoltaics: From the laboratory to the marketplace [DE91-002151] N91-26588
Multiple-frequency SAW devices for chemical sensing and materials characterization [DE91-010856] N91-26888
Transmission electron microscopy of the CVD diamond film/substrate interface [AD-A234790] N91-26956
Symposium E: Properties of 2-6 semiconductors. Bulk crystals, epitaxial films, quantum well structures [AD-A234835] N91-26957
High temperature superconducting films and crystals [AD-A235234] N91-26965
Process for the controlled growth of single-crystal films of silicon carbide polytypes on silicon carbide wafers [NASA-CASE-LEW-15222-1] N91-26966

Microwave properties of high transition temperature superconducting thin films
[NASA-CR-185842] N91-26976
High-T(sub c) thin-film magnetometer
[DE91-011828] N91-26981
Thin film alloys on semiconductor substrates
[DE91-012355] N91-26985
HREM study of heteroepitaxial interfaces in the TiO2/Al2O3 system
[DE91-012473] N91-26986

THIN PLATES
Buckling of laminated composite plates
[ITN-91-85101] N91-26232

THIN WALLED SHELLS
Comparisons of backscattering from cylindrical shells described by thin shell and elasticity theories
[AD-A234745] N91-26475

THREE BODY PROBLEM
Spatial rotations of a satellite in a circular three-body problem for the case of general resonance N91-26164

THREE DIMENSIONAL BODIES
Proceedings of the First Workshop on 3-D Optical Memories
[AD-A234732] N91-27003

THREE DIMENSIONAL COMPOSITES
Investigation into the effect of heat treatment on the thermal conductivity of 3-D carbon/carbon fiber composites
[DE91-010388] N91-26240

THREE DIMENSIONAL FLOW
Numerical investigations in three-dimensional internal flows
[NASA-CR-188615] N91-26114
Viscous flow simulations of internal store carriage and separation
[NASA-CR-185343] N91-26123
Methods to enhance the accuracy of finite volume schemes 2
[FFA-147] N91-26466
Direct and large-eddy simulations of three-dimensional compressible Navier-Stokes turbulence
[AD-A233717] N91-26470

THREE DIMENSIONAL MODELS
Development and verification of global/local analysis techniques for laminated composites
[NASA-CR-185060] N91-26238
Development and verification of a physical cloud-moisture model for use in general circulation models
[AD-A234751] N91-26643

THRUST CHAMBERS
Method of injecting fluid propellants into a rocket combustion chamber
[NASA-CASE-LEW-14846-2] N91-26200

THULIUM
Energy levels and branching ratios of Tm(3)+ in ten garnet laser materials
[AD-A235274] N91-26514

THYROID GLAND
Functional activity of hypophyseal-thyroid system during 370-day antiorthostatic hypokinesia N91-26691

TILES
Bidirectional reflectance distribution (BRDF) of NASA shuttle tiles
[AD-A235115] N91-26188
Long-rod penetration of confined ceramic tiles
[AD-A234312] N91-26534

TILT ROTOR AIRCRAFT
Civil tiltrotor missions and applications. Phase 2: The commercial passenger market
[NASA-CR-177576] N91-26126

TIME DEPENDENCE
Development and verification of a physical cloud-moisture model for use in general circulation models
[AD-A234751] N91-26643
A system and language environment for scientific computing
[AD-A233747] N91-26772
Adaptive component methods for time dependent PDE's
[AD-A233776] N91-26775

TIME MEASUREMENT
Using mappings to prove timing properties
[AD-A234404] N91-26780

TIME SERIES ANALYSIS
Spectral and correlation analysis with applications to middle-atmosphere radars N91-26619
Analysis of wave characteristics in extreme seas
[AD-A234538] N91-26660
The SYNOP experiment: Inverted echo sounder data report for June 1989 to September 1990
[AD-A234625] N91-26662

TISSUES (BIOLOGY)
Wound healing by cultured skin cells and growth factors
[AD-A235300] N91-26730

TITANIUM
Materials/microstructures characterization
[AD-A233751] N91-26295
Chemistry on an atomic scale of ion-beam modified surfaces
[AD-A233707] N91-26891

TITANIUM ALLOYS
Titanium alloy integrated centrifugal impeller 5 coordinate computer assisted manufacturing technology
[AD-A234797] N91-26300
Fundamentals of mechanical behavior in intermetallic compounds
[AD-A235016] N91-26301
Mechanical properties of spray atomized SiC particle reinforced aluminum-titanium alloys
[AD-A235231] N91-26306
Environmental embrittlement of ordered intermetallic alloys at room temperature in moist atmospheres
[DE91-012051] N91-26321
Oxidation resistant coatings for titanium alloys and titanium alloy matrix composites
[NASA-CASE-LEW-15155-1] N91-26375

TITANIUM OXIDES
HREM study of heteroepitaxial interfaces in the TiO2/Al2O3 system
[DE91-012473] N91-26986

TOBACCO
Airliner cabin environment: Contaminant measurements, health risks, and mitigation options
[PB91-159384] N91-26746

TOILETS
Method and apparatus for waste collection and storage
[NASA-CASE-MSC-21025-3] N91-26747

TOKAMAK DEVICES
Comparison of dimensionally similar discharges with similar heat deposition discharges
[DE91-011740] N91-26938
Statistical properties of intrinsic topological noise in tokamaks
[DE91-011741] N91-26939

TOLERANCES (PHYSIOLOGY)
Effectiveness of ice-vest cooling in prolonging work tolerance time during heavy exercise in the heat for personnel wearing Canadian forces chemical defence ensembles
[AD-A235273] N91-26758

TOMOGRAPHY
The analysis of a rocket tomography measurement of the N2+3914A emission and N2 ionization rates in an auroral arc
[NASA-CR-188622] N91-26596
Ocean acoustic tomography and telemetry
[AD-A233826] N91-26659

TOPOGRAPHY
Results of morphometric analysis of the Tesserae surface of Venus according to Venera-15 and -16 data N91-26176
Have graben wall scarps accumulated sand and dust on Mars? N91-27062
The aeolian wind tunnel N91-27065

TOPOLOGY
Space platform power system hardware testbed
[NASA-CR-185839] N91-26204
A nonrecursive order N preconditioned conjugate gradient: Range space formulation of MDOF dynamics N91-27099

TOROIDAL DISCHARGE
Statistical properties of intrinsic topological noise in tokamaks
[DE91-011741] N91-26939

TOROIDAL PLASMAS
Statistical properties of intrinsic topological noise in tokamaks
[DE91-011741] N91-26939

TORPEDOES
Vertical incidence backscatter and surface forward scattering from near-surface bubbles
[AD-A234432] N91-26880

TORQUE MOTORS
Magnetostrictive angular positioning motor
[AD-D014858] N91-26536

TORSION
Dynamics of elastic bending and torsion of hingeless rotors with dynamic stall
[AD-A234775] N91-26134
Ring-torsional polarons in polyaniline and polyparaphenylene sulfide
[AD-A234384] N91-26345

TOTAL OZONE MAPPING SPECTROMETER
Nimbus-7 TOMS Antarctic ozone atlas: August - December 1990
[NASA-RP-1264] N91-26651

TOUGHNESS
Microalloyed steel preforms
[AD-A234039] N91-26296
Strength and microstructure of ceramics
[AD-A235424] N91-26374

TOWERS
Structural concept studies for a horizontal cylindrical lunar habitat and a lunar guyed tower N91-27117

TOXIC HAZARDS
Ecological exposure and effects of airborne toxic chemicals: An overview
[PB91-148460] N91-26594

TOXICITY
Regeneration of whetlerite for adsorbing toxic pollutants from air
[AD-D014859] N91-26753

TOXICITY AND SAFETY HAZARD
Ecological exposure and effects of airborne toxic chemicals: An overview
[PB91-148460] N91-26594

TRACE ELEMENTS
The chemistry and mineralogy of Mars soil and dust N91-27058
Solutions to problems of weathering in Antarctic eucrites N91-27113

TRACKING (POSITION)
Calculation of the pointing accuracy of spacecraft equipment using autonomous measurements of the angular position of the object of investigation N91-26167

TRACKING FILTERS
TRACE trajectory analysis and orbit determination program. Volume 13: Square root information filtering and smoothing
[AD-A234957] N91-26183

TRAINING ANALYSIS
A Rome Laboratory guide to basic training in TQM analysis techniques
[AD-A233855] N91-26993

TRAINING DEVICES
Training effectiveness of an intelligent tutoring system for a propulsion console trainer N91-27097

TRAINING EVALUATION
A Rome Laboratory guide to basic training in TQM analysis techniques
[AD-A233855] N91-26993

TRAJECTORIES
Spatial rotations of a satellite in a circular three-body problem for the case of general resonance N91-26164

TRAJECTORY ANALYSIS
The effect of sabot wheelbase and position on the launch dynamics of fin-stabilized kinetic energy ammunition
[AD-A234945] N91-26118
TRACE trajectory analysis and orbit determination program. Volume 13: Square root information filtering and smoothing
[AD-A234957] N91-26183

TRAJECTORY OPTIMIZATION
Apparatus for guiding a missile
[AD-D014866] N91-26147
Evolution of some types of Earth satellite orbits N91-26163
Constrained trajectory optimization for kinematically redundant arms
[NASA-CR-183477] N91-26527

TRANQUILIZERS
Attention span, anxiety, and benzodiazepine receptors
[AD-A234549] N91-26716

TRANSDUCERS
Evaluation of environmentally aged polymer/composite material by ultrasonic inspection
[AD-A235343] N91-26231
The wavenumber-frequency filtering characteristics of compliant layers
[AD-A234768] N91-26561

TRANSFER ORBITS
The effects of space debris on solar propulsion
[AD-A235257] N91-26192

TRANSFORMATIONS (MATHEMATICS)
Iterated transform image compression
[AD-A233655] N91-26769
Gabor transforms and neural networks for automatic target recognition
[DE91-011919] N91-26834

TRANSFORMERS
High-T(sub c) thin-film magnetometer
[DE91-011828] N91-26981

TRANSISTOR CIRCUITS
Monolithic integration semiconductor and superconductor components
[AD-A234986] N91-26959

Superconducting high T(sub c) thin film vortex-flow transistor, phase 1
[AD-A235025] N91-26962

TRANSISTORS
Superconducting high T(sub c) thin film vortex-flow transistor, phase 1
[AD-A235025] N91-26962

TRANSITION FLOW
Hydroacoustics of intermittent boundary-layer flow: A review
[AD-A235092] N91-26883

TRANSITION METALS
Partial oxidation of light alkanes in transition-metal ion containing zeolites
[DE91-008202] N91-26243
Study of intermediates from transition metal excited-state electron-transfer reactions
[DE91-012182] N91-26324

TRANSITION TEMPERATURE
Microwave properties of high transition temperature superconducting thin films
[NASA-CR-185842] N91-26976
Defects in decomposed YBa2Cu4O8 (124) superconductor after rapid annealing
[DE91-010597] N91-26979

TRANSLATIONAL MOTION
One-dimensional translation measurement of speckle from rough rotating objects in ultraviolet illumination
[AD-A233719] N91-26919

TRANSMISSION
The instrumental principles of MST radars and incoherent scatter radars and the configuration of radar system hardware N91-26616

TRANSMISSION LINES
High temperature superconducting planar circuit structures for high frequency applications
[AD-A234335] N91-26445

TRANSMISSION LOSS
The wavenumber-frequency filtering characteristics of compliant layers
[AD-A234768] N91-26561

TRANSMISSIONS (MACHINE ELEMENTS)
Magnetic field generator
[AD-D014869] N91-26449

TRANSMITTANCE
FTIR studies of water and ammonia decomposition on silicon surfaces
[AD-A234637] N91-26265

TRANSMITTERS
The instrumental principles of MST radars and incoherent scatter radars and the configuration of radar system hardware N91-26616

TRANSONIC FLOW
Methods to enhance the accuracy of finite volume schemes 2
[FFA-147] N91-26466

TRANSPARENCE
High performance transparency design
[AD-A234456] N91-26133

TRANSPIRATION
Transpiration cooled ultraviolet sol-gel silica optics
[AD-A235426] N91-26934

TRANSPORT PROPERTIES
Gel solidified microinterface between two immiscible electrolytes applied to amperometric detection of picrate and tetramethylammonium
[AD-A235260] N91-26280
Transport processes and interfacial phenomena in an evaporating meniscus
[DE91-005561] N91-26284
Ionically and electronically conductive composite polymer membranes
[AD-A234587] N91-26349
Electronic and ionic transport in processable conducting polymers
[AD-A234597] N91-26352
Transport and fate of acetone in an outdoor model stream, Stennis Space Center near Bay St. Louis, Mississippi
[PB91-154674] N91-26600
Simulation of precipitation scavenging in a three-dimensional global model
[DE91-011531] N91-26606

TRANSPORTATION NETWORKS
Civil tiltrotor missions and applications. Phase 2: The commercial passenger market
[NASA-CR-177576] N91-26126

TREADMILLS
Physiological and perceptual responses to load carrying in female subjects using internal and external frame backpacks
[AD-A234941] N91-26722
Mechanics, impact loads and EMG on the space shuttle treadmill N91-27112

TRENDS
Trends in certification procedures and design analysis N91-26158

TRIBOLOGY
A tribological investigation of the graphite-to-diamond-like behavior of amorphous carbon films ion-beam-deposited on ceramic substrates
[DE91-010816] N91-26379

TRINITROTOLUENE
Molecular mechanics calculations for nitro and amino substituted conjugated systems containing oxygen and nitrogen
[AD-A233928] N91-26389

TROPICAL METEOROLOGY
An overview of tropical circulation
[AD-A234984] N91-26645

TROPICAL REGIONS
An overview of tropical circulation
[AD-A234984] N91-26645
The tropical Pacific Ocean's heat budget during a cold event, from a numerical model N91-26657

TROPOSPHERE
Middle Atmosphere Program. Handbook for MAP. Volume 30: International School on Atmospheric Radar
[NASA-CR-188623] N91-26613
The instrumental principles of MST radars and incoherent scatter radars and the configuration of radar system hardware N91-26616
Statistical characteristics of MST radar echoes and its interpretation N91-26617
Data acquisition and processing N91-26618
Applications of MST radars: Meteorological applications N91-26622

TUNABLE LASERS
Elementary reaction rate measurements at high temperatures by tunable-laser flash-absorption
[DE91-011850] N91-26516
Tunable excimer lasers
[DE91-011399] N91-26522
Development of a subpicosecond, tunable LiCAF (Cr:LiCaAlF6) laser
[DE91-012082] N91-26526

TUNGSTEN
Chemistry on an atomic scale of ion-beam modified surfaces
[AD-A233707] N91-26891

TUNGSTEN ALLOYS
Lifetimes and failure mechanisms of W/Re hairpin filaments
[AD-A235199] N91-26305

TUNING
Tunable excimer lasers
[DE91-011399] N91-26522
Aircraft interior noise reduction by alternate resonance tuning
[NASA-CR-185453] N91-26889

TURBINE BLADES
Investigation of hot streak migration and film cooling effects on the heat transfer in rotor/stator interacting flows
[AD-A235420] N91-26145

TURBINE PUMPS
ALS liquid hydrogen turbopump: Advanced Development Program
[NASA-CR-183730] N91-26196

TURBOCOMPRESSORS
Investigation of axial positioning for flexural compressors
[NASA-CR-185711] N91-26544

TURBOMACHINERY
Improved modeling and performance of squeeze film damper bearings
[AD-A233694] N91-26531
Computation of broadband mixing noise from turbomachinery
[AD-A233991] N91-26878

TURBULENCE
Viscous flow simulations of internal store carriage and separation
[NASA-CR-185343] N91-26123
Improved reduction of gust loads data for gust intensity N91-26153
Gust design procedures N91-26155
Turbulent processes of mass-loading of new ions on Venus and Mars and the problems of numerical models of the interaction of solar wind with these planets. 1: Characteristics of the flow of solar wind around the planets N91-26174
Direct and large-eddy simulations of three-dimensional compressible Navier-Stokes turbulence
[AD-A233717] N91-26470
Dynamics of face and annular seals with two-phase flow
[NASA-CR-4256] N91-26479
JPRS report: Science and technology. USSR: Earth sciences
[JPRS-UES-91-003] N91-26582
Effect of turbulence on impurity observation in upper atmosphere using lidar method N91-26584
Target parameter estimation N91-26620
Incoherent scatter radar observations of the ionosphere N91-26623

TURBULENCE MODELS
The kinematics of turbulent boundary layer structure
[NASA-TM-103859] N91-26465

TURBULENT BOUNDARY LAYER
The kinematics of turbulent boundary layer structure
[NASA-TM-103859] N91-26465
The delay of turbulent boundary layer separation by oscillatory active control
[ITN-91-85104] N91-26482
Boundary layer parameterization for a global spectral model
[AD-A235310] N91-26635
Hydroacoustics of intermittent boundary-layer flow: A review
[AD-A235092] N91-26883
Boundary layer transition noise art
[AD-A235093] N91-26884

TURBULENT DIFFUSION
Description of the RIVM/KNMI puff dispersion model
[KNMI-177] N91-26638

TURBULENT FLOW
Direct and large-eddy simulations of three-dimensional compressible Navier-Stokes turbulence
[AD-A233717] N91-26470
Basic studies of microstructure of combusting turbulent flows
[AD-A234222] N91-26471
Investigation of laminar, fully developed flow in annulus by finite difference model
[ITN-91-85116] N91-26483

TURBULENT JETS
Control of an axisymmetric turbulent jet by multi-modal excitation
[NASA-TM-104483] N91-26121
Laboratory modelling of the dynamics of coastal upwelling
[AD-A234987] N91-26664

TWINNING
Materials/microstructures characterization
[AD-A233751] N91-26295

TWO FLUID MODELS
Turbulent processes of mass-loading of new ions on Venus and Mars and the problems of numerical models of the interaction of solar wind with these planets. 1: Characteristics of the flow of solar wind around the planets N91-26174

TWO PHASE FLOW
Dynamics of face and annular seals with two-phase flow
[NASA-CR-4256] N91-26479
Simulation of pore scale porous media flow using lattice gas methods
[DE91-004829] N91-26484

U

U.S.S.R.
USSR Space Life Sciences Digest, issue 29
[NASA-CR-3922(34)] N91-26669
USSR Space Life Sciences Digest, issue 30
[NASA-CR-3922(36)] N91-26670
JPRS report: Science and technology. USSR: Life sciences
[JPRS-ULS-91-010] N91-26683

U.S.S.R. SPACE PROGRAM
JPRS report: Science and technology. USSR: Space
[JPRS-USP-91-002] N91-26162
Survey of the principal results of medical research in the flight program of the second main expedition aboard the Mir orbiting complex N91-26686
State-of-the-art automated evaluation of functional state of the body in the space program and preventive medicine N91-26687

ULTRAHIGH FREQUENCIES
Evaluation of the MARISAT satellite UHF wideband channel
[AD-A233666] N91-26408

ULTRAHIGH VACUUM
Chemistry on an atomic scale of ion-beam modified surfaces
[AD-A233707] N91-26891

ULTRASHORT PULSED LASERS
Laser switched power linac
[AD-A234581] N91-26507

ULTRASONIC FLAW DETECTION
Evaluation of environmentally aged polymer/composite material by ultrasonic inspection
[AD-A235343] N91-26231
Methods for determining crack depth
[AD-A234799] N91-26562
ULTRASONIC TESTS
Evaluation of environmentally aged polymer/composite material by ultrasonic inspection
[AD-A235343] N91-26231
Methods for determining crack depth
[AD-A234799] N91-26562
ULTRASONICS
Progress in ultrasonic measurements research in 1990: Transient sources for acoustic emission work
[AD-A234965] N91-26882
Bulk wave characterization of high T(sub c) superconductors
[AD-A234649] N91-26954
ULTRAVIOLET PHOTOMETRY
UV aurora mapping in corrected geomagnetic coordinates
[ITN-91-85106] N91-26636
ULTRAVIOLET RADIATION
UV aurora mapping in corrected geomagnetic coordinates
[ITN-91-85106] N91-26636
ULTRAVIOLET SPECTRA
The analysis of a rocket tomography measurement of the N2+3914A emission and N2 ionization rates in an auroral arc
[NASA-CR-188622] N91-26596
UNDERWATER ACOUSTICS
A boundary scattering strength extraction algorithm for the analysis of long-range reverberation data
[AD-A233721] N91-26877
Hydroacoustics of intermittent boundary-layer flow: A review
[AD-A235092] N91-26883
Underwater scattering of sound
[AD-A235097] N91-26885
UNITED STATES
Publications of the Executive Office of the President, January 20, 1989 to December 31, 1990
[PB91-127423] N91-26998
UNIVERSITY PROGRAM
Northeast Artificial Intelligence Consortium (NAIC). Volume 1: Executive summary
[AD-A234880] N91-26815
NASA/ASEE Summer Faculty Fellowship Program, 1990, Volume 1
[NASA-CR-185637-VOL-1] N91-27088
NASA/ASEE Summer Faculty Fellowship Program, 1990, volume 2
[NASA-CR-185637-VOL-2] N91-27103
UNIX (OPERATING SYSTEM)
UNIX (tm) in high energy physics: What we can learn from the initial experiences at Fermilab
[DE91-011976] N91-26914
CRUSH: The NSI data compression utility N91-27032
Integrating UNIX workstation into existing online data acquisition systems for Fermilab experiments
[DE91-011974] N91-27044
A system for UNIX command retrieval using a multilayered neural network
[DE91-012105] N91-27045
UNSTEADY AERODYNAMICS
State space models for aeroelastic and viscoelastic systems
[AD-A234730] N91-26117
Viscous flow simulations of internal store carriage and separation
[NASA-CR-185343] N91-26123
Gust design procedures N91-26155
UPPER ATMOSPHERE
Measurements of the longitudinal movements of O(+) ions in the subauroral upper atmosphere from the Aureol 3 satellite N91-26171
Effect of turbulence on impurity observation in upper atmosphere using lidar method N91-26584
Development of a Vector Spherical Harmonic (VSH) model of the neutral thermosphere
[AD-A234744] N91-26631
UPPER IONOSPHERE
Measurements of the longitudinal movements of O(+) ions in the subauroral upper atmosphere from the Aureol 3 satellite N91-26171
UPWELLING WATER
Laboratory modelling of the dynamics of coastal upwelling
[AD-A234987] N91-26664
Phytoplankton abundance in relation to Lagrangian paths
[AD-A233728] N91-26672
USER MANUALS (COMPUTER PROGRAMS)
Composite database interface users manual
[AD-A235327] N91-26230
Improved Point Analysis Model (IPAM) (users guide)
[AD-A235305] N91-26649
The NASA/MSFC global reference atmospheric model: 1990 version (GRAM-90). Part 1: Technical/users manual
[NASA-TM-4268] N91-26654
The High Resolution Profiler (HRP): User's guide and software modifications documentation
[AD-A234640] N91-26663
BaRT manual version 3.0
[AD-A234528] N91-26784
NFEARS: A nonlinear adaptive finite element solver. Part 2: User's manual
[AD-A234416] N91-26842
USER REQUIREMENTS
Illuminance and luminance distributions of a prototype ambient illumination system for Space Station Freedom
[NASA-TM-103541] N91-26193
HORACE: Presentation-level protocol standard for digital transmission of monochrome television images
[AD-A235276] N91-26428
The High Resolution Profiler (HRP): User's guide and software modifications documentation
[AD-A234640] N91-26663
Expert system explanation: The user perspective
[AD-A233739] N91-26749
NSIUWG: Science networking retreat N91-27010
User support services and network application development: An overview N91-27015
NASA's use of FTS2000 services N91-27018
Requirements management: A CSR's perspective N91-27027
Overview of the NSI User Support Office (NSI USO) N91-27028
The NSINIC on-line system N91-27029
NSI conference support N91-27031
UTILITIES
Queueing systems with orbiting customers
[ITN-91-85112] N91-26868

V

VACUUM
Work performed experiments: 1989-1990
[AD-A235221] N91-26457
VACUUM CHAMBERS
Saltation threshold detection in a wind tunnel by the measurement of the net electrostatic charge N91-27070
VACUUM SYSTEMS
Vacuum design for a superconducting mini-collider
[DE91-011964] N91-26975
VALVES
Method of injecting fluid propellants into a rocket combustion chamber
[NASA-CASE-LEW-14846-2] N91-26200
Method and apparatus for waste collection and storage
[NASA-CASE-MSC-21025-3] N91-26747
VAN DER WAAL FORCES
Cationic polymerization within van der Waals clusters of the form (CH2=R)n where R=CH2, CF2 and CHCH3
[AD-A234233] N91-26255
VANADIUM ALLOYS
Environmental embrittlement of ordered intermetallic alloys at room temperature in moist atmospheres
[DE91-012051] N91-26321
VAPOR DEPOSITION
Magnetron sputter deposition of boron and boron carbide
[DE91-011194] N91-26241
Desorption product yields following Cl2 adsorption on Si(111)7x7: Coverage and temperature dependence
[AD-A234635] N91-26264
A program in the chemistry of electronic materials. Task 1: New organometallic precursors for the low pressure chemical vapor deposition of refractory materials for electronics
[AD-A234315] N91-26342
Surface etching and roughening in integrated processing of thermal oxides
[AD-A234960] N91-26456
Radio frequency and microwave plasma for optical thin film deposition
[DE91-012081] N91-26525
Research on stable, high-efficiency amorphous silicon multijunction modules
[DE91-002159] N91-26591
Chemistry on an atomic scale of ion-beam modified surfaces
[AD-A233707] N91-26891
Transmission electron microscopy of the CVD diamond film/substrate interface
[AD-A234790] N91-26956
HREM study of heteroepitaxial interfaces in the TiO2/Al2O3 system
[DE91-012473] N91-26986
VAPOR PHASES
Ceramic fiber coating development and demonstration
[AD-A234773] N91-26358
A study of the gas phase chemistry of solid propellants using a microprobe mass spectrometer (MPMS) system: Initial development of the MPMS system
[AD-A234839] N91-26393
A study of the gas phase chemistry of solid propellants using a microprobe mass spectrometer (MPMS) system: Preliminary results for solid fuels (HTPB/Zecorez and BAMO/NMMO), single-base propellant (M10) and an RDX-Based propellant (BLX-9)
[AD-A234840] N91-26394
VARIATIONS
Incoherent scatter radar observations of the ionosphere N91-26623
VAX COMPUTERS
MultiNet TCP/P/IP for VAX/VMS update N91-27020
CRUSH: The NSI data compression utility N91-27032
VECTOR ANALYSIS
Peptide transport through the blood-brain barrier
[AD-A233753] N91-26708
Weighted least squares estimation for Aalen's additive risk model
[AD-A235250] N91-26852
VECTORS (MATHEMATICS)
On the sensitivity of solutions of parametrized equations
[AD-A234265] N91-26838
Method and apparatus for second-rank tensor generation
[NASA-CASE-NPO-17512-1-CU] N91-26918
VEGETABLES
Higher plants as part of biological human life support system N91-26693
VEGETATION
Ecological exposure and effects of airborne toxic chemicals: An overview
[PB91-148460] N91-26594
VEGETATION GROWTH
Free-air carbon dioxide enrichment: A new approach to research on carbon exchange processes
[DE91-012074] N91-26609
JPRS Report: Science and technology. USSR: Life sciences
[JPRS-ULS-91-009] N91-26688
Higher plants as part of biological human life support system N91-26693
VELOCITY DISTRIBUTION
The delay of turbulent boundary layer separation by oscillatory active control
[ITN-91-85104] N91-26482
VENERA SATELLITES
Results of morphometric analysis of the Tesserae surface of Venus according to Venera-15 and -16 data N91-26176
VENUS SURFACE
Results of morphometric analysis of the Tesserae surface of Venus according to Venera-15 and -16 data N91-26176
VERBAL COMMUNICATION
Induced pictorial representations
[AD-A234548] N91-26735
Using genetic algorithms to select and create features for pattern classification
[AD-A235165] N91-26792
VERTEBRAE
Computer tomography measurement of vertebral bones and muscles after extended manned space flights N91-26690
VERTEBRATES
Mathematical problems concerning rhythmic processes
[AD-A234588] N91-26845
VERTICAL DISTRIBUTION
Evaluation of the Navy oceanic vertical aerosol model using lidar and PMS particle-size spectrometers
[AD-A233653] N91-26625
Characterization of vertical electric fields and associated voltages induced on an overhead power line from close artificially initiated lightning
[DE91-010781] N91-26656
VERTICAL ORIENTATION
Sea test development of laser altimeter
[AD-A233824] N91-26498
VERY LARGE SCALE INTEGRATION
VHSIC electronics and the cost of Air Force avionics in the 1990s
[RAND-R-3843-AF] N91-26143

VERY LONG BASE INTERFEROMETRY
Evolution of some types of Earth satellite orbits N91-26163
VERY LOW FREQUENCIES
Omega/VLF signal coverage database development [AD-A235226] N91-26129
VLF nighttime data analysis [AD-A234006] N91-26417
VESTA ASTEROID
Study of the properties of the autonomous optical navigation of a space probe in a rendezvous with an asteroid N91-26169
VESTIBULAR NYSTAGMUS
Vestibular reactions and intersensory interactions in weightlessness: Results of Optokinez experiment N91-26698
VESTIBULES
State and forms of adaptation of vestibular function after space flights N91-26706
Combined effect of noise and vibration on cells of auditory and vestibular apparatus N91-26707
VESTS
Effect of a passive cooling vest on tension/anxiety and fatigue in a high heat and high humidity naval environment [AD-A234657] N91-26755
Effectiveness of ice-vest cooling in prolonging work tolerance time during heavy exercise in the heat for personnel wearing Canadian forces chemical defence ensembles [AD-A235273] N91-26758
VHSIC (CIRCUITS)
VHSIC electronics and the cost of Air Force avionics in the 1990s [RAND-R-3843-AF] N91-26143
VIBRATION
Photoexcitation spectroscopy of pernigraniline [AD-A233841] N91-26250
Field work and dispersion relations of excitations on fractals [AD-A234953] N91-26455
The delay of turbulent boundary layer separation by oscillatory active control [ITN-91-85104] N91-26482
Combined effect of noise and vibration on cells of auditory and vestibular apparatus N91-26707
Advanced Dynamic Anthropomorphic Manikin (ADAM) design report [AD-A234761] N91-26756
VIBRATION DAMPING
Establishment of a remotely piloted helicopter test flight program for higher harmonic control research [AD-A234978] N91-26135
Improved modeling and performance of squeeze film damper bearings [AD-A233694] N91-26531
The wavenumber-frequency filtering characteristics of compliant layers [AD-A234768] N91-26561
The relationship of traditional damping measures for materials with high damping capacity [AD-A235347] N91-26568
VIBRATION EFFECTS
Combined effect of noise and vibration on cells of auditory and vestibular apparatus N91-26707
VIBRATIONAL SPECTRA
The stepwise dissociation of NH3 on the Si(111)-(7x7) surface: Low temperature dissociative adsorption and thermal effects [AD-A235009] N91-26274
VIEWING
Incorporation of shuttle CCT parameters in computer simulation models N91-27096
VIKING LANDER SPACECRAFT
Martian surface materials N91-27073
Sand and dust issues for the MESUR mission N91-27080
Dust in the Mars atmosphere N91-27082
VIKING MARS PROGRAM
The effects of atmospheric dust on observations of Martian surface albedo N91-27072
Magnetic and electrical properties of Martian particles N91-27074
VIKING ORBITER SPACECRAFT
Thermal and albedo mapping of the north and south polar regions of Mars N91-27076
VINYL POLYMERS
Block patterning of the metallization of polyvinylidene fluoride transducers [AD-D014872] N91-26450
VINYLIDENE
The development of piezoelectric poly(vinylidene fluoride) sensors for measuring peel stresses in adhesive joints [AD-A233880] N91-26559
VIRUSES
Molecular studies of cytokine induction [AD-A235326] N91-26731
A study of murine bone marrow cells cultured in bioreactors which create an environment which simulated microgravity N91-27101
VISCOELASTICITY
State space models for aeroelastic and viscoelastic systems [AD-A234730] N91-26117
Effect of a viscoelastic interface on the transverse behavior of fiber-reinforced composites [AD-A233986] N91-26212
Viscoelastic behavior of elastomeric membranes [AD-A234496] N91-26560
VISCOSITY
Experimental techniques in the field of low density aerodynamics [AGARD-AG-318(E)] N91-26124
Effect of a viscoelastic interface on the transverse behavior of fiber-reinforced composites [AD-A233986] N91-26212
Lubricants at low temperatures [AD-A234536] N91-26348
Changes in rheologic indices of blood and hemodynamics during 14-day antiorthostatic hypokinesia N91-26692
Viscosity methods in optimal control of distributed systems. The Bellman equation [AD-A234646] N91-26812
VISCOUS FLOW
Viscous flow simulations of internal store carriage and separation [NASA-CR-185343] N91-26123
VISIBILITY
Visual sensitivities and discriminations and their role in aviation [AD-A234866] N91-26740
Incorporation of shuttle CCT parameters in computer simulation models N91-27096
VISION
Visual accommodation in cosmonauts N91-26697
Young and older observers show similar perceived contrast functions for isoluminant stimuli [AD-A233766] N91-26709
A Conference on Eye Movements and Visual Cognition [AD-A234754] N91-26739
VISUAL DISCRIMINATION
Visual sensitivities and discriminations and their role in aviation [AD-A234866] N91-26740
VISUAL PERCEPTION
Induced pictorial representations [AD-A234548] N91-26735
A Conference on Eye Movements and Visual Cognition [AD-A234754] N91-26739
VOCODERS
Intelligibility of digital speech masked by noise: Normal hearing and hearing impaired listeners [AD-A234852] N91-26427
VOICE COMMUNICATION
Opportunities for advanced speech processing in military computer-based systems [AD-A233724] N91-26412
Intelligibility of digital speech masked by noise: Normal hearing and hearing impaired listeners [AD-A234852] N91-26427
VOICE DATA PROCESSING
Opportunities for advanced speech processing in military computer-based systems [AD-A233724] N91-26412
Uncertainty handling at speech/natural language interface, volume 1 [AD-A234310] N91-26422
VOLT-AMPERE CHARACTERISTICS
Quantum limited quasiparticle mixers at 100 GHz [DE91-011894] N91-26973
VOLTAGE CONVERTERS (DC TO DC)
High-power converters for space applications [NASA-CR-187116] N91-26461
VORTICES
A study of high speed flows in an aircraft transition duct [NASA-TM-104449] N91-26122
The kinematics of turbulent boundary layer structure [NASA-TM-103859] N91-26465
Direct and large-eddy simulations of three-dimensional compressible Navier-Stokes turbulence [AD-A233717] N91-26470
Theoretical studies of the kinematics, dynamics, stability, and control of unsteady/vortical flows [AD-A235190] N91-26477
Laboratory modelling of the dynamics of coastal upwelling [AD-A234987] N91-26664

W

WAFERS
Non-destructive evaluation of residual stresses in thin films via x ray diffraction topography methods [AD-A235328] N91-26552
Process for the controlled growth of single-crystal films of silicon carbide polytypes on silicon carbide wafers [NASA-CASE-LEW-15222-1] N91-26966
Process for the homoepitaxial growth of single-crystal silicon carbide films on silicon carbide wafers [NASA-CASE-LEW-15223-1] N91-26967
WALLS
Testing of a composite thermal structure to insulate the drivers of a large scale blast/thermal simulator [AD-A234014] N91-26213
Aircraft interior noise reduction by alternate resonance tuning [NASA-CR-185453] N91-26889
WALSH FUNCTION
Optimal Walsh modulations in the presence of Doppler [AD-A233723] N91-26411
WARFARE
Progress with neural network gulf streams [AD-A233810] N91-26658
Space doctrine [AD-A234971] N91-26866
WARNING SYSTEMS
KC-135 ground collision avoidance system questionnaire [AD-A234385] N91-26125
Evaluation of the C/EC/KC-135 Ground Collision Avoidance System (GCAS), study 1 [AD-A235301] N91-26130
Northeast Artificial Intelligence Consortium (NAIC). Volume 9: A planner system for the application of indications and warning [AD-A234888] N91-26823
WASTE DISPOSAL
Method and apparatus for waste collection and storage [NASA-CASE-MSC-21025-3] N91-26747
WASTE WATER
Transport and fate of acetone in an outdoor model stream, Stennis Space Center near Bay St. Louis, Mississippi [PB91-154674] N91-26600
WATER
Water solubility of bis(2-ethylhexyl) hydrogen phosphite [AD-A234561] N91-26259
Raman spectroscopy study of solvation structure in acetonitrile/water mixtures [AD-A234921] N91-26271
Abrasive-waterjet machining of isogrid structures [AD-A234626] N91-26405
Ricochet of sphere off water [ITN-91-85102] N91-26480
Investigating combustion as a method of processing inedible biomass produced in NASA's biomass production chamber [NASA-TM-103821] N91-26759
Impact of Mars sand on dust on the design of space suits and life support equipment: A technology assessment N91-27079
WATER BALANCE
A review of precipitation-related aspects of West Antarctic meteorology N91-26574
Development of advanced methods based on stable isotope technology for studies of exercise in heat [AD-A234670] N91-26719
WATER IMMERSION
COLDEX-86: Physical work capacity during prolonged cold water immersion at 6.1 msw [AD-A233767] N91-26710
COLDEX-86: Fluid and electrolyte changes during prolonged cold water immersion [AD-A233768] N91-26711
COLDEX-86: Summary of the experimental protocol and general results [AD-A234031] N91-26715
WATER POLLUTION
Transport and fate of acetone in an outdoor model stream, Stennis Space Center near Bay St. Louis, Mississippi [PB91-154674] N91-26600

WATER QUALITY
Transport and fate of acetone in an outdoor model stream, Stennis Space Center near Bay St. Louis, Mississippi
[PB91-154674] N91-26600
WATER SPLITTING
FTIR studies of water and ammonia decomposition on silicon surfaces
[AD-A234637] N91-26265
Design of a lunar oxygen production plant N91-27109
WATER WAVES
Research in nonlinear water waves
[AD-A235410] N91-26478
Sloshing response in a tank containing two liquids
[DE91-011844] N91-26487
Analysis of wave characteristics in extreme seas
[AD-A234538] N91-26660
Directional characteristics of waves in shallow water
[AD-A234568] N91-26661
WAVE DISPERSION
Field work and dispersion relations of excitations on fractals
[AD-A234953] N91-26455
WAVE EQUATIONS
Backscattering from rough interfaces and the parabolic approximation
[AD-A235184] N91-26886
WAVE FUNCTIONS
Theoretical studies of potential energy surfaces and computational methods
[DE91-011126] N91-26902
WAVE GENERATION
An experimental and numerical study of wavemaker dissipation in the process of direct generation of the resonant sloshing waves in a rectangular tank
[ITN-91-85103] N91-26481
WAVE INTERACTION
Energy migration, motion and order in synthetic polymers
[AD-A234403] N91-26346
An experimental and numerical study of wavemaker dissipation in the process of direct generation of the resonant sloshing waves in a rectangular tank
[ITN-91-85103] N91-26481
A numerical study of blocking N91-26640
Backscattering from rough interfaces and the parabolic approximation
[AD-A235184] N91-26886
WAVE PROPAGATION
Thermoelastic wave propagation in laminated composites N91-26209
Atmospheric propagation of laser beams
[AD-A234314] N91-26501
Determination of SBS induced damage limits in large fused silica optics for intense, time varying laser pulses
[DE91-012080] N91-26518
NDE pattern recognition of LSS states via wave propagation
[AD-A234772] N91-26549
Gravity waves and instabilities in the lower and middle atmosphere N91-26621
Bulk wave characterization of high T(sub c) superconductors
[AD-A234649] N91-26954
WAVE REFLECTION
A multichannel seismic investigation of variations in crustal structure in the western North Atlantic
[AD-A235245] N91-26634
WAVEFORMS
Complex envelope properties, interpretation, filtering, and evaluation
[AD-A234478] N91-26844
Progress in ultrasonic measurements research in 1990: Transient sources for acoustic emission work
[AD-A234965] N91-26882
WAVEGUIDE LASERS
Quasi-CW excimer laser, phase 2
[AD-A234771] N91-26509
WEAK ENERGY INTERACTIONS
Gauge bosons and heavy quarks: Proceedings of Summer Institute on Particle Physics
[DE91-011248] N91-26907
WEAK INTERACTIONS (FIELD THEORY)
Weak interactions and presupernova evolution
[DE91-011543] N91-27052
WEAPON SYSTEMS
The wild weasel development programs, one run, one hit, one error
[RAND-P-7661-RGS] N91-26431
Application of software tools in embedded computers within military systems to enhance software reliability, quality assurance, and maintenance
[AD-A234555] N91-26785
WEAR RESISTANCE
Lubricants at low temperatures
[AD-A234536] N91-26348
WEAR TESTS
Sliding wear-testing and data analysis strategies for advanced engineering ceramics
[DE91-009524] N91-26383
Performance evaluation of a novel erosion-resistant pump design
[DE91-008201] N91-26528
WEATHER
Surface Observation Climatic Summaries (SOCS) for Kodiak, Alaska
[AD-A235182] N91-26646
Surface observation climatic summaries for Tonopah test range, Nevada
[AD-A235228] N91-26648
WEATHER FORECASTING
In the energy active region of the ocean N91-26583
Applications of MST radars: Meteorological applications N91-26622
Improved Point Analysis Model (IPAM) (users guide)
[AD-A235305] N91-26649
WEATHERING
Solutions to problems of weathering in Antarctic eucrites N91-27113
WEDGES
Comparison of sound pressure in a wedge-shaped ocean as predicted by an image method and a PE model
[AD-A234191] N91-26879
WEIGHTING FUNCTIONS
The weighted uni-dimensional similarities problem with least absolute value metric is NP-Hard
[AD-A235060] N91-26849
Weighted least squares estimation for Aalen's additive risk model
[AD-A235250] N91-26852
WEIGHTLESSNESS
Hormonal regulators of calcium metabolism following space flights of various durations N91-26689
Computer tomography measurement of vertebral bones and muscles after extended manned space flights N91-26690
Vestibular reactions and intersensory interactions in weightlessness: Results of Optokinez experiment N91-26698
Effects of 13 day space flight on skeletal muscles and neuromuscular junctions in rats N91-26703
Method and apparatus for waste collection and storage
[NASA-CASE-MSC-21025-3] N91-26747
WEIGHTLESSNESS SIMULATION
Diagnostic utility of continuous noninvasive blood pressure monitoring (Penaz method) in gravity-induced blood redistribution N91-26705
Proceedings of the 12th Annual Meeting of the UIPS Commission on Gravitational Physiology
[AD-A235337] N91-26732
WELDED JOINTS
Investigations into fracture mechanics failure concepts with thermomechanically rolled steels
[BLL-OA-TRANS-4238-(6196.3)] N91-26556
WELDING
Laser applications in machining slab materials
[AD-A233823] N91-26497
Shell hoop prestress generated by welding
[DE91-011892] N91-26571
WHISKER COMPOSITES
Reaction processing of ceramic particulate and whisker composites
[AD-A234951] N91-26225
Characterization of mechanical damage mechanisms in ceramic composite materials
[NR-032-553] N91-26235
Response of whisker-reinforced ceramic matrix composites to dynamic compressive loading N91-26236
WHITE DWARF STARS
The light curve of the magnetic star AM - Herculis
[ITN-91-85108] N91-27049
WHITE NOISE
Low frequency noise in resonant Josephson soliton oscillators
[DE91-011911] N91-26464
Lyapunov exponents and rotation numbers of linear systems with real noise
[AD-A234729] N91-26846
WIND (METEOROLOGY)
Description of the RIVM/KNMI puff dispersion model
[KNMI-177] N91-26638
Radar-aeolian roughness project
[NASA-CR-4378] N91-27056
WIND DIRECTION
Directional characteristics of waves in shallow water
[AD-A234568] N91-26661
WIND EFFECTS
Wind abrasion on Mars N91-27064
The aeolian wind tunnel N91-27065
Saltation threshold detection in a wind tunnel by the measurement of the net electrostatic charge N91-27070
Saltation threshold reduction due to the electrostatic agglomeration of fine particles N91-27071
WIND SHEAR
Description of the RIVM/KNMI puff dispersion model
[KNMI-177] N91-26638
WIND TUNNEL TESTS
Performance optimization of helicopter rotor blades
[NASA-TM-104054] N91-26137
The delay of turbulent boundary layer separation by oscillatory active control
[ITN-91-85104] N91-26482
Sand and Dust on Mars
[NASA-CP-10074] N91-27057
Saltation threshold detection in a wind tunnel by the measurement of the net electrostatic charge N91-27070
Saltation threshold reduction due to the electrostatic agglomeration of fine particles N91-27071
WIND TUNNELS
The aeolian wind tunnel N91-27065
WIND VELOCITY
Development and verification of a physical cloud-moisture model for use in general circulation models
[AD-A234751] N91-26643
WINDOWS (APERTURES)
Transpiration cooled ultraviolet sol-gel silica optics
[AD-A235426] N91-26934
WINDSHIELDS
High performance transparency design
[AD-A234456] N91-26133
WINGS
Calculated aerodynamics of wings in severe maneuver
[AD-A235241] N91-26120
WIRE
Lifetimes and failure mechanisms of W/Re hairpin filaments
[AD-A235199] N91-26305
WORDS (LANGUAGE)
A physiologically motivated front end for speech recognition
[AD-A233727] N91-26414
WORK CAPACITY
COLDEX-86: Physical work capacity during prolonged cold water immersion at 6.1 msw
[AD-A233767] N91-26710
WORKLOADS (PSYCHOPHYSIOLOGY)
Effect of shift work of air traffic controllers on sympathetic nervous system N91-26700
Task analysis and workload prediction for the MH-47E mission and a comparison with CH-47D workload predictions. Volume 2: Appendixes A through N
[AD-A235249] N91-26757
Effectiveness of ice-vest cooling in prolonging work tolerance time during heavy exercise in the heat for personnel wearing Canadian forces chemical defence ensembles
[AD-A235273] N91-26758
WORKSTATIONS
Omega system Performance Assessment and Coverage Evaluation (PACE) workstation design and implementation, volume 1
[AD-A235225] N91-26128
Omega/VLF signal coverage database development
[AD-A235226] N91-26129
Integrating UNIX workstation into existing online data acquisition systems for Fermilab experiments
[DE91-011974] N91-27044
WOUND HEALING
Wound healing by cultured skin cells and growth factors
[AD-A235300] N91-26730

X

X RAY ABSORPTION
High temperature superconducting films and crystals
[AD-A235234] N91-26965
X RAY DIFFRACTION
Non-destructive evaluation of residual stresses in thin films via x ray diffraction topography methods
[AD-A235328] N91-26552
X RAY IMAGERY
The 1980 solar maximum mission event listing
[NASA-TM-4287] N91-27087
X RAY INSPECTION
X ray tomographic inspection of printed wiring assemblies and electrical components
[AD-A234748] N91-26548

X RAY LASERS
X ray laser program
[AD-A234390] N91-26504
Saturation and kinetic issues for optical-field-ionized plasma x ray lasers
[DE91-012079] N91-26517
X ray spot motion during 220 ps laser pulses
[DE91-012111] N91-26519
X RAY SCATTERING
Photons and neutrons
[DE91-010980] N91-26906
X RAYS
X ray structure of polyanilines
[AD-A233848] N91-26332
X ray spot motion during 220 ps laser pulses
[DE91-012111] N91-26519
X ray-computed tomography for inspecting industrial parts
[DE91-011390] N91-26554
The 1980 solar maximum mission event listing
[NASA-TM-4287] N91-27087
XENON CHLORIDE LASERS
Quasi-CW excimer laser, phase 2
[AD-A234771] N91-26509

Y

YAG LASERS
SUNLITE program. Sub-Hertz relative frequency stabilization of two diode laser pumped Nd:YAG lasers locked to a Fabry-Perot interferometer
[NASA-CR-184957] N91-26520
YTTRIUM OXIDES
Diagnostic studies of YBa2Cu3O(7-delta) laser ablation
[DE91-011382] N91-26515
Development of high Tc (greater than 110K) Bi, Tl and Y-based materials as superconducting circuit elements
[NASA-CR-188581] N91-26948
Formation of intermediate compounds during reduced pressure calcination of Y-Ba-Cu-O precursor
[DE91-011179] N91-26971

Z

ZEOLITES
Partial oxidation of light alkanes in transition-metal ion containing zeolites
[DE91-008202] N91-26243
ZINC-BROMIDE BATTERIES
Proof-of-concept zinc/bromine electric vehicle battery
[DE91-011767] N91-26463
ZIRCONIUM ALLOYS
The cryogenic mechanical properties of Vintage 3 Al-Li-Zr alloy 2090-T81
[DE91-011897] N91-26311
ZIRCONIUM OXIDES
India-stabilized zirconia coating for composites
[AD-D014857] N91-26224
Transformation toughening of ceramics
[AD-A234926] N91-26359
A tribological investigation of the graphite-to-diamond-like behavior of amorphous carbon films ion-beam-deposited on ceramic substrates
[DE91-010816] N91-26379
ZOOPLANKTON
SEEP 2 zooplankton data report: Winter, spring and summer collections at mooring 3 during 1988
[DE91-012077] N91-26668

Typical Personal Author Index Listing

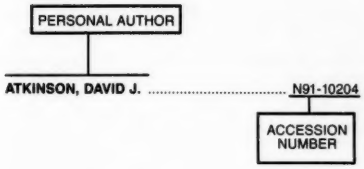

Listings in this index are arranged alphabetically by personal author. The accession number denotes the number by which the citation is identified.

A

AARON, SUSAN N91-27031
AARONS, JULES N91-26632
ABDELKARIM, M. H. N91-26585
ABDI, F. F. N91-26133
ACHENBACH, J. D. N91-26212
ACKERS, GARY K. N91-26723
ADAMOVICH, B. A. N91-26687
ADAMS N91-26851
ADOLPH, H. G. N91-26363
AGAH-TEHRANI, A. N91-26215
N91-26216
AGRAWAL, DHARMA P. N91-26801
AGRAWAL, GOVIND N91-26496
AHO, I. N91-26593
AKAU, R. L. N91-26486
AKUNDI, MURTY A. N91-27089
ALBARES, D. J. N91-26930
ALBERTI, J. C. N91-26385
ALDERTON, DAVID L. N91-27005
ALEKHINA, T. P. N91-26693
ALEKSEYEV, V. N. N91-26698
ALEXANDER, H. N91-26126
ALLEGRE, J. N91-26124
ALLEN, CHRISTOPHER W. N91-26257
ALLEN, JAMES F. N91-26824
ALLEY, RICHARD B. N91-26579
ALLOCK, H. R. N91-26344
ALYEA, F. N. N91-26654
AMENDT, P. N91-26517
ANASTASI, ROBERT F. N91-26231
ANCHEV, A. A. N91-26166
ANDERSON, CHARLES E., JR. N91-26534
ANDERSON, G. L. N91-26559
ANDERSON, GARY L. N91-26533
ANDERSON, JOHN B. N91-26578
ANDERSON, M. U. N91-26399
ANDERSON, MICHAEL A. N91-26786
ANG, J. A. N91-26187
ANTOLOVICH, STEPHEN D. N91-26304
ARMSTRONG, ROBERT L. N91-26501
ARMSTRONG, WILBUR C. N91-26201
ARMSTRONG, WILLIAM N91-26227
ARNOLD, FRED E. N91-26357
ARNOLDUS, HENK F. N91-26894
ASAY, B. W. N91-26399
ASAY, J. R. N91-26186
ATANASOV, V. A. N91-26166
ATKESON, CHRISTOPHER G. N91-26813
ATKINSON, LEE A. N91-26665
ATLURI, SATYA N. N91-26190
ATTIYA, HAGIT N91-26780
AUBURN, P. R. N91-26260
AUCLAIR, R. A. N91-27004
AUFDERHEIDE, M. B. N91-27052
AURANDT, RICHARD G. N91-26115

B

BABAKOVA, L. L. N91-26703
BABAN, FARZAD N91-26115
BAILEY, J. L. N91-26474
BAILEY, MICHAEL P. N91-26858
BAIN, B. N91-26758
BAKER, C. F. N91-26240
BAKER, CHARLES K. N91-26354
BAKER, IAN N91-26322
N91-26586
BAKER, S. R. N91-26746
BALACHANDRAN, U. N91-26971
N91-26979
BALANDINA, T. N. N91-26694
BALWALLY, NANDAKUMAR M. N91-26451
BANIN, A. N91-27058
BANNEROT, RICHARD B. N91-27088
N91-27103
BANTA, GUY R. N91-26755
BAO, YOULIN N91-26300
BAR-COHEN, YOSEPH N91-26550
BARER, A. S. N91-26699
BARKER, J. R. N91-26594
BARKER, L. M. N91-26186
BARLETTA, W. A. N91-26975
BARNEA, RAM N91-26760
BARNES, DANIEL C. N91-26147
BARNES, NORMAN P. N91-26514
BARNES, RON N91-27090
BARNES, TERENCE J. N91-26154
N91-26158
BARRETT, DAVID J. N91-26222
BARRON, EMMANUEL N. N91-26812
BARSANTI, M. L. N91-26492
BART, STEPHEN F. N91-26446
BARTIE, K. M. N91-26139
BARTOL, AILEEN M. N91-26756
BARWEY, DINESH N91-26134
BASSO, T. S. N91-26588
BASTIAANSSEN, W. G. M. N91-26585
BASU, PRITHWISH N91-26479
BAYEVSKIY, R. M. N91-26687
BAYSAL, OKTAY N91-26123
N91-26488
BAZAN, GUILLERMO C. N91-26365
BEATTY, PAUL A. N91-26479
BECKER, LEE N91-26800
BEELER, RICHARD M. N91-26479
BELFIORE, J. S. N91-26189
BENFORD, GREGORY N91-26457
BENNISON, S. J. N91-26374
BENSON, A. N91-26591
BENTLEY, C. R. N91-26576
BERARD, EDWARD V. N91-26766
BERNARD, J. J. N91-26124
BERNAYS, D. J. N91-26410
BERRA, P. B. N91-26826
BERRY, D. N91-26126
BERRY, G. F. N91-26946
BERSENEVA, A. P. N91-26687
BERSHAD, NEIL J. N91-26859
BEVER, G. A. N91-26432
BHAT, P. K. N91-26591
BHATNAGAR, R. N91-26910
BHATT, R. T. N91-26233
BHATTI, N. N91-26595
BIBARSOV, P. SH. N91-26177
BIBRING, J. P. N91-26175
BIEDENBENDER, M. D. N91-26436
BIERBAUM, CARL R. N91-26757
BILELLO, JOHN C. N91-26552
BILES, JOHN N91-26822
BINDSCHADLER, ROBERT A. N91-26573
BINKOWSKI, F. S. N91-26598
BIRD, S. L. N91-26602
BIRDSALL, THEODORE G. N91-26659
BIRKNER, BJORN N91-26944
BIRMAN, KENNETH P. N91-26804
BISHOP, PHILLIP A. N91-27091
BLAEDEL, K. L. N91-26381
BLAIR, D. S. N91-26385
BLANCHARD, CHERYL R. N91-26235
N91-26236
N91-26237
BLAU, P. J. N91-26383
BLISS, DONALD B. N91-26889
BLOOMFIELD, HARVEY S. N91-26592
BOCHENKOV, A. A. N91-26684
BOCKHEIM, JAMES G. N91-26577
BODO, G. N91-26698
BOGOMOLOV, V. V. N91-26178
N91-26686
BOLSTED, J. N91-26463
BORNSTEIN, JONATHAN A. N91-26118
BOSS, R. D. N91-26769
BOSSI, RICHARD H. N91-26548
BOTTONI, M. N91-26489
BOURNE, JOHN N91-26551
BOURNE, L. C. N91-26981
BOWEN, KENNETH N91-26825
BOWERSOX, V. C. N91-26607
BOYD, ERNEST J. N91-27092
BOYLE, BRIAN N91-27051
BOZICH, S. N91-26279
BRACKER, A. S. N91-26265
BRANDON, JONATHAN N91-26867
BRASLAVETS, R. I. N91-26168
BRECKENRIDGE, F. R. N91-26882
BRENNER, M. J. N91-26113
BRESLAV, I. S. N91-26699
BREUS, T. K. N91-26174
BRIDGES, WENDELL J. N91-26147
BRINDLEY, WILLIAM J. N91-26375
BRITTEN, J. N91-26525
BROCK, DAVID L. N91-26535
BRODERSEN, A. J. N91-26551
BRODSKY, MARA N91-26296
BROMWICH, DAVID H. N91-26574
BROOKS, RODNEY A. N91-26446
BROWN, CHRISTOPHER M. N91-26832
BROWN, D. S. N91-26602
BROWN, GEORGE E., JR. N91-27046
BROWN, I. G. N91-26974
BROWN, R. C. N91-26283
BROWN, S. N91-26591
BRULE, JAMES F. N91-26815
BRUSASCO, R. M. N91-26525
BU, XIN YA N91-26234
BUCK, F. N91-26433
BUCKLEY, WILLIAM H. N91-26660
BUGROV, S. A. N91-26178
N91-26686
BUHL, PETER N91-26634
BUONANNO, M. A. N91-26220
BURCHELL, T. D. N91-26240
BURCHETT, S. N. N91-26570
BURGMAN, H. A. N91-26467
BURKE, M. G. N91-26314
BURKE, THOMAS G. N91-26714
BURLUKA, O. N91-26179
BURR, RALPH G. N91-26755
BURROUGHS, C. B. N91-26561
N91-26887
BURSTEN, B. E. N91-26905
BURSZTYN, DIZZA N91-26553
BUSSEY, DIRK T. N91-26444
BUSSI, PHILIPPE N91-26964
BUTLER, J. N. N91-26914
BUTLER, JOHN M. N91-26355
BUTTON, ROBERT M. N91-26202
BYER, R. L. N91-26520
BYRD, R. H. N91-26777

C

CAIRNS, JOHN, JR. N91-26603
CALCOTE, H. F. N91-26273
CAMBANIS, STAMATIS N91-26860
CAMERON, CARIG P. N91-26225
CAMPBELL, J. H. N91-26525
CAMPBELL, L. A. N91-26183
CANAVAN, G. H. N91-26871
CAPRILE, BRUNO N91-26810
CARD, VICTOR N91-26154
N91-26158
CARDONA, A. H. N91-26981

CARIGNAN, CRAIG R. N91-26527
CARLETON, ANDREW M. N91-26574
CARLETON, F. B. N91-26388
CARLSON, S. N91-27050
CARMAN, H. S., JR. N91-26909
CARR, JON R. N91-26147
CARR, T. D. N91-27047
CARTER, G. M. N91-26410
CASSADY, JOSEPH N91-26198
CELMINS, ILMARS N91-26118
CEPHAS, KIA N91-26259
CERUTI, M. G. N91-27004
CHAIKEN, JOSEPH N91-26927
CHAMBERS, KATHLEEN C. N91-26744
CHAMBERS, W. F. N91-26798
CHAN, H. M. N91-26374
CHANDA, T. N91-26306
CHANDRASEKARAN, B. N91-26865
CHANG, E. I. N91-26792
CHANG, H. L. M. N91-26986
CHANG, LI W. N91-26784
CHANG, S. L. N91-26946
CHANG, Y. W. N91-26487
CHANTIKUL, P. N91-26374
CHAO, A. W. N91-26917
CHARTOFF, RICHARD P. N91-26355
CHEBOTAREV, R. P. N91-26177
CHEN, C. H. N91-26524
CHEN, G. N91-26567
CHEN, J. L. S. N91-26467
CHEN, K. C. N91-26953
CHEN, P. J. N91-26274
CHEN, R. N91-26963
CHEN, SHIYI N91-26484
CHEN, T. N. N91-26530
CHENG, C. C. N91-26248
CHEPLICK, J. M. N91-26602
CHERNOV, A. A. N91-26167
CHESSON, CHARLES V., II N91-26755
CHHABILDAS, L. C. N91-26186
CHIANG, J. F. N91-26220
CHICK, C. J. N91-26256
CHIEN, T. H. N91-26489
CHILCOTT, GARY A. N91-26866
CHILDS, DARA W. N91-26541
CHO, B. H. N91-26204
CHO, HYUN-NAM N91-26365
CHO, S. Y. N91-26283
CHOU, Y. T. N91-26983
CHOW, CHUEN-YEN N91-26477
CHOW, TA-TUNG N91-26778
CHOYKE, W. J. N91-26252
CHRISTEN, D. N91-26982
CHRISTENSEN, PHILIP R. N91-27059
CHRISTMAN, R. F. N91-26601
CHRISTOPHOROU, L. G. N91-26911
CHU, D. N91-26311
CHU, NHI-ANH N91-26802
CHU, TAK-KIN N91-26925
CHUNG, SOON M. N91-26826
CHVYAKIN, V. A. N91-26684
CHYLEK, PETR N91-26502
CIARAVINO, VICTOR N91-26677
CIVALE, L. N91-26982
CLAFFY, GEORGE J. N91-26196
CLANCY, R. T. N91-27060
N91-27072
CLARK, ARTHUR E. N91-26536
CLARK, G. A. N91-26834
CLARK, G. M. N91-26133
CLARK, L. SCOTT N91-27033
CLARKE, J. N91-26464
N91-26981
CLARKE, NORMAN P. N91-26406
CLARKE, THEODORE C. N91-27024
CLAUSER, JOHN F. N91-26896
CLEMEN, L. N91-26252
CLINE, NEAL N91-27021
CLOUGH, R. L. N91-26382
COFFEY, D. N91-26292
COFFEY, D. W. N91-26242
COFFEY, H. E. N91-27083
N91-27084
N91-27085
N91-27086
COHEN, GERALD C. N91-26797
COHEN, J. B. N91-26290
COHEN, PAUL R. N91-26819
N91-26828
COHEN, S. N91-26272
COLAIANNI, M. L. N91-26274
COLCLOUGH, M. S. N91-26981
COLE, ARTHUR N. N91-26404
COLLETTE, T. W. N91-26601
COLLINS, G. N91-26551
COLTRIN, M. E. N91-26285
COMBES, M. N91-26175
COMPTON, R. N. N91-26909
CONG, NGUYEN HUU N91-26835
CONNER, KELLY J. N91-26541
CONRY, SUSAN E. N91-26818
N91-26819
CONSAGA, JOHN P. N91-26392
CONWAY, TERRY L. N91-26717
COOLBAUGH, M. T. N91-26253
N91-26255
COON, P. A. N91-26262
N91-26263
N91-26264
N91-26267
COOPER, A. W. N91-26498
COOPER, BARBARA H. N91-26899
COOPER, DAVID G. N91-26923
COOPER, JOHN N91-26505
COOPER, RANDY N91-26461
COPLIN, K. A. N91-27002
COPPOLA, ANTHONY N91-26993
N91-26994
CORRIGAN, ROBERT D. N91-26543
COUCH, W. N91-27051
COUPRY, GABRIEL N91-26153
COYNE, J. T. N91-26755
CRAIG, ALAN N91-27003
CRATCH, P. N91-26433
CRAWFORD, F. N91-27050
CRISTENSEN, C. P. N91-26509
CRITTENDEN, E. C., JR. N91-26498
CROCKETT, THOMAS W. N91-26767
CROFT, W. B. N91-26820
N91-26828
N91-27006
CROMACK, K. N91-26331
CRONAN, TERRY A. N91-26717
CROSLEY, JOHN K. N91-26754
CUNNOLD, D. M. N91-26654
CYPRYK, MAREK N91-26370

D

DAHL, P. H. N91-26880
DAHLBURG, J. P. N91-26470
DAHLBURG, R. B. N91-26470
DALLMAN, MARY F. N91-26720
DALRYMPLE, MATHIEU A. N91-26738
DALTON, LARRY R. N91-26364
DANA, ROGER A. N91-26418
DANDL, R. A. N91-26942
DANDRIDGE, ANTHONY N91-26924
DANFORD, M. D. N91-26312
DANISZEWSKI, EDWARD J. N91-26444
DANTZIG, GEORGE B. N91-26788
N91-26789
DARCHIYEVA, L. A. N91-26172
DARLINGTON, DANIEL N. N91-26720
DAS, G. P. N91-26308
DAS, PANKAJ K. N91-26430
DAVIS, P. A. N91-27062
DAVIS, ROGER L. N91-26145
DAVIS, WILLIAM H. N91-26184
DAY, WILLIAM B. N91-26811
DEAN, WILLIAM E. N91-26138
DEBANY, WARREN H., JR. N91-26441
DEBOO, J. C. N91-26938
DECKER, JENNIE J. N91-26743
N91-27007
N91-27008
DEGTYAREV, V. I. N91-26173
DEHART, C. N91-26591
DEHOFF, RONALD N91-26205
DEITZ, VICTOR R. N91-26753
DEJONGE, J. B. N91-26152
DELAHOUSSAYE, PAUL R. N91-26950
DELCUETO, J. N91-26591
DELEEUW, F. A. A. M. N91-26638
DELEMAN, BERNARD N91-26449
DEMAIN, A. L. N91-26680
DEMAR, PHIL N91-27025
DEMBEK, A. A. N91-26344
DEMORZHI, M. S. N91-26703
DEMPSEY, BARRY J. N91-26161
DENTON, GEORGE H. N91-26577
DEPAULA, RAMON N91-27119
DERENDYAYEVA, T. A. N91-26693
DESANTO, JOHN A. N91-26426
DESROCHERS, GEORGE R. N91-26128
DETRICK, ROBERT S. N91-26634
DEUSTER, P. A. N91-26711
N91-26715
DEUTY, S. N91-26204
DEVATY, ROBERT P. N91-26219
DEXTER, JAMES L. N91-26505
N91-26923
DEY, DIPAK K. N91-26547
DHARANI, L. R. N91-26382
DIBATTISTA, JOHN N91-27119
DICKEY, J. N91-26469
DIEFFENBACH, CARL W. N91-26731
DIEMAND, DEBORAH N91-26348
DIGIROLAMO, ROBERT D. N91-26149
DILLARD, D. A. N91-26559
DILLON, A. C. N91-26265
N91-26266
N91-26267
DILLON, M. P. N91-26382
DINWIDDIE, R. B. N91-26240
DMITRIADI, D. N91-26179
DOANE, GEORGE B., III N91-26201
DOBROVOLSKIS, A. N91-27056
DODONOV, V. V. N91-26893
DOIRON, SCOTT D. N91-26651
DOLLAR, MAREK N91-26303
DOMMANUS, H. M. N91-26489
DONLEY, SHAWN T. N91-26149
DOONG, S. H. N91-26214
DORNEY, DANIEL J. N91-26145
DORRIS, S. E. N91-26971
DOSS, HANI N91-26546
DOUBT, T. J. N91-26710
N91-26711
N91-26715
DOYLE, J. H. N91-26798
DOZOIS, CLAUDE G. N91-26633
DRAGONETTE, LOUIS R. N91-26475
DRESCHEL, T. W. N91-26759
DRESSER, M. J. N91-26248
N91-26252
DRIELS, MORRIS R. N91-26532
DRIGA, M. D. N91-26185
DRISCOLL, J. F. N91-26278
DUCKWORTH, R. JAMES N91-26800
DUDEK, F. E. N91-26675
DUNCAN, JOHN C. N91-26748
DUNCAN, S. N91-26741
DUNN, MARTY N91-26227
DURKOT, M. J. N91-26728
DUTKA, A. J. N91-26715
DUTKA, ANDREW J. N91-26673
DYE, CRAIG J. N91-26743
DYE, R. C. N91-26515
DYMEK, STANISLAW N91-26303

E

EARTHMAN, JAMES C. N91-26307
EBERMAN, BRIAN N91-26535
ECKEL, M. N91-26556
EDDY, DOUGLAS R. N91-26738
EDDY, M. M. N91-26981
EDER, D. C. N91-26517
EDMOND, J. A. N91-26439
EDWARDS, STEPHEN N91-26770
EGETH, HOWARD N91-26742
EGGERT, K. N91-26484
EIDLER, P. N91-26463
EISELE, U. N91-26557
EISINGER, MAGDALENA N91-26730
EITZEN, D. G. N91-26882
EK, M. N91-26635
EL-SAYED, M. A. N91-26249
EL-SAYED, MOSTAFA A. N91-26247
ELDRIDGE, J. I. N91-26233
ELIAHOU, SHAUL N91-26590
ELLIS, D. E. N91-26290
ELLIS, STEPHEN R. N91-26142
EMILIANI, M. L. N91-26226
EMMONS, DONALD A. N91-26443
ENGEL, THOMAS N91-26269
EPPERSON, J. E. N91-26294
EPSTEIN, A. J. N91-26244
N91-26250
N91-26251
N91-26330
N91-26331
N91-26332
N91-26333
N91-26335
N91-26336
N91-26337
N91-26339
N91-26340
N91-26345
EPSTEIN, ARTHUR J. N91-26334
ERBER, T. N91-26563
ERDEMIR, A. N91-26379
ESAREY, E. N91-26503
ESENER, SADIK N91-27003
ESKOW, ELIZABETH N91-26778

ESPOSITO, L. N91-26175
ESTEROWITZ, LEON N91-26506
ESTLER, R. C. N91-26515
ESTRADA, ARTHUR T. N91-26864
ETZKORN, J. W. N91-26525
EVANS, T. E. N91-26939

F

FAETH, G. M. N91-26278
FALSETTI, CHRISTINE M. N91-27012
FAORO, J. E. N91-26214
FEILD, C. N91-26982
FEINGOLD, GRAHAM N91-26652
FENG, LIANG N91-26148
FENG, WILLIAM W. N91-26223
N91-26560
FERBER, M. K. N91-26242
FERGUSON, D. C. N91-27068
FERNAU, M. E. N91-26604
FETROW, FRED N91-27118
FIELDS, ERIK N91-26662
FILER, ELIZABETH D. N91-26514
FINDLAY, J. G. N91-26468
FISCHER, R. P. N91-26492
FISHER, GENE N91-26797
FISHER, R. J. N91-26653
FISHER, VERNIE G. N91-26427
FISHER, Y. N91-26769
FLAGG, C. N. N91-26668
FLAGG, R. S. N91-27047
FLAHERTY, JOSEPH E. N91-26850
FLAMM, DAVID S. N91-26833
FLIFLET, A. W. N91-26492
FLOYD, STEPHEN A. N91-26806
FLYNN, ANITA M. N91-26446
FOELL, W. K. N91-26595
FOLKERS, JOHN P. N91-26302
FOLTYN, S. R. N91-26515
FONG, C. Y. N91-26977
FONG, E. N. N91-27000
FONG, S. O. N91-26228
FORD, DONNIE R. N91-26806
FORSYTHE, K. W. N91-26411
FORTE, V. A., JR. N91-26728
FORTMANN, R. C. N91-26746
FORTNEY, L. R. N91-26912
FOX, MARYE A. N91-26246
FRANCHI, R. E. N91-26877
FRANKLIN, M. J. N91-26316
FRAZIER, W. E. N91-26306
FREAR, D. R. N91-26319
FREEMAN, ARTHUR J. N91-26239
N91-26298
FREITAS, JOHN E. N91-26247
FRICK, S. E. N91-26882
FRIEDMAN, M. N91-26448
FRINCKE, DEBORAH N91-26797
FROMM, DAVID M. N91-26877
FU, C. L. N91-26325
FU, YANSONG N91-26206
FUJIEDA, I. N91-26904
FUKAO, SHOICHIRO N91-26613
FUNTOVA, I. I. N91-26687

G

GABRIELI, H. N91-26433
GADDIS, L. N91-27056
GAGE, MARK N91-26205
GAIER, J. R. N91-27061
GAILLARD, M. K. N91-26992
GAINES, G. L. N91-26980
GALLAGHER, P. K. N91-26333
GALLIANO, J. A. N91-26655
GALLUP, R. F. N91-26977
GALPERIN, YU. I. N91-26171
GAMACHE, ROBERT R. N91-26633
GAMMA, L. O. N91-26999
GANPANTSEROVA, O. F. N91-26175
GAO, Y. N91-26979
N91-26986
GAO, YUANPING N91-26382
GAONKAR, GOPAL H. N91-26134
GARNER, JAMES M. N91-26116
GARVEY, JAMES F. N91-26253
N91-26255
N91-26343
GARY, J. PATRICK N91-27009
N91-27015
N91-27030
GAYVERT, ROBERT T. N91-26830
GAZENKO, O. G. N91-26686
GEBALLE, THEODORE H. N91-26965
GEIL, P. H. N91-26338
GENT, ALAN N. N91-26210
GEORGE, M. H. N91-26721
GEORGE, S. M. N91-26262
N91-26263
N91-26264
N91-26265
N91-26266
N91-26267
N91-26508
GEORGE, THOMAS F. N91-26455
N91-26875
N91-26893
N91-26894
N91-26963
GEORGIYEVSKIY, V. S. N91-26705
GEORGOPOULOS, P. N91-26597
GESTELAND, R. F. N91-26676
GHAFOOR, ARIF N91-26826
GHANDEHARI, MOSTAFA N91-26840
GIBBS, H. N91-26799
GIBBS, HYATT M. N91-26926
GILAT-CYGEILMAN, RIVKA N91-26232
GILL, ROBERT J. N91-26273
GILMOUR, PHILLIP N91-26948
GINDER, J. M. N91-26250
N91-26340
N91-26345
N91-27002
GINEVAN, M. E. N91-26746
GINSBERG, JERRY H. N91-26476
GIROLAMO, HENRY N91-26752
GIROSI, FEDERICO N91-26782
N91-26810
GLADDEN, E. N91-26997
GLADYSHEV, V. A. N91-26171
GLASER, JOHN N91-26156
GLATTER, I. N91-26358
GLAUDELL, GENE A. N91-27048
GLENDINNING, S. G. N91-26943
GOLD, BERNARD N91-26414
GOLDHABER, G. N91-27051
GOLDMAN, T. N91-26915
GOLDSMITH, WERNER N91-26564
GOLDSTEIN, J. I. N91-27053
GOLDSTEIN, STANLEY H. N91-27088
N91-27103
GOLOMBEK, M. P. N91-27062
GONCHAROV, I. B. N91-26692
GONZALEZ, J. A. N91-26437
GOO, GEE-IN N91-26450
GOODING, JAMES L. N91-27063
GOODMAN, JOHN M. N91-26416
GORDON, MARK S. N91-26366
GORDON, W. L. N91-26976
GOROSHKOVA, N. V. N91-26175
GOSHAW, A. T. N91-26912
GOSSELIN, DAVE N91-26800
GOSZ, M. N91-26212
GOTTLIEB, C. N91-26286
GOTTWALD, JAMES A. N91-26889
GOVINDAN, T. R. N91-26989
GRABERT, GREGORY N91-26948
GRAESSER, E. J. N91-26568
GRAHAM, R. A. N91-26399
GRATE, JAY W. N91-26254
GREELEY, RONALD N91-27056
N91-27057
N91-27064
N91-27071
N91-27081
GREEN, PETER N91-26800
GREENMAN, W. B. N91-27047
GREICHEN, K. R. N91-26554
GREINER, HELEN N91-26539
GRIFFIN, ANSELM C. N91-26373
GRIFFIN, O. HAYDEN, JR. N91-26238
GRIGORYEV, A. I. N91-26178
N91-26686
GRIGORYEV, S. A. N91-26171
GRISSON, WILLIAM M. N91-26197
GROSS, K. C. N91-26863
GROVER, J. R. N91-26253
GROVER, PAUL E. N91-26545
GROVES, SCOTT E. N91-26223
GRUBIN, H. L. N91-26989
GRUNAU, D. N91-26484
GRUTZECK, M. W. N91-26279
GUCCIONE, SALVADORE J., JR. N91-26674
GUEST, G. E. N91-26942
GUHA, S. N91-26322
GUIMARAES, PATRICIA T. N91-26651
GUL, V. YE. N91-26453
GUPTA, K. K. N91-26113
GUPTA, P. N91-26262
N91-26263
N91-26264
N91-26265
GUPTA, RADHA R. N91-26129
GURALNICK, S. A. N91-26563
GYEKENYESI, JOHN Z. N91-26234

H

HABERLE, ROBERT M. N91-27057
N91-27082
HABTE-MARIAM, YITBAREK N91-26361
HACHEM, NABIL I. N91-26826
HAERTLING, GENE H. N91-26948
HAGEDORN, K. E. N91-26556
HAGFORS, TOR N91-26623
HAJALI, RAMI N91-26218
HALL, C. A. N91-26187
HALL, J. S. N91-26763
HALL, JEFFERY L. N91-26281
HALL, RALPH M. N91-27046
HALL, ROBERT J. N91-26791
HALLANDER, J. E. N91-26887
HALLENBECK, JOHN M. N91-26673
HALLET, BERNARD N91-26628
HALLOCK, GARY A. N91-26944
HALLOCK, R. B. N91-26949
HAMEED, S. N91-26606
HAMILTON, DAVID B. N91-26757
HAMILTON, N. N91-27050
HAN, M. Y. N91-26266
HANDY, J. N91-27075
HANN, RAIFORD E. N91-26872
HANN, S. W. N91-26943
HANSEN, J. B. N91-26464
HARDGREAVES, T. A. N91-26492
HARDING, L. B. N91-26902
HARIHARAN, RAMAKRISHNAN N91-26328
HARRIS, D. N91-26997
HARRIS, J. M N91-26207
HARRIS, J. M. N91-26268
N91-26271
N91-26676
HARRISON, R. J. N91-26902
HART, JIM N91-27010
HART, MAXWELL M. N91-27093
HARVEY, J. A. N91-26293
HASHISH, MOHAMED N91-26405
HASSOUN, JOHN A. N91-26125
N91-26130
HATFIELD, WILLIAM E. N91-26951
HAUER, ROBERT L. N91-26543
HAUSERMAN, W. B. N91-26528
HAUSMANN, JOHN C., JR. N91-26727
HAW, JAMES F. N91-26282
HAWICK, K. A. N91-26294
HAWKE, R. S. N91-26187
HAWTHORNE, J. F. N91-26907
HAWWA, MUHAMMAD A. N91-26209
HAYES, B. C. N91-26193
HAZELBECK, D. N91-26358
HAZEN, VERNON L. N91-26756
HE, QIANYUAN N91-26562
HEDGES, L. V. N91-26741
HEIMANN, PAUL J. N91-26234
HELLWARTH, ROBERT W. N91-26929
HEMBREE, STEPHEN C. N91-26671
HENCHMAN, MICHAEL N91-26940
HENDREY, G. R. N91-26609
HENESIAN, M. A. N91-26523
HERDMAN, T. L. N91-26117
HERMAN, R. G. N91-26243
HERNANDEZ, J. E. N91-26834
HERON, W. J. N91-26253
HERRON, WILLIAM J. N91-26343
HESSLER, J. P. N91-26516
HEWETT, C. A. N91-26950
HEWETT, MARLE D. N91-26140
HIHARA, L. H. N91-26220
HILL, N. W. N91-26293
HILLARD, G. B. N91-27068
HINKLE, C. R. N91-26759
HITCHCOCK, GARY N91-26672
HITE, GERALD E. N91-27094
HOCKING, W. K. N91-26620
HODGDON, JAMES A. N91-26755
HOFFMAN, M. Z. N91-26324
HOHENWARTER, G. K. N91-26962
HOLAHAN, PATRICIA K. N91-26677
HOLCOMB, LEE N91-27119
HOLDEMAN, J. D. N91-26146
HOLLANDER, MYLES N91-26546
HOLLER, ROGER A. N91-26537
HOLLINGSWORTH, R. N91-26591
HOLMES, J. T. N91-26398
HOLST, T. N91-26464
HOLTSLAG, A. A. N91-26635

HOLTZBERG, F. N91-26982
HOOD, RAY N91-27119
HOOK, AUDREY A. N91-26773
HOOKER, JOHN C. N91-27095
HORDINSKY, J. R. N91-26721
HORTON, J. A. N91-26322
HOSKING, F. M. N91-26570
HOTA, NAVEEN N91-26784
HOU, P. Y. N91-26974
HOUBOLT, JOHN C. N91-26150
HOUSTON, J. E. N91-26495
HOVER, G. L. N91-26751
HOWARD, DAVID E. N91-26459
HOWE, JAMES M. N91-26301
HOWE, JOHN B. N91-26644
HOYLE, S. N91-26279
HOYT, R. W. N91-26728
HSU, N. N. N91-26882
HSUEH, KESYIN F. N91-26329
HU, QING N91-26973
N91-26991
HUANG, H. C. N91-26189
HUBBARD, C. M. N91-26242
HUBBARD, G. S. N91-27080
HUBER, C. C. N91-26608
HUDSON, JOHN A. N91-26449
HUFFER, FRED W. N91-26852
HUGHES, PHIL N91-26203
HUGHES, W. J. N91-26561
HUGHES, WILLIAM F. N91-26479
HUMENIK, K. E. N91-26863
HUNNICUTT, M. L. N91-26207
HUNTER, PAUL N91-27119
HUNTSBERGER, TERRY N91-27096
HURWITZ, FRANCES I. N91-26234
HUSSAIN, FAZLE N91-26471
HUTTENLOCHER, JANELLEN N91-26741
HWANG, SEUNG J. N91-26303

I

IGNATYUK, A. N. N91-26707
IKELS, KENNETH G. N91-26136
ILYINA-KAKUYEVA, YE. I. N91-26703
INFANGER, GERD N91-26789
INLOW, MARK N91-26725
INTERRANTE, L. V. N91-26342
ISAACS, R. G. N91-26189
ISAYEV, G. G. N91-26699
ISHIDA, HATSUO N91-26964
ISIK, CAN N91-26422
ISRAELI, EITAN N91-26869
ITOH, TATSUO N91-26445
IU, KAI-KONG N91-26382
IVAKHNENKO, I. N91-26462
IVANOV, A. P. N91-26692
IVANOV, M. A. N91-26176
IVANOVA, I. YE. N91-26693
IVANOVA, T. A. N91-26172
IVASHKIN, V. V. N91-26169
IVERSEN, J. D. N91-27056
N91-27065
IVES, J. T. N91-26676
IWANICKO, E. N91-26591

J

JACKSON, LENORE A. N91-27009
N91-27028
JACOBS, E. W. N91-26769
JACOBS, MICHAEL J. N91-26427
JACOBS, STANLEY S. N91-26575
JACOBS, STEPHEN N91-26921
JACOBY, ANAT N91-26749
N91-26808
JAKOSKY, BRUCE M. N91-27066
JANG, GUANG-WAY N91-26329
JANGHORBANI, MORTEZA N91-26719
JANKOWSKI, A. N91-26241
JARVAISE, JEANNE M. N91-26143
JARVIS, ROBERT L. N91-26387
JAYNES, E. T. N91-26420
JEFFRIES, W. R., III N91-26654
JENKINS, JAMES N91-27119
JENSEN, BRIAN J. N91-26377
N91-26378
JENSEN, D. R. N91-26625
JENSSEN, H. P. N91-26521
JESSUP, E. R. N91-26854
JEWULSKI, J. R. N91-26970
JOHANSEN, J. D. N91-26949
JOHNSON, ARDEN P. N91-26589
JOHNSON, BURGESS N91-26959
JOHNSON, D. L. N91-26654
JOHNSON, DEBRA STEELE N91-27097
JOINER, R. G. N91-26416
JOLLY, C. A. N91-26353
JONES, MEDLINDA D. N91-26589
JONES, ROBERT L. N91-26224
JONES, T. E. N91-26728
JORY, H. R. N91-26942
JOYCE, G. N91-26503
JOYCE, S. A. N91-26495
JOZEFOWICZ, M. E. N91-26332
JUERGENSEN, H. N91-26436
JULISCH, P. N91-26557
JUSTUS, C. G. N91-26654

K

KABITSKIY, YE. N. N91-26691
KACHELMYER, A. L. N91-26411
KAEGI, EMIL M. N91-26115
KALLIANPUR, GOPINATH N91-26860
KAN, YE. L. N91-26700
KANDER, ILAN N91-26460
KANE, R. L. N91-26604
KANKAM, M. DAVID N91-26870
KANN, K. N91-26690
KAPITULNIK, AHARON N91-26965
KAPLAN, D. I. N91-27067
KAPOOR, VIK J. N91-26434
N91-26436
KARGER, A. N91-26676
KARIMI, AMIR N91-27098
KASI, S. R. N91-26272
KAST, B. A. N91-26936
KATO, SUSUMU N91-26614
KAUFFMAN, JOEL M. N91-26499
KAZAKOV, G. T. N91-26704
KAZANOVSKAYA, I. N91-26695
KEDZIERAWSKI, ANDRZEJ WLADYSLAW N91-26876
KEE, R. J. N91-26285
KEEFE, L. R. N91-26119
KEEGAN, K. D. N91-27076
KEFFER, CHARLES E. N91-26637
KELLEY, PAUL L. N91-26920
KELLY, J. N91-26374
KELLY, PATTIE L. N91-27007
KELLY, THOMAS JEROME N91-27054
KENNEALY, JOHN P. N91-27048
KEPLER, KEITH D. N91-26951
KEPPLER, E. E. N91-26295
KERBACHER, JAMES J. N91-26677
KERLEY, G. I. N91-26186
KERSEY, ALAN D. N91-26924
KERSTEN, R. T. N91-26525
KEY, J. N91-26666
KHALFAN, H. N91-26777
KHURGIN, J. N91-26960
KIERSTEAD, J. A. N91-26990
KIGGANS, J. O. N91-26242
KILKENNY, J. D. N91-26943
KILLEEN, TIMOTHY L. N91-26631
KILLINGSWORTH, PAUL S. N91-26143
KIM, H. J. N91-26467
KIM, HYEONGDONG N91-26944
KIM, HYOUN-EE N91-26380
KIM, J. N91-26635
KIM, JONG R. N91-26879
KING, DAVID Q. N91-26198
KINGSTON, J. J. N91-26981
KINNEY, GILBERT F. N91-26837
KIRK, JOHN N91-26722
KIRK, MARTIN L. N91-26951
KISER, J. D. N91-26233
KITAMURA, K. N91-26937
KITSOPOULOS, T. N. N91-26256
KITZMILLER, CHARLES T. N91-26786
KLENART, JOHN N91-27019
KLIER, K. N91-26243
KLIPEC, KATHERINE N91-26833
KLOBUCHAR, J. A. N91-26416
KLOSTERMEYER, JUERGEN N91-26621
KLOTS, C. E. N91-26909
KNOTT, W. M. N91-26759
KNOWLTON, T. M. N91-26468
KOBAYASHI, A. S. N91-26229
KOEHLER, B. G. N91-26262
N91-26263
N91-26264
N91-26508
KOERT, PETER N91-26630
KOHLMAN, WILLIAM G. N91-26360
KOHN, ROBERT V. N91-26843
KOLB, C. E. N91-26283
KOLECKI, J. C. N91-27068
KONRAD, C. H. N91-26187
KOONTZ, M. D. N91-26746
KOPELL, N. N91-26845
KORNILOVA, L. N. N91-26698
N91-26706
KOSANOVICH, M. N91-26529
KOSS, D. A. N91-26299
KOSZORU, ARTHUR A. N91-26391
KOTOVSKAYA, A. R. N91-26705
KOVALENKO, YE. A. N91-26694
KOVARIK, F. N91-26484
KOWALSKI, JOSEPH F. N91-26756
KOZLOVSKAYA, I. B. N91-26178
N91-26686
KRALL, J. N91-26448
KRALLIS, K. N91-26388
KRASILNIKOV, P. S. N91-26164
KRAUKLIS, A. N91-26695
KRAUT, ROBERT E. N91-26787
KRISTIANSEN, M. N91-26382
KROES, ROGER L. N91-26968
KROTOV, V. P. N91-26704
KRUEGER, ARLIN J. N91-26651
KRUKEMYER, T. H. N91-26317
KRUKONIS, VAL J. N91-26341
KRUSE, ROBERT J. N91-26548
KRYMSKIY, A. M. N91-26174
KSANFORMALITI, L. V. N91-26175
KUHN, G. D. N91-26119
KUPRIYANOV, V. A. N91-26700
KURDILA, ANDREW J. N91-27099
KUROKAWA, KO N91-27007
N91-27008
KUZINA, V. I. N91-26705
KUZNETSOV, S. L. N91-26702
KWAN, S. N91-26279
KWOK, MUNSON A. N91-26115
KWON, S. N91-26278
KYRAZIS, D. T. N91-26518

L

LACOVARA, R. C. N91-27100
LAGEN, NICHOLAS T. N91-26159
LAGUTIN, M. F. N91-26584
LAI, M. C. N91-26146
LAIBINIS, PAUL E. N91-26302
LALLEMENT, PIERRE N91-26630
LAM, D. J. N91-26986
LAM, JUAN F. N91-26926
LANCASTER, N. N91-27056
LANDRAM, C. S. N91-26485
LANDRY, JOSEPH F. N91-26923
LANE, P. V. Z. N91-26668
LANGE, FRED F. N91-26221
LANGE, J. P. N91-26243
LANGER, S. H. N91-26519
LANKFORD, JAMES, JR. N91-26235
N91-26236
N91-26237
N91-26534
LARKO, DAVID E. N91-26651
LAROSA, J. N91-26279
LARSEN, M. F. N91-26622
LARSON, D. C. N91-26293
LARSON, N. M. N91-26293
LASSILA, K. E. N91-26903
LASTER, R. N91-26489
LATANISION, R. M. N91-26220
LATHABAI, S. N91-26374
LAU, SONIE N91-26796
LAU, STEPHEN N91-26479
LAU, Y. Y. N91-26448
LAUCHLE, G. C. N91-26883
LAVERNIA, E. J. N91-26306
LAVERNIA, ENRIQUE J. N91-26307
LAVERY, DAVID N91-27119
LAWLESS, BROTHER DESALES N91-27101
LAWVER, B. S. N91-26834
LAYNE, CHARLES S. N91-27102
LEACH, RODMAN N. N91-27056
N91-27069
N91-27070
N91-27071
N91-27081
LEADBETTER, M. R. N91-26860
LEAKEAS, C. L. N91-26941
LEAVITT, DENNIS D. N91-26726
LEE, BURTRAND N91-26948
LEE, F. C. N91-26204
LEE, J. N91-26605
LEE, J. L. N91-26643
LEE, PETER C. N91-26458
LEE, S. W. N91-27060
N91-27072
LEE, T. R. N91-26208
N91-26277
N91-26302

LEHOCZKY, SANDOR L. N91-26968
LEIB, TERRY K. N91-26678
LEITNER, ARNOLD N91-26913
LENG, J. M. N91-26250
N91-27002
LEON, MARK N91-27013
LEREAH, YOSSI N91-26969
LESSER, VICTOR R. N91-26819
N91-26820
N91-26831
LESUER, D. R. N91-26318
LEV, BRIAN N91-27029
LEVER, A. B. N91-26206
N91-26260
N91-26261
LEVINE, RICHARD R. N91-26754
LEVY, MOISES N91-26954
LEVY, P. W. N91-26990
LEVY, SAUL Y. N91-26763
LEWIN, K. F. N91-26609
LEWIS, TOM N91-27046
LI, GANG N91-26857
LI, XIPING N91-26511
LI, Y. N91-26979
LI, Z. Y. N91-26875
LICATA, J. P. N91-27087
LICHON, PAUL G. N91-26198
LICHTENBERGER, K. S. N91-26984
LIDOV, M. L. N91-26163
LIEHR, M. N91-26272
N91-26456
LIGHT, BONNIE N91-26919
LIM, BENG-HONG N91-26764
LIN, D. L. N91-26875
N91-26963
LIN, JIANN N91-26243
LINDEN, SHWN-MEEI N91-26355
LING, HAO N91-26944
LIOU, K. N. N91-26643
LIPFERT, F. W. N91-26609
N91-26610
LIPPMANN, RICHARD P. N91-26414
N91-26792
N91-26795
LITOVCHENKO, V. N91-26462
LITZINGER, THOMAS A. N91-26393
N91-26394
LIU, C. T. N91-26321
N91-26323
N91-26983
LIU, FUPING N91-26586
LIU, HUA-KUANG N91-26918
LIU, XIUYUN N91-26511
LLOYD, CHARLES J. N91-26743
LOH, E. N91-26484
LOHRENZ, MAURA C. N91-26587
LONG, CHARLES E. N91-26661
LONGBOTHAM, HAROLD N91-26729
LOTT, S. N91-26463
LOTTES, S. A. N91-26946
LUEY, KENNETH T. N91-26305
LUKENS, JAMES N91-26952
LUKES, A. N91-26287
LUKYANYUK, V. YU. N91-26705
LURMANN, F. R. N91-26597
LUSEBRINK, HELMUT N91-26155
LUSHER, J. A. N91-26540
LUZZI, DAVID E. N91-26356
LYNCH, NANCY A. N91-26780

M

MA, D. C. N91-26487
MA, YU-QUIANG N91-26875
MACDIARMID, ALAN G. N91-26244
N91-26245
N91-26251
N91-26329
N91-26330
N91-26331
N91-26333
N91-26334
N91-26335
N91-26336
N91-26337
N91-26339
N91-26340
N91-26345
N91-26347
MACKENZIE, J. D. N91-26276
MAHRT, L. N91-26635
MAIDANIK, G. N91-26469
MAKEIG, SCOTT N91-26725
MAKOWIECKI, D. N91-26241
MALKUS, D. S. N91-26472
MALOZEMOFF, A. P. N91-26982
MANG, M. N. N91-26344
MANGELSDORFF, A. D. N91-26736
MANHEIMER, WALLACE M. N91-26425
MANKO, OLGA V. N91-26893
MANNA, ZOHAR N91-26774
MANNING, JAMES M. N91-26712
MANOHAR, S. K. N91-26245
N91-26330
N91-26347
MAPLE, M. B. N91-26953
MARBOE, R. C. N91-26884
MARCINKOWSKI, SLAWOMIR J. N91-26826
MARCZYNSKI, THADDEUS J. N91-26716
MARSHALL, C. N91-26591
MARSHALL, D. B. N91-26359
MARTIN, CHARLES R. N91-26349
N91-26367
MARTIN, RODERICK H. N91-26569
MARTIN, S. J. N91-26888
MARVIN, H. N91-27050
N91-27051
MARVIN, MARK N91-26405
MARWICK, A. D. N91-26982
MARYNICK, DENNIS S. N91-26352
MASLANIK, J. A. N91-26666
MASNOVI, JOHN N91-26234
MASON, T. O. N91-26290
MASTERS, J. G. N91-26245
N91-26251
N91-26331
N91-26332
N91-26347
MASUI, H. N91-26260
MATTHEWS, JOHN D. N91-26406
MATYJASZEWSKI, KRZYSZTOF N91-26368
N91-26369
N91-26370
N91-26371
N91-26372
MAUNEY, JON N91-26801
MAXWORTHY, T. N91-26664
MAYNARD, SHAWN N91-26282
MAZDIYASNI, K. S. N91-26953
MAZOR, EDI N91-26483
MAZUMDAR, PRANAB K. N91-26565
MCCALL, R. P. N91-26250
N91-26340
N91-27002
MCCONNELL, S. O. N91-26880
MCCUE, L. F. N91-26213
MCCUNE, J. E. N91-26120
MCDADE, IAN C. N91-26596
MCDANIEL, G. L. N91-26999
MCDANIEL, S. T. N91-26886
MCDONALD, CATHERINE W. N91-26773
MCELFRESH, M. W. N91-26982
MCGREEVY, MICHAEL WALLACE N91-26142
MCGUIRE, J. M. N91-26601
MCKEAGUE, IAN W. N91-26852
MCKENNA, EDWARD N91-26626
MCKERNAN, M. A. N91-26241
MCKINLEY, RICHARD L. N91-26427
MCKOY, VINCENT N91-26898
MCLANDRICH, M. N. N91-26930
MCLAREN, A. S. N91-26666
MCMURRY, P. H. N91-26598
MCNEESE, MICHAEL D. N91-26748
MCPHAIL, A. T. N91-26949
MCWHORTER, ALAN L. N91-26958
MEARS, C. A. N91-26973
N91-26991
MEDELIUS, P. J. N91-26656
MEIER, M. L. N91-26318
MELAD, CHEMESSE N91-26481
MELISSINOS, A. C. N91-26507
MELNIKOVA, G. K. N91-26453
MELTZ, MARTIN L. N91-26677
MENDILLO, MICHAEL N91-26632
MENKER, LAVERN J. N91-26995
MENTOR, D. N91-26591
MENYUK, NORMAN N91-26920
MERKLE, K. L. N91-26979
N91-26986
MESSICK, L. J. N91-26436
MESZTENYI, CHARLES K. N91-26842
MEUSER, R. B. N91-26571
MEYER, ROBERT A. N91-26818
N91-26819
MICHAEL, J. R. N91-26319
MICHALSKI, K. A. N91-26423
MICHALSON, BILL N91-26800
MIKHAYLOV, V. M. N91-26705
MIKLICH, A. H. N91-26981
MILES, R. N91-26463
MILLER, HARVEY I. N91-26713
MILLER, JAMES N91-26921
MILLER, M. K. N91-26314
MILLER, WILLIAM V. N91-26540
MILNE, E. A. N91-26498
MINK, RICHARD B. N91-26673
MINOR, THOMAS C. N91-26391
MINSTER, B. N91-26612
MITO, T. N91-26937
MIZUKAMI, S. N91-26937
MODESTINO, JAMES N91-26821
MOELLER, MARTIN N91-26370
MOHAMED, F. A. N91-26306
MOIR, R. W. N91-26947
MOLINELLI, EUGENE N91-26658
MOLLEY, P. A. N91-26936
MONSERUD, DAVID N91-26405
MONTEIRO, S. N91-26975
MONTEMERLO, MELVIN N91-27119
MONTGOMERY, ELLYN T. N91-26663
MONTGOMERY, F. N91-26358
MONTGOMERY, L. C. N91-26711
MOOK, DEAN T. N91-26558
MOON, FRANCIS C. N91-26191
MOORE, H. J. N91-27073
MOORE, J. A. N91-26342
MOORE, R. E. N91-26362
MOORHEAD, A. J. N91-26380
MORAN, B. N91-26212
MORAN, C. N91-26386
MORE, K. L. N91-26242
MOREY, WILLIAM A. N91-26725
MORGAN, J. N91-26530
MORGAN, PAUL N91-27104
MORGAN, STEVEN H. N91-26313
MORISSETTE, S. L. N91-26971
MORITA, HIROSHI N91-26247
MOROZ, V. I. N91-26175
MORRILL, THOMAS H. N91-26987
MORRIS, BRUCE L. N91-26534
MORRIS, J. W., JR. N91-26311
MORRIS, ROBERT A. N91-27105
MORRIS, S. N91-26605
MORRISON, CLYDE A. N91-26514
MORRISON, P. W. N91-26524
MORSE, R. E. N91-26999
MOSER, T. J. N91-26594
MOSS, FRANK N91-26512
MOTOJIMA, O. N91-26937
MPITSOS, GEORGE J. N91-26737
MUENCHAUSEN, R. E. N91-26515
MUENZEN, JEANNE L. N91-26794
MUHLEMAN, D. O. N91-27060
MUKERJI, I. N91-26681
MUKHERJEE, A. K. N91-26318
MUKHOPADHYAY, NITIS N91-26547
MULLER, R. A. N91-27050
N91-27051
MULLICAN, R. C. N91-26193
MUNCILL, GREGORY N91-26658
MURPHY, BRIAN P. N91-26756
MURPHY, MICHAEL G. N91-27106
MURRI, GRETCHEN BOSTAPH N91-26569
MURRILL, STEVEN R. N91-26447
MURROW, HAROLD N. N91-26151
MUSICH, M. A. N91-26528
MUTTER, JOHN C. N91-26634

N

NAGDA, N. L. N91-26746
NAGPAL, P. N91-26322
NAGY, J. N91-26609
NAINANI, KRISHAN N91-26800
NAKAMOTO, K. N91-26937
NARIMOUSA, S. N91-26664
NARZIYEV, M. N91-26177
NASH, J. K. N91-26517
NASH, PHILIP N91-26303
NAVARD, SHARON E. N91-27107
NAWAB, HAMID N91-26831
NEIR, R. N91-26126
NEKHOROSHEV, A. S. N91-26707
NELSON, J. J. N91-27087
NETTE, HERBERT L. N91-26454
NETZER, AVITAL N91-26853
NEUBEK, DEBORAH J. N91-27108
NEUMARK, DANIEL M. N91-26256
N91-26900
NEWMAN, L. N91-26607
NEY, ADDIE N91-27049
NG, KENNEY N91-26795
NGUYEN, R. N91-26436
NGUYEN, THAO K. N91-26414
NI, YUJING N91-26808
NICHOLLS, J. N91-26916

NIEDERLEHNER, B. R. N91-26603
NIEMAN, G. W. N91-26310
NIEMCZYK, M. P. N91-26980
NIKITIN, YE. I. N91-26694
NIKKEL, D. J., JR. N91-26381
NIKOLASHIN, G. F. N91-26705
NIR, DAVID N91-26998
NIRENBURG, SERGEI N91-26823
NISHRI, BOAZ N91-26482
NIXON, CHARLES W. N91-26427
NIXON, D. N91-26119
NOBACK, ROEL N91-26157
NOCK, L. A. N91-26363
NOGAR, N. S. N91-26515
NOON, J. N91-26204
NOQUES, JEAN-LUC N91-26934
NORTON, K. N91-26358
NOSKOV, V. B. N91-26689
NOVAK, L. N91-26705
NOVAK, MARK E. N91-26444
NOVINSKI, JOHN A. N91-26499
NOWACK, MARK L. N91-26131
NUTTALL, ALBERT H. N91-26844

O

OFFENBERG, M. N91-26456
OGANOV, V. S. N91-26690
OGILBY, P. R. N91-26382
OLEYNIK, G. N91-27044
OLHOEFT, G. R. N91-27074
OLIGER, JOSEPH N91-26772
N91-26775
N91-26836
OLSON, D. A. N91-26985
OLSON, W. L. N91-26981
OLTMAN-SHAY, JOAN M. N91-26661
OLTON, DAVID N91-26742
ONEIL, HAROLD F., JR. N91-26807
N91-26808
ONEIL, M. P. N91-26980
OPALKA, KLAUS O. N91-26473
ORALTAY, RIZA GURCAN N91-26611
ORENBERG, J. B. N91-27075
N91-27077
ORLOFF, TOBIAS N91-26767
ORTEGA, J. P. N91-26554
OSBORNE, T. N91-26938
OSIF, T. L. N91-26970
OSKAM, JOHN H. N91-26365
OSTERGAARD, JENS N91-26424
OTTO, J. N91-26525
OU, S. C. N91-26643
OUYANG, JIANGBO N91-26261
OWENS, JAY N91-26490
OZMIDOV, R. V. N91-26583

P

PACE, N. N91-26732
PACIESAS, WILLIAM S. N91-26407
PAIGE, D. A. N91-27076
PALEKAR, V. N91-26291
PALMER, RONALD W. N91-26750
PALMOUR, J. W. N91-26439
PAN, CHENGZHI N91-26511
PAQUET, V. N91-26525
PARDEE, R. N91-26997
PARISH, THOMAS R. N91-26574
PARK, J. N. N91-26461
PARK, LEE Y. N91-26365
PARTRIDGE, WILLIAM M. N91-26708
PARVEZ, M. N91-26344
PARZEN, EMANUEL N91-26873
PATIL, A. N91-26204
PATTERSON, F. G. N91-26526
PAUL, DOUGLAS B. N91-26414
PAULIUS, L. N91-26953
PEARCE, R. P. N91-26639
PEARSON, DALE S. N91-26221
PEASE, ADAM N91-26800
PEEBLES, D. E. N91-26320
PEGG, D. J. N91-26908
PEIFER, W. R. N91-26253
PEIFER, WILLIAM R. N91-26255
PEIO, KAREN J. N91-26748
PELLENBARG, ROBERT E. N91-26259
PELTON, JOSEPH N. N91-26182
PENN, LANNING M. N91-26651
PENNER, J. E. N91-26606
PENNISI, JOSEPH M. N91-26430
PENNYPACKER, C. N91-27050
N91-27051
PENYAZ, YA. N91-26705
PEPE, KEVIN N91-26658
PEREZ-DAVIS, M. E. N91-27061
PERLMUTTER, S. N91-27050
N91-27051
PERRY, M. D. N91-26526
PESTOV, I. D. N91-26178
PETERS, J. W. N91-26228
PETERS, TIMOTHY J. N91-26415
PETERSEN, R. N91-26463
PETROVA, YE. V. N91-26175
PEYGHAMBARIAN, N. N91-26799
PHILLIPS, DAVID N91-26346
PHILLIPS, J. E. N91-26561
PHILLIPS, R. C. N91-26524
PICHUMANI, RAMANI N91-26836
PIERCE, D. G. N91-26972
PINSKY, MARK N91-26846
PITRE, RICHARD N91-26877
PITT, COLIN G. N91-26949
PIVNENKO, A. D. N91-26584
PIVOVAROV, M. L. N91-26170
PLATT, R. H. N91-26655
PLAUT, RAYMOND H. N91-26558
PLEMMONS, ROBERT J. N91-26790
PLOSTINS, PETER N91-26118
PLOURDE, J. V. N91-26751
PLUMMER, MICHAEL D. N91-26839
N91-26841
PLYASOVA-BAKUNINA, I. A. N91-26697
POEPPEL, R. B. N91-26971
POFFIO, TOMASO N91-26810
POGGIO, TOMASO N91-26782
POLLACK, J. B. N91-27077
POLYCHRONIDIS, JOHN E. N91-26673
POMERANTZ, MARTIN N91-26351
N91-26352
POMETOV, YU. D. N91-26705
POMPHREY, RICK B. N91-27022
POPE, DAVID P. N91-26356
POPOV, G. V. N91-26173
PORTER, LINDA N91-27025
POUGET, J. P. N91-26332
POWELL, J. ANTHONY N91-26966
N91-26967
POWELL, RICHARD C. N91-26500
POZDNYAKOV, O. M. N91-26703
POZHARSKAYA, L. G. N91-26689
PRAIRIE, M. R. N91-26398
PRASAD, PARAS N. N91-26897
PRASANNA, G. N. N91-26803
PRESCOTT, W. N91-26612
PRESTON, D. R. N91-27045
PREZYNA, L. A. N91-26258
PRICE, PAMELA E. N91-26650
PRITCHARD, DAVID E. N91-26494
N91-26895
PROBER, D. E. N91-26973
N91-26991
PROCTOR, T. M. N91-26882
PROSCHAN, FRANK N91-26546
PRUITT, JOHN S. N91-26890
PUR, RICHARD A. N91-26161
PURSLEY, MICHAEL B. N91-26409

Q

QIU, Y. J. N91-26258
QIU, YONG-JIAN N91-26350
N91-26354
QUARLES, G. J. N91-26506

R

RABITZ, ARNOLDO N91-26636
RABITZ, H. R. N91-26283
RADHAKRISHNAN, RAMALINGAM N91-27109
RADLINSKI, RONALD P. N91-26475
RAEISAENEN, A. V. N91-26973
N91-26991
RAFFIN, M. N91-26124
RAHAMAN, M. N. N91-26362
RAINEY, V. S. N91-26294
RAJAN, PERIASAMY K. N91-27110
RAJESHWAR, KRISHNAN N91-26352
RAKHMAN-ZADE, YA. Z. N91-26327
RAKHMANOV, A. S. N91-26690
RALLS, JOHN A. N91-26627
RAMAN, GANESH N91-26121
RAMSAY, J. B. N91-26399
RAMSEY, CONNIE L. N91-26784
RAMSEY, P. N91-26241
RAMULU, MAMIDALA N91-26227
RASDORF, WILLIAM J. N91-26230
RASH, CLARENCE E. N91-26754
RASNUSSEN, K. N91-27056
RASTOGI, PRABHAT K. N91-26619
RATHBUN, R. E. N91-26600
RAUCH, JEFFREY S. N91-26870
RAY, A. N91-26332
N91-26335
RAY, JAYANTA K. N91-26328
RAYNER, KEITH N91-26739
REBER, R. N91-26126
REECE, GARLAND D. N91-26159
REEVES, R. R. N91-26342
REGAN, DAVID N91-26740
REICHERT, BRUCE A. N91-26122
REID, N. W. N91-26607
REIF, JOHN N91-26765
REINISCH, BODO W. N91-26627
REINTJES, JOHN F. N91-26505
N91-26923
REISS, DONALD A. N91-26968
REMICK, R. J. N91-26970
REMINGTON, B. A. N91-26943
REMO, JOHN L. N91-26922
REN, ZHONGSHU N91-26300
REPENKOVA, L. G. N91-26692
RESHOTKO, ELI N91-26121
REYES, F. N91-27047
REYNOLDS, J. R. N91-26258
REYNOLDS, JOHN R. N91-26350
N91-26351
N91-26352
N91-26353
N91-26354
REYNOLDS, W. H. N91-26751
RHEINBOLDT, WERNER C. N91-26838
N91-26842
RHODY, HARVEY E. N91-26822
N91-26830
RICCO, A. J. N91-26888
RICE, EDWARD J. N91-26121
RICE, ROY W. N91-26225
RICHARDS, P. L. N91-26973
N91-26991
RICLES, JAMES M. N91-27111
RIDING, G. H. N91-26344
RIGGLE, PETER N91-26544
RIMKUS, W. A. N91-26946
RITCHEY, NATHAN P. N91-26849
RIZAYEV, N. U. N91-26327
ROBBINS, FREDERICK W. N91-26391
ROBE, R. Q. N91-26751
ROBERTS, J. M. N91-26607
ROBINS, C. B. N91-26413
ROBINSON, G. C. N91-26572
ROBINSON, M. B. N91-26265
N91-26266
N91-26267
ROBINSON, STEPHEN KERN N91-26465
ROBLE, RAYMOND G. N91-26631
RODEBACK, G. W. N91-26498
ROETTGER, JUERGEN N91-26616
ROGERS, JOHN S. N91-26806
ROIDT, R. M. N91-26467
ROLFE, S. T. N91-26572
ROMESBURG, L. N. N91-26999
ROMIG, A. D., JR. N91-26319
ROSE, M. S. N91-26728
ROSE, WILLIAM C. N91-26114
ROSEN, M. D. N91-26517
ROSENFIELD, AZRIEL N91-26848
ROSS, JOHN N91-26270
ROTH, P. M. N91-26597
ROUGE, CARL J. N91-26375
ROUNDS, FRED N91-27011
N91-27041
N91-27042
ROUSH, T. L. N91-27077
ROWE, JOSEPH N91-26669
N91-26670
ROWLEN, K. L. N91-26271
ROYDEN, L. N91-26612
ROZHDESTVENSKAYA, M. K. N91-26453
RUBIN, DAVID N91-26442
RUBINSTEIN, M. N91-26656
RUBLOFF, G. W. N91-26456
RUEB, JUSTIN D. N91-26125
N91-26130
RUEHL, KAREN N91-26370
RUGGLES, A. N91-26530
RUPLEY, F. M. N91-26285
RUSHBY, JOHN N91-26814
RUSSELL, R. A. N91-26971
RUSSELL, YVONNE N91-27012
RUTH, CARL R. N91-26391
RYAN, JAMES E. N91-26587
RYCKMAN, S. J., JR. N91-26608
RYDER, D. E. N91-26555

S

SABLE, D. N91-26204
SACKMAN, JEROME L. N91-26564
SADOWAY, DONALD N91-26955
SAFFMAN, P. G. N91-26478
SAGER, J. C. N91-26759
SALES, GARY S. N91-26627
SANDERS, D. E. N91-26309
SANDERSON, ARTHUR N91-26821
SANDS, T. N91-26985
SARID, D. N91-26799
SARMA, BIMAL N91-26954
SARWATE, DILIP V. N91-26409
SASSEEN, T. N91-27050
SATO, TORU N91-26615
SAULNIER, GARY J. N91-26430
SAUNDERS, S. N91-27056
SAUVE, J. L. N91-26187
SAVINA, V. P. N91-26694
SAWCHUK, ALEXANDER A. N91-26931
N91-26932
SCHANTZ, RICHARD E. N91-26429
SCHEER, E. M. N91-26347
SCHEROCMAN, JAMES A. N91-26402
SCHERR, ELLIOT M. N91-26329
SCHETZINA, J. F. N91-26957
SCHIFLETT, SAMUAL E. N91-26738
SCHILL, J. P. N91-27004
SCHLAIKJER, CARL R. N91-26589
SCHLICHTING, J. J. F. M. N91-26788
SCHMITZ, D. N91-26436
SCHNABEL, ROBERT B. N91-26777
N91-26778
SCHNEIDER, DONALD A. N91-26722
SCHNEIDER, J. J. N91-26139
SCHNEIDER, STEVEN J. N91-26200
SCHNETZER, G. H. N91-26653
SCHOENFELD, THILO N91-26466
SCHOFIELD, K. N91-26288
SCHOLES, R. N91-26126
SCHROCK, RICHARD R. N91-26365
SCHRODER, KENNETH J. N91-26429
SCHWARTING, E. M. N91-26668
SCOTT, COURTNEY J. N91-26651
SCOTT, DAN N91-27018
SCOTT, JAMES G. N91-26135
SCULLY, J. R. N91-26320
SEED, W. R. N91-26408
SEGLETES, STEVEN B. N91-26988
SEIBERT, JOHN F. N91-26211
SEIDMAN, DAVID N. N91-26891
SEIGEL, R. W. N91-26310
SEILER, ED N91-27032
SEINFELD, J. H. N91-26597
SELF, CHARLES T. N91-26447
SEMENOV, B. KH. N91-26685
SENSENBRENNER, F. JAMES, JR. N91-27046
SENTMAN, D. D. N91-27078
SERLIN, V. N91-26448
SETH, VINAY K. N91-26934
SHA, W. T. N91-26489
SHAHINPOOR, MO N91-26533
SHAKHOV, YE. M. N91-26165
SHAKOCIUS, AARON M. N91-26136
SHALAEV, VALDIMIR M. N91-26455
SHALKHAUSER, K. A. N91-26436
SHAMES, P. N91-27023
SHANKAR, U. N91-26598
SHAPIRO, STUART C. N91-26816
N91-26817
SHARP, TOM N91-26282
SHARVIT, MOSHE N91-26868
SHAUB, R. L. N91-26555
SHAYDOROV, YU. I. N91-26693
SHEALY, ROBIN N91-26862
SHECHTMAN, DAN N91-26956
SHEN, D. S. N91-26591
SHEN, Y. N91-26489
SHENFIL, L. Z. N91-26453
SHEPARD, R. N91-26902
SHERWOOD, R. J. N91-26834
SHESHUKOV, S. S. N91-26173
SHI, H. N91-26979
SHIMP, NANCY R. N91-26196
SHIN, JAIWON N91-26490
SHINOHARA, H. N91-26937
SHIRANE, G. N91-26906
SHOOCKRON, JOSEPH N91-26480
SHORT, ROBERT D. N91-26630
SHREVE, STEVEN E. N91-26861
SHULTZ, D. J. N91-26600
SIEGEL, R. W. N91-26978
SIKKA, DIGVIJAY I. N91-26827
SILVERMAN, A. N. N91-26990
SILVESTER, JOHN N91-26419
SIMONDS, CHARLES H. N91-27079
SIMS, STEVEN A. N91-26355
SINGER, R. M. N91-26863
SIPRIKOVA, N. I. N91-26453
SIZEMORE, T. N91-26204
SKIBA, I. A. N91-26697
SKIBINSKI, MARK N91-26192
SLATER, HOWARD N91-26490
SLONE, JAMES C., JR. N91-26449
SMAGIN, D. M. N91-26584
SMIALEK, JAMES L. N91-26375
SMITH, A. E. N91-26608
SMITH, B. K. N91-26495
SMITH, C. N91-27050
SMITH, C. E. N91-26146
SMITH, C. R. N91-26420
SMITH, D. J. N91-26710
N91-26711
N91-26715
SMITH, DENNIS A. N91-26459
SMITH, DONALD E. N91-26763
SMITH, PAUL N91-27119
SMITH, S. L. N91-26668
SMITH, STEVEN T. N91-26677
SMITH, THOMAS MICHAEL N91-26657
SMOAK, B. L. N91-26711
SNYDER, DANIEL E. N91-26748
SNYDER, HARRY L. N91-26743
N91-27007
N91-27008
SOCIE, D. F. N91-26214
SOKOL, YE. A. N91-26699
SOLCHER, H. N91-26416
SOLOVYEV, V. S. N91-26171
SOMMEIJER, B. P. N91-26835
SONDER, RAINER N91-26155
SORNATALE, FRANK N91-26645
SOSNOVETS, E. N. N91-26172
SOUFFLOT, A. N91-26175
SOUTH, D. W. N91-26804
SPAINHOUR, LISA K. N91-26230
SPARKS, C. J., JR. N91-26323
SPEICH, D. M. N91-27087
SPERBER, K. R. N91-26606
SPRANGLE, P. N91-26503
SPRINGER, JOHN M. N91-26313
SPROULL, STEVEN J. N91-26351
SQUIRES, WILLIAM G. N91-27112
SRIHARI, SARGUR N. N91-26817
SRINIVASAN, R. N91-26297
STADTMUELLER, W. N91-26557
STANNY, ROBERT R. N91-26725
STEEL, DUNCAN G. N91-26926
STEGEMAN, G. I. N91-26799
STEIER, W. H. N91-26931
STEIN, LYNN A. N91-26809
STEINBERG, M. N91-26288
N91-26605
STEPANOV, V. V. N91-26702
STEPHENS, D. W. N91-26600
STEPHENS, J. J. N91-26570
STEPHENSON, MARK S. N91-26427
STEWART, CLAYTON V. N91-26630
STICKEL, MARK E. N91-26814
STICKLE, W. F. N91-26353
STILES, GERALD J. N91-26431
STOCKMAN, H. W. N91-26486
STOCKMAN, MARK I. N91-26455
STONE, LYDIA RAZRAN N91-26669
N91-26670
STONE, R. S. N91-26666
STONEKING, D. E. N91-26440
STOUKIDES, M. N91-26289
STOUT, WILLIAM N91-26862
STRACHOTINSKY, CHRISTIAN N91-26913
STRAIT, MELISSA M. N91-27113
STRANDBERG, G. W. N91-26680
STRAUSS, KURT N91-26144
STRECKERT, H. N91-26358
STREETER, LYNN A. N91-26787
STREETS, D. G. N91-26595
STRICKER, LAWRENCE J. N91-27005
STRINGER, J. N91-26974
STROME, DAVID R. N91-26738
STUIVER, MINZE N91-26577
STUPIN, D. M. N91-26554
STURM, D. N91-26557
STURR, JOSEPH F. N91-26709
SUJANANI, M. N91-26284
SUK, MINSOO N91-26829
SUN, Y. N91-26245
N91-26251
N91-26331
N91-26347
SUREK, T. N91-26588
SUSOEFF, A. R. N91-26187
SUTTON, JOHN F. N91-26438
SUZUKI, DAVID E. N91-26199
SVEC, W. A. N91-26980
SWANSON, D. B. N91-26337
SWANSON, GARY J. N91-26933
SWEENEY, D. N91-26433
SWEET, D. N91-26126
SWIGGER, KATHLEEN M. N91-26808
SWINDEMAN, R. W. N91-26317
SWITALA, M. N91-26379
SZE, R. C. N91-26522

T

TAI, D. Y. N91-25600
TAKAGI, Y. N91-26229
TAKAHATA, K. N91-26937
TAKEYAMA, MASAO N91-26323
TALPALLIKAR, M. V. N91-26146
TAM, CHRISTOPHER N91-26878
TAN, XIANXIANG N91-26493
TANG, JANE N91-26633
TANG, Y. N91-26487
TANKESLEY, LAWRENCE N91-26505
TANNER, R. L. N91-26607
TARASOV, I. K. N91-26178
N91-26686
N91-26698
N91-26706
TARRANT, JANICE M. N91-26527
TATEM, P. A. N91-26474
TATSUOKA, KIKUMI N91-26847
TATSUOKA, MAURICE N91-26847
TAVIK, GREGORY C. N91-26761
TAVROW, LEE S. N91-26446
TAYA, MINORU N91-26227
TAYLOR, M. J. N91-26950
TAYLOR, P. A. N91-26248
N91-26252
TAYLOR, V. L. N91-26382
TEAS, DON C. N91-26881
TEETER, RONALD N91-26669
N91-26670
TENCATI, RON N91-27016
TENG, HONG N91-26215
N91-26216
TERNOVOY, S. K. N91-26690
TESCHE, T. W. N91-26597
TETER, JOSEPH P. N91-26536
THADDEUS, P. N91-26286
THEISS, T. J. N91-26572
THOMAS, G. J. N91-26978
THOMPSON, ANTHONY W. N91-26301
THOMPSON, DANNIELLA MUHEIM N91-26238
THOMPSON, GERALD L. N91-26849
THOMPSON, J. R. N91-26982
THOMPSON, JOANIE N91-27027
THOMPSON, P. N91-26126
THOMSON, E. M. N91-26656
THORNTON, J. N91-26588
THORNTON, WILLIAM E., JR. N91-26747
THORSNESS, J. B. N91-26525
TICHY, JOHN A. N91-26531
TIEFENBOECK, WILHELM N91-26913
TIEGS, T. N. N91-26242
TIERNEY, J. W. N91-26291
TIETZE, KAREN J. N91-27114
TINGEY, D. T. N91-26594
TIPTON, CHARLES W. N91-26447
TKACHENKO, V. K. N91-26697
TOLBERT, A. K. N91-27087
TOLLIN, G. N91-26682
TORKELSON, JAMES E. N91-26589
TRAVIS, B. N91-26484
TRAVOR, BRUCE W. N91-26537
TREJO, LEONARD J. N91-26725
TRENARY, MICHAEL N91-26452
TREW, R. J. N91-26440
TROJAN, KATHLEEN L. N91-26951
TRUCANO, T. G. N91-26186
TRUSSELL, C. W. N91-26496
TRUSTY, C. N91-26601
TRUSTY, GARY L. N91-26919
TSAI, P. K. N91-26953
TSAI, TSU-TZU N91-26357
TSCHANZ, J. N91-26608
TSENG, JOHN J. N91-26351
TSUDA, TOSHITAKA N91-26618
TURNER, N. L. N91-26745
TURNER, VERNON R. N91-26403
TUROCZY, WILLIAM R. N91-26785
TURSUNOVA, D. R. N91-26327
TVERSKAYA, L. V. N91-26172
TVERSKY, BARBARA N91-26735

TWARDOWSKI, T. E. N91-26338
TWERSKY, VICTOR N91-26885
TZENG, REN-YOW N91-26640

U

UHDE-LACOVARA, J. N91-27115
UM, CHUNG-IN N91-26893
UMAN, MARTIN A. N91-26642
N91-26656
UPADHYAYA, SHAMBHU J. N91-26817

V

VAEWIG, ROBERT L. N91-26115
VAIDYANATHAN, GOPAL N91-26255
VALDIMIROFF, T. N91-26390
VALENTINE, TIM N91-27046
VANCAMP, WARREN N91-27014
VANCE, L. STUART N91-27020
VANCHAU, KIET N91-26217
VANDERHOUWEN, P. J. N91-26835
VANDERVORST, H. A. N91-26768
VANORDEN, KARL F. N91-26709
VANRHEINECK-LEYSSIUS, H. J. N91-26638
VANSCHALKWIJK, WALTER N91-26589
VANSCHILFGAARDE, MARK N91-26901
VANYSEK, P. N91-26280
VANZYL, J. N91-27056
VARACALLE, D. J., JR. N91-26326
VARSHNEY, PRAMOD K. N91-26827
VASEY, A. R. N91-26187
VASHKOVYAK, M. A. N91-26163
VAUCHER, CHRISTOPHER A. N91-26629
VAUCHER, GAIL T. N91-26629
VAUGHAN, WILLIARD S. N91-26733
VENKATA, RAMANA N91-26836
VERVER, G. H. L. N91-26638
VIL-VILYAMS, I. F. N91-26705
VILLASENOR, TONY N91-27017
VINTER, STEPHEN T. N91-26429
VISKOE, D. A. N91-26554
VITEK, VACLAV N91-26356
VLADIMIROFF, T. N91-26389
VOELKER, L. S. N91-26113
VOGELSONG, RICHARD D. N91-26475

W

WACHI, Y. N91-26937
WADDINGTON, EDWIN N91-26628
WAIGHT, KENNETH T., III N91-26650
WALDINGER, RICHARD J. N91-26814
WALKER, JAMES D. N91-26534
WALKER, W. D. N91-26912
WALL, S. N91-27056
WALLACE, R. J. N91-26943
WALLACE, R. M. N91-26248
N91-26252
WALLACE, TOM N91-26630
WALSH, JOANNE L. N91-26137
WALTERS, DONALD L. N91-26629
WALTON, J. J. N91-26606
WALTZ, R. E. N91-26938
WANG, FEI N91-26350
WANG, LI-PING N91-27050
WANG, LI-SHENG N91-26401
WANG, S. S. N91-26214
WANG, SU S. N91-26218
WANG, Z. H. N91-26335
WANGEMANN, ROBERT T. N91-26926
WARD, K. J. N91-26385
WASHBURN, J. N91-26985
WASIELEWSKI, M. R. N91-26980
WASSERSTEIN, MICHAEL N91-26935
WATERS, THOMAS A. N91-26450
WATKINS, JAMES J. N91-26341
WATTS, D. R. N91-26662
WAYNER, P. C., JR. N91-26284
WEBB, GRAHAM N91-26304
WEBSTER, STEVE L. N91-26160
WEDDENDORF, BRUCE N91-26542
WEERTMAN, J. R. N91-26310
WEGNER, P. J. N91-26523
WEI, R. N91-26379
WEI, YEN N91-26328
N91-26329
WEILAND, T. L. N91-26518
WEINBERG, F. J. N91-26388
WEINBERG, R. P. N91-26715
WEINBERG, W. H. N91-26248
WEINBERGER, NORMAN M. N91-26734
WEINER, M. M. N91-26421
WEINSHALL, DAPHNA N91-26781
WEINSTEIN, C. J. N91-26412
WEISS, H. N91-26245
WEISS, I. N91-26297
WEISS, ISAAC N91-26874
WEISS, R. B. N91-26676
WEISS, VOLKER N91-26815
WEITZ, ERIC N91-26892
WELLS, R. L. N91-26949
WELLSTOOD, F. C. N91-26464
N91-26981
WEN, DIANZHONG N91-26300
WENDER, I. N91-26291
WENHUA, LI N91-26148
WENZEL, STUART W. N91-26254
WERCINSKI, P. F. N91-27080
WETS, ROGER N91-26793
WHEELER, R. M. N91-26759
WHILLANS, IAN N91-26580
WHITBY, E. R. N91-26598
WHITE, BRUCE R. N91-27081
WHITE, D. C. N91-26316
WHITE, MICHAEL N91-26370
WHITE, RICHARD M. N91-26254
WHITE, RICHARD P., JR. N91-26756
WHITEMORE, HENRY B. N91-26747
WHITESIDES, GEORGE M. N91-26208
N91-26277
N91-26302
WIHSTUTZ, VOLKER N91-26846
WILBUR, P. N91-26379
WILCOX, D. R. N91-26491
WILDE, PETER N91-26466
WILKE, R. J. N91-26667
WILKERSON, J. B. N91-26139
WILKS, S. C. N91-26517
WILLIAMS, D. B. N91-27053
WILLIAMS, F. W. N91-26474
WILLIAMS, JAMES H., JR. N91-26549
WILLIAMS, RAYMOND N91-27116
WILSON, SCOTT C. N91-26577
WINDSOR, C. G. N91-26294
WINHOLTZ, R. A. N91-26566
WINICK, K. A. N91-26410
WISE, M. L. N91-26262
N91-26263
N91-26267
WITT, AUGUST N91-26961
WITZANI, JOSEF N91-26913
WNEK, G. E. N91-26258
WOLBER, DAVE N91-26797
WOLFE, ROBERT R. N91-26724
WONG, A. L. N91-26207
N91-26268
WONG, C. R. N91-26568
WOOD, B. E. N91-26188
WOODMAN, RONALD F. N91-26617
WOOLF, BEVERLY N91-26816
WORKING, DENNIS C. N91-26378
WORSHAM, A. H. N91-26973
N91-26991
WORTHINGTON, T. K. N91-26982
WU, M. S. N91-26278
WU, X. D. N91-26515
WYATT, M. N91-26529

X

XU, J. N91-26280
XU, WANQING N91-26493

Y

YACCARINO, K. N91-26463
YAMAMOTO, J. N91-26937
YAN, JERRY C. N91-26796
YAN, SHEN N91-26928
YAN, Y. N91-26856
YANAGI, N. N91-26937
YANG, HONG N91-26833
YANG, SHUMEI N91-26679
YAO, M. N91-26472
YARNELL, K. N91-27004
YATES, J. T., JR. N91-26274
N91-26275
YAVROUIAN, A. H. N91-26386
YE, H. J. N91-26250
N91-27002
YEGOROV, A. D. N91-26178
N91-26686
YEH, POCHI N91-26926
YEON, KYU-HWANG N91-26893
YEPISHKIN, A. K. N91-26701
YETTER, R. A. N91-26283
YIN, JOHN N91-27039
YIN, PAUL K. N91-27117
YOUNG, MICHAEL A. N91-26779
YOUNG, R. P. N91-26188
YU, K. M. N91-26985
YU, S. L. N91-26983
YUE, J. N91-26333
YULDASHEV, A. YU. N91-26327
YUREK, AILEEN M. N91-26924
YUST, C. S. N91-26383

Z

ZACKS, S. N91-26857
ZAFF, BRIAN S. N91-26748
ZANG, T. A. N91-26470
ZANLEY, NANCY L. N91-27038
ZAPLATYNSKY, I. N91-26376
ZEIDLER, JAMES R. N91-26950
ZEISSE, CARL R. N91-26950
ZHAI, MING N91-26511
ZHANG, E. N91-26928
ZHANG, J. N91-27053
ZHANG, T. J. N91-26986
ZHANG, XIAOPING N91-26497
ZHAO, Y. N91-26256
ZHARKOV, A. V. N91-26175
ZHONG, Z. N91-26333
ZHOU, B. N91-26983
ZHOU, J. N91-26567
ZHU, HONG N91-26351
ZHU, MEIJUAN N91-26493
ZHU, QINGLIN N91-26181
ZHUK, V. I. N91-26165
ZIEGLER, D. P. N91-26315
ZININ, L. V. N91-26171
ZUREK, R. W. N91-27082

Typical Corporate Source Index Listing

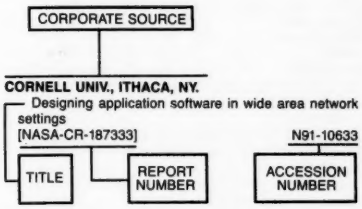

Listings in this index are arranged alphabetically by corporate source. The title of the document provides the user with a brief description of the subject matter. The report number helps to indicate the type of document cited (e.g., NASA report, translation, NASA contractor report). The accession number denotes the number by which the citation is identified. The titles are arranged under each corporate source in ascending accession number order.

A

ADVISORY GROUP FOR AEROSPACE RESEARCH AND DEVELOPMENT, NEUILLY-SUR-SEINE (FRANCE).
Experimental techniques in the field of low density aerodynamics
[AGARD-AG-318(E)] N91-26124
Manual on the flight of flexible aircraft in turbulence
[AGARD-AG-317] N91-26150
Digital signal conditioning for flight test, volume 19
[AGARD-AG-160-VOL-19] N91-26432

AEROCHEM RESEARCH LABS., INC., PRINCETON, NJ.
Computer modeling of soot formation comparing free radical and ionic mechanisms
[AD-A235007] N91-26273

AERODYNE RESEARCH, INC., BILLERICA, MA.
Boron combustion model development with kinetic sensitivity analysis and measurement of key chemical rate parameters
[AD-A235309] N91-26283

AEROJET ELECTROSYSTEMS CO., AZUSA, CA.
Proceedings of the 12th Annual Meeting of the UIPS Commission on Gravitational Physiology
[AD-A235337] N91-26732

AEROJET-GENERAL CORP., SACRAMENTO, CA.
Development of life prediction capabilities for liquid propellant rocket engines. Post-fire diagnostic system for the SSME system architecture study
[NASA-CR-187112] N91-26205

AEROJET TECHSYSTEMS CO., SACRAMENTO, CA.
ALS liquid hydrogen turbopump: Advanced Development Program
[NASA-CR-183730] N91-26196

AERONAUTICAL RESEARCH INST. OF SWEDEN, STOCKHOLM.
Methods to enhance the accuracy of finite volume schemes 2
[FFA-147] N91-26466

AERONAUTICAL SYSTEMS DIV., WRIGHT-PATTERSON AFB, OH.
KC-135 ground collision avoidance system questionnaire
[AD-A234385] N91-26125
Evaluation of the C/EC/KC-135 Ground Collision Avoidance System (GCAS), study 1
[AD-A235301] N91-26130
A look at digital nose wheel steering
[AD-A233944] N91-26131
Results of the aeronautical systems division critical process team on integrated product development
[AD-A235419] N91-26995

AEROSPACE CORP., EL SEGUNDO, CA.
Pressure distribution and induced force field on a conical nozzle due to impingement of a normal jet into the supersonic cross-flow
[AD-A233981] N91-26115
TRACE trajectory analysis and orbit determination program. Volume 13: Square root information filtering and smoothing
[AD-A234957] N91-26183
Lifetimes and failure mechanisms of W/Re hairpin filaments
[AD-A235199] N91-26305
Application of a conjugate gradient method to the synthesis of phase-only planar arrays
[AD-A233756] N91-26415

AEROSPACE MEDICAL RESEARCH LABS., WRIGHT-PATTERSON AFB, OH.
Intelligibility of digital speech masked by noise: Normal hearing and hearing impaired listeners
[AD-A234852] N91-26427
An advanced knowledge and design acquisition methodology: Application for the pilot's associate
[AD-A233700] N91-26748

AIR FORCE ENVIRONMENTAL TECHNICAL APPLICATIONS CENTER, SCOTT AFB, IL.
Surface Observation Climatic Summaries (SOCS) for Kodiak, Alaska
[AD-A235182] N91-26646
Surface observation climatic summaries for Norton AFB, California
[AD-A235227] N91-26647
Surface observation climatic summaries for Tonopah test range, Nevada
[AD-A235228] N91-26648

AIR FORCE GEOPHYSICS LAB., HANSCOM AFB, MA.
Sounding rocket flight data summary
[AD-A233656] N91-26626

AIR FORCE GLOBAL WEATHER CENTRAL, OFFUTT AFB, NE.
Improved Point Analysis Model (IPAM) (users guide)
[AD-A235305] N91-26649

AIR FORCE HISTORICAL RESEARCH CENTER, MAXWELL AFB, AL.
Personal papers in the United States Air Force Historical Research Center, 5th edition
[PB91-156380] N91-26999

AIR FORCE INST. OF TECH., WRIGHT-PATTERSON AFB, OH.
Application of transformational ideas to automatic flight control design
[AD-A234758] N91-26148
Chinese space science and technology (selected articles)
[AD-A234798] N91-26180
Prime Minister Li Peng talks with representatives to a discussion meeting on satellite applications and applied satellite technology about the development of our country's activities in space
[AD-A234801] N91-26181
Titanium alloy integrated centrifugal impeller 5 coordinate computer assisted manufacturing technology
[AD-A234797] N91-26300
Method of obtaining phenol-furfural resins
[AD-A233746] N91-26327
Methods of obtaining an electrical contact
[AD-A234800] N91-26453
Methods for determining crack depth
[AD-A234799] N91-26562
Optical methods of measuring the roughness of the surfaces of high precision steel balls
[AD-A234796] N91-26928

AIR FORCE OCCUPATIONAL AND ENVIRONMENTAL HEALTH LAB., BROOKS AFB, TX.
Composite fiber hazards
[AD-A233924] N91-26211

AIR FORCE SYSTEMS COMMAND, GRIFFISS AFB, NY.
Synthetic metals: A novel role for organic polymers
[AD-A233862] N91-26334
A Rome Laboratory guide to basic training in TQM analysis techniques
[AD-A233855] N91-26993

AIR FORCE SYSTEMS COMMAND, WRIGHT-PATTERSON AFB, OH.
WPG-3u model microprocessor controlled rotating beryllium mirror scanning camera and its applications
[AD-A234802] N91-26493
Laser applications in machining slab materials
[AD-A233823] N91-26497
Array-typed, sealed-off mini tea CO2 laser
[AD-A234804] N91-26511
ROBOT: A journal of Chinese Society of Automation
[AD-A234808] N91-26538

AIR WAR COLL., MAXWELL AFB, AL.
Space doctrine
[AD-A234971] N91-26866

ALABAMA UNIV., HUNTSVILLE.
Propulsion stability codes for liquid propellant propulsion systems developed for use on a PC computer
[NASA-CR-184983] N91-26201
Gamma ray astronomy
[NASA-CR-187774] N91-26407
Theoretical and experimental studies relevant to interpretation of auroral emissions
[NASA-CR-188491] N91-26637
Applications of artificial intelligence to mission planning
[NASA-CR-187953] N91-26806

ALABAMA UNIV., TUSCALOOSA.
Techniques for determining total body water using deuterium oxide N91-27091

ALMA COLL., MI.
Solutions to problems of weathering in Antarctic eucrites N91-27113

ALPINE GEOPHYSICS, PLACERVILLE, CA.
Improvement of procedures for evaluating photochemical models
[PB91-160374] N91-26597

ALUMINUM CO. OF AMERICA, ALCOA CENTER, PA.
Current distribution modeling for novel alumina electrolysis
[DE91-010060] N91-26315

AMERICAN TELEPHONE AND TELEGRAPH CO., NEW YORK, NY.
FTS2000 network architecture N91-27019

AMES LAB., IA.
Cross-linking and modification of cytochrome c with redox-active metal complexes
[DE91-012023] N91-26287
Epitaxy of metal atoms on metal surfaces: Deposition and diffusion
[DE91-011142] N91-26309
Electronic excitation transport in photosynthesis and crystal and molecular structures of porphyrin compounds
[DE91-012024] N91-26679
Nonperturbative behavior of quarks
[DE91-011905] N91-26903
Magnetic relaxation, flux pinning and, critical currents in superconductors
[DE91-012022] N91-26984

ANACAPA SCIENCES, INC., FORT RUCKER, AL.
Task analysis and workload prediction for the MH-47E mission and a comparison with CH-47D workload predictions. Volume 2: Appendixes A through N
[AD-A235249] N91-26757

ANALYSIS AND TECHNOLOGY, INC., NEW LONDON, CT.
Evaluation of night vision goggles for maritime search and rescue
[AD-A233798] N91-26751

ANALYTIC SCIENCES CORP., READING, MA.
Omega system Performance Assessment and Coverage Evaluation (PACE) workstation design and implementation, volume 1
[AD-A235225] N91-26128
Omega/VLF signal coverage database development
[AD-A235226] N91-26129

APPLIED MICROWAVE PLASMA CONCEPTS, CARLSBAD, CA.
Development of a tactical high-power microwave source using the Plasma Electron Microwave Source (PEMS) concept
[AD-A234967] N91-26942

APPLIED RESEARCH LAB., STATE COLLEGE, PA.
Boundary layer transition noise art
[AD-A235093] N91-26884
ARCO POWER TECHNOLOGIES, INC., WASHINGTON, DC.
System concept and analysis of an Artificial Ionospheric Mirror (AIM) radar
[AD-A234289] N91-26630
ARGONNE NATIONAL LAB., IL.
Chemical phase separation in binary iron-chromium alloys
[DE91-010282] N91-26294
Adsorption of ammonia on iron clusters
[DE91-011125] N91-26308
Mechanical behavior of nanocrystalline Cu, Pd, and Ag samples
[DE91-011747] N91-26310
A tribological investigation of the graphite-to-diamond-like behavior of amorphous carbon films ion-beam-deposited on ceramic substrates
[DE91-010816] N91-26379
Sloshing response in a tank containing two liquids
[DE91-011844] N91-26487
Implementation of the flow-modulated skew-upwind difference scheme in the COMMIX-1C code: A first assessment
[DE91-011168] N91-26489
Elementary reaction rate measurements at high temperatures by tunable-laser flash-absorption
[DE91-011850] N91-26516
Acid rain in Asia
[DE91-011160] N91-26595
AQUIS: An air quality and permit information management system
[DE91-011750] N91-26608
Pumping system fault detection and diagnosis utilizing pattern recognition and fuzzy inference techniques
[DE91-011849] N91-26863
Theoretical studies of potential energy surfaces and computational methods
[DE91-011126] N91-26902
Multi-dimensional computer simulation of MHD combustor hydrodynamics
[DE91-011851] N91-26946
Formation of intermediate compounds during reduced pressure calcination of Y-Ba-Cu-O precursor
[DE91-011179] N91-26971
On the nature of grain boundary structures in nanophase materials
[DE91-010285] N91-26978
Defects in decomposed YBa2Cu4O8 (124) superconductor after rapid annealing
[DE91-010597] N91-26979
Efficient photoinduced charge separation and storage in the solid state, rates, energetics, and spin-polarization
[DE91-010727] N91-26980
Critical currents in proton irradiated YBa2Cu3O(7-delta) crystals
[DE91-011835] N91-26982
HREM study of heteroepitaxial interfaces in the TiO2/Al2O3 system
[DE91-012473] N91-26986
ARIZONA STATE UNIV., TEMPE.
Radar-aeolian roughness project
[NASA-CR-4378] N91-27056
The distribution of particulate material on Mars N91-27059
Wind abrasion on Mars N91-27064
Effect of pressure on electrostatic processes on Mars N91-27069
Saltation threshold detection in a wind tunnel by the measurement of the net electrostatic charge N91-27070
Saltation threshold reduction due to the electrostatic agglomeration of fine particles N91-27071
ARIZONA UNIV., TUCSON.
Photochemical energy conversion by membrane-bound photoredox systems
[DE91-012171] N91-26682
Part 1: Ultrafast logic and multiple-beam optical parallel processing using nonlinear etalons. Part 2: Novel devices for all-optical computing. Part 3: Novel nonlinear semiconductor structures for signal processing and optical computing
[AD-A233410] N91-26799
ARMY AEROMEDICAL RESEARCH LAB., FORT RUCKER, AL.
SPH-4 aircrew helmet impact protection improvements 1970-1990
[AD-A233784] N91-26750
Visual and field-of-view evaluation of the M-43 protective mask with prescription eyepieces
[AD-A234592] N91-26754
ARMY ARMAMENT RESEARCH, DEVELOPMENT AND ENGINEERING CENTER, PICATINNY ARSENAL, NJ.
Rail circuit augmentation
[AD-A234944] N91-26184
Application of software tools in embedded computers within military systems to enhance software reliability, quality assurance, and maintenance
[AD-A234555] N91-26785
ARMY ARMAMENT RESEARCH, DEVELOPMENT AND ENGINEERING CENTER, WATERVLIET, NY.
Microalloyed steel preforms
[AD-A234039] N91-26296
ARMY ARMAMENT RESEARCH AND DEVELOPMENT COMMAND, DOVER, NJ.
Molecular mechanics calculations for nitro and amino substituted conjugated systems containing oxygen and nitrogen
[AD-A233928] N91-26389
Modification of the user friendly thermodynamic code to include the effects of minor species
[AD-A233929] N91-26390
ARMY AVIATION SYSTEMS COMMAND, HAMPTON, VA.
Effect of initial delamination on Mode 1 and Mode 2 interlaminar fracture toughness and fatigue fracture threshold
[NASA-TM-104079] N91-26569
ARMY BIOMEDICAL RESEARCH AND DEVELOPMENT LAB., FORT DETRICK, MD.
US Army Biomedical Research and Development Laboratory
[AD-A233664] N91-26671
ARMY COLD REGIONS RESEARCH AND ENGINEERING LAB., HANOVER, NH.
Lubricants at low temperatures
[AD-A234536] N91-26348
International State-of-the-Art Colloquium on Low-Temperature Asphalt Pavement Cracking
[AD-A233663] N91-26402
Rotating multicylinder method for the measurement of cloud liquid-water content and droplet size
[AD-A234780] N91-26644
ARMY CONSTRUCTION ENGINEERING RESEARCH LAB., CHAMPAIGN, IL.
Research in nonlinear water waves
[AD-A235410] N91-26478
ARMY ENGINEER WATERWAYS EXPERIMENT STATION, VICKSBURG, MS.
Geogrid reinforced base course for flexible pavements for light aircraft: Literature review and test section design
[DOT/FAA/RD-90/28] N91-26160
ARMY HEALTH CARE STUDIES AND CLINICAL INVESTIGATION ACTIVITY, FORT SAM HOUSTON, TX.
Proceedings of the 7th User's Stress Workshop
[AD-A234583] N91-26736
ARMY LAB. COMMAND, FORT MONMOUTH, NJ.
The role of EEPROM devices in upcoming ISDN applications
[AD-A234837] N91-26454
ARMY LAB. COMMAND, WATERTOWN, MA.
Evaluation of environmentally aged polymer/composite material by ultrasonic inspection
[AD-A235343] N91-26231
ARMY NATICK LABS., MA.
Mechanical properties of polycarbonate-polysulfone and polycarbonate-polyetherimide blends
[AD-A234939] N91-26360
Physiological and perceptual responses to load carrying in female subjects using internal and external frame backpacks
[AD-A234941] N91-26722
ARMY NATICK RESEARCH AND DEVELOPMENT COMMAND, MA.
Notional helmet concepts: A survey of near-term and future technologies
[AD-A234475] N91-26752
ARMY RESEARCH INST. OF ENVIRONMENTAL MEDICINE, NATICK, MA.
Level of dietary fat does not affect fuel oxidation or ondurance exercise performance of soldiers
[AD-A235194] N91-26728
ARMY WAR COLL., CARLISLE BARRACKS, PA.
What fuels our future?
[AD-A233674] N91-26387
Space support for airland battle-future
[AD-A233868] N91-26864
ARNOLD ENGINEERING DEVELOPMENT CENTER, ARNOLD AIR FORCE STATION, TN.
Bidirectional reflectance distribution (BRDF) of NASA shuttle tiles
[AD-A235115] N91-26188
ATMOSPHERIC AND ENVIRONMENTAL RESEARCH, INC., CAMBRIDGE, MA.
Satellite data derived estimates of erosion parameters for reentry vehicles
[AD-A234792] N91-26189
AUBURN UNIV., AL.
Strategies for parallel AI implementations
[AD-A234449] N91-26811

B

BALLISTIC RESEARCH LABS., ABERDEEN PROVING GROUND, MD.
Aerodynamics of a 0.60 caliber electromagnetic projectile
[AD-A234660] N91-26116
The effect of sabot wheelbase and position on the launch dynamics of fin-stabilized kinetic energy ammunition
[AD-A234945] N91-26118
A new high-progressivity/high-density propulsion concept: Partially cut multiperforated stick propellant
[AD-A234255] N91-26391
Optical studies of the flow start-up processes in four convergent-divergent nozzles
[AD-A234552] N91-26473
An analysis on the stability of the Mie-Gruneisen equation of state for describing the behavior of shock-loaded materials
[AD-A233827] N91-26988
BATTELLE COLUMBUS LABS., OH.
Electromagnetic launch technology assessment. Scientific basis and unified treatment: Forces and electromechanical power conversion (analytical and numerical methods)
[AD-A235028] N91-26185
BATTERY ENGINEERING, INC., HYDE PARK, MA.
Improvement in the capacity and safety of lithium/inorganic electrolyte sulfur dioxide rechargeable cells, phase 2
[AD-A235303] N91-26589
BBN SYSTEMS AND TECHNOLOGIES CORP., CAMBRIDGE, MA.
Architectures for a high performance distributed operating system
[AD-A235333] N91-26429
BELL COMMUNICATIONS RESEARCH, INC., MORRISTOWN, NJ.
Coordination in large scale software development
[AD-A234898] N91-26787
BIONETICS CORP., COCOA BEACH, FL.
Investigating combustion as a method of processing inedible biomass produced in NASA's biomass production chamber
[NASA-TM-103821] N91-26759
BOEING AEROSPACE AND ELECTRONICS CO., SEATTLE, WA.
X ray tomographic inspection of printed wiring assemblies and electrical components
[AD-A234748] N91-26548
BOEING CANADA, TORONTO (ONTARIO).
Analysis by the statistical discrete gust method N91-26156
BOEING COMMERCIAL AIRPLANE CO., SEATTLE, WA.
Civil tiltrotor missions and applications. Phase 2: The commercial passenger market
[NASA-CR-177576] N91-26126
BOEING COMPUTER SERVICES CO., SEATTLE, WA.
Electronic design process
[AD-A234709] N91-26786
BOEING HELICOPTER CO., PHILADELPHIA, PA.
Technology needs for high-speed rotorcraft, volume 1
[NASA-CR-177585] N91-26139
BOEING MILITARY AIRPLANE DEVELOPMENT, SEATTLE, WA.
Structured representation for requirements and specifications
[NASA-CR-187522] N91-26797
BOSTON UNIV., MA.
Study of intermediates from transition metal excited-state electron-transfer reactions
[DE91-012182] N91-26324
The effects of magnetic storm phases on F-layer irregularities from auroral to equatorial latitudes
[AD-A235170] N91-26632
Mathematical problems concerning rhythmic processes
[AD-A234588] N91-26845
General relativistic continuum mechanics and the post-Newtonian equations of motion N91-26987
BRANDEIS UNIV., WALTHAM, MA.
The chemical modification of plasmas
[AD-A234448] N91-26940

BROOKHAVEN NATIONAL LAB., UPTON, NY.
An assessment of CO2 greenhouse gas mitigation technologies
[DE91-011972] N91-26605
Relationships between PAN and ozone at sites in eastern North America
[DE91-011728] N91-26607
Free-air carbon dioxide enrichment: A new approach to research on carbon exchange processes
[DE91-012074] N91-26609
The impact of atmospheric damage to materials on consumers: News you can use
[DE91-012075] N91-26610
Inorganic carbon surveys of oceanic basins
[DE91-011132] N91-26667
SEEP 2 zooplankton data report: Winter, spring and summer collections at mooring 3 during 1988
[DE91-012077] N91-26668
Photons and neutrons
[DE91-010980] N91-26906
Thermoluminescence kinetics of pyrite (FeS2)
[DE91-011710] N91-26990

C

CALIFORNIA INST. OF TECH., PASADENA.
An experimental investigation of structure, mixing, and combustion in compressible turbulent shear layers
[AD-A235278] N91-26281
Improvement of procedures for evaluating photochemical models
[PB91-160374] N91-26597
Studies of resonantly enhanced multiphoton ionization processes in molecules
[AD-A235217] N91-26898
Overview of the NASA astrophysics data system N91-27022

CALIFORNIA UNIV., BERKELEY.
Flexural plate wave devices for chemical analysis
[AD-A234129] N91-26254
Study of the low-lying electronic states of Si2 and Si2(-) using negative ion photodetachment techniques
[AD-A234336] N91-26256
Dynamic energy absorption of sandwich structures by inelastic deformation
[AD-A234903] N91-26564
Neutral atom deBroglie-wave interferometry
[AD-A234624] N91-26896
Negative ion photodetachment as a probe of the transition state region: The I + HI reaction
[AD-A235297] N91-26900

CALIFORNIA UNIV., BERKELEY. LAWRENCE BERKELEY LAB.
The cryogenic mechanical properties of Vintage 3 Al-Li-Zr alloy 2090-T81
[DE91-011897] N91-26311
Low frequency noise in resonant Josephson soliton oscillators
[DE91-011911] N91-26464
Shell hoop prestress generated by welding
[DE91-011892] N91-26571
Fluorescence spectroscopy of excitation transfer in Photosystem 1
[DE91-011867] N91-26681
A study of signal generation and charge collectionin a-Si:H diodes for radiation imaging
[DE91-010243] N91-26904
Quantum limited quasiparticle mixers at 100 GHz
[DE91-011894] N91-26973
Study of the effect of reactive element addition by implanting metal ions in a pre-formed oxide layer
[DE91-011916] N91-26974
High-T(sub c) thin-film magnetometer
[DE91-011828] N91-26981
Thin film alloys on semiconductor substrates
[DE91-012355] N91-26985
Quantum limited quasiparticle mixers at 100 GHz
[DE91-011826] N91-26991
Supersymmetry breaking from superstrings and the gauge hierarchy
[DE91-011899] N91-26992
Preliminary estimates of core-collapse supernova rates from the Berkeley automated supernova search
[DE91-011824] N91-27050
The Berkeley/Anglo-Australian Observatory high-redshift supernova search
[DE91-012348] N91-27051

CALIFORNIA UNIV., DAVIS.
Nonlinear stochastic optimization solution procedures and incomplete information
[AD-A235242] N91-26793
Martian dust threshold measurements: Simulations under heated surface conditions N91-27081

CALIFORNIA UNIV., IRVINE.
Grain boundary cavitation processes in a Ni3Al alloy at elevated temperatures
[AD-A235279] N91-26307
Work performed experiments: 1989-1990
[AD-A235221] N91-26457
Mechanisms of adaptive information processing
[AD-A234435] N91-26734
Statistical analysis of stochastic gradient based algorithms
[AD-A234545] N91-26859

CALIFORNIA UNIV., LOS ANGELES.
Laser ionic multiphoton dissociation of some acrylate clusters
[AD-A233801] N91-26247
Size dependence of gaseous cluster reactivity and evaporation dynamics as a mechanistic probe
[AD-A233811] N91-26249
International collaboration program on innovative chemical processing of superior electronic and optical materials
[AD-A235030] N91-26276
Laboratory modelling of the dynamics of coastal upwelling
[AD-A234987] N91-26664
Intracellular physiology of the rat suprachiasmatic nucleus: Electrical properties, neurotransmission, and effects of neuromodulators
[AD-A234442] N91-26675
Peptide transport through the blood-brain barrier
[AD-A233753] N91-26708
Expert system explanation: The user perspective
[AD-A233739] N91-26749
Measurement expert system effectiveness
[AD-A234359] N91-26807
Evaluation of expert systems: A review of the literature
[AD-A234360] N91-26808
Science network resources: Distributed systems N91-27021
Thermal and albedo mapping of the north and south polar regions of Mars N91-27076
Electrostatic fields in a dusty Martian environment N91-27078

CALIFORNIA UNIV., SAN DIEGO, LA JOLLA.
Proceedings of the First Workshop on 3-D Optical Memories
[AD-A234732] N91-27003
Development of load-dependent Ritz vector method for structural dynamic analysis of large space structures N91-27111

CALIFORNIA UNIV., SAN FRANCISCO.
The effect of catecholamines on arterial blood pressure and heart rate
[AD-A234755] N91-26720

CALIFORNIA UNIV., SANTA BARBARA.
Effect of surface forces on the rheology of particle-liquid systems and the consolidation of ceramic powders
[AD-A234375] N91-26221
The chemistry of sodium with sulfur in flames
[DE91-002060] N91-26288

CALSPAN-BUFFALO UNIV. RESEARCH CENTER, NY.
Strategies for parallel AI implementations
[AD-A234449] N91-26811

CARNEGIE-MELLON UNIV., PITTSBURGH, PA.
Fundamentals of mechanical behavior in intermetallic compounds
[AD-A235016] N91-26301
Catalysts and initiators as instruments controlling structure of polymers with inorganic backbone
[AD-A235350] N91-26368
Polysilanes, synthesis, modification, and properties
[AD-A235351] N91-26369
Synthesis and characterization of polysilanes
[AD-A235357] N91-26370
Preparation of inorganic and organometallic polymers with controlled structures
[AD-A235359] N91-26371
Anionic ring-opening polymerization of cyclotetrasilanes
[AD-A235360] N91-26372
Dynamics of face and annular seals with two-phase flow
[NASA-CR-4256] N91-26479
The weighted uni-dimensional similarities problem with least absolute value metric is NP-Hard
[AD-A235060] N91-26849
Singular and bang-bang stochastic control
[AD-A234752] N91-26861

CASE WESTERN RESERVE UNIV., CLEVELAND, OH.
Spectral and correlation analysis with applications to middle-atmosphere radars N91-26619
An induction time approach to surface induced crystallization in polyethylene/poly (e-caprolactone) melt
[AD-A235102] N91-26964
Microwave properties of high transition temperature superconducting thin films
[NASA-CR-185842] N91-26976

CATHOLIC UNIV. OF AMERICA, WASHINGTON, DC.
Long-term prediction test procedure for most ICs, based on linear response theory
[NASA-CR-185843] N91-26462

CENTER FOR MATHEMATICS AND COMPUTER SCIENCE, AMSTERDAM (NETHERLANDS).
NUMVEC FORTRAN library manual. Chapter: Partial differential equations. Routine: ICGG3D
[CWI-NM-R9018] N91-26768
Stability of collocation-based Runge-Kutta-Nystroem methods
[CWI-NM-R9016] N91-26835

CHICAGO UNIV., IL.
Development of advanced methods based on stable isotope technology for studies of exercise in heat
[AD-A234670] N91-26719
Categories and particulars: Prototype effects in estimating spatial location
[AD-A234955] N91-26741

CINCINNATI UNIV., OH.
Thermoelastic wave propagation in laminated composites N91-26209
MMIC integration technology investigation
[NASA-CR-188035] N91-26434
Four-to-one power combiner for 20 GHz phased array antenna using RADC MMIC phase shifters N91-26435
A gravitationally consistent second-order analytic secular solution for the point-mass motion of the eight principal planets N91-27054

CITY OF HOPE MEDICAL CENTER, DUARTE, CA.
Evaluation of liposome-encapsulated Hemoglobin/LR16 formulation as a potential blood substitute
[AD-A233973] N91-26714

CIVIL AVIATION AUTHORITY, REDHILL (ENGLAND).
Trends in certification procedures and design analysis N91-26158

CLARK-ATLANTA UNIV., GA.
Organosilicon polymers incorporating the bicyclo(2.2.2)-octane moiety
[AD-A234966] N91-26361

CLEMSON UNIV., SC.
Applications of MST radars: Meteorological applications N91-26622
Polyhedral approaches for solving 0-1 polynomial programming problems
[AD-A235219] N91-26851
Development of high Tc (greater than 110K) Bi, Tl and Y-based materials as superconducting circuit elements
[NASA-CR-188581] N91-26948

COAST GUARD ACADEMY, NEW LONDON, CT.
Structural concept studies for a horizontal cylindrical lunar habitat and a lunar guyed tower N91-27117

COASTAL ENGINEERING RESEARCH CENTER, VICKSBURG, MS.
Directional characteristics of waves in shallow water
[AD-A234568] N91-26661

COLORADO SCHOOL OF MINES, GOLDEN.
Backscattering enhancement from rough surfaces
[AD-A234707] N91-26426

COLORADO STATE UNIV., FORT COLLINS.
Template synthesis of polymeric and metal microtubules
[AD-A235307] N91-26367

COLORADO UNIV., BOULDER.
Theoretical studies of the kinematics, dynamics, stability, and control of unsteady/vortical flows
[AD-A235190] N91-26477
Lead detection and mapping with reference to relationships between scale, sensor characteristics, surface conditions and atmospheric properties
[AD-A235121] N91-26666
A theoretical and experimental study of the symmetric rank one update
[AD-A233965] N91-26777
A software package for unconstrained optimization using tensor methods
[AD-A233989] N91-26778
Recent studies of the optical properties of dust and cloud particles in the Mars atmosphere and the interannual frequency of global dust storms N91-27060
Measurements of dust on Mars to be obtained from upcoming missions N91-27066
The effects of atmospheric dust on observations of Martian surface albedo N91-27072

COMMITTEE ON SCIENCE, SPACE AND TECHNOLOGY (U.S. HOUSE).
National Aeronautics and Space Administration Multiyear Authorization Act of 1991 N91-27046

COMPUTER SCIENCES CORP., ATHENS, GA.
Preliminary testing, evaluation and sensitivity analysis for the Terrestrial Ecosystem Exposure Assessment Model (TEEAM)
[PB91-161711] N91-26602

COMPUTER SCIENCES CORP., RESEARCH TRIANGLE PARK, NC.
Modal aerosol dynamics modeling
[PB91-161729] N91-26598
CONNECTICUT UNIV., STORRS.
Fixed sample and sequential problems with applications in reliability
[AD-A234547] N91-26547
CONSULTANTS CHOICE, INC., ATLANTA, GA.
OSIRRUS: Oceanic symbolic image representation, recognition and understanding software
[AD-A235112] N91-26665
CONTEL TECHNOLOGY CENTER, CHANTILLY, VA.
Advanced Satellite Research Project: SCAR Research Database. Bibliographic analysis
[NASA-CR-186086] N91-26182
COORDINATING RESEARCH COUNCIL, INC., ATLANTA, GA.
Survey of current aircraft engine conditions
[AD-A235143] N91-26144
CORNELL UNIV., ITHACA, NY.
Nonlinear dynamics and control of flexible structures
[AD-A235186] N91-26191
Incoherent scatter radar observations of the ionosphere N91-26623
The process group approach to reliable distributed computing
[NASA-CR-188498] N91-26804
Charge exchange in ion-surface scattering at hyperthermal (10-100 eV) and keV energies
[AD-A235233] N91-26899
CORVALLIS ENVIRONMENTAL RESEARCH LAB., OR.
Ecological exposure and effects of airborne toxic chemicals: An overview
[PB91-148460] N91-26594
CREE RESEARCH, INC., DURHAM, NC.
Development and testing of radiation and electromagnetic pulse hardened silicon carbide based electronics
[AD-A233744] N91-26439

D

DARTMOUTH COLL., HANOVER, NH.
The examination of dislocations in ice
[AD-A233716] N91-26586
DAVID TAYLOR RESEARCH CENTER, BETHESDA, MD.
Reflection of incident pressure waves by ribbed panels
[AD-A233671] N91-26469
The relationship of traditional damping measures for materials with high damping capacity
[AD-A235347] N91-26568
Analysis of wave characteristics in extreme seas
[AD-A234538] N91-26660
DAYTON UNIV., OH.
Chemical synthesis study of deuterated epoxy resins
[AD-A234666] N91-26355
DEFENCE AND CIVIL INST. OF ENVIRONMENTAL MEDICINE, DOWNSVIEW (ONTARIO).
Effectiveness of ice-vest cooling in prolonging work tolerance time during heavy exercise in the heat for personnel wearing Canadian forces chemical defence ensembles
[AD-A235273] N91-26758
DEFENCE RESEARCH ESTABLISHMENT, OTTAWA (ONTARIO).
Evaluation of the MARISAT satellite UHF wideband channel
[AD-A233666] N91-26408
DEFENSE LOGISTICS AGENCY, ALEXANDRIA, VA.
Forecasting digital microcircuit obsolescence
[AD-A234573] N91-26451
Quality effectiveness sensing technique release 3.0
[AD-A233651] N91-26545
DELAWARE UNIV., NEWARK.
The tropical Pacific Ocean's heat budget during a cold event, from a numerical model N91-26657
Inverse scattering problems for acoustic waves in an inhomogeneous medium N91-26876
DEPARTMENT OF DEFENSE EXPLOSIVES SAFETY BOARD, ALEXANDRIA, VA.
Minutes of the 24th Explosives Safety Seminar, volume 1
[AD-A235005] N91-26395
Minutes of the 24th Explosives Safety Seminar, volume 2
[AD-A235006] N91-26396
DEPARTMENT OF ENERGY, WASHINGTON, DC.
Global climate change: A discussion of major uncertainties
[DE91-011746] N91-26604
Large scale computing in the Energy Research Programs
[DE91-012128] N91-26805
DEPARTMENT OF THE NAVY, WASHINGTON, DC.
Apparatus for guiding a missile
[AD-D014866] N91-26147
India-stabilized zirconia coating for composites
[AD-D014857] N91-26224
Bonding agent for composite propellants
[AD-D014876] N91-26392
High power klystron amplifier
[AD-D014862] N91-26448
Magnetic field generator
[AD-D014869] N91-26449
Block patterning of the metallization of polyvinylidene fluoride transducers
[AD-D014872] N91-26450
A narrow-bandwidth unstable resonator laser cavity
[AD-D014865] N91-26505
A room-temperature, flashpumped, 2.09 micron solid state laser
[AD-D014871] N91-26506
Magnetostrictive angular positioning motor
[AD-D014858] N91-26536
Vehicle steering device
[AD-D014861] N91-26537
Regeneration of whetlerite for adsorbing toxic pollutants from air
[AD-D014859] N91-26753
An ultraviolet optical isolator utilizing the KDP-isomorphs
[AD-D014860] N91-26923
Improved inline fiber optic sensor arrays
[AD-D014864] N91-26924
Design for electronic spectrally tunable infrared detector
[AD-D014877] N91-26925
DEUTSCHE AIRBUS G.M.B.H., HAMBURG (GERMANY, F.R.).
Gust design procedures N91-26155
DOUGLAS AIRCRAFT CO., INC., LONG BEACH, CA.
Nondestructive Evaluation (NDE) of fiberglass marine structures state-of-the art review
[AD-A234785] N91-26550
DUKE UNIV., DURHAM, NC.
Computational complexity and efficiency in electro-optical computing system
[AD-A235013] N91-26765
Aircraft interior noise reduction by alternate resonance tuning
[NASA-CR-185453] N91-26889
Studies of interactions between elementary particles and nuclei
[DE91-012300] N91-26912
Preparation of a novel gallium arsenide single-source precursor having the empirical formula AsCl3Ga2
[AD-A233704] N91-26949

E

EDGERTON, GERMESHAUSEN AND GRIER, INC., IDAHO FALLS, ID.
Current distribution modeling for novel alumina electrolysis
[DE91-010060] N91-26315
EDUCATIONAL TESTING SERVICE, PRINCETON, NJ.
Response latency measures for biographical inventories
[AD-A235010] N91-27005
EISCAT SCIENTIFIC ASSOCIATION, KIRUNA (SWEDEN).
The instrumental principles of MST radars and incoherent scatter radars and the configuration of radar system hardware N91-26616
ENVIRONMENTAL RESEARCH LAB., ATHENS, GA.
Multispectral identification of potentially hazardous byproducts of ozonation and chlorination. Part 1: Studies of chromatographic and spectroscopic properties of MX
[PB91-161703] N91-26601
Preliminary testing, evaluation and sensitivity analysis for the Terrestrial Ecosystem Exposure Assessment Model (TEEAM)
[PB91-161711] N91-26602
ENVIROSYSTEMS SUPPLY, INC., FORT MYERS, FL.
National Bureau of Standards Publications 1977-1987. Volume 2: Indexes
[PB91-136515] N91-26997
ERG SYSTEMS, INC., SAINT JAMES, NY.
Full surface testing of grazing incidence mirrors
[AD-A234005] N91-26922
EXECUTIVE OFFICE OF THE PRESIDENT, WASHINGTON, DC.
Publications of the Executive Office of the President, January 20, 1989 to December 31, 1990
[PB91-127423] N91-26998

F

FEDERAL AVIATION ADMINISTRATION, SEATTLE, WA.
Certification procedures and requirements N91-26154
FEDERAL AVIATION ADMINISTRATION, WASHINGTON, DC.
Utilization of emergency medical kits by air carriers
[AD-A234784] N91-26721
FERMI NATIONAL ACCELERATOR LAB., BATAVIA, IL.
UNIX (tm) in high energy physics: What we can learn from the initial experiences at Fermilab
[DE91-011976] N91-26914
Providing a computing environment for a high energy physics workshop
[DE91-012049] N91-26916
Integrating UNIX workstation into existing online data acquisition systems for Fermilab experiments
[DE91-011974] N91-27044
FISK UNIV., NASHVILLE, TN.
US and foreign alloy cross-reference database
[NASA-CR-184166] N91-26313
FLORIDA ATLANTIC UNIV., BOCA RATON.
Dynamics of elastic bending and torsion of hingeless rotors with dynamic stall
[AD-A234775] N91-26134
FLORIDA INST. OF TECH., MELBOURNE.
A design for an intelligent monitor and controller for space station electrical power using parallel distributed problem solving N91-27105
FLORIDA STATE UNIV., TALLAHASSEE.
Statistical aspects of reliability, maintainability, and availability
[AD-A234546] N91-26546
Computation of broadband mixing noise from turbomachinery
[AD-A233991] N91-26878
FLORIDA UNIV., GAINESVILLE.
Comparison of the RF frequency spectra of HEMP and lightning
[AD-A234306] N91-26642
A catalog of high resolution Jovian decametric radio noise burst spectra, volume 1 N91-27047
FORDHAM UNIV., NEW YORK, NY.
A study of murine bone marrow cells cultured in bioreactors which create an environment which simulated microgravity N91-27101
FREQUENCY AND TIME SYSTEMS, INC., BEVERLY, MA.
Tactical quartz oscillator development
[AD-A234308] N91-26443

G

G AND C SYSTEMS, INC., SAN JUAN CAPISTRANO, CA.
Autonomous aircraft initiative study
[NASA-CR-186013] N91-26140
GELTECH, INC., ALACHUA, FL.
Transpiration cooled ultraviolet sol-gel silica optics
[AD-A235426] N91-26934
GENERAL ACCOUNTING OFFICE, WASHINGTON, DC.
Unmanned aerial vehicles. Medium range system components do not fit
[AD-A234131] N91-26132
Aerospace plane technology: Research and development efforts in Europe. Report to the Chairman, Committee on Science, Space, and Technology, House of Representatives
[GAO/NSIAD-91-194] N91-26141
Weather satellites: Action needed to resolve status of the US Geostationary Satellite Program. Report to the Chairman, Committee on Science, Space, and Technology, House of Representatives
[GAO/NSIAD-91-252] N91-26194
Air Force stock fund: Hydrazine sales consistent with the Commercial Space Launch Act. Report to the Chairman, Committee on Science, Space and Technology, House of Representatives
[GAO/NSIAD-91-196] N91-26397
Commercial use of space: Many grantees making progress, but NASA oversight could be improved. Report to the Chair, Subcommittee on VA, HUD, and Independent Agencies, Committee on Appropriations, U.S. Senate
[GAO/NSIAD-91-142] N91-26400
GENERAL ATOMIC CO., SAN DIEGO, CA.
Ceramic fiber coating development and demonstration
[AD-A234773] N91-26358
Comparison of dimensionally similar discharges with similar heat deposition discharges
[DE91-011740] N91-26938
Statistical properties of intrinsic topological noise in tokamaks
[DE91-011741] N91-26939

High-temperature ceramic superconductors
[AD-A234620] N91-26953
GENERAL ELECTRIC CO., SCHENECTADY, NY.
High-power converters for space applications
[NASA-CR-187116] N91-26461
Biological synthesis of substituted o-aminophenols
[AD-A234910] N91-26678
GEOLOGICAL SURVEY, DENVER, CO.
Transport and fate of acetone in an outdoor model stream, Stennis Space Center near Bay St. Louis, Mississippi
[PB91-154674] N91-26600
Magnetic and electrical properties of Martian particles N91-27074
GEOLOGICAL SURVEY, MENLO PARK, CA.
Martian surface materials N91-27073
GEOMET TECHNOLOGIES, INC., GERMANTOWN, MD.
Airliner cabin environment: Contaminant measurements, health risks, and mitigation options
[PB91-159384] N91-26746
GEORGIA INST. OF TECH., ATLANTA.
Studies in modeling, dynamics, and control of space structures
[AD-A235059] N91-26190
Cyclic deformation, damage, and effects of environment in the Ni3Al ordered alloy at elevated temperature
[AD-A235168] N91-26304
Analysis of knowledge-based expert systems as tools for construction design
[AD-A234473] N91-26404
Improved algorithms for transient and steady-state fluid-structure interaction
[AD-A235172] N91-26476
GEORGIA TECH RESEARCH INST., ATLANTA.
Advanced Microwave Precipitation Radiometer (AMPR) for remote observation of precipitation
[NASA-CR-184165] N91-26655
GEORGIA UNIV., ATHENS.
Electronic software submittal/distribution N91-27033
COSMIC: Software catalog 1991 edition diskette format N91-27036
GLASSTECH SOLAR, INC., GOLDEN, CO.
Research on stable, high-efficiency amorphous silicon multijunction modules
[DE91-002159] N91-26591
GORDON RESEARCH CONFERENCES, INC., KINGSTON, RI.
Gordon Research Conference on Composites
[AD-A233778] N91-26210
GRACE (W. R.) AND CO., COLUMBIA, MD.
Reaction processing of ceramic particulate and whisker composites
[AD-A234951] N91-26225

H

HARRY DIAMOND LABS., ADELPHI, MD.
An electron-beam dose deposition experiment: TIGER 1-D simulation code versus thermoluminescent dosimetry
[AD-A234507] N91-26447
Energy levels and branching ratios of Tm(3)+ in ten garnet laser materials
[AD-A235274] N91-26514
HARVARD UNIV., CAMBRIDGE, MA.
Fundamental studies of carbenes and hydrocarbon radicals
[DE91-011029] N91-26286
HONEYWELL, INC., BLOOMINGTON, MN.
Monolithic integration semiconductor and superconductor components
[AD-A234986] N91-26959
HOUSTON BAPTIST UNIV., TX.
Nonlinear systems dynamics in cardiovascular physiology: The heart rate delay map and lower body negative pressure N91-27095
HOUSTON UNIV., CLEAR LAKE, TX.
Object-oriented requirements analysis: A quick tour
[NASA-CR-187919] N91-26766
HOUSTON UNIV., TX.
Basic studies of microstructure of combusting turbulent flows
[AD-A234222] N91-26471
NASA/ASEE Summer Faculty Fellowship Program, 1990, Volume 1
[NASA-CR-185637-VOL-1] N91-27088
Compound estimation procedures in reliability N91-27090
Training effectiveness of an intelligent tutoring system for a propulsion console trainer N91-27097
NASA/ASEE Summer Faculty Fellowship Program, 1990, volume 2
[NASA-CR-185637-VOL-2] N91-27103
Fuzzy logic control system to provide autonomous collision avoidance for Mars rover vehicle N91-27106
Developing a taxonomy for mission architecture definition N91-27108
HUGHES AIRCRAFT CO., EL SEGUNDO, CA.
Investigation of polybenzocyclobutene resins in multilayer thin films for electronic packaging
[AD-A235223] N91-26228
HUMAN ENGINEERING LABS., ABERDEEN PROVING GROUND, MD.
The effects of display failures and symbol rotation on visual search and recognition performance
[AD-A235035] N91-26743
The effects of character size, modulation, polarity, and font on reading and search performance in matrix-addressable displays
[AD-A235033] N91-27007
The effect of rotation on legibility of dot-matrix characters
[AD-A235034] N91-27008
HYPRESS, INC., ELMSFORD, NY.
Superconducting high T(sub c) thin film vortex-flow transistor, phase 1
[AD-A235025] N91-26962

I

IDAHO NATIONAL ENGINEERING LAB., IDAHO FALLS.
An analytical methodology to predict the coating characteristics of plasma-sprayed ceramic powders
[DE91-010088] N91-26326
IIT RESEARCH INST., LANHAM, MD.
Requirements for developing Embedded Real-Time Trusted Computer System (ERT-TCSs)
[AD-A234325] N91-26762
ILLINOIS INST. OF TECH., CHICAGO.
Microstructure, plastic deformation and mechanical properties of mechanically alloyed NiAl and NiAl based alloys
[AD-A235135] N91-26303
The hysteresis and incremental collapse of complex structures: A paradigm for the fatigue failure of materials
[AD-A234831] N91-26563
ILLINOIS UNIV., CHICAGO.
Scanning tunnelling microscope for boron surface studies
[AD-A234716] N91-26452
Attention span, anxiety, and benzodiazepine receptors
[AD-A234549] N91-26716
Underwater scattering of sound
[AD-A235097] N91-26885
ILLINOIS UNIV., URBANA.
Guidelines for design, construction, and evaluation of airport pavement drainage
[DOT/FAA/RD-90/31] N91-26161
Spread spectrum communication networks
[AD-A233696] N91-26409
On measures of misconception stability
[AD-A234952] N91-26847
Computational methods and software for differential equations and their applications
[DE91-012172] N91-26855
A procedure to detect item bias present simultaneously in several items
[AD-A235252] N91-26862
ILLINOIS UNIV., URBANA-CHAMPAIGN.
Effect of a viscoelastic interface on the transverse behavior of fiber-reinforced composites
[AD-A233986] N91-26212
Development of a test system and experimental method for in-plane biaxial compressive deformation and failure of fiber composite materials
[AD-A234062] N91-26214
A model for wet filament winding of composite cylinders with arbitrary thickness
[AD-A234102] N91-26215
Interfacial slippage of a unidirectional fiber composite under longitudinal shearing
[AD-A234186] N91-26216
Static and cyclic compressive fatigue of thermoplastic-matrix composite in ambient and moisture environments
[AD-A234187] N91-26217
Nonlinear behavior of fiber composite materials and its effect on the postbuckling response of laminated plates
[AD-A234203] N91-26218
Characterization studies of fluorinated epoxy resins: Naval experimental resin C8/1SA as a structural material and for use in blends and composites
[AD-A234188] N91-26338
IMPERIAL COLL. OF SCIENCE AND TECHNOLOGY, LONDON (ENGLAND).
Energy migration, motion and order in synthetic polymers
[AD-A234403] N91-26346
Laser initiated ignition of liquid propellant
[AD-A233777] N91-26388
INFORMATION SYSTEMS AND TECHNOLOGY CENTER, WRIGHT-PATTERSON AFB, OH.
Ada compiler validation summary report: Certification number: 9000703W1.11014, Silicon Graphics 4D ADA Iris-4D/380 (host) Iris-4D/380 (target)
[AD-A233714] N91-26771
Ada compiler validation summary report: Certificate number 900703W1.11015, Silicon Graphics 4D Ada, Iris-4D/220S (host) Iris-4D/220S (target)
[AD-A233786] N91-26776
INSTITUTE FOR COMPUTER APPLICATIONS IN SCIENCE AND ENGINEERING, HAMPTON, VA.
A parallel rendering algorithm for MIMD architectures
[NASA-CR-187571] N91-26767
INSTITUTE FOR DEFENSE ANALYSES, ALEXANDRIA, VA.
An approach for constructing reusable software components in Ada
[AD-A233662] N91-26770
Ada software portability and level 2 system simulator integration issues
[AD-A233757] N91-26773
INSTITUTE OF ELECTRICAL AND ELECTRONICS ENGINEERS, NEW YORK, NY.
The First Nonlinear Optics: Materials, Phenomena, and Devices Conference
[AD-A234733] N91-26926
INSTITUTE OF GAS TECHNOLOGY, CHICAGO, IL.
Determination of flow-regime boundaries for cohesive particles
[DE91-010552] N91-26468
Solid-state proton conductors
[DE91-002050] N91-26970
INSTITUTO GEOFISICO DEL PERU, LIMA.
Statistical characteristics of MST radar echoes and its interpretation N91-26617
INTERNATIONAL BUSINESS MACHINES CORP., YORKTOWN HEIGHTS, NY.
Chemistry of fluorine in the oxidation of silicon
[AD-A234959] N91-26272
Surface etching and roughening in integrated processing of thermal oxides
[AD-A234960] N91-26456
INTERNATIONAL COUNCIL OF SCIENTIFIC UNIONS, KYOTO (JAPAN).
Middle Atmosphere Program. Handbook for MAP. Volume 30: International School on Atmospheric Radar
[NASA-CR-188623] N91-26613
IOWA STATE UNIV. OF SCIENCE AND TECHNOLOGY, AMES.
Computer modeling of soot formation comparing free radical and ionic mechanisms
[AD-A235007] N91-26273
A numerical study of blocking N91-26640
The aeolian wind tunnel N91-27065

J

JACKSON STATE UNIV., MS.
Infrared and visible laser double resonance studies of vibrational energy transfer processes in polyatomic molecules
[DE91-012162] N91-26910
JAYCOR, VIENNA, VA.
Depressed collector experiments on a quasioptical gyrotron
[AD-A234559] N91-26492
JET PROPULSION LAB., CALIFORNIA INST. OF TECH., PASADENA.
Additives for high temperature liquid lubricants
[DE91-011018] N91-26386
Atmospheric InfraRed Sounder (AIRS): Science and measurement requirements
[NASA-TM-104977] N91-26624
Method and apparatus for second-rank tensor generation
[NASA-CASE-NPO-17512-1-CU] N91-26918
Galileo: The Earth encounter N91-27024
Have graben wall scarps accumulated sand and dust on Mars? N91-27062
Dust in the Mars atmosphere N91-27082
JOHNS HOPKINS UNIV., BALTIMORE, MD.
Studies of mutant hemoglobins to define types of modifications useful in the design of blood substitutes
[AD-A234997] N91-26723
Neural mechanisms of attention
[AD-A235003] N91-26742
Material engineering of novel semiconductor structures
[AD-A235014] N91-26960
JOHNSON CONTROLS, INC., MILWAUKEE, WI.
Proof-of-concept zinc/bromine electric vehicle battery
[DE91-011767] N91-26463

JOHNSON MATTHEY ENVIRONMENTAL PRODUCTS, WAYNE, PA.
Development of a low temperature catalytic combustor for small gas turbine applications
[PB91-161273] N91-26529
JOINT DATA SYSTEMS SUPPORT CENTER, WASHINGTON, DC.
Software requirements specification for the Mapping And Graphic Information Capability (MAGIC). Volume 4: Geographic mapping CSCI
[AD-A235275] N91-26794
JOINT PUBLICATIONS RESEARCH SERVICE, ARLINGTON, VA.
JPRS report: Science and technology. USSR: Space
[JPRS-USP-91-002] N91-26162
Evolution of some types of Earth satellite orbits N91-26163
Spatial rotations of a satellite in a circular three-body problem for the case of general resonance N91-26164
Oscillations of a small-mass satellite probe caused by aerodynamic and gravitational forces N91-26165
Analysis of necessary and sufficient conditions for the equilibrium stability of a gyrostatic satellite N91-26166
Calculation of the pointing accuracy of spacecraft equipment using autonomous measurements of the angular position of the object of investigation N91-26167
Analytical algorithms to solve an inverse navigation problem for a system of satellites N91-26168
Study of the properties of the autonomous optical navigation of a space probe in a rendezvous with an asteroid N91-26169
Fluid damping of the oscillations of satellites with a large magnetic moment N91-26170
Measurements of the longitudinal movements of O(+) ions in the subauroral upper atmosphere from the Aureol 3 satellite N91-26171
Dynamics of equatorial and polar boundaries of penetration of solar protons with energy about 1 MeV into magnetosphere during strong magnetic storm N91-26172
Modelling the dynamics of fluxes of electrons with energies 30-300 keV in geostationary orbit N91-26173
Turbulent processes of mass-loading of new ions on Venus and Mars and the problems of numerical models of the interaction of solar wind with these planets. 1: Characteristics of the flow of solar wind around the planets N91-26174
Characteristics of aerosol in the atmosphere of Mars according to data from the KRFM experiment N91-26175
Results of morphometric analysis of the Tesserae surface of Venus according to Venera-15 and -16 data N91-26176
Determination of the masses and densities of meteoroids from radar observations from one point N91-26177
Review of primary medical results of year-long flight on Mir station N91-26178
Limited current capabilities for cosmonaut rescue N91-26179
JPRS report: Science and technology. USSR: Earth sciences
[JPRS-UES-91-002] N91-26581
JPRS report: Science and technology. USSR: Earth sciences
[JPRS-UES-91-003] N91-26582
In the energy active region of the ocean N91-26583
Effect of turbulence on impurity observation in upper atmosphere using lidar method N91-26584
JPRS report: Science and technology. USSR: Life sciences
[JPRS-ULS-91-010] N91-26683
Pharmacological correction of functional condition of Army Air Force flyers in hot climate with asparkam N91-26684
Risk factors and prediction of syncopic states in flyers N91-26685
Survey of the principal results of medical research in the flight program of the second main expedition aboard the Mir orbiting complex N91-26686
State-of-the-art automated evaluation of functional state of the body in the space program and preventive medicine N91-26687
JPRS Report: Science and technology. USSR: Life sciences
[JPRS-ULS-91-009] N91-26688
Hormonal regulators of calcium metabolism following space flights of various durations N91-26689
Computer tomography measurement of vertebral bones and muscles after extended manned space flights N91-26690
Functional activity of hypophyseal-thyroid system during 370-day antiorthostatic hypokinesia N91-26691
Changes in rheologic indices of blood and hemodynamics during 14-day antiorthostatic hypokinesia N91-26692
Higher plants as part of biological human life support system N91-26693
Biochemical aspects of human adaptation to combined effect of antiorthostasis, decreased barometric pressure, and increased oxygen content N91-26694
Individual stereotypes of human neuropsychic prognostic activity in problem situations with different probability structures N91-26695
JPRS report: Science and technology. USSR: Life sciences
[JPRS-ULS-91-011] N91-26696
Visual accommodation in cosmonauts N91-26697
Vestibular reactions and intersensory interactions in weightlessness: Results of Optokinez experiment N91-26698
Effect of excess respiratory resistance on physical performance and cardiorespiratory function N91-26699
Effect of shift work of air traffic controllers on sympathetic nervous system N91-26700
Physical and psychogenic sequelae of impact acceleration on tracking performance of operators N91-26701
Reaction of human skeletal muscle fibers to 370 day antiorthostatic hypokinesia combined with physical exertion N91-26702
Effects of 13 day space flight on skeletal muscles and neuromuscular junctions in rats N91-26703
Effect of 7 day antiorthostatic hypokinesia on cardiac pumping action in monkeys N91-26704
Diagnostic utility of continuous noninvasive blood pressure monitoring (Penaz method) in gravity-induced blood redistribution N91-26705
State and forms of adaptation of vestibular function after space flights N91-26706
Combined effect of noise and vibration on cells of auditory and vestibular apparatus N91-26707

K

KANSAS STATE UNIV., MANHATTAN.
The effects of deuterium on static posture control N91-27102
KRUG LIFE SCIENCES, INC., SAN ANTONIO, TX.
Review of audition literature: Selection of acoustic signals for use in the synthesis of auditory space
[AD-A234579] N91-26881
KYOTO UNIV. (JAPAN).
Historical aspects of radar atmospheric dynamics N91-26614
Radar principles N91-26615
Data acquisition and processing N91-26618
Target parameter estimation N91-26620

L

LAMONT-DOHERTY GEOLOGICAL OBSERVATORY, PALISADES, NY.
Sea-level response to ice sheet evolution: An ocean perspective N91-26575
A multichannel seismic investigation of variations in crustal structure in the western North Atlantic
[AD-A235245] N91-26634
LAWRENCE LIVERMORE NATIONAL LAB., CA.
Performance of hypervelocity armatures with replenished metal vapor plasmas
[DE91-011931] N91-26187
On the finite-strain-invariant failure criterion for composites
[AD-A234493] N91-26223
Magnetron sputter deposition of boron and boron carbide
[DE91-011194] N91-26241
Strain enhanced microstructural evolution
[DE91-011921] N91-26318
Numerical simulations of the indentation of glass with implications to ductile grinding
[DE91-011512] N91-26381
Shock response of Detasheet
[DE91-010923] N91-26399
Computational model for optimizing longitudinal fin heat transfer in laminar internal flows
[DE91-005070] N91-26485
Saturation and kinetic issues for optical-field-ionized plasma x ray lasers
[DE91-012079] N91-26517
Determination of SBS induced damage limits in large fused silica optics for intense, time varying laser pulses
[DE91-012080] N91-26518
X ray spot motion during 220 ps laser pulses
[DE91-012111] N91-26519
Precision high-power solid-state laser diagnostics for target-irradiation studies and target-plane irradiation modeling
[DE91-012036] N91-26523
Radio frequency and microwave plasma for optical thin film deposition
[DE91-012081] N91-26525
Development of a subpicosecond, tunable LiCAF (Cr:LiCaAlF6) laser
[DE91-012082] N91-26526
Viscoelastic behavior of elastomeric membranes
[AD-A234496] N91-26580
Simulation of precipitation scavenging in a three-dimensional global model
[DE91-011531] N91-26606
Plate motion and deformation
[DE91-010466] N91-26612
Gabor transforms and neural networks for automatic target recognition
[DE91-011919] N91-26834
Planar indirect-drive Rayleigh-Taylor experiments on Nova
[DE91-011967] N91-26943
HYLIFE-2 inertial confinement: Fusion power plant design
[DE91-012089] N91-26947
Vacuum design for a superconducting mini-collider
[DE91-011964] N91-26975
The electronic structure of the ionic insulator sodium nitrite
[DE91-009766] N91-26977
A system for UNIX command retrieval using a multilayered neural network
[DE91-012105] N91-27045
Weak interactions and presupernova evolution
[DE91-011543] N91-27052
LEHIGH UNIV., BETHLEHEM, PA.
Partial oxidation of light alkanes in transition-metal ion containing zeolites
[DE91-008202] N91-26243
LOCKHEED CORP., HOUSTON, TX.
Impact of Mars sand on dust on the design of space suits and life support equipment: A technology assessment N91-27079
LOCKHEED ENGINEERING AND SCIENCES CO., WASHINGTON, DC.
USSR Space Life Sciences Digest, issue 29
[NASA-CR-3922(34)] N91-26669
USSR Space Life Sciences Digest, issue 30
[NASA-CR-3922(36)] N91-26670
LOS ALAMOS NATIONAL LAB., NM.
Investigation of a Hamiltonian with two sources of anisotropy: The Dzyaloshinskii-Moriya and single-size interactions
[DE91-011381] N91-26292
Simulation of pore scale porous media flow using lattice gas methods
[DE91-004829] N91-26484
Diagnostic studies of YBa2Cu3O(7-delta) laser ablation
[DE91-011382] N91-26515
Tunable excimer lasers
[DE91-011399] N91-26522
X ray-computed tomography for inspecting industrial parts
[DE91-011390] N91-26554
Boost-phase kill versus midcourse discrimination: The grand inquisitor's solution
[DE91-011744] N91-26871
An active particle accelerator
[DE91-011404] N91-26915
LOUISIANA STATE UNIV., NEW ORLEANS.
Metabolic changes and hemodynamic dysfunction following hypothermic shock
[AD-A233942] N91-26713
LOWELL UNIV., MA.
Meteor scatter communication between Thule and Station Nord, Greenland
[AD-A234440] N91-26424
Technique for measuring ionospheric irregularities generated by high power oblique HF heating of the F-region
[AD-A233883] N91-26627
ARTIST tape output formats
[AD-A235173] N91-26633
LOYOLA UNIV., CHICAGO, IL.
Viscosity methods in optimal control of distributed systems. The Bellman equation
[AD-A234646] N91-26812

M

MAINE UNIV., ORONO.
Late Wisconsin and early holocene glacial history, inner Ross Embayment, Antarctica N91-26577
MANKATO STATE COLL., MN.
Mathematical modeling of the flow field and particle motion in a rotating bioreactor at unit gravity and microgravity N91-27092

MANTECH ENVIRONMENTAL TECHNOLOGY, INC., RESEARCH TRIANGLE PARK, NC.
Ecological exposure and effects of airborne toxic chemicals: An overview
[PB91-148460] N91-26594
MARY HARDIN-BAYLOR UNIV., BELTON, TX.
An Air Revitalization Model (ARM) for Regenerative Life Support Systems (RLSS) N91-27093
MARYLAND UNIV., COLLEGE PARK.
Geometry, dynamics and control of coupled systems N91-26401
NFEARS: A nonlinear adaptive finite element solver. Part 2: User's manual
[AD-A234416] N91-26842
Understanding object classes: Modeling and matching
[AD-A235027] N91-26848
High order differentiation filters that work
[AD-A234504] N91-26874
MASSACHUSETTS INST. OF TECH., CAMBRIDGE.
Calculated aerodynamics of wings in severe maneuver
[AD-A235241] N91-26120
Isotropic exchange in the platinum-catalyzed reduction of olefins in protic solvents
[AD-A234828] N91-26208
Corrosion of graphite aluminum metal matrix composites
[AD-A234322] N91-26220
The reduction by deuterium on platinum black of exo-2-norbornyl and endo-2-norbornyl to norbornane-2-d occurs with predominant retention of configuration
[AD-A235057] N91-26277
Heterogeneous catalysis on platinum and self-assembled monolayers on metal and metal oxide surfaces
[AD-A235055] N91-26302
Living ring-opening metathesis polymerization of 7-oxa-2,3-difunctionalized norbornenes and norbornadienes by Mo(CHCMe2R) (N-2,6-C6H3-i-Pr2) (O-t-Bu)2 and Mo(CHCMe2R) (N-2,6-C6H3-i-Pr2) (OCMe2CF3)2
[AD-A235235] N91-26365
Piezoelectric micromotors for microrobots
[AD-A234423] N91-26446
Atom wave interferometer
[AD-A234863] N91-26494
New laser materials for laser diode pumping
[NASA-CR-187786] N91-26521
Line kinematics for whole-arm manipulation
[AD-A234422] N91-26535
Passive and active grasping with a prehensile robot end-effector
[AD-A235085] N91-26539
Waiting algorithms for synchronization in large-scale multiprocessors
[AD-A234985] N91-26764
Using mappings to prove timing properties
[AD-A234404] N91-26780
The shape of shading
[AD-A234419] N91-26781
Continuous stochastic cellular automata that have a stationary distribution and no detailed balance
[AD-A234421] N91-26782
Program improvement by automatic redistribution of intermediate results
[AD-A235086] N91-26791
Structure driven multiprocessor compilation of numeric problems
[AD-A234653] N91-26803
Imagination and situated cognition
[AD-A234420] N91-26809
Extensions of a theory of networks and learning: Outliers and negative examples
[AD-A234425] N91-26810
Using modular neural networks with local representations to control dynamic systems
[AD-A234700] N91-26813
Experiments with trapped atoms
[AD-A234580] N91-26895
Electrochemically modulated superconductivity
[AD-A234703] N91-26955
Luminescence and lasing in II-VI semiconductors
[AD-A235019] N91-26961
MASSACHUSETTS INST. OF TECH., LEXINGTON.
Wideband heterodyne spatial tracking for optical space communications
[AD-A233722] N91-26410
Optimal Walsh modulations in the presence of Doppler
[AD-A233723] N91-26411
Opportunities for advanced speech processing in military computer-based systems
[AD-A233724] N91-26412
A test vector generator for a radar signal processor
[AD-A233725] N91-26413
A physiologically motivated front end for speech recognition
[AD-A233727] N91-26414
Using genetic algorithms to select and create features for pattern classification
[AD-A235165] N91-26792
A comparative study of the practical characteristics of neural network and conventional pattern classifiers
[AD-A235345] N91-26795
Analysis of nonlinear optical frequency conversion
[AD-A233726] N91-26920
Binary optics technology: Theoretical limits on the diffraction efficiency of multilevel diffractive optical elements
[AD-A235404] N91-26933
Solid state research
[AD-A234836] N91-26958
MASSACHUSETTS UNIV., AMHERST.
A Conference on Eye Movements and Visual Cognition
[AD-A234754] N91-26739
Retrieval using plausible inference
[AD-A235015] N91-27006
MAX-PLANCK-INST. FUER AERONOMIE, KATLENBURG-LINDAU (GERMANY, F.R.).
Gravity waves and instabilities in the lower and middle atmosphere N91-26621
MAXWELL LABS., INC., SAN DIEGO, CA.
High-power converters for space applications
[NASA-CR-187116] N91-26461
MESOSCALE ENVIRONMENTAL SIMULATIONS AND OPERATIONS, INC., TROY, NY.
The development of an improved convective initiation scheme for Mesoscale numerical weather prediction models, phase 1
[AD-A235417] N91-26650
MICHIGAN UNIV., ANN ARBOR.
Turbulent premixed hydrogen/air flames
[AD-A235109] N91-26278
Non-destructive evaluation of residual stresses in thin films via x ray diffraction topography methods
[AD-A235328] N91-26552
The analysis of a rocket tomography measurement of the N2+3914A emission and N2 ionization rates in an auroral arc
[NASA-CR-188622] N91-26596
Development of a Vector Spherical Harmonic (VSH) model of the neutral thermosphere
[AD-A234744] N91-26631
Ocean acoustic tomography and telemetry
[AD-A233826] N91-26659
MIDWEST RESEARCH INST., GOLDEN, CO.
Photovoltaics: From the laboratory to the marketplace
[DE91-002151] N91-26588
Research on stable, high-efficiency amorphous silicon multijunction modules
[DE91-002159] N91-26591
MINNESOTA UNIV., MINNEAPOLIS.
Modal aerosol dynamics modeling
[PB91-161729] N91-26598
MISSION RESEARCH CORP., NASHUA, NH.
CBSD version 2 component models of the IR celestial background
[AD-A235372] N91-27048
MISSION RESEARCH CORP., SANTA BARBARA, CA.
Propagation of RF signals through structured ionization: The general model
[AD-A234051] N91-26418
MISSISSIPPI VALLEY STATE UNIV., ITTA BENA.
Planetary spacecraft cost modeling utilizing labor estimating relationships N91-27116
MISSOURI UNIV., ROLLA.
Pressureless densification of ceramic matrix composites
[AD-A235031] N91-26362
MISSOURI UNIV., SAINT LOUIS.
Chaotic and bifurcating nonlinear systems driven by noise with applications to laser dynamics
[AD-A234841] N91-26512
MITRE CORP., BEDFORD, MA.
Input impedance and gain of monopole elements with disk ground planes on flat earth
[AD-A234284] N91-26421
MITRE CORP., MCLEAN, VA.
Functional baseline specification for ATC data link service implementation in the host computer system
[DOT/FAA/CT-91/12] N91-26433
MOREHOUSE COLL., ATLANTA, GA.
Liquid film cooling in rocket engines
[AD-A234288] N91-26197

N

NATIONAL AERONAUTICS AND SPACE ADMINISTRATION, WASHINGTON, DC.
National research and education network N91-27017
Report of the 90-day study on human exploration of the Moon and Mars
[NASA-TM-102999] N91-27055
NASA information sciences and human factors program
[NASA-TM-4291] N91-27119
NATIONAL AERONAUTICS AND SPACE ADMINISTRATION. AMES RESEARCH CENTER, MOFFETT FIELD, CA.
Format and basic geometry of a perspective display of air traffic for the cockpit
[NASA-TM-86680] N91-26142
The kinematics of turbulent boundary layer structure
[NASA-TM-103859] N91-26465
Parallel processing and expert systems
[NASA-TM-103886] N91-26796
NSIUWG: Science networking retreat N91-27010
NSI organization and highlights N91-27011
Customer requirements process N91-27012
NSI engineering review N91-27013
Backbone upgrades and DEC equipment replacement N91-27014
NSI white pages project: X.500 directory service N91-27039
NSI customer service representatives and user support office: NASA Science Internet N91-27040
The NASA Science Internet: An integrated approach to networking N91-27041
NSI directed to continue SPAN's functions N91-27042
Sand and Dust on Mars
[NASA-CP-10074] N91-27057
The chemistry and mineralogy of Mars soil and dust N91-27058
Derivation of mid-infrared (5-25 microns) optical constants of some silicates and palagonite N91-27077
Sand and dust issues for the MESUR mission N91-27080
Dust in the Mars atmosphere N91-27082
NATIONAL AERONAUTICS AND SPACE ADMINISTRATION. GODDARD SPACE FLIGHT CENTER, GREENBELT, MD.
Synchronous demodulator
[NASA-CASE-GSC-13179-1] N91-26438
West Antarctic Ice Sheet Initiative. Volume 2: Discipline Reviews
[NASA-CP-3115-VOL-2] N91-26573
Nimbus-7 TOMS Antarctic ozone atlas: August - December 1990
[NASA-RP-1264] N91-26651
Proceedings of the Second Annual NASA Science Internet User Working Group Conference
[NASA-CP-3117] N91-27009
User support services and network application development: An overview N91-27015
NSI security task: Overview N91-27016
NSIUWG security sub-group N91-27026
Overview of the NSI User Support Office (NSI USO) N91-27028
The NSINIC on-line system N91-27029
The Internet resources guide and the Automatic Login Executor (ALEX) N91-27030
CRUSH: The NSI data compression utility N91-27032
The NASA master directory quick reference guide N91-27034
A guide to NASA's Pilot Land Data System (PLDS) N91-27035
The 1990 solar maximum mission event listing
[NASA-TM-4287] N91-27087
NATIONAL AERONAUTICS AND SPACE ADMINISTRATION. HUGH L. DRYDEN FLIGHT RESEARCH FACILITY, EDWARDS, CA.
Development of an integrated aeroservoelastic analysis program and correlation with test data
[NASA-TP-3120] N91-26113
NATIONAL AERONAUTICS AND SPACE ADMINISTRATION. JOHN F. KENNEDY SPACE CENTER, COCOA BEACH, FL.
Investigating combustion as a method of processing inedible biomass produced in NASA's biomass production chamber
[NASA-TM-103821] N91-26759
NATIONAL AERONAUTICS AND SPACE ADMINISTRATION. LYNDON B. JOHNSON SPACE CENTER, HOUSTON, TX.
Method and apparatus for waste collection and storage
[NASA-CASE-MSC-21025-3] N91-26747

Chemistry and mineralogy of Martian dust: An explorer's primer N91-27063
Engineering knowledge requirements for sand and dust on Mars N91-27067

NATIONAL AERONAUTICS AND SPACE ADMINISTRATION. LANGLEY RESEARCH CENTER, HAMPTON, VA.

Performance optimization of helicopter rotor blades [NASA-TM-104054] N91-26137
Measurement of atmospheric turbulence N91-26151
Liquid cooled supersonic total temperature probe [NASA-CASE-LAR-14435-1-CU] N91-26159
Effect of molecular weight on polyphenylquinoxaline properties [NASA-TM-104100] N91-26377
LaRC-ITPI/arylene ether copolymers [NASA-TM-104099] N91-26378
Effect of initial delamination on Mode 1 and Mode 2 interlaminar fracture toughness and fatigue fracture threshold [NASA-TM-104079] N91-26569

NATIONAL AERONAUTICS AND SPACE ADMINISTRATION. LEWIS RESEARCH CENTER, CLEVELAND, OH.

Control of an axisymmetric turbulent jet by multi-modal excitation [NASA-TM-104483] N91-26121
A study of high speed flows in an aircraft transition duct [NASA-TM-104449] N91-26122
CFD analysis of jet mixing in low NOx flametube combustors [NASA-TM-104466] N91-26146
Method of injecting fluid propellants into a rocket combustion chamber [NASA-CASE-LEW-14846-2] N91-26200
Development and testing of a source subsystem for the supporting development PMAD DC test bed [NASA-TM-104510] N91-26202
Investigation of interfacial shear strength in SiC/Si3N4 composites [NASA-TM-103739] N91-26233
Polymeric routes to silicon carbide and silicon oxycarbide CMC [NASA-TM-104372] N91-26234
Oxidation resistant coatings for titanium alloys and titanium alloy matrix composites [NASA-CASE-LEW-15155-1] N91-26375
Method of preparing a thermal barrier coating [NASA-CASE-LEW-14999-2] N91-26376
Submicron gate InP power MISFET's with improved output power density at 18 and 20 GHz N91-26436
Applied high-speed imaging for the icing research program at NASA Lewis Research Center [NASA-TM-104415] N91-26490
Removable hand hold [NASA-CASE-LEW-15196-1] N91-26543
A reliability and mass perspective of SP-100 Stirling cycle lunar-base powerplant designs [NASA-TM-103736] N91-26592
Comparative survey of dynamic analyses of free-piston Stirling engines [NASA-TM-104491] N91-26870
A model for the scattering of high-frequency electromagnetic fields from dielectrics exhibiting thermally-activated electrical losses [NASA-TM-104376] N91-26872
Process for the controlled growth of single-crystal films of silicon carbide polytypes on silicon carbide wafers [NASA-CASE-LEW-15222-1] N91-26966
Process for the homoepitaxial growth of single-crystal silicon carbide films on silicon carbide wafers [NASA-CASE-LEW-15223-1] N91-26967
Effects of Martian dust on power system components N91-27061
Electrical system/environment interactions on the planet Mars N91-27068

NATIONAL AERONAUTICS AND SPACE ADMINISTRATION. MARSHALL SPACE FLIGHT CENTER, HUNTSVILLE, AL.

Illuminance and luminance distributions of a prototype ambient illumination system for Space Station Freedom [NASA-TM-103541] N91-26193
The corrosion protection of 2219-T87 aluminum by anodizing [NASA-TM-103540] N91-26312
Control circuitry using electronic emulation of a synchro signal for accurate control of position and rate of rotation for shafts [NASA-CASE-MFS-28458-1] N91-26459
Double face sealing device [NASA-CASE-MFS-28521-1] N91-26542
The NASA/MSFC global reference atmospheric model: 1990 version (GRAM-90). Part 1: Technical/users manual [NASA-TM-4268] N91-26654
Crystal growth in a microgravity environment [NASA-CASE-MFS-28473-1] N91-26968
NASA's use of FTS2000 services N91-27018
NASA/SPAN and DOE/ESnet-DECnet transition strategy for DECnet OSI/phase 5 N91-27025

NATIONAL AERONAUTICS AND SPACE ADMINISTRATION. PASADENA OFFICE, CA.

Method and apparatus for second-rank tensor generation [NASA-CASE-NPO-17512-1-CU] N91-26918

NATIONAL AEROSPACE LAB., AMSTERDAM (NETHERLANDS).

Matching of PSD-design loads N91-26157

NATIONAL AEROSPACE LAB., EMMELOORD (NETHERLANDS).

Acquisition of statistical gust load data by commercial airplanes N91-26152

NATIONAL GEOPHYSICAL DATA CENTER, BOULDER, CO.

Solar-geophysical data number 556, December 1990. Part 1: (Prompt reports). Data for November, October 1990, and late data [PB91-152140] N91-27083
Solar-geophysical data number 556, December 1990. Part 2: (Comprehensive reports). Data for June 1990 and miscellaneous [PB91-152157] N91-27084
Solar geophysical data number 551, July 1990. Part 1: (Prompt reports). Data for June, May 1990 and late data [PB91-160713] N91-27085
Solar-geophysical data number 551, July 1990. Part 2: (Comprehensive reports). Data for January 1990 and miscellaneous [PB91-160721] N91-27086

NATIONAL INST. FOR FUSION SCIENCE, NAGOYA (JAPAN).

Design and fabrication of forced-flow coils as an R/D program for large helical device [NIFS-81] N91-26937

NATIONAL INST. FOR OCCUPATIONAL SAFETY AND HEALTH, CINCINNATI, OH.

Physiological responses to the wearing of protective equipment and respirators: Effects of hot, humid inspired air on work of breathing [PB91-152884] N91-26745

NATIONAL INST. OF STANDARDS AND TECHNOLOGY, GAITHERSBURG, MD.

Strength and microstructure of ceramics [AD-A235424] N91-26374
Center for electronics and electrical engineering. Technical progress bulletin covering center programs, July to September 1990, with 1991 CEEE events calendar [PB91-159749] N91-26437
Progress in ultrasonic measurements research in 1990: Transient sources for acoustic emission work [AD-A234965] N91-26882
Absorbed-dose calibration of ionization chambers in a Co-60 gamma-ray beam [PB91-132290] N91-26890
Transmission electron microscopy of the CVD diamond film/substrate interface [AD-A234790] N91-26956
Proceedings of the Object-Oriented Database Task Group Workshop [PB91-157198] N91-27000

NATIONAL OCEANIC AND ATMOSPHERIC ADMINISTRATION, MIAMI, FL.

Hurricane Research Division fiscal year 1990 programs-fiscal year 1991 projections [PB91-153452] N91-26641

NAVAL ACADEMY, ANNAPOLIS, MD.

Summary of research academic departments, October 1990 [AD-A234353] N91-27118

NAVAL AIR DEVELOPMENT CENTER, WARMINSTER, PA.

Flight control law synthesis using neural network theory [AD-A234990] N91-26149
An anisotropic laminated damped plate theory [AD-A234446] N91-26222
Mechanical properties of spray atomized SiC particle reinforced aluminum-titanium alloys [AD-A235231] N91-26306

NAVAL BIODYNAMICS LAB., NEW ORLEANS, LA.

A statistical analysis of -X rhesus head kinematics [AD-A233977] N91-26674

NAVAL CIVIL ENGINEERING LAB., PORT HUENEME, CA.

Liquid water production from atmospheric sources [AD-A235090] N91-26406
Advanced material handling equipment controls [AD-A235091] N91-26540

NAVAL HEALTH RESEARCH CENTER, SAN DIEGO, CA.

Smoking, exercise, and physical fitness [AD-A234658] N91-26717
Methylphenidate and pemoline: Effects on sleepiness and mood during sleep deprivation [AD-A234659] N91-26718
Effect of a passive cooling vest on tension/anxiety and fatigue in a high heat and high humidity naval environment [AD-A234657] N91-26755

NAVAL MEDICAL RESEARCH INST., BETHESDA, MD.

The Trendelenburg position after cerebral air embolism in dogs: Effects on the somatosensory evoked potential, intracranial pressure, and blood-brain barrier [AD-A233809] N91-26673
Young and older observers show similar perceived contrast functions for isoluminant stimuli [AD-A233766] N91-26709
COLDEX-86: Physical work capacity during prolonged cold water immersion at 6.1 msw [AD-A233767] N91-26710
COLDEX-86: Fluid and electrolyte changes during prolonged cold water immersion [AD-A233768] N91-26711
COLDEX-86: Summary of the experimental protocol and general results [AD-A234031] N91-26715

NAVAL OCEAN SYSTEMS CENTER, SAN DIEGO, CA.

De-embedding millimeter-wave integrated circuits with TRL [AD-A234194] N91-26442
Backplane bus distributed realtime clock synchronization [AD-A234476] N91-26491
Evaluation of the Navy oceanic vertical aerosol model using lidar and PMS particle-size spectrometers [AD-A233653] N91-26625
Iterated transform image compression [AD-A233655] N91-26769
Thickness measurements of silicon films using partial coherence interferometry [AD-A235211] N91-26930
Ohmic contacts to semiconducting diamond [AD-A234130] N91-26950
On-line magnetic tape Library Inventory Tracking And Reporting (LITAR) system [AD-A234934] N91-27004

NAVAL OCEANOGRAPHIC AND ATMOSPHERIC RESEARCH LAB., BAY SAINT LOUIS, MS.

The Navy standard compressed aeronautical chart database [AD-A235340] N91-26587

NAVAL POSTGRADUATE SCHOOL, MONTEREY, CA.

Establishment of a remotely piloted helicopter test flight program for higher harmonic control research [AD-A234978] N91-26135
Sea test development of laser altimeter [AD-A233824] N91-26498
Adaptive control of direct drive dexterous robotic hand with bilateral tactile sensing [AD-A233980] N91-26532
Atmospheric optical turbulence measurements taken at Anderson Mesa, Flagstaff, Arizona between 10-19 July 1990 [AD-A234190] N91-26629
Primes: The first 2400 prime numbers [AD-A233979] N91-26837
Covering a closed curve with a given total curvature [AD-A234342] N91-26840
Maximization on matroids with random weights [AD-A233978] N91-26858
Comparison of sound pressure in a wedge-shaped ocean as predicted by an image method and a PE model [AD-A234191] N91-26879

NAVAL RESEARCH LAB., WASHINGTON, DC.

Flexural plate wave devices for chemical analysis [AD-A234129] N91-26254
Water solubility of bis(2-ethylhexyl) hydrogen phosphite [AD-A234561] N91-26259
The Effect of the Ionosphere on Radiowave Signals and Systems Performance Based on Ionospheric Effects Symposium [AD-A233797] N91-26416
Plasma reflectors for electronic beam steering in radar systems [AD-A234560] N91-26425
Direct and large-eddy simulations of three-dimensional compressible Navier-Stokes turbulence [AD-A233717] N91-26470
Use of a zone model for validation of a horizontal ceiling/floor vent algorithm [AD-A234553] N91-26474
Depressed collector experiments on a quasioptical gyrotron [AD-A234559] N91-26492
Frequency upshifting of laser pulses by ionization fronts [AD-A234354] N91-26503

X ray laser program
[AD-A234390] N91-26504
Testing the One-Port Random Access Memory (1PRAM) module of TRW's CPUAX signal processing superchip
[AD-A234127] N91-26761
NRL connection machine Fortran library
[AD-A234121] N91-26779
BaRT manual version 3.0
[AD-A234528] N91-26784
An implementation of the singular value decomposition on the connection machine CM-2
[AD-A234124] N91-26802
A boundary scattering strength extraction algorithm for the analysis of long-range reverberation data
[AD-A233721] N91-26877
One-dimensional translation measurement of speckle from rough rotating objects in ultraviolet illumination
[AD-A233719] N91-26919
Materials Science and Engineering, 1989 publications
[AD-A234087] N91-27001

NAVAL SURFACE WARFARE CENTER, SILVER SPRING, MD.
Synthesis of energetic single phase and multi-phase polymers
[AD-A235104] N91-26363

NAVAL UNDERWATER SYSTEMS CENTER, NEW LONDON, CT.
Comparisons of backscattering from cylindrical shells described by thin shell and elasticity theories
[AD-A234745] N91-26475
Complex envelope properties, interpretation, filtering, and evaluation
[AD-A234478] N91-26844

NAVY PERSONNEL RESEARCH AND DEVELOPMENT CENTER, SAN DIEGO, CA.
The P300 component of the auditory event-related potential: Interlaboratory consistency and test-retest reliability
[AD-A235114] N91-26725

NEVADA UNIV., RENO.
Numerical investigations in three-dimensional internal flows
[NASA-CR-188615] N91-26114
Growth, evaporation and melting of ice crystals: Implications for radiation, atmospheric dynamics and particle scavenging N91-26611

NEW MEXICO STATE UNIV., LAS CRUCES.
Atmospheric propagation of laser beams
[AD-A234314] N91-26501

NEW MEXICO UNIV., ALBUQUERQUE.
Dynamic stability of flexible robot manipulators
[AD-A234297] N91-26533

NEW YORK UNIV., NEW YORK.
Mathematical topics in the modelling and identification of multicomponent continua
[AD-A234471] N91-26843

NIELSEN ENGINEERING AND RESEARCH, INC., MOUNTAIN VIEW, CA.
The effects of compressibility on a supersonic mixing layer
[AD-A234992] N91-26119

NORTH AMERICAN AIRCRAFT OPERATIONS, LOS ANGELES, CA.
High performance transparency design
[AD-A234456] N91-26133

NORTH CAROLINA STATE UNIV., RALEIGH.
Composite database interface users manual
[AD-A235327] N91-26230
Active devices for monolithic millimeter-wave integrated circuits
[AD-A234033] N91-26140
Parallel algorithms for least squares and related computations
[AD-A235018] N91-26790
Strategies for reliable and real time execution on a heterogeneous multiprocessor
[AD-A234114] N91-26801
Symposium E: Properties of 2-6 semiconductors. Bulk crystals, epitaxial films, quantum well structures
[AD-A234835] N91-26957

NORTH CAROLINA UNIV., CHAPEL HILL.
Multispectral identification of potentially hazardous byproducts of ozonation and chlorination. Part 1: Studies of chromatographic and spectroscopic properties of MX
[PB91-161703] N91-26601
Research in stochastic processes
[AD-A234650] N91-26860
Strong exchange coupling in lanthanide bis(phthalocyaninato) sandwich compounds
[AD-A234466] N91-26951

NORTH DAKOTA STATE UNIV., FARGO.
Second Mini-Conference on Key Problems in Silicon Chemistry
[AD-A235243] N91-26366

NORTH DAKOTA UNIV., GRAND FORKS.
Performance evaluation of a novel erosion-resistant pump design
[DE91-008201] N91-26528

NORTHEAST ARTIFICIAL INTELLIGENCE CONSORTIUM, SYRACUSE, NY.
Northeast Artificial Intelligence Consortium (NAIC). Volume 1: Executive summary
[AD-A234880] N91-26815
Northeast Artificial Intelligence Consortium (NAIC). Volume 2: Discussing, using, and recognizing plans
[AD-A234881] N91-26816
Northeast Artificial Intelligence Consortium (NAIC). Volume 3: The Versatile Maintenance Expert System (VMES)
[AD-A234882] N91-26817
Northeast Artificial Intelligence Consortium (NAIC). Volume 4: Distributed artificial intelligence for communications network management
[AD-A234883] N91-26818
Northeast Artificial Intelligence Consortium (NAIC). Volume 5: Distributed planning for dynamic environments in the presence of time constraints
[AD-A234884] N91-26819
Northeast Artificial Intelligence Consortium (NAIC). Volume 6: Building an intelligent assistant: The acquisition, integration, and maintenance of complex distributed tasks
[AD-A234885] N91-26820
Northeast Artificial Intelligence Consortium (NAIC). Volume 7: Automatic photointerpretation
[AD-A234886] N91-26821
Northeast Artificial Intelligence Consortium (NAIC). Volume 8: Artificial intelligence applications to speech recognition
[AD-A234887] N91-26822
Northeast Artificial Intelligence Consortium (NAIC). Volume 9: A planner system for the application of indications and warning
[AD-A234888] N91-26823
Northeast Artificial Intelligence Consortium (NAIC). Volume 10: Time oriented problem solving
[AD-A234889] N91-26824
Northeast Artificial Intelligence Consortium (NAIC). Volume 11: Knowledge base maintenance
[AD-A234890] N91-26825
Northeast Artificial Intelligence Consortium (NAIC). Volume 12: Computer architecture for very large knowledge bases
[AD-A234891] N91-26826
Northeast Artificial Intelligence Consortium (NAIC). Volume 18: A distributed artificial intelligence approach to information fusion and object classification
[AD-A234892] N91-26827
Northeast Artificial Intelligence Consortium (NAIC). Volume 14: Knowledge base retrieval using plausible inference
[AD-A234893] N91-26828
Northeast Artificial Intelligence Consortium (NAIC). Volume 15: Strategies for coupling symbolic and numerical computation in knowledge base systems
[AD-A234894] N91-26829
Northeast Artificial Intelligence Consortium (NAIC). Volume 16: Intelligent signal processing techniques for multi-sensor surveillance systems
[AD-A234895] N91-26830
Northeast Artificial Intelligence Consortium (NAIC). Volume 17: High-level adaptive signal processing
[AD-A234896] N91-26831
Northeast Artificial Intelligence Consortium (NAIC). Volume 13: Image understanding and intelligent parallel systems
[AD-A234897] N91-26832

NORTHWESTERN UNIV., EVANSTON, IL.
Energetics, bonding mechanism and electronic structure of metal/ceramic interfaces
[DE91-009787] N91-26239
Defect clustering and related properties of oxides
[DE91-011072] N91-26290
Quantum mechanical approach to understanding microstructural and mechanical properties of intermetallics
[AD-A234702] N91-26298
NATO advanced research workshop on Measurement of Residual and Applied Stress Using Neutron Diffraction
[AD-A235103] N91-26566
Lyapunov exponents and rotation numbers of linear systems with real noise
[AD-A234729] N91-26846
Chemistry on an atomic scale of ion-beam modified surfaces
[AD-A233707] N91-26891
High energy density systems in cryogenic media: The production and reaction of atoms and radicals
[AD-A233785] N91-26892

NOVA UNIV., FORT LAUDERDALE, FL.
Phytoplankton abundance in relation to Lagrangian paths
[AD-A233728] N91-26672

NTI, INC., DAYTON, OH.
Aircrew Evaluation Sustained Operations Performance (AESOP): A triservice facility for technology transition
[AD-A234626] N91-26738

O

OAK RIDGE NATIONAL LAB., TN.
Investigation into the effect of heat treatment on the thermal conductivity of 3-D carbon/carbon fiber composites
[DE91-010388] N91-26240
Microstructure development during microwave annealing of dense silicon nitride
[DE91-012069] N91-26242
Measurement of the nitrogen total cross section from 0.5 eV to 50 MeV and analysis of the 433-keV resonance
[DE91-012222] N91-26293
Effect of bacterial biofilms on carbon steel pit propagation in phosphate containing medium
[DE91-010806] N91-26316
Performance of a 22Cr-20Ni-18Co-Fe alloy for service to 870 C
[DE91-011366] N91-26317
Environmental embrittlement of ordered intermetallic alloys at room temperature in moist atmospheres
[DE91-012051] N91-26321
TEM in-situ straining of B2 compounds
[DE91-012062] N91-26322
Microstructure and hardness of NiAl/Ni2AlX two-phase ordered intermetallic alloys
[DE91-012068] N91-26323
The role of electronic structure in the mechanical behavior of aluminides
[DE91-012508] N91-26325
Strength of SiC- and Si-N-C-ceramic fibers exposed to high-temperature gaseous environments
[DE91-011099] N91-26380
Sliding wear-testing and data analysis strategies for advanced engineering ceramics
[DE91-009524] N91-26383
Ceramic technology for advanced heat engines project
[DE91-010451] N91-26384
In-situ monitoring of laser ablation of superconductors
[DE91-012057] N91-26524
Preliminary test results from the HSST shallow-crack fracture toughness program
[DE91-010147] N91-26572
Characterization of vertical electric fields and associated voltages induced on an overhead power line from close artificially initiated lightning
[DE91-010781] N91-26656
Introduction to Session 2: Applied biological research
[DE91-012067] N91-26680
A divide and conquer approach to the nonsymmetric eigenvalue problem
[DE91-011085] N91-26854
Correlation in photodetachment
[DE91-011369] N91-26908
Negative ion formation by Rydberg electron transfer: Isotope-dependent rate constants
[DE91-012058] N91-26909
Electron-excited molecule interactions
[DE91-012227] N91-26911
Effect of boron addition on recrystallization and grain growth in Ni3Al polycrystals
[DE91-011966] N91-26963
Catalog of data bases and reports
[DE91-011516] N91-27043

OESTERREICHISCHES FORSCHUNGSZENTRUM SEIBERSDORF G.M.B.H., VIENNA.
A test of the IAEA code of practice for absorbed dose determination in photon and electron beams
[OEFZS-4565] N91-26913

OFFICE NATIONAL D'ETUDES ET DE RECHERCHES AEROSPATIALES, PARIS (FRANCE).
Improved reduction of gust loads data for gust intensity N91-26153

OFFICE OF NAVAL RESEARCH, ARLINGTON, VA.
Cognitive and neural sciences division 1990 programs
[AD-A233773] N91-26733

OFFICE OF TECHNOLOGY ASSESSMENT, WASHINGTON, DC.
Changing by degrees: Steps to reduce greenhouse gases
[PB91-163428] N91-26599

OHIO STATE UNIV., COLUMBUS.
Impedance profiling: A convenient technique for determining the redox or protonic acid doping characteristics of conducting polymers
[AD-A233941] N91-26337
A review of precipitation-related aspects of West Antarctic meteorology N91-26574
Glacial dynamics (glaciology) N91-26580
Generic tasks for knowledge-based problem solving: Extension and new directions
[AD-A234925] N91-26865
Molecular orbital studies of the bonding in heavy element organometallics
[DE91-010915] N91-26905
OKLAHOMA STATE UNIV., STILLWATER.
Laser spectroscopy characterization of materials for frequency agile solid state laser systems
[AD-A233916] N91-26500
OLD DOMINION UNIV., NORFOLK, VA.
Viscous flow simulations of internal store carriage and separation
[NASA-CR-185343] N91-26123
Navier-Stokes calculations of scramjet-nozzle-afterbody flowfields
[NASA-CR-185356] N91-26488
OREGON STATE UNIV., CORVALLIS.
Boundary layer parameterization for a global spectral model
[AD-A235310] N91-26635
OREGON STATE UNIV., NEWPORT.
Parallel processing and learning: Variability and chaos in self-organization of activity in groups of neurons
[AD-A234589] N91-26737
OVERSEAS RELATIONS BRANCH TRANSLATION SERVICE, LONDON (ENGLAND).
Investigations into fracture mechanics failure concepts with thermomechanically rolled steels
[BLL-OA-TRANS-4238-(6196.3)] N91-26556
Load-bearing capacity of large pipes with circumferential defects under tensile stress: Comparison of experiments with calculated estimates
[BLL-OA-TRANS-4233-(6196.3)] N91-26557

P

PACIFIC NORTHWEST LAB., RICHLAND, WA.
Quality Assurance Manual
[DE91-012618] N91-26555
PENNSYLVANIA STATE UNIV., UNIVERSITY PARK.
Computer modeling of soot formation comparing free radical and ionic mechanisms
[AD-A235007] N91-26273
Microstructure, porosity, and mechanical property relationships of calcium-silicate-hydrate
[AD-A235191] N91-26279
Advanced processing and properties of high performance alloys
[AD-A234746] N91-26299
Synthesis and structure of small-molecule cyclic phosphazenes bearing ortho-substituted aryloxy and phenoxy substituents
[AD-A234377] N91-26344
A study of the gas phase chemistry of solid propellants using a microprobe mass spectrometer (MPMS) system: Initial development of the MPMS system
[AD-A234839] N91-26393
A study of the gas phase chemistry of solid propellants using a microprobe mass spectrometer (MPMS) system: Preliminary results for solid fuels (HTPB/Zecorez and BAMO/NMMO), single-base propellant (M10) and an RDX-Based propellant (BLX-9)
[AD-A234840] N91-26394
The wavenumber-frequency filtering characteristics of compliant layers
[AD-A234768] N91-26561
Ice cores and SeaRISE: What we do (and don't) know N91-26579
Hydroacoustics of intermittent boundary-layer flow: A review
[AD-A235092] N91-26883
Backscattering from rough interfaces and the parabolic approximation
[AD-A235184] N91-26886
Acoustic radiation from fluid-loaded, ribbed cylindrical shells excited by different types of concentrated mechanical drives
[AD-A235324] N91-26887
PENNSYLVANIA UNIV., PHILADELPHIA.
New developments in the synthesis and doping of polyacetylene and polyaniline
[AD-A233702] N91-26244
Polyaniline: Synthesis and properties of pernigraniline
[AD-A233706] N91-26245
Photoexcitation spectroscopy of pernigraniline
[AD-A233841] N91-26250
Polyaniline: Allowed oxidation states
[AD-A233842] N91-26251
Interaction of cationic polypeptides with electroactive polypyrrole/poly(styrenesulfonate) and poly(N-methylpyrrole)/poly(styrenesulfonate) films
[AD-A234469] N91-26258
Synthesis, polymerization and thermal properties of a new acetylene-terminated Schiff base
[AD-A233806] N91-26328
Thermal transitions and mechanical properties of the films of chemically prepared polyaniline
[AD-A233807] N91-26329
Polyaniline: Pernigraniline, an isolable intermediate in the conventional chemical synthesis of emeraldine
[AD-A233840] N91-26330
Light induced electron spin resonance in polyaniline
[AD-A233847] N91-26331
X ray structure of polyanilines
[AD-A233848] N91-26332
Thermal stabilities of polyanilines
[AD-A233849] N91-26333
Electron localization in polyaniline and its derivatives
[AD-A233934] N91-26335
Structure, order and the metallic state in polyaniline and its derivatives
[AD-A233935] N91-26336
Impedance profiling: A convenient technique for determining the redox or protonic acid doping characteristics of conducting polymers
[AD-A233941] N91-26337
Novel concepts in electronic polymers: Polyaniline and its derivatives
[AD-A234214] N91-26339
Spectroscopy and photoexcitation spectroscopies of polyaniline: A model system for new phenomena
[AD-A234215] N91-26340
Ring-torsional polarons in polyaniline and polyparaphenylene sulfide
[AD-A234384] N91-26345
Polyaniline: Oriented films and fibers
[AD-A234414] N91-26347
Plasticity of single crystalline Al3X intermetallic compounds
[AD-A234699] N91-26356
Photoinduced absorption and erasable optical information storage in polyanilines
[AD-A234108] N91-27002
PHASEX CORP., LAWRENCE, MA.
Supercritical fluid processing of propellant polymers
[AD-A234285] N91-26341
PHILADELPHIA COLL. OF PHARMACY AND SCIENCE, PA.
High pulse-energy flashlamp-pumpable laser dyes
[AD-A233837] N91-26499
Assessment of the pharmacodynamics of intranasal, intravenous and oral scopolamine N91-27114
PHILLIPS LAB., EDWARDS AFB, CA.
The effects of space debris on solar propulsion
[AD-A235257] N91-26192
Engine cycle analysis for a particle bed reactor nuclear rocket
[AD-A235258] N91-26199
Parametric studies of dense plasma focus for fusion space propulsion with D-He3
[AD-A234578] N91-26941
PITTSBURGH ENERGY TECHNOLOGY CENTER, PA.
MHD contractors' review meeting
[DE91-011295] N91-26945
PITTSBURGH UNIV., PA.
Far- and mid-infrared properties of metal-insulator composite materials
[AD-A234264] N91-26219
Adsorption and decomposition of acetylene on Si(100)-(2x1)
[AD-A233808] N91-26248
Adsorption and thermal behavior of ethylene on Si(100)-(2x1)
[AD-A234098] N91-26252
The stepwise dissociation of NH3 on the Si(111)-(7x7) surface: Low temperature dissociative adsorption and thermal effects
[AD-A235009] N91-26274
Surface chemistry of silicon: The behavior of dangling bonds
[AD-A235011] N91-26275
The synthesis of methanol by a novel method
[DE91-011131] N91-26291
On the sensitivity of solutions of parametrized equations
[AD-A234265] N91-26838
NFEARS: A nonlinear adaptive finite element solver. Part 2: User's manual
[AD-A234416] N91-26842
PLANNING SYSTEMS, INC., MCLEAN, VA.
Progress with neural network gulf streams
[AD-A233810] N91-26658
POTOMAC PHOTONICS, INC., LANHAM, MD.
Quasi-CW excimer laser, phase 2
[AD-A234771] N91-26509
PRAIRIE VIEW AGRICULTURAL AND MECHANICAL COLL., TX.
Design of a lunar oxygen production plant N91-27109
PRATT AND WHITNEY AIRCRAFT, WEST PALM BEACH, FL.
Fiber coating by sputtering for high temperature composites
[AD-A234994] N91-26226
PRC SYSTEMS SERVICES CO., EDWARDS, CA.
Autonomous aircraft initiative study
[NASA-CR-186013] N91-26140
PRINCETON UNIV., NJ.
Acceleration insensitive resonators
[AD-A235400] N91-26458
H-infinity-optimal control for distributed parameter systems
[AD-A234931] N91-26833
PUERTO RICO UNIV., MAYAGUEZ.
Fatigue crack tip plastic strain range measurement studies in two titanium alloys
[AD-A234973] N91-26565

Q

QUEST INTEGRATED, INC., KENT, WA.
Abrasive-waterjet machining of isogrid structures
[AD-A234628] N91-26405

R

RADIAN CORP., SACRAMENTO, CA.
Improvement of procedures for evaluating photochemical models
[PB91-160374] N91-26597
RAND CORP., SANTA MONICA, CA.
How low can an unmanned air vehicle fly?
[RAND-P-7680-RGS] N91-26138
VHSIC electronics and the cost of Air Force avionics in the 1990s
[RAND-R-3843-AF] N91-26143
The wild weasel development programs, one run, one hit, one error
[RAND-P-7661-RGS] N91-26431
RANGE COMMANDERS COUNCIL, WHITE SANDS MISSILE RANGE, NM.
IRIG standard format for Global Positioning System (GPS) data for post-operation interrange exchange
[AD-A234932] N91-26127
HORACE: Presentation-level protocol standard for digital transmission of monochrome television images
[AD-A235276] N91-26428
READING UNIV. (ENGLAND).
Coordination of mesoscale meteorological research between ASL and European groups
[AD-A233586] N91-26639
RENSSELAER POLYTECHNIC INST., TROY, NY.
Transport processes and interfacial phenomena in an evaporating meniscus
[DE91-005561] N91-26284
A program in the chemistry of electronic materials. Task 1: New organometallic precursors for the low pressure chemical vapor deposition of refractory materials for electronics
[AD-A234315] N91-26342
Spread spectrum communications emulator design
[AD-A235403] N91-26430
Improved modeling and performance of squeeze film damper bearings
[AD-A233694] N91-26531
Numerical methods for singularly perturbed differential equations with applications
[AD-A235188] N91-26850
RHODE ISLAND UNIV., NARRAGANSETT.
The SYNOP experiment: Inverted echo sounder data report for June 1989 to September 1990
[AD-A234625] N91-26662
RICE UNIV., HOUSTON, TX.
Marine record of late quaternary glacial-interglacial fluctuations in the Ross Sea and evidence for rapid, episodic sea level change due to marine ice sheet collapse N91-26578
ROCHESTER UNIV., NY.
Proceedings of the Optoelectronic Workshop 27: Semiconductor Lasers and Their Applications
[AD-A233779] N91-26496
Laser switched power linac
[AD-A234581] N91-26507

Proceedings of the Optoelectronic Workshop 25: Liquid Crystal Materials and Devices for Opto-Electronic Applications
[AD-A233780] N91-26921

ROCKEFELLER UNIV., NEW YORK, NY.
Carboxyalkylated hemoglobin as a potential blood substitute
[AD-A233822] N91-26712

ROCKET RESEARCH CORP., REDMOND, WA.
Arcjet endurance test program
[AD-A235232] N91-26198

ROCKWELL INTERNATIONAL CORP., NEWBURY PARK, CA.
Multigigahertz semiconductor lasers
[AD-A234776] N91-26510

ROCKWELL INTERNATIONAL SCIENCE CENTER, THOUSAND OAKS, CA.
Transformation toughening of ceramics
[AD-A234926] N91-26359

ROME AIR DEVELOPMENT CENTER, GRIFFISS AFB, NY.
Digital logic testing and testability
[AD-A234123] N91-26441
RADC cathode life test facility
[AD-A234309] N91-26444
Measuring the quality of knowledge work
[AD-A235354] N91-26994

ROYAL NETHERLANDS METEOROLOGICAL INST., DE BILT.
Description of the RIVM/KNMI puff dispersion model
[KNMI-177] N91-26638

RUTGERS UNIV., NEW BRUNSWICK, NJ.
Content addressable memory project
[AD-A234524] N91-26763

S

SAN FRANCISCO STATE UNIV., CA.
Reflectance spectroscopy of palagonite and iron-rich montmorillonite clay mixtures: Implications for the surface composition of Mars N91-27075

SANDIA NATIONAL LABS., ALBUQUERQUE, NM.
Hypervelocity launch capabilities to over 10.4 km/s
[DE91-010859] N91-26186
Surface Chemkin (version 3.7): A FORTRAN package for analyzing heterogeneous chemical kinetics at a solid-surface-gas-phase interface
[DE91-010840] N91-26285
Grain boundary chemistry in Al-Cu metallizations as determined by analytical electron microscopy
[DE91-012007] N91-26319
Metastable pitting corrosion of aluminum, Al-Cu, and Al-Si thin films in dilute HF solutions and its relevancy to the processing of integrated circuit interconnections
[DE91-012014] N91-26320
Polymer characterization using singlet oxygen phosphorescence as a spectroscopic probe
[DE91-011735] N91-26382
Process monitoring of polyurethane foam using Fourier transform infrared spectroscopy
[DE91-010578] N91-26385
Commercializing solar hydrogen production
[DE91-011232] N91-26398
Proof-of-concept zinc/bromine electric vehicle battery
[DE91-011767] N91-26463
Benchmark study between FIDAP and a cellular automata code
[DE91-011224] N91-26486
Interfacial force sensor with force-feedback control
[DE91-004897] N91-26495
Residual stresses in metal/ceramic brazes: Effect of creep on finite element analysis results
[DE91-011233] N91-26570
The 1990 Sandia rocket-triggered lightning field tests at Kennedy Space Center, Florida
[DE91-011263] N91-26653
Quantitative analysis procedures for Task 8
[DE91-009684] N91-26798
Multiple-frequency SAW devices for chemical sensing and materials characterization
[DE91-010856] N91-26888
Automatic target recognition using acousto-optic image correlator
[DE91-011499] N91-26936
A temperature dependent SPICE macro-model for power MOSFETs
[DE91-011737] N91-26972
Investigation of plessite in iron meterorites and laboratory Fe-Ni(P) alloys
[DE91-010858] N91-27053

SCHOOL OF AEROSPACE MEDICINE, BROOKS AFB, TX.
Refurbishing AV-8 on-board oxygen generation system beds
[AD-A235083] N91-26136
Administrative guide for the flight surgeon and the aeromedical technician: Performing medical examinations
[AD-A235178] N91-26727

SCIENCE RESEARCH LAB., INC., SOMERVILLE, MA.
Scaling CW electron beam pumped rare gas lasers to ultra-high average power
[AD-A235120] N91-26513

SCIENTIFIC RESEARCH ASSOCIATES, INC., GLASTONBURY, CT.
Quantum devices and structures
[AD-A235298] N91-26989

SLOAN-KETTERING INST. FOR CANCER RESEARCH, NEW YORK, NY.
Wound healing by cultured skin cells and growth factors
[AD-A235300] N91-26730

SONOMA TECHNOLOGY, INC., SANTA ROSA, CA.
Improvement of procedures for evaluating photochemical models
[PB91-160374] N91-26597

SOUTH CAROLINA UNIV., COLUMBIA.
Incorporation of shuttle CCT parameters in computer simulation models N91-27096

SOUTHWEST RESEARCH INST., SAN ANTONIO, TX.
Characterization of mechanical damage mechanisms in ceramic composite materials
[NR-032-553] N91-26235
Response of whisker-reinforced ceramic matrix composites to dynamic compressive loading N91-26236
Fragmentation of brittle materials at high rates of loading N91-26237
Long-rod penetration of confined ceramic tiles
[AD-A234312] N91-26534

SPACE TELESCOPE SCIENCE INST., BALTIMORE, MD.
Using HST: From proposal to science N91-27023

SRI INTERNATIONAL CORP., MENLO PARK, CA.
Engineering for artificial intelligence software
[AD-A234793] N91-26814
Ab initio molecular dynamics simulations of surfaces and interfaces
[AD-A235315] N91-26901

ST SYSTEMS CORP., LANHAM, MD.
Constrained trajectory optimization for kinematically redundant arms
[NASA-CR-183477] N91-26527
The 1980 solar maximum mission event listing
[NASA-TM-4287] N91-27087

STANFORD LINEAR ACCELERATOR CENTER, CA.
Gauge bosons and heavy quarks: Proceedings of Summer Institute on Particle Physics
[DE91-011248] N91-26907

STANFORD UNIV., CA.
Comparison of hydrogen desorption kinetics from Si(111)7x7 and Si(100)2x1
[AD-A234633] N91-26262
Comparison of H2 desorption kinetics from Si(111)7x7 and Si(100)2x1
[AD-A234634] N91-26263
Desorption product yields following Cl2 adsorption on Si(111)7x7: Coverage and temperature dependence
[AD-A234635] N91-26264
FTIR studies of water and ammonia decomposition on silicon surfaces
[AD-A234637] N91-26265
Diethylsilane decomposition on silicon surfaces studied using transmission FTIR spectroscopy
[AD-A234638] N91-26266
Adsorption and decomposition of diethylsilane on silicon surfaces
[AD-A234639] N91-26267
Theory and experimental and chemical instabilities
[AD-A234916] N91-26270
Laser-induced desorption of H2 from Si(111)7x7
[AD-A234636] N91-26508
SUNLITE program. Sub-Hertz relative frequency stabilization of two diode laser pumped Nd:YAG lasers locked to a Fabry-Perot interferometer
[NASA-CR-184957] N91-26520
Induced pictorial representations
[AD-A234548] N91-26735
A system and language environment for scientific computing
[AD-A233747] N91-26772
Deductive programming synthesis
[AD-A233770] N91-26774
Adaptive component methods for time dependent PDE's
[AD-A233776] N91-26775
Converting a converging algorithm into a polynomially bounded algorithm
[AD-A234961] N91-26788
Large-scale stochastic linear programs: Importance sampling and Benders decomposition
[AD-A234962] N91-26789
Symbolic expressions of composite grid structures
[AD-A233794] N91-26836
Weighted least squares estimation for Aalen's additive risk model
[AD-A235250] N91-26852
High temperature superconducting films and crystals
[AD-A235234] N91-26965

STATE UNIV. COLL. OF NEW YORK, BUFFALO.
Propagators for quantum oscillator chains
[AD-A234467] N91-26893

STATE UNIV. OF NEW YORK, ALBANY.
Cluster beam analysis via photoionization
[AD-A234111] N91-26253
Effect of aerosols on laser-induced breakdown
[AD-A234324] N91-26502

STATE UNIV. OF NEW YORK, BINGHAMTON.
The distribution of the size and number of shadows cast on a line segment in a Poisson random field
[AD-A233697] N91-26857

STATE UNIV. OF NEW YORK, BUFFALO.
Cationic polymerization within van der Waals clusters of the form (CH2=R)n where R=CH2, CF2 and CHCH3
[AD-A234233] N91-26255
Cluster beam deposition of high temperature materials
[AD-A234358] N91-26343
Field work and dispersion relations of excitations on fractals
[AD-A234953] N91-26455
Trimodal random-field Ising systems in a transverse field
[AD-A235038] N91-26875
Resonance fluorescence spectrum of an atom near a phase conjugator
[AD-A234535] N91-26894
Molecular engineering dynamics of electron transport and nonlinear optical interaction in Langmuir-Blodgett films of organic semiconductor heterostructure
[AD-A235001] N91-26897
Polaron ground state in a double heterostructure of polar crystals
[AD-A235037] N91-26963

STATE UNIV. OF NEW YORK, STONY BROOK.
Study of Josephson effect arrays as sources at 1 THz
[AD-A234526] N91-26952

STERLING FEDERAL SYSTEMS, INC., MOFFETT FIELD, CA.
NSI operations center N91-27038

STERLING SOFTWARE, MOFFETT FIELD, CA.
Requirements management: A CSR's perspective N91-27027
NSI conference support N91-27031

STEVENS INST. OF TECH., HOBOKEN, NJ.
Applications of formal simulation languages in the control and monitoring subsystems of Space Station Freedom N91-27100
High accuracy optical rate sensor N91-27115

SUPERCONDUCTING SUPER COLLIDER LAB., DALLAS, TX.
Normalization of the parameterized Courant-Snyder matrix
[DE91-012554] N91-26856
Coherent beam-beam effects
[DE91-012512] N91-26917

SYRACUSE UNIV., NY.
Uncertainty handling at speech/natural language interface, volume 1
[AD-A234310] N91-26422
Content addressable memory project
[AD-A234524] N91-26763
Design and construction of apparatus for optical switch evaluation
[AD-A234765] N91-26927

SYSTEMS RESEARCH LABS., INC., DAYTON, OH.
Materials/microstructures characterization
[AD-A233751] N91-26295
Aircrew Evaluation Sustained Operations Performance (AESOP): A triservice facility for technology transition
[AD-A234626] N91-26738
Advanced Dynamic Anthropomorphic Manikin (ADAM) design report
[AD-A234761] N91-26756

T

TECHNICAL RESEARCH CENTRE OF FINLAND, ESPOO.
Absorption heat pump in heating and cooling systems of buildings
[DE91-752988] N91-26593

TECOGEN, INC., WALTHAM, MA.
Variable speed gas engine-driven air compressor system. Phase 1: System analysis
[PB91-159533] N91-26530

TEL-AVIV UNIV. (ISRAEL).
Buckling of laminated composite plates
[ITN-91-85101] N91-26232
Calculation of the conductance of two dimensional narrow wires
[ITN-91-85109] N91-26460
Ricochet of sphere off water
[ITN-91-85102] N91-26480
An experimental and numerical study of wavemaker dissipation in the process of direct generation of the resonant sloshing waves in a rectangular tank
[ITN-91-85103] N91-26481
.The delay of turbulent boundary layer separation by oscillatory active control
[ITN-91-85104] N91-26482
Investigation of laminar, fully developed flow in annulus by finite difference model
[ITN-91-85116] N91-26483
Quality by design using statistically planned experiments
[ITN-91-85119] N91-26553
Investigation and characterization of ITO/poly-Si photovoltaic junctions
[ITN-91-85105] N91-26590
UV aurora mapping in corrected geomagnetic coordinates
[ITN-91-85106] N91-26636
On the evolution of raindrop spectra and their effect on the atmosphere below cloud base: Numerical models and comparisons with observations
[ITN-91-85113] N91-26652
Sitting posture analysis. An experimental optimisation approach
[ITN-91-85114] N91-26760
Spectral recovery of discontinuous data
[ITN-91-85115] N91-26853
A sequential Jackson network with feedback
[ITN-91-85111] N91-26867
Queueing systems with orbiting customers
[ITN-91-85112] N91-26868
Creation of uncertainty in repeated two-person non-zero-sum games
[ITN-91-85118] N91-26869
Temporal and spatial correlations in images distorted by a random medium
[ITN-91-85107] N91-26935
Crystallization of thin films of amorphous germanium alloys
[ITN-91-85110] N91-26969
Heuristics for a flow-shop model with parallel machines and setup times
[ITN-91-85117] N91-26996
The light curve of the magnetic star AM - Herculis
[ITN-91-85108] N91-27049
TELECOMMUNICATION SCIENCE ASSOCIATES, INC., SAN DIEGO, CA.
VLF nighttime data analysis
[AD-A234006] N91-26417
TENNESSEE TECHNOLOGICAL UNIV., COOKEVILLE.
Design of optimal correlation filters for hybrid vision systems N91-27110
TEXAS A&M UNIV., COLLEGE STATION.
Thermal degradation chemistry of poly(diphenoxy phosphazene)
[AD-A235264] N91-26282
Ionically and electronically conductive composite polymer membranes
[AD-A234587] N91-26349
Radiation, scattering, and guidance of electromagnetic fields by arbitrarily shaped structures embedded in layered dielectric media
[AD-A234434] N91-26423
Rotordynamic and leakage characteristics of a 4-stage brush seal
[AD-A235336] N91-26541
Stabilization and control problems in structural dynamics
[AD-A235189] N91-26567
Proton arc doses to the primate head
[AD-A235134] N91-26726
Comparison change analysis
[AD-A233690] N91-26873
A nonrecursive order N preconditioned conjugate gradient: Range space formulation of MDOF dynamics N91-27099
TEXAS A&M UNIV., GALVESTON.
Photographic image enhancement N91-27094
TEXAS LUTHERAN COLL., SEGUIN.
Mechanics, impact loads and EMG on the space shuttle treadmill N91-27112
TEXAS UNIV., ARLINGTON.
Electroactive, near infrared absorbing nickel bis(dithiolene) complex polycarbonates and polyurethanes
[AD-A234595] N91-26350
Processable polymers and copolymers of 3-alkylthiophenes and their blends
[AD-A234596] N91-26351
Electronic and ionic transport in processable conducting polymers
[AD-A234597] N91-26352
Surface characterization of electrically conducting nickel tetrathiooxalate/poly(vinyl alcohol) composites
[AD-A234598] N91-26353
Electrochemically induced charge and mass transport in polypyrrole/poly(styrene sulfonate) molecular composites
[AD-A234599] N91-26354
TEXAS UNIV., AUSTIN.
Surface mediated photocatalysis
[AD-A233748] N91-26246
High temperature superconducting planar circuit structures for high frequency applications
[AD-A234335] N91-26445
Near field interaction of microwave signals with a bounded plasma plume
[NASA-CR-185358] N91-26944
TEXAS UNIV., GALVESTON.
Pharmacological sparing of protein in burn injury
[AD-A235026] N91-26724
TEXAS UNIV., SAN ANTONIO.
Interaction of ionizing radiation, genetically active chemicals, and radiofrequency radiation in human and rodent cells
[AD-A234747] N91-26677
Analysis of visual loss from retinal lesions
[AD-A235268] N91-26729
Reexamination of METMAN, recommendations on enhancement of LCVG, and development of new concepts for EMU heat sink N91-27098
TGV, INC., SANTA CRUZ, CA.
MultiNet TCP/P/IP for VAX/VMS update N91-27020
Software product description N91-27037
THERMO-SYSTEMS, INC., SAINT LOUIS, MO.
Testing of a composite thermal structure to insulate the drivers of a large scale blast/thermal simulator
[AD-A234014] N91-26213
THIOKOL CORP., BRIGHAM CITY, UT.
Follow-on cable coupling lightning test. Volume 2: Appendixes A, B, C, and D
[NASA-CR-184124] N91-26195
Technical Evaluation Motor No. 7 (TEM-7)
[NASA-CR-184163] N91-26203
TUFTS UNIV., MEDFORD, MA.
Electrocatalytic study of ammonia synthesis and methane dimerization in high temperature solid electrolyte cells
[DE91-009797] N91-26289

U

UNIFORMED SERVICES UNIV. OF THE HEALTH SCIENCES, BETHESDA, MD.
Molecular studies of cytokine induction
[AD-A235326] N91-26731
UNISYS CORP., RESTON, VA.
Software Technology for Adaptable, Reliable Systems (STARS), UR60-IRIS-Ada toolset. User's guide (draft)
[AD-A234445] N91-26783
UNITED TECHNOLOGIES RESEARCH CENTER, EAST HARTFORD, CT.
Investigation of hot streak migration and film cooling effects on the heat transfer in rotor/stator interacting flows
[AD-A235420] N91-26145
UNIVERSITY OF NORTHERN ARIZONA, FLAGSTAFF.
Evaluation of geophysical properties of the lunar regolith for the design of precursor scientific missions for the space exploration initiative N91-27104
UNIVERSITY OF NORTHERN ILLINOIS, DE KALB.
Gel solidified microinterface between two immiscible electrolytes applied to amperometric detection of picrate and tetramethylammonium
[AD-A235260] N91-26280
UNIVERSITY OF SOUTHERN CALIFORNIA, LOS ANGELES.
Design of polymers with semiconductor, NLO, and structural properties
[AD-A235215] N91-26364
Adaptive spread spectrum networks
[AD-A234084] N91-26419
Integration of neurobiological and computational analyses of the neural network essentials for conditioned taste aversion
[AD-A235164] N91-26744
Studies of optical beam phase-conjugation and electromagnetic scattering process
[AD-A234830] N91-26929
Center for the Integration of Optical C
[AD-A235277] N91-26931
Research instrumentation for optical computing
[AD-A235335] N91-26932
UNIVERSITY OF SOUTHERN MISSISSIPPI, HATTIESBURG.
Novel liquid crystalline polymers as nonlinear optical materials
[AD-A235371] N91-26373
UTAH UNIV., SALT LAKE CITY.
Structure of alkylated silica surfaces: Quenching of fluorescence from covalently bound pyrene
[AD-A234642] N91-26207
Surface diffusion at the liquid-solid interface: Quenching of fluorescence from pyrene covalently bound to methylated silica
[AD-A234645] N91-26268
Raman spectroscopy study of solvation structure in acetonitrile/water mixtures
[AD-A234921] N91-26271
Development and verification of a physical cloud-moisture model for use in general circulation models
[AD-A234751] N91-26643
Imaging of fluorescent and chemiluminescent DNA hybrids using a 2-D CCD camera
[AD-A234641] N91-26676

V

VANDERBILT UNIV., NASHVILLE, TN.
Research on intelligent fault detection and repair advisory systems
[AD-A235267] N91-26551
Matching theory. A sampler: From Denes Koenig to the present
[AD-A234321] N91-26839
Extending matchings in graphs: A survey
[AD-A234392] N91-26841
VARIAN ASSOCIATES, PALO ALTO, CA.
Development of a tactical high-power microwave source using the Plasma Electron Microwave Source (PEMS) concept
[AD-A234967] N91-26942
VERMONT UNIV., BURLINGTON.
Regio- and stereochemical control in substitution reactions of cyclophosphazenes
[AD-A234376] N91-26257
VIRGINIA COMMONWEALTH UNIV., RICHMOND.
Evaluating the effect of accuracy ratios on the percent of calibrations which are out of tolerance N91-27107
VIRGINIA POLYTECHNIC INST., BLACKSBURG.
Nonlinear oscillations of mechanical systems under multifrequency parametric excitation
[AD-A233800] N91-26558
VIRGINIA POLYTECHNIC INST. AND STATE UNIV., BLACKSBURG.
State space models for aeroelastic and viscoelastic systems
[AD-A234730] N91-26117
Space platform power system hardware testbed
[NASA-CR-185839] N91-26204
Development and verification of global/local analysis techniques for laminated composites
[NASA-CR-185060] N91-26238
The development of piezoelectric poly(vinylidene fluoride) sensors for measuring peel stresses in adhesive joints
[AD-A233880] N91-26559
Adaptation and resistance of ecosystems to stress
[AD-A234576] N91-26603

W

WASHINGTON UNIV., RICHLAND.
Investigation of axial positioning for flexural compressors
[NASA-CR-185711] N91-26544
WASHINGTON UNIV., SAINT LOUIS, MO.
Theory of radar target discrimination
[AD-A234172] N91-26420
WASHINGTON UNIV., SEATTLE.
Damage accumulation in advanced metal matrix composites under thermal cycling
[AD-A235002] N91-26227
Dynamic fracture responses of Al2O3, Si3N4, and SiC(w)/Al2O3
[AD-A235286] N91-26229
A combined XPS-ISS modulated molecular beam investigation of the reactions of oxygen and fluorine with silicon surfaces
[AD-A234867] N91-26269
A basic guide to overlay design using nondestructive testing equipment data
[AD-A234472] N91-26403

Process study of sorted patterns on Arctic soils
[AD-A234089] N91-26628
Vertical incidence backscatter and surface forward scattering from near-surface bubbles
[AD-A234432] N91-26880

WEA, CAMBRIDGE, MA.
NDE pattern recognition of LSS states via wave propagation
[AD-A234772] N91-26549

WEATHER WING (1ST), HICKAM AFB, HI.
An overview of tropical circulation
[AD-A234984] N91-26645

WESTINGHOUSE ELECTRIC CORP., PITTSBURGH, PA.
Precipitation in Alloy 718: A combined AEM and APFIM investigation
[DE91-009918] N91-26314
Advanced study in solid transport: Rheological behavior of dense suspension
[DE91-009428] N91-26467

WHITAKER COLL., MA.
The shape of shading
[AD-A234419] N91-26781
Extensions of a theory of networks and learning: Outliers and negative examples
[AD-A234425] N91-26810

WINAND STARING CENTRE, WAGENINGEN (NETHERLANDS).
Application of thematic mapper images to determine regional evaporation from the playas in the western desert of Egypt
[REPT-31] N91-26585

WISCONSIN UNIV., MADISON.
Analytical solution of plane Poiseuille flow of a Johnson-Segalman fluid
[AD-A234313] N91-26472
Terrestrial geophysics in the SeaRISE project
N91-26576

WISCONSIN UNIV., MILWAUKEE.
Bulk wave characterization of high T(sub c) superconductors
[AD-A234649] N91-26954

WOODS HOLE OCEANOGRAPHIC INST., MA.
The High Resolution Profiler (HRP): User's guide and software modifications documentation
[AD-A234640] N91-26663

WORCESTER POLYTECHNIC INST., MA.
Translating expert system rules into Ada code with validation and verification
[NASA-CR-187505] N91-26800

WRIGHT RESEARCH DEVELOPMENT CENTER, WRIGHT-PATTERSON AFB, OH.
Synthesis and properties of rigid-rod benzobisazole polymers containing benzothiazole pendent groups
[AD-A234742] N91-26357

WRIGHT STATE UNIV., DAYTON, OH.
Mechanical behavior and flow mechanisms in refractory metal composition
[AD-A234701] N91-26297

X

XAVIER UNIV. OF LOUISIANA, NEW ORLEANS.
LIF and emission studies of copper and nitrogen
N91-27089

Y

YORK UNIV., DOWNSVIEW (ONTARIO).
Visual sensitivities and discriminations and their role in aviation
[AD-A234866] N91-26740

YORK UNIV. (ONTARIO).
Molecular orientation of the silver tetra neopentoxy phthalo cyanine and stearic acid mixed Langmuir-Blodgett film and its chemical and electrochemical behaviour
[AD-A234601] N91-26206
The control of orbital mixing in ruthenium complexes containing quinone related ligands
[AD-A234602] N91-26260
Tetra neopentoxy phthalo cyanine Langmuir-Blodgett films: Spectroscopy at the air/water interface
[AD-A234603] N91-26261

Typical Contract Number Index Listing

Listings in this index are arranged alphanumerically by contract number. Under each contract number the accession numbers denoting documents that have been produced as a result of research done under that contract are arranged in ascending order. The accession number denotes the number by which the citation is identified.

AF PROJ. 2301 ..... N91-26926
AF PROJ. 2302 ..... N91-26190
N91-26227
N91-26563
AF PROJ. 2303 ..... N91-26270
N91-26349
N91-26366
N91-26898
N91-26899
AF PROJ. 2304 ..... N91-26117
N91-26546
N91-26547
N91-26551
N91-26567
N91-26729
N91-26790
N91-26793
N91-26812
N91-26833
N91-26845
N91-26846
N91-26848
N91-26850
N91-26851
N91-26859
N91-26861
N91-26865
N91-27006
AF PROJ. 2305 ..... N91-26765
N91-26813
N91-26960
N91-27003
AF PROJ. 2306 ..... N91-26279
N91-26298
N91-26301
N91-26304
N91-26356
N91-26362
N91-26955
AF PROJ. 2307 ..... N91-26120
AF PROJ. 2308 ..... N91-26281
AF PROJ. 2310 ..... N91-26643
AF PROJ. 2312 ..... N91-26603
N91-26675
N91-26716
N91-26732
N91-26737
AF PROJ. 2313 ..... N91-26735
N91-26739
N91-26741
N91-26742
AF PROJ. 2338 ..... N91-26441
N91-26994
AF PROJ. 2484 ..... N91-26361
AF PROJ. 3056 ..... N91-26192
AF PROJ. 3058 ..... N91-26199
N91-26941
AF PROJ. 3442 ..... N91-26452
AF PROJ. 3482 ..... N91-26932
AF PROJ. 3484 ..... N91-26191
N91-26297
N91-26303
N91-26931
AF PROJ. 7184 ..... N91-26748
AF PROJ. 7231 ..... N91-26427
AF PROJ. 7659 ..... N91-26626
AF PROJ. 7930 ..... N91-26136
AF PROJ. 9993 ..... N91-26993
AF-AFOSR-ISSA-91-002 ..... N91-26374
AF-AFOSR-0009-89 ..... N91-26955
AF-AFOSR-0017-90 ..... N91-26845
AF-AFOSR-0020-84 ..... N91-26190
AF-AFOSR-0033-90 ..... N91-26301
AF-AFOSR-0039-87 ..... N91-26898
AF-AFOSR-0040-88 ..... N91-26546
AF-AFOSR-0056-90 ..... N91-26675
AF-AFOSR-0059-89 ..... N91-26227
AF-AFOSR-0062-89 ..... N91-26356
AF-AFOSR-0069-88 ..... N91-26899
AF-AFOSR-0073-90 ..... N91-26739
AF-AFOSR-0074-88 ..... N91-26117
AF-AFOSR-0075-89 ..... N91-26861
AF-AFOSR-0076-89 ..... N91-26735
AF-AFOSR-0092-86 ..... N91-26848
AF-AFOSR-0093-86 ..... N91-26859
AF-AFOSR-0110-90 ..... N91-27006
AF-AFOSR-0120-87 ..... N91-26270
AF-AFOSR-0123-87 ..... N91-26361
AF-AFOSR-0133-90 ..... N91-26931
AF-AFOSR-0141-85 ..... N91-26472
AF-AFOSR-0144-87 ..... N91-26551
AF-AFOSR-0146-89 ..... N91-26452
AF-AFOSR-0152-90 ..... N91-26303
AF-AFOSR-0153-90 ..... N91-26366
AF-AFOSR-0155-88 ..... N91-26281
AF-AFOSR-0156-85 ..... N91-26850
AF-AFOSR-0157-86 ..... N91-26120
AF-AFOSR-0162-87 ..... N91-26304
AF-AFOSR-0166-87 ..... N91-26269
AF-AFOSR-0171-89 ..... N91-26563
AF-AFOSR-0173-87 ..... N91-26349
AF-AFOSR-0175-89 ..... N91-26932
AF-AFOSR-0178-90 ..... N91-27003
AF-AFOSR-0191-90 ..... N91-26851
AF-AFOSR-0197-90 ..... N91-26926
AF-AFOSR-0202-86 ..... N91-26812
AF-AFOSR-0204-90 ..... N91-26297
AF-AFOSR-0205-89 ..... N91-26833
AF-AFOSR-0211-90 ..... N91-26191
AF-AFOSR-0218-90 ..... N91-26741
AF-AFOSR-0225-89 ..... N91-26547
AF-AFOSR-0250-89 ..... N91-26865
AF-AFOSR-0256-88 ..... N91-26846
AF-AFOSR-0262-89 ..... N91-26737
AF-AFOSR-0263-88 ..... N91-26603
AF-AFOSR-0267-90 ..... N91-26362
AF-AFOSR-0272-85 ..... N91-26793
AF-AFOSR-0285-88 ..... N91-26790
AF-AFOSR-0294-87 ..... N91-26643
AF-AFOSR-0320-90 ..... N91-26732
AF-AFOSR-0328-87 ..... N91-26507
AF-AFOSR-0334-87 ..... N91-26567
AF-AFOSR-0346-88 ..... N91-26298
AF-AFOSR-0364-87 ..... N91-26716
AF-AFOSR-0379-89 ..... N91-26960
AF-AFOSR-0386-87 ..... N91-26765
AF-AFOSR-0395-87 ..... N91-26279
AF-AFOSR-0435-89 ..... N91-26307
AF-AFOSR-0481-89 ..... N91-26742
AF-AFOSR-0490-89 ..... N91-26729
AF-AFOSR-0500-89 ..... N91-26813
ARB-A832-103 ..... N91-26597
ARPA ORDER 6049 ..... N91-26185
ARPA ORDER 6808 ..... N91-26358
ARPA ORDER 7412-A N91-26503
ARPA ORDER 9520 ..... N91-26961
ATD-89-GNC-1504 ..... N91-26140
DA PROJ. 1L1-61102-AH-45 ..... N91-26233
DA PROJ. 1L1-61102-AH-52 ..... N91-26360
DA PROJ. 1L1-61102-BH-57 ..... N91-26210
DA PROJ. 1L1-62120-AH-25 ..... N91-26213
N91-26473
DA PROJ. 1L1-62618-AH-80 ..... N91-26118
N91-26223
N91-26230
N91-26391
N91-26560
N91-26988
DA PROJ. 1L1-62705-AH-94 ..... N91-26589
DA PROJ. 1L1-62716-AH-70 ..... N91-26743
N91-27007
N91-27008
DA PROJ. 2Q2-63007-A-793 ..... N91-26757
DA PROJ. 3M1-61102-BS-12 ..... N91-26708
DA PROJ. 3M1-61102-BS-15 ..... N91-26671
N91-26719
DA PROJ. 3M1-62772-A-874 ..... N91-26723
DA PROJ. 3M1-62787-A-874 ..... N91-26730
DA PROJ. 3M4-63764-B-995 ..... N91-26709
DA PROJ. 3S1-62772-A-874 ..... N91-26724
DA PROJ. 4A1-61102-AT-24 ..... N91-26644
DA PROJ. 4A7-62730-AT-42 ..... N91-26402
DA PROJ. 4E1-61102-BS-04 ..... N91-26671
DAAA15-86-C-0098 ..... N91-26213
DAAG29-85-K-0251 ..... N91-26586
DAAH01-88-C-0131 ..... N91-26185
DAAL01-88-C-0845 ..... N91-26589
DAAL03-01-G-0006 ..... N91-26210
DAAL03-86-D-0001 ..... N91-26420
DAAL03-86-G-0041 ..... N91-26559
DAAL03-86-G-0056 ..... N91-26440
DAAL03-86-G-0063 ..... N91-26891
DAAL03-86-K-0173 ..... N91-26496
N91-26921
DAAL03-87-K-0037 ..... N91-26134
DAAL03-87-K-0049 ..... N91-26552
DAAL03-87-K-0058 ..... N91-26628
DAAL03-87-K-0093 ..... N91-26502
DAAL03-87-K-0097 ..... N91-26409
DAAL03-87-K-0113 ..... N91-26531
DAAL03-87-K-0114 ..... N91-26533
DAAL03-87-K-0125 ..... N91-26458
DAAL03-87-K-0144 ..... N91-26501
DAAL03-88-K-0012 ..... N91-26246
DAAL03-88-K-0025 ..... N91-26500
DAAL03-88-K-0050 ..... N91-26419
DAAL03-88-K-0068 ..... N91-26534
DAAL03-88-K-0086 ..... N91-26777
N91-26778
DAAL03-89-K-0024 ..... N91-26426
DAAL03-89-K-0129 ..... N91-26857
DAAL03-89-K-0142 ..... N91-26801
DAAL03-89-K-0160 ..... N91-26499
DAAL03-90-G-0069 ..... N91-26873
DACA76-85-C-0010 ..... N91-26781
N91-26782
N91-26810
DACA88-85-M-0271 ..... N91-26161
DACA88-85-M-0786 ..... N91-26161
DACW88-85-D-0004 ..... N91-26161
DAJA45-87-C-0010 ..... N91-26388
DAJA45-90-C-0009 ..... N91-26639
DAJA87-87-C-0031 ..... N91-26346
DAMD17-87-C-7030 ..... N91-26724
DAMD17-87-C-7137 ..... N91-26708
DAMD17-87-C-7235 ..... N91-26719
DAMD17-88-C-8014 ..... N91-26723
DAMD17-88-C-8105 ..... N91-26730
DAMD17-88-C-81699 ..... N91-26712
DARPA ORDER 6177 ..... N91-26774
DASG60-90-C-0061 ..... N91-26513
DCA100-89-C-0015 ..... N91-26794
DE-AC02-76CH-00016 ..... N91-26316
N91-26605
N91-26607
N91-26609
N91-26610
N91-26667
N91-26668
N91-26906
N91-26990
DE-AC02-76CH-03000 ..... N91-26914
N91-26916
N91-27044
DE-AC02-83CH-10093 ..... N91-26588
N91-26591
DE-AC02-89ER-40486 ..... N91-26856

N91-26917
DE-AC03-76SF-00098 ..... N91-26311
N91-26464
N91-26571
N91-26681
N91-26904
N91-26973
N91-26974
N91-26981
N91-26985
N91-26991
N91-26992
N91-27050
N91-27051
DE-AC03-76SF-00515 ..... N91-26907
DE-AC03-89ER-51114 ..... N91-26938
N91-26939
DE-AC04-76DP-00789 ..... N91-26186
N91-26285
N91-26319
N91-26320
N91-26382
N91-26385
N91-26398
N91-26399
N91-26463
N91-26486
N91-26495
N91-26570
N91-26653
N91-26798
N91-26888
N91-26936
N91-26972
N91-27053
DE-AC04-76DR-00789 ..... N91-26978
DE-AC04-88AL-54304 ..... N91-26463
DE-AC05-76OR-00033 ..... N91-26322
DE-AC05-84OR-21400 ..... N91-26240
N91-26242
N91-26293
N91-26314
N91-26316
N91-26317
N91-26321
N91-26322
N91-26323
N91-26325
N91-26380
N91-26383
N91-26384
N91-26524
N91-26572
N91-26656
N91-26680
N91-26854
N91-26908
N91-26909
N91-26911
N91-26982
N91-26983
N91-27043
DE-AC06-76RL-01830 ..... N91-26555
DE-AC07-76ID-01570 ..... N91-26326
DE-AC21-88MC-24216 ..... N91-26970
DE-AC22-88PC-88949 ..... N91-26467
DE-AC22-88PC-88951 ..... N91-26468
DE-AI02-89CE-90023 ..... N91-26386
DE-AI05-83ER-40017 ..... N91-26503
DE-AS05-76ER-03065 ..... N91-26912
DE-FC07-89ID-12848 ..... N91-26315
DE-FG02-84ER-45097 ..... N91-26290
DE-FG02-85ER-13396 ..... N91-26849
DE-FG02-86ER-13529 ..... N91-26905
DE-FG02-86ER-13603 ..... N91-26324
DE-FG02-86ER-13631 ..... N91-26682
DE-FG02-86ER-45256 ..... N91-26983
DE-FG02-87ER-25026 ..... N91-26855
DE-FG02-88ER-13912 ..... N91-26286
DE-FG02-88ER-40388 ..... N91-27052
DE-FG02-88ER-45372 ..... N91-26239
DE-FG02-89CE-90048 ..... N91-26289
DE-FG02-89ER-14045 ..... N91-26284
DE-FG05-88ER-13925 ..... N91-26910
DE-FG21-86MC-23135 ..... N91-26288
DE-FG22-86PC-90526 ..... N91-26243
DE-FG22-89PC-89786 ..... N91-26291
DE-FG22-89PC-89864 ..... N91-26528
DNA001-87-C-0169 ..... N91-26418
DNA001-87-C-0180 ..... N91-26642
DOTS59-89-C-00082 ..... N91-26746
DTCG23-89-C-20008 ..... N91-26128
N91-26129
DTCG39-89-C-E10G56 ..... N91-26751
DTCG39-89-R-80812 ..... N91-26550
DTFA01-89-C-00001 ..... N91-26433
DTFA01-89-Z-02029 ..... N91-26160
EPA-68-01-7365 ..... N91-26598
F04611-89-C-0013 ..... N91-26198
F04611-89-C-0042 ..... N91-26341
F04701-88-C-0089 ..... N91-26115
N91-26183
N91-26305
N91-26415
F04704-90-C-0033 ..... N91-26405
F19628-81-C-0148 ..... N91-26443
F19628-86-K-0039 ..... N91-26952
F19628-88-C-0014 ..... N91-27048
F19628-88-D-0031 ..... N91-26783
F19628-88-K-0001 ..... N91-26635
F19628-88-K-0004 ..... N91-26424
F19628-89-C-0174 ..... N91-26630
F19628-89-K-0026 ..... N91-26631
F19628-90-C-0002 ..... N91-26410
N91-26411
N91-26412
N91-26413
N91-26414
N91-26792
N91-26795
N91-26920
N91-26933
N91-26958
F19628-90-C-0048 ..... N91-26189
F19628-90-K-0029 ..... N91-26633
F29638-87-K-0012 ..... N91-26627
F30602-85-C-0008 ..... N91-26815
N91-26816
N91-26817
N91-26818
N91-26819
N91-26820
N91-26821
N91-26822
N91-26823
N91-26824
N91-26825
N91-26826
N91-26827
N91-26828
N91-26829
N91-26830
N91-26831
N91-26832
F30602-87-D-0093 ..... N91-26429
F30602-87-D-0094 ..... N91-26814
F30602-88-D-0025 ..... N91-26430
N91-26940
F30602-88-D-0026 ..... N91-26811
F30602-88-D-0027 ..... N91-26422
N91-26763
N91-26927
F33615-85-C-0535 ..... N91-26756
F33615-86-C-3414 ..... N91-26133
F33615-86-C-5013 ..... N91-26295
F33615-87-C-0001 ..... N91-26786
F33615-87-C-0610 ..... N91-26677
F33615-87-C-2737 ..... N91-26892
F33615-87-D-0601 ..... N91-26738
F33615-87-D-0627 ..... N91-26726
F33615-88-C-2908 ..... N91-26541
F33615-88-C-5404 ..... N91-26548
F33615-88-C-5509 ..... N91-26228
F33615-89-C-0603 ..... N91-26881
F49620-85-C-0013 ..... N91-26197
F49620-85-C-0144 ..... N91-26860
F49620-86-C-0008 ..... N91-26143
F49620-87-C-0097 ..... N91-26897
F49620-87-C-0100 ..... N91-26364
F49620-87-K-0011 ..... N91-26276
F49620-88-C-0002 ..... N91-26740
F49620-88-C-0003 ..... N91-26119
F49620-88-C-0004 ..... N91-26965
F49620-88-C-0007 ..... N91-26273
F49620-88-C-0016 ..... N91-26678
F49620-88-C-0027 ..... N91-26929
F49620-88-C-0035 ..... N91-26961
F49620-88-C-0036 ..... N91-26549
F49620-88-C-0048 ..... N91-26283
F49620-88-C-0068 ..... N91-26373
F49620-88-C-0092 ..... N91-26509
F49620-88-C-0098 ..... N91-26477
F49620-88-C-0102 ..... N91-26942
F49620-88-C-0131 ..... N91-26564
F49620-89-C-0031 ..... N91-26359
F49620-89-C-0064 ..... N91-26565
F49620-89-C-0066 ..... N91-26226
F49620-89-C-0078 ..... N91-26358
F49620-90-C-0054 ..... N91-26962
F49620-90-C-0055 ..... N91-26934
F49620-90-C-0057 ..... N91-26650
F49620-90-C-0061 ..... N91-26989
GRI-5087-293-1565 ..... N91-26529
GRI-5089-291-1846 ..... N91-26530
GTRI PROJ. A-8013 ..... N91-26655
MAP-HANDBOOK-30 ..... N91-26613
MDA903-87-C-0523 ..... N91-26757
MDA903-89-C-0003 ..... N91-26770
N91-26773
NAGW-1378 ..... N91-27072
NAG1-664 ..... N91-26123
NAG1-675 ..... N91-26238
NAG1-722 ..... N91-26889
NAG1-811 ..... N91-26488
NAG1-839 ..... N91-26520
NAG1-924 ..... N91-26521
NAG1-964 ..... N91-26800
NAG1-1108 ..... N91-26948
NAG2-593 ..... N91-26804
NAG3-166 ..... N91-26479
NAG3-749 ..... N91-26234
NAG5-670 ..... N91-26596
NAG5-864 ..... N91-26462
NAG5-1038 ..... N91-26544
NAG5-1232 ..... N91-26204
NAG8-078 ..... N91-26654
NAG8-717 ..... N91-26806
NAG8-834 ..... N91-26637
NASW-4292 ..... N91-26669
N91-26670
NASW-4520 ..... N91-26182
NAS1-18586 ..... N91-26797
NAS1-18605 ..... N91-26767
NAS2-12393 ..... N91-26126
NAS2-12722 ..... N91-26140
NAS2-13041 ..... N91-26139
NAS3-24816 ..... N91-26490
NAS3-25800 ..... N91-26461
NAS3-25834 ..... N91-26146
NAS3-25883 ..... N91-26205
NAS5-29373 ..... N91-26651
NAS5-30440 ..... N91-26527
NAS8-30490 ..... N91-26195
N91-26203
NAS8-36166 ..... N91-26313
NAS8-36955 ..... N91-26201
N91-26407
NAS8-37142 ..... N91-26655
NAS8-37593 ..... N91-26196
NAS10-11624 ..... N91-26759
NCC2-346 ..... N91-27057
NCC2-507 ..... N91-26114
NCC3-40 ..... N91-26976
NCC3-63 ..... N91-26234
NCC3-127 ..... N91-26944
NCC3-167 ..... N91-26434
NCC9-16 ..... N91-26766
NGT-44-005-803 ..... N91-27088
N91-27089
N91-27090
N91-27091
N91-27092
N91-27093
N91-27094
N91-27095
N91-27096
N91-27097
N91-27098
N91-27099
N91-27100
N91-27101
N91-27102
N91-27103
N91-27104
N91-27105
N91-27106
N91-27107
N91-27108
N91-27109
N91-27110
N91-27111
N91-27112
N91-27113
N91-27114
N91-27115
N91-27116
N91-27117
NR PROJ. RH2-1522 ..... N91-26474
NR PROJ. RR0-1109 ..... N91-26470
NR PROJ. RR0-4108 ..... N91-26280
N91-26731
NR PROJ. RR0-4204 ..... N91-26862
NR PROJ. RR0-4206 ..... N91-26749
N91-26847
NR PROJ. RV3-6121 ..... N91-26769
NR PROJ. RZ6-6512 ..... N91-26406
NSF AST-89-20861 ..... N91-27047
NSF CCR-86-11442 ..... N91-26780

NSF CCR-89-07654 ..... N91-26838
NSF CCR-89-15206 ..... N91-26780
NSF DMR-88-19885 ..... N91-26334
NSF DMS-87-12058 ..... N91-26472
NSF DMS-89-07264 ..... N91-26472
NSF DMS-89-13089 ..... N91-26788
NSF ECS-89-06260 ..... N91-26789
NSF IRI-87-19394 ..... N91-26781
NSG-7415 ..... N91-27056
N00014-80-C-1116 ..... N91-26566
N00014-80-C-9455 ..... N91-26842
N00014-82-K-0260 ..... N91-26248
N91-26252
N91-26274
N91-26275
N00014-82-K-0612 ..... N91-26367
N00014-84-C-0123 ..... N91-26235
N00014-84-G-0201 ..... N91-26206
N91-26260
N91-26261
N00014-84-K-0017 ..... N91-26659
N00014-84-K-0713 ..... N91-26476
N00014-85-K-0124 ..... N91-26535
N91-26781
N91-26782
N91-26809
N91-26810
N00014-85-K-0168 ..... N91-26780
N00014-85-K-0169 ..... N91-26842
N00014-85-K-0198 ..... N91-26849
N00014-85-K-0488 ..... N91-26839
N91-26841
N00014-85-K-0632 ..... N91-26342
N00014-85-K-0685 ..... N91-26446
N00014-85-K-0808 ..... N91-26219
N00014-86-K-0290 ..... N91-26847
N00014-86-K-0381 ..... N91-26299
N00014-86-K-0395 ..... N91-26749
N91-26807
N00014-86-K-0685 ..... N91-26535
N91-26539
N00014-86-K-0719 ..... N91-26799
N00014-87-C-0515 ..... N91-26225
N00014-87-K-0040 ..... N91-26672
N00014-87-K-0074 ..... N91-26634
N00014-87-K-0326 ..... N91-26229
N00014-87-K-0495 ..... N91-26256
N91-26900
N00014-87-K-0670 ..... N91-26471
N00014-87-K-0698 ..... N91-26278
N00014-87-K-0809 ..... N91-26664
N00014-87-K-0825 ..... N91-26764
N91-26780
N00014-88-C-0714 ..... N91-26953
N00014-88-K-0059 ..... N91-26720
N00014-88-K-0075 ..... N91-26280
N00014-88-K-0084 ..... N91-26512
N00014-88-K-0239 ..... N91-26282
N00014-88-K-0279 ..... N91-26843
N00014-88-K-0483 ..... N91-26253
N91-26255
N91-26343
N00014-88-K-0487 ..... N91-26791
N00014-88-K-0731 ..... N91-26277
N91-26302
N00014-88-R-0330 ..... N91-26964
N00014-89-C-0104 ..... N91-26272
N91-26456
N00014-89-C-6027 ..... N91-26665
N00014-89-J-1006 ..... N91-26445
N00014-89-J-1041 ..... N91-26257
N00014-89-J-1073 ..... N91-26663
N00014-89-J-1207 ..... N91-26494
N00014-89-J-1238 ..... N91-26393
N91-26394
N00014-89-J-1296 ..... N91-26744
N00014-89-J-1350 ..... N91-26247
N91-26249
N00014-89-J-1412 ..... N91-26207
N91-26268
N91-26271
N91-26676
N00014-89-J-1489 ..... N91-26803
N00014-89-J-1542 ..... N91-26365
N00014-89-J-1545 ..... N91-26949
N00014-89-J-1588 ..... N91-26220
N00014-89-J-1627 ..... N91-26852
N00014-89-J-1659 ..... N91-26788
N91-26789
N00014-89-J-1734 ..... N91-26951
N00014-89-J-1754 ..... N91-26632
N00014-89-J-1759 ..... N91-26457
N00014-89-J-1815 ..... N91-26772
N91-26775
N91-26836
N00014-89-J-1836 ..... N91-26878
N00014-89-J-1988 ..... N91-26780
N00014-89-J-3124 ..... N91-26713
N00014-89-J-3202 ..... N91-26809
N00014-89-K-0072 ..... N91-27005
N00014-89-K-0132 ..... N91-26901
N00014-90-C-0037 ..... N91-26439
N00014-90-C-0226 ..... N91-26959
N00014-90-C-0246 ..... N91-26922
N00014-90-C-1278 ..... N91-26957
N00014-90-C-2354 ..... N91-26510
N00014-90-C-6007 ..... N91-26658
N00014-90-F-0001 ..... N91-26882
N00014-90-F-0011 ..... N91-26956
N00014-90-J-1025 ..... N91-26838
N91-26842
N00014-90-J-1041 ..... N91-26885
N00014-90-J-1186 ..... N91-26368
N91-26369
N91-26370
N91-26371
N91-26372
N00014-90-J-1193 ..... N91-26455
N91-26875
N91-26893
N91-26894
N91-26963
N00014-90-J-1281 ..... N91-26262
N91-26263
N91-26264
N91-26265
N91-26266
N91-26267
N91-26508
N00014-90-J-1311 ..... N91-26731
N00014-90-J-1320 ..... N91-26350
N91-26351
N91-26352
N91-26353
N91-26354
N00014-90-J-1344 ..... N91-26772
N91-26775
N91-26836
N00014-90-J-1441 ..... N91-26221
N00014-90-J-1475 ..... N91-26896
N00014-90-J-1548 ..... N91-26662
N00014-90-J-1559 ..... N91-26244
N91-26245
N91-26250
N91-26251
N91-26258
N91-26328
N91-26329
N91-26330
N91-26331
N91-26332
N91-26333
N91-26334
N91-26335
N91-26336
N91-26337
N91-26339
N91-26340
N91-26345
N91-27002
N00014-90-J-1568 ..... N91-26662
N00014-90-J-1642 ..... N91-26895
N00014-90-J-1648 ..... N91-26714
N00014-90-J-1815 ..... N91-26734
N00014-90-J-1840 ..... N91-26666
N00014-90-J-1940 ..... N91-26862
N00014-91-J-1046 ..... N91-26780
N00014-91-J-1194 ..... N91-26344
N00014-91-J-1197 ..... N91-26423
N00014-91-J-1222 ..... N91-26874
N00039-84-C-0211 ..... N91-26774
N00039-88-C-0051 ..... N91-26561
N91-26883
N91-26884
N91-26887
N00039-88-C-0054 ..... N91-26880
N00140-88-C-0677 ..... N91-26145
N62269-88-C-0253 ..... N91-26355
N66001-88-D-0033 ..... N91-26417
SWRI PROJ. 8124 ..... N91-26235
W-31-109-ENG-38 ..... N91-26294
N91-26308
N91-26310
N91-26379
N91-26487
N91-26489
N91-26516
N91-26595
N91-26604
N91-26608
N91-26863
N91-26902
N91-26946
N91-26971
N91-26978
N91-26979
N91-26980
N91-26982
N91-26986
W-7405-ENG-36 ..... N91-26292
N91-26484
N91-26515
N91-26522
N91-26554
N91-26871
N91-26915
W-7405-ENG-48 ..... N91-26187
N91-26223
N91-26241
N91-26318
N91-26381
N91-26485
N91-26517
N91-26518
N91-26519
N91-26523
N91-26525
N91-26526
N91-26560
N91-26606
N91-26612
N91-26834
N91-26943
N91-26947
N91-26975
N91-26977
N91-27045
N91-27052
W-7405-ENG-82 ..... N91-26287
N91-26309
N91-26679
N91-26903
N91-26984
151-01-60-03 ..... N91-27057
474-42-10 ..... N91-26202
488-80-04-01 ..... N91-26800
505-35-31 ..... N91-26142
505-59-53 ..... N91-26465
505-62-00 ..... N91-26872
505-62-52 ..... N91-26121
505-62-91 ..... N91-26122
505-63-01-05 ..... N91-26569
505-63-31 ..... N91-26234
505-63-36-06 ..... N91-26137
505-63-50-01 ..... N91-26377
N91-26378
505-64-10-07 ..... N91-26797
505-64-54 ..... N91-26796
505-66-71 ..... N91-26140
505-90-52-01 ..... N91-26767
506-41-3F N91-26461
510-01-0A N91-26233
532-06-37 ..... N91-26139
533-02-51 ..... N91-26113
537-02-21 ..... N91-26146
549-03-31-50 ..... N91-26800
590-13-11 ..... N91-26592
N91-26870
591-41-21 ..... N91-26479
656-63-00 ..... N91-27009

Typical Report Number Index Listing

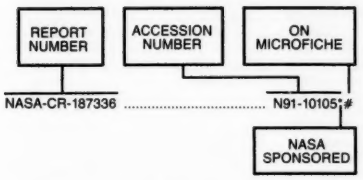

Listings in this index are arranged alphanumerically by report number. The accession number denotes the number by which the citation is identified. An asterisk (*) indicates that the item is a NASA report. A pound sign (#) indicates that the item is available on microfiche.

A-85126 ..... N91-26142* #
A-91077 ..... N91-26796* #
A-91123 ..... N91-26465* #
A-91130 ..... N91-27057* #
A-91159 ..... N91-26139* #

AAMRL-TR-90-023 ..... N91-26756 #
AAMRL-TR-90-026 ..... N91-26427 #
AAMRL-TR-90-060 ..... N91-26748 #

AD-A233410 ..... N91-26799 #
AD-A233586 ..... N91-26639 #
AD-A233651 ..... N91-26545 #
AD-A233653 ..... N91-26625 #
AD-A233655 ..... N91-26769 #
AD-A233656 ..... N91-26626 #
AD-A233662 ..... N91-26770 #
AD-A233663 ..... N91-26402 #
AD-A233664 ..... N91-26671 #
AD-A233666 ..... N91-26408 #
AD-A233671 ..... N91-26469 #
AD-A233674 ..... N91-26387 #
AD-A233690 ..... N91-26873 #
AD-A233694 ..... N91-26531 #
AD-A233696 ..... N91-26409 #
AD-A233697 ..... N91-26857 #
AD-A233700 ..... N91-26748 #
AD-A233702 ..... N91-26244 #
AD-A233704 ..... N91-26949 #
AD-A233706 ..... N91-26245 #
AD-A233707 ..... N91-26891 #
AD-A233714 ..... N91-26771 #
AD-A233716 ..... N91-26586 #
AD-A233717 ..... N91-26470 #
AD-A233719 ..... N91-26919 #
AD-A233721 ..... N91-26877 #
AD-A233722 ..... N91-26410 #
AD-A233723 ..... N91-26411 #
AD-A233724 ..... N91-26412 #
AD-A233725 ..... N91-26413 #
AD-A233726 ..... N91-26920 #
AD-A233727 ..... N91-26414 #
AD-A233728 ..... N91-26672 #
AD-A233739 ..... N91-26749 #
AD-A233744 ..... N91-26439 #
AD-A233746 ..... N91-26327 #
AD-A233747 ..... N91-26772 #
AD-A233748 ..... N91-26246 #
AD-A233751 ..... N91-26295 #
AD-A233753 ..... N91-26708 #
AD-A233756 ..... N91-26415 #
AD-A233757 ..... N91-26773 #
AD-A233766 ..... N91-26709 #
AD-A233767 ..... N91-26710 #
AD-A233768 ..... N91-26711 #
AD-A233770 ..... N91-26774 #
AD-A233773 ..... N91-26733 #
AD-A233776 ..... N91-26775 #
AD-A233777 ..... N91-26388 #
AD-A233778 ..... N91-26210 #
AD-A233779 ..... N91-26496 #
AD-A233780 ..... N91-26921 #
AD-A233784 ..... N91-26750 #
AD-A233785 ..... N91-26892 #
AD-A233786 ..... N91-26776 #
AD-A233794 ..... N91-26836 #
AD-A233797 ..... N91-26416 #
AD-A233798 ..... N91-26751 #
AD-A233800 ..... N91-26558 #
AD-A233801 ..... N91-26247 #
AD-A233806 ..... N91-26328 #
AD-A233807 ..... N91-26329 #
AD-A233808 ..... N91-26248 #
AD-A233809 ..... N91-26673 #
AD-A233810 ..... N91-26658 #
AD-A233811 ..... N91-26249 #
AD-A233822 ..... N91-26712 #
AD-A233823 ..... N91-26497 #
AD-A233824 ..... N91-26498 #
AD-A233826 ..... N91-26659 #
AD-A233827 ..... N91-26988 #
AD-A233837 ..... N91-26499 #
AD-A233840 ..... N91-26330 #
AD-A233841 ..... N91-26250 #
AD-A233842 ..... N91-26251 #
AD-A233847 ..... N91-26331 #
AD-A233848 ..... N91-26332 #
AD-A233849 ..... N91-26333 #
AD-A233855 ..... N91-26993 #
AD-A233862 ..... N91-26334 #
AD-A233868 ..... N91-26864 #
AD-A233880 ..... N91-26559 #
AD-A233883 ..... N91-26627 #
AD-A233916 ..... N91-26500 #
AD-A233924 ..... N91-26211 #
AD-A233928 ..... N91-26389 #
AD-A233929 ..... N91-26390 #
AD-A233934 ..... N91-26335 #
AD-A233935 ..... N91-26336 #
AD-A233941 ..... N91-26337 #
AD-A233942 ..... N91-26713 #
AD-A233944 ..... N91-26131 #
AD-A233965 ..... N91-26777 #
AD-A233973 ..... N91-26714 #
AD-A233977 ..... N91-26674 #
AD-A233978 ..... N91-26858 #
AD-A233979 ..... N91-26837 #
AD-A233980 ..... N91-26532 #
AD-A233981 ..... N91-26115 #
AD-A233986 ..... N91-26212 #
AD-A233989 ..... N91-26778 #
AD-A233991 ..... N91-26878 #
AD-A234005 ..... N91-26922 #
AD-A234006 ..... N91-26417 #
AD-A234014 ..... N91-26213 #
AD-A234031 ..... N91-26715 #
AD-A234033 ..... N91-26440 #
AD-A234039 ..... N91-26296 #
AD-A234051 ..... N91-26418 #
AD-A234062 ..... N91-26214 #
AD-A234084 ..... N91-26419 #
AD-A234087 ..... N91-27001 #
AD-A234089 ..... N91-26628 #
AD-A234098 ..... N91-26252 #
AD-A234102 ..... N91-26215 #
AD-A234108 ..... N91-27002 #
AD-A234111 ..... N91-26253 #
AD-A234114 ..... N91-26801 #
AD-A234121 ..... N91-26779 #
AD-A234123 ..... N91-26441 #
AD-A234124 ..... N91-26802 #
AD-A234127 ..... N91-26761 #
AD-A234129 ..... N91-26254 #
AD-A234130 ..... N91-26950 #
AD-A234131 ..... N91-26132 #
AD-A234172 ..... N91-26420 #
AD-A234186 ..... N91-26216 #
AD-A234187 ..... N91-26217 #
AD-A234188 ..... N91-26338 #
AD-A234190 ..... N91-26629 #
AD-A234191 ..... N91-26879 #
AD-A234194 ..... N91-26442 #
AD-A234203 ..... N91-26218 #
AD-A234214 ..... N91-26339 #
AD-A234215 ..... N91-26340 #
AD-A234222 ..... N91-26471 #
AD-A234233 ..... N91-26255 #
AD-A234255 ..... N91-26391 #
AD-A234264 ..... N91-26219 #
AD-A234265 ..... N91-26838 #
AD-A234284 ..... N91-26421 #
AD-A234285 ..... N91-26341 #
AD-A234288 ..... N91-26197 #
AD-A234289 ..... N91-26630 #
AD-A234297 ..... N91-26533 #
AD-A234306 ..... N91-26642 #
AD-A234308 ..... N91-26443 #
AD-A234309 ..... N91-26444 #
AD-A234310 ..... N91-26422 #
AD-A234312 ..... N91-26534 #
AD-A234313 ..... N91-26472 #
AD-A234314 ..... N91-26501 #
AD-A234315 ..... N91-26342 #
AD-A234321 ..... N91-26839 #
AD-A234322 ..... N91-26220 #
AD-A234324 ..... N91-26502 #
AD-A234325 ..... N91-26762 #
AD-A234335 ..... N91-26445 #
AD-A234336 ..... N91-26256 #
AD-A234342 ..... N91-26840 #
AD-A234353 ..... N91-27118 #
AD-A234354 ..... N91-26503 #
AD-A234358 ..... N91-26343 #
AD-A234359 ..... N91-26807 #
AD-A234360 ..... N91-26808 #
AD-A234375 ..... N91-26221 #
AD-A234376 ..... N91-26257 #
AD-A234377 ..... N91-26344 #
AD-A234384 ..... N91-26345 #
AD-A234385 ..... N91-26125 #
AD-A234390 ..... N91-26504 #
AD-A234392 ..... N91-26841 #
AD-A234403 ..... N91-26346 #
AD-A234404 ..... N91-26780 #
AD-A234414 ..... N91-26347 #
AD-A234416 ..... N91-26842 #
AD-A234419 ..... N91-26781 #
AD-A234420 ..... N91-26809 #
AD-A234421 ..... N91-26782 #
AD-A234422 ..... N91-26535 #
AD-A234423 ..... N91-26446 #
AD-A234425 ..... N91-26810 #
AD-A234432 ..... N91-26880 #
AD-A234434 ..... N91-26423 #
AD-A234435 ..... N91-26734 #
AD-A234440 ..... N91-26424 #
AD-A234442 ..... N91-26675 #
AD-A234445 ..... N91-26783 #
AD-A234446 ..... N91-26222 #
AD-A234448 ..... N91-26940 #
AD-A234449 ..... N91-26811 #
AD-A234456 ..... N91-26133 #
AD-A234466 ..... N91-26951 #
AD-A234467 ..... N91-26893 #
AD-A234469 ..... N91-26258 #
AD-A234471 ..... N91-26843 #
AD-A234472 ..... N91-26403 #
AD-A234473 ..... N91-26404 #
AD-A234475 ..... N91-26752 #
AD-A234476 ..... N91-26491 #
AD-A234478 ..... N91-26844 #
AD-A234493 ..... N91-26223 #
AD-A234496 ..... N91-26560 #
AD-A234504 ..... N91-26874 #
AD-A234507 ..... N91-26447 #
AD-A234524 ..... N91-26763 #
AD-A234526 ..... N91-26952 #
AD-A234528 ..... N91-26784 #
AD-A234535 ..... N91-26894 #
AD-A234536 ..... N91-26348 #
AD-A234538 ..... N91-26660 #
AD-A234545 ..... N91-26859 #
AD-A234546 ..... N91-26546 #
AD-A234547 ..... N91-26547 #
AD-A234548 ..... N91-26735 #
AD-A234549 ..... N91-26716 #
AD-A234552 ..... N91-26473 #

AD-A234553 ..... N91-26474 #
AD-A234555 ..... N91-26785 #
AD-A234559 ..... N91-26492 #
AD-A234560 ..... N91-26425 #
AD-A234561 ..... N91-26259 #
AD-A234568 ..... N91-26661 #
AD-A234573 ..... N91-26451 #
AD-A234576 ..... N91-26603 #
AD-A234578 ..... N91-26941 #
AD-A234579 ..... N91-26881 #
AD-A234580 ..... N91-26895 #
AD-A234581 ..... N91-26507 #
AD-A234583 ..... N91-26736 #
AD-A234587 ..... N91-26349 #
AD-A234588 ..... N91-26845 #
AD-A234589 ..... N91-26737 #
AD-A234592 ..... N91-26754 #
AD-A234595 ..... N91-26350 #
AD-A234596 ..... N91-26351 #
AD-A234597 ..... N91-26352 #
AD-A234598 ..... N91-26353 #
AD-A234599 ..... N91-26354 #
AD-A234601 ..... N91-26206 #
AD-A234602 ..... N91-26260 #
AD-A234603 ..... N91-26261 #
AD-A234620 ..... N91-26953 #
AD-A234624 ..... N91-26896 #
AD-A234625 ..... N91-26662 #
AD-A234626 ..... N91-26738 #
AD-A234628 ..... N91-26405 #
AD-A234633 ..... N91-26262 #
AD-A234634 ..... N91-26263 #
AD-A234635 ..... N91-26264 #
AD-A234636 ..... N91-26508 #
AD-A234637 ..... N91-26265 #
AD-A234638 ..... N91-26266 #
AD-A234639 ..... N91-26267 #
AD-A234640 ..... N91-26663 #
AD-A234641 ..... N91-26676 #
AD-A234642 ..... N91-26207 #
AD-A234645 ..... N91-26268 #
AD-A234646 ..... N91-26812 #
AD-A234649 ..... N91-26954 #
AD-A234650 ..... N91-26860 #
AD-A234653 ..... N91-26803 #
AD-A234657 ..... N91-26755 #
AD-A234658 ..... N91-26717 #
AD-A234659 ..... N91-26718 #
AD-A234660 ..... N91-26116 #
AD-A234666 ..... N91-26355 #
AD-A234670 ..... N91-26719 #
AD-A234699 ..... N91-26356 #
AD-A234700 ..... N91-26813 #
AD-A234701 ..... N91-26297 #
AD-A234702 ..... N91-26298 #
AD-A234703 ..... N91-26955 #
AD-A234707 ..... N91-26426 #
AD-A234709 ..... N91-26786 #
AD-A234716 ..... N91-26452 #
AD-A234729 ..... N91-26846 #
AD-A234730 ..... N91-26117 #
AD-A234732 ..... N91-27003 #
AD-A234733 ..... N91-26926 #
AD-A234742 ..... N91-26357 #
AD-A234744 ..... N91-26631 #
AD-A234745 ..... N91-26475 #
AD-A234746 ..... N91-26299 #
AD-A234747 ..... N91-26677 #
AD-A234748 ..... N91-26548 #
AD-A234751 ..... N91-26643 #
AD-A234752 ..... N91-26861 #
AD-A234754 ..... N91-26739 #
AD-A234755 ..... N91-26720 #
AD-A234758 ..... N91-26148 #
AD-A234761 ..... N91-26756 #
AD-A234765 ..... N91-26927 #
AD-A234768 ..... N91-26561 #
AD-A234771 ..... N91-26509 #
AD-A234772 ..... N91-26549 #
AD-A234773 ..... N91-26358 #
AD-A234775 ..... N91-26134 #
AD-A234776 ..... N91-26510 #
AD-A234780 ..... N91-26644 #
AD-A234784 ..... N91-26721 #
AD-A234785 ..... N91-26550 #
AD-A234790 ..... N91-26956 #
AD-A234792 ..... N91-26189 #
AD-A234793 ..... N91-26814 #
AD-A234796 ..... N91-26928 #
AD-A234797 ..... N91-26300 #
AD-A234798 ..... N91-26180 #
AD-A234799 ..... N91-26562 #
AD-A234800 ..... N91-26453 #
AD-A234801 ..... N91-26181 #
AD-A234802 ..... N91-26493 #
AD-A234804 ..... N91-26511 #
AD-A234808 ..... N91-26538 #
AD-A234828 ..... N91-26208 #
AD-A234830 ..... N91-26929 #
AD-A234831 ..... N91-26563 #
AD-A234835 ..... N91-26957 #
AD-A234836 ..... N91-26958 #
AD-A234837 ..... N91-26454 #
AD-A234839 ..... N91-26393 #
AD-A234840 ..... N91-26394 #
AD-A234841 ..... N91-26512 #
AD-A234852 ..... N91-26427 #
AD-A234863 ..... N91-26494 #
AD-A234866 ..... N91-26740 #
AD-A234867 ..... N91-26269 #
AD-A234880 ..... N91-26815 #
AD-A234881 ..... N91-26816 #
AD-A234882 ..... N91-26817 #
AD-A234883 ..... N91-26818 #
AD-A234884 ..... N91-26819 #
AD-A234885 ..... N91-26820 #
AD-A234886 ..... N91-26821 #
AD-A234887 ..... N91-26822 #
AD-A234888 ..... N91-26823 #
AD-A234889 ..... N91-26824 #
AD-A234890 ..... N91-26825 #
AD-A234891 ..... N91-26826 #
AD-A234892 ..... N91-26827 #
AD-A234893 ..... N91-26828 #
AD-A234894 ..... N91-26829 #
AD-A234895 ..... N91-26830 #
AD-A234896 ..... N91-26831 #
AD-A234897 ..... N91-26832 #
AD-A234898 ..... N91-26787 #
AD-A234903 ..... N91-26564 #
AD-A234910 ..... N91-26678 #
AD-A234916 ..... N91-26270 #
AD-A234921 ..... N91-26271 #
AD-A234925 ..... N91-26865 #
AD-A234926 ..... N91-26359 #
AD-A234931 ..... N91-26833 #
AD-A234932 ..... N91-26127 #
AD-A234934 ..... N91-27004 #
AD-A234939 ..... N91-26360 #
AD-A234941 ..... N91-26722 #
AD-A234944 ..... N91-26184 #
AD-A234945 ..... N91-26118 #
AD-A234951 ..... N91-26225 #
AD-A234952 ..... N91-26847 #
AD-A234953 ..... N91-26455 #
AD-A234955 ..... N91-26741 #
AD-A234957 ..... N91-26183 #
AD-A234959 ..... N91-26272 #
AD-A234960 ..... N91-26456 #
AD-A234961 ..... N91-26788 #
AD-A234962 ..... N91-26789 #
AD-A234965 ..... N91-26882 #
AD-A234966 ..... N91-26361 #
AD-A234967 ..... N91-26942 #
AD-A234971 ..... N91-26866 #
AD-A234973 ..... N91-26565 #
AD-A234978 ..... N91-26135 #
AD-A234984 ..... N91-26645 #
AD-A234985 ..... N91-26764 #
AD-A234986 ..... N91-26959 #
AD-A234987 ..... N91-26664 #
AD-A234990 ..... N91-26149 #
AD-A234992 ..... N91-26119 #
AD-A234994 ..... N91-26226 #
AD-A234997 ..... N91-26723 #
AD-A235001 ..... N91-26897 #
AD-A235002 ..... N91-26227 #
AD-A235003 ..... N91-26742 #
AD-A235005 ..... N91-26395 #
AD-A235006 ..... N91-26396 #
AD-A235007 ..... N91-26273 #
AD-A235009 ..... N91-26274 #
AD-A235010 ..... N91-27005 #
AD-A235011 ..... N91-26275 #
AD-A235013 ..... N91-26765 #
AD-A235014 ..... N91-26960 #
AD-A235015 ..... N91-27006 #
AD-A235016 ..... N91-26301 #
AD-A235018 ..... N91-26790 #
AD-A235019 ..... N91-26961 #
AD-A235025 ..... N91-26962 #
AD-A235026 ..... N91-26724 #
AD-A235027 ..... N91-26848 #
AD-A235028 ..... N91-26185 #
AD-A235030 ..... N91-26276 #
AD-A235031 ..... N91-26362 #
AD-A235033 ..... N91-27007 #
AD-A235034 ..... N91-27008 #
AD-A235035 ..... N91-26743 #
AD-A235037 ..... N91-26963 #
AD-A235038 ..... N91-26875 #
AD-A235055 ..... N91-26302 #
AD-A235057 ..... N91-26277 #
AD-A235059 ..... N91-26190 #
AD-A235060 ..... N91-26849 #
AD-A235083 ..... N91-26136 #
AD-A235085 ..... N91-26539 #
AD-A235086 ..... N91-26791 #
AD-A235090 ..... N91-26406 #
AD-A235091 ..... N91-26540 #
AD-A235092 ..... N91-26883 #
AD-A235093 ..... N91-26884 #
AD-A235097 ..... N91-26885 #
AD-A235102 ..... N91-26964 #
AD-A235103 ..... N91-26566 #
AD-A235104 ..... N91-26363 #
AD-A235109 ..... N91-26278 #
AD-A235112 ..... N91-26665 #
AD-A235114 ..... N91-26725 #
AD-A235115 ..... N91-26188 #
AD-A235120 ..... N91-26513 #
AD-A235121 ..... N91-26666 #
AD-A235134 ..... N91-26726 #
AD-A235135 ..... N91-26303 #
AD-A235143 ..... N91-26144 #
AD-A235164 ..... N91-26744 #
AD-A235165 ..... N91-26792 #
AD-A235168 ..... N91-26304 #
AD-A235170 ..... N91-26632 #
AD-A235172 ..... N91-26476 #
AD-A235173 ..... N91-26633 #
AD-A235178 ..... N91-26727 #
AD-A235182 ..... N91-26646 #
AD-A235184 ..... N91-26886 #
AD-A235186 ..... N91-26191 #
AD-A235188 ..... N91-26850 #
AD-A235189 ..... N91-26567 #
AD-A235190 ..... N91-26477 #
AD-A235191 ..... N91-26279 #
AD-A235194 ..... N91-26728 #
AD-A235199 ..... N91-26305 #
AD-A235211 ..... N91-26930 #
AD-A235215 ..... N91-26364 #
AD-A235217 ..... N91-26898 #
AD-A235219 ..... N91-26851 #
AD-A235221 ..... N91-26457 #
AD-A235223 ..... N91-26228 #
AD-A235225 ..... N91-26128 #
AD-A235226 ..... N91-26129 #
AD-A235227 ..... N91-26647 #
AD-A235228 ..... N91-26648 #
AD-A235231 ..... N91-26306 #
AD-A235232 ..... N91-26198 #
AD-A235233 ..... N91-26899 #
AD-A235234 ..... N91-26965 #
AD-A235235 ..... N91-26365 #
AD-A235241 ..... N91-26120 #
AD-A235242 ..... N91-26793 #
AD-A235243 ..... N91-26366 #
AD-A235245 ..... N91-26634 #
AD-A235249 ..... N91-26757 #
AD-A235250 ..... N91-26852 #
AD-A235252 ..... N91-26862 #
AD-A235257 ..... N91-26192 #
AD-A235258 ..... N91-26199 #
AD-A235260 ..... N91-26280 #
AD-A235267 ..... N91-26551 #
AD-A235268 ..... N91-26729 #
AD-A235273 ..... N91-26758 #
AD-A235274 ..... N91-26514 #
AD-A235275 ..... N91-26794 #
AD-A235276 ..... N91-26428 #
AD-A235277 ..... N91-26931 #
AD-A235278 ..... N91-26281 #
AD-A235279 ..... N91-26307 #
AD-A235284 ..... N91-26282 #
AD-A235286 ..... N91-26229 #
AD-A235297 ..... N91-26900 #
AD-A235298 ..... N91-26989 #
AD-A235300 ..... N91-26730 #
AD-A235301 ..... N91-26130 #
AD-A235303 ..... N91-26589 #
AD-A235305 ..... N91-26649 #
AD-A235307 ..... N91-26367 #
AD-A235309 ..... N91-26283 #
AD-A235310 ..... N91-26635 #
AD-A235315 ..... N91-26901 #
AD-A235324 ..... N91-26887 #
AD-A235326 ..... N91-26731 #
AD-A235327 ..... N91-26230 #
AD-A235328 ..... N91-26552 #
AD-A235333 ..... N91-26429 #
AD-A235335 ..... N91-26932 #
AD-A235336 ..... N91-26541 #
AD-A235337 ..... N91-26732 #
AD-A235340 ..... N91-26587 #
AD-A235343 ..... N91-26231 #
AD-A235345 ..... N91-26795 #

AD-A235347 ..... N91-26568 #
AD-A235350 ..... N91-26368 #
AD-A235351 ..... N91-26369 #
AD-A235354 ..... N91-26994 #
AD-A235357 ..... N91-26370 #
AD-A235359 ..... N91-26371 #
AD-A235360 ..... N91-26372 #
AD-A235371 ..... N91-26373 #
AD-A235372 ..... N91-27048 #
AD-A235400 ..... N91-26458 #
AD-A235403 ..... N91-26430 #
AD-A235404 ..... N91-26933 #
AD-A235410 ..... N91-26478 #
AD-A235417 ..... N91-26650 #
AD-A235419 ..... N91-26995 #
AD-A235420 ..... N91-26145 #
AD-A235424 ..... N91-26374 #
AD-A235426 ..... N91-26934 #

AD-D014857 ..... N91-26224 #
AD-D014858 ..... N91-26536 #
AD-D014859 ..... N91-26753 #
AD-D014860 ..... N91-26923 #
AD-D014861 ..... N91-26537 #
AD-D014862 ..... N91-26448 #
AD-D014864 ..... N91-26924 #
AD-D014865 ..... N91-26505 #
AD-D014866 ..... N91-26147 #
AD-D014869 ..... N91-26449
AD-D014871 ..... N91-26506 #
AD-D014872 ..... N91-26450
AD-D014876 ..... N91-26392
AD-D014877 ..... N91-26925

AD-E040002 ..... N91-26587 #
AD-E501362 ..... N91-26770 #
AD-E951634 ..... N91-26420 #

AEDC-TR-91-1 ..... N91-26197 #

AEDC-TSR-91-V1 ..... N91-26188 #

AEROCHEM-TP-495 ..... N91-26273 #

AFGWC/TN-91/001 ..... N91-26649 #

AFHRL-TP-90-34 ..... N91-26786 #

AFOEHL-EI00178MGA ..... N91-26211 #

AFOSR-91-0199TR ..... N91-26932 #
AFOSR-91-0225TR ..... N91-26358 #
AFOSR-91-0229TR ..... N91-26273 #
AFOSR-91-0230TR ..... N91-26549 #
AFOSR-91-0231TR ..... N91-26929 #
AFOSR-91-0233TR ..... N91-26564 #
AFOSR-91-0234TR ..... N91-26565 #
AFOSR-91-0235TR ..... N91-26477 #
AFOSR-91-0236TR ..... N91-26678 #
AFOSR-91-0237TR ..... N91-26740 #
AFOSR-91-0238TR-PHASE-2 ..... N91-26509 #
AFOSR-91-0239TR ..... N91-26860 #
AFOSR-91-0240TR ..... N91-26942 #
AFOSR-91-0242TR ..... N91-26742 #
AFOSR-91-0243TR ..... N91-26737 #
AFOSR-91-0245TR ..... N91-26741 #
AFOSR-91-0246TR ..... N91-26897 #
AFOSR-91-0247TR ..... N91-26845 #
AFOSR-91-0248TR ..... N91-26190 #
AFOSR-91-0250TR ..... N91-26191 #
AFOSR-91-0251TR ..... N91-26361 #
AFOSR-91-0252TR ..... N91-26865 #
AFOSR-91-0253TR ..... N91-26790 #
AFOSR-91-0254TR ..... N91-26848 #
AFOSR-91-0255TR ..... N91-26739 #
AFOSR-91-0256TR ..... N91-26269 #
AFOSR-91-0257TR ..... N91-26279 #
AFOSR-91-0261TR ..... N91-26227 #
AFOSR-91-0262TR ..... N91-26861 #
AFOSR-91-0264TR ..... N91-26567 #
AFOSR-91-0265TR ..... N91-26850 #
AFOSR-91-0267TR ..... N91-26643 #
AFOSR-91-0269TR ..... N91-26452 #
AFOSR-91-0270 ..... N91-26349 #
AFOSR-91-0271TR ..... N91-27003 #
AFOSR-91-0272TR ..... N91-26117 #
AFOSR-91-0273TR ..... N91-26926 #
AFOSR-91-0274TR ..... N91-26846 #
AFOSR-91-0275TR ..... N91-26547 #
AFOSR-91-0276TR ..... N91-26546 #
AFOSR-91-0277TR ..... N91-26859 #
AFOSR-91-0278TR ..... N91-26812 #
AFOSR-91-0281TR ..... N91-26955 #
AFOSR-91-0283TR ..... N91-26716 #
AFOSR-91-0284TR ..... N91-26735 #
AFOSR-91-0358TR ..... N91-26833 #
AFOSR-91-0376TR ..... N91-26675 #
AFOSR-91-0377TR ..... N91-26603 #
AFOSR-91-0378TR ..... N91-26507 #
AFOSR-91-0379TR ..... N91-26563 #
AFOSR-91-0380TR ..... N91-26120 #
AFOSR-91-0381TR ..... N91-26793 #
AFOSR-91-0382TR ..... N91-26270 #
AFOSR-91-0383TR ..... N91-26366 #
AFOSR-91-0387TR ..... N91-26283 #
AFOSR-91-0388TR ..... N91-26961 #
AFOSR-91-0389TR ..... N91-26989 #
AFOSR-91-0390TR-PHASE-1 ..... N91-26962 #
AFOSR-91-0391TR ..... N91-26276 #
AFOSR-91-0395TR ..... N91-27006 #
AFOSR-91-0396TR ..... N91-26960 #
AFOSR-91-0397TR ..... N91-26765 #
AFOSR-91-0398TR ..... N91-26307 #
AFOSR-91-0399TR ..... N91-26362 #
AFOSR-91-0400TR ..... N91-26301 #
AFOSR-91-0442TR ..... N91-26732 #
AFOSR-91-0443TR ..... N91-26965 #
AFOSR-91-0445TR ..... N91-26899 #
AFOSR-91-0446TR ..... N91-26304 #
AFOSR-91-0448TR ..... N91-26374 #
AFOSR-91-0449TR ..... N91-26303 #
AFOSR-91-0450TR ..... N91-26298 #
AFOSR-91-0451TR ..... N91-26297 #
AFOSR-91-0452TR ..... N91-26813 #
AFOSR-91-0453TR ..... N91-26356 #
AFOSR-91-0493TR-PHASE-1 ..... N91-26650 #
AFOSR-91-0495TR ..... N91-26934 #
AFOSR-91-0496TR ..... N91-26898 #
AFOSR-91-0497TR ..... N91-26364 #
AFOSR-91-0498TR ..... N91-26373 #
AFOSR-91-0499TR ..... N91-26551 #
AFOSR-91-0500TR ..... N91-26851 #
AFOSR-91-0501TR ..... N91-26729 #

AGARD-AG-160-VOL-19 ..... N91-26432 #
AGARD-AG-317 ..... N91-26150 #
AGARD-AG-318(E) ..... N91-26124 #

AI-M-1168 ..... N91-26782 #
AI-M-1220 ..... N91-26810 #
AI-M-1255 ..... N91-26535 #
AI-M-1264 ..... N91-26781 #
AI-M-1269 ..... N91-26446 #
AI-M-1277 ..... N91-26809 #

AI-TR-1235 ..... N91-26539 #
AI-TR-1251 ..... N91-26791 #

AL-TR-90-069 ..... N91-26198 #

ANL/CP-70073 ..... N91-26902 #
ANL/CP-70076 ..... N91-26516 #
ANL/CP-70860 ..... N91-26294 #
ANL/CP-70929 ..... N91-26978 #
ANL/CP-71092 ..... N91-26971 #
ANL/CP-71156 ..... N91-26979 #
ANL/CP-71255 ..... N91-26863 #
ANL/CP-71726 ..... N91-26608 #
ANL/CP-71865 ..... N91-26986 #
ANL/CP-72194 ..... N91-26980 #
ANL/CP-72383 ..... N91-26595 #
ANL/CP-72401 ..... N91-26487 #
ANL/CP-72421 ..... N91-26489 #
ANL/CP-72657 ..... N91-26379 #
ANL/CP-72791 ..... N91-26310 #
ANL/CP-72859 ..... N91-26604 #
ANL/CP-72897 ..... N91-26946 #
ANL/CP-72968 ..... N91-26982 #

ANL/PP-66981 ..... N91-26308 #

APL-UW-TR-9022 ..... N91-26880 #

APTI-5005 ..... N91-26630 #

ARAED-TR-91001 ..... N91-26390 #
ARAED-TR-91002 ..... N91-26389 #

ARB-R-91/453 ..... N91-26597 #

ARCCB-TR-91012 ..... N91-26296 #

ARFSD-TR-91007 ..... N91-26785 #
ARFSD-TR-91008 ..... N91-26184 #

ARI-RN-91-35-VOL-2 ..... N91-26757 #

ARO-23056.1-GS ..... N91-26586 #
ARO-23759.3-EG-F ..... N91-26559 #
ARO-23788.2-EL-F ..... N91-26440 #
ARO-23804.1-MS-F ..... N91-26891 #
ARO-24376.4-GS ..... N91-26628 #
ARO-24626.209-PH-UIR ..... N91-26496 #
ARO-24626.210-PH-UIR ..... N91-26921 #
ARO-24720.24-EG ..... N91-26558 #
ARO-24738.7-EG ..... N91-26134 #
ARO-24803.5-GS ..... N91-26502 #
ARO-24839.7-EG ..... N91-26531 #
ARO-24867.8-EG ..... N91-26533 #
ARO-24923.9-MA ..... N91-26778 #
ARO-24923.10-MA ..... N91-26777 #
ARO-25003.1-GS ..... N91-26501 #
ARO-25077.6-MS ..... N91-26552 #
ARO-25169.13-CH ..... N91-26246 #
ARO-25289.7-EG ..... N91-26458 #
ARO-25342.28-EL ..... N91-26409 #
ARO-25347.2-MA ..... N91-26857 #
ARO-25478.19-PH ..... N91-26500 #
ARO-25507-31-EL ..... N91-26419 #
ARO-26067.5-MS-A ..... N91-26534 #
ARO-26150.3-EL ..... N91-26801 #
ARO-26275.3-GS ..... N91-26426 #
ARO-27514.2-CH ..... N91-26499 #
ARO-27574.4-MA ..... N91-26873 #
ARO-28321.1-MS-CF ..... N91-26210 #

ASD-TR-90-5010 ..... N91-26125 #
ASD-TR-90-5014 ..... N91-26995 #
ASD-TR-90-5018 ..... N91-26131 #
ASD-TR-91-5004-STUDY-1 ..... N91-26130 #

ASI690-329-90-II-VOL-2 ..... N91-26757 #

ASME-91-GT-217 ..... N91-26146* #

ASMI-CR-RD-AS-91-6 ..... N91-26420 #

AVF-VSR-383.0291 ..... N91-26771 #
AVF-VSR-384.0291 ..... N91-26776 #

AVSCOM-TR-91-B-005 ..... N91-26569* #
AVSCOM-TR-91-C-008 ..... N91-26233* #

B-233745 ..... N91-26194 #

BLL-OA-TRANS-4233-(6196.3) ..... N91-26557 #
BLL-OA-TRANS-4238-(6196.3) ..... N91-26556 #

BMO-TR-91-03 ..... N91-26405 #

BNL-44234 ..... N91-26667 #
BNL-45864 ..... N91-26607 #
BNL-45968 ..... N91-26668 #
BNL-45993 ..... N91-26906 #
BNL-46045 ..... N91-26605 #
BNL-46062 ..... N91-26609 #
BNL-46065 ..... N91-26610 #
BNL-46067 ..... N91-26990 #

BRL-CR-655 ..... N91-26223 #
BRL-CR-656 ..... N91-26560 #
BRL-CR-658 ..... N91-26213 #
BRL-CR-663 ..... N91-26230 #

BRL-MR-3907 ..... N91-26116 #

BRL-TR-3189 ..... N91-26391 #
BRL-TR-3214 ..... N91-26988 #
BRL-TR-3215 ..... N91-26473 #
BRL-TR-3225 ..... N91-26118 #

CAR-TR-545 ..... N91-26874 #

CBIP-M-60 ..... N91-26781 #

CBIP-46 ..... N91-26810 #

CCI-G89-0056-01 ..... N91-26665 #

CERC-TR-91-1 ..... N91-26661 #

CLASSIC-91-25 ..... N91-26836 #

CMC-GIT-90-1 ..... N91-26190 #

CMS-TSR-90-24 ..... N91-26472 #

CONF-900593-2 ..... N91-26326 #
CONF-900799 ..... N91-26907 #
CONF-900936-28 ..... N91-26974 #
CONF-900944-42 ..... N91-26981 #
CONF-900944-43 ..... N91-26973 #
CONF-900944-44 ..... N91-26464 #
CONF-901008-11 ..... N91-26570 #
CONF-901105-114 ..... N91-26294 #
CONF-901105-115 ..... N91-26978 #
CONF-901105-116 ..... N91-26979 #
CONF-901105-123 ..... N91-26985 #

CONF-901155-7 ..... N91-26291 #
CONF-901184-1 ..... N91-26383 #
CONF-901219-14 ..... N91-26947 #
CONF-901244-3 ..... N91-26495 #
CONF-901293-1 ..... N91-26522 #
CONF-910123-28 ..... N91-26523 #
CONF-910192-1 ..... N91-26982 #
CONF-910202-12 ..... N91-26971 #
CONF-910202-14 ..... N91-26310 #
CONF-910202-15 ..... N91-26311 #
CONF-910217-1 ..... N91-26834 #
CONF-910279-14 ..... N91-26385 #
CONF-910318-16 ..... N91-26588 #
CONF-910340-8 ..... N91-26571 #
CONF-910373-SUMM ..... N91-26916 #
CONF-910373-4 ..... N91-26914 #
CONF-910373-6 ..... N91-27044 #
CONF-910402-13 ..... N91-26382 #
CONF-910402-15 ..... N91-26909 #
CONF-910406-6 ..... N91-26319 #
CONF-910406-7 ..... N91-26320 #
CONF-910406-9 ..... N91-26986 #
CONF-910430-2 ..... N91-26242 #
CONF-910450-8 ..... N91-26936 #
CONF-910485-1 ..... N91-26379 #
CONF-910503-9 ..... N91-26293 #
CONF-910505-12 ..... N91-26915 #
CONF-910505-34 ..... N91-26975 #
CONF-910550-1-EXTD-ABST ..... N91-26680 #
CONF-910595-9 ..... N91-26526 #
CONF-910602-22 ..... N91-26572 #
CONF-910602-31 ..... N91-26317 #
CONF-910602-39 ..... N91-26487 #
CONF-910608-2 ..... N91-26292 #
CONF-910609-13 ..... N91-26938 #
CONF-910609-14 ..... N91-26939 #
CONF-910614-3 ..... N91-26314 #
CONF-910645-2 ..... N91-26240 #
CONF-910648-2 ..... N91-26863 #
CONF-910651-8 ..... N91-26946 #
CONF-910659-13 ..... N91-26608 #
CONF-910659-17 ..... N91-26609 #
CONF-910659-18 ..... N91-26610 #
CONF-910711-6 ..... N91-26911 #
CONF-910731-1 ..... N91-26380 #
CONF-910739-1 ..... N91-26485 #
CONF-910739-2 ..... N91-26284 #
CONF-910759-1 ..... N91-26484 #
CONF-910771-2 ..... N91-26854 #
CONF-8907240-1 ..... N91-26612 #
CONF-9006343-1 ..... N91-26992 #
CONF-9007117-4 ..... N91-26525 #
CONF-9007188-2 ..... N91-26990 #
CONF-9008204-1 ..... N91-26903 #
CONF-9010138-2 ..... N91-26316 #
CONF-9010227-3 ..... N91-26186 #
CONF-9010243-17 ..... N91-26906 #
CONF-9010287-8 ..... N91-26518 #
CONF-9011198-1 ..... N91-27050 #
CONF-9011198-3 ..... N91-27051 #
CONF-9101100-1 ..... N91-27052 #
CONF-9102101-1 ..... N91-26315 #
CONF-9102104-1 ..... N91-26980 #
CONF-9102110-1 ..... N91-26595 #
CONF-9102112-ABSTS ..... N91-26945 #
CONF-9103131-4 ..... N91-26399 #
CONF-9103134-3 ..... N91-27053 #
CONF-9103164-1 ..... N91-26398 #
CONF-9104106-5 ..... N91-26604 #
CONF-9104163-6 ..... N91-26656 #
CONF-9104164-4 ..... N91-26517 #
CONF-9104192-3 ..... N91-26515 #
CONF-9104192-4 ..... N91-26524 #
CONF-9104202-4 ..... N91-26486 #
CONF-9104226-1 ..... N91-26489 #
CONF-9104231-1 ..... N91-26241 #
CONF-9104234-2 ..... N91-26991 #
CONF-9104240-1 ..... N91-26187 #
CONF-9104241-1 ..... N91-26943 #
CONF-9104242-1 ..... N91-26908 #
CONF-9105162-2 ..... N91-26902 #
CONF-9105162-3 ..... N91-26516 #
CONF-9105166-1 ..... N91-26554 #
CONF-9105169-1 ..... N91-26972 #
CONF-9106116-3 ..... N91-26888 #
CONF-9106146-3 ..... N91-26322 #
CONF-9106146-4 ..... N91-26983 #
CONF-9106146-5 ..... N91-26321 #
CONF-9106146-6 ..... N91-26323 #
CONF-9106146-7 ..... N91-26325 #
CONF-9107104-1 ..... N91-26606 #

CRC-573 ..... N91-26144 #

CRREL-SR-91-5 ..... N91-26402 #

CRREL-TD-90-1 ..... N91-26348 #

CRREL-91-2 ..... N91-26644 #

CS-TR-2639 ..... N91-26874 #

CU-CS-489-90 ..... N91-26777 #
CU-CS-491-90 ..... N91-26778 #

CWI-NM-R9016 ..... N91-26835 #
CWI-NM-R9018 ..... N91-26768 #

CWRU/DMS/TR-38 ..... N91-26964 #

DCA/JDSSC-SRS-1-90-VOL-4 ..... N91-26794 #

DCIEM-91-06 ..... N91-26758 #

DE91-002050 ..... N91-26970 #
DE91-002060 ..... N91-26288 #
DE91-002151 ..... N91-26588 #
DE91-002159 ..... N91-26591 #
DE91-004829 ..... N91-26484 #
DE91-004897 ..... N91-26495 #
DE91-005070 ..... N91-26485 #
DE91-005561 ..... N91-26284 #
DE91-008201 ..... N91-26528 #
DE91-008202 ..... N91-26243 #
DE91-009428 ..... N91-26467 #
DE91-009524 ..... N91-26383 #
DE91-009684 ..... N91-26798 #
DE91-009766 ..... N91-26977 #
DE91-009787 ..... N91-26239 #
DE91-009797 ..... N91-26289 #
DE91-009918 ..... N91-26314 #
DE91-010060 ..... N91-26315 #
DE91-010088 ..... N91-26326 #
DE91-010147 ..... N91-26572 #
DE91-010243 ..... N91-26904 #
DE91-010282 ..... N91-26294 #
DE91-010285 ..... N91-26978 #
DE91-010388 ..... N91-26240 #
DE91-010451 ..... N91-26384 #
DE91-010466 ..... N91-26612 #
DE91-010552 ..... N91-26468 #
DE91-010578 ..... N91-26385 #
DE91-010597 ..... N91-26979 #
DE91-010727 ..... N91-26980 #
DE91-010781 ..... N91-26656 #
DE91-010806 ..... N91-26316 #
DE91-010816 ..... N91-26379 #
DE91-010840 ..... N91-26285 #
DE91-010856 ..... N91-26888 #
DE91-010858 ..... N91-27053 #
DE91-010859 ..... N91-26186 #
DE91-010915 ..... N91-26905 #
DE91-010923 ..... N91-26399 #
DE91-010980 ..... N91-26906 #
DE91-011018 ..... N91-26386 #
DE91-011029 ..... N91-26286 #
DE91-011072 ..... N91-26290 #
DE91-011085 ..... N91-26854 #
DE91-011099 ..... N91-26380 #
DE91-011125 ..... N91-26308 #
DE91-011126 ..... N91-26902 #
DE91-011131 ..... N91-26291 #
DE91-011132 ..... N91-26667 #
DE91-011142 ..... N91-26309 #
DE91-011160 ..... N91-26595 #
DE91-011168 ..... N91-26489 #
DE91-011179 ..... N91-26971 #
DE91-011194 ..... N91-26241 #
DE91-011224 ..... N91-26486 #
DE91-011232 ..... N91-26398 #
DE91-011233 ..... N91-26570 #
DE91-011248 ..... N91-26907 #
DE91-011263 ..... N91-26653 #
DE91-011295 ..... N91-26945 #
DE91-011366 ..... N91-26317 #
DE91-011369 ..... N91-26908 #
DE91-011381 ..... N91-26292 #
DE91-011382 ..... N91-26515 #
DE91-011390 ..... N91-26554 #
DE91-011399 ..... N91-26522 #
DE91-011404 ..... N91-26915 #
DE91-011499 ..... N91-26936 #
DE91-011512 ..... N91-26381 #
DE91-011516 ..... N91-27043 #
DE91-011531 ..... N91-26606 #
DE91-011543 ..... N91-27052 #
DE91-011710 ..... N91-26990 #
DE91-011728 ..... N91-26607 #
DE91-011735 ..... N91-26382 #
DE91-011737 ..... N91-26972 #
DE91-011740 ..... N91-26938 #
DE91-011741 ..... N91-26939 #

DE91-011744 ..... N91-26871 #
DE91-011746 ..... N91-26604 #
DE91-011747 ..... N91-26310 #
DE91-011750 ..... N91-26608 #
DE91-011767 ..... N91-26463 #
DE91-011824 ..... N91-27050 #
DE91-011826 ..... N91-26991 #
DE91-011828 ..... N91-26981 #
DE91-011835 ..... N91-26982 #
DE91-011844 ..... N91-26487 #
DE91-011849 ..... N91-26863 #
DE91-011850 ..... N91-26516 #
DE91-011851 ..... N91-26946 #
DE91-011867 ..... N91-26681 #
DE91-011892 ..... N91-26571 #
DE91-011894 ..... N91-26973 #
DE91-011897 ..... N91-26311 #
DE91-011899 ..... N91-26992 #
DE91-011905 ..... N91-26903 #
DE91-011911 ..... N91-26464 #
DE91-011916 ..... N91-26974 #
DE91-011919 ..... N91-26834 #
DE91-011921 ..... N91-26318 #
DE91-011931 ..... N91-26187 #
DE91-011964 ..... N91-26975 #
DE91-011966 ..... N91-26983 #
DE91-011967 ..... N91-26943 #
DE91-011972 ..... N91-26605 #
DE91-011974 ..... N91-27044 #
DE91-011976 ..... N91-26914 #
DE91-012007 ..... N91-26319 #
DE91-012014 ..... N91-26320 #
DE91-012022 ..... N91-26984 #
DE91-012023 ..... N91-26287 #
DE91-012024 ..... N91-26679 #
DE91-012036 ..... N91-26523 #
DE91-012049 ..... N91-26916 #
DE91-012051 ..... N91-26321 #
DE91-012057 ..... N91-26524 #
DE91-012058 ..... N91-26909 #
DE91-012062 ..... N91-26322 #
DE91-012067 ..... N91-26680 #
DE91-012068 ..... N91-26323 #
DE91-012069 ..... N91-26242 #
DE91-012074 ..... N91-26609 #
DE91-012075 ..... N91-26610 #
DE91-012077 ..... N91-26668 #
DE91-012079 ..... N91-26517 #
DE91-012080 ..... N91-26518 #
DE91-012081 ..... N91-26525 #
DE91-012082 ..... N91-26526 #
DE91-012089 ..... N91-26947 #
DE91-012105 ..... N91-27045 #
DE91-012111 ..... N91-26519 #
DE91-012128 ..... N91-26805 #
DE91-012162 ..... N91-26910 #
DE91-012171 ..... N91-26682 #
DE91-012172 ..... N91-26855 #
DE91-012182 ..... N91-26324 #
DE91-012222 ..... N91-26293 #
DE91-012227 ..... N91-26911 #
DE91-012300 ..... N91-26912 #
DE91-012348 ..... N91-27051 #
DE91-012355 ..... N91-26985 #
DE91-012473 ..... N91-26986 #
DE91-012508 ..... N91-26325 #
DE91-012512 ..... N91-26917 #
DE91-012554 ..... N91-26856 #
DE91-012618 ..... N91-26555 #
DE91-752988 ..... N91-26593 #

DLA-91-P00177 ..... N91-26451 #
DLA-91-P90272 ..... N91-26545 #

DNA-TR-90-9 ..... N91-26418 #
DNA-TR-90-101 ..... N91-26642 #

DOE/CE-90023/T1 ..... N91-26386 #
DOE/CE-90048/2 ..... N91-26289 #

DOE/ER-0496P ..... N91-26805 #
DOE/ER-03065/T8 ..... N91-26912 #
DOE/ER-13529/5 ..... N91-26905 #
DOE/ER-13603/4 ..... N91-26324 #
DOE/ER-13631/T1 ..... N91-26682 #
DOE/ER-13912/3 ..... N91-26286 #
DOE/ER-13925/2 ..... N91-26910 #
DOE/ER-25026/T3 ..... N91-26855 #
DOE/ER-45097/6 ..... N91-26290 #
DOE/ER-45372/2 ..... N91-26239 #

DOE/MC-23135/2980 ..... N91-26288 #
DOE/MC-24218/2957 ..... N91-26970 #

DOE/PC-88949/T8 ..... N91-26467 #
DOE/PC-88951/7 ..... N91-26468 #

DOE/PC-89864/T2 ..... N91-26528 #
DOE/PC-90526/T2 ..... N91-26243 #

DOT-P-15-89-5 ..... N91-26746 #

DOT/FAA/AM-91/2 ..... N91-26721 #

DOT/FAA/CT-91/12 ..... N91-26433 #

DOT/FAA/RD-90/28 ..... N91-26160 #
DOT/FAA/RD-90/31 ..... N91-26161 #

DR-5-3 ..... N91-26195* #

DREO-TN-90-25 ..... N91-26408 #

DTRC-SR-1309 ..... N91-26660 #

DTRC-91/006 ..... N91-26469 #

DTRC/SME-91/05 ..... N91-26568 #

DU/DC/TR-19 ..... N91-26949 #

D6-55699-1-PHASE-2 ..... N91-26126* #

E-4999 ..... N91-26479* #
E-5974 ..... N91-26592* #
E-5979 ..... N91-26233* #
E-6040-1 ..... N91-26872* #
E-6054 ..... N91-26234* #
E-6243 ..... N91-26121* #
E-6246 ..... N91-26490* #
E-6290 ..... N91-26122* #
E-6313 ..... N91-26146* #
E-6348 ..... N91-26870* #
E-6378 ..... N91-26202* #

ECS-SS3900 ..... N91-26195* #

EGG-M-90209 ..... N91-26326 #
EGG-M-91092 ..... N91-26315 #

ENF-TM-90-6 ..... N91-26131 #

EPA/600/3-91/001 ..... N91-26594 #
EPA/600/3-91/019 ..... N91-26602 #
EPA/600/3-91/020 ..... N91-26598 #
EPA/600/4-91/004 ..... N91-26601 #

ESD-TR-90-117 ..... N91-26413 #
ESD-TR-90-118 ..... N91-26795 #
ESD-TR-90-119 ..... N91-26958 #
ESD-TR-90-133 ..... N91-26412 #
ESD-TR-90-134 ..... N91-26411 #
ESD-TR-90-139 ..... N91-26414 #
ESD-TR-90-140 ..... N91-26920 #
ESD-TR-90-144 ..... N91-26792 #
ESD-TR-90-147 ..... N91-26410 #
ESD-TR-90-188 ..... N91-26933 #

ETN-91-99100 ..... N91-26638
ETN-91-99409 ..... N91-26835 #
ETN-91-99411 ..... N91-26768 #
ETN-91-99440 ..... N91-26585 #
ETN-91-99496 ..... N91-26913 #

FFA-147 ..... N91-26466 #

FNAL/C-91/83 ..... N91-26916 #
FNAL/C-91/86 ..... N91-27044 #
FNAL/C-91/91 ..... N91-26914 #

FTD-ID(RS)T-0466-90 ..... N91-26538 #
FTD-ID(RS)T-0550-90 ..... N91-26497 #
FTD-ID(RS)T-0754-90 ..... N91-26300 #
FTD-ID(RS)T-0958-90 ..... N91-26327 #
FTD-ID(RS)T-1062-90 ..... N91-26562 #
FTD-ID(RS)T-1080-90 ..... N91-26453 #
FTD-ID(RS)T-1181-90 ..... N91-26511 #
FTD-ID(RS)T-1272-90 ..... N91-26928 #
FTD-ID(RS)T-1273-90 ..... N91-26180 #
FTD-ID(RS)T-1276-90 ..... N91-26148 #
FTD-ID(RS)T-1277-90 ..... N91-26493 #
FTD-ID(RS)T-1368-90 ..... N91-26181 #

GA-A-20448 ..... N91-26939 #
GA-A-20466 ..... N91-26938 #

GA-C-20422 ..... N91-26358 #

GA-C19466 ..... N91-26953 #

GAO/NSIAD-91-2 ..... N91-26132 #
GAO/NSIAD-91-142 ..... N91-26400 #
GAO/NSIAD-91-194 ..... N91-26141 #

GAO/NSIAD-91-196 ..... N91-26397 #
GAO/NSIAD-91-252 ..... N91-26194 #

GEOMET-IE-2096 ..... N91-26746 #

GL-SR-264 ..... N91-26626 #

GL-TR-90-0145 ..... N91-26631 #
GL-TR-90-0190 ..... N91-26633 #
GL-TR-90-0206 ..... N91-26627 #
GL-TR-90-0248 ..... N91-26424 #
GL-TR-90-0267 ..... N91-26630 #
GL-TR-90-0288 ..... N91-26626 #
GL-TR-90-0317 ..... N91-26189 #
GL-TR-90-0328 ..... N91-27048 #

GR-7670-1162(NP) ..... N91-26783 #

GRI-90/0339 ..... N91-26529 #
GRI-91/0001 ..... N91-26530 #

H-1543 ..... N91-26113* #
H-1609 ..... N91-26140* #

HCSCIA-CR91-001 ..... N91-26736 #

HDL-TM-91-3 ..... N91-26447 #

HDL-TR-2196 ..... N91-26514 #

HEL-TM-4-91 ..... N91-26743 #
HEL-TM-5-91 ..... N91-27008 #
HEL-TM-6-91 ..... N91-27007 #

ICASE-IR-91-3 ..... N91-26767* #

ICMA-91-157-PT-2 ..... N91-26842 #
ICMA-91-158 ..... N91-26838 #

IDA-D-898 ..... N91-26773 #

IDA-P-2378 ..... N91-26770 #

IDA/HQ-90-36708 ..... N91-26773 #
IDA/HQ-90-035362 ..... N91-26770 #

IIT-5-54718-1 ..... N91-26303 #

INT-PATENT-CLASS-H03D-1/04 ..... N91-26438*

IRIG-STANDARD-164-91 ..... N91-26127 #

IS-M-663 ..... N91-26903 #

IS-T-1513 ..... N91-26679 #
IS-T-1522 ..... N91-26287 #
IS-T-1530 ..... N91-26309 #
IS-T-1543 ..... N91-26984 #

ISBN-0-8330-1026-3 ..... N91-26143 #
ISBN-92-835-0613-8 ..... N91-26124 #
ISBN-92-835-0617-0 ..... N91-26150 #
ISBN-92-835-0621-9 ..... N91-26432 #

ISSN-0915-633X ..... N91-26937 #
ISSN-0924-3062 ..... N91-26585 #

ITN-91-85101 ..... N91-26232
ITN-91-85102 ..... N91-26480
ITN-91-85103 ..... N91-26481
ITN-91-85104 ..... N91-26482
ITN-91-85105 ..... N91-26590
ITN-91-85106 ..... N91-26636
ITN-91-85107 ..... N91-26935
ITN-91-85108 ..... N91-27049
ITN-91-85109 ..... N91-26460
ITN-91-85110 ..... N91-26969
ITN-91-85111 ..... N91-26867
ITN-91-85112 ..... N91-26868
ITN-91-85113 ..... N91-26652
ITN-91-85114 ..... N91-26760
ITN-91-85115 ..... N91-26853
ITN-91-85116 ..... N91-26483
ITN-91-85117 ..... N91-26996
ITN-91-85118 ..... N91-26869
ITN-91-85119 ..... N91-26553

JPL-D-6665 ..... N91-26624* #

JPRS-UES-91-002 ..... N91-26581 #
JPRS-UES-91-003 ..... N91-26582 #

JPRS-ULS-91-009 ..... N91-26688 #
JPRS-ULS-91-010 ..... N91-26683 #
JPRS-ULS-91-011 ..... N91-26696 #

JPRS-USP-91-002 ..... N91-26162 #

KGC4-M-2 ..... N91-26196* #

KNMI-177 ..... N91-26638

LA-UR-90-3782 ..... N91-26484 #
LA-UR-91-1077 ..... N91-26522 #
LA-UR-91-1196 ..... N91-26554 #
LA-UR-91-1267 ..... N91-26515 #
LA-UR-91-1275 ..... N91-26292 #
LA-UR-91-1287 ..... N91-26915 #

LA-11858-MS ..... N91-26871 #

LBL-28891 ..... N91-26464 #
LBL-28892 ..... N91-26981 #
LBL-28991 ..... N91-26973 #
LBL-29313 ..... N91-26992 #
LBL-29395 ..... N91-26311 #
LBL-29522 ..... N91-26974 #
LBL-29546 ..... N91-26991 #
LBL-29702 ..... N91-26571 #
LBL-29862 ..... N91-26985 #
LBL-30136 ..... N91-26681 #
LBL-30291 ..... N91-26904 #
LBL-30590 ..... N91-27050 #
LBL-30591 ..... N91-27051 #

LC-89-70202 ..... N91-26143 #

M-657 ..... N91-26654* #

MEMS-ALC-14 ..... N91-26301 #

MIT/LCS/TM-412.C ..... N91-26780 #

MIT/LCS/TR-498 ..... N91-26764 #
MIT/LCS/TR-502 ..... N91-26803 #

MRC-R-1262R ..... N91-26418 #

MSRR-560 ..... N91-26849 #

MTL-TR-91-10 ..... N91-26231 #

MTR-M90-92 ..... N91-26421 #

MTR-90W00164 ..... N91-26433 #

NA-89-1122L ..... N91-26133 #

NADC-90066-60 ..... N91-26222 #
NADC-90119-60 ..... N91-26306 #
NADC-91004-60 ..... N91-26149 #
NADC-91016-60 ..... N91-26355 #

NAS 1.15:4268 ..... N91-26654* #
NAS 1.15:4287 ..... N91-27087* #
NAS 1.15:4291 ..... N91-27119* #
NAS 1.15:86680 ..... N91-26142* #
NAS 1.15:102999 ..... N91-27055* #
NAS 1.15:103540 ..... N91-26312* #
NAS 1.15:103541 ..... N91-26193* #
NAS 1.15:103736 ..... N91-26592* #
NAS 1.15:103739 ..... N91-26233* #
NAS 1.15:103821 ..... N91-26759* #
NAS 1.15:103859 ..... N91-26465* #
NAS 1.15:103886 ..... N91-26796* #
NAS 1.15:104054 ..... N91-26137* #
NAS 1.15:104079 ..... N91-26569* #
NAS 1.15:104099 ..... N91-26378* #
NAS 1.15:104100 ..... N91-26377* #
NAS 1.15:104372 ..... N91-26234* #
NAS 1.15:104376 ..... N91-26872* #
NAS 1.15:104415 ..... N91-26490* #
NAS 1.15:104449 ..... N91-26122* #
NAS 1.15:104466 ..... N91-26146* #
NAS 1.15:104483 ..... N91-26121* #
NAS 1.15:104491 ..... N91-26870* #
NAS 1.15:104510 ..... N91-26202* #
NAS 1.15:104977 ..... N91-26624* #
NAS 1.26.184124 ..... N91-26195* #
NAS 1.26:3922(34) N91-26669*
NAS 1.26:3922(36) N91-26670*
NAS 1.26:4256 ..... N91-26479* #
NAS 1.26:4378 ..... N91-27056* #
NAS 1.26:177576 ..... N91-26126* #
NAS 1.26:177585 ..... N91-26139* #
NAS 1.26:183477 ..... N91-26527* #
NAS 1.26:183730 ..... N91-26196* #
NAS 1.26:184163 ..... N91-26203* #
NAS 1.26:184165 ..... N91-26655* #
NAS 1.26:184166 ..... N91-26313* #
NAS 1.26:184957 ..... N91-26520* #
NAS 1.26:184983 ..... N91-26201* #

NAS 1.26:185060 ..... N91-26238* #
NAS 1.26:185343 ..... N91-26123* #
NAS 1.26:185356 ..... N91-26488* #
NAS 1.26:185358 ..... N91-26944* #
NAS 1.26:185453 ..... N91-26889* #
NAS 1.26:185637-VOL-1 ..... N91-27088* #
NAS 1.26:185637-VOL-2 ..... N91-27103* #
NAS 1.26:185711 ..... N91-26544* #
NAS 1.26:185839 ..... N91-26204* #
NAS 1.26:185842 ..... N91-26976* #
NAS 1.26:185843 ..... N91-26462* #
NAS 1.26:186013 ..... N91-26140* #
NAS 1.26:186086 ..... N91-26182* #
NAS 1.26:187112 ..... N91-26205* #
NAS 1.26:187116 ..... N91-26461* #
NAS 1.26:187505 ..... N91-26800* #
NAS 1.26:187522 ..... N91-26797* #
NAS 1.26:187571 ..... N91-26767* #
NAS 1.26:187774 ..... N91-26407*
NAS 1.26:187786 ..... N91-26521* #
NAS 1.26:187919 ..... N91-26766* #
NAS 1.26:187953 ..... N91-26806* #
NAS 1.26:188035 ..... N91-26434* #
NAS 1.26:188491 ..... N91-26637* #
NAS 1.26:188498 ..... N91-26804* #
NAS 1.26:188581 ..... N91-26948* #
NAS 1.26:188615 ..... N91-26114* #
NAS 1.26:188622 ..... N91-26596* #
NAS 1.26:188623 ..... N91-26613* #
NAS 1.55:3115-VOL-2 ..... N91-26573* #
NAS 1.55:3117 ..... N91-27009* #
NAS 1.55:10074 ..... N91-27057* #
NAS 1.60:3120 ..... N91-26113* #
NAS 1.61:1264 ..... N91-26651* #
NAS 1.71:LAR-14435-1-CU ..... N91-26159* #
NAS 1.71:LEW-14999-2 ..... N91-26376* #
NAS 1.71:LEW-15155-1 ..... N91-26375* #
NAS 1.71:LEW-15196-1 ..... N91-26543* #
NAS 1.71:LEW-15222-1 ..... N91-26966* #
NAS 1.71:LEW-15223-1 ..... N91-26967* #
NAS 1.71:MFS-28458-1 ..... N91-26459* #
NAS 1.71:MFS-28473-1 ..... N91-26968* #
NAS 1.71:MFS-28521-1 ..... N91-26542* #
NAS 1.71:14846-2 ..... N91-26200* #

NASA-CASE-GSC-13179-1 ..... N91-26438*

NASA-CASE-LAR-14435-1-CU ..... N91-26159* #

NASA-CASE-LEW-14846-2 ..... N91-26200* #
NASA-CASE-LEW-14999-2 ..... N91-26376* #
NASA-CASE-LEW-15155-1 ..... N91-26375* #
NASA-CASE-LEW-15196-1 ..... N91-26543* #
NASA-CASE-LEW-15222-1 ..... N91-26966* #
NASA-CASE-LEW-15223-1 ..... N91-26967* #

NASA-CASE-MFS-28458-1 ..... N91-26459* #
NASA-CASE-MFS-28473-1 ..... N91-26968* #
NASA-CASE-MFS-28521-1 ..... N91-26542* #

NASA-CASE-MSC-21025-3 ..... N91-26747*

NASA-CASE-NPO-17512-1-CU N91-26918*

NASA-CP-3115-VOL-2 ..... N91-26573* #
NASA-CP-3117 ..... N91-27009* #
NASA-CP-10074 ..... N91-27057* #

NASA-CR-3922(34) N91-26669*
NASA-CR-3922(36) N91-26670*
NASA-CR-4256 ..... N91-26479* #
NASA-CR-4378 ..... N91-27056* #
NASA-CR-177576 ..... N91-26126* #
NASA-CR-177585 ..... N91-26139* #
NASA-CR-183477 ..... N91-26527* #
NASA-CR-183730 ..... N91-26196* #
NASA-CR-184124 ..... N91-26195* #
NASA-CR-184163 ..... N91-26203* #
NASA-CR-184165 ..... N91-26655* #
NASA-CR-184166 ..... N91-26313* #
NASA-CR-184957 ..... N91-26520* #
NASA-CR-184983 ..... N91-26201* #
NASA-CR-185060 ..... N91-26238* #
NASA-CR-185343 ..... N91-26123* #
NASA-CR-185356 ..... N91-26488* #
NASA-CR-185358 ..... N91-26944* #
NASA-CR-185453 ..... N91-26889* #
NASA-CR-185637-VOL-1 ..... N91-27088* #
NASA-CR-185637-VOL-2 ..... N91-27103* #
NASA-CR-185711 ..... N91-26544* #
NASA-CR-185839 ..... N91-26204* #
NASA-CR-185842 ..... N91-26976* #
NASA-CR-185843 ..... N91-26462* #
NASA-CR-186013 ..... N91-26140* #
NASA-CR-186086 ..... N91-26182* #
NASA-CR-187112 ..... N91-26205* #
NASA-CR-187116 ..... N91-26461* #
NASA-CR-187505 ..... N91-26800* #
NASA-CR-187522 ..... N91-26797* #
NASA-CR-187571 ..... N91-26767* #
NASA-CR-187774 ..... N91-26407*
NASA-CR-187786 ..... N91-26521* #
NASA-CR-187919 ..... N91-26766* #
NASA-CR-187953 ..... N91-26806* #
NASA-CR-188035 ..... N91-26434* #
NASA-CR-188491 ..... N91-26637* #
NASA-CR-188498 ..... N91-26804* #
NASA-CR-188581 ..... N91-26948* #
NASA-CR-188615 ..... N91-26114* #
NASA-CR-188622 ..... N91-26596* #
NASA-CR-188623 ..... N91-26613* #

NASA-RP-1264 ..... N91-26651* #

NASA-TM-4268 ..... N91-26654* #
NASA-TM-4287 ..... N91-27087* #
NASA-TM-4291 ..... N91-27119* #
NASA-TM-86680 ..... N91-26142* #
NASA-TM-102999 ..... N91-27055* #
NASA-TM-103540 ..... N91-26312* #
NASA-TM-103541 ..... N91-26193* #
NASA-TM-103736 ..... N91-26592* #
NASA-TM-103739 ..... N91-26233* #
NASA-TM-103821 ..... N91-26759* #
NASA-TM-103859 ..... N91-26465* #
NASA-TM-103886 ..... N91-26796* #
NASA-TM-104054 ..... N91-26137* #
NASA-TM-104079 ..... N91-26569* #
NASA-TM-104099 ..... N91-26378* #
NASA-TM-104100 ..... N91-26377* #
NASA-TM-104372 ..... N91-26234* #
NASA-TM-104376 ..... N91-26872* #
NASA-TM-104415 ..... N91-26490* #
NASA-TM-104449 ..... N91-26122* #
NASA-TM-104466 ..... N91-26146* #
NASA-TM-104483 ..... N91-26121* #
NASA-TM-104491 ..... N91-26870* #
NASA-TM-104510 ..... N91-26202* #
NASA-TM-104977 ..... N91-26624* #

NASA-TP-3120 ..... N91-26113* #

NATICK/TR-91/017 ..... N91-26752 #
NATICK/TR-91/023 ..... N91-26722 #
NATICK/TR-91/025 ..... N91-26360 #

NBDL-89R006 ..... N91-26674 #

NCEL-R-931 ..... N91-26540 #

NCEL-TN-1825 ..... N91-26406 #

NEAR-TR-421 ..... N91-26119 #

NHRC-90-23 ..... N91-26755 #
NHRC-90-41 ..... N91-26718 #
NHRC-90-43 ..... N91-26717 #

NIFS-81 ..... N91-26937 #

NIST/SP-250/40 ..... N91-26890 #
NIST/SP-790-VOL-2 ..... N91-26997 #

NISTIR-4488 ..... N91-27000 #
NISTIR-4496 ..... N91-26437 #

NMRI-90-116 ..... N91-26673 #
NMRI-90-132 ..... N91-26715 #
NMRI-90-133 ..... N91-26711 #
NMRI-90-135 ..... N91-26710 #
NMRI-91-09 ..... N91-26709 #

NOARL-CR-019 ..... N91-26658 #

NOARL-8 ..... N91-26587 #

NOSC-TD-2042 ..... N91-26417 #

NOSC-TR-1372 ..... N91-26930 #

NOSC/TD-2020 ..... N91-26442 #
NOSC/TD-2055 ..... N91-26950 #
NOSC/TD-2057 ..... N91-27004 #

NOSC/TR-1391 ..... N91-26625 #
NOSC/TR-1400 ..... N91-26491 #
NOSC/TR-1408 ..... N91-26769 #

NPRDC-TR-91-6 ..... N91-26725 #

NPS-MA-91-003 ..... N91-26840 #
NPS-PH-91-003 ..... N91-26837 #
NPS-PH-91-006 ..... N91-26498 #
NPS-PH-91-007 ..... N91-26629 #

NPSOR-91-06 ..... N91-26858 #

NPS69-90-06 ..... N91-26532 #

NR-032-553 ..... N91-26235 #

NRL-MR-6737 ..... N91-26503 #
NRL-MR-6775 ..... N91-26761 #
NRL-MR-6778 ..... N91-26784 #
NRL-MR-6795 ..... N91-26259 #
NRL-MR-6799 ..... N91-26470 #
NRL-MR-6807 ..... N91-26779 #
NRL-MR-6809 ..... N91-26425 #
NRL-MR-6811 ..... N91-26474 #
NRL-MR-6815 ..... N91-26254 #
NRL-MR-6817 ..... N91-26504 #

NRL-PUB-195-6000 ..... N91-27001 #

NRL-9142 ..... N91-26877 #
NRL-9293 ..... N91-26919 #
NRL-9318 ..... N91-26802 #

NUSC-TD-8835 ..... N91-26475 #

NUSC-TR-8827 ..... N91-26844 #

OCNR-114290-17 ..... N91-26733 #

OEFZS-4565 ..... N91-26913 #

ONT-90-165 ..... N91-26877 #

ORNL/CDIAC-34/R1 ..... N91-27043 #

ORNL/TM-11719 ..... N91-26384 #

OTA-O-482 ..... N91-26599 #

PB91-127423 ..... N91-26998 #
PB91-132290 ..... N91-26890 #
PB91-136515 ..... N91-26997 #
PB91-148460 ..... N91-26594 #
PB91-152140 ..... N91-27083 #
PB91-152157 ..... N91-27084 #
PB91-152884 ..... N91-26745 #
PB91-153452 ..... N91-26641 #
PB91-154674 ..... N91-26600 #
PB91-156224 ..... N91-26624* #
PB91-156380 ..... N91-26999 #
PB91-157198 ..... N91-27000 #
PB91-159384 ..... N91-26746 #
PB91-159533 ..... N91-26530 #
PB91-159749 ..... N91-26437 #
PB91-160374 ..... N91-26597 #
PB91-160713 ..... N91-27085 #
PB91-160721 ..... N91-27086 #
PB91-161273 ..... N91-26529 #
PB91-161703 ..... N91-26601 #
PB91-161711 ..... N91-26602 #
PB91-161729 ..... N91-26598 #
PB91-163428 ..... N91-26599 #

PL-TR-91-2031 ..... N91-26635 #
PL-TR-91-3001 ..... N91-26192 #
PL-TR-91-3002 ..... N91-26199 #
PL-TR-91-3003 ..... N91-26341 #
PL-TR-91-3014 ..... N91-26941 #

PNL-MA-70 ..... N91-26555 #

PSI-TR-545445 ..... N91-26658 #

PSU-AFOSR-91-1 ..... N91-26279 #

PSU-ARL-TM-90-320 ..... N91-26887 #

PSU/ARL-TM-91-81 ..... N91-26884 #
PSU/ARL-TM-91-104 ..... N91-26886 #

PSU/ARL-TR-91-004 ..... N91-26561 #

PUBL-911520 ..... N91-26203* #

PWA-FR-21539 ..... N91-26226 #

QUEST-TR-508 ..... N91-26405 #

R/D-5462-AN-01 ..... N91-26388 #
R/D-5718-CH-01 ..... N91-26346 #
R/D-6323-EN-01 ..... N91-26639 #

RADC-TR-90-220 ..... N91-26952 #
RADC-TR-90-232 ..... N91-26443 #
RADC-TR-90-290 ..... N91-26763 #
RADC-TR-90-342 ..... N91-26940 #
RADC-TR-90-404-VOL-1 ..... N91-26815 #
RADC-TR-90-404-VOL-2 ..... N91-26816 #
RADC-TR-90-404-VOL-3 ..... N91-26817 #
RADC-TR-90-404-VOL-4 ..... N91-26818 #
RADC-TR-90-404-VOL-5 ..... N91-26819 #
RADC-TR-90-404-VOL-6 ..... N91-26820 #
RADC-TR-90-404-VOL-7 ..... N91-26821 #
RADC-TR-90-404-VOL-8 ..... N91-26822 #
RADC-TR-90-404-VOL-9 ..... N91-26823 #
RADC-TR-90-404-VOL-10 ..... N91-26824 #
RADC-TR-90-404-VOL-11 ..... N91-26825 #
RADC-TR-90-404-VOL-12 ..... N91-26826 #
RADC-TR-90-404-VOL-13 ..... N91-26832 #
RADC-TR-90-404-VOL-14 ..... N91-26828 #
RADC-TR-90-404-VOL-15 ..... N91-26829 #
RADC-TR-90-404-VOL-16 ..... N91-26830 #
RADC-TR-90-404-VOL-17 ..... N91-26831 #
RADC-TR-90-404-VOL-18 ..... N91-26827 #
RADC-TR-90-412-VOL-1 ..... N91-26422 #
RADC-TR-90-415 ..... N91-26811 #
RADC-TR-90-417 ..... N91-26927 #
RADC-TR-90-424 ..... N91-26814 #

RAND-P-7661-RGS ..... N91-26431 #
RAND-P-7680-RGS ..... N91-26138 #

RAND-R-3843-AF ..... N91-26143 #

RCC-164-91 ..... N91-26127 #
RCC-210-91 ..... N91-26428 #

REPT-1 ..... N91-26714 #
REPT-1-5-36452 ..... N91-26477 #
REPT-1WW/TN-90/001 ..... N91-26645 #
REPT-3 ..... N91-26958 #
REPT-15 ..... N91-27118 #
REPT-28-3-PHASE-1 ..... N91-26650 #
REPT-31 ..... N91-26585 #
REPT-90SRD008 ..... N91-26461* #
REPT-91 ..... N91-26658 #
REPT-91A01040-VOL-2 ..... N91-26573* #
REPT-91B00089 ..... N91-27009* #
REPT-91B00095 ..... N91-27087* #
REPT-91B00103 ..... N91-26651* #
REPT-91SRD001 ..... N91-26678 #
REPT-0092F-PHASE-2 ..... N91-26509 #
REPT-1990 ..... N91-26958 #
REPT-1990-1 ..... N91-26244 #
REPT-1990-7 ..... N91-26245 #
REPT-1990-13 ..... N91-26330 #
REPT-1990-14 ..... N91-26347 #
REPT-1990-15 ..... N91-26251 #
REPT-1990-16 ..... N91-26337 #
REPT-1990-18 ..... N91-26331 #
REPT-1990-20 ..... N91-26332 #
REPT-1990-22 ..... N91-26250 #
REPT-1990-23 ..... N91-26333 #
REPT-1990-34 ..... N91-26328 #
REPT-1990-35 ..... N91-26329 #
REPT-1990-36 ..... N91-26258 #
REPT-1991-3 ..... N91-26862 #
REPT-1991-5 ..... N91-26334 #
REPT-1991-6 ..... N91-26339 #
REPT-1991-7 ..... N91-26340 #
REPT-021535-1-F ..... N91-26659 #

RIVM-222501001 ..... N91-26638

RL-TR-91-6 ..... N91-26441 #
RL-TR-91-10 ..... N91-26444 #
RL-TR-91-19 ..... N91-26429 #
RL-TR-91-29 ..... N91-26993 #
RL-TR-91-32 ..... N91-26430 #
RL-TR-91-48 ..... N91-26994 #

SAND-90-0973C ..... N91-26570 #
SAND-90-1704 ..... N91-26798 #
SAND-90-2331C ..... N91-26936 #
SAND-90-2474C ..... N91-26186 #
SAND-90-2558C ..... N91-26495 #
SAND-90-2926 ..... N91-26653 #
SAND-90-2994C ..... N91-26398 #
SAND-90-3144C ..... N91-26320 #
SAND-90-8003 ..... N91-26285 #
SAND-91-0063C ..... N91-26888 #
SAND-91-0160C ..... N91-26486 #
SAND-91-0422C ..... N91-26972 #
SAND-91-0469C ..... N91-26385 #
SAND-91-0563C ..... N91-27053 #
SAND-91-0632C ..... N91-26399 #
SAND-91-0933C ..... N91-26319 #
SAND-91-0988C ..... N91-26382 #

SAND-91-7029 ..... N91-26463 #

SC71002.AR ..... N91-26359 #

SERI/TP-211-3971 ..... N91-26588 #
SERI/TP-214-4292 ..... N91-26591 #

SGD-551-PT-1 ..... N91-27085 #
SGD-551-PT-2 ..... N91-27086 #
SGD-556-PT-1 ..... N91-27083 #
SGD-556-PT-2 ..... N91-27084 #

SLCET-TR-88-0845-F-PHASE-2 ..... N91-26589 #
SLCET-TR-91-5 ..... N91-26454 #

SR-1 ..... N91-26630 #
SR-1 ..... N91-26631 #
SR-1 ..... N91-27048 #
SR-3 ..... N91-26424 #

SRA-R91-910032-F ..... N91-26989 #

SRL-05-F-1991 ..... N91-26513 #
SRL-6921-F ..... N91-26295 #

SSC-353 ..... N91-26660 #

SSCL-302 ..... N91-26856 #
SSCL-346 ..... N91-26917 #

SSD-TR-91-03 ..... N91-26415 #
SSD-TR-91-05 ..... N91-26115 #
SSD-TR-91-06 ..... N91-26305 #
SSD-TR-91-07-VOL-13 ..... N91-26183 #

STARS-RC-01310/001/00 ..... N91-26783 #

SU-CLASSIC-MANUSCRIPT-91-26 ..... N91-26775 #
SU-CLASSIC-MANUSCRIPT-91-27 ..... N91-26772 #

SU-SLAC-378 ..... N91-26907 #

SU-SOL-91-4 ..... N91-26789 #
SU-SOL-91-5 ..... N91-26788 #

SU-TR-14 ..... N91-26508 #
SU-TR-15 ..... N91-26264 #
SU-TR-17 ..... N91-26263 #
SU-TR-18 ..... N91-26265 #
SU-TR-19 ..... N91-26267 #
SU-TR-21 ..... N91-26266 #
SU-TR-22 ..... N91-26262 #
SU-TR-441 ..... N91-26852 #

SUNY/AB/TR-20 ..... N91-26255 #

SWRI-06-8124 ..... N91-26235 #

TACTEC-R-6266 ..... N91-26185 #

TCS-TP-89-368 ..... N91-26417 #

TIM-5834-2-2-VOL-1 ..... N91-26128 #
TIM-5834-3-1 ..... N91-26129 #

TL-SEAL-4-90 ..... N91-26541 #

TM-91-78 ..... N91-26883 #

TR-2 ..... N91-26302 #
TR-2 ..... N91-26344 #
TR-2 ..... N91-26857 #
TR-3 ..... N91-26220 #
TR-3 ..... N91-26277 #
TR-6 ..... N91-26208 #
TR-7 ..... N91-26900 #
TR-12 ..... N91-26365 #
TR-14 ..... N91-26272 #
TR-15 ..... N91-26456 #
TR-16 ..... N91-26257 #
TR-18 ..... N91-26299 #
TR-18 ..... N91-26343 #
TR-21 ..... N91-26253 #
TR-23-ONR ..... N91-26271 #
TR-24-ONR ..... N91-26268 #
TR-25 ..... N91-26352 #
TR-25-ONR ..... N91-26207 #
TR-26 ..... N91-26353 #
TR-26-ONR ..... N91-26676 #
TR-27 ..... N91-26354 #
TR-28 ..... N91-26350 #
TR-30 ..... N91-26351 #
TR-30 ..... N91-26566 #
TR-37 ..... N91-26248 #
TR-38 ..... N91-26252 #
TR-38 ..... N91-26260 #

TR-39 ..... N91-26206 #
TR-39 ..... N91-26274 #
TR-40 ..... N91-26261 #
TR-40 ..... N91-26275 #
TR-59 ..... N91-26367 #
TR-67 ..... N91-26247 #
TR-68 ..... N91-26249 #
TR-91-1216 ..... N91-26804* #
TR-133 ..... N91-26873 #
TR-827 ..... N91-26413 #
TR-892 ..... N91-26792 #
TR-893 ..... N91-26414 #
TR-894 ..... N91-26795 #
TR-904 ..... N91-26412 #
TR-905 ..... N91-26411 #
TR-907 ..... N91-26920 #
TR-910 ..... N91-26410 #
TR-914 ..... N91-26933 #
TR-0059(9320)-1-VOL-13 ..... N91-26183 #
TR-0090(5925-05)-1 ..... N91-26415 #
TR-0090(5930-01)-2 ..... N91-26115 #
TR-0090(5945-09)-1 ..... N91-26305 #
TR-1990-12 ..... N91-26345 #
TR-1990-17 ..... N91-27002 #
TR-1990-19 ..... N91-26335 #
TR-1990-21 ..... N91-26336 #
TR-901008-5 ..... N91-26439 #

TR4489-096-90 ..... N91-26530 #

TSI-8152-BRL ..... N91-26213 #

TWR-17659 ..... N91-26203* #
TWR-60187 ..... N91-26195* #

UBUFFALO/DC/91/TR-44 ..... N91-26893 #
UBUFFALO/DC/91/TR-45 ..... N91-26894 #
UBUFFALO/DC/91/TR-46 ..... N91-26455 #
UBUFFALO/DC/91/TR-48 ..... N91-26875 #
UBUFFALO/DC/91/TR-49 ..... N91-26963 #

UCB-PTH-90/30 ..... N91-26992 #

UCRL-CR-106563 ..... N91-26318 #
UCRL-CR-106691 ..... N91-26977 #

UCRL-ID-106838 ..... N91-26381 #
UCRL-ID-107120 ..... N91-26519 #

UCRL-JC-105102 ..... N91-26947 #
UCRL-JC-105105 ..... N91-26525 #
UCRL-JC-105107 ..... N91-26518 #
UCRL-JC-105362 ..... N91-26834 #
UCRL-JC-105437 ..... N91-26485 #
UCRL-JC-105594 ..... N91-26975 #
UCRL-JC-105738 ..... N91-26517 #
UCRL-JC-106107 ..... N91-26606 #
UCRL-JC-106571 ..... N91-26241 #
UCRL-JC-106597 ..... N91-27052 #
UCRL-JC-106652 ..... N91-26943 #
UCRL-JC-106677 ..... N91-26612 #
UCRL-JC-106786 ..... N91-26523 #
UCRL-JC-106828 ..... N91-26187 #
UCRL-JC-106926 ..... N91-26526 #

UCRL-LR-107023 ..... N91-27045 #

UDR-TR-90-31 ..... N91-26355 #

UIUC-NCCMR-89-0013 ..... N91-26338 #
UIUC-NCCMR-90-06 ..... N91-26214 #
UIUC-NCCMR-90-07 ..... N91-26212 #
UIUC-NCCMR-90-09 ..... N91-26217 #
UIUC-NCCMR-90-10 ..... N91-26218 #
UIUC-NCCMR-91-01 ..... N91-26216 #
UIUC-NCCMR-91-02 ..... N91-26215 #

ULRF-457/CAR ..... N91-26633 #
ULRF-458/CAR ..... N91-26627 #
ULRF-462/CAR ..... N91-26424 #

URI/GSO-TR-91-2 ..... N91-26662 #

US-PATENT-APPL-SN-035401 ..... N91-26747*
US-PATENT-APPL-SN-056014 ..... N91-26147 #
US-PATENT-APPL-SN-059796 ..... N91-26449
US-PATENT-APPL-SN-178258 ..... N91-26392
US-PATENT-APPL-SN-215136 ..... N91-26450
US-PATENT-APPL-SN-310992 ..... N91-26918*
US-PATENT-APPL-SN-392174 ..... N91-26747*
US-PATENT-APPL-SN-414815 ..... N91-26438*
US-PATENT-APPL-SN-464100 ..... N91-26925
US-PATENT-APPL-SN-516943 ..... N91-26506 #
US-PATENT-APPL-SN-579921 ..... N91-26537 #
US-PATENT-APPL-SN-589230 ..... N91-26224 #
US-PATENT-APPL-SN-597847 ..... N91-26923 #

US-PATENT-APPL-SN-598513 ..... N91-26505 #
US-PATENT-APPL-SN-607345 ..... N91-26536 #
US-PATENT-APPL-SN-627163 ..... N91-26753 #
US-PATENT-APPL-SN-641843 ..... N91-26924 #
US-PATENT-APPL-SN-641997 ..... N91-26448 #
US-PATENT-APPL-SN-657586 ..... N91-26542* #
US-PATENT-APPL-SN-662684 ..... N91-26376* #
US-PATENT-APPL-SN-682160 ..... N91-26375* #
US-PATENT-APPL-SN-687606 ..... N91-26543* #
US-PATENT-APPL-SN-690144 ..... N91-26159* #
US-PATENT-APPL-SN-709907 ..... N91-26200* #
US-PATENT-APPL-SN-710192 ..... N91-26459* #
US-PATENT-APPL-SN-717447 ..... N91-26968* #
US-PATENT-APPL-SN-718314 ..... N91-26967* #
US-PATENT-APPL-SN-718315 ..... N91-26966* #

US-PATENT-CLASS-83-203 ..... N91-26747*
US-PATENT-CLASS-83-206 ..... N91-26747*
US-PATENT-CLASS-83-277 ..... N91-26747*
US-PATENT-CLASS-83-282 ..... N91-26747*
US-PATENT-CLASS-83-614 ..... N91-26747*
US-PATENT-CLASS-83-649 ..... N91-26747*
US-PATENT-CLASS-102-402 ..... N91-26449
US-PATENT-CLASS-149-19.1 ..... N91-26392
US-PATENT-CLASS-244-3.17 ..... N91-26147 #
US-PATENT-CLASS-307-353 ..... N91-26438*
US-PATENT-CLASS-310-366 ..... N91-26450
US-PATENT-CLASS-329-349 ..... N91-26438*
US-PATENT-CLASS-329-361 ..... N91-26438*
US-PATENT-CLASS-350-353 ..... N91-26918*
US-PATENT-CLASS-350-354 ..... N91-26918*
US-PATENT-CLASS-350-358 ..... N91-26918*
US-PATENT-CLASS-357-30 ..... N91-26925
US-PATENT-CLASS-364-713 ..... N91-26918*
US-PATENT-CLASS-364-822 ..... N91-26918*
US-PATENT-CLASS-364-837 ..... N91-26918*
US-PATENT-CLASS-364-841 ..... N91-26918*

US-PATENT-4,939,407 ..... N91-26450
US-PATENT-4,944,815 ..... N91-26392
US-PATENT-4,993,325 ..... N91-26449
US-PATENT-4,993,662 ..... N91-26147 #
US-PATENT-4,996,579 ..... N91-26925
US-PATENT-5,005,457 ..... N91-26747*
US-PATENT-5,005,954 ..... N91-26918*
US-PATENT-5,015,963 ..... N91-26438*

USAARL-91-11 ..... N91-26750 #
USAARL-91-13 ..... N91-26754 #

USAFETAC/DS-90/231 ..... N91-26646 #
USAFETAC/DS-90/232 ..... N91-26648 #
USAFETAC/DS-90/234 ..... N91-26647 #

USAFSAM-SR-90-5 ..... N91-26727 #

USAFSAM-TP-90-22 ..... N91-26136 #
USAFSAM-TP-90-24 ..... N91-26726 #
USAFSAM-TP-90-26 ..... N91-26738 #

USAFSAM-TR-90-18 ..... N91-26677 #
USAFSAM-TR-90-33 ..... N91-26881 #

USCG-D-01-91 ..... N91-26751 #
USCG-D-02-91 ..... N91-26550 #

USCG/ONSCEN-02.1-91-VOL-1 ..... N91-26128 #
USCG/ONSCEN-03-91 ..... N91-26129 #

USGS/WRI-89-4141 ..... N91-26600 #

USNA-3910-3 ..... N91-27118 #

UW-ME-91-001 ..... N91-26227 #

UWA/DME/TR-91/5 ..... N91-26229 #

VPI-E-91-12 ..... N91-26238* #

VTT/LVIS-20009 ..... N91-26593 #

WBS-4B102-11-10 ..... N91-26195* #

WHOI-91-01 ..... N91-26663 #

WL-TR-91-2013 ..... N91-26541 #

WP-89-90-11 ..... N91-26849 #

WRDC-TR-90-2112 ..... N91-26892 #
WRDC-TR-90-3061 ..... N91-26133 #
WRDC-TR-90-4091 ..... N91-26548 #
WRDC-TR-90-4092 ..... N91-26357 #
WRDC-TR-90-4110 ..... N91-26295 #
WRDC-TR-90-4135 ..... N91-26228 #

Appendix

NASA SCIENTIFIC AND TECHNICAL INFORMATION PROGRAM PRODUCTS AND SERVICES

The NASA Scientific and Technical Information (STI) Program provides for the collection and announcement of aerospace-related reports and literature obtained worldwide through agreements and exchanges. The result of the collection is the comprehensive NASA STI Database that covers aeronautics, space, and supporting disciplines.

The STI Database, documents generated or obtained by NASA, and products and services derived from or supporting the database are made available to the NASA research community and to the public. Descriptions and sources of these items are presented in the following pages.

Scientific and Technical Aerospace Reports (*STAR*) is an abstract journal, listing citations with abstracts for aerospace-related reports obtained from worldwide sources. *STAR* is issued on the 8th and 23rd of each month and announces current documents that have been entered into the NASA STI Database during the previous two weeks. The reports are of the following types:

- NASA, NASA contractor, and NASA grantee reports;
- Reports issued by other U.S. Government agencies, domestic and foreign institutions, universities, and private firms;
- Translations in report form;
- NASA-owned patents and patent applications;
- Other U.S. Government agency and foreign patents and patent applications;
- Domestic and foreign dissertations and theses.

Journal, book, and conference literature, journal translations, and certain foreign dissertations having the same subject scope as *STAR* are announced in a companion journal, *International Aerospace Abstracts* (*IAA*). *IAA* is issued on the 1st and 15th of each month and is available from the American Institute of Aeronautics and Astronautics, Technical Information Service, 555 West 57th Street, 12th Floor, New York, NY 10019.

ELIGIBILITY AND REGISTRATION FOR NASA STI PRODUCTS AND SERVICES

Organizations of the type listed below that have registered with NASA can receive products and services.

- NASA offices and installations, contractors, subcontractors, grantees, and consultants;
- Other U.S. Government agencies and their contractors;
- Libraries in the United States that have arrangements with NASA to maintain collections of NASA documents for public reference;
- Other organizations in the United States having a need for NASA documents in work related to aeronautics and space research;
- Organizations abroad that have established reciprocal documents exchange arrangements with NASA.

Only the central service points or central points of document acquisition and control within qualified organizations are eligible to register for NASA STI products and services. Domestic organizations that may be eligible to receive various classes of NASA publications and services should address their requests for registration or further information to:

NASA Center for AeroSpace Information
ATTN: Registration Services
P.O. Box 8757
BWI Airport, MD 21240
301-621-0153

Organizations abroad should direct requests to:

National Aeronautics and Space Administration
Director, Scientific and Technical Information Program
Code NTT
Washington, DC 20546
USA
703-271-5640

SUBJECT SCOPE

The subject scope of *STAR* and *IAA* includes all aspects of aeronautics and space research and development, supporting basic and applied research, and applications. Aerospace aspects of Earth resources, energy development, conservation, oceanography, environmental protection, urban transportation, and other topics of high national priority are also covered.

HOW TO USE *STAR* SUBJECT CATEGORIES

Abstracts in *STAR* are categorized by 10 major subject divisions that are divided further into 76 specific subject categories. The subject divisions and categories are listed in the Table of Contents together with a note for each that defines its scope and provides any cross-references. For example:

16 SPACE TRANSPORTATION
Includes passenger and cargo space transportation, e.g., shuttle operations; and space rescue techniques. For related information see also *03 Air Transportation and Safety* and *18 Spacecraft Design, Testing and Performance.* For space suits see *54 Man/System Technology and Life Support.*

CROSS-REFERENCES

Individual *STAR* abstracts are not ordinarily cross-referenced, except for certain conference reports or book translations that have had separate abstracts written for their component papers or chapters. Citations and abstracts of the components follow immediately after those of the parent document. When the subject content of a component differs sufficiently from the general content of the parent, a cross-reference citation also is printed at the end of the category to which it normally would have been assigned if it were independent.

DOCUMENTS ON MICROFICHE

Documents available on microfiche are designated by a pound sign (#) following the accession number.

LIMITED REPRODUCIBILITY

A note of limited reproducibility appears in the citation, if there are factors affecting the reproducibility of more than 20% of the document. These factors include faint or broken type, color photographs, black and white photographs, foldouts, dot matrix print, or some other factor that limits the reproducibility of the document. This notation also appears on the microfiche header with the specific factor checked off on a list visible in the second frame.

COLOR COPIES

An increasing number of NASA scientific and technical reports are being produced with color graphs, charts, illustrations, and photographs. An indication that a document has color pages follows the source and pricing (SAP) information in the *STAR* citation.

Registered users of the NASA Scientific and Technical Information Program will receive ordered documents with color at no additional cost, as long as stock copies of the document are available. Otherwise, an additional fee of $2.00 per color page will be charged. The NASA Center for AeroSpace Information staff will contact registered users to determine individual user's needs.

NASA PATENTS AND PATENT APPLICATIONS

Patents and patent applications owned by NASA are announced in *STAR* under appropriate subject categories and are referenced in the *STAR* indexes. In the Report/Accession Number Index, patents are indexed by the NASA Case Number, and the U.S. Patent Class. Patent applications are indexed by the NASA Case Number and the U.S. Patent Application Serial Number.

Printed copies of patents (which are not microfiched) are available for purchase from the U.S. Patent and Trademark Office.

NASA patent application specifications are sold in both paper copy and microfiche by the National Technical Information Service (NTIS). The US-Patent-Appl-SN-number should be used in ordering either paper copy or microfiche from NTIS.

When ordering patents, the U.S. Patent Number should be used, and payment must be remitted in advance, by money order or check payable to the Commissioner of Patents and Trademarks. Prepaid purchase coupons for ordering are also available from the U.S. Patent and Trademark Office.

The patents and patent applications announced in *STAR* are owned by NASA and are available for royalty-free licensing. Requests for licensing terms and further information should be addressed to:

National Aeronautics and Space Administration
Associate General Counsel for Intellectual Property
Code GP
Washington, DC 20546

SOURCES FOR DOCUMENTS

One or more sources from which a document announced in *STAR* is available to the public is given in each citation. The most commonly indicated sources and their acronyms or abbreviations are listed on page A-6. If the publication is available from a source other than those listed, the publisher and address will be displayed on the availability line or in combination with the corporate source line.

Avail: NTIS. Sold by the National Technical Information Service. Prices for hard copy (HC) and microfiche (MF) are indicated by a price code following the letters HC or MF in the *STAR* citation. Current values for the price codes are given in the tables on page A-7.

Initially distributed microfiche under the NTIS SRIM (Selected Research in Microfiche) is available at greatly reduced unit prices. For this service and for information concerning subscription to NASA printed reports, consult the NTIS Subscription Section, Springfield, VA 22161.

NOTE ON ORDERING DOCUMENTS: When ordering NASA publications (those followed by the * symbol), use the N accession number. NASA patent applications (only the specifications are offered) should be ordered by the US-Patent-Appl-SN number. Non-NASA publications (no asterisk) should be ordered by the AD, PB, or other *report number* shown on the last line of the citation, not by the N accession number. It is also advisable to cite the title and other bibliographic identification.

Avail: SOD (or GPO). Sold by the Superintendent of Documents, U.S. Government Printing Office, in hard copy. The current price and order number are given following the availability line. (NTIS will fill microfiche requests, as indicated above, for those documents identified by a # symbol.)

Avail: BLL (formerly NLL): British Library Lending Division, Boston Spa, Wetherby, Yorkshire, England. Photocopies available from this organization at the price shown. (If none is given, address inquiry to the BLL.)

Avail: DOE Depository Libraries. Organizations in U.S. cities and abroad that maintain collections of Department of Energy reports, usually in microfiche form, are listed in *Energy Research Abstracts*. Services available from the DOE and its depositories are described in a booklet, *DOE Technical Information Center - Its Functions and Services* (TID-4660), which may be obtained without charge from the DOE Technical Information Center.

Avail: ESDU. Pricing information on specific data, computer programs, and details on Engineering Sciences Data Unit (ESDU) topic categories can be obtained from ESDU International Ltd. Requesters in North America should use the Virginia address while all other requesters should use the London address, both of which are on page A-6.

Avail: Fachinformationszentrum, Karlsruhe. Sold by the Fachinformationszentrum Energie, Physik, Mathematik GMBH, Eggenstein Leopoldshafen, Federal Republic of Germany, at the price shown in deutschmarks (DM).

Avail: HMSO. Publications of Her Majesty's Stationery Office are sold in the U.S. by Pendragon House, Inc. (PHI), Redwood City, CA. The U.S. price (including a service and mailing charge) is given, or a conversion table may be obtained from PHI.

Avail: NASA Public Document Rooms. Documents so indicated may be examined at or purchased from the National Aeronautics and Space Administration, Public Documents Room (Room 126), 600 Independence Ave., S.W., Washington, DC 20546, or public document rooms located at NASA installations, and the NASA Pasadena Office at the Jet Propulsion Laboratory.

Avail: Univ. Microfilms. Documents so indicated are dissertations selected from *Dissertation Abstracts* and are sold by University Microfilms as xerographic copy (HC) and microfilm. All requests should cite the author and the Order Number as they appear in the citation.

Avail: US Patent and Trademark Office. Sold by Commissioner of Patents and Trademarks, U.S. Patent and Trademark Office, at the standard price of $1.50 each, postage free. (See discussion of NASA patents and patent applications below.)

Avail: (US Sales Only). These foreign documents are available to users within the United States from the National Technical Information Service (NTIS). They are available to users outside the United States through the International Nuclear Information Service (INIS) representative in their country, or by applying directly to the issuing organization.

Avail: USGS. Originals of many reports from the U.S. Geological Survey, which may contain color illustrations, or otherwise may not have the quality of illustrations preserved in the microfiche or facsimile reproduction, may be examined by the public at the libraries of the USGS field offices whose addresses are listed on page A-6. The libraries may be queried concerning the availability of specific documents and the possible utilization of local copying services, such as color reproduction.

Avail: Issuing Activity, or Corporate Author, or no indication of availability. Inquiries as to the availability of these documents should be addressed to the organization shown in the citation as the corporate author of the document.

FEDERAL DEPOSITORY LIBRARIES: To provide the general public with greater access to U.S. Government publications, Congress established the Federal Depository Library Program under the Government Printing Office (GPO), with 52 regional depositories responsible for permanent retention of material, inter-library loan, and reference services. (These libraries are not sales outlets.) At least one copy of nearly every NASA and NASA-sponsored publication, either in printed or microfiche format, is received and retained by the 52 regional depositories. A list of the regional GPO libraries, appears on page A-8. A local library can contact a regional depository library to help locate specific reports, or direct contact may be made by an individual.

PUBLIC COLLECTION OF NASA DOCUMENTS

An extensive collection of NASA and NASA-sponsored publications is maintianed by the British Library Lending Divison, Boston Spa, Wetherby, Yorkshire, England, for public access. The British Library Lending Division also has available many of the non-NASA publications cited in *STAR*.

European requesters may purchase facsimile copy or microfiche of NASA and NASA-sponsored documents, those identified by both the symbols # and * from ESA—Information Retrieval Service, European Space Agency, 8-10 rue Mario-Nikis, 75738 Paris CEDEX 15, France.

SUBMITTING DOCUMENTS

All users of this abstract service are urged to forward reports to be considered for announcement in *STAR*. This will aid NASA in its efforts to provide the fullest possible coverage of all scientific and technical publications that might support aeronautics and space research and development. If you have prepared relevant reports (other than those you will transmit to NASA, DOD, or DOE through the usual contract- or grant-reporting channels), please send them for consideration to the NASA Center for AeroSpace Information, P.O. Box 8757, BWI Airport, MD 21240.

Reprints of journal articles, book chapters, and conference papers are also welcome. These will be considered for announcement in *STAR*'s companion journal, *IAA*.

You may specify a particular source to be included in a report announcement if you wish; otherwise the report will be placed on a public sale at the National Technical Information Service. Copyrighted publications will be announced but not distributed or sold.

PURCHASE OF *STAR*

STAR is publicly available on annual subscription from the Superintendent of Documents, U.S. Government Printing Office, Washington, DC 20402.

STAR is available to registered users on annual subscription from the NASA Center for AeroSpace Information, ATTN: Registration Services, P.O. Box 8757, BWI Airport, MD 21240.

Microfiche of the abstract sections of *STAR* are available, on annual subscription only, from NTIS as PB91-911300, Attn: Subscriptions, 5285 Port Royal Road, Springfield, VA 22161. Annual subscription rates are $85.00 North America; $170.00 foreign. Abstract sections for previous years retroactive to 1964 are available at the current rates.

ADDRESSES OF ORGANIZATIONS

American Institute of Aeronautics and Astronautics
Technical Information Service
555 West 57th Street, 12th Floor
New York, New York 10019

British Library Lending Division,
Boston Spa, Wetherby, Yorkshire,
England

Commissioner of Patents and Trademarks
U.S. Patent and Trademark Office
Washington, DC 20231

Department of Energy
Technical Information Center
P.O. Box 62
Oak Ridge, Tennessee 37830

European Space Agency-Information Retrieval Service
ESRIN
Via Galileo Galilei
00044 Frascati (Rome) Italy

Engineering Sciences Data Unit International
P.O. Box 1633
Manassas, Virginia 22110

Engineering Sciences Data Unit International, Ltd.
251-259 Regent Street
London, W1R 7AD, England

Fachinformationszentrum Energie, Physik, Mathematik
GMBH
7514 Eggenstein Leopoldshafen
Federal Republic of Germany

Her Majesty's Stationery Office
P.O. Box 569, S.E. 1
London, England

NASA Center for AeroSpace Information
P.O. Box 8757
BWI Airport, Maryland 21240

National Aeronautics and Space Administration
Scientific and Technical Information Program (NTT)
Washington, DC 20546

National Technical Information Service
5285 Port Royal Road
Springfield, Virginia 22161

Pendragon House, Inc.
899 Broadway Avenue
Redwood City, California 94063

Superintendent of Documents
U.S. Government Printing Office
Washington, DC 20402

University Microfilms
A Xerox Company
300 North Zeeb Road
Ann Arbor, Michigan 48106

University Microfilms, Ltd.
Tylers Green
London, England

U.S. Geological Survey Library National Center
MS 950
12201 Sunrise Valley Drive
Reston, Virginia 22092

U.S. Geological Survey Library
2255 North Gemini Drive
Flagstaff, Arizona 86001

U.S. Geological Survey
345 Middlefield Road
Menlo Park, California 94025

U.S. Geological Survey Library
Box 25046
Denver Federal Center, MS914
Denver, Colorado 80225

NTIS PRICE SCHEDULES

(Effective January 1, 1991)

Schedule A
STANDARD PRICE DOCUMENTS AND MICROFICHE**

PRICE CODE	NORTH AMERICAN PRICE	FOREIGN PRICE
A01	$ 8.00	$ 16.00
A02	11.00	22.00
A03	15.00	30.00
A04-A05	17.00	34.00
A06-A09	23.00	46.00
A10-A13	31.00	62.00
A14-A17	39.00	78.00
A18-A21	45.00	90.00
A22-A25	53.00	106.00
A99	*	*
N01	60.00	120.00
N02	59.00	118.00
N03	20.00	40.00

Schedule E
EXCEPTION PRICE DOCUMENTS AND MICROFICHE**

PRICE CODE	NORTH AMERICAN PRICE	FOREIGN PRICE
E01	$10.00	$ 20.00
E02	12.00	24.00
E03	14.00	28.00
E04	16.50	33.00
E05	18.50	37.00
E06	21.50	43.00
E07	24.00	48.00
E08	27.00	54.00
E09	29.50	59.00
E10	32.50	65.00
E11	35.00	70.00
E12	38.50	77.00
E13	41.00	82.00
E14	45.00	90.00
E15	48.50	97.00
E16	53.00	106.00
E17	57.50	115.00
E18	62.00	124.00
E19	69.00	138.00
E20	80.00	160.00
E99	*	*

* Contact NTIS for price quote.

** Effective January 1, 1991, the microfiche copy of any new document entering the NTIS collection will be priced the same as the paper copy of the document.

IMPORTANT NOTICE

NTIS Shipping and Handling Charges

U.S., Canada, Mexico — ADD $3.00 per TOTAL ORDER

All Other Countries — ADD $4.00 per TOTAL ORDER

Exceptions — Does NOT apply to:

ORDERS REQUESTING NTIS RUSH HANDLING

ORDERS FOR SUBSCRIPTION OR STANDING ORDER PRODUCTS *ONLY*

NOTE: Each additional delivery address on an order requires a separate shipping and handling charge.

FEDERAL REGIONAL DEPOSITORY LIBRARIES

ALABAMA

AUBURN UNIV. AT MONTGOMERY LIBRARY
Documents Dept.
7300 University Drive
Montgomery, AL 36117-3596
(205) 244-3650 FAX: (205) 244-0678

UNIV. OF ALABAMA
Amelia Gayle Gorgas Library
Govt. Documents
Box 870266
Tuscaloosa, AL 35487-0266
(205) 348-6046 FAX: (205) 348-8833

ARIZONA

DEPT. OF LIBRARY, ARCHIVES, AND PUBLIC RECORDS
Federal Documents
Third Floor State Capitol
1700 West Washington
Phoenix, AZ 85007
(602) 542-4121 FAX: (602) 542-4400; 542-4500

ARKANSAS

ARKANSAS STATE LIBRARY
State Library Services
One Capitol Mall
Little Rock, AR 72201
(501) 682-2869

CALIFORNIA

CALIFORNIA STATE LIBRARY
Govt. Publications Section
914 Capitol Mall - P.O. Box 942837
Sacramento, CA 94237-0001
(916) 322-4572 FAX: (916) 324-8120

COLORADO

UNIV. OF COLORADO - BOULDER
Norlin Library
Govt. Publications
Campus Box 184
Boulder, CO 80309-0184
(303) 492-8834 FAX: (303) 492-2185

DENVER PUBLIC LIBRARY
Govt. Publications Dept. BS/GPD
1357 Broadway
Denver, CO 80203
(303) 571-2135

CONNECTICUT

CONNECTICUT STATE LIBRARY
231 Capitol Avenue
Hartford, CT 06106
(203) 566-4971 FAX: (203) 566-3322

FLORIDA

UNIV. OF FLORIDA LIBRARIES
Documents Dept.
Library West
Gainesville, FL 32611-2048
(904) 392-0366 FAX: (904) 392-7251

GEORGIA

UNIV. OF GEORGIA LIBRARIES
Govt. Documents Dept.
Jackson Street
Athens, GA 30602
(404) 542-8949 FAX: (404) 542-6522

HAWAII

UNIV. OF HAWAII
Hamilton Library
Govt. Documents Collection
2550 The Mall
Honolulu, HI 96822
(808) 948-8230 FAX: (808) 956-5968

IDAHO

UNIV. OF IDAHO LIBRARY
Documents Section
Moscow, ID 83843
(208) 885-6344 FAX: (208) 885-6817

ILLINOIS

ILLINOIS STATE LIBRARY
Reference Dept.
300 South Second
Springfield, IL 62701-1796
(217) 782-7596 FAX: (217) 524-0041

INDIANA

INDIANA STATE LIBRARY
Serials/Documents Section
140 North Senate Avenue
Indianapolis, IN 46204
(317) 232-3678 FAX: (317) 232-3728

IOWA

UNIV. OF IOWA LIBRARIES
Govt. Publications Dept.
Washington & Madison Streets
Iowa City, IA 52242
(319) 335-5926 FAX: (319) 335-5830

KANSAS

UNIV. OF KANSAS
Govt. Documents & Map Library
6001 Malatt Hall
Lawrence, KS 66045-2800
(913) 864-4660 FAX: (913) 864-5380

KENTUCKY

UNIV. OF KENTUCKY LIBRARIES
Govt. Publications/Maps Dept.
Lexington, KY 40506-0039
(606) 257-3139 FAX: (606) 257-1563; 257-8379

LOUISIANA

LOUISIANA STATE UNIV.
Middleton Library
Govt. Documents Dept.
Baton Rouge, LA 70803
(504) 388-2570 FAX: (504) 388-6992

LOUISIANA TECHNICAL UNIV.
Prescott Memorial Library
Govt. Documents Dept.
305 Wisteria Street
Ruston, LA 71270-9985
(318) 257-4962 FAX: (318) 257-2447

MAINE

TRI-STATE DOCUMENTS DEPOSITORY
Raymond H. Fogler Library
Govt. Documents & Microforms Dept.
Univ. of Maine
Orono, ME 04469
(207) 581-1680

MARYLAND

UNIV. OF MARYLAND
Hornbake Library
Govt. Documents/Maps Unit
College Park, MD 20742
(301) 454-3034 FAX: (301) 454-4985

MASSACHUSETTS

BOSTON PUBLIC LIBRARY
Govt. Documents Dept.
666 Boylston Street
Boston, MA 02117
(617) 536-5400 ext. 226
FAX: (617) 267-8273; 267-8248

MICHIGAN

DETROIT PUBLIC LIBRARY
5201 Woodward Avenue
Detroit, MI 48202-4093
(313) 833-1440; 833-1409
FAX: (313) 833-5039

LIBRARY OF MICHIGAN
Govt. Documents Unit
P.O. Box 30007
Lansing, MI 48909
(517) 373-0640 FAX: (517) 373-3381

MINNESOTA

UNIV. OF MINNESOTA
Wilson Library
Govt. Publications Library
309 19th Avenue South
Minneapolis, MN 55455
(612) 624-5073 FAX: (612) 626-9353

MISSISSIPPI

UNIV. OF MISSISSIPPI
J.D. Williams Library
Federal Documents Dept.
106 Old Gym Bldg.
University, MS 38677
(601) 232-5857 FAX: (601) 232-5453

MISSOURI

UNIV. OF MISSOURI - COLUMBIA
Ellis Library
Govt. Documents
Columbia, MO 65201
(314) 882-6733 FAX: (314) 882-8044

MONTANA

UNIV. OF MONTANA
Maureen & Mike Mansfield Library
Documents Div.
Missoula, MT 59812-1195
(406) 243-6700 FAX: (406) 243-2060

NEBRASKA

UNIV. OF NEBRASKA - LINCOLN
D.L. Love Memorial Library
Documents Dept.
Lincoln, NE 68588
(402) 472-2562

NEVADA

UNIV. OF NEVADA
Reno Library
Govt. Publications Dept.
Reno, NV 89557
(702) 784-6579 FAX: (702) 784-1751

NEW JERSEY

NEWARK PUBLIC LIBRARY
U.S. Documents Div.
5 Washington Street - P.O. Box 630
Newark, NJ 07101-0630
(201) 733-7812 FAX: (201) 733-5648

NEW MEXICO

UNIV. OF NEW MEXICO
General Library
Govt. Publications Dept.
Albuquerque, NM 87131-1466
(505) 277-5441 FAX: (505) 277-6019

NEW MEXICO STATE LIBRARY
325 Don Gaspar Avenue
Santa Fe, NM 87503
(505) 827-3826 FAX: (505) 827-3820

NEW YORK

NEW YORK STATE LIBRARY
Documents/Gift & Exchange Section
Federal Depository Program
Cultural Education Center
Albany, NY 12230
(518) 474-5563 FAX: (518) 474-5786

NORTH CAROLINA

UNIV. OF NORTH CAROLINA - CHAPEL HILL
CB#3912, Davis Library
BA/SS Dept.—Documents
Chapel Hill, NC 27599
(919) 962-1151 FAX: (919) 962-0484

NORTH DAKOTA

NORTH DAKOTA STATE UNIV. LIBRARY
Documents Office
Fargo, ND 58105
(701) 237-8886 FAX: (701) 237-7138
In cooperation with Univ. of North Dakota, Chester Fritz Library
Grand Forks

OHIO

STATE LIBRARY OF OHIO
Documents Dept.
65 South Front Street
Columbus, OH 43266
(614) 644-7051 FAX: (614) 752-9178

OKLAHOMA

OKLAHOMA DEPT. OF LIBRARIES
U.S. Govt. Information Div.
200 NE 18th Street
Oklahoma City, OK 73105-3298
(405) 521-2502, ext. 252, 253
FAX: (405) 525-7804

OKLAHOMA STATE UNIV.
Edmon Low Library
Documents Dept.
Stillwater, OK 74078
(405) 744-6546 FAX: (405) 744-5183

OREGON

PORTLAND STATE UNIV.
Millar Library
934 SW Harrison - P.O. Box 1151
Portland, OR 97207
(503) 725-3673 FAX: (503) 725-4527

PENNSYLVANIA

STATE LIBRARY OF PENN.
Govt. Publications Section
Walnut St. & Commonwealth Ave. - P.O. Box 1601
Harrisburg, PA 17105
(717) 787-3752

SOUTH CAROLINA

CLEMSON UNIV.
Cooper Library
Public Documents Unit
Clemson, SC 29634-3001
(803) 656-5174 FAX: (803) 656-3025
In cooperation with Univ. of South Carolina, Thomas Cooper Library, Columbia

TENNESSEE

MEMPHIS STATE UNIV. LIBRARIES
Govt. Documents
Memphis, TN 38152
(901) 678-2586 FAX: (901) 678-2511

TEXAS

TEXAS STATE LIBRARY
United States Documents
P.O. Box 12927 - 1201 Brazos
Austin, TX 78711
(512) 463-5455 FAX: (512) 463-5436

TEXAS TECH. UNIV. LIBRARY
Documents Dept.
Lubbock, TX 79409
(806) 742-2268 FAX: (806) 742-1920

UTAH

UTAH STATE UNIV.
Merrill Library & Learning Resources Center, UMC-3000
Documents Dept.
Logan, UT 84322-3000
(801) 750-2684 FAX: (801) 750-2677

VIRGINIA

UNIV. OF VIRGINIA
Alderman Library
Govt. Documents
Charlottesville, VA 22903-2498
(804) 924-3133 FAX: (804) 924-4337

WASHINGTON

WASHINGTON STATE LIBRARY
Document Section
MS AJ-11
Olympia, WA 98504-0111
(206) 753-4027 FAX: (206) 753-3546

WEST VIRGINIA

WEST VIRGINIA UNIV. LIBRARY
Govt. Documents Section
P.O. Box 6069
Morgantown, WV 26506
(304) 293-3640

WISCONSIN

ST. HIST. SOC. OF WISCONSIN LIBRARY
Govt. Publications Section
816 State Street
Madison, WI 53706
(608) 262-2781 FAX: (608) 262-4711
In cooperation with Univ. of Wisconsin-Madison, Memorial Library

MILWAUKEE PUBLIC LIBRARY
Documents Div.
814 West Wisconsin Avenue
Milwaukee, WI 53233
(414) 278-2167 FAX: (414) 278-2137

WYOMING

WYOMING STATE LIBRARY
Supreme Court & Library Bldg.
Govt. Publications
Cheyenne, WY 82002
(307) 777-5920 FAX: (307) 777-6289

National Aeronautics and
Space Administration
Code NTT
Washington, D.C.
20546

Official Business

Penalty for Private Use, $300

SPECIAL FOURTH-CLASS RATE
POSTAGE & FEES PAID
NASA
PERMIT No. G27

NASA
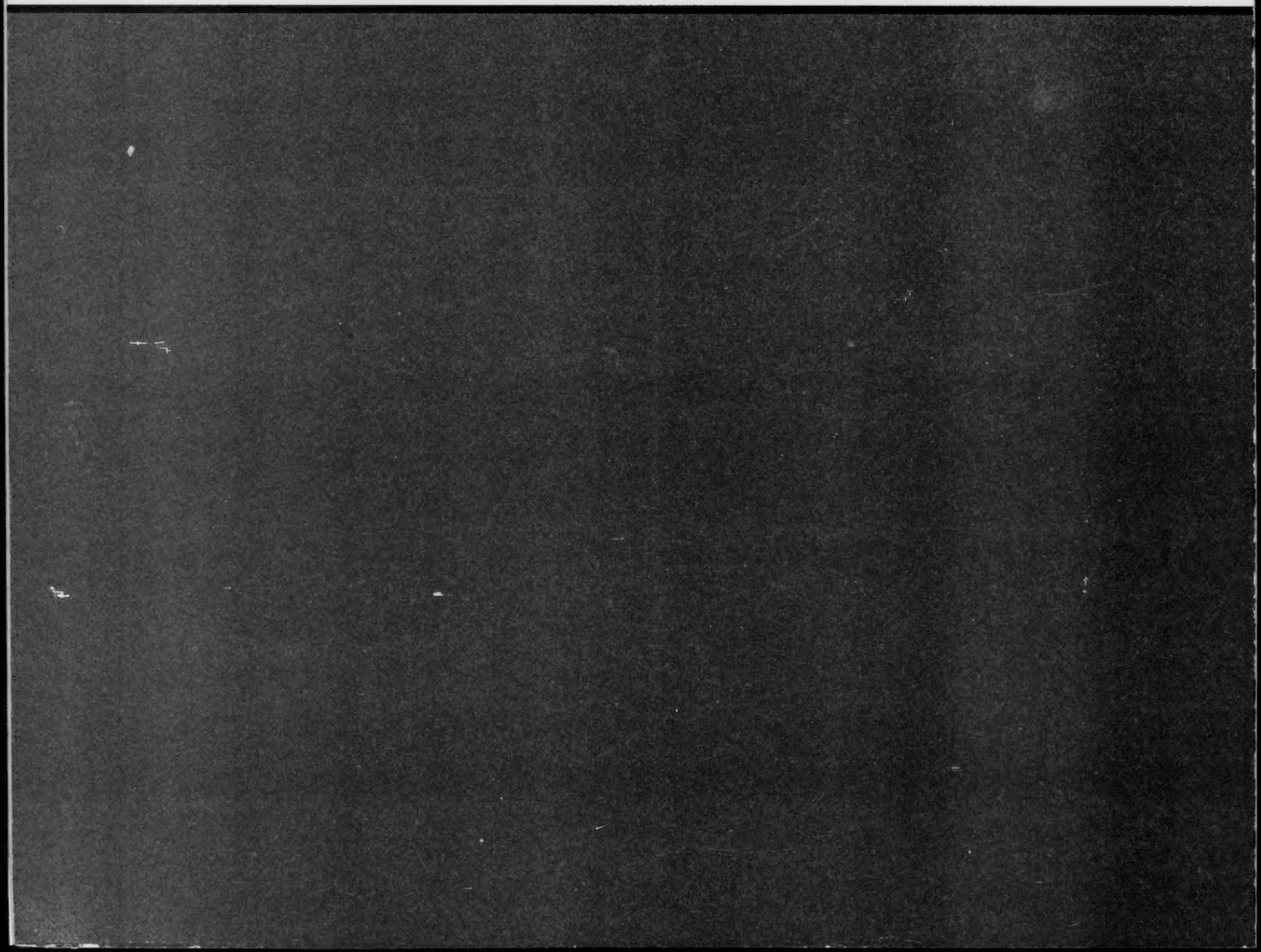
POSTMASTER: If Undeliverable (Section 158 Postal Manual) Do Not Return